EFFECTS OF MOLASSES, BACTERIAL INOCULANT AND ENZYME + BACTERIAL INOCULANT ADDITION ON SILAGE CHARACTERISTICS, IN VITRO ORGANIC MATTER DIGESTIBILITY AND METABOLISABLE ENERGY CONTENT OF GRASS SILAGE

GUL, S.[1*] – COSKUNTUNA, L.[2]

[1]*Plant and Animal Production Department, Vocational School of Technical Sciences, Namik Kemal University, TR-59030 Tekirdag, Turkey*

[2]*Department of Animal Science, Faculty of Agriculture, Namik Kemal University, TR-59030 Tekirdag, Turkey*

**Corresponding author*
e-mail: sgul@nku.edu.tr; phone: +90-282-250-4014; fax: +90-282-250-9934

(Received 25th Mar 2022; accepted 11th Jul 2022)

Abstract. This study was carried out to evaluate molasses, microbial inoculant and microbial inoculant + enzyme (MICROBIOS) *(Lactobacillus plantarum, Lactobacillus brevis, Propionibacterium shermanii, Enterococcus faecium, Bacillus subtilis, Pediococcus acidilactici* and alpha–Amylase (*A. oryzae*), cellulase and hemicellulose (*A. niger*)) addition as silage additives on nutrient contents, in vitro organic matter digestibility (IVOMD) and metablisable energy (ME) of grass silage. The material mixed with additive was pressed in (1.0-1 L) glass jars. Each application consisted of three parallel. Three jars per treatment from all group were analayzed on day 2, 7, 21, 60 for chemical, in vitro digestibility organic matter, metebolisable energy and cell wall contents. According to the analysis; control, molasses, enzyme + inoculant and inoculant groups of dry matter (DM) 26.59, 26.47, 27.00, 26.65, pH 4.75, 4.38, 4.29, 4.04 were found. Additives (molasses, microbial inoculant, enzyme + microbial inoculant) were able to ensure fermentation quality. Particularly inoculant and inoculant + enzyme improved the digestibility organic matter and metabolisable energy contents of silage.
Keywords: *grass, silage additive, feed value, cell wall, minerals*

Introduction

Silage is the main forms of preserved grass and other forages for livestock in Europe and North America (Randby et al., 2015). Pasture grasses is moderately suitable to ensiling due to their botanical composition and low water-soluble carbohydrate contents (Gul et al., 2008; Yuksel, 2019; Arslan et al., 2020). In order to improve feeding value and silage preservation different additives (such as: bacterial inoculant, molasses, enzyme, grains etc.) have been applied (Keady, 2000). Molasses which are the rich sugars and fermentable carbohydrate contents and are also easily handled all over the world. Molasses improved silage fermentation characteristics such as pH and lactic acid concentration (Baytok and Muruz, 2003; Burenook et al., 2012). Enzymes have been used as additives either alone or in combination with lactic acid bacteria (LAB). Enzymes show hemiselluloytic and celluloytic activites. Thus, these activities solubilize the cell wall carbohydrates, increasing the substrate availability for LAB, and after all improve the silage fermentation quality (McDonald et al., 1991; Rinne et al., 2020). Bacterial inoculants contain one or more type of homofermentative LAB that are fast and efficient of lactic acid. The main purpose of using homofermentative LAB inoculants is to improve the nutritional value and to reduce the risk of clostridial fermentations (Driehuis et al., 2001; Muck et al., 2017).

http://www.aloki.hu ● ISSN 1589 1623 (Print) ● ISSN 1785 0037 (Online)
DOI: http://dx.doi.org/10.15666/aeer/2005_36993707

This study was carried out to evaluate the effects molasses, microbial inoculants and enzyme + microbial inoculants as silage additives on nutrient contents, in vitro organic matter digestibility and metabolizable energy value of grass silage.

Material and methods

The study was conducted in Tekirdag (41.0°N, 27.5°E), western Turkey located at about 5 m altitude above sea level and with a total precipitation of 482 mm on average and an annual mean temperature of 10.5 °C. Proportions of the Gramineae, Leguminoseae and other plant families in the pasture grasses were 50.3-51.0%, 31.3-34.8% and 14.2-18.4% of the flora, respectively (Altin et al., 2010). Forage was chopped (1.0-1.5 cm theoretical length of cut). Silage materials were divided into four trial groups for the control, molasses, inoculant and enzyme + inoculant treatments. (1) The chopped forage treatment control; (2) treatment mollases; applied at rate of 5% of fresh forage. (3) inoculant, a mixture of lactic acid bacteria (LAB) consisting of Lactobacillus plantarum and Enterococcus faecium applied at a rate of 6.00 log10 cfu LAB·g-1 of fresh forage (Pioneer 1188, USA). (4) Treatment enzyme + inoculant: enzym as, a mixture of enzymes consisting of cellulase, amylase, hemicellulase and pentosanase enzymes applied at a rate of 0.01 mg·g-1 of fresh forage (Enzyme, Global Nutritech 41600 Kandira, Kocaeli-Turkey), On the day of the experiment, molasses, inoculants and enzymes were suspended in 10 ml of tap water and the whole suspension was sprayed over 5 kg (wet weight) of the chopped forage spread over a 1 × 4 m area. All additives were applied to the forages in a uniform manner with constant mixing (Ozduven et al., 2009, 2010). The material mixed with additive was pressed in (1.0-1 L) glass jars (Weck, Wher-Oftlingen, Germany) equipped with lids that enabled gas release only. The jars were stored under constant room temprature (20 ± 1 °C). Three jars per treatment from all group were sampled on day 2, 7, 21, 60 for analayses of chemical, cell wall contents, in vitro organic matter digestibility and metabolisable energy contents of grass silages.

Analytical procedure

Chemical analyses were performed on triplicate samples. The fresh and silage samples were dried at 60 °C for 72 h in a fanassisted oven. After drying samples were ground through a 1 mm screen for chemical analysis. The dry matter (DM) was determined by drying the samples at 105 °C for 4 h. Crude protein and ash contents of samples were determined according to the methods of AOAC (1990). Neutral detergent fibre (NDF), acid detergent fibre (ADF) and acid detergent lignin (ADL) content determined as described by Van Soest et al. (1991). Metabolisable eenergy (ME) content of fresh and silage samples were calculated from the chemical composition Anonymous (1991). In vitro OMD contents of silages were determined according to the enzyme method reported by Naumann and Bassler (1993). For this purpose, pepsin enzyme (Merck, 0.7 FIP-U/g, Germany) and cellulase enzyme obtained from Trichoderma viride microorganisms (Merck, Onozuka R10; Germany) were used. Ammonia nitrogen (NH_3-N) and pH values fresh and silage samples were determined according to Anonymous (1986). Lactic acid (LA) was determined by the spectrophotometric (Shimadzu UV_12 ol, Kyoto Japan) method Barker and Summerson (1941). Fermentation losses during storage were estimated by weight loss, calculated separately for each jar by the difference in the weight at the beginning and end of the ensiling period. Ca and P content of samples were determined to the methods of AOAC (1990).

http://www.aloki.hu ● ISSN 1589 1623 (Print) ● ISSN 1785 0037 (Online)
DOI: http://dx.doi.org/10.15666/aeer/2005_36993707

Statistical analysis

Statistical analyses were performed with the general linear model (GLM) procedure of Duncan's multiple range test performed with the Statistical Analysis System. Software (SAS, Cary, NC).

$$Y_{ijk} = \mu + a_i + b_j + a_{bij} + e_{ijk} \quad \text{(Eq.1)}$$

Y_{ij} = studied traits; μ = overall mean; $a_{i\,=}$ = effect of b factor; e_{ij} = error; b_j = effect of b factor; ($a_{bij)\ (a*b)}$ = interaction effect.

For all statistical comparisons, a probability level of $P < 0.05$ was accepted as statistically significant. When significant associations were identified, the mean values for each effect were contrasted using Duncan test.

Results

Nutrient content of the silage is presented in *Table 1*. It was determined that the effects of the applications on the DM contents on the 7th and 60th days of the silages were insignificant. The DM contents on the 2nd and 21st days of the silages were determined as 28.43-29.92%, 24.50%-26.03%, respectively, and the difference between the treatments was statistically significant ($P < 0.05$).

CP contents of the silages were determined with the lowest 6.61% DM in the inoculant application on the 21st day, while the highest value was detected on the 21st day with the molasses application with 7.71% DM. The differences between the applications were found to be statistically significant ($P < 0.05$).

The lowest pH value was found with 4.04 in the inoculant group on the 60th day, the highest pH value with 5.39 on the 2nd day of the control group. When the pH contents of the silages were evaluated, the differences between the applications were found to be statistically significant ($P < 0.01$).

LA and WSC contents of silages were determined in the range of 3.29%-3.54% DM, 5.50%-28.50% g/kg DM in all treatment groups, and the differences between treatment groups were statistically insignificant.

The lowest NH_3-N contents of the study were found in the control group on the 7th day with 75.68% g/kgTN and the highest in the control group on the 2nd day with 83.54 g/kgTN. Differences between the 21st and 60th day treatment groups were found to be statistically significant ($P < 0.05$) (*Table 2*).

NDF, ADF and ADL contents of silages were determined in the range of 58.72%-60.22% DM, 44.55%-45.60% DM, 9.23%-10.16% DM in all treatment groups. and the differences between treatment groups were statistically insignificant (*Table 3*).

In vitro organic matter digestion (IVOMD) and metabolic energy (ME) contents of grass silages were determined and given in *Table 4*. In the study OMD value ranged between 49.85%-58.72% respectively. The highest OMD was determined as 58.72% in the inoculants + enzyme group ($P < 0.01$).

ME contents of silages ranged between 1.42%-1.71MJ/kg DM respectively. The highest ME contents was determined as 1.71% MJ/kg DM in the inoculants group ($P < 0.01$) (*Table 4*).

Ca and P contents of silages were determined and given in *Table 5*. In the study P value ranged between 0.26%-0.30% respectively. The highest P contents was determined as 0.30% in the inoculants group ($P < 0.01$).

http://www.aloki.hu ● ISSN 1589 1623 (Print) ● ISSN 1785 0037 (Online)
DOI: http://dx.doi.org/10.15666/aeer/2005_36993707

Table 1. *Results of the chemical analyses of the grass silages*

Day	Treatment	DM %	Weight loss %	pH	CP %(DM)	CF %(DM)
2	C	28.76 b	0.54 b	5.39 a	7.46	31.50 b
	M	28.43 b	0.65 b	5.02 b	7.27	28.58 ab
	E + I	28.60 b	0.86 a	4.40 d	7.12	32.81 c
	I	29.92 a	0.54 b	4.47 c	7.33	33.42 a
	SEM	0.238	0.050	0.153	0.063	0.721
	P	0.033	0.040	0.000	0.316	0.004
7	C	28.45	0.66 ab	5.17 a	7.50 a	34.05 a
	M	28.81	0.59 b	4.89 b	7.63 a	30.51 c
	E + I	28.52	0.75 a	4.06 d	6.78 b	31.82 b
	I	28.59	0.58 b	4.53 c	6.85 b	32.90 ab
	SEM	0.108	0.028	0.156	0.151	0.507
	P	0.763	0.043	0.000	0.021	0.005
21	C	26.03 a	0.51 b	4.65 a	7.66 a	32.97 a
	M	24.50 b	0.56 ab	4.57 b	7.71 a	31.15 b
	E + I	25.50 ab	0.60 ab	4.20 d	7.07 ab	32.36 ab
	I	25.48 ab	0.64 a	4.50 c	6.61 b	32.78 ab
	SEM	0.226	0.020	0.064	0.184	0.312
	P	0.070	0.078	0.000	0.029	0.119
60	C	26.59	0.55 ab	4.75 a	6.99	33.43
	M	26.47	0.59 ab	4.38 b	7.14	32.19
	E + I	27.00	0.51 b	4.29 c	6.77	33.32
	I	26.65	0.63 a	4.04 d	6.90	33.16
	SEM	0.112	0.186	0.097	0.073	0.242
	P	0.465	0.054	0.000	0.386	0.279

$P < 0.05$, $P < 0.01$
DM: dry matter, CP: crude protein, CF: crude fiber, C: control, M: molasses, I: inoculant, E + I: enzyme + inoculant

Discussion

In this study addition of molasses, inoculant, and enzyme + inoculants were significantly affected DM contents (2nd and 21st days) of the silages (*Table 1*) ($P < 0.05$). The higher DM contents in the silages might be related to the readily additives. Additives (molasses, inoculant, and enzyme + inoculants) improve the fermentation and thus preventing the undesirable fermentation of silage and DM loses.

Silage dry matter content is similar to the findings of Bureenok et al. (2012), Khota et al. (2016), Ofori and Nartey (2018); Rinne et al. (2020). It was found to be lower than the findings of Gul et al. (2008), Vendramini et al. (2016), Randby et al. (2015) and Arslan et al. (2020). The difference between the DM findings of the study and the literature findings is due to the plant composition, soil structure and the different additives used.

For good silage fermentation aerobic requirements and reduced pH should be ensured. The pH value usually drops through the fermentation of lactic acid Van Soest (1994). Inoculant + enzyme, inoculant and molasses, added silage groups showed a

http://www.aloki.hu ● ISSN 1589 1623 (Print) ● ISSN 1785 0037 (Online)
DOI: http://dx.doi.org/10.15666/aeer/2005_36993707

significant decrease in pH value compared to the control group (*Table 1*) ($P < 0.01$). The lowest pH value was obtained on day 60th with the addition of inoculant.

Table 2. *Results of the chemical analyses of the grass silages*

Day	Treatment	NH3-N g/kgTN	LA %(DM)	WSC g/kgDM
2	C	83.54	3.29	28.00
	M	77.44	3.31	27.00
	E + I	80.67	3.33	28.50
	I	79.18	3.38	25.00
	SEM	1.044	0.016	1.042
	P	0.195	0.325	0.754
7	K	75.68	3.37	19.50
	M	78.39	3.40	18.00
	E + I	77.55	3.32	20.50
	I	79.68	3.35	18.50
	SEM	0.667	0.014	0.895
	P	0.173	0.335	0,.850
21	C	79.13 a	3.40	13.00
	M	77.43 bc	3.40	11.50
	E + I	78.84 ab	3.42	9.50
	I	76.64 c	3.43	10.50
	SEM	0.414	0.012	0.789
	P	0.034	0.923	0.829
60	K	76.20 b	3.54	7.50
	M	78.37 a	3.52	5.50
	E + I	76.50 b	3.51	6.50
	I	78.83 a	3.51	6.50
	SEM	0.43	0.012	0.626
	P	0.030	0.846	0.827

$P < 0.05$, $P < 0.01$
WSC: water soluble carbohydrates, LA: lactic acid, NH3-N: ammonia nitrogen, C: control, M: molasses I: inoculant, E + I: enzyme + inoculant

Table 3. *Cell wall contents of the grass silages (% DM)*

Day	Treatment	NDF	ADF	ADL
60	C	60.20	44.82	9.83
	M	58.72	45.35	9.23
	E + I	59.90	44.55	10.00
	I	60.22	45.60	10.16
	SEM	0.343	0.225	0.207
	P	0.440	0.384	0.481

NDF: nötral detergan fiber, ADF: acid detergen fiber, ADL: acid detergen lignin, C: control, M: molasses, I: inoculant, E + I: enzyme + inoculant

http://www.aloki.hu ● ISSN 1589 1623 (Print) ● ISSN 1785 0037 (Online)
DOI: http://dx.doi.org/10.15666/aeer/2005_36993707

Table 4. *In vitro OMD and ME contents of grass silage*

Day	Treatment	IVOMD %	ME MJ kg DM
60	C	53.34 bc	1.58 b
	M	49.85 c	1.42 c
	E + I	58.72 a	1.69 ab
	I	56.14 b	1.71 a
	SEM	1.307	0.045
	P	0.016	0.005

P < 0.05, P < 0.01
OMD: organic matter digestibility, ME: metabolize energy, C: control, M: molasses, I: inoculant, E + I: enzyme + inoculant

Table 5. *Mineral matter contents of grass silage (%)*

Day	Treatment	P	Ca
60	C	0.29 ab	0.54
	M	0.26 b	0.53
	E + I	0.26 b	0.45
	I	0.30 a	0.54
	SEM	0.071	0.025
	P	0.000	0.630

P < 0.05, P < 0.01
C: control, M: molasses, I: inoculant, E + I: enzyme + inoculant

The pH values of the silages are similar to the study findings used as additives such as arion vulgaris (Randby et al., 2015), *Lactobacillus buchneri* (Driehuis et al., 2001), fibrolytic enzyme (Rinne et al., 2020) and molasses (Vendramini et al., 2010). At the same time, the pH findings of the study, which used Lactic acid + acetic acid (Vendramini et al., 2016), cassava foilage (Mao et al., 2018) and enzyme as additives (Arslan et al., 2020) were found to be lower than the study findings used, but higher than the study findings using lactic acid and molasses (Bureenok et al., 2012) as additives. The difference between the study findings and previous study findings is due to the additives used and the plant composition.

In this study it was emphasized that use of silage additives induced a decrease CP contents of treatment groups as compared to control group. The highest CP content was found in the molasses group day of 21st.

The research findings were lower than the findings of Khota et al. (2016) who use cellulose and inoculant as additives, Baba et al. (2018) who use corn, soy, molasses and Arslan et al. (2020) who use molasses, oak tannins barley. The difference between research findings and previous study findings is due to the plant composition, soil structure and additives used.

NH_3-N content should not exceed 100 g/kg total nitrogen (Van Soest et al., 1991). All the treatments silage groups met these criteria. This study result emphasized that additives unchanged NH_3-N concentration as compared to control groups. The highest NH_3-N contents found in control group day of 2nd. In accordance with our silage results Arslan et al. (2020) indicated that use of 25 g/kg molasses addition unchanged NH_3-N concentration of silage.

http://www.aloki.hu ● ISSN 1589 1623 (Print) ● ISSN 1785 0037 (Online)
DOI: http://dx.doi.org/10.15666/aeer/2005_36993707

In this study the highest OMD and ME contents were established in enzyme + inoculant silage group. Our study results accordance with Kaya et al. (2009 a) emphasized 40 g/kg barley or 20 g/kg molasses addition increase the organic matter digestion. Another study conducted by Kaya et al. (2009b) was found that 25 g/kg and 50 g/kg barley addition to grass silage did not affect organic matter digestion. Arslan et al. (2020) results indicated that oak tannin extracts, previously fermented juice (OTE and PFE) addition decreased OMD and ME values. Difference may be based on variety, additives and used different in vitro methods.

Ca and P contents of the study are given in *Table 5*. The highest P content was detected in inoculant application.

The additives used did not change the Ca content of the silages. The highest Ca content was found in the control and inoculant group. Tomaz et al. (2018) emphasized that Ca and P content did not change in their study using inoculant as an additive. The reason why the research findings are lower than those of Tomaz et al. (2018) is due to the amount of Ca and P contained in meadow grass and soil.

Conclusion

As a result of the study, it was determined that use of inoculant, molasses, enzyme + inoculant as silage additive improved the nutrient contents and silage fermentation quality. In vitro organic matter digestion and metabolic energy values of grass silage molasses followed the effect of inoculant.

Acknowledgements. This work was supported by Namik Kemal University NKUBAP.00.MB.AR.12.01 foundation Turkey. The authors would like to express thanks for this financial support to Namık Kemal University, Scientific Research Project Commission.

REFERENCES

[1] Altin, M., Tuna C., Gur, M. (2010): Effects of fertilizer application on forage production and botanical composition of floodplain and steppe rangelands of Tekirdag. – Journal of Tekirdag Agricultural Faculty, 7(2): 191-198.

[2] Anonymus (1986): The Analysis of Agricultural Material. Reference Book. – H.M. Stationery Office, London, pp. 427-428.

[3] Anonymus (1991): Animal Feeds - Determination of Metabolizable Energy (Chemical Method). – Turkish Standards Institute (TSE), Publ. No. 9610, 1-3, Ankara.

[4] AOAC. (1990): Official Methods of Analysis. 15th Ed. – Association of Official Analytical Chemists, Arlington, Virginia.

[5] Arslan, C., Tufan, T., Avcı, M., Kaplan, O., Uyarlar, C. (2020): Effects of molasses, barley, oak tannins extracts and previously fermented juice addition on silage characteristics, in vitro organic matter digestibility and metabolisable energy content of grass silage. – Fresenius Environmental Bulletin 29(8): 6533-6542.

[6] Baba, M., Nasir, A., Kabiru, A., Erakpotobor, M., Umar, G. A. (2018): Effects of additives and their levels of inclusion on nutritive value of silage made from elephant grass (Penisetum purpureum). – Nigeria Journal of Food 45(2): 352-362.

[7] Barker, S. B., Summerson, W. H. (1941): The colorimetric determination of lactic acid in biological material. – Journal of Biological Chemistry 138: 535-554. DOI: 10.1016/S0021-9258(18)51379-x.

http://www.aloki.hu ● ISSN 1589 1623 (Print) ● ISSN 1785 0037 (Online)
DOI: http://dx.doi.org/10.15666/aeer/2005_36993707

[8] Baytok, E., Muruz, H. (2003): The effects of formic acid or formic acid plus molasses additives on the fermentation quality and DM and ADF degradabilities of grass silage. – Turkish Journal of Veterinary and Animal Sciences 27(2): 425-431.
[9] Bureenok, S., Yuangklang, C., Vasupen, K., Schonewille, J. T., Kawamoto, Y. (2012): The effects of additives in Napier grass silages on chemical composition, feed intake, nutrient digestibility and rumen fermentation. – Asian Australian Journal of Animal Science 25: 1248-1254. DOI: 10.5713/ajas2012.12081.
[10] Driehuis, F., Oude Elferink, S. J. W. H., Van, Wikselaar. (2001): Fermentation characteristics and aerobic stability of grass silage inoculated with Lactobacillus buchneri, with or without homofermentative lactic acid bacteria. – Grass and Forage Science 56: 330-343. DOI: 10.1046/j.1365-2494.2001.00282.x.
[11] Gul, M., Yörük, M. A., Karaoğlu, M., Macit, M. (2008): Influence of microbial inoculant and molasses and their combination on fermentation characteristics and ruminal degradability of grass silages. – Ataturk University Journal of Agricultural Faculty 39(2): 201-207.
[12] Kaya, I., Unal, Y., Sahin, T. (2009a): The effects of certain additives on the grass silage quality, digestibility and rumen parameters in rams. – Journal of Animal and Veterinary Advances 8(9): 1780-1783. ISSN: 1680-5593.
[13] Kaya, I., Unal, Y., Elmali, D. A. (2009b): Effects of different additives on the quality of grass silage and rumen degradability and rumen parameters of the grass silages in rams. – Journal of the Faculty of Veterinary Medicine, Kafkas University 15(1): 19-24. DOI: 10.9775/kvfd.2008.44-A.
[14] Keady, T. W. J. (2000): Beyond the Science: What the Farmer Looks for in the Production of Silage. – In: Lyons, T. P., Jacques, K. A. (ed.) Biotechnology in the Feed Industry. Proceedings of Alltech's 16th Annual Symposium, Lexington, Kentucky, USA. Nottingham University Press, Nottingham, pp. 439-452.
[15] Khota, W., Pholsen, S., Higgs, D., Cait, Y. (2016): Natural lactic acid bacteria population of tropical grasses and their fermentation factor analysis of silage prepared with cellulase and inoculant. – Journal of Dairy Science 99: 9768-9781. DOI: 10.3168/jds-11180.
[16] Mao, L., Xuejuan, Z. I., Tang, J., Zhou, H., Cai, Y. (2018): Silage fermentation, chemical composition and ruminal degradation of king grass, cassava foliage and their mixture. – Japanese Society of Grassland Science 65: 205-215. DOI: 10.1111/grs.12235.
[17] McDonald, P., Henderson, A. R., Heron, S. J. E. (1991): The Biochemistry of Silage. Second Ed. – Chalcombe Publications, Marlow.
[18] Muck, R. E., Nadeau, E. M. G., McAllister, T. A. Conteras-Govea, F. E., Sanros, M. C., Kung, L. Jr. (2017): Silage review: recent advances and future uses of silage additives. – Journal of Dairy Science 101: 3980-4000.10.3168/jds.2017-13839.
[19] Naumann, C., Bassler, R. (1993): Die Chemische Untersuchung von Futtermitteln. – ln: Naumann, C. et al. (eds.) VDLUFA Methodenbuch. Band III. 3. Erg. VDLUFA, Darmstadt.
[20] Ofori, A. D., Nartey, M. A. (2018): Nutritive value of Napier grass ensiled using molasses as an additive. – The International Journal of Engineering and Science 7(9Ver.II): 45-50. DOI: 10.9790/1813-0709024550.
[21] Ozduven, M. L., Koc, F., Polat, C., Coskuntuna, L. (2009): The effects of lactic acid bacteria and enzyme mixture inoculants on fermentation and nutrient digestibility of sunflower silage. – Journal of the Faculty of Veterinary Medicine, Kafkas University 15(2): 195-199.
[22] Ozduven, M. L., Onal, Z. K., Koc, F., Coskuntuna, L. (2010): The effects of bacterial inoculants and/or enzymes on the fermentation, aerobic stability and in vitro dry and organic matter digestibility characteristics of triticale silages. – Journal of the Faculty of Veterinary Medicine, Kafkas University 16(5): 751-756.
[23] Randby, Å. T., Gismervik, K., Andersen, A., Skaar, I. (2015): Effect of invasive slug populations (Arion vulgaris) on grass silage I. Fermentation quality, in-silo losses and

http://www.aloki.hu ● ISSN 1589 1623 (Print) ● ISSN 1785 0037 (Online)
DOI: http://dx.doi.org/10.15666/aeer/2005_36993707

aerobic stability. – Animal Feed Science and Technology 199: 10-19. DOI: 10.1016/J.ANIFEEDSCI.2014.09.026.

[24] Rinne, M., Winquist, E., Pihlajaniemi, V., Niemi, P., Sppälä, Siika-aho, M. (2020): Fibrolytic enzyme treatment prior to ensiling increased press-juice and crude protein yield from grass silage. – Bioresource Technology 299: 122572. DOI: 10.1016/j.biortech.2019.122572.

[25] Statical Analysis Sistem. (2005): SAS User's Guide: Statistics. Version 6. – SAS Institute, Cary, NC.

[26] Tomaz, P. K., Araujo de, L. C., Sanches, L. A., Santos-Araujo, S. N., Lima de, T. O., Lino, A. de A., Ferreira, E. M. (2018): Effect of sward height on the fermentability coefficient and chemical composition of Guinea grass silage. – Grass Forage Science 73: 588-598. DOI: 10.1111/gfs.12349.

[27] Van Soest, P. J., Robertson, J. B., Lewis, B. A. (1991): Methods for dietary fiber, neutral detergent fiber, and nonstarch polysaccharides in relation to animal nutrition. – Journal of Dairy Science 74: 3583-3597. DOI: 10.3168/jds.S0022-0302(91)78551-2.

[28] Van Soest, P. J. (1994): Nutritional Ecology of the Ruminant. 2nd Ed. – Cornell University Press, Ithaca.

[29] Vendramini, J. M. B., Desogan, A. A., Siveira, L. A., Sollenberger, L. E., Queitoz, O. C. M., Anderson, W. F. (2010): Nutritive value and fermentation parameters of warm-season grass silage. – The Professional Animal Scientist 26: 193-200. DOI: vivo.ufl.edu/individual/n1862820440.

[30] Vendramini, J. M. B., Aguiar, A. D., Adesogan, A. T., Sollen-berger, L. E., Alves, E., Galzerano, L, Salvo, P., Valente, A. L., Ar-riola, K. G., Ma, Z. X., Oliveira, F. C. L. (2016): Effects of: enotype, wilting, and additives on the nutritive value and fermentation of bermudagrass silage. – Journal of Animal Science 94: 3061-3071.

[31] Yuksel, O. (2019): Determination of some physical and chemical characteristics of giant miscanthus (miscanthus x giganteus) silages harvested at different development stages. – Fresenius Environmental Bulletin 28: 4226-4231.

http://www.aloki.hu ● ISSN 1589 1623 (Print) ● ISSN 1785 0037 (Online)
DOI: http://dx.doi.org/10.15666/aeer/2005_36993707

SPATIAL VARIATION IN BENTHIC DIATOM COMMUNITIES IN RELATION TO SALINITY IN THE ARID DRÂA RIVER BASIN (SOUTHERN MOROCCO)

LAZRAK, K.[1] – TAZART, Z.[1] – BERGER, E.[2] – MOUHRI, K.[1] – LOUDIKI, M.[1*]

[1]Water, Biodiversity and Climate Change Laboratory, Phycology, Biotechnology and Environmental Toxicology Research Unit, Faculty of Sciences Semlalia, University Cadi Ayyad, Av. Prince My Abdellah P.O. Box 2390, Marrakech 40000, Morocco
(e-mails: khawla.lazrak.15@gmail.com, zakaria.tazart@gmail.com, mouhri@uca.ac.ma)

[2]iES Landau, Institute for Environmental Sciences, University of Koblenz-Landau, Landau, Germany
(e-mail: berger@uni-landau.de)

**Corresponding author*
e-mail: loudiki@uca.ac.ma; phone: +212-666-935-826; fax: +212-524-436-769
ORCID: 0000-0002-3624-9225

(Received 9th Feb 2022; accepted 10th Jun 2022)

Abstract. Many arid rivers worldwide are under increasing human pressures amplified by hydrological drought and climate change. The Oued Drâa River, Southern Morocco, suffers greatly from global warming and human activities' impacts leading to extreme changes in water salinity. This study aims to investigate spatial changes of benthic diatom community composition in the Drâa river and their relation to environmental factors especially water salinity. The results showed that salinity generally increases from upstream to downstream. A total of 86 diatom taxa belonging to 44 genera were recorded. The Upper Drâa sites were poorly productive in biomass and had diatom communities significantly different from those of the Middle Drâa. The Canonical Correspondence Analysis (CCA) showed that salinity, ion contents, pH and nutrients were the most important structuring factors of diatom assemblages. Oued El Malleh, the most natural salty site of Upper Drâa, was dominated by halotolerant diatoms, whereas the Iriri freshwater stream was characterized by halophobic and oligohaline species. However, the diatom composition of Middle Drâa sites was dominated by halophilic species that tolerate moderate salinity from anthropogenic sources. This survey provides a first inventory of the benthic diatom assemblages of Drâa river and highlights their spatial variability and sensitivity to environmental impacts.
Keywords: *desert river, Drâa basin, diatom assemblages, diversity, spatial distribution, salinity*

Introduction

Desert rivers are highly dynamic systems characterized by changing flow regime, hydromorphological and physicochemical features (Kingsford and Thompson, 2006; Harms et al., 2018). These rivers with intermittent flow are strongly shaped by contrasting hydrological events (drought and floods) and are abundant in arid, Mediterranean and North African regions where they are commonly called "wadis" (Wheater and Al Weshah, 2002; Sen, 2008). They are part of the so-called intermittent rivers and ephemeral streams (IRES) that share the common characteristics of water scarcity, cessation of surface flow at some point of time and space as well as high spatial and temporal variability of habitats during the hydrological cycle (Stanley et al., 1997; Datry et al., 2017). In arid and semi-arid regions such North Africa, human pressures on riverscapes are particularly strong and several activities may affect the

http://www.aloki.hu ● ISSN 1589 1623 (Print) ● ISSN 1785 0037 (Online)
DOI: http://dx.doi.org/10.15666/aeer/2005_37093736

river flow regimes often modified by dam construction, surface and groundwater abstraction and land uses (Malmqvist and Rundle, 2002; Vörösmarty et al., 2010).

The Drâa river, southern Morocco, is one of the most arid river basins in the world spanning from the High Atlas Mountains to the Sahara Desert in the south, with increasing aridity along a north southeast direction (Carrillo-Rivera et al., 2013). Owing to the increasing frequency of dry years and prolonged dry periods, the sustainability of the water supply (drinking water and irrigation) and the oases of the Middle Drâa valley is strongly threatened. Both climate change and the overuse of water resources in the catchment area are leading to falling groundwater levels and increasing salinization of soils and waterways (Speth et al., 2010; Johannsen et al., 2016). In addition, rivers in the Drâa basin are mostly ephemeral, depending on rainfall or snowmelt, and are often naturally saline due to high evaporation and geology (primary salinization) (Bailey et al., 2006). However, this salinization is amplified, especially in the downstream, through anthropogenic changes in the hydrologic cycle (e.g. dams) and in catchment land-use (e.g. agriculture, intensive irrigation) (secondary salinization) (Potapova and Charles, 2003; Cañedo-Argüelles et al., 2013; Nhiwatiwa et al., 2017). Increased salinization in this intermittent river also endangers ecosystem services such as drinking water quality and agricultural yields (Stevenson and Smol, 2015; Berger et al., 2019).

Salinization of rivers is known to affect the species composition of riverine biota through a reduction in biodiversity (Williams, 1987; Piscart et al., 2005; Cañedo-Argüelles et al., 2013; Schröder et al., 2015). For instance, when salinity levels increase, some species react sensitively potentially leading to population decline or disappearance (Williams and Williams, 1998; Piscart et al., 2006). Chemical changes such as variations in salinity affect the physiological response of species in aquatic ecosystems, namely diatoms (Bere and Tundisi, 2011a). In rivers and streams, benthic diatoms are the most widespread, diverse and species-rich group of benthic algae (Lowe and LaLiberte, 2017). Therefore, they form a large portion of total algal biomass and a major source of energy for aquatic food webs as primary producers (Stevenson et al., 1996; Pan et al., 1999). Photosynthesis by periphytic algae, in general, and diatoms in particular, provides oxygen to aerobic organisms (Lowe and LaLiberte, 2017), so that any change in their composition and structure can affect the growth, development, survival and reproduction of many organisms in aquatic ecosystems (Campeau et al., 1994).

Moreover, diatoms are considered as an excellent bioindicator for water quality monitoring (Lange-Bertalot, 1979; Potapova and Charles, 2005; Centis et al., 2010; Stevenson and Smol, 2015). Because they are very sensitive to physical, chemical, pollution and salinity disturbances, their composition and abundance respond to several environmental factors such as nutrients, pH and conductivity (Potapova and Charles, 2002). Benthic diatom-based assessments to quantify river pollution and impairment have been used worldwide, especially in EU countries and the USA (Charles et al., 2021).

Despite the importance of the Drâa basin as one of the most important oasis areas in South of Morocco, benthic algal and diatoms communities in particular, remain poorly understood compared to other aquatic groups such as fish (Qninba et al., 2011; Clavero et al., 2015, 2017), turtles (Loulida et al., 2019), aquatic and semi-aquatic plants (Mostakim et al., 2020), mammals (Riesco et al., 2020) and invertebrates (Berger et al., 2021). Therefore, this study aims to investigate the diversity of benthic diatoms communities in this desert intermittent river and to assess the salinity effects

http://www.aloki.hu ● ISSN 1589 1623 (Print) ● ISSN 1785 0037 (Online)
DOI: http://dx.doi.org/10.15666/aeer/2005_37093736

on their composition and spatial distribution. This information allows us to better understand the autecology of diatoms in IRES in relation to salinity (conductivity and major ions). Our hypotheses were that, changes in salinity would be reflected in diatom community composition which could be used as bioindicator of salinization and human impacts.

Material and methods

Study area and sampling sites

The study was carried out in the Drâa river basin (~115,000 km²) located in southern Morocco (*Fig. 1*). This river is formed by the confluence of several perennial, intermittent and ephemeral rivers and streams from High Atlas such Dades, Imini, Iriri, El Malleh and from Anti Atlas such Ait Douchen (Warner et al., 2013). The Drâa river basin is subdivided into three sub-basins the Upper Drâa, the Middle Drâa and the Lower Drâa. The Upper Drâa subcatchment is part of the Ouarzazate province, extends from the High Atlas summits to outlet at the Mansour-Eddahbi (ME) reservoir, while the Middle Drâa, belonging to the Zagora province, is drained from ME dam up to the M'hamid oasis (Schulz et al., 2008). The altitude of the basin ranges from 450 to 4071 m above sea level (Diekkrüger et al., 2012). The area is characterized by an increasing north-southeast aridity gradient with average annual precipitation ranging from 600 to 700 mm on the southern slopes of the High Atlas Mountains in the north to 200 mm in the valley, and 60 mm in the southern section, whereas evaporation is very important, varying between 2000 and 3000 mm/year (Karmaoui et al., 2015). Regarding hydrological regime of the Drâa river, the Upper Drâa valley has an undisturbed natural hydrological regime of the semi-arid subtropics, except for Iriri stream, which has been recently (2013) regulated by the Sultan Moulay Ali Cherif dam, while the hydrology of the Middle Drâa subcatchment is controlled by water releases from the ME dam. The Upper and Middle Drâa sub-basins are more densely populated especially alongside the rivers, owing to the water availability for drinking and irrigation (Diekkrüger et al., 2012). The Middle Drâa valley is mainly rural and its economic activities remains highly dependent on irrigated agriculture, oasis and tourism (Karmaoui et al., 2014).

Sampling of benthic diatoms was carried out in March 2018 at seven sites (*Fig. 1* and *Appendix 1*). Three sites (S1, S2 and S3) in the Upper Drâa streams (Iriri, El Malleh and Ait Douchen respectively) and four sites (S4, S5, S 6 and S7) in the Middle Drâa valley (oued Drâa at Kasbah Tamnogalt, Taghzout, Zagoura and Tamgroute localities). *Table 1* provides description of the sampling sites, their substrate type and vegetation.

Hydrological and physicochemical parameters

At each sampling site, water temperature (°C), dissolved oxygen (mg/L), pH, electrical and conductivity (µS/cm) and salinity (g/L) were measured *in situ* at the time of sampling using a Hanna HI98194 multi-parameter device (Hanna Instruments, USA). Flow velocity (m/s) and flow rate (m^3 /s) were determined using current meter (OTT hydromet GmbH, Germany) by taking three measurements across the width of the river for each site.

Water samples from each site were collected in PVC bottles (1 L) already well rinsed, and stored in cooler for transport to the laboratory. According to Rodier et al.

http://www.aloki.hu ● ISSN 1589 1623 (Print) ● ISSN 1785 0037 (Online)
DOI: http://dx.doi.org/10.15666/aeer/2005_37093736

(2009) analytical methods, the water samples were measured for ammonium (NH_4^+), orthophosphate (PO_4^{3-}), total alkalinity (HCO_3^-), total hardness ($CaCO_3$), sulfate (SO_4^{2-}) and chloride (Cl^-).

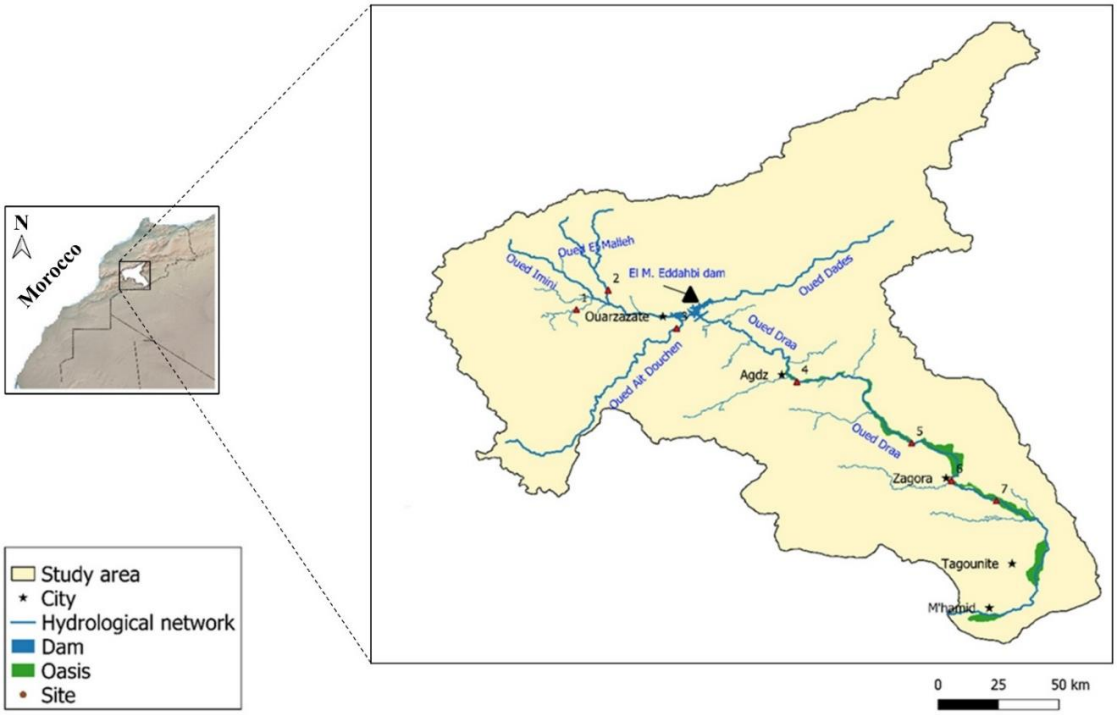

Figure 1. *Location of the study area and sampling sites in Drâa basin*

Table 1. *Description of sampling sites*

Sub-basins	Streams	Sampling site	Coordinates	Altitude (m)	Localization	Substratum type	Vegetation
Upper Drâa	Iriri	1	N: 30°93'75.7" W: 007°21'06.3"	1234	Three Km downstream of the Sultan Moulay Ali Cherif dam	Stones, pebbles and muddy sediments	Aquatic macrophytes, filamentous algae
Upper Drâa	El Malleh	2	N: 31°00'39.6" W: 007°06'0.2"	1028	downstream of Ait Benhaddou Kasbah	Pebbles, silts, clays and muds	*Phragmites australis* and *Tamarix gallica*
Upper Drâa	Ait Douchen	3	N: 30°52'13.7" W: 006°50'54.0"	874	Oued Ait Douchen (near to Tarmigte locality)	Stones, clays and silts	Abundance of vegetation composed mainly of *Nerium oleander*, herbaceous, *Potamogeton nodosus* and filamentous algae floating on the surface
Middle Drâa	Drâa	4	N: 30°40'26.4'' W: 006°24'21,599"	908	Downstream of Agdz (Kasbah Tamnogalt locality)	Sands, clays strewn with stones and pebbles	Highly developed, *Tamarix gallica, Nerium oleander* and *Juncus acutus*
Middle Drâa	Drâa	5	N: 30°26'55.3" W: 005°59'3.1"	781	Just before Ternata oasis (Taghzout locality)	Stones and pebbles	*Phoenix dactylifera* (oasis), *Arundo donax* and *Acacia tortilis*
Middle Drâa	Drâa	6	N: 30°32'23.6" W: 005°83'23.0"	711	At the Zagora city	Stones, pebbles and muddy deposits	Highly degraded vegetation due to human disturbance
Middle Drâa	Drâa	7	N: 30°14'12,5" W: 5°40'21"	678	20 km downstream of the Zagora city (Tamgroute locality)	Stones and pebbles	Highly developed, *Tamarix gallica*

http://www.aloki.hu ● ISSN 1589 1623 (Print) ● ISSN 1785 0037 (Online)
DOI: http://dx.doi.org/10.15666/aeer/2005_37093736

Benthic diatoms sampling

Epilithic biofilm was sampled at each site by brushing stones with a toothbrush. Prior to sampling of epilithic surfaces, all substrata were gently shaken in stream water to remove any loosely attached sediments and non-epilithic diatoms. The pebble to cobble sized rocks/stones were randomly collected at different points of each sampling site across a 100 m long section to sample all microhabitats in riffles and pools. After brushed, the resulting periphytic suspensions were combined into single sample per site. For quantitative sampling, the biofilm sample was obtained by brushing a defined surface (at least 10 × 10 cm) of the substratum. All samples were divided into defined amounts, placed in labelled plastic bottles and preserved in Lugol solution, except for subsamples subjected to chlorophyll *a* analysis, and all transported to the laboratory for qualitative and quantitative analysis.

Treatment and taxonomic identification of diatoms

After homogenization of biofilm samples, an aliquot from each site was digested using concentrated hydrogen peroxide (30%) and hydrochloric acid (35%) to remove organic matter and calcium carbonates. After repeated rinsing and centrifugation with distilled water, the cleaned diatom suspensions were then mounted on glass slide using Naphrax® (IR = 1.7) high refractive mounting medium for taxonomic identification and counting. Diatoms slides were observed under 400–1000× magnification using a Motic BA210 light microscope (Motic®, China) and species were identified based on (Krammer and Lange-Bertalot, 1986; Krammer and Lange-Bertalot, 1988; Krammer, 1991a, 1991b). Diatom synonymy was updated by Algaebase (Guirry and Guirry, 2020). A minimum of 400 diatom valves were counted from each slide to calculate the relative abundance (in %) of diatom species. Only those taxa with an abundance more than 1% of the total sample were included for further statistical analysis.

Diatom total abundance

To determine the diatom total abundance (cells.cm^{-2}), a known surface of each homogenous biofilm sample was placed in a glass slide (24 × 60 mm). The total of diatom valves was counted from each slide at 1000× magnification using a Motic BA210 light microscope (Motic®, China). Diatom abundance was expressed in number of cells.cm^{-2}.

Diatom diversity and similarity indices

Diatom species richness (S), Shannon diversity index (H') (Shannon and Weaver, 1963), Pielou's species evenness (E) (Pielou, 1966) and Simpson's diversity index (SDI) (also known as Species Diversity Index) (Simpson, 1949) were calculated. H' is more subtle to rare species than SDI, gave more weight to common species, while E gave an indication of the equitability of species in the population (homogeneity). Similarity in taxonomic composition of diatom community between the sites was analyzed using Sorensen index (Sorensen, 1948). The formulas are as follows (*Eqs. 1, 2, 3* and *4*):

Shannon–Weaver diversity (H') index:

$$H' = -\sum P_i log_2 P_i ; \quad P_i = {}^{n_i}/_{N} \qquad \text{(Eq.1)}$$

http://www.aloki.hu ● ISSN 1589 1623 (Print) ● ISSN 1785 0037 (Online)
DOI: http://dx.doi.org/10.15666/aeer/2005_37093736

where n_i = number of individuals of species *i*; *N* = total number of individuals in the site.

Pielou's evenness index (E):

$$E = {H'}/{log_2 S} \quad \text{(Eq.2)}$$

where *H*': Shannon index; *S*: number of species present.

Simpson Diversity Index (SDI):

$$SDI = 1 - \sum p^2 \quad \text{(Eq.3)}$$

where *p* = the proportion (*n*/*N*) of individuals of one particular species found (*n*) divided by the total number of individuals found (*N*).

Sorensen (Qs) index:

$$Q_s = {2j}/{a + b} \quad \text{(Eq.4)}$$

where *a* = total number of species at site A; *b* = total number of species at site B; *j* = total number of common species between the two sites A and B.

Biofilm biomass

Dry weight measurement

A known surface of each homogenous biofilm sample was centrifugated at 6000 rpm for 15 min, then the pellet was dried in an oven at 105 °C to constant weight (dry weight, W1) using a previously weighed porcelain capsules (W0). The biofilm dry weight (DW) was then calculated on the basis of the difference between W1 and W0 and values expressed as mg dw.cm^{-2}**.** The porcelain capsules were then transferred to a muffle furnace type N3/R (Nabertherm®, Germany) at 550 °C and ashed for 5 h. Ash-free dry weight (AFDW) (i.e. organic matter dry mass) was calculated by the difference between the weight of the residue calcined at 550 °C (W2) and (W1).

Chlorophyll a analysis

Biofilm biomass was determined by measuring Chlorophyll *a* (Chl-*a*) content according to the protocol of (Millerioux, 1975). Chlorophyll *a* content was measured spectrophotometrically by recording absorbance at 630, 664 and 750 nm and using the equation of Jeffrey and Humphrey (1975), as follows (*Eq. 5*):

$$Chl - a\left({\mu g}/{ml}\right) = 11.47(A_{630} \times A_{750}) - 0.4(A_{664} \times A_{750}) \quad \text{(Eq.5)}$$

Chlorophyll *a* is expressed in µg/ml and converted to µg/cm².

Statistical analysis

The analysis of water physicochemical and algal biomass parameters was done in triplicate and the results are given in mean ± standard error (SE). Pearson's correlation was used to determine the relationships between environmental variables and diatom diversity indices (species richness S, H', E and SDI). One-way analysis of variance

http://www.aloki.hu ● ISSN 1589 1623 (Print) ● ISSN 1785 0037 (Online)
DOI: http://dx.doi.org/10.15666/aeer/2005_37093736

ANOVA and Tukey's honest significance test were used to find significant differences between sampling sites. Canonical correspondence analysis (CCA) was performed to assess the correlations between diatom assemblages and environmental variables and identify the main explanatory factors for their diversity and distribution (Šmilauer and Lepš, 2014). The Pearson correlation and cluster dendrogram were carried out using PAST version 4.02. The ANOVA was performed using SPSS Statistics, Version 23.0. The CCA analysis was carried out using Canoco software version 5.

Results

Hydrological and physicochemical parameters

The hydrological and physicochemical parameters measured *in situ* or in laboratory (mean ± SD) are reported in *Table 2*.

Table 2. *Physicochemical and hydrological parameters of sampled sites*

Parameter	Site 1	Site 2	Site 3	Site 4	Site 5	Site 6	Site 7
Water T (°C)	22.8	21.7	15.9	18.4	26.6	22.3	20.3
pH	8.7	7.77	8.22	7.89	7.9	7.96	7.91
EC ($\mu S.cm^{-1}$)	385.5	7090	1154	2050	5670	4533	3110
Salinity ($g.L^{-1}$)	0.194	4.187	0.704	1.211	2.961	2.561	1.798
Dissolved oxygen ($mg.L^{-1}$)	8.64	8.4	9.26	9.1	12.56	9.22	6.99
NH_4^+($\mu g.L^{-1}$)	24.36±0.003	0±0.00	5.96±0.001	22.87±0.001	0±0.00	11.43±0.003	13.42±0.00
PO_4^{3-}($\mu g.L^{-1}$)	44.88±3.73	52.53±1.30	181.30±37.98	47.38±3.92	72.53±20.06	28.25±0.37	90.88±4.38
HCO_3^- ($mg.L^{-1}$)	194±2.82	132±5.65	190±2.82	184± 5.60	78±2.82	172±5.65	164±5.65
$CaCO_3$(mg. L^{-1})	178.67±6.11	1832±0.00	429.33±4.61	793.33±2.30	693.33±2.30	1492±0.00	546.66±2.30
SO_4^{2-}($mg.L^{-1}$)	8.97±0.067	77.39±0.87	10.45±0.68	31.82±0.22	19.73±0.13	46.41±2.60	30.58±0.93
Cl^- ($g.L^{-1}$)	0.02±0.008	1.88±0.00	0.16±0.008	0.29±0.008	1.29±0.00	0.96±0.008	0.47±0.01
Flow velocity ($m.s^{-1}$)	0.7544±0.12	0.603±0.15	0.0134±0.5	0.390±0.25	0.327±0.25	0.288±0.3	0.146±0.2
Flow rate ($m^3.s^{-1}$)	1.30±0.25	0.9±0.2	0.0104±0.06	0.708±0.25	0.315±0.85	0.32±1.58	0.269±0.105

The hydrological variables showed spatial variation and significant differences between the Upper Drâa and Middle Drâa sites. The flow velocity values varied between 0.7544 $m.s^{-1}$ in site 1 and 0.146 $m.s^{-1}$ in site 7 with a significantly decreasing upstream-downstream gradient. In the downstream part of the Ait Douchene (site 3), the stream was mainly dominated by large pools and the water flow is extremely low (0.0134 $m.s^{-1}$). The Upper Drâa sites showed highest flow rates compared to the Middle Drâa sites which are regulated by the large ME reservoir and by small weirs throughout the southern oases. These hydraulic systems cause significant changes in runoff and a great hydro-morphological heterogeneity of the surface flow and habitats which was mostly reduced to isolated or weakly connected pools with varying degrees of intermittency.

The water physicochemical parameters showed spatial variability and significant differences between the Upper Drâa and Middle Drâa sites. The electrical conductivity values showed spatial variability ranging from 385.5 $\mu S.cm^-$ to 7090 $\mu S.cm^{-1}$. Except for site 2 of Oued El Malleh with a significantly high salinity (4.187 g/L), water conductivity and salinity increase gradually from the Upper to the Middle Drâa basin. The major anions (Cl^-, SO_4^{2-}, CO_3^-) showed the same spatial variation with the highest contents in oued El Malleh and the Middle Drâa downstream sites. The water pH ranged from 7.77 to 8.7 with highest values at sites 1 and 3. Ammonium concentrations were

http://www.aloki.hu ● ISSN 1589 1623 (Print) ● ISSN 1785 0037 (Online)
DOI: http://dx.doi.org/10.15666/aeer/2005_37093736

very low at all sampling sites, however sites 1 (24.36 µg.L^{-1}), site 4 (22.87 µg.L^{-1}) and site 7 (13.42 µg.L^{-1}) had the highest values compared to the other sites. For phosphorus, site 3 had the highest content (181.30 µg.L^{-1}) compared to the other sites, followed by site 7 (97.88 µg.L-1), both of these sites recorded values greater than 76 µg.L^{-1} which indicates a highly productive or eutrophic system according to The Trophic Status Classification of U.S. Streams (Stackpoole et al., 2019).

Benthic diatoms diversity analysis

Diatom composition

A total of 86 diatom species belonging to 44 genera were identified in all prospected sites as illustrated in *Table 3*. There were a few taxa that could not be identified to the species level because of their very small size, which requires further in-depth morphological investigations. These unidentified species belong mainly to the genera *Navicula* and *Nitzschia*. The Drâa phytobenthic community was mostly represented by pennate diatoms while centric diatoms were represented by only two taxa ~~only~~ (*Fig. 2*). The highest number of taxa belonged to *Nitzschia* (15 species) followed by *Navicula* (9 species), *Caloneis* (4 species), *Amphora* and *Sellaphora* with 3 species for each one.

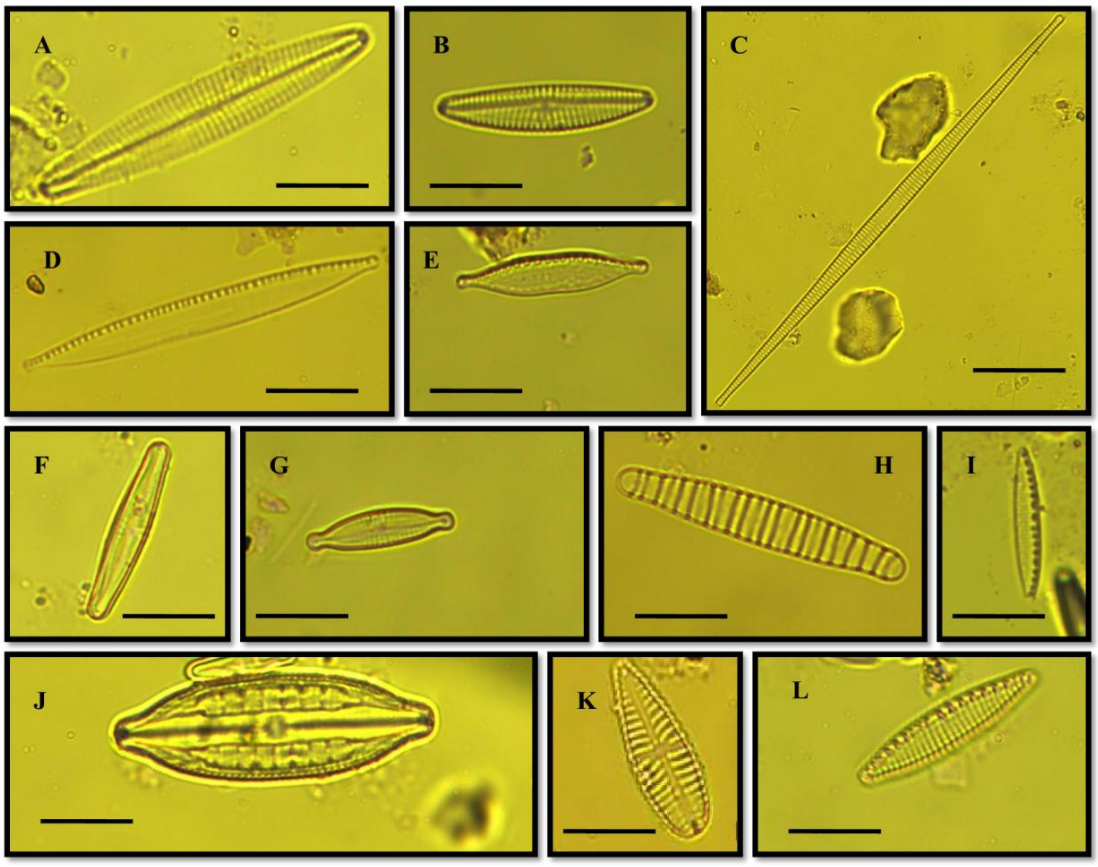

Figure 2. *LM photomicrographs of some characteristic diatoms. A: Haslea stundlii; B: Navicymbula pusilla; C: Ulnaria acus; D: Nitzschia palea; E: Nitzschia elegantula; F: Achnanthidium minutissimum; G: Encyonopsis microcephala; H: Diatoma moniliformis; I: Nitzschia frustulum; J: Mastogloia smithii; K: Gomphonella olivacea; L: Homoeocladia amphibia. Scale bar:10 µm*

http://www.aloki.hu ● ISSN 1589 1623 (Print) ● ISSN 1785 0037 (Online)
DOI: http://dx.doi.org/10.15666/aeer/2005_37093736

Table 3. *List of the identified diatoms in the sampling sites. (+) presence*

Taxon/site	Code	1	2	3	4	5	6	7
Pennate diatoms								
G/Achnanthidium								
Achnanthidium minutissimum (kützing) Czarnecki	ADMI	+	+	+	+	+	+	+
G/Amphora								
Amphora coffeaeformis var. *acutiuscula* (Kützing) Rabenhorst	ACOFA		+					
Amphora inariensis Krammer	AINA					+		
Amphora pediculus (Kützing) Grunow	APED			+	+	+		
G/Anomoeoneis								
Anomoeoneis vitrea (Grunow) R.Ross	AVIT				+	+	+	
G/Bacillaria								
Bacillaria paxillifera (O.F.Müller) T.Marsson	BPAX				+			
G/Caloneis								
Caloneis amphisbaena (Bory) Cleve	CAMH			+	+	+	+	+
Caloneis macedonica Hustedt	CMAC							+
Caloneis silicula (Ehrenb.) Cleve	CSIL			+	+	+	+	
Caloneis thermalis (Grunow) Krammer	CTHE				+			
G/Cocconeis								
Cocconeis pediculus Ehrenberg	CPED	+		+	+			
Cocconeis placentula Ehrenberg	CPLA	+		+	+	+		
G/Craticula								
Craticula riparia (Hustedt) Lange-Bertalot	CRIP			+				
Craticula subminuscula (Manguin) C.E.Wetzel & Ector	CSUB		+	+				
G/Ctenophora								
Ctenophora pulchella (Ralfs ex Kützing) D.M.Williams & Round	CPUL		+	+				
G/Cymatopleura								
Cymatopleura solea (Brébisson) W.Smith	CSOL			+				
G/Cymbella								
Cymbella affinis (Krammer)	CAFF	+	+		+	+	+	+
Cymbella proxima Reimer	CPRO			+		+		
G/Cymbopleura								
Cymbopleura amphicephala (Nägeli ex Kützing) Krammer	CAMP		+		+	+		
G/Diatoma								
Diatoma moniliformis (Kützing) D.M.Williams	DMON	+		+	+	+	+	+
G/Diploneis								
Diploneis elliptica (Kützing) Cleve	DELL				+	+		
Diploneis ovalis (Hilse) Cleve	DOVA	+			+	+	+	+
G/Encyonopsis								
Encyonopsis microcephala (Grunow) Krammer	EMIC	+	+	+	+	+	+	+
G/Entomoneis								
Entomoneis paludosa (W.Smith) Reimer	EPAL				+		+	+
G/Epithemia								
Epithemia sorex Kützing	ESOR			+				
G/Fallacia								
Fallacia pygmaea (Kützing) Stickle & D.G.Mann	FPYG			+	+	+	+	
G/Fragilaria								
Fragilaria capucina var. *vaucheriae* (Kützing) Lange-Bertalot	FCAPV	+			+	+	+	+
Fragilaria crotonensis Kitton	FCRO	+						
G/Geissleria								
Geissleria acceptata (Hust.) Lange-Bert. and Metzeltin	GACC		+					
G/Gomphonella								
Gomphonella olivacea (Hornemann) Rabenhorst	GOLI	+		+	+	+		
Gomphonella calcarea (Cleve) R.Jahn & N.Abarca	GCAL	+		+				
G/Gomphonema								

http://www.aloki.hu ● ISSN 1589 1623 (Print) ● ISSN 1785 0037 (Online)
DOI: http://dx.doi.org/10.15666/aeer/2005_37093736

Gomphonema angustum C.Agardh	GANG	+		+	+			
Gomphonema parvulum (Kützing) Kützing	GPAR	+		+		+	+	+
G/Gyrosigma								
Gyrosigma scalproides (Rabenhorst) Cleve	GSCA	+	+				+	
G/Halamphora								
Halamphora coffeaeformis (C.Agardh) Mereschkowsky	HCOF		+					
Halamphora veneta (Kützing) Levkov	HVEN			+				
G/Hantzschia								
Hantzschia amphioxys (Ehrenberg) Grunow	HAMP							+
Hantzschia virgata (Roper) Grunow	HVIR							+
G/Haslea								
Haslea stundlii (Hustedt) Blanco, Borrego-Ramos & Olenici	HSTU		+			+	+	
G/Homoeocladia								
Homoeocladia amphibia (Grunow) Kuntze	HAMP			+				
G/Luticola								
Luticola mutica (Kützing) D.G.Mann	LMUT		+					
G/Mastogloia								
Mastogloia elliptica (C.Agardh) Cleve	MELL		+			+		
Mastogloia smithii Thwaites ex W.Smith	MSMI		+				+	
G/Melosira								
Melosira varians C.Agardh	MVAR	+			+			
G/Navicula								
Navicula cryptocephala Kützing	NCRY				+			
Navicula cryptotenella Lange-Bertalot	NCRT	+	+		+	+		
Navicula gregaria Donkin	NGRE		+		+			+
Navicula phyllepta Kützing	NPHY	+	+		+	+	+	
Navicula recens (Lange-Bertalot) Lange-Bertalot	NREC		+		+			
Navicula tripunctata (O.F.Müller)Bory	NTRI		+	+			+	
Navicula veneta Kützing	NVEN		+	+			+	+
Navicula sp1	NSP1			+				
Navicula sp2	NSP2			+				
G/Navicymbula								
Navicymbula pusilla (Grunow) Krammer	NPUS		+			+	+	+
G/Navigeia								
Navigeia decussis (Østrup) Bukhtiyarova	NDEC		+	+				
G/Nitzschia								
Nitzschia bergii Cleve-Euler	NBER		+		+	+		+
Nitzschia clausii Hantzsch	NCLA		+		+			
Nitzschia communis Rabenhorst	NCOM		+					
Nitzschia constricta (Kützing)	NCON	+	+	+	+	+		
Nitzschia denticula Grunow	NDEN					+	+	+
Nitzschia dissipata (Kützing) Rabenhorst	NDIS				+	+		+
Nitzschia dubia W.Smith	NDUB		+		+			
Nitzschia elegantula Grunow	NELE		+			+	+	+
Nitzschia frustulum (Kützing) Grunow	NFRU		+					
Nitzschia homburgiensis Lange-Bertalot	NHOM							+
Nitzschia inconspicua Grunow	NINC			+				
Nitzschia microcephala Grunow	NMIC		+					+
Nitzschia palea (kützing) W. smith	NPAL		+	+	+	+	+	+
Nitzschia tryblionella Hantzsch	NTRY				+			
Nitzschia sp.	NSPE		+			+	+	+
G/Planothidium								
Planothidium lanceolatum (Brébisson ex Kützing) Lange-Bertalot	PLAN			+	+			
G/Pseudostaurosira								
Pseudostaurosira brevistriata (Grunow) D.M.Williams & Round	PBRE			+	+			+
G/Tabularia								

http://www.aloki.hu ● ISSN 1589 1623 (Print) ● ISSN 1785 0037 (Online)
DOI: http://dx.doi.org/10.15666/aeer/2005_37093736

Tabularia fasciculata (C.Agardh) D.M.Williams & Round	TFAS	+		+	+	+	+	+
G/Tryblionella								
Tryblionella calida (Grunow) D.G.Mann	TCAL				+		+	+
G/Rhoicosphenia								
Rhoicosphenia abbreviata (C.Agardh) Lange-Bertalot	RABB	+	+	+	+			
G/Rhopalodia								
Rhopalodia gibba (Ehrenberg) Otto Müller	RGIB	+		+	+	+	+	+
Rhopalodia gibberula (Ehrenberg) Otto Müller	RGBB		+		+			+
G/Sellaphora								
Sellaphora bacillum (Ehrenberg) D.G.Mann	SBAC			+				
Sellaphora pupula (Kützing) Mereschkovsky	SPUP			+		+	+	
Sellaphora stroemii (Hustedt) H.Kobayasi	SSTR				+	+		
G/Surirella								
Surirella brebissonii Krammer& Lange-Bertalot	SBRE		+					
Surirella peisonis Pantocsek	SPEI			+				
G/Ulnaria								
Ulnaria acus (Kützing) Lange-Bertalot	UACU			+	+	+	+	
Ulnaria ulna (Nitzsch) Lange-Bertalot	UULN	+			+	+	+	+
Centric diatoms								
G/Cyclotella								
Cyclotella meneghiniana Kützing	CMEN			+	+	+	+	+
G/Pantocsekiella								
Pantocsekiella ocellata (Pantocsek) K.T.Kiss & Ács	POCE	+			+	+	+	+
Total species = 86		23	35	39	45	38	31	31

Species richness and diversity indices

The species richness (S), Shannon–Weaver diversity (H'), Pielou's species evenness (E) and Simpson indices of diatom community are shown in *Table 4*. The highest species richness was found in Middle Drâa at site 4 (45 taxa), while the lowest value was recorded in the Upper Drâa at site 1 (23 taxa). The Shannon index was much higher in Middle Drâa sites (especially at S4 and S5) and rather low in the upstream sites of the basin (2.19 at site 1). Similarly, the highest species evenness values were recorded in the Middle Drâa sites (0.74 at site 5). Simpson diversity index followed the same trend as Shannon index with the highest diversity value at site 4.

The Pearson correlation analysis was further used to elucidate the relationships between diatoms diversity indices (H', SDI and E) and the environmental variables (*Fig. 3*). The results showed that diatom species richness was negatively correlated with pH (r = -0.61). No significant correlation was detected between diatom species richness and salinity or major ions contents.

Table 4. *Species richness (S), Shannon–Weaver diversity (H'), Pielou's species evenness (E) and Simpson indices of diatom community in each sampling site*

Indices	S1	S2	S3	S4	S5	S6	S7
Species richness (S)	23	35	39	45	38	31	31
Shannon (H')	2.19	2.47	2.49	2.72	2.70	2.51	2.38
Evenness (E)	0.70	0.69	0.68	0.71	0.74	0.73	0.69
Simpson (SDI)	0.85	0.85	0.86	0.91	0.89	0.87	0.83

http://www.aloki.hu ● ISSN 1589 1623 (Print) ● ISSN 1785 0037 (Online)
DOI: http://dx.doi.org/10.15666/aeer/2005_37093736

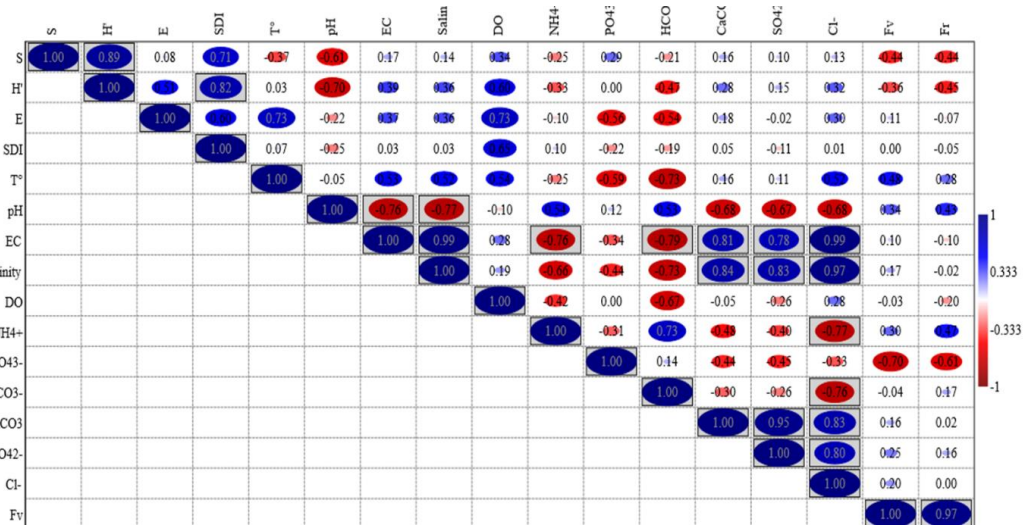

Figure 3. *Pearson correlation coefficient values of biological indices with environmental variables. S. Species richness, H'. Shannon index, E. Evenness, SDI. Simpson index, Sal. Salinity, EC. Conductivity, Fv. Flow velocity, Fr. Flow rate. Boxed Circle with coloration: correlation is significant at the 0.05 level (2-tailed). blue circle: positive correlation, red: negative correlation*

In order to compare the different sites and to evaluate the variation of benthic diatom diversity along the upstream-downstream gradient, we calculated the Sorensen similarity index. The results of the inter-sites similarity matrix are given in *Table 5*. The most similar sites (Qs ranging from 0.53 to 0.72) are located in the Middle Drâa, whereas the least similar are those of the Upper Drâa, particularly sites 2 and 3. *Figure 4* shows a dendrogram grouping the sampling sites according to their similarities. The dendogram distinguished three clusters. The first cluster corresponds to site 3 characterized by diatoms only found at this site namely *Cymatopleura solea*, *Epithemia sorex, Homoeocladia amphibia, Halamphora veneta* and *Nitzschia inconspicua*. The second cluster includes all the sites of Middle Drâa (4, 5, 6 and 7) plus the site 1 of Upper Drâa. All these sites were characterized by numerous common diatom species such as *Cymbella affinis, Diploneis ovalis*, *Diatoma moniliformis, Pantocsekiella ocellata, Ulnaria ulna* and *Fragilaria capucina* var. *vaucheriae.* The third cluster corresponds to site 2 characterized by typical halotolerant species such as *Nitzschia frustulum*, *Nitzschia communis*, *Halamphora coffeaeformis*, *Geissleria acceptata, Luticola mutica* and *Surirella brebissonii.* Only *Achnanthidium minutissimum* and *Encyonopsis microcephala* were common to all sites with variable relative abundances.

Table 5. *Sorenson similarity matrix of the studied sites*

	S1	**S2**	**S3**	**S4**	**S5**	**S6**	**S7**
S1	**1**	0.28	0.42	0.57	0.52	0.48	0.44
S2	0.28	**1**	0.27	0.38	0.38	0.39	0.33
S3	0.42	0.27	**1**	0.48	0.47	0.43	0.31
S4	0.57	0.38	0.48	**1**	0.66	0.53	0.56
S5	0.52	0.38	0.47	0.66	**1**	0.72	0.58
S6	0.48	0.39	0.43	0.53	0.72	**1**	0.68
S7	0.44	0.33	0.31	0.56	0.58	0.68	**1**

http://www.aloki.hu ● ISSN 1589 1623 (Print) ● ISSN 1785 0037 (Online)
DOI: http://dx.doi.org/10.15666/aeer/2005_37093736

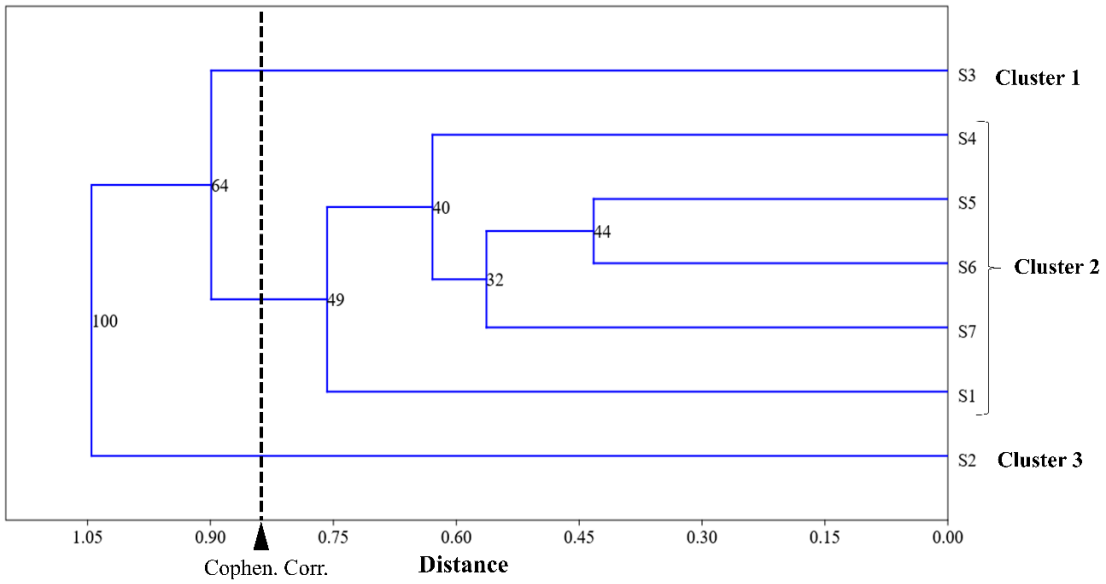

Figure 4. *Cluster dendrogram of inter-sites similarity. Cophenetic correlation coefficient at 0.86*

Quantitative diatoms analysis

Diatoms relative abundance

The distribution of diatom species relative abundances varied significantly between the different sites (*Fig. 5*). The diatom community of site 1 was mainly dominated by *Gomphonella olivacea* (26%), *Diatoma moniliformis* (25%), *Cymbella affinis* (16%) and *Ulnaria ulna* (14%). In site 2, *Nitzschia frustulum* was the most dominant species (30%) and was only found at this site followed by *Achnanthidium minutissimum* (18%), *Mastogloia smithii* (11%), *Navicymbula pusilla* (10%) and *Nitzschia microcephala* (8%). *Gomphonema angustum*, *Achnanthidium minutissimum, Encyonopsis microcephala, Homoeocladia amphibia* and *Nitzschia inconspicua* were the dominant species at site 3 with 25%, 23%, 16%, 7% and 5%, respectively. In site 4, *Ulnaria ulna* (21%), *Diatoma moniliformis* (16%) *Fragilaria capucina var. vaucheriae* (16%), *Cyclotella meneghiniana* (9%), *Tabularia fasciculata* (8%) and *Nitzschia dissipata* (7%) were the dominant species. At site 5, the abundant species were *Nitzschia elegantula* (21%), *Achnanthidium minutissimum* (17%) and *Encyonopsis microcephala* (14%). *Achnanthidium minutissimum* was the most dominant species in site 6 (28%) followed by *Nitzschia elegantula* (13%), *Gomphonema parvulum* (11%) and *Ulnaria ulna* (11%). This latter species also dominated (27%) the diatom assemblage at site 7 followed by *Rhopalodia gibba* (12%), *Navicula veneta* (9%) and *Nitzschia palea* (6%).

Biofilm total biomass

The biofilm biomass parameters (DW, AFDW, Chl *a* and cell diatoms.cm^{-2}) showed spatial variation and significant differences ($p < 0.05$) were observed between the sampling sites (*Table 6*). The biofilm DW showed a significant difference between all study sites with the lowest values (ranging from 0.32 to 3.06 mg/cm²), observed in

http://www.aloki.hu ● ISSN 1589 1623 (Print) ● ISSN 1785 0037 (Online)
DOI: http://dx.doi.org/10.15666/aeer/2005_37093736

the Upper Drâa sites (S1, S2 and S3) and the highest values (ranging from 20.2 to 87.67 mg/cm²) in the Middle Drâa sites except for site 6 where the DW was extremely low (3.82 mg/cm²). The AFDW showed the same variation with the highest value found in site 7 (77.37 ± 0.01 mg/cm²) and the lowest value in site 1 (0.32 ± 0.01 mg/cm²). Similarly, the chlorophyll *a* concentration showed significant spatial variation between the Upper Drâa and Middle Drâa sites. The number of cell diatoms per cm^2 showed a significant difference between all sampling sites with the lowest value (1091.51 cells.cm^{-2}) observed in site 1 and the highest one (13627.75 cells.cm^{-2}) in site 4.

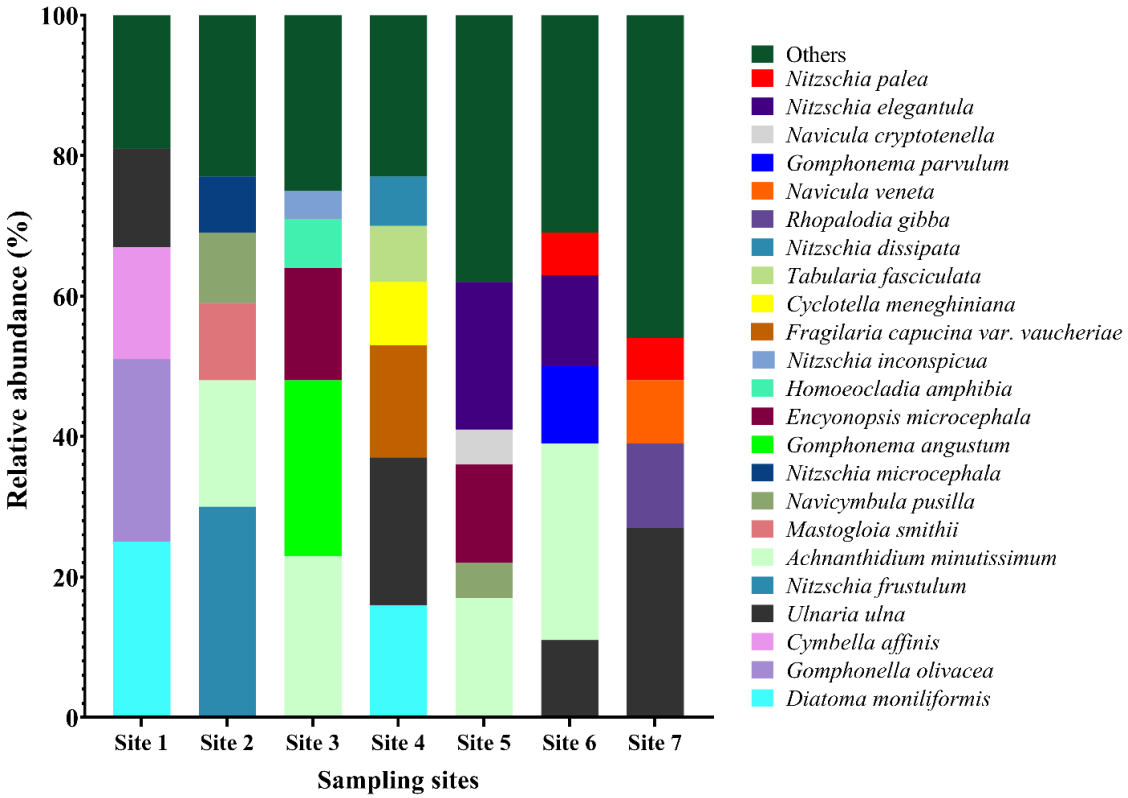

Figure 5. *Relative abundances of main diatoms species in each sampling site*

Table 6. *Biofilm biomass expressed as dry weight, ash−free dry weight, chlorophyll a and number of diatom cells per cm^2 in each sampling sites*

Sampling site	Biofilm DW mg.cm^{-2}	AFDW mg.cm^{-2}	Chlorophyll a µg.cm^{-2}	Diatom cells.cm^{-2}
1	0.32 ± 0.01^{a}	0.31 ± 0^{a}	0.04 ± 0^{a}	1092 ± 2.3^{a}
2	3.06 ± 0.01^{c}	2.73 ± 0.01^{c}	0.15 ± 0^{c}	2376 ± 75.7^{b}
3	2.17 ± 0.02^{b}	1.71 ± 0.1^{b}	0.11 ± 0.01^{b}	1263 ± 72.91^{c}
4	39.19 ± 0.02^{f}	33.54 ± 0.1^{e}	0.62 ± 0^{f}	13628 ± 122.86^{g}
5	20.2 ± 0.01^{e}	17.09 ± 0.01^{d}	0.30 ± 0^{d}	11854 ± 6.62^{f}
6	3.82 ± 0.01^{d}	2.64 ± 0^{c}	0.1 ± 0^{b}	8075 ± 94.12^{e}
7	87.67 ± 0.01^{g}	77.37 ± 0.01^{f}	0.61 ± 0^{f}	6400 ± 138.14^{d}

Values with the same letter were not significantly different according to Tukey's test ($p > 0.05$)

http://www.aloki.hu ● ISSN 1589 1623 (Print) ● ISSN 1785 0037 (Online)
DOI: http://dx.doi.org/10.15666/aeer/2005_37093736

Relationships between diatom community composition and environmental parameters

Canonical correspondence analysis (CCA) was used to investigated the relationships between diatom assemblages and environmental variables. Among 86 taxa inventoried, 39 species with relative abundance higher than 1% were included in this analysis. The ordination of dominant diatom species and their determining environmental factors in the CCA diagram is given in *Figure 6*.

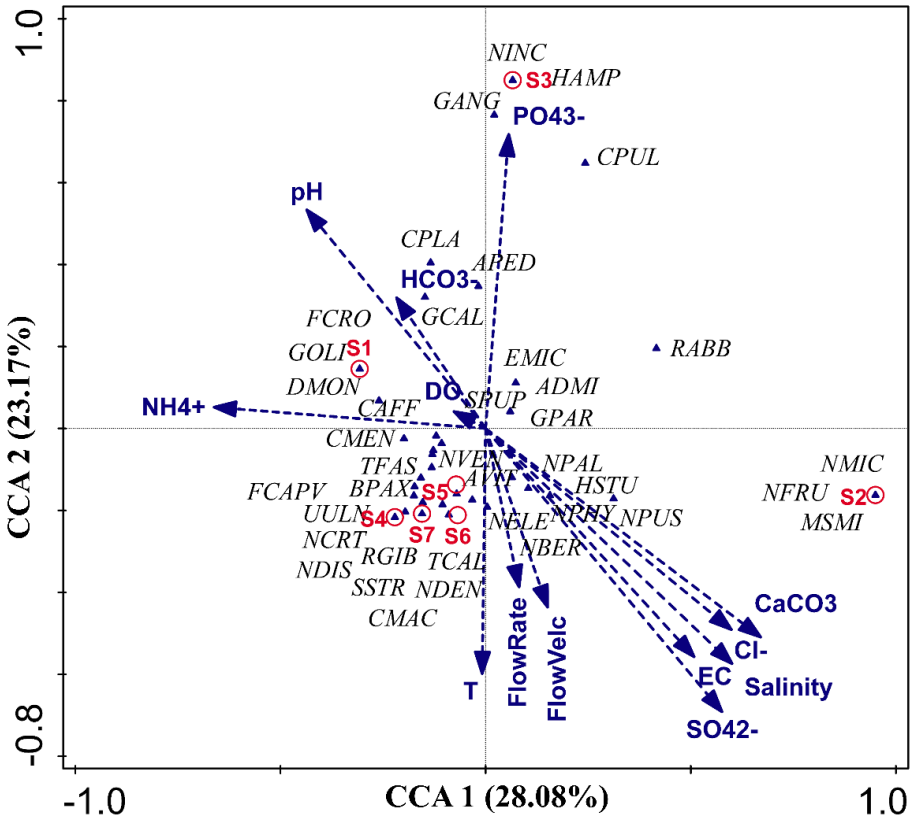

Figure 6. *Canonical correspondence analysis (CCA) ordination diagram of benthic diatoms and environmental variables (arrows) in the seven sampling sites. The direction of the arrow indicates the direction of maximum correlation, and length the strength of this correlation; DO: Dissolved oxygen, T: Temperature, FlowVelc: Flow velocity, SO42-: Sulfate, CaCO3: Total hardness, Cl-: Chloride, EC: Conductivity, HCO3-: total alkalinity, PO43-: Orthophosphate, NH4+: Ammonium ion. The species codes are represented in Table 3*

The first two axes F1 and F2 explained 51.1% of the variance in the data found. The first axis F1 with 28.01% of total variance was related to conductivity, salinity, SO_4^{2-}, Cl^-, $CaCO_3$ and ammonium ion (NH_4^+). The second axis F2 with 23.17% of total variance where PO_4^{3-} and pH have the highest contribution. The SO_4^{2-} value was the largest positive correlation with first axis followed by the salinity, $CaCO_3$ and Cl^-, and the NH_4^+ was largest negative with the first axis, while the PO_4^{3-} value was the largest positive correlation with second axis followed by pH. The arrow lengths in CCA ordination showed that the distribution of benthic diatoms was mainly affected by salinity, major ions (SO_4^{2-}, Cl^-, $CaCO_3$) and nutrients (PO_4^{3-}, NH_4^+). CCA axis 1 and 2 separated the Middle Drâa river sites (S4, S5, S6 and S7) from the Upper Drâa sites (S1,

http://www.aloki.hu ● ISSN 1589 1623 (Print) ● ISSN 1785 0037 (Online)
DOI: http://dx.doi.org/10.15666/aeer/2005_37093736

S2 and S3) into four clusters. The first cluster includes site 1 characterized by high values of pH and NH_4^+ where the biofilm was dominated by freshwater diatoms such as *Fragilaria crotonensis, Gomphonella olivacea, Diatoma moniliformis* and *Cocconeis placentula.* The second cluster corresponds to site 2 characterized by high values of EC, salinity, Cl^-, SO_4^{2-} and $CaCO_3$ where the biofilm was marked by euryhaline and halotolerant diatoms namely *Nitzschia frustulum*, *Mastogloia smithii* and *Nitzschia microcephala.* The cluster 3 includes site 3 marked by low current velocity with high values of PO_4^{3-} and pH and characterized by *Nitzschia inconspicua*, *Homoeocladia amphibia, Gomphonema angustum* and *Ctenophora pulchella.* The cluster 4 includes all Middle Drâa sites 4, 5, 6 and 7 highly impacted by agricultural and domestic activities (six downstream palm oases) and characterized by a gradual increase in water salinity. Diatom assemblages in these sites were characterized by a mixture of halophilic and eutrophic taxa namely *Rhopalodia gibba*, *Tryblionella calida*, *Sellaphora stroemii, Nitzschia dissipata, Cyclotella meneghiniana, Navicula cryptonella, Ulnaria ulna*, *Nitzschia palea*, *Nitzschia elegantula, Navicula veneta, Bacillaria paxillifera, Anomoeoneis vitrea, Fragilaria capucina* var. *vaucheriae.*

It is interesting to note that halophilic diatom species (e.g., *Nitzschia elegantula, Nitzchia bergii*, *Navicymbula pusilla* and *Haslea stundlii*) were commonly found in some brackish sites of the Middle Drâa and site 2 and were mainly related to high values of SO_4^{2-}, EC, salinity, $CaCO_3$ and Cl^-.

Discussion

Arid rivers provide important services to humans and society such as drinking water, domestic and irrigation water, food (fish), climate regulation, and recreation (Malmqvist and Rundle, 2002; Vörösmarty et al., 2010; Berger et al., 2019). These environmental stressors contribute in various ways to water physicochemical changes, including salinization.

The physico-chemical analysis showed a spatial variability with a gradual increase of water salinity and ions composition along the Drâa river. Overall, the water salinity showed an increasing gradient in the Drâa river, especially downstream of the Mansour Eddahbi dam. Previous studies have highlighted the rise of salinity along the course of the Drâa from the ME dam to the downstream area through the succession of six large oases (Warner et al., 2013). During the last decades, the salinity of Draa river has increased due to water abstraction, land use, irrigation and sequence of drought episodes (Warner et al., 2013). This salinization originates from natural (geological) and various anthropogenic drivers further is significantly amplified by climate changes. Indeed, the modeling and climate scenario for the period 2000-2029 showed a mean decrease in precipitation (-11%) and especially snowfall (-31%) in the Upper Draa valley leading to a significant decrease in runoff and available water resources (Johannsen et al., 2016). In a recent paper, Berger et al. (2021) have monitored the changes in the water surface area (calculated from satellite images) of ME reservoir from 2015 until 2020 as a proxy for surface water availability in the Draa valley. By referring to these data, the time of water and diatoms sampling coincided with a period of receding water availability in the valley.

The total ion content in the river can be reflected by the conductivity (EC) as a good indicator. The lowest value (385.5 $\mu S.cm^{-1}$) was observed in oued Iriri (site 1) a freshwater perennial stream located at the Upper Drâa basin that drains surface

http://www.aloki.hu ● ISSN 1589 1623 (Print) ● ISSN 1785 0037 (Online)
DOI: http://dx.doi.org/10.15666/aeer/2005_37093736

discharge originating in the High Atlas Mountain to the Mansour Eddahbi reservoir. The high EC value (7090 $\mu S.cm^{-1}$), was measured in oued El Malleh (Site 2) followed by the Middle Drâa river (S5 with 5670 $\mu S.cm^{-1}$). Oued El Malleh, an ephemeral stream depending on rainfall or snowmelt, was characterized by high salt water content. Numerous previous studies have indicated that El Malleh stream is characterized by significantly high salinity with high content of Cl^- and SO_4^{2-} (Schulz et al., 2008; Warner et al., 2013; Clavero et al., 2017). The site 5 located just before the oasis of Ternata (Ouled Yaoub) is also rather salty which could be due to the high salinity of the soil (about 5.6 mS. cm^{-1}) (Schulz et al., 2008).

On the other hand, nutrient contents (NH_4^+ and PO_4^{3-}) are rather high, especially in certain sites of Middle Drâa affected by direct human impact (diffuse wastes, washing clothes and animal keeping). Our findings are in agreement with Berger et al. (2021) who found that of the 92% of farmers in the Upper Drâa assess water quality as good for agricultural production while only 67% in the Northern Middle Drâa think that water has good quality for agriculture, decreasing to 35% in the Southern Middle Drâa.

The spatial variability of water temperature in Drâa river depends on aquatic stages, degrees of intermittency, river depth and time of measurement. Indeed, the lowest temperature value was measured in isolated or weakly connected pools such as site 3 (15.9 °C) and the highest value was recorded in eurheic habitats with surface flow and abundant riffles as site 1 (22.8 °C).

Despite the low number of samples, this first study of benthic diatoms of Drâa river highlighted significant diatom species richness dominated by pennate taxa. The analysis of diatom composition revealed the presence of 86 diatom species belonging to 44 genera. Among the 26 genera observed, *Nitzschia* and *Navicula* were the genera with the highest number of species. The common species to all sites were *Achnanthidium minutissimum and Encyonopsis microcephala* which are cosmopolitan, in particular *A. minutissimum.* This later diatom is a very ubiquitous species showing a wide range of ecological tolerance and can be found in all types of watercourse (Krammer, 1991b; Taylor et al., 2007; Bey and Ector, 2013; Hofmann et al., 2013; Stubbington et al., 2019).

The spatial variability of benthic diatoms showed that oued Iriri (site 1) had the lowest species richness. This could be due to competition (especially for light and nutrients) with the well-developed macrophytes in this site as well as high flow velocity and water releases from the dam. Conversely, site 4 of the Middle Drâa, has the highest species richness, which can be explained by the low flow and the frequency of pools microhabitats compared to riffle. Stubbington et al. (2017) state that taxa richness in temperate rivers can initially increase when the flow ceases and pools form, as lentic colonists join lotic refugees, and then decrease as results of poor habitat suitability, reduced water quality and intensive biotic interactions. Shannon, Simpson and Pielou's diversity indices showed relatively higher diversity and structural stability within the diatom communities especially in the Middle Drâa river. No significant correlation was detected between diatom species richness and salinity or major ions contents. In contrast, diatoms diversity index (Shannon–Weaver diversity index) and species richness were negatively correlated with pH. As species richness was rather similar between the study sites, it is not sufficient to significantly differentiate them (i.e., it cannot differentiate between abundant and rare species and two sites with different salinity could have the same species richness). However, the composition of diatom communities was affected by salinity and major ions contents as the relative abundance

http://www.aloki.hu ● ISSN 1589 1623 (Print) ● ISSN 1785 0037 (Online)
DOI: http://dx.doi.org/10.15666/aeer/2005_37093736

of some diatom taxa was significantly correlated with salinity and major ions contents. For instance, *Mastogloia smithii* (abundant at site 2) and *Navicymbula pusilla* (abundant at site 2 and site 5) were positively correlated ($r \geq 0.76$) with conductivity, salinity and chloride. In addition, *Nitzshia frustulum* and *Nitzshia microcephala* that were abundant at site 2 had a positive correlation ($r = 0.84$) with sulfate concentration. However, salinity was negatively correlated with *Cymbella affinis* ($r = -0.80$) that was abundant at site 1.

The analysis of inter-sites similarity and its illustration in a dendogram separated the sampling sites into three clusters. The cluster including El Malleh site (site 2) is the least similar to any other sites owing to the presence of characteristic euryhaline and halotolerant diatoms such as *Nitzschia frustulum*, *Nitzschia communis*, *Halamphora coffeaeformis*, *Geissleria acceptata, Luticola mutica* and *Surirella brebissonii* usually found in electrolyte-rich and brackish waters (Lange-Bertalot, 1996; Taylor et al., 2007). The cluster of site 3, downstream of Ait Douchen intermittent stream with abundant pools, was characterized by both eutrophic and halophilic diatoms that were found only in this site such *as Cymatopleura solea, Epithemia sorex, Homoeocladia amphibia, Halamphora veneta, Craticula riparia*, *Surirella peisonis* and *Nitzschia inconspicua*. Some of these species are characteristic of eutrophic habitats (Taylor et al., 2007; Delgado et al., 2012) while others such as *Epithemia sorex*, *Craticula riparia*, *Surirella peisonis* were found in brackish water rich of HCO_3^- (Krammer and Lange-Bertalot, 1999; Bey and Ector, 2013; Hofmann et al., 2013). The clustering of the Middle Drâa sites and Iriri stream (site 1) in the same group can be explained by the presence of several common species such as *Diatoma moniliformis*, *Cymbella affinis*, *Diploneis ovalis, Ulnaria ulna, Rhopalodia gibba* and *Fragilaria capucina var. vaucheriae* characteristic of freshwaters habitats (Reynolds et al., 2002; Taylor et al., 2007; Padisák et al., 2009).

The CCA analysis showed that diatoms spatial distribution in Drâa basin appear to be mainly determined by variations in ion composition (SO_4^{2-}, Cl^-, $CaCO_3$), salinity, pH, nutrient content (PO_4^{3-}, NH_4^+) (*Fig. 5*). Previous studies have highlighted the effects of these environmental variables on changes in diatom composition in lotic and lentic ecosystems (Potapova and Charles, 2003; Bere and Tundisi, 2009, 2011a; Smucker and Vis, 2011; Bere and Mangadze, 2014; Ingebrigtsen et al., 2016; Mangadze et al., 2017).

Based on CCA results, site 2 (Oued El Malleh), which was the most saline, was associated with high levels of Cl-, SO_4^{2-}, CaCO3, salinity and was characterized by diatoms known by their preference for electrolyte-rich waters and brackish habitats (Taylor et al., 2007; Sivaci et al., 2008; Lengyel et al., 2015). Site 3 with abundant pools in downstream of Ait douchen high level of PO_4^{3-} and pH was characterized by the occurence of eutrophic taxa such as *Nitzschia inconspicua*, *Homoeocladia amphibia* which are a good indicator of a high level of trophic pollution (Van Dam et al., 1994; Taylor et al., 2007; Delgado et al., 2012; Shen et al., 2018), while *Ctenophora pulchella* can be found in waters affected by industrial and mining wastes (Taylor et al., 2007). Site 1 (Iriri stream) with low salt concentrations, high values of pH and NH_4^+ was characterized by oligohaline and oligo- to mesotrophic diatoms (Saros et al., 2003, 2005; Ranković et al., 2006; Taylor et al., 2007; Licursi et al., 2016). *Gomphonella olivacea* is considered as a good indicator of eutrophic waters with moderate conductivity (Krammer and Lange-Bertalot, 1999; Bey and Ector, 2013; Hofmann et al., 2013). Similary, *Diatoma moniliformis* has been described as representative species of eu-polytrophic conditions (Schneider et al., 2000). While *Cocconeis placentula* lives in

http://www.aloki.hu ● ISSN 1589 1623 (Print) ● ISSN 1785 0037 (Online)
DOI: http://dx.doi.org/10.15666/aeer/2005_37093736

freshwater/brackish habitats and is considered as an alkaliphilous species (Pienitz et al., 1991; Vouilloud, 2003).

The Middle Drâa river sites (S4, S5, S6 and S7) with moderate salt and nutrients contents were characterized by diatom assemblage frequently observed in eutrophic and/or electrolyte rich waters (Reynolds et al., 2002; Fránková-Kozáková et al., 2007; Taylor et al., 2007; Padisák et al., 2009). *Nitzschia palea* was considered as a representative species of eutrophic and very heavily polluted to extremely polluted waters with moderate to high electrolyte content (Van Dam et al., 1994; Krammer and Lange-Bertalot, 1999; Taylor et al., 2007; Bey and Ector, 2013; Hofmann et al., 2013). It has also been associated with high conductivity and eutrophication sites in Brazil (Bere and Tundisi, 2011b), South Africa (Mangadze et al., 2017) and China (Shen et al., 2018). *Ulnaria ulna* has been considered as a dominant species in moderate and high trophic levels (Krammer and Lange-Bertalot, 2000; Taylor et al., 2007; Bey and Ector, 2013; Hofmann et al., 2013). *Nitzschia elegantula* has been described as representative species of electrolyte rich waters (Taylor et al., 2007).

The effects of ionic strength and salinity on diatom communities structure can be impacted by combined effects of environmental factors namely nutrients contents and eutrophication (Bere and Tundisi, 2011a). Moreover, Saros and Fritz (2000) showed that nutrient enrichment can broaden the high end of a taxon's salinity tolerance range. However, the separation of ionic strength and conductivity effects from other variables on diatom communities has not been thoroughly studied in situ. This study provides additional data and baseline information on salinity impacts on diatom assemblages in an intermittent desert river in southern Morocco.

Conclusion

This exploratory survey provides a first inventory, data ecology and distribution of the benthic diatom assemblages in arid Drâa river, South of Morocco. The physico-chemical parameters monitoring showed a spatial variability with a gradual increase of water salinity and ions composition along the Drâa river. This study reveals the existence of a significant diatom richness (86 taxa) and notable differences between the Middle Drâa valley which had diatom communities significantly different from those of the Upper Drâa streams with higher diversity and evenness of taxa.

The composition and spatial distribution of benthic diatoms was mainly determined by salinity, ion content (chloride and sulfate), pH, flow velocity and nutrients (NH_4^+, PO_4^{3-}). Thus, benthic diatoms are a good tool for monitoring ecological quality of intermittent rivers and ephemeral streams (IRES) during the period of water stability. We therefore recommend in-depth studies including spatio-temporal monitoring of benthic diatoms with other groups of algae taking into account other factors such as hydrological drought (dry phase and aquatic stage) that have been shown to influence benthic diatoms assemblage structure in intermittent river, but which were not assessed in this study.

Acknowledgements. We gratefully acknowledge the German Ministry of Education and Research (BMBF) for financial support in the framework of the projects: SALIDRÂA-01DH17002 and SALIDRÂAjuj-01UU1906. The first project was funded in the framework of The Moroccan-German Programme for Scientific Research (PMARS III) —2016–2018. Also, we are very grateful for the constructive critique of anonymous reviewers.

http://www.aloki.hu ● ISSN 1589 1623 (Print) ● ISSN 1785 0037 (Online)
DOI: http://dx.doi.org/10.15666/aeer/2005_37093736

REFERENCES

[1] Bailey, P. C. E., Boon, P. I., Blinn, D. W., Williams, W. D. (2006): Salinisation as an Ecological Perturbation to Rivers, Streams and Wetlands of Arid and Semi-Arid Regions. – In: Kingsford, R. (ed.) Ecology of Desert Rivers .Cambridge University Press, Cambridge, pp. 280-314.

[2] Bere, T., Tundisi, J. G. (2011a): Influence of ionic strength and conductivity on benthic diatom communities in a tropical river (Monjolinho), São Carlos-SP, Brazil. – Hydrobiologia 661: 261-276.

[3] Bere, T., Tundisi, J. G. (2011b): Influence of land-use patterns on benthic diatom communities and water quality in the tropical Monjolinho hydrological basin, São Carlos-SP, Brazil. – Water Sa 37: 93-102.

[4] Bere, T., Tundisi, J. G. (2009): Weighted average regression and calibration of conductivity and pH of benthic diatom assemblages in streams influenced by urban pollution–São Carlos/SP, Brazil. – Acta Limnol. Bras 21: 317-325.

[5] Bere, T., Mangadze, T. (2014): Diatom communities in streams draining urban areas: community structure in relation to environmental variables. – Tropical Ecology 55: 271-281.

[6] Berger, E., Frör, O., Schäfer, R. B. (2019): Salinity impacts on river ecosystem processes: a critical mini-review. – Philosophical Transactions of the Royal Society B 374: 20180010.

[7] Berger, E., Bossenbroek, L., Beermann, A. J., Schäfer, R. B., Znari, M., Riethmüller, S., Sidhu, N., Kaczmarek, N., Benaissa, H., Ghamizi, M. (2021): Social-ecological interactions in the Draa River Basin, southern Morocco: towards nature conservation and human well-being using the IPBES framework. – Science of the Total Environment 769: 144492.

[8] Bey, M. Y., Ector, L. (2013): Atlas of River Diatoms the Rhone Alpes Region. – Agence Française pour la Biodiversité, Vincennes (in French).

[9] Campeau, S., Murkin, H. – R., Titman, R. D. (1994): Relative importance of algae and emergent plant litter to freshwater marsh invertebrates. – Canadian Journal of Fisheries and Aquatic Sciences 51: 681-692.

[10] Cañedo-Argüelles, M., Kefford, B. J., Piscart, C., Prat, N., Schäfer, R. B., Schulz C-J. (2013): Salinisation of rivers: an urgent ecological issue. – Environmental Pollution 173: 157-167.

[11] Carrillo-Rivera, J. J., Ouysse, S., Hernández-Garcia, G. J. (2013): Integrative approach for studying water sources and their vulnerability to climate change in semi-arid regions (Drâa Basin, Morocco). – Int J Water Resour Arid Environ 2: 26-36.

[12] Centis, B., Tolotti, M., Salmaso, N. (2010): Structure of the diatom community of the River Adige (North-Eastern Italy) along a hydrological gradient. – Hydrobiologia 639: 37-42.

[13] Charles, D. F., Kelly, M. G., Stevenson, R. J., Poikane, S., Theroux, S., Zgrundo, A., Cantonati, M. (2021): Benthic algae assessments in the EU and the US: striving for consistency in the face of great ecological diversity. – Ecological Indicators 121: 107082.

[14] Clavero, M., Esquivias, J., Qninba, A., Riesco, M., Calzada, J., Ribeiro, F., Fernández, N., Delibes, M. (2015): Fish invading deserts: non-native species in arid Moroccan rivers. – Aquatic Conservation: Marine and Freshwater Ecosystems 25: 49-60.

[15] Clavero, M., Qninba, A., Riesco, M., Esquivias, J., Calzada, J., Delibes, M. (2017): Moroccan desert rivers: fish on the arid extreme of Mediterranean streams. – FiSHMED 3: 21.

[16] Datry, T., Singer, G., Sauquet, E., Capdevilla, D. J., Von Schiller, D., Subbington, R., Magrand, C., Paril, P., Milisa, M., Acuña, V. (2017): Science and management of intermittent rivers and ephemeral streams (SMIRES). – Research Ideas and Outcomes 3: 23.

http://www.aloki.hu ● ISSN 1589 1623 (Print) ● ISSN 1785 0037 (Online)
DOI: http://dx.doi.org/10.15666/aeer/2005_37093736

[17] Delgado, C., Pardo, I., García, L. (2012): Diatom communities as indicators of ecological status in Mediterranean temporary streams (Balearic Islands, Spain). – Ecological Indicators 15: 131-139.
[18] Diekkrüger, B., Busche, H., Klose, A., Klose, S., Rademacher, C., Schulz, O. (2012): Impact of global change on hydrology and soil degradation—scenario analysis for the semi-arid Drâa catchment (South Morocco). – River Basins and Change: 21-26.
[19] Fránková-Kozáková, M., Marvan, P., Geriš, R. (2007): Halophilous diatoms in Czech running waters: Pleurosira laevis and Bacillaria paxillifera. – In: Proceedings of the 1st Central European Diatom Meeting. Berlin, Germany, pp. 39-44.
[20] Guiry, M. D., Guiry, G. M. (2022): AlgaeBase. – World-Wide Electronic Publication, National University of Ireland, Galway. https://www.algaebase.org (accessed on 8 Feb 2022).
[21] Harms, T. K., Sponseller, R. A., Grimm, N. B. (2018): Desert Streams. – In: Jørgensen, S. E., Fath, B. D. (eds.) Encyclopedia of Ecology. Elsevier, Amsterdam, pp. 439-446.
[22] Hofmann, G., Lange-Bertalot, H., Werum, M. (2013): Diatomeen im Süßwasser-Benthos von Mitteleuropa. 2. Corrected Edition. – Koeltz Scientific Books, Königstein.
[23] Ingebrigtsen, R. A., Hansen, E., Andersen, J. H., Eilertsen, H. C. (2016): Light and temperature effects on bioactivity in diatoms. – Journal of Applied Phycology 28: 939-950.
[24] Jeffrey, S. W., Humphrey, G. F. (1975): New spectrophotometric equations for determining chlorophylls a, b, c1 and c2 in higher plants, algae and natural phytoplankton. – Biochemie und Physiologie der Pflanzen 167: 191-194.
[25] Johannsen, I. M., Hengst, J. C., Goll, A., Höllermann, B., Diekkrüger, B. (2016): Future of water supply and demand in the Middle Drâa Valley, Morocco, under climate and land use change. – Water 8: 313.
[26] Karmaoui, A., Messouli, M., Khebiza, Y. M., Ifaadassan, I. (2014): Environmental vulnerability to climate change and anthropogenic impacts in dryland, (pilot study: Middle Draa Valley, South Morocco). – Journal of Earth Science & Climatic Change: 1.
[27] Karmaoui, A., Ifaadassan, I., Messouli, M., Khebiza, M. Y. (2015): Characterization of common environmental indicators of the Moroccan Oasean Biome. Pilot study in the reserve biosphere of Oases in Southern Morocco. – Adv. Res 5: 1-15.
[28] Kingsford, R. T., Thompson, J. R. (2006): Desert or Dryland Rivers of the World. An Introduction. – Cambridge University Press, Cambridge.
[29] Krammer, K. (1991a). Suβwasserflora von Mitteleuropa. Bacillariophyceae. 3. Teil: Centrales, Fragilariaceae, Eunotiaceae. Süβwasserflora von Mitteleuropa. – Gustav Fischer Verlag, Stuttgart.
[30] Krammer, K. (1991b). Bacillariophyceae 4. Teil: Achnanthaceae, Kritische Erganzungen zu Navicula (Lineolatae) und Gomphonema. Süβwasserflora von Mitteleuropa 2. – Gustav Fischer Verlag, Stuttgart.
[31] Krammer, K., Lange-Bertalot, H. (1986): 1986: Bacillariophyceae. 1. Teil: Naviculaceae. – In: Ettl, H., Gerloff, J., Heynig, H. and Mollenhauer, D. (eds.) Süßwasser flora von Mitteleuropa, Band 2/1. Gustav Fischer Verlag, Stuttgart.
[32] Krammer, K., Lange-Bertalot, H. (1988): Süsswasser-Flora von Mitteleuropa. Bacillariophyceae, 2. Teil: Epithemiaceae, Surirellaceae. – Gustav Fischer Verlag, Stuttgart.
[33] Krammer, K., Lange-Bertalot, H. (1999): Süßwasserflora von Mitteleuropa II: 1, Bacillariophyceae. Naviculaceae. – Gustav Fischer Verlag, Stuttgart.
[34] Krammer, K., Lange-Bertalot, H. (2000): 'Centrales','Fragilariaceae','Eunotiaceae'. – Spektrum, Heidelberg.
[35] Lange-Bertalot, H. (1979): Pollution tolerance of diatoms as a criterion for water quality estimation. – Nova Hedwigia, Beih. 64: 285-304.

http://www.aloki.hu ● ISSN 1589 1623 (Print) ● ISSN 1785 0037 (Online)
DOI: http://dx.doi.org/10.15666/aeer/2005_37093736

[36] Lange-Bertalot, H. (1996): Indicators of oligotrophy. 800 taxa representative of three ecologically distinct lake types. Carbonate buffered-oligodys-trophic-weakly buffered soft water. – Iconogr. Diatomol 2: 390.
[37] Lengyel, E., Kovács, A. W., Padisák, J., Stenger-Kovács, C. (2015): Photosynthetic characteristics of the benthic diatom species Nitzschia frustulum (Kützing) Grunow isolated from a soda pan along temperature-, sulfate-and chloride gradients. – Aquatic Ecology 49: 401-416.
[38] Licursi, M., Gomez, N., Sabater, S. (2016): Effects of nutrient enrichment on epipelic diatom assemblages in a nutrient-rich lowland stream, Pampa Region, Argentina. – Hydrobiologia 766: 135-150.
[39] Loulida, S., Naimi, M., Znari, M., Bendami, S. (2019): Tolerance to salinity and dehydration in the Sahara Desert blue-eyed turtle, Mauremys leprosa saharica (Testudines: Geoemydidae) from a brackish pond in the Lower Draa basin, southern Morocco. – African Journal of Herpetology 68: 58-76.
[40] Lowe, R. L., LaLiberte, G. D. (2017): Benthic Stream Algae: Distribution and Structure. – In: Hauer, F., Lamberti, G. (eds.) Methods in Stream Ecology. Volume 1. Elsevier, Amsterdam, pp. 193-221.
[41] Malmqvist, B., Rundle, S. (2002): Threats to the running water ecosystems of the world. – Environmental Conservation 29: 134-153.
[42] Mangadze, T., Wasserman, R. J., Dalu, T. (2017): Use of diatom communities as indicators of conductivity and ionic composition in a small austral temperate river system. – Water, Air, & Soil Pollution 228: 1-11.
[43] Millerioux, G. (1975): Projet alpin OCDE pour la lutte contre l'eutrophisation. Lacs du massif central francais. IV. Le lac d'Aydat, interrelations entre parametres. – OCDE, Paris.
[44] Mostakim, L., Fetnassi, N., Rassam, H., Benaissa, H., Berger, E., Ghamizi, M. (2020): Assessment of aquatic and semi-aquatic plants in arid regions: testing factors affecting riparian plant distribution in the Draa Basin, Morocco. – EurAsian Journal of BioSciences 14: 4735-4741.
[45] Nhiwatiwa, T., Dalu, T., Brendonck, L. (2017): Impact of irrigation based sugarcane cultivation on the Chiredzi and Runde Rivers quality, Zimbabwe. – Science of the Total Environment 587: 316-325.
[46] Padisák, J., Crossetti, L. O., Naselli-Flores, L. (2009): Use and misuse in the application of the phytoplankton functional classification: a critical review with updates. – Hydrobiologia 621: 1-19.
[47] Pan, Y., Stevenson, R. J., Hill, B. H., Kaufmann, P. R., Herlihy, A. T. (1999): Spatial patterns and ecological determinants of benthic algal assemblages in Mid-Atlantic streams, USA. – Journal of Phycology 35: 460-468.
[48] Pielou, E. C. (1966): Species-diversity and pattern-diversity in the study of ecological succession. – Journal of Theoretical Biology 10: 370-383.
[49] Pienitz, R., Lortie, G., Allard, M. (1991): Isolation of lacustrine basins and marine regression in the Kuujjuaq area, northern Québec, as inferred from diatom analysis. – Géographie Physique et Quaternaire 45: 155-174.
[50] Piscart, C., Moreteau, J.-C., Beisel J-N. (2005): Biodiversity and structure of macroinvertebrate communities along a small permanent salinity gradient (Meurthe River, France). – Hydrobiologia 551: 227-236.
[51] Piscart, C., Usseglio-Polatera, P., Moreteau, J.-C. B. (2006): The role of salinity in the selection of biological traits of freshwater invertebrates. – Archiv für Hydrobiologie: 185-198.
[52] Potapova, M. G., Charles, D. F. (2002): Benthic diatoms in USA rivers: distributions along spatial and environmental gradients. – Journal of Biogeography 29: 167-187.
[53] Potapova, M., Charles, D. F. (2003): Distribution of benthic diatoms in US rivers in relation to conductivity and ionic composition. – Freshwater Biology 48: 1311-1328.

http://www.aloki.hu ● ISSN 1589 1623 (Print) ● ISSN 1785 0037 (Online)
DOI: http://dx.doi.org/10.15666/aeer/2005_37093736

[54] Potapova, M., Charles, D. F. (2005): Choice of substrate in algae-based water-quality assessment. – Journal of the North American Benthological Society 24: 415-427.
[55] Qninba, A., Lieron, V., Dieuleveut, T., Amairat, M., Yahyaoui, A. (2011): Sur la présence de l'Anguille Anguilla anguilla (Linnaeus, 1758) dans l'Oued Tissint, un affluent de l'Oued Dr'a (Maroc). – Bulletin Institut Scientifique Rabat 33: 65-66.
[56] Ranković, B., Simić, S., Bogdanović, D. (2006): Phytoplankton as indicator of water quality of lakes Bubanj and Šumarice during autumn. – Prirodno-Matematički Fakultet, Univerzitet k Kragujevcu, Kragujevac.
[57] Reynolds, C. S., Huszar, V., Kruk, C., Naselli-Flores, L., Melo, S. (2002): Towards a functional classification of the freshwater phytoplankton. – Journal of Plankton Research 24: 417-428.
[58] Riesco, M., Delibes, M., Calzada, J., Esquivias, J., Qninba, A., Clavero, M. (2020): Desert otters: Distribution, habitat use and feeding ecology in arid rivers of Morocco. – Journal of Arid Environments 178: 104165.
[59] Rodier, J., Legube, B., Merlet, N., Brunet, R., Mialocq, J. C., Leroy, P., Houssin, M., Lavison, G., Bechemin, C., Vincent, M. (2009): L'analyse de l'eau-9e éd. Eaux naturelles, eaux résiduaires, eau de mer. – Dunod, Paris, pp. 564-571.
[60] Saros, J. E., Fritz, S. C. (2000): Nutrients as a link between ionic concentration/composition and diatom distributions in saline lakes. – Journal of Paleolimnology 23: 449-453.
[61] Saros, J. E., Interlandi, S. J., Wolfe, A. P., Engstrom, D. R. (2003): Recent changes in the diatom community structure of lakes in the Beartooth Mountain Range, USA. – Arctic, Antarctic, and Alpine Research 35: 18-23.
[62] Saros, J. E., Michel, T. J., Interlandi, S. J., Wolfe, A. P. (2005): Resource requirements of Asterionella formosa and Fragilaria crotonensis in oligotrophic alpine lakes: implications for recent phytoplankton community reorganizations. – Canadian Journal of Fisheries and Aquatic Sciences 62: 1681-1689.
[63] Schneider, S., Schranz, C., Melzer, A. (2000): Indicating the trophic state of running waters by submersed macrophytes and epilithic diatoms: exemplary implementation of a new classification of taxa into trophic classes. – Limnologica-Ecology and Management of Inland Waters 30: 1-8.
[64] Schröder, M., Sondermann, M., Sures, B., Hering, D. (2015): Effects of salinity gradients on benthic invertebrate and diatom communities in a German lowland river. – Ecological Indicators 57: 236-248.
[65] Schulz, O., Reichert, B., Diekkrüger, B. (2008): L'approche IMPETUS: Recherche et outils pour la gestion de l'eau. – http://hdl.handle.net/123456789/31401.
[66] Sen, Z. (2008): Wadi Hydrology. – CRC Press, Boca Raton, FL.
[67] Shannon CB, Weaver, W. (1963): The Mathematical Theory of Communication. – Univ. of Illinois Press, Urbana, IL.
[68] Shen, R., Ren, H., Yu, P., You, Q., Pang, W., Wang, Q. (2018): Benthic diatoms of the Ying River (Huaihe River Basin, China) and their application in water trophic status assessment. – Water 10: 1013.
[69] Simpson, E. H. (1949): Measurement of diversity. – Nature 163: 688.
[70] Sivaci, E. R., Cankaya, E., Kilinc, S., Dere, S. (2008): Seasonal assessment of epiphytic diatom distribution and diversity in relation to environmental factors in a karstic lake (Central Turkey). – Nova Hedwigia 86: 215-230.
[71] Šmilauer, P., Lepš, J. (2014): Multivariate Analysis of Ecological Data Using CANOCO 5. – Cambridge University Press, Cambridge.
[72] Smucker, N. J., Vis, M. L. (2011): Contributions of habitat sampling and alkalinity to diatom diversity and distributional patterns in streams: implications for conservation. – Biodiversity and Conservation 20: 643-661.

http://www.aloki.hu ● ISSN 1589 1623 (Print) ● ISSN 1785 0037 (Online)
DOI: http://dx.doi.org/10.15666/aeer/2005_37093736

[73] Sorensen, T. A. (1948): A method of establishing groups of equal amplitude in plant sociology based on similarity of species content and its application to analyses of the vegetation on Danish commons. – Biol. Skar. 5: 1-34.
[74] Speth, P., Christoph, M., Diekkrüger, B. (2010): Impacts of Global Change on the Hydrological Cycle in West and Northwest Africa. – Springer Science & Business Media, Berlin.
[75] Stackpoole, S. M., Stets, E. G., Sprague, L. A. (2019): Variable impacts of contemporary versus legacy agricultural phosphorus on US river water quality. – Proceedings of the National Academy of Sciences 116(41): 20562-20567.
[76] Stanley, E. H., Fisher, S. G., Grimm, N. B. (1997): Ecosystem expansion and contraction in streams. – BioScience 47: 427-435.
[77] Stevenson, R. J., Smol, J. P. (2015): Use of Algae in Ecological Assessments. – In: Wehr, J. D., Sheath, R. G. (eds.) Freshwater Algae of North America. Elsevier, Amsterdam, pp. 921-962.
[78] Stevenson, R. J., Bothwell, M. L., Lowe, R. L., Thorp, J. H. (1996): Algal Ecology: Freshwater Benthic Ecosystem. – Academic Press, Cambridge, MA.
[79] Stubbington, R., England, J., Wood, P. J., Sefton, C. E. M. (2017): Temporary streams in temperate zones: recognizing, monitoring and restoring transitional aquatic-terrestrial ecosystems. Wiley Interdisciplinary Reviews. – Water 4: e1223.
[80] Stubbington, R., Paillex, A., England, J., Barthès, A., Bouchez, A., Rimet, F., Sánchez-Montoya, M. M., Westwood, C. G., Datry, T. (2019): A comparison of biotic groups as dry-phase indicators of ecological quality in intermittent rivers and ephemeral streams. – Ecological Indicators 97: 165-174.
[81] Taylor, J. C., Prygiel, J., Vosloo, A., de la Rey, P. A., van Rensburg, L. (2007): Can diatom-based pollution indices be used for biomonitoring in South Africa? A case study of the Crocodile West and Marico water management area. – Hydrobiologia 592: 455-464.
[82] Van Dam, H., Mertens, A., Sinkeldam, J. (1994): A coded checklist and ecological indicator values of freshwater diatoms from the Netherlands. – Netherland Journal of Aquatic Ecology 28: 117-133.
[83] Vörösmarty, C. J., McIntyre, P. B., Gessner, M. O., Dudgeon, D., Prusevich, A., Green, P., Glidden, S., Bunn, S. E., Sullivan, C. A., Liermann, C. R. (2010): Global threats to human water security and river biodiversity. – Nature 467: 555-561.
[84] Vouilloud, A. A. (2003): Catálogo de diatomeas continentales y marinas de Argentina. –
[85] Warner, N., Lgourna, Z., Bouchaou, L., Boutaleb, S., Tagma, T., Hsaissoune, M., Vengosh, A. (2013): Integration of geochemical and isotopic tracers for elucidating water sources and salinization of shallow aquifers in the sub-Saharan Drâa Basin, Morocco. – Applied Geochemistry 34: 140-151.
[86] Wheater, H., Al Weshah, R. (2002): Hydrology of wadi systems. – Technical Documents in Hydrology No. 55. UNESCO, Paris
[87] Williams, W. D. (1987): Salinization of rivers and streams: an important environmental hazard. – Ambio 15: 180-185.
[88] Williams, D. D., Williams, N. E. (1998). Aquatic insects in an estuarine environment: densities, distribution and salinity tolerance. – Freshwater Biology 39: 411-421.

http://www.aloki.hu ● ISSN 1589 1623 (Print) ● ISSN 1785 0037 (Online)
DOI: http://dx.doi.org/10.15666/aeer/2005_37093736

APPENDIX

Appendix 1. *Photos of the sampling sites:*

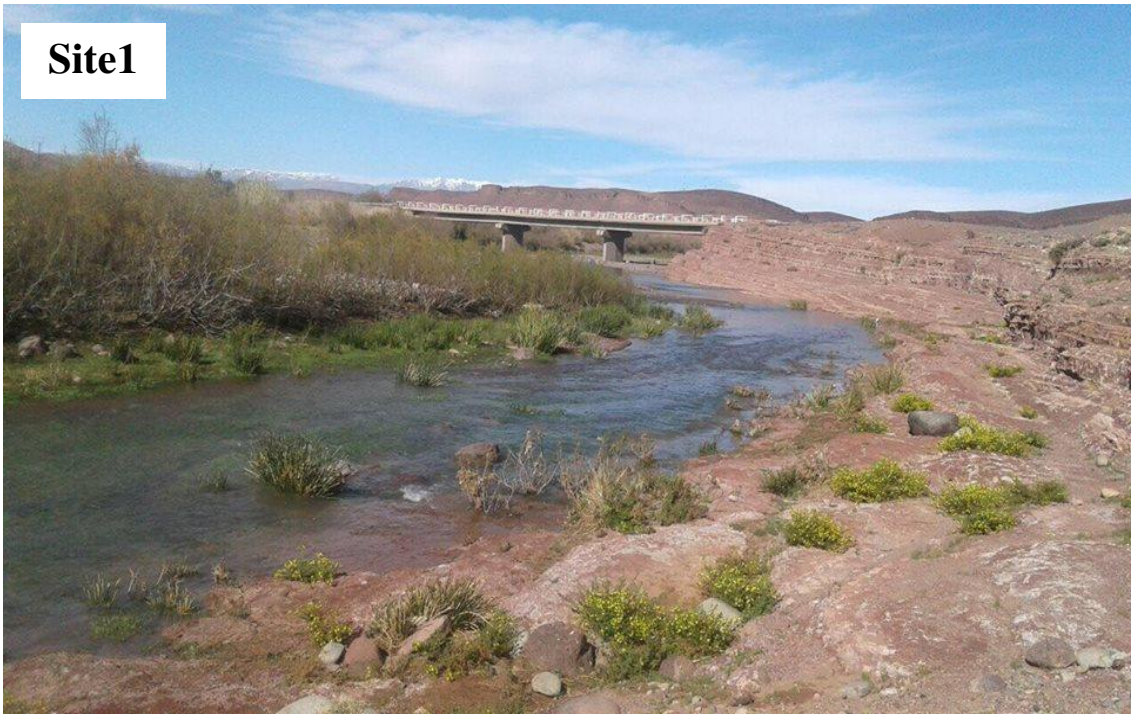

http://www.aloki.hu ● ISSN 1589 1623 (Print) ● ISSN 1785 0037 (Online)
DOI: http://dx.doi.org/10.15666/aeer/2005_37093736

http://www.aloki.hu ● ISSN 1589 1623 (Print) ● ISSN 1785 0037 (Online)
DOI: http://dx.doi.org/10.15666/aeer/2005_37093736

http://www.aloki.hu ● ISSN 1589 1623 (Print) ● ISSN 1785 0037 (Online)
DOI: http://dx.doi.org/10.15666/aeer/2005_37093736

http://www.aloki.hu ● ISSN 1589 1623 (Print) ● ISSN 1785 0037 (Online)
DOI: http://dx.doi.org/10.15666/aeer/2005_37093736

ACUTE PHYTOTOXICITY OF FOUR COMMON PHARMACEUTICALS ON THE GERMINATION AND GROWTH OF *Lactuca sativa* L.

CHAN-KEB, C. A.[1] – AGRAZ-HERNÁNDEZ, C. M.[2] – GUTIÉRREZ-ALCÁNTARA, E. J.[1] – AKE-CANCHÉ, B.[1] – TIRADO-TORRES, D.[3] – RUIZ-HERNÁNDEZ, J.[1] – SARABIA-ALCOCER, B.[4] – GÓMEZ-SOLANO, M. I.[1] – MOO-CHIM, D. J.[1] – LOPEZ-GUTIERREZ, T. J.[1] – PÉREZ-BALAN, R. A.[1*]

[1]*Facultad de Ciencias Químico Biológicas, Universidad Autónoma de Campeche, Avenida Ing. Humberto Lanz Cárdenas S/N, Colonia Ex Hacienda Kalá, C.P. 24085 San Francisco de Campeche, Campeche, México*

[2]*Instituto EPOMEX. Universidad Autónoma de Campeche. Av. Heroe de Nacozari #480. Campus 6 de Investigaciones. C.p. 24029 San Francisco de Campeche, Campeche, México*

[3]*Departamento de Ingeniería Civil, División de Ingenierías, Campus Guanajuato, Universidad de Guanajuato, Av. Juarez N° 77, Col. Centro, Guanajuato, Gto., México*

[4]*Facultad de Medicina, Universidad Autónoma de Campeche,Av Patricio Trueba de Regil, Lindavista CTM, 24096 Campeche, Campeche, México*

[*]*Corresponding author*
e- mail: roaperez@uacam.mx; phone: +52-981-811-9800 (ext. 2010110)

(Received 18th Feb 2022; accepted 20th Jun 2022)

Abstract. The pharmaceutical industry has provided an extraordinary variety of drugs that have improved human health, yet the incorrect final disposal of drugs has been released into the environment. In this research, the phytotoxic effect of four pharmaceutical products exposed to five concentrations was evaluated, using *Lactuca sativa*, and the percentage of germination, stem, and root length were evaluated. The four pharmaceuticals used in this bioassay caused inhibitory effects on root growth, elongation of hypocotyls, and germination of *Lactuca sativa* seeds. The greatest inhibition effect occurred from 10 to 1000 mg L^{-1}, likewise significant differences, and interaction ($p \leq 0.05$) were observed between concentrations and drugs. Ranitidine was the drug that had the greatest phytotoxic effect on the inhibition of germination and root growth of *Lactuca sativa*. The results obtained in this study could contribute as a reference to future chronic studies with *Lactuca sativa*, as well as to prevent or reduce the impact on ecosystems and agricultural soils.
Keywords: *drugs, toxicity, ranitidine, bioassay, contaminants*

Introduction

Currently, the consumption of pharmaceutical products has been increasing due to the increase in the world population as a basic need for the improvement of human health, however, the incorrect final disposal of medicines has been released into the environment (Arnold et al., 2013; Vasquez et al., 2014; Christou et al., 2019). Moreover, pharmaceuticals are generally discharged into the environment through contaminated wastewater and biosolids in different environmental compartments such as rivers, water tables, coastal areas, as well as in agricultural soils (Singh et al., 2018). In addition, pharmaceutical residues in rainy seasons can be transported by terrestrial runoff that reaches surface waters or can also infiltrate the soil, thus generating the dispersion of the pharmaceutical pollutant in other environmental compartments of the subsoil (Edwards

http://www.aloki.hu ● ISSN 1589 1623 (Print) ● ISSN1785 0037 (Online)
DOI: http://dx.doi.org/10.15666/aeer/2005_37373746

et al., 2009; Bártíková et al., 2016; Hurtado et al., 2016). Most research conducted on ecotoxicology has focused on aquatic organisms (e.g., phytoplankton, marine bacteria, algae, crustaceans, or fish) and very few studies on soil-dwelling organisms (e.g., invertebrates, plants, soil bacteria, and fungi). There are other studies, but only for phytoremediation purposes or to determine possible human exposure through trophic transfer (Carvalho et al., 2014). However, the effects of toxicity documented with pharmaceuticals on land plants are rare (Hillis et al., 2011; Carvalho et al., 2014; Bártíková et al., 2016). Some studies conducted with pharmaceutical products such as paracetamol were classified as harmful to the copepod *Tisbe battagliai* (Trombini et al., 2016) and exhibited toxicity to a variety of other aquatic species such as the unicellular algae *Pseudokirchneriella subcapitata,* the cyanobacterium *Cylindrospermopsis raciborskii* (Nunes et al., 2014). Ibuprofen can accumulate in the soil and cause toxic effects on plants in their development (Schmidt, 2015) or inhibition of root growth (González and Boltes, 2014), depending on the type of species. On the other hand, amoxicillin has been determined to stimulate photosynthetic activity and microcystin production of *Microcystis aeruginosa* (Liu et al., 2016). This pharmaceutical product was also able to induce oxidative stress in zebrafish (*Dania rerio*) (Oliveira et al., 2013). Amoxicillin has also shown toxicity to terrestrial organisms affecting photosynthetic processes in wheat (*Triticum* aestivum) (Opri et al., 2013).

The *Lactuca sativa* seed toxicity bioassay is a 120-hour static acute toxicity test, which evaluates the phytotoxic effects of pure compounds or complex mixtures on the process of seed germination and seedling development in the first days of growth (Bowers et al., 1996). The success or fitness of a seedling to settle in a certain environment is of great importance to ensure the survival of the species. The evaluation of the development of the radicle and hypocotyl are representative indicators to determine the establishment and development capacity of a plant (Priac et al., 2017). The use of bioassays with plants represents a fast and economical method for the characterization of the toxicity of environmental samples (Chan-Keb et al., 2018). Therefore, the objective of this study is to determine the acute toxic effects of the exposure of four pharmaceutical products to different concentrations in the germination and elongation of the radicle and hypocotyl of lettuce (*Lactuca sativa* L.).

Materials and methods

Characterization of pharmaceutical products and experimental design with Lactuca sativa

The experiment was conducted at the Faculty of Chemical Biological Sciences of the Autonomous University of Campeche, Mexico. The sowing of the lettuce seeds and the analysis of the samples were carried out in February 2019.

For the realization of the bioassay*, Lactuca sativa* seeds (Vita-Los Molinos) were used, four pharmaceutical products were used (bezafibrate, hydrochlorothiazide, losartan, and ranitidine) of Sigma Aldrich, the physicochemical properties are shown in *Table 1*. For this bioassay, 1 liter of 1000 mg L^{-1} (w/v) stock solution of each of the four drugs was prepared with distilled water.

For the determination of acute toxicity, 5 treatments per drug were performed with concentrations of 0.01, 0.1, 1, 10, and 1000 mg L^{-1} that were obtained from successive dilutions in triplicate and for the negative growth, control distilled water was used, for a total of 80 experimental units.

http://www.aloki.hu ● ISSN 1589 1623 (Print) ● ISSN1785 0037 (Online)
DOI: http://dx.doi.org/10.15666/aeer/2005_37373746

Table 1. *Physicochemical properties of the four drugs*

Chemical group	Compound	Drug class	Formula molecular	Molecular weight (g mol^{-1})	PKa	CAS Registration Number	ATC
H2 Antagonist	Ranitidine	Anti-ulcer agents	$C_{13}H_{22}N_4O_3S$	314.404	7.8	66357-35-5	A02BA02
PPAR-alpha agonist	Bezafibrato	Lipid-lowering agents	$C_{19}H_{20}ClNO_4$	361.8	3.83	41859-67-0	C10AB02
Diuretics; Sodium chloride symporter inhibitors	Hydrochlorothiazide	Antihypertensive agents;	$C_7H_8ClN_3O_4S_2$	297.7	7.9	58-93-5	C03AA03
Angiotensin II receptor blockers type 1	Losartan	Antiarrhythmic agents; Antihypertensive agents	$C_{22}H_{23}ClN_6O$	422.9	5.5	114798-26-4	C09CA01

ATC: For its acronym in English refers: Anatomy, Therapeutics, Chemical Classification System

http://www.aloki.hu ● ISSN 1589 1623 (Print) ● ISSN1785 0037 (Online)
DOI: http://dx.doi.org/10.15666/aeer/2005_37373746

For each unit, 25 seeds of *Lactuca sativa* (Vita - Los Molinos) were placed in a polyethylene container (petri dish) 90 mm in diameter, with filter paper (Whatman® No. 3) at the bottom as support. Subsequently, 10 ml of each of the concentrations of the aqueous solution were applied. All units were kept at a controlled room temperature of 24 ± 1°C for 120 hours (5 days) as set by the EPA for phytotoxicity testing. At the end of the exposure period, the number of germinated seeds was counted and the length of the root and hypocotyls was measured. As response variables, the mean and standard deviation of radicle length and hypocotyls were determined in the negative controls and each treatment (exposure concentration) (*Figure 1*). In addition, the percentage of germination (*%G*) of the seeds for each concentration concerning the negative control was determined according to the equation of Chan-Keb et al. (2018), *Eq. (1)*.

$$\% G = (\text{No. of sprouted seedlings in each concentration} * 100) / \text{No. of germinated seedlings in the control} \quad \text{(Eq.1)}$$

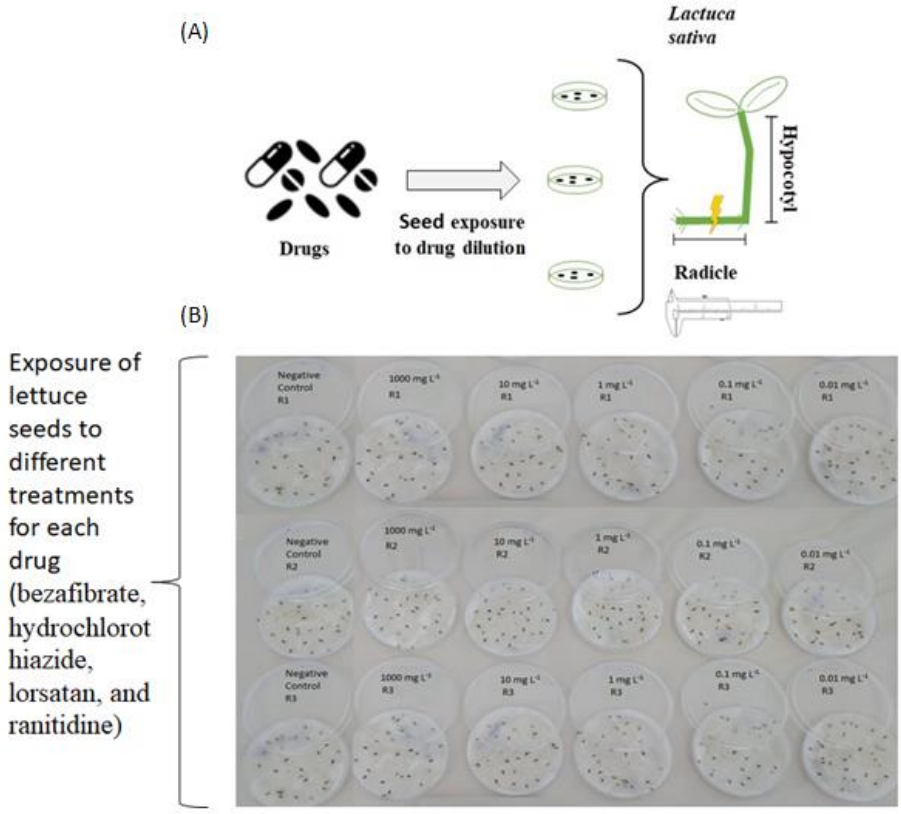

Figure 1. *(A) Experimental diagram of the exposure of Lactuca sativa seeds to drug dilutions; (B) Exposure of Lactuca sativa seeds to different treatments for each drug*

Statistical analysis

To evaluate the toxicity effect of pharmaceutical products on the morphometric variables (seed germination, root elongation, and hypocotyl) in *Lactuca sativa,* we compared the treatments and the four drugs exposed, to determine the variation or interaction of these two factors, applying a two-way ANOVA. Before this comparison

http://www.aloki.hu ● ISSN 1589 1623 (Print) ● ISSN1785 0037 (Online)
DOI: http://dx.doi.org/10.15666/aeer/2005_37373746

analysis, the normality of the variables was validated with the method of Shapiro and Wilks (1965), with a significance level $\alpha = 0.05$, not complying with the assumption of normal distribution, the data were transformed using the Box-Cox method so that the variables will present the assumptions of normal distribution (Zar, 2010). *Post-hoc* analysis was realized with least significant difference (LSD) Fisher test. All statistical analyses were performed with the STATISTICA V.12 program (©Copyright StatSoft, Inc., Palo Alto, CA, USA, 1984–2014).

Results

Figure 2 shows the data of the percentage of germination of lettuce seeds concerning the negative control with distilled water. Seeds germinated in the negative control were considered 100% germination. In the treatments, the phytotoxic effect was observed when drugs exposure concentration increased. The low germination was statistically significant in all treatments with regard to control ($p \leq 0.05$, *Table 2*). For bezafibrate, hydrochlorothiazide and losartan the effect on decrease germination was noticeable from the exposure of 10 to 1000 mg L^{-1}, in addition, ranitidine shown the lowest germination to concentrations of 0.01 to 1000 mg L^{-1}, where decrease of 61 to 41% are observed when increasing the concentration of exposure (*Figure 2*).

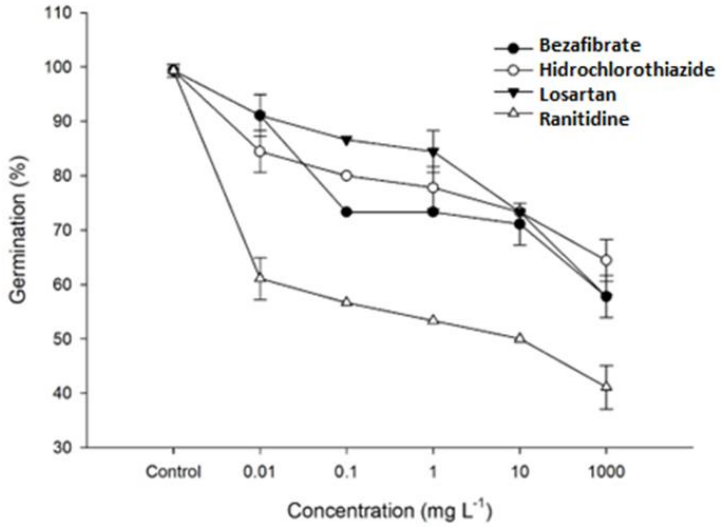

Figure 2. *Average germination of Lactuca sativa seeds between the concentrations of the 4 drugs exposed. The error bars represent the standard deviation*

Exposure to different concentrations of the 4 drugs also showed a decrease in the development of root length and the hypocotyls of lettuce (*Figure 3A and 3B*). When performing a 2-way ANOVA, significant differences were observed between drugs and exposure concentrations in the average development of root length and hypocotyls of *Lactuca sativa* (*Table 2*). From the above, considering all the concentrations of the 4 drugs, a decrease in the elongation of the radicles were observed concerning the control, being the treatment at 1000 mg L^{-1} the greatest effect was presented (*Figure 3A*); it was also observed in the treatments exposed with ranitidine they were notorious in terms of the decrease in root elongation.

http://www.aloki.hu ● ISSN 1589 1623 (Print) ● ISSN1785 0037 (Online)
DOI: http://dx.doi.org/10.15666/aeer/2005_37373746

Table 2. *Two-way analysis of variance concerning germination, root length, and hypocotyls of Lactuca sativa between concentrations (Control, 0.01, 0.1, 1, 10, and 1000 mg L^{-1}) and exposure to 4 drugs (bezafibrate, hydrochlorothiazide, losartan, and ranitidine), with a significance level of $p<0.05$*

Parameter	Factor	Gl	F	P
Germination (%)	Concentration	5	258.09	<0001
	Drug	3	174.89	<0001
	Concentration * Drug	15	10.42	<0001
	Error	48		
Root length (mm)	Concentration	5	1420.09	<0001
	Drug	3	11.99	<0001
	Concentration * Drug	15	2.43	<0.010
	Error	48		
Hypocotyl length (mm)	Concentration	5	2569.93	<0001
	Drug	3	119.14	<0001
	Concentration * Drug	15	9.92	<0001
	Error	48		

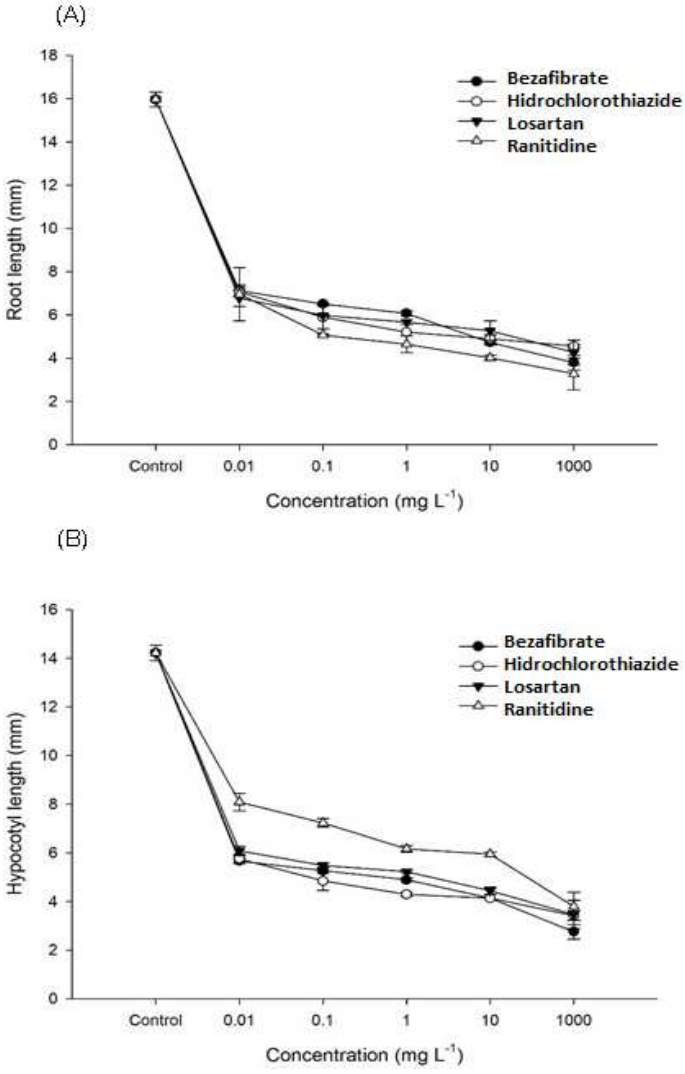

Figure 3. *Average growth in (A) root length; (B) length of the hypocotyl of Lactuca sativa between the concentration exposed to 4 drugs. The error bars represent the standard deviation*

http://www.aloki.hu ● ISSN 1589 1623 (Print) ● ISSN1785 0037 (Online)
DOI: http://dx.doi.org/10.15666/aeer/2005_37373746

In *Figure 3B* see that the bezafibrate, hydrochlorothiazide, and losartan shown significative less hypocotyls length that ranitidine effect in concentrations of 0.01 to 100 mg L^{-1}, however, for 1000 mg concentrations do not significate differences were observed among all drugs.

Discussion

In general terms, germination, root length, and hypocotyls of *Lactuca sativa* showed a decrease concerning control, this is due to the phytotoxic effect of the 4 drugs to which they were exposed different concentrations, which were absorbed through the roots. The results in the germination of *Lactuca sativa* seeds show that there was a greater phytotoxic effect caused by ranitidine when the exposure concentration increased compared to the 3 drugs (bezafibrate, hydrochlorothiazide, and losartan) and control, this may be due to the sensitivity of lettuce seeds to ranitidine. Similar findings have been reported by authors such as Rade et al. (2019) where they performed an individual toxic evaluation and the mixture of three pharmaceutical products (paracetamol, ibuprofen, and amoxicillin) in the germination and growth of seeds in *Lactuca sativa*, where they determined that the lowest amount of germination occurred in the drug ibuprofen and the mixture of the 3 drugs (Rade et al., 2019). Moreover, authors such as Biruk et al. (2017) found that lettuce seeds were more sensitive to extracts containing inorganic elements than organic extracts.

The phytotoxic effect on the radicle and hypocotyl of lettuce was greater at concentrations of 10 to 1000 mg L^{-1} in the four drugs exposed. This is due to the absorption of drugs that are bioavailable in aqueous solution, through the roots, as the main route for transfer and direct contact, where the influx of nutrients and water in lettuce is also regulated, that is, the morphology, anatomy, and biomass production of the roots is also associated with the effect on the absorption of drugs (Rodriguez-Ruiz et al., 2015), as presented in this study.

When comparing the effects of ranitidine on radicular and hypocotyl length in lettuce, it was observed that the toxic effect was greater in the roots than in the length of the hypocotyls, therefore, we described that the root was more sensitive to aqueous solutions of ranitidine, due to direct contact in the absorption of the drug generating physiological stress. In this regard, Gómez-Oliván et al. (2014) mention that the presence of isolated drugs in the soil can induce oxidative stress in plants and influence their antioxidant defenses giving rise to different responses (phytotoxic effects), this will depend on the drug, its concentration and the sensitivity of the plant species (Carvalho et al., 2014; Marsoni et al., 2014; Minden et al., 2017). On the other hand, Christou et al. (2019) mention that the bioaccumulation of contaminants in plant tissues depends on the type of soil, the physicochemical properties of the contaminants, and the interactions of these factors, as well as the type of species.

Based on the results obtained from this research, more future studies can be carried out on chronic phytotoxic effects in *Lactuca sativa* considering other types of indicators to be evaluated, different concentrations of drugs or similar to those found in the environment, to contribute to the environmental regulations that allow establishing the permissible limits of discharge of residual drains that contain drug residues and thus be able to prevent or mitigate short-, medium- and long-term impacts on coastal areas, rivers, soils, and crops.

http://www.aloki.hu ● ISSN 1589 1623 (Print) ● ISSN1785 0037 (Online)
DOI: http://dx.doi.org/10.15666/aeer/2005_37373746

Conclusions

This study describes the phytotoxic effect of four drugs where 3 are commonly used (bezafibrate, hydrochlorothiazide, and losartan) and one (ranitidine) that was banned from use and excluded since 2019 for marketing and consumption by the U.S. Food and Drug Administration (FDA), due to its classification as a carcinogen. Phytotoxicity caused by the drugs was related to inhibitory effects on a radicle, hypocotyl elongation, and seed germination in *Lactuca sativa*. Exposure to ranitidine aqueous solution exerted a greater effect on seed germination and root elongation in lettuce. Based on the results of this study, the phytotoxic effect of ranitidine that it can cause in a plant species such as *Lactuca sativa* is verified and described for the first time. The test used allowed the identification of different levels of phytotoxicity in the samples of drugs in aqueous solution, in addition, the bioassay with *Lactuca sativa* proved to be efficient, sensitive, economical, fast, and reproducible. Likewise, the results of our research could contribute as reference information for future chronic studies with *Lactuca sativa* and other drugs.

REFERENCES

[1] Arnold, K. E., Boxall, A. B. A., Brown, A. R., Cuthbert, R. J., Gaw, S., Hutchinson, T. H., Jobling, S., Madden, J. C., Metcalfe, C. D., Naidoo, V., Shore, R. F., Smits, J. E., Taggart, M. A., Thompson, H. M. (2013): Assessing the exposure risk and impacts of pharmaceuticals in the environment on individuals and ecosystems. – Biol. Lett. 9.

[2] Bártíková, H., Podlipná, R., Skálová, L. (2016): Veterinary drugs in the environment and their toxicity to plants. – Chemosphere 144: 2290-2301. https://doi.org/10.1016/j. chemosphere.2015.10.137.

[3] Biruk, L. N., Moretton, J., Fabrizio de Iorio, A., Weigandt, C., Etcheverry, J., Filippetto, J., Magdaleno, A. (2017): Toxicity and genotoxicity assessment in sediments from the Matanza- iachuelo river basin (Argentina) under the influence of heavy metals and organic contaminants. – Ecotoxicol. Environ. Saf. 135: 302-311.

[4] Bowers, N., Pratt, J. R., Beeson, D., Lewis, M. (1997): Comparative evaluation of soil toxicity using lettuce seeds and soil ciliates. – Environ. Toxicol. Chem. 16: 207-213.

[5] Carvalho, P. N., Basto, M. C. P., Almeida, C. M. R., Brix, H. (2014): A review of plantpharmaceutical interactions: from uptake and effects in crop plants to phytoremediation in constructed wetlands. – Environ. Sci. Pollut. Res. 21: 11729-11763.

[6] Chan-Keb, C. A., Agraz-Hernández, C. M., Perez-Balan, R. A., Gómez-Solano, M. I., Maldonado-Montiel, T. D., Ake-Canche, B., Gutiérrez-Alcántara, E. J. (2018): Acute toxicity of water and aqueous extract of soils from Champotón river in *Lactuca sativa* L. – Toxicology reports 5: 593-597.

[7] Christou, A., Kyriacou, M. C., Georgiadou, E. C., Papamarkou, R., Hapeshi, E., Karaolia, P., Michael, C., Fotopoulos, V., Fatta-Kassinos, D. (2019): Uptake and bioaccumulation of threewidely prescribed pharmaceutically active compounds in tomato fruits andmediated effects on fruit quality attributes. – Sci. Total Environ. 647: 1169-1178.

[8] Edwards, M., Topp, E., Metcalfe, C. D., Li, H., Gottschall, N., Bolton, P., Curnoe, W., Payne, M., Beck, A., Kleywegt, S., Lapen, D. R. (2009): Pharmaceutical and personal care products in tile drainage following surface spreading and injection of dewatered municipal biosolids to an agricultural field. – Sci. Total, Environ. 407(14): 4220-4230.

[9] Gómez-Oliván, L. M., Neri-Cruz, N., Galar-Martínez, M., Islas-Flores, H., García-Medina, S. (2014): Binary mixtures of diclofenac with paracetamol, ibuprofen, naproxen, and acetylsalicylic acid and these pharmaceuticals in isolated forminduce oxidative stress on Hyalella azteca. – Environ. Monit. Assess. 186: 7259-7271.

http://www.aloki.hu ● ISSN 1589 1623 (Print) ● ISSN1785 0037 (Online)
DOI: http://dx.doi.org/10.15666/aeer/2005_37373746

[10] González-Naranjo, V., Boltes, K. (2014): Toxicity of ibuprofen and perfluorooctanoic acid for risk assessment of mixtures in aquatic and terrestrial environments. – International Journal of Environmental Science and Technology 11(6): 1743-1750.
[11] Hillis, D. G., Fletcher, J., Solomon, K. R., Sibley, P. K. (2011): Effects of ten antibiotics on seed germination and root elongation in three plant species. – Arch. Environ. Contam. Toxicol. 60: 220-232.
[12] Hurtado, C., Domínguez, C., Pérez-Babace, L., Cañameras, N., Comas, J., Bayona, J. M. (2016): Estimate of uptake and translocation of emerging organic contaminants from irrigation water concentration in lettuce grown under controlled conditions. – J. Hazard. Mater. 305: 139-148.
[13] Liu, Y., Chen, S., Zhang, J., Gao, B. (2016): Growth, microcystin-production and proteomic responses of Microcystis aeruginosa under long-term exposure to amoxicillin. – Water Res. 93: 141-152.
[14] Marsoni, M., De Mattia, F., Labra, M., Bruno, A., Bracale, M., Vannini, C. (2014): Uptake and effects of amixture of widely used therapeutic drugs in *Eruca sativa* L. and *Zea mays* L. plants. – Ecotoxicol. Environ. Saf. 108: 52-57.
[15] Minden, V., Deloy, A., Volkert, A. M., Leonhardt, S. D., Pufal, G. (2017): Antibiotics impact plant traits, even at small concentrations. – AoB Plants 9: plx010.
[16] Nunes, B., Antunes, S. C., Santos, J., Martins, L., Castro, B. B. (2014): Toxic potential of paracetamol to freshwater organisms: a headache to environmental regulators? – Ecotoxicol. Environ. Saf. 107: 178-185.
[17] OECD: Guideline for the Testing of Chemicals. Proposal for Updating Guideline 208. – Available online: http://www.oecd.org/hemicalsafety/testing/33653757.pdf. Accessed November 2017.
[18] Opris, O., Copaciu, F., Soran, M. L., Ristoiu, D., Niinemets, U., Copolovici, L. (2013): Influence of nine antibiotics on key secondary metabolites and physiological characteristics in *Triticum aestivum*: leaf volatiles as a promising new tool to assess toxicity. – Ecotoxicol. Environ. Saf. 87: 70-79.
[19] Priac, A., Badot, P.-M., Crini, G. (2017): Treated wastewater phytotoxicity assessment using Lactuca sativa: focus on germination and root elongation test parameters - Évaluation de la phytotoxicite'eaux de rejets via Lactuca sativa: paramètres des tests de germination et d'e´longation. – Comp. Rend. Biol. 340(3): 188-194.
[20] Rede, D., Santos, L. H., Ramos, S., Oliva-Teles, F., Antão, C., Sousa, S. R., Delerue-Matos, C. (2019): Individual and mixture toxicity evaluation of three pharmaceuticals to the germination and growth of Lactuca sativa seeds. – Science of the total environment 673: 102-109.
[21] Rhaul, S., McDonough, S., Ladewig, J. C. L., Soares, A. M. V. M., Nogueira, A. J. A., Domingues, I. (2013): Effects of oxytetracycline and amoxicillin on development and biomarkers activities of zebrafish (Danio rerio). – Environ. Toxicol. Pharmacol. 36(3): 903-912.
[22] Rodriguez-Ruiz, A., Etxebarria, J., Boatti, L. Marigómez, I. (2015): Scenario-targeted toxicity assessment through multiple endpoint bioassays in a soil posing unacceptable environmental risk according to regulatory screening values. – Environ. Sci. Pollut. Res. 22: 13344-13361.
[23] Schmidt, W., Redshaw, C. H. (2015): Evaluation of biological endpoints in crop plants after exposure to non-steroidal anti-inflammatory drugs (NSAIDs): implications for phytotoxicological assessment of novel contaminants. – Ecotoxicol. Environ. Saf. 112: 212-222.
[24] Shapiro, S. S., Wilks, M. B. (1965): An Analysis of Variance Test for Normality. – Biometrika 52(3/4): 591-611.
[25] Singh, V., Pandey, B., Suthar, S. (2018): Phytotoxicity of amoxicillin to the duckweed Spirodela polyrhiza: growth, oxidative stress, biochemical traits and antibiotic degradation. – Chemosphere 201: 492-502.

http://www.aloki.hu ● ISSN 1589 1623 (Print) ● ISSN1785 0037 (Online)
DOI: http://dx.doi.org/10.15666/aeer/2005_37373746

[26] Trombini, C., Hampel, M., Blasco, J. (2016): Evaluation of acute effects of four pharmaceuticals and their mixtures on the copepod *Tisbe battagliai*. – Chemosphere 155: 319-328.
[27] Vasquez, M. I., Lambrianides, A., Schneider, M., Kümmerer, K., Fatta-Kassinos, D. (2014): Environmental side effects of pharmaceutical cocktails: what we know and what we should know. – J. Hazard. Mater. 279: 169-189.
[28] Zar, J. H. (2010): Biostatistical Analysis. – 5th Edition, Pearson Prentice-Hall, Upper Saddle River, NJ.

http://www.aloki.hu ● ISSN 1589 1623 (Print) ● ISSN1785 0037 (Online)
DOI: http://dx.doi.org/10.15666/aeer/2005_37373746

EFFECTS OF NITROGEN APPLICATION RATE UNDER DIFFERENT GROWING SEASON PRECIPITATION LEVELS ON WATER AND NITROGEN UTILIZATION EFFICIENCIES, GRAIN YIELD, AND QUALITY IN DRYLAND WHEAT (*TRITICUM AESTIVUM* L.)

HAO, R.[1,2#] – NOOR, H.[1,2#] – WANG, P.[1,2] – REN, A.[1,2] – HAN, X.[1,2] – ZHONG, R.[1,2] – SUN, M.[1,2*] – GAO, Z.[1,2]

[1]*College of Agriculture, Shanxi Agriculture University, No.1, Minxian South Road, Taigu, 030801 Shanxi, China*

[2]*State Key Laboratory of Sustainable Dryland Agriculture (Taigu District, Shanxi Province), Shanxi Agricultural University, No. 1, Mingxian South Road, Taigu District, Jinzhong City, Shanxi Province, China*
(phone: +86-183-2975-5208)

[#]*These authors contributed equally to this work*

[*]*Corresponding author*
e-mail: sm_sunmin@126.com; phone: +86-136-2354-1985

(Received 5th Mar 2022; accepted 20th Jun 2022)

Abstract. High interannual variability of precipitation and unbalanced N application rate has a considerable impact on wheat (*Triticum aestivum* L.) production in the drylands of the Loess Plateau, China. In this study, we conducted field experiments in Wenxi County, Shanxi Province, under six N application rates (0, 90, 120, 150, 180, and 210 kg ha^{-1}) for three consecutive years from 2014 to 2017. The years were classified as the wet (2014–2015), dry (2015–2016), and normal growing seasons (2016–2017) based on total precipitation during the growth period. The results showed that in the wet growing season, the optimum N application rate was 180 kg ha^{-1}, improved the total water consumption during the growth period by 1.9%-13.8%, the spike number by 0.6%–10.9%, the yield by 2.8%–14.3%, N recovery efficiency (NRE) by 15.2%–47.0%, and the economic by 4.4%–21.1%. In the normal and dry growing seasons, the optimum N application rate was 150 kg ha^{-1}, the total water consumption increased during the growth period by 0.5%–16.3%, the spike number by 0.9%–19.8%, the yield by 0.3%–23.3%, water use efficiency by 2.5%–12.9%, and NRE by 12.9%–59.1%, the economic improved by 0.6%–74.7%.
Keywords: *Loess Plateau, wheat cultivation, amount of precipitation, water use efficiency, nitrogen fertilizer recovery efficiency*

Introduction

Dryland farming accounts for one third of the cultivated area in China. Approximately 40% of the cultivated land in the Loess Plateau is dryland, covering an area of 63×104 ha^{-1} (Yang et al., 2021). Winter wheat production in this dryland is of importance in ensuring regional food security (Ren et al., 2016; Liu et al., 2021). In the Loess Plateau dryland, where irrigation is not available, precipitation is the only source of water for wheat production. Precipitation levels are low and unevenly distributed, and summer rainfall accounts for approximately 60% of the annual precipitation (Ren et al., 2016). Furthermore, annual precipitation fluctuates considerably (Yang et al., 2021). Because of limited water resources, the main planting approach in this area is to plant one crop (winter wheat) per year and leave the land fallow in the summer (Sun et al., 2019;

http://www.aloki.hu ● ISSN 1589 1623 (Print) ● ISSN 1785 0037 (Online)
DOI: http://dx.doi.org/10.15666/aeer/2005_37473762

Yu et al., 2021). In recent years, the frequency, duration, and severity of drought in this area have increased substantially due to climate change (Jiang et al., 2016; Yu et al., 2021). Drought is the main limiting factor of winter wheat production in the drylands of the Loess Plateau (Wang et al., 2019).

Soil fertility, especially N levels, in the Loess Plateau dryland is low (Cao et al., 2017). While the rainfall in wheat growing season is generally scarce, extensive yearly variabilities make it difficult to synchronize the soil N supply capacity with the wheat growth demand (Mon et al., 2016). The imbalance of soil water and N supply is the main cause of low and unstable wheat yield in the dryland (Zhang et al., 2017). The application of N fertilizers can significantly increase grain yield and water use efficiency (WUE) of winter wheat (Xia et al., 2016). Li et al. (2022) showed that fertilizers can reduced the effect of soil moisture on productivity in dryland soil while improving the wheat yield and WUE. The effects of water and N on crop yield are synergistic rather than individual. As the effects of water on yield and grain quality are influenced by N fertilizer, yield responses to N fertilizers vary with the annual precipitation level. A study on N application rate in the Loess Plateau for four consecutive years showed that when 180 kg N ha^{-1} was applied, wheat yield in the dry years increased by 14.0% relative to no N application, whereas it increased by 32.8% in the wet years (Wang et al., 2018).

Excessive N fertilization can have negative effects on crop yield and the environment (Lai et al., 2022). Several studies in the Loess Plateau have shown that N application rates of 75–150 kg ha^{-1} could result in a higher yield and higher N use efficiency (NUE), but the positive effects are considerably reduced when the N application rate exceeds 210 kg ha^{-1} (Li et al., 2022). The excessive use of N fertilizers poses several negative effects on the environment (Liu et al., 2016). A study in the Loess Plateau has shown that with the use of controlled release nitrogen fertilizers, the crop yield, NUE, and accounts returns increased by 8.5%, 10.9%, and 11.3%, respectively (Xu et al., 2021). Another study on N application rates in the Loess Plateau reported that the application of an appropriate amount of N fertilizer increased the content and composition of wheat proteins, leading to an improvement in baking quality of wheat flour (Raymbek et al., 2017). With an increase in the N application rate, the investment on N fertilizer increases. Appropriate N application should be determined based on the economic return (Liu et al., 2019). Furthermore, a survey of farmers in dry farming areas in the Loess Plateau in 2011 showed that 42% of the farmers applied more than 200 kg ha^{-1} N, and achieved an average yield of 4,500 kg ha^{-1} (Cao et al., 2017). Apparently, the amount of N applied by farmers in the area exceeds the level of N required to achieve high yield. Considering the variety of agricultural practices, outlining an effective guidance on how to apply fertilizers according to varying annual precipitation for improved grain yield and quality as well as high water and fertilizer use efficiency in the dryland wheat region of the Loess Plateau is essential for the farmers and has been the focus of many studies.

Previous studies have shown that optimizing N application in different growth periods and precipitation amounts can effectively improve yield and increase the efficiencies of water and N use (Wang et al., 2018; Xu et al., 2021). However, the problem of blind fertilization to achieve high yield, efficient water and N use, and sustainable winter wheat cropping system still exists in most areas of the Loess Plateau (Cao et al., 2017) due to the lack of systematic and comprehensive observation of precipitation and N fertilizer application during the growth period. In this study, field experiments with different N application rates (0–210 kg ha^{-1}) on dryland wheat were conducted for three consecutive years in the experimental site in the eastern part of the Loess Plateau, Shanxi Province,

http://www.aloki.hu ● ISSN 1589 1623 (Print) ● ISSN 1785 0037 (Online)
DOI: http://dx.doi.org/10.15666/aeer/2005_37473762

China. We aimed to determine (1) the effects of N application rates on growth, N accumulation of the plant, grain yield, grain quality, economic return, WUE, and NRE in the three years with differing growing season precipitation levels. (2) The optimal N application rates were determined based on grain yield, grain quality, and economic return in planting years with different growing season precipitation levels.

Materials and Methods

Experimental site

The experiment was carried out in the experimental site of Shanxi Agricultural University in Wenxi County, Shanxi Province, China (110°59′–111°37′E, 35°09′-35°34′N, *Figure 1*) in 2014–2017. Basic nutrients in the 0–20-cm layer of the calcareous cinnamon soil are shown in *Table 1*.

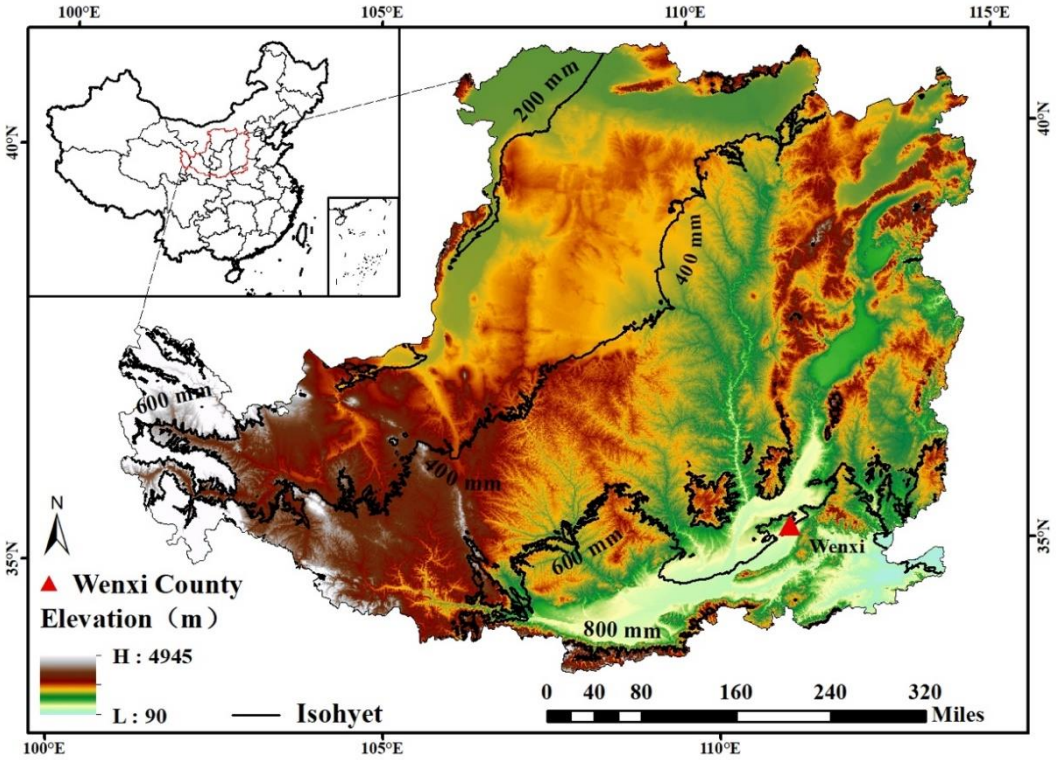

Figure 1. *Study area. Elevation and isohyet on the Loess Plateau in China*

Table 1. *Soil nutrient content in the 0–20-cm soil layer before wheat sowing*

Year	Organic matter (g kg^{-1})	Alkali-hydrolyzable nitrogen (g kg^{-1})	Available phosphorus (mg kg^{-1})	Available potassium (mg kg^{-1})	PH (2.5:1)
2014–2015	9.9	38.2	21.0	112.5	8.2
2015–2016	11.9	38.6	24.6	108.9	8.4
2016–2017	15.3	38.1	28.1	117.6	8.1

http://www.aloki.hu ● ISSN 1589 1623 (Print) ● ISSN 1785 0037 (Online)
DOI: http://dx.doi.org/10.15666/aeer/2005_37473762

Experimental design and field management

A completely randomized design was used in the experiment with six application rates of N fertilizer (0, 90, 120, 150, 180, and 210 kg ha^{-1}) and three replicates. The plot size was 4 m × 20 m. Before sowing, 150 kg P_2O_5 ha^{-1} and 150 kg K_2O ha^{-1} were evenly applied to the plots. Winter wheat seeds (variety Yunhan 20410) were sown in early October each year. A rotary seeder (2BMF-12/6; Dandong Virtue River Technology Co., Ltd., Shandong Province, China, *Figure 2*) was used for strip sowing. Straw residues from the previous season were plowed into the soil to a depth of 10–15 cm with the rotary seeder, and N fertilizer (urea content of 46% N) was applied at six rates (0, 90, 120, 150, 180, and 210 kg ha^{-1}) underneath the seeds. The sowing depth was 3–5 cm, row width was 12–13 cm, and plant spacing was 2–3 cm. Artificial herbicide was sprayed in the spring; before jointing, powdery mildew, red spiders, and aphids were controlled by UAV. *Fusarium* head blight was controlled at the anthesis stage. At the initial stage of filling, aphids and other pests were controlled. Wheat plants were harvested in early June in the following year.

Figure 2. *Wheat strip sowing and emergence of seedlings in the experimental site. Note: The picture on the left shows the strip sowing machine and the picture on the right shows the emergence of seedlings one month after sowing*

Classification of annual precipitation

Annual precipitation was used to classify the growing season using the drought index (DI). DI = (P – M)/σ [22]; where P is the growing season precipitation (mm), M is the average growing season precipitation from 2009 to 2019 (the value of M is 434.7 mm), and σ is the mean square deviation of the multiyear mean precipitation. The planting year of 2014–2015 was classified as a wet growing season, 2015–2016 as a dry growing season, and 2016–2017 as a normal growing season (*Table 2*).

Table 2. *Classification of year type for three planting seasons from 2014 to 2017*

Year	Growing season precipitation (mm)	Drought index (DI)	Growing season type
2014–2015	516.7	0.69	Wet
2015–2016	342.9	-0.78	Dry
2016–2017	406.3	-0.24	Normal

DI, drought index (DI < -0.35 classified as a dry growing season, DI > 0.35 as a wet growing season, and -0.35 ≤ DI ≤ 0.35 as a normal growing season)

http://www.aloki.hu ● ISSN 1589 1623 (Print) ● ISSN 1785 0037 (Online)
DOI: http://dx.doi.org/10.15666/aeer/2005_37473762

Measurement of soil moisture content and evapotranspiration and calculation of WUE

Soil samples from a depth of 200 cm was collected after harvesting the previous wheat crop. Soil samples (0–200 cm) were also collected by drilling in the pre-sowing, pre-wintering, jointing, anthesis, and maturity stages. Fresh soil weight was recorded, and then the soil was dried to a constant weight at 105 °C. Soil moisture content was calculated as a percentage of the difference between dry and wet weight (Ren et al., 2021).

Precipitation (mm) and consumption of soil water stored (mm) in the 0–200 cm layer were used to calculate crop water consumption in different growth periods. The total crop water consumption from sowing to plant maturity corresponds to the evapotranspiration (ET) rate for a given cropping season. ET was calculated using the following equation (Dong et al., 2019):

$$\mathrm{ET} = \mathrm{S}i + \mathrm{P}r + \mathrm{K} \quad \text{(Eq.1)}$$

where Si is the sum of soil water consumption (mm) in all growth stages, Pr is the sum of precipitation (mm) in all growth stages, K is groundwater recharge (mm), and K is negligible when the groundwater depth is greater than 2.5 m.

WUE was calculated as grain yield (kg ha^{-1}) /crop water consumption (mm) (Sadras and Lawson, 2012).

Measurement of grain yield and its components

Wheat plots of 0.667 m^2 were randomly selected at maturity to determine yield components (spike number, grain number, and 1000 grain weight). For the grain yield measurements, a 20 m^2 area in each plot was harvested at maturity.

Measurement of grain protein and starch content and calculation of NUE

Wheat grains were ground to flour using a miniature high speed grinder (FZ102; Beijing, China). The total N content in the flour was determined using the colorimetric method described by Ren et al. (2019), and the total grain protein content was obtained by multiplying the total N by 5.7. Albumin, globulin, gliadin, and glutenin were isolated by continuous extraction and N contents were determined using the same colorimetric method (Ren et al., 2019). Starch content was determined by hydrolyzing starch into glucose with hydrochloric acid and measuring the glucose using the enthrone colorimetry method described by Ren et al. (2021).

NRE, the plant N uptake per kilogram of N fertilizer applied, was calculated using the following equation (Wang et al., 2019):

$$\mathrm{NRE}\ (\%) = \{[\text{N uptake at treat plot (kg ha–1)} - \text{N uptake at N0 plot (kg ha–1)}] / \text{Fertilizer N application rate (kg ha}^{-1})\} \times 100 \quad \text{(Eq.2)}$$

Calculation of economic return

The economic return and the yield income were calculated in terms of United States dollar (USD) per hectare using the following equations:

$$\text{Economic return (USD ha}^{-1}) = \text{yield income (USD ha}^{-1}) - \text{production cost (USD ha}^{-1}) \quad \text{(Eq.3)}$$

http://www.aloki.hu ● ISSN 1589 1623 (Print) ● ISSN 1785 0037 (Online)
DOI: http://dx.doi.org/10.15666/aeer/2005_37473762

$$\text{Yield income} = \text{grain yield (kg ha}^{-1}) \times \text{market price (USD ha}^{-1}) \quad \text{(Eq.4)}$$

The market price of winter wheat was 0.34 USD kg^{-1} and the production cost (*Table 3*) included the input of seeds, fertilizers, and field management (USD ha^{-1}) (Duc-Anh et al., 2018).

Table 3. *Production cost of winter wheat*

Seed and fertilizer cost (USD·kg^{-1})				Field management (USD·ha^{-1})				
Urea	Superphosphate	Potassium sulfate	Seed	Tillage	Sowing	Reaping	Weed	Spraying pesticide
0.3	0.26	0.6	0.7	139.2	116.0	116.0	162.4	69.6

Statistical analyses

All procedures were performed using SAS software (SAS, 2008, NC, USA) to calculate the analysis of variance. The significance of differences was tested using the least significant difference, and the significance level was set at $\alpha = 0.05$.

Results

Effects of N application rates on water consumption by dryland wheat in the three years with different growing season precipitation levels

Water consumption by winter wheat during the growth period was significantly affected by the annual precipitation level. The average total water consumption (ET) under all N application rates in the wet growing season was the highest among the three cropping years (*Table 4*). The water consumption during the growth period increased until reaching the optimal N application rate and then decreased with the increasing rate. The highest water consumption in the growth period was observed at 180 kg ha^{-1} for the wet growing season and at 150 kg ha^{-1} for the normal and dry growing season.

Effects of N application rates on yield components, yield, and WUE of dryland wheat in the three years with different growing season precipitation levels

The average number of spikes for all N application rates (from 0 to 210 kg ha^{-1}) in the wet growing season was significantly higher than that in the normal or dry growing season (*Table 5*). The spike number and grain number per spike peaked at 150 kg ha^{-1} in all growing seasons except for the highest number of spikes obtained at the N application rate of 180 kg ha^{-1} in the wet growing season (*Table 5*). The highest yield was recorded at 180 kg ha^{-1} in the wet growing season and 150 kg ha^{-1} in normal and dry growing season (*Table 5*). The N application rate of 180 kg ha^{-1} in the wet growing season increased the yield by 2.9% relative to 150 kg ha^{-1}, whereas the rate of 210 kg ha^{-1} reduced yield by 8.0%. In both the normal and dry growing seasons, the N application rate of 150 kg ha^{-1} increased the yield by at least 10.2% relative to 120 kg ha^{-1}. The WUE was the highest at 150 kg ha^{-1} in all three years studied (*Figure 3*) and in the dry growing season, it was approximately 40% lower than that in wet or normal growing season. These results indicated that the N application rates of 180 and 150 kg ha^{-1} are adequate for achieving high yield in the wet growing season and in both normal and dry growing season, respectively. The spike number was found to be a major contributor to the high yield.

http://www.aloki.hu ● ISSN 1589 1623 (Print) ● ISSN 1785 0037 (Online)
DOI: http://dx.doi.org/10.15666/aeer/2005_37473762

Table 4. *Effects of N application rates on crop water consumption (mm) in the four growth stages in the three planting years with different growing season precipitation levels*

Growing season type	N application rate (kg ha^{-1})	SS-WS	WS-JS	JS-AS	AS-MS	ET
Wet growing season	0	44.7 e	144.1 d	107.5 e	95.3 a	391.5 d
	90	48.8 d	155.7 c	112.0 d	88.3 b	404.8 c
	120	52.3 c	160.0 bc	118.6 c	85.1 c	416.0 b
	150	54.8 bc	164.9 b	124.0 b	80.2 d	423.9 b
	180	57.5 ab	171.7 a	128.6 a	96.3 a	454.0 a
	210	59.7 a	176.6 a	118.9 c	89.9 b	445.2 a
	Mean	53.0 ± 5.6	162.2 ± 11.7	118.3 ± 7.7	89.2 ± 6.1	422.6 ± 23.8
Normal growing season	0	56.8 e	124.9 d	84.6 e	97.3 a	363.7 e
	90	60.7 c	124.3 d	90.9 d	87.4 b	363.3 e
	120	58.4 d	137.8 c	100.7 c	89.9 b	386.8 d
	150	67.5 a	141.1 ab	109.3 a	98.3 a	416.1 a
	180	65.7 b	144.0 a	105.6 b	98.8 a	414.1 b
	210	65.1 b	138.0 bc	104.2 b	98.6 a	406.0 c
	Mean	62.4 ± 4.4	135.0 ± 8.4	99.2 ± 9.5	95.1 ± 5.0	391.7 ± 24.2
Dry growing season	0	30.6 d	85.4 d	79.9 e	98.1 a	294.0 f
	90	33.8 c	90.4 c	86.4 d	99.3 a	309.9 e
	120	39.3 b	90.6 c	96.6 c	99.3 a	325.8 d
	150	48.4 a	107.5 a	104.8 a	90.8 b	351.4 a
	180	45.6 a	104.9 a	101.1 b	89.7 b	341.3 b
	210	41.0 b	96.6 b	100.4 b	97.3 a	335.4 c
	Mean	39.8 ± 6.8	95.9 ± 8.8	94.9 ± 9.6	95.7 ± 4.4	326.3 ± 21.2
F value						
precipitation growing season (P)		1590.7**	11628.4**	7401.0**	461.6**	11620.0**
N application rate (N)		181.2**	450.2**	1875.5**	85.5**	1239.3**
P×N		8.5**	22.3**	28.8**	198.2**	21.5**

ET, evapotranspiration during the entire growth period. SS-WS, the period from sowing to pre-wintering. WS-JS, the growth period from pre-wintering to jointing. JS-AS, the period from jointing to anthesis. AS-MS, the period from anthesis to maturity. Different letters in the same column of a given year indicate that the difference between treatments was significant ($P < 0.05$). * and ** denote a significant difference at 5% and 1%, respectively

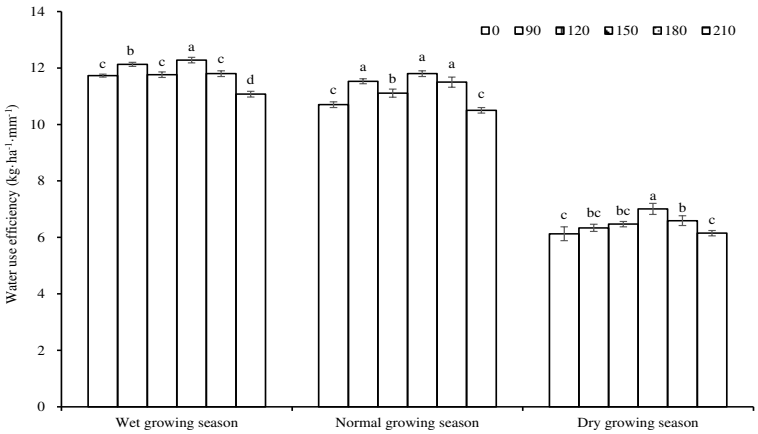

Figure 3. *Effects of N application rates on water use efficiency of dryland wheat in the three planting years with different growing season precipitation levels. Note: Error bars in the figure represent standard errors. Different letters represent a significant difference ($P < 0.05$) between the N application rates in a given year. In the legend, 0, 90, 120, 150, 180, and 210 represent different N application rates, and the unit is kg ha^{-1}*

http://www.aloki.hu ● ISSN 1589 1623 (Print) ● ISSN 1785 0037 (Online)
DOI: http://dx.doi.org/10.15666/aeer/2005_37473762

Table 5. *Effects of N application rates on yield and its components of dryland wheat in the three cropping years with different growing season precipitation levels*

Growing season type	N application rate (kg ha^{-1})	Spike number (10^4 ha^{-1})	Grain number per spike	1000-grain weight	Yield (kg ha^{-1})
Wet growing season	0	480.0 d	31.1 cd	39.6 b	4592.3 e
	90	514.0 b	30.9 d	38.9 c	4909.7 d
	120	526.5 ab	31.1 cd	39.7 b	4893.8 d
	150	536.0 a	32.3 a	39.7 b	5205.2 b
	180	539.0 a	32.5 a	40.3 a	5357.1 a
	210	499.0 c	31.4 bc	38. 9 c	4929.3 d
	Mean	515.8 ± 22.9	31.6 ± 0.7	39.5 ± 0.6	4981.2 ± 267.6
Normal growing season	0	397.8 d	31.6 bc	38.9 d	3878.3 d
	90	428.6 c	31.3 cd	38.6 e	4188.6 c
	120	441.6 bc	31.0 d	39.6 b	4296. 9 b
	150	496.1 a	32.2 a	40.0 a	4801.3 a
	180	491.2 a	31.9 ab	39.7 b	4786.6 a
	210	443.6 b	31.0 d	38.7 e	4367.6 b
	Mean	449.8 ± 37.7	31.5 ± 0.5	39.2 ± 0.6	4386.5 ± 357.2
Dry growing season	0	225.3 d	30.4 e	37.3 de	1801.9 d
	90	251.1 bc	30.7 d	37.3 de	1963.6 c
	120	246.9 c	30.2 f	37.4 d	2107.8 b
	150	268.6 a	31.6 a	39.5 a	2350.5 a
	180	265.4 ab	31.4 b	39.2 b	2316.6 a
	210	248.5 c	30.9 cd	37.2 e	2099.3 b
	Mean	251.0 ± 15.5	30.9 ± 0.6	38.0 ± 1.0	2106.6 ± 208.3
F value					
precipitation growing season (P)		16532.2**	151.6**	668.8**	48477.7**
N application rate (N)		264.7**	155.3**	227.4**	796.8**
P×N		26.4**	11.9**	32.4**	27.3**

Different letters in the same column of a given growing season indicate that the difference between treatments was significant ($P < 0.05$). * and ** denote a significant difference at 5% and 1%, respectively

Effects of N application rates on plant N accumulation and NRE of dryland wheat in the three years with different growing season precipitation levels

With an increase in the N application rate from 0 to 210 kg ha^{-1}, plant N accumulation and NRE peaked at 180 kg ha^{-1} in the wet growing season, whereas in the normal and dry growing season it peaked at 150 kg ha^{-1} (*Figure 4A and 4B*). Plant N accumulation at 180 kg ha^{-1} in the wet growing season was 9.1% higher than that at 150 kg ha^{-1}, but it was 4.1% lower than that at 210 kg ha^{-1} (*Figure 4A*). Compared to plant N accumulation, the NRE at 180 kg ha^{-1} in the wet growing season was 18.0 % higher than that at 150 kg ha^{-1}, but was 29.8% lower than that at 210 kg ha^{-1} (*Figure 4B*). In the normal and dry growing season, plant N accumulation at 150 kg ha^{-1} was at least 13.0% higher than that at 120 kg ha^{-1} (*Figure 4A*) and NRE was at least 24.8% higher (*Figure 4B*). These results indicated that the N application rate of 180 kg ha^{-1} in the wet growing season can lead to the highest plant N accumulation level and NRE, and the N application rate of 150 kg ha^{-1} can help achieve the highest plant N accumulation level and NRE in normal and dry growing season.

http://www.aloki.hu ● ISSN 1589 1623 (Print) ● ISSN 1785 0037 (Online)
DOI: http://dx.doi.org/10.15666/aeer/2005_37473762

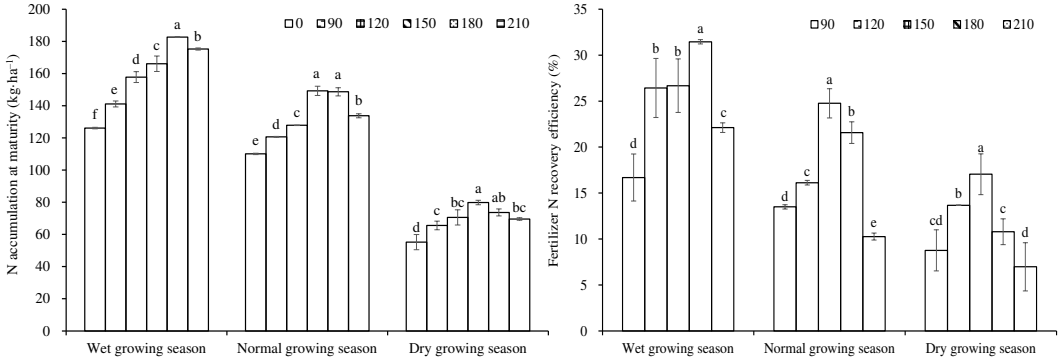

Figure 4. *Effects of N application rates on plant N accumulation (A) and fertilizer N recovery efficiency(B) of dryland wheat in the three planting years with different annual precipitation levels. Note: Error bars in the figure represent standard errors. Different letters represent a significant difference ($P < 0.05$) between the N application rates in a given year. In the legend, 0, 90, 120, 150, 180, and 210 represent different N application rates, and the unit is kg ha^{-1}*

Effects of N application rates on grain quality of dryland wheat in the three years with different growing season precipitation levels

In the three planting years, different growing season precipitation levels significantly affected the total grain protein content, protein composition, and starch content. The content of total grain protein and composition of proteins on average of all N application rates were the highest in the dry growing season followed by the normal growing season and the wet growing season (*Table 6*). In contrast, the starch content was the highest in the wet growing season followed by the normal growing season and the dry growing season (*Table 6*). The total grain protein content and protein composition peaked at 180 kg N ha^{-1} in the wet growing season (*Table 6*), whereas the total grain protein content and protein composition peaked at 150 kg N ha^{-1} in the normal and dry growing season (*Table 6*). In the wet growing season, the protein content at 180 kg N ha^{-1} was 2.5% higher than that at 150 kg N ha^{-1}, and there was no significant difference in the protein content between 180 and 210 kg N ha^{-1}. In the normal and dry growing season, at least 3.8% increase in protein content was found at 150 kg N ha^{-1} relative to that at 120 kg N ha^{-1} (*Table 6*). In contrast to protein content, the starch content in grains peaked at 180 kg N ha^{-1} in all growing season tested (*Figure 5*). The effects of N application rate and year type (based on precipitation) on the four proteins tested were similar (*Table 6*). These results indicated that higher annual precipitation can lead to more starch accumulation in grain, but lower grain protein content and protein composition. The N application rate of 180 kg ha^{-1} can result in the highest total grain protein content and protein composition in the wet growing season, whereas the N application rate of 150 kg ha^{-1} can result the highest total grain protein content and protein composition in both normal and dry growing season.

Effects of N application rates on economic returns of dryland wheat in the three years with different growing season precipitation level

Positive economic return peaked at the N application rate of 180 kg ha^{-1} in the wet growing season and at 150 kg ha^{-1} in the normal growing season. However, in the dry growing season negative returns were recorded across all N application rates (*Figure 6*). The lowest negative return was observed at the N application rate of 150 kg ha^{-1} in the

http://www.aloki.hu ● ISSN 1589 1623 (Print) ● ISSN 1785 0037 (Online)
DOI: http://dx.doi.org/10.15666/aeer/2005_37473762

dry growing season (*Figure 6*). In the wet growing season, the economic return at 180 kg N ha^{-1} was 4.6% higher than that at 150 kg N ha^{-1}, whereas it was 16% higher than that at 210 kg N ha^{-1}. In both normal and dry growing season, the economic return at 150 kg N ha^{-1} was at least 25.2% higher than that at 120 kg N ha^{-1}. These results indicated that the optimal rates of N applied can increase economic returns in normal and wet growing season and reduce the economic loss in the dry growing season.

Table 6. *Effects of N rates in three planting years with different precipitation during growth period on protein content and composition of dryland wheat*

Growing season type	N rate (kg ha^{-1})	Albumin (%)	Globulin (%)	Gliadin (%)	Glutenin (%)	Total protein content (%)
Wet growing season	0	2.18 e	1.05 d	3.21 e	3.13 e	9.57 e
	90	2.22 d	1.14 c	3.62 d	3.67 d	10.65 d
	120	2.26 c	1.19 b	3.78 c	3.92 c	11.15 c
	150	2.32 b	1.23 ab	3.92 b	4.21 b	11.68 b
	180	2.38 a	1.27 a	3.98 a	4.34 a	11.97 a
	210	2.36 a	1.25 a	3.94 b	4.32 a	11.87 a
	Mean	2.29±0.08	1.19±0.08	3.74±0.29	3.93±0.47	11.15±0.92
Normal growing season	0	2.21 e	1.21 e	4.16 e	4.34 d	11.92 f
	90	2.28 d	1.23 de	4.20 d	4.42 c	12.13 e
	120	2.31 d	1.25 cd	4.25 c	4.48 b	12.29 d
	150	2.47 a	1.33 a	4.38 a	4.59 a	12.77 a
	180	2.42 b	1.30 ab	4.32 b	4.50 b	12.54 b
	210	2.36 c	1.27 bc	4.29 b	4.51 b	12.43 c
	Mean	2.34±0.09	1.27±0.04	4.27±0.08	4.47±0.09	12.35±0.30
Dry growing season	0	2.24 d	1.42 c	4.25 d	4.24 e	13.54 f
	90	2.39 c	1.42 c	4.32 c	4.36 d	13.96 d
	120	2.38 c	1.45 bc	4.37 c	4.45 c	13.83 e
	150	2.50 a	1.53 a	4.51 a	4.66 a	14.51 a
	180	2.46 ab	1.50 a	4.45 b	4.56 b	14.18 b
	210	2.43 bc	1.46 b	4.42 b	4.51 b	14.04 c
	Mean	2.40±0.09	1.47±0.05	4.39±0.10	4.46±0.15	14.01±0.33
F value						
precipitation growing season (P)		217.0**	288.5**	2937.3**	1960.2**	15246.8**
N rate (N)		388.0**	29.9**	264.9**	528.0**	912.3**
P×N		47.8**	1.9	76.2**	149.6**	195.3**

Different letters in the same column of a given growing season indicate that the difference between treatments was significant ($P < 0.05$). * and ** denote the significant difference at 5% and 1%, respectively

Correlation analysis of water consumption and yield, grain quality, and N accumulation of dryland wheat at different growth stages under different precipitation types of N application rates

Under the condition of N application rate of 0–210 kg ha^{-1} in the wet growing season, sowing to pre-wintering, pre-wintering to jointing, and jointing to anthesis water consumption were significantly correlated with grain protein, starch content and nitrogen accumulation (*Table 7*). Jointing to anthesis water consumption was significantly correlated with spike number, grain number per spike and yield. In the normal growing season, water consumption of sowing to pre-wintering and jointing to anthesis was significantly correlated with spike number, yield, grain protein, starch content, and N accumulation. Water consumption of pre-wintering to jointing was significantly correlated with grain protein, starch content and N accumulation. In the dry growing

http://www.aloki.hu ● ISSN 1589 1623 (Print) ● ISSN 1785 0037 (Online)
DOI: http://dx.doi.org/10.15666/aeer/2005_37473762

season, water consumption of sowing to pre-wintering and pre-wintering to jointing was significantly correlated with grain starch content. Water consumption of jointing to anthesis was significantly correlated with spike number, yield, grain protein content, and N accumulation.

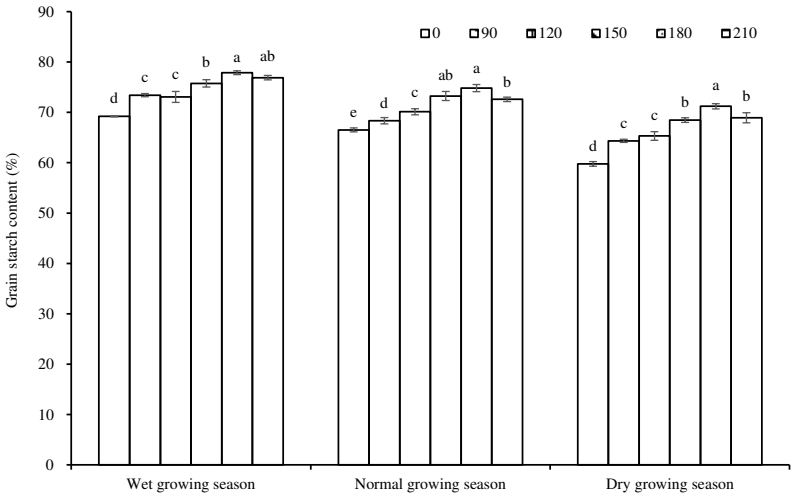

Figure 5. *Effects of N application rates on grain starch content of dryland wheat in the three planting years with different growing season precipitation levels. Note: Error bars in the figure represent standard errors. Different letters represent a significant difference ($P < 0.05$) between the N application rates in a given year. In the legend, 0, 90, 120, 150, 180, and 210 represent different N application rates, and the unit is kg ha^{-1}*

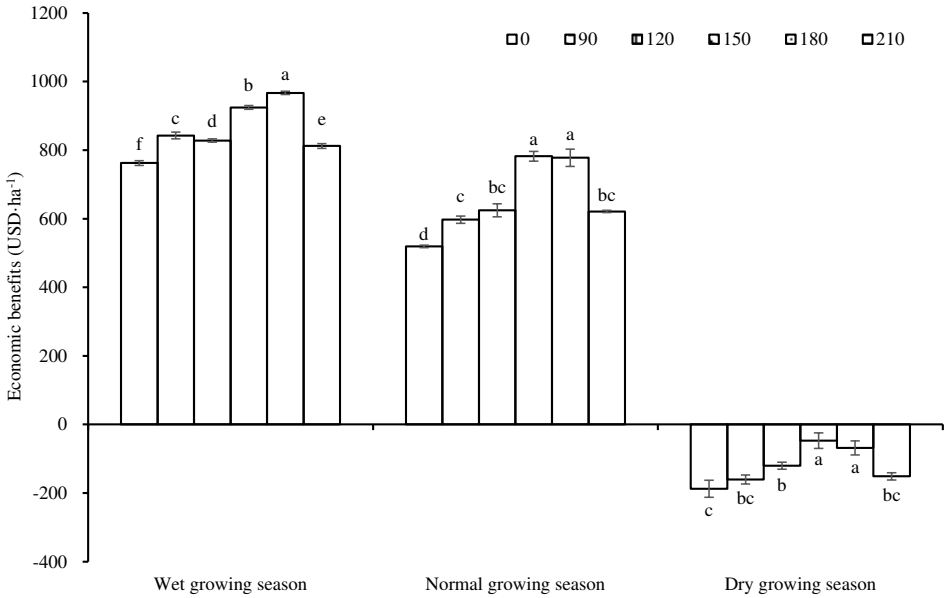

Figure 6. *Effects of N application rates on economic returns of dryland wheat in the three planting years with different growing season precipitation levels. Note: Error bars in the figure represent standard errors. Different letters represent a significant difference ($P < 0.05$) between the N application rates in a given year. In the legend, 0, 90, 120, 150, 180, and 210 represent different N application rates, and the unit is kg ha^{-1}*

http://www.aloki.hu ● ISSN 1589 1623 (Print) ● ISSN 1785 0037 (Online)
DOI: http://dx.doi.org/10.15666/aeer/2005_37473762

Table 7. *Relationship between plant water consumption and yield, grain protein content, grain starch content, and N accumulation at different growth stages*

Growing season type	Factor	SS-WS	WS-JS	JS-AS	AS-MS
Wet growing season	Spike number	0.5085	0.5001	0.8455*	-0.4119
	Grain number per spike	0.6215	0.5882	0.8833**	0.0061
	1000-grain weight	0.0844	0.0206	0.5512	0.2453
	Yield	0.7140	0.7124	0.9462**	-0.1617
	Grain protein content	0.9639**	0.9605**	0.9107**	-0.2713
	Grain starch content	0.9419**	0.9553**	0.8810**	-0.1144
	N accumulation at maturity	0.9702**	0.9585**	0.9295**	-0.0977
Normal growing season	Spike number	0.8366*	0.6818	0.8693*	0.3820
	Grain number per spike	0.3853	0.0172	0.1932	0.4971
	1000-grain weight	0.3101	0.4593	0.5472	0.3281
	Yield	0.8579*	0.7044	0.8839**	0.3936
	Grain protein content	0.8207*	0.7641*	0.8748**	0.4532
	Grain starch content	0.9278**	0.8708**	0.972**	0.5164
	N accumulation at maturity	0.8766**	0.7686*	0.9141**	0.4638
Dry growing season	Spike number	0.7008	0.6575	0.8032*	-0.3042
	Grain number per spike	0.5735	0.6464	0.6039	-0.4432
	1000-grain weight	0.5070	0.4706	0.5921	-0.2111
	Yield	0.8103*	0.7130	0.9104**	-0.4026
	Grain protein content	0.6252	0.6055	0.7453	-0.2983
	Grain starch content	0.9575**	0.9318**	0.9632**	-0.7060
	N accumulation at maturity	0.7236	0.6104	0.8694*	-0.2669

SS-WS, the period from sowing to pre-wintering. WS-JS, the growth period from pre-wintering to jointing. JS-AS, the period from jointing to anthesis. AS-MS, the period from anthesis to maturity. * and ** denote a significant difference at 5% and 1%, respectively

Discussion

Optimal N application rates for high yield vary among the years with different growing season precipitation levels

As the growing season precipitation varied in the three cropping years studied, the optimal N application rates were also different among these years (*Table 2*). In the wet growing season, the optimal N application rate for high yield was 180 kg ha^{-1}, whereas 150 kg ha^{-1} ensured the high yield in normal and dry growing season (*Table 5*). The application of 180 kg N ha^{-1} in the wet growing season could increase the yield by 2.9% relative to that of 150 kg N ha^{-1}, and the application of 150 kg N ha^{-1} in normal and dry growing season could increase the yield by at least 11.4% relative to that of 120 kg N ha^{-1} (*Table 5*). The increase in the yield is most likely correlated to the increased water consumption, due to the optimal N amounts, at jointing anthesis stage, which promotes the development of tillers, thereby increases the number of panicles per unit area (*Table 4*). The optimal rates fertilization in different precipitation years can also reduce production costs (*Figure 4*) and environmental pollution Noor et al. (2022). The higher yield and lower production cost can boost economic return (*Fig. 4*). Liu et al. (2019) reported that the highest grain yield and higher economic returns and environmental benefits can be achieved at the optimal N application rate.

http://www.aloki.hu ● ISSN 1589 1623 (Print) ● ISSN 1785 0037 (Online)
DOI: http://dx.doi.org/10.15666/aeer/2005_37473762

Optimal N application rates under different annual precipitation levels improve grain quality in dryland wheat production

Our results showed that increasing N up to the optimal rate enhanced the total grain protein content and protein composition in all years studied regardless of growing season precipitation level (*Table 6*). In the wet growing season, the application of 180 kg N ha^{-1} could increase the grain protein content by 2.5% relative to 150 kg N ha^{-1}, and the application of 150 kg N ha^{-1} in both normal and dry growing season could increase grain protein content by at least 3.8% relative to 120 kg N ha^{-1} (*Table 6*). Similar to grain protein content, the starch content in grain was enhanced with increasing N up to the optimal rates in both wet and normal growing season (*Figure 3*). Optimal N application increased the water consumption of SS-WS, WS-JS, JS-AS plants, resulting in increased grain protein and starch content (*Table 7*). In the wet growing season, the higher starch content in grain was associated with the lower content of grain protein, whereas in the dry growing season, the lower starch content in the grain was associated with the higher content of grain protein (*Table 6 and Figure 3*). This is a result of the "dilution effect"; as the grain protein content is relatively constant, an increase in grain starch content reduces the grain protein content (Eser et al., 2020). In addition, the content of grain protein in dry and normal growing season was higher than that in the wet growing season (*Table 6*). A higher grain content results in not only a higher market price, leading to a higher economic return (Alghory et al., 2018), but also a higher nutritional value for human consumption (Farinde et al., 2021).

Optimal N application rates for different precipitation growing season maximizes WUE and NUE for sustainable wheat production in dryland

The optimal N application rate in the normal and dry growing season led to the highest WUE (*Figure 1*). However, in the wet growing season, the optimum N application rate resulted in the highest yield and water consumption during the growing period of crops t, but the highest WUE was not achieved. The optimal N application rates under different precipitation conditions could also increase NRE (*Figure 2B*) by at least 18.0% relative to the lower N application rate (*Figure 2*). When the higher rate (210 kg N ha^{-1} in the wet growing season or 180 kg N ha^{-1} in the normal and dry growing season) was applied, NRE was reduced by 12.9%–36.8% (*Figure 2*). Excess N fertilization results in the accumulation of residual N in the soil (Noor et al., 2021). The residual N could be lost due to runoff, erosion, and leaching, or through denitrification and volatilization (Habbib et al., 2017), leading to environmental pollution. The rational application of N fertilizer based on annual precipitation improves WUE and NRE, making wheat production sustainable in the dryland in the Loess Plateau.

The annual precipitation levels fluctuate considerably in the Loess Plateau, as observed in this study and that by Yang et al. (2021). Precipitation is also unevenly distributed within a year. Summer rainfall accounts for approximately 60% of yearly precipitation (Ren et al., 2019). The amount of soil water stored at sowing stage could be used as a guide for applying the basal amount of fertilizer. Additional N fertilization as top dressing could be applied when rainfall is higher than expected in the growth season. The implementation of this "basal and top dressing" strategy based on monitoring the progression of seasonal rainfall can further improve the yield, grain quality, NUE, WUE, and the farmers' profitability in wheat production.

http://www.aloki.hu ● ISSN 1589 1623 (Print) ● ISSN 1785 0037 (Online)
DOI: http://dx.doi.org/10.15666/aeer/2005_37473762

Conclusions

When the N application rate was 180 kg ha^{-1} in a wet growing season, compared with other N application rates, the jointing to anthesis water consumption increased along with the total water consumption, the spike number and yield, and the NRE, while the protein content and starch content of the grain increased at the same time, thus the economic benefit increased. When the combined N application rate of dryland wheat was 150 kg ha^{-1} in the normal and dry growing season, compared with other N application rates, the jointing to anthesis water consumption, total water consumption, spike number at maturity, and yield all increased, the WUE and NRE improved, and the protein content of the grain also increased, ultimately increasing the economic benefits. In summary, the optimal N application rate varies with the annual precipitation. The recommended N application rate is 180 kg ha^{-1} in the wet growing season and 150 kg ha^{-1} in the normal and dry growing season. The optimal N application rate in different precipitation growing seasons can improve the growth period water consumption, yield, WUE, NRE, and grain quality, resulting in economic benefits for the farmers of dryland wheat.

Acknowledgements. The authors would like to thank the Shanxi Agricultural University and State Key Laboratory of Sustainable Dryland Agriculture for providing all the means needed to carry out this project.

REFERENCES

[1] Alghory, A., Yazar, A. (2018): Evaluation of net return and grain quality characteristics of wheat for various irrigation strategies under the Mediterranean climatic conditions. – Agric Water Manag. 203: 395-404.

[2] Cao, H., Wang, Z., He, G., Dai, J., Huang, M., Wang, S., Luo, L., Sadras, V. O., Malhi, S. S. (2017): Tailoring NPK fertilizer application to precipitation for dryland winter wheat in the Loess Plateau. – Field Crops Research 209: 88-95.

[3] Coskun, D., Britto, D. T., Shi, W., Kronzucker, H. J. (2017): Nitrogen transformations in modern agriculture and the role of biological nitrification inhibition. – Nature Plants 3(6): 17074.

[4] Dong, Z., Zhang, X., Li, J., Zhang, C., Wei, T., Yang, Z., Cai, T., Zhang, P., Ding, R., Jia, Z. (2019): Photosynthetic characteristics and grain yield of winter wheat (*Triticum aestivum* L.) in response to fertilizer, precipitation, and soil water storage before sowing under the ridge and furrow system: A path analysis. – Agric for Meteorol. 272-273: 12-19. doi:10.1016/j.agrformet.2019.03.015.

[5] Duc-Anh, A., Shahbaz, M., Zheng, B., Christopher, J. T., Chapman, S. C., Chenu, K. (2018): Direct and Indirect Costs of Frost in the Australian Wheatbelt. – Ecol Econ. 150: 122-136. doi:10.1016/j.ecolecon.2018.04.008.

[6] Eser, A., Kassai, K. M., Kato, H., Kunos, V., Tarnava, A., Jolankai, M. (2020): Impact of nitrogen topdressing on the quality parameters of winter wheat (*Triticum aestivum* L.) yield. – Acta Aliment 49: 244-253.

[7] Farinde, E. O., Dauda, T. O., Obatolu, V. A. (2021): Heteroscedasticity analysis of nixtamalization effect on nutrients, digestibility, and functional properties of quality protein maize and indigenous local maize flour. – Journal of Food Processing and Preservation 45(4): e15303.

[8] Habbib, H., Hirel, B., Verzeaux, J., Roger, D., Lacoux, J., Lea, P., Dubois, F., Tétu, T. (2017): Investigating the combined effect of tillage, nitrogen fertilization and cover crops on nitrogen use efficiency in winter wheat. – Agronomy 7(4): 66. doi:10.3390/agronomy7040066.

http://www.aloki.hu ● ISSN 1589 1623 (Print) ● ISSN 1785 0037 (Online)
DOI: http://dx.doi.org/10.15666/aeer/2005_37473762

[9] Hu, Y., Hao, D., Wang, Z., Fu, W. (2017): Effect of long-term fertilization on winter wheat yield from the dry land under different precipitation patterns. – Journal of applied ecology 28(01): 135-141. doi: 10.13287/j.1001-9332.201701.016.
[10] Jiang, C., Wang, F., Zhang, H., Dong, X. (2016): Quantifying changes in multiple ecosystem services during 2000–2012 in the Loess Plateau, China, as a result of climate variability and ecological restoration. – Ecological Engineering 97: 258-271. doi: 10.1016/j.ecoleng.2016.10.030.
[11] Lai, X., Yang, X., Wang, Z., Shen, Y., Ma, L. (2022): Productivity and water use in forage-winter wheat cropping systems across variable precipitation gradients on the Loess Plateau of China. – Agricultural Water Management 259: 107250.
[12] Lehnert, N., Musselman, B. W., Seefeldt, L. C. (2021): Grand challenges in the nitrogen cycle. – Chemical Society Reviews 50(6): 3640-3646.
[13] Li, Y., Huang, G., Chen, Z., Xiong, Y., Huang, Q., Xu, X., Huo, Z. (2022): Effects of irrigation and fertilization on grain yield, water and nitrogen dynamics and their use efficiency of spring wheat farmland in an arid agricultural watershed of Northwest China. – Agricultural Water Management 260: 107277. doi: 10.1016/j.agwat.2021.107277.
[14] Liu, H., Wang, Z. H., Yu, R., Li, F. C., Li, K. Y., Cao, H. B., Yang, M. H. (2016): Optimal nitrogen input for higher efficiency and lower environmental impacts of winter wheat production in China. – Agric Ecosyst Environ. 224: 1-11. doi: 10.1016/j.agee.2016.03.022.
[15] Liu, Z., Yu, N., Camberato, J. J., Gao, J., Liu, P., Zhao, B., Zhang, J. (2019): Crop production kept stable and sustainable with the decrease of nitrogen rate in North China Plain: An economic and environmental assessment over 8 years. – Sci Rep 9: 19335.
[16] Liu, X., Dong, W., Jia, S., Liu, Q., Li, Y., Hossain, M. E., Liu, E., Kuzyakov, Y. (2021): Transformations of N derived from straw under long-term conventional and no-tillage soils: A 15N labelling study. – Science of The Total Environment 786: 147428. doi: 10.1016/j.scitotenv.2021.147428.
[17] Mon, J., Bronson, K., Hunsaker, D., Thorp, K., White, J., French, A. (2016): Interactive effects of nitrogen fertilization and irrigation on grain yield, canopy temperature, and nitrogen use efficiency in overhead sprinkler irrigated durum wheat. – Field Crops Research 191: 54-65.
[18] Noor, H., Wang, Q., Sun, M., Lin, W., Ren, A. X., Feng, Y., Yu, S. B., Ding, P. C., Gao, Z. Q. (2021): Effects of sowing methods and nitrogen rates on photosynthetic characteristics, yield and quality of winter wheat. – Photosynthetica 59(2): 277-285.
[19] Noor, H., Sun, M., Lin, W., Gao, Z. (2022): Effect of Different Sowing Methods on Water Use Efficiency and Grain Yield of Wheat in the Loess Plateau, China. – Water 14: 577.
[20] Raymbek, A., Saunikov, E., Kenenbayev, S., Ramazanova, S. (2017): Protein content changes in wheat grain as influenced by nitrogen fertilization. – Agrochimica –Pisa 61: 180-189. doi:10.12871/00021857201732.
[21] Ren, X., Zhang, P., Chen, X., Guo, J., Jia, Z. (2016): Effect of different mulches under rainfall concentration system on corn production in the semiarid areas of the Loess Plateau. – Sci Rep 6: 19019. doi:10.1038/srep19019.
[22] Ren, A., Sun, M., Xue, L., Deng, Y., Wang, P., Lei, M., Xue, J., Lin, W., Yang, Z., Gao, Z. (2019): Spatiotemporal dynamics in soil water storage reveals effects of nitrogen inputs on soil water consumption at different growth stages of winter wheat. – Agricultural Water Management 216: 379-389. doi:10.1016/j.agwat.2019.01.023.
[23] Ren, J., Ren, A. X., Lin, W., Noor, H., Khan, S., Dong, S. F., Sun, M., Gao, Z. Q. (2021): Nitrogen fertilization and precipitation affected wheat nitrogen use efficiency and yield in the semiarid region of the Loess Plateau in China. – J Soil Sci Plant Nutr. 2021: 285. doi:10.1007/s42729-021-00671-1.
[24] Rui, W., Ying, W., Hu, Y., Dang, T., Guo, S. (2021): Divergent responses of tiller and grain yield to fertilization and fallow precipitation: Insights from a 28-year long-term experiment in a semiarid winter wheat system. – Journal of Integrative Agriculture 20(11): 3003-3011. doi: 10.1016/S2095-3119(20)63296-8.

http://www.aloki.hu ● ISSN 1589 1623 (Print) ● ISSN 1785 0037 (Online)
DOI: http://dx.doi.org/10.15666/aeer/2005_37473762

[25] Sadras, V. O., Lawson, C. (2012): Nitrogen and water use efficiency of Australian wheat varieties released between 1958 and 2007. – Eur J Agron 46: 34-41. doi: 10.1016/j.eja.2012.11.008.
[26] Sun, L., Wang, R., Li, J., Wang, Q., Lyu, W., Wang, X., Cheng, K., Zhang, X. (2019): Reasonable fertilization improves the conservation tillage benefit for soil water use and yield of rainfed winter wheat: a case study from the Loess Plateau. – Field Crops Research 242: 107589. doi: 10.1016/j.fcr.2019.107589.
[27] Van Grinsven, H. J. M., Ebanyat, P., Glendining, M., Gu, B., Hijbeek, R., Lam, S. K., Lassaletta, L., Mueller, N. D. (2022): Establishing long-term nitrogen response of global cereals to assess sustainable fertilizer rates. – Nature Food 3(2): 122-132.
[28] Wang, L., Palta, J. A., Chen, W., Chen, Y. L., Deng, X. P. (2018): Nitrogen fertilization improved water use efficiency of winter wheat through increasing water use during vegetative rather than grain filling. – Agric Water Manag 197: 41-53. doi:10.1016/j.agwat.2017.11.010.
[29] Wang, X., Wang, B., Xu, X. (2019): Effects of largescale climate anomalies on trends in seasonal precipitation over the Loess Plateau of China from 1961 to 2016. – Ecological Indicators 107: 105643. doi:10.1016/j.ecolind.2019.105643.
[30] Wang, B., Guo, C., Wan, Y., Li, J., Ju, X., Cai, W., You, S., Qin, X., Wilkes, A., Li, Y. (2019): Air warming and CO2 enrichment increase N use efficiency and decrease N surplus in a Chinese double rice cropping system. – Sci Total Environ 19: 136063. doi:10.1016/j.scitotenv.2019.136063.
[31] Xia, L., Ti, C., Li, B., Xia, Y., Yan, X. (2016): Greenhouse gas emissions and reactive nitrogen releases during the life-cycles of staple food production in China and their mitigation potential. – Science of the Total Environment 556: 116-125.
[32] Xu, X., He, P., Wei, J., Cui, R., Sun, J., Qiu, S. (2021): Use of controlled-release urea to improve yield, nitrogen utilization, and economic return and reduce nitrogen loss in wheat maize crop rotations. – Agronomy Basel 11(4): 723.
[33] Yang, Y., Li, M., Wu, J., Pan, X., Gao, C., Tang, D. W. S. (2021): Impact of Combining Long-Term Subsoiling and Organic Fertilizer on Soil Microbial Biomass Carbon and Nitrogen, Soil Enzyme Activity, and Water Use of Winter Wheat. – Frontiers in Plant Science 12: 788651-788651.
[34] Yu, S., Khan, S., Mo, F., Ren, A., Lin, W., Feng, Y., Dong, S., Ren, J. (2021): Determining optimal nitrogen input rate on the base of fallow season precipitation to achieve higher crop water productivity and yield. – Agricultural Water Management 246: 106689.
[35] Zhang, H., Yu, X., Jin, Z., Zheng, W., Zhai, B., Li, Z. (2017): Improving grain yield and water use efficiency of winter wheat through a combination of manure and chemical nitrogen fertilizer on the Loess plateau, China. – Journal of Soil Science & Plant Nutrition 17(2): 461-474.

http://www.aloki.hu ● ISSN 1589 1623 (Print) ● ISSN 1785 0037 (Online)
DOI: http://dx.doi.org/10.15666/aeer/2005_37473762

APPROPRIATE SUBSURFACE DRIP IRRIGATION DEPTH CAN IMPROVE THE PHOTOSYNTHETIC CAPACITY AND INCREASE THE ECONOMIC COEFFICIENT OF COTTON WITHOUT PLASTIC MULCHING

DUAN, J.[1#] – WANG, G.[2#] – WANG, J.[2] – HAO, X.[2] – LUO, H.[1*] – YANG, G.[3*]

[1]*College of Agronomy, Shihezi University, Shihezi, Xinjiang 832000, China*

[2]*Xinjiang Academy of Agricultural Reclamation Sciences, Shihezi, Xinjiang 832000, China*

[3]*College of Plant Science and Technology, Huazhong Agricultural University, Wuhan, Hubei 430070, China*

[#]*These authors contributed equally to this work.*

[*]*Corresponding authors*
e-mail: luohonghai@shzu.edu.cn, ygzh9999@mail.hzau.edu.cn
phone: +86-133-4546-6760; +86-139-9555-3884

(Received 7th Mar 2022 ; accepted 20th Jun 2022)

Abstract. Residual film pollution in fields is the main problem affecting the sustainable development of agriculture. Cultivation without plastic mulching is the best way to reduce the accumulation of residual film. Therefore, we investigated the effects of three depths of embedded drip irrigation belts (10 cm, 15 cm and 20 cm) on the photosynthetic traits and yield of cotton without plastic mulching. From Biologische Bundesanstalt, Bundessortenamt and Chemical industry (BBCH) 65 to 75, the cotton leaf area of the 10 cm and 15 cm treatments decreased by 45.0% and 25.4%, respectively, while the cotton leaf area of the 20 cm treatment increased by 8.3%. With increasing depth, the SPAD value, net photosynthetic rate, intercellular CO_2 concentration, transpiration rate, stomatal conductance, quantum efficiency of PSII, electron transport rate, photochemical quenching coefficient and maximal quantum yield of PSII photochemistry increased. Compared with the 10 cm and 15 cm treatments, the biological yield of the 20 cm treatment was 51% and 33% higher, and the seed cotton yield was 15% and 2% highter, but the economic coefficient was 24%, lower. Hence, 15 cm is the optimum depth to enhance the photosynthetic capacity and ensure the maximum economic coefficient of cotton without plastic mulching.
Keywords: *diffused pollution, growth, photosynthesis, localized irrigation, yield*

Introduction

Cotton is an important fiber and oil crop worldwide (Constable and Bange, 2015). China is one of the world's major cotton producers (Wang et al., 2020). Film mulching technology has made an important contribution to the development of the cotton industry in Xinjiang, the most important high-quality cotton production base in China (Li et al., 2004; He et al., 2018). However, the promotion and use of plastic mulching have not only brought huge economic benefits but have also contributed to residual film pollution in cotton fields, seriously affecting seedling emergence and the development of the root system of cotton, and thus reducing cotton yield. Therefore, preventing and/or controlling residual film pollution is a matter of great urgency (Zhang et al., 2016; Gao et al., 2019). Compared with degradable plastic film mulching and plastic film recovery, cultivation without plastic mulching is the most direct and effective way to reduce the accumulation of residual film.

http://www.aloki.hu ● ISSN 1589 1623 (Print) ● ISSN1785 0037 (Online)
DOI: http://dx.doi.org/10.15666/aeer/2005_37633777

Due to the loss of the beneficial effects of mulching film, including increasing the temperature and preserving moisture, cotton in fields without plastic mulching is faced with problems such as a delayed sowing date, evaporation of soil water and yield reduction. Based on previous studies, we assumed that the above problems can be solved by using early-maturing cotton cultivars, reasonable chemical regulation and increasing sowing density under subsurface drip irrigation (Dong et al., 2005; Chen et al., 2018). Subsurface drip irrigation technology can effectively control the retention of irrigation water in the root zone of crops via drip irrigation belts embedded in the soil (Ayars et al., 2015). Compared with traditional surface drip irrigation, subsurface drip irrigation can significantly improve the water use efficiency and yield of cotton in drought regions (Kalfountzos et al., 2006; Çetin et al., 2021).

Improving photosynthetic performance is of great significance for improving cotton production potential. The key to improving the photosynthetic capacity of cotton without plastic mulching is to optimize the spatial distribution of soil water. The main factors affecting soil water movement include the soil texture, depth of the embedded drip irrigation belt, irrigation amount and drip hole flow under subsurface drip irrigation (Amali et al., 1997). In recent years, many researchers have carried out studies on the characteristics of soil water and salt transport, the arrangement of drip irrigation belts, irrigation quotas and irrigation frequency under subsurface drip irrigation and have proposed reasonable irrigation systems and cultural practices (Grabow et al., 2006; Elmaloglou and Diamantopoulos, 2013; Yao et al., 2021). Since subsurface drip irrigation achieves water conservation through the soil layer above the drip irrigation belt and the depth of the embedded drip irrigation belt has a significant effect on soil water transport and crop water absorption and utilization (Guo et al., 2020), it is important to explore the influence of the embedded belt depth on crop growth and the underlying mechanisms. Khalilian et al. (2000) noted that the embedded depth of a drip irrigation belt had an effect on cotton yield. Chen (2017) found that when the drip irrigation belt is embedded in an appropriate position, it can not only meet the normal water demand of crops but can also significantly reduce soil evaporation and inhibit the growth of weeds.

However, there are few studies on the effects of different depths of embedded drip irrigation belts on the photosynthetic characteristics and yield of cotton without plastic mulching. Therefore, the purpose of the study was to determine the responses of the relative water content of cotton leaves, leaf area, leaf mass per area, SPAD value, chlorophyll fluorescence parameters, gas exchange parameters and yield to three different embedded belt depth treatments using a Xinjiang self-bred early-maturing cotton cultivar, Xinluzao 74 (*Gossypium hirsutum* L.), and adopting the same row spacing cultivation mode of 76 cm without plastic mulching. This study also included correlation analysis of photosynthetic characteristics and yield to provide a theoretical basis and technical support for high-efficiency production of cotton without plastic mulching in Xinjiang.

Materials and methods

Experimental site and cultivar

The experiments were conducted at the Shihezi Experimental Observation Station of Crop Water Efficiency, Ministry of Agriculture/Soil and Water Institute of Xinjiang Academy of Agricultural Reclamation Sciences, Shihezi, Xinjiang, China (86°09’ E, 45°38’ N) from April to October 2019. The average altitude of this area is 430 m. The texture of the soil at the experimental site is loam, and the soil had the following initial

http://www.aloki.hu ● ISSN 1589 1623 (Print) ● ISSN1785 0037 (Online)
DOI: http://dx.doi.org/10.15666/aeer/2005_37633777

characteristics: 7.86 pH, 23 g kg^{-1} organic matter, 29 mg kg^{-1} available phosphorus, and 174 mg kg^{-1} available potassium in the 0−20 cm layer. The average bulk density from 0−100 cm was 1.40 g cm^{-3}, the field capacity was 24.0%, and the groundwater depth was less than 10 m. During the growing period, the total precipitation was 98.2 mm, with 7 events with an effective precipitation greater than 5 mm. From May 1 to August 31, the daily mean maximum temperature was 30.9°C, and the daily mean minimum temperature was 16.2°C. The daily mean temperature from April to October was 18.7°C. The meteorological indexes during the growing period of 2019 at the experimental site were all at the average levels for the past decade. Xinluzao 74 (*Gossypium hirsutum* L.), an early-maturing cotton cultivar, was used in the experiment and was provided by the Cotton Research Institute of Shihezi Academy of Agricultural Sciences (the growth period is 120 days, the prefrost flowering rate is highter than 95%, and the cultivar's strong growth potential and stress resistance are suitable to allow machine picking).

Experimental design and management

The experiments were conducted in a randomized block design with three different embedded belt depth treatments (Li et al., 2017): D_1 (10 cm), D_2 (15 cm), and D_3 (20 cm). The plot size was 45.6 m^2 (10 m × 4.56 m), with three replications. An anti-siphon dripline (*DripNet*, *Netafim*, Israel) was adopted, with an emission rate of 1.0 L h^{-1}, and the drop head spacing was 30 cm. Drip irrigation belts were laid with a spacing of 1.52 m with one drip irrigation belt covering two rows. The total irrigation amount was 262.5 mm (Liu, 2006) (*Table 1*).

Table 1. *Irrigation cycles and irrigation amount*

Date	Irrigation amount [mm]		
	D_1	D_2	D_3
06-15	18.0	18.0	18.0
06-22	18.0	18.0	18.0
06-29	18.0	18.0	18.0
07-01	21.0	21.0	21.0
07-03	21.0	21.0	21.0
07-05	21.0	21.0	21.0
07-09	24.0	24.0	24.0
07-15	24.0	24.0	24.0
07-21	27.0	27.0	27.0
07-27	27.0	27.0	27.0
08-07	21.0	21.0	21.0
08-20	15.0	15.0	15.0
08-30	7.5	7.5	7.5
Total	262.5	262.5	262.5

Seeds were sown 38 cm from the horizontal drip irrigation belt on 3 May 2019, 2.0–3.0 cm deep and with a 76 cm equal row spacing. Pendimethalin (2700~3000ml ha^{-1}) was sprayed evenly on the soil on 26 April for weed control. After sowing, irrigation was carried out twice, with 15.0 mm each time. Seedlings were thinned to 5 cm after cotyledon flattening to maintain a planting density of 265,000 plants ha^{-1}. The basal fertilizers were urea (N 46%, mass fraction, the same below) applied at 150 kg ha^{-1} and phosphate fertilizer (P_2O_5 45%) applied at 225 kg ha^{-1}. Urea (N 46%; 525 kg ha^{-1}; the ratio for the

http://www.aloki.hu ● ISSN 1589 1623 (Print) ● ISSN1785 0037 (Online)
DOI: http://dx.doi.org/10.15666/aeer/2005_37633777

seedling, budding, flowering and boll-setting stages was 1:4:5) and potassium dihydrogen phosphate (P_2O_5 52%, K_2O 34%; 150 kg ha^{-1}; the ratio at the budding, flowering and boll-setting stages was 4:6) were applied with water throughout the whole growth period. Disease and insect control was carried out three times, in the full bud stage (late June), in the full flowering stage (mid-July) and in the full boll stage (late July). The initial application consisted of acetamiprid (0.22 kg ha^{-1}) and abamectin etoxazole (0.32 kg ha^{-1}). The second application consisted of acetamiprid (0.27 kg ha^{-1}) and abamectin etoxazole (0.18 kg ha^{-1}). The third application consisted of nitenpyram pymetrozine (0.46 kg ha^{-1}), acetamiprid (0.46 kg ha^{-1}), abamectin (0.23 kg ha^{-1}) and emamectin benzoate (0.46 kg ha^{-1}). A defoliation/ripening agent (thidiazuron, 195 ml ha^{-1}; ethephon, 1380 ml ha^{-1}) was sprayed on 22 September. The second application (ethephon, 870 ml ha^{-1}) was carried out on 8 October. Other field management practices were conducted according to local practices (*Figure 1*).

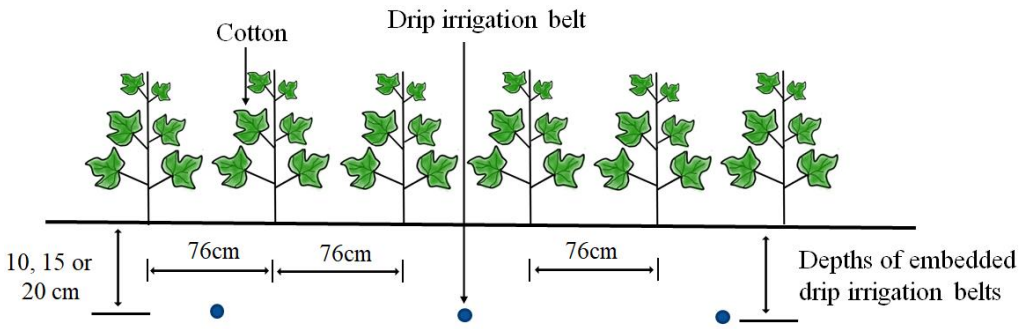

Figure 1. *Schematic diagram of the planting mode at the experimental site*

Leaf area

The proportion method was used to measure the whole leaf area of cotton (Shi, 2012). In Biologische Bundesanstalt, Bundessortenamt and Chemical industry (BBCH) stages 52 (1st floral bud detectable ('match-head square')), 61 (beginning of flowering ('early bloom'): 5-6 blooms/7.5 meter of row), 65 (main phase of flowering ('mid bloom'): 11 or more blooms/7.5 meter of row) and 75 (approximately 50% of bolls have attained their final size) (Munger, 1998), a 6-mm-hole punch was used to remove 40 small round pieces from all leaves of each plant, and these pieces were put into craft paper bags and weighed after oven drying at 105°C for 30 min followed by drying at 80°C to a constant weight. The leaf area of a whole plant was determined as follows:

$$\text{Leaf area of a whole plant} = \frac{\text{dry leaf weight of the whole plant} \times \text{circular leaf area}}{\text{circular dry weight}} \quad \text{(Eq.1)}$$

Leaf relative water content

The relative water content of the functional leaves of the cotton main stem (fourth or third leaf from the top) was measured at BBCH 52, 61, 65 and 85 (approximately 50% of bolls open). Five round pieces were collected using a hole punch to avoid leaf veins, and the fresh weight (FW) was determined by weighing; the process was repeated 4 times. The round pieces were immersed in distilled water for 24 h to saturate the tissue with water. The material was removed from the distilled water, absorbent paper was used to

http://www.aloki.hu ● ISSN 1589 1623 (Print) ● ISSN1785 0037 (Online)
DOI: http://dx.doi.org/10.15666/aeer/2005_37633777

absorb the surface moisture, and the saturated fresh weight (SFW) was determined by weighing. Then the samples were placed in water for 1 h, and the SFW was determined again. The materials were dried in an oven at 105°C for 30 min followed by drying at 80°C to a constant weight for dry weight (DW) determination. The relative water content (RWC) was calculated as follows:

$$\mathrm{RWC} = \frac{\mathrm{FW-DW}}{\mathrm{SFW-DW}} \times 100\% \quad \text{(Eq.2)}$$

Leaf mass per area

At BBCH 52, 61, 65, 75 and 79 (approximately 90% of bolls attained their final size), a 6 mm hole punch was used to remove 5 small round pieces from the functional leaves of the cotton (fourth or third leaf from the top), and these pieces were put into craft paper bags and dried in an oven at 105°C for 30 min followed by drying at 80°C to a constant weight and were then weighed. The specific leaf weight was calculated as follows:

$$\text{Leaf mass per area} = \frac{\text{circular dry weight}}{\text{circular leaf area}} \quad \text{(Eq.3)}$$

Leaf SPAD value

Four plants with uniform growth from each treatment group were selected at BBCH 52, 61, 65, 75 and 79. The chlorophyll (SPAD) concentrations of the main stem functional leaves were measured by a SPAD instrument (*SPAD-502Plus, KONICA MINOLTA*, Chiyoda-ku, Tokyo, Japan) from 10:00 to 11:00 on the same day, and the average value of five points measured per leaf was calculated.

Leaf gas exchange

The net photosynthetic rate (P_N), stomatal conductance (g_s), intercellular CO_2 concentration (C_i) and transpiration rate (E) of the functional leaves (fourth or third leaf from the top) of cotton with good growth were measured at BBCH 52, 61, 65, 75 and 79 by using an open-type photosynthetic measurement system (*LI-6800*, *LI-COR*, Lincoln, NE, USA) with steady light intensity (1800 μmol m^{-2} s^{-1}), and the temperature was controlled to 32°C. The ambient CO_2 concentration was basically stable at 400 μmol mol^{-1}, and the relative humidity was 30~32%. Each treatment was measured 4 times.

Chlorophyll fluorescence parameters

The chlorophyll fluorescence parameters of the functional leaves of the main stem were measured at BBCH 52, 61, 65, 75 and 79 using a pulse-amplitude modulation portable fluorometer (*Mini-PAM*, *Heinz Walz GmbH*, Effeltrich, Germany). The measurement indexes included the maximal quantum yield of PSII photochemistry (F_v/F_m), quantum efficiency of PSII (Y_{II}), electron transport rate (ETR), photochemical quenching coefficient (q_P) and nonphotochemical quenching coefficient (NPQ).

http://www.aloki.hu ● ISSN 1589 1623 (Print) ● ISSN1785 0037 (Online)
DOI: http://dx.doi.org/10.15666/aeer/2005_37633777

Economic coefficient

The middle section of each plot was designated (2×1.52) m^2 as the test production area at BBCH 85 (130 days after seedling emergence), and the yield was calculated according to the actual harvest yield. At the same time, four plants with uniform growth were selected in each treatment group. Samples were taken from 6 tissues, i.e., leaves, stems, roots, buds, flowers and bolls, put into craft paper bags, and dried in an oven at 105°C for 30 min followed by drying at 80°C to a constant weight. The dry weight was measured to calculate the biological yield. The economic coefficient was calculated as follows:

$$\text{Economic coefficient} = \frac{\text{seed cotton yield}}{\text{biological yield}} \quad \text{(Eq.4)}$$

Statistical analysis

The experiment was laid out in a randomized block design with three different embedded belt depth treatments: D_1 (10 cm), D_2 (15 cm) and D_3 (20 cm). The plot size was 10 × 4.56 m^2 with three replications. *Microsoft Excel 2010* and *SigmaPlot 14.0* (*Systat Software Inc*., San Jose, CA, USA) were employed for data processing and drawing the figures, respectively. *SPSS 23* (*SPSS Inc*., Chicago, IL, USA) was used for one-way analysis of variance (ANOVA). The significance of differences between the treatment means was determined using Duncan's test at the $P < 0.05$ level in the same period.

Results

Leaf area and leaf mass per area

The experimental results (*Figure 2*) showed that from BBCH 52 to 75, the cotton leaf area in the D_1 and D_2 treatments first increased and then decreased. From BBCH 65 to 75, the cotton leaf area in the D_1 and D_2 treatments decreased by 45.0% and 25.4%, respectively, while that in the D_3 treatment increased by 8.3%.

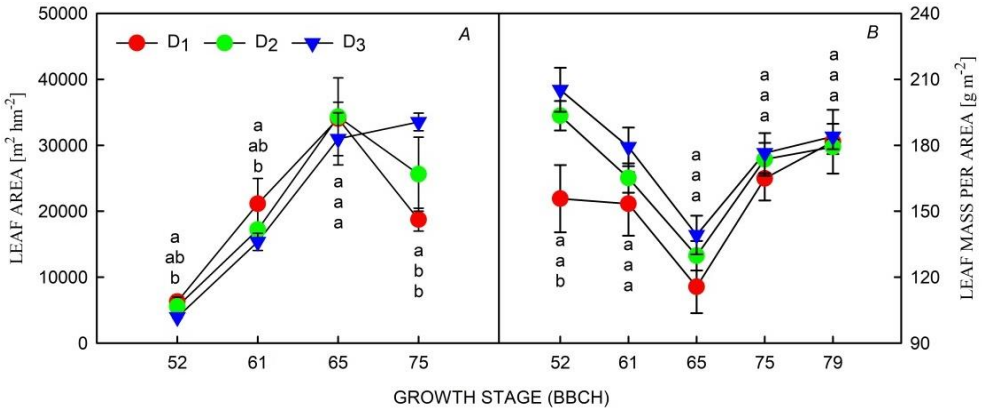

Figure 2. *Effect of the embedded drip irrigation belt depth on the leaf area and leaf mass per area of cotton at BBCH 52, 61, 65, 75 and 79. The treatments D_1, D_2 and D_3 represent embedded belt depths of 10, 15 and 20 cm, respectively. Error bars show the standard error (SE) of the means. Different lowercase letters in the figure indicate statistical significance at the P = 0.05 level within the same stage. Leaf SPAD values and relative water contents*

http://www.aloki.hu ● ISSN 1589 1623 (Print) ● ISSN1785 0037 (Online)
DOI: http://dx.doi.org/10.15666/aeer/2005_37633777

The depth of the embedded drip irrigation belt had an effect only on the leaf mass per area at BBCH 52, with values 24.2% and 31.8% higher in the respective D_2 and D_3 treatments than in the D_1 treatment.

The study showed that the depth of the embedded drip irrigation belt had a significant impact on the SPAD at BBCH 52, 61 and 79 (*Figure 3*). The greater embedded belt depth under D_3 resulted in a significantly higher SPAD value than that under D_1, and D_2 was significantly different from D_3 only at BBCH 61.

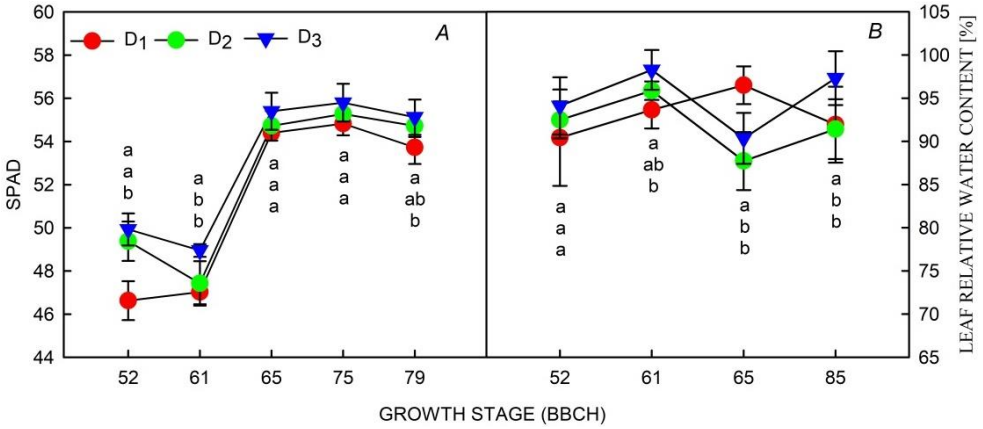

Figure 3. *Effect of embedded drip irrigation belt depth on the SPAD value and relative water content of cotton at BBCH 52, 61, 65, 75 and 79. The treatments D_1, D_2 and D_3 represent embedded belt depths of 10, 15 and 20 cm, respectively. Error bars show the standard error (SE) of the means. Different lowercase letters in the figure indicate statistical significance at the P = 0.05 level within the same stage*

There was no significant difference in leaf RWC among all treatments at BBCH 52. From BBCH 61 to 65, the relative water content of cotton leaves in D_2 and D_3 decreased by 8.5% and 8.1%, respectively, while that in D_1 increased by 3%. From BBCH 65 to 85, the relative water content of cotton leaves in D_2 and D_3 increased by 4.2% and 7.7%, respectively, while that in D_1 decreased by 4.7%.

Gas exchange parameters

The net photosynthetic rate (P_N), intercellular CO_2 concentration (C_i) and transpiration rate (E) of functional cotton leaves increased as the embedment depth increased after BBCH 61 (*Figure 4*). There was no significant difference among all treatments at BBCH 61. Stomatal conductance (g_s) increased with increasing depth of the embedded drip irrigation belt, and the g_s in D_3 was significantly different from that in D_2 only at BBCH 61; there was no significant difference in the other stages.

Chlorophyll fluorescence parameters

The results (*Figure 5*) showed that the depth of the embedded drip irrigation belt had a significant effect only on the maximal quantum yield of PSII photochemistry (F_v/F_m) at BBCH 79, and the values under the D_3 treatments were 1.8% higher than those under D_1. The quantum efficiency of PSII (Y_{II}), the electron transport rate (ETR) and the photochemical quenching coefficient (q_P) increased with increasing belt depth, and D_3 resulted in significantly higher values than D_1. The depth of the belt had a significant

http://www.aloki.hu ● ISSN 1589 1623 (Print) ● ISSN1785 0037 (Online)
DOI: http://dx.doi.org/10.15666/aeer/2005_37633777

effect only on the nonphotochemical quenching coefficient (NPQ) of cotton leaves at BBCH 61, with 10.4% and 18.0% lower values in D_2 and D_3, respectively, compared with those in D_1.

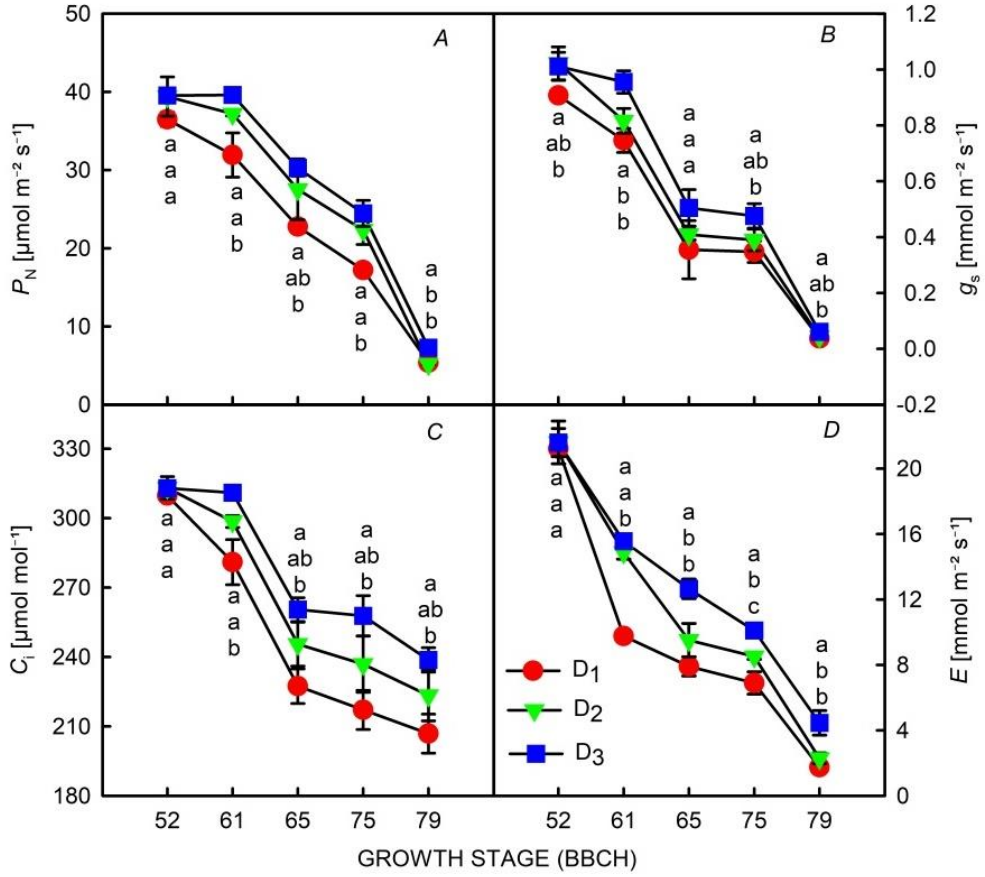

Figure 4. *Effect of the embedded drip irrigation belt depth on cotton gas exchange parameters at BBCH 52, 61, 65, 75 and 79. The treatments D_1, D_2 and D_3 represent embedded belt depths of 10, 15 and 20 cm, respectively. P_N, g_s, C_i and E represent the net photosynthetic rate, stomatal conductance, intercellular CO_2 concentration and transpiration rate, respectively. Error bars show the standard error (SE) of the means. Different lowercase letters in the figure indicate statistical significance at the P = 0.05 level within the same stage.*

Biological yield, seed cotton yield and economic coefficient

The experiment showed that compared with D_1 and D_2, the biological yield of D_3 increased by 51% and 33%, and the seed cotton yield increased by 15% and 2%, but the economic coefficient decreased by 24% and 24%, respectively (*Figure 6*). There was no significant difference in seed cotton yield between D_3 and D_2.

Correlation analysis between photosynthetic parameters and cotton yield

Seed cotton yield was positively correlated with g_s at BBCH 52 and 61, Y_{II} and ETR at BBCH 65 and 79, q_P at BBCH 61 and 65, P_N and E at BBCH 61 and 75, and C_i at BBCH 61 to 75. Seed cotton yield was negatively correlated with NPQ at BBCH 61 and 65 (Table 2). Biological yield was positively correlated with F_v/F_m at BBCH 79, Y_{II} at BBCH 52 and 79, ETR and q_P at BBCH 52 to 79, P_N at BBCH 61, 75 and 79, E and C_i at

http://www.aloki.hu ● ISSN 1589 1623 (Print) ● ISSN1785 0037 (Online)
DOI: http://dx.doi.org/10.15666/aeer/2005_37633777

BBCH 61 to 79, and g_s at BBCH 61. There was a significant negative correlation between biological yield and NPQ at BBCH 61. The economic coefficient was negatively correlated with F_v/F_m at BBCH 65, Y_{II} at BBCH 79, ETR and q_P at BBCH 52, 75 and 79, P_N at BBCH 61, g_s at BBCH 61 and 79, C_i at BBCH 75 and 79, and E at BBCH 65 and 79. There was a significant positive correlation between the cotton economic coefficient and NPQ at BBCH 61 (*Table 2*).

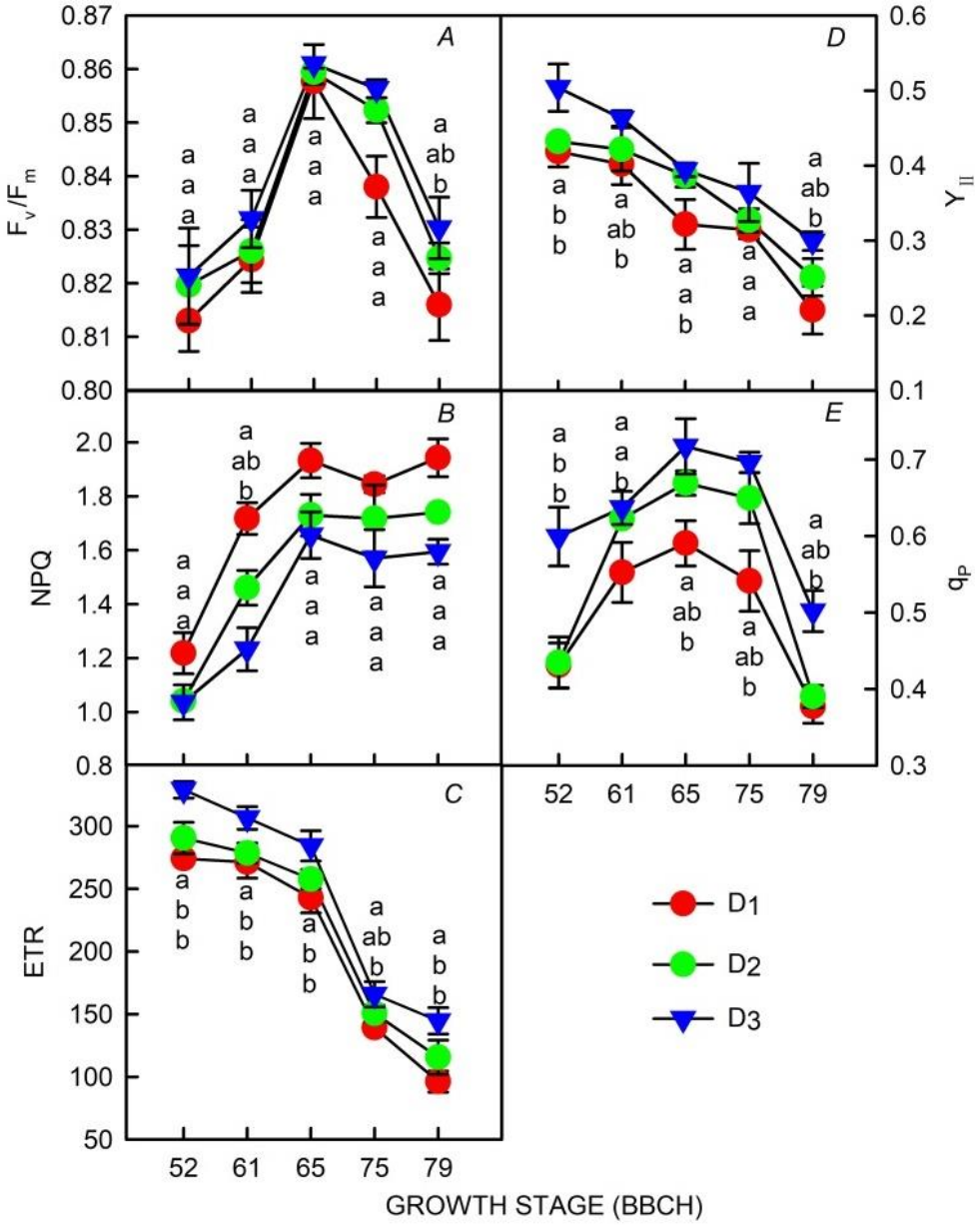

Figure 5. *Effect of embedded drip irrigation belt depth on the cotton chlorophyll fluorescence parameters at BBCH 52, 61, 65, 75 and 79. The treatments D_1, D_2 and D_3 represent embedded belt depths of 10, 15 and 20 cm, respectively. F_v/F_m, NPQ, ETR, Y_{II} and q_P represent the maximal quantum yield of PSII photochemistry, the nonphotochemical quenching coefficient, the electron transport rate, the quantum efficiency of PSII and the photochemical quenching coefficient, respectively. Error bars show the standard error (SE) of the means. Different lowercase letters in the figure indicate statistical significance at the P = 0.05 level within the same stage*

http://www.aloki.hu ● ISSN 1589 1623 (Print) ● ISSN1785 0037 (Online)
DOI: http://dx.doi.org/10.15666/aeer/2005_37633777

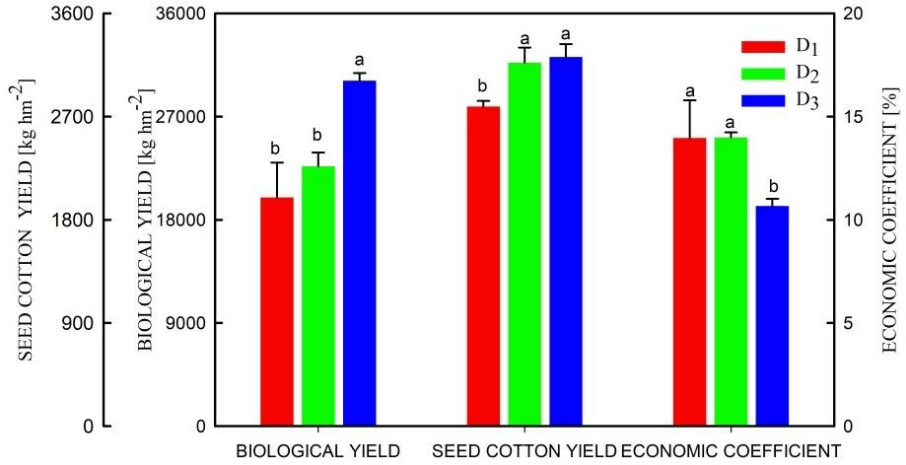

Figure 6. *Effect of embedded drip irrigation belt depth on the biological yield, seed cotton yield and economic coefficient of cotton. The treatments D_1, D_2 and D_3 represent embedded belt depths of 10, 15 and 20 cm, respectively. Error bars show the standard error (SE) of the means. Different lowercase letters in the figure indicate statistical significance at the P = 0.05 level within the same stage*

Table 2. *Correlation analysis between photosynthetic parameters and yield of cotton at different growth stages*

Growth stage (BBCH)	Parameter	F_v/F_m	Y_{II}	NPQ	ETR	q_P	P_N [μmol m^{-2} s^{-1}]	C_i [μmol mol^{-1}]	g_s [mmol m^{-2} s^{-1}]	E [mmol m^{-2} s^{-1}]
52	Seed cotton yield	0.371	0.653	-0.341	0.589	0.558	0.453	0.399	0.810 **	0.327
	Biological yield	0.270	0.738 *	-0.051	0.857 **	0.873 **	0.487	0.166	0.476	0.133
	Economic coefficient	-0.138	-0.537	-0.147	-0.831 **	-0.837 **	-0.482	0.030	-0.291	-0.054
61	Seed cotton yield	0.311	0.460	-0.697*	0.656	0.740*	0.825**	0.724*	0.712*	0.953**
	Biological yield	0.386	0.604	-0.808**	0.779*	0.678*	0.847**	0.759*	0.854**	0.741*
	Economic coefficient	-0.289	-0.538	0.712*	-0.610	-0.569	-0.772*	-0.628	-0.776*	-0.546
65	Seed cotton yield	0.317	0.791*	-0.720*	0.760*	0.712*	0.573	0.690*	0.490	0.632
	Biological yield	0.551	0.659	-0.663	0.773*	0.722*	0.621	0.754*	0.462	0.802**
	Economic coefficient	-0.677*	-0.515	0.547	-0.587	-0.633	-0.504	-0.617	-0.230	-0.676*
75	Seed cotton yield	0.540	0.476	-0.291	0.641	0.602	0.803**	0.729*	0.595	0.798**
	Biological yield	0.270	0.600	-0.532	0.786*	0.692*	0.711*	0.839**	0.625	0.764*
	Economic coefficient	0.005	-0.448	0.598	-0.736*	-0.681*	-0.576	-0.755*	-0.444	-0.555
79	Seed cotton yield	0.628	0.720*	-0.392	0.747*	0.380	0.422	0.658	0.331	0.606
	Biological yield	0.679*	0.912**	-0.546	0.834**	0.781*	0.731*	0.807**	0.666	0.865**
	Economic coefficient	-0.589	-0.884**	0.592	-0.684*	-0.826**	-0.620	-0.756*	-0.709*	-0.813**

* Significant correlation at the 0.05 level (bilateral). ** Significant correlation at the 0.01 level (bilateral).

http://www.aloki.hu ● ISSN 1589 1623 (Print) ● ISSN1785 0037 (Online)
DOI: http://dx.doi.org/10.15666/aeer/2005_37633777

Discussion

Regulation of cotton photosynthetic characteristics by embedded drip irrigation belt depth

The depth of irrigation and fertilization can affect the photosynthesis of the aboveground parts of crops and thus affect yield formation in fields without plastic mulching (He, 2001). The leaf is the main organ for photosynthesis. Maintaining appropriate leaf area dynamics at each growth stage of crops is critical for improving yield (Maddonni et al., 2001). The results of this experiment showed that compared with BBCH 65, the leaf area at BBCH 75 decreased by 45.0% and 25.4% in D_1 and D_2, respectively, and increased by 8.3% in D_3, indicating that an increase in the depth of the embedded drip irrigation belt led to an increase in leaf area after BBCH 65 and prevented premature senescence. Combined with the fact that the relative water content in D_2 and D_3 was significantly lower than that in D_1 at BBCH 65 in this experiment, this indicates that the water consumption of cotton plants in the D_2 and D_3 treatments was relatively high during this stage, and D_2 and D_3 maintained stronger growth potential in the later growth stage than D_1. In addition, in this experiment, the relative water content of cotton leaves at BBCH 52, 61 and 85 and the SPAD value at BBCH 52, 61 and 79 significantly increased with increasing belt depth, indicating that an increase in belt depth is beneficial to maintaining the water supply of cotton plants and improving the physiological activity of cotton leaves (Poorter et al., 2009; Sampathkumar et al., 2013; Ni et al., 2014).

Kahlaoui et al. (2011) found that subsurface drip irrigation increased tomato leaf area and chlorophyll content compared to drip irrigation. Han (2018) found that a suitable embedded belt depth (15 cm) could increase the soil volumetric water content, photosynthetic rate and stomatal conductance of pakchoi leaves. In this experiment, the net photosynthetic rate, intercellular CO_2 concentration and stomatal conductance of functional cotton leaves in D_3 from BBCH 61 to 79 were significantly higher than those in D_1 but were not significantly different from those in D_2. This indicated that increasing the depth of the embedded drip irrigation belt in the range of 10-20 cm could enhance the carbon assimilation ability of cotton leaves.

Chlorophyll fluorescence characteristics are closely related to each process of photosynthesis and can reflect the intrinsic characteristics of photosynthesis (Olaf and Jan, 1990). Liu (2020) found that an increase in the soil water content under subsurface drip irrigation could improve F_v/F_m, q_P, and ETR and reduce the NPQ of alfalfa. In this experiment, increasing the depth of the embedded drip irrigation belt significantly increased the Y_{II}, ETR, q_P and F_v/F_m of cotton leaves at BBCH 79 and reduced the NPQ at BBCH 61, which is basically consistent with the results presented by Liu. These results indicate that both increasing the depth of the embedded drip irrigation belt and increasing the soil water content can enhance the light energy conversion and utilization efficiency of cotton leaves and reduce light energy and heat dissipation.

Adjustment of the embedded drip irrigation belt depth for cotton yield

Compared with surface irrigation, subsurface drip irrigation can significantly reduce soil evaporation, realize the rational distribution of water and fertilizer in the root zone, and improve the utilization efficiency of water and fertilizer, thus achieving the purpose of increasing crop yields (Meshkat et al., 2000). Çetin and Kara (2019) evaluated the water productivity, economic water productivity and land economic productivity of cotton and concluded that a subsurface drip irrigation system with a lateral pipe depth of

http://www.aloki.hu ● ISSN 1589 1623 (Print) ● ISSN1785 0037 (Online)
DOI: http://dx.doi.org/10.15666/aeer/2005_37633777

40 cm had higher economic benefits than surface drip irrigation. Çetin et al. (2021) also found that the net income under subsurface drip irrigation was significantly higher than that under surface drip irrigation. However, compared with drip irrigation under mulch, cotton cultivated without plastic mulching grew slowly in the early stage and tended to produce insufficient bolls. In this experiment, because some bolls did not open normally after spraying of the defoliating agent in D_3, the seed cotton yield increased only by 2% compared with D_2, and the difference was not significant. Liu et al. (2015) found that potato yield first increased and then decreased with increasing depth of the embedded drip irrigation belt in the range of 10–50 cm and reached the maximum yield when the depth was 30 cm. When the depth was greater than 30 cm, the potato emergence process lagged, which is consistent with the results of this study. The results indicated that the deep embedding of the drip irrigation belt would inhibit the growth and development of cotton in the early stage, delay the growth process, and then have an adverse effect on production.

Photosynthesis is the basis of yield formation. In this experiment, the correlation analysis between the photosynthetic parameters and yield showed that g_s, Y_{II}, ETR, q_P, P_N, C_i, E, and F_v/F_m were positively correlated with the seed cotton yield and biological yield and were negatively correlated with the economic coefficient. NPQ was negatively correlated with the seed cotton yield and biological yield and positively correlated with the economic coefficient. These results indicate that increasing the photosynthetic capacity of cotton leaves can further increase the biological yield and seed cotton yield but reduce its economic coefficient under the experimental conditions.

Compared with surface irrigation, subsurface drip irrigation can increase the soil moisture content in the crop root zone (Meshkat et al., 2000). According to the research of Al-Othman et al. (2020), subsurface drip irrigation without plastic mulching can reduce water consumption compared with surface drip irrigation with plastic mulching, and a proper belt depth can significantly optimize root distribution and improve root activity (Lamm et al., 2021). The depth of the embedded drip irrigation belt should be optimized to avoid damage by cultivation or other equipment and to meet the needs of seed germination and seedling growth. In addition, it should also be based on soil texture, drip irrigation belt specification, pipeline combination, irrigation quota and frequency and other factors. In this study, the optimal depth of the embedded drip irrigation belt in the experimental site was 15 cm within the range of 10–20 cm under the same soil texture, irrigation quota, irrigation frequency and other factors. However, at the determined depth of the embedded drip irrigation belt, how to optimize the irrigation mode for the growth period, tap the biological water-saving potential of cotton, and realize efficient water-saving production of cotton without plastic mulching needs further exploration.

Conclusion

Under the irrigation system in this study, the increase in the embedded drip irrigation belt depth at the experimental site was beneficial for increasing the leaf area of cotton without plastic mulching in the later growth stage, promoting the accumulation of photosynthetic pigments, improving the photosynthetic rate, transpiration rate, stomatal conductance and light energy conversion efficiency, and enhancing the photosynthetic capacity of cotton leaves. The biological yield was significantly increased under the 20 cm embedded belt depth, but there was no significant difference in seed cotton yield between the 15 cm and 20 cm depth treatments due to the significant reduction in the

http://www.aloki.hu ● ISSN 1589 1623 (Print) ● ISSN1785 0037 (Online)
DOI: http://dx.doi.org/10.15666/aeer/2005_37633777

economic coefficient. Overall, D_2 (15 cm) was the most suitable embedded belt depth to maximize cotton yield without plastic mulching.

Acknowledgements. This project was supported by the National Natural Science Foundation of China (32160512) and Scientific and Technological Innovation Team of Soil Nutrient and Fertilizer Efficient Utilization in Xinjiang Academy of Agricultural Reclamation Sciences.

REFERENCES

[1] Al-Othman, A. A., Mattar, M. A., Alsamhan, M. A. (2020): Effect of mulching and subsurface drip irrigation on soil water status under arid environment. – Spanish Journal of Agricultural Research 18: 1201.
[2] Amali, S., Rolston, D. E., Fulton, A. E., Hanson, B. R., Phene, C. J., Oster, J. D. (1997): Soil water variability under subsurface drip and furrow irrigation. – Irrigation Science 17: 151-155.
[3] Ayars, J. E., Fulton, A., Taylor, B. (2015): Subsurface drip irrigation in California - here to stay? – Agricultural Water Management 157: 39-47.
[4] Çetin, O., Kara, A. (2019): Assessment of water productivity using different drip irrigation systems for cotton. – Agricultural Water Management 223: 105693.
[5] Çetin, Ö., Üzen, N., Temiz, M. G., Altunten, H. (2021): Improving cotton yield, water use and net income in different drip irrigation systems using real-time crop evapotranspiration. – Polish Journal of Environmental Studies 30: 4463-4474.
[6] Chen, Y. (2017): Discussion on the development and application of underground drip irrigation technology and existing problems. – Gansu Science and Technology 33: 128-130.
[7] Chen, Z., Tao, X., Khan, A., Tan, D. K. Y., Luo, H. (2018): Biomass accumulation, photosynthetic traits and root development of cotton as affected by irrigation and nitrogen-fertilization. – Frontiers in plant science 9: 173.
[8] Constable, G., Bange, M. (2015): The yield potential of cotton (*Gossypium hirsutum* L.). – Field Crops Research 182: 98-106.
[9] Dong, H., Li, W., Tang, W., Li, Z., Zhang, D., Niu, Y. (2005): Yield, quality and leaf senescence of cotton grown at varying planting dates and plant densities in the Yellow River Valley of China. – Field Crops Research 98: 106-115.
[10] Elmaloglou, S., Diamantopoulos, E. (2013): Simulation of soil water dynamics under subsurface drip irrigation from line sources - ScienceDirect. – Agricultural Water Management 27: 4131-4148.
[11] Gao, H., Yan, C., Liu, Q., Ding, W., Chen, B. (2019): Effects of plastic mulching and plastic residue on agricultural production: A meta-analysis. – Science of The Total Environment 651: 484-492.
[12] Grabow, G. L., Huffman, R. L., Evans, R. O., Jordan, D. L., Nuti, R. C. (2006): Water distribution from a subsurface drip irrigation system and dripline spacing effect on cotton yield and water use efficiency in a coastal plain soil. – Transactions of the Asabe 49: 1823-1835.
[13] Guo, X., Yang, H., Tai, J., Li, R., Zhang, M. (2020): Advances in crop shallow buried drip irrigation technology. – Journal of Inner Mongolia University for Nationalities 35: 80-84.
[14] Han, S. (2018): Soil water infiltration characteristics of different depths of moistube and its effect on crops. – Hebei University of Engineering, Hebei (in Chinese).
[15] He, H. (2001): Crop water and nitrogen use and optimum irrigation technical parameters under subsurface drip irrigation. – Northwest Agriculture & Forestry University, Shanxi (in Chinese).

http://www.aloki.hu ● ISSN 1589 1623 (Print) ● ISSN1785 0037 (Online)
DOI: http://dx.doi.org/10.15666/aeer/2005_37633777

[16] He, H., Wang, Z., Guo, L., Zheng, X., Zhang, J., Li, W., Fan, B. (2018): Distribution characteristics of residual film over a cotton field under long-term film mulching and drip irrigation in an oasis agroecosystem. – Soil and Tillage Research 180: 194-203.
[17] Kahlaoui, B., Hachicha, M., Rejeb, S., Rejeb, M. N., Hanchi, B., Misle, E. (2011): Effects of saline water on tomato under subsurface drip irrigation: nutritional and foliar aspects. – Journal of soil science and plant nutrition 11: 69-86.
[18] Kalfountzos, D., Alexiou, I., Kotsopoulos, S., Zavakos, G., Vyrlas, P. (2006): Effect of Subsurface Drip Irrigation on Cotton Plantations. – Water Resources Management 21: 1341-1351.
[19] Khalilian, A., Sullivan, M. J., Smith, W. B. (2000): Lateral depth placement and deep tillage effects in a subsurface drip irrigation system for cotton. – In: Proceedings of the Fourth Decennial National Irrigation Symposium, Phoenix, AZ, USA, 14–16 November: 641-646.
[20] Lamm, F. R., Colaizzi, P. D., Sorensen, R. B., Bordovsky, J. P., Dougherty, M., Balkcom, K., Zaccaria, D., Bali, K. M., Rudnick, D. R., Peters, R. T. (2021): A 2020 vision of subsurface drip irrigation in the U.S. – Transactions of the Asabe 64: 1319-1343.
[21] Li, F., Wang, P., Wang, J., Xu, J. (2004): Effects of irrigation before sowing and plastic film mulching on yield and water uptake of spring wheat in semiarid Loess Plateau of China. – Agricultural Water Management 67: 77-88.
[22] Li, X., Shi, J., Wang, S., Zuo, Q. (2017): Numerical simulation and analysis on depth of disposable tape in cotton field under subsurface drip irrigation in Xinjiang, China. – Transactions of the Chinese Society of Agricultural Machinery 48: 191-198, 222.
[23] Liu, Y. (2006): Application and effect analysis of subsurface drip irrigation in water-saving irrigation of cotton. – Water Conservancy Science and Technology and Economy 12: 831-832.
[24] Liu, J. (2020): Effects of water stress on photosynthetic physiological characteristics and quality of Alfalfa. – Gansu Agricultural University, Gansu (in Chinese).
[25] Liu, X., Wan, S., Feng, D., Jiang, S., Kang, Y., Liu, S. (2015): Response of potato yield and irrigation water use efficiency under subsurface drip irrigation at various lateral depths. – Journal of Irrigation and Drainage 34: 63-66.
[26] Maddonni, G. A., Otegui, M. E., Cirilo, A. G. (2001): Plant population density, row spacing and hybrid effects on maize canopy architecture and light attenuation. – Field Crops Research 71: 183-193.
[27] Meshkat, M., Warner, R. C., Workman, S. R. (2000): Evaporation reduction potential in an undisturbed soil irrigated with surface drip and sand tube irrigation. – Transactions of the ASAE 43: 79-86.
[28] Munger, P., Bleiholder, H., Hack, H., Hess, M., Stauß, R., van den Boom, T., Weber, E. (1998): Phenological Growth Stages of the Cotton Plant (*Gossypium hirsutum* L.): Codification and Description according to the BBCH Scale. – Journal of Agronomy and Crop Science 180: 143-149.
[29] Ni, J., Wang, W., Yu, S., Dai, S. (2014): Effects of drought stress on some physiological and biochemical indices of Kapok leaves. – Chinese Journal of Tropical Crops 35: 2020-2024.
[30] Olaf, V. K., Jan, F. H. S. (1990): The use of chlorophyll fluorescence nomenclature in plant stress physiology. – Photosynthesis Research 25: 147-150.
[31] Poorter, H., Niinemets, U., Poorter, L., Wright, I. J., Villar, R. (2009): Causes and consequences of variation in leaf mass per area (LMA): a meta-analysis. – The New phytologist 182: 565-588.
[32] Sampathkumar, T., Pandian, B. J., Jeyakumar, P., Manickasundaram, P. (2013): Effect of deficit irrigation on yield, relative leaf water content, leaf proline accumulation and chlorophyll stability index of cotton–maize cropping sequence. – Experimental Agriculture 50: 407-425.

http://www.aloki.hu ● ISSN 1589 1623 (Print) ● ISSN1785 0037 (Online)
DOI: http://dx.doi.org/10.15666/aeer/2005_37633777

[33] Shi, W. (2012): Effects of plant densities on cotton dry matter accumulation and distribution, yield and fiber quality. – Nanjing Agricultural University, Jiangsu (in Chinese).
[34] Wang, X., Li, H., Wang, Y., Wang, Y. (2020): Analysis of world cotton production and trade pattern under the background of trade dispute. – Agricultural Outlook 16: 95-99.
[35] Yao, J., Qi, Y., Li, H., Shen, Y. (2021): Effects of the irrigation quota and drip irrigation pipes spacing on growth and development of summer maize with subsurface drip irrigation. – Chinese Journal of Eco-Agriculture 29: 1502-1511.
[36] Zhang, D., Liu, H., Hu, W., Qin, X., Ma, X., Yan, C., Wang, H. (2016): The status and distribution characteristics of residual mulching film in Xinjiang, China. – Journal of Integrative Agriculture 15: 2639-2646.

http://www.aloki.hu ● ISSN 1589 1623 (Print) ● ISSN1785 0037 (Online)
DOI: http://dx.doi.org/10.15666/aeer/2005_37633777

DIFFERENCES IN GRAIN YIELD AND GRAIN QUALITY TRAITS OF WINTER TRITICALE DEPENDING ON THE VARIETY, FERTILIZER AND WEATHER CONDITIONS

LALEVIĆ, D.[1*] – MILADINOVIĆ, B.[2] – BIBERDŽIĆ, M.[1] – VUKOVIĆ, A.[1] – MILENKOVIĆ, L.[1]

[1]*University of Priština – Kosovska Mitrovica, Faculty of Agriculture, Kopaonička bb, 38219 Lešak, Serbia*

[2]*Forest Administration of Montenegro, Miloša Tošića 4, 84210 Pljevlja, Montenegro*

[*]*Corresponding author*
e-mail: dragana.lalevic@pr.ac.rs; phone: +381-655-626-592

(Received 10th Mar 2022; accepted 11th Jul 2022)

Abstract. The research conducted in the north of Montenegro in the period from 2017-2019 aimed to examine the impact of different fertilizer variants on the yield and grain quality traits in four varieties of winter triticale. The research included the control and three variants of nitrogen fertilization: 60 kg ha^{-1} (N_1), 100 kg ha^{-1} (N_2) and 120 kg ha^{-1} (N_3). In all fertilizer variants, in addition to nitrogen, another 100 kg of ha^{-1} phosphorus and potassium were used. The results of the research showed that all examined varieties reacted positively to the application of mineral nutrition both by changing the productive characteristics and by changing the grain quality. The greatest positive effect on all examined parameters that affect productivity had the variant of fertilization in which nitrogen was used in the amount of 120 kg ha^{-1}. The variety PKB Vožd had the highest yield (5.79 t ha^{-1}) in both years of research, while the cultivar Favorit had the lowest yield (4.67 t ha^{-1}). The variance analysis clearly indicated that the individual effects of variety and fertilization, as well as the effects of the interaction between variety x fertilization and fertilization x year on grain yield in the examined winter triticale varieties were significant ($p<0.01$).
Keywords: *triticale, mineral nutrition, nitrogen, productive characteristics, grain quality*

Introduction

The emergence of a new, more demanding range of triticale, accompanied by constant changes in agroecological conditions and soil characteristics, especially when we talk about its fertility, emphasizes the need to research the mineral nutrition of triticale while determining optimal amounts and ratios of nutrients in specific agroecological conditions. The increase in the number of inhabitants, accompanied by the problem that the world production of basic cereals intended for human consumption is not in proportion to the number of the human population, has produced the need to find new ways of production. Also, the current pandemic has shown how important each country's own production, compared to the import of goods, is in overcoming the global crisis. Created with the idea of combining the good properties of wheat and rye by intergenus hybridization, triticale is characterized today by the existence of a large number of varieties marked by high tolerance to adverse biotic and abiotic factors (Massimi et al., 2016) which reduces the requirements for chemical protection (Losert, 2017) and fertilization. On the other hand, triticale provides high grain yields and high biomass even in marginal environments that cannot be used for growing food crops (Bezabih et al., 2019; Kucukozdemir et al., 2021), but also in arid areas that are becoming more widespread due to global climate change (Blum, 2014; Cantale et al., 2016). High productivity with lower initial investments, better adaptation to moist,

http://www.aloki.hu ● ISSN 1589 1623 (Print) ● ISSN1785 0037 (Online)
DOI: http://dx.doi.org/10.15666/aeer/2005_37793792

acidic and alkaline soils with the lack of nutrients compared to other cereals, good grain quality with high protein content (Epure et al., 2015; Bezabih et al., 2019) are some of the properties of triticale. Triticale is an excellent component for preparing feed mixtures and can partially or completely replace other, more expensive nutrients, and thanks to nutritional values higher than corn, breeders and livestock experts have so far recommended it in the diet of all domestic animals (Đekić et al., 2012), while Glamočlija et al. (2018) point out that it has given the best results so far in the diet of poultry and dairy cattle. Mature grain can be used, but also green, ensiled, alone or in combination with other ensiled legumes. Despite the fact that the problems of mineral nutrition have been researched a lot and that there are a lot of available results, many questions will always be relevant, while some will reappear in a new form. In support of this is the fact that the results of experiments with fertilization are directly or indirectly influenced by numerous factors, including climatic conditions of the region and year, soil fertility, fertilization preceding crops, nutrient composition, time and manner of its introduction, etc. (Kirchev et al., 2014; Gerdzhikova, 2014; Madić et al., 2015; Terzić et al., 2018).

According to Jaćimović et al. (2012) for achieving adequate quality and yield of small grains, one of the key factors is a well-balanced mineral diet where the full effect of NPK nutrients can be achieved only if other factors that model yield are brought to optimum, especially weather conditions of the growing season (Janušauskaite, 2014). Dumbravă et al. (2016) state that one of the most important agro-technical factors on which the grain yield depends and enables farmers to use the production potential of cereals is mineral nutrition, with special emphasis on the use of nitrogen due to its impact on grain yield and quality. Namely, high grain yield of good quality in intensive agricultural production can be achieved only in the conditions of application of a sufficient amount of nitrogen in the periods of vegetation when it is most needed by plants (Janušauskaite, 2013). Nikolić et al. (2012), Novak et al. (2019) and Hirzel et al. (2020) state that among the nutrients, nitrogen certainly has the greatest impact on yield elements and its quality, both through its presence in the soil and its deficiency, which in critical phases can lead to irreversible loss of yield (Estrada-Campuzano et al., 2012), so this justifies the fact that its impact on the yield is the subject of numerous studies. When we talk about the quantities of mineral fertilizers, different data are given in the literature precisely because of the different conditions of the survey, climatic and soil factors, variety potential, preceding crop (Gerdzhikova et al., 2017; Darguza and Gaile, 2020).

Therefore, the production of small grains requires constant improvement when we talk about nutrient intake systems, and we should always take into account its economic moments.

Montenegro, despite the favorable climatic conditions for the cultivation of cereals and the available arable land that can be used for these purposes, meets its needs in cereals mainly from imports. The importance of triticale cultivation intended for domestic animals in the hilly and mountainous area of northern Montenegro requires the need for more detailed study and popularization of this type of grain with the aim of its fuller use in large-scale production. According to Peltonen-Sainio et al. (2009), the prevalence of winter cereals in the northern regions will be much higher in the future than at present. Taking into account that plant nutrition, i.e. nutrient intake is more regional in nature, that agricultural producers do not have enough information about the use of nitrogen fertilizers, its amounts in soil and that the research is conducted in rural

http://www.aloki.hu ● ISSN 1589 1623 (Print) ● ISSN1785 0037 (Online)
DOI: http://dx.doi.org/10.15666/aeer/2005_37793792

areas, the aim is to determine optimal fertilization systems which would result in high and stable yields of satisfactory quality. The results of the research would enable giving reliable recommendations to producers of this type of grain for variety selection and determining optimal quantities of the most important nutrients in a specific production area, because the production potential of the variety can be used only by applying varietal agrotechnics, by educating producers and faster transfer of scientific knowledge into production.

Materials and methods

In order to examine the effect of different amounts of nitrogen in combination with phosphorus and potassium on the productivity and protein content of triticale grain, an experiment was set up in the vicinity of Bijelo Polje (Montenegro) at 43°05'25"N and 19°46'10"E, at an altitude of 562 m. The experiment set up according to a random block system in four repetitions was performed in the period from 2017-2019. The size of the elementary plot was 6 m^2 (3x2 m). The land on which the survey was performed belongs to the type of Eutric Cambisol on alluvial and colluvial deposits with low carbonate content (2.38-2.45%), which is a characteristic of most of these lands in the Lim river valley. The soil is humic (3.37-3.98%), low pH value (pH (KCl) = 5.01-4.94) with low content of easily accessible phosphorus and potassium (below 10 mg 100 g^{-1} soil).

Four varieties of winter triticale (Kg-20, Favorit, Tango and PKB Vožd) were used as test material, of which the first two were selected at the Center for Small Grains in Kragujevac (Serbia), the variety Tango was created at the Center for Agricultural and Technological research in Zajecar (Serbia) and the variety PKB Vožd in the Institute PKB (Padinska Skela – Serbia). Sowing in both years of research was done manually in the optimal time for this area (second decade of October) with a row spacing of 12.5 cm and sowing density of 600 germinated seeds per m^2. Additional tillage performed just before sowing was preceded by basic tillage at a depth of 25 cm. The research included the control and three variants of nitrogen fertilization: 60 kg ha^{-1} (N_1), 100 kg ha^{-1} (N_2) and 120 kg ha^{-1} (N_3), where nitrogen was used in the form of calcium-ammonium nitrate (KAN - 27% N). In all fertilizer variants, in addition to nitrogen, another 100 kg of ha^{-1} phosphorus in the form of super phosphate and 100 kg of ha^{-1} potassium in the form of 60% potassium salt were used. Fertilizers were used so that the entire amount of phosphorus and potassium together with half of nitrogen fertilizers was applied in the autumn period together with pre-sowing soil preparation, and the other half in fertilization in mid-March in the phase of full flowering of plants. Other production technology applied to the experiment was standard. The harvest was carried out manually in the phase of full maturity in the middle of July, during which the measured grain yield was corrected to 14% moisture. Also, the values of hectoliter weight were determined by measuring 48 samples on a hectoliter scale (volume 250 ml) and the mass of 1000 grains. The nitrogen content in the grain of the tested triticale cultivars was determined by the Kjeldah method, whereby the obtained values were multiplied by a coefficient of 6.25.

The obtained results presented through average values were statistically processed by the method of variance analysis, where the significance of differences in treatment environments was tested by LSD test, at significance thresholds of 1 and 5%, using WASP 2.0 Statistics Software Package (free version, Indian Council of Agricultural

http://www.aloki.hu ● ISSN 1589 1623 (Print) ● ISSN1785 0037 (Online)
DOI: http://dx.doi.org/10.15666/aeer/2005_37793792

Research [ICAR] - Central Coastal Agricultural Research Institute [CCARI], Ela, Goa, India).

Climatic data of the experimental area

Meteorological conditions, air temperatures and precipitation for crop growing seasons are shown in *Table 1*. The data for the research period (2017-2019) clearly show that the years in which the research was conducted differed in temperature and quantity and distribution of precipitation between each other and with a perennial average.

Table 1. *Climatic data of the region (2017-2019 growing seasons)*

Month	Temperature (°C)			Precipitation (mm)		
	Year		Long term average (1991-2020)	Year		Long term average (1991-2020)
	2017/18	2018/19		2017/18	2018/19	
October	10.4	13.5	10.8	50.1	38.0	85.7
November	5.1	7.0	5.5	88.9	119.7	100.0
December	1.8	0.8	0.8	158.4	49.1	89.9
January	2.6	-1.2	-0.4	38.2	71.9	63.6
February	2.4	2.9	1.6	114.7	60.2	77.6
March	6.4	7.0	5.7	103.2	13.6	67.7
April	15.0	11.8	10.4	39.5	44.0	70.9
May	15.3	13.2	14.6	101.7	230.2	81.4
June	18.9	20.6	18.4	90.8	125.1	72.4
July	20.4	20.5	20.1	79.0	97.7	69.3
Mean / total	9.8	9.6	8.7	864.5	849.5	778.5

The average air temperature and the amount of precipitation during the vegetation period in both years of research was higher than the multi-year average. In the first year of research (2017/18), the average air temperature was 1.12 °C higher compared to the multi-year average, while in the second year of research (2018/19) the difference was 0.86 °C. Large amounts of precipitation in the second year of research in May, June and July compared to the first year of research, but also the long-term average, adversely affected both plant development and the process of their maturation, which resulted in lower yields.

Results and discussion

The data obtained during the research showed the existence of significant differences in the values of the mass of 1000 grains of the examined triticale cultivars (*Table 2*).

Also, it was noticed that the environmental conditions as well as certain nutrients significantly affected the observed trait. Average values for all variants of fertilization show that the variety PKB Vožd in both years of research achieved the highest mass of 1000 grains and it amounted to 49.8 g and 48.5 g, respectively. The lowest average mass of 1000 grains, in both years of research, was recorded in the cultivar Favorit. The results of two years of research show that the average mass of 1000 grains for all varieties was the highest in the variant where nitrogen was used in the amount of 120 kg ha^{-1} and it was 44.3 g in the first year and 43.2 g in the second, which is in accordance with the results of Oral et al. (2018) who point out that even the smallest

http://www.aloki.hu ● ISSN 1589 1623 (Print) ● ISSN1785 0037 (Online)
DOI: http://dx.doi.org/10.15666/aeer/2005_37793792

amounts of nitrogen used in triticale cultivation affect a significant increase in the value of this trait.

Table 2. *Thousand grain weight (g) of triticale as affected by varieties, nitrogen application and year*

Variety (A)	Year (C) 2017/18 Fertilization variant (B)					2018/19 Fertilization variant (B)				
	0	N_1	N_2	N_3	Average	0	N_1	N_2	N_3	Average
Kg-20	33.5	36.2	37.0	38.6	36.3	33.7	36.7	37.0	38.8	36.5
Favorit	31.0	34.8	35.4	36.0	34.3	30.8	33.0	35.4	36.0	33.8
Tango	45.1	47.9	47.8	49.0	47.4	42.4	46.1	46.0	47.2	45.4
PKBVožd	43.8	49.2	52.6	53.8	49.8	45.1	48.1	50.0	50.9	48.5
Average	38.3	42.0	43.2	44.3	41.9	38.0	41.0	42.1	43.2	41.0

Anova Table

Source of variation	Degrees of freedom	Sum of squares	Mean sum of squares	F cal	F prob
Replications	3	6.370	2.123	-	-
Factor A	3	392.947	130.982	166.851***	0.000
Factor B	3	5216.678	1738.893	2215.081***	0.000
Factor C	1	1.033	1.033	1.316ns	0.254
AxB	9	68.644	7.627	9.716***	0.000
AxC	3	28.401	9.467	12.059***	0.000
BxC	3	212.457	70.819	90.213***	0.000
AxBxC	9	38.385	4.265	5.433***	0.000
Error	93	73.007	0.785	-	-
Total	127	6037.923	-	-	-

		A	B	C	AxB	AxC	BxC	AxBxC
Lsd	0.05	0.440	0.440	0.311	0.880	0.622	0.622	1.244
	0.01	0.583	0.583	0.412	1.165	0.824	0.824	1.648

0 – control (without fertilization), N_1 - 60 kg ha^{-1} of nitrogen, N_2 - 100 kg ha^{-1} of nitrogen, N_3 - 120 kg ha^{-1} of nitrogen. ***Significant at $p < 0.01$; ns – non-significant

And while the values of the mass of 1000 grains in our research and the research of Oral et al. (2018) increase with the increasing amount of nitrogen used in fertilization (36.4 g - N_0 to 38.0 g – N_3 (120 kg ha^{-1} N)), Bielski et al. (2020) based on their research, state that even the use of small amounts of nitrogen in fertilization leads to a significant increase in the mass of 1000 grains. The mentioned authors obtained the highest mass of 1000 grains when using the least amount of nitrogen (40 kg ha^{-1}), while a further increase in the amount of nitrogen resulted in so-called post fertilization diminution of grains followed by a decrease in the mass of 1000 grains. Accordingly, the results of these authors show that the use of nitrogen in the amount of 120 kg ha^{-1} caused a significant decrease in the value of 1000 grains and that a similar trend was observed with a further increase in nitrogen (160 kg ha^{-1}). In contrast, the results of the study by Dumbravă et al. (2016) showed that the highest values of mass of 1000 grain were recorded on non-fertilized variants where the number of grains per ear and the number of ears per m^2 were lower and that this property significantly depends on other yield parameters. By analysis of variance, individual influences of cultivar and fertilization on the mass of 1000 grains were significant at the 0.01 level, as well as the effects of interaction of cultivars x fertilization, cultivar x years, fertilization x years and cultivar x

http://www.aloki.hu ● ISSN 1589 1623 (Print) ● ISSN1785 0037 (Online)
DOI: http://dx.doi.org/10.15666/aeer/2005_37793792

fertilization x years. The individual effect of the year on the mass of 1000 grains in the observed varieties of winter triticale was not statistically significant.

The results of our research show that the use of mineral fertilizers caused a significant increase in hectoliter weight compared to the control, but that a similar trend was observed with increasing doses of nitrogen. Jelić et al. (2013) point out that the hectoliter weight in small grains is the trait which is genetically defined but also strongly modified by the nutrient status of the environment and weather conditions. On the other hand, the results of Dumbravă et al. (2016) indicate that hectolitre weight, in addition to quantity, is largely conditioned by the distribution of nitrogen fertilizers during vegetation, where they obtained the highest values of this trait on non-fertilized treatments with the lowest number of spikes / m^2 followed by the lowest number of grains per spike.

From the data in *Table 3*, it can be seen that the variety Tango, on average in both years of research, achieved the highest hectoliter weight and it amounted to 70.9 kg hl^{-1} in the first and 67.9 kg hl^{-1} in the second year of research.

Table 3. *Hectolitre weight (kg hl^{-1}) of triticale as affected by varieties, nitrogen application and year*

Variety (A)	Year (C)									
	2017/18					2018/19				
	Fertilization variant (B)					Fertilization variant (B)				
	0	N_1	N_2	N_3	Average	0	N_1	N_2	N_3	Average
Kg-20	66.7	68.3	72.5	74.4	70.5	63.3	65.9	66.9	68.0	66.0
Favorit	65.4	68.1	70.2	71.1	68.7	62.3	64.4	65.6	67.0	64.8
Tango	66.1	71.0	73.5	73.2	70.9	65.0	66.3	70.0	70.5	67.9
PKBVožd	66.5	70.3	69.9	71.1	69.4	65.6	65.1	68.0	69.3	67.0
Average	66.2	69.4	71.5	72.4	69.9	64.0	65.4	67.6	68.7	66.4

Anova Table

Source of variation	Degrees of freedom	Sum of squares	Mean sum of squares	F cal	F prob
Replications	3	9.604	3.201	-	-
Factor A	3	848.487	282.829	277.985^{***}	0.000
Factor B	3	147.523	49.174	48.332^{***}	0.000
Factor C	1	0.546	0.546	0.537^{ns}	0.466
AxB	9	76.018	8.446	8.302^{***}	0.000
AxC	3	2.732	0.911	0.895^{ns}	0.447
BxC	3	59.486	19.829	19.489^{***}	0.000
AxBxC	9	35.662	3.962	3.895^{***}	0.000
Error	93	94.621	1.017	-	-
Total	127	1274.679	-	-	-

		A	B	C	AxB	AxC	BxC	AxBxC
Lsd	0.05	0.501	0.501	0.354	1.002	0.708	0.708	1.416
	0.01	0.663	0.663	0.469	1.326	0.938	0.938	1.876

0 – control (without fertilization), N_1 - 60 kg ha^{-1} of nitrogen, N_2 - 100 kg ha^{-1} of nitrogen, N_3 - 120 kg ha^{-1} of nitrogen. ***Significant at $p < 0.01$; ns – non-significant

The analysis of variance determined very highly significant statistical effects of variety and fertilization on the achieved values of hectoliter weight as well as the interaction of variety x fertilization, fertilization x years and variety x fertilization x years. The individual effect of year as well as the effects of interactions between variety × year on hectoliter weight in the studied winter triticale varieties were statistically

http://www.aloki.hu ● ISSN 1589 1623 (Print) ● ISSN1785 0037 (Online)
DOI: http://dx.doi.org/10.15666/aeer/2005_37793792

nonsignificant. This confirms the fact that hectoliter grain weight is a complex property controlled by a large number of genes, that it is conditioned by the genotype and whose values can vary significantly according to soil tillage, preceding crop and nitrogen fertilization conditions (Dumbravă et al., 2016; Kucukozdemir et al., 2019).

Studies have shown that mineral nutrition specifically affects the yield and its components in the tested varieties. Also, statistically significant differences in yield height and between examined varieties were observed. Grain yield on average for all cultivars and variants of fertilization in the first year of research was 5.43 t ha^{-1} and was higher compared to the second year of research, thanks to more favorable meteorological conditions, which is in accordance with the results of Studnicki et al. (2019) who pointed out that the variety, meteorological conditions in certain years and agro-ecological conditions of the region are the main factors influencing the yield. Dumbrava et al. (2016) add the importance of tillage and crop fertilization, with a special emphasis on nitrogen fertilization. Our results are in agreement with the results of Estrada-Campuzano et al. (2012) and Wójcik-Gront et al. (2021) who state that generally, starting in May, both spring and winter triticale prefer drier conditions with higher solar radiation to obtain higher yields. Certainly, the importance of applied agricultural techniques during plant breeding should not be neglected. The average grain yield, for all varieties in both years of research, was the lowest in the control and amounted to 3.56 t ha^{-1} in the first and 3.25 t ha^{-1} in the second year of research (*Table 4*).

Table 4. *Grain yield (t ha^{-1}) of triticale as affected by varieties, nitrogen application and year*

Variety (A)	Year (C)									
	2017/18					2018/19				
	Fertilization variant (B)					Fertilization variant (B)				
	0	N_1	N_2	N_3	Average	0	N_1	N_2	N_3	Average
Kg-20	3.58	5.20	5.71	6.55	5.26	3.10	5.09	5.46	5.99	4.91
Favorit	3.02	4.95	5.35	5.75	4.77	2.91	4.44	5.31	5.63	4.57
Tango	3.75	5.70	6.39	6.91	5.69	3.41	5.14	6.08	6.80	5.36
PKBVožd	3.89	6.14	6.81	7.20	6.01	3.60	5.15	6.51	7.08	5.58
Average	3.56	5.50	6.06	6.60	5.43	3.25	4.95	5.84	6.37	5.10

Anova Table

Source of variation	Degrees of freedom	Sum of squares	Mean sum of squares	F cal	F prob
Replications	3	2.280	0.760	-	-
Factor A	3	119.733	39.911	360.531***	0.000
Factor B	3	64.016	21.339	192.760***	0.000
Factor C	1	0.158	0.158	1.423ns	0.236
AxB	9	15.538	1.726	15.596***	0.000
AxC	3	0.194	0.065	0.584 ns	0.627
BxC	3	3.955	1.318	11.910***	0.000
AxBxC	9	0.736	0.082	0.739 ns	0.673
Error	93	10.295	0.111	-	-
Total	127	216.905	-	-	-

		A	B	C	AxB	AxC	BxC	AxBxC
Lsd	0.05	0.165	0.165	0.117	0.330	0.234	0.234	0.467
	0.01	0.219	0.219	0.155	0.438	0.309	0.309	0.619

0 – control (without fertilization), N_1 - 60 kg ha^{-1} of nitrogen, N_2 - 100 kg ha^{-1} of nitrogen, N_3 - 120 kg ha^{-1} of nitrogen. ***Significant at $p < 0.01$; ns – non-significant

http://www.aloki.hu ● ISSN 1589 1623 (Print) ● ISSN1785 0037 (Online)
DOI: http://dx.doi.org/10.15666/aeer/2005_37793792

Fertilization in both experimental years significantly affected the increase in average yield ($p < 0.01$). The same trend was noticed with the application of fertilizers with increasing amounts of nitrogen, so the grain yield achieved on fertilization variants in which nitrogen was used in the amount of 120 kg ha^{-1} was higher than the average yields on all other fertilization variants ($p < 0.01$). The lowest average yield, observed for all variants of fertilization in both years of testing, had the variety Favorit (4.77 t ha^{-1} in the first and 4.57 t ha^{-1} in the second year), and the highest variety PKB Vožd (in the first 6.01 t ha^{-1}, and in the second 5.58 t ha^{-1}). The PKB Vožd variety had a significantly higher grain yield in both years compared to other tested varieties in contrast to the previously obtained results of Lalević et al. (2019) when we talk about this area, where the Tango variety stood out as the most productive variety. Precisely such results indicate the importance of repeating the research in an area with a comparative examination of some other varieties in order to single out the one that best suits the area in terms of yield and quality.

The results of the analysis of variance clearly indicate that the individual effects of variety and fertilization, as well as the effects of the interaction between variety x fertilization and fertilization x year on grain yield in the examined winter triticale varieties indicate the existence of a significant ($p < 0.01$). Variance analysis indicated that the individual effect of year as well as the effects of interactions between cultivar × fertilization x year on grain in our study were not statistically significant. The importance of fertilization in agricultural production has been emphasized by other authors, and Nogalska et al. (2012) point out that fertilization has the strongest impact on increasing yields, while Ivanova and Tsenov (2014 a,b) add meteorological conditions during the year to fertilization. While Gerdzhikova et al. (2017) recommend nitrogen doses of 80 to 120 kg ha^{-1} in production when triticale growing after legume predecessors and 180 kg ha^{-1} of nitrogen after the cereal precursors and sunflower and on poorer soils, Ivanova and Tsenov (2014 a,b) state that new varieties of triticale respond to an increase in the amount of fertilizer by increasing productivity. Oral (2018) points out that for the realization of high genetic potential for yield, plants need nitrogen, especially in the early stages of development, and Alazmani (2015) calls nitrogen a key element in plant nutrition whose intake directly affects the increase in yield. The influence of phosphorus and potassium on the grain yield should certainly not be neglected, considering that the soil on which the experiment was performed is poor in the mentioned elements, as a result of which they must be added in the form of fertilizers. Phosphorus and potassium from the used fertilizers move slowly through the soil, are not subject to leaching and usually remain in the soil layer where they are introduced and available to plants for a long time. However, one should also take into account the economic and ecological justification of the application of larger quantities of mineral fertilizers in the cultivation of plants, since their large quantities can often be the cause of ecosystem pollution, agricultural inefficiency (Wójcik-Gront, 2018) and nitrogen leaching (Roques et al., 2017).

According to the results of many researchers, triticale is a cereal that is characterized by a high content of protein in the grain, and that is exactly one of its most important positive properties. The protein content in the grain of the tested triticale cultivars in our study ranged from 11.08% in the cultivar Tango on the variant without fertilization in the second year of research to 14.64% in the cultivar Favorit on the variant using 100 kg ha^{-1} nitrogen in the first year of research. The values in *Table 5*. show that the

http://www.aloki.hu ● ISSN 1589 1623 (Print) ● ISSN1785 0037 (Online)
DOI: http://dx.doi.org/10.15666/aeer/2005_37793792

established values of protein content in the grain differed both between the examined varieties and between the variants of fertilization and the years of research.

Table 5. *Protein content (%) of triticale as affected by varieties, nitrogen application and year*

Variety (A)	Year (C)									
	2017/18					2018/19				
	Fertilization variant (B)					Fertilization variant (B)				
	0	N_1	N_2	N_3	Average	0	N_1	N_2	N_3	Average
Kg-20	12.15	14.35	14.51	13.68	13.67	12.53	13.96	13.21	12.34	13.01
Favorit	12.24	14.41	14.64	13.74	13.76	12.72	14.12	13.39	13.07	13.32
Tango	11.87	14.06	13.57	13.12	13.15	11.08	12.94	12.45	12.08	12.14
PKBVožd	11.84	13.77	13.84	13.19	13.16	11.16	12.92	12.51	12.36	12.24
Average	12.02	14.15	14.14	13.43	13.43	11.87	13.48	12.89	12.46	12.68

Anova Table

Source of variation	Degrees of freedom	Sum of squares	Mean sum of squares	F cal	F prob
Replications	3	2.211	0.737	-	-
Factor A	3	25.148	8.383	18.768^{***}	0.000
Factor B	3	39.148	13.049	29.216^{***}	0.000
Factor C	1	0.195	0.195	0.437^{ns}	0.510
AxB	9	56.570	6.286	14.073^{***}	0.000
AxC	3	0.586	0.195	0.437^{ns}	0.727
BxC	3	0.336	0.112	0.251^{ns}	0.861
AxBxC	9	0.508	0.056	0.126^{ns}	0.999
Error	93	41.539	0.447	-	-
Total	127	166.242	-	-	-

		A	B	C	AxB	AxC	BxC	AxBxC
Lsd	0.332	0.332	0.235	0.664	0.469	0.469	0.939	0.332
	0.439	0.439	0.311	0.879	0.621	0.621	1.243	0.439

0 – control (without fertilization), N_1 - 60 kg ha^{-1} of nitrogen, N_2 - 100 kg ha^{-1} of nitrogen, N_3 - 120 kg ha^{-1} of nitrogen. ***Significant at $p < 0.01$; ns – non-significant

Analysis of variance showed that the protein content in grain in all tested varieties in both years of research on fertilized variants was higher ($p < 0.01$) compared to those achieved in the control (variant without fertilization), with the highest average protein content in all varieties, observed using the lowest dose of nitrogen (60 kg ha^{-1}). A further increase in the amount of nitrogen simultaneously accompanied by an increase in yield led to a decrease in grain protein content in varieties Tango and PKB Vožd while varieties Kg-20 and Favorit had the highest protein content in grain in the variant where nitrogen was used in 100 kg ha^{-1}, but only in the first year. These differences were not statistically significant. On average, the Favorit variety had the highest protein content in both years of research. At the same time, the mentioned variety achieved the lowest yield.

On the other hand, the lowest average protein content was found in the grain of the Tango variety. Flajšman et al. (2020) based on their research found that the use of mineral nitrogen reduces the protein content, which is contrary to the results of La Menza et al. (2017). The data in *Table 5* indicate a statistically highly significant influence of variety specificity and fertilization on the protein content in the grain and

http://www.aloki.hu ● ISSN 1589 1623 (Print) ● ISSN1785 0037 (Online)
DOI: http://dx.doi.org/10.15666/aeer/2005_37793792

that the same tendency was observed in the interactions of varieties x fertilization. The individual effect of year and the effects of interactions between cultivar x fertilization, fertilization x year and cultivar × fertilization x year on grain protein content in the studied winter triticale varieties was statistically nonsignificant. Our results partially confirm the results of Janušauskaitė (2014) who stated that the yield and quality of triticale in addition to fertilization also depends on climatic conditions, and Salehi and Arzani (2013) add the influence of genotype. The fact that we have established significant differences in the mentioned trait in different cultivars, and on the same variants of fertilization, indicates how much influence the genotype can have on the protein content in the grain.

The results of two-year research, based on the Pearson coefficient, indicate the existence of a negative correlation between grain yield and protein content in grain ($r = -0.92$; $R^2 = 0.85$, *Figure 1*), which is in line with the results of Salehi and Arzani (2013) who also noticed in their experiments the appearance of a negative correlation between the mentioned quantities ($r = -0.92$ or $r = -0.72$) and that this is a well-known fact when it comes to cereals. In contrast, Kara and Uysal (2009) stated in their paper that the results of their research indicate the existence of a significant ($p < 0.01$) positive association ($r^2 = 0.451$) between grain protein content and triticale grain yield.

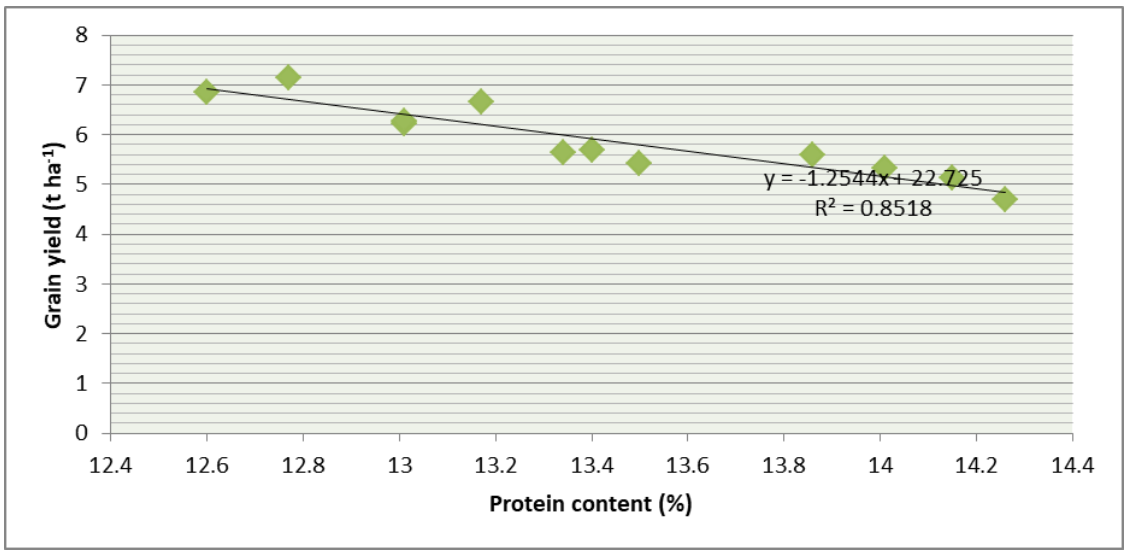

Figure 1. *Relationship between grain yield and protein content over two years*

Precisely because of that, protein yield per unit area is of special importance, so in our research it was on average for all varieties from 0.38 t ha^{-1} in the control variant in the second year of research to 0.89 t ha^{-1} in the first year and in the variant where nitrogen was used in the amount of 120 kg ha^{-1}. If we look at the varieties individually, then we can point out that the PKB Vožd variety achieved the highest protein yield and that it was the highest in the variant of fertilization where nitrogen was used in the amount of 120 kg ha^{-1} in both years of research (*Figure 2*). In this regard, he singles out the PKB Vožd variety as the most suitable for the conditions in which the research was conducted.

http://www.aloki.hu ● ISSN 1589 1623 (Print) ● ISSN1785 0037 (Online)
DOI: http://dx.doi.org/10.15666/aeer/2005_37793792

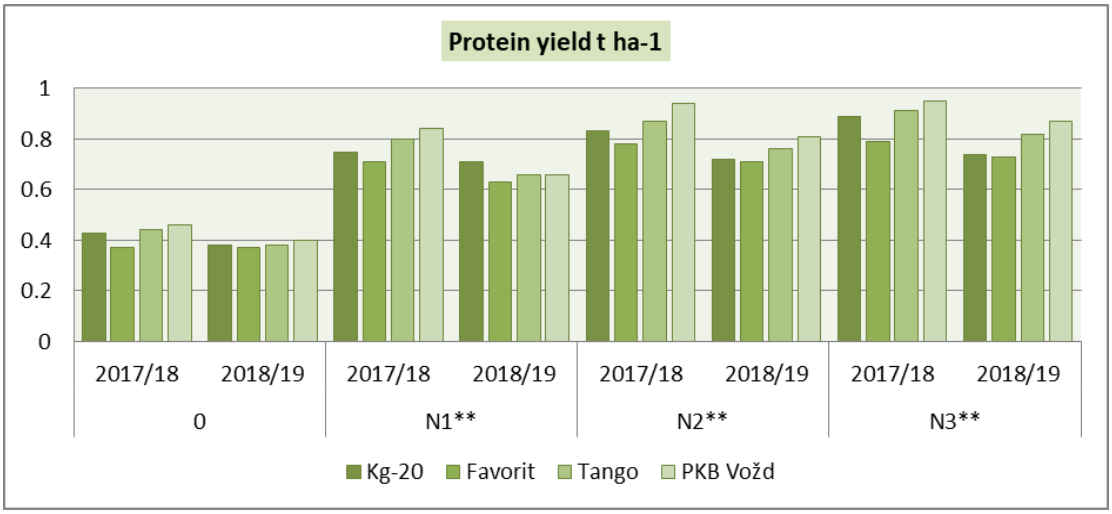

Figure 2. *Protein yield (t ha^{-1}) depending on variety, year and fertilization variant. 0 – control; N_1 - 60 kg ha^{-1}, 100 kg ha^{-1} P_2O_5, 100 kg ha^{-1} K_2O; N_2 - 100 kg ha^{-1}, 100 kg ha^{-1} P_2O_5, 100 kg ha^{-1} K_2O; N_3 - 120 kg ha^{-1}, 100 kg ha^{-1} P_2O_5, 100 kg ha^{-1} K_2O. ** significant at $p<0.05$*

Conclusion

The results of examining the influence of variety and different fertilizer variants on yield, yield components and protein content in triticale grain during the two-year period indicate the existence of differences in the achieved results both between the varieties and between the fertilization variants.

The PKB Vožd variety and the use of nitrogen in the amount of 120 kg ha^{-1} in combination with phosphorus and potassium in the amount of 100 kg ha^{-1} in the observed conditions gives the best results in terms of yield.

When we talk about quality parameters, the mentioned variety had the highest mass of 1000 grains in both years of research. The results of two years of research show that the average mass of 1000 grains for all varieties was the highest in the variant where nitrogen was used in the amount of 120 kg ha^{-1}.

The highest hectoliter weight, on average in both years of research, achieved the variety Tango.

On average, the Favorit variety had the highest protein content in both years of research.

Variety PKB Vožd had the highest protein yield per unit area, which, in addition to the highest grain yield and mass of 1000 grains, recommends it for wider production in this production area. Variance analysis indicated that the individual effect of variety, fertilization, as well as the effects of interaction between variety x fertilization and fertilization x year, for all observed traits in the examined winter triticale varieties were statistical significant ($p<0.01$). The year did not have a statistically significant influence on the values of the observed parameters.

http://www.aloki.hu ● ISSN 1589 1623 (Print) ● ISSN1785 0037 (Online)
DOI: http://dx.doi.org/10.15666/aeer/2005_37793792

REFERENCES

[1] Alazmani, A. (2015): Evaluation of yield and yield components of barley varieties to nitrogen. – International Journal of Agriculture and Crop Sciences IJACS 8(1): 52-54.
[2] Bezabih, A., Girmay, G., Lakewu, A. (2019): Performance of triticale varieties for the marginal highlands of Wag-Lasta, Ethiopia. – Cogent Food & Agriculture 5: 1-11.
[3] Bielski, S., Romaneckas, K., Šarauskis, E. (2020): Impact of Nitrogen and Boron Fertilization on Wimter Triticale Productivity Parameters. – Agronomy 10: 279.
[4] Blum, A. (2014): The abiotic stress response and adaptation of triticalea review. – Cereal Research Communication 42: 359-375. doi:10.1556/CRC.42.2014.3.1.
[5] Cantale, C., Petrazzuolo, F., Correnti, A., Farneti, A., Felici, F., Latini, A., Galeffi, P. (2016): Triticale for bionergy production. – Agriculture and Agricultural Science Procedia 8: 609-616.
[6] Darguza, M., Gaile, Z. (2020): The effect of crop rotation and soil tillage on winter wheat yield. – In Annual 26th International Scientific Conference Research for Rural Development, Jelgava, Latvia: Latvia University of Life Sciences and Technologies 35: 14-21. doi: 10.22616/rrd.26.2020.002.
[7] Đekić, V., Mitrović, S., Šefer, D., Obradović, S., Vukašinović, M. (2012): The effect of different varietes of triticale on the product characteristics in broiler chickens. – Veterinarski glasnik 66(5-6): 345-353.
[8] Dumbravă, M., Ion, V., Epure, L. I., Băsa, A. G., Ion, N., Dusa, E. M. (2016): Grain yield and yield components at triticale under different technological conditions. – Agriculture and Agricultural Science Procedia 10: 94-103.
[9] Epure, L. I., Ion, V., Băşa, A. Gh., Dumbrava, M., Epure, D. G., Temocico, G. (2015): Results regarding the biomass yield at triticale undre different technological conditions. – Book of Proceedings, Sixth International Agricultural Syposium „Agrosym 2015“: 273-278.
[10] Estrada-Campuzano, G., Slafer, G. A., Miralles, D. J. (2012): Differences in yield, biomass and their components between triticale and wheat grown under contrasting water and nitrogen environments. – Field Crops Research 128: 167-179.
[11] Flajšman, M., Mihelič, R., Kolmanič, A., Kocjan Ačko, D. (2020): Influence of soil amended with zeolite and/or mineral N on agronomic performance and soil mineral N dynamics in a soybean–winter triticale crop rotation field experiment. – Cereal Research Communications 48: 239-246.
[12] Gerdzhikova, M. (2014): Influence of N fertilization and predecessors on triticale yield structure characteristics. – Balkan Agriculture Congress, September 08-11, 2014, Edirne, Turkey, Turkish Journal of Agricultural and Natural Sciences, Special Issue 2: 1922-1932.
[13] Gerdzhikova, M., Grozeva, N., Pavlov, D., Tzanova, M. (2017): Effect of nitrogen fertilization in Triticale (X Triticosecale wittm.), cultivated after different predecessors, nitrogen uptake and efficiency. – AGROFOR International Journal 2(3): 147-156.
[14] Glamočlija, N., Starčević, M., Ćirić, J., Šefer, D., Glišić, M., Baltić, Ž., Marković, R., Spasić, M., Glamočlija, Đ. (2018): The importance of triticale in animal nutrition. – Veterinary Journal of Republic of Srpska (Banja Luka) XVIII(1): 73-94. doi: 10.7251/VETJ1801073G.
[15] Hirzel, J., Paredes, M., Becerra, V., Donoso, G. (2020): Response of direct seeded rice to increasing rates of nitrogen, phosphorus, and potassium in two paddy rice soils. – Chilean Journal of Agricultural Research 80(2): 263-273. doi:10.4067/S0718-58392020000200263.
[16] Ivanova, A., Tsenov, N. (2014a): Production potential of new triticale varieties grown in the region of Dobrudzha. – Agricultural Science and Technology 6: 243-246.
[17] Ivanova, A., Tsenov, N. (2014b): Comparative evaluation of triticale cultivars grown in the region of Dobrudzha. – Agricultural Science and Technology 6: 387-391.

http://www.aloki.hu ● ISSN 1589 1623 (Print) ● ISSN1785 0037 (Online)
DOI: http://dx.doi.org/10.15666/aeer/2005_37793792

[18] Jaćimović, G., Malešević, M., Aćin, V., Hristov, N., Marinković, B., Crnobarac, J., Latković, D. (2012): Winter wheat yield and yield components depending on the level of nitrogen, phosphorus and potassium fertilization. – Annals of Agronomy 36(1): 72-80. (In Serbian).
[19] Janušauskaite, D. (2013): Spring triticale yield formation and nitrogen use efficiency as affected by nitrogen rate and its splitting. – Zemdirbyste 100: 383-392.
[20] Janušauskaitė, D. (2014): Analysis of grain yield and its components in spring triticale under different N fertilization regimes. – Zemdirbyste 101: 381-388.
[21] Jelić, M., Dugalić, G., Milivojević, J., Đekić, V. (2013): Effect of liming and fertilization on yield and quality of oat (*Avena sativa* L.) on an acid Luvisol soil. – Romanian Agricultural Research 30: 239-248.
[22] Kara, B., Uysal, N. (2009): Influence on Grain Yield and Grain Protein Content of Late-Season Nitrogen Application in Triticale. – Journal of Animal and Veterinary Advances 8(3): 579-586.
[23] Kirchev, H., Delibaltova, V., Matev, A., Kolev, T., Yanchev, I. (2014): Analysis of productivity of triticale varieties grown in Thrace and Dobrudja depending on nitrogen fertilization. – Journal of Mountain Agriculture on the Balkans 17(2): 328-335.
[24] Küçüközdemir, Ü., Dumlu, B., Yalcın, Z., Karagöz, H. (2019): Determination of Yield, Quality and Winter Hardiness Characteristics of Some Triticale (xTriticosecale Wittmack) Genotypes in Pasinler and Erzincan Locations. – Ekin Journal of Crop Breeding and Genetics 5(2): 74- 83.
[25] Küçüközdemir, Ü., Dumlu, B., Karagöz, H., Yılmaz, O. (2021): Determination of yield and cold hardiness of some triticale (xTriticosecale Wittmack) genotypes in Eastern Anatolia Region. – Journal of Agricultural Production 2(1): 26-31.
[26] Lalević, D., Biberdžić, M., Ilić, S. Z., Milenković, L., Stojiljković, J. (2019): Productivity and quality of grains of triticale varieties at various quantities of mineral nutrition. – Journal of Agricultural Sciences 64(4): 341-352.
[27] La Menza, N. C., Monzon, J. P., Specht, J. E., Grassini, P. (2017): Is soybean yield limited by nitrogen supply? – Field Crops Research 213: 204-212.
[28] Losert, D. (2017): Phenotypic, Genetic, and Genomic Assessment of Triticale Lines and Hybrids. – Dissertation, University of Hohenheim, Faculty of Agriculture: p.7.
[29] Madic, M., Đurovic, D., Paunovic, A., Jelic, M., Kneževic, D., Govedarica, B. (2015): Effect of nitrogen fertilizer on grain weight per spike in triticale under conditions of central Serbia. – Sixth International Scientific Agricultural Symposium "Agrosym 2015", Jahorina, Bosnia and Herzegovina, October 15-18, 2015. Book of Proceedings: 483-487.
[30] Massimi, M., Al-Rifaee, M. K., Alrusheidat, J., Dakheel, A., Ismail, F., Al-Ashgar, Y. (2016): Salttolerant Triticale (X Triticosecale Witt) Cultivation in Jordan as a New Forage Crop. – American Journal of Experimental Agriculture 12(2): 1-7.
[31] Nikolić, O., Zivanović, T., Jelić, M., Đalović, I. (2012): Interrelationships between grain nitrogen content and other indicators of nitrogen accumulation and utilization efficiency in wheat plants. – Chilean Journal of Agricultural Research 72: 111-116.
[32] Nogalska, A., Czapla, J., Skwierawska, M. (2012): Effect of multicomponent fertilizers on spring triticale yield, the content and uptake of micronutrients. – Journal of Elementology 17: 95-104.
[33] Novak, L., Liubych, V., Poltoretskyi, S., Andrushchenko, M. (2019): Technological indices of spring wheat grain depending on the nitrogen supply. – Modern Development Paths of Agricultural Production: Trends and Innovations: 753-761. DOI: 10.31388/2220-8674-2019-1-55.
[34] Oral, E. (2018): Effect of nitrogen fertilization levels on grain yield and yield components in triticale based on AMMI and GGE biplot analysis. – Applied Ecology and Environmental Research 16(4): 4865-4878.

http://www.aloki.hu ● ISSN 1589 1623 (Print) ● ISSN1785 0037 (Online)
DOI: http://dx.doi.org/10.15666/aeer/2005_37793792

[35] Peltonen-Sainio, P., Jauhiainen, L., Laurila, I. P. (2009): Cereal yield trends in northern European conditions: Changes in yield potential and its realization. – Field Crops Research 110: 85-90.
[36] Roques, S. E., Kindred, D. R., Clarke, S. (2017): Triticale out-performs wheat on range of UK soils with a similar nitrogen requirement. – The Journal of Agricultural Science 155: 261-281.
[37] Salehi, M., Arzani, A. (2013): Grain quality traits in triticale influenced by field salinity stress. – Australian Journal of Crop Science 7(5): 580-587.
[38] Studnicki, M., Derejko, A., Wójcik-Gront, E., Kosma, M. (2019): Adaptation patterns of winter wheat cultivars in agro-ecological regions. – Scientia Agricola 76(2): 148-156.
[39] Terzic, D., Djekic, V., Jevtic, S., Popovic, V., Jevtic, A., Mijajlovic, J., Jevtic, A. (2018): Effect of long term fertilization on grain yield and yield components of winter triticale. – The Journal of Animal & Plant Sciences 28(3): 830-836.
[40] Wójcik-Gront, E. (2018): Variables influencing yield-scaled Global Warming Potential and yield of winter wheat production. – Field Crop Research 227: 19-29.
[41] Wójcik-Gront, E., Studnicki, M. (2021): Long-Term Yield Variability of Triticale (×Triticosecale Wittmack) Tested Using a CART Model. – Agriculture 11(2): 2-12.

http://www.aloki.hu ● ISSN 1589 1623 (Print) ● ISSN1785 0037 (Online)
DOI: http://dx.doi.org/10.15666/aeer/2005_37793792

LOW TEMPERATURE AND VEGETATION EFFECTS ON THE SOIL BACTERIAL COMMUNITIES STRUCTURE IN HIGH MOUNTAINOUS AND COLD BIOTOPES IN KYRGYZSTAN

DOOLOTKELDIEVA, T. D.[1*] – BEKTURGANOVA, B. S.[2] – BOBUSHEVA, S. T.[1]

[1]*Plant Protection Department, The Kyrgyz-Turkish Manas University, Ch. Aytmatov street, 56, Bishkek city 720044, Kyrgyzstan*

[2]*Ecology Department, The Kyrgyz National Agrarian University of Skryabin, Mederov Street, 54, Bishkek city 720055, Kyrgyzstan*

[*]*Corresponding author*
e-mail: tdoolotkeldieva@gmail.com; phone: +916-312-552-501-668; fax: +916-312-541-935

(Received 10th Mar 2022; accepted 11th Jul 2022)

Abstract. It is well known that soil microorganisms play essential roles in the biogeochemical cycling of biogenic elements and soil-forming processes. However, little is known about the effect of the vegetation type on the bacterial community structures in soils from cold regions. For these reasons, we have analysed the bacterial communities of eight biotopes covered with different plants and two biotopes without vegetation in the Son-Kull Valley as the coldest corner in Kyrgyzstan. Using the culture-depended and culture-independent (16S rRNA gene sequencing) methods, we found 4 phylum (Actinobacteria- 55.0%, *Proteobacteria*- 30%, *Firmicutes*- 13%, and *Bacteroides*- 2%) and 5 classes of the bacterial community, with dominant classes of *Actinomycetia* (60.03%), *Gammaproteobacteria* (25.0%), Bacilli (10.0%), *Bacteroidia* (3.0%) and *Alphaproteobacteria* (2.0%). The dominant generalist genera were *Arthrobacter, Pseudomonas, Actinobacter, Dermacoccus, Brevibacterium,* and *Micrococcus.* The results have confirmed that bacterial community structures were significantly affected by the vegetation type and environment factor, such as temperature. The diversity of the bacterial community was higher in the rhizosphere of succulent vegetation with a short lifespan, that is, in ephemerals, and with a high content of organic matter, like manure, in soil. The soil under the snow harboured the highest proportion of uncultured bacteria, representing *Actinobacteria* phylum.
Keywords: *environment factor, soil-forming bacteria, 16S rRNA gene of bacterial diversity, dominant soil bacterial phylotypes and classes*

Introduction

In some regions on Earth, the temperature can reach 30 °C or more in summer. However, in areas with a temperate climate, the soil temperature never reaches 20 °C, and the temperature drops below freezing in winter in many regions. In these cold regions, harsh climatic conditions, such as sudden changes in temperature, strong winds, ultraviolet radiation and an acute lack of moisture, significantly reduce the primary production of organic matter and thereby determine soil formation characteristics (Brambilla et al., 2001; Smith et al., 2006; Olubukola et al., 2009; Yang et al., 2015; Zhang et al., 2016). Cold ecosystems are susceptible to climate change, and microorganisms play a critical ecological role in these habitats; therefore, understanding their role and potential has a significant environmental and scientific importance (Margesin and Collin, 2019; Collins and Margesin, 2019).

These cold environments are colonised by cold-adapted, psychrophilic and psychrotolerant microorganisms, which can grow at temperatures of 0 °C and below (Gray and Williams, 1971; Neufeld and Mohn, 2005; Anesio et al., 2009; Mackelprang

http://www.aloki.hu ● ISSN 1589 1623 (Print) ● ISSN 1785 0037 (Online)
DOI: http://dx.doi.org/10.15666/aeer/2005_37933815

et al., 2011; Harding et al., 2011; Ghiglione et al., 2012; Crump et al., 2012; Lee et al., 2013; Larose et al., 2013; Cuthbertson et al., 2017).

These cold-adapted soil fungi and bacteria take a leading role; they perform biochemical processes, drive the cycling of biogenic elements (e.g., carbon, nitrogen, phosphorus, potassium) necessary for plant nutrition in the soil, decompose plant residue and form organic matter in the ground (Goodfellow and Williams, 1983; Holmalahti et al., 1994; Wynn-Williams, 1996; Hill et al., 2011; Bottos, et al., 2014; Lysak et al., 2018).

Bacteria contribute to the decomposition of plant residue by producing a range of extracellular hydrolytic enzymes that can degrade animal and plant polymers, including lignin, cellulose, chitin and other organic compounds (Eisenlord and Zak, 2010).

Psychrotrophic bacteria are usually found in temperate climate soils, and, as a rule, they grow in a wide temperature range (Ingram, 1965; Druce and Thomas, 1970). To survive and thrive in harsh conditions, they have developed a series of adaptations in particular cellular components and biochemical pathways involved in metabolism to compensate for the negative effects of low temperatures (Larose et al., 2013; Boetius et al., 2015).

Soil type, soil pH and cover vegetation can influence the distribution of different bacterial species population in soil habitat (Matsukawa et al., 2007; Han et al., 2007; Hayakawa, 2008; Xu et al., 2014). Assessing and measuring the biodiversity of soil bacteria in relation to local vegetation can reveal the ecological role and function of bacteria in soil formation and ecosystem integrity (Babalola et al., 2007; Xu et al., 2014). Extreme cold environments are mainly dependent on microbial activities because this climate restricts higher plants and animals (Dhakar and Pandey, 2020).

The high-altitude Son-Kul valley is a unique and not yet explored corner of the globe for microbiological biodiversity, which determines the processes of decay and transformation of plant organic matter at low-temperature conditions. This territory is highly elevated; it includes the high-mountainous basin of Son-Kul Lake surrounded by mountains and is located at more than 3000 m above sea level. The average annual air temperature is minus 2 °C. In July, summer is rainy and cold with an average monthly temperature of 7–10 °C. The Son-Kul basin soils are subalpine, alpine, meadow-steppe and meadow (Mamytov, 1974, 1996).

In this work, we aimed to study the quantitative content and biodiversity structure of the heterotrophic bacterial block responsible for organic decomposition residues in different biotopes of the Son-Kul valley, focusing on various altitudinal belts. The overall goal was to understand the functioning of this coldest corner of the globe.

Materials and Methods

The soil types in the Son-Kul valley of Kyrgyzstan, described by A. Mamytov (1974, 1996)

On the one hand, the Son-Kul valley soils have chestnut and chernozem features, and on the other hand, they have subalpine and alpine mountain-steppe features. Due to the high elevation of the territory, the soil-forming process takes place during a short growing season. These soils are well-sod, humus-rich and have a light alkaline reaction.

Mountain meadow subalpine soils are formed under subalpine meadow vegetation, which is dominated by meadow timothy grass, bluegrass, fescue, sedge and so on. Such soils contain significant humus (8–15%). They are leached from carbonates and have a pH of 6.5–7.0. These soils are well structured.

http://www.aloki.hu ● ISSN 1589 1623 (Print) ● ISSN 1785 0037 (Online)
DOI: http://dx.doi.org/10.15666/aeer/2005_37933815

Mountain meadow steppe alpine soils are formed under alpine meadow-steppes. They are characterized by a dark grey colour of the humus horizon, a lumpy-granular structure. Meadow-steppe-alpine soils are rich in humus (10-11%). The grounds are carbonate from the surface, the amount of CO_2 in the humus horizon does not exceed 1.5-3.0%. The reaction of the soil solution is neutral or slightly alkaline. These soils belong to medium and heavy loams according to the mechanical components.

Mountain meadow alpine soils are formed under alpine meadows on northern (shaded) slopes of ridges in the alpine belt zone. They are characterised by a dark grey and black colour, granular structure and good sodding. The soils are characterised by a high content of total nitrogen (0.6-0.8%), gross phosphorus (0.25-0.40%) and potassium (2.6-4.0%). Mountain meadow alpine soils are containing a humus of 6.7-8.13%.

Alpine semi peaty soils of cobresia barrens exhibit strong turfiness at the upper horizon, which has a dark colour, and resemble peat. They are rich in humus (up to 20%), with deep penetration along with the profile. They are characterised by a neutral reaction of the soil environment (pH = 7.0-7.4) or a weakly alkaline reaction (pH = 7.7-8.4).

Sampling site description and sample collection

The study area was located in the Son-Kul valley. The valley includes the alpine lake Son-Kul, the Son-Kul Too ridge to the north and the Borbor Alabas and Moldo Too mountains to the south (*Fig. 1*). The valley lies at an altitude of 3,016 m and has an area of about 270 km^2 and a volume of 2.64 km^3. The lake's maximum length is 29 km, its breadth is about 18 km and the deepest point is 13.2 m. It is the second-largest lake in Kyrgyzstan, after Issyk Kul, and the largest freshwater lake in Kyrgyzstan. The mean temperature in the lake basin is −3.5 °C (25.7 °F), with a mean temperature of −20 °C (−4 °F) in January and 11 °C (52 °F) in July.

A) B)

Figure 1. *A) A map of the Son–Kul valley (Latitude: 41° 49' 59.99" N, Longitude: 75° 09' 60.00" E) and (B) a view of the lake*

Annual precipitation averages 300–400 mm from April to October and 100–150 mm from November to March. Snow cover in the lake basin persists for 180 to 200 days a year. In winter, the lake surface freezes, and the ice can be up to 1–1.2 m thick. The ice on Son-Kul begins to thaw in mid to late April and completely disappears by late May (Ramsar Sites Information Service, 2011).

Samples were taken from the rhizosphere soil and the soil without vegetation in the summer (middle of July) from 10 biotopes. Samples were taken at every 100 m, moving

http://www.aloki.hu ● ISSN 1589 1623 (Print) ● ISSN 1785 0037 (Online)
DOI: http://dx.doi.org/10.15666/aeer/2005_37933815

from the lakeshore to the top of the subalpine and alpine belts of the Kondoy Too mountain range, which has permafrost in the summer. A detailed description of the investigation sites is given in *Table 1*.

Table 1. *Soil sampling sites in the Son-Kul valley*

Site and sample numbers	Description of localities and covered vegetation	Soil type	Air temperature ° C	Soil temperature ° C	Altitude, meter above sea level and GPS coordinates	pH soil
SK-1	The coast of Lake Son-Kol (10 m from the beach). Vegetation - low-grass meadows dominated by the common skullcap (*Scutellaria galericulata)*	Alpine semi-peaty soils	18.1	8.3	3027; 41°50' 45.620" N and 75°9'07.877" E	7.77
SK-2	Terrain 100 m from the coast of Son-Kul. Meadow undersized Forbes associations. Dominated by edelweiss (*Leontopodium fedschen-kaanum*).	Mountain-meadow-steppe-alpine soils	18.1	10.0	3031; 41°50' 45.611" N and 75°9'07.890" E	7.17
SK-3	The depression between the foothills of the ridge "Suuk Kolot" 1.5 km from the lake, meadow forb vegetation, yellow geraniums and tulips dominate.	Mountain-meadow-steppe-alpine soils	15.3	8.0	3095; 41°50' 45.286" N and 75°9'07.974" E	7.67
SK-4	The Suuk Kolot ridge. Vegetation meadow, peat-bog cereal communities dominate	Mountain-meadow alpine soils	9.3	7.3	3200; 41°50' 45. 123" N and 75°9'07.995" E	8.28
SK-5	Floodplain banks of the Uzun-Bulak River. Meadow vegetation, feather grass and geranium prevail	Mountain-meadow-steppe-alpine soils	9.4	9.5	3088; 41°50' 42. 279" N and 75°9'04. 410" E	8.115
SK-6	Uzun-Bulak. Heavily used for livestock, the soil is fertilised with manure, dominated by dandelion (*Taraxacum officinale*) and cinquefoil.	Mountain-meadow-steppe-alpine soils	9.0	8.6	3103; 41°50' 42. 224" N and 75°9'04. 465" E	7.93
SK- 7	Foothill area "Kondoy Too"southern ridge, low-growing mountain-valley vegetation, labiate associations dominate	Mountain-meadow alpine soils	8.1	8.4	3141; 41°50' 42. 0.19" N and 75°9'03. 636" E	7.59
SK-8	Top of the Kondoy Too mountain, near a mountain glacier. Alpine meadows. A dense thicket of wild onion association and yellow tulips.	Mountain-meadow alpine soils	11.16	8.9	3222; 41°50' 41. 929" N and 75°9'03.407" E	6.32
SK-9	Top of the Kondoy Too mountain, soil under a glacier, soil moisture 100%. No vegetation.	Mountain-meadow alpine soils	11.7.	0.0	3243, 41°50' 41. 937" N and 75°9'03.380" E	6.59
SK-10	Top of the mountain "Kondoy Too", soil under a melting glacier, humidity soil - 100%, without vegetation	Mountain-meadow alpine soils	10.7	3.0	3244; 41°50' 41. 963" N and 75°9'03.310" E	6.50

http://www.aloki.hu ● ISSN 1589 1623 (Print) ● ISSN 1785 0037 (Online)
DOI: http://dx.doi.org/10.15666/aeer/2005_37933815

Three repeating plots were randomly selected for each type of vegetation. The size of each plot was ~20 m × 20 m. A soil sample was taken from the depth of the root system (5–20 cm) under the dominant plant species in each plot with a soil drill (5 cm in diameter). Before sampling, the top 2-3 cm of sod was removed. Selection was carried out in good weather, in the morning before the onset of heat or at the end of the day, so the sample was as dry as possible. The resulting samples were mixed and formed the average specimen. Each mixed piece was composed of 5 individual samples taken from 5 points. The mass of the sample for analysis was 300-400 g. Notes were attached to all samples, which contained all their characteristics: the exact place of taking and the plot area.

The samples were stored in double sterile plastic bags, labelled and transported to the laboratory. The samples were conserved in an incubator with ice bags during transportation. The soil samples were frozen at −80 °C until nucleic acid extraction. The samples were air-dried at room temperature, separated from roots and debris and passed through a 2-mm plastic sieve before chemical and microbiological analysis. The pH was determined using a pH meter (Thermo Scientific, Orion Laboratory Products) and exchangeable and hydrolytic acidity were measured by titration with KCl and CH_3COONa, respectively (soil: solution ratio of 1:2.5). Carbon and nitrogen content was measured using a soil elemental analyser (ElvaX Plus spectrometer, Elvatech Ltd., Canada). All physical-chemical and biological parameters were analysed in triplicate at a minimum (n = 3–6). Soil classification was performed according to Mamytov (1971, 1996).

Isolation of bacteria from soil by cultivation-dependent approach

To isolate bacteria species from the soil, soil samples were analyzed using the acetate selection protocol of Travers et al. and the methods of soil microbiology and biochemistry (Zvyagintsev, 1991) with some modifications. Samples of 10 g were prepared from each soil sample and ground in a sterile porcelain mortar for 5 min in aseptic conditions. After grinding, the soil sample was washed in sterile water. Ten milliliters of Luria-Bertani broth, 1 g from each soil sample, was added and buffered with sodium acetate (0.25 M, pH 6.8) in a 125-ml flask. The broth was incubated in a shaker at 200 rpm for 4 h at 28 °C. A 1-ml aliquot was spread on nutrient agar plates (NA), and incubated at 15^0, 20 ^{o} and 28 °C for 48–72 h. The colonies were subcultured on new NA plates until pure cultures were obtained, and they were kept at 4 °C for further identification.

The colonies were subjected to Gram staining, and the results were analysed along with colony shape and bacterial movement. The isolated bacterial cultures were studied for their ability to grow on meat-peptone broth (MPB), meat-peptone agar (MPA), oxidative-fermentative (OF) medium and catalase. Conventional tests were performed, such as protein hydrolysis, reduction of nitrates to nitrites, reduction of nitrates to nitrogen, indole production (tryptophane), fermentation (glucose), arginine dihydrolase, gelatin hydrolysis and the urea breath test. The phenotypic and biochemical characteristics of the isolates were established according to the determinants (Bergey's Manual of Determinative Bacteriology, 2004). Isolated bacteria were grouped on the basis of their morphological, biochemical and physiological characteristics.

For isolation and cultivation of bacteria, semi-differential media compositions were used: NutriSelect™ Plus (Merck KGaA) nutrient agar for microbiology (15 g L^{-1} agar; 1 g L^{-1} meat extract; 5 g L^{-1} peptone; 5 g L^{-1} sodium chloride; 2 g L^{-1} yeast extract); King medium (20 g protease peptone #3 (Difco); 1.5 g K_2HPO_4; 1.5 g $MgSO_4 \cdot 7H_2O$; 10 mL

http://www.aloki.hu ● ISSN 1589 1623 (Print) ● ISSN 1785 0037 (Online)
DOI: http://dx.doi.org/10.15666/aeer/2005_37933815

glycerol; 15 g agar; 1 L distilled water); and starch ammonium agar medium or ISP Medium No. 4 (10 g L^{-1} soluble starch; 1 g L^{-1} dipotassium phosphate; 1 g L^{-1} magnesium sulphate heptahydrate; 1 g L^{-1} sodium chloride; 2 g L^{-1} ammonium sulphate; 2 g L^{-1} calcium carbonate; 0.001 g L^{-1} ferrous sulphate heptahydrate; 0.001 g L^{-1} manganous chloride $7H_2O$; 0.001 g L^{-1} zinc sulphate $7H_2O$; 20 g L^{-1} agar; pH 7.2 ± 0.2; 25 °C).

To identify the bacteria species, modern special keys were used (Bergey's Manual of Systematics of Archaea and Bacteria, 2015). Pictures of bacterial cells were obtained using a microscopy camera (Motic Images Plus, Version 2.0 ML, Quick Start Guide, 163 Series Compound Biological Microscopes).

Determination of the colonies united form (CUF) of bacteria on nutrient medium per g soil

To calculate the number of microorganisms in soil using the inoculation method, two conditions must be met: the soil suspension from which the dilution is carried out must contain only single free-floating cells, and each cell, once on the nutrient medium, must produce a colony (Zvyagintsev, 1991).

The following method was used to determine the number of bacterial colony-forming units (CFU) per gram of soil. Under aseptic conditions, 1 g of soil was moistened to a paste and ground with a rubber pestle for 5 min. After preliminary dispersion of the ground, dilutions of the soil suspension were prepared. Plating was carried out at dilutions from 1:2 to 1:100,000, depending on the group of microorganisms, type of soil, season and soil moisture. The most accurate calculation is obtained when 50–200 CFU develop on a plate. The seeded cups were turned upside down and placed in a thermostat at 15^0, 20^o and 28 °C.

Bacterial colony counting on NA in Petri dishes was conducted at 7 days for the r-strategies group and at 10 days for the K-strategies group. Colonies were usually counted using a magnifying glass device without opening the Petri dishes. For convenience, the positions of the counted colonies were marked with dots on the underside of the dish using a glass marker. Having counted the number of colonies on all parallel plates, the average number of colonies per plate was determined and then recalculated per 1 g of air-dried and dried soil, according to the *formula (1)*:

With a large number

$$N = C / [V \times (n1 + 0, 1 \text{ X } n2) \times d] \quad \text{(Eq.1)}$$

where,
N = Number of CUF microorganisms in 1 g
C = Total number of CUF in all counted Petri dishes
V = Volume transferred to Petri dishes (1 ml)
n1 = Number of Petri dishes counted from the first dilution
n2 = Number of Petri dishes counted from the second dilution
d = Dilution factor of more concentrated than the 2 consecutive dilutions from which the calculation is made (10^{-2}). Based on the results obtained, the number of microorganisms per gram soil was calculated.

http://www.aloki.hu ● ISSN 1589 1623 (Print) ● ISSN 1785 0037 (Online)
DOI: http://dx.doi.org/10.15666/aeer/2005_37933815

Isolation of microorganisms from soil by cultivation-independent methods

DNA extraction, PCR amplification and sequencing of bacteria

DNA was extracted from the enrichment cultures during the active phase of microbial growth, using the Ultraclean Soil DNA Isolation Kit (Mo Bio Laboratories, Carlsbad, CA, USA) and alternative protocol developed by the Mo Bio Laboratories. To process soil samples, 5 g of soil was mixed with 10 to 30 mL of phosphate-buffered saline (PBS) to create homogenized slurry. Samples were mixed for 1 hour at room temperature and then centrifuged for 5 minutes at 123×g. The supernatant was removed and centrifuged at 20 000×g for 15 minutes. The supernatant was then carefully discarded, and the pellet was resuspended in 1 mL of PBS. To extract DNA, 700 uL of the resuspended soil extraction pellet was processed. The purified bacteria were incubated in meat peptone medium (MPM) for 2days at 25°C. Cells were harvested at the early exponential growth phase, and their DNA was then extracted by the alternative protocol of the Mo Bio Laboratories. Successful DNA extraction was determined by agarose gel electrophoresis (1.0% agarose). Amplification was performed with a Multi Gene Thermal Cycler (TC9600-G/TC, Labnet International, Edison, New Jersey, USA), using a 25 uL mixture containing 15 uL of PCR MasterMix (Taq DNA poly- merase, $MgCl_2$, deoxyribonucleotide triphosphate, and reaction buffer), 2 uL of each primer,1 uL of template DNA, and 1 uL of H_2O. The amplification program was used as the follows: 94°C for 5minutes, 35 cycles at 94°C for 30 seconds, 55°C for 30 seconds, 72°C for 60 seconds, and 72°C for 7 minutes. PCR products were electrophoresed in a 1.0% agarose gel and visualized using the BioDoc-It Imaging Systems (Ultra-Violet Products Ltd) after ethidium bromide staining. To control contamination, we used a negative control reaction, and sterile water was added as a matrix. Almost full-length fragments of 16Sp RNA genes were amplified using the primers 16S-27F (27f 5'-AGAGTT TGA TCC TGG CTC AG-3') and 16S-1492 R (5'-GGTTAC CTT CTT ACG ACT T-3'). Sequence analysis was performed by the Macrogen Company (10F World Meridian Center, Seoul, Korea), and sequences were edited with Applied Biosystems 3730XL sequencers. Only sequences with more than 700 nucleotides were used for diversity analyses. The phylogenetic relatedness among different sites was determined using the cluster environment. The 16S ribosomal RNA (rRNA) gene sequences were deposited in the GenBank and DB of the National Center for Biotechnology Information nucleotide sequence databases.

Statistical analysis

The Shannon index was used to determine the complete species composition of the bacterial community, including the abundant rare species at the studied sites. The Simpson index was used to characterise the community by the dominant group of species.

The obtained data were statistically processed using SPSS version 25 (IBM, USA).

Results

The ecological features of the Son-Kul valley that serve as habitats for plants and soil microorganisms

Seven altitude zones are conventionally distinguished in Kyrgyzstan. Son-Kul is located in subalpine and alpine areas, where subalpine and alpine meadows are

http://www.aloki.hu ● ISSN 1589 1623 (Print) ● ISSN 1785 0037 (Online)
DOI: http://dx.doi.org/10.15666/aeer/2005_37933815

widespread. The regional vegetation types vary with altitude (Tsekanov, 1979; Golovkova, 1990) in the Son-Kul basin. Soil organic carbon density ranged from 9.73 to 35.21 kg m ^{2} at 0–60 cm at the hill scale (Mamytov, 1974). The climate and vegetation change with every 100–200 m of ascent into the mountains. Only a few plant species are found in the glacial belt. The conditions here are very harsh, as they are in the tundra, and the plants that grow here do so in response to this natural and climatic zone. There is permafrost under the topsoil at the mountaintops. There are famous high-mountain pastures; in the alpine belt, they are covered with turf grasses, feather grass, fescue and grasses. Some plants grow only at certain altitudes; for example, edelweiss is not found below 2,000 m. Alpine tundra is found above 3,000 m, where the vegetation is poorer and more monotonous. Plants cover the soil, but not entirely. They are found in spots, ribbons and rings.

Density of bacterial colonies found in the studied biotopes of the Son-Kul valley

Number of bacterial species found growing at different temperatures

A total of 320 bacterial isolates belonging to various morphological groups and genera were isolated from the biotopes. They were cultivated in MPA at 0, 5, 15, 20 and 28 °C for 15 days. As *Figure 2* shows, the growth ability of the bacterial populations isolated from the 10 biotopes under the range of temperature conditions was significantly different. Of the isolates, 5.0% could grow at 0 °C, and these were found in the SK-9 and SK-10 site samples, which were permafrost and snow. When tested at 5 °C, 20% of the isolated bacterial populations grew, and they were isolated mainly from sites SK-8 and SK-9. About 30% of the natural isolates grew at 15 °C, and 35% established colony growth at 20 °C. These isolates were from locations other than SK-8, SK-9 and SK-10. At 28 °C, about 5.0% of the isolates could grow, representing species from sites SK-6, SK-5, and SK-2 (*Fig. 2*).

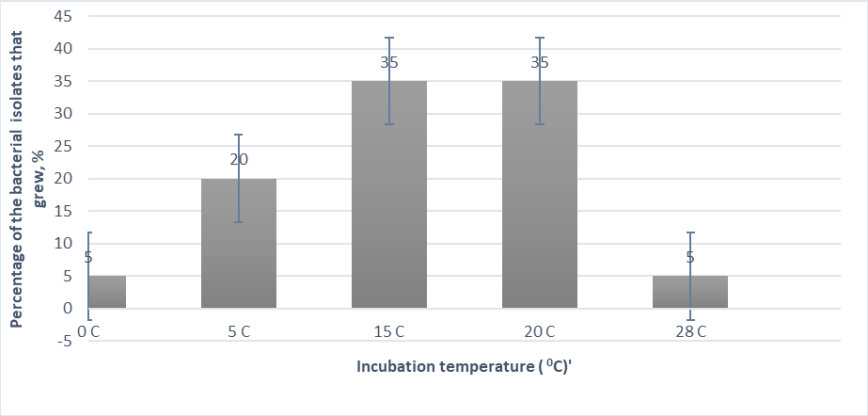

Figure 2. *The proportion of bacterial isolates found to grow at different temperatures. Values are given as mean ± SD, n = 3, significantly different at P ≤ .05*

The number of bacterial colony-forming units (CFU) able to grow at a temperature of 15-20 ^{0} C in the studied soils of the Son-Kul Valley

The number of ammonifying bacteria able to grow at 15–20 °C was examined in this study. We focused on this temperature range because these are the optimal temperatures

http://www.aloki.hu ● ISSN 1589 1623 (Print) ● ISSN 1785 0037 (Online)
DOI: http://dx.doi.org/10.15666/aeer/2005_37933815

at which heterotrophic, ammonifying bacteria are actively involved in the decomposition of fresh plant residue in the short summer period. The number of bacteria capable of decomposing organic residue in the different biotopes ranged from 4.3×10^3 to 25.3×10^3 CFU/g of soil, indicating a generally low bacterial biomass in this high-mountain region. The Uzun-Bulak soils were found to have the highest content of ammonifying bacteria: 25.3×10^3 CFU/g of soil. The lowest concentrations were found in the SK-9 and SK-10 samples, which were taken after the glacier melted (3,244 m.a.s.l.), with 3×10^2 CFU/g of soil (*Fig. 3*).

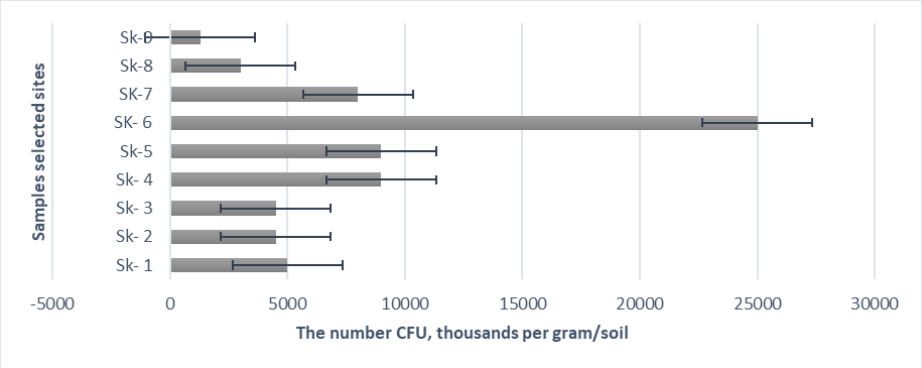

Figure 3. *The number of colony-forming unites (CFU) of heterotrophic bacteria in the studied soil biotopes of the Son-Kul Valley. Values are given as mean ± SD, n = 3, significantly different at P ≤ .05.*

Rhizosphere bacteria living around plant root systems and directly involved in the transformation of plant root exudates into mineral compounds were studied. However, the findings suggest that these bacterial communities have insignificant biomass due to low temperatures and sharp daily fluctuations. Significantly, high numbers of bacteria were found at the Uzun-Bulak site, where the soil was enriched with animal manure; a stall of sheep and a cow that grazed daily in the pasture were housed here at night each year. The annual introduction of animal protein into the soil promoted the activation of ammonifying bacteria and an increase in their biomass in this biotope.

Soil bacterial biodiversity determined using molecular identification

The molecular identification results show that during the summer, in high-altitude soils of the Son-Kul valley were dominated by the Firmicutes, Actinobacteria, Gammaproteobacteria, Betaproteobacteria genetic groups. The findings show that bacterial species composition differs in soils under different vegetation cover according to the terrain's altitude.

The SK-1 site (the coast of Son-Kul, 10 m from the beach) is located at 3,027 m.a.s.l. This site was covered with low-grass meadows dominated by the common skullcap (*Scutellaria galericulata)*. At this site, in the skullcap's rhizosphere, spore-forming bacteria were dominant, namely representatives of the phylum Firmicutes*: Bacillus sp, Bacillus pumilus, Bacillus safensis, and Bacillus altidudinus.* Also, non-spore-forming representatives of the same phylogenetic group were present: *Lactobacillus rhamnosus, Coprococcus eutactus, Dorea longicaten and Heliobacterium modesticaldum Ice1*. Phylum Actinobacteria representatives made up an insignificant share*: Collinsella aerofaciens, Dermacoccus sp. and Micrococcus* sp. (*Fig. 4*).

http://www.aloki.hu ● ISSN 1589 1623 (Print) ● ISSN 1785 0037 (Online)
DOI: http://dx.doi.org/10.15666/aeer/2005_37933815

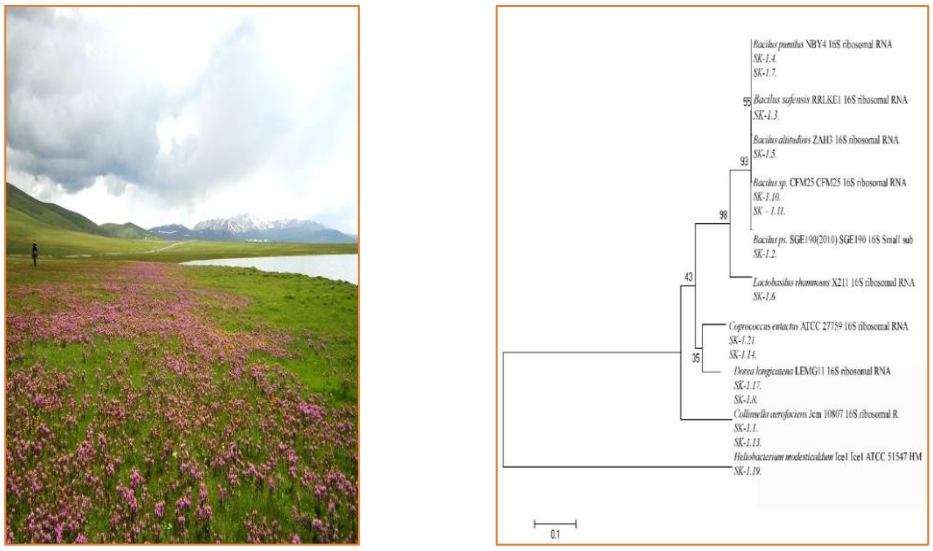

A B

Figure 4. *A- SK-1 site view; B- Phylogenetic tree of bacteria found in the soils of the Son-Kul Valley at the SK-1 site based on the analysis of 16SrRNA sequences. Each group contains at least > 97% sequence similarity available in the GenBank database*

The SK-2 site (100 m from the coast of Son-Kul) is located at 3,031 m.a.s.l. This site was covered with vegetation of meadow undersized Forbes associations and dominated by edelweiss (*Leontopodium fedschen-kaanum*). At this site, under the edelweiss population and in the rhizosphere of the alpine flowers, only non-spore-forming bacteria from the class Gammaproteobacteria (phylum Proteobacteria) were found: *Pseudomonas putida*, *Pseudomonas fluorescens*, *Pseudomonas migulae*, *Pseudomonas tolaasii*, *Pseudomonas corrugata*, *Pseudomonas thivervalensis*, *Pseudomonas chlororaphis subsp. aurantiaca*, *Pseudomonas brassicacearum* and *Pseudomonas* sp. (*Fig. 5*).

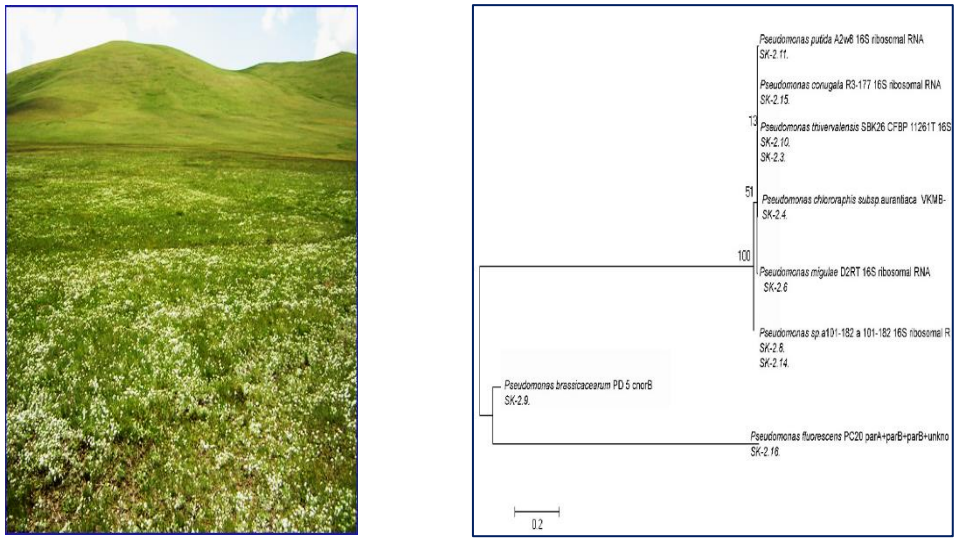

A B

Figure 5. *A- SK-2 site view; B- Phylogenetic tree of bacteria found in the soils of the Son-Kul Valley at the SK-2 site based on the analysis of 16SrRNA sequences. Each group contains at least > 97% sequence similarity available in the GenBank database*

http://www.aloki.hu ● ISSN 1589 1623 (Print) ● ISSN 1785 0037 (Online)
DOI: http://dx.doi.org/10.15666/aeer/2005_37933815

The SK-3 site (the depression between the foothills of the Suuk Kolot ridge, 1.5 km from the lake) is located at 3,095 m.a.s.l. This site is covered with meadow forb vegetation, and yellow geraniums (*Geranium maculatum*) and tulips (*Tulipa kaufmanniana*) dominate. At this site, under the geranium and tulip populations, in the rhizospheres of the alpine flowers, the same bacteria of the genus *Pseudomonas* were found as at SK-2, namely *P. thivervalensis* and *P. chlororaphis*. In contrast to SK-2, other species were found at SK-3: *Pseudomonas mandeli*, *Pseudomonas mediterranea*, *Pseudomonas frederiksbergensis*, *Pseudomonas borealis*, *Pseudomonas syringae*, *Pseudomonas collierea*, *Pseudomonas brenneri*, *Pseudomonas marginalis* and *Pseudomonas lin.* It is well-known that non-spore-forming bacteria, as active ammonifiers, decompose fresh plants. Therefore, their complete dominance in these two biotopes indicates their active involvement in the process of ammonification in high-mountain areas (*Fig. 6*).

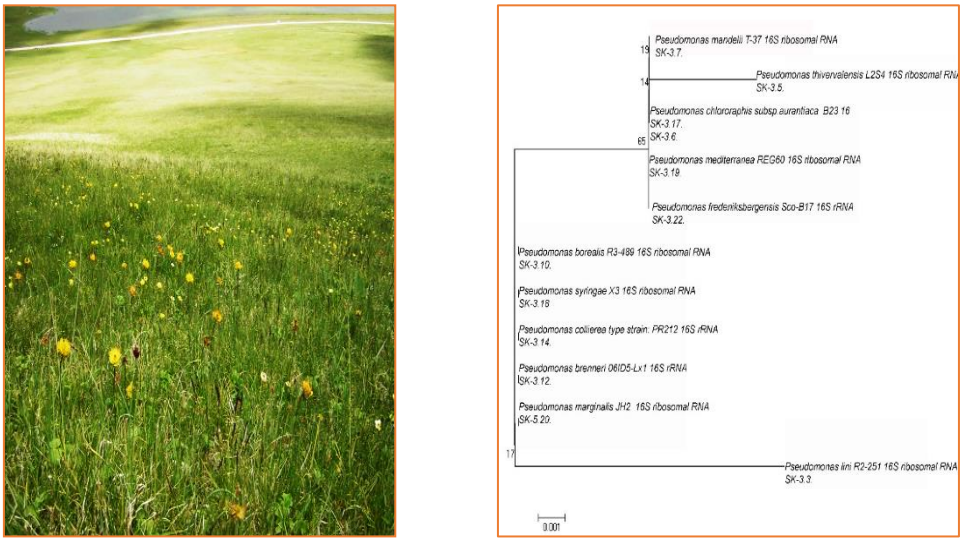

A B

Figure 6. *A- SK-3 site view; B- Phylogenetic tree of bacteria found in the soils of the Son-Kul Valley at the SK-3 site based on the analysis of 16SrRNA sequences. Each group contains at least > 97% sequence similarity available in the GenBank database*

The SK-4 site (the Suuk Kolot ridge) is located at 3,200 m.a.s.l. This site is covered with meadow vegetation, and peat-bog cereal communities are dominant. At this site, in the peat-bog cereal rhizospheres, it was found that representatives of the Actinobacteria phylum were dominant: *Arthrobacter sp.*, *Arthrobacter luteolus*, *Arthrobacter koreensis*, *Nocardia sp.*, *NanoD*, *Arthrobacter sp. everest*, *Arthrobacter gandavensis* and *Arthrobacter citreus*, as well as uncultivated bacteria: *Uncultural bacterium* (*Fig. 7*).

The SK-5 site, floodplain banks of the Uzun-Bulak River is located at an altitude of 3088 m.a.s.l., meadow vegetation, feather grass (Nassella tenuissima) and geranium (Geranium maculatum) are prevailed. At the SK-5 site, species of class Gammaproteobacteria (phylum Proteobacteria) predominate: *Stenotrophomonas rhizophila*, *Stenotrophomonas maltophilia*, *Stenotrophomonas sp.* and *uncultured Stenotrophomonas.* There are also significant representatives of the genus *Xanthomonas*: *Xanthomonas oryzae pv. oryzae* and *Xanthomonas bacterium IK1.* Representatives of other phyla were found in small amounts. For example, from Actinobacteria:

http://www.aloki.hu ● ISSN 1589 1623 (Print) ● ISSN 1785 0037 (Online)
DOI: http://dx.doi.org/10.15666/aeer/2005_37933815

Arthrobacter sp., from Firmicutes: *Brevibacterium sp.* and from *Bacteria: Uncultured bacterium sp.* (*Fig. 8*).

A B

Figure 7. *A- SK-4 site view; B- Phylogenetic tree of bacteria found in the soils of the Son-Kul Valley at the SK-4 site based on the analysis of 16SrRNA sequences. Each group contains at least > 97% sequence similarity available in the GenBank database*

A B

Figure 8. *A- SK-5 site view; B- Phylogenetic tree of bacteria found in the soils of the Son-Kul Valley at the SK-5 site based on the analysis of 16SrRNA sequences. Each group contains at least > 97% sequence similarity available in the GenBank database*

The SK-6 site (Uzun-Bulak) is located at 3,103 m.a.s.l. This site is heavily used for livestock. The soil is fertilised with manure, and the vegetation is dominated by dandelion (*Taraxacum officinale*) and cinquefoil (*Potentilla reptans*). At this site, almost 95% of the bacterial community was found to consist of representatives of the Actinobacteria

http://www.aloki.hu ● ISSN 1589 1623 (Print) ● ISSN 1785 0037 (Online)
DOI: http://dx.doi.org/10.15666/aeer/2005_37933815

phylum. However, within this phylogenetic group, rich genera and species diversity were found. The following six genera were found to make up the given proportions of the bacterial community: *Dermacoccus* (46.15%), *Terracoccus* (23.076%), *Janibacter* (7.6%), *Luteipulveratus* (7.6%), *Intrasporangium* (7.6%) and *Yimella* (7.6%). Genus *Dermacoccus* was represented by the following species: *Dermacoccus profundi*, *Dermacoccus barathni*, *Dermacoccus abyssi*, *Dermacoccus nishinomiyaensis* and *Dermacoccus sp. Ellin.* The following species were found in the genus *Terracoccus*: *Terracoccus sp. WPCB166*, *Terracoccus lapilli typestrain* and *Terracoccus terrae.* The genera *Intrasporangium*, *Janibacter*, *Luteipulveratus* and *Yimella* were all represented by one species each: *Intrasporangium calvum*, *Janibacter sp. BSi20546*, *Luteipulveratus mongoliensis* and *Yimella lutea*, respectively (*Fig. 9*).

A B

Figure 9. *A- SK-6 site view; B- Phylogenetic tree of bacteria found in the soils of the Son-Kul Valley at the SK-6 site based on the analysis of 16SrRNA sequences. Each group contains at least > 97% sequence similarity available in the GenBank database*

The SK-7 site (the Kondoy Too southern ridge foothills) is located at 3,141 m.a.s.l. It has low-growing mountain-valley vegetation, and labiate associations (*Labiatae*) are dominant. A rich diversity of bacteria from phyla Firmicutes, Actinobacteria, Proteobacteria (classes: Gammaproteobacteria and Alphaproteobacteria) and Bacteria was identified at this site. The Firmicutes phylum was found to be the richest in terms of species diversity and number, with the following species found: *Paenibacillaceae bacterium Ts2*, *Brevibacterium frigoritolerans*, *Sporosarcina sp. CL3.9*, *Eubacterium* sp. 11–12 and *Firmicutes bacterium*. The second richest phylum was found to be Actinobacteria, represented by: *Micrococcineae bacterium BF.10*, *Corynebacterineae bacterium* CL1.15 and *Arthrobacter sp.* 210_15. This was followed by the *Bacteria* phylum with: *glacial ice bacterium G500K-17*, *Antarctic bacterium L2* and *marine sponge bacterium plate OTU5*. The rest of the phylogenetic groups were represented by one species each. From the Gammaproteobacteria class was *Lysobacter sp*. CL4.11, and from the Alphaproteobacteria class was *Rhizobium sp.* CL4.3. At this site, bacteria were represented mainly by species associated with plant root systems (e.g., *Paenibacillaceae*)

http://www.aloki.hu ● ISSN 1589 1623 (Print) ● ISSN 1785 0037 (Online)
DOI: http://dx.doi.org/10.15666/aeer/2005_37933815

and species related to plants living in peaty-soddy soils (e.g., *Sporosarcina sp.*, *Micrococcineae* bacterium and *Corynebacterineae* bacterium) (*Fig. 10*). These species have been found in similar peat soils in other countries (Cousin et al., 2010).

A B

Figure 10. *A- SK-7 site view; B- Phylogenetic tree of bacteria found in the soils of the Son-Kul Valley at the SK-7 site based on the analysis of 16SrRNA sequences. Each group contains at least > 97% sequence similarity available in the Genebank database*

The SK-8 site (the top of the Kondoy Too mountain) is located at 3,222 m.a.s.l. and near a mountain glacier. The alpine meadow vegetation consists of a dense thicket of wild onion association (*Allium stellatum*) and yellow tulips (*Tulipa sylvestris*). At this site, up to 99% of the detected microbial community consisted of representatives of the phylum Actinobacteria: *Rhodococcus* sp. RE 59, *Rhodococcus groberulus*, *Rhodococcus gingshengii L-10*, *Rhodococcus bonitorelans*, *Rhodococcus erythropolis*, *Rhodococcus sp.*, *Nocardia coeliaca*, *Nocardia globerula*, *Nocardia bacteruim PhyCEM*, *Nocardia bacterium KDV*, *Nocardia smegmatus str. actinobacterium CH21i* and *uncultured actinobacterium*, and phylum Bacteroidetes (marine bacterium WP02-3-63) (*Fig. 11*).

The SK-9 site (the top of the Kondoy Too mountain) is located at 3,243 m.a.s.l and consisted of soil under a glacier. The soil moisture level was 100%, the soil pH was 6.5 and the temperature was 0.0 °C. There is no vegetation. At this site, only microbial communities from the Actinobacteria phylum and *Paenarthrobacter* genus (Syn. *Arthrobacter* genus) were found: *Paenarthrobacter ilicis*, *Arthrobacter oxydans*, *Paenarthrobacter histidinolovorans*, *Arthrobacter boritolerans*, *Paenarthrobacter nicotinovorans*, *Arthrobacter aurescens*, *A. luteolus*, *Paenarthrobacter nitroguajacolicus*, *A. citreus* and *Pseudarthrobacter chlorophenolicus*. Among the identified species, a glacier-dwelling species was found: *Glacial ice bacterium* (*Fig. 12*).

The SK-10 site is located at the top of the mountain "Kondoy Too", at an altitude of 3244 m.a.s.l, soil under glacier, soil moisture - 100%, no vegetation. Soil type is mountain-light brown, with pH -6.5 and temperature 3.0 ^{0}C. There is no vegetation. At this site, the same microbial communities from the Actinobacteria phylum as at the SK-9 site were identified (*Fig. 13*).

http://www.aloki.hu ● ISSN 1589 1623 (Print) ● ISSN 1785 0037 (Online)
DOI: http://dx.doi.org/10.15666/aeer/2005_37933815

A B

Figure 11. *A- SK-8 site view; B- Phylogenetic tree of bacteria found in the soils of the Son-Kul Valley at the SK-8 site based on the analysis of 16SrRNA sequences. Each group contains at least > 97% sequence similarity available in the GenBank database*

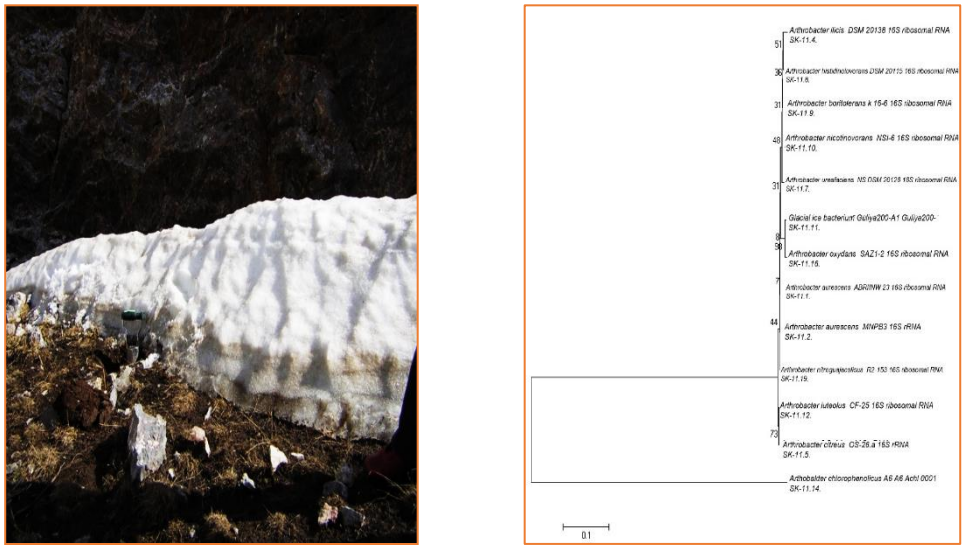

A B

Figure 12. *A- SK-9 site view; B- Phylogenetic tree of bacteria found in the soils of the Son-Kul Valley at the SK-9 site based on the analysis of 16SrRNA sequences. Each group contains at least > 97% sequence similarity available in the GenBank database*

Analysis of 16S rRNA revealed the DNA sequences and identities of the bacterial species within the communities directly after soil extraction. It also allowed us to examine the biodiversity of the species and their distribution among the different ecological niches in the studied biotopes. Representatives of four phyla were identified in total, with the diverse *Actinobacteria* phylum dominating (about 55% of the total), then the *Proteobacteria* (30%), *Firmicutes* (13%) and *Bacteroides* (2%) phyla (*Fig. 14*).

http://www.aloki.hu ● ISSN 1589 1623 (Print) ● ISSN 1785 0037 (Online)
DOI: http://dx.doi.org/10.15666/aeer/2005_37933815

A B

Figure 13. *A- SK-10 site view; B- Phylogenetic tree of bacteria found in the soils of the Son-Kul Valley at the SK-10 site based on the analysis of 16SrRNA sequences. Each group contains at least > 97% sequence similarity available in the GenBank database*

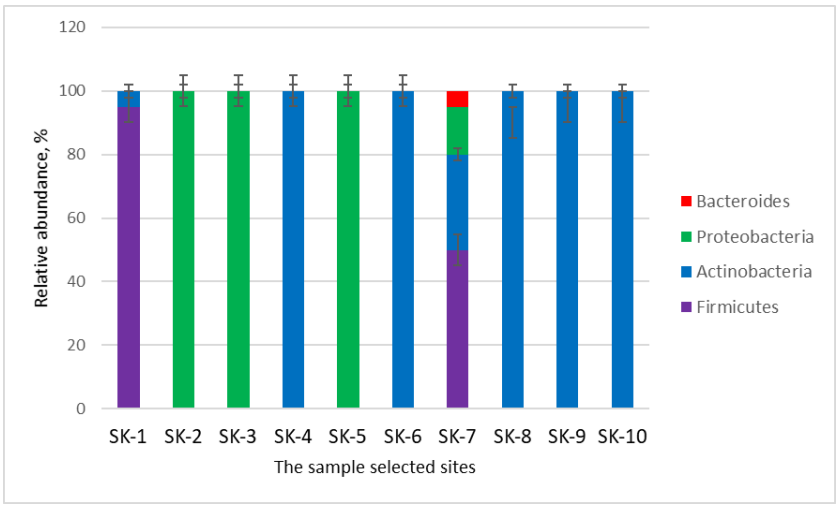

Figure 14. *The bacterial community composition at the phylotype level for the 10 sample sites. Values are given as mean ± SD, n = 3, significantly different at P ≤ .05*

When we analysed the obtained bacterial communities at the class level, each studied biotope under a specific plant species had distinctive bacterial biodiversity. The proportion of *Actinomycetia* class representatives was found to be high compared to the other classes identified. Species from the *Gammaproteobacteria* class were the second most frequently occurring, and species from the classes *Alphaproteobacteria* and *Bacteroidia* were found in insignificant proportions under the vegetation of alpine steppe meadow biotopes (*Fig. 15*).

http://www.aloki.hu ● ISSN 1589 1623 (Print) ● ISSN 1785 0037 (Online)
DOI: http://dx.doi.org/10.15666/aeer/2005_37933815

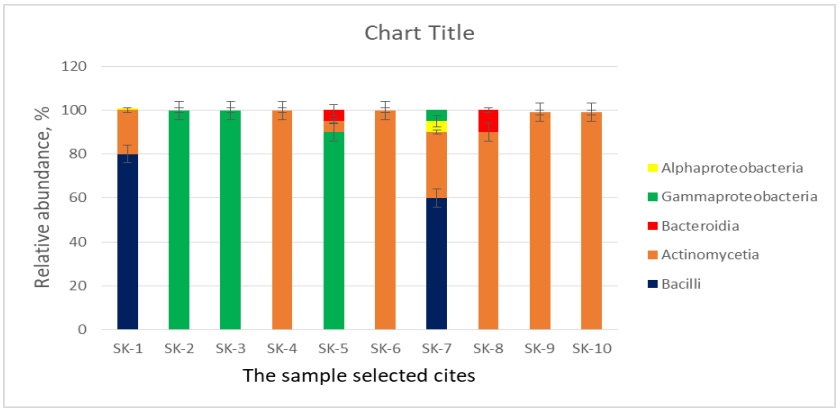

Figure 15. *The bacterial community composition at the classes level for the 10 sample sites. Values are given as mean ± SD, n = 3, significantly different at P ≤ .05*

As the results of the analysis of the Shannon and Simpson index showed that the richness and diversity occurring species was low in this study region (*Figs. 16 and 17*).

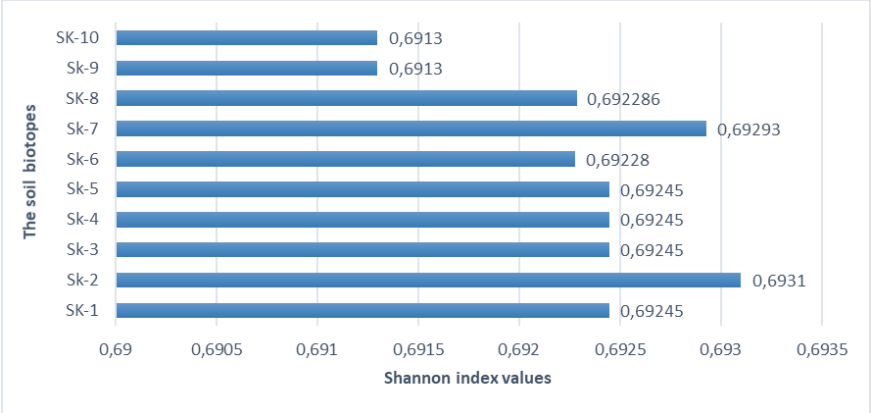

Figure 16. *Histogram of bacterial species probability distribution for the soil biotopes on Shannon index. Values are given as mean ± SD, n = 3, significantly different at P ≤ .05*

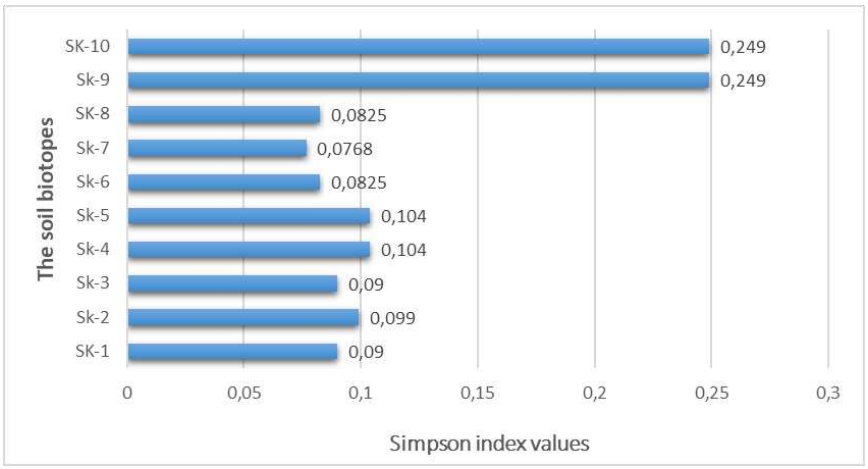

Figure 17. *Histogram of bacterial species probability distribution for the soil biotopes on Simpson index index. Values are given as mean ± SD, n = 3, significantly different at P ≤ .05*

http://www.aloki.hu ● ISSN 1589 1623 (Print) ● ISSN 1785 0037 (Online)
DOI: http://dx.doi.org/10.15666/aeer/2005_37933815

Discussion

The studied soils of the Son-Kul high-mountain ecosystem were found to have different physicochemical and biological characteristics; therefore, these different soil habitats reflected the phenotypic differences of the microorganisms inhabiting the soil. The vegetation found in the Son-Kul basin region varies according to altitude (Mamytov, 1971; Tsekanov, 1979; Golovkova, 1990).

Soil organic matter affects soil functions and is a critical component of the global carbon cycle (Pataki et al., 2003; Houghton, 2007). Our results show that the number of ammonifying bacteria capable of growing at 15–20 °C and participating in the decomposition of plant litter was low in the collected samples, indicating a slower decay rate of new organic matter in soils of this cold ecosystem. The highest numbers of ammonifying bacteria were recorded at site SK-6, where the soil is rich in organic matter and covered under dense meadow vegetation. The lowest numbers of isolated bacteria were recorded in soils under a glacier (sites SK-9 and SK-10). At these sites, the ground has a low organic matter content, there is an absence of vegetation and the temperature is constantly below zero. Many studies have reported intermediate bacterial concentration values from glacier sites (Skidmore et al., 2000; Zhang et al., 2002; Foght et al., 2004). In mid-latitude environments, mountain snow bacterial concentrations have been reported to range from 3×10^3 cells/ml (Bauer et al., 2002) to around 4×10^5 cells/ml (Alfreider et al., 1996; Sattler et al., 2001; Segawa et al., 2005).

In most cold habitats, nutrient concentrations are low, and temperatures are typically high enough to support microbial growth and activity for only one to two months a year. Under these conditions, psychrotrophic microbes predominate that can withstand extreme temperatures and a lack of moisture for a long time (Larkin et al., 1970; Groudieva et al., 2004). Our results align with these earlier findings—most of the detected bacterial isolates were found to be psychrotrophic. Among the detected isolates, 35% grew well at 15 °C and a further 35% grew well at 20 °C. Thus, 70% of the bacterial species obtained in this study can be considered psychrotrophic. Furthermore, we assume that these bacteria that are capable of growing in a medium temperature range (15–20 °C) are the main bacteria responsible for the degradation and mineralization of plant residue during the short warm summer period. This is a reasonable assumption, given that other studies have proven that bacterial isolates from Arctic snow samples can degrade organic compounds found there at moderate temperature (17 °C) after 24 h of incubation (Amato et al., 2006).

Analysis of 16S rRNA revealed the DNA sequences and identities of the bacterial species within the communities directly after soil extraction. It also allowed us to examine the biodiversity of the species and their distribution among the different ecological niches in the studied biotopes. Representatives of four phyla were identified in total, with the diverse *Actinobacteria* phylum dominating (about 55% of the total), then the *Proteobacteria* (30%), *Firmicutes* (13%) and *Bacteroides* (2%) phyla (*Fig. 14*). Many other studies have also reported a high diversity of Actinobacteria in extreme habitats, such as marine sediments (Duran et al., 2015; Zhang et al., 2019), volcanic caves (Riquelme et al., 2015), deposits of cold springs (Yang et al., 2015), microbial mats of hot springs (Jiang et al., 2012), glacial forelands (Zhang et al., 2016b), lakes (Parveen et al., 2011) and deserts (Ding et al., 2013).

According to available literature, plant communities had different effects on archaea and bacteria in biotopes. Species richness and evenness of the plant community can have direct and indirect impacts on the structure of the soil bacterial community (Lamb et al.,

http://www.aloki.hu ● ISSN 1589 1623 (Print) ● ISSN 1785 0037 (Online)
DOI: http://dx.doi.org/10.15666/aeer/2005_37933815

2011). A more homogeneous plant community increases the abundance of bacteria increases the potential of nitrification processes, here the mechanism of influence of plant evenness in the structural biodiversity of soil bacteria lies in the complementarity of root exudate profiles (Lamb et al., 2011). Other scientists also argue that the genotype of plants is of some importance in creating the species and genetic composition of soil microorganisms (Babalola et al., 2007). Plants and their associated microbial communities have evolved complex adaptations to cold stress. Microbial communities can increase plant resistance to harsh environmental conditions (Compant et al., 2019; Marian et al., 2022).

Our results also confirmed that vegetation cover influences the composition of bacterial biodiversity in the rhizosphere. Each studied biotope under a specific plant species had distinctive bacterial biodiversity. The obtained results showed a certain regularity in the distribution of the bacterial species, genera and classes under the vegetation. For example, under perennial cereals and many other plants, bacteria from the genus *Bacillus* (Bacilli class) dominated as active ammonifiers involved in decomposing plant residue. In another example, under succulent meadow vegetation, which has a short vegetation period, species from the Gammaproteobacteria class dominated, mainly species of *Pseudomonas*. As altitude increased and soil temperature decreased, *Arthrobacter* species from the Actinomycetia class were predominately found under alpine meadow plants (*Fig. 15*).

Our results align with those of others who have also found that specific phylogenetic groups, such as Betaproteobacteria, Gammaproteobacteria, Firmicutes, Actinobacteria and Alphaproteobacteria, are associated with cold environments (Christner et al., 2001; Zhang et al., 2002; Brinkmeyer et al., 2003; Groudieva et al., 2004; Miteva and Brenchley, 2005; Amato et al., 2006; Chica et al., 2019).

Phylogenetic analysis in several metagenomic studies has shown that Actinobacteria are the most common and predominant phylotype; its populations may be cosmopolitan, dominat in different geographical areas (Buckley and Schmidt, 2002; Smith et al., 2006; Aislabie et al., 2006, 2008). *Artrobacter* and related organisms differ in that they form coccoid cells during the stationary growth phase or under starvation conditions (Cure and Keddie, 1973). Some soil species of *Arthrobacter* can withstand long periods of in suti starvation, which explains their wide distribution in soils at fluctuating low temperatures (Ensign, 1970).

As the results of the analysis of the Shannon and Simpson index showed that the richness and diversity occurring species was low in this study region (*Figs. 16 and 17*) compared to other ecosystems where the temperature is more suitable for the activity of soil bacteria, and the natural biodiversity of species is high. For example, when compared with data on the richness and diversity of bacterial communities in ecosystems in typical temperature regions, the highest biodiversity was noted in the grassland ecosystem (4.5-5.0 Shannon Index) and desert (5.0-5.5 Shannon Index), probably reflecting the relationship between community structure and plant species. The diversity in samples obtained from farmland and tree grove ecosystems was narrower than the others (Zhang et al., 2019).

Conclusion

Results obtained suggest that as one moves up the slope, the soil biogenicity decreases, reaching a minimum in the soils of the Alpine belt. Here, the low temperature of the earth

http://www.aloki.hu ● ISSN 1589 1623 (Print) ● ISSN 1785 0037 (Online)
DOI: http://dx.doi.org/10.15666/aeer/2005_37933815

is already a deterrent to bacterial activity. The decomposition of organic residues is slow with a high plant litter accumulation. The results also suggest that the mineralization of organic residues in the soils of high-mountain intermontane depressions is extremely slow due to the lack of heat and moisture. Here, *Artrobacter* and *Actinobacteria* group bacteria are predominantly distributed, using mineral forms of nitrogen as a source of nitrogen nutrition, indicating soil microflora's weak ammonifying activity.

Finally, our studies have shown although the active layer of alpine high mountain soils is directly exposed to extreme environmental conditions, harboured significant microbial diversity, that has an activity for a short time at moderate temperature, their role in nutrient cycling is essential.

REFERENCES

[1] Aislabie, J. M., Chhour, K.-L., Saul, D. J., Miyauchi, S., Ayton, J., Paetzold, R. F., Balks, M. R. (2006): Dominant bacteria in soils of Marble Point and Wright Valley, Victoria Land, Antarctica. – Soil Biology and Biochemistry 38: 3041-3056.

[2] Aislabie, J. M., Jordon, S., Barker, G. M. (2008): Relation between soil classification and bacterial diversity in soils of the Ross Sea region, Antarctica. – Geoderma 144: 9-20.

[3] Alfreider, A., Pernthaler. J., Amann, R., Sattler, B., Glockner, F. O., Wille, A., Psenner, R. (1996): Community analysis of the bacterial assemblages in the winter cover and pelagic layers of a high mountain lake by in situ hybridization. – Applied and Environmental Microbiology 62: 2138-3144.

[4] Amato, P., lle Hennebelle, R., Magand, O., Sancelme, M., Delort, A. M., Barbante, C., Boutron, C., Ferrari, C. (2006): Bacterial characterization of the snow cover at Spitzberg, Svalbard. – FEMS 59: 255-264.

[5] Anesio, A. M., Hodson, A. J., Fritz, A., Psenner, R., Sattler, B. (2009): High microbial activity on glaciers: importance to the global carbon cycle. – Global Change Biology 15: 955-960.

[6] Babalola, O. O., Sanni, A. I., Odhiambo, G. D., Torto, B. (2007): Plant growth-promoting rhizobacteria do not pose any deleterious effect on cowpea and detectable amounts of ethylene are produced. – World Journal of Microbiology & Biotechnology 23: 747-752.

[7] Bauer, H., Kasper-Giebl, A., Loflund, M., Giebl, H., Hitenberger, R., Zibuschka, F., Puxbaum, H. (2002): The contribution of bacterial and fungal spores to the organic carbon content of cloud water, precipitation and aerosols. – Atmospheric Research 64: 109-119.

[8] Bergey's Manual of Systematic Bacteriology (2004): The Proteobacteria. – Volume 2. Garrity, G. M. (ed.), Publisher Springer, USA.

[9] Bergey's Manual of Systematics of Archaea and Bacteria (2015): Publisher Hoboken, New Jersey.

[10] Boetius, A., Anesio, A., Deming, J., Mikucki, J. A., Rapp, J. Z. (2015): Microbial ecology of the cryosphere: sea ice and glacial habitats. – Nature Reviews Microbiology 13: 677-690.

[11] Bottos, E., Scarrow, J., Archer, S., McDonald, I., Cary, S (2014): Bacterial community structures of Antarctic soils. – In: Cowan, D. (ed.) Antarctic Terrestrial Microbiology: Physical and Biological Properties of Antarctic Soils. Springer: Heidelberg, Germany.

[12] Brambilla, E., Hippe, H., Hagelstein, A., Tindall, B. J., Stackerbrandt, E. (2001): 16S rDNAdiversity of cultured and uncultured prokaryotes of a mat sample from Lake Fryxell, McMurdo Dry Valleys, Antarctica. – Extremophiles 5(1): 23-33.

[13] Brinkmeyer, R., Knittel, K., Jürgens, J., Weyland, H., Amann, R., Helmke, E. (2003): Diversity and structure of bacterial communities in Arctic versus Antarctic pack ice. – Applied and Environmental Microbiology 69: 6610-6619.

http://www.aloki.hu ● ISSN 1589 1623 (Print) ● ISSN 1785 0037 (Online)
DOI: http://dx.doi.org/10.15666/aeer/2005_37933815

[14] Buckley, D. H., Schmidt, T. M. (2002): Exploring the biodiversity of soil: a microbial rain forest. – In: Staley, J. T., Reyenbach, A.-L. (eds.) Biodiversity of Microbial Life. New York, NY, USA: Wiley-Liss.
[15] Chica, E., Buela, L., Valdez, A., Villena, P., Pena, D., Yarzábal, L. A. (2019): Metagenomic survey of the bacterial communities in the rhizosphere of three Andean tuber crops. – Symbiosis 79: 141-50.
[16] Christner, B. C., Mosley-Thompson, E., Thompson, L. G., Reeve, J. N. (2001): Isolation of bacteria and 16S rDNAs from Lake Vostok accretion ice. – Environmental Microbiology 3: 570-577.
[17] Collins, T., Margesin, R. (2019): Psychrophilic lifestyles: mechanisms of adaptation and biotechnological tools. – Applied Microbiology and Biotechnology. https://doi.org/10.1007/s00253-019-09659-5.
[18] Compant, S., Samad, A., Faist, H., Sessitsch, A. (2019): A review on the plant microbiome: ecology, functions, and emerging trends in microbial application. – Journal of Advanced Research 19: 29-37.
[19] Cousin, S., Brambilla, E., Stackebrandt, E. (2010): Spatial Bacterial Diversity in a Recent Freshwater Tufa Deposit. – Geomicrobiology Journal 27(4): 275-291.
[20] Crump, B. C., Amaral-Zettler, L. A., Kling, G. W. (2012): Microbial diversity in arctic freshwaters is structured by inoculation of microbes from soils. – International Society for Microbial Ecology 6: 1629-1639.
[21] Cure, G. L., Keddie, R. M. (1973): Methods for the morphological examination of aerobic coryneform bacteria. – In: Board, R. C., Lovelock, D. M. (eds.) Sampling - Microbiological Monitoring of Environments. Academic Press, London, pp. 123-135.
[22] Cuthbertson, L., Amores-Arrocha, H., Malard, L. A., Els, N., Sattler, B., Pearce, D. A. (2017): Characterisation of Arctic bacterial communities in the air above Svalbard. – Biology 6: 29.
[23] Dhakar, K., Pandey, A. (2020): Microbial Ecology from the Himalayan Cryosphere Perspective. – MDPI Microorganisms 8: 257.
[24] Ding, D., Chen, G. C., Wang, B. C., Wang, Q. L., Liu, D. M., Peng, M., Shi, P. (2013): Culturable actinomycetes from desert ecosystem in northeast of Qinghai-Tibet plateau. – Annals of Microbiology 63: 259-266.
[25] Druce, R. G., Thomas, S. B. (1970): An ecological study of psychrotrophic bacteria in soil, water, grass, and hay. – Journal of Applied Microbiology 31: 290-301.
[26] Duran, R., Bielen, A., Paradzik, T., Gassie, C., Pustijanac, E., Cagnon, C., Hamer, B., Vujaklija, D. (2015): Exploring Actinobacteria assemblages in coastal marine sediments under contrasted human influences in the west Istria sea, Croatia. – Environmental Science and Pollution Research 22: 15215-15229.
[27] Eisenlord, S. D., Zak, D. R. (2010): Simulated atmospheric nitrogen deposition alters actinobacterial community composition in forest soils. – Soil Science Society of American Journal 74: 1157-1166.
[28] Ensign, J. C. (1970): Long-term starvation survival of rod and spherical cells of Arthrobacter crystallopoietes. – Journal of Bacteriology 103(3): 569-77.
[29] Foght, J., Aislabie, J., Turner, S., Brown, C. E., Ryburn, J., Saul, D. J., Lawson, W. (2004): Culturable bacteria in subglacial sediments and ice from two southern hemisphere glaciers. – Microbiological Ecology 47: 329-340.
[30] Ghiglione, J.-F., Galand, P. E., Pommier, T., Pedrós-Alió, C., Maas, E. W., Bakker, K., Bertilson, S., Kirchman, D. L., Lovejoy, C., Yager, P. L., Murray, A. E. (2012): Pole-to-pole biogeography of surface and deep marine bacterial communities. – Proceedings of the National Academy of Sciences of the United States of America 109(43): 17633-17638.
[31] Golovkova, A. G. (1990): Vegetation of Kyrgyzstan. – Frunze, Ilim.
[32] Goodfellow, M., Williams, S. T. (1983): Ecology of actinomycetes. – Annual Review of Microbiology 37: 189-216.

http://www.aloki.hu ● ISSN 1589 1623 (Print) ● ISSN 1785 0037 (Online)
DOI: http://dx.doi.org/10.15666/aeer/2005_37933815

[33] Gray, T. R. G., Williams, S. T. (1971): Soil microorganisms. – Oliver and Boyd, Edinburgh.
[34] Groudieva, T., Kambourova, M., Yusef, H., Royter, M., Grote, R., Trinks, H., Antranikian, G. (2004): Diversity and cold-active hydrolytic enzymes of culturable bacteria associated with Artic sea ice, Spitzbergen. – Extremophiles 8: 475-488.
[35] Han, X. M., Wang, R. Q., Liu, R., Wang, M. C., Zhou, J., Guo, W. H. (2007): Effects of vegetation type on soil microbial community structure and catabolic diversity assessed by polyphasic methods in North China. – Journal of Environmental Sciences China 19: 1228-1234.
[36] Harding, T., Jungblut, A. D., Lovejoy, C., Vincent, W. F. (2011): Microbes in high Arctic snow and implications for the cold biosphere. – Applied and Environmental Microbiology 77: 3234-3243.
[37] Hayakawa, M. (2008): Studies on the isolation and distribution of rare actinomycetes in soil. – Actinomycetologica 22: 12-19.
[38] Hill, P., Krištùfek, V., Dijkhuizen, L., Boddy, C., Kroetsch, D., van Elsas, J. D. (2011): Land use intensity controls actinobacterial community structure. – Microbiological Ecology 61: 286-302.
[39] Holmalahti, J., Wright, A., Raatikainen, O. (1994): Variations in the spectra of biological activities of actinomycetes isolated from different soils. – Letters in Applied Microbiology 18: 144-146.
[40] Houghton, R. A. (2007): Balancing the global carbon budget. – Annual Review of Earth and Planetary Sciences 35: 313-347.
[41] Ingram, M. (1965): Psychrophilic and psychrotrophic microorganisms. – Annales de l'Institut Pasteur de Lille 16: 111-118.
[42] Jiang, H., Dong, C. Z., Huang, Q., Wang, G., Fang, B., Zhang, C., Dong, H. (2012): Actinobacterial diversity in microbial mats of five hot springs in central and central-eastern Tibet, China. – Geomicrobiology Journal 29(6): 520-527.
[43] Lamb, E. G., Kennedy, N., Siciliano, S. D. (2011): Effects of plant species richness and evenness on soil microbial community diversity and function. – Plant and Soil 338: 483-495.
[44] Larkin, J. M. (1970): Seasonal incidence of bacterial temperature types in Lousiana soil and water. – Journal of Applied Microbiology 20: 286-288.
[45] Larose, C., Dommergue, A., Vogel, T. M. (2013): The dynamic arctic snow pack: an unexplored environment for microbial diversity and activity. – Biology 2: 317-330.
[46] Lee, S.-H., Jang, I., Chae, N., Choi, T., Kang, H. (2013): Organic layer serves as a hotspot of microbial activity and abundance in Arctic tundra soils. – Microbiological Ecology 65: 405-414.
[47] Lysak, V., Maksimova, I. A., Nikitin, D. A., Ivanova, A. E., Kudinova, A. G., Soina, V. S., Marfenina, O. E. (2018): Soil microbial communities of eastern Antarctica. – Moscow University Biological Sciences Bulletin 73: 104-112.
[48] Mackelprang, R., Waldrop, M. P., DeAngelis, K. M., David, M. M., Chavarria, K. L., Blazewicz, S. J., Rubin, E. M., Jansson, J. K. (2011): Metagenomic analysis of a permafrost microbial community reveals a rapid response to thaw. – Nature 480: 368-371.
[49] Mamytov, A. (1974): Soils of the Kirghiz SSR. – Ilim Publishing, Frunze.
[50] Mamytov, A. (1996): Soil resources and issues of the land cadaster of the Kyrgyz Republic. Monograph. – Publishing house "Kyrgyzstan», Frunze.
[51] Margesin, R., Collin, T. (2019): Microbial ecology of the cryosphere (glacial and permafrost habitats: current knowledge). – Applied Microbiology and Biotechnology 103: 2537-2549. https://doi.org/10.1007/s00253-019-09631-3.
[52] Marian, M., Licciardello, G., Vicelli, B., Pertot, I., Perazzolli, M. (2022): Ecology and potential functions of plant-associated microbial communities in cold environments. – FEMS Microbiology Ecology 98: fiab.161.
[53] Matsukawa, E., Nakagawa, Y., Iimura, Y., Hayakawa, M. (2007): Stimulatory effect of indole-3-acetic acid on aerial mycelium formation and antibiotic production in Streptomyces spp. – Actinomycetologica 21: 32-39.

http://www.aloki.hu ● ISSN 1589 1623 (Print) ● ISSN 1785 0037 (Online)
DOI: http://dx.doi.org/10.15666/aeer/2005_37933815

[54] Miteva, V. I., Brenchley, J. E. (2005): Detection and isolation of ultra-small microorganisms from a 120,000-year-old Green-land glacier ice core. – Applied and Environmental Microbiology 71: 7806-7818.
[55] Neufeld, J. D., Mohn, W. W. (2005): Unexpectedly high bacterial diversity in arctic tundra relative to boreal forest soils, revealed by serial analysis of ribosomal sequence tags. – Applied and Environmental Microbiology 71: 5710-5718.
[56] Olubukola, O. B., Bronwyn, M. K., Marilize, L. R., Andrew, E. C., Craig, C., Stephanie, G. B., Don, A. C. (2009): Phylogenetic analysis of actinobacterial populations associated with Antarctic Dry Valley mineral soils. – Environmental Microbiology 11(3): 566-76.
[57] Parveen, B., Reveilliez, J. P., Mary, I., Ravet, V., Bronner, G., Mangot, J. F., Domaizon, I., Debroas, D. (2011): Diversity and dynamics of free-living and particle-associated betaproteobacteria and actinobacteria in relation to phytoplankton and zooplankton communities. – FEMS Microbiology Ecology 77: 461-476.
[58] Pataki, D. E. (2003): Tracing changes in ecosystem function under elevated carbon dioxide conditions. – BioScience 53: 805-818.
[59] Ramsar Sites Information Service (2011): Son–Kol Lake. – Ramsar site no. 1943.
[60] Riquelme, C., Marshall, H. J. J., Enes, D. M. L. N., Miller, A. Z., Kooser, A., Northup, D. E., Jurado, V., Fernandez, O., Saiz-Jimenez, C., Cheeptham, N. (2015): Actinobacterial Diversity in Volcanic Caves and Associated Geomicrobiological Interactions. – Frontiers in Microbiology 6.
[61] Sattler, B., Puxbaum, H., Psenner, R. (2001): Bacterial growth in super cooled cloud droplets. – Geophysical Research Letters 28: 239-242.
[62] Segawa, T., Miyamoto, K., Ushida, K., Agata, K., Okada, N., Kohshima, S. (2005): Seasonal change in bacterial flora and biomass in mountain snow from Tateyama Mountains, Japan, analyzed by 16SrRNA gene sequencing and real-time PCR. – Applied and Environmental Microbiology 71: 123-130.
[63] Skidmore, M. L., Foght, J. M., Sharp, M. J. (2000): Microbial life beneath a high Arctic glacier. – Applied and Environmental Microbiology Journal 66: 3214-3220.
[64] Smith, J. J., Tow, L. A., Stafford, W., Cary, C., Cowan, D. A. (2006): Bacterial diversity in three different Antarctic cold desert mineral soils. – Microbiological Ecology 51: 413-421.
[65] Tsekanov, A. S. (1979): Ecological and Biological Basis for Improving the Pastures of the Highlands of the Inner Tien Shan. – Frunze, Ilim.
[66] Wynn-Williams, D. (1996): Antarctic microbial diversity: The basis of polar ecosystem processes. – Biodiversity conservation 5: 1271-1293.
[67] Xu, Z. F., Hansen, M. A., Hansen, L. H., Jacquiod, S., Sorensen, S. J. (2014): Bioinformatic approaches reveal metagenomic characterization of soil microbial community. – PLoS One 9: e93445.
[68] Yang, J., Li, X. Y., Huang, L. Q., Jiang, H. C. (2015): Actinobacterial diversity in the sediments of five cold springs on the Qinghai-Tibet plateau. – Frontiers in Microbiology 6: 1345.
[69] Zhang, X. J., Yao, T. D., Ma, X. J., Wang, N. L. (2002): Microorganisms in a high altitude glacier in Tibet. – Folia Microbiol 47: 241-245.
[70] Zhang, B., Wu, X., Zhang, W., Chen, X., Zhang, G., Ai, X., Sun, L., Zhang, B., Liu, G., Chen, T., Dyson, P. (2016): Diversity and succession of actinobacteria in the forelands of the Tianshan glacier, China. – Geomicrobiology Journal 33: 716-723.
[71] Zhang, B., Wu, X., Tai, X., Sun, L., Wu, M., Zhang, W., Chen, X., Zhang, G., Chen, T., Liu, G., Dyson, P. (2019): Variation in Actinobacterial Community Composition and Potential Function in Different Soil Ecosystems Belonging to the Arid Heihe River Basin of Northwest China. – Frontiers in Microbiology 10: 2209.
[72] Zvyagintsev, D. G. (1991): Methods of Soil Microbiology and Biochemistry. – MSU, Moscow.

http://www.aloki.hu ● ISSN 1589 1623 (Print) ● ISSN 1785 0037 (Online)
DOI: http://dx.doi.org/10.15666/aeer/2005_37933815

BEE POLLEN AN ALTERNATIVE TO GROWTH PROMOTERS FOR POULTRY PRODUCTION-A REVIEW

NEMAULUMA, M. F. D. – NG'AMBI, J. W. – KOLOBE, S. D. – MALEMATJA, E. – MANYELO, T. G. – CHITURA, T.*

Department of Agricultural Economics and Animal Production, University of Limpopo, Private Bag X1106, Sovenga 0727, South Africa

**Corresponding author*
e-mail: teedzai.chitura@ul.ac.za

(Received 14th Mar 2022; accepted 11th Jul 2022)

Abstract. Globally, the use of natural products as remedies for poultry health calls for a systematic exploration of their potential. Furthermore, there is an increasing popularity and utilization of bee-based products due to their inherent benefits. The current review was aimed at analysing empirical results, biological activities and secondary metabolites of bee pollen that are beneficial to the poultry industry. Eligible literature was retrieved from different databases. The findings from the literature search indicated that bee-collected pollen has received attention from researchers owing to its positive effects as a possible growth promoter in poultry production. It contains antioxidants, antimicrobials, emulsifiers, vitamins and minerals which can meet the biochemical and functional needs of poultry flocks. We identified a minimum of 17 research articles that captured various observations on the effects of bee pollen in poultry. The most common observations were on growth performance and gastrointestinal morphology. The search results also indicated that there are several factors such as floral species, climatic conditions and soil types which influence the nutritional composition of bee pollen. Studies gathered revealed that the antioxidant properties found in bee pollen are due to the phenolic compounds it possesses. Overall, there is a lack of empirical evidence on the health effects of supplementing bee pollen indicating a major knowledge gap that requires more research.
Keywords: *antimicrobials, antioxidants, beekeeping, gastrointestinal, growth performance*

Introduction

Antibiotics have been in use for many years as targets against enteric microorganisms in an effort to improve the health and performance of chickens (Babaei et al., 2016). The inclusion of antibiotics in poultry diets was reported to improve feed utilisation, thereby improving growth among other positive attributes. However, use of antibiotics at sub-therapeutic doses is associated with the development of antibiotic resistance (WHO, 2017). Antibiotic resistance is a worldwide problem which affects the animal production industry (Selaledi et al., 2020). This concern caused the European Commission in 2006 to ban the use of antibiotics as growth promoters. The ban did cause implications such as an increase in the incidence of animal diseases and reduced livestock production (Cheng et al., 2014).

There is an increasing risk of bacteria developing resistance to synthetic antibiotics in food animal production (Masud et al., 2020). Bacteria such as *Acinetobacter spp*, *Eschericha coli*, *Klebsiella spp* and *Salmonela spp* are tremendously resistant to most synthetic antibiotics (Carlet et al., 2012). *Salmonella serovars* and *Campylobacter spp* are most common in poultry meat and are well-known causes of zoonotic diseases (Hafez and Attia, 2020). Frequent use of synthetic antibiotics promotes the development of antimicrobial resistance which therefore affects the health of animals, consumers, the quality of the product and promotes an unsafe environment (CDC, 2021). Concerns

http://www.aloki.hu ● ISSN 1589 1623 (Print) ● ISSN1785 0037 (Online)
DOI: http://dx.doi.org/10.15666/aeer/2005_38173832

associated with the continued and unregulated use of antibiotics have been raised in several countries including Brazil, Russia, India, China and South Africa (Willams-Nguyen et al., 2016). Over the recent past years, research has focused on natural antibiotics such as plant extracts as alternatives and a possible solution to the challenge of antibiotic resistance in the poultry industry (Seal et al., 2013). Plant extracts are commonly known as phytogenic feed additives due to the various biological properties they have (Gheisar and Kim, 2017; Selaledi et al., 2020). Specifically, the metabolites found in bee pollen possess biological properties such as antioxidant, antibacterial, anticarcinogenic activity, hepatoprotective and cardioprotective (Li et al., 2018).

Literature reports have revealed that bee pollen has positive effects on the immunity, growth, gut health as well as improving the quality and safety of food production (Wang et al., 2007; Cheng, 2009; Hashmi et al., 2012; Haščík et al., 2013). Due to the high bioactive compounds, phytochemicals from plants have also shown possibilities in treatment of coronaviruses that are infectious to animals and also humans (Attia et al., 2020). Bee pollen as a natural agent could be a possible candidate to treat such diseases (Ali and Kunugi, 2021). Furthermore, bee pollen has been reported to have protective actions on the gastrointestinal of poultry (Liu et al., 2010). Bee pollen increases growth performance as well as the population of *Lactobacillus spp* and *Enterococcus spp* in the caeca of broiler chickens. Supplementation of bee pollen in chicken diets increases the weight and length of the small intestine (duodenum, jejenum and ileum) in chickens (Wang et al., 2007). According to Babaei et al. (2016), supplementation of bee pollen in Japanese quails improves their growth performance. Such findings can be used to improve development of chickens at an early age through supplementation of bee pollen (Hascik et al., 2017). These findings may suggest that bee pollen could be a possible natural antibiotic candidate to substitute synthetic antibiotics in poultry production. Therefore, this review aims to provide a comprehensive understanding of the potential use of bee pollen in poultry production.

Materials and methods

The literature search was facilitated using the key words such as “antibiotics”, “pollen”, “bee collected pollen”, feed additives, natural substances, “poultry”, “immunity”, “microbial health”, “processing techniques”. The literature was acquired from recent articles from (2017-2021) that were published in different journals. However, there are articles that are years older but were used in the recent articles from the above time range. We focused on peer reviewed articles published on bee pollen use in poultry production. Databases were accessed using electronic data sources such as Research gate, Science direct, Cross Ref and Google scholar. In addition, phytochemical, antioxidant, phenolic and antibacterial effect were used to generate data for the biological activity and phytochemical aspects of this review.

Results and discussion

Anatomy and structure of bee pollen

Bee pollen is considered to be a natural substance which is acquired from the pollen of different botanical plants through the mixture of bee saliva and nectar (Oliveira et al., 2013; Attia et al., 2014). There are male reproductive organs in the pollen which are

http://www.aloki.hu ● ISSN 1589 1623 (Print) ● ISSN1785 0037 (Online)
DOI: http://dx.doi.org/10.15666/aeer/2005_38173832

located in the anthers of botanical plants (Bogdanov, 2016b). Within the anthers of the seed, there is about 2.5-250 μm grain of bee pollen (Komosinska-Vassev et al., 2015). It is called "the life giving dust" by the ancient Egyptians due to its nutritional value (Bishop, 2002).

This grain is surrounded by doubled layer of cell wall. The cell contains a rich cellulose cell which includes an inner cell (intine) and outer cell (exine) which extremely has a hard outer cover (Komosinska-Vassev et al., 2015; Bogdanov, 2016). Plant species of pollen grains are usually different in terms of size, colour, weight and shape (Shubharani et al., 2013). Pollen grains are usually bright yellow to black in colour. This may be due to the different plant species that honey bees collect their pollen from Dubtsova (2009). Since bee pollen is harvested from different plant species, the overall composition of bee pollen varies and is affected (Hsu et al., 2021). This also goes to the taste, bee pollen has a sweet and floral taste depending on the plants that bees gather pollen (Johnson, 2021). However, according to our understanding, studies on whether different kinds of pollen may affect poultry production are limited. There is about 10% nectar bee pollen collected from plants containing an average of 20-30 g water per 100 g like any other freshly collected plant extract spoilage occurs from humidity and freezing is a required method for bee pollen preservation, and drying is best done with an electrical oven (Bogdanov, 2016b).

Economic effects of bee pollen supplementation in poultry diets

According to Elahi et al. (2022), feed costs account for approximately 60% to 80% of the total production cost encountered in poultry farming. Therefore, there is a need to find ways to reduce such high costs. The use of alternative feed ingredients from locally available and affordable sources can help to lower the costs of poultry feeds. Insect based meals such as bee pollen can be a sustainable solution for the poultry industry (Al-Qazzaz and Ismail, 2016). According to Elahi et al. (2022) the use of lower doses of bee products in poultry feeds could bring a beneficial effect on the growth and health of poultry. Ricigliano et al. (2022) and Mazorodze (2020) reported that bee keeping plays vital roles which include it being an excellent tool for the eradication of poverty especially in rural based communities. Land requirements for beekeeping practices are very limited thereby making this practice to be ideal for small holder farmers with limited resources. However, beekeeping has its fair share of challenges such as the emergence and transmission of diseases, pets and changes in climate factors which may adversely affect the viability of beekeeping (Masehela, 2017). The use of bee pollen as a feed supplement for poultry production can help to reduce production costs since it can be produced with locally available resources thereby also boosting local economies (Gratzer et al., 2021). Furthermore, there is a high local demand for bee based products in most developing countries (Hilmi et al., 2019). In some African countries, bee products such as bee pollen may the main source of income for impoverished families. To the best of our knowledge, there is limited information on the economic benefits of supplementing bee pollen in poultry diets.

Supplementation of bee pollen in poultry production

Natural products in poultry feeds have received a great amount of attention and have been encouraged to be incorporated in poultry feed ingredients (Farag and El-Rayes, 2016). Bee pollen has, however, shown positive effects in the growth performance of poultry (Hascik et al., 2017). Additionally, bee pollen includes vital nutrients that are beneficial to the health and growth performance of animals and humans (Hsu et al., 2021).

http://www.aloki.hu ● ISSN 1589 1623 (Print) ● ISSN1785 0037 (Online)
DOI: http://dx.doi.org/10.15666/aeer/2005_38173832

Health issues in humans such as prostrate problems have shown to ease with the use of bee pollen (Shoskes, 2002). Damaged tissues are easily repaired also reducing toxicity in the body (Moria et al., 2011). It has been reported that bee pollen is able to support the immune system of human and also have anti-aging effects (Estevinho et al., 2012). The vital nutrients that bee pollen contains such as the high protein content, essential amino acids, fats, unsaturated fatty acids, carbohydrates and minerals may be the reason behind health and growth improvements in poultry (Farag and El-Rayes, 2016). During the early development of growth bee pollen has shown to affect the villi of the small intestine in the size and length (Wang et al., 2007). Such information may prove that the digestive system may be improved during early stages of a chick's life (Hascik et al., 2017). Published data has indicated that bee pollen contains nutrients to assist broilers during periods of heat stress (Hascik et al., 2017). The mechanism of bee pollen action may be attributed to its strong antibacterial action, also with the high amount of micronutrients that have a positive effect on the health and metabolism of chickens (Viuda-Martos et al., 2008). The use of natural substances as possible candidates to replace synthetic antibiotic has received great attention over the past decades (Seal et al., 2013). Several studies have shown that bee pollen includes vital nutrients such as minerals, vitamins and proteins are beneficial to the health and growth performance of humans and animals (Haščík et al., 2013; Abdelnour et al., 2018; Kostic, 2019; Lika et al., 2021).

Wang et al. (2007) stated that bee pollen could be a promising alternative as a beneficial supplement in poultry diets to counteract the challenges that occur during the early stages of a chick. Furthermore, it has been reported that bee pollen increases animal growth, promotes quality and safe products and improves the immunity and health of poultry (Haščík et al., 2017). Haščík et al. (2012) reported that supplementation of bee pollen could increase the weights of the body, carcass and giblets in broiler chickens. Positive results were recorded with fatty acid composition in quail meat (Seven et al., 2016). Improvements on blood parameters and reduced serum uric acid, creatinine triglycerides as well as cholesterol have been reported following supplementation of bee pollen in broiler diets (Farag and El-Rayes, 2016).

Nutritional profile and chemical composition of bee pollen

Nowadays consumers are quite observant about the quality and safety of poultry products (Abdel-Moneim et al., 2020). Supplements from phytogenic feed additives have positive effects that are essential in the growth performance and health of animals through polyphenol content found in plant extracts (Batiha et al., 2020). Polyphenol compounds are found in several parts of plants including grains, flowers (Abdel-Moneim et al., 2020). Bee pollen consists of important nutrients, trace elements and polyphenols including flavonoids (Li et al., 2018). Polyphenol compounds found in bee pollen consists of immunomodulators, anti-flammantory, antioxidant, antimicrobial activities (Lipinski et al., 2017). These compounds in natural substances have improved the growth (Luo et al., 2018) and egg quality in poultry (Galli et al., 2018). Gut health and antioxidant levels in poultry have increased through the use of natural products consisting of polyphenols (Nm et al., 2018). There are several factors that the chemical composition of bee pollen such as the plant species that are used to make the bee pollen and geographical location (Liolios et al., 2019; Mayda et al., 2020). Notable metabolites in bee pollen include an average of 22.7% protein content (Khalifa et al., 2020), 30.8% carbohydrates, 5.1% lipids as essential fatty acids, 1.6% phenolic compounds, 0.6% vitamins and 1% carotenoids (Komosinska- Vassev et al., 2015).

http://www.aloki.hu ● ISSN 1589 1623 (Print) ● ISSN1785 0037 (Online)
DOI: http://dx.doi.org/10.15666/aeer/2005_38173832

The composition of bee pollen is dependant also on the type of soil and beekeeping practices (Nogueira et al., 2012; Urcan et al., 2017). Soil that is healthy should consist of balanced nutrients having the correct pH, enough water holding capacity, a high microbial activity and should be free from toxins of pesticides and herbicides (Magdoff and Van Es, 2021). However, there are new methods such as the use of organic matter on the improving of the quality of soil (FAO, 2005). Literature reviewed indicates that the average digestibility of carbohydrates in bee pollen is 4% and 53% digestibility for the proteins (Franchi, 1997). Freshly collected pollen contains 15-30% water content (Castagna et al., 2020). When bee pollen grains are dissolved in water, nutrient availability as well as digestibility are increased by 60-80% (Kieliszek et al., 2018). Total dry matter digestibility of bee pollen at freshly collected is 62%, enzymatic pretreatment, 85%, dry thermal pretreatment, 89%, wet thermal pretreatment 92% and alkaline pretreatment digestibility, 98% (Benavides et al., 2017). Nutritional profiles and chemical compositions of bee pollen are presented in *Table 1*.

Table 1. *Nutritional profiles and chemical compositions of bee pollen*

Chemical analysis	Percentage (%)	Authors
Component		
Dry matter	90.32 97.17	Farag & El-Rayes, 2016 Zeedan *et al*., 2017
Moisture	19.0 ~20-30	Hsu *et al*., 2021 Luo *et al*., 2021
Lipids	5.1 4.09 3 4-7	Khalifa *et al*., 2020 Farag & El-Rayes, 2016 Bogdanov, 2016b Bogdanov, 2016a
Protein	19.23 22.7 15-29.07 16-29 5-60	Farag & El-Rayes, 2016 Addi, 2018 Kedzia & Holderna- Kedzia, 2012 Odoux *et al*., 2012 Bogdanov, 2016a
Carbohydrates	30.8 62.82 13-55	Kedzia & Holderna-Kedzia, 2012 Farag & El-Rayes, 2016 Bogdanov, 2016a
Ash	1.27 3.28 2.83	Kedzia & Holderna-Kedzia, 2012 Farag & El-Rayes, 2016 Zeedan *et al*., 2017
Fibres	0.90 1.17 0.3-20	Farag & El-Rayes, 2016 Zeedan *et al*., 2017 Bogdanov, 2016a

http://www.aloki.hu ● ISSN 1589 1623 (Print) ● ISSN1785 0037 (Online)
DOI: http://dx.doi.org/10.15666/aeer/2005_38173832

Phenolic compounds in bee pollen

Bee pollen contains polyphenolic compounds such as phenolic acids and flavonoids which are responsible for the numerous biological activities possessed by bee pollen (Rocchetti et al., 2019). The total content of the polyphenols in bee pollen range from 3-5% depending on the plant origin (Campos et al., 2005). The high polyphenols properties found in bee pollen protect health and immunity in poultry (Ali and Kunugi, 2021). Phenolic acids (0.19%) and flavonoids are polyphenols which are responsible for the numerous biological activities found in bee pollen (Rzepecka-Stojko et al., 2015).

The bio- availability of phenolic compounds in bee pollen is beneficial to the health of animals and humans (Omar et al., 2016). Flavonoids have been reported to constitute about 1.6% of the polyphenolic content of bee pollen with the most common ones being catechins, leucothocyanidins, quercetin, kaempferol and isorhamnetin. Flavonoids are well known for their high antioxidants properties (Pascoal et al., 2014; Komosinska–Vasser et al., 2015; Kostić, 2019). The most common phenolic acids in bee pollen are p-coumaric, chlorogenic and ferulic acids (Kocot et al., 2018). The antiproliferative properties of polyphenols found in bee pollen set a balance on cell proliferation (Preemratanachai and Chanchao, 2014). Glycosides are usually in occurrence as flavonoids in bee pollen and they can be 2.5% in total content (Kieliszek et al., 2018). The composition of phenolic compounds in bee pollen largely depends on the plant species that are used to make the pollen as well as the geographical conditions such as soil types among other factors (Addi, 2018). Absorption of polyphenols depends on the physicochemical properties. The best absorption takes place in the gastrointestinal tract in forms that are soluble in water. However, absorption of polyphenols is based on the structural type of both phenolic acids and flavonoids (Rzepecka-Stojko et al., 2015).

Within the structure of phenolic acids, benzoic and cinnamic acid are the most common. However, cinnamic acid contains antioxidants that are more effective. Hydroxyl groups play an important role in determining the total amount of antioxidant activity (Rzepecka-Stojko et al., 2015). The presence of phenols enhance taste, texture and nutritional content of the diet and this help maximize the growth, health and safety of the animals (Batiha et al., 2020). However, the low bioavaliabity and slow absorption in the gut should further be investigated in poultry production (Abdel-Moneim et al., 2020).

When poultry birds are under stressful conditions, this affects their chromosome causing no production of free radicals such as reactive nitrogen species (RNS) and reactive oxygen species (ROS) (Lipinski et al., 2017). The most effective polyphenols to help with production of free radicals are flavonoids, which are essential since they prevent injuries to occur in poultry bodies (Prochazkova et al., 2011)

Effects of bee pollen in poultry feeds on growth performance and gut morphology

Several studies have emphasized on the use of bee pollen in poultry diets to improve nutrition, health and growth performance while decreasing toxins (Hegazi et al., 2012). The antioxidant compounds, known to be free radical scavengers in bee pollen eliminate toxins in the animal body (Campos et al., 2003). The high levels of polyphenols and tannins that bee pollen possess play a vital role as protective agents and antioxidants that are key to the health of animals (Ali and Kunugi, 2021). Studies have shown that bee pollen can help to reduce stress levels in birds through the reduction of oxidative stress markers thereby enhancing the capacity of the antioxidant system of birds (Ketkar et al.,

http://www.aloki.hu ● ISSN 1589 1623 (Print) ● ISSN1785 0037 (Online)
DOI: http://dx.doi.org/10.15666/aeer/2005_38173832

2015). Early chick nutrition is important during the early stages of a chick's life for optimal growth (Riva and Panisello, 2020). *In vivo* feeding trials conducted in chicks to explore the nutritional properties of bee pollen reported that bee pollen can play an important role in early chick nutrition through improved growth and immune stimulation (Malayo˘glu et al., 2010). Bee pollen is rich in essential amino acids, unsaturated fatty acids, carbohydrates and minerals which act as catalysts in improving body weight gain in birds (Farag and El-Rayes, 2016). Reports have revealed that bee pollen supplementation in diets of birds can enhance the initial development of the gastrointestinal tract and the process of digestion (Toman et al., 2015; Haščík et al., 2017).

Bee pollen is composed of several nutrient components such as amino acids, vitamins, hormones, minerals, enzymes and coenzymes that are important for digestion and production of cells (Wang et al., 2007). The glands of the small intestine play an important role in absorption of nutrients which therefore increases development and growth of the gut (Wang et al., 2007). Bee pollen contains enzymes which assist in the process of digestion to improve feed conversion ratio and due to its palatability it increases feed intakes in broiler chickens (Haščík et al., 2012). Feed conversion improvement in broilers may be due to the vitamins, amino acids, hormones and minerals found in bee pollen (Farag and El-Rayes, 2016).

Further findings show that bee pollen consists of nutrients that are essential for improved digestion and growth of cells in broiler chickens (Wang et al., 2007). Basim et al. (2006) and Kročko et al. (2012) evaluated the effects of bee pollen supplementation on the crop of chickens and reported reduced counts of bacteria of the *Enterobacteriaceae* family which supports the antibacterial properties of bee pollen. Similar observations were found for the ileum and caecum (Haščík et al., 2013). According to several literatures, decrease in *Enterobacteriaceae* counts in the gastrointestinal tract of chickens may be due to the antibacterial properties of bee pollen (Kumova et al., 2002; Basim et al., 2006). However, there is scarce literature on bee pollen antibacterial properties on poultry gut health. Several studies have reported the effect of bee pollen supplementation on growth performance and gut morphology in poultry diets. *Table 2*, *Table 3* and *Table 4* present findings from several studies that investigated the effects of bee pollen supplementation in poultry diets on growth performance, gut morphology and gut health.

The potential for large scale bee pollen production and processing technologies in developing countries

Apiculture is an agricultural practice that can be carried out with minimum pollution to the environment (Kohsaka et al., 2017; Paray et al., 2020). Beekeepers are developing business skills and using new innovations in the beekeeping industry. Apiculture can thrive in environments where plant production is not sustainable due to factors such as land type (Paray et al., 2020). Bee products can contribute to income generation, development and sustainability of food security strategies in developing countries around the world (FAO, 2018; Zheng et al., 2018). Pollen sources for bee pollen production varies in different countries and regions due to environmental impacts. In South Africa, pollen sources include purple echium, macadamia, maize and pine trees. Protein content for eucalyptus species differ from 17%-30% (Louw, 2022). China, Australia and Argentina are the biggest producers of bee pollen (Estevinho et al., 2012). According to CNCAGR 2011, China has 6 million *Apis mellifera* colonies. The total amount of honey produced yearly is 450,000 metric tons which a third is exported to countries like Japan, United Kingdom, Belgium and Spain (Fang, 2015, 2016). In Africa, Ethopia is amongst

http://www.aloki.hu ● ISSN 1589 1623 (Print) ● ISSN1785 0037 (Online)
DOI: http://dx.doi.org/10.15666/aeer/2005_38173832

the top producers of honey (CSA, 2020) with a total of 53782 tons of honey (FAO, STAT, 2020). South Africa is a diverse country with several landscapes consisting of several plants and pollinators (Mittermeier et al., 2011). In 2017, South Africa has produced a total amount of 1500 tons of honey. However, several factors that are playing a role in low production of bee products include the high prevalence of pathogens, low and erratic rainfall and veld fires and this is why it is mostly imported from other countries such as China (Langenhoven, 2018). South African production and marketing of bee products is still at a very low level for it to be able to meet the consumer demands (Preuss, 2019; Hall, 2020). This therefore makes South Africa a net importer of bee products from China and the neighbouring African countries (Hall, 2020).

Table 2. *Observations on the effect of bee pollen supplementation in poultry diets on growth performance*

Poultry species	Levels	Observations	Authors
Broiler chicken	2%	There was an increase in average daily gain by 15.6%	Hosseini *et al*., 2016
Broiler chicken	0.6%	Improved body weight gain	Farag & El-Rayes, 2016
Japanese quails	0.5%	Increase in growth performance and weight gain	Babaei *et al*., 2016
Broiler chickens	0.5-1.5%	Improved growth performance and carcass traits	DeOliveria *et al*., 2013
Broiler chickens	0.04%	Bee pollen increased growth performance and body weights in broilers	Haščík *et al*., 2012
Broiler chickens	0.2%, 0.4%,0.6%	Improved body weight gain by 8.14%, 8.86% and 11.65% compared to the control birds	Abdelnour *et al*., 2018
Broiler chicken	0.05-0.15%	Average daily feed intake were increased	Hosseini *et al*., 2016
Broiler chicken	0.002%	No increase in feed conversion ratio under high ambient temperature	Hosseini *et al*., 2016
Broiler chicken	0.6%	Improved feed conversion ratios under high ambient temperature compared to the control group	Farag & El-Rayes, 2016
Laying hens and quails	0.05-0.15%	Egg production and performance was improved	Abuoghaba,2018; Desoky & Kamel, 2018

http://www.aloki.hu ● ISSN 1589 1623 (Print) ● ISSN1785 0037 (Online)
DOI: http://dx.doi.org/10.15666/aeer/2005_38173832

Table 3. *Observations on the effects of bee pollen supplementation in poultry diets on gastrointestinal tract morphology*

Poultry species	Levels	Observations	Authors
Broiler chicken	0.001%	Improved length and weight of intestinal villi	Wang *et al*., 2007
Broiler chicken	0.1-1.5%	Increased villus length and villus length: crypt length	Fazayeli-Rad *et al*., 2015
Broiler chicken	1.5%	Jejenum crypt depth was increased	Fazayeli-Rad *et al*, 2015
Broiler chicken		The lengths of small intestine were longer	Haščík *et al*., 2013
Broiler chicken	1.5%	Weights of spleen increased in broiler diets	Wang *et al*., 2005
Broiler chicken	0.6%	Weights of the gizzard and liver increased by 2.21% and 2.07%	Song *et al*., 2005; Wang *et al*., 2007
Broiler chicken	0.6%	Increased weights thymus, bursa and spleen	Farag & El-Rayes, 2016

Table 4. *Observations on the effects of bee pollen supplementation in poultry diets on gastrointestinal tract health*

Poultry Species	Levels	Observations	Authors
Broiler chicken	0.6%	High levels of bee pollen supplementation revealed low bacterial colonization in the crop	Kročko *et al*., 2012
Broiler chicken	0.6%	Reduction of bacterial colonization in the ileum and caecum	Haščík *et al*., 2013
Broiler chicken	4.5%	Low number of Enterobacteriaceae family in the ileum and caecum than the control and other experimental groups	Kročko *et al*., 2012

Generally, there is an increase in innovative drying technologies that conserve the good quality of bee products in most part of the world. However, processing techniques that can effectively improve the nutritional value and quality of the product are still highly required (Luo et al., 2021). This is why bee pollen after collection should be processed to avoid microbial development and help keep the physicochemicals (Palla et al., 2018). To maintain the nutrition value of bee pollen and other products, different processing techniques are critical such as drying (Thakur and Nanda, 2018), pulverization (Kostić et al., 2017), freeze drying (Ghosh and Jung, 2020), use of vacuum to extract impurities (Thakur and Nanda, 2018; Mayda et al., 2020), storage in bags at 4^{o}C (Zuluaga-Dominguez and Quicazan, 2019) and in areas that are dark at ±20^{o}C (Araujo et al., 2017). Bee pollen as a feed ingredient requires to understand ways on storing and preserving to avoid losing all the nutrients it possess (Kostic et al., 2020). Factors such as humidity, temperature, gas atmosphere and pressure of oxygen affects the viability of pollen

http://www.aloki.hu ● ISSN 1589 1623 (Print) ● ISSN1785 0037 (Online)
DOI: http://dx.doi.org/10.15666/aeer/2005_38173832

(Stanely and Linskens, 1974). For the poultry bodies to function and the chemical process to take place, there is a certain amount of nutrients required in diets of animals which are antioxidants, antimicrobials, emulsifiers, vitamins and minerals (Kostic et al., 2020). Of these techniques, drying is a very important technique that controls the moisture and new drying techniques such as IR radiation which influences the quality and colour of bee pollen are being developed (Luo et al., 2021).

Conclusion and recommendation

Bacterial resistance to commercially available antibiotics is a global concern. Naturally available products such as bee pollen have potential to replace commercial antibiotics. The high safety margin of natural products as compared to commercial remedies has made them popular as animal feed additives particularly in the developing countries in an effort to strike a balance between profitability and the safety of animal products. Bee pollen has shown that it can be a promising natural growth promoter to improve growth, performance, quality and safe products in poultry production. It contains bioactive ingredients with various properties that have revealed to play a vital role in development and growth in poultry. A few studies have been conducted showing different levels of supplementation in poultry diets. Bee pollen supplementation of 0.6% showed to have a tremendous outcome on the body weights and improvement of gut morphology of broiler chickens. This level of supplementation could be recommended in poultry diets. However, more studies should be conducted to further investigate improvements in growth performances on poultry birds. Diverse beekeeping strategies need to be introduced especially in developing countries so as to be able to meet the demands for bee pollen and other related products.

Acknowledgements. The authors would like to acknowledge the Department of Agricultural Economics and Animal Production, University of Limpopo for internet and other resources that were critical to develop this review article.

Authors' Contributions. MFDN, JWN and TC gathered the literature. SDK, EM and TGM contributed to manuscript write up. MFDN, JWN and TC finalized the manuscript. All the authors approved the final version of the manuscript.

Conflict of Interests Declaration. All the authors do not have any conflicts of interests to declare.

REFERENCES

[1] Abdel-Moneim, A. M. E., Shehata, A. M, Alzahrani, S. O. (2020): The role of polyphenols in poultry nutrition. – Journal of Animal Physiology and Animal Nutrition 104: 1851-1866.
[2] Abdelnour, S. A., El-Hack, M. E. A., Alagawany, M., Farag, M. R., ElNesr, S. S. (2018): Beneficial impacts of bee pollen in animal production, reproduction and health. – Journal of Animal Physiology and Animal Nutrition 103: 477-484.
[3] Abuoghaba, A. A. K. (2018): Egg Production, Egg Quality Traits and Some Hematological Parameters of Sinai Chicken Strain Treated with Different Levels of Bee Pollen. – Journal of Egyptian Poultry Science 38: 427-438.
[4] Addi, A. (2018): Proximate composition and antioxidant power of bee collected pollen from moist Afromontan forests in southwest Ethiopia. – Agricultural Science Research Journal 7: 83-95.

http://www.aloki.hu ● ISSN 1589 1623 (Print) ● ISSN1785 0037 (Online)
DOI: http://dx.doi.org/10.15666/aeer/2005_38173832

[5] Ali, A. M., Kunugi, H. (2021): Propolis, Bee Honey, and Their Components Protect against Coronavirus Disease 2019 (COVID-19): A Review of In Silico, In Vitro, and Clinical Studies. – Molecules 26(5): 1232.
[6] Al-Qazzaz, M. F., Ismail, D. B. (2016): Insect meal as a source of protein in animal diet. – Animal Nutrition and Feed Technology 16: 527-547.
[7] Araujo, J. S., Chambo, E. D., Costa, M., Cavalcante da Silva, S. M. P., Lopes de Carvalho, C. A. L., Estevinho, L. M. (2017): Chemical composition and biological activities of mono- and heterofloral bee pollen of different geographical origins. – International Journal of Molecular Sciences 18(5): 921.
[8] Attia, Y. A., Al-Hamid, A. B. D., Ibrahim, A. E. M., Al-Harthi, S., Bovera, M. A., Elnaggar, A. S. (2014): Productive performance, biochemical and hematological traits of broiler chickens supplemented with propolis, bee pollen, and mannan oligosaccharides continuously or intermittently. – Livestock Science 164: 87-95.
[9] Attia, Y. A., Mahmoud, A., Farag, M. R., Alkhatib, F. M., Khafaga, A. F., Abdel-Moneim, A.-M. E., Asiry, K. A., Mesalam, N. M., Shafi, M. E., Al-Harthi, M. A., El-Hack, M. E. A. (2020): Phytogenic products and phytochemicals as a candidate strategy to improve tolerance to COVID-19. – Frontiers in Veterinary Science.
[10] Babaei, S., Rahimi, S., Torshizi, M. K., Tahmasebi, G., Miran, S. N. (2016): Effects of propolis, royal jelly, honey and bee pollen on growth performance and immune system of Japanese quails. – Veterinary Research Forum 1: 13-20.
[11] Basim, E., Basim, H., Özcan, M. (2006): Antibacterial activities of Turkish pollen and propolis extracts against plant bacterial pathogens. – Journal of Food Engineering 77(4): 992-996.
[12] Batiha, G. E. S., Beshbishy, A. W., Wasef, L., Elewa, Y. H. A., El-Hack, M. E. A., Taha, A. E., Al-Sagheer, A. A., Devkota, H. P., Tufarelli, V. (2020): Uncaria tomentosa (Willd. ex Schult.) DC.: A review on chemical constituents and biological activities. – Applied Science 10(8): 2668.
[13] Benavides, G. R., Quicazán, M., Toro, C. (2017): Digestibility and availability of nutrients in bee pollen applying different pretreatments. – Ingeniería y Competitividad 19: 119-128.
[14] Bishop, H. (2002): Behind the Bee's Knees. – Gastronomica 3(3): 19-24.
[15] Bogdanov, S. (2016a): Pollen: Production, Nutrition and Health: A Review. – Bee Product Science.
[16] Bogdanov, S. (2016b): Pollen: Collection, Harvest, Composition, Quality. – Bee Product Science.
[17] Campos, M. G., Webby, R. F., Markham, K. R., Mitchell, K. A., da Cunha, A. P. (2003): Age-induced diminution of free radical scavenging capacity in bee pollens and the contribution of constituent flavonoids. – Journal of Agricultural and Food Chemistry 51: 742-745.
[18] Campos, M., Bogdanov, S., Almeida-Muradian, L., Szczesna, T., Mancebo, Y., Frigerio, C., Ferreira, F. (2008): Pollen composition and standardisation of analytical methods. – J. Apic. Res. Bee. W. 47: 156-163.
[19] Carlet, J., Jarlier, V., Harbarth, S. (2012): Ready for a world without antibiotics. The Pensières Antibiotic Resistance Call to Action. – Antimicrobial Resistance and Infection Control 1: 11.
[20] Castagna, A., Benelli, G., Conte, G., Sgherri, C., Signorini, F., Nicolella, C., Ranieri, A., Canale, A. (2020): Drying Techniques and Storage: Do They Affect the Nutritional Value of Bee-Collected Pollen? – Molecules 25: 4925.
[21] Centers for Disease Control and Prevention (2021): Antibiotic resistance, food and food animals. – Content source: Centers for Disease Control and Prevention, National Center for Emerging and Zoonotic Infectious Diseases (NCEZID), Division of Foodborne, Waterborne, and Environmental Diseases (DFWED).
[22] Cheng, Y. (2009): Effect of bee-collected pollen on the growth of immune organs of miscellaneous broilers. – Journal of Animal and Feed Sciences 30: 23-24.

http://www.aloki.hu ● ISSN 1589 1623 (Print) ● ISSN1785 0037 (Online)
DOI: http://dx.doi.org/10.15666/aeer/2005_38173832

[23] Cheng, G., Hao, H., Xie, S., Wang, X., Dai, M., Huang, L., Yuan, Z. (2014): Antibiotic alternatives: the substitution of antibiotics in animal husbandry? – Frontiers in Microbiology 5: 217.
[24] CSA. (2020): Livestock and Livestock Characteristics. – Federal Democratic Republic of Ethiopia Central Statistical Agency: Agricultural Sample Survey (Private Peasant Holdings).
[25] De Oliveira, M., Da Silva, D., Loch, F., Martins, P., Dias, D., Simon, G. (2013): Effect of bee pollen on the immunity and tibia characteristics in broilers. – Revista Brasileira de Ciencia Avicola 15(4): 323-327.
[26] Desoky, A., Kamel, N. (2018): Egg Production Performance, Blood Biochemical and Immunological Response of Laying Japanese Quail Fed Diet Supplemented with Propolis and Bee Pollen. – Egyptian Journal of Nutrition and Feeds 21(2): 549-557.
[27] Dubtsova, E. A. (2009): Structure biological properties of honey, pollen and royal jelly and their possible use in nutrition therapy. – Clinical and Experimental Gastroenterology 3: 36-41.
[28] Elahi, U., Xu, C., Wang, J., Lin, J., Wu, S., Zhang, H., Qi, G. (2022): Insect meal as a feed ingredient for poultry. – Animal Bioscience 35.
[29] Estevinho, L. M., Rodrigues, S., Pereira, A. P., Feás, X. (2012): Portuguese bee pollen: palynological study, nutritional and microbiological evaluation. – International Journal of Food Science and Technology 47: 429-35.
[30] Fang, B. B. (2015): The review of Chinese bee products market of 2014 and the forecast of 2015. – Apiculture of China 66(5): 16-17.
[31] Fang, B. B. (2016): The review of Chinese bee products market of 2015 and the forecast of 2016. – Apiculture of China 67(5): 12-13.
[32] FAO (2005): Status of research and application of crop biotechnologies in developing countries: Preliminary assessment. – Food and Agriculture Organization of the United Nations, 2005, Rome.
[33] FAO (2018): Ethiopia: report on feed inventory and feed balance. – FAO, Food and Agriculture Organization of the United Nations, Rome, Italy.
[34] Farag, S. A., El-Rayes, T. K. (2016): Effect of bee pollen supplementation on performance, carcass traits and blood parameters of broiler chickens. – Asian Journal of Animal and Veterinary Advances 11(3): 68-77.
[35] Fazayeli-Rad, A. R., Afzali, N., Farhangfar, H., Asghari, M. R. (2015): Effect of bee pollen on growth performance, intestinal morphometry and immune status of broiler chicks. – European Poultry Science 79.
[36] Franchi, G. G. (1997): Microspectrophotometric evaluation of digestibility of pollen grains. – Plant Foods for Human Nutrition 50(2): 115-26.
[37] Galli, G. M., Da Silva, A. S., Biazus, A. H., Reis, J. H., Boiago, M. M., Topazio, J. P., Migliorini, M. J., Guarda, N. S., Moresco, R. N., Ourique, A. F., Santos, C. G., Lopes, L. S., Baldissera, M. D., Stefani, L. M. (2018): Feed addition of curcumin to laying hens showed anticoccidial effect, and improved egg quality and animal health. – Research in Veterinary Science 118: 101-106.
[38] Gheisar, M. M., Kim, I. H. (2017): Phytobiotics in poultry and swine nutrition-A review. – Italian Journal of Animal Science 17: 92-99. doi.org/10.1080/1828051X.2017.1350120.
[39] Ghosh, S., Jung, C. (2020): Changes in nutritional composition from bee pollen to pollen patty used in bumblebee rearing. – Journal of Asia-Pacific Entomology 3(3): 701-708.
[40] Gratzer, K., Wakjira, K., Fiedler, S., Brodschneider, R. (2021): Challenges and perspectives for beekeeping in Ethiopia. A review. – Agronomy for Sustainable Development 41.
[41] Hafez, M. H., Attia, Y. A. (2020): Challenges to the poultry industry: Current perspectives and strategic future after the COVID-19 outbreak. – Frontiers in Veterinary Science.
[42] Hall, G. (2020): The Sticky Situation: Honey adulteration and quality in South Africa: how to tackle this problem. – South African Bee Journal 92: 3.

http://www.aloki.hu ● ISSN 1589 1623 (Print) ● ISSN1785 0037 (Online)
DOI: http://dx.doi.org/10.15666/aeer/2005_38173832

[43] Haščík, P., Elimam, I., Garlík, J., Kačániová, M., Čuboň, J., Bobko, M., Abdulla, H. (2012): Impact of bee pollen as feed supplements on the body weight of broiler Ross 308. – African Journal of Biotechnology 11(89): 15596-15599.
[44] Haščík, P., Elimam, I., Garlík, J., Kačániová, M., Čuboň, J., Bobko, M., Vavrišinová, K., Arpášová, H. (2013): The effect of bee pollen as dietary supplement on meat chemical composition for broiler Ross 308. – Acta Universitatis Agriculturae et Silviculturae Mendelianae Brunensis 61(1): 71-76.
[45] Haščík, P., Pavelkova, A., Bobko, M., Trembecká, L., Elimam, I., Capcarova, M. (2017): The effect of bee pollen in chicken diet. – World's Poultry Science Journal 73(3): 643-650.
[46] Hashmi, M. S., Haščík, P., Eliman, I., Garlík, J., Bobko, M., Kačániová, M. (2012): Effects of Bee Pollen on the Technical and Allocative Efficiency of Meat Production of Ross 308 Broiler. – International Journal of Poultry Science 11(11): 689-695.
[47] Hegazi, A. G., Abd El Hady, F. K., Abd Allah, F. A. (2000): Chemical composition and antimicrobial activity of European propolis. – Zeitschrift fur Naturforschung. C, Journal of biosciences 55(1-2): 70-75.
[48] Hilmi, M., Bradbear, N., Mejia, D. (2019): Beekeeping and sustainable livelihoods. – FAO, Rome.
[49] Hosseini, S. M., Vakili Azghandi, M., Ahani, S., Nourmohammad, R. (2016): Effect of bee pollen and propolis (bee glue) on growth performance and biomarkers of heat stress in broiler chickens reared under high ambient temperature. – Journal of Animal and Feed Sciences 25(1): 45-51.
[50] Hsu, P. S., Wu, T. H., Huang, M. Y., Wang, D. Y., Wu, M. C. (2021): Nutritive Value of 11 Bee Pollen Samples from Major Floral Sources in Taiwan. – Foods 10(9): 2229.
[51] Johnson, J. (2021): Bee pollen: Benefits, uses, side effects and more. – Reviewed by Ritcher, R. D. Nutrition. Medical news today, newsletter.
[52] Kačániová, M., Rovná, K., Arpášová, H., Hleba, L., Petrová, J., Haščík, P., Cuboň, J., Pavel, A. (2013): The effects of bee pollen extracts on the broiler chicken's gastrointestinal microflora. – Veterinary Science Research Journal 95: 34-37.
[53] Kędzia, B., Hołderna-Kędzia, E. (2012): New studies on biological properties of pollen. – Postepy Fitoter 1: 48-54.
[54] Ketkar, S., Rathore, A. S., Kandhare, A., Lohidasan, S., Bodhankar, S., Paradkar, A., Mahadik, K. (2015): Alleviating exercise-induced muscular stress using neat and processed bee pollen: Oxidative markers, mitochondrial enzymes, and myostatin expression in rats. – Integrative Medicine Research 4: 147-160.
[55] Khalifa, S. A. M., Elashal, M., Kieliszek, M., Ghazala, N. E., Farag, M. A., Saeed, A. (2020): Recent insights into chemical and pharmacological studies of bee bread. – Trends in Food Science and Technology 97: 300-316.
[56] Kieliszek, M., Piwowarek, K., Kot, A. M., Błazejak, S., Chlebowska-Smigiel, A., Wolska, I. (2018): Pollen and bee ´ bread as new health-oriented products: A review. – Trends in Food Science & Technology 71: 170-180.
[57] Kocot, J., Kiełczykowska, M., Luchowska-Kocot, D., Kurzepa, J., Musik, I. (2018): Antioxidant potential of propolis, bee pollen and royal jelly: Possible medical application. – Oxidative Medicine and Cellular Longevity 2018: 7074209.
[58] Kohsaka, R., Park, M. S., Uchiyama, Y. (2017): Beekeeping and honey production in Japan and South Korea: Past and Present. – Journal of Ethnic Foods 4(2): 72-79.
[59] Komosinska–Vassev, K., Olczyk, P., Kazmierczak, J., Mencner, L., Olczyk, K. (2015): Bee pollen: Chemical composition and therapeutic application. – Evidence-Based Complementary and Alternative Medicine 2015: 297425.
[60] Kostić, A. Ž. (2019): Polyphenolic profile and antioxidant properties of bee-collected pollen from sunflower (*Helianthus annuus* L.) plant. – Lebensmittel-Wissenschaft Technologie 112: 108244.
[61] Kostić, A. Ž., Pešić, M. B., Trbović, D., Petronijević, R., Dramićanin, A. M., Milojković-Opsenica, D. M. (2017): The fatty acid profile of Serbian bee-collected pollen – a

http://www.aloki.hu ● ISSN 1589 1623 (Print) ● ISSN1785 0037 (Online)
DOI: http://dx.doi.org/10.15666/aeer/2005_38173832

chemotaxonomic and nutritional approach. – Journal of Apicultural Research 56(5): 533-542.
[62] Kostić, A., Milinčić, D., Barać, M., Ali Shariati, M., Tešić, Z., Pešić, M. (2020): The application of pollen as a functional food and feed ingredient - The present and perspectives. – Biomolecules 10(1): 84.
[63] Kročko, M., Čanigová, M., Bezeková, J., Lavová, M., Haščík, P., Ducková, V. (2012): Effect of nutrition with propolis and bee pollen supplements on bacteria colonization pattern in gastrointestinal tract of broiler chickens. – Lucr. Stiint. Zooteh. Biotehnology 45: 63-67.
[64] Kumova, U., Korkmaz, A., Avci, B. C., Ceyran, G. (2002): An important bee product: propolis. – Uludag Apiculture Journal 2: 10-24.
[65] Langenhoven, N. (2018): Supplementary feeding – the new norm in beekeeping. – South African Bee Journal 90(1): 10-16.
[66] Li, Q. Q., Wang, K., Marcucci, M. C., Sawaya, A. C. H. F., Hu, L., Xue, X. F., Wu, L. M., Hu, F. L. (2018): Nutrient-rich bee pollen: A treasure trove of active natural metabolites. – Journal of Functional Foods 49: 472-484.
[67] Lika, E., Kostic, M., Vještica, S., Milojević, I., Puvača, N. (2021): Honeybee and Plant Products as Natural Antimicrobials in Enhancement of Poultry Health and Production. – Sustainability (Basel) 13(15): 8467.
[68] Liolios, V., Tananaki, C., Papaioannou, A., Kanelis, D., Rodopoulou, M. A., Argena, N. (2019): Mineral content in monofloral bee pollen: Investigation of the effect of the botanical and geographical origin. – Journal of Food Measurement and Characterization 13(3): 1674-1682.
[69] Lipiński, K., Mazur, M., Antoszkiewicz, Z., Purwin, C. (2017): Polyphenols in monogastric nutrition – A review. – Annals of Animal Science 17(1): 41-58.
[70] Liu, G., Yan, W., Zeng, Z. (2010): Application of bee pollen on the Gallus feed. – Mifeng. Zazhi 3: 22-29.
[71] Louw, M. (2022): Bees and pollination. Beekeeping in South Africa.
[72] Luo, J., Song, J., Liu, L., Xu, B., Tian, G., Yang, Y. (2018): Effect of epi-gallocatechin gallate on growth performance and serum biochemical metabolites in heat-stressed broilers. – Poultry Scienece 97(2): 599-606.
[73] Luo, X., Dong, Y., Gu, C., Zhang, X., Ma, H. (2021): Processing Technologies for Bee Products: An Overview of Recent Developments and Perspectives. – Frontiers in Nutrition 8: 834.
[74] Magdoff, F., Van Es, H. (2021): Building soils for better crops. Ecological management for healthy soils. – Sustainable Agriculture Research and Education, 4th edition.
[75] Malayoglu, H. B., Baysal, S., Misirlioglu, Z., Polat, M., Yilmaz, H., Turan, N. (2010): Effects of oregano essential oil with or without feed enzymes on growth performance, digestive enzyme, nutrient digestibility, lipid metabolism and immune response of broilers fed on wheat–soybean meal diets. – British Poultry Science 51: 67-80.
[76] Masehela, T. (2017): An assessment of different beekeeping practices in South Africa based on their needs (bee forage use), services (pollination services) and threats (hive theft and vandalism). – Thesis for: PhD Entomology.
[77] Masud, A. A., Rousham, E. K., Islam, M. A., Alam, M. U., Rahman, M., Mamun, A. A., Sarker, S., Asaduzzaman, M., Unicomb, L. (2020): Drivers of Antibiotic Use in Poultry Production in Bangladesh: Dependencies and Dynamics of a Patron-Client Relationship. – Frontiers in Veterinary Science 28: 7-78.
[78] Mayda, N., Özkök, A., Bayram, N. E., Gerçek, Y. C., Sorkun, K. (2020): Bee bread and bee pollen of different plant sources: Determination of phenolic content, antioxidant activity, fatty acid and element profiles. – Journal of Food Measurement and Characterization 14: 1795-1809.
[79] Mazorodze, B. (2020): The contribution of apiculture towards rural income in Honde Valley Zimbabwe. – AgEcon Search.

http://www.aloki.hu ● ISSN 1589 1623 (Print) ● ISSN1785 0037 (Online)
DOI: http://dx.doi.org/10.15666/aeer/2005_38173832

[80] Mittermeier, R. A., Turner, W. R., Larsen, F. W., Brooks, T. M., Gascon, C. (2011): Global biodiversity conservation: The critical role of hotspots. – In: Zachos, F. E., Habel, J. C. (eds.) Biodiversity hotspots. Heidelberg: Springer, pp. 3-22.
[81] Morais, M., Moreira, L., Feás, X., Estevinho, L. M. (2011): Honeybee-collected pollen from five Portuguese natural parks: Palynological origin, phenolic content, antioxidant properties and antimicrobial activity. – Food and Chemical Toxicology 49: 1096-1101.
[82] Nm, J., Joseph, A., Maliakel, B., Im, K. (2018): Dietary addition of a stan-dardized extract of turmeric (TurmaFEEDTM) improves growth per-formance and carcass quality of broilers. – Journal of Animal Science and Technology 60(1): 8.
[83] Nogueira, C., Iglesias, A., Sanchez, X., Estevinho, L. (2012): Commercial Bee Pollen with Different Geographical Origins: A Comprehensive Approach. – International Journal of Molecular Sciences 13(9): 11173-11187.
[84] Odoux, J. F., Feuillet, D., Aupinel, P., Loublier, Y., Tasei, J. N., Mateescu, C. (2012): Territorial biodiversity and consequences on physico-chemical characteristics of pollen collected by honey bee colonies. – Apidologie 43: 561-575.
[85] Oliveira, M. C., Silva, D. M., Loch, F. C., Martins, P. C., Dias, D. M. B., Simon, G. A. (2013): Effect of bee pollen on the immunity and Tibia characteristics in broilers. – Brazilian Journal of Poultry Science 15(4): 323-328.
[86] Omar, W. A. W., Azhar, N. A., Fadzilah, N. H., Kamal, N. N. S. N. (2016): Bee pollen extract of Malaysian stingless bee enhances the effect of cisplatin on breast cancer cell lines. – Asian Pacific Journal of Tropical Biomedicine 6(3): 265-269.
[87] Palla, M., Turrini, A., Sbrana, C., Signorini, F., Nicolella, C., Benelli, G., Canale, A., Giovannetti, M., Agnolucci, M. (2018): Honeybee-collected pollen for human consumption: Impact of post-harvest conditioning on the microbiota. – Agrochimica 62(1): 55-66.
[88] Paray, B., Kumari, I., Hajam, Y., Sharma, B., Kumar, R., Albeshr, M., Farah Mand Khan, J. M. (2020): Honeybee nutrition and pollen substitutes: A review. – Saudi Journal of Biological Sciences 28.
[89] Pascoal, A., Rodrigues, S., Teixeira, A., Feas, X., Estevinho, L. M. (2014): Biological activities of commercial bee pollens: Antimicrobial, antimutagenic, antioxidant and anti-inflammatory. – Food and Chemical Toxicology 63: 233-239.
[90] Preuss, H. (2019): South African beekeepers are declining despite robust honey demand. – Business Report.
[91] Procházková, D., Boušová, I., Wilhelmová, N. (2011): Antioxidant and prooxidant properties of flavonoids. – Fitoterapia 82(4): 513-523.
[92] Ricigliano, V., Williams, S., Oliver, R. (2022): Effects of different artificial diets on commercial honey bee colony performance, health biomarkers, and gut microbiota. – BMC Veterinary Research 18: 52.
[93] Riva, S., Panisello, T. (2020): The importance of early nutrition in broiler chickens: Hydrated gels enriched with nutrients, an innovative feeding system. – Animal Husbandry, Dairy and Veterinary Science 4.
[94] Rocchetti, G., Castiglioni, S., Maldarizzi, G., Carloni, P., Lucini, L. (2019): UHPLC-ESI-QTOF-MS phenolic profiling and antioxidant capacity of bee pollen from different botanical origin. – International Journal of Food Science and Technology 54: 335-346.
[95] Rzepecka-Stojko, A., Stojko, J., Kurek-Górecka, A., Górecki, M., Kabała-Dzik, A., Kubina, R., Moździerz, A., Buszman, E. (2015): Polyphenols from Bee Pollen: Structure, Absorption. – Metabolism and Biological Activity Molecules 20(12): 21732-49.
[96] Seal, B., Lillehoj, H., Donovan, D. (2013): Alternatives to antibiotics: A symposium on the challenges and solutions for animal production. – Animal health research reviews / Conference of Research Workers in Animal Diseases 14: 1-10.
[97] Selaledi, L. A., Hassan, Z. H., Manyelo, T. G., Mabelebele, M. (2020): The Current Status of the Alternative Use to Antibiotics in Poultry Production: An African Perspective. – Antibiotics 9: 9.

http://www.aloki.hu ● ISSN 1589 1623 (Print) ● ISSN1785 0037 (Online)
DOI: http://dx.doi.org/10.15666/aeer/2005_38173832

[98] Seven, P. T., Sur Arslan, A., Seven, ˙I., Gökçe, Z. (2016): The effects of dietary bee pollen on lipid peroxidation and fatty acids composition of Japanese quails (Coturnix coturnix japonica) meat under different stocking densities. – Journal of Applied Animal Research 44: 487-491.
[99] Shoskes, D. A., Albakri, Q., Thomas, K. (2002): Cytokine polymorphisms in men with chronic prostatitis/chronic pelvic pain syndrome: association with diagnosis and treatment response. – Journal of Urology 168(1): 331-335.
[100] Shubharani, R., Roopa, P., Sivaram, V. (2013): Pollen morphology of selected bee forage plants. – Global Journal of Bio-Science and Biotechnology 2(1): 82-90.
[101] Song, Y. F., Wang, J., Li, S. H., Shang, C. F. (2005): Effect of bee pollen on the development of digestive gland of broilers. – Animal Husbandry & Veterinary Medicine 37: 14-17.
[102] Stanley, R. G., Linskens, H. F. (1974): Pollen: Biology Biochemistry and Management. – Springer, Berlin.
[103] Thakur, M., Nanda, V. (2018): Assessment of physico-chemical properties, fatty acid, amino acid and mineral profile of bee pollen from India with a multivariate perspective. – Journal of Food and Nutrition Research 57: 328-340.
[104] Toman, R., Hajkova, Z., Hluchy, S. (2015): Changes in Intestinal Morphology of Rats Fed with Different Levels of Bee Pollen. – Pharmacognosy Communications *5*: 261-264.
[105] Urcan, A., Marghitas, L., Dezmirean, D., Bobis, O., Bonta, V., Muresan, C., Mărgăoan, R. (2017): Chemical Composition and Biological Activities of Beebread-Review. – Bulletin of the University of Agricultural Sciences and Veterinary Medicine Cluj-Napoca Animal Science and Biotechnologies 74(1): 6.
[106] Viuda-Martos, M., Ruiz-Navajas, Y., Fernández-López, J., Pérez-Alvarez, J. A. (2008): Functional properties of honey, propolis, and royal jelly. – Journal of Food Science 73(9): R117-24.
[107] Wang, J., Jin, G., Zheng, Y., Li, S., Wang, H. (2005): Effect of bee pollen on development of immune organ of animal. – Zhongguo Zhong Yao Za Zhi 30: 1532-1536.
[108] Wang, J., Li, S., Wang, Q., Xin, B., Wang, H. (2007): Trophic effect of bee pollen on small intestine in broiler chickens. – Journal of Medicinal Food 10(2): 276-280.
[109] Williams-Nguyen, J., Sallach, J. B., Bartelt-Hunt, S., Boxall, A. B., Durso, L. M., Mclain, J. E., Singer, R. S., Snow, D. D., Zilles, J. L. (2016): Antibiotics and antibiotic resistance in agroecosystems: state of the science. – Journal of Environmental Quality 45: 394-406.
[110] Zeedan, K., Battaa, A. M., Elneney, B. A., Abuoghaba, A. A., El-Kholy, K. (2017): Effect of bee pollen at different levels as natural additives on immunity & productive performance in rabbit males. – Egyptian Poultry Science Journal 37: 213-231.
[111] Zheng, H-Q., Cao, L-F., Huang, S., Neumann, P., Hu, F. (2018): Current Status of the Beekeeping Industry in China. – In: Asian Beekeeping in the 21st Century, pp. 129-158.
[112] Zuluaga-Dominguez, C. M., Quicazan, M. (2019): Effect of fermentation on structural characteristics and bioactive compounds of bee-pollen based food. – Journal of Apicultural Science 63: 209-222.

http://www.aloki.hu ● ISSN 1589 1623 (Print) ● ISSN1785 0037 (Online)
DOI: http://dx.doi.org/10.15666/aeer/2005_38173832

CARBONACEOUS DISINFECTION BY-PRODUCTS IN LOW SUVA WATERS: OCCURRENCE, FORMATION POTENTIAL, AND HEALTH RISK ASSESSMENT

OZGUR, C.[1] – KAPLAN-BEKAROGLU, S. S.[2*]

[1]*Sutculer Prof. Dr. Hasan Gurbuz Vocational School, Isparta University of Applied Sciences, Isparta, Turkey*

[2]*Environmental Engineering Department., Suleyman Demirel University, Isparta, Turkey*

**Corresponding author*
e-mail: sulebekaroglu@sdu.edu.tr; phone: +90-246-351-2900; fax: +90-246-351-2901

(Received 17th Mar 2022; accepted 11th Jul 2022)

Abstract. This study aims (1) to determine the regulated carbonaceous disinfection by-products formation potentials under five disinfection scenarios for extremely low specific ultraviolet absorbance water sources, (2) to monitor the spatial and temporal variations of carbonaceous disinfection by-products in two full-scale drinking water distribution system for one-year, and (3) to evaluate carcinogenic and non-carcinogenic health risks of carbonaceous disinfection by-products through multi-pathways. Formation potentials of trihalomethanes and haloacetic acids were in the order of chlorination > ozonation/chlorination > chloramination > ozonation/chloramination > ozonation. Trihalomethanes were the most prevalent disinfection by-products followed by haloacetic acids. Chloroform was the dominant species of trihalomethanes, whereas trichloroacetic acid and dichloroacetic acid were the predominant species of haloacetic acids. No clear seasonality changes in carbonaceous disinfection by-products level were observed in water source with lower dissolved organic carbon values, and higher carbonaceous disinfection by-products values were observed in summer for water sources with higher dissolved organic carbon values. Also, there were no clear correlations between carbonaceous disinfection by-products formations and tested surrogate water quality parameters. Although the non-cancer risk of carbonaceous disinfection by-products was below permissible recommended levels, the average lifetime carcinogenic risk levels for trihalomethanes and haloacetic acids were 6.9E-05 and 5.8E-05, respectively, which were above the negligible risk level.

Keywords: *chlorination, haloacetic acids, multi-pathways exposure, occurrence, SUVA, total lifetime cancer risk, trihalomethanes*

Abbreviations: ANT: Antalya; APR: April; AT: Average Time; AUG: August; BAA: Bromoacetic Acid; BDCM: Bromodichloromethane; BW: Body Weight; C-DBPs: Carbonaceous Disinfection By-Products; C_{air}: THM Concentrations in The Air; CDI: Chronic Daily Intake; CF: Chloroform; Cl: Chlorine; CR: The Cancer Risk; CRT: The Total Cancer Risk; C_w: Concentrations of C-DBPs in Water; DBAA: Bibromoacetic Acid; DBCAA: Dibromochloroacetic Acid; DBCM: Dibromochloromethane; DBP: Disinfection By-Product; DCAA: Dichloroacetic Acid; DEC: December; DOC: Dissolved Organic Carbon; DPD: N, N-Diethyl-P-Phenylenediamine; DS: Distribution System; DUVA: Differential UV Absorbance; ED: Exposure Duration; EF: Exposure Frequency; ET: Exposure Time; FEB: February; FP: Formation Potential; GC/ECD: Gas Chromatography-Electron Capture Detector; HAA: Haloacetic Acid; HI: The Hazard Index; IR: Inhalation Rate; ISP: Isparta; JAN: January; JUL: July; JUN: June; KUM: Kumluca; MAR: March; MCL: Maximum Contaminant Level; MRL: Minimum Reporting Limit; MtBE: Methyl Tert-Butyl Ether; NOM: Natural Organic Matter; NOV: November; OCT: October; PC: Permeability Constant in Water; r: Correlation Coefficient; RfD: Reference Dose; SA: Skin Area; SEP: September; SF: Slope Factors; SUVA: Specific Ultraviolet Absorbance; TBAA: Tribromoacetic Acid; TBM: Tribromomethane; TCAA: Trichloroacetic Acid; TCM: Trichloromethane; The USA: The United States of America; THM: Trihalomethane; TSI: Turkish Statistical Institute; USEPA: United States Environmental Protection Agency; UV: Ultraviolet; UV_{254}: 254 nm Ultraviolet

http://www.aloki.hu ● ISSN 1589 1623 (Print) ● ISSN 1785 0037 (Online)
DOI: http://dx.doi.org/10.15666/aeer/2005_38333851

Introduction

The most used method for disinfection is chlorination for water supplies to ensure microbial quality of drinking water, and it has been playing an essential role in preventing waterborne microbial diseases (String et al., 2020). Complex reactions between disinfectants with precursors can unintentionally form carbonaceous disinfection by-products (C-DBPs) which are classified as possible carcinogens to humans (Mashau et al., 2018; Ates et al., 2020). People may be exposed to C-DBPs by multi-pathways such as ingestion, dermal absorption, inhalation. Several studies have found links between C-DBPs exposure and cancer risk of brain, bladder, colon, and rectum (Du et al., 2021). Studies focused on the health risks of C-DBPs through multi-pathways exposure in different countries showed that the cumulative cancer risk was relatively higher than the negligible risk level (1.0E-06) (Wang et al., 2007; Siddique et al., 2015; Zhang et al., 2018). Also, C-DBPs were also shown to induce reproductive and neurotoxicological adverse effects as a result of C-DBPs (Du et al., 2021).

Trihalomethanes (THMs) were the first C-DBPs class to be detected in chlorinated drinking water in 1974 (Rook, 1974). C-DBPs have been intensively studied, mainly for the conditions affecting their formation, precursors, toxicity, and their adverse health impacts in waters with high specific ultraviolet absorbance (SUVA) value (Tak and Vellanki, 2018; Ates et al.,2020). More than 800 species of disinfection by-products (DBPs) are reported in disinfected water (Ding and Chu, 2017; Sui et al., 2022). THMs and haloacetic acids (HAAs) make up 25% of the total halogenated DBPs are the predominant classes formed after chlorination (Krasner et al., 2016a; Hao et al., 2017). Four THMs have been regulated in most of the countries around the world. Additionally, five HAAs, chlorite, and bromate are also regulated in The United States of America (The USA) (Krasner et al., 2016a). According to the DBPs Stage 2 Rule, maximum contaminant level (MCL) for total THMs at 80 µg/L at each point of the distribution system (DS) by United States Environmental Protection Agency (USEPA). Also, MCL is set 60 µg/L for total HAAs at each sampling point in the DS (USEPA, 2006).

Chlorine is the most widely used chemical disinfectant worldwide. However, alternative disinfectants or disinfection scenarios are used to seek for control and reduction of the formation of C-DBPs, especially the regulated C-DBPs. Alternative disinfectants may reduce the formation of C-DBPs, but they may lead the formation of different classes of DBPs with higher toxicity. The type and amount of disinfectant used in the drinking water treatment are some of the significant parameters that affect the DBPs formation (Ebsa and Dibaba, 2022). However, various factors and conditions influence the formation and speciation of DBPs in very complex ways. The species and concentration of DBPs depend on the type of water source (Rodriguez et al., 2003), contact time and DS length (Tian et al., 2017), temperature (Uyak et al., 2014), and other physicochemical properties of water (Bond et al., 2015). The formation potentials (FPs) tests are important to determine indirectly the amount of DBPs precursors. The majority of DBPs studies investigated formation potentials of waters that have higher SUVA values (>2-3 mg/L) (Tak and Vellanki, 2018). Also, FPs studies based on real waters have generally been limited to chlorination and only for THMs formation. Also, there is a limited study about the FPs tests in low SUVA waters under different disinfection scenarios to examine the presence of C-DBPs precursors in water. Therefore, there is a need to determine the formation and occurrence of DBPs in low SUVA waters. Most of the water supplies in Turkey had low SUVA values. Ates et al.

http://www.aloki.hu ● ISSN 1589 1623 (Print) ● ISSN 1785 0037 (Online)
DOI: http://dx.doi.org/10.15666/aeer/2005_38333851

(2007) performed a comprehensive THMs and HAAs formation study in Turkey at 29 different water sources using chlorine as a disinfectant. Kitis et al. (2010) found that the water sources in the Antalya region were characterized by low organic content, low SUVA, and low bromide (Br^-) concentrations. The main purpose of the study is (i) to determine the FPs of THMs and HAAs using different disinfection scenarios in water sources, specifically, with low SUVA values; and (ii) to monitor THMs and HAAs in two different full-scale DSs (Isparta and Kumluca DSs) (iii) to estimate the lifetime cancer and non-cancer risk of C-DBPs through multiple pathways such as ingestion, dermal absorption, and inhalation. The results will contribute to improve the knowledge regarding FPs of THMs and HAAs about under different disinfection scenarios to determine indirectly the amount of DBPs precursors in low SUVA waters. To decrease C-DBPs in the coming years, the use of alternative disinfectants will be inevitable in the legislation that they will become even stricter in the future. This study is the first study for comparison of different disinfection scenarios for C-DBPs formation in low SUVA waters with tracking spatio-temporal occurrence and assessment of cancer/non-cancer risk of THMs and HAAs through ingestion, dermal absorption, and inhalation routes in Turkey.

Methods

Water sources and sampling strategy

The selected water sources and DSs are in the south of Turkey are used in this study. The first water source is Egirdir Lake in Isparta city located 915 meters above sea level, which is a drinking water source that supplies approximately 265,000 people. The second water source is the Karaagac water source, located 900 meters above sea level which is a drinking water source for approximately 50,000 people, on the west side of Antalya city. In addition to the FPs tests, C-DBPs were monitored in two DSs: Isparta DS and Kumluca DS that is supplied from Egirdir Lake and Karaagac Water Source, respectively. Water samples were collected monthly from two full-scale water DSs between October 2017 and November 2018. To have representative samples from the DSs, different 5 points along the DSs were selected from the closest to the disinfection unit to the farthest. Distribution points for Isparta and Kumluca DSs were numbered from 1 to 5 (one is the closest point, 5 is the farthest point). The distance between the disinfection unit of the Isparta water treatment plant and the furthest point of the water distribution system is approximately 25 kilometers, and the drinking water distribution system of Kumluca is approximately 10 kilometers. In both water DSs, chlorine is used as a disinfectant (Ozgur, 2019). Water samples were quenched using 1:1 sodium sulphite (Na_2SO_3 (Sigma Aldrich)) to end the disinfectant activity. All samples were transferred to the lab and analyzed as soon as possible (no later than 2 days). Analytic methods of selected water quality parameters are shown in *Table 1*. The SUVA is calculated by dividing the ultraviolet (UV) absorbance of the sample (in cm^{-1}) by the dissolved organic carbon (DOC) of the sample (in mg/L) and then multiplying by 100 cm/M. THMs and HAAs analyses were carried out in three repetitions for twelve months at ten points in two separate water distribution networks. Moreover, C-DBPs formation potential tests in both water sources were performed in triplicate over twelve months. Statistical analysis of the water quality data was performed based on t-statistics and 95% confidence intervals were calculated from parallel tests and triplicate measurements.

http://www.aloki.hu ● ISSN 1589 1623 (Print) ● ISSN 1785 0037 (Online)
DOI: http://dx.doi.org/10.15666/aeer/2005_38333851

Table 1. *Water quality parameters and methods*

Parameter	Measurement methods	Instruments	Minimum detection limit
pH	SM 4500 H +	Multi 340i, WTW, Weilheim-Germany	
Temperature	SM 2550		
Free chlorine	Colorimeter/DPD	Pocket Colorimeter™ II, HACH, Colorado, USA	0.1 mg/L
Dissolved organic carbon (DOC)	SM* 5310B	TOC-L Series, Shimadzu, Kyoto, Japan	0.1 mg/L
UV absorbance	SM 5910	BioSpec 1601 UV-Vis Spectrophotometer, Shimadzu, Kyoto, Japan	± 0.005 cm^{-1}
Br^-	USEPA Method 300	The Dionex ICS-3000 Ion Chromatography, California, USA	0.01 mg/L
SUVA	Calculation		

Formation potential tests and analysis of disinfection by products

FPs tests were conducted under five different disinfection scenarios, (1) chlorination, (2) chloramination, (3) ozonation, (4) ozonation/chlorination, and (5) ozonation/chloramination. All FPs tests were conducted in triplicates using 130 mL headspace free amber glass bottles. Chlorine was prepared from a stock sodium hypochlorite solution (10-15%) (Merck). The chloramine stock solution was prepared by mixing very slowly (drop by drop) 500 mg/L chlorine solution to a 500 mg/L ammonium sulphate solution at a pH 9 to a mass ratio of 3.5:1 chlorine/ammonium sulfate (Cl_2/N). Free chlorine and chloramine were determined using N, N-Diethyl-P-Phenylenediamine (DPD) ferrous titrimetric method (APHA, 1995). The chlorine and chloramine dose in the FPs test was determined using *Equations 1* and *2* respectively. Ozone was produced with Degremont Technologies (North America, The USA), Ozonia LAB2B model ozone generator (producing up to 10 g/h using oxygen), and ozone gas was applied 1:1 (Ozone/DOC) ratio according to DOC concentrations. All FP tests were carried out at room temperature in a dark and cool environment for 72 h as previously performed by Krasner (2009). After 72 h, the oxidant concentration in the samples was quenched with sodium sulphite ($Cl_2 : Na_2SO_3$ 1:1). Ozonation + chlorination and ozonation and chloramination scenarios were performed by applying chlorine or chloramine on ozonated water samples. In these processes, the Ozone/DOC ratio was used as 1:1. Ozone concentration in water was measured using AccuVac® Ampules (HACH). Dilutions were made according to DOC concentration (Krasner, 2009).

$$Cl_2(mg/L) = 3 * DOC + 8 * NH_3^- - N * NO_2^- - N + 10 \quad \text{(Eq.1)}$$

$$NH_2Cl(mg/L) = 3 * DOC + 5 * NO_2^- - N \quad \text{(Eq.2)}$$

THMs analysis was performed by USEPA Method 551.1 with inconsequential modifications (USEPA, 1995). A total of six calibration standards (1, 5, 10, 25, 50, and 75 µg/L) were prepared. The minimum reporting limit for THMs measurements was 0.5 µg/L. HAA was analyzed by liquid/liquid extraction using methyl tert-butyl ether (MtBE), followed by derivatization with acidic methanol, and analyzed by gas chromatography-electron capture detector (GC/ECD) (Agilent 6890) according to the USEPA method 552.2 (USEPA, 1995). Standard solutions at concentrations ranging from 0.1 to 2000 µg/L were prepared for the HAAs calibration curve. The minimum

http://www.aloki.hu ● ISSN 1589 1623 (Print) ● ISSN 1785 0037 (Online)
DOI: http://dx.doi.org/10.15666/aeer/2005_38333851

reporting limit (MRL) for HAAs species measurements was 1.0 µg/L. To eliminate the effects of extraction efficiency, water samples were extracted according to the same protocol as the calibration standards. Agilent 6890 gas chromatograph with an electron capture detector was used for both THMs and HAAs measurements.

Cancer risk assessment

The cancer risks (CR) from THMs and HAAs were estimated with calculation using chronic daily intake (CDI) and the corresponding slope factor (SF) (Wang et al., 2019). The total cancer risk (CRT) was the sum of the cancer risks for each species of THMs and HAAs from different exposure pathways. Little's inhalation model was used to the concentrations of THMs in the air in this study (Little, 1992). Parameters used in Little's theory are provided in Ates et al. (2020) study. *Table 2* shows input parameters in cancer/non-cancer risk assessment of THMs and HAAs. The input parameters related on specific to population characteristics were used to represent the accurate assessment using Turkish Statistical Institute (TSI) reports (Ates et al., 2020; TSI, 2022). CR and chronic daily intake (CDI) for each exposure pathway were calculated according to *Equations 3–5:*

$$CR_{ingestion} = CDI_{ingestion} * SF_{ingestion} = \frac{C_w * IR * EF * ED}{(BW * AT)} * SF_{ingestion} \quad \text{(Eq.3)}$$

$$CR_{inhalation} = CDI_{inhalation} * SF_{inhalation} = \frac{C_{air} * IR_a * EF * ED * ET}{BW * AT} * SF_{inhalation} \quad \text{(Eq.4)}$$

$$CR_{dermal} = CDI_{dermal} * SF_{dermal} = (C_w * SA * PC * EF * ED * ET * CF) / (BW * AT) \quad \text{(Eq.5)}$$

Non-cancer risk assessment

The hazard index (HI) was used to estimate the non-carcinogenic risk due to ingestion and dermal and HI of six compounds was calculated by CDI of each compound dividing the reference dose (RfD) according to *Equations 6–7*. Non-cancer risk for inhalation route could not be performed since the RfD values for C-DBPs compounds are not yet evaluated (Kumari and Gupta, 2018). The sum of HI of all each species forms the HI of each pathway. Then the sum of total HI through all the two pathways was the cumulative non-cancer risk of DBPs. Generally, sum of HI < 1 means low non-carcinogenic risk, and sum of HI ≥ 1 means high non-carcinogenic risk.

$$HI_{ingestion} = CDI_{ingestion\ for\ each\ specie}/RfD \quad \text{(Eq.6)}$$

$$HI_{dermal} = CDI_{dermal\ for\ each\ specie}/RfD \quad \text{(Eq.7)}$$

Results and discussion

Water characteristics

During the sampling period, samples were collected from Egirdir Lake and Karaagac Water Source and 10 points from Isparta DS and Kumluca DS. The pH values in water sources were in the range of 7.70-8.54. In Isparta DS and Kumluca DS samples, the pH values of all sampling points vary in the range of 7.12-8.62. The results showed that changes on pH values were quite narrow. When the relationship between pH and DBPs

http://www.aloki.hu ● ISSN 1589 1623 (Print) ● ISSN 1785 0037 (Online)
DOI: http://dx.doi.org/10.15666/aeer/2005_38333851

are determined, it is seen that water sources with high pH value cause more DBPs formation (Hung et al., 2017). The average water temperature measured in the Egirdir Lake and Karaagac were 16.4 °C and 14.7 °C, respectively. The maximum water temperature in Isparta DS is 27 °C, the maximum water temperature in Kumluca DS is 28 °C. pH and temperature parameters complied with the water quality standards set by the "Regulation on Waters Intended for Human Consumption" published by the Ministry of Health of Turkey (Ministry of Health Turkey, 2005).

Table 2. *Input parameters in assessment of THMs and HAAs*

Parameters	Unit	Value/distribution					Data source
		Male			Female		
Concentrations of C-DBPs in water (C_w)	mg/L						This study
Ingestion rate (IR_W)	L/d	2					Pan et al., 2014
Exposure frequency (EF)	d/y	365					Pan et al., 2014
Exposure duration (ED)	y	75.6			81		TSI, 2022
Body weight (BW)	kg	77.4			68.4		TSI, 2022
Average time (AT)	d	75.6×365			81×365		TSI, 2022
Skin area (SA)	cm^2	18900			17700		TSI, 2022
Permeability constant in water (PC)	cm/h	0.16 Trichloromethane (TCM)					Zhang et al., 2018
		0.18 Bromodichloromethane (BDCM)					
		0.20 Dibromochloromethane (DBCM)					
		0.21 Tribromomethane (TBM)					
Exposure time (ET)	h/day	0.12			0.13		
THM concentrations in the air (C_{air})	mg/L	Model calculations					Little, 1992
Inhalation rate (IR_a)	m^3/h	0.84			0.66		Pan et al., 2014
Slope factors (SF)	$(mg/kg/day)^{-1}$		TCM	BDCM	DBCM	TBM	Dobaradaran et al., 2020
		Oral ingestion	0.061	0.062	0.084	0.0079	
		Dermal	0.0305	0.0633	0.14	0.0132	
		Inhalation	0.0805	0.13	0.084	0.00385	
		Oral ingestion	DCAA		TCAA		
			0.05		0.07		
Reference dose (RfD)	mg/kg.d	TCM	1.0×10^{-2}				
		BDCM	2.0×10^{-2}				
		DBCM	2.0×10^{-2}				
		TBM	2.0×10^{-2}				
		DCAA	4.0×10^{-3}				
		TCAA	2.0×10^{-2}				

Among water quality parameters monitored, DOC, SUVA and free chlorine were particularly the most important ones that affect the formation of C-DBPs. The water characterization results showed that natural waters used in the FPs tests covered a wide range of average DOC (0.58 mg/L (Karaagac Water Source) and 3.52 mg/L (Egirdir Lake). However, average DOC numbers were quite different, average values of $SUVA_{254}$ of Egirdir Lake and Karaagac Natural Water are approximately 1.0 L/mg-m (between 0.66-1.73 L/mg-L values). For DS samples, average SUVA values were calculated as 1.21 mg/L (Isparta DS) and 0.79 mg/L (Kumluca DS), respectively. The SUVA is a parameter that can be calculated according to the ratio between UV_{254} and DOC. In the studies conducted, it was stated that the waters with a value of < 1.5-2.0 L/mg-m of SUVA generally contain hydrophilic, non-humic and small molecular

http://www.aloki.hu ● ISSN 1589 1623 (Print) ● ISSN 1785 0037 (Online)
DOI: http://dx.doi.org/10.15666/aeer/2005_38333851

weight NOM fragments (Lee and Park, 2022). The UV absorbance measured at a wavelength of 254 nm generally indicates DOM structures containing aromatic DOM fragments and/or unsaturated carbon-carbon bonds in water (Faixo et al., 2021). Bromide values were below measurable levels in all water sources and DSs (Data not shown). Similar results in terms of bromide levels have been found at surface waters in Turkey (Baytak et al., 2008). Another important parameter measured in DS samples is the residual free chlorine concentration. The lowest and highest residual free chlorine concentrations measured in Isparta DS range between 0.10-1.24 mg/L. The highest free chlorine concentration was measured at Isp 1, the closest sampling point to the disinfection unit, and the 0.10 mg/L free chlorine concentration was measured at Isp 4. As it moves away from the disinfection unit, the residual free chlorine concentration decreases because of reactions with organic matter content and decreases depending on the length of the distribution system. However, this free chlorine level did not change in Kumluca DS. This is because of the low organic matter content of Kumluca DS. Average DOC of Kumluca DS is 0.3 mg/L. Since DOC and SUVA values were low, chlorine demand was low in Kumluca DS. The selected characteristics of water samples are summarized in *Table 3*.

Table 3. *Water quality data with annual descriptive statistics (average, minimum, maximum) during 12 months of sampling*

Sampling point	pH			Temperature (°C)			Residual free chlorine (mg/L)			DOC (mg/L)			UV absorbance (cm^{-1})			SUVA (L/mg-m)		
	Min.	Max.	Ave.	Min.	Max.	Ave.	Min.	Max.	Ave.	Min.	Max.	Ave.	Min.	Max.	Ave.	Min.	Max.	Ave.
Egirdir L.	7.75	8.54	8.32	8.6	25.0	16.3	NA	NA	NA	2.71	4.02	3.52	0.024	0.048	0.034	0.66	1.40	0.98
Karaagac W.S.	7.70	8.42	8.15	11.4	20.5	14.7	NA	NA	NA	0.37	0.98	0.58	0.003	0.023	0.008	0.47	1.73	1.03
Isparta 1	7.52	8.43	8.15	6.8	26.0	14.9	0.48	1.24	0.77	1.07	3.60	2.25	0.016	0.049	0.027	0.83	2.24	1.28
Isparta 2	7.69	8.47	8.21	8.0	26.0	15.9	0.50	0.92	0.68	1.24	3.44	2.25	0.015	0.039	0.026	0.76	2.02	1.21
Isparta 3	7.63	8.62	8.23	8.1	25.0	16.6	0.15	0.49	0.32	1.44	2.88	2.13	0.012	0.033	0.024	0.74	2.08	1.15
Isparta 4	7.81	8.62	8.21	8.6	23.0	16.8	0.10	0.62	0.23	1.46	3.12	2.11	0.006	0.035	0.024	0.41	2.01	1.15
Isparta 5	7.37	8.46	8.19	6.3	27.0	15.7	0.12	0.61	0.35	1.29	2.98	2.18	0.011	0.041	0.026	0.57	2.17	1.25
Kumluca 1	7.12	8.35	8.08	13.6	28.0	19.0	0.10	0.37	0.19	0.17	0.42	0.25	0.001	0.004	0.002	0.56	1.38	0.88
Kumluca 2	7.41	8.38	8.09	11.9	21.0	16.2	0.10	0.30	0.15	0.23	0.51	0.31	0.001	0.005	0.003	0.40	1.61	0.82
Kumluca 3	7.50	8.50	8.13	11.6	16.0	14.1	0.10	0.33	0.22	0.19	0.43	0.32	0.001	0.005	0.003	0.30	1.39	0.78
Kumluca 4	7.55	8.45	8.13	11.9	19.0	15.4	0.10	0.42	0.18	0.20	0.41	0.30	0.001	0.002	0.002	0.24	1.00	0.64
Kumluca 5	7.60	8.35	8.09	4.0	28.0	18.4	0.10	0.41	0.16	0.19	0.38	0.30	0.001	0.004	0.003	0.37	1.58	0.83

*NA: Not available. No chlorine was applied for source water. Min: minimum, Max: maximum, Ave: average

Formation potential of C-DBPs in low SUVA source waters

The FPs of THMs and HAAs of Egirdir Lake and Karaagac water source are shown in *Table 4*. In both tested water sources, the FPs of THMs and HAAs were in the order of chlorination > ozonation/chlorination > chloramination > ozonation/chloramination > ozonation. The maximum FPs of THMs and HAAs concentrations measured in Egirdir Lake were 120 µg/L and 101 µg/L, respectively. The maximum HAAs and THMs FPs concentrations in Karaagac were 44 µg/L and 26 µg/L, respectively. For all disinfection scenarios, C-DBPs concentrations in Karaagac Natural Water were lower than Egirdir Lake. This is expected since DOC values of Karaagac was 0.58 mg/L and DOC values of Egirdir Lake was 3.52 mg/L with similar SUVA values. Precursors reactivity was quantified by specific C-DBPs yields, or µg of C-DBPs formed per mg of DOC to evaluate formation potential of different water sources. Determination of specific C-DBPs yields is important in terms of comparing water sources based on reactivity. The

http://www.aloki.hu ● ISSN 1589 1623 (Print) ● ISSN 1785 0037 (Online)
DOI: http://dx.doi.org/10.15666/aeer/2005_38333851

highest THM formation of 1 mg DOC in Egirdir Lake and Karaagac water is 37 and 119 µg THM/mg for only chlorination, respectively. Similarly, 1 mg of dissolved organic carbon forms 29 µg HAA/mg DOC, while Karaagac water forms 49 µg HAA/mg DOC. This comparison indicates Egirdir Lake had relatively lower precursors reactivity and Karaagac Natural Water has more potential for C-DBPs formation with lower organic matter content than Egirdir Lake. Trichloromethane (TCM) was the dominant species in both water bodies and the speciation in THMs followed the order: TCM > bromodichloromethane (BDCM) > dibromochloromethane (DBCM) > tribromomethane (TBM).

Table 4. *THMs and HAAs formation potentials under different disinfection scenarios for 12 months (µg/L)*

Scenario	DBPs FP	NOV	DEC	JAN	FEB	MAR	APR	MAY	JUN	JUL	AUG	SEP	OCT
Chlorination	THM_4_E	95	87	73	82	84	120	110	88	95	101	91	76
	THM_4_K	30	31	37	28	30	36	37	44	34	36	27	35
	HAA_9_E	69	58	84	63	65	76	70	101	76	78	89	73
	HAA_9_K	16	17	15	12	16	18	20	18	14	19	19	26
Ozonation/chlorination	THM_4_E	46	49	41	39	37	50	45	49	47	44	54	45
	THM_4_K	22	21	25	25	27	26	25	30	30	32	18	26
	HAA_9_E	35	31	42	30	35	39	37	50	36	42	45	39
	HAA_9_K	17	18	16	14	17	19	22	19	17	20	21	22
Chloramination	THM_4_E	30	35	34	28	27	32	42	41	34	32	35	34
	THM_4_K	21	23	19	10	21	25	28	23	12	25	17	19
	HAA_9_E	23	27	26	22	23	25	32	31	26	28	37	32
	HAA_9_K	11	12	10	5	11	12	14	12	6	13	11	17
Ozonation/chloramination	THM_4_E	15	11	16	18	11	18	13	19	22	13	12	11
	THM_4_K	13	10	14	17	13	16	12	17	20	16	9	11
	HAA_9_E	12	8	12	14	12	13	10	14	17	14	15	12
	HAA_9_K	7	5	8	9	7	8	6	10	11	8	9	7
Ozonation	THM_4_E	7	9	5	5	9	8	11	6	6	11	14	7
	THM_4_K	2	2	1	5	2	2	2	1	6	2	4	3
	HAA_9_E	5	7	4	4	5	6	8	5	5	6	9	10
	HAA_9_K	1	1	1	3	1	1	1	1	4	1	3	2

E: Egirdir Lake, K: Karaagac Water Source

The dominant HAAs species were trichloroacetic acid (TCAA) in all disinfection scenarios. In similar previous studies, the dominant HAAs species were dichloroacetic acid (DCAA) and TCAA in most of the tested waters in Turkey (Ates et al., 2007). The minimum C-DBPs FP was obtained after ozonation only and the bromide levels were below the detection limit. Similar to our study, it has been reported that the average THMs formation decreased to 10 µg/L after ozonation alone (Vedugo et al., 2020). Pre-ozonation reduces C-DBPs formation and similar results were reported in other studies (Uyak et al., 2014; Meite et al., 2015; Krasner et al., 2016b; Vedugo et al., 2020). The decrease in C-DBPs formation after ozonation/pre-ozonation has been attributed that when pre-ozonation is performed, natural organic materials break down the hydrophobic components into hydrophilic components in high SUVA waters (Vedugo et al., 2020). The results showed that THMs and HAAs formation in chloramination was about 3 times lower than chlorination. Chloramination resulted in lower formation C-DBPs, attributing that the oxidation potential of chloramine is lower than chlorine

http://www.aloki.hu ● ISSN 1589 1623 (Print) ● ISSN 1785 0037 (Online)
DOI: http://dx.doi.org/10.15666/aeer/2005_38333851

(Sfynia et al., 2020). Goslan et al. (2009) found that THMs formation with chlorine is 2 times higher than with chloramine. Also, earlier studies reported HAAs after chlorination were 3 times higher than after chloramination (Goslan et al., 2009; Behbahami et al., 2018; Bougeard et al., 2020). Brominated THMs concentrations were considerably lower than chlorinated ones since the bromide concentration was less than 10 µg/L for both water sources. However, the highest brominated THMs concentrations were detected only after ozonation. One-year-long monitoring was performed to evaluate seasonal changes of C-DBPs formation potential the presence of typical drinking water disinfectants. The C-DBPs formation potential for Egirdir Lake varied with changes in seasons. The highest C-DBPs formation potential concentration was determined for both THMs and HAAs in spring and summer months, which could be attributed to the higher concentrations of dissolved organic matter and temperature at that time. No clear seasonality in C-DBPs formation potential for Karaagac Natural Water was observed.

Occurrence of C-DBPs in distribution systems

The seasonal variations of THMs in Isparta DS sampling points are presented in *Figure 1*. The highest THMs average was 41 µg/L in summer and the lowest THMs was 31 µg/L in winter in Isparta DS. A similar temporal trend has been reported in several previous studies (Rodriguez et al., 2003; Scheili et al., 2015). As expected, the total concentrations of THMs in the DSs were lower than those produced in the FPs tests which are attributed to the high disinfectant dose and the long contact time in the FPs tests. Increased THMs concentrations in summer are explained with higher water temperature and higher DOC concentration. In addition, since the sustainability of microbial water quality is more difficult in hot seasons than in cold seasons, higher chlorine doses are used in DSs and a significant increase in free chlorine demand and higher THMs concentrations especially in summer and autumn seasons observed (Rodriguez et al., 2011; Sfynia et al., 2022). Rodriguez et al. (2003) found a good correlation between residual chlorine, temperature and THMs formation in summers. The seasonal variation of THMs in Kumluca distribution points are presented in *Figure 2*. The highest THMs concentrations detected in Kumluca DS was 11 µg/L and the lowest THMs concentration was 3 µg/L. The average THMs concentrations calculated at Kumluca DS sampling points are 7 µg/L. As expected in the Kumluca DS, less THMs formation was observed than Isparta DS. This is explained with the lower UV absorbance and DOC values of Kumluca DS compared to Isparta DS. TCM accounted for average 73% of the THMs in all samples, implying that TCM was dominant species of THMs in both DSs, which is consistent with other similar studies (Summerhayes et al., 2011; Duan et al., 2020). A meaningful seasonal variation could not find in Kumluca DS. The slightly higher THM formation was observed in winter for Kumluca DS. In the Kumluca DS. The seasonal variation of HAAs in Isparta distribution points are presented in *Figure 3*. In Isparta DS, the highest HAAs concentration was 29 µg/L in summer and the lowest HAAs concentration was 18 µg/L in winter. The mean HAA_9 concentrations obtained in the spring and summer seasons were 23 and 22 µg/L, respectively. Rodriguez et al. (2004) found that HAAs concentration was 4 times higher in summer than in winter. The main mechanism responsible for the reduction of HAAs concentration throughout the distribution system is thought to be the biodegradation mechanism produced by the biofilm layer resulting from reduced chlorine concentration (Uyak et al., 2014; Behbahami et al., 2018). The

http://www.aloki.hu ● ISSN 1589 1623 (Print) ● ISSN 1785 0037 (Online)
DOI: http://dx.doi.org/10.15666/aeer/2005_38333851

most dominant HAAs species in the Isparta DS were TCAA and DCAA. Similarly, it was reported that the dominant HAAs species are TCAA or DCAA when surface waters were used as water sources and chlorine was disinfectant (Rodriguez et al., 2004; Muellner et al., 2007; Bougeard et al., 2020). In present study, other HAA species were low due to the very low bromine level (below detection levels). In most studies, while CAA can be measured in many surface waters sources, bromoacetic acid (BAA), dibromoacetic acid (DBAA), dibromochloroacetic acid (DBCAA), tribromoacetic acid (TBAA) could not be measured in chlorine use either in surface water sources or groundwater sources in low bromide levels (Alomirah et al., 2020). The seasonal variation of HAAs in Kumluca distribution points are presented in *Figure 4*. The highest HAAs value measured in Kumluca DS was 8 µg/L at KUM 1 and the lowest HAA value was 2 µg/L at KUM 2. Low HAA concentrations were expected due to low DOC concentrations and low initial chlorine dose.

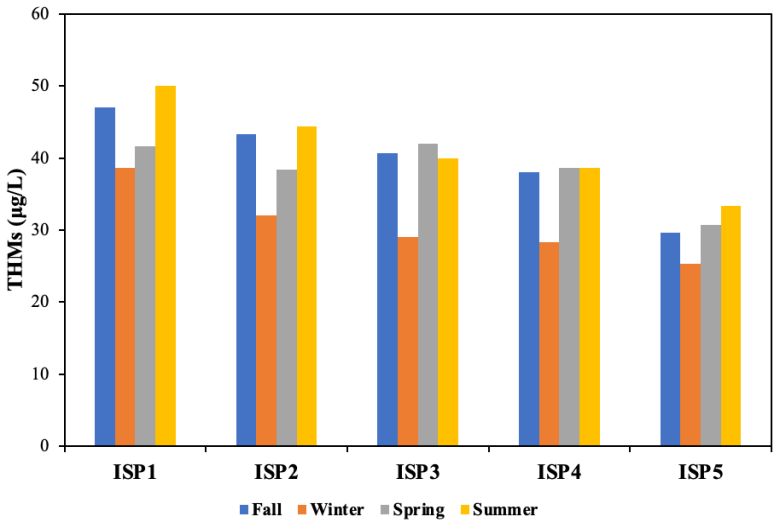

Figure 1. *Seasonal average concentrations of THMs in Isparta distribution system sampling points. (Sampling point 1 is the closest while 5 is the farthest sampling point)*

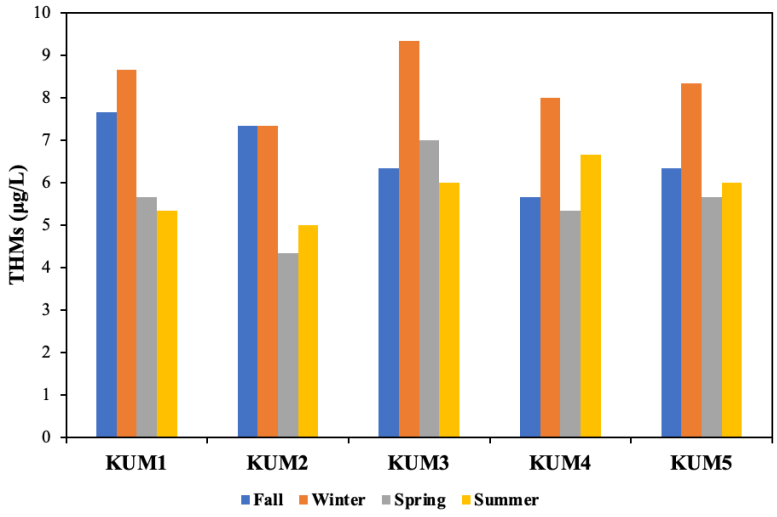

Figure 2. *Seasonal average concentrations of THMs in Kumluca distribution system sampling points. (Sampling point 1 is the closest while 5 is the farthest sampling point)*

http://www.aloki.hu ● ISSN 1589 1623 (Print) ● ISSN 1785 0037 (Online)
DOI: http://dx.doi.org/10.15666/aeer/2005_38333851

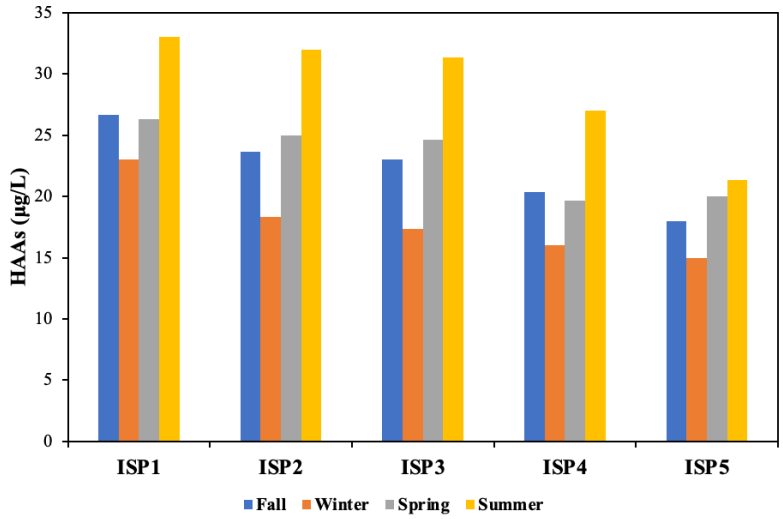

Figure 3. *Seasonal average concentrations of HAAs in Isparta distribution points. (Sampling point 1 is the closest while 5 is the farthest sampling point)*

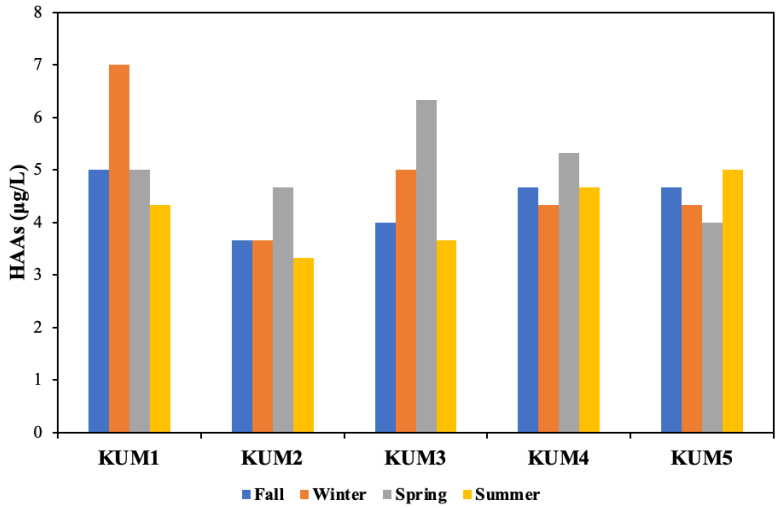

Figure 4. *Seasonal average concentrations of HAAs in Kumluca distribution points (Sampling point 1 is the closest while 5 is the farthest sampling point)*

Correlations between surrogate parameters and DBPs

Analyses of C-DBPs in water treatment plants and DSs are expensive, complicated and time-consuming, and require specialized laboratories and know-how. A key aim of many studies has been to find a surrogate readily measurable water quality parameters to predict C-DBP formation. Among the water quality parameters, DOC, UV_{254}, SUVA, and differential ultraviolet absorbance (DUVA) are the most associated surrogate parameters (Li et al., 2017). At this stage of the study, data analysis was performed with surrogate of the water quality parameters (such as pH, temperature, free chlorine, DOC, UV_{254}, SUVA) with THMs and HAAs in DSs. Pearson's correlation matrix was used to perform data analysis. *Table 5* present the correlation coefficients among total THMs and its species with surrogate parameters. Although strong correlations were reported between THMs formation with DOC, SUVA, UV_{254},

http://www.aloki.hu ● ISSN 1589 1623 (Print) ● ISSN 1785 0037 (Online)
DOI: http://dx.doi.org/10.15666/aeer/2005_38333851

and differential UV absorbance in the DBPs literature, THMs and its species did not correlate well with almost all parameters. THMs were low correlations with DOC and free chlorine with 0.26 and 0.35 correlations coefficients, respectively. Especially SUVA and UV did not correlate well with the formation and speciation of THMs and HAAs. The results may explain that low- or non-UV-absorbing NOM moieties play important roles in the formation of C-DBPs in waters with low SUVA waters. Fu et al. (2017) found low correlations ($r = < 0.25$) between DBPs types and water quality parameters. *Table 6* present the correlation coefficients among total HAAs and its species with surrogate parameters. Like THMs results, low correlations ($r = < 0.3$) were found between HAAs types and water quality parameters. Studies in the literature reported that Pearson correlation (P) values for the DOC and the chlorine dosages are 0.786 and 0.865 for HAAFPs, respectively for high SUVA waters (Alver and Kılıc, 2018). Ates et al. (2007) reported that no strong correlations between SUVA and HAAs formations were found in low SUVA waters. These different trends showed that the effectiveness of surrogate parameters in correlating with C-DBPs formation is water specific. Kumluca water distribution systems, Pearson Correlation Matrix between THMs and parameters did not yield significant results (Data not shown). For the Kumluca water distribution system, this situation can be explained by the very low total organic concentration in groundwater (Kitis et al., 2010). According to the Pearson correlation matrix in the Kumluca water DS, the lower correlation between THMs and free chlorine can be explained by the fact that the DS length is quite short, and the chlorine demand of the water is very low. The reason of poor correlation between chlorine and THMs formation is because of relatively little organic matter in the sample.

Table 5. *The Pearson's correlations matrices of surrogate parameters and THMs in Isparta DS*

	THM	TCM	BDCM	DBCM	TBM	pH	Temp.	Free Cl.	DOC	UV	SUVA
THM	1										
TCM	0.68	1									
BDCM	0.30	-0.34	1								
DBCM	0.47	0.54	-0.27	1							
TBM	-0.14	-0.59	0.03	-0.13	1						
pH	-0.02	-0.33	0.50	-0.17	0.06	1					
Free Cl.	0.35	0.17	0.17	0.05	0.02	-0.03	-0.15	1			
DOC	0.26	-0.20	0.58	0.07	0.14	0.39	0.42	-0.01	1		
UV	-0.15	-0.31	-0.02	-0.05	0.42	0.03	-0.10	0.15	0.18	1	
SUVA	-0.33	-0.13	-0.37	-0.12	0.19	-0.15	-0.37	0.13	-0.47	0.73	1

The relationship between THM and HAA concentrations detected in the Isparta DS and the measured water quality parameters was evaluated with the Pearson correlation matrix is statistically significant ($\alpha < 0.05$). While a positive correlation was found between DOC - free chlorine and THM formation, a negative correlation was found between SUVA - UV and THM formation. Regression analysis was not statistically significant ($\alpha > 0.05$) for THM and HAA in the Kumluca distribution system.

http://www.aloki.hu ● ISSN 1589 1623 (Print) ● ISSN 1785 0037 (Online)
DOI: http://dx.doi.org/10.15666/aeer/2005_38333851

Table 6. *The Pearson's correlations matrices of surrogate parameters and HAAs in Isparta DS*

	HAA	CAA	BAA	DCAA	BCAA	TCAA	DBAA	BDCAA	DBCAA	TBAA	pH	Temp.	Free Cl.	DOC	UV	SUVA
HAA	1															
CAA	-0.25	1														
TCAA	0.53	0.08	1													
DCAA	0.45	-0.23	-0.27	1												
BCAA	0.13	-0.27	-0.37	0.04	1											
BAA	-0.02	-0.19	-0.42	-0.12	0.88	1										
DBAA	-0.40	0.01	-0.21	-0.20	-0.15	-0.14	1									
BDCAA	-0.01	-0.23	-0.18	0.06	0.10	0.16	0.08	1								
DBCAA	-0.10	0.06	-0.23	0.19	-0.05	-0.12	0.10	-0.06	1							
TBAA	0.19	-0.29	-0.38	0.41	-0.11	-0.20	0.10	0.02	0.18	1						
pH	-0.23	0.16	-0.29	0.00	0.26	0.25	-0.05	0.03	0.03	-0.14	1					
Free Cl.	0.30	-0.07	0.10	0.00	0.32	0.13	0.12	-0.02	-0.02	0.12	-0.03	-0.15	1			
DOC	0.12	-0.02	0.02	0.05	0.32	0.27	-0.39	-0.11	0.12	-0.22	0.39	0.42	-0.01	1		
UV	-0.19	0.25	0.09	-0.14	-0.10	-0.12	0.21	-0.11	0.07	-0.28	0.03	-0.10	0.15	0.18	1	
SUVA	-0.31	0.17	-0.02	-0.15	-0.23	-0.23	0.52	0.01	0.00	-0.12	-0.15	-0.37	0.13	-0.47	0.73	1

Cancer risk and non-cancer risk assessment

Figure 5 shows the lifetime cancer risk of THMs for males and females through different exposure pathways in Isparta DS. The highest values of the total cumulative cancer risk posed by exposure to THMs for males and females in Isparta DS were 8.3E-05 and 8.1E-05, respectively. The average values of total lifetime cancer risks for males were 1.77% higher than those for females. The average lifetime total cancer risk was 60–70 times higher than negligible cancer risk (1.0E-06). The lifetime cancer risk for total THMs through each pathway in both males and females exceeds 1.0E-06, the negligible cancer risk level recommended by USEPA. Inhalation exposure made the most contribution (average 59%) to the total lifetime risk, followed by ingestion (average 29%), whereas dermal absorption showed the least contribution (average 12%) for both males and females. Similarly, the inhalation route was the most prominent exposure pathway to lifetime cancer risk in the studies of multi-pathway risk assessment for THMs (Siddique et al., 2015; Kujlu et al., 2020). However, other studies found that ingestion was the main contributor pathway (Uyak, 2006; Kumari et al., 2015; Mishaqa et al., 2022). The average total cancer risk for HAAs for males and females was calculated as 3.3E-05 and 4.4E-05 respectively (Data not shown). TCAA was the compound contributing the most (80%) to the total CDI of HAAs, followed by DCAA (20%) though ingestion. The average values of the total lifetime cancer risk posed by exposure to THMs for males and females in Kumluca DS were 1.4E-05 and 1.2E-05, respectively. The average values of the total lifetime cancer risk posed by exposure to HAAs for males and females in Kumluca DS were 7.6E-06 and 7.6E-06, respectively (data not shown).

Table 7 shows the average specific cancer risks for each THM species through different pathways for Isparta DS. While BDCM made the highest percentage contribution of the total risk through ingestion, TCM is the main contribution to the total risk through both inhalation and dermal adsorption. These results are explained by the product of the concentration of individual THMs and its SF of exposure pathways (Kumari et al., 2015; Mishaqa et al., 2022). The total cancer risk through ingestion for THMs followed the order: BDCM (61%) > TCM (23%) > DBCM (14%) > TBM (2%). A similar trend of higher BDCM percent contribution through ingestion has been

http://www.aloki.hu ● ISSN 1589 1623 (Print) ● ISSN 1785 0037 (Online)
DOI: http://dx.doi.org/10.15666/aeer/2005_38333851

observed in previous studies (Lee et al., 2004; Uyak et al., 2006). TCM made the highest percentage contribution (52%) to average lifetime cancer risk through dermal exposure, followed by BDCM (23%), DBCM (14%), and TBM (2%). The percentage contribution of each THMs to the cancer risk though inhalation followed the pattern: TCM (70%) > BDCM (26%) > DBCM (3%) > TBM (1%). In several studies, it is shown that TCM was the major contributor for inhalation route since TCM has a lower boiling point than other THMs (Uyak et al., 2006; Wang et al., 2019).

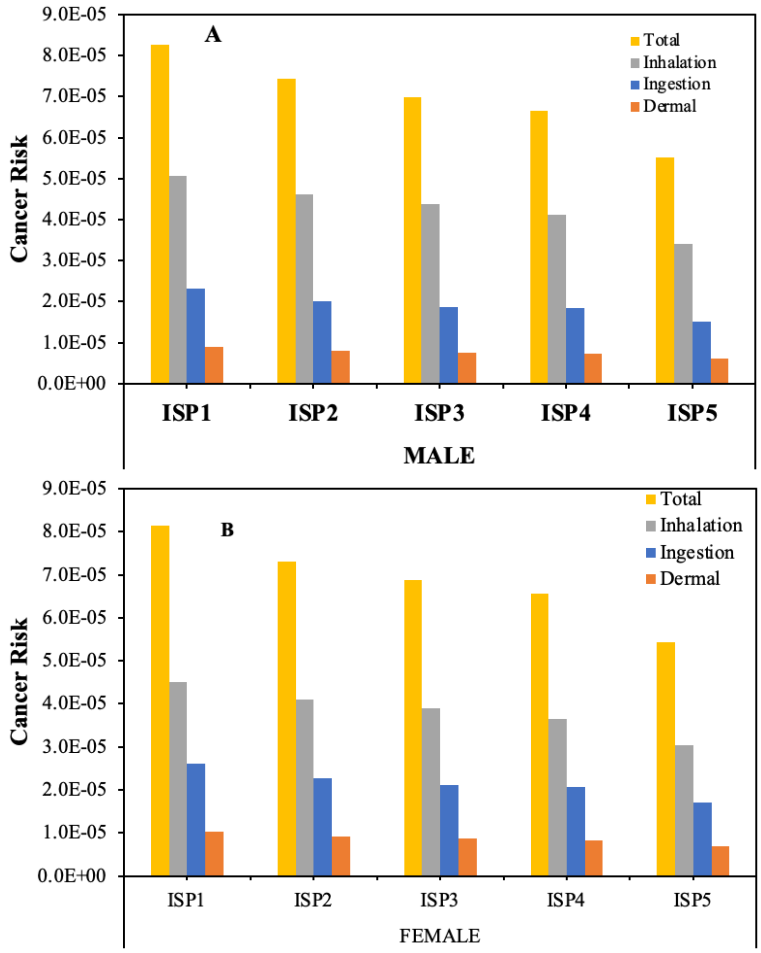

Figure 5. *Lifetime cancer risk of THMs through all exposure routes in males (A) and females (B) for Isparta DS*

For the non-carcinogenic risk, the total HI of C-DBPs through ingestion (A) and dermal (B) for Isparta DS are provided in *Figure 6*. The total HI of C-DBPs from all exposure routes was ranged from 0.18 to 0.25. Dermal exposure resulted in slightly HI than ingestion route. The major HI of THMs and HAAs via dermal exposure was the HI of TCAA. Of the four THMs compounds, TCM had the highest HI value for both dermal and ingestion routes. HI values of THMs species followed an order of TCM > DBCM > TBM > DCBM for both dermal and ingestion routes. For HAA species, TCAA had a higher HI value than DCAA. In conclusion, the non-carcinogenic risk of C-DBPs in the distribution system was less than 1, which was in the allowable range for C-DBPs. Similar results were reported in the studies from Kumari et al.

http://www.aloki.hu ● ISSN 1589 1623 (Print) ● ISSN 1785 0037 (Online)
DOI: http://dx.doi.org/10.15666/aeer/2005_38333851

(2015) and Wang et al. (2019). For Kumluca HI of C-DBPs through dermal and ingestion exposure were 0.033, meaning they were in the allowable range.

Table 7. *Specific cancer risks for each THM species for Isparta DS*

		Male				Female			
		TCM	**BDCM**	**DBCM**	**TBM**	**TCM**	**BDCM**	**DBCM**	**TBM**
Ingestion	ISP1	5E-06	1E-05	3E-06	4E-07	6E-06	2E-05	4E-06	5E-07
	ISP2	5E-06	1E-05	3E-06	3E-07	5E-06	1E-05	3E-06	3E-07
	ISP3	5E-06	1E-05	3E-06	3E-07	5E-06	1E-05	3E-06	3E-07
	ISP4	4E-06	1E-05	3E-06	3E-07	5E-06	1E-05	3E-06	4E-07
	ISP5	4E-06	9E-06	2E-06	3E-07	4E-06	1E-05	3E-06	3E-07
Dermal	ISP1	5E-06	3E-06	1E-06	2E-07	5E-06	3E-06	1E-06	2E-07
	ISP2	4E-06	3E-06	1E-06	1E-07	5E-06	3E-06	1E-06	1E-07
	ISP3	4E-06	2E-06	1E-06	1E-07	5E-06	3E-06	1E-06	1E-07
	ISP4	4E-06	2E-06	1E-06	1E-07	4E-06	3E-06	1E-06	2E-07
	ISP5	3E-06	2E-06	9E-07	1E-07	4E-06	2E-06	1E-06	1E-07
Inhalation	ISP1	4E-05	1E-05	1E-06	7E-08	3E-05	1E-05	1E-06	6E-08
	ISP2	3E-05	1E-05	1E-06	5E-08	3E-05	1E-05	1E-06	4E-08
	ISP3	3E-05	1E-05	1E-06	4E-08	3E-05	1E-05	1E-06	4E-08
	ISP4	3E-05	1E-05	1E-06	5E-08	3E-05	1E-05	1E-06	5E-08
	ISP5	2E-05	9E-06	1E-06	5E-08	2E-05	8E-06	8E-07	5E-08

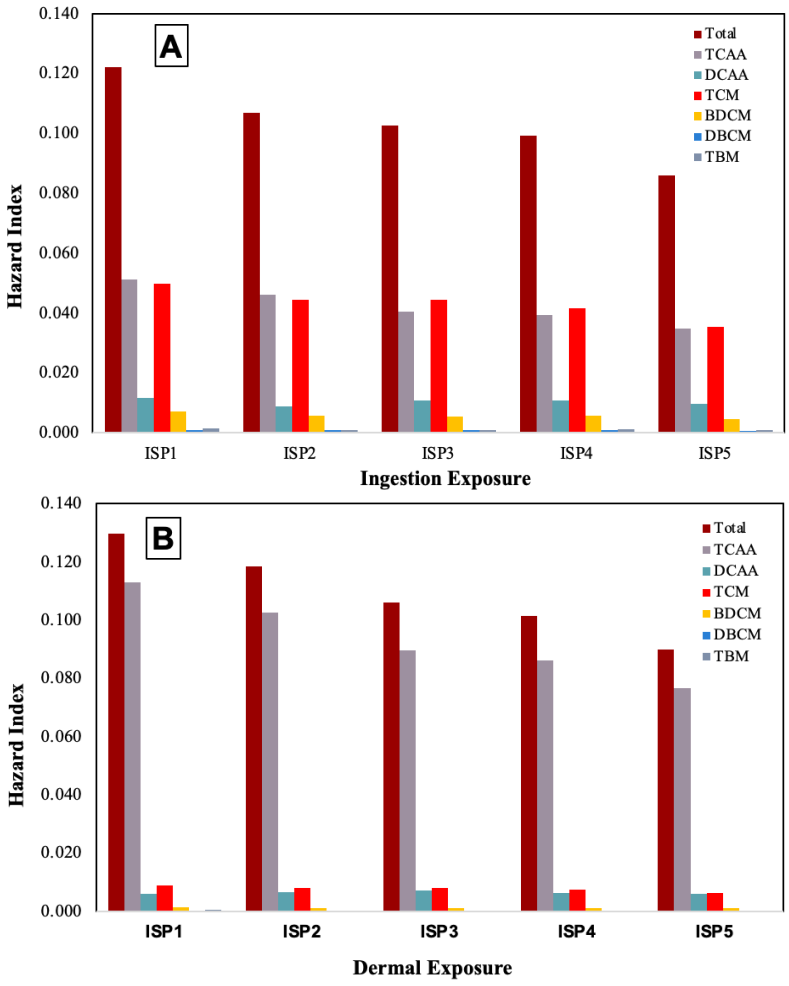

Figure 6. *Lifetime hazard index of C-DBPs through ingestion (A) and dermal exposure (B) for Isparta DS*

http://www.aloki.hu ● ISSN 1589 1623 (Print) ● ISSN 1785 0037 (Online)
DOI: http://dx.doi.org/10.15666/aeer/2005_38333851

Conclusions

In this study, a systematic investigation was conducted for tracking spatio-temporal occurrence and formation potential of C-DBPs in low SUVA water sources. Also one of objectives of this study was to evaluate the lifetime cancer risk and the hazard index caused by THMs and HAAs. Results of FPs tests showed that chlorination produced the highest THMs and HAAs followed by in the order of ozonation/chlorination, ozonation/chlorination, chloramination, ozonation/chloramination and ozonation. Pre-ozonation may be recommended for the drinking water treatment plants, in consideration of trade-off control of C-DBPs in case of low bromide ion levels. Disinfectants can react not only with NOM and other organic pollutants but also with inorganic compounds form DBPs. Therefore, greater variety of DBPs precursors may form greater quantity and variety of DBPs. Further studies are required to explain and understand better the underlying chemical reaction with precursors and disinfectants in low SUVA waters. A one-year-long monitoring was conducted to evaluate the concentrations of THMs and HAAs in the presence of chlorine for DSs which are low SUVA waters. According to Pearson correlation coefficients, the C-DBPs formation prediction capability of DOC, UV and SUVA were weak in waters with low SUVA waters. Overall, it is apparent that C-DBPs formation in low-SUVA waters may not be estimated by simple surrogate parameters. Although the non-cancer risk of C-DBPs was below permissible recommended levels, the average lifetime carcinogenic risk levels for THMs and HAAs in Isparta DS were 6.9E-05 and 5.8E-05, respectively, which is higher than negligible risk level (1.0E-06). The results of THMs cancer risk reveal that the ingestion had the highest impact on lifetime cancer risk. Males were found to be at a slightly greater risk of cancer, and the values was found relatively close. The non-carcinogenic hazard index of THMs via dermal was found higher than ingestion. The study would benefit the water management authority and health departments to control the level of C-DBPs. Besides C-DBPs, future studies must focus on improving our understanding of emerging DBPs formation in low SUVA waters (both laboratory-scale and full-scale studies).

Acknowledgment. This work was supported by the Suleyman Demirel University Scientific Research Projects (Project Number 4722-D2-16).

REFERENCES

[1] Alomirah, H. F., Al-Zenki, S. F., Alaswad, M. C., Alruwaih, N. A., Wu, Q., Kannan, K. (2020): Elevated concentrations of bromate in Drinking water and groundwater from Kuwait and associated exposure and health risks. – Environmental Research 181: 108885.

[2] Alver, A., Kılıc, A. (2018): Catalytic ozonation by iron coated pumice for the degradation of natural organic matters. – Catalysts 8(5): 219-239.

[3] APHA (1995): Standard Methods for the Examination of Water and Wastewater. 19th Ed. – American Public Health Association Inc., New York.

[4] Ates, N., Kaplan, S. S., Sahinkaya, E., Kitis, M., Dilek, F. B., Yetis, U. (2007): Occurrence of disinfection by-products in low DOC surface waters in Turkey. – Journal of Hazardous Materials142: 526-534.

[5] Ates, N., Kaplan-Bekaroglu, S. S., Dadaser-Celik, F. (2020): spatial/temporal distribution and multi-pathway cancer risk assessment of trihalomethanes in low TOC and high bromide groundwaters. – Environ Science: Process Impacts.22: 1-10.

http://www.aloki.hu ● ISSN 1589 1623 (Print) ● ISSN 1785 0037 (Online)
DOI: http://dx.doi.org/10.15666/aeer/2005_38333851

[6] Baytak, D., Sofuoglu, A., Inal, F., Sofuoglu, S. C. (2008): Seasonal variation in drinking water concentrations of disinfection by-products in İzmir and associated human health risks. – Science Total Environment 407: 286-296.
[7] Behbahani, M., Lin, B., Phares, T. L., Seo, Y. (2018): Understanding the impact of water distribution system conditions on the biodegradation of haloacetic acids and expression of bacterial dehalogenase genes. – Journal of Hazardous Materials 351: 293-300.
[8] Bond, T., Templeton, M. R., Kamal, N. H. M., Graham, N., Kanda, R. (2015): Nitrogenous disinfection byproducts in English drinking water supply systems: occurrence, bromine substitution and correlation analysis. – Water Research 85: 85-94.
[9] Bougeard, C. M. M., Goslan, E. H., Jefferson, B., Parsons, S. A. (2020): Comparison of the disinfection by-product formation potential of treated waters exposed to chlorine and monochloramine. – Water Research 44: 729-740.
[10] Ding, S., Chu, W. (2017): Recent advances in the analysis of nitrogenous disinfection by-products. – Trends in Environmental Analytical Chemistry 14: 19-27.
[11] Dobaradaran, S., Shabankareh, F. E., Tekle-Röttering, A., Keshtkar, M., Karbasdehi, V. N., Abtahi, M., Gholamnia, R., Saeedi, R. (2020): Age-sex specific and cause-specific health risk and burden of disease induced by exposure to trihalomethanes (THMs) and haloacetic acids (HAAs) from drinking water: an assessment in four urban communities of Bushehr Province, Iran. – Environ Research 182: 109062.
[12] Du, Y. J., Zhao, L., Ban, J., Zhu, J. Y., Wang, S. W., Zhu, X., Zhang, Y., Huang, Z., Li, T. (2021): Cumulative health risk assessment of disinfection by-products in drinking water by different disinfection methods in typical regions of China. – Science Total Environment 770: 144662.
[13] Duan, X., Liao, X., Chen, J., Xie, S., Qi, H., Li, F., Yuan, B. (2020): THMs, HAAs and NAs production from culturable microorganisms in pipeline network by ozonation, chlorination, chloramination and joint disinfection strategies. – Science of the Total Environment, Volume 744: 140833.
[14] Ebsa, D. G., Dibaba, W. T. (2022): Assessment of drinking water treatment and disinfection by-products. – South African Journal of Chemical Engineering 41: 85-92.
[15] Faixo, S., Gehin, N., Balayssac, S., Gilard, V., Mazeghrane, S., Haddad, M., Gaval, G., Paul, E., Garrigues, J. C. (2021): Current trends and advances in analytical techniques for the characterization and quantification of biologically recalcitrant organic species in sludge and wastewater: a review. – Analytica Chimica Acta, Volume 1152: 338284.
[16] Fu, J., Lee, W. N., Coleman, C., Nowack, K., Carter, J., Huang, C. H. (2017): Removal of disinfection byproduct (DBP) precursors in water by two-stage biofiltration treatment. – Water Research 123: 224-235.
[17] Goslan, E. H., Krasner, S. W., Bower, M., Rocks, S. A., Holmes, P., Levy, L. S., Parsons, S. A. (2009): A comparison of disinfection by-products found in chlorinated and chloraminated drinking waters in Scotland. – Water Research 43: 4698-4706.
[18] Hao, R., Zhang, Y., Du, T., Yang, L., Adeleye, A. S., Li, Y. (2017): Effect of water chemistry on disinfection by-product formation in the complex surface water system. – Chemosphere 172: 384-391.
[19] Hung, Y. C., Waters, B. W., Yemmireddy, V. K., Huang, C. H. (2017): pH effect on the formation of THM and HAA disinfection byproducts and potential control strategies for food processing. – Journal of Integrative Agriculture 16(12): 2914-2923.
[20] Kitis, M., Yigit, N. O., Harman, B. I., Muhammetoglu, H., Muhammetoglu, A., Karadirek, I. E., Demirel, I., Ozden, T., Palanci, I. (2010): Occurrence of trihalomethanes in chlorinated groundwaters with very low natural organic matter and bromide concentrations. – Environmental Forensics 11: 264-274.
[21] Krasner, S. W. (2009): The formation and control of emerging disinfection by-products of health concern. – Philosophical Transactions of the Royal Society A 367: 4077-4095.
[22] Krasner, S. W., Kostopoulou, M., Toledano, M. B., Wright, J., Patelarou, E., Kogevinas, M., Villanueva, C. M., Carrasco-Turigas, G., Marina, L. S., Fernandez-Somoano, A.,

http://www.aloki.hu ● ISSN 1589 1623 (Print) ● ISSN 1785 0037 (Online)
DOI: http://dx.doi.org/10.15666/aeer/2005_38333851

Ballaster, F., Tardon, A., Grazuleviciene, R., Danileviciute, A., Cordier, S., Costet, N., Righi, E., Aggazzotti, G., Stephanou, E. G., Kargaki, S., Nieuwenhuijsen, M. J. (2016a): Occurrence of DBPs in drinking water of European regions for epidemiology studies. – J. Am. Water Works Assoc. 108: 501-512.

[23] Krasner, S. W., Weinberg, H. S., Richardson, S. D., Pastor, S. J., Chinn, R., Sclimenti, M. J., Onstad, G. D., Thruston, Jr. A. D. (2016b): The occurrence of a new generation of disinfection by-products. – Environmental Science Technology 40: 7175-7185.

[24] Kujlu, R., Mahdavianpour, M., Ghanbari, F. (2020): Multi-route human health risk assessment from trihalomethanes in drinking and non-drinking water in Abadan, Iran. – Environmental Science and Pollution Research 27: 42621-42630.

[25] Kumari, M., Gupta, S. K. (2018): Age dependent adjustment factor (ADAF) for the estimation of cancer risk through trihalomethanes (THMs) for different age group. An innovative approach. – Ecotoxicology and Environmental Safety148: 960-968.

[26] Kumari, M., Gupta, S. K., Mishra, B. (2015): Multi-exposure cancer and non-cancer risk assessment of trihalomethanes in drinking water supplies–a case study of Eastern region of India. – Ecotoxicology and Environmental Safety 113: 433-438.

[27] Lee, S., Park, J. (2022): Identification of dissolved organic matter origin using molecular level analysis methods. – Water 14: 1317.

[28] Li, W. T., Cao, M. J., Young, T., Ruffino, B., Dodd, M., Li, A. M., Kotshin, G. (2017): Application of UV absorbance and fluorescence indicators to assess the formation of biodegradable dissolved organic carbon and bromate during ozonation. – Water Research 111: 154-162.

[29] Little, J. C. (1992): Applying the two-resistance theory to contaminant volatilization in showers. – Environmental Science Technology 26: 1341-1349.

[30] Mashau, F., Ncube, E. J., Voyi, K. (2018): Association between exposure to drinking water disinfection by products and adverse pregnancy outcomes in South Africa. – Journal Water Health 16(2): 181-196.

[31] Meite, L., Fotsing, M., Barbeau, B. (2015): Efficacy of ozone to reduce chlorinated disinfection by-products in Quebec (Canada) drinking water facilities. – Ozone Science Engineering 37: 1-12.

[32] Ministry of Health (2005): Regulation on Waters Intended for Human Consumption. – Ankara, Turkey.

[33] Mishaqa, E. I., Radwan, E. K., Ibrahim, M. B. M., Hegazy, T. A., Ibrahim, M. S. (2022): Multi-exposure human health risks assessment of trihalomethanes in drinking water of Egypt. – Environmental Research 207: 112643.

[34] Muellner, M. G., Wagner, E. D., Mccalla, K., Richardson, S. D., Woo, Y. T., Plewa, M. J. (2007): Haloacetonitriles vs. regulated haloacetic acids: are nitrogen-containing DBPs more toxic? – Environmental Science Technology 41: 645-651.

[35] Ozgur, C. (2019): Formation of Carbonaceous and Nitrogenous Disinfection By Products in Different Water Sources and Distribution Systems. – Suleyman Demirel University, Graduate School of Natural and Applied Sciences, Department of Environmental Engineering, Kaskelen.

[36] Pan, S., An, W., Li, H., Su, M., Zhang, J., Yang, M. (2014): Cancer risk assessment on trihalomethanes and haloacetic acids in drinking water of China using disability adjusted life years. – Journal Hazardous Materials 280: 288-294.

[37] Rodriguez, M. J., Serodes, J. B. (2011): Spatial and temporal evolution of trihalomethanes in three water distribution systems. – Water Research 35: 1572-1586.

[38] Rodriguez, M. J., Vinette, Y., Serodes, J. B., Bouchard, C. (2003): Trihalomethanes in drinking water of greater Québec region (Canada): occurrence, variations and modelling. – Environmental Monitoring and Assessment 89: 69-93.

[39] Rodriguez, M. J., Serodes, J. B., Levallois, P. (2004): Behavior of trihalomethanes and haloacetic acids in a drinking water distribution system. – Water Research 38: 4367-4382.

http://www.aloki.hu ● ISSN 1589 1623 (Print) ● ISSN 1785 0037 (Online)
DOI: http://dx.doi.org/10.15666/aeer/2005_38333851

[40] Rook, J. J. (1974): Formation of haloforms during chlorination of natural water. – Water Treatment Examination 23: 234-243.
[41] Scheili, A., Rodriguez, M. J., Sadiq, R. (2015): Seasonal and spatial variations of source and drinking water quality in small municipal systems of two Canadian regions. – Science Total Environment 508: 514-524.
[42] Sfynia, C., Bond, T., Kanda, R., Templeton, M. R. (2020): The formation of disinfection by-products from the chlorination and chloramination of amides. – Chemosphere 248: 1-12.
[43] Sfynia, C., Bond, T., Kanda, R., Templeton, M. R. (2022): Simultaneous prediction of trihalomethanes, haloacetic acids, haloacetonitriles and haloacetamides using simulated distribution system tests. – Environ. Sci.: Water Res. Technol 8: 742-756.
[44] Siddique, A., Saied, S., Mumtaz, M., Hussain, M. M., Khwaja, H. A. (2015): Multipathways human health risk assessment of trihalomethane exposure through drinking water. – Ecotoxicology and Environmental Safety 116: 129-136.
[45] String, G. M., Gutierrez, E. V., Lantagne, D. S. (2020): Laboratory efficacy of surface disinfection using chlorine against Vibrio cholerae. – Journal Water Health 18(6): 1009-1019.
[46] Sui, S., Liu, H., Yang, X. (2022): Research progress of the endocrine-disrupting effects of disinfection byproducts. – Journal of Xenobiotics 12: 145-157.
[47] Summerhayes, R. J., Morgan, G. G., Lincoln, D., Edwars, H. P., Earnest, A., Rahman, Md. B., Byleveld, P., Cowie, C. T., Beard, J. R. (2011): Spatio-temporal variation in trihalomethanes in New South Wales. – Water Research 45: 5717-5726.
[48] Tak, S., Vellanki, P. (2018): Natural organic matter as a precursor to disinfection by-products and its removal using conventional and advanced processes: state of the art review. – Journal Water Health 16: 681-703.
[49] Tian, Y., Guo, H., Wang, Y., Liu, Y., Shan, J. (2017): Behavior of haloacetic acids in drinking water distribution systems. – Transactions of Tianjin University 23: 93-99.
[50] Turkish Statistical Institute (TSI): http://www.tuik.gov.tr. – Accessed February 2022.
[51] U. S. Environmental Protection Agency (USEPA) (1995): Method 551.1: Determination of chlorination disinfection byproducts, chlorinated solvents, and halogenated pesticides/herbicides in drinking water by liquid-liquid extraction and gas chromatography with electron-capture detection. Revision 1.0. – Cincinnati, OH.
[52] U. S. Environmental Protection Agency (2006): National primary drinking water regulations: stage 2 disinfectants and disinfection by-products rule: final rule. Federal Register 71(2). – USEPA, Washington, DC, pp. 387-493.
[53] Uyak, V. (2006): Multi-pathway risk assessment of trihalomethanes exposure in Istanbul drinking water supplies. – Environment International 32(1): 2-21.
[54] Uyak, V., Soylu, S., Topal, T., Karapinar, N., Ozdemir, K., Ozaydin, S., Avsar, E. (2014): Spatial and seasonal variations of disinfection byproducts (DBPs) in drinking water distribution systems of İstanbul city, Turkey. – Environmental Forensics 15: 190-205.
[55] Vedugo, E. M., Gifford, M., Glover, C., Cuthbertson, A. A., Trenholm, R. A., Kimura, S. Y., Liberatore, H. K., Richardson, S. D., Stanford, B. D., Summer, R. S., Dickenson, E. R. V. (2020): Controlling disinfection byproducts from treated wastewater using adsorption with granular activated carbon: impact of pre-ozonation and pre-chlorination. – Water Research X 9: 100068.
[56] Wang, G. S., Deng, Y. C., Lin, T. F. (2007): Cancer risk assessment from trihalomethanes in drinking water. – Sci. Total Environ 387(1-3): 86-95.
[57] Wang, Y., Zhu, G., Engel, B. (2019): Health risk assessment of trihalomethanes in water treatment plants in Jiangsu Province, China. – Ecotoxicology and Environmental Safety 170: 346-354.
[58] Zhang, H., Chang, S., Wang, L., Wang, W. (2018): Estimating and comparing the cancer risks from THMs and low-level arsenic in drinking water based on disability-adjusted life years. – Water Research 145: 83-93.

http://www.aloki.hu ● ISSN 1589 1623 (Print) ● ISSN 1785 0037 (Online)
DOI: http://dx.doi.org/10.15666/aeer/2005_38333851

STUDY ON THE SPATIOTEMPORAL VARIABILITY OF SOIL NUTRIENTS AND THE FACTORS AFFECTING THEM: ECOLOGICALLY FRAGILE AREAS OF THE LOESS PLATEAU, CHINA

XIA, L. H.[1] – LI, L.[2] – LIU, J.[3]*

[1]*Institute of Land Engineering and Technology, Shaanxi Provincial Land Engineering Construction Group Co., Ltd., Xi'an 710075, China*
(e-mail: 18092729601@163.com)

[2]*Agricultural Inspection and Testing Center of Shaanxi Province, Xi'an 710014, China*
(e-mail: 576427877@qq.com)

[3]*College of Natural Resources and Environment, Northwest Agriculture and Forestry University, Yangling 712100, China*

**Corresponding author*
e-mail: liujing@nwafu.edu.cn

(Received 18th Mar 2022; accepted 11th Jul 2022)

Abstract. The spatial variability of soil nutrients can improve the yield per unit area of food crops and protect the agricultural ecological environment. Geostatistics and geographic information system (GIS) technology were applied to analyse the spatiotemporal variability and main influencing factors in soil organic matter (SOM) and soil total nitrogen (STN) in ecologically fragile regions of the Loess Plateau, China. The results showed that the mean SOM and STN contents significantly increased in the past 40 years. Compared to the 1980 data, both SOM and STN global Moran's I indices are lower, with less spatial structure and an increased role for stochastic factors. The centre of gravity of soil nutrients in the study area mainly to the south-east, a reduction in the area of the ellipse and a tendency to concentrate the spatial distribution of nutrients. And it was concluded that the variation in nutrients was mainly influenced by fertiliser management practices. Therefore, a long time series of soil nutrient study is of great research value to clarify the soil nutrient status of the study area and to improve the efficiency of arable land use, as well as providing a theoretical basis for precision agriculture.
Keywords: *cultivated land, geostatistics, geographic information system, centre of gravity*

Introduction

Cultivated land soil nutrients are essential nutrients for plant growth and development and are important for ensuring the quality of cultivated land and grain yield (Keskinen et al., 2019). Soil organic matter (SOM) and soil total nitrogen (STN) are important factors that determine soil fertility, agricultural product yield and quality. Due to the combined effects of soil type, topography and human activities, soil nutrients have a high degree of spatial variability (Huang et al., 2012; Wang et al., 2009). Studying the temporal and spatial variability laws of soil nutrients has important theoretical and practical guiding significance for precise nutrient management and the promotion of farmland ecological and economic benefits.

In the early 2000s, domestic scholars began to use geostatistics combined with GIS technology to explore the spatiotemporal variability laws of soil characteristics (Xu et al., 2004). Some studies have been conducted at different spatial scales, such as the scale of farmland or paddy field (Duan et al., 2020; Liu et al., 2004, 2014), the

http://www.aloki.hu ● ISSN 1589 1623 (Print) ● ISSN 1785 0037 (Online)
DOI: http://dx.doi.org/10.15666/aeer/2005_38533872

watershed scale (Wei et al., 2008), and county or larger scales (Chen et al., 2016; Hu et al., 2014; Osat et al., 2016). Recently, an increasing number of studies have focused on the spatiotemporal variability of soil nutrients, e.g., for an agricultural county located in the southern Loess Plateau, China (Chen et al., 2016), five subcatchments in the Ping Gu intermontane basin in Beijing (Zhuo et al., 2019), and the hilly area of the Taihu Lake basin of China (Liao et al., 2017). These studies have provided more in-depth descriptions of the spatiotemporal change process of soil nutrients.

With its advantage of interpolation, the geostatistics method has been widely used in the study of soil spatial variability (Aghasi et al., 2017; Foroughifar et al., 2013). Most scholars have successfully used spatial autocorrelation analysis (Blanchet et al., 2017) and semivariogram analysis (Liu et al., 2013) to describe the spatial variability of soils. However, to date, most studies on the spatiotemporal variability of soil nutrients have used only two phases of data (Guo et al., 2001; Chuai et al., 2012; Wang et al., 2012), and there have been few reports comparing three phases of data with a longer time span. In addition, current studies generally use semivariograms to quantitatively describe spatial characteristics (Hoffmann et al., 2014), and few studies have analysed the spatiotemporal variability laws of soil nutrients from different perspectives. This limited approach will result in researchers not fully understanding the laws of spatiotemporal variability of soil nutrients, which will introduce uncertainty to the formulation of regional soil management measures.

Therefore, this study selects Baishui County, which is a typical region ecologically fragile regions of the Loess Plateau, China, as the research area. The SOM and STN contents in 1980, 2007 and 2020 are employed as the research objects. This study is based on geostatistics and Geographic Information System (GIS) technology, using spatial autocorrelation and Centre of gravity models to reveal the dynamics of the spatial distribution of SOM and STN, and to explore the main factors of nutrient content variation.

The main objectives of this study are (1) to characterise and compare the spatial variability of farmland SOM and STN in the dry plateau area of Weibei; (2) to quantify their spatial distributions and temporal changes; and (3) to clarify the main factors influencing the spatial variability of SOM and STN. Under the current situation of uneven distribution of nutrients in cultivated land, improve the use efficiency of low-nutrient cultivated land, protect the use efficiency of high-nutrient cultivated land, and provide a realistic basis for precision agriculture.

Materials and methods

Description of the study area

Baishui County is located in the transition zone between the Guanzhong Plain and the North Shaanxi Plateau, China, between 109°16′-109°45′ E and 35°4′-35°27′ N (*Fig. 1*). The total area of the district is 986.6 km^2, of which the cultivated area is 525.4 km^2, accounting for 53.2% of the total area. The area is high in the northwest and low in the southeast, with an altitude between 440 m and 1500 m. Baishui County has a temperate continental monsoon climate, an average annual temperature of 11.4 °C, and an average annual precipitation of 577.8 mm. Due to the cutting of each branch gully of the Luo River and Baishui River, the study area has criss-crossed gullies and broken topography. The dominant soil types include loessial soil and cumulic cinnamon soil.

http://www.aloki.hu ● ISSN 1589 1623 (Print) ● ISSN 1785 0037 (Online)
DOI: http://dx.doi.org/10.15666/aeer/2005_38533872

Data collection

Soil data, including the SOM and STN utilised in this study, were obtained from three soil sampling surveys: The second national soil survey in 1980, the 2007 survey of cultivated land quality in Shaanxi Province, and the 2020 survey of cultivated land quality in Shaanxi Province. The three datasets were named "Soil attribute-1980", "Soil attribute-2007" and "Soil attribute-2020". The average temperature and climate data were obtained from the Resource and Environment Science Data Center of CAS with a spatial resolution of 1 km×1 km and time taken from 2020.

In the 1980 soil survey, 2007 soil survey and 2020 soil survey, 154 farmland topsoil samples, 156 farmland topsoil samples and 73 farmland topsoil samples (0-20 cm), respectively, were collected from May to June (dry season) after the summer grain harvest. The sampling location was determined by the main topography, soil type and distribution of the sample plot, and the Global Positioning System (GPS) was employed to record the points while avoiding roads, residential areas and other easily disturbed areas when sampling. At each sampling point, 6-8 points were randomly selected and mixed into a soil sample. The collected soil samples were ventilated and dried, and the impurities were removed and finely ground for determination of the SOM and STN content.

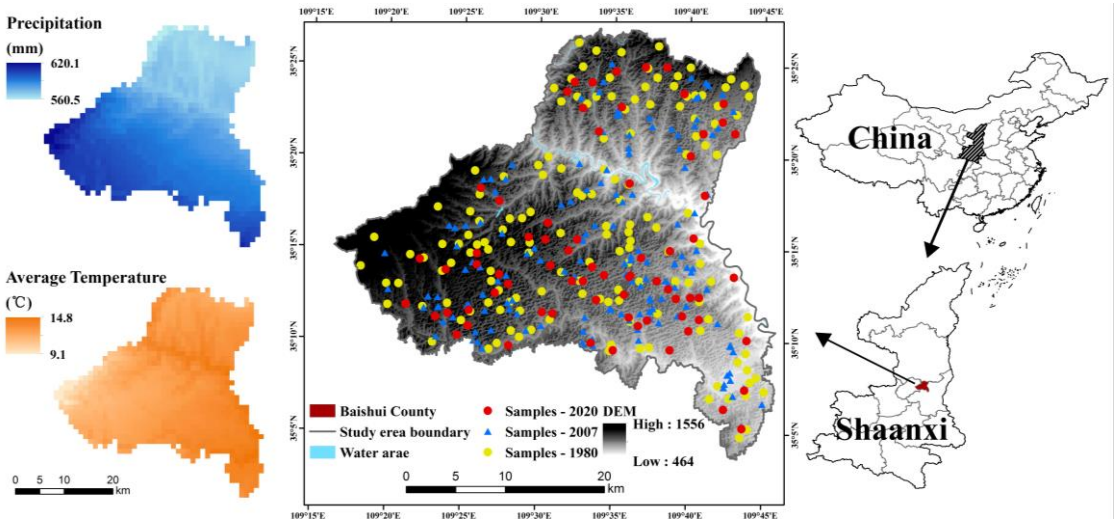

Figure 1. *Map of the soil sample distribution*

In the 1980 soil survey, the SOM content of all 154 soil samples was obtained by the $K_2Cr_2O_7$-H_2SO_4 oxidation method, and the STN of 152 samples was measured by the Kjeldahl method (Agricultural Chemistry Committee of China, 1983). According to this method, the SOM and STN of the soil samples from the 2007 and 2020 surveys were analysed. The sampling point distribution is shown in *Figure 1*.

Data processing and analysis

Data processing

The existence of outliers and the non-normal distribution of data can easily cause the proportional effect of the variogram and increase the estimation error. In this study, we applied the A±3s method to eliminate outliers, where A denotes the average value for

http://www.aloki.hu ● ISSN 1589 1623 (Print) ● ISSN 1785 0037 (Online)
DOI: http://dx.doi.org/10.15666/aeer/2005_38533872

each variable and s is its standard deviation (Liu et al., 2009). Data that exceed the value (A±3s) were obtained from the raw dataset; we replaced them with the maximum or minimal value of the dataset without outliers. In SPSS 20.0, a one-sample normality test (K-S test) was performed on the sample data after removing outliers. The R-language was applied to perform Box-Cox conversion of the data that did not conform to a normal distribution. The converted data passed the K-S test. The specific parameters are shown in *Table 1*.

Table 1. *Soil nutrient description statistics of cultivated land in three periods (g kg^{-1})*

Variables	Samples	Mean ± standard deviation	Minimum	Maximum	Coefficient of variation (%)	P_{k-s}
SOM-1980	154	10.53 ± 2.36	4.71	17.74	22.4	0.14*
STN-1980	152	0.60 ± 0.09	0.32	1.05	15.6	0.40*
SOM-2007	156	12.49 ± 5.01	2.60	26.40	38.47	0.78*
STN-2007	156	0.64 ± 0.37	0.18	1.11	37.16	0.74*
SOM-2020	73	15.42 ± 4.23	7.96	27.53	27.23	0.43*
STN-2020	73	0.73 ± 0.19	0.38	1.32	27.26	0.74*

Level of significance: * P < 0.05

In this study, we compiled descriptive statistics of soil nutrients using Excel 2016 and performed Kriging interpolation to estimate the spatial distribution and spatial changes of SOM and STN in different years. We calculated the global Moran's I values using ArcGIS 10.6. Sample-independent t tests and a correlation analysis were carried out using SPSS 16.0. A geostatistics analysis was performed by GS + 9.0.

Spatial autocorrelation analysis

Spatial autocorrelation refers to the potential dependence of the same variable at different spatial positions and is a statistical method used to test the correlation between adjacent positions of the studied variables in space (Gelaw et al., 2014). When judging the spatial autocorrelation, the global Moran's I index is often employed to reflect the spatial autocorrelation of the study area. The calculation formula is as follows:

$$I = \frac{n}{S_0} \times \frac{\sum_{i=1}^{n}\sum_{j=1}^{n} w_{ij}(x_i-\bar{x})(x_j-\bar{x})}{\sum_{i=1}^{n}(x_i-\bar{x})^2} \quad \text{(Eq.1)}$$

where n is the total number of samples, Wij is the symmetric binomial spatial weight matrix, and X_i and X_j are the measured values of spatial variable X at different positions i and j, respectively. The value of I ranges from -1 to 1. When I > 0, it means that there is a positive spatial correlation, and larger values indicate stronger spatial correlation. When I < 0, it means there is a negative spatial correlation, and smaller values indicate more obvious spatial differences (Darand et al., 2017).

Semivariogram analysis

The semivariogram is a commonly used function in geostatistical analysis. It can accurately describe the characteristics of the spatial variability of a study area based on known sample points. The semivariogram can reveal the internal relations of variables,

http://www.aloki.hu ● ISSN 1589 1623 (Print) ● ISSN 1785 0037 (Online)
DOI: http://dx.doi.org/10.15666/aeer/2005_38533872

and the relationship between spatial points in different distances and different directions can be used to obtain the spatial distribution law of variables, which makes the spatial interpolation more accurate (Awais et al., 2017); its calculation formula is as follows:

$$r(h) = \frac{1}{2N(h)} \sum_{i=1}^{N(h)} [Z(x_i) - Z(x_i + h)]^2 \quad \text{(Eq.2)}$$

where h is the spatial interval of the sampling points, N (h) is the number of samples with interval distance h, and $Z(x_i)$ and $Z(x_i + h)$ are the measured values of spatial variable Z(x) at the different positions of xi and xi + h, respectively (Balaguer-Beser et al., 2013). There are three important parameters in the semivariogram: the nugget value (C_0), the sill value ($C_0 + C$) and the range (A). When the step size of h is 0, then r(h) is the nugget value. As the step size of h increases, the semivariogram tends to be in a stable state. At this time, r(h) is the sill value and h is the range (Onyejekwe et al., 2016).

Centre of gravity models and standard deviational ellipse

The centre of gravity model is mostly used to study the process of change in the spatial location of a geographical element in the process of regional development. The model reflects the changing trend of the spatial element through the direction, distance and speed of the centre of gravity migration. This paper uses a centre of gravity model to reveal the spatial aggregation characteristics and trends of soil nutrients. Its calculation formula is as follows:

$$\overline{X} = \sum_{i=1}^{n} M_i X_i / \sum_{i=1}^{n} M_i \quad \text{(Eq.3)}$$

$$\overline{Y} = \sum_{i=1}^{n} M_i X_i / \sum_{i=1}^{n} M_i \quad \text{(Eq.4)}$$

where $\overline{X}$, $\overline{Y}$ are the soil nutrient coordinates at the beginning of the study; M_i is the nutrient content of the ith sample point, g kg^{-1}; X_i, Y_i denote the coordinates of the ith sample point.

The standard deviation ellipse is a visual representation of the state of aggregation of soil nutrients and their tendency to shift, and consists mainly of the angle of rotation θ, the standard deviation along the major axis (long axis) and the standard deviation along the minor axis (short axis). The long half-axis of the ellipse indicates the direction of the soil nutrient distribution and the short half-axis indicates the extent of the soil nutrient distribution. In this study, standard deviation ellipses were constructed to reflect the spatial pattern of soil nutrients on the basis of the centre of gravity model.

Results

Descriptive statistics

The descriptive statistical results of the data after eliminating the outliers in the three periods are summarised in *Table 1*. It can be seen that the average contents of SOM and STN of the cultivated soil in the study area in 1980 were 10.53 g kg^{-1} and 0.60 g kg^{-1}, respectively. In 2007, the average SOM content and STN content in the cultivated soil in the study area were 12.49 g kg^{-1} and 0.64 g kg^{-1}, respectively; in 2020, the corresponding values were 15.42 and 0.73 g kg^{-1}, respectively. Compared with 1980,

http://www.aloki.hu ● ISSN 1589 1623 (Print) ● ISSN 1785 0037 (Online)
DOI: http://dx.doi.org/10.15666/aeer/2005_38533872

the average SOM content and STN content in 2007 increased by 2.48 g kg^{-1} and 0.04 g kg^{-1}, respectively. From 2007 to 2020, the contents of the two nutrients increased by 2.41 g kg^{-1} and 0.09 g kg^{-1}, respectively. Although the data do not depend on the sample t test, the mean value presents a significant difference (*Table 2*). The coefficient of variability of the soil nutrients in the cultivated land in the study area in the three phases was between 15.6 and 38.47%, which indicated moderate variability.

Table 2. *Significance test of soil nutrients in 1980, 2007 and 2020*

Variables	P		Variables	P
SOM (1980-2007)	0.005**		SOM (2007-2020)	0.002**
STN (1980-2007)	0.03*		STN (2007-2020)	0.021*

Level of significance: * $P < 0.05$; ** $P < 0.01$

Spatial autocorrelation analysis

The spatial statistical results of the soil nutrients of the cultivated land in the three phases are shown in *Table 3*. It can be seen from the table that the global Moran's I index of SOM and STN decreased from 0.41 and 0.44 to 0.26 and 0.17, respectively, from 1980 to 2007. In 2020, the global Moran's I index of SOM and STN were 0.25 and 0.21, respectively. By normalizing the global Moran' s I index, all Z values were greater than 2.56, which indicates that at the current sampling density, the three-stage SOM and STN show a very significant positive spatial correlation at the 0.01 statistic level, and their spatial distribution is characterised by agglomeration. By further comparing the global Moran's I index, the global Moran's I index of SOM and STN in 2007 and 2020 is higher than that of SOM and STN in 1980. This finding shows that SOM and STN in 1980 have stronger spatial dependence and better spatial structure, with weaker random variability.

Geostatistics analysis

The optimal fitting of the theoretical model revealed that SOM-1980, STN-1980, SOM-2020 and STN-2020 fit the exponential model, while SOM-2007 and STN-2007 conform to the linear model. The coefficient of determination (r^2) is between 0.785 and 0.995; the proximity of these values to 1 indicates that the excellent fit of the semivariogram (*Fig. 2*). The parameters of the model are listed in *Table 3* (i.e., nugget, sill and nugget/sill ratio). The nugget/sill ratio of SOM and STN in the three periods ranges from 42.27 to 76.14%, which indicates that the spatial correlation is moderate and the spatial continuity is average. The nugget/sill ratios of SOM and STN in 2007 were 76.14% and 66.56%, respectively, which is higher than in 1980 (SOM with 42.95% and STN with 42.27%). The nugget/sill ratio of SOM and STN in 2020 has not changed substantially from 2007 and is also higher than that in 1980. The strong spatial variability in 2007 and 2020 indicates that they may be affected by more external factors, such as fertilization and irrigation. These results are consistent with the analysis results of the global Moran's I values.

The spatial range of soil SOM and STN in the three periods is 5050 to 17,350 m, which is considerably larger than the average sampling interval (2500-4000 m). This finding shows that the number of sampling points in the three periods is sufficient for analysing the spatial distribution of nutrients on the county scale.

http://www.aloki.hu ● ISSN 1589 1623 (Print) ● ISSN 1785 0037 (Online)
DOI: http://dx.doi.org/10.15666/aeer/2005_38533872

Table 3. *Semivariance model of soil nutrients in three periods and Moran's I index*

Variables	Model	Nugget (C_0)	Sill ($C_0 + C$)	Nugget/sill (%)	Range (m)	R^2	Moran's I	Z
SOM-1980	E	0.1188	0.2766	42.95	6470	0.995	0.41**	32.36
STN-1980	E	0.0238	0.0563	42.27	5050	0.957	0.44**	35.48
SOM-2007	L	2.129	2.796	76.14	17350	0.867	0.26**	24.89
STN-2007	L	0.0547	0.0823	66.56	16280	0.816	0.17**	19.06
SOM-2020	E	0.0748	0.1315	56.88	9950	0.824	0.25**	24.96
STN-2020	E	0.0304	0.0638	47.64	11800	0.785	0.21**	17.56

E is the exponential model, L is the linear model
Level of significance: ** $P < 0.01$

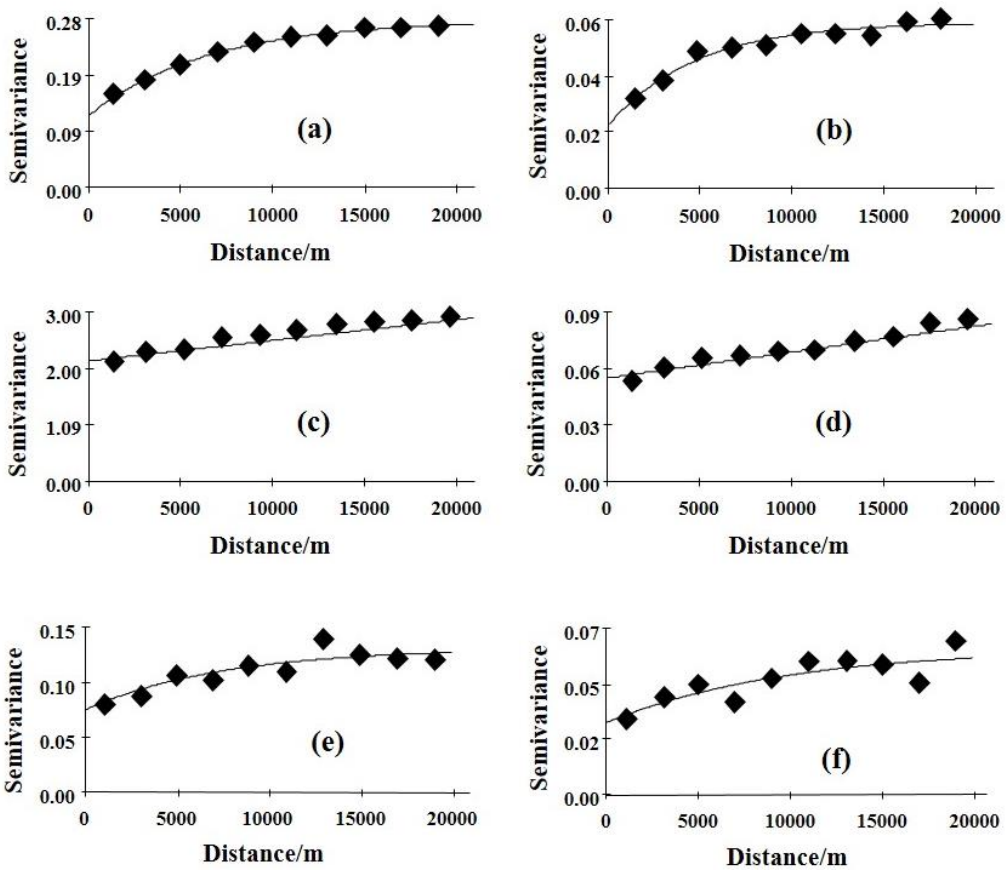

Figure 2. *Fitted models of SOM and STN in 1980 (a-b), 2007 (c-d), and 2020 (e-f). SOM: soil organic matter; STN: soil total nitrogen*

Spatial distribution characteristics

The spatial interpolation results of soil SOM and STN in the three periods are shown in *Figure 3*. It can be seen from the figure that the spatial distribution characteristics of soil SOM content in the three phases are similar: the distribution characteristics are low in the northwest and high in the southeast (*Fig. 3a-c*). In 1980, the SOM content in the study area was at a low-medium level, while the content in the central region was relatively low. The area with a content greater than 13 g kg^{-1} was only 1.47 km^2. In

http://www.aloki.hu ● ISSN 1589 1623 (Print) ● ISSN 1785 0037 (Online)
DOI: http://dx.doi.org/10.15666/aeer/2005_38533872

2007, the soil SOM content in the study area increased steadily, and the area with a content greater than 13 g kg^{-1} increased to 228.06 km^2. In 2020, the SOM content increased significantly, which shows high spatial distribution characteristics in the east and low spatial distribution characteristics in the west. Only 78.98 km^2 remained in the study area where the SOM content was less than 13 g kg^{-1} (*Table A1* in the *Appendix*).

As SOM and STN have a significant positive correlation, they show similar spatial distribution characteristics (*Fig. 3d-f*). In 1980, the content of STN was low and mostly concentrated from 0.55 to 0.65 g kg^{-1}. In 2007, the STN content was distributed in blocks, and the content in some areas increased significantly, mainly in the southern part of the study area. In 2020, the STN content was at a relatively high level, with a content greater than 0.75 g kg^{-1} concentrated in the southeast part of the study area, with an area of 165.37 km^2, which accounts for 30.88% of the total study area (*Table A2*).

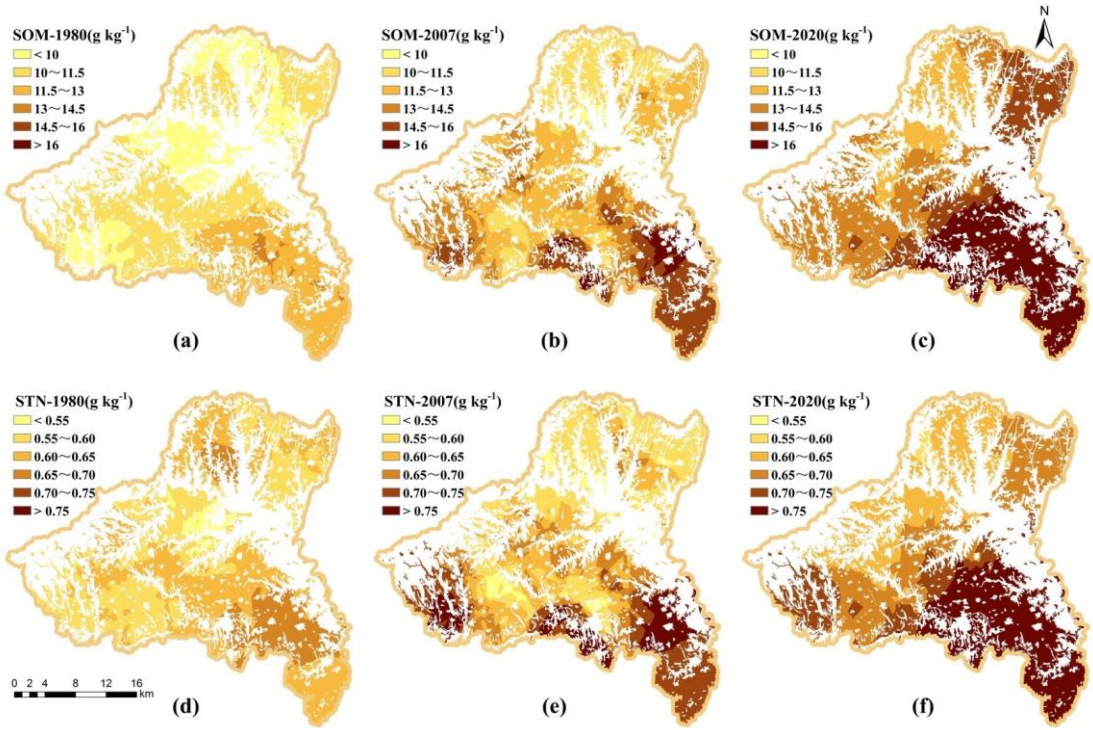

Figure 3. *Distribution map of SOM and STN in three different periods (a – f). SOM: soil organic matter; STN: soil total nitrogen*

Temporal and spatial characteristics

We employed the ArcGIS vector mask extraction tool and raster calculator to calculate the rate of change according to the formula "(x2007-x1980)/x1980 and (x2020-x2007)/x2007". The results are shown in *Figure 4*.

From 1980 to 2007, the soil SOM and STN content in the study area showed an overall increasing trend, but the degree of change was different in different regions. The area where the SOM increased accounted for 94.97% of the study area, with an area of 499.07 km^2. Compared with SOM, the increase in STN was relatively weak, and the increase was mainly concentrated in the range 0-15%, which accounts for 44.55% of the total area. The data reveals that 31.14% of the cultivated land exhibits a decrease in STN content (*Table A3*).

http://www.aloki.hu ● ISSN 1589 1623 (Print) ● ISSN 1785 0037 (Online)
DOI: http://dx.doi.org/10.15666/aeer/2005_38533872

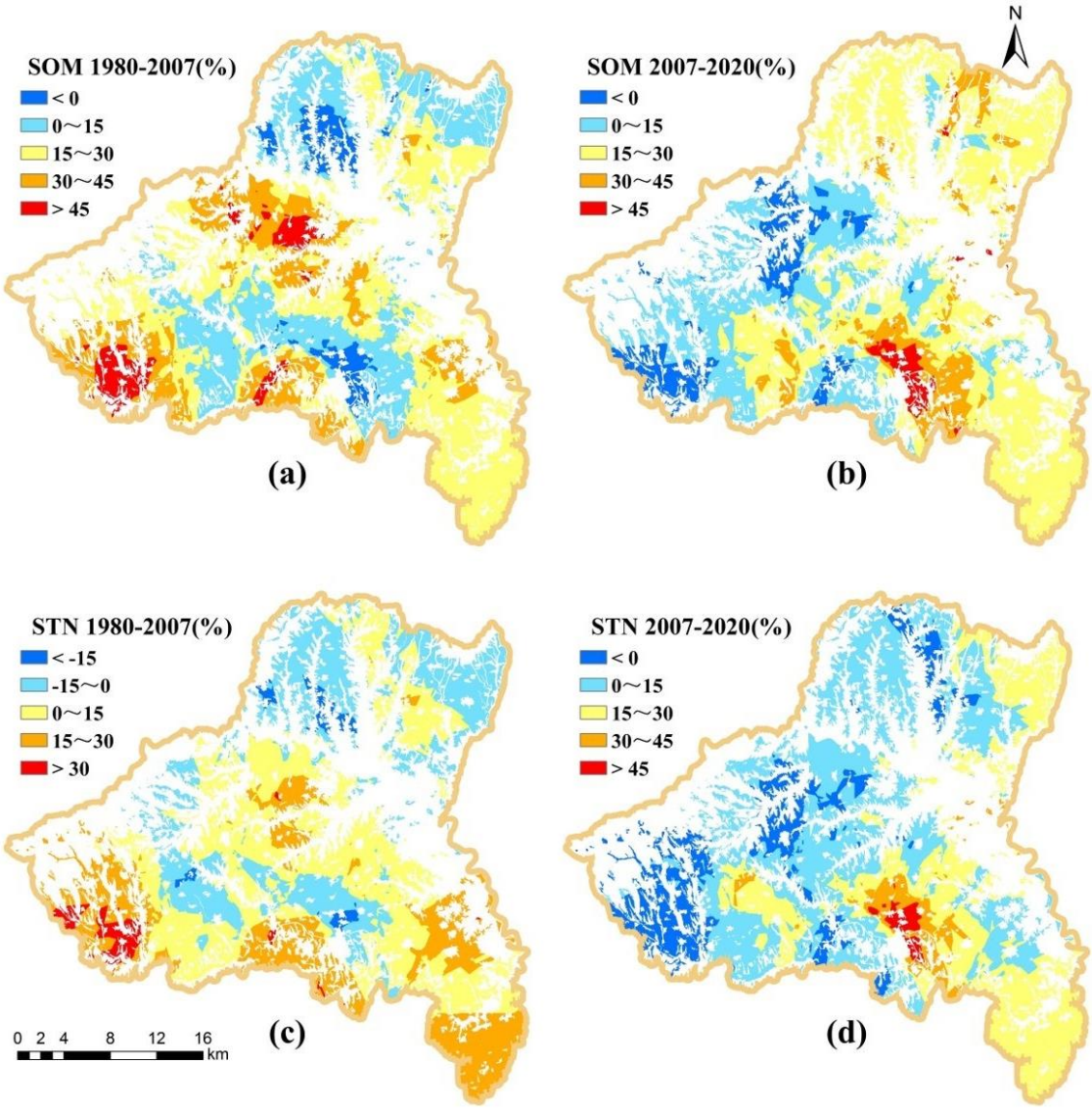

Figure 4. *Spatial distribution map of SOM (a) and STN (b) changes in Baishui County from 1980 to 2007, and the spatial distribution map of the changes in soil SOM (c) and STN (d) Baishui County from 2007 to 2020. SOM: soil organic matter; STN: soil total nitrogen*

From 2007 to 2020, the content of SOM and STN in the study area increased steadily, with a relatively large increase in the east and a relatively small increase in the west. The SOM and STN content decreased in only a few areas. The growth rates of SOM and STN are similar, and the growth rates are mainly concentrated from 0 to 30%, which accounts for 79.52% of the study area and 79.75% of the study area, respectively (*Table A4*).

Centre of gravity models and standard deviational ellipse

The centre of gravity model was used to obtain the direction and distance of soil nutrient centre of gravity migration for each period respectively, and the results are shown in *Tables 4* and *5* and *Figure 5,* which show that the nutrient changes in the study area are mainly divided into the following two stages:

http://www.aloki.hu ● ISSN 1589 1623 (Print) ● ISSN 1785 0037 (Online)
DOI: http://dx.doi.org/10.15666/aeer/2005_38533872

From 1980-2007, the centre of gravity of soil nutrients shifted towards southeast. Since the 1980s, farmers have been practising intensive farming and have begun to focus on land management, so the centre of gravity of soil nutrients has moved a long way. From 2007 to 2020, the centre of gravity of soil nutrients as a whole shifted 922.96 m and 1030.95 m to the southeast, respectively, a relatively short distance (*Table 4*). The centre of gravity as a whole shifted to the south-east as the lower ground made it easier for people to cultivate. In summary, it can be seen that the centre of gravity of soil nutrients in the study area has generally shifted to the south-east over the past 40 years, with a decreasing trend in the distance shifted.

Table 4. *Soil nutrient gravity shift 1980-2020*

Shift of gravity centre	SOM		STN	
	1980-2007	2007-2020	1980-2007	2007-2020
Moving direction	South-east	South-east	South-east	South-east
Movement distance (m)	3579.31	922.76	3903.31	1030.95

Table 5. *Changes in standard deviational ellipse parameters for soil nutrients 1980-2020*

Year	SOM			STN		
	1980	2007	2020	1980	2007	2020
Rotation (°)	56.32	72.63	61.98	51.49	70.71	63.66
Standard deviation along the x-axis (km)	14.72	13.38	13.29	14.58	13.49	13.31
Standard deviation along the y-axis (km)	13.48	11.63	12.32	13.25	11.59	12.37
Ellipse area (km^2)	623.69	514.61	489.24	618.76	514.61	491.54

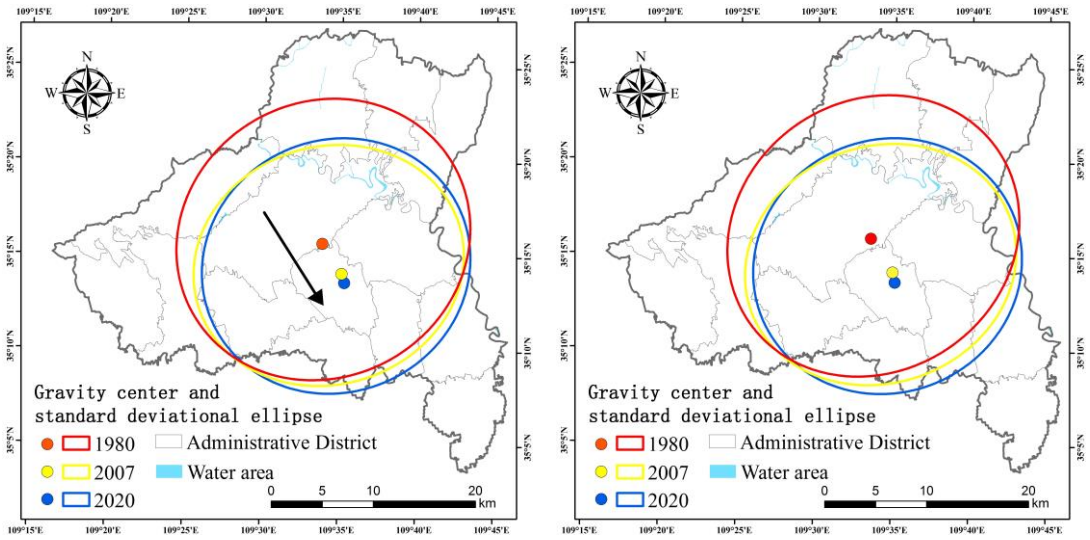

Figure 5. *Soil nutrient gravity shift 1980-2020*

As can be seen from *Figure 5,* there is a certain directionality to the change in the standard deviation ellipse in the study area, which correlates with the shift in the centre of gravity. Throughout the study period, the angle of rotation shows an 'increasing-

http://www.aloki.hu ● ISSN 1589 1623 (Print) ● ISSN 1785 0037 (Online)
DOI: http://dx.doi.org/10.15666/aeer/2005_38533872

decreasing' pattern, with an increasing spatial distribution in the southeast. As can be seen from *Table 5,* the area of the standard deviation ellipse gradually decreases, indicating that the spatial distribution of soil nutrients in the study area gradually tends to concentrate and the nutrient content becomes more stable.

Discussion

Temporal changes in SOM and STN

The distribution patterns of soil SOM and STN in the study area are similar. During the 38-year period from 1980 to 2020, the content of soil SOM and STN in Baishui County increased significantly. Generally, some agricultural practices can reduce soil carbon by soil disturbance and mineralization (Ma et al., 2016a). Some studies have focused on the impact of land use changes on SOM and STN content. For example, the conversion from cultivated land to orchard land increases the risk of nutrient loss in the watershed (Chen et al., 2019). Compared with farmland, the organic matter and total nitrogen content in the surface soil of orchard land increases (Lu et al., 2016). When the original grassland is changed to vegetable land (Kong et al., 2006), both the soil organic carbon (SOC) content and STN content increase. More research focuses on the impact of agricultural activities on SOM and STN content. In Kansas, the application of animal droppings (Schlegel et al., 2017) and the presence of plateau pikas in the Qinghai-Tibet Plateau significantly (Yu et al., 2017) increased the STN and SOC content. The average SOC content and STN content in the Tai Lake Basin increased during a 20-year period (1980-2000) (Liu et al., 2014a); and the STN and SOM content in the ecologically fragile area of the Loess Plateau increased (Guan et al., 2020). These findings show that fertilization measures and planting management methods may cause changes in soil nutrients. Therefore, it can be seen that the transformation of land use patterns and various agricultural practices will affect the soil SOM content and STN content to varying degrees. In this study, the general increase in SOM and STN content may be attributed to the implementation of the household contract responsibility system, the distribution of land to households, the widespread use of fertilizers, the improvements in irrigation and drainage facilities, and the intensive cultivation of farmers.

Among the major apple-producing areas in the country, Baishui County is the only county that meets the seven indicators used to identify the most suitable apple production areas, and the region has very superior natural conditions. Therefore, apples have become the main agricultural industry in the county. For apples, the content of organic matter in the soil is very important. It can not only improve the quality of apples but also fertilize the soil and improve the soil environment. The SOM content in the study area showed an increasing trend, which provided a strong guarantee for increasing apple output, rural residents' incomes and sustainable agricultural development.

Temporal changes of their spatial variability

Judging from the variability of the soil nutrients in the study area, the coefficient of variability of the nutrients in the three phases is between 15.6 and 38.47%, and the spatial heterogeneity is weak. From the spatial autocorrelation and semivariogram analysis, we obtain the same analysis results for the three-phase SOM and STN. The nugget/sill ratios of SOM and STN in 2007 and 2020 are higher, and the global Moran's I index is lower, which indicates that the spatial autocorrelation of SOM and STN is

http://www.aloki.hu ● ISSN 1589 1623 (Print) ● ISSN 1785 0037 (Online)
DOI: http://dx.doi.org/10.15666/aeer/2005_38533872

weakened, the distribution tends to be fragmented, and the proportion of random variability increases.

The global Moran's I index describes the spatial aggregation characteristics of the research variables from the perspective of correlation and uses the standard deviation of the approximate normal distribution hypothesis in random conditions to standardise it to determine whether the spatial autocorrelation is significant (or extremely significant). However, the global Moran's I index cannot provide a basis for spatial interpolation and is unable to adequately describe the spatial patterns of variables (Martin et al., 2014). A semivariogram can better compensate for the lack of interpolation of a spatial autocorrelation analysis. A semivariogram can not only quantitatively reveal the spatial correlation degree of regional variables and the scale range of spatial variability using indicators such as the block base ratio and variable range but also perform Kriging interpolation on a parameter basis; however, it cannot provide a statistical test for positive and negative spatial correlation significance, such as Moran's I standardised Z value (Ma et al., 2016).

Factors that influence an increase in SOM and STN

Topographic influence

To explore the influence of topography, the average SOM and STN content of different elevations and topography types were calculated (*Tables 6* and *7*). From 1980 to 2007, additional SOM and STN were accumulated in low-altitude areas. For example, SOM and STN content increased by 2.422 g kg^{-1} and 0.051 g kg^{-1} (<600 m), and high-altitude areas only increased by 1.899 g kg^{-1} and 0.034 g kg^{-1} (>900 m). This pattern also appeared from 2007 to 2020. This phenomenon may be caused by flat terrain in low-altitude areas, excessive agricultural production activities, and excessive fertilization, which produced greater biological residues and nitrogen accumulation in the soil (Zhu et al., 2019).

Table 6. *Average SOM and STN content (g kg^{-1}) at different elevations. SOM: soil organic matter; STN: soil total nitrogen*

Variables	Elevation			
	< 700 m	**700-800 m**	**800-900 m**	**> 900 m**
SOM-1980	11.511 ± 2.374	11.230 ± 2.446	9.986 ± 2.309	10.429 ± 1.975
SOM-2007	13.933 ± 4.132	13.503 ± 5.779	12.148 ± 4.315	12.328 ± 4.537
SOM-2020	17.091 ± 2.895	17.717 ± 4.936	14.419 ± 3.671	13.281 ± 2.487
Increment (1980-2007)	2.422	2.273	2.162	1.899
Increment (2007-2020)	3.158	4.214	2.271	0.953
STN-1980	0.618 ± 0.087	0.635 ± 0.091	0.592 ± 0.090	0.601 ± 0.081
STN-2007	0.669 ± 0.217	0.663 ± 0.261	0.629 ± 0.203	0.635 ± 0.249
STN-2020	0.811 ± 0.131	0.821 ± 0.223	0.683 ± 0.135	0.653 ± 0.145
Increment (1980-2007)	0.051	0.028	0.037	0.034
Increment (2007-2020)	0.142	0.158	0.054	0.018

Table 7 shows the comparison results of the changes in the SOM and STN content for different landform types. From 1980 to 2007, the SOM and STN content in the

http://www.aloki.hu ● ISSN 1589 1623 (Print) ● ISSN 1785 0037 (Online)
DOI: http://dx.doi.org/10.15666/aeer/2005_38533872

valley terrace increased by 2.747 g kg^{-1} and 0.031 g kg^{-1}, respectively, while the increase in SOM and STN content in the middle mountain were negative. The changes in the SOM and STN content from 2007 to 2020 also showed this pattern.

Table 7. *Average SOM and STN content (g kg^{-1}) for different terrains. SOM: soil organic matter; STN: soil total nitrogen*

Variables	Topography		
	Valley terrace	**Loess tableland**	**Middle mountain**
SOM-1980	10.881 ± 2.394	10.496 ± 2.109	10.982 ± 2.949
SOM-2007	13.628 ± 3.754	12.881 ± 4.142	10.400 ± 4.537
SOM-2020	17.354 ± 4.152	15.627 ± 4.210	11.278 ± 3.285
Increment (1980-2007)	2.747	2.385	-0.582
Increment (2007-2020)	3.726	2.746	0.878
STN-1980	0.606 ± 0.077	0.605 ± 0.086	0.590 ± 0.103
STN-2007	0.637 ± 0.193	0.632 ± 0.247	0.540 ± 0.249
STN-2020	0.750 ± 0.008	0.721 ± 0.185	0.574 ± 0.213
Increment (1980-2007)	0.031	0.027	-0.05
Increment (2007-2020)	0.113	0.089	0.034

The study revealed that the valleys and rivers located in the valley terrace of the study area have flat terrain with relatively satisfactory farming performance, which greatly improves the supply and utilization of carbon and nitrogen in the soil (Weihrauch and Opp, 2018). According to the survey results, the use of chemical fertilizers has increased steadily in recent years. The combined application of phosphate fertilizers and organic fertilizers, the increase in agricultural production input and the high degree of cultivation and maturation facilitate the accumulation of organic matter, which causes a steady increase in the SOM content in the study area.

Soil-type influence

The main soil types in Baishui County mainly include cumulic cinnamon soil and loessial soil. The effects of two soil types on the SOM and STN content were calculated separately (*Fig. 6*). It can be seen from the figure that there are significant differences in the content of SOM and STN in the two soil types. For example, in 1980, the average SOM content and STN content of Cumulic cinnamon soil were 10.704 g kg^{-1} and 0.612 g kg^{-1}, respectively, while the average SOM content and STN content of loessial soil were only 9.985 g and 0.558 g kg^{-1}. From 1980 to 2007, the SOM content and STN content of cinnamon soil increased to 13.266 g kg^{-1} and 0.648 g kg^{-1}, respectively, and the SOM content and STN content of loess soil increased to 12.916 g kg^{-1} and 0.642 g kg^{-1}, respectively. From 2007 to 2020, the SOM and STN content in the two soil types also showed an increasing trend. These differences could be attributed to the different textures, parent materials, and soil formation processes that are associated with these soil types.

Cumulic cinnamon soil is a kind of anthropogenic soil that is neutral to slightly alkaline, has a deep plough layer, and has excellent water and fertility retention (Yan et al., 2019). Loessial soil is loose and soft with a light soil colour. Due to the lack of

http://www.aloki.hu ● ISSN 1589 1623 (Print) ● ISSN 1785 0037 (Online)
DOI: http://dx.doi.org/10.15666/aeer/2005_38533872

obvious profile development and serious soil erosion, loessial soil has weak water and fertilizer retention capabilities (Xin et al., 2016). Therefore, cumulic cinnamon soil has a higher SOM and STN content. Therefore, it can be concluded that soil type also has a substantial influence on the spatial changes of farmland SOM and STN.

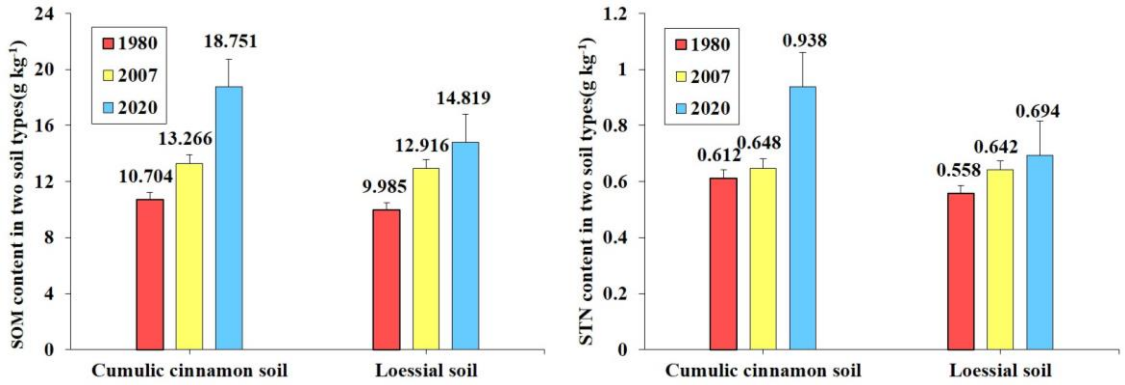

Figure 6. *Bar graphs for average SOM and STN content for two different soil types. SOM: soil organic matter; STN: soil total nitrogen*

Impact of land use practices

In addition to the influence of soil type, changes in land use patterns should not be ignored. In the 1980s, the land use pattern in Baishui county was mainly dry land. With the construction and improvement of farmland water conservancy facilities, dry land gradually decreased, watered land increased, and the effective irrigated area of arable land increased significantly. As can be seen from *Figure 7,* from 1980 to 2007, except for the soil STN decreased under dryland-watered conditions, all the others showed an increase; from 2007 to 2020, the soil nutrient content increased regardless of the change in cropland use, with the highest increase in cropland maintained as watered land for a long time, with SOM and STN increasing by 3.74 g kg^{-1} and 0.148 g kg^{-1} respectively. Due to the favourable irrigation conditions on the watered land and the fine tillage management, the soil nutrient content increased significantly. It shows that the change in the use of arable land leads to a different pattern of change in soil nutrient content.

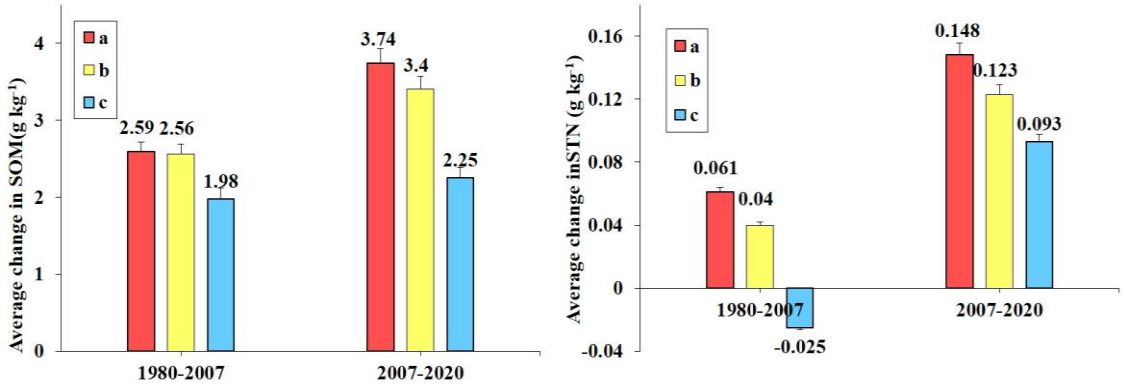

Figure 7. *Changes in soil nutrients in arable land under different land use practices. (a) Watered land-Watered land; (b) Dryland-Dryland; (c) Dryland-Watered land*

http://www.aloki.hu ● ISSN 1589 1623 (Print) ● ISSN 1785 0037 (Online)
DOI: http://dx.doi.org/10.15666/aeer/2005_38533872

Farming management practice influence

In agricultural production, various farming practices, such as fertilizer application, irrigation, and crop residue returned to the field can significantly affect the SOM and STN dynamic change. In 1980, the lower SOM and STN contents on farmland reflected a long cultivation history with little or no fertilizer input (2542 t in 1980). Most crop residues were also taken off and used as fuel for cooking and heating. Since the early 1980s the Household Responsibility System has been implemented. The farmers were then given the authority to manage the contracted land, including all decisions regarding production. In order to get higher yield, more chemical fertilizers were used by farmers. After reviewing the Shaanxi Statistical Yearbook (Shaanxi Provincial Bureau of Statistics, 1980-2020), the amount of chemical fertilizer used in the study area increased from 2,542 t in 1980 to 70,643 t in 2020. Meanwhile, there has been a significant increase of organic manure applications and return of crop residues into the soil. It is clear that the use of organic manure and higher chemical fertilizers inevitably resulted in increased cropland SOM and STN levels.

In addition, with the development of irrigation and water conservation activities, many non-irrigated farmlands were transformed into irrigated lands, especially in the low-elevation areas. To reveal the irrigation effect, the average SOM and STN contents for different cropland types are calculated and their increment is shown in *Figure 8*. During the period from 1980 to 2020, the highest increment of SOM was in the cropland that changed from dry land to irrigated land, whereas for STN the largest increase occurred for the irrigated land (over the whole period). Generally speaking, SOM and STN in irrigated cropland increased relatively most. Thus, it can be seen that irrigation has a clear influence on the change of farmland SOM and STN.

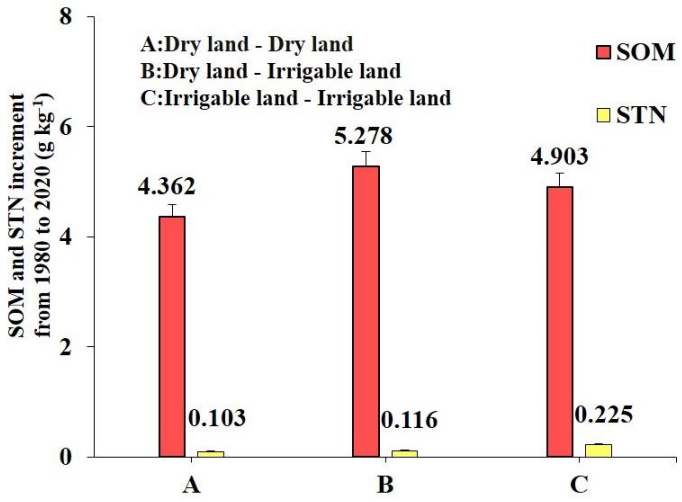

Figure 8. *Average increase of SOM and STN content between 1980 and 2020 for different cropland types. SOM: soil organic matter; STN: soil total nitrogen*

Conclusions

In this study, a combination of geostatistical and GIS techniques was used to quantitatively study and explore the spatial and temporal variability characteristics of the SOM and STN of cultivated soils in Baishui County, a typical region in ecologically fragile regions of the Loess Plateau, China. The main findings are as follows:

http://www.aloki.hu ● ISSN 1589 1623 (Print) ● ISSN 1785 0037 (Online)
DOI: http://dx.doi.org/10.15666/aeer/2005_38533872

1. The average SOM content increased by 2.48 g kg^{-1} and 2.41 g kg^{-1} during 1980-2007 and 2007-2020, respectively, and the average STN content increased by 0.04 g kg^{-1} and 0.09 g kg^{-1}, respectively.

2. The coefficients of variability of soil nutrients on cultivated land in three years ranged between 15.6% and 38.5%, which represented moderate variability. Compared with 1980, the SOM and STN contents in 2007 and 2020 showed a higher nugget/sill ratio and a lower global Moran's I index, which indicates the spatial variability and weak spatial structure of SOM and STN.

3. The centre of gravity of soil nutrients generally shifted towards southeast, moving 922.96 m and 1030.95 m respectively. The spatial distribution pattern of the soil nutrient standard deviation ellipse is consistent with the direction of distribution in the study area, shifting to the southeast. The Rotation show an "increasing-decreasing" pattern of change, with the oval area decreasing and the spatial distribution of soil nutrients tending to concentrate.

4. We also found moderate spatial variation in both SOM and STN content as a result of a combination of intrinsic factors (topography, soil type, and land use patterns) and extrinsic factors (agricultural management practices). However, the main factors causing nutrient variation was agricultural management practices.

Acknowledgements. This research was supported by the National Natural Science Foundation (grant number 42071240) and Analysis of the Evolution of Spatial and Temporal Patterns of Arable Land in the Northern Weibei Dry Plateau Area and its Driving Forces (DJNY2022-36).

REFERENCES

[1] Aghasi, B., Jalalian, A., Khademi, H., Toomanian, N. (2017): Sub-basin scale spatial variability of soil properties in Central Iran. – Arabian Journal of Geosciences 10. https://doi.org/10.1007/s12517-017-2921-4.

[2] Agricultural Chemistry Committee of China (1983): Conventional Methods of Soil and Agricultural Chemistry Analysis. – Science Press, Beijing (in Chinese).

[3] Awais, M., Arshad, M., Shah, S. H. H., Anwar-ul-Haq, M. (2017): Evaluating groundwater quality for irrigated agriculture: spatio-temporal investigations using GIS and geostatistics in Punjab, Pakistan. – Arabian Journal of Geosciences 10. https://doi.org/10.1007/s12517-017-3280-x.

[4] Balaguer-Beser, A., Ruiz, L. A., Hermosilla, T., Recio, J. A. (2013): Using semivariogram indices to analyse heterogeneity in spatial patterns in remotely sensed images. – Computers & Geosciences 50: 115-127. https://doi.org/10.1016/j.cageo.2012.08.001.

[5] Blanchet, G., Libohova, Z., Joost, S., Rossier, N., Schneider, A., Jeangros, B., Sinaj, S. (2017): Spatial variability of potassium in agricultural soils of the canton of Fribourg, Switzerland. – Geoderma 290: 107-121. https://doi.org/10.1016/j.geoderma.2016.12.002.

[6] Chen, T., Chang, Q., Liu, J., Clevers JGPW (2016): Spatio-temporal variability of farmland soil organic matter and total nitrogen in the southern Loess Plateau, China: a case study in Heyang County. – Environmental Earth Sciences 75. https://doi.org/10.1007/s12665-015-4786-8.

[7] Chen, Z., Wang, L., Wei, A., Gao, J., Lu, Y., Zhou, J. (2019): Land-use change from arable lands to orchards reduced soil erosion and increased nutrient loss in a small catchment. – Science of the Total Environment 648: 1097-1104. https://doi.org/10.1016/j.scitotenv.2018.08.141.

http://www.aloki.hu ● ISSN 1589 1623 (Print) ● ISSN 1785 0037 (Online)
DOI: http://dx.doi.org/10.15666/aeer/2005_38533872

[8] Chuai, X. W., Huang, X. J., Wang, W. J., Zhang, M., Lai, L., Liao, Q. L. (2012): Spatial variability of soil organic carbon and related factors in Jiangsu Province, China. – Pedosphere 22: 404-414. https://doi.org/10.1016/s1002-0160(12)60026-5.

[9] Darand, M., Dostkamyan, M., Rehmanic, M. I. A. (2017): Spatial autocorrelation analysis of extreme precipitation in Iran. – Russian Meteorology and Hydrology 42: 415-424. https://doi.org/10.3103/s1068373917060073.

[10] Duan, L. X., Li, Z. W., Xie, H. X., Li, Z. M., Zhang, L., Zhou, Q. (2020): Large-scale spatial variability of eight soil chemical properties within paddy fields. – Catena 188. https://doi.org/10.1016/j.catena.2019.104350.

[11] Foroughifar, H., Jafarzadeh, A. A., Torabi, H., Pakpour, A., Miransari, M. (2013): Using geostatistics and geographic information system techniques to characterize spatial variability of soil properties, including micronutrients. – Communications in Soil Science and Plant Analysis 44: 1273-1281. https://doi.org/10.1080/00103624.2012.758279.

[12] Gelaw, A. M., Singh, B. R., Lal, R. (2014): Soil organic carbon and total nitrogen stocks under different land uses in a semi-arid watershed in Tigray, Northern Ethiopia. – Agric. Ecosyst. Environ. 188(15): 256-263. https://doi.org/10.1016/j.agee.2014.02.035.

[13] Guan, Y., Zhou, W., Bai, Z., Cao, Y., Huang, Y., Huang, H. (2020): Soil nutrient variations among different land use types after reclamation in the Pingshuo opencast coal mine on the Loess Plateau, China. – Catena 188. https://doi.org/10.1016/j.catena.2019.104427.

[14] Guo, X. D., Fu, B. J., Ma, K. M., Chen, L. D., Wang, J. (2001): Spatio-temporal variability of soil nutrients in the Zunhua Plain, Northern China. – Physical Geography 22: 343-360. https://doi.org/10.1080/02723646.2001.10642748.

[15] Hoffmann, U., Hoffmann, T., Jurasinski, G., Glatzel, S., Kuhn, N. J. (2014): Assessing the spatial variability of soil organic carbon stocks in an alpine setting (Grindelwald, Swiss Alps). – Geoderma 232: 270-283. https://doi.org/10.1016/j.geoderma.2014.04.038.

[16] Hu, K. L., Wang, S. Y., Li, H., Huang, F., Li, B. G. (2014): Spatial scaling effects on variability of soil organic matter and total nitrogen in suburban Beijing. – Geoderma 226: 54-63. https://doi.org/10.1016/j.geoderma.2014.03.001.

[17] Huang, Y. L., Chen, L. D., Fu, B. J., Huang, Z. L., Gong, J., Lu, X. X. (2012): Effect of land use and topography on spatial variability of soil moisture in a gully catchment of the Loess Plateau, China. – Ecohydrology 5: 826-833. https://doi.org/10.1002/eco.273.

[18] Keskinen, R., Nyambura, M., Heikkinen, J., Sila, A., Eurola, M., Towett, E., Shepherd, K., Esala, M. (2019): Readily available concentrations of selected micronutrients and harmful metals in soils of Sub-Saharan Africa. – Geoderma 347: 203-209. https://doi.org/10.1016/j.geoderma.2019.04.014.

[19] Kong, X., Zhang, F., Wei, Q., Xu, Y., Hui, J. (2006): Influence of land use change on soil nutrients in an intensive agricultural region of North China. – Soil & Tillage Research 88: 85-94. https://doi.org/10.1016/j.still.2005.04.010.

[20] Liao, K. H., Lai, X. M., Zhou, Z. W., Zhu, Q. (2017): Applying fractal analysis to detect spatio-temporal variability of soil moisture content on two contrasting land use hillslopes. – Catena 157: 163-172. https://doi.org/10.1016/j.catena.2017.05.022.

[21] Liu, X. M., Xu, J. M., Zhang, M. K., Zhou, B. (2004): Effects of land management change on spatial variability of organic matter and nutrients in paddy field: a case study of Pinghu, China. – Environmental Management 34: 691-700. https://doi.org/10.1007/s00267-004-0053-6.

[22] Liu, X. M., Zhang, W. W., Zhang, M. H., Ficklin, D. L., Wang, F. (2009): Spatio-temporal variations of soil nutrients influenced by an altered land tenure system in China. – Geoderma 152: 23-34. https://doi.org/10.1016/j.geoderma.2009.05.022.

[23] Liu, Q., Xie, W. J., Xia, J. B. (2013): Using semivariogram and Moran's i techniques to evaluate spatial distribution of soil micronutrients. – Communications in Soil Science and Plant Analysis 44: 1182-1192. https://doi.org/10.1080/00103624.2012.755999.

http://www.aloki.hu ● ISSN 1589 1623 (Print) ● ISSN 1785 0037 (Online)
DOI: http://dx.doi.org/10.15666/aeer/2005_38533872

[24] Liu, L.-L., Zhu, Y., Liu. X.-J., Cao W.-X., Xu, M., Wang, X.-K., Wang, E.-L. (2014a): Spatiotemporal changes in soil nutrients: a case study in Taihu region of China. – Journal of Integrative Agriculture 13. https://doi.org/10.1016/s2095-3119(13)60528-6.

[25] Liu, Z. J., Zhou, W., Shen, J. B., He, P., Lei, Q. L., Liang, G. Q. (2014b): A simple assessment on spatial variability of rice yield and selected soil chemical properties of paddy fields in South China. – Geoderma 235: 39-47. https://doi.org/10.1016/j.geoderma.2014.06.027.

[26] Lu, Y., Chen, Z., Kang, T., Zhang, X., Bellarby, J., Zhou, J. (2016): Land-use changes from arable crop to kiwi-orchard increased nutrient surpluses and accumulation in soils. – Agriculture Ecosystems & Environment 223: 270-277. https://doi.org/10.1016/j.agee.2016.03.019.

[27] Ma, J. C., He, P., Xu, X. P., He, W. T., Liu, Y. X., Yang, F. Q., Chen, F., Li, S. T., Tu, S. H., Jin, J. Y., Johnston, A. M., Zhou, W. (2016a): Temporal and spatial changes in soil available phosphorus in China (1990-2012). – Field Crops Research 192: 13-20. https://doi.org/10.1016/j.fcr.2016.04.006.

[28] Ma, K., Zhang, Y., Tang, S., Liu, J. (2016b): Spatial distribution of soil organic carbon in the Zoige alpine wetland, northeastern Qinghai-Tibet Plateau. – Catena 144: 102-108. https://doi.org/10.1016/j.catena.2016.05.014.

[29] Martin, M. P., Orton, T. G., Lacarce, E., Meersmans, J., Saby, N. P. A., Paroissien, J. B., Jolivet, C., Boulonne, L., Arrouays, D. (2014): Evaluation of modelling approaches for predicting the spatial distribution of soil organic carbon stocks at the national scale. – Geoderma 223-225(1): 97-107. https://doi.org/10.1016/j.geoderma.2014.01.005.

[30] Onyejekwe, S., Kang, X., Ge, L. (2016): Evaluation of the scale of fluctuation of geotechnical parameters by autocorrelation function and semivariogram function. – Engineering Geology 214: 43-49. https://doi.org/10.1016/j.enggeo.2016.09.014.

[31] Osat, M., Heidari, A., Karimian Eghbal, M., Mahmoodi, S. (2016): Spatial variability of soil development indices and their compatibility with soil taxonomic classes in a hilly landscape: a case study at Bandar village, Northern Iran. – Journal of Mountain Science 13: 1746-1759. https://doi.org/10.1007/s11629-016-3952-0.

[32] Schlegel, A. J., Assefa, Y., Bond, H. D., Haag, L. A., Stone, L. R. (2017): Changes in soil nutrients after 10 years of cattle manure and swine effluent application. – Soil & Tillage Research 172: 48-58. https://doi.org/10.1016/j.still.2017.05.004.

[33] Shaanxi Provincial Bureau of Statistics (1980-2017): Statistical Yearbook of Baishui. – China Statistics Press, Beijing (in Chinese).

[34] Wang, Y. Q., Zhang, X. C., Zhang, J. L., Li, S. J. (2009): Spatial Variability of soil organic carbon in a watershed on the Loess Plateau. – Pedosphere 19: 486-495. https://doi.org/10.1016/s1002-0160(09)60141-7.

[35] Wang, Z., Liu, G. B., Xu, M. X., Zhang, J., Wang, Y., Tang, L. (2012): Temporal and spatial variations in soil organic carbon sequestration following revegetation in the hilly Loess Plateau, China. – Catena 99: 26-33. https://doi.org/10.1016/j.catena.2012.07.003.

[36] Wei, J. B., Xiao, D. N., Zeng, H., Fu, Y. K. (2008): Spatial variability of soil properties in relation to land use and topography in a typical small watershed of the black soil region, northeastern China. – Environmental Geology 53: 1663-1672. https://doi.org/10.1007/s00254-007-0773-z.

[37] Weihrauch, C., Opp, C. (2018): Ecologically relevant phosphorus pools in soils and their dynamics: the story so far. – Geoderma 325: 183-194. https://doi.org/10.1016/j.geoderma.2018.02.047.

[38] Xin, Z. B., Qin, Y. B., Yu, X. X. (2016): Spatial variability in soil organic carbon and its influencing factors in a hilly watershed of the Loess Plateau, China. – Catena 137: 660-669.https://doi.org/10.1016/j.catena.2015.01.028.

[39] Xu, X., Zhang, H., Zhang, O. (2004): Development of check-dam systems in gullies on the Loess Plateau, China. – Environ Sci Policy 7: 79-86. https://doi.org/10.1016/j.envsci.2003.12.002.

http://www.aloki.hu ● ISSN 1589 1623 (Print) ● ISSN 1785 0037 (Online)
DOI: http://dx.doi.org/10.15666/aeer/2005_38533872

[40] Yan, P., Peng, H., Yan, L. B., Zhang, S. Y., Chen, A. M., Lin, K. R. (2019): Spatial variability in soil pH and land use as the main influential factor in the red beds of the Nanxiong Basin, China. – Peerj 7. https://doi.org/10.7717/peerj.6342.
[41] Yu, C., Pang, X. P., Wang, Q., Jin, S. H., Shu, C. C., Guo, Z. G. (2017): Soil nutrient changes induced by the presence and intensity of plateaupika (Ochotona curzoniae) disturbances in the Qinghai-Tibet Plateau, China. – Ecological Engineering 106: 1-9. https://doi.org/10.1016/j.ecoleng.2017.05.029.
[42] Zhu, M., Feng, Q., Qin, Y., Cao, J., Zhang, M., Liu, W., Deo, R. C., Zhang, C., Li, R., Li, B. (2019): The role of topography in shaping the spatial patterns of soil organic carbon. – Catena 176: 296-305. https://doi.org/10.1016/j.catena.2019.01.029.
[43] Zhuo, Z. Q., Xing, A., Li, Y., Huang, Y. F., Nie, C. J. (2019): Spatio-temporal variability and the factors influencing soil-available heavy metal micronutrients in different agricultural sub-catchments. – Sustainability 11. https://doi.org/10.3390/su11215912.

APPENDIX

Table A1. *Statistical table of SOM in three periods*

SOM ($g\ kg^{-1}$)	1980		2007		2020	
	Area (km^2)	Percentage (%)	Area (km^2)	Percentage (%)	Area (km^2)	Percentage (%)
< 10	144.64	27.53	4.27	0.8	-	-
10-11.5	236.81	45.06	102.54	19.51	-	-
11.5-13	135.02	25.69	190.59	36.27	78.98	15.03
13-14.5	9.02	1.72	105.69	20.11	180.61	34.37
14.5-16	-	-	102.57	19.52	105.04	19.99
> 16	-	-	19.83	3.77	160.86	30.61

SOM: soil organic matter

Table A2. *Statistical table of total nitrogen content in three periods*

STN ($g\ kg^{-1}$)	1980		2007		2020	
	Area (km^2)	Percentage (%)	Area (km^2)	Percentage (%)	Area (km^2)	Percentage (%)
< 0.55	15.74	3.00	22.60	4.30	-	-
0.55-0.6	201.05	38.26	158.49	30.16	5.90	1.10
0.6-0.65	228.90	43.56	124.34	23.66	128.66	24.03
0.65-0.7	79.80	15.19	71.54	13.61	151.34	28.26
0.7-0.75	-	-	93.58	17.81	74.23	13.86
> 0.75	-	-	54.96	10.46	165.37	30.88

Table A3. *Area and percentage of soils with increased SOM and STN contents between 1980 and 2007*

Variables and item	Different categories of content increase (%)					
	<-15	-15-0	0-15	15-30	30-45	>45
SOM						
Area (km^2)	-	26.42	157.56	218.32	98.98	24.21
Percentage (%)	-	5.03	29.98	41.55	18.84	4.61
STN						
Area (km^2)	8.22	155.42	234.12	117.13	10.61	-
Percentage (%)	1.56	29.58	44.55	22.29	2.02	-

SOM: soil organic matter; STN: soil total nitrogen

http://www.aloki.hu ● ISSN 1589 1623 (Print) ● ISSN 1785 0037 (Online)
DOI: http://dx.doi.org/10.15666/aeer/2005_38533872

Table A4. *Area and percentage of soils with increased SOM and STN contents between 2007 and 2020*

Variables and item	Different categories of content increase (%)					
	<-15	**-15-0**	**0-15**	**15-30**	**30-45**	**>45**
SOM						
Area (km^2)		43.28	150.73	267.18	53.02	11.29
Percentage (%)		8.24	28.68	50.84	10.09	2.15
STN						
Area (km^2)		75.79	248.36	170.71	23.87	6.75
Percentage (%)		14.42	47.26	32.49	4.54	1.28

SOM: soil organic matter; STN: soil total nitrogen

http://www.aloki.hu ● ISSN 1589 1623 (Print) ● ISSN 1785 0037 (Online)
DOI: http://dx.doi.org/10.15666/aeer/2005_38533872

RELATIONSHIP OF CHANGES IN THE STEM AND LEAF MORPHOLOGY, NUTRIENT AND ENDOGENOUS HORMONE CONTENTS AND FLOWER BUD NUMBER OF *POPULUS EUPHRATICA* OLIV.

GUO, X. F.[1,2,3] – ZHAI, J. T.[1,2,3] – ZHANG, S. H.[1] – LI, Z. J.[1,2,3*]

[1]*Key Laboratory of Protection and Utilization of Biological Resources in Tarim Basin Xinjiang Production and Construction Corps, Alar, Xinjiang 843300, China*

[2]*Desert Poplar Research Center of Tarim University, Alar, Xinjiang 843300, China*

[3]*College of Life Science, Tarim University, Alar, Xinjiang 843300, China*

[*]*Corresponding author*
e-mail: lizhijun0202@126.com; phone: +86-997-468-1202

(Received 12th Nov 2021; accepted 11th Jul 2022)

Abstract. During *Populus euphratica* ontogeny, the morphological changes of stems and leaves, nutrient and endogenous hormone contents were significantly different, but the relationship between these changes and the number of flower buds was not clear. We counted the number of *P. euphratica* flower buds, and measured the morphological of the stems and leaves nutrient and endogenous hormone contents at different ontogeny to clarify the change trends in the morphology and nutrient and endogenous hormone contents of stems and leaves and mutual relationships in the flower bud number throughout the ontogeny. The results showed that in diameter 4, flower buds and broad-ovate leaves appeared meanwhile, indicating that *P. euphratica* had entered the reproductive growth stage. Between diameter 4 to 12, stem length, leaf number and leaf C/N gradually decreased, and leaf area, leaf nitrogen, organic carbon, and ZR contents gradually increased, indicating diameters 4-12 represent the stage during which vegetative growth and reproductive growth cooccur in *P. euphratica*. In diameter 14, flower bud number increased significantly, while leaf shape index and stem diameter decreased. *P. euphratica* began to enter the vigorous reproductive growth stage. In addition, correlations were found between leaf and stem nitrogen, phosphorus, organic carbon, GA_3, ABA, IAA contents, leaf C/N and leave and stem morphology was closely related to the ontogeny; the change in coordination significantly affected the flower bud number. The synergistic changes in the nutrient and endogenous hormone contents in *P. euphratica* stems and leaves regulate the morphology of stems and leaves and flower bud number and directly or indirectly aaffect the transition from vegetative growth to reproductive growth.
Keywords: *leaf shape index, nitrogen, organic carbon, ABA, phase change*

Introduction

The transition from vegetative growth to reproductive growth is marked by flower bud differentiation; initiation of flowering is the standard for dividing juvenile from adult (Guo et al., 2008; Hao et al., 2017). The morphology of stems and leaves can also be used to measure the growth and development of trees (Besford et al., 1996; Zhang et al., 1997; Jin et al., 1998; Du et al., 2018). Research shows that petiole roughness and the leaf shape index have been considered for use as markers of the juvenile stage in peach trees (Zhang et al., 1997). *Malus hupehensis* leaves in the juvenile stage have deep cracks and straight lateral veins; in the adult stage, the leaf crack disappears, and the lateral veins become pliable and parabolic (Jin et al., 1998). In the model plant *Arabidopsis thaliana*, the shift to maturity is marked by a decrease in leaf hairs on the leaf blade after a certain age. The development of early flowers is often accompanied by

http://www.aloki.hu ● ISSN 1589 1623 (Print) ● ISSN1785 0037 (Online)
DOI: http://dx.doi.org/10.15666/aeer/2005_38733891

a reduction in leaf hairs (Besford et al., 1996). During this transition, the nutrient and hormone content of leaves and stems also changed significantly. Xu et al. (2018) measured the nutrient contents in overwintering stems of *Styrax tonkinensis* Craib ex Hartw. and established a relationship between nutrient levels and blossom number. The results showed that a high carbohydrate content was beneficial to the flowering of *Styrax tonkinensis* Craib ex Hartw. Changes in the contents and equilibrium values of endogenous hormones such as gibberellin (GA_3), indole acetic acid (IAA), abscisic acid (ABA) and zeatin (ZR) regulate the amount of flowering on each branch and the stage transitions of trees (Munoz et al., 2012; Gao et al., 2012; Feng et al., 2014; Zhu et al., 2015; Hassankhah et al., 2018; Yu et al., 2019). GA increased the number of flowers per branch and significantly changed the vegetative branch to flowering branch ratio in the next year (Munoz et al., 2012; Hassankhah et al., 2018).

P. euphratica exhibits heteromorphism, showing only strip leaves in the seedling stage, followed by lanceolate ovate and broad-ovate leaves that gradually appear with ontogeny (Li et al., 2021). Previous studies have shown that there is a certain relationship between leaf morphology and flowering of *P. euphratica* (Huang et al., 2010a,b). The appearance of broad-ovoid leaves, stems length, leaves number, total nitrogen content in leaves, stems and leaves C/N ratio and ZR content in leaves could be used as indicators of the transition from juvenile to the adult stage of *P. euphratica* (Li et al., 2015b). Feng et al. (2014) showed that the total N content of *P. euphratica* varied with the location and growth stage of leaves, and the leaf shape index decreased with the increase of total N content. Li et al. (2017) showed that the leaf shape index of *P. euphratica* decreased gradually from the bottom to the top of the crown, and the broad-ovoid leaves were mostly distributed at the top of the crown, while GA_3 content showed a significant positive correlation with the leaf shape index, indicating that GA_3 content was closely related to the emergence of broad-ovoid leaves. Most studies showed that there was a certain correlation between the morphological and nutrients and endogenous hormone contents in stems and leaves. But the relationship between the morphological, nutrients, endogenous hormones contents in stems and leaves and the number of flower buds was not clear.

This study hypothesized that there was a correlation between leaf morphology, nutrient and endogenous hormone content and the number of flower buds. At the different stages of the investigation, individual stems of *P. euphratica* were assessed for their flower bud number, stem and leaf morphological characteristics, stem and leaf nutrients and endogenous hormone contents. The changes in stem and leaf morphology as well as in flower bud number and nutrient and endogenous hormone contents with tree development and their mutual relationships were analyzed to reveal the roles of the morphological and physiological characteristics of the stems and leaves of *P. euphratica* in the reproductive growth.

Materials and methods

Study site, plant material and experimental design

The study area is located on the northwest edge of the Tarim Basin, Alar, Xinjiang, China (81°17′56.52″E，40°32′36.90″N). The area of the artificial *P. euphratica* forest was 180.6 hectares, the spacing of plants and rows was 1.20 m×4.20 m, and the average tree height was 6.41 m. The forest included 355 strains of *P. euphratica* in different

http://www.aloki.hu ● ISSN 1589 1623 (Print) ● ISSN1785 0037 (Online)
DOI: http://dx.doi.org/10.15666/aeer/2005_38733891

stages of development (different ages). This region experiences hot, dry weather and little rainfall throughout the year. The average temperature is 10.8°C, the average annual precipitation is 50 mm, and the potential evaporation is 1900 mm, with average annual sunshine hours of 2900 h, making it a typical temperate desert climate.

In the area of the artificial *P. euphratica* forest located on the northwest edge of the Tarim Basin, Xinjiang, China (81°17′56.52″E，40°32′36.90″N), all *Populus euphratica* trees with DBHs above 2 cm were investigated. The mean DBH (diameter at breast height, D) and mean age (A) of each class diameter of *Populus euphratica* fit the following relationship: $A = 13.679 / (1 + 3.3476 \times \exp(-0.2099 D))$ (Gu et al., 2013). The trees were sorted into age diameters as determined by their diameter. The DBH of each plant was rounded to the nearest 2 cm, and nine class diameters were established: 2, 4, 6, 8, 10, 12, 14, 16 and 18 cm. A total of 27 *P. euphratica* plants were selected from the 2 cm diameter to the 18 cm diameter, with 3 plants in each diameter taken for sampling; of these, 21 were flowering plants, sampling at year level (*Table 1*).

Table 1. *Distribution of diameter class, DBH and age*

Diameter class	2	4	6	8	10	12	14	16	18
Average DBH	2.44	3.99	5.95	7.85	9.79	11.99	14.08	15.66	17.40
Average age	4.13	5.20	6.48	7.72	8.65	10.33	10.52	11.63	11.33

The crown of the sample tree is divided into 5 layers from base to top. One-year-old stems were randomly selected from each layer from the east, south, west and north directions, and 20 stems were collected from each sample tree. All leaves from the base to the end of each stem were taken as the sample leaves. The collected stems were brought back to the laboratory, and the number of leaves and flowers per stem were counted. All nodal leaves from the base to the end of each stem were selected for stem and leaf morphological measurement and nutrient and endogenous hormone content measurement.

Determination of morphological indicators of flower buds, stems and leaves

Leaves (with petioles) were taken from the same stem and arranged in the order in which they grew on the stem. The stems, leaves and flower buds were scanned by an MRS-9600TFU2 scanner (made in Microtek). The measurements of stems (length and roughness) and leaves (leaf length, leaf width, leaf area, petiole length and leaf perimeter) were obtained by an LA-S plant image analyzer (made in Hangzhou wseen), and the leaf shape index (length/width) was calculated, the leaf shape index larger, the leaf shape tends to be round.

Determination of nutrient contents of flower buds, stems and leaves

All the stems of the same grade were combined, and all the leaves taken from the stems of each grade were combined. The mixed samples were rinsed with tap water and then rinsed with deionized water twice. They were dried in the shade and then placed in an oven. The samples were subjected to enzymolysis at 105°C for 10 min and then dried to a constant weight at 65°C. After the dried samples were removed from the oven, they were quickly ground through a 100-mesh sieve with a plant grinder for the determination of their total nitrogen, total phosphorus, total potassium and organic

http://www.aloki.hu ● ISSN 1589 1623 (Print) ● ISSN1785 0037 (Online)
DOI: http://dx.doi.org/10.15666/aeer/2005_38733891

carbon contents. The total nitrogen content was determined by the Kjeldahl method. The total phosphorus content was determined by the molybdenum antimony colorimetric method. The total potassium content was determined by ammonium acetate extraction-flame photometry. The low-temperature external thermal potassium dichromate oxidation method determined the organic carbon content.

Determination of the endogenous hormone contents of flower buds, stems and leaves

All the stems of the same grade were combined, and all the leaves taken from the stems of each grade were combined. And in the day, approximately 0.2 g of the fresh mixed sample was weighed, quickly frozen with liquid nitrogen and stored in an ultralow-temperature refrigerator at -80°C for later use. The contents of indole acetic acid (IAA), zeatin (ZR), gibberellin (GA_3) and abscisic acid (ABA) were determined by an enzyme-linked immunosorbent assay. This part of the testing work was performed by China Agricultural University.

Statistical analyses

SPSS 25.0 was used to perform one-way ANOVA, correlation analysis, path analysis and stepwise regression analysis. The differences in leaf morphology, nutrient and endogenous hormone content and number of flower buds among different class diameters were analyzed, and the factors that had direct or indirect influences on the morphology of stems and leaves and the number of flower buds were identified. And differences were considered significant at $\alpha = 0.05$ by Tukey's test.

Results

The morphology of stems and leaves and the flower bud number changed with developmental stage

With increasing class diameter, the leaf shape index, stem length and leaf number (*Figure 1b*) gradually decreased, while the stem diameter, flower bud number, leaf area, leaf perimeter (*Figure 1f*) and petiole length gradually increased (*Figure 1a-h*). From 4 diameter, flower buds and broad ovate leaves appeared at the same time, and stems became significantly shorter, indicating that *P. euphratica* individuals began to enter reproductive growth (*Figure S1*). From 4 diameter to 12 diameter, flower buds number gradually increased, the differences were not significant (*Figure 1a*). While the leaf shape index gradually decreased (*Figure 1d*), stems became thicker (*Figure 1g*), leaf area (*Figure 1c*), petiole length (*Figure 1e*) and leaf length (*Figure 1h*) increased, and it was a significant difference. When the flower buds number increased significantly to 1.36, *P. euphratica* individuals entered the vigorous reproductive growth stage and stems reached the thickest state, 0.42 cm.

Characteristic changes in stem and leaf nutrient contents with developmental stage

As shown in *Figure 2a-j*, with increasing class diameter, the contents of total nitrogen, phosphorus, potassium (*Figure 2e,f*) and organic carbon in stems and leaves increased gradually, while the C/N ratio of stems and leaves decreased gradually. The results showed that the total nitrogen content of leaves (*Figure 2b*) and the organic carbon content of stems (*Figure 2g*) increased significantly, and the C/N ratio of stems and leaves (*Figure 2i,j*) decreased significantly when flower buds appeared at the

http://www.aloki.hu ● ISSN 1589 1623 (Print) ● ISSN1785 0037 (Online)
DOI: http://dx.doi.org/10.15666/aeer/2005_38733891

beginning of 4 diameter. From 4 to 12 diameter, the number of flower buds gradually increased (*Figure 1a*), the leaf shape index gradually decreased (*Figure 1d*), the leaf area gradually increased (*Figure 1c*), and the stems became thicker and shorter (*Figure 1g,h*), and the total nitrogen contents in stems and leaves (*Figure 2a,b*), total phosphorus in stems and leaf (*Figure 2c,d*) organic carbon (*Figure 2g,h*) gradually increased, the C/N ratio of stems and leaves (*Figure 2i,j*) unchanged, and the differences were not significant. When the flower buds' number of 14 diameter increased significantly, the total nitrogen content and total phosphorus content of leaves also increased significantly and reached the maximum value of 1.38%, 0.62%, 46.20% and 39.77%, respectively.

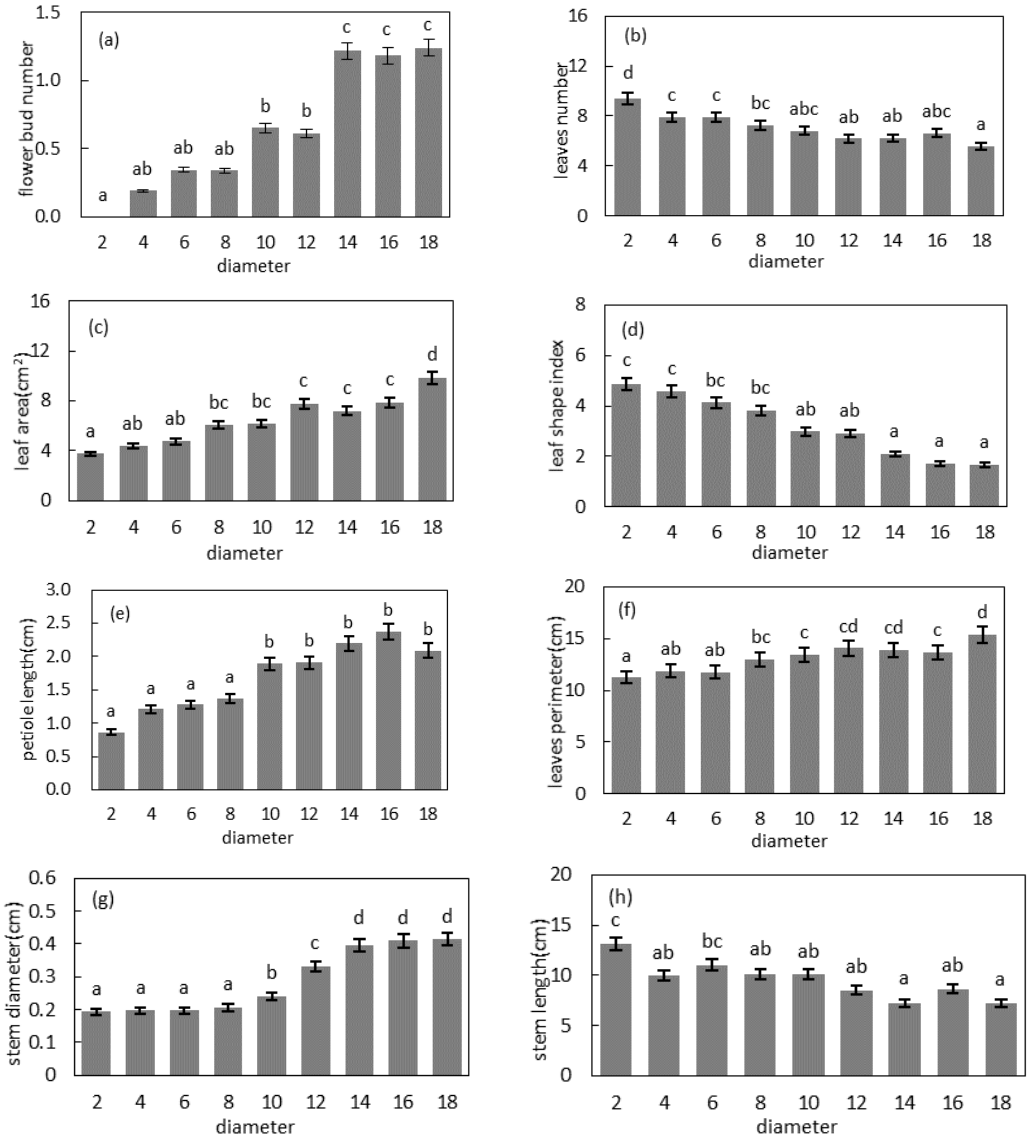

Figure 1. *Variation of leaf and stem morphology and flower bud number with ontogenetic stage of Populus euphratica. (a) flower bud number, (b) leaves number, (c) leaf area, (d) leaf shape index, (e) petiole length, (f) leaves perimeter, (g) stem diameter, (h) stem length, Different lowercase letters indicate significant, according to Tukey's test after one-way ANOVA at a significance level of $P < 0.05$, the bar chart represents the mean, the error line represents ± standard deviation*

http://www.aloki.hu ● ISSN 1589 1623 (Print) ● ISSN1785 0037 (Online)
DOI: http://dx.doi.org/10.15666/aeer/2005_38733891

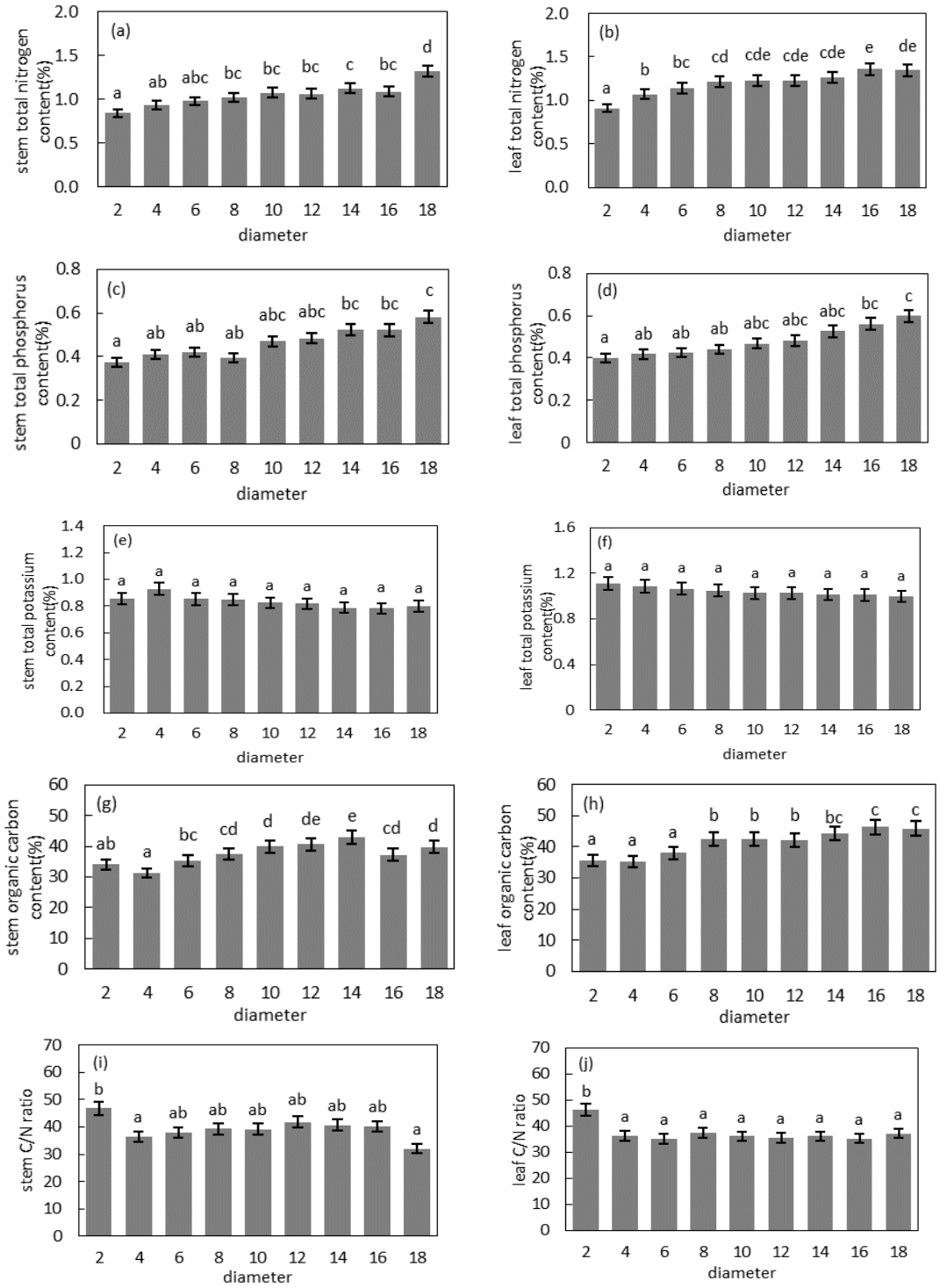

Figure 2. *Variation of leaf and stem nutrient content with individual development stages of Populus euphratica. (a) stem total nitrogen content, (b) leaf total nitrogen content, (c) stem total phosphorus content, (d) leaf total phosphorus content, (e) stem total potassium content, (f) leaf total potassium content, (g) stem organic carbon content, (h) leaf organic carbon content, (i) stem C/N ratio, (j) leaf C/N ratio, Different lowercase letters indicate significant, according to Tukey's test after one-way ANOVA at a significance level of $P < 0.05$, the bar chart represents the mean, the error line represents ± standard deviation*

http://www.aloki.hu ● ISSN 1589 1623 (Print) ● ISSN1785 0037 (Online)
DOI: http://dx.doi.org/10.15666/aeer/2005_38733891

Characteristic changes in stem and leaf endogenous hormone content with developmental stage

The contents of endogenous hormones in the stems and leaves changed among the different class diameters. The analysis showed that the content of GA_3 in stems (*Figure 3c*) and the contents of GA_3 and IAA in leaves (*Figure 3b,d*) decreased with increasing class diameter, while the content of ABA in stems (*Figure 3e*) increased with increasing class diameter. The contents of IAA and ZR in stems (*Figure 3a,g*) first decreased and then increased with the increasing class diameter, and the content of ZR in leaves (*Figure 3h*) first increased and then decreased with increasing class diameter (*Figure 3a-h*). However, ZR content in leaves (*Figure 3h*) increased significantly with the appearance of 4 diameter flower buds, while 4-12 diameter flower buds gradually increased (*Figure 1a*), leaf shape index gradually decreased (*Figure 1d*), leaf area gradually increased (*Figure 1c*), stems became thicker and shorter (*Figure 1g,h*), and the contents of GA_3, IAA and ABA in stems (*Figure 3c,a,e*) decreased significantly. ZR content in leaves (*Figure 3h*) decreased significantly when the number of 14 diameter flower buds increased significantly.

Correlation analysis of leaf morphology, nutrient and endogenous hormone content with DBH and flower buds number

Correlation analysis showed (*Tables 2, 3*) that the morphology of stems and leaves, nutrient and endogenous hormone content was closely related to DBH (diameter at breast height) of *P. euphratica*. The leaf number, leaf shape index and stem length were negatively correlated with DBH of *P. euphratica*. Leaf area, petiole length, leaf circumference, stem diameter, flower buds number, total nitrogen, total phosphorus and organic carbon in stems and leaves were positively correlated with DBH of *P. euphratica*. There was a significant positive correlation between leaf ZR and DBH of *P. euphratica*, and a significant negative correlation between stem ABA and DBH of *P. euphratica*.

Correlation analysis showed (*Table 4*) that morphological nutrients and endogenous hormone contents of stems and leaves were closely related to the number of flower buds. However, there was a significant negative correlation between leaves number, leaf shape index, stem length and flower bud number, leaf area, leaf perimeter, petiole length and stem diameter were positively correlated with the number of flower buds, suggesting that the increase of leaf area, leaf perimeter, petiole length, stem diameter and the decrease of leaf number, leaf shape index and stem length were phenotypic characteristics of the increase of flower bud number. The contents of total nitrogen, total phosphorus and organic carbon in stems and leaves were positively correlated with the flower buds number, while the C/N ratio in leaves was negatively correlated with the flower buds number. The total nitrogen content and organic carbon content in stems and leaves increased with the growth of *P. euphratica* and the decrease of leaf C/N ratio promoted the increase of flower bud quantity. The results showed that total nitrogen in stems and leaves, organic carbon content and leaf C/N ratio synergistically promoted the reproductive growth of *P. euphratica*. There was a significant negative correlation between ABA and the number of flower buds, and a significant positive correlation between ZR and the number of flower buds. The results showed that the decrease of ABA content in stems and the increase of ZR content in leaves with the ontogeny of *P. euphratica* promoted the increase of the number of flower buds and the reproductive

http://www.aloki.hu ● ISSN 1589 1623 (Print) ● ISSN1785 0037 (Online)
DOI: http://dx.doi.org/10.15666/aeer/2005_38733891

growth of *P. euphratica*. Four endogenous hormones played a synergistic role in the reproductive growth of *P. euphratica*.

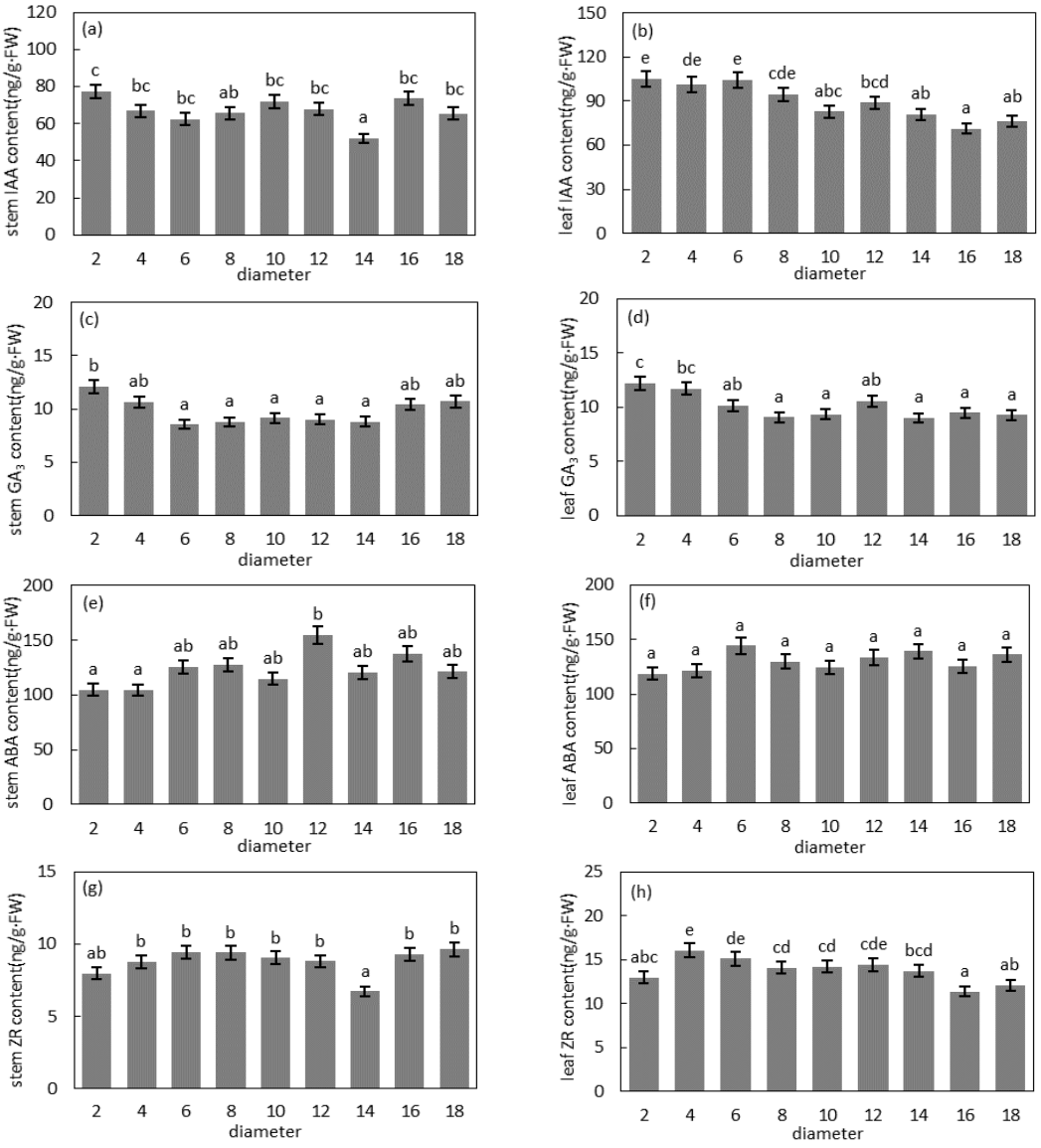

Figure 3. *Variation of leaf and stem endogenous hormone content with individual development stages of Populus euphratica. (a) stem IAA content, (b) leaf IAA content, (c) stem GA_3 content, (d) leaf GA_3 content, (e) stem ABA content, (f) leaf ABA content, (g) stem ZR content, (h) leaf ZR content, Different lowercase letters indicate significant, according to Tukey's test after one-way ANOVA at a significance level of $P < 0.05$, the bar chart represents the mean, the error line represents ± standard deviation*

Main factors affecting stem and leaf morphology and flower bud number

There was a certain correlation between the flower bud number and the morphology, nutrient contents, and endogenous hormone contents of stems and leaves. To screen for the factors that had a significant effect on the flower bud number, path analysis was conducted on the morphology, nutrient contents, and endogenous hormone contents of

http://www.aloki.hu ● ISSN 1589 1623 (Print) ● ISSN1785 0037 (Online)
DOI: http://dx.doi.org/10.15666/aeer/2005_38733891

stems and leaves and the flower bud number (*Table S1*). The results showed that the magnitude of the direct effects of the different factors on the flower bud number could be ranked as follows: stem total nitrogen >leaf total nitrogen >leaf number >leaf organic carbon >leaf ABA >stem length >leaf C/N ratio >stem total phosphorus >leaf total phosphorus >petiole length >leaf area >leaf perimeter >stem diameter >leaf ZR >leaf shape index > stem C/N ratio >stem total potassium >stem ABA >leaf total potassium >leaf GA_3 >stem ZR >stem organic carbon >leaves IAA >stem IAA >stem GA_3. Among them, the contents of endogenous hormones and nutrients in stems and leaves also indirectly affected the number of flower buds by affecting the morphology of stems and leaves.

Table 2. *Pearson correlated with the stem and leaf morphology and diameter of Populus euphratica*

Coefficient of association	DBH	leaves number	leaf shape index	leaf area	petiole length	leaves perimeter	stem length	stem diameter
DBH	1							
crown height	0.95**							
leaves number	-0.66**	1						
leaf shape index	-0.81**	0.57**	1					
leaf area	0.75**	-0.57**	-0.82**	1				
petiole length	0.62**	-0.30**	-0.48**	0.44**	1			
leaves perimeter	0.55**	-0.34**	-0.45**	0.47**	0.51**	1		
stem length	-0.61**	0.65**	0.48**	-0.49**	-0.28*	-0.40**	1	
stem diameter	0.92**	-0.60**	-0.79**	0.73**	0.53**	0.50**	-0.67**	1

The asterisks $^{**}P < 0.01$; $^{*}P < 0.05$

Table 3. *Pearson correlated with the stem and leaf nutrient, endogenous hormones content and diameter of Populus euphratica*

Coefficient of association	**DBH**	**Coefficient of association**	**DBH**	**Coefficient of association**	**DBH**
leaf N	0.73**	stem P	0.41**	stem ZR	-0.08
leaf P	0.50**	stem K	-0.05	stem ABA	-0.37*
leaf K	-0.27	stem Organic carbon	0.63**	leaf GA_3	-0.12
leaf Organic carbon	0.82**	stem C/N	-0.04	leaf IAA	0.01
leaf C/N	-0.22	stem GA_3	-0.21	leaf ZR	0.31*
stem N	0.48**	stem IAA	-0.17	leaf ABA	-0.16

The asterisks $^{**}P < 0.01$; $^{*}P < 0.05$

In the stepwise regression analysis, the contents of endogenous hormones and nutrients in stems and leaves were taken as independent variables, and the morphology of stems and leaves and the flower bud number were taken as the dependent variables. The results showed that there was a very significant linear relationship between the dependent variable Y and the independent variable X (*Table 5*). Leaf total nitrogen, stem total phosphorus and stem IAA content directly affected flower bud number, and

http://www.aloki.hu ● ISSN 1589 1623 (Print) ● ISSN1785 0037 (Online)
DOI: http://dx.doi.org/10.15666/aeer/2005_38733891

leaf total nitrogen also directly affected leaf number and petiole length. In addition, the stem and leaf total nitrogen contents, organic carbon content, and GA_3 content, stem ABA content and leaf C/N ratio indirectly affected the flower bud number by directly affecting the morphology of stems and leaves, promoting reproductive growth.

Table 4. *Pearson correlated with the stem and leaf morphology, nutrient, endogenous hormones content and flower bud number of Populus euphratica*

coefficient of association	flower bud number	coefficient of association	flower bud number	coefficient of association	flower bud number	coefficient of association	flower bud number	coefficient of association	flower bud number
leaves number	-0.53**	stem length	-0.46**	leaf Organic carbon	0.59**	stem Organic carbon	0.45**	stem ABA	-0.46**
leaf shape index	-0.54**	stem roughness	0.58**	leaf C/N	-0.28*	stem C/N	-0.19	leaf GA_3	-0.27
leaf area	0.51**	leaf N	0.54**	stem N	0.48**	stem GA_3	-0.38**	leaf IAA	-0.04
petiole length	0.48**	leaf P	0.40**	stem P	0.34**	stem IAA	-0.02	leaf ZR	0.27
leaves perimeter	0.41**	leaf K	-0.17	stem K	-0.19	stem ZR	-0.01	leaf ABA	-0.28

The asterisks $^{**}P < 0.01$; $^{*}P < 0.05$. gibberellin (GA_3), indole acetic acid (IAA), abscisic acid (ABA), zeatin (ZR), total nitrogen (N), total phosphorus (P), total potassium (K), carbon/ nitrogen (C/N)

Table 5. *Optimum regression models for prediction of stem and leaf morphology and flower bud number of Populus euphratica*

Dependent variable (Y)	Regression equation	R	R^2	F	Sig.
Y_1	$Y_1=-0.62+1.29X_1+1.31X_2-0.02X_3$	0.75	0.56	17.11	0.00
Y_2	$Y_2=16.63-0.14X_4-3.28X_1$	0.61	0.38	12.63	0.00
Y_3	$Y_3=6.71-0.21X_5+0.10X_6+0.10X_7$	0.82	0.67	27.88	0.00
Y_4	$Y_4=-354.16+23.51X_5+473.25X_8-60.24X_9$	0.75	0.57	17.77	0.00
Y_5	$Y_5=7.07+15.26X_1-0.06X_7$	0.65	0.43	15.57	0.00
Y_6	$Y_6=178.15-2.27X_5+6.79X_{10}-43.99X_8$	0.66	0.43	10.47	0.00
Y_7	$Y_7=-1.43+0.14X_5-0.30X_9+0.95X_8$	0.87	0.76	43.06	0.00

Y_1,flower bud number; Y_2,leaves number; Y_3,leaf shape index; Y_4,leaf area; Y_5,petiole length; Y_6,stem length; Y_7,stem diameter ; X_1,leaf N; X_2,stem P; X_3,stem IAA; X_4,stem organic carbon; X_5,leaf organic carbon; X_6,leaf C/N; X_7,stem ABA; X_8,stem N; X_9,stem GA_3; X_{10},leaf GA_3.Sig=Significant at $p< 0.05$, R=coefficient of association R^2 = coefficient of determination

Discussion

Relationship of morphological changes of stems and leaves on the flower buds number

There were significant differences in leaf morphology, nutrient and endogenous hormone contents and flower bud number at different diameters (Feng et al., 2014; Li et al., 2015b; Han et al., 2021). Zheng et al. (2015) showed that with the increase of tree age and canopy level (from base to top), the length of new stems, the number of stems and leaf shape index decreased gradually, while the leaf area and leaf dry weight increased gradually. Our results were consistent with that. The increase in flower bud

http://www.aloki.hu ● ISSN 1589 1623 (Print) ● ISSN1785 0037 (Online)
DOI: http://dx.doi.org/10.15666/aeer/2005_38733891

number, leaf area, leaf perimeter, petiole length and stem diameter was closely related to the increase in diameter rank. At the same time, the increase in leaf area, leaf perimeter, petiole length, stem diameter and leaf shape index was closely related to the increase in flower bud number. Consistent with the results of De et al. (2016), traits of different plant organs (leaves, stems and roots) have a high degree of functional coordination and are highly correlated with physiological key traits. Leaf shape and leaf area can be used as markers for growth and development (England et al., 2006). The results of this study showed that flower buds and broad-ovoid leaves appeared at the same time in the 4-diameter order (5.20 years of age) (*Figure. S1*), and the stems length and the number of leaves per branch decreased significantly in this diameter order, suggesting that the emergence of broad-ovoid leaves and the shortening of stems were indicators of the reproductive growth of *P. euphratica*. Wang et al. (2019) showed that to cope with energy demand at the breeding stage, leaves of *P. euphratica* adopted an adaptive strategy of gradually changing from strip leaves to oval leaves with the increase of tree age and realized the transition from vegetative growth to reproductive growth through coordinated changes of stems and leaves. When the leaf shape index decreased and the leaf area increased during the growth and development, most of the leaves were broad ovate. The broad oval leaves of *P. euphratica* have a stronger photosynthetic capacity (Zhai et al., 2020), which can fix more carbon, and the structural basis of leaf area and branch thickness can effectively improve photosynthetic efficiency, material transport and storage capacity (Runion et al., 2017; Han et al., 2019), provides material and energy for the reproductive growth of *P. euphratica* (Liu et al., 2016).

Relationship of changes in the nutrient contents of stems and leaves on the flower buds number

Morphological manifestations lag behind their physiological and biochemical triggers. When obvious morphological changes such as flowering are observed, the internal physiological and biochemical environment has already undergone great changes (Guo et al., 2008). N, P and K are three essential nutrients for plant growth, and N and P are important components of macromolecules (proteins, nucleic acids, etc.) (Krapp et al., 2012). K can activate enzymes related to energy metabolism, protein synthesis and solute transport. High N, P and K levels can promote cell division and size and have certain regulatory effects on flower bud differentiation and morphological changes in stems and leaves (Kirkby et al., 2010). Feng et al. (2014) showed that the total N content of *P. euphratica* promoted the increase of leaf area and the decrease of leaf shape index, thus promoting the emergence of broad-ovoid leaves. Zhang et al. (2017) showed that the nutrient contents of N, P and K from dormancy to flowering in flower buds increased significantly at the flowering stage. The results of this study showed that the growth of flower buds and broad ovoid leaves was promoted by the significant increase of total N content in leaves and organic carbon content in stems.

Carbon and nitrogen metabolism plays an important role in plant growth and development. Carbon and nitrogen interact and restrict each other to coordinate the process of plant growth and development (Barney et al., 1989). According to the C/N theory, flowering is controlled by the vegetative state, and a high carbohydrate to nitrogen ratio is necessary for flowering (Corbesier et al., 2002). It was found that C/N of *Dimocarpus longan* Lour., *Syzygium samarangense* (Bl.) Merr. et Perry and *Litchi chinensis* Sonn. increased significantly during the initiation of flower buds (Matsumoto

http://www.aloki.hu ● ISSN 1589 1623 (Print) ● ISSN1785 0037 (Online)
DOI: http://dx.doi.org/10.15666/aeer/2005_38733891

et al., 2007; Sritontip et al., 2008). This suggests that an appropriate C/N balance can promote the reproductive transition in plants (Liu et al., 2015). C/N promoted the differentiation of flower buds but also regulated the morphological changes in stems and leaves. The high level of carbohydrates in the shoot tip promoted an increase in the leaf number and flower bud height as well as the ratio of leaf width to flower bud height; these changes were conducive to the initiation of flower bud differentiation (Li et al., 2019). Li et al. (2015a) showed that starch metabolism in the leaves of *P. euphratica* played a regulatory role in the changes in leaf length and width. Starch is a high molecular-weight carbohydrate, and the higher the content of organic carbon, the higher the content of starch. In this study, *P. euphratica* ontogenesis exhibited a significant correlation with the total P, organic carbon, and total N contents in leaves; the leaf total N significantly influenced stem morphology, and the number of flower buds and the stem and leaf organic carbon contents significantly influenced stem and leaf morphology. These results indicate that the synergistic effects of total N, total P and organic carbon in leaves and stems promoted the transition from vegetative growth to reproductive growth.

Relationship of changes in the endogenous hormone contents of stems and leaves on the flower buds number

The physiological effects of different hormones promote or antagonize each other, and their effects involve various processes, such as synthesis, transportation, and metabolism. Plant growth and development are often the results of the comprehensive action of the balance of multiple hormones (Hsu et al., 1999). A certain level of IAA in flower buds is conducive to nutrient input and differentiation (Zhao et al., 2020). Mo et al. (2020) found that low levels of IAA and GA_3 and high levels of ABA were conducive to flower bud differentiation and could accelerate the transition from the physiological differentiation stage to the morphological differentiation stage. ABA and ZR are a diameter of hormones that promote the transition of the plant body into maturity. The transition from the seedling to mature stages in trees requires a lower GA level and a higher ABA level (Chen et al., 2020). Wang et al. (2020) studied the changes in endogenous hormones during flower bud differentiation in female *Ginkgo biloba* L. and showed that the GA_3 content reached a peak at the beginning of flower bud differentiation. According to the study by Ma et al. (2021), ABA reached its peak at the flowering stage of *Phalaenopsis aphrodite* H. G. Reichenbach, and the content of ABA in leaves was one of the main factors affecting the number of flower buds. A low IAA content before flower bud differentiation can reduce sugar loss, increase starch accumulation and prepare the plant for flower formation. After entering the physiological differentiation stage of flower buds, increased IAA content is conducive to nutrient input and promotes flower bud differentiation (Du et al., 2021). Meanwhile, an exogenous IAA treatment also showed that a low concentration of IAA was necessary for flower bud initiation, while a high concentration of IAA inhibited flower bud initiation (Zhao et al., 2020). It was further proved that IAA content was the main factor promoting the increase of flower buds per shoot. In this study, the decrease of IAA content in branches and leaves was closely related to the significant increase in the number of flower buds, and the IAA content in branches directly affected the number of flower buds. The results showed that IAA content in branches and leaves increased the reproductive capacity of *P. euphratica*.

http://www.aloki.hu ● ISSN 1589 1623 (Print) ● ISSN1785 0037 (Online)
DOI: http://dx.doi.org/10.15666/aeer/2005_38733891

Differences in the GA content in the leaf primordium in aquatic and terrestrial environments determine the *Rorippa indica* L. changes in their leaf shape (Bengera et al., 2012; Nakayama et al., 2014; Nakayama et al., 2017). GA_3 not only terminates vegetative growth but also promotes flower bud formation in woody plants (Goldberg-Moeller et al., 2013). ABA is involved mainly in the establishment and maintenance of the terrestrial morphological characteristics of heteromorphic plants (Wanke et al., 2011). Studies have shown that *P. euphratica* regulates the dormancy and germination of winter buds through the interaction of ABA, GA_3, and ZR, and promotes stem and leaf growth through the interaction of IAA, ABA, and ZR (Xu et al., 2007). The content of IAA in leaves decreased gradually with increasing tree age, while the contents of ABA and ZR in leaves showed an overall increasing trend, and the content of GA_3 in leaves showed a trend of first increasing and then decreasing (Li et al., 2017). Zheng et al. (2015) showed that the leaf shape index of *P. euphratica* gradually decreased from the bottom to the top of the crown and that broad-ovate leaves were distributed mostly at the top of the crown; the GA_3 content was significantly positively correlated with the leaf shape index, indicating that the GA_3 content was closely related to the emergence of broad-ovate leaves. In this study, the GA_3 content of stems and leaves had a direct and significant effect on the morphology of stems and leaves. Flower buds appeared in the 4 cm class diameter, when *P. euphratica* entered the reproductive growth stage, and the content of ZR in leaves increased significantly. In the 4-12 cm class diameteres, the number of flower buds increased gradually, the leaf area increased, the leaf shape index gradually decreased, *P. euphratica* entered the stage of vegetative growth and reproductive growth, and the GA_3 content of stems and leaves decreased gradually. The results indicated that leaf ZR content promotes the reproductive growth of *P. euphratica* and that the GA_3 content of stems and leaves promotes reproductive growth mainly by affecting vegetative growth in the stage during which vegetative growth and reproductive growth cooccur.

Cells transmit light signals through the cytokinin signal transduction pathway, and lightly regulates leaf initiation by activating cytokinin signals and affecting the efflux-dependent IAA gradient (Li et al., 2020). In this study, only the ABA and ZR contents in the stems and leaves were significantly correlated with the ontogenetic development of *P. euphratica*. It was inferred that endogenous hormones in the stems and leaves did not affect the ontogenetic stage of *P. euphratica* because IAA induces changes in the balance of other hormones (Nakayama et al., 2017). Therefore, the effect of IAA on the flower bud number during the phase change in *P. euphratica* may be due to the signaling function of IAA. The hormone balance of *P. euphratica* in the juvenile stage was changed, to make the transition to adulthood; at the same time, the hormones distributed nutrients to meet the needs of *P. euphratica* during its stage transition.

Conclusions

The flower buds and broad ovoid leaves of 4 diameter (5.20 years old) appeared simultaneously, indicating that P. euphratica had entered the reproductive growth stage, and 14 diameter (10.52 years old) had entered the vigorous reproductive growth stage. The leaf and stem morphology and the total nitrogen, total phosphorus and organic carbon contents changed synergistically with developmental stages. The leaf total nitrogen, stem total phosphorus and stem IAA contents significantly affected the number of flower buds, and the stem total nitrogen, organic carbon, GA_3 content, stem

http://www.aloki.hu ● ISSN 1589 1623 (Print) ● ISSN1785 0037 (Online)
DOI: http://dx.doi.org/10.15666/aeer/2005_38733891

ABA content and leaf C/N ratio significantly affected the morphology of stems and leaves and indirectly affected the number of flower buds. We believe that the synergistic changes in the nutrient and endogenous hormone contents of *P. euphratica* stems and leaves regulate the morphology of stems and leaves as well as the flower bud number and directly or indirectly affect the transition from vegetative growth to reproductive growth. Therefore, the synergistic changes among the influencing factors should be considered in the study of the transition between plant growth and development stages.

Acknowledgements. This work was financially supported by the National Natural Sciences Foundation of China (31860198, 31060026, U1803231).

Author contributions. Xuefei Guo had the main responsibility for data collection, analysis and writing, Juntuan Zhai and Shanhe Zhang had a significant contribution to data analysis, and Zhijun Li (the corresponding author) had the overall responsibility for experimental design and project management.

Conflict of interests. The authors declare that they have no conflict of interests.

REFERENCES

[1] Barney, P. E., Bush, L. P., Tso, T. C. (1989): Physiology and biochemistry of tobacco plant. 2. physiological disorder-mineral nutrients. – Beitrage Zur Tabakforschung International 14: 211-236.
[2] Bengera, H., Shwartz, I., Shao, M., Shani, E., Estelle, M., Ori, N. (2012): ENTIRE and GOBLET promote leaflet development in tomato by modulating auxin response. – Plant J 70: 903-915.
[3] Besford, R. T., Hand, P., Peppitt, S. D., Richardson, C. M., Thomas, B. (1996): Phase change in Prunus avium-differences between juvenile and mature shoots identified by 2-dimensional protein separation and in vitro translation of mRNA. – Journal of Plant Physiology 147: 534-538.
[4] Chen, C., Yu, F. Y. (2020): Research Progress on Flower Bud Differentiation of Trees. – Scientia Silvae Sinicae 56: 119-129.
[5] Corbesier, L., Bernier, G., Périlleux, C. (2002): C:N ratio increases in the phloem sap during floral transition of the long day plants Sinapis alba and Arabidopsis thaliana. – Plant and Cell Physiology 43: 684-688.
[6] De la Riva, E. G., Tosto, A., Pérez-Ramos, I. M., Navarro-Fernández, C. M., Olmo, M., Anten, N. P., Marañón, T., Villar, R. (2016): A plant economics spectrum in Mediterranean forests along environmental gradients: is there coordination among leaf, stem and root traits? – Journal of Vegetation Science 27: 187-199.
[7] Du, F., Guan, C., Jiao, Y. (2018): Molecular Mechanisms of Leaf Morphogenesis. – Mol. Plant 11: 1117-1134.
[8] Du, L. Y., Zheng, N., Li, J. J., Yu, J. L., Zhou, C. L. (2021): Changes in endogenous hormones during flower bud differentiation in Cerasus subhirtella'Autumnalis'. – Journal of Forest and Environment 41: 51-59.
[9] England, J. R., Attiwill, P. M. (2006): Changes in leaf morphology and anatomy with tree age and height in the broadleaved evergreen species, Eucalyptus regnans F. Muell. – Trees 20: 79-90.
[10] Feng, M., Huang, W. J., Li, Z. J. (2014): Relationship of leaf shape change and leaf nutrient contents in Populus Euphratica. – Chinese Journal of Ecology 33: 1467-1473.
[11] Gao, Y., Liu, H., Dong, N. G., Pei, D. (2012): Temporal and spatial pattern of indole-3-acetic acid occurrence during walnut pistillate flower bud differentiation as revealed by

http://www.aloki.hu ● ISSN 1589 1623 (Print) ● ISSN1785 0037 (Online)
DOI: http://dx.doi.org/10.15666/aeer/2005_38733891

immunohistochemistr. – Journal of the American Society for Horticultural Science 137: 283-289.

[12] Goldberg-Moeller, R., Shalom, L., Shlizerman, L., Samuels, S., Zur, N., Ophir, R., Blumwald, E., Sadka, A. (2013): Effects of gibberellin treatment during flowering induction period on global gene expression and the transcription of flowering-control genes in Citrus buds. – Plant Sci. 198: 46-57.

[13] Gu, Y. Y., Zhang, S. Q., Li, Z. J. (2013): Relationship between Diameter at Breast Height and Age of Endangered Species Populus Euphratica Oliv. – Journal of Tarim University 25: 11-21.

[14] Guo, C. H., Kan, X. Y. (2008): Progress in Phase Change During Tree Development. – Letters in Biotechnology 19: 784-786.

[15] Han, H., Shan, L. F., Wang, S. L., Shi, S., Feng, J. Z. (2019): Photosynthesis Characteristics of Heteromorphic Leaves of Populus euphratica. – Journal of MUC (Natural Sciences Edition) 28: 5-11.

[16] Han, X. L., Zhai, J. T., Gai, Z. S., Li, Z. J. (2021): The relationship between the morphological and structural changes of Populus euphratica oliv. and endogenous hormone contents. – Applied Ecology and Environmental Research 19: 2259-2280.

[17] Hao, J. Q., Yue, N., Zheng, C. X. (2017): Analysis of changes in anatomical characteristics and physiologic features of heteromorphic leaves in a desert tree, Populus euphratica. – Acta Physiologiae Plantarum 39: 160.

[18] Hassankhah, A., Rahemi, M., Mozafari, M. R., Vahdati, K. (2018): Flower development in walnut: altering the flowering pattern by gibberellic acid application. – Notulae Botanicae Horti Agrobotanici Cluj-Napoca 46: 700-706.

[19] Hsu, Y. M., Tseng, M. J., Lin, C. H. (1999): The fluctuation of carbohydrates and nitrogen compounds in flooded wax-apple trees. – Botanical Bulletin Academia Sinica 40: 193-198.

[20] Huang, W. J., Li, Z. J., Yang, Z. P., Bai, G. Z. (2010a): The structural traits of Populus euphratica heteromorphic leaves and their correlations. – Acta Ecologica Sinica 30: 4636-4642.

[21] Huang, W. J., Li, Z. J., Yang, Z. P., Liang, J. Y., Bai, G. Z. (2010b): Heteromorphic leaf structural characteristics and their correlations with diameter at breast height of Populus euphratica. – Chinese Journal of Ecology 29: 2347-2352.

[22] Jin, Y. F., Li, Z. L., Chen, D. M. (1998): Leaf contents of polyamines, RNA/DNA and soluble protein related to phase change of crabapple seedlings. – Acta Agriculturae Zhejiangensis 10: 264-267.

[23] Kirkby, E A. (2010): Research on potassium in agriculture: Needs and prospects. – Plant Soil 335: 155-180.

[24] Krapp, A., Castaings, L. (2012): Plant adaptation to nitrogen availability. – Biol Aujourdhui 206: 323-335.

[25] Li, J. H., Feng, M., Li, Z. J. (2015a): Carbohydrate, Soluble Protein and Morphometric Changes of Leaves of Populus euphratica Oliv. Individuals under Different Developmental Stages. – Bulletin of Botanical Research 35: 521-527.

[26] Li, J. H., Liu, S. F., Li, Z. J. (2015b): Morphometric changes in branches, leaves and flower buds of Populus euphratica at different development stages. – Chinese Journal of Ecology 34: 941-946.

[27] Li, Y. L., Zhang, X., Feng, M., Han, Z. J., Li, Z. J. (2017): Characteristics of Endhormones in Leaf Blade of Populus euphratica Heteromorphic Leaves. – Journal of Tarim University 29: 7-13.

[28] Li, Z. J., Fu, B. C., Wang, Y. S., Lu, Y. M. (2019): Characteristics of external morphology and nutrients in flower bud differentiation of Hemerocallis. – Molecular plant breeding 17: 6135-6141.

[29] Li, G. J., Hu, S. Q., Yang, J. J., Hou, H. W. (2020): Advances of heterophylly studies in plants. – Plant Physiology Journal 56: 2067-2078.

http://www.aloki.hu ● ISSN 1589 1623 (Print) ● ISSN1785 0037 (Online)
DOI: http://dx.doi.org/10.15666/aeer/2005_38733891

[30] Li, Z. J., Jiao, P. P., Wu, Z. H., Zhai, J. T., Zhang, X., Zhang, S. H., Gai, Z. S., Guo, X. F., (2021): Heterophylly and growth adaptation strategies of Populus euphratica and Populus pruinose. – Science press, Beijing, China.
[31] Liu, Y. P., Yang, J., Yang, M. F. (2015): Pathways of flowering regulation in plants. – Chinese Journal of Biotechnology 31: 1553-1566.
[32] Liu, S. F., Jiao, P. P., Li, Z. J. (2016): Diversifolious Types and Spatiotemporal Characteristics of Populus pruinosa Schrenk. – Aridzone Research 33: 1098-1103.
[33] Ma, X. H., Liu, H. J., Zhan, Q. L., Hu, Q. D., Qian, R. J. (2021): Dynamic Changes of Endogenous Hormones in Leaves of Phalaenopsis amabilis During Flower Forcing Process. – Journal of Agriculture 11: 57-61.
[34] Matsumoto, T. K., Tsumura, T., Zee, F. (2007): Exploring the mechanism of potassium chlorate-induced flowering in Dimocarpus longan. – Acta Horticultural 738: 451-457.
[35] Mo, W. J., Zhang, J. J., Yang, S. B., Xu, Y., Yuan, C. G., Liu, Y. X. (2020): Flower bud differentiation and dynamic changes of endogenous hormone in Prunus domestica × areniaca'Fengweineigui'. – Journal of China Agricultural University 25: 54-61.
[36] Munoz-Fambuena, N., Mesejo, C., Gonzlez-Mas, M. C., Iglesias, D. J., Millo, E. P., Agustí, M. (2012): Gibberellic acid reduces flowering intensity in sweet orange (*Citrus sinensis* L. Osbeck) by repressing CiFT gene expression. – Journal of Plant Growth Regulations 31: 529-536.
[37] Nakayama, H., Nakayama, N., Seiki, S., Kojima, M., Sakakibara, H., Sinha, N., Kimura, S. (2014): Regulation of the KNOX-GA gene module induces heterophyllic alteration in North American Lake Cress. – Plant Cell 26: 4733-4748.
[38] Nakayama, H., Sinha, N. R., Kimura, S. (2017): How Do Plants and Phytohormones Accomplish Heterophylly, Leaf Phenotypic Plasticity, in Response to Environmental Cues. – Frontiers in Plant Science 8: 1717.
[39] Runions, A., Tsiantis, M., Prusinkiewicz, P. (2017): A common developmental program can produce diverse leaf shapes. – New Phytol. 216: 401-418.
[40] Sritontip, C., Khaosumain, Y., Changjaraja, S., Changjeraja, R. (2008): Effects of light intensity and potassium chlorate on photosynthesis and flowering in 'Do' longan. – Acta Horticulturae 787: 285-288.
[41] Wang, W. J., Lü, H., Zhong, Y. M., Chen, L. J., Li, J. W., Ma, Q. (2019): Relationship between heteromorphic leaf traits of Populus euphratica and its individual development. – Journal of Beijing Forestry University 41: 62-69.
[42] Wang, J. H., Li, G., Che, S. C., Ren, G. F., Ren, B. B., Qiu, L. F., Zhong, L. (2020): Changes of Endogenous Hormones during Female Floral Bud Differentiation of *Ginkgo biloba* L. in Beijing Region and Determination of the Initiation Time. – Journal Anhui Agricultural Science 48: 118-123.
[43] Wanke, D. (2011): The ABA-mediated switch between submersed and emersed lifestyles in aquatic macrophytes. – J Plant Res. 124: 467-475.
[44] Xu, S. L., Feng, J. Z., Jiang, L., Zhang, C. L. (2007): Variation of Saccharides in Young Leaves of Populus Euphratica in E Jina County. – Journal of the CUN (Natural Science Edition) 16: 210-216.
[45] Xu, L. P., Yu, F. Y. (2018): Physiological characteristics during bud development of Styrax tonkinensis. – Jiangsu Agricultural Sciences 46: 120-123.
[46] Yu, X., Deng, Q. E., Li, J. A. (2019): Relationship between endogenous hormones contents and flowering process in Camellia oleifera 'Tiecheng No.1'. – Nonwood Forest Research 37: 149-154.
[47] Zhai, J. T., Li, Y. L., Han, Z. J., Li, Z. J. (2020): Morphological, structural and physiological differences in heteromorphic leaves of Euphrates poplar during development stages and at crown scales. – Plant Biology 22: 366-375.
[48] Zhang, L. B., Liu, G. S., Wang, X. M., Yuan, Z. Y. (1997): Relationship Between Leaf Characters Juvenile Span on Shenzhmitao Peach Seedlings. – Journal of Fruit Science 14: 28-3l.

http://www.aloki.hu ● ISSN 1589 1623 (Print) ● ISSN1785 0037 (Online)
DOI: http://dx.doi.org/10.15666/aeer/2005_38733891

[49] Zhang, X., Lu, R. H., Liang, J. Y., Zhou, Z. L., Li, Z. J. (2017): Spatial Distribution of Reproductive Shoots and Dynamic Change of Nutrient Contents of Populus euphratica. – Aridzone Research 34: 95-103.
[50] Zhao, S. L., Wei, Y. R., Pang, H. G., Du, Y. N., Xu, J. F., Li, Y. L., Zhang, H. X., Zhang, J. G., Zhang, Y. X. (2020): Effects of spraying plant growth regulator and leaf picking on flower bud differentiation of pear tree. – China Fruits 3: 61-64.
[51] Zhao, Z. H., Zhang, R., Yan, L., Liang, W. H., Liao, J. M., Lan, Z. Q., Tan, X. B. (2020): Changes of Endogenous Hormones in Castanea mollissima Flower Bud Differentiation. – Guangxi Foreatry Science 49: 518-523.
[52] Zheng, Y. Q., Feng, M., Li, Z. J. (2015): Investigation of bud burst, shoot growth and leaf expansion in Populus euphratica of different ages. – Acta Ecologica Sinica 35: 1198-1207.
[53] Zhu, Z. J., Jiang, C. H., Shi, Y. H., Chen, W. Q., Chen, N. L., Zhao, M. J., Wu, W. J. (2015): Variations of endogenous hormones in lateral buds of olive trees (Olea europaea) during floral induction and flower-bud differentiation. – Scientia Silvae Sinicae 51: 32-39.

http://www.aloki.hu ● ISSN 1589 1623 (Print) ● ISSN1785 0037 (Online)
DOI: http://dx.doi.org/10.15666/aeer/2005_38733891

APPENDIX

Table S1. *Path coefficient analysis of stem and leaf morphology,nutrients,endogenous hormones and flower bud number of Populus euphratica*

Effect of factors	Direct effect	Indirect effects																						
		leaves number	leaf shape index	leaf area	petiole length	Leaves perimeter	stem length	stem diameter	leaf N	leaf P	leaf K	leaf Organic carbon	leaf C/N	stem N	stem P	stem K	stem Organic carbon	stem C/N	stem GA_3	stem IAA	stem ZR	stem ABA	leaf GA_3	leaf IAA	leaf ZR	leaf ABA
leaves number	-0.411		-0.090	0.119	-0.072	-0.049	0.213	-0.107	0.265	-0.042	0.013	-0.164	-0.057	-0.149	0.046	-0.025	-0.026	-0.015	-0.006	-0.006	-0.003	-0.021	0.004	0.004	-0.032	0.042
leaf shape index	-0.157	-0.235		0.152	-0.107	-0.080	0.163	-0.148	0.363	-0.090	0.017	-0.225	-0.062	-0.197	0.060	-0.006	-0.031	-0.010	-0.006	-0.004	0.007	-0.030	0.010	-0.005	-0.052	0.069
leaf area	-0.201	0.244	0.119		0.109	0.094	-0.161	0.132	-0.291	0.080	-0.018	0.187	0.049	0.274	-0.103	0.022	0.027	-0.019	0.009	0	-0.008	0.036	-0.006	0	0.045	-0.108
petiole length	0.215	0.138	0.078	-0.102		0.103	-0.102	0.102	-0.281	0.096	-0.014	0.157	0.066	0.165	-0.074	0.013	0.019	-0.009	0.003	0	-0.012	0.036	-0.024	0.011	0.023	-0.080
leaves perimeter	0.179	0.113	0.071	-0.105	0.124		-0.120	0.092	-0.269	0.091	-0.010	0.118	0.074	0.089	-0.032	-0.001	0.011	0.010	0.005	-0.001	-0.013	0.013	-0.024	0.003	0.038	-0.008
stem length	0.279	-0.314	-0.092	0.116	-0.079	-0.077		-0.125	0.220	-0.038	0.011	-0.146	-0.050	-0.220	0.069	-0.028	-0.021	0.009	-0.009	0.003	0.007	-0.024	0.025	0	-0.039	0.043
stem diameter	0.175	0.250	0.133	-0.151	0.126	0.094	-0.198		-0.319	0.097	-0.021	0.244	0.027	0.208	-0.093	0.014	0.029	0	0.010	0.001	0.001	0.037	-0.018	0.002	0.042	-0.083
leaf N	-0.519	0.210	0.110	-0.113	0.117	0.093	-0.118	0.108		0.095	-0.006	0.188	0.160	0.156	-0.016	-0.003	0.022	0.009	0.003	0.004	-0.007	0.014	-0.005	-0.004	0.055	-0.011
leaf P	0.224	0.078	0.063	-0.072	0.092	0.072	-0.048	0.076	-0.219		-0.029	0.170	-0.004	0.132	-0.112	0.017	0.006	-0.027	0.001	0	-0.007	0.021	-0.004	0.007	0.004	-0.030
leaf K	0.068	-0.080	-0.039	0.054	-0.045	-0.026	0.044	-0.053	0.047	-0.097		-0.101	0.038	-0.007	0.046	-0.050	-0.004	-0.002	-0.002	-0.004	0.013	-0.012	0.009	-0.006	0.015	0.032
leaf Organic carbon	0.312	0.216	0.114	-0.120	0.108	0.068	-0.130	0.137	-0.313	0.122	-0.022		-0.027	0.126	-0.067	0.025	0.032	0.020	0.001	0.005	0.001	0.021	0	0	0.054	-0.055
leaf C/N	-0.243	-0.097	-0.040	0.040	-0.059	-0.055	0.057	-0.019	0.341	0.004	-0.011	0.035		-0.111	-0.025	0.026	-0.002	0.018	-0.003	-0.002	0.012	0.001	0.010	0.002	-0.018	-0.042
stem N	0.547	0.112	0.057	-0.101	0.065	0.029	-0.112	0.067	-0.148	0.054	-0.001	0.072	0.049		-0.158	0.031	0.016	-0.098	0.003	0.002	-0.002	0.024	-0.006	0.011	0.011	-0.060
stem P	-0.225	0.085	0.042	-0.092	0.070	0.026	-0.085	0.072	-0.037	0.111	-0.014	0.092	-0.027	0.383		0.058	0.010	-0.083	0.005	0	0.003	0.036	-0.008	0.008	-0.018	-0.078
stem K	-0.128	-0.079	-0.007	0.034	-0.022	0.001	0.060	-0.019	-0.013	-0.029	0.027	-0.060	0.049	-0.132	0.102		-0.007	0.026	0.001	0.004	0.003	-0.008	0.007	-0.003	0.035	0.068
stem Organic carbon	0.050	0.218	0.097	-0.109	0.081	0.041	-0.116	0.104	-0.234	0.028	-0.005	0.200	0.009	0.173	-0.047	0.018		0.055	0	0	0.019	0.031	-0.007	0.005	0.040	-0.077
stem C/N	0.145	0.043	0.011	0.027	-0.014	0.012	0.017	0.000	-0.032	-0.042	-0.001	0.044	-0.030	-0.367	0.129	-0.023	0.019		-0.003	-0.002	0.014	-0.003	0.001	-0.007	0.027	0.020
stem GA_3	-0.027	-0.092	-0.035	0.066	-0.025	-0.032	0.097	-0.067	0.052	-0.004	0.004	-0.017	-0.022	-0.060	0.043	0.003	-0.001	0.015		-0.001	0.001	-0.034	0.024	0	0.012	0.121
stem IAA	-0.042	-0.059	-0.014	0.002	-0.001	0.002	-0.018	-0.004	0.049	0.001	0.007	-0.039	-0.010	-0.030	-0.001	0.013	0	0.006	-0.001		-0.015	-0.001	-0.012	-0.009	-0.036	0.014
stem ZR	-0.064	-0.020	0.017	-0.024	0.040	0.036	-0.030	-0.002	-0.053	0.024	-0.014	-0.006	0.044	0.018	0.012	0.006	-0.015	-0.033	0.001	-0.010		0.005	-0.012	0.015	0.020	-0.002
stem ABA	-0.080	-0.110	-0.059	0.091	-0.097	-0.030	0.083	-0.080	0.089	-0.058	0.010	-0.081	0.003	-0.166	0.103	-0.012	-0.020	0.005	-0.011	0.000	0.004		0.027	-0.022	0.029	0.222
leaf GA_3	0.066	-0.026	-0.024	0.019	-0.077	-0.066	0.105	-0.047	0.042	-0.014	0.009	0	-0.037	-0.050	0.027	-0.014	-0.005	0.001	-0.010	0.008	0.011	-0.032		-0.017	0.029	0.046
leaf IAA	-0.047	0.036	-0.018	0.000	-0.051	-0.010	0.002	-0.006	-0.039	-0.033	0.008	0.001	0.009	-0.125	0.038	-0.008	-0.005	0.020	0	-0.008	0.021	-0.038	0.024		0.008	0.113
leaf ZR	0.159	0.083	0.051	-0.057	0.032	0.043	-0.068	0.047	-0.181	0.005	0.007	0.106	0.027	0.039	0.025	-0.029	0.013	0.025	-0.002	0.010	-0.008	-0.015	0.012	-0.003		0.066
leaf ABA	0.296	-0.058	-0.037	0.074	-0.058	-0.005	0.040	-0.049	0.020	-0.023	0.007	-0.059	0.035	-0.111	0.060	-0.029	-0.013	0.010	-0.011	-0.002	0	-0.060	0.010	-0.018	0.036	

http://www.aloki.hu ● ISSN 1589 1623 (Print) ● ISSN1785 0037 (Online)
DOI: http://dx.doi.org/10.15666/aeer/2005_38733891

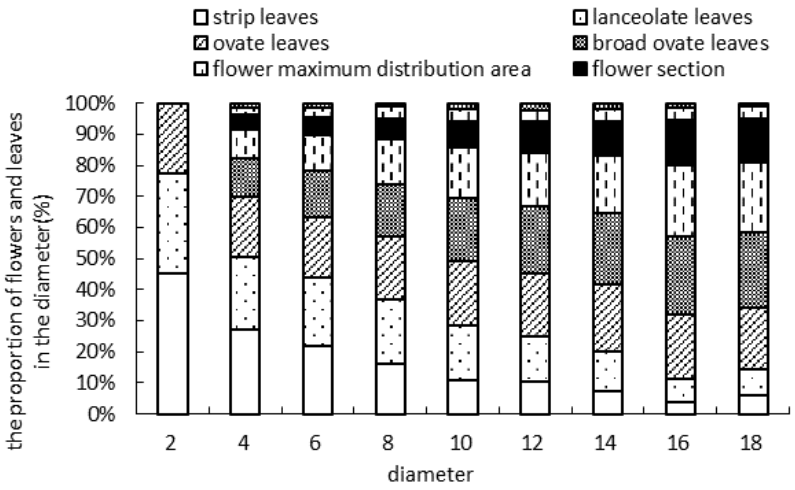

Figure S1. *Overlaps of spatiotemporal distribution of heteromorphic leaves and flower buds in Populus euphratica. X-axis is the ontogenetic stage and Y-axis represent the proportion of flowers and leaves in the diameter*

http://www.aloki.hu ● ISSN 1589 1623 (Print) ● ISSN1785 0037 (Online)
DOI: http://dx.doi.org/10.15666/aeer/2005_38733891

EFFECTS OF ZINC OXIDE NANOPARTICLES ON GERMINATION AND SEEDLING ESTABLISHMENT OF PEA (*PISUM SATIVUM)* AND BEANS *(PHASEOLUS VULGARIS)*

BASAHI, M. A.

College of Sciences and Arts – Sajer, Shaqra University, Riyadh, Saudi Arabia
(e-mail: mbasahi@su.edu.sa; phone: +966-58-222-3689)

(Received 17th Dec 2021; accepted 21st Mar 2022)

Abstract. The number of studies on nanomaterials, the ecological significance and the possible ecotoxicity have been increased over the last decade. Nanoparticles have been considered a potential health risk and a massive menace to the environment. The aim of the study was to explore the effect of zinc oxide nanoparticles on the growth, metabolism, stress and defense systems during seed germination and seedling development. Pea (*Pisum sativum* L. var. Alicia), white beans [*Phaseolus vulgaris* L. 'Snowdon' (Pv1)] and red beans [*Vigna angularis* 'adzuki bean' (Pv2)]. Seeds were germinated for 5 days. Seedlings were then transplanted into several trays filled with nutrient solution for 15 days. At harvest, plants were divided into leaves, stems and roots. Application of ZnO nanoparticles (150 mg/L and 300 mg/L) improved vegetable production. The antioxidant activities in cytosolic, chloroplast, and mitochondrial compartments varied according to ZnO doses, organs and plant species. Significant changes were found caused by genetic variability. A gradation of quantitative differences in ZnO-NPs resistance is more typically observed between plant genotypes.
Keywords: cellular responses, environmental risk, genotypes, harmful effects, nanomaterials, resistance, tolerance, yield losses

Introduction

Agricultural practice has shown that certain substances promote plant growth and development. These substances, of natural or anthropogenic origin, allow for better absorption of nutrients (Missaoui et al., 2020). Among these substances are nanoparticles with dimensions smaller than 100 nm (Missaoui et al., 2017, 2018; Chemingui et al., 2019a, b; 2021; Guey et al., 2020). Publications often present discordant results (Dietz et al., 2011; Missaoui et al., 2021). Indeed, studies on plants show both beneficial and harmful effects (Larue, 2011). Nanoparticles (NPs) stimulate plant growth and represent an interesting potential in agriculture (Missaoui et al., 2021). The results obtained depend on the type of nanoparticles and their properties (Ghafariyan et al., 2013; Missaoui et al., 2017), but also on the plant species and their stage of development, time and doses (Ma et al., 2013). They are expressed indirectly via mineral nutrition, by improving the bioavailability of mineral elements, or directly, by the assimilation of organic molecules that modify biochemical processes and plant cell metabolism. These effects are either positive or negative depending on the experimental conditions. Several levels of variability are involved in the study of the biological impact of NPs. Reducing the application of fertilizers and biocides on crops limits the risks of soil, groundwater and watercourse pollution, and would reduce the energy and environmental costs associated with the production and distribution of agrochemicals (Koller, 2004). However, minimizing environmental risk often implies yield losses. Modern agriculture uses techniques that would allow a reduction in the use of chemical inputs without affecting crop yields or farmers' incomes. For these different reasons, we present in this work the results of the treatment of pea and bean seedlings

http://www.aloki.hu ● ISSN 1589 1623 (Print) ● ISSN 1785 0037 (Online)
DOI: http://dx.doi.org/10.15666/aeer/2005_38933909

with the aim of analyzing the biological, physiological and cellular responses. We asked the following questions: is it a general response for both plants? Could it be a kind of plant resistance, or is it a genetically controlled tolerance?

'Resistance' and 'tolerance' are the terms used to denote the ability of the plant manage the stress, be it biotic or abiotic. A plant is considered resistant when it has the ability to exclude, hinder or overcome the effects of a given pathogen or another damaging factor. A plant may be resistant to one pathogen or condition but not others. Tolerance is the ability of a plant to be colonized by a pathogen or exposed to an abiotic factor without dying or demonstrating disease symptoms (Cooper, 2007; Catiempo et al., 2021). According to the definition of Koch et al. (2016), plant resistance can be categorized into three categories: antibiosis, antixenosis or non-preference, and tolerance. Antibiotic plant traits negatively impact a pest's biology through increases in mortality, reduced growth, longevity, and fecundity. Antixenosis, often referred to as non-preference, is a host-expressed trait that has adverse effects on insect behavior. In essence, insects have a non-preference for antixenotic hosts, and a preference for susceptible ones. Tolerance traits reduce the negative effects of herbivory on plant fitness after herbivory has occurred, all the while maintaining insect populations similar to those seen on susceptible plants. In an evolutionary context, tolerance is defined as the slope of the line describing the association between fitness and level of damage for a set of genetically related plants (Strauss and Agrawal, 1999). In agronomic situations, tolerant crop varieties are able to withstand injury and produce acceptable yields (Qiu et al., 2011). From an ecological perspective, tolerant plants can maintain fitness in response to pest injury. Both antibiosis and antixenosis involve a plant response and a pest response (Peterson et al., 2017). However, in the case of tolerance only a plant response is involved. Therefore, there is a nonreciprocal process associated with tolerance (Smith, 2005).

The two major mechanisms of plant defense against Zinc oxide nanoparticles are resistance (the ability to limit ZnO-NPs-plant interactions) and tolerance (the ability to reduce the effect of ZnO-NPs on plant metabolism regardless of the dose of ZnO-NPs). Qualitative differences in stress resistance can be observed when multiple specimens are compared after treated by the ZnO-NPs at similar levels in similar environments. A gradation of quantitative differences in ZnO-NPs resistance is more typically observed between plant genotypes.

The purpose of this research is to understand and explain the variable effects of zinc oxide nanoparticles on *Pisum sativum* and *Phaseolus vulgaris* seedlings.

Materials and methods

Genotypes tested comprised three commercial cultivars in Saudi Arabia. Seeds of pea (*Pisum sativum* L. var. Alicia), white beans [*Phaseolus vulgaris* L. 'Snowdon' (Pv1)] and red beans [*Vigna angularis* 'adzuki bean' (Pv2)] were disinfected with sodium hypochlorite (2%) for 10 min, washed thoroughly with distilled water and then germinated in Petri dishes (10 seeds/Petri dish) on 2 sheets of moist filter paper for 5 days at 25 °C (Basahi, 2018).

The seedlings were transplanted into several trays filled with nutrient solution (Hoagland and Arnon, 1950). pH 6.5 was evaluated as optimum for hydroponic culture Aeration was provided by a modular aerator. The temperature was about 25 °C. The luminosity was 150 lx. Relative humidity was 50%. The photoperiod was

http://www.aloki.hu ● ISSN 1589 1623 (Print) ● ISSN 1785 0037 (Online)
DOI: http://dx.doi.org/10.15666/aeer/2005_38933909

8 h. Seedlings were imbibed with distilled water (control) or treated with 150 mg/L and 300 mg/L ZnO nanoparticles (<50 nm particle size (BET), Purity = 99.9%, Sigma-Aldrich, St. Louis, MO, USA; *Table 1*) for 15 days. Nutrient solutions were changed every four days during the experiment. The dissolution of zinc oxide (ZnO) nanoparticles (NPs) is a key step controlling their environmental fate, bioavailability, and toxicity. ZnO nanoparticles were not soluble at pH 6.5 (Copur, 2010). The different treatments used were presented in *Table 2*. At harvest (20-days old; phenophase: plant growth during spring), plants were divided into leaves, stems and roots, dried for 8 days at 70 °C for dry weight determination or kept in ultra-deep freezer at -80 °C for biochemical studies.

As for morphological parameters axis length, (2) length of internodes, (3) root length, (4) number of secondary roots, (5) leaf area, and (6) number of leaves were determined. Leaf area had been measured using CI-202 portable laser leaf area meter.

For the determination of chlorophylls, they were extracted by grinding 100 mg fresh leaves in 5 mL ethanol (80%) using a mortar and after 72 h in the dark and at 4 °C, the absorbance was measured at 663 and 645 nm (Lichtenthaler and Welburn, 1983). Pigment contents (chlorophyll a (Cha) and chlorophyll b (Chb)) (mg g^{-1} FW) were determined using a spectrophotometer (Lamba 2, PerkinElmer, Waltham, MA, USA).

Cytosol, chloroplasts, and mitochondria were isolated according to method described by Smiri et al. (2009). Enzyme activities expressed as units per gram of fresh weight Ug^{-1} FW and determined using spectrophotometer (Lamba 2, PerkinElmer, Waltham, MA, USA).

Table 1. *Size, surface area and form of ZnO-NPs obtained from Sigma-Aldrich*

Properties of ZnO-NPs (677450 - Zinc oxide; Sigma-Aldrich)	
Quality level	For non-regulated applications with no change notification requirements
Purity	99.9% Based on trace metals analysis
Form	Nanopowder
Contains	6% Al as dopant
Reaction suitability	Reagent type: catalyst Core: zinc
Particle size	< 50 nm (BET)
Surface area	> 10.8 m2/g
Safety information	
Symbol	GHS09
Signal word	Warning
Hazard statements	H410
Precautionary statements	P273 - P391 - P501
Personal protective equipment	Dust mask type N95 (US), Gloves

Table 2. *The different treatments*

Treatments	***Pisum sativum***	***Phaseolus vulgaris***	***Vigna angularis***
Controls (ZnO (0 g/L))	CPs	CPv1	CPv2
ZnO (150 mg/L)	ZnO-1Ps	ZnO-1Pv1	ZnO-1Pv2
ZnO (300 mg/L)	ZnO-2Ps	ZnO-2Pv1	ZnO-2Pv2

http://www.aloki.hu ● ISSN 1589 1623 (Print) ● ISSN 1785 0037 (Online)
DOI: http://dx.doi.org/10.15666/aeer/2005_38933909

Guaiacol peroxidase (GPOX) activity was measured according to Fielding and Hall (1978). The enzyme extract was added to the reaction mixture containing 50 mM of potassium phosphate (pH 7.0), 10 mM of H_2O_2, and 9 mM of guaiacol. Enzyme activity was estimated by the increase in absorbance at 470 nm. GPOX activity was determined using the extinction coefficient of 26.6 $mM^{-1}\,cm^{-1}$. One unit of GPOX activity was defined as the amount of enzyme that caused the formation of 1 μM of tetraguaiacol per minute under the assay conditions. Catalase (CAT) was measured according to Aebi (1984). The enzyme extract was added to the reaction mixture containing 50 mM of potassium phosphate buffer (pH 7.0), 10 mM of H_2O_2, and 1 mM of dithiothreitol (DTT). The enzyme activity was quantified by recording the decrease in absorbance at 240 nm. CAT activity was determined using the extinction coefficient of 39.4 $mM^{-1}\,cm^{-1}$. One unit of CAT activity was defined as the amount of enzyme required to decay 1 μM of hydrogen peroxide/min/mg protein under the assay conditions.

Seedling data were arcsine transformed before statistical analysis to ensure homogeneity of variance (Ahmed and Khan, 2010). For statistical analysis, the factors were the species and the ZnO concentrations. The effects of the tested factors on growth, productivity, chlorophyll metabolism, oxidative stress and antioxidant systems were analysed. Post hoc tests were performed to compare treatment means.

Results

ZnO-NPs treatments have significant effects on stem growth and the number of internodes of two tested plants (*Fig. 1A, B*). The variability of the results could be explained by the tolerance of the ZnO-NPs, which depends on the genetic variability of the plants (interspecific variability). These results could be explained by a Zn-dependent control of stem growth (intraspecific variability). Results in *Figure 1C* showed the variation in root lengths. The ZnO (150 mg/L) and ZnO (300 mg/L) treatments give the longest roots in pea, which reach 30 cm and 35 cm, respectively, and significantly different from the control (15 cm). In white beans, which are more sensitive to contamination of the nutrient medium by ZnO-NPs, root development regressed by more than 20% compared to the control. These results proved that the effectiveness of treatment with ZnO-NPs depended on the applied dose in both varieties of beans (inter- and/or intra-specific variability). No significant effect of ZnO-NPs on the number of roots was recorded for the three species (*Fig. 1D*). The impact of nanoparticle on plant varied in relation to its size, concentration, and exposure methodology. Based on the available reports, we proposed the possible implication of the same mechanism against ZnO-NPs stress for Fabaceae plants. It is a general response for both plants.

Results in *Table 3* show significant effects of ZnO-NPs varying within the same species. This was a kind of specific resistance. Results presented in *Table 4* showed a significant variation in responses between species. We suggested a genetic control of ZnO-NPs induced growth. The results presented in *Figure 1E* and *F* show that the addition of ZnO-NPs induced leaf area and number of plant leaves after 20 days of development in hydroponic environments.

Water content, fresh weight and dry weight varied significantly when plants were exposed to ZnO-NPs (*Fig. 2*). The application of zinc oxide nanoparticles induced an

http://www.aloki.hu ● ISSN 1589 1623 (Print) ● ISSN 1785 0037 (Online)
DOI: http://dx.doi.org/10.15666/aeer/2005_38933909

excessive accumulation of water in plant organs. The highest levels were highlighted for the ZnO- treatment (150 mg/L). The treatment of beans with ZnO-NPs (300 mg) kept organ water contents of control levels. pea dry weight showed no significant effect when changed ZnO-NPs dose, in contrary for beans (*Table 5*). The responses varied significantly among the three species (*Table 6*).

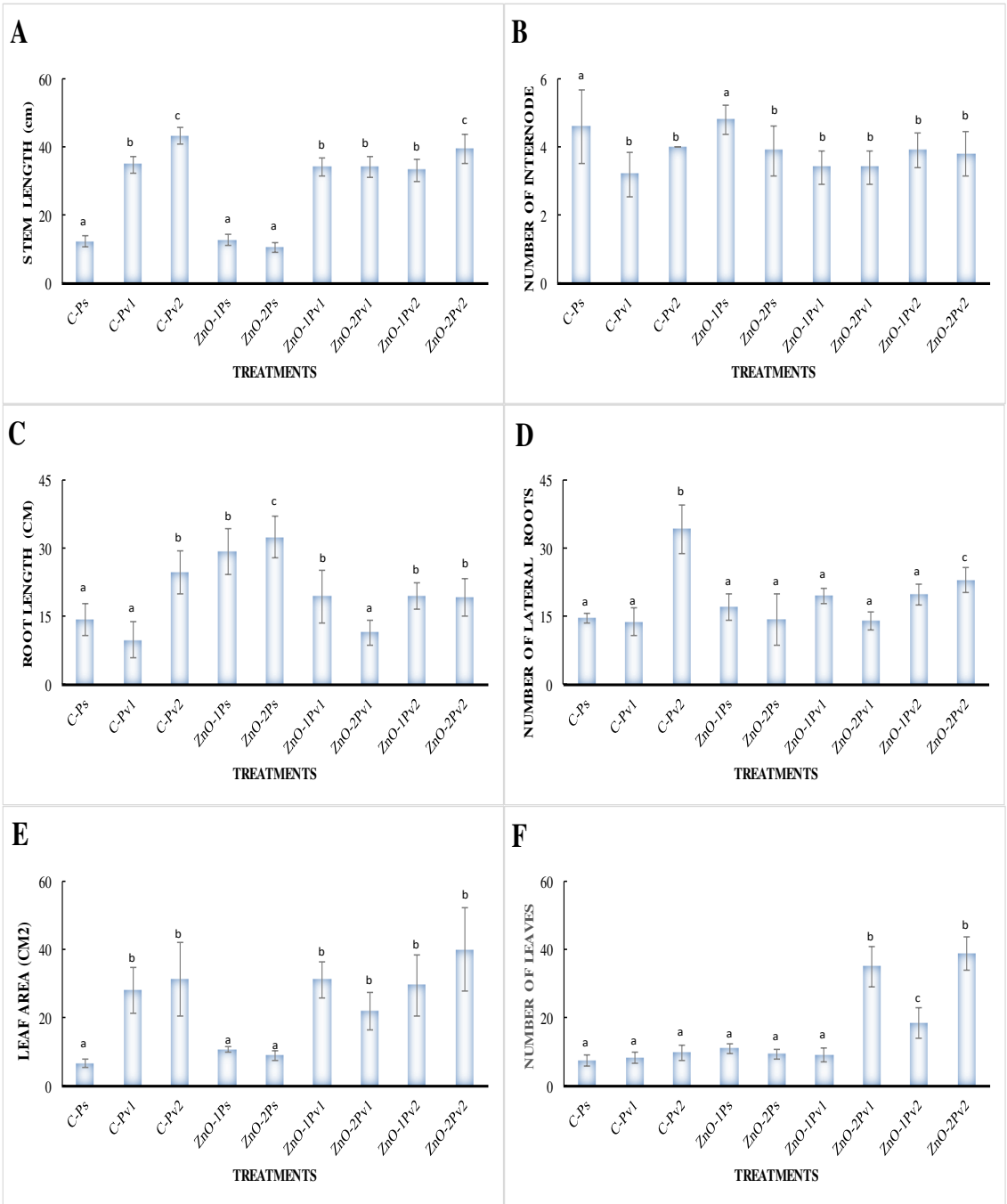

Figure 1. *(A) Stem length, (B) Number of enter node, (C) Root length, (D) Number of lateral roots, (E) Leaf area and (F) Number of leaves of pea [Pisum sativum L. (Ps)] and beans [Phaseolus vulgaris L. (Pv1) and Vigna angularis (Pv2)] Grown in water (C) or exposed to 150 mg/L (ZnO-1) or 300 mg/L (ZnO-2) of Zinc oxide. Data are the means of 5 repetitions (±SE). Different letters represent significant differences at $p < 0.05$*

http://www.aloki.hu ● ISSN 1589 1623 (Print) ● ISSN 1785 0037 (Online)
DOI: http://dx.doi.org/10.15666/aeer/2005_38933909

Table 3. *The effects of the ZnO concentrations on the growth*

Independent variables	C-Ps	ZnO-1Ps	ZnO-2Ps	C-Ps*ZnO-1Ps	C-Ps*ZnO-2Ps	ZnO-1Ps*ZnO-2Ps	Error
df	5	5	5	25	25	25	
***Pisum sativum* L.**	144.74**	588.65**	390.99**	319.06**	148.76**	1243.68**	MS=3
Independent variables	C-Pv1	ZnO-1Pv1	ZnO-2Pv1	C-Pv1*ZnO-1Pv1	C-Pv1*ZnO-2Pv1	ZnO-1Pv1*ZnO-2Pv1	Error
df	5	5	5	25	25	25	
***Phaseolus vulgaris* L. (Pv1)**	485.03**	158.63**	242.91**	350.34**	765.98**	158.24**	MS=3
Independent variables	C-Pv2	ZnO-1Pv2	ZnO-2Pv2	C-Pv2*ZnO-1Pv2	C-Pv2*ZnO-2Pv2	ZnO-1Pv2*ZnO-2Pv2	Error
df	5	5	5	25	25	25	
***Vigna angularis* (Pv2)**	485.03**	158.63**	242.91**	350.34**	765.98**	158.24**	MS=3

Asterisks indicate statistical significance (P < 0.05)

Table 4. *The effects of the species on the growth.*

Independent variables	**Ps*Pv1**	**Ps*Pv2**	**Pv1*Pv2**	**Ps*Pv1*Pv2**
df	25	25	25	125
Control	200.06**	675.23**	992.72**	1293.18***
Zno-1	802.75**	812.20**	430.70**	389.77***
ZnO-2	275.66**	422.88**	295.61**	199.06***
Error	MS=3	MS=3	MS=3	MS=2

Asterisks indicate statistical significance (P < 0.05)

Table 5. *The effects of the ZnO concentrations on the productivity*

Independent variables	C-Ps	ZnO-1Ps	ZnO-2Ps	C-Ps*ZnO-1Ps	C-Ps*ZnO-2Ps	ZnO-1Ps*ZnO-2Ps	Error
df	5	5	5	25	25	25	
***Pisum sativum* L.**	4056.00**	-	-	4056.00**	4056.00**	-	MS=3
Independent variables	C-Pv1	ZnO-1Pv1	ZnO-2Pv1	C-Pv1*ZnO-1Pv1	C-Pv1*ZnO-2Pv1	ZnO-1Pv1*ZnO-2Pv1	Error
df	5	5	5	25	25	25	
***Phaseolus vulgaris* L. (Pv1)**	29.36**	86.65**	25.20**	40.08**	15.01**	70.07**	MS=3
Independent variables	C-Pv2	ZnO-1Pv2	ZnO-2Pv2	C-Pv2*ZnO-1Pv2	C-Pv2*ZnO-2Pv2	ZnO-1Pv2*ZnO-2Pv2	Error
df	5	5	5	25	25	25	
***Vigna angularis* (Pv2)**	31.63**	32.64**	48.75**	12.25**	25.49**	19.40**	MS=3

Asterisks indicate statistical significance (P < 0.05)

http://www.aloki.hu ● ISSN 1589 1623 (Print) ● ISSN 1785 0037 (Online)
DOI: http://dx.doi.org/10.15666/aeer/2005_38933909

Table 6. *The effects of the species on the productivity*

Independent variables	Ps*Pv1	Ps*Pv2	Pv1*Pv2	Ps*Pv1*Pv2
df	25	25	25	125
Control	4056.00**	1767.65**	17.72**	17.72***
Zno-1	86.65**	32.64**	416.17**	416.17***
ZnO-2	25.20**	48.75**	79.59**	79.59***
Error	MS=4	MS=4	MS=3	MS=3

Asterisks indicate statistical significance (P < 0.05)

The results in *Figure 3* showed a significant reduction in chl a and b levels after treatment with nanoparticles (ZnO-NPs) compared to the control on 20-day-old pea leaves. Treatment of beans with ZnO-NPs (300 mg) maintains values of the controls. Chlorophyll metabolism (mg/L) showed significant changes under 0-300 mg/L of Zinc oxide (*Table 7*). The significant variations between species in response to nanoparticles shows that these responses are genetically controlled at the level of chlorophyll metabolism (*Table 8*).

In the stems, the results in *Figure 4* showed responses significantly changed according to the cell organelle (compartment) and the dose of nanoparticle. The cytosolic isoforms have the highest activity for ZnO treatment (150 mg/L), followed by the mitochondrial isoforms for ZnO treatment (300 mg/L). In leaves, significant responses are recorded after ZnO treatment in the different analyzed cell compartments. The ZnO treatment (300 mg/L) stimulated GPOX activity in the mitochondria and chloroplasts by 80% compared to the control. The ZnO treatment (150 mg/L) stimulated activity in the cytosol and mitochondria by 50%. The addition of ZnO nanoparticles in the roots gives the highest stimulation. The addition of ZnO-NPs induced GPOX activity in both bean varieties. The effect of ZnO-NPs varied according to the applied dose and the involved isoforms. The activities of the cytosolic and chloroplastic isoforms increased proportionally with increasing doses of NPs-ZnO. They are inversely proportional to the dose in the mitochondria. Several studies showed the role of peroxidases in the response to various stimuli. At the root level, peroxidases do not behave in the same way. These peroxidases were stimulated after treatment with ZnO-NPs in a dose-proportional manner in red beans, but inversely proportional in the white variety. In the root mitochondria we did not see any significant effects. Metabolic adaptation can be based either on the functioning of the primitive pathways which would have been preserved in the higher plants and which would allow an active metabolism (mitochondrial pathway) or, on the contrary, on the establishment of a slowed-down life (cytosolic pathway). In both cases, it is the maintenance of certain metabolic balances that must be fundamental to produce adaptation. Results of GPOX activities and their interactions with resistance and tolerance under 0-300 mg/L of Zinc oxide were presented in *Tables 9* and *10*. It appear that control of oxidative stress induced by ZnO nanoparticles varied significantly due to applicable dose and species.

http://www.aloki.hu ● ISSN 1589 1623 (Print) ● ISSN 1785 0037 (Online)
DOI: http://dx.doi.org/10.15666/aeer/2005_38933909

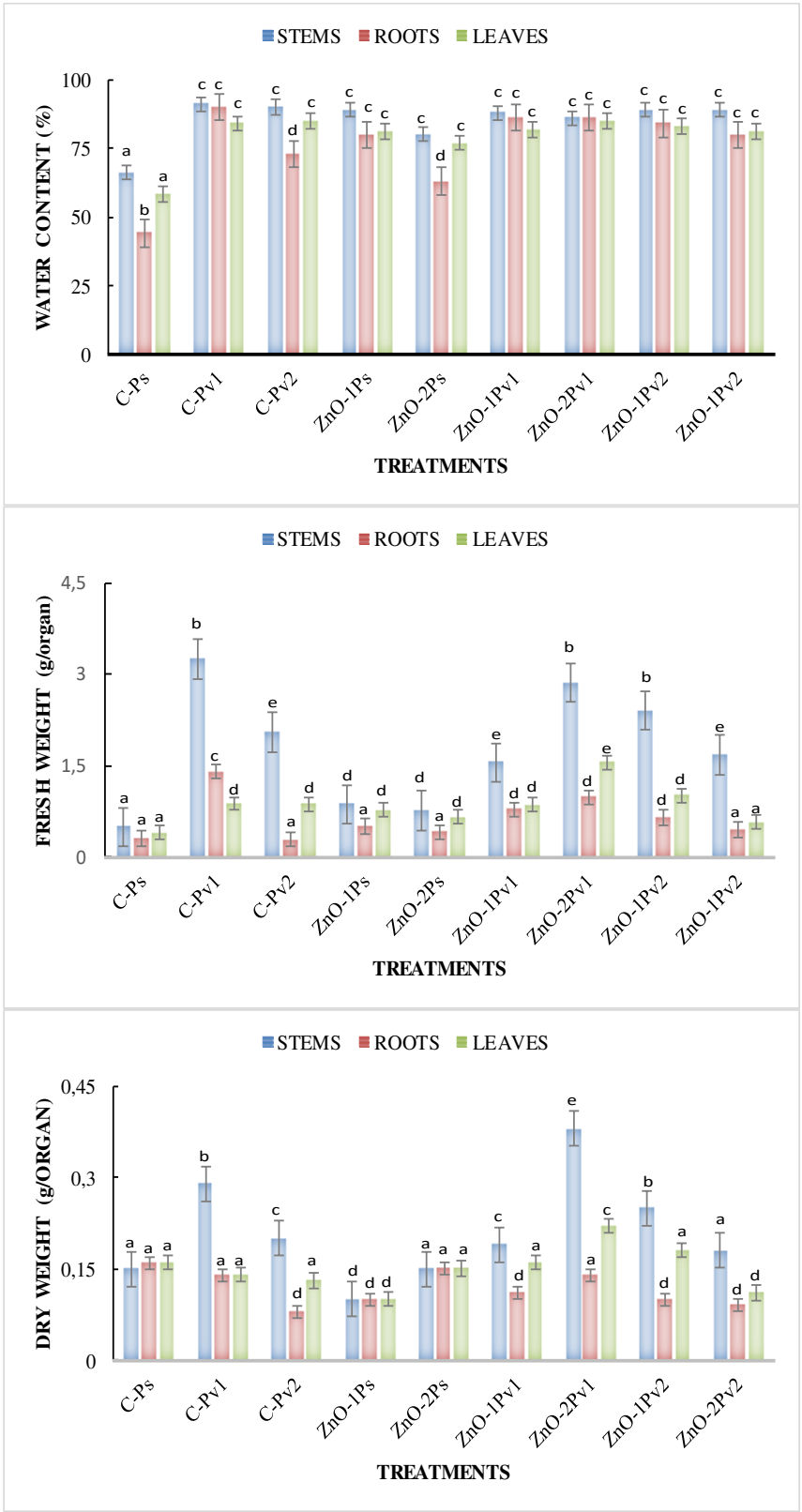

Figure 2. *(A) Water content, (B) Fresh weight and (C) Dry weight of pea [Pisum sativum L. (Ps)] and beans [Phaseolus vulgaris L. (Pv1) and Vigna angularis (Pv2)] Grown in water (C) or exposed to 150 mg/L (ZnO-1) or 300 mg/L (ZnO-2) of Zinc oxide. Data are the means of 5 repetitions (±SE). Different letters represent significant differences at $p < 0.05$*

http://www.aloki.hu ● ISSN 1589 1623 (Print) ● ISSN 1785 0037 (Online)
DOI: http://dx.doi.org/10.15666/aeer/2005_38933909

The ZnO treatment (300 mg/L) stimulated catalase activity at the cytosol level by 115% compared to control (*Fig. 5*). The ZnO (150 mg/L) and ZnO (300 mg/L) treatment stimulates this activity in the chloroplast by 200%. At leaf level, cytosolic isoforms have the highest activity for ZnO treatment (150 mg/L), followed by mitochondrial isoforms for ZnO treatment (150 mg/L). At the root level, the addition of ZnO nanoparticles stimulates catalase activity, especially for the cytosolic and mitochondrial isoforms. ZnO-NPs treatment inhibited the cytosolic and chloroplastic catalase activities in a dose-dependent manner in both bean varieties, but inhibited the cytosolic catalase activity of the red variety and the mitochondrial catalase activity of the white variety. Catalase activity in roots was induced by ZnO-NPs. The cytosolic catalase activities were induced by 50-100% for the red variety and 75-170% in the white variety in the presence of ZnO-NPs. Mitochondrial catalase activities were induced after seed soaking or irrigation of plants in the white variety. Catalase activities are regulated by ZnO-NPs (*Tables 11* and *12*).

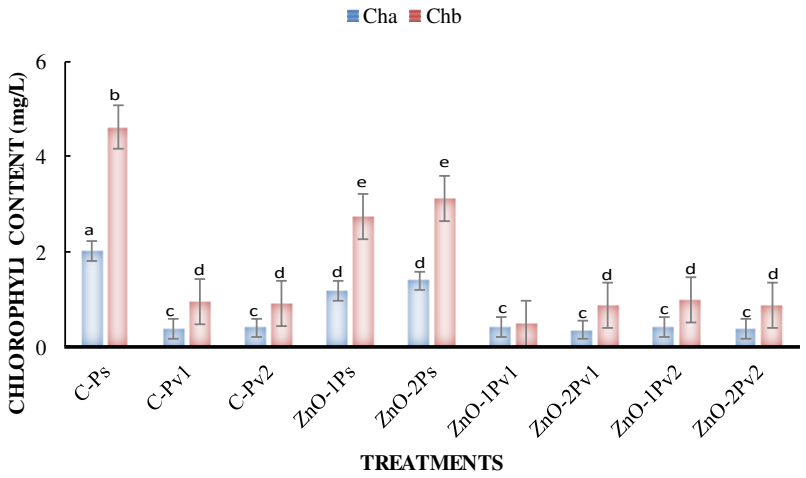

Figure 3. *Chlorophyll a and b of pea [Pisum sativum L. (Ps)] and beans [Phaseolus vulgaris L. (Pv1) and Vigna angularis (Pv2)] Grown in water (C) or exposed to 150 mg/L (ZnO-1) or 300 mg/L (ZnO-2) of Zinc oxide. Data are the means of 5 repetitions (±SE). Different letters represent significant differences at p < 0.05*

Table 7. *The effects of the ZnO concentrations on the chlorophyll metabolism*

Independent variables	C-Ps	ZnO-1Ps	ZnO-2Ps	C-Ps*ZnO-1Ps	C-Ps*ZnO-2Ps	ZnO-1Ps*ZnO-2Ps	Error
df	5	5	5	25	25	25	
***Pisum sativum* L.**	31.59**	30.16**	32.34**	31.59**	31.59**	32.34**	MS=4
Independent variables	C-Pv1	ZnO-1Pv1	ZnO-2Pv1	C-Pv1*ZnO-1Pv1	C-Pv1*ZnO-2Pv1	ZnO-1Pv1*ZnO-2Pv1	Error
df	5	5	5	25	25	25	
***Phaseolus vulgaris* L. (Pv1)**	27.77**	442.99**	27.57**	27.77**	27.77**	27.77**	MS=4
Independent variables	C-Pv2	ZnO-1Pv2	ZnO-2Pv2	C-Pv2*ZnO-1Pv2	C-Pv2*ZnO-2Pv2	ZnO-1Pv2*ZnO-2Pv2	Error
df	5	5	5	25	25	25	
***Vigna angularis* (Pv2)**	30.37**	27.72**	29.92**	30.37**	30.37**	27.72**	MS=4

Asterisks indicate statistical significance (P < 0.05)

http://www.aloki.hu ● ISSN 1589 1623 (Print) ● ISSN 1785 0037 (Online)
DOI: http://dx.doi.org/10.15666/aeer/2005_38933909

Table 8. *The effects of the species on the chlorophyll metabolism*

Independent variables	**Ps*Pv1**	**Ps*Pv2**	**Pv1*Pv2**	**Ps*Pv1*Pv2**
df	25	25	25	125
Control	31.59**	31.59**	27.77**	27.77***
Zno-1	30.16**	30.16**	27.72**	27.72***
ZnO-2	32.34**	32.34**	27.57**	27.57***
Error	MS=4	MS=4	MS=4	MS=4

Asterisks indicate statistical significance (P < 0.05)

Table 9. *The effects of the ZnO concentrations on the oxidative stress metabolism*

Independent variables	C-Ps	ZnO-1Ps	ZnO-2Ps	C-Ps*ZnO-1Ps	C-Ps*ZnO-2Ps	ZnO-1Ps*ZnO-2Ps	Error
df	5	5	5	25	25	25	
***Pisum sativum* L.**	6495.47**	61.00**	70.13**	45750.20**	149808.10**	802.95**	MS=3
Independent variables	C-Pv1	ZnO-1Pv1	ZnO-2Pv1	C-Pv1*ZnO-1Pv1	C-Pv1*ZnO-2Pv1	ZnO-1Pv1*ZnO-2Pv1	Error
df	5	5	5	25	25	25	
***Phaseolus vulgaris* L. (Pv1)**	84.53**	61.00**	70.13**	332.78**	130.38**	2579.92**	MS=3
Independent variables	C-Pv2	ZnO-1Pv2	ZnO-2Pv2	C-Pv2*ZnO-1Pv2	C-Pv2*ZnO-2Pv2	ZnO-1Pv2*ZnO-2Pv2	Error
df	5	5	5	25	25	25	
***Vigna angularis* (Pv2)**	24.82**	37.31**	209.07**	1213.30**	216.46**	169.33**	MS=3

Asterisks indicate statistical significance (P < 0.05)

Table 10. *The effects of the species on the oxidative stress metabolism*

Independent variables	**Ps*Pv1**	**Ps*Pv2**	**Pv1*Pv2**	**Ps*Pv1*Pv2**
df	25	25	25	125
Control	23715.68**	3984.47**	70.44**	70.44***
Zno-1	336.22**	24.34**	365.24**	365.24***
ZnO-2	580.86**	1552.89**	143.98**	143.98***
Error	MS=3	MS=3	MS=3	MS=3

Asterisks indicate statistical significance (P < 0.05)

http://www.aloki.hu ● ISSN 1589 1623 (Print) ● ISSN 1785 0037 (Online)
DOI: http://dx.doi.org/10.15666/aeer/2005_38933909

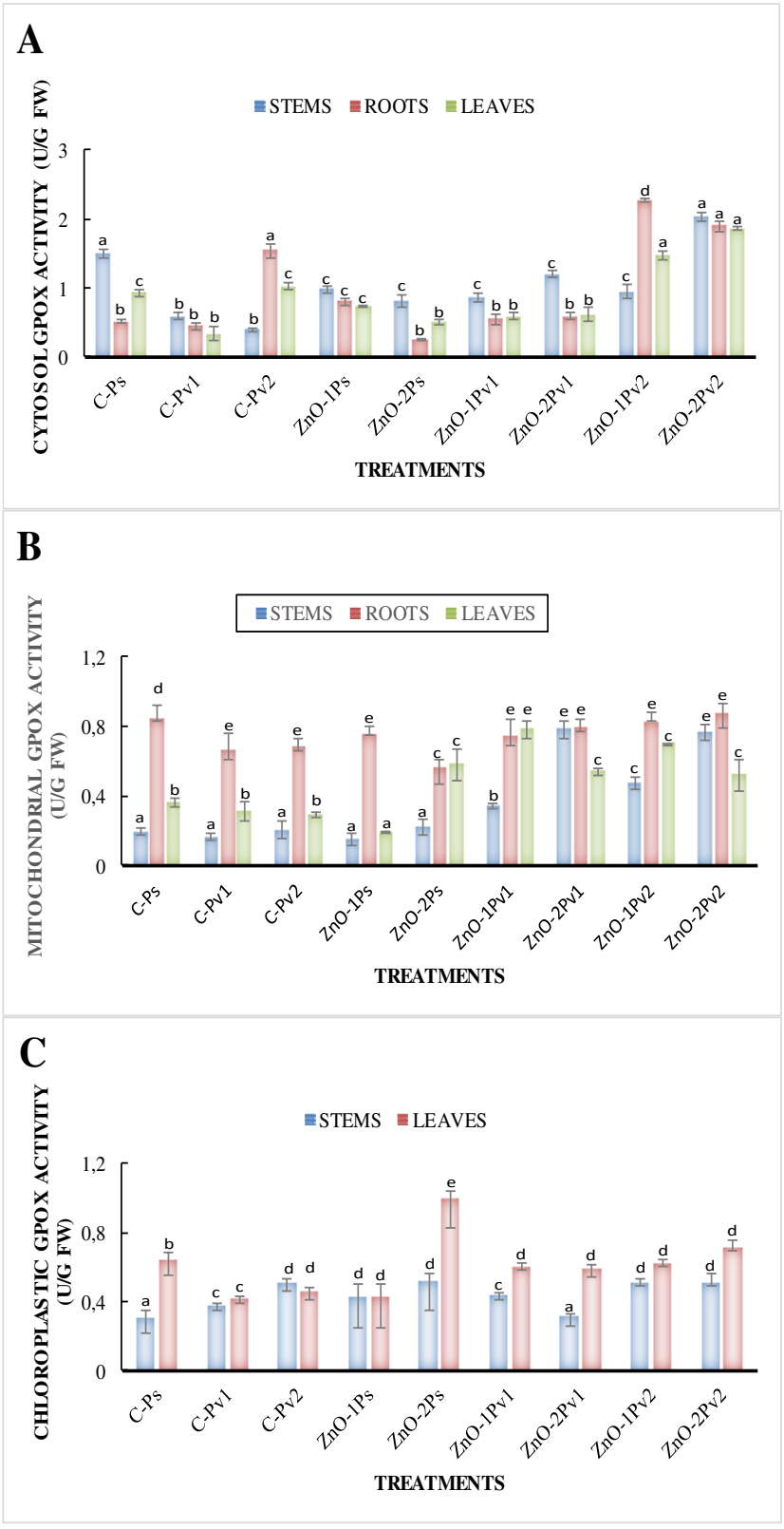

Figure 4. *Guaiacol peroxidase activity in (A) Cytosol, (B) Mitochondria and (C) Chloroplast of pea [Pisum sativum L. (Ps)] and beans [Phaseolus vulgaris L. (Pv1) and Vigna angularis (Pv2)] Grown in water (C) or exposed to 150 mg/L (ZnO-1) or 300 mg/L (ZnO-2) of Zinc oxide. Data are the means of 5 repetitions (±SE). Different letters represent significant differences at* $p < 0.05$

http://www.aloki.hu ● ISSN 1589 1623 (Print) ● ISSN 1785 0037 (Online)
DOI: http://dx.doi.org/10.15666/aeer/2005_38933909

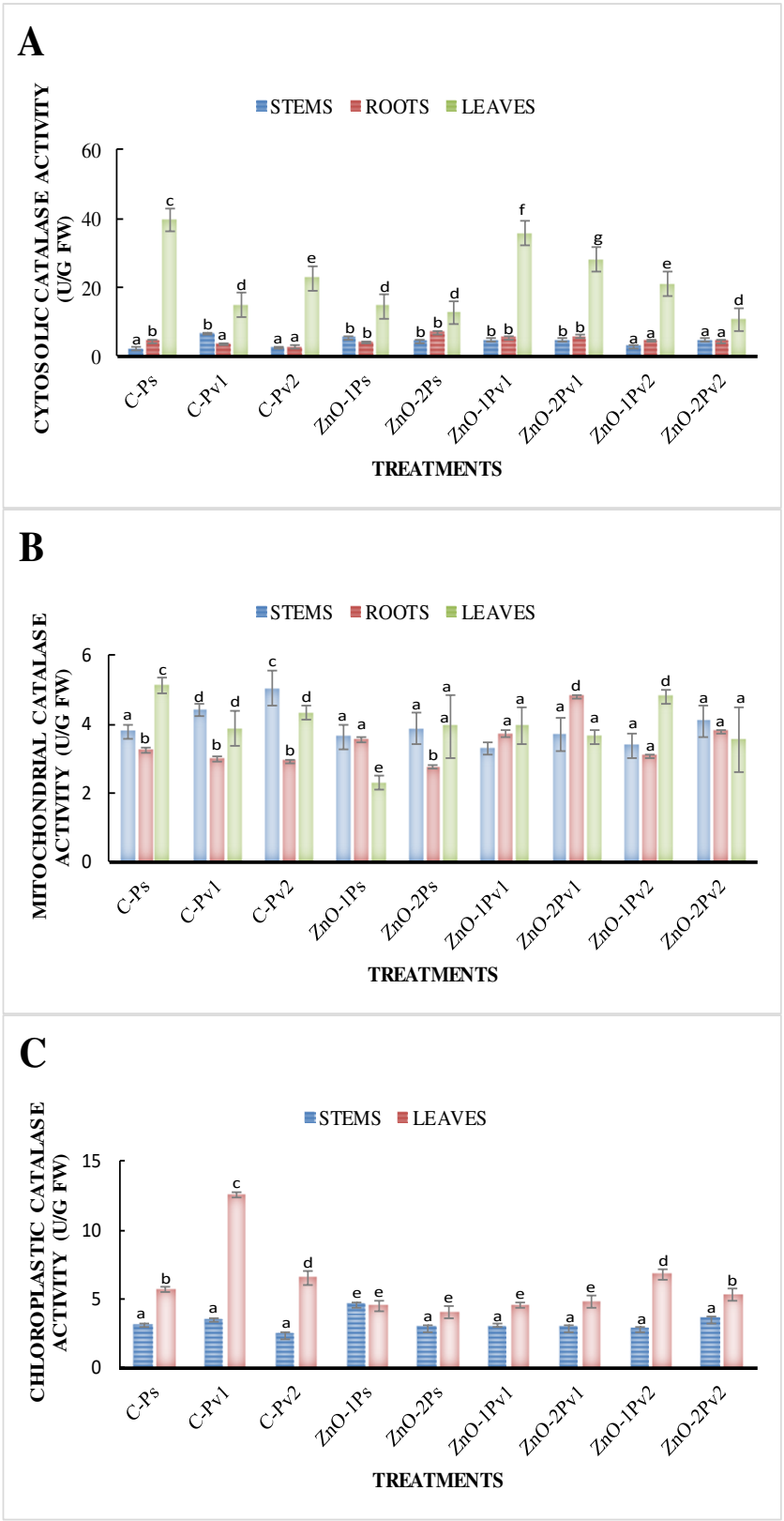

Figure 5. *Catalase activity in (A) Cytosol, (B) Mitochondria and (C) Chloroplast of pea [Pisum sativum L. (Ps)] and beans [Phaseolus vulgaris L. (Pv1) and Vigna angularis (Pv2)] Grown in water (C) or exposed to 150 mg/L (ZnO-1) or 300 mg/L (ZnO-2) of Zinc oxide. Data are the means of 5 repetitions (±SE). Different letters represent significant differences at $p < 0.05$*

http://www.aloki.hu ● ISSN 1589 1623 (Print) ● ISSN 1785 0037 (Online)
DOI: http://dx.doi.org/10.15666/aeer/2005_38933909

Table 11. *The effects of the ZnO concentrations on the antioxidant systems*

Independent variables	C-Ps	ZnO-1Ps	ZnO-2Ps	C-Ps*ZnO-1Ps	C-Ps*ZnO-2Ps	ZnO-1Ps*ZnO-2Ps	Error
df	5	5	5	25	25	25	
***Pisum sativum* L.**	7.27**	15.01**	9.48**	15.64**	9.41**	21.28**	MS=3
Independent variables	C-Pv1	ZnO-1Pv1	ZnO-2Pv1	C-Pv1*ZnO-1Pv1	C-Pv1*ZnO-2Pv1	ZnO-1Pv1*ZnO-2Pv1	Error
df	5	5	5	25	25	25	
***Phaseolus vulgaris* L. (Pv1)**	45.70**	77.31**	10.66**	30.17**	80.40**	180.32**	MS=3
Independent variables	C-Pv2	ZnO-1Pv2	ZnO-2Pv2	C-Pv2*ZnO-1Pv2	C-Pv2*ZnO-2Pv2	ZnO-1Pv2*ZnO-2Pv2	Error
df	5	5	5	25	25	25	
***Vigna angularis* (Pv2)**	17.49**	12.83**	72.59**	35.48**	72.59**	864.12**	MS=3

Asterisks indicate statistical significance (P < 0.05)

Table 12. *The effects of the species on the antioxidant systems*

Independent variables	**Ps*Pv1**	**Ps*Pv2**	**Pv1*Pv2**	**Ps*Pv1*Pv2**
df	25	25	25	125
Control	122.63**	87.56**	34.19**	34.19***
Zno-1	53.47**	5.82**	175.35**	175.35***
ZnO-2	4.76**	22769.41**	1213.21**	1213.21***
Error	MS=3	MS=3	MS=3	MS=3

Asterisks indicate statistical significance (P < 0.05)

Discussion

The obtained results showed that the sensitivity of the two varieties changed from one genotype to the other. This study was consistent with several studies on the differential sensitivity of legumes to metals (Siddiqui et al., 2015). These results suggested that enzymatic antioxidant system responses (GPOX and catalase) are carried out by isoforms specific to each compartment. The stimulation of the defense system after application of each stimulus could also explain the improved growth of pea plants.

Significant changes were due to genetic variability. All the results obtained show that this was a genetic control of the responses of pea and bean plants to the enrichment of the environment by nanoparticles. The dose of ZnO controlled intensity of the responses of each plant. In previous research, application of zinc oxide nanoparticles induced growth of *Brassica juncea* (Mazumder et al., 2020) and reduced genetic impairment under salt stress in tomato (*Solanum lycopersicum* L. 'Linda') (Hosseinpour et al., 2020). Researchers analyzed the impact of zinc oxide nanoparticles on cytotoxicity, genotoxicity and mRNA expression in tomato (Sun et al., 2020a, b) and barley

http://www.aloki.hu ● ISSN 1589 1623 (Print) ● ISSN 1785 0037 (Online)
DOI: http://dx.doi.org/10.15666/aeer/2005_38933909

(*Hordeum vulgare* L.) seedlings Plaksenkova et al. (2020). Missaoui et al. (2021) showed that TiO_2 affected growth due to changes in nanoparticle availability and accumulation. Faizan et al. (2019) showed that effective use of zinc oxide nanoparticles through root dipping on the performance of growth, quality, photosynthesis and antioxidant system in tomato. Zinc oxide nanoparticles disturbed germination and seedling growth in *Allium cepa* L. (Tymoszuk and Wojnarowicz, 2020). Alabdallah and Alzahrani (2020) described the potential mitigation effect of ZnO nanoparticles on *Abelmoschus esculentus* L. metabolism under salt stress conditions.

Nanoparticles alter the plant's capacity to absorb and transport some nutrients. NPs produced increases in the contents of Mg, Zn and Mn, and a decline in the contents of Fe and Cu in leaves and stems (Missaoui et al., 2021). Physiological disturbances could be correlated with exposure to ZnO-NPs. The application of ZnO-NPs in agriculture has indicated variable impacts on plant growth (Rajpu et al., 2021). Biomass accumulation in the vegetative growth phase of a plant can therefore be regarded as the ultimate expression of its metabolic performance. Taking into account the various studies on the effects of zinc nanoparticles on plants, it appeared that there was an interaction between metabolism, growth and stress. The distribution of metabolites between growth, production of defense compounds and storage compounds therefore has to be very tightly regulated.

Conclusions

We evaluated the effectiveness of nanoparticles by studying the interaction of ZnO-NPS with plant production (growth and photosynthesis) and the defense system (oxidative stress and enzymatic antioxidant system: GPOX and CAT) of pea (*Pisum sativum* var. Alicia), white bean (*Phaseolus vulgaris* L.) and red bean (*Vigna angularis*) seedlings. We analyzed the responses on the basis of genetic variability (tolerance) and within the same species (resistance). We used the results of the analyses for the prediction of growth control, metabolism and defense mechanisms against the presence of ZnO-NPs in the three species.

An application of ZnO-NPs increased plant production. These responses vary according to ZnO-NPs doses. A positive dose effect in root and a negative dose effect in stem. We suggested that there was a specificity of responses for each organ. These responses could be due to the anatomical and functional properties of the different tested organs.

The antioxidant system responses were carried out by specific isoforms of each compartment. The responses of the cytosolic, chloroplast and mitochondrial isoforms varied according to ZnO-NPs doses. Stimulation of the defense system after application of ZnO-NPs could also explain the improved plant growth. ZnO-dependent root control varied in the two bean varieties. This work will be continued in the future with more genotypes of pea and beans. We used actually for the present work the genotypes available in the region.

http://www.aloki.hu ● ISSN 1589 1623 (Print) ● ISSN 1785 0037 (Online)
DOI: http://dx.doi.org/10.15666/aeer/2005_38933909

REFERENCES

[1] Aebi, H. (1984): Catalase *in vitro*. Chap. 13. – In: Packer, L. (ed.) Oxygen Radicals in Biological Systems. Methods in Enzymology 105. Elsevier, Amsterdam, pp. 121-126. https://doi.org/10.1016/S0076-6879(84)05016-3.

[2] Ahmed, M. Z., Khan, M. A. (2010): Tolerance and recovery responses of playa halophytes to light, salinity and temperature stresses during seed germination. – Flora 205(11): 764-771. https://doi.org/10.1016/j.flora.2009.10.003.

[3] Alabdallah, N. M., Alzahrani, H. S. (2020): The potential mitigation effect of ZnO nanoparticles on [*Abelmoschus esculentus* L. Moench] metabolism under salt stress conditions. – Saudi Journal of Biological Sciences 27(11): 3132-3137. DOI: 10.1016/j.sjbs.2020.08.005.

[4] Basahi, M. A. (2018): Seed germination of the halophyte Anabasis setifera (Amaranthaceae) from Saudi Arabia. – Botany 96: 643-651. https://doi.org/10.1139/cjb-2018-0053.

[5] Catiempo, R. L., Photchanachai, S., Bayogan, E. R. V., Chalermchai, W. (2021): Impact of hydropriming on germination and seedling establishment of sunflower seeds at elevated temperature. – Plant, Soil and Environment 67: 491-498. https://doi.org/10.17221/163/2021-PSE.

[6] Chemingui, H., Missaoui, T., Mzali, J. C., Smiri, M., Hafiane, A., Yatmaz, H. C. (2019a): Facile green synthesis of zinc oxide nanoparticles (ZnO NPs): Antibacterial and photocatalytic activities. – Materials Research Express 6(10): 1050B4. https://doi.org/10.1088/2053-1591/ab3cd6.

[7] Chemingui, H., Smiri, M., Missaoui, T., Hafiane, A. (2019b): Zinc oxide nanoparticles induced oxidative stress and changes in the photosynthetic apparatus in fenugreek (*Trigonella foenum graecum* L.). – Bulletin of Environmental Contamination and Toxicology 102: 477-485. https://doi.org/10.1007/s00128-019-02590-5.

[8] Chemingui, H., Chékir, M. J., Missaoui, T., Konyar, M., Smiri, M., Cengiz, Y. H., Hafiane, A. (2021): Characteristic of Er-doped zinc oxide layer: application to color removal of synthetic dye solution. – Desalination and Water Treatment 402-413. DOI: https://doi.org/10.5004/dwt.2021.26644.

[9] Cooper, J. (2007): Basic terminology and definitions in plant pathology. – https://s3.wp.wsu.edu/uploads/sites/2054/2014/04/TermsandDefinitions_001.pdf.

[10] Dietz, D. M., Laplant, Q., Watts, E. L., Hodes, G. E., Russo, S. J., Feng, J., Oosting, R. S., Vialou, V., Nestler, E. J. (2011): Paternal transmission of stress-induced pathologies. – Biological Psychiatry 70: 408-414. DOI: 10.1016/j.biopsych.2011.05.005.

[11] Faizan, M., Faraz, A., Hayat, S. (2019): Effective use of zinc oxide nanoparticles through root dipping on the performance of growth, quality, photosynthesis and antioxidant system in tomato. – Journal of Plant Biochemistry and Biotechnology 29: 553-567. DOI: 10.1007/s13562-019-00525-z.

[12] Fielding, J. L., Hall, J. L. (1978): Biochemical and cytochemical study of peroxidase activity in roots of *Pisum sativum*: i. a comparison of dab-peroxidase and guaiacol-peroxidase with particular emphasis on the properties of cell wall activity. – Journal of Experimental Botany 29(4): 969-981. https://doi.org/10.1093/jxb/29.4.969.

[13] Ghafariyan, M. H., Malakouti, M. J., Dadpour, M. R., Stroeve, P., Mahmoudi, M. (2013): Effects of magnetite nanoparticles on soybean chlorophyll. – Environmental Science & Technology 47(18): 10645-52. DOI: 10.1021/es402249b.

[14] Guey, F., Smiri, M., Chemingui, H., Dekhil, A. B., Elarbaoui, S., Hafiane, A. (2020): Remove of humic acid from water using magnetite nanoparticles. – European Journal of Advanced Chemistry Research 1: 4-9. DOI: http://dx.doi.org/10.24018/ejchem.

[15] Hoagland, D. R., Arnon, D. I. (1950): The water culture method for growing plants without soil. – California Agricultural Experiment Station 347: 1-32.

http://www.aloki.hu ● ISSN 1589 1623 (Print) ● ISSN 1785 0037 (Online)
DOI: http://dx.doi.org/10.15666/aeer/2005_38933909

[16] Hosseinpour, A., Haliloglu, K., Cinisli, T. K., Ozkan, G., Ozturk, H. I., Pour-Aboughadareh, A., Poczai, P. (2020): Application of zinc oxide nanoparticles and plant growth promoting bacteria reduces genetic impairment under salt stress in tomato (*Solanum lycopersicum* L. 'Linda'). – Agriculture 10: 521. https://doi.org/10.3390/agriculture10110521.

[17] Koch, K. G., Chapman, K., Louis, J., Heng-Moss, T., Sarath, G. (2016): plant tolerance: a unique approach to control hemipteran pests. – Frontiers in Plant Science 7. DOI: 10.3389/fpls.2016.01363.

[18] Koller, E. (2004): Traitement des pollutions industrielles. – Technical and Engineering Collection - Environment and Safety Series. Paris, pp. 59-90. https://www.eyrolles.com/BTP/Livre/traitement-des-pollutions-industrielles-9782100521043/.

[19] Larue, C., Khodja, H., Herlin-Boime, N., Brisset, F., Flank, A. M., Fayard, B., Chaillou, S., Carrière, M. (2011): Investigation of titanium dioxide nanoparticles toxicity and uptake by plants. – Journal of Physics: Conference Series 304: 012057.

[20] Lichtenthaler, H. K., Wellburn, A. R. (1983): Determinations of total carote-noids and chlorophylls a and b of leaf extracts in different solvents. – Biochemical Society Transactions 11591-11603. https://doi.org/10.1042/bst0110591.

[21] Ma, C., Chhikara, S., Xing, B., Musante, C., White, J. C., Dhankher, O. P. (2013): Physiological and molecular response of *Arabidopsis thaliana* (L.) to nanoparticle cerium and indium oxide exposure. – American Chemical Society Sustainable Chemistry & Engineering 1(7): 768-778. https://doi.org/10.1021/sc400098h.

[22] Mazumder, J. A., Khan, E., Perwez, M., Gupta, M., Kumar, S., Raza, K., Sardar, M. (2020): Exposure of biosynthesized nanoscale ZnO to *Brassica juncea* crop plant: morphological, biochemical and molecular aspects. – Scientific Reports 10: 8531. https://doi.org/10.1038/s41598-020-65271-y.

[23] Missaoui, T., Smiri, M., Chemingui, H., Hafiane, A. (2017): Effects of nanosized titanium dioxide on the photosynthetic metabolism of fenugreek (*Trigonella foenum graecum* L.). – Comptes Rendus Biologies 340(11-12): 499-511. DOI: 10.1016/j.crvi.2017.09.004.

[24] Missaoui, T., Smiri, M., Chemingui, H., Jbira, E., Hafiane, A. (2018): Regulation of mitochondrial and cytosol antioxidant systems of fenugreek (*Trigonella foenum graecum,* L.) exposed to nanosized titanium dioxide. – Bulletin of Environmental Contamination and Toxicology 101: 326-337. https://doi.org/10.1007/s00128-018-2414-5.

[25] Missaoui, T., Smiri, M., Chemingui, H., Alhalili, Z., Hafiane, A. (2020): Disturbance in mineral nutrition of fenugreek grown in water polluted with nanosized titanium dioxide. – Bulletin of Environmental Contamination and Toxicology 106: 327-333. DOI: https://doi.org/10.1007/s00128-020-03051-0.

[26] Missaoui, T., Smiri, M., Chemingui, H., Hafiane, A. (2021): Effect of nanosized TiO_2 on redox properties in fenugreek (*Trigonella foenum graecum* L.) during germination. – Environmental Processes 8: 843-867. https://doi.org/10.1007/s40710-020-00493-w.

[27] Peterson, R. K. D., Varella, A. C., Higley, L. G. (2017): Tolerance: the forgotten child of plant resistance. – PeerJ 5: e3934. DOI: 10.7717/peerj.3934.

[28] Plaksenkova, I., Kokina, I., Petrova, A., Jermaļonoka, M., Gerbreders, V., Krasovska, M. (2020): The impact of zinc oxide nanoparticles on cytotoxicity, genotoxicity, and miRNA expression in barley (*Hordeum vulgare* L.) seedlings. – Scientific World Journal 1-13. DOI: 10.1155/2020/6649746.

[29] Qiu, Y., Guo, J., Jing, S., Tang, M., Zhu, L., He, G. (2011): Identification of antibiosis and tolerance in rice varieties carrying brown plant hopper resistance genes. – Entomologia Experimentalis et Applicata 141:224-231. DOI: 10.1111/j.1570-7458.2011.01192.x.

[30] Rajput, V. D., Minkina, T., Fedorenko, A., Chernikova, N., Hassan, T., Mandzhieva, S., Sushkova, S., Lysenko, V., Soldatov, M. A., Burachevskaya, M. (2021): Effects of zinc

http://www.aloki.hu ● ISSN 1589 1623 (Print) ● ISSN 1785 0037 (Online)
DOI: http://dx.doi.org/10.15666/aeer/2005_38933909

oxide nanoparticles on physiological and anatomical indices in spring barley tissues. – Nanomaterials 11: 1722. https://doi.org/10.3390/nano11071722.

[31] Siddiqui, M. H., Al-Whaibi, M. H., Firoz, M., Al-Khaishany, M. Y. (2015): Nanotechnology and plant sciences. Nanoparticles and their impact on plants. – Springer, Cham, pp. 19-35.

[32] Smiri, M., Chaoui, A., El Ferjani, E. (2009): Respiratory metabolism in the embryonic axis of germinating pea seed exposed to cadmium. – Journal of Plant Physiology 166: 259-269. https://doi.org/10.1016/j.jplph.2008.05.006.

[33] Smith, C. M. (2005): Plant Resistance to Arthropods: Molecular and Conventional Approaches. – Springer, Dordrecht.

[34] Strauss, S. Y., Agrawal, A. A. (1999): The ecology and evolution of plant tolerance to herbivory. – Trends in Ecology & Evolution 14: 179-185. DOI: 10.1016/s0169-5347(98)01576-6.

[35] Sun, L., Wang, Y., Wang, R., Wang, R., Zhang, P., Ju, Q., Xu, J. (2020a): Physiological, transcriptomic and metabolomic analyses reveal zinc oxide nanoparticles modulate plant growth in tomato. – Environmental Science: Nano 7: 3587-3604. DOI: 10.1039/d0en00723d.

[36] Sun, S., Guo, Z., Liu, L., Xiangnan, L. (2020b): Nano-ZnO-induced drought tolerance is associated with melatonin synthesis and metabolism in maize. – International Journal of Molecular Sciences 21(3): 782. DOI: 10.3390/ijms21030782.

[37] Tymoszuk, A., Wojnarowicz, J. (2020): Zinc oxide and zinc oxide nanoparticles impact on in vitro germination and seedling growth in *Allium cepa* L. – Materials 13(12): 2784. DOI: 10.3390/ma13122784.

http://www.aloki.hu ● ISSN 1589 1623 (Print) ● ISSN 1785 0037 (Online)
DOI: http://dx.doi.org/10.15666/aeer/2005_38933909

EFFECTS OF SOIL EXOGENOUS NITROGEN ON BAMBOO (*DENDROCALAMUS LATIFLORUS* MUNRO) SHOOTS, PHOTOSYNTHETIC CHARACTERISTICS, AND NITROGEN METABOLISM

FAN, L.[1] – TARIN, M. W. K.[2] – HAN, Y.[1] – LI, B.[1] – RONG, J.[1] – CHEN, L.[1] – HE, T.[1] – ZHENG, Y.[1*]

[1]*College of Forestry, Fujian Agriculture and Forestry University Fuzhou, Fujian 350002, People's Republic of China*

[2]*College of Arts & College of Landscape Architecture, Fujian Agriculture and Forestry University, Fuzhou, Fujian 350002, People's Republic of China*

[*]*Corresponding author*
e-mail: zys1960@163.com; phone: +86-50-397-265

(Received 14th Feb 2022; accepted 10th Jun 2022)

Abstract. Nitrogen (N) is an essential nutrient element that is involved in almost every aspect of a plant's physiological mechanism. Therefore, the current research aims to determine the optimal amount of N fertilizer for bamboo seedlings for better nutrient management practices to minimize N pollution in bamboo forests. We evaluated the physiological response of *Dendrocalamus latiflorus* Munro grown under five varying levels of N fertilizer; such as N0, N1, N2, N3, N4, and N5 (0, 1.50, 3.00, 4.50, 6.00, and 7.50 $g \cdot pot^{-1}$, respectively). N4 treatment had a significant effect on the number of shoots, which was greatly correlated with net photosynthetic rate (P_n) and photosynthetic pigment including carotenoid (Car), total chlorophyll (Chls), and Chl a per b ratio (Chl a/b) as well as N-related indices [leaf N, leaf ammonium N (NH_4^+-N), and nitrate reductase (NR)]. N supply significantly increased soil carbon and N contents, which could be conducive to the accumulation of leaf chlorophyll content, improving leaf photosynthesis mechanism, and accelerating N metabolism and conversion through an enzymatic reaction. Overall, the N application of 6.00 $g \cdot pot^{-1}$ was advantageous to improving physiological characteristics and shoot production of seedlings, which provided a theoretical basis for improving bamboo nitrogen use efficiency and high-yield cultivation.
Keywords: *nitrogen application, bamboo seedlings, photosynthetic physiological characteristics, nitrogen-related enzyme activity*

Introduction

Nitrogen (N) is an essential macronutrient element that is required by plants in higher amounts relative to other essential nutrients (Kirova et al., 2005). N is involved in almost every aspect of a plant's physiological metabolism being a most essential nutritional component (Kishorekumar et al., 2020a). At the physiological level, N may trigger both the nitrate (NO_3^-) assimilatory mechanism and the regulation of carbon (C) metabolism that can provide C skeletons and reductants for this process (Stitt, 1999). At the developmental stage, N regulates activities such as leaf expansion (Walch-Liu et al., 2000), root branching (Forde and Lorenzo, 2002), and resource allocation between axillary bud and root growth (Scheible et al., 1997). N and other elements in the plant are responsible for the synthesis of amino acids, proteins, nucleic acids, chlorophyll, and other compounds (Talukder et al., 2016; Wen et al., 2020). Furthermore, N can also regulate the adaptation mechanism of plants to the environment and play an important role in the adaptation of plants to adversity (Krouk et al., 2010). Simultaneously, exogenous N can significantly affect the N metabolism in plants as well as a certain

http://www.aloki.hu ● ISSN 1589 1623 (Print) ● ISSN1785 0037 (Online)
DOI: http://dx.doi.org/10.15666/aeer/2005_39113926

degree of impact on its related enzymatic activities, thereby affecting plant growth (Xing et al., 2018).

N, being a necessary component, has the potential to change plant proteins as well as plant photosynthesis (Kishorekumar et al., 2020b; Liu et al., 2020). In general, when the N concentration increases, the leaf's photosynthetic rate (P_n) and transpiration rate (T_r) increase while the intercellular CO_2 concentration (C_i) decreases (Li et al., 2017; Mu and Chen, 2021). Furthermore, increasing the amount of N fertilizer can also increase the leaf's chlorophyll contents and alleviate the reduction in photosynthetic efficiency (Zhou et al., 2017a). Previous studies have shown that N fertilizer application can effectively increase the chlorophyll contents and net photosynthetic rate of agricultural or horticultural crops, such as rice (Kurai et al., 2011; Zhou et al., 2017b), wheat (Kataria and Guruprasad, 2015), peanut (Liu et al., 2019), etc. As a result, in the current research, we attempt to gain insight into the photosynthetic capacity of *Dendrocalamus latiflorus* Munro grown under varying N levels.

Soil is a part of the ecosystem, where the contents of essential nutrients can not only reveal the utilization of soil nutrients but also explore the regulatory and metabolic balance mechanisms of elements such as C and N in plants and soil (Kleinhenz et al., 2003). Since, both C and N are essential nutrient elements in the soil and are required for plant growth and development (Krapp and Castaings, 2012). Plants uptake the nutrients from the soil via roots, which are greatly influenced by the external environment, especially by fertilizers (Bargaz et al., 2018). Therefore, the nutritional changes (C and N) in plants can explore the nutrient distribution ratio and status of plants, as well as the internal connection between soil and plants.

N metabolism is one of the important physiological metabolic processes in plants (O'Brien et al., 2016). Nitrate reductase (NR) is the main N metabolizing enzyme of higher plants. The metabolic enzyme activity of plant leaves and roots is related to the accumulation of N in plants (Fu et al., 2020a). Glutamine synthetase (GS) is the first enzyme to be isolated, purified, and identified from plants, and it is also the first enzyme to be found to be related to the storage form of plant N (Seabra and Carvalho, 2015). GS converts the inorganic ammonia absorbed by plants into an organic form in glutamine (Gln) and glutamic acid (Glu) as N donors in the biosynthesis of N-containing organics in higher plants (Yang et al., 2016). NR and GS are all inducible enzymes that affect the metabolism and transformation of N in plants, which play an important role in the absorption and transformation of nutrient elements to affect plant growth.

Fertilization is an important measure to improve bamboo cultivation. As one of the main factors affecting bamboo growth, N has a great influence on the growth and development of bamboo. Previous research has shown that optimum N fertilization can effectively improve the photosynthetic capacity, growth, and productivity of shoots and timber in bamboo forests (Xu et al., 2014; Gao et al., 2016). At present, N fertilization in bamboo forests is relatively systematic in China, but the phenomenon of soil deterioration and environmental degradation caused by fertilization still exists (Zhu and Chen, 2002). Increased use of N fertilizers will also exacerbate the increase in nitrous oxide (N_2O) emissions from the soil (Xu et al., 2014). In order to increase the yield of bamboo forests and protect the ecological environment, it is necessary to further improve the utilization efficiency of N fertilizer in bamboo forests.

D. latiflorus Munro has become the main cultivated bamboo species for shoots in China by the features of its strong adaptability, long shoot period, and high yield of bamboo shoots. *D. latiflorus* Munro has a large leaf area and continuous rainfall in the

http://www.aloki.hu ● ISSN 1589 1623 (Print) ● ISSN1785 0037 (Online)
DOI: http://dx.doi.org/10.15666/aeer/2005_39113926

early stage of bamboo shoots in southern China, which would exacerbate the lack of sunlight in the forest understory. Nutrient management can also alleviate the stress caused by low light, improve the photosynthetic capacity of bamboo, and increase its productivity. Therefore, in the current study, *D. latiflorus* Munro seedlings were established under various levels of N-based fertilizer, to assess its efficacy on shoot growth. The study will provide valuable insights into optimum N requirements for the growth of *D. latiflorus* Munro seedlings. The main goals of our experiment were (i) to distinguish the effect of different levels of N on physiological and biochemical attributes of the seedlings; (ii) to identify the effect of N application on soil properties and the growth pattern in the seedlings; (iii) to determine the reasonable amount of N applied to bamboo shoots.

Material and Methods

Study sites

The greenhouse experiment was carried out in the greenhouse of the College of Forestry, Fujian Agriculture and Forestry (*Fig. 1*). The study site was located (119°13′51.18″ E, 26°05′4.35″ N) in Fuzhou, Fujian province, China, where the average solar radiation per year was 1246 kW·hm^{-2}. The maximum temperature in the greenhouse was controlled below 35°C, and the relative air humidity was kept above 85%.

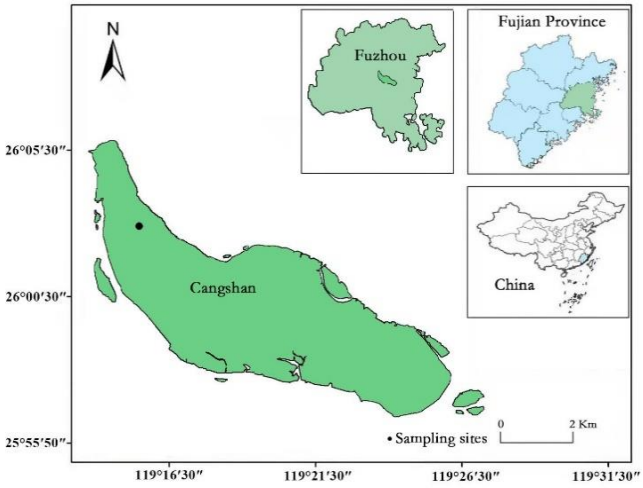

Figure 1. *The geographical location of Fujian Agriculture and Forestry University*

Plant material and soil

Three-year-old seedlings of *D. latiflorus* were grown in PVC pots with a diameter of 30 cm and a height of 33 cm. The potting substrate material was yellow soil and peat (volume ratio 3:1) with a weight of 15 kg per pot. The basic properties of soil were as follows: pH value, 5.77; organic C, 13.67 g·kg^{-1}; total N, 0.35 g·kg^{-1}; total phosphorus (P), 0.50 g·kg^{-1}; total potassium (K), 50.01 g·kg^{-1}. The basic growth attributes of *D. latiflorus* Munro seedlings cultured from October 2018 were as follows: mean height, 105.51 cm; mean DBH, 4.67 mm; north-south crown, 71.11 cm; east-west crown, 68.95 cm.

http://www.aloki.hu ● ISSN 1589 1623 (Print) ● ISSN1785 0037 (Online)
DOI: http://dx.doi.org/10.15666/aeer/2005_39113926

Experiment design

In the current research, we used five N treatment combinations; N0, N1, N2, N3, N4, and N5, like 0, 1.50, 3.00, 4.50, 6.00, and 7.50 g of N in each pot, respectively. N was applied three times such as April (30%), May (40%), and June (30%), respectively in 2019. The amount of exogenous N applied to the seedlings of *D. latiflorus* Munro has been presented in *Table 1*. All treatments were replicated 15 times. Three months later when nitrogen was completely added, leaf gas exchange parameters were measured, after that, the leaf tissues were collected for the estimation of chlorophyll content, N-related indices, and C content. Soil samples were also collected to measure N-related indices and C content. The experiment started in April and ended in October.

Table 1. *The amount of exogenous N (g·pot^{-1}) applied to D. latiflorus Munro seedlings*

Fertilization times	**Treatments (g·pot^{-1})**					
	CK	N1	N2	N3	N4	N5
I (April)	0	0.45	0.90	1.35	1.80	2.25
II (May)	0	0.60	1.20	1.80	2.40	3.00
III (June)	0	0.45	0.90	1.35	1.80	2.25
Total amount	0	1.50	3.00	4.50	6.00	7.50

Urea (mass fraction 46%) was applied as N fertilizer, calcium superphosphate (P_2O_5, mass fraction 12%), and potassium chloride (K_2O, mass fraction 60%) were used as phosphate and potassium fertilizer, respectively. Among them, phosphate and potassium fertilizer were applied only once, and the dosages were 6.00 and 1.50 g·pot^{-1}, respectively. Weeding and other cultural practices were carried out regularly during the entire experiment.

Investigation of the number of bamboo shoots

After every two days, the number of shoots from each replicate was recorded from beginning to end. The bamboo shoots (semi-lignified state) were harvested after they attained a height of approximately 50 cm (*Fig. 2*). The bamboo shoots were not retained in shooting initial-phase and metaphase, and new bamboo shoots were retained at the end of shooting. The purpose of cutting bamboo shoots was to remove the apical dominance of the bamboo shoots and stimulate the germination of dormant shoots at the base of the bamboo stump.

Figure 2. *Schematic diagram of bamboo shoots growth of D. latiflorus Munro seedlings*

http://www.aloki.hu ● ISSN 1589 1623 (Print) ● ISSN1785 0037 (Online)
DOI: http://dx.doi.org/10.15666/aeer/2005_39113926

Determination of leaf gas exchange parameters and chlorophyll content

Li-6400 photosynthesis system (Li-Cor Inc., Lincoln, USA) was used to determine the gas exchange parameters, including P_n, C_i, T_r, stomatal conductance (*Cond*), and water use efficiency (WUE) from 2-3 mature functional leaves during consecutive sunny days. The LED (red and blue) light source was used with 1600 $\mu mol \cdot m^{-2} \cdot s^{-1}$ photosynthetically active radiation (PAR). The seedlings were measured from all replicates, however, before the measurement, the sampling leaves were induced under a light intensity of 1600 $\mu mol \cdot m^{-2} \cdot s^{-1}$ PAR for 20-30 min.

Following the assessment of gas exchange parameters, fresh leaves were cut to determine the concentrations of the photosynthetic pigments. After the separation of the midrib, the fresh leaves were cut into pieces and weighed 0.20 g. A mixed solution (pure acetone: absolute ethanol: distilled water = 4.5: 4.5:1) of 25 ml (Gao, 2006) was used to extract the photosynthetic pigments directly in the dark for 48 h. Chlorophyll a (Chl a), b (Chl b), total chlorophylls (Chls), and carotenoid (Car) contents were calculated by optical density (OD) values according to the equations of Lichtenthaler (1987), and the ratios of chlorophyll a per b ratio (Chl a/b) and carotenoid per total chlorophyll ratio (Car/Chls) were further calculated.

Determination of leaf N indices and C content

After the extraction of leaf chlorophyll, part of fresh leaves was chopped, mixed, weighed, stored in liquid N, and then stored at -80°C refrigerator for measuring. Fresh leaves were used to estimate the activities of leaf Gs and NR, leaf ammonium N (NH_4^+-N), and nitrate N (NO_3^--N) using the kit manufactured by Suzhou Keming Biotechnology Co., Ltd. After chopping and mixing, another part of fresh leaves was oven-dried at 105°C for 15 minutes and later at 85°C to dry to constant weight. Furthermore, the dried samples were grinded with an ultra-high-speed pulverizer (HUANGCHENG HC-300Y, China) and sieved through a 0.15 mm sieve. The total C and N contents were determined using an element analyzer (VARIO MAX, ELEMENTAR, Germany), and their ratio was further calculated.

Determination of soil C and N indices

Similarly, the fresh soil samples were taken from a distance of 10 cm and a depth of 10 cm around the bamboo stump. After removing stones and roots, each soil sample was separated into two portions: One portion was used to determine soil NH_4^+-N and NO_3^--N using the chemical kits. The other was air-dried, grinded, and sieved to 0.15 mm to determine total C and N contents using an element analyzer (VARIO MAX, ELEMENTAR, Germany), and their ratios were also calculated.

Data analysis

All the data were expressed as means and standard errors. Analysis of variance (one-way ANOVA) was performed using SPSS 20.0 to determine the effect of N treatments, and Tukey HSD test was used to identify significant differences (α=0.05) between mean values. The statistical data was adopted for principal component analysis (PCA) to analyze relationships among the number of shoots, leaf biochemical attributes, and soil C and N properties under different N treatments. Origin 9.5 and Prism 8.0 were used for graphical illustrations and Microsoft Excel-2016 was used for the table.

http://www.aloki.hu ● ISSN 1589 1623 (Print) ● ISSN1785 0037 (Online)
DOI: http://dx.doi.org/10.15666/aeer/2005_39113926

Results

Impact of N application on the number of bamboo shoots

We noticed that N application significantly influenced the number of bamboo shoots (*Fig. 3*). *D. latiflorus* Munro established under N4 treatment increased their shoots up to 68.75% (P<0.05) compared to N0.

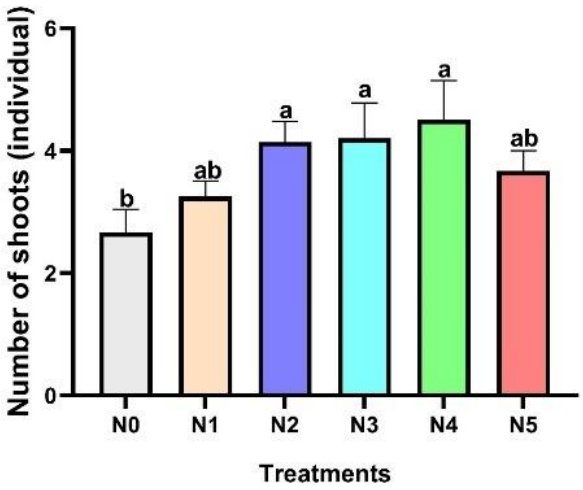

Figure 3. *Impact of various N application rates on the number of bamboo seedlings. N0: 0 g·pot^{-1}, N1: 1.50 g·pot^{-1}, N2: 3.00 g·pot^{-1}, N3: 4.50 g·pot^{-1}, N4: 6.00 g·pot^{-1}, and N5: 7.50 g·pot^{-1}, respectively. Different letters indicate significant differences ($P < 0.05$) in the mean between different nitrogen treatments and ± denotes the standard errors of the means (SE) (n = 4)*

Leaf photosynthetic pigments concentrations under various N application rates

Under various N application rates, the leaves photosynthetic pigments (Car, Chls, and Chl a/b) concentrations increased as depicted in *Figure 4*. Compared to N0, under N4 and N5 treatments, significant increases of 100.00% and 109.60%, 99.08% and 110.52% (P<0.05) respectively were observed for Chls and Car (*Fig. 4A–B*). N3 treatment exhibited the maximum Chl a/b compared to other treatments (*Fig. 4C*). Besides, for Car/Chls, seedlings established under the N application did not show any difference (*Fig. 4D*).

Leaf gas exchange parameters under various N application rates

The N application had a significant (P<0.05) effect on leaf P_n (*Fig. 5A*). Specifically, N4 and N5 treatments resulted in a significant rise in leaf P_n relative to N0, whereas N4 was found the most effective over all other treatments combinations. In addition, the rise in *Cond* was parallel to the N application rate (*Fig. 5B*) and seedlings established under N4 treatment greatly (P<0.05) enhanced their leaf *Cond* (106.57%) as compared to N0. In contrast, compared to N0, none of N based treatments influenced the C_i and T_r significantly (*Fig. 5C and D*). Besides, seedlings under N4 treatment exhibited a relatively greater (P<0.05) *WUE* compared to N1 and N2 treatments (*Fig. 5E*).

http://www.aloki.hu ● ISSN 1589 1623 (Print) ● ISSN1785 0037 (Online)
DOI: http://dx.doi.org/10.15666/aeer/2005_39113926

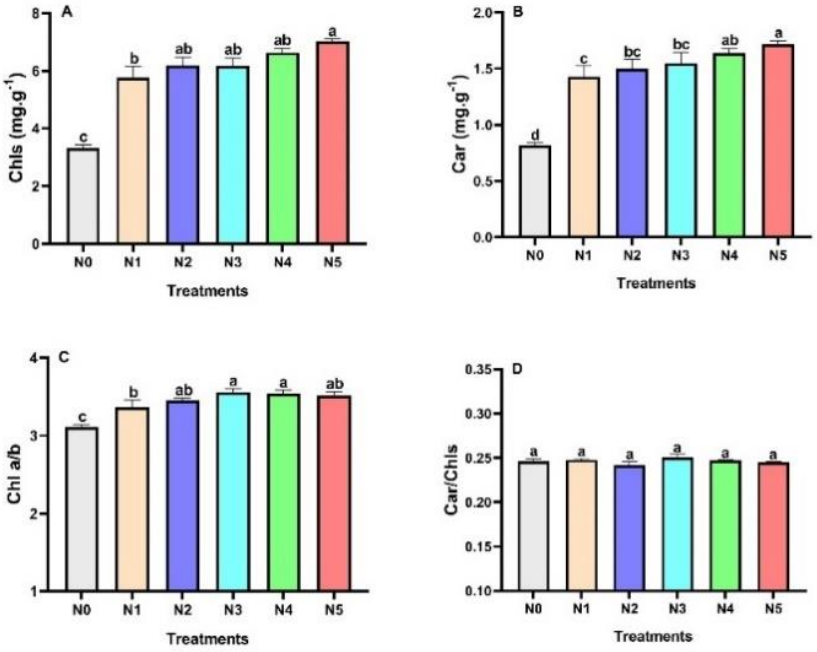

Figure 4. *Leaf photosynthetic pigments under different N application rates. (A) Chls – total chlorophylls, (B) Car – carotenoids, (C) Chl a/b – chlorophyll a per b ratio, and (D) Car/Chls – carotenoid per total chlorophylls ratio, respectively. N0: 0 g·pot^{-1}, N1: 1.50 g·pot^{-1}, N2: 3.00 g·pot^{-1}, N3: 4.50 g·pot^{-1}, N4: 6.00 g·pot^{-1}, and N5: 7.50 g·pot^{-1}, respectively. Different letters indicate significant differences ($P < 0.05$) in the mean between different N treatments and ± denotes the standard errors of the means (SE) (n = 4)*

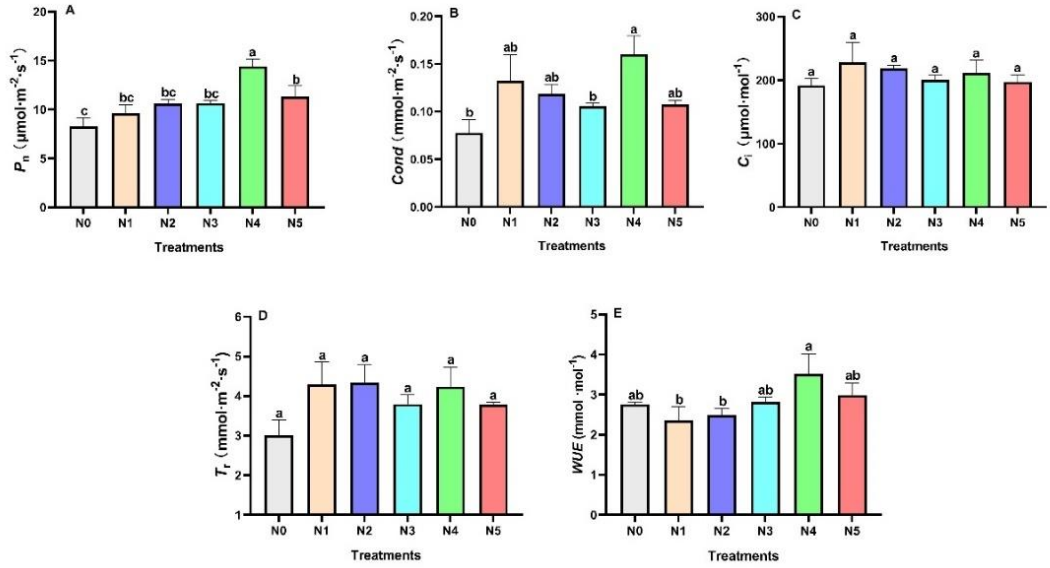

Figure 5. *Leaf gas exchange parameters under different N application rates. (A) P_n – net photosynthetic rate, (B) Cond – stomatal conductance, (C) C_i – intercellular CO_2 concentration, (D) T_r – transpiration rate, and (E) WUE – Water use efficiency, respectively. N0: 0 g·pot^{-1}, N1: 1.50 g·pot^{-1}, N2: 3.00 g·pot^{-1}, N3: 4.50 g·pot^{-1}, N4: 6.00 g·pot^{-1}, and N5: 7.50 g·pot^{-1}, respectively. Different letters indicate significant differences ($P < 0.05$) in the mean between different N treatments and ± denotes the standard errors of the means (SE) (n = 4)*

http://www.aloki.hu ● ISSN 1589 1623 (Print) ● ISSN1785 0037 (Online)
DOI: http://dx.doi.org/10.15666/aeer/2005_39113926

The N and C indices of leaf and soil under various N application rates

Compared to N0, N-treated seedlings accumulated significantly (P<0.05) greater soil N and C contents (*Fig. 6*). Overall, the seedlings treated in N4 treatment responded with maximum concentrations for leaf N and C contents (31.97 and 433.23 g·kg^{-1}, respectively) (*Fig. 6A and B*). In contrast, N5 treatment for the contents of soil N and C were significantly (P<0.05) higher relative to other treatments (*Fig. 6D and E*). Except for N5, the leaf C/N decreased under N application as the level of concentration increased (*Fig. 6C*). Additionally, seedlings amended with N4 treatment responded with maximum soil C/N (*Fig. 6F*).

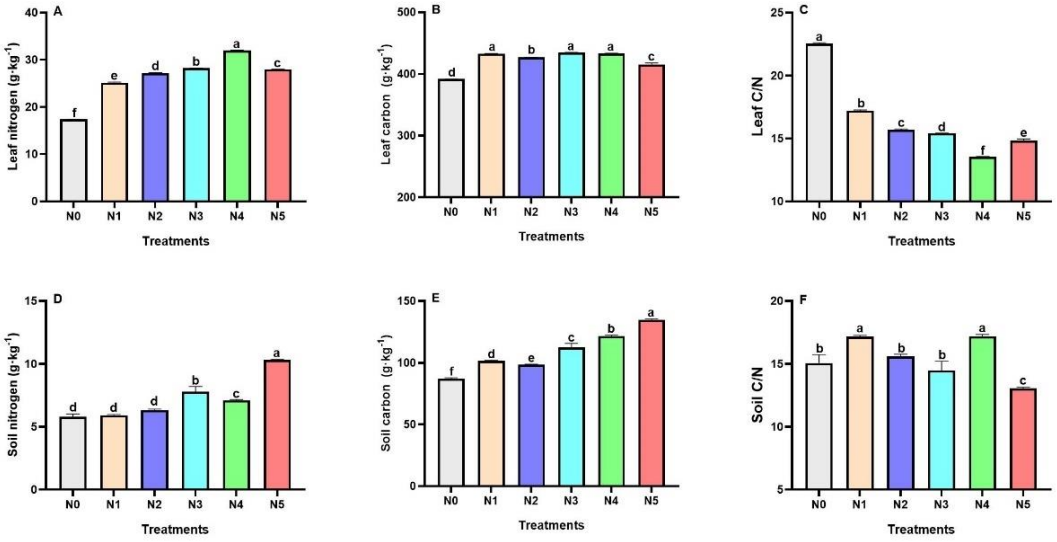

Figure 6. *Total nitrogen and carbon indices of leaf and soil under different N application rates. (A) leaf nitrogen content, (B) leaf carbon content, (C) leaf C/N - leaf carbon per nitrogen ratio, (D) soil total nitrogen content, (E) soil total carbon content, and (F) soil C/N – soil carbon per nitrogen ratio, respectively. N0: 0 g·pot^{-1}, N1: 1.50 g·pot^{-1}, N2: 3.00 g·pot^{-1}, N3: 4.50 g·pot^{-1}, N4: 6.00 g·pot^{-1}, and N5: 7.50 g·pot^{-1}, respectively. Different letters indicate significant differences (P < 0.05) in the mean between different N treatments and ± denotes the standard errors of the means (SE) (n = 4)*

Leaf GS and NR activities under various N application rates

The activities of leaf GS and NR were influenced by N application (*Fig. 7*). Compared to N0, GS activities greatly (P<0.05) increased by 140.55% and 121.13% under N3 and N4 treatments (*Fig. 7A*). However, seedlings established under the N application did not show any significant difference for NR (*Fig. 7B*).

Leaf and soil NH_4^+-N and NO_3^--N under various N application rates

N application determined higher leaf NH_4^+-N in seedlings compared to N0 (*Fig. 8A*). N1, N2, and N3 treatments showed a significant (P<0.05) impact on soil NH_4^+-N, while N4 decreased soil NH_4^+-N by 18.88% compared to N0 (*Fig. 8C*). In contrast, there was a decline under N application amended seedlings for leaf and soil NO_3^--N (*Fig. 8B and D*).

http://www.aloki.hu ● ISSN 1589 1623 (Print) ● ISSN1785 0037 (Online)
DOI: http://dx.doi.org/10.15666/aeer/2005_39113926

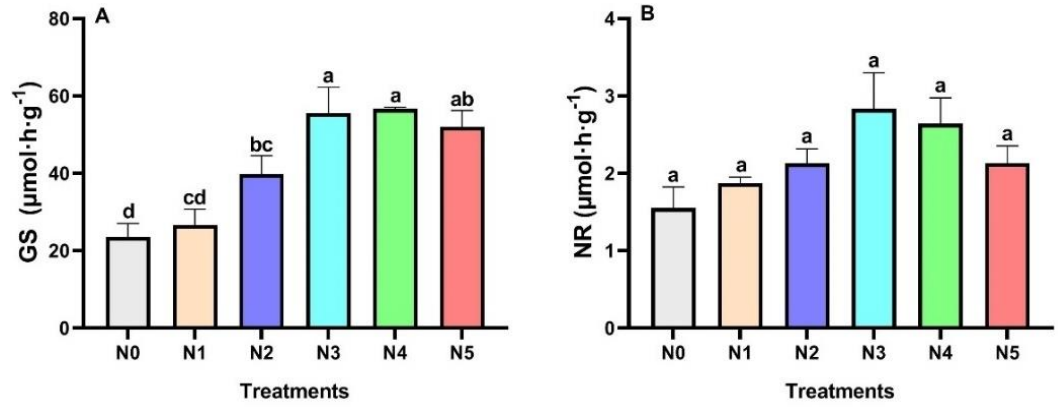

Figure 7. *The activities of leaf GS and NR under different N application rates. (A) GS – glutamine synthetase and (B) NR – nitrate reductase. N0: 0 g·pot^{-1}, N1: 1.50 g·pot^{-1}, N2: 3.00 g·pot^{-1}, N3: 4.50 g·pot^{-1}, N4: 6.00 g·pot^{-1}, and N5: 7.50 g·pot^{-1}, respectively. Different letters indicate significant differences ($P < 0.05$) of mean between different N treatments and ± denotes the standard errors of the means (SE) (n = 4)*

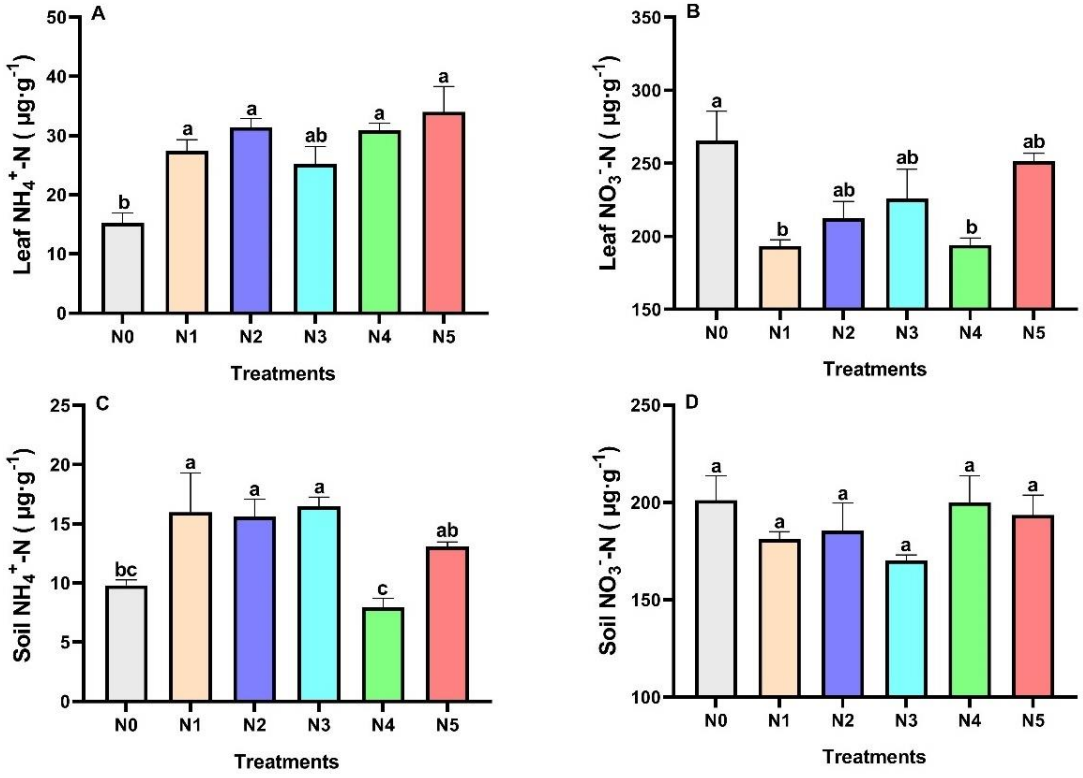

Figure 8. *The contents of NH_4^+-N and NO_3^--N of leaf and soil under different N application rates. (A) leaf NH_4^+-N – leaf ammonium N, (B) leaf NO_3^--N – leaf nitrate N, (C) soil NH_4^+-N – soil ammonium N, and (D) soil NO_3^--N – soil nitrate N, respectively. N0: 0 g·pot^{-1}, N1: 1.50 g·pot^{-1}, N2: 3.00 g·pot^{-1}, N3: 4.50 g·pot^{-1}, N4: 6.00 g·pot^{-1}, and N5: 7.50 g·pot^{-1}, respectively. Different letters indicate significant differences ($P < 0.05$) in the mean between different N treatments and ± denotes the standard errors of the means (SE) (n = 4)*

http://www.aloki.hu ● ISSN 1589 1623 (Print) ● ISSN1785 0037 (Online)
DOI: http://dx.doi.org/10.15666/aeer/2005_39113926

Evaluation of all indices under different N treatments by principal component analysis (PCA)

PCA revealed that the cumulative variance contribution rate of the first two principal components reached 74.47%, suggesting an overall variation of the data (*Fig. 9*). PC1 showed that the number of shoots had a highly positive correlation with photosynthetic pigments (Car, Chls, and Chl a/b), gas exchange parameters (P_n, *Cond*, T_r, and *WUE*), and C and N metabolism related indices (GS, NR, LC, LN, L-NH_4^+, and S-NH_4^+). Except for LC/N, L-NO_3^-, and S-NO_3^-, all indices exhibited with PC1 were favorable following N4 treatment, whereas N0 was correlated with LC/N, S-NO_3^-, and S-NO_3^-.

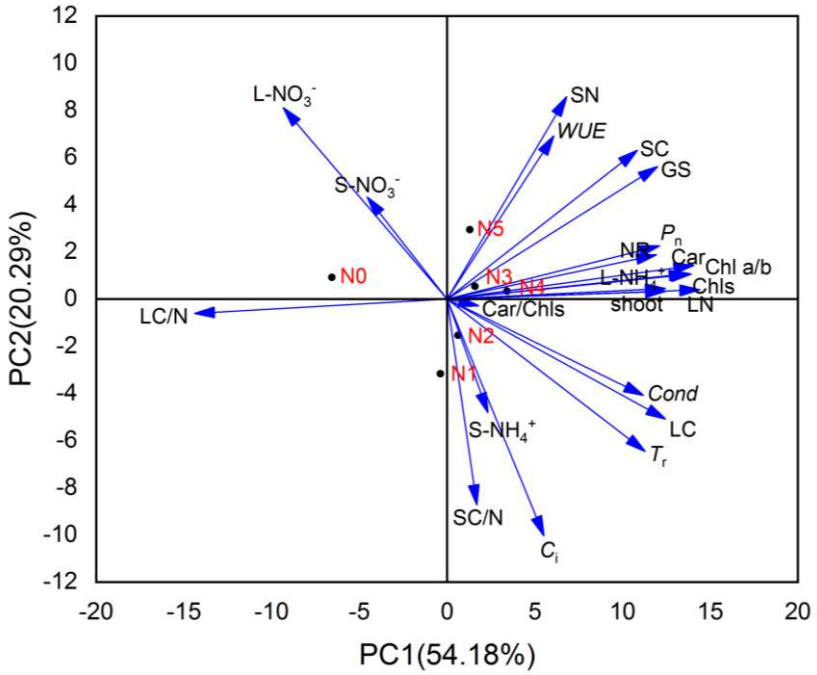

Figure 9. *Biplot of principal component analysis of the first two principal components of all tested parameters and N levels. Shoot – the number of shoots, Chls – total chlorophylls, Car – carotenoid, Chl a/b – chlorophyll a per b ratio, Car/Chls – carotenoid per total chlorophyll ratio, P_n – net photosynthetic rate, Cond – stomatal conductance, C_i – intercellular CO_2 concentration, T_r – transpiration rate, WUE – water use efficiency, GS – glutamine synthetase, NR – nitrate reductase, LN – leaf nitrogen, LC – leaf carbon, LC/N – leaf C per N ratio, SN – soil nitrogen, SC – soil carbon, SC/N – soil C per N ratio, L-NH_4^+ – leaf ammonium N, L-NO_3^- – leaf nitrate N, S-NH_4^+ – soil ammonium N, and S-NO_3^- – soil nitrate N, respectively. N0: 0 g·pot^{-1}, N1: 1.50 g·pot^{-1}, N2: 3.00 g·pot^{-1}, N3: 4.50 g·pot^{-1}, N4: 6.00 g·pot^{-1}, and N5: 7.50 g·pot^{-1}, respectively*

Discussion

In the current study, we noticed that different N levels impacted the number of shoots, leaf photosynthetic characteristics, and soil and leaf N-related indices in *D. latiflorus* Munro seedlings. The optimal N application can substantially increase leaf N and photosynthetic pigments, as well as improve plant photosynthetic efficiency and leaf physiological activities (Peng et al., 2021). The increase in soil C and N contents is conducive to the accumulation of leaf chlorophyll content, improving leaf photosynthetic

http://www.aloki.hu ● ISSN 1589 1623 (Print) ● ISSN1785 0037 (Online)
DOI: http://dx.doi.org/10.15666/aeer/2005_39113926

capacity, and accelerating C and N metabolism and conversion (Manna et al., 2005; Zhang et al., 2019) ultimately increasing the number of shoots, which was also confirmed by our research.

The formation of bamboo shoots is inseparable from the intensity of photosynthesis, N utilization, and transportation (Dordas and Sioulas, 2008). Increasing the application of N fertilizer to some extent may increase the chlorophyll contents, prolong the function period of the leaves, and improve the photosynthetic efficiency, thereby increasing the production capacity of the plant (Liu et al., 2019; Fu et al., 2020b). The current study concluded that N application enhanced the chlorophyll accumulation and improved the photosynthetic efficiency in leaves. For instance, N4 treatment had a positive effect on the accumulation of leaf chlorophylls and P_n in leaves, indicating that optimal N supply can effectively increase leaf chlorophyll contents, which was conducive to improving the photosynthesis mechanism of *D. latiflorus* Munro seedlings.

In plants, nutrient elements play a vital role in maintaining leaf C balance and sustaining photosynthetic efficiency (Matthews et al., 2017). In the current research, N application significantly increased P_n to fix relatively large amounts of C for photosynthesis, which is closely related to N assimilation and metabolic processes (Huang et al., 2013; Zhang et al., 2017). We reported that N4 was advantageous compared to other N treatments in terms of increasing P_n to enhance the C sequestration ability of *D. latiflorus* Munro. Higher *Cond* leads to enhancing leaf photosynthetic biochemical pathways and the accumulation of photosynthetic products (Lichtenthaler et al., 2007a,b). Compared with N0, the values of *Cond*, C_i, T_r, and *WUE* increased to a certain degree of N treatments, which can improve photosynthetic performance in the growth of the seedlings.

N application can effectively increase the contents and reserves of soil organic C and total N content (Huang et al., 2013). The C/N in the soil can reflect the utilization efficiency of the soil, and the application of fertilizer can affect the nutrient element in the soil (Vitousek, 1982). In our research, N treatments significantly improved N availability and increased soil N contents. Similarly, N provided a carbon source and improved the environment in the soil, which promoted the conversion of organic C and increased the organic C content (Cheng et al., 2020), where all N treatments significantly increased soil C content compared to N0. Additionally, previous studies have shown that there is a positive correlation between soil C and N content and crop yield (Wang et al., 2019; Zhang et al., 2019). Our research found that the number of shoots, SC, and SN all had positive correlations. In addition, some studies have shown that the application of N fertilizer significantly increases the N accumulation in leaves, thereby reducing the C/N of the leaves (Liu et al., 2014; Wu et al., 2019), which is consistent with our research. These changes would be conducive to increasing productivity, as well as changing the degradation and mineralization of leaves, which in turn would be conducive to the return of C and N to the soil (Stubbs et al., 2009; Pierik et al., 2011), to ensure the supply essential nutrient to meet the needs of bamboo shoot production.

NR and GS are the key enzymes for N assimilation and ammonia assimilation in plant physiological processes (Xie et al., 2014; Lin et al., 2017). Zhu et al. (2016) found that fertilization can effectively promote the N metabolism of *Phyllostachys edulis*, and enhance the activities of both NR and GS, which is related to the direct promotion of fertilizers and the absorption of N by plants. Our research came to the same conclusion that the activities of NR and GS were enhanced with the application of N fertilization, which can improve the transformation of N metabolism directly. Furthermore, N

http://www.aloki.hu ● ISSN 1589 1623 (Print) ● ISSN1785 0037 (Online)
DOI: http://dx.doi.org/10.15666/aeer/2005_39113926

application would encourage plants to absorb more N to synthesize more NR and GS indirectly.

Compared to N0, the soil and leaf NH_4^+-N was at a significant level under N supply. Soil NH_4^+-N was greatly reduced under N4 treatment in comparison to soil NO_3^--N, indicating that roots of seedlings had higher absorption of NH_4^+-N. The enhanced NR activity under N application could promote the reduction of NO_3^- to more NH_4^+ (Maeda et al., 2014), which possibly promoted to accumulation of NH_4^+-N of leaves in our research. Additionally, compared with other N treatments, the enhanced activity of GS under N4 treatment could be conducive to catalyzing inorganic NH_4^+-N to produce more organic N, which could provide sufficient N not only for bamboo shoot production but also to synthesize more chlorophyll to ensure the photosynthesis of seedlings (Cruz et al., 1993). However, leaf and soil NO_3^--N had an insignificant negative correlation with bamboo shoots, which had an adverse effect on shoots. Our research was consistent with the previous findings that NH_4^+-N can promote leaf chlorophyll synthesis and increase plant production (Sanchez-Zabala et al., 2015; Heuermann et al., 2021).

The PCA analyzed with strong correlations may be screened out and can be used to assess *D. latiflorus* Munro adaptation to varying N levels. According to the PCA results, N4 treatment seems to be advantageous for shoots growth, owing to increased leaf photosynthetic characteristics and soil nutrient availability. In addition, the increased number of bamboo shoots under N4 treatment exhibited strong correlations with chlorophylls pigments and leaf N-related indices, which may regulate the photosynthesis mechanism and promote N accumulation in *D. latiflorus* Munro to fulfill the requirements of a greater number of bamboo shoots.

Conclusions

Exogenous N has varying degrees of influence on the photosynthetic characteristics, nutritional element contents, and N metabolism-related indices of *D. latiflorus* Munro seedlings. We concluded that applying N fertilizer (6 $g \cdot pot^{-1}$) to maximize the growth and shoot production of *D. latiflorus* Munro seedlings was advantageous. We elucidated the N absorption mechanism of the bamboo seedlings as well as the related physiological change mechanism after the application of N fertilizer. These findings not only provide a theoretical basis for improving the N utilization efficiency of *D. latiflorus* Munro but also the production of high-yield and high-quality bamboo shoots in the future.

Competing interests. The authors declare that they have no competing interests.

Acknowledgments. This work was supported by the the "National Key R&D Program of China" (2021YFD2200501).

REFERENCES

[1] Bargaz, A., Lyamlouli, K., Chtouki, M., Zeroual, Y., Dhiba, D. (2018): Soil microbial resources for improving fertilizers efficiency in an integrated plant nutrient management system. – Frontiers in Microbiology 9. DOI: 10.3389/fmicb.2018.01606.

[2] Cheng, C., Wu, Z., Huang, Q., Han, C., Zhong, W. (2020): Effect of organic matter promotion on nitrogen-cycling genes and functional microorganisms in acidic red soils. – Environmental Science 41: 2468-2475. DOI: 10.13227/j.hjkx.201911013.

http://www.aloki.hu ● ISSN 1589 1623 (Print) ● ISSN1785 0037 (Online)
DOI: http://dx.doi.org/10.15666/aeer/2005_39113926

[3] Cruz, C., Lips, S. H., Martins-Loucao, M. A. (1993): The effect of nitrogen source on photosynthesis of carob at high CO_2 concentrations. – Physiologia Plantarum 89: 552-556. DOI: 10.1111/j.1399-3054.1993.tb05212.x.
[4] Dordas, C. A., Sioulas, C. (2008): Safflower yield, chlorophyll content, photosynthesis, and water use efficiency response to nitrogen fertilization under rainfed conditions. – Industrial Crops and Products 27: 75-85. DOI: 10.1016/j.indcrop.2007.07.020.
[5] Forde, B., Lorenzo, H. (2002): The nutritional control of root development. – In: Interactions in the Root Environment: An Integrated Approach. Springer Netherlands, Dordrecht. DOI: 10.1007/978-94-010-0566-1_6.
[6] Fu, W., Wang, Y., Ye, Y., Zhen, S., Zhou, B., Wang, Y., Hu, Y., Zhao, Y., Huang, Y. (2020a): Grain yields and nitrogen use efficiencies in different types of stay-green maize in response to nitrogen fertilizer. – Plants 9: 474. DOI: 10.3390/plants9040474.
[7] Fu, Y., Zhang, Z., Yang, X., Wang, C., Lan, T., Tang, X., Chen, G., Zeng, J., Yuan, S. (2020b): Nitrate reductase is a key enzyme responsible for nitrogen-regulated auxin accumulation in Arabidopsis roots. – Biochemical and Biophysical Research Communications 532: 633-639. DOI: 10.1016/j.bbrc.2020.08.057.
[8] Gao, J. (2006): Experimental guide of plant physiology. – Higher Education Press, Beijing, pp. 76.
[9] Gao, P., Zuo, Z., Zhang, R., Qiu, Y., He, R., Gao, R., Gui, R. (2016): Optimum nitrogen fertilization for Phyllostachys edulis productivity and photosynthetic response. – Agronomy Journal 108: 448-458. DOI: 10.2134/agronj2015.0324.
[10] Heuermann, D., Hahn, H., von Wirén, N. (2021): Seed yield and nitrogen efficiency in oilseed rape after ammonium nitrate or urea fertilization. – Frontiers in Plant Science 11. DOI: 10.3389/fpls.2020.608785.
[11] Huang, W., Siemann, E., Yang, X., Wheeler, G. S., Ding, J. (2013): Facilitation and inhibition: changes in plant nitrogen and secondary metabolites mediate interactions between above-ground and below-ground herbivores. – Proceedings of the Royal Society B: Biological Sciences 280: 20131318. DOI: 10.1098/rspb.2013.1318.
[12] Kataria, S., Guruprasad, K. N. (2015): Exclusion of solar UV radiation improves photosynthetic performance and yield of wheat varieties. – Plant Physiology and Biochemistry 97: 400-411. DOI: 10.1016/j.plaphy.2015.10.001.
[13] Kirova, E., Nedeva, D., Nikolova, A., Ignatov, G. (2005): Changes in the biomass production and total soluble protein spectra of nitrate-fed and nitrogen-fixing soybeans subjected to gradual water stress. – Plant, Soil and Environment 51: 237-242.
[14] Kishorekumar, R., Bulle, M., Wany, A., Gupta, K. J. (2020a): An overview of important enzymes involved in nitrogen assimilation of plants. – In: Methods in molecular biology. DOI: 10.1007/978-1-4939-9790-9_1.
[15] Kishorekumar, R., Bulle, M., Wany, A., Gupta, K. J. (2020b): An overview of important enzymes involved in nitrogen assimilation of plants. – In: Methods in molecular biology. DOI: 10.1007/978-1-4939-9790-9_1.
[16] Kleinhenz, V., Milne, J., Walsh, K. B., Midmore, D. J. (2003): A case study on the effects of irrigation and fertilization on soil water and soil nutrient status, and on growth and yield of bamboo (Phyllostachys pubescens) shoots. – Journal of Bamboo & Rattan (VSP International Science Publishers).
[17] Krapp, A., Castaings, L. (2012): Réponses des plantes à la disponibilité en azote. – Biologie Aujourd'hui 206: 323-335. DOI: 10.1051/jbio/2012031.
[18] Krouk, G., Crawford, N. M., Coruzzi, G. M., Tsay, Y.-F. (2010): Nitrate signaling: adaptation to fluctuating environments. – Current Opinion in Plant Biology 13: 265-272. DOI: 10.1016/j.pbi.2009.12.003.
[19] Kurai, T., Wakayama, M., Abiko, T., Yanagisawa, S., Aoki, N., Ohsugi, R. (2011): Introduction of the ZmDof1 gene into rice enhances carbon and nitrogen assimilation under low-nitrogen conditions. – Plant Biotechnology Journal 9: 826-837. DOI: 10.1111/j.1467-7652.2011.00592.x.

http://www.aloki.hu ● ISSN 1589 1623 (Print) ● ISSN1785 0037 (Online)
DOI: http://dx.doi.org/10.15666/aeer/2005_39113926

[20] Li, Q., Peng, C., Wu, J., Hänninen, H., Yao, H., Zhang, R., Song, X., Ying, Y. (2017): Nitrogen Deposition Enhances Photosynthesis in Moso Bamboo but Increases Susceptibility to Other Stress Factors. – Frontiers in Plant Science 8: 1-11. DOI: 10.3389/fpls.2017.01975.
[21] Lichtenthaler, H. K. (1987): Chlorophylls and carotenoids: pigments of photosynthetic biomembranes. – Methods in Enzymology 148: 350-382.
[22] Lichtenthaler, H. K., Ač, A., Marek, M. V., Kalina, J., Urban, O. (2007a): Differences in pigment composition, photosynthetic rates and chlorophyll fluorescence images of sun and shade leaves of four tree species. – Plant Physiology and Biochemistry 45: 577-588. DOI: 10.1016/j.plaphy.2007.04.006.
[23] Lichtenthaler, H. K., Fatbardha, B., Gabriele, L. (2007b): Chlorophyll fluorescence imaging of photosynthetic activity in sun and shade leaves of trees. – Photosynthesis Research 93: 235-244. DOI: 10.1007/s11120-007-9174-0.
[24] Lin, Y., Zhang, J., Gao, W., Chen, Y., Li, H., Lawlor, D. W., Paul, M. J., Pan, W. (2017): Exogenous trehalose improves growth under limiting nitrogen through upregulation of nitrogen metabolism. – BMC Plant Biology 17: 247. DOI: 10.1186/s12870-017-1207-z.
[25] Liu, C.-W., Sung, Y., Chen, B.-C., Lai, H.-Y. (2014): Effects of nitrogen fertilizers on the growth and nitrate content of Lettuce (*Lactuca sativa* L.). – International Journal of Environmental Research and Public Health 11: 4427-4440. DOI: 10.3390/ijerph110404427.
[26] Liu, Z., Gao, F., Yang, J., Zhen, X., Li, Y., Zhao, J., Li, J., Qian, B., Yang, D., Li, X. (2019): Photosynthetic characteristics and uptake and translocation of nitrogen in peanut in a wheat-peanut rotation system under different fertilizer management regimes. – Frontiers in Plant Science 10. DOI: 10.3389/fpls.2019.00086.
[27] Liu, N., Zhang, S., Huang, Y., Cai, H., Zhu, X. (2020): Understory and canopy additions of nitrogen differentially affect carbon and nitrogen metabolism of Psychotria rubra in an evergreen broad-leaved forest. – Science of The Total Environment 724: 138183. DOI: 10.1016/j.scitotenv.2020.138183.
[28] Maeda, S., Konishi, M., Yanagisawa, S., Omata, T. (2014): Nitrite transport activity of a novel HPP family protein conserved in cyanobacteria and chloroplasts. – Plant and Cell Physiology 55: 1311-1324. DOI: 10.1093/pcp/pcu075.
[29] Manna, M. C., Swarup, A., Wanjari, R. H., Ravankar, H. N., Mishra, B., Saha, M. N., Singh, Y. V., Sahi, D. K., Sarap, P. A. (2005): Long-term effect of fertilizer and manure application on soil organic carbon storage, soil quality and yield sustainability under sub-humid and semi-arid tropical India. – Field Crops Research 93: 264-280. DOI: 10.1016/j.fcr.2004.10.006.
[30] Matthews, J. S. A., Vialet-Chabrand, S. R. M., Lawson, T. (2017): Diurnal variation in gas exchange: The balance between carbon fixation and water Loss. – Plant Physiology 174: 614-623. DOI: 10.1104/pp.17.00152.
[31] Mu, X., Chen, Y. (2021): The physiological response of photosynthesis to nitrogen deficiency. – Plant Physiology and Biochemistry 158: 76-82. DOI: 10.1016/j.plaphy.2020.11.019.
[32] O'Brien, J. A., Vega, A., Bouguyon, E., Krouk, G., Gojon, A., Coruzzi, G., Gutiérrez, R. A. (2016): Nitrate transport, sensing, and responses in plants. – Molecular Plant 9: 837-856. DOI: 10.1016/j.molp.2016.05.004.
[33] Peng, J., Feng, Y., Wang, X., Li, J., Xu, G., Phonenasay, S., Luo, Q., Han, Z., Lu, W. (2021): Effects of nitrogen application rate on the photosynthetic pigment, leaf fluorescence characteristics, and yield of indica hybrid rice and their interrelations. – Scientific Reports 11: 7485. DOI: 10.1038/s41598-021-86858-z.
[34] Pierik, M., Ruijven, J. V., Bezemer, T. M., Geerts, R., Berendse, F. (2011): Recovery of plant species richness during long-term fertilization of a species-rich grassland. – Ecology 92: 1393-1398.

http://www.aloki.hu ● ISSN 1589 1623 (Print) ● ISSN1785 0037 (Online)
DOI: http://dx.doi.org/10.15666/aeer/2005_39113926

[35] Sanchez-Zabala, J., González-Murua, C., Marino, D. (2015): Mild ammonium stress increases chlorophyll content in Arabidopsis thaliana. – Plant Signaling & Behavior 10: e991596. DOI: 10.4161/15592324.2014.991596.
[36] Scheible, W. R., Gonzalez-Fontes, A., Lauerer, M., Muller-Rober, B., Caboche, M., Stitt, M. (1997): Nitrate acts as a signal to induce organic acid metabolism and repress starch metabolism in Tobacco. – The Plant Cell 15: 783-798. DOI: 10.1105/tpc.9.5.783.
[37] Seabra, A. R., Carvalho, H. G. (2015): Glutamine synthetase in medicago truncatula, unveiling new secrets of a very old enzyme. – Frontiers in Plant Science 6. DOI: 10.3389/fpls.2015.00578.
[38] Stitt, M. (1999): Nitrate regulation of metabolism and growth. – Current Opinion in Plant Biology 2: 178-186. DOI: 10.1016/S1369-5266(99)80033-8.
[39] Stubbs, T. L., Kennedy, A. C., Reisenauer, P. E., Burns, J. W. (2009): Chemical composition of residue from cereal crops and cultivars in dryland ecosystems. – Agronomy Journal 101: 538-545. DOI: 10.2134/agronj2008.0107x.
[40] Talukder, P., Dedkova, L. M., Ellington, A. D., Yakovchuk, P., Lim, J., Anslyn, E. V., Hecht, S. M. (2016): Synthesis of alanyl nucleobase amino acids and their incorporation into proteins. – Bioorganic & Medicinal Chemistry 24: 4177-4187. DOI: 10.1016/j.bmc.2016.07.008.
[41] Vitousek, P. (1982): Nutrient cycling and nutrient use efficiency. – The American Naturalist 119: 553-572. DOI: 10.1086/283931.
[42] Walch-Liu, P., Neumann, G., Bangerth, F., Engels, C. (2000): Rapid effects of nitrogen form on leaf morphogenesis in tobacco. – Journal of Experimental Botany 51: 227-237. DOI: 10.1093/jexbot/51.343.227.
[43] Wang, T., Ding, N., Li, L., Zhou, H., Shang, L. (2019): Combining chemical fertilizer with organic manure or straw increase the yield stability and sustainability of maize and wheat in Loess Plateau of east Gansu Province. – Journal of Plant Nutrition and Fertilizers 25: 1817-1826.
[44] Wen, B., Xiao, W., Mu, Q., Li, D., Chen, X., Wu, H., Li, L., Peng, F. (2020): How does nitrate regulate plant senescence? – Plant Physiology and Biochemistry 157: 60-69. DOI: 10.1016/j.plaphy.2020.08.041.
[45] Wu, Y., Zhao, B., Li, Q., Kong, F., Du, L., Zhou, F., Shi, H., Ke, Y., Liu, Q., Feng, D., Yuan, J. (2019): Non-structural carbohydrates in maize with different nitrogen tolerance are affected by nitrogen addition. – PLoS ONE 14: 1-19. DOI: 10.1371/journal.pone.0225753.
[46] Xie, J., Bai, X., Li, Y., Sun, C., Qian, H., Fu, Z. (2014): The effect of glufosinate on nitrogen assimilation at the physiological, biochemical and molecular levels in *Phaeodactylum tricornutum*. – Ecotoxicology 23: 1430-1438. DOI: 10.1007/s10646-014-1285-8.
[47] Xing, Y., Guo, S., Chen, X., Du, D., Liu, M., Xiao, Y., Zhang, T., Zhu, M., Zhang, Y., Sang, X., He, G., Wang, N. (2018): Nitrogen metabolism is affected in the nitrogen-deficient rice mutant esl4 with a calcium-dependent protein kinase gene mutation. – Plant and Cell Physiology. DOI: 10.1093/pcp/pcy169.
[48] Xu, S., Fu, X., Ma, S., Bai, Z., Xiao, R., Li, Y., Zhuang, G. (2014): Mitigating nitrous oxide emissions from tea field soil using bioaugmentation with a trichoderma viride biofertilizer. – The Scientific World Journal 2014: 1-9. DOI: 10.1155/2014/793752.
[49] Yang, X., Nian, J., Xie, Q., Feng, J., Zhang, F., Jing, H., Zhang, J., Dong, G., Liang, Y., Peng, J., Wang, G., Qian, Q., Zuo, J. (2016): Rice ferredoxin-dependent glutamate synthase regulates nitrogen-carbon metabolomes and is genetically differentiated between japonica and indica Subspecies. – Molecular Plant 9: 1520-1534. DOI: 10.1016/j.molp.2016.09.004.
[50] Zhang, R., Wu, J., Li, Q., Hänninen, H., Peng, C., Yao, H., Song, X., Ying, Y. (2017): Nitrogen deposition enhances photosynthesis in moso bamboo but increases susceptibility to other stress factors. – Frontiers in Plant Science 8. DOI: 10.3389/fpls.2017.01975.

http://www.aloki.hu ● ISSN 1589 1623 (Print) ● ISSN1785 0037 (Online)
DOI: http://dx.doi.org/10.15666/aeer/2005_39113926

[51] Zhang, X. Z., Gao, H. J., Peng, C., Qiang, L. I., Zhu, P., Gao, Q. (2019): Variation trend of soil organic carbon, total nitrogen and the stability of maize yield in black soil under long-term organic fertilization. – Journal of Plant Nutrition and Fertilizers 25: 1473-2532.
[52] Zhou, W., Lv, T., Yang, Z., Wang, T., Fu, Y., Chen, Y., Hu, B., Ren, W. (2017a): Morphophysiological mechanism of rice yield increase in response to optimized nitrogen management. – Scientific Reports 7: 17226. DOI: 10.1038/s41598-017-17491-y.
[53] Zhou, W., Lv, T., Yang, Z., Wang, T., Fu, Y., Chen, Y., Hu, B., Ren, W. (2017b): Morphophysiological mechanism of rice yield increase in response to optimized nitrogen management. – Scientific Reports 7: 17226. DOI: 10.1038/s41598-017-17491-y.
[54] Zhu, Z., Chen, D. (2002): Nitrogen fertilizer use in China-contributions to food production, impacts on the environment and best management strategies. – Nutrient Cycling in Agroecosystems 63: 117-127. DOI: 10.1023/A:1021107026067.
[55] Zhu, Q. G., Jin, A. W., Lou, Y. H., Luo, J. (2016): Effect of fertilization on root acid phosphatase and nitrogen metabolism of Phyllostachys heterocycla cv. pubescens. – Journal of Fujian Forestry Science and Technology 1:30-34.

http://www.aloki.hu ● ISSN 1589 1623 (Print) ● ISSN1785 0037 (Online)
DOI: http://dx.doi.org/10.15666/aeer/2005_39113926

EFFECTS OF SINGLE AND COMBINED STRESS OF CU OR ZN ON THE PHOTOSYNTHETIC FLUORESCENCE CHARACTERISTICS OF *VALLISNERIA NATANS*

GAO, G. Q.* – YANG, W. H. – ZENG, K. H. – HU, L. – WANG, X. L. – LIU, Z. M.

School of Civil and Architecture Engineering, Nanchang Institute of Technology, NO. 289 Tianxiang Road, Nanchang, 330099 Jiangxi, China
(phone: +86-791-8209-6402; fax: +86-791-8812-6772)

**Corresponding author*
e-mail: 342823307@qq.com; phone: +86-130-3723-2216

(Received 19th Feb 2022; accepted 10th Jun 2022)

Abstract. For investigating the response of chlorophyll fluorescence characteristics under single and combined of Cu or Zn stress, *Vallisneria natans* was selected as the experimental subject. *V. natans* was cultured 21 days under six concentration levels of Cu or Zn. The results showed that *Fv/Fm*, *Fv/Fo*, *Y (II)* and *qP* increased, and other indicators were almost unchanged in low- concentration treatment (Cu≤0.4mg/L, Zn≤4.0mg/L, Cu+Zn≤0.2+2.0 mg/L). *V. natans* could still maintain normal growth within such a range of heavy metal concentration, and it could maintain relatively a high photosynthetic activity. When heavy metal concentration was higher than the above concentration, the photosynthetic activity was inhibited. *Fv/Fm*, *Fv/Fo*, *Y (II)* and *qP* decreased gradually with the increasing stress concentration and stress time, while *Y(NO)*, *Y (NPQ)*, and *qN* showed different degrees of increase. The combined stress of Cu and Zn had a synergistic effect on the photosynthetic activity. *V. natans* can be used for ecological restoration of polluted water with low concentration of Cu and Zn.
Keywords: *Vallisneria natans, heavy metal stress, chlorophyll fluorescence parameter, synergistic effect*

Introduction

Heavy metals such as Cu, Cd, Pb and Cr are very common environmental pollutants, which can negatively and profoundly impact on the species diversity in aquatic ecosystems (Xing et al., 2013; Ji et al., 2018). Certain physiological variables of plants can be positively stimulated by the treatment of heavy metals with low concentration and with a relatively short period of time. However, long-term and high-concentration single heavy metal stress will show strong toxicity to aquatic plants (Gao et al., 2019a). Both Cu and Zn are essential trace elements for plant growth (Nagajyoti et al., 2010). Cu with optimum level can positively influence the production of chlorophyll and development of reproductive organs, while excessive copper will stifle the growth of plant roots, thus reducing the extraction ability of plant roots for other nutrients (Xue et al., 2010). Zn plays an important role in regulating osmotic pressure, maintaining metabolism and promoting substances synthesis in plants. Like Cu, when its concentration reaches a certain threshold, Zn can inhibit plant growth or even cause plant death (Ji et al., 2017).

Vallisneria natans is a very common submerged plant in rivers and lakes in China, and it is considered to be one of the effective species for solving heavy metal pollution in water bodies (Gao et al., 2019b). China has a large number of rivers and lakes in which the pollution of heavy metals is quite complicated. The poisoning effect of submerged plants often comes from the combined stress of multiple heavy metals (Xing et al., 2017). Currently, a large number of studies on submerged plants mainly focus on the enrichment of heavy metals (Upadhyay et al., 2014; Ahmad et al., 2016; Borisova et al., 2017) and

http://www.aloki.hu ● ISSN 1589 1623 (Print) ● ISSN1785 0037 (Online)
DOI: http://dx.doi.org/10.15666/aeer/2005_39273938

physiological indicators (Wang et al., 2012). The researches on the fluorescence characteristics of plant chlorophyll are mostly limited to single heavy metal stress in a short period of time, and there are few literature-related to combined stress. In this study, the effects of single and combined heavy metal (using Cu and Zn as pollutants) on chlorophyll fluorescence parameters of *V. natans* were investigated to illuminate the response mechanism of the photosynthetic system, thus providing some guidance for ecological restoration of heavy metal polluted water bodies.

Materials and Methods

Experimental materials

V. natans and bottom mud required for the experiment were collected from Poyang Lake. After removing debris from the bottom mud, it was evenly spread in a plastic square box (length 34.0 cm, width 22.5 cm, height 10 cm), and the thickness of bottom mud is 8 cm. Individuals of *V. natans* with relatively intact leaves and robust growth were selected. The leaf length and the root length was trimmed to 15 cm and 3 cm, respectively. After the attachments on the leaf surface were washed away, these plants were evenly planted in plastic boxes (12 plants per box), and then these plastic boxes were placed in glass tanks (length 40 cm, width 40 cm, height 50 cm). Tap water was added into the tanks to a height of 40 cm for pre-cultivation of submerged plants, and these plants was used for experiments after the plants' growth status was stable (*Figure 1*).

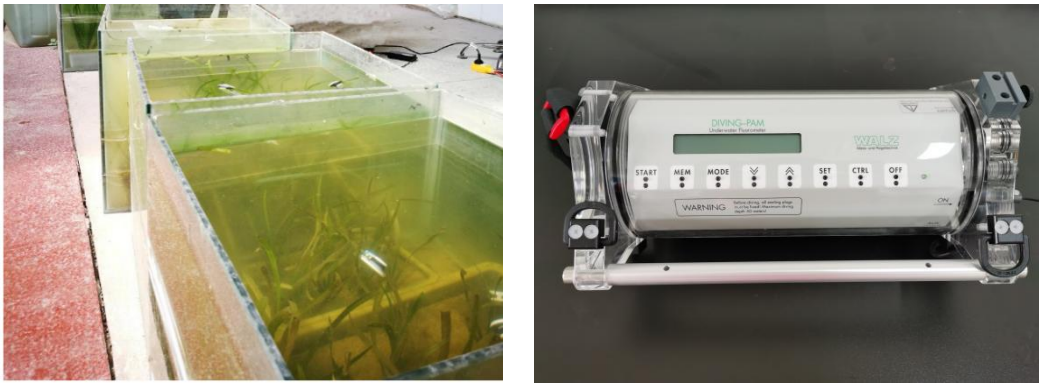

Figure 1. *Diagram of the experimental culture and equipment*

Experimental design

Pre-experiment: Different concentrations of $CuSO_4$ and $ZnSO_4$ solution were added into the glass tanks for treatment. The concentrations of Cu and Zn were divided into different levels (5.0 mg/L, 10.0 mg/L, 15.0 mg/L and 20.0 mg/L for Cu; 5.0 mg/L, 10.0 mg/L, 20.0 mg/L, 40.0 mg/L, 50.0 mg/L, 75.0 mg/L and 100.0 mg/L for Zn). Root and leaf damage of the experimental subjects were recorded every 24 h. The results were shown in *Table 1*.

When 5.0 mg/L and 10.0 mg/L concentrations of Cu were applied, the total damage of *V. natans* was 11 and 14, respectively. In contrast, when the same total damage occurred, the applied concentrations of Zn were 50.0 mg/L and 100.0 mg/L, respectively. It demonstrated that the toxicity of Cu for *V. natans* was around ten times higher than that

http://www.aloki.hu ● ISSN 1589 1623 (Print) ● ISSN1785 0037 (Online)
DOI: http://dx.doi.org/10.15666/aeer/2005_39273938

of Zn. Naturally, the concentrations of Cu and Zn should be configured according to 1:10 in water body.

Table 1. *Influence of Cu or Zn stress on the growth of V. natans*

Concentration of heavy metals (mg/L)		0 h		24 h		48 h		72 h		Total damage
		Root damage	Leaf damage	Root damage	Leaf damage	Root damage	Leaf damage	Root damage	Leaf damage	
Cu	5	1	1	1	1	1	1	3	2	11
	10	1	1	1	1	2	2	3	3	14
	15	1	1	2	2	3	2	3	3	17
	20	1	1	2	2	2	4	4	4	20
Zn	5	1	1	1	1	1	1	1	1	8
	10	1	1	1	1	1	1	1	1	8
	20	1	1	1	1	1	1	1	2	9
	40	1	1	1	1	1	1	2	2	10
	50	1	1	1	1	1	2	2	2	11
	75	1	1	1	2	2	2	2	2	13
	100	1	1	1	2	2	2	2	3	14

Root damage: 1 represents normal growth (the roots are long and robust); 2 represents mild damage (part of the root tip is deformed, and the color of root hair turns darker);3 represents moderate damage (the color of taproot turns black). 4 represents severe damage (the root system is completely black, and lots of roots fall off).
Leaf damage: 1 represents normal growth (the leaves are smooth and flat, and the color is emerald green). 2 represents mild damage (the green color of the leaves fades, and the chlorosis phenomenon occurs). 3 represents moderate damage (shrinkage and fold occurs in certain parts of the leaves). 4 represents severe damage (the leaves are completely chlorotic and withered)

Formal experiment: $CuSO_4$ and $ZnSO_4$ solutions were added into the glass tank for single or combined stress treatments. Five treatment groups were set up according to different concentrations, and a control group (CK) was set at the same time (*Table 2*). There were three replicates for each treatment group. Photosynthetic fluorescence was measured every 7 days after stress cultivation, and the experimental period was 21 days in total. The temperature of water is between 22 and 29 ℃ and PH was 6.8. The experiment was completed from May to June in 2021.

Table 2. *Concentration settings of Cu and Zn in water*

Heavy metal	Treatment group concentration (mg/L)					
	CK	T1	T2	T3	T4	T5
Cu	0	0.2	0.4	0.6	0.8	1.0
Zn	0	2.0	4.0	6.0	8.0	10.0
Cu+Zn	0+0	0.1+1.0	0.2+2.0	0.3+3.0	0.4+4.0	0.5 +5.0

Measuring method

The leaf fluorescence parameters were measured by the underwater modulation fluorescence instrument (Diving-PAM). Three plants were randomly selected from each treatment group, and the leaves were clamped with dark leaf clamps. Wincontrol software was used for data acquisition after dark adaptation for 20 min. The specific measurement method was included in the literature (Gao et al., 2019a).

http://www.aloki.hu ● ISSN 1589 1623 (Print) ● ISSN1785 0037 (Online)
DOI: http://dx.doi.org/10.15666/aeer/2005_39273938

Data analysis

The experimental result is expressed as the form of mean ± standard error. Excel 2017 is used in the processing and drawing of experimental data. SPSS 19.0 software is used to conduct one-way analysis of variance. The SNK method is used for multiple comparison analysis. Two-way analysis of variance was used to judge whether the interactions of factors were significant.

Result and Analysis

Effects of Cu or Zn on plant growth

There was no significant difference in plant height after single metal stress (Cu≤0.4 mg/L or Zn≤4 mg/L) compared with CK. The combined stress of Cu and Zn (0.1+1.0 mg/L) was beneficial to plant growth, and had antagonistic effect on plant growth. When the concentration exceeded T2 group, the plant growth was significantly inhibited and showed a significant downward trend ($P < 0.05$); Under combined stress, the decline was the most.

Effects of Cu or Zn on Fv/Fm and Fv/Fo

After the stress treatment, *Fv/Fm* and *Fv/Fo* of *V. natans* were measured, and the change trend of *Fv/Fm and Fv/Fo* was analyzed. The results were shown in *Fig. 2*.

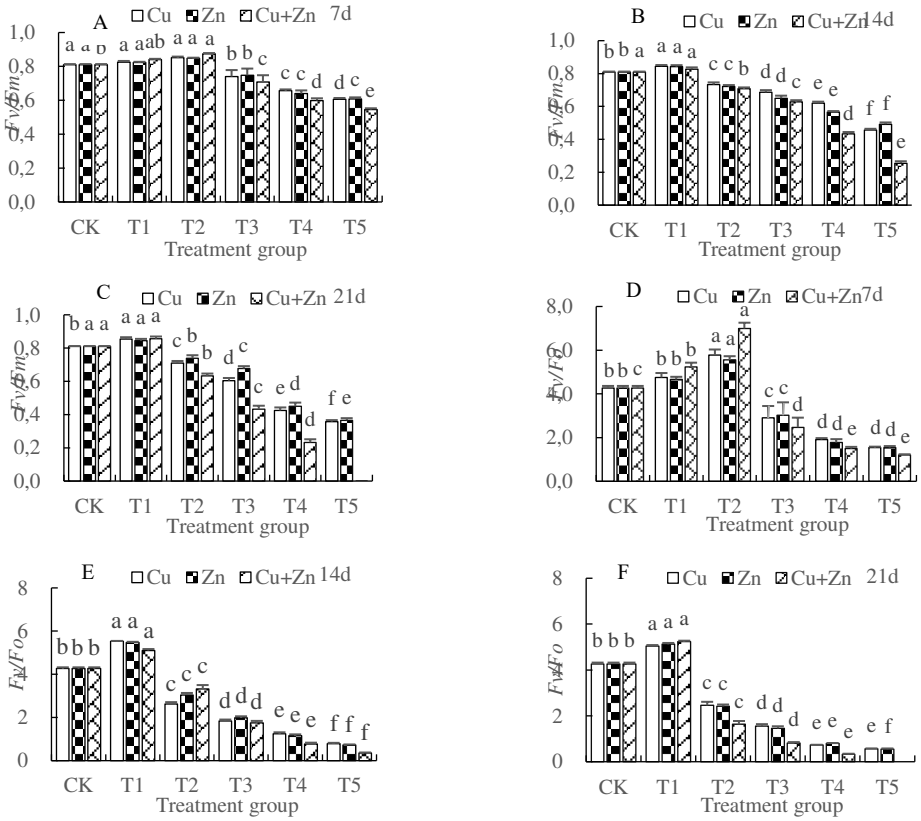

Figure 2. *Effects of different heavy metal concentrations on Fv/Fm and Fv/Fo. Note: Different lowercase letters in each line indicate significant differences at P <0.05 among different treatment groups*

http://www.aloki.hu ● ISSN 1589 1623 (Print) ● ISSN1785 0037 (Online)
DOI: http://dx.doi.org/10.15666/aeer/2005_39273938

After 7 days' stress, *Fv/Fm* and *Fv/Fo* showed an upward trend when heavy metal concentration was lower than that of T2, then these two variables decreased gradually. The changes of *Fv/Fm* and *Fv/Fo* under low concentration treatment were insignificant, and the minimum values were all observed in T5 group. Compared with CK, for T5 group, *Fv/Fm* decreased by 25.10%, 24.98% and 32.57%, and *Fv/Fo* decreased by 63.82%, 63.66% and 71.77%. For subjects with 14 days' and 21 days' cultivation, only *Fv/Fm* and *Fv/Fo* in T1 group were slightly higher than that of CK, and the values of other groups decreased significantly according to the increase of heavy metal concentrations. For subjects of T5 group with 14 days' cultivation, *Fv/Fm* were 56.34%, 60.74% and 31.44% of CK, and *Fv/Fo* were 18.28%, 17.18% and 8.25% of CK. For subjects with 21 days' cultivation, *Fv/Fm* and *Fv/Fo* in different groups changed more widely, and these two parameters stressed by combined stress in T5 group couldn't be determined. Overall, heavy metals had significant effects on *Fv/Fm* and *Fv/Fo* ($P<0.05$), and the amplitude of variation of *Fv/Fo* was higher than that of *Fv/Fm*. The impact caused by single stress of Cu or Zn was lower than that of combined stress.

Effects of Cu or Zn stress on Y(II), Y(NPQ) and Y(NO)

As shown in *Fig. 3*, *Y(II)* increased gradually when applied concentration was lower than that of T2. When the concentration was higher than that of T2, *Y(II)* decreased significantly. Compared with the single stress of Cu or Zn, the variation amplitude of *Y(II)* resulted from combined stress was relatively greater. In addition, *Y(II)* in T2 and T5 groups were 1.12 and 0.64 times of those in CK, respectively. It meant that the transfer of photosynthetic electrons of *V. natans* could be improved by the treatment of heavy metals with low concentration (≤T2), and the treatment could also enhance the effective quantum yield to a certain extent. However, the high concentration would damage the reaction of photosynthetic system inside *V. natans*, thus influencing the photosynthesis. Among the three types of heavy metal stress, the combined stress had the greatest impact on *Y(II)*.

For subjects with 7 days' cultivation, when applied concentration was higher than that of T2, *Y(II)* increased with the increase of the heavy mental concentration. The minimum values of *Y(II)* were all observed in the T5 group for all three types of stress, and these values were 72.60%, 72.87% and 63.51% of CK. *Y(NO)* and *Y(NPQ)* change insignificantly in T2 group ($P>0.05$). However, in T3, T4, and T5 groups, two values mentioned above showed a different degree of upward trend. In T5 group, *Y(NO)* and *Y(NPQ)* under combined stress were 1.64 and 3.40 times that of CK. For subjects within 21 days' cultivation, *Y(II)* decreased significantly, and *Y(NO)* increased dramatically with the increase of heavy metal concentrations. The impact caused by combined stress was significantly higher than that of single stress of Cu or Zn. The increase of *Y(NPQ)* was much greater than that of *Y(NO)*. After 21 days' cultivation, *Y(II)*, *Y(NO)* and *Y(NPQ)* treated by combined stress couldn't be determined in T5 group.

Effects of Cu or Zn stress on qP and qN

As shown in *Fig. 4*, the values of *qP* in T1 group were higher than that of CK. The longer stress time of heavy metals would cause a greater decrease of *qP*. For subjects with 21 days' cultivation, *qP* couldn't be determined in T5 group under combined stress. For subjects with 14 days' cultivation, *qN* slightly increased with the increase of heavy metal concentrations until the applied concentration was higher than that of T2. For subjects with 21 days' cultivation, *qN* showed an upward trend under the single stress, while the

http://www.aloki.hu ● ISSN 1589 1623 (Print) ● ISSN1785 0037 (Online)
DOI: http://dx.doi.org/10.15666/aeer/2005_39273938

same parameter under combined stress increased first, reaching the maximum value (0.617) in T3 group, and then decreased. The value of *qN* in T5 group couldn't be determined. The variation amplitude of *qN* resulted from combined stress was relatively greater.

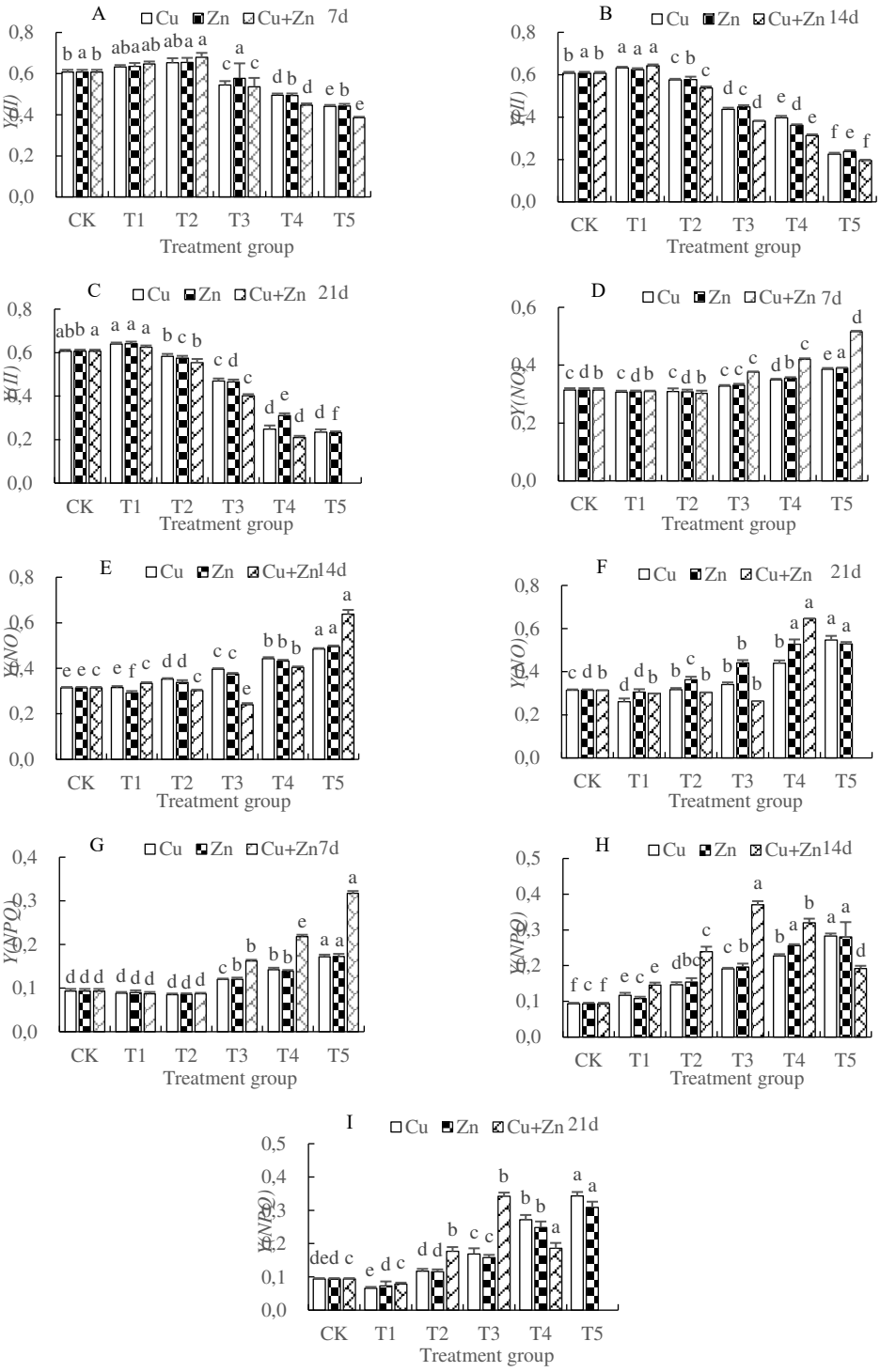

Figure 3. *Effects of different heavy metal concentrations on Y(II), Y(NO)and Y(NPQ). Note: Different lowercase letters in each line indicate significant differences at P＜0.05 among different treatment groups*

http://www.aloki.hu ● ISSN 1589 1623 (Print) ● ISSN1785 0037 (Online)
DOI: http://dx.doi.org/10.15666/aeer/2005_39273938

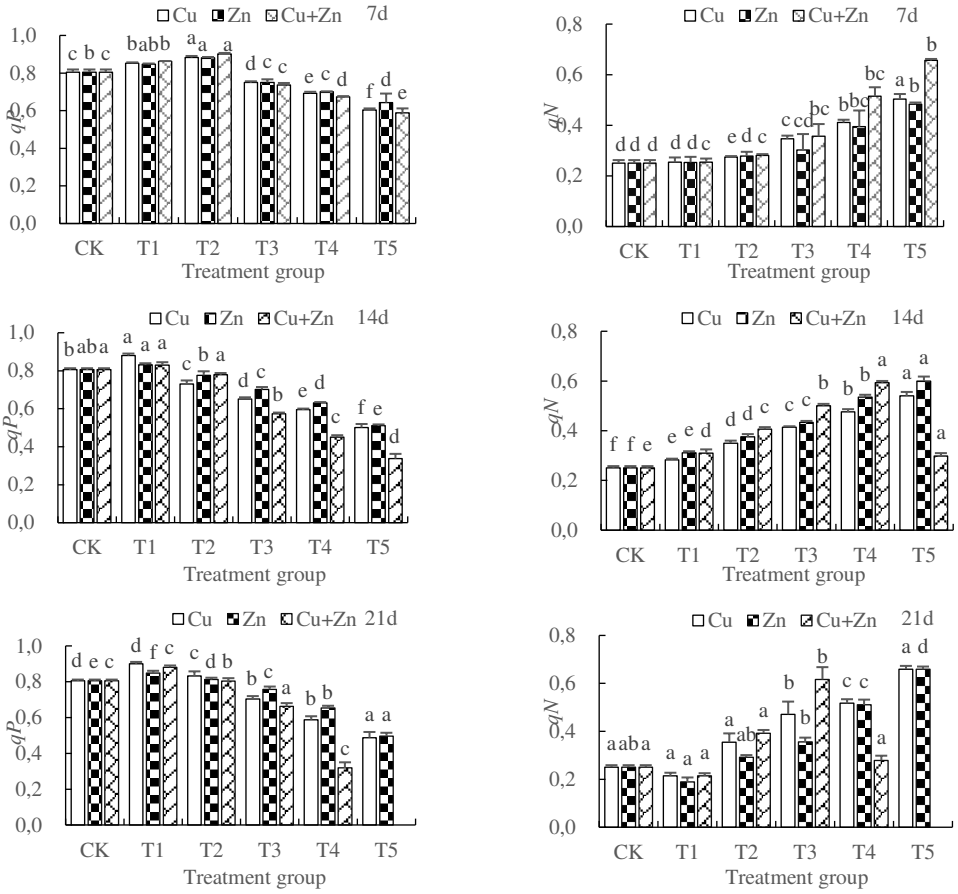

Figure 4. *Effects of different heavy metal concentrations on qP and qN. Note: Different lowercase letters in each line indicate significant differences at P<0.05 among different treatment groups*

Correlation analysis of various indexes

According to Pearson correlation analysis (*Table 3*), for subjects within 14 days' cultivation, the correlation between *Fv/Fm*, *Fv/Fo* and heavy metal concentrations was insignificant. For subjects with 14 to 21 days' cultivation, a significant negative correlation was observed for the single stress of Cu or Zn. Under combined stress of Cu and Zn, there was also a very significant negative correlation between *Fv/Fm*, *Fv/Fo* and heavy metal concentrations at the level of $P<0.01$. A significant negative correlation between *Fv/Fo* and heavy metal concentrations could be observed from the data of all three types of treatment. For subjects with 7 days' cultivation, the correlation between *Y(II)* and heavy metal concentrations was insignificant. For subjects with 14 days' cultivation, the negative correlation was significant for single stress and was extremely significant for combined stress. For subjects with 21 days' cultivation, the negative correlation was extremely significant for both single stress of Cu and combined stress, and was significant for the single stress of Zn. *Y(NO)* in the whole cultivation stage was significantly and positively correlated with heavy metal concentrations at the $P<0.05$ level. For subjects within 14 days' cultivation, a significant positive correlation was observed for the single stress of Cu or Zn. The positive correlation observed was extremely significant within 14-21 days. The correlation was insignificant for combined

http://www.aloki.hu ● ISSN 1589 1623 (Print) ● ISSN1785 0037 (Online)
DOI: http://dx.doi.org/10.15666/aeer/2005_39273938

stress. For subjects within 7 days' cultivation, there was no significant correlation between *qP* and heavy metal concentrations, while after 7 days' cultivation, a significant negative correlation was observed. *qN* was significantly and positively correlated with heavy metal concentrations under the single stress, while the correlation was not significant under combined stress.

Table 3. *Correlation of various indicators under Cu or Zn stress*

	Indicator	***Fv/Fm***	***Fv/Fo***	***Y(II)***	***Y(NO)***	***Y(NPQ)***	***qP***	***qN***
7d	Cu	-0.872	-0.789	-0.858	0.694*	0.856*	-0.827	0.871*
	Zn	-0.870	-0.807	-0.800	0.706*	0.861*	-0.800	0.820*
	Cu+Zn	-0.869	-0.724	-0.842	0.858*	0.876	-0.817	0.825*
14d	Cu	-0.937	-0.899	-0.940*	0.975*	0.984*	-0.932*	0.987*
	Zn	-0.964	-0.918	-0.951*	0.937*	0.930*	-0.933*	0.989*
	Cu+Zn	-0.955	-0.941	-0.963**	0.668*	0.580	-0.947*	0.473
21d	Cu	-0.959*	-0.927**	-0.924**	0.864*	0.929**	-0.867*	0.950*
	Zn	-0.937*	-0.921**	-0.943*	0.939*	0.921**	-0.869*	0.922*
	Cu+Zn	-0.950**	-0.893**	-0.919**	0.622*	0.666	-0.827*	0.437

* indicates significant correlation at $P<0.05$. ** indicates extremely significant correlation at $P<0.01$

According to the two-way ANOVA (*Table 4*), Cu had an extremely significant effect on *Fv/Fo* and *Y(II)* ($P < 0.01$). It had significant effect on *Fv/Fm, Y(II), Y(NO), Y(NPQ), qP* and *qN* ($P < 0.05$). Zn had an extremely significant effect on *Fv/Fm* and *Y (II)* ($P < 0.01$), and had a significant effect on *Fv/Fo, Y(NPQ) and qP* ($P < 0.05$). From the mean square value, the difference between groups caused by the change of Cu was greater than that caused by Zn. The interaction effect of the two factors only had an extremely significant effect on *Fv/Fm, Fv/Fo* and *Y(II)* ($P < 0.01$). It had a significant effect on *Y(II)* and *qP* ($P < 0.05$). The difference between groups caused by combined stress was the largest.

Table 4. *Variance analysis of Cu, Zn and their interaction on physiological indexes*

Parameters	**Cu**		**Zn**		**Cu×Zn**	
	F	***P***	**F**	***P***	**F**	***P***
Fv/Fm	45.428	0.017*	36.521	0.009**	68.526	0.007**
Fv/Fo	37.645	0.008**	31.432	0.007*	57.435	0.009**
Y(II)	46.273	0.009**	21.435	0.005**	31.971	0.015*
Y(NO)	1.439	0.024*	10.366	0.161	21.765	0.126
Y(NPQ)	7.578	0.043*	8.163	0.018*	4.462	0.208
qP	31.301	0.032*	3.750	0.042*	1.756	0.027*
qN	7.406	0.045*	2.953	0.143	0.873	0.234

*Represents a significant correlation at 0.05 level (bilateral). * * Represents a very significant correlation at the level of 0.01 (bilateral)

http://www.aloki.hu ● ISSN 1589 1623 (Print) ● ISSN1785 0037 (Online)
DOI: http://dx.doi.org/10.15666/aeer/2005_39273938

Discussion

Heavy metals can affect the normal activities of chloroplasts and thylakoids of *V. natans*, interfere with the synthesis of chlorophyll and control the electron transfer of PSII, thus causing changes in the photosynthetic activity and fluorescence parameters (Kalaji et al., 2016).

Fv/*Fm* is the maximum light quantum yield, which indicates the relative light energy used in photosynthesis. It can be used to evaluate the adaptability of plants to abiotic stress environment (Li et al., 2016). For subjects within 7 days' cultivation under the stress of heavy metals, *Fv*/*Fm* and *Fv*/*Fo* showed an upward trend when applied concentration was lower than that of T2. Low concentration of heavy metals could promote the antioxidant enzyme system and increased the activity of antioxidant enzymes in plant body which is beneficial to resist oxidative damage (Li et al., 2016), so a small amount of Cu and Zn could promote the growth of *V. natans.*

However, for subjects within 7-14 days' cultivation, *Fv*/*Fm* and *Fv*/*Fo* increased only when applied concentration was lower than that of T1. It meant the same treatment concentration would also have a certain degree of inhibitory effect on *V. natans* under long-term stress. When the concentration of heavy metals exceeded the threshold, *Fv/Fm* and *Fv*/*Fo* showed a downward trend for all three types of stress. There were two reasons: the increase of the heavy metal concentration lead to the decrease of protein activity on the chloroplast thylakoid membrane of the leaves (Assche and Clijsters, 1990). This hindered electron transfer, thus reducing the number of electrons involved in CO_2 fixation in photosynthesis, thus *Fv*/*Fm* decreased (Gao et al., 2019a). The high concentration of heavy metals would interfere with the photosystem reaction center of *V. natans*, and affected the activity of the photosynthetic system by controlling the electrons at the water cracking end, resulting in the decrease of fluorescence level and the decrease of *Fv*/*Fo* (Rai et al., 2016). In this study, *Fv*/*Fo* had a greater range of change, indicating that Cu and Zn had a much greater impact on the water cracking end than *Fv*/*Fm*. For the groups treated with the same concentration of heavy metals, the variation ranges of *Fv*/*Fm* and *Fv*/*Fo* under combined stress was larger than that under single stress, and there was significant difference between Cu and Zn groups. This might be related to the types of heavy metals. Cu can affect the chlorophyll content, and Zn can adjust the balance of cell osmotic pressure (Zhang et al., 2016). Low-concentration treatment would not cause too much negative impact on plants, but with the increase of Zn concentration, the osmotic pressure balance was broken in plants, which aggravated the toxicity to chloroplasts and interfered with the photosynthesis (Momchil et al., 2018). High concentration of Zn could also hinder the synthesis of certain proteins, weaken the resistance of the plant itself, and increase the toxicity of other heavy metals (Xu et al., 2006).

Light quantum of adsorbed by PS II reaction center transferred and dissipated in effective quantum yield *Y(II)*, non-photochemical quenching coefficient *qN*, and regulated energy dissipation quantum *Y(NPQ)* (Qian et al., 2011). The values of *Y(II)* always increased first and then decreased, while the values of *Y(NO)* and *Y(NPQ)* hardly changed when applied concentration was lower than that of T2. However, when the concentration was higher than that of T2, *Y(NO)* and *Y(NPQ)* increased significantly for the subjects within 14 days' cultivation, and the rise of *Y(NPQ)* was higher than *Y(NO)*. It indicated that heavy metal stress at this time had already threatened the growth of *V. natans*, and plants consumed too much energy through self-regulation to resist unfavorable conditions (Gao et al., 2019a). For the subject with 14 to 21 days' cultivation under the combined stress, *Y(NO)* and *Y(NPQ)* had a decline in high concentration

http://www.aloki.hu ● ISSN 1589 1623 (Print) ● ISSN1785 0037 (Online)
DOI: http://dx.doi.org/10.15666/aeer/2005_39273938

treatment. The possible reason is that due to the long-term, high-concentration heavy metal stress, the normal physiological activity of *V. natans* was interfered, resulting in the weakening of the photosynthetic ability (Ozffidan et al., 2018). The energy conversion and electron transfer in the photosystem under combined stress were more severely affected. It might be that the presence of Zn promoted the absorption of Cu by plants, which made plants suffer more from the outside environment. Similarly, the variation of increasing trend of *Y(NO)* and *Y(NPQ)* caused by combined stress was greater than by single stress.

The values of *qP* decreased significantly with the increase of the concentration of heavy metals, indicating that the electron flow from the oxidation side of PS II to the reaction center was inhibited in the photosystem, which further caused a decrease in the rate of photosynthesis (Wang et al., 2010; Sun et al., 2020). The variation of *qP* caused by combined stress was greater, which indicated the combined stress has a greater impact on the actinic photoelectron transport of *V. natans.* When applied concentration was lower than that of T2, the values of *qN* hardly changed. The possible reason was that the heavy metal concentration was low, which didn't affect the normal physiological activities of plants (Mobin and Khan, 2014). However, when applied concentration increased to a higher level (>T2), the values of *qN* increased gradually. It means that the PSII reaction center of leaves absorbs light energy for natural pigments, mostly for heat dissipation (Hou et al., 2018). The increase of *qN* has a positive effect on the protection of plants themselves. For subjects with 21 days' cultivation, *qP* and *qN* couldn't be determined in T5 group treated by combined stress. This means the plant photosynthetic function is completely impaired.

Conclusions

V. natans could still have normal photosynthetic activity in the water environment with low concentration of heavy metals (Cu≤0.4 mg/L, Zn≤4.0 mg/L, Cu+Zn≤0.2+2.0 mg/L). *Fv/Fm*, *Fv/Fo*, *Y(II)* and *qP* increased slightly, so it could promote the photosynthetic cooperation of plants to a certain extent, and the other indicators were almost unchanged. Under the stress of higher concentration of heavy metals, the tolerance of *V. natans* to combined stress was smaller than that of single stress. Therefore, in the three stress treatments, the inhibition of combined stress on the photosynthetic activity was the highest, and had a synergistic effect.

Acknowledgements. This study was supported by Jiangxi Provincial Technology Department (20212BAB204402, 20203BBGL73228), the University Students Innovation and Entrepreneurship Training Program of Jiangxi Province in 2022 (S202211319008) and National Natural Science Foundation of China (51369024).

REFERENCES

[1] Ahmad, S. S., Reshi, Z. A., Shah, M. A., Rashid, I., Ara, R. A., Syed, M. A. (2016): Heavy metal accumulation in the leaves of *Potamogeton natans* and *Ceratophyllum demersum in* a Himalayan RAMSAR site: management implications. – Wetlands Ecology Management 24: 469-475.

[2] Assche, F. V., Clijsters, H. (1990): Effects of metals on enzymes activity in plant. – Plant Cell and Environment 13(3): 195-206.

http://www.aloki.hu ● ISSN 1589 1623 (Print) ● ISSN1785 0037 (Online)
DOI: http://dx.doi.org/10.15666/aeer/2005_39273938

[3] Borisova, G. G., Chukina, N. V., Maleva, M. G., Levchenko, U. A. (2017): Accumulation of heavy metals in leaves of submerged hydrophytes (*Elodea canadensis Michx*. and *Potamogeton perfoliatus* L.) and their responses to the effect of the wastewater of a metallurgical plant. – Inland Water Biology 10(2): 176-181.

[4] Gao, G. Q., Zeng, K. H., Ji, Y., Li, W., Wang, Y. (2019a): Effects of lead stress on the chlorophyll content and photosynthetic fluorescence characteristics of *Vallisneria natans*. – Applied Ecology Environment Research 17(2): 4171-4181.

[5] Gao, G. Q., Jian, M. F., Lu, L., Ji, Y., Wang, X. L., Wang, Y. (2019b): Effects of Cu^{2+} or Cd^{2+} stress on photosynthetic pigment and photosynthetic fluorescence characteristics of *Potamogeton malaianus*. – Chinese Journal of Applied and Environmental Biology 25(3): 517-523.

[6] Hou, X. L., Han, H., Cai, L. P., Ma, X., Zhou, C., Wang, G., Meng, F. (2018): Pb stress effects on leaf chlorophyll fluorescence, antioxidative enzyme activities, and organic acid contents of *Pogonatherum crinitum* seedlings. – Flora 240: 82-88.

[7] Ji, Y., Zhang, J., Li, X. L., Peng, Y. W., Cai, G. T., Gao, G. Q., Wu, J. Q., Liu, J. L. (2017): Biomarker responses of rice plants growing in a potentially toxic element polluted region: a case study in the Le'an region. – Chemosphere 187: 97-105.

[8] Ji, Y., Wu, P. J., Zhang, J., Zhou, Y. F., Zhang, S. F., Cai, G. T., Gao, G. Q. (2018): Heavy metal accumulation, risk assessment and integrated biomarker responses of local vegetables: a case study along the Le'an river. – Chemosphere 199: 361-371.

[9] Kalaji, H. M., Jajoo, A., Oukarroum, A., Brestic, M., Zivcak, M., Samborska, I. A., Cetner, M. D., Lukasik, I., Goltsev, V., Ladle, R. J. (2016): Chlorophyll a fluorescence as a tool to monitor physiological status of plants under abiotic stress conditions. – Acta Physiologia Plantarum 38(4): 1-11.

[10] Li, W. L., Zhang, G. S., Cheng, X. Y. (2016): Stress effect and response mechanism of Cd^{2+}, Cu^{2+}, Zn^{2+} and Pb^{2+} on *Potamogeton crispus* L. growth. – Journal of Food Science and Biotechnology 35(9): 1001-1007.

[11] Mobin, M., Khan, N. A. (2007): Photosynthetic activity, pigment composition and antioxidative response of two mustard (*Brassica juncea*) cultivars differing in photosynthetic capacity subjected to cadmium stress. – Journal of plant physiology 164(5): 601-610.

[12] Momchil, P., Lyubka, K., Andon, V., Jaco, V., Vasilij, G. (2018): Effects of different metals on photosynthesis: Cadmium and Zinc affect chlorophyll fluorescence in Durum Wheat. – International Journal of Molecular medicine 19(3): 787-798.

[13] Nagajyoti, P. C., Lee, K. D., Sreekanth, T. V. M. (2010): Heavy metals, occurrence and toxicity for plants: a review RID D-5207-2011. – Environmental Chemistry Letters 8(3): 199-216.

[14] Ozfidan-Konakci, C., Yildiztugay, E., Bahtiyar, M., Kucukoduk, M. (2018): The humic acid-induced changes in the water status, chlorophyll fluorescence and antioxidant defense systems of wheat leaves with cadmium stress. – Ecotoxicology and environmental safety 155: 66-75.

[15] Qian, Y. Q., Zhou, X. X., Hai, L., Sun, Z. Y., Ju, G. S. (2011): Rapid light-response curves of PS II chlorophyll fluorescence parameters in leaves of *Salix leucopithecia* subjected to cadmium-ion stress. – Acta Ecologica Sinica 31(20): 6134-6142.

[16] Rai, R., Agrawal, M., Agrawal, S. B. (2016): Impact of heavy metals on physiological processes of plants: with special reference to photosynthetic system. – Springer Singapore.

[17] Sun, C., Xu, Y., Hu, N., Ma, Y., Zhao, Y. (2020): To evaluate the toxicity of atrazine on the freshwater microalgae *Chlorella sp*. using sensitive indices indicated by photosynthetic parameters. – Chemosphere 244: 125-136.

[18] Upadhyay, A. K., Singh, N. K., Rai, U. N. (2014): Comparative metal accumulation potential of *Potamogeton pectinatus* L. and *Potamogeton crispus* L.: role of enzymatic and non-enzymatic antioxidants in tolerance and detoxification of metals. – Aquatic Botany 117(5): 27-32.

http://www.aloki.hu ● ISSN 1589 1623 (Print) ● ISSN1785 0037 (Online)
DOI: http://dx.doi.org/10.15666/aeer/2005_39273938

[19] Wang, L., Yang, H. Q., Fan, W. G., Zhang, Z. (2010): Effect of $CdCl_2$ treatment on photosynthetic rate and chlorophyll fluorescence parameters in *Malus Hupehensis* leaves. – Scientia Agricultura Sinica 43(15): 3176-3183.
[20] Wang, P. F., Zhang, S. H., Wang, C., Lu, J. (2012): Effects of Pb on the oxidative stress and antioxidant response in a Pb bioaccumulator plant *Vallisneria natans*. – Ecotoxicology and Environment Safety 78: 28-34.
[21] Xing, W., Wu, H. P., Hao, B. B., Huang, W. M., Liu, G. H. (2013): Bioaccumulation of heavy metals by submerged macrophytes: looking for hyperaccumulators in eutrophic lakes. – Environment Science Technology 47(9): 4695-4703.
[22] Xing, W., Bai, G. L., Wu, H. P., Liu, H., Liu, G. H. (2017): Effect of submerged macrophytes on metal and metalloid concentrations in sediments and water of the Yunnan Plateau lakes in China. – Journal of Soils and Sediments 17(10): 1-10.
[23] Xu, Q. S., Shi, G. X., Wang, X., Wu, G. R. (2006): Generation of active oxygen and change of antioxidant enzyme activity in Hydrilla verticillata under Cd, Cu and Zn stress. – Acta Hydrobiologica Sinica 30(1): 107-112.
[24] Xue, P. Y., Li, G. X., Liu, W. J., Yan, C. Z. (2010): Copper uptake and translocation in a submerged aquatic plant *Hydrilla verticillata* (L.f.) Royle. – Chemosphere 81(9): 1098-1103.
[25] Zhang, W. B., Xie, Y., Huang, R., Qian, W., Wang, J. (2016): Effects of water pollution of copper on the chlorophyll fluorescence parameters and the growth of Eichhornia crassipes. – Journal of Fujian Normal University (Natural Science Edition) 32(2): 55-61.

http://www.aloki.hu ● ISSN 1589 1623 (Print) ● ISSN1785 0037 (Online)
DOI: http://dx.doi.org/10.15666/aeer/2005_39273938

ASSESSING GENETIC DIVERSITY AND POPULATION STRUCTURE ANALYSIS IN UPLAND COTTON GERMPLASM THROUGH MICROSATELLITES

ÇELIK, S.

Department of Forestry, Genç Vocational School, Bingol University, Genç-Bingol 12500, Turkey
(e- mail: sadettincelik@bingol.edu.tr; phone: +90-535-070-6739; fax: +90-426-216-0029)

(Received 5th Mar 2022; accepted 23rd Aug 2022)

Abstract. Genetic diversity analyses were performed on 96 genotypes using 20 SSR markers to determine the genetic diversity and population structure of the genotypes of *Gossypium hirsutum* L. cotton at the molecular level. As a result of the bioinformatic analysis, 126 alleles ranging from 3 to 12 were produced for 20 SSR markers, with an average of 6.3 alleles per locus. In gene diversity analysis, the highest value was 0.4478 and the lowest value was 08.13, the mean GD was 0.2419. The PIC value ranged between 0.08 and 0.28, with a mean of 0.20. The genetic distance between the Upland cotton genotypes was calculated as the highest 0.973 and the lowest 0.156. According to the UPGMA method, the dendrogram obtained and the genotypes were divided into six main clusters. The optimum K number was K = 3 according to the analysis performed in the STRUCTURE v2.3.4 program examining the population structure. Accordingly, the genotypes used in the analysis were divided into three different groups. This information can be used in the development of mapping populations, in the selection of parents to be used in cultivar development breeding programs through crossbreeding, and in determining the polymorphic levels of SSR markers.
Keywords: A*llele, PIC, SSR, Gossypium hirsutum*

Introduction

Upland cotton (*Gossypium hirsutum* L.) is cultivated for its natural fibers and seeds. In addition to providing raw materials to many industries, it is also the main source of income for millions of people (FAO, 2021). There are approximately 50 cultivars of *Gossypium spp.* (Canbell et al., 2009) and 4 of them are cultivated. Two of the cultured ones are allotetraploid (2n = 4x = 52), while the other two are diploid (2n = 2x = 26). Most of the world cotton production is composed of allotetraploid cultivars, *G. hirsutum* L. and *G. bardabance* L. (Wendel et al., 1992). While the cultivation of Upland cotton, which has the highest adaptation, cultivation and spread in the world, is 90% of the world cotton production, the cultivation rate of *G. barbadense* L. is 8%, and the cultivation rate of *G. herbaceum* L. and *G. Arboretum* L. together is 2% (Abdurakhmonov et al., 2012; Zhang et al., 2008). Upland cotton (*G. hirsutum* L.) is superior in its high yield and wide adaptability, but poor in quality, disease and pest resistance. The second most cultivated cotton, *G. barbadense* L. (Sea-island), is resilient against diseases and pests, and high in quality, but has a low yield and limited adaptation abilities (Wang et al., 2008).

Very important agricultural parameters, such as high yield and wide adaptability of Upland cotton, have also improved other weaknesses, allowing biotic and abiotic disease and pest resistance breeding programs to focus on this cotton type (Seyoum et al., 2018). Underlying a successful and sustainable cultivar development breeding program is the wide cultivar of genetic resources from commercial cultivars, wild or foreign cultivars (McCarty et al., 2006) that breeders use when selecting parents

http://www.aloki.hu ● ISSN 1589 1623 (Print) ● ISSN 1785 0037 (Online)
DOI: http://dx.doi.org/10.15666/aeer/2005_39393953

(Glaszmann et al., 2010). On the other hand, limited genetic variation of upland cotton genotypes limits variation development breeding programs (Paterson et al., 2004; Abdurakhmonov et al., 2012; Brown, 1983). Huang et al. (2002) put forward that genetic diversity is the basis of a successful breeding program, and limited genetic diversity has a negative effect on breeding programs to have cultivars that are resistant to biotic stress factors such as adaptation, diseases and pests, and abiotic stress factors such as drought, salinity and frost. Limited genetic variation causes the cotton cultivars to be prone to epidemic diseases and frail against climate change (Brown, 1983). Some studies have shown that *G. hirsutum* L. cotton cultivars shows the greatest genetic diversity among all other cultivars (Wendel et al., 1992), and the level of genetic diversity is higher than the other three cultivars (Wendel et al., 1992; Abdurakhmonov et al., 2012) but this has not been seen in current cultivars (Van Esbroeck et al., 1999).

Events such as the genetic drift in cotton variations, the founder effect, migration and gene flow, mate selection, and population bottleneck at the mutation, isolation (separation) and domestication phases (Iqbal et al., 2001), using low genetic breeding materials through crossbreeding in variation development breeding studies (May et al., 1995; Bowman et al., 1996; Wendel et al., 1992; Brubaker et al., 1999) cause changes in allele frequencies in the gene pool and consequently decrease the genetic diversity as well (Haw, 2013; Anonymous, 2021; Purves et al., 2003; California University, 2016). In addition, breeding studies conducted with close relatives cause decreases in genetic variation (Wendel et al., 1992; Esbroeck et al., 1999).

Choosing the right parents, the first step in developing resistant/tolerant cultivars to biotic and abiotic stress conditions through crossbreeding, increases the success of breeding programs. For this, parents should be chosen from those who are as far from each other as possible in terms of kinship. This is possible through genetic diversity analysis. Genetic diversity analyses are conducted using morphological and pedigree data (May et al., 1995; Van Esbroeck et al., 1999), biochemical markers (Wendel et al., 1992) and DNA-based markers (Yu et al., 2012). However, since morphological and pedigree data are affected by the environment (Huang et al., 2002), DNA-based markers in genetic diversity analyses are being used more frequently as they are not affected by the environment, can give safer results and are reproducible.

Molecular markers such as RFLP (Restriction fragment length polymorphism) (Ulloa et al., 2005), RAPD (Random amplified polymorphic DNA) (Mumtaz et al., 2010; Sapkal et al., 2011), AFLP (Amplified fragment length polymorphism) (Rana et al., 2005; Badigannavar et al., 2012), ISSR (Intersimple sequence repeats) (Noormohammadi et al., 2011) and SSRs (Simple sequence repeats) (Chen and Du, 2006; Abdurakhmonov et al., 2009; Cai et al., 2014; Tyagi et al., 2014; Zhao et al., 2014) are being used in genetic diversity analysis. However, SSR markers are used in cultivar fingerprinting, Association mapping, QTL mapping and Marker-assisted selection (MAS), especially in genetic diversity analyses, due to their advantages such as being multiallelic and highly polymorphic, their abundance in the plant genome and their ease of use (Reddy et al., 2001; Zhang et al., 2008). SSR markers can be effectively used in *Gossypium spp*. Germplasm resources to do molecular characterization (Liu et al., 2000; Lacape et al., 2007; Sun et al., 2009; Zhang et al., 2005; Reddy et al., 2001).

The aim of this study is to use 96 worldwide *Gossypium hirsutum* L. cotton cultivars germplasm genotypes to assess the genetic diversity, genetic distance, and population structure analyses.

http://www.aloki.hu ● ISSN 1589 1623 (Print) ● ISSN 1785 0037 (Online)
DOI: http://dx.doi.org/10.15666/aeer/2005_39393953

Materials and methods

Plant materials

A set of 96 genotypes of *Gossypium hirsutum* L., located at Agricultural Biotechnology germplasm, Faculty of Agricultural of Kahramanmaraş Sütçü İmam University (Turkey/Kahramanmaraş), collected from different locations worldwide, and which are known for their fiber quality, fiber yield, seed cotton yield, adaptation, number of bolls, important economic parameters such as earliness and tolerance to biotic and abiotic stress conditions were used in the study.

DNA extraction and SSR genotyping

Genomic DNA isolation was performed by taking 0.5 g leaf samples from true young leaves of cotton genotypes and using the Cetyl trimethyl ammonium bromide (CTAB) method developed by Zhang and Stewart (2000). Leaf samples were kept at -80 °C until isolation. DNA isolation was performed after physical grinding with liquid nitrogen, and the control of DNAs was tested by being executed in 1% agarose gel. To clean dirty DNA, Proteinase K enzyme was used, and they have been purified from histone proteins wrapped around the DNAs. Concentrations of DNA were determined by using the Nanodrop spectrophotometer (Thermo fisher).

Genetic diversity analyses of commercial cultivars of 96 *G. hirsutum* L. cotton were carried out using 24 Simple Sequence Repeat (SSR) markers distributed on 26 chromosomes of Upland cotton genome (AD genome). It can be said that in previous studies, of the 20 microsatellites that gave polymorphic bands, 7 belonged to BNL, 5 belonged to JESPR and 8 belonged to NAU marker types were used. The primer sequences of the SSR markers are available in the CottonGene (http://www.cottongene.org) and Cotton Marker (http://www.cottonmarker.org) databases.

PCR amplification, PCR solution and gel electrophoresis were performed according to the technique specified by Zhang and Stewart (2000). Reaction volume of 15 μL^{-1} was used for each PCR cycle. The PCR reaction mixture has 0.75 µL-1 dNTP (Conc.10 mM), 1.5 μL^{-1} 10X PCR buffer, 1 μL^{-1} forward primer, 1 μL^{-1} reverse primer, 0.5 μL^{-1} Taq DNA polymerase. PCR protocol consists of the following stages: Denaturation at 94 °C for 5 min, then at 94 °C with 34 cycles for 1 min, at 60 °C for 1 min, annealing at 72 °C for 2 min, and the extension at 72 °C for 7 min. (Conc.5 U/µL, 2 μL^{-1} template DNA (Conc. 25 ng/μL^{-1}), 8.25 µL ddH2O (double-distilled) components).

PCR products were horizontally electrophoresed with 1% agarose in 1X TBE (Tris-Borate-EDTA) buffer solution. The length of the tapes was measured using a 100-bp DNA ladder. After electrophoresis, the gels were kept in ethidium bromide solution for 20 min and visualized in a UV (Ultraviolet) device.

Data analysis

For alleles amplified by the SSR marker loci, if the bands were present, then they were scored as "1", and if not, as "0". Alleles amplified by each SSR marker locus were assigned letters such as A, B, and C. Parameters such as the number of alleles, genetic diversity (heterozygosity) (Nei, 1972) and Polymorphic information content (PIC; Botstein et al., 1980) were calculated using the PowerMarker ver. 3.25 program (Liu and Muse, 2005) with the scored alleles. Gene diversity (GD) of a locus is accepted as the response of expected heterozygosity (*He*). It shows the expected heterozygosity ratio of

http://www.aloki.hu ● ISSN 1589 1623 (Print) ● ISSN 1785 0037 (Online)
DOI: http://dx.doi.org/10.15666/aeer/2005_39393953

genotypes based on Hardy-Weinberg equilibrium as a measure of the genetic diversity of the population (Nei, 1973). The genetic distance in phylogenetics (Nei et al., 1983) was calculated based on the dissimilarity coefficient of the SSR markers between genotypes. A phylogenetic tree was created using the genetic distance coefficients matrix obtained from POPGENE 1.31 ver. (Yeh et al., 1999) program, and the clustering analysis for all the genotypes in the main and subgroups were conducted using the Unweighted Pair Group Method of Arithmetic Mean (UPGMA) technique. MEGA_11.0.10 ver. program was used in creating, interpreting and organizing the phylogenetic tree (Tamura et al., 2021). PIC value shows the number of alleles at each locus and the distinctive features of the markers through the relative frequencies of alleles in the population (Pei et al., 2010). PIC calculation was based on the formula given below:

$$PIC = 1-\Sigma(Pi)^2$$

The P-value is the frequency of the i^{th} allele of the 96 Upland cotton genotypes subject to the analyses (Weir, 1996).

Population structure

For clustering analysis of genotypes, a Bayesian model-based (Bayesian Model-Based (MBB) STRUCTURE ver. 2.3.4 program using co-dominant genotypic data was used (Pritchard et al., 2010). The subpopulation number (K) of the Upland cotton germplasm genotypes was obtained by calculating the ΔK (Evanno et al., 2005) value. The K value was adjusted between 2-10 and 5 repetitions were made for each K. The STRUCTURE program settings, Leng of Burning Periods and the iteration number of Markov Chain Monte Carlo (MCMC) was set as 10.000-100.000 (Chen et al., 2012; Zoric et al., 2012). Optimum K value was identified for the population. The Compressing results as a zip format were uploaded to the web-based "STRUCTURE HARVESTER" platform (Earl and Von Holdt, 2012).

Results and discussion

Phylogenetic analysis and genetic diversity

In genetic diversity analyses performed on 96 genotypes of Upland cotton, 24 SSR markers were used, 83.3% (20) of them produced polymorphic bands, 12.5% (3) monomorphic bands and 4.2% (1) did not produce any. 126 alleles were produced from 24 SSR markers in total: 6 from BNL0852, 8 from BNL1317, 12 from BNL1690, 4 from BNL1694, 11 from BNL3031, 5 from BNL3140, 6 from BNL3255, 6 from JESPR65, 6 from JESPR114, 6 from JESPR300, 9 from JESPR0092, 7 from JESPR0122, 3 from NAU0923, 9 from NAU2173, NAU2196, 5 from NAU4024, 6 from NAU1037, 6 from NAU1093, 4 from NAU1248, 3 and 4 from NAU2302 markers. For SSR markers that produced polymorphic bands, a mean of 6.3 alleles per locus was produced, while the marker producing the most alleles was BNL1690 (12), while the marker producing the least allele was NAU2196 (3) (*Table 1; Fig. 1*). Similar results were also produced in literature. 5.6 alleles (Lacape et al., 2007), 5.08 (Zhang et al., 2011), and 6.9 alleles (Moiana et al., 2012) were obtained per SSR locus. Liu et al. (2000a) amplified 62 loci in cotton using 56 polymorphic microsatellites and produced a total of 325 alleles, with a mean of 5 alleles per locus. Bertini et al. (2006), in their

http://www.aloki.hu ● ISSN 1589 1623 (Print) ● ISSN 1785 0037 (Online)
DOI: http://dx.doi.org/10.15666/aeer/2005_39393953

genetic diversity analysis in cotton using 31 SSR primary farmers, reproduced 31 loci and duplicated BNL1964 and BNL3408 markers in two loci. They also obtained a total of 66 alleles, with an average of 2.13 alleles per microsatellite locus. Liu et al. (2000b) reproduced 2 loci with SSR primers. Gutiérrez et al. (2002) also reproduced 69 loci using 60 polymorphic SSRs and produced a total of 139 alleles, with a mean of 2 alleles per locus. Due to cotton's allotetraploid genomic structure, SSR primer pairs appear to reproduce multiple loci (Fang et al., 2013). Zhao et al. (2015) reported 2-5 alleles per SSR locus, with a mean of 2.26. Most of the SSR primers used in the study reproduced multiple marker loci polymorphically. In our study, the average allele amount per locus and the total number of alleles were higher than previous genetic diversity analyses (Bertini et al., 2006; Ai et al., 2017; Fang et al., 2013) performed on the same cotton cultivars. It is thought that this may be due to the use of SSR markers with broad-spectrum genetic diversity that show high polymorphism in genetic mapping.

In our study, the Polymorphic information content (PIC) value, which gives information about each SSR primer pair, ranged from 0.12 to 0.35, with a mean of 0.20 (*Table 1; Fig. 1*). As expected in the study, gene diversity (GD) values were higher than PIC values. The PIC values are always lower than the diversity (or *He*) values, and the proliferation of alleles and the increase in the flatness in allele frequencies (the low probability of individuals having similar heterozygous genotypes) bring the PIC value closer to the GD values. Luo et al. (2019) produced similar values in their study as well. These results are similar to the studies of Ai et al. (2017) who found 0.25 mean PIC, Fang et al. (2013) who found 0.29 mean PIC, Rungis et al. (2005) who found 0.37 mean PIC and Bertini et al., who found 0.40 mean PIC in 53 *G. hirsutum* L. cotton genotypes. Tiyagi et al. (2014) found mean PIC values of 0.17 for upland cotton and 0.16 PIC values for *G. barbadense* cotton cultivars in their genetic diversity analyses using *G. hirsutum* and *G. barbadense* cotton cultivars and obtained results similar to our study. A PIC value of "1" indicates that the marker is polymorphic, and a value of "0" indicates that it is a monomorphic marker. At the same time, PIC values of 0.5 and above have the potential to give more information about the marker, if they are between 0.5 and 0.25, they are medium, and if they are less than 0.25, they give very less information about the marker (Tiyagi et al., 2014). Polymorphic information content (PIC) is an analysis that measures the informativeness of the markers used in the analysis (Guo and Elston, 1999). The PIC value was first defined by Botstein et al. (1980) as a measure of the informative trait of a marker independent of the mode of inheritance of the associated trait. Other researchers also identified PIC as a measurement of polymorphism of SSR markers (Gupta and Vershey, 2000; Shete et al., 2000; Botstein et al., 1980). Liu et al. (2000b) obtained PIC values in cotton ranging between 0.05-0.082, with a mean of 0.31. Guang and Xiong-Ming (2006) obtained a mean of 3.6 alleles, between 2 and 8 per primer. PIC values ranged between 0.278-0.865 with a mean of 0.62. The fact that the PIC values in our study were lower than some studies in the literature may be due to genetic diversity analyses being conducted using cultured commercial cultivars. Iqbal et al. (1997) and Tatineni et al. (1996) concluded in their research that genetic diversity is low in molecular diversity studies conducted using the cultured cotton cultivars. The low biodiversity in cultivated Upland cotton is due to bottleneck events during the domestication phase (Brubaker and Wendel, 1994; Wendel and Cronn, 2003; May et al., 1995; Iqbal et al., 2001). However, developments in the technology of obtaining transgenic cotton also contribute to the decrease in the level of genetic diversity in other cotton growing countries, especially in the USA (Zhang et al., 2005).

http://www.aloki.hu ● ISSN 1589 1623 (Print) ● ISSN 1785 0037 (Online)
DOI: http://dx.doi.org/10.15666/aeer/2005_39393953

Table 1. *Polymorphic SSR marker properties used in this study*

No.	Primer name	Primer sequences	Repeat motify	Location	Allele no.	Gene diver (GD)	PIC
1	BNL0852	F: TGCTTTCAGCCAATGACTTG R: AACAATGCCCCCAATATTCA	(CA)13	Chr9.	6	0.3185	0.27
2	BNL1317	F: AAAAATCAGCCAAATTGGGA R: CGTCAACAATTGTCCCAAGA	(AG)14	Chr6.	8	0.2474	0.21
3	BNL1690	F: TTTGTCTTTCTGTTACCAAATGG R: CCAGGAAATTTGAGGTGGAA	(GA)10	Chr9	12	0.0813	0.08
4	BNL1694	F: CGTTTGTTTTCGTGTAACAGG R: TGGTGGATTCACATCCAAAG	(AG)19, (TC)19	Chr1.	4	0.3462	0.27
5	BNL3031	F: AGGCTGACCCTTTAAGGAGC R: AACCAACTTTTCCAACACCG	(AG)27	D09.	11	0.2547	0.22
6	BNL3140	F: CACCATTGTGGCAACTGAGT R: GGAAAAGGGAAAGCCATTGT	(GA)11	A09.	5	0.2960	0.24
7	BNL3255	F: GACAGTCAAACAGAACAGATATGC R: TTACACGACTTGTTCCCACG	(GC)6, AT(AC)14	A08.	6	0.4478	0.35
8	JESPR0065	F: CCACCCAATTTAAGAAGAAATTG R: GGTTAGTTGTATTAGGGTCGTTG	(GAA)25	A05.	6	0.3495	0.28
9	JESPR 114	F: GATTTAAGGTCTTTGATCCG R: CAAGGGTTAGTAGGTGTGTATAC	(GT)12	D10.	6	0.3117	0.26
10	JESPR 300	F: CGCATCACAAACCAAACAC R: CGGAAAATGATGATGATGAAGAAG	(CTT)5, (CAT)6	Chr8.	6	0.2306	0.20
11	JESPR0092	F: GGGACCTCTATTGAATAGCTGGAG R: CTCTTGGCATCATTAGTTCCTGG	(GAA)23	D12.	9	0.2324	0.20
12	JESPR0122	F: GCTGCTGGTTTTACTTGTTGG R: CTATGGTGGAGGAGCAACAAC	(CAT)5	Chr05.	7	0.1357	0.12
13	NAU0923	F: GGAATTCAAGGTTGAAGGAG R: CCTCTTCTTTGGCTCTGAAA	(TCTTTT)4	Chr6	3	0.3138	0.26
14	NAU2173	F: GCCAAATAGGTCACACACAA R: AGCGAGAAGGAGACAGAAAA	AAG (17)	NA	9	0.2054	0.17
15	NAU2196	F: TCAAGAAAACATGCCTGCTA R: CTATTTGCTCGTTGTTGACG	CAT (4)	Chr7.	3	0.3306	0.27
16	NAU4024	F: ACAAGCATCTTCATGGACCT R: AGAAGGATGATGCAAAGAGG	(GTC)6	Chr5	5	0.2345	0.20
17	NAU1037	F: CACCTTCACCTAACCATCAA R: GAAGAATTGCGAGAAGAGGA	(CTGCCA)3	-	6	0.1570	0.14
18	NAU1093	F: TGTGATGAAGAACCCTCTCA R: AAATGGCGTGCTTGAAATAC	(TA)14	-	6	0.1831	0.16
19	NAU1248	F: AATGTCAGCTGCCTATTTCC R: AAGACAGGCGATGTCATCTT	(TCTTCC)3	Chr5.	4	0.2281	0.20
20	NAU2302	F: CAAACCGTCAAATGAGACAA R: GCCTCTAAGGGTCCCTACTC	AT(12); GA (10)	Chr12	4	0.2419	0.20
Mean				-	6.3	0.2419	0.20
Total				-	126	-	-

In the current study, the genetic diversity varied between 0.08130 and 0.4478, with a mean of 0.2419 (*Table 1; Fig. 1*). While BNL3255, JESPR0065 and NAU2196 showed the highest genetic diversity values, BNL1690, JESPR0122 and NAU1037 markers showed the lowest genetic diversity values (*Table 1*). There are studies with similar results in the literature. Seyoum et al. (2017) obtained genetic diversity values ranging from 0.020 to 0.492, with a mean of 0.279. The low genetic diversity in genetic diversity studies conducted using the upland cotton may be due to the fact that the developed upland cotton cultivars were obtained using very few genotypes (Chen and Du, 2006; Du et al., 2007). Rungis et al. (2005) stated that the bottleneck events occurring in the first stage of modern upland cotton cultivar developments lead to a

http://www.aloki.hu ● ISSN 1589 1623 (Print) ● ISSN 1785 0037 (Online)
DOI: http://dx.doi.org/10.15666/aeer/2005_39393953

significant decrease in the level of genetic diversity in upland cotton cultivars. Low genetic diversity studies were carried out on Upland cotton cultivars (Tiyagi et al., 2014; Campbell et al., 2009; Abdurakhmonov et al., 2008). Heterozygosity levels of marker data can be calculated by averaging the similarity frequencies of alternative alleles (Heterozygosity, *H*: 0.9 or 0.5 values indicate high heterozygosity, while *H*: 0.1 indicates low heterozygosity (Li et al., 2007).

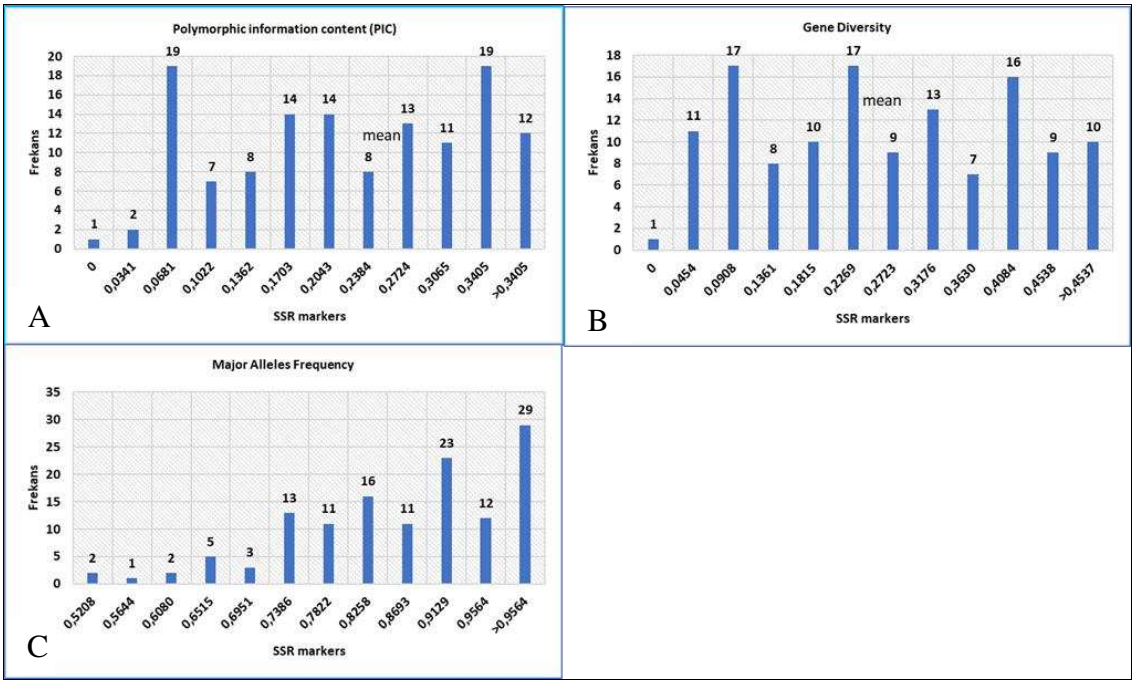

Figure 1. *(A) Polymorphic information content (PIC), (B) genetic diversity (GD), (C) major alleles frequency (MAF)*

The genetic distance between the Upland cotton genotype pairs was based on the pairwise matching technique of Nei (1972), and the genetic distance values between the Upland cotton genotypes varied between 0.973 and 0.015. The highest genetic distance was between 308 (Campo) and DPL-5614 and Israel-2 (0.9730). These were followed by 308 (Campo) and Stoneville 506 with 0.9322 genetic distance value, and the values between DP 5111, Nazilli 303 and 93 FF 01 and Nazilli 303 genotypes. The lowest genetic distance values were obtained between Delcerro and 4SP, CA-228; DPL50-DPL5409, DPL5614- DPL50 and DPL50- ERŞAN-92 genotypes. The low genetic distance between them is directly proportional to the degree of relation. Similar studies have been carried out in the literature. The similarity coefficient ranged between 0.407 and 0.767, with a mean value of 0.587 (Hancı and Gokçe., 2016). Nas et al. (2011) recorded a GD coefficient as low as 0.40 between the two cultivars and stated that this might be due to these cultivars being closely related. In addition, the genetic distance between heterogeneous genotypes (generally wild cultivars) should be higher than homogeneous (breeding genotypes) genotypes (Hinze et al., 2017). The genetic distance in the genetic diversity analyses performed in the F_2 cotton population varied between 0.06-0.34 (Gutierrez et al., 2002). The genetic distance between genotypes of the Upland cotton cultivars is higher than the F_2 segregation population from the same mother and father, due to the possibility of having different parents. The genetic

http://www.aloki.hu ● ISSN 1589 1623 (Print) ● ISSN 1785 0037 (Online)
DOI: http://dx.doi.org/10.15666/aeer/2005_39393953

distance between *G. hirsutum* and *G. barbadense* varies between 42-54% (Kebede et al., 2007). Lacape et al. (2007) revealed that there is a higher genetic distance between *G. hirsutum* and *G. barbadense* (GD = 0.89-0.91). Analyses with highly polymorphic SSR markers showed a high difference between G. *hirsutum* and G. *tomentosum* (D:0.71-0.75) and between G. *barbadense* and G. *tomentosum* (D:0.80) (Lacape et al., 2007). Kebede et al. (2007) also stated that the genetic distance between genotypes belonging to cotton genome groups such as A and D varies between 29-42%. The genetic distance between those included in the AD tetraploid cotton group also varies between 0.80-0.88 (Liu et al., 2000).

Ninety-six upland cotton cultivars were divided into 6 main groups in phylogenetic tree analysis conducted in the MEGA_11.0.10 computer program using short tandem repeat markers (*Fig. 2*). The groups are as follows: Flash genotype in an independent group, Marcell leaf brown, israil 2, Paymaster 2379, Acala 552, DP 388, Dulcerro, 308 (Campo), 153 F, and 111 glandless genotypes in first group, TX0091-2, STV 474, PI 528420, STV-132, Acala Prema, Lockette genotypes in the second group, Okra 201, Nazilli 503, Mn nair 235-612, Acala 172, 93 FF01, 919 (leader) genotypes in the third group, Acala 1517-D, PI 528872 (SEALAND 3), Acala 1517-99, Nazilli 87, STV-506, DPL-529, Acala 3080, Is 10, Orgosta 644 genotypes in the fourth group, Tamcot Luxor and Sahel 1 genotypes in the fifth group, Cabu cs 2-1-8-3, Deltapine 5111, BA 525, STV 373, Deltapine 419, Celia, PI 529128 (Acala 1517 D) and Deltapine 50 genotypes in the sixth group. The remaining 63 genotypes formed subsets among themselves and clustered in a separate sixth group (*Fig. 2*). Similar studies were conducted in the literature. Ulah et al. (2012) stated that their dendrogram built using 19 Bt cotton genotypes was divided into three main groups and two independent groups, Fang et al. (2013) stated that 193 upland cotton genotypes formed 15 main groups and two independent groups, and Erdal (2018) stated that the genotypes were clustered in four main groups in dendrogram, and formed 8 subgroups.

Population structure analysis in MBB subpopulations

Using the STRUCTURE v 2.3.4 ver. (Pritchard et al., 2000) program, the structure of the cotton populations and the genetic relationship between 96 upland cotton (*G. Hirsutum* L.) cultivars obtained from different countries were tried to be revealed. The K value shows the number of the clusters obtained in cluster analysis using genotypic data. The most suitable K values was calculated via the log likelihood of the data and to find the value of optimum K (Number of subpopulations), the number of clusters was plotted against Delta K ($\triangle$K), which indicates the highest peak point to K = 3. Two peaks occurred at K = 5 and K = 9. Since this provides information about these two different populations, it is important. According to Seyoum et al. (2018), the entire germplasm population was divided into three subpopulations in their clustering analysis conducted using the STRUCTURE program. Population structure analysis shows that the highest population number $\triangle$K value is K = 3, and the whole population is divided into 3 subpopulations (*Figs. 2* and *3*).

Population structure analyzes are the guides for understanding genetic diversity and for association mapping studies and for planning the future. Since the presence of population structure data in Association mapping (AM) analyses may cause incorrect marker-trait matching, testing the population structure is the first step in establishing a correct marker-trait match and determining the gene/genes controlling the trait (Eltaher et al., 2018). While the number of subpopulations could not be determined in the Ln (K)

http://www.aloki.hu ● ISSN 1589 1623 (Print) ● ISSN 1785 0037 (Online)
DOI: http://dx.doi.org/10.15666/aeer/2005_39393953

plot in the study (*Fig. 3a*), 3 groups (G1, G2, G3) were determined based on the optimum ΔK value (*Fig. 3b*). However, these three clusters happen to be mixed significantly (*Fig. 3c*). Each group is indicated by a color. Similar results were obtained in the phylogenetic tree (Neighbor-joining tree). Groups of different colors show that they were bred in different geographic locations (Tiyagi et al., 2014). Ai et al. (2017) has also reported similar results. Population structure and determining the relationship between Upland cotton genotypes are of great importance for the development, characterization and maintenance of genotypes. Results of our study are similar with the studies of Jia et al. (2014b) and Ai et al. (2017) who divided the genotypes into three groups as a result of STRUCTURE analyses using Upland cotton genotypes originated in China. Although Mei et al. (2013) divided Upland cotton genotypes into two subsets as a result of MBB structure analysis even though they used Upland cottons originated in China, Tiyagi et al. (2014) used upland cotton cultivars originating from the USA and the genotypes were divided into five main populations. It is thought that the difference here may be due to the cotton genotype type, the breeding stage and the geographical location of breeding.

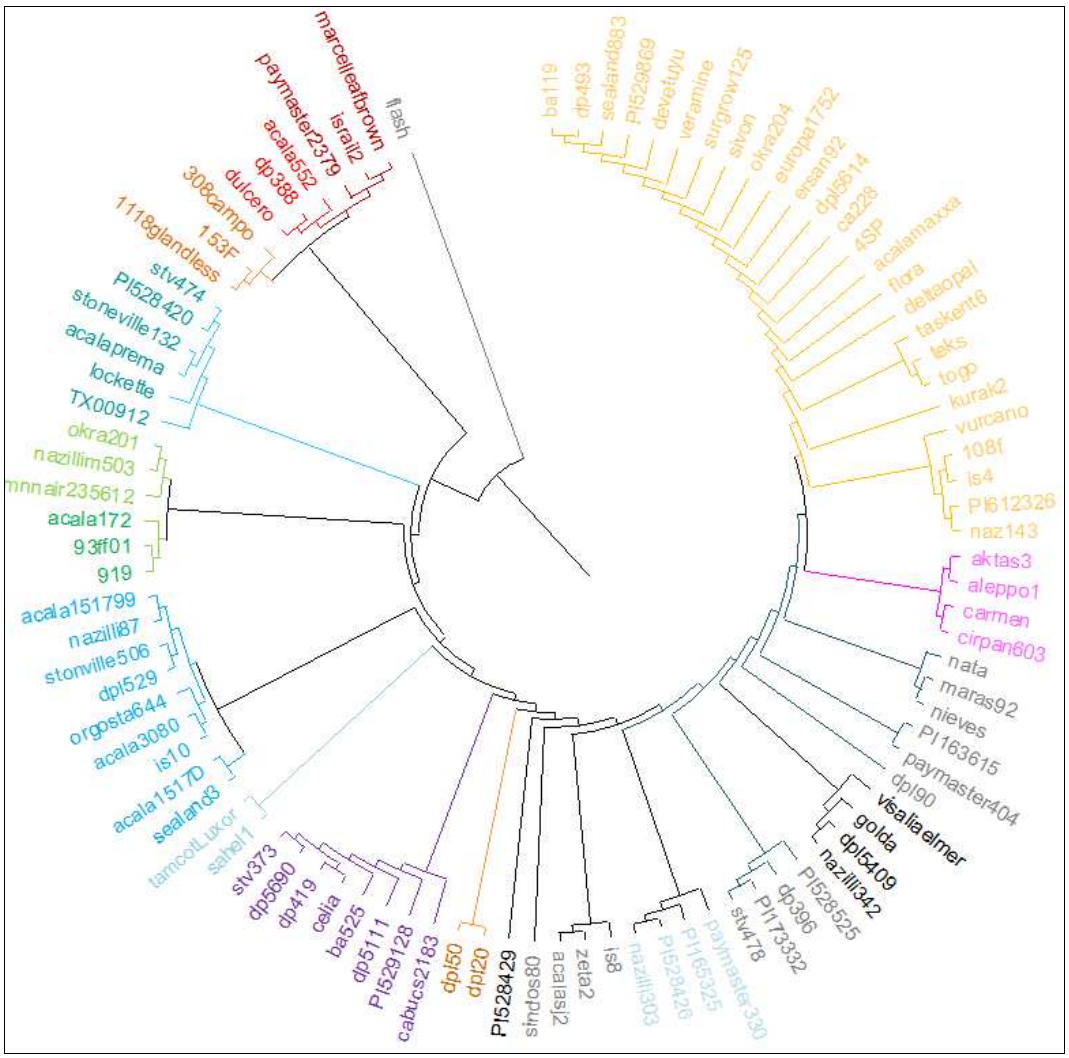

Figure 2. *Cluster analyses of 96 upland cotton genotypes using unweighted pair group of arithmetic mean (UPGMA) Basid Neil's 1972 in MEGA_11.0.10 (Tamura et al., 2021). Six major clusters were obtained.*

http://www.aloki.hu ● ISSN 1589 1623 (Print) ● ISSN 1785 0037 (Online)
DOI: http://dx.doi.org/10.15666/aeer/2005_39393953

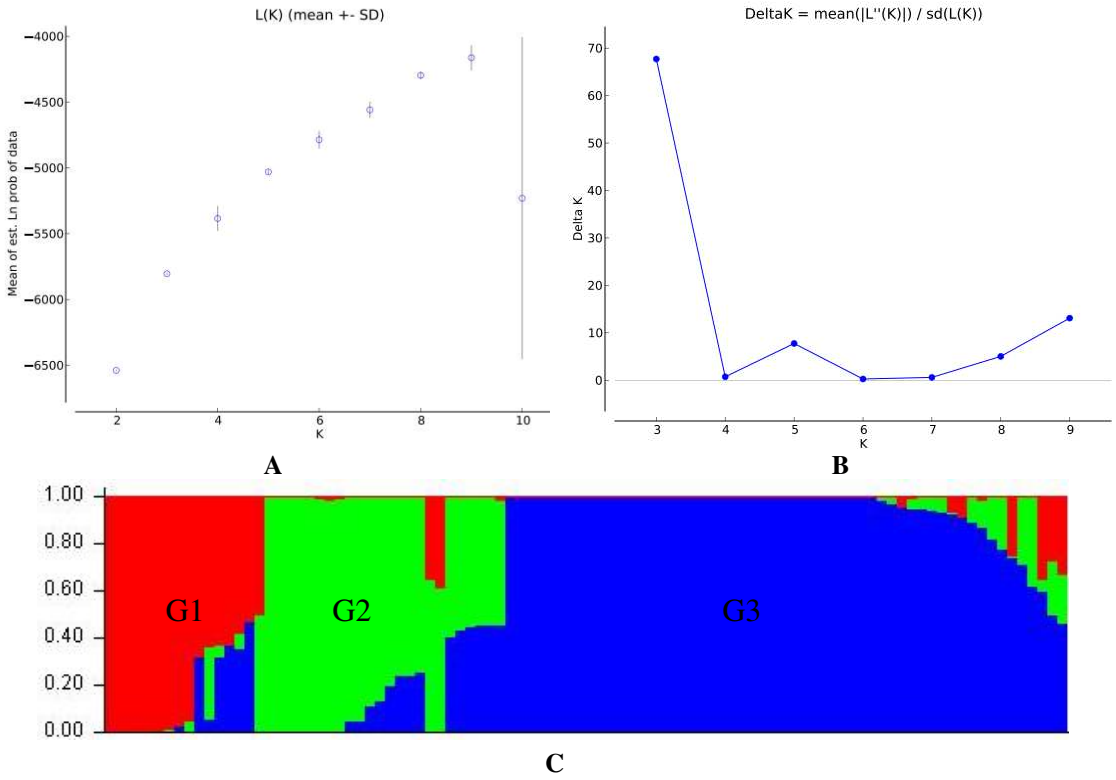

Figure 3. *(A) The plot of Ln (probability of data) analysis in the population structure. (B) Estimating the number of subpopulations DK value (⊿K) using Evanno et al. (2005) method. (C) The Q-plot indicates the Model-based Bayesian (MBB) structure clustering of a panel of 96 upland cotton genotypes. Each vertical bar represents a genotype. Each color represents the estimated member individuals of each K group*

Conclusions

Genetic diversity results from modification of the plant's genome to adapt to changing environmental conditions. As a result of such modifications, differences occur in the genomes of plants and Microsatellites, which can detect these differences, are used in genetic diversity analyses in cotton plants thanks to their high polymorphic capabilities. As expected, in the study, the PIC values were lower than gene diversity values. Polymorphic levels of SSR markers were found to be high and PIC values that provide information about the marker were calculated using the PowerMarker program. The genetic distance between the Upland cotton genotypes was similar to the literature. As a result of UPGMA analysis, genotypes were divided into 6 main clusters and a total of 5 large clusters were formed. The sixth major cluster covers the vast majority of cotton genotypes. In the analysis of the population structure, the clusters were divided into 3 groups depending on the geographical regions, but the genotypes were partially mixed with each other due to the use of the parents obtained from different geographic locations in breeding programs. The genetic diversity, which is generally low, is getting lower. Genetic diversity analyzes and population structure analyses enable benefitting from genetic variation in genomic studies. Considering the other economic characteristics of the genotypes that are genetically far from each other, the development of resistant cultivars against biotic and abiotic diseases and pests can be used as parents in breeding programs using marker-assisted selection technology. In

http://www.aloki.hu ● ISSN 1589 1623 (Print) ● ISSN 1785 0037 (Online)
DOI: http://dx.doi.org/10.15666/aeer/2005_39393953

addition, SSR markers, whose polymorphic levels are determined, can enable the development of mapping populations for genetic mapping such as high-resolution linkage mapping and Association mapping.

Acknowledgements. The author is grateful to associate Prof. Dr. Adem Bardak for providing cotton germplasm materials, and Osman Yiğit for the assistance on laboratory analyses in Kahramanmaraş Sütçü Imam University, Agricultural Biotechnology Laboratory.

REFERENCES

[1] Abdurakhmonov, I., Kohel, R., Yu, J., Pepper, A., Abdullaev, A., Kushanov, F. et al. (2008): Molecular diversity and association mapping of fiber quality traits in exotic G. hirsutum L. germplasm. – Genomics 92: 478-487.

[2] Abdurakhmonov, I., Saha, S., Jenkins, J., Buriev, Z., Shermatov, S., Scheffler, B. et al. (2009): Linkage disequilibrium based association mapping of fiber quality traits in G. hirsutum L. variety germplasm. – Genetica 136: 401-417.

[3] Abdurakhmonov, I. Y., Buriev, Z. T., Shermatov, S. E., Abdullaev, A. A., Urmonov, K., Kushanov, F., Egamberdiev, S. S., Shapulatov, U., Abdukarimov, A., Saha, S., Jenkins, J. N., Kohel, R. J., Yu, J. Z., Pepper, A. E., Kumpatla, S. P., Ulloa, M. (2012): Genetic Diversity in *Gossypium* Genus. – In: Caliskan, M. (ed.) Genetic Diversity in Plants 7. InTech, London, pp. 313-338.

[4] Ai, X., Liang, Y., Wang, J., Zheng, J., Gong, Z., Guo, J., Qu, Y. (2017): Genetic diversity and structure of elite cotton germplasm (*Gossypium hirsutum* L.) using genome-wide SNP data. – Genetica 145(4): 409-416.

[5] Anonymous (2021): Genetic drift and the founder effect. – Evolution. http://www.pbs.org/wgbh/evolution/library/06/3/l_063_03.html.

[6] Badigannavar, A., Myers, G. O., Jones, D. C. 2012 Molecular diversity revealed by AFLP Markers in upland cotton genotypes. – J. Crop Improvement 26: 627-640.

[7] Bertini, C. H., Schuster, I., Sediyama, T., Barros, E. G. D., Moreira, M. A. (2006): Characterization and genetic diversity analysis of cotton cultivars using microsatellites. – Genetics and Molecular Biology 29: 321-329.

[8] Botstein, D., White, R. L., Skolnick, M., Davis, R. W. (1980): Construction of a genetic linkage map in man using restriction fragment length polymorphisms. – Am J Hum Genet 32: 314-331.

[9] Bowman, D. T., May, O. L., Calhoun, D. S. (1996): Genetic base of upland cotton cultivars released between 1970 and 1990. – Crop Sci 36: 577-581.

[10] Brown, W. L. (1983): Genetic diversity and genetic vulnerability: an appraisal. – Econ Bot 37: 4-12.

[11] Brubaker, C. L., Wendel, J. F. (1994): Re-evaluating the origin of domesticated cotton (Gossypium hirsutum: Malvaceae) using nuclear restriction fragment length polymorphisms (RFLPs). – Am J Bot 81: 1309-1326.

[12] Brubaker, C. L., Bourland, F. M., Wendel, J. F. (1999): The Origin and Domestication of Cotton. – In: Smith C. W., Cothren J. T. (eds.) Cotton: Origin, History, Technology, and Production. Wiley, New York, pp 3-32.

[13] Cai, C. P., Ye, W. X., Zhang, T. Z., Guo, W. Z. (2014): Association analysis of fiber quality traits and exploration of elite alleles in Upland cotton cultivars/accessions (*Gossypium hirsutum* L.). – J. Integr. Plant Biol. 56: 51-62.

[14] Campbell, B. T., Williams, V. E., Park, W. (2009): Using molecular markers and field performance data to characterize the Pee Dee cotton germplasm resources. – Euphytica 169: 285-301.

http://www.aloki.hu ● ISSN 1589 1623 (Print) ● ISSN 1785 0037 (Online)
DOI: http://dx.doi.org/10.15666/aeer/2005_39393953

[15] Chen, G., Du, X. M. (2006): Genetic diversity of source germplasm of upland cotton in China as determined by SSR marker. – Acta Genet. Sinica 33: 1-10.
[16] Chen, X., Min, D., Yasir, T. A., Hu, Y. G. (2012): Genetic diversity, population structure and linkage disequilibrium in elite Chinese winter wheat investigated with SSR markers. – PLoS One 7: e44510.
[17] Du, X. M., Zhou, Z. L., Jia, Y. H., Liu, G. Q. (2007): Collection and conservation of cotton germplasm in China (English abstract). – CNKI Cotton Sci. 19: 346-353.
[18] Earl, D. A., vonHoldt, B. M. (2012): Structure harvester: a website and program for visualizing structure output and implementing the Evanno method. – Conserv. Genet. Resour. 4: 359-361.
[19] Eltaher, S., Sallam, A., Belamkar, V., Emara, H. A., Nower, A. A., Salem, K. F. M. et al. (2018): Genetic diversity and population structure of F3:6 Nebraska winter wheat genotypes using genotyping-by-sequencing. – Front. Genet. 9: 76.
[20] Erdal, Ş. (2018): Determination of genetic distances of inbred maize lines. – Derim 35(1): 73-80.
[21] Esbroeck, G. V., Bowman, D. T., May, O. L., Calhoun, D. S. (1999): Genetic similarity indices for ancestral cotton cultivars and their impact on genetic diversity estimates of modern cultivars. – Crop Sci. 39: 323-328.
[22] Evanno, G., Regnaut, S., Goudet, J. (2005): Detecting the number of clusters of individuals using the software STRUCTURE: a simulation study. – Mol Ecol 14: 2611-2620.
[23] Fang, D. D., Hinze, L. L., Percy, R. G., Li, P., Deng, D., Thyssen, G. (2013): A microsatellite-based genome-wide analysis of genetic diversity and linkage disequilibrium in Upland cotton (*Gossypium hirsutum* L.) cultivars from major cotton-growing countries. – Euphytica 191(3): 391-401.
[24] FAO (2021): https://www.fao.org/land-water/databases-and-software/crop-information/cotton/en/ – Access: 12.10.2021.
[25] Glaszmann, J. C., Kilian, B., Upadhyaya, H. D., Varshney, R. K. (2010): Accessing genetic diversity for crop improvement. – Curr. Opin. Plant Biol. 13: 167-173.
[26] Guang, C. H. E. N., Xiong-Ming, D. U. (2006): Genetic diversity of source germplasm of upland cotton in China as determined by SSR marker analysis. – Acta Genetica Sinica 33(8): 733-745.
[27] Guo, X., Elston, R. (1999): Linkage information content of polymorphic genetic markers. – Human Heredity 49(2): 112-118.
[28] Gupta, P. K., Varshney, R. K. (2000): The development and use of microsatellite markers for genetic analysis and plant breeding with emphasis on bread wheat. – Euphytica 113: 163-185.
[29] Gutierrez, O. A., Basu, S., Saha, S., Jenkins, J. N., Shoemaker, D. B., Cheatham, C. L., McCarty, J. C. (2002): Genetic distance among selected cotton genotypes and its relationship with F2 performance. – Crop Science 42: 1841-1847.
[30] Hanci, F., Gökçe, A. F. (2016): Molecular characterization of Turkish onion germplasm using SSR markers. – Czech Journal of Genetics and Plant Breeding 52(2): 71-76.
[31] Haw, J. (2013): Northern elephant seals: increasing population, decreasing biodiversity. – Scientific American. http://blogs.scientificamerican.com/expeditions/northern-elephant-seals increasing-population-decreasing-biodiversity/.
[32] Hinze, L. L., Hulse-Kemp, A. M., Wilson, I. W., Zhu, Q. H., Llewellyn, D. J., Taylor, J. M., Stelly, D. M. (2017): Diversity analysis of cotton (Gossypium hirsutum L.) germplasm using the CottonSNP63K Array. – BMC Plant Biology 17(1): 1-20.
[33] Huang, X., Börner, A., Röder, M., Ganal, M. (2002): Assessing genetic diversity of wheat (Triticum aestivum L.) germplasm using microsatellite markers. – Theoretical and Applied Genetics 105(5): 699-707.

http://www.aloki.hu ● ISSN 1589 1623 (Print) ● ISSN 1785 0037 (Online)
DOI: http://dx.doi.org/10.15666/aeer/2005_39393953

[34] Iqbal, M. J., Aziz, N., Saeed, N. A., Zafar, Y. (1997): Genetic diversity evaluation of some elite cotton varieties by RAPD analysis. – Theoretical and Applied Genetic 94: 139-144.
[35] Iqbal, A. E., Reddy, O. U. K., El-Zik, K. M., Pepper, A. E. (2001): A genetic bottleneck in the 'evolution under domestication' of upland cotton *Gossypium hirsutum* L. examined using DNA fingerprinting. – Theor Appl Genet. 103: 547-554.
[36] Jia, Y. H., Sun, J. L., Wang, X. W., Zhou, Z. L., Pan, Z. E., He, S. P. et al. (2014b): Molecular diversity and association analysis of drought and salt tolerance in *G. hirsutum* L. germplasm. – J. Integr. Agric. 30: 1845-1853.
[37] Kebede, H., Burow, G., Dani, R. G., Allen, R. D. (2007): A-genome cotton as a source of genetic variability for upland cotton (*Gossypium hirsutum*). – Genetic Resources and Crop Evolution 54(4): pp. 885-895.
[38] Lacape, J. M., Dessauw, D., Rajab, M., Noyer, J. L., Hau, B. (2007): Microsatellite diversity in tetraploid *Gossypium* germplasm: assembling a highly informative genotyping set of cotton SSRs. – Molecular Breeding 19(1): 45-58.
[39] Li, Y., Li, Y., Han, K., Wang, Z., Hou, W., Zeng, Y. et al. (2007): Estimation of multilocus linkage disequilibria in diploid populations with dominant markers. – Genetics 176: 1811-1821.
[40] Liu, K., Muse, S. V. (2005): PowerMarker: an integrated analysis environment for genetic marker analysis. – Bioinformatics 21: 2128-2129.
[41] Liu, S., Cantrell, R. G., McCarty-Jr, J. C., Stewart, J. Mc. D. (2000a): Simple sequence repeat based assessment of genetic diversity in cotton race stock accessions. – Crop Science 40: 1459-1469.
[42] Liu, S., Saha, S., Stelly, D., Burr, B., Cantrell, R. G. (2000b): Chromosomal assignment of microsatellite loci in cotton. – Journal of Heredity 91: 326-332.
[43] Luo, Z., Brock, J., Dyer, J. M., Kutchan, T., Schachtman, D., Augustin, M., Abdel-Haleem, H. (2019): Genetic diversity and population structure of a Camelina sativa spring panel. – Frontiers in Plant Science 10: 184.
[44] May, O. L., Bowman, D. T., Calhoun, D. S. (1995): Genetic diversity of U.S. upland cotton cultivars released between 1980 and 1990. – Crop Sci 35: 1570-1574.
[45] McCarty, J. C., Wu, J., Jenkins, J. N. (2006): Genetic diversity for agronomic and fiber traits in day-neutral accessions derived from primitive cotton germplasm. – Euphytica 148: 283-293.
[46] Mei, H., Zhu, X., Zhang, T. (2013): Favorable QTL alleles for yield and its components identified by association mapping in Chinese Upland cotton cultivars. – PLoS One 8: e82193.
[47] Moiana, L. D., Filho, P. S. V., Gonçalves-Vidigal, M. C., Carvalho, L. P. (2012): Genetic diversity and population structure of cotton (*Gossypium hirsutum* L. race latifolium H.) using microsatellite markers. – Afr. J. Biotechnol. 11: 11640-11647.
[48] Mumtaz, A. S., Naveed, M., Shinwari, Z. K. (2010): Assessment of genetic diversity and germination pattern in selected cotton genotypes of Pakistan. – Pak. J. Bot. 42: 3949-3956.
[49] Nas, M. N., Bolek, Y., Bardak, A. (2011): Genetic diversity and phylogenetic relationships of Prunus microcarpa CA Mey. subsp. tortusa analyzed by simple sequence repeats (SSRs). – Scientia Horticulturae 127(3): 220-227.
[50] Nei, M. (1972): Genetic distance between populations. – Am. Nat. 106 283-292.
[51] Nei, M. (1973): Analysis of gene diversity in subdivided populations. – Proc. Natl. Acad. Sci. USA 70: 3321-3323.
[52] Nei, M. (1987): Molecular Evolutionary Genetics. – Columbia University Press, New York.
[53] Nei, M., Tajima, F., Tateno, Y. (1983): Accuracy of estimated phylogenetic trees from molecular data. II. Gene frequency data. – J Mol Evol 19: 153-170.

http://www.aloki.hu ● ISSN 1589 1623 (Print) ● ISSN 1785 0037 (Online)
DOI: http://dx.doi.org/10.15666/aeer/2005_39393953

[54] Noormohammadi, Z., Jesvaghani, F. S., Sheidai, M., Farahani, F., Alishah, O. (2011): Inter simple sequence repeats (ISSR) and random amplified polymorphic DNA (RAPD) analyses of genetic diversity in Mehr cotton cultivar and its crossing progenies. – Afr. J. Biotechnol. 10: 11839-11847.
[55] Paterson, A., Boman, R., Brown, S., Chee, P., Gannaway, J., Gingle, A. et al. (2004): Reducing the genetic vulnerability of cotton. – Crop Sci. 44: 1900-1901.
[56] Pei, Z., Gao, J. Q., Chen, J., Wie, Z., Li, F., Luo, L., Shi, B., Ding, S., Sun, S. (2010): Genetic diversity of elite sweet sorghum genotypes assessed by SSR markers. – Biologia Plantarum 54(4): 653-658.
[57] Pritchard, J. K., Stephens, M., and Donnelly, P. (2000): Inference of population structure using multilocus genotype data. – Genetics 155: 945-959.
[58] Purves, W. K., Sadava, D., Orians, G. H., Heller, H. C. (2003): Genetic drift may cause large changes in small populations. – In: Purves, W. K. et al. (eds.) Life: The Science of Biology. Sinauer, Sunderland, MA, pp. 468-469.
[59] Rana, M. K., Singh, V. P., Bhat, K. V. (2005): Assessment of genetic diversity in upland cotton (Gossypium hirsutum L.) breeding lines by using amplified fragment length polymorphism (AFLP) markers and morphological characteristics. – Genet. Resour. Crop Evol. 52: 989-997.
[60] Reddy, O. U. K., Pepper, A. E., Abdurakhmonov, I., Saha, S., Jenkins, J. N., Brooks, T. D. (2001): New dinucleotide and trinucleotide microsatellite markers for cotton genomic research. – J. Cotton Sci. 5: 103-113.
[61] Rungis, D., Llewellyn, D., Dennis, E. S., Lyon, B. R. (2005): Simple sequence repeat (SSR) markers reveal low levels of polymorphism between cotton (Gossypium hirsutum L.) cultivars. – Australian Journal of Agricultural Research 56(3): 301-307.
[62] Sapkal, D. R., Sutar, S. R., Thakre, P. B., Patil, B. R., Paterson, A. H., Waghmare, V. N. (2011): Genetic diversity analysis of maintainer and restorer accessions in Upland cotton (*Gossypium hirsutum* L.). – J. Plant Biochem. Biotechnol. 20: 20-28.
[63] Seyoum, M., Du, X. M., He, S. P., Jia, Y. H., Pan, Z., Sun, J. L. (2017): Analysis of genetic diversity and population structure in upland cotton (*Gossypium hirsutum* L.) germplasm using simple sequence repeats. – Journal of Genetics 97(2): 513-522.
[64] Shete, S., Tiwari, H., Elston, R. C. (2000): On estimating the heterozygosity and polymorphism information content value. – Theor. Popul. Biol. 57: 265-271.
[65] Sun, D. L., Sun, J. L., Jia, Y. H., Ma, Z. Y., Du, X. M. (2009): Genetic diversity of colored cotton analyzed by simple sequence repeat markers. – Int. J. of Plant Sci. 170: 76-82.
[66] Tamura, K., Stecher, G., Kumar S. (2021): MEGA 11: Molecular Evolutionary Genetics Analysis Version 11. – Molecular Biology and Evolution. https://doi.org/10.1093/molbev/msab120.
[67] Tatineni, V., Cantrell, R. G., Davis, D. D. (1996): Genetic diversity in elite cotton germplasm determined by morphological characteristics and RAPDs. – Crop Science 36: 186-192.
[68] Tyagi, P., Gore, M. A., Bowman, D. T., Cambell, B. T., Udall, J. A., Kuraparthy, V. (2014): Genetic diversity and population structure in the US Upland cotton (*Gossypium hirsutum* L.). – Theor Appl. Genet. 127: 283-295.
[69] Ullah, I., Iram, A., Iqbal, M. Z., Nawaz, M., Hasni, S. M., Jamil, S. (2012): Genetic diversity analysis of Bt cotton genotypes in Pakistan using simple sequence repeat markers. – Genetics and Molecular Research 11(1): 597-605.
[70] Ulloa, M., Saha, S., Jenkins, J. N., Meredith Jr, W. R., McCarty Jr, J. C., Stelly D. M. (2005): Chromosomal assignment of RFLP linkage groups harboring important QTLs on an intraspecific cotton (*Gossypium hirsutum* L.) join map. – J. Hered. 96: 132-144.
[71] University of California Museum of Paleontology (2016): Bottlenecks and founder effects. – Understanding Evolution. http://evolution.berkeley.edu/evolibrary/article/bottlenecks_01.

http://www.aloki.hu ● ISSN 1589 1623 (Print) ● ISSN 1785 0037 (Online)
DOI: http://dx.doi.org/10.15666/aeer/2005_39393953

[72] Van Esbroeck, G. A., Bowman, D. T., May, O. L., Calhoun, D. S. (1999): Genetic similarity indices for ancestral cotton cultivars and their impact on genetic diversity estimates of modern cultivars. – Crop Sci 39: 323-328.
[73] Wang, H. M., Lin, Z. X., Zhang, X. L., Chen, W., Guo, X. P., Nie, Y. C., Li, Y. H. (2008): Mapping and quantitative trait loci analysis of Verticillium wilt resistance genes in cotton. – Journal of Integrative Plant Biology 50(2): 174-182.
[74] Weir, B. S. (1996): Genetic Data Analysis II: Methods for Discrete Population Genetic Data. 2nd ed. – Sinauer Associates Inc., Sunderland, MA.
[75] Wendel, J. F., Cronn, R. C. (2003): Polyploidy and the evolutionary history of cotton. – Adv Agron 78: 139-186.
[76] Wendel, J., Brubaker, C., Percival, A. (1992): Genetic diversity in Gossypium hirsutum and the origin of upland cotton. – Am J Bot 79: 1291-1310.
[77] Yeh, F. C., Yang, R. C., Boyle, T. (1999): POPGENE. Microsoft Windows Based Freeware for Population Genetic Analysis. Release 1.31. – University of Alberta, Edmonton.
[78] Yu, J. Z., Fang, D. D., Kohel, R. J., Ulloa, M., Hinze, L. L., Percy, R. G., Zhang, J., Chee, P., Scheffler, B. E., Jones, D. C. (2012): Development of a core set of SSR markers for the characterization of gossypium germplasm. – Euphytica 187: 203-213.
[79] Zhang, J., Stewart, J. M. (2000): Economical and rapid method for extracting cotton genomic DNA. – J Cotton Sci 4(3): 193-201.
[80] Zhang, J., Lu, Y., Cantrell, R. G., Hughs, E. (2005): Molecular markers diversity and field performance in commercial cotton cultivars evaluated in the Southwestern USA. – Crop Sci 45: 1483-1490.
[81] Zhang H. B., Li Y., Wang B., Chee P. W. (2008): Recent advances in cotton genomics. – Int. J. Plant Genomics 20.
[82] Zhang, Y., Wang, X. F., Li, Z. K., Zhang, G. Y., Ma Z. Y. (2011): Assessing genetic diversity of cotton cultivars using genomic and newly developed expressed sequence tag-derived microsatellite markers. – Genet. Mol. Res. 10: 1462-1470.
[83] Zhao, Y. L., Wang, H. M., Chen, W., Li, Y. H. (2014): Genetic structure, linkage disequilibrium and association mapping of Verticillium wilt resistance in elite cotton (*Gossypium hirsutum* L.) germplasm population. – PLoS One 9: e86308.
[84] Zhao, Y. L., Wang, H. M., Chen, W., Li, Y. H., Gong, H. Y., Sang, X. H. (2015): Genetic diversity and population structure of elite cotton (*Gossypium hirsutum* L.) germplasm revealed by SSR markers. – Plant Syst. Evol. 301: 327-336.
[85] Zoric, M., Dodig, D., Kobiljski, B., Quarrie, S., Barnes, J. (2012): Population structure in a wheat core collection and genomic loci associated with yield under contrasting environments. – Genetica 140: 259-275.

ELECTRONIC APPENDIX

This manuscript has an electronic appendix with the genotypes' properties.

http://www.aloki.hu ● ISSN 1589 1623 (Print) ● ISSN 1785 0037 (Online)
DOI: http://dx.doi.org/10.15666/aeer/2005_39393953

ETHNOBOTANICAL STUDY ON TRADED MEDICINAL PLANTS AND HERBAL MARKET ANALYSES IN GAZIANTEP/TURKEY

PALABAŞ UZUN, S.[1*] – ŞIMŞIR BOZDAĞ, R.[2]

[1]*Department of Forest Engineering, Faculty of Forestry, Kahramanmaraş Sütçü Imam University, Kahramanmaraş, Turkey*

[2]*Graduate School of Natural and Applied Sciences, Kahramanmaraş Sütçü Imam University, Kahramanmaraş, Turkey*
(phone: +90-533-660-9810; fax: +90-344-300-1712)

[*]*Corresponding author*
e-mail: seyran@ksu.edu.tr; phone: +90-533-660-9810; fax: +90-344-300-1712

(Received 9th Mar 2022; accepted 20th Jun 2022)

Abstract. Herbal markets are the meeting point of the local people and allow quick information exchange about medicinal plants. In this study, it is aimed both to investigate the traditional uses of medicinal plants traded in Gaziantep herbal markets and to make a detailed evaluation of the selected herbal markets. Data about herbal markets and medicinal plants were collected through semi-structured and open-ended questionnaires from herbalists and customers. Ethnobotanical data were analysed using indices such as; Frequency of Citation (FC), Cultural Importance Index (CI), Relative Frequency of Citation (RFC), and species Use Value (UV). Totally, 58 species (belonging 30 families) out of which 10 imported were surveyed from 14 selected herbal markets to be used as traditional medicines. *Mentha* x *piperita* (147), *Thymus* sp. (141), and *Tilia platyphyllos* (132) were determined to have the highest FC values. According to the results of the study, the density of customers in herbal markets, the variety and quality of products sold, and the number of herbal markets has increased in recent years. It has been determined that the average operating age of the herbal market is 34.7 years, the average number of employees is 2.6, and the average annual turnover of the markets is 166,772,888TL (US$42,762,279, currency in 2017).
Keywords: *traditional knowledge, market characteristics, FC, CI, Turkey*

Introduction

Although molecular biology and computerized drug design are developing rapidly, medicinal plants continue to play a dominant role in the healthcare system for approximately 80 percent of the world's population is living in developing countries. At the same time, in developed countries, which make up the remaining 20 percent of the population, natural products and medicines derived from herbs are an important part of health systems (Bussmann, 2002). Realizing that natural compounds cannot be replaced by synthetic products, the treatment with medicinal plants, which lost interest in the past due to synthetic drugs, has become more common in recent years. Among the reasons of the increasing demand for medicinal plants are people's dissatisfaction with their medical treatments, their desire to add quality to living standards by reducing the side effects of the drugs they use, and cultural heritage (Prance, 1991). According to WHO (2013), herbal medicines and traditional therapies are the main sources of health care system and are sometimes the only sources of care for millions of people.

Today, the concentration of people in city centers and the decrease in access to plants have led to an increase in the demand for herbal markets. Herbal markets not only facilitate people's access to medicinal and aromatic plants, but also contribute to the transfer of cultural heritage and traditional knowledge about plants to future generations

http://www.aloki.hu ● ISSN 1589 1623 (Print) ● ISSN 1785 0037 (Online)
DOI: http://dx.doi.org/10.15666/aeer/2005_39553976

(Ji et al., 2020). In recent years, many research has been done documenting traditional knowledge in herbal markets (Bussmann et al., 2016; Carvalho et al., 2018; Jin et al., 2018; Franco et al., 2020; Nanogulyan et al., 2020; Palabaş-Uzun and Koca, 2020; Ötnü and Akan, 2020; Łuczaj et al., 2021). Research conducted in herbal markets provides a fast and effective communication with people who sell and use plants. At the same time, these markets are meeting point and allow rapid information exchange on the names of the plant materials sold, their ethnobotanical characteristics, uses and benefits (Łuczaj et al., 2021).

Gaziantep, whose history dates back to 5600 BC, has also been the center of various civilizations. The first humans lived in caves were found in Dülük (Doliche), 12 km north of the city center. The historical ruins of many ancient settlements from the Hellenistic, Roman and Byzantine periods have survived to the present day in Gaziantep. It is possible to encounter traces of all these civilizations in the cultural life of the city. The role of Turkmen tribes is more dominant in today's traditional life of the city, which has lived through the Turkish-Islamic and Ottoman periods (Yüksel, 2007; Şahin, 2011; Gürsel, 2015).

The city, whose commercial volume and popularity increased with the GAP (Southeastern Anatolian project), actually had a strategic importance before the project due to its geographical location. Gaziantep is located on the historical "Silk Road" connecting the Near East, the Middle East and the Far East. In addition, being at an important crossroad connecting the western region of the country with neighboring countries in the east and southeast, has increased its geographical importance of the province since the past. While this historical caravan route connecting Asia to Europe formed the basis of the city's productivity and commercial capability, it also formed the foundations of the city's cultural richness (Yüksel, 2007; Külek, 2010). The cultural richness of the city is also reflected in its gastronomy and Gaziantep cuisine has been added to the Creative Cities Network list by UNESCO in 2015 and has taken its deserved place among the world cuisines (Uçuk and Kayran, 2020). The characteristic feature of Gaziantep cuisine comes from the different spices used in the dishes. The most important secret of tastes, liked by almost everyone comes from the high aroma and taste of herbal and animal products grown in the region under natural conditions.

To date, no studies have been conducted to evaluate the herbal markets, which have an important role in Gaziantep's cultural life. With this study, it is aimed both to make a detailed evaluation of the herbal markets of the province and to determine the relative importance of the medicinal plants traded. For this purpose, we tried to determine the plant species that are frequently used in the treatment of diseases and to perform analysis of the documented data using quantitative ethnobotanical indices. In addition, this study reveals the sales volume of herbal markets and their quantitative and qualitative change in the last five years.

Materials and methods

Location of the study site

Gaziantep province, located on Turkey's Syrian border, is between 37031′ North latitude and 38001′ East longitude at the intersection of the Mediterranean and Southeastern Anatolia regions (*Figure 1*). A large part of the province located in the west of the Southeastern Anatolia region. Gaziantep city center is built on the Gaziantep

http://www.aloki.hu ● ISSN 1589 1623 (Print) ● ISSN 1785 0037 (Online)
DOI: http://dx.doi.org/10.15666/aeer/2005_39553976

Plateau, which is considered higher than its surroundings, and its altitude is 850 m on average (Çakır, 2009).

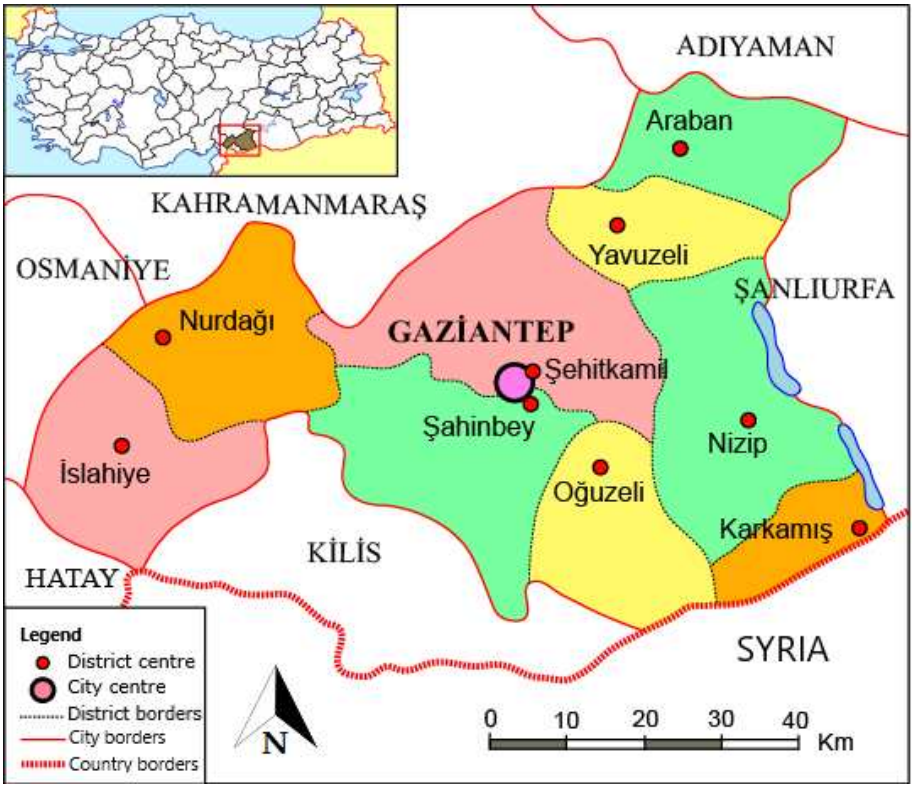

Figure 1. *Geographical location of the study area*

Gaziantep province, which hosts approximately 2264 taxa belonging to 115 family, is located in the Mediterranean phytogeographical region (MAF, 2021). Steppe vegetation is common throughout the study area. In addition, forest vegetation mostly formed by oak communities, and maquis vegetation, are also observed (Çakır, 2009). In Gaziantep, an area of 370,736 hectares is agricultural land. Of these areas, 195,110 hectares are fruit lands and 7,277 hectares are vegetables. The largest area in orchard lands belongs to pistachio (*Pistacia vera* L.) plantations (127,087 ha) and 31% of Turkey's pistachio production is provided by Gaziantep.

Gaziantep is the most populous city of the Southeastern Anatolia region. Gaziantep population is 2,101,157 according to 2020 data and 50.49% of the population is men and 49.51% is women (TUIK, 2020). The majority of the population of Gaziantep consists of the Turkish (75%), followed by the Kurdish minority (20%), and a small minority (5%) of Arabs and Circassians (Güllü, 2009; URL-1, 2022).

Ethnobotanical data collection

Herbal markets have been important components of trade life since ancient times in the province of Gaziantep, which is on the Silk Road. The culture of the grand bazaar, where many herbal markets and spice sellers trade together, still continues in the province. In the present study, ethnobotanical data were collected through face-to-face interviews during the herbal market visits held at regular intervals between 2016 and 2017. In total,

http://www.aloki.hu ● ISSN 1589 1623 (Print) ● ISSN 1785 0037 (Online)
DOI: http://dx.doi.org/10.15666/aeer/2005_39553976

14 herbal market vendors and 160 customers were interviewed in Gaziantep. The interviewees were selected only from those who wanted to participate in the survey, and no distinction was made between the interviewees.

Questionnaires; designed to collect detailed data about each taxa, such as its uses, vernacular name, parts used and preparation methods. Data were obtained by semi-structured questionnaires and open-ended interviews. The questionnaire consisted of two parts (*Appendix I*), with the first part including demographic information about the informants (*Table 1*). One of the herbalists we interviewed was female and thirteen were male. Six herbalists were between the ages of 18-35, five were between 36 and 50 years old, and three were over 51. Four herbalists were primary school graduates, seven were secondary school graduates and three were university graduates. Out of the 160 customers interviewed, 89 were male and 71 were female. 46 of these customers were aged between 18 and 35; 60 were aged between 36 and 50, and 54 were aged 51 years or older. Seventy-two customers graduated from primary school, 49 from secondary school, and 39 from university. The second part of the questionnaire mostly consisted of questions measuring the professional knowledge of the herbalists, such as: how do they buy their products; what are the top-selling plant taxa, where or from whom they buy the products they sell; how often do they buy medicinal plants; how do they get information about plants; and are they aware of the laws regarding the collection, processing and sale of plants; what is the most important criteria that customers pay attention when purchasing medicinal plants. We also asked about the changes they have observed in the medicinal plant market in the last 5 years. For customers, the second part consisted of information about the name of the plant, plant part used, the method of use, and the list of diseases being treated (*Appendix II*).

Table 1. *Demographic profile of informants*

Variables	Category	Herbalist	Customer	Total Number of Informants	Percentage
Age					
	18-35	6	46	52	29.9
	36-50	5	60	65	37.3
	above 51	3	54	57	32.8
Gender					
	Male	13	89	102	58.6
	Female	1	71	72	41.4
Education					
	Primary	4	72	76	43.7
	Secondary	7	49	56	32.2
	Higher	3	39	42	24.1

Samples were taken from the plant materials, reported by the informants, and their identifications were made in the Herbarium KASOF (Kahramanmaraş Sütçü Imam University, Faculty of Forestry Herbarium). Plant parts have been stored in Herbarium KASOF. Since the samples stored in the herbarium were just dried plant parts (not a complete sample), the herbarium number could not be given. The study examines, not all products sold in herbal markets, only medicinal plants whose use is mentioned by informants. Herbal products such as resins, oils, and juices were not included in this study.

http://www.aloki.hu ● ISSN 1589 1623 (Print) ● ISSN 1785 0037 (Online)
DOI: http://dx.doi.org/10.15666/aeer/2005_39553976

Ethnobotanical data analyses

The collected data from the field studies were entered into Microsoft Excel© spreadsheets. For analysis of data; Frequency of Citation (FC), Cultural Importance (CI), Relative Frequency of Citation (RFC), and species Use Value (UV) were calculated.

Frequency of citation (FC)

FC allows to assess the relative cultural importance of a species or group of species (Heinrich et al., 2009). In order to determine the FC value, which is defined as an absolute number, herbalist and local people were asked the medicinal uses of plants. In this study, two types of FC values were determined: FC and FC_{event}. FC is obtained by reporting the number of participants citing a plant species for different diseases. Therefore, it ranges from 0 (if none of the informants used this plant species) to 160 (if all used this plant species in different uses). FC_{event} explains the number of participants using a species for a particular disease and FC_{event} refers to the citation frequency for only one disease (Mehrnia et al., 2021).

Cultural importance index (CI)

Cultural Importance Index (CI) was calculated according to following equation (*Eq.1*) for each taxon (Tardio and Pardo-de-Santayana, 2008):

$$CI = \sum_{U=U1}^{U_{NC}} \sum_{i=i1}^{i_N} \frac{UR_{Ui}}{N} \qquad \text{(Eq.1)}$$

where, *U*= use category; *N*= the number of participants in the survey, *NC* = total number of different use categories; *i* varying from only one use to the total number of uses; *UR* = total number of use reports.

Relative frequency of citation (RFC)

The RFC was calculated using the *Eq.2* according to Vitalini et al. (2013):

$$RFC = \frac{FC}{N} \qquad (0 < \text{RFC} < 1) \qquad \text{(Eq.2)}$$

where "FC" is the number of informants mentioning the use of the species and "N" is the total number of informants in the survey.

Use value (UV)

The number of the use-reports for each taxon was used for the calculation of the use value. It was calculated by the *Eq.3* given below (Trotter and Logan, 1986):

$$UV = \frac{U}{n} \qquad \text{(Eq.3)}$$

where "U" is the number of uses mentioned by each informant for a given taxa and "n" is the number of informants who cited the plant species.

http://www.aloki.hu ● ISSN 1589 1623 (Print) ● ISSN 1785 0037 (Online)
DOI: http://dx.doi.org/10.15666/aeer/2005_39553976

Results

Herbal market characteristics and traditional knowledge

We asked herbalists the changes they have observed in herbal markets in the last five years. Accordingly, 43% of herbalists said that the number of customers increased, 71% said that the quality and standardization of the products increased, 71% said that the number of products demanded by customers increased, 79% said that the price of the products increased; and 64% stated that the number of herbal markets in the market has increased (*Table 2*). According to *Table 2*, herbalists did not mention a significant improvement (50%) regarding the inspections in the production and sale of products.

Table 2. *Changes observed in the medicinal plant market in the last five years*

	Increase		**Decrease**		**Steady**	
	Herbalist Number	Ratio (%)	Herbalist Number	Ratio (%)	Herbalist Number	Ratio (%)
Number of customers	6	43	4	29	4	29
Quality and standardization of the products	10	71	0	0	4	29
Product variety	10	71	0	0	4	29
Product price	11	79	0	0	3	21
Inspections	7	50	0	0	7	50
Number of herbal markets	9	64	2	14	3	22

During the herbal market visits, we observed that many of the products sold do not have a collection and expiration date, that the products were not properly stored, and that some products were too old to be beneficial for health. Increasing the inspections of the provincial health directorates in order to eliminate such deficiencies will contribute to the development and amelioration of the herbal markets. In addition, it is thought that herbalists gave subjective answers to some of the questions we asked, such as the number of customers, due to their professional concerns.

Traditional knowledge about processing of medicinal plants is learned from vendors' masters/teachers or parents (Ji et al., 2020). When we asked the herbalists how they get the information about medicinal plants, seven of them said that they learned it from their master and seven herbalists said that they were self-taught. None of the herbalists have a university degree or any certificate related to their profession. When customers come to herbalists, they sometimes come to buy a plant and sometimes to find healing for their diseases. For this reason, herbalists who will suggest a treatment about plants must have a certain level of knowledge. When we examined the frequency of herbalists who buy medicinal plants, they reported that they buy medicinal plants once a week (43%), once a month (36%), every three months (14%), and once a year (7%).

Herbal markets in Gaziantep have been popular places since the past due to the history and rich cuisine of the province. Many of the herbalists we wanted to interview for the survey did not want to participate in due to financial concerns. Some herbalists who accepted the interview did not want to give information about their income. According to interviews, it has been determined that the average operating age of the herbal market is 34.7 years, the average number of employees is 2.6, and the average annual turnover of the markets is 166,772,888TL (US$42,762,279, currency in 2017). The annual average

http://www.aloki.hu ● ISSN 1589 1623 (Print) ● ISSN 1785 0037 (Online)
DOI: http://dx.doi.org/10.15666/aeer/2005_39553976

turnover of the herbal markets is calculated according to the average of nine responding herbalists. Five of the herbalists did not answer this question, and there is a wide variation in the income of the respondents. In addition, according to the statements of eleven herbalists, their monthly income varies between 800TL (US$205) and 10,000TL (US$2,564), and their average income has been determined as 2,745TL (US$704). In 2017, the per capita monthly income in Turkey was US$883 (TUİK, 2018). Ten of the herbalists stated that they do not have any other source of income. A significant difference was also observed between the monthly incomes of the herbalists who participated in the interview. The location of the herbal market could be important in its income. Gaziantep is a city of gastronomy and museums and hosts an increasing number of tourists every year. Since most of the tourists visit historical spice shops and herbal markets, the sales rates of herbalists situated in near touristic bazaars is much higher than others.

The vast majority of herbalists participated in the survey stated that they bought the products from vendors and in processed form. Only one herbalist stated that he collected the products from nature, and one herbalist stated that he bought them as unprocessed. Also, majority of herbalists (57%) stated that they were not aware of the laws regarding the collecting, processing and selling of plants. When we examined the storage methods of medicinal plants sold by herbalists, it was determined that they mostly prefer to store them in gunny bags (40%) followed by storing it in paper boxes (27%), plastic boxes (15%), plastic bags (12%) and finally in glass jars (6%), respectively. We also asked about the most important criteria that customers pay attention to when purchasing medicinal plants. Herbalist indicated that quality (31%), price (31%), expiry date (19%) and trademark (11%) are the most important criteria respectively. During the field survey, we observed that the products were exhibited open to all kinds of contamination and some of them did not have an expiry date on storage bags. Failure to paying attention to the storage and hygiene conditions of the products also threatens public health. It is necessary to increase the frequency of inspections and herbalists should be trained about these improper practices.

Medicinal plant diversity, plant parts and their preparations

We identified 58 medicinal plant taxa belonging to 30 families as a result of our interviews with herbalists and customers from 14 herbal markets in the Gaziantep city. We were able to identify 56 plant samples in species level and 2 samples in genus level. The plant family with the most taxa represented was *Lamiaceae* (11 taxa). *Asteraceae* was the second most common plant family with six taxa while *Rosaceae* was the third rank with five taxa. Other frequently used families include *Malvaceae* (4 taxa); *Apiaceae* and *Fabaceae* (3 taxa); and *Cupressaceae*, *Anacardiaceae*, *Lauraceae*, *Zingiberaceae* (2 taxa) (*Figure 2*). The following families have only one taxon: *Equisetaceae*, *Aquifoliaceae*, *Caryophyllaceae*, *Ericaceae*, *Hypericaceae*, *Juglandaceae*, *Myrtaceae*, *Nitrariaceae*, *Oleaceae*, *Orchidaceae*, *Papaveraceae*, *Piperaceae*, *Ranunculaceae*, *Santalaceae*, *Solanaceae*, *Theaceae*, *Urticaceae*, and *Zygophyllaceae*.

Customers reported the use of 85 plant parts from 58 taxa and the leaves were the most frequently cited plant parts. The parts cited by customers were; leaves (27%), followed by fruits and flowers (each of 14%), seeds (13%), shoots (12%), roots (8%), aerial parts (4%), bark, cones and rhizomes (each of 2%), and tuber (1%), respectively (*Figure 3*).

The annual average weight for the 10 top-selling taxa by 14 herbalists were as follows: Mint (*Mentha* x *piperita* L.) 878 kg, Licorice (*Glycyrrhiza glabra* L.) 579 kg, Ginger (*Zingiber officinale* Roscoe) 301 kg, Thyme (*Thymus* sp.) 274 kg, Carob (*Ceratonia*

http://www.aloki.hu ● ISSN 1589 1623 (Print) ● ISSN 1785 0037 (Online)
DOI: http://dx.doi.org/10.15666/aeer/2005_39553976

siliqua L.) 222 kg, Senna (*Senna alexandrina* Mill.) 216 kg, Linden (*Tilia platyphyllos* Scop.) 214 kg, Sage (*Salvia officinalis* L.) 120 kg, Common Nettle (*Urtica dioica* L.) 98 kg and Chamomile (*Matricaria chamomilla* L.) 68 kg. Also, herbalists stated that the preferred medicinal plants differ according to the seasons; Licorice in summer, Linden in autumn and winter, and Green Tea (*Camellia sinensis* (L.) Kuntze) in spring were the top-selling taxa.

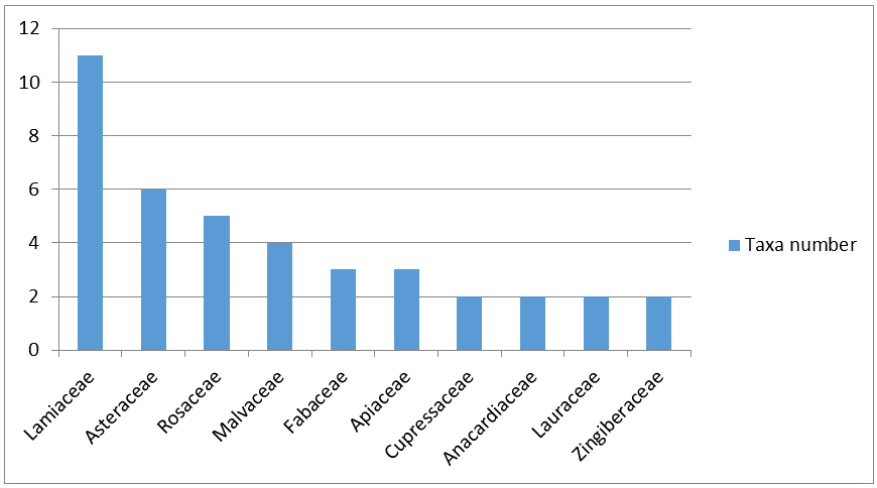

Figure 2. *Richest plant families with their number of taxa*

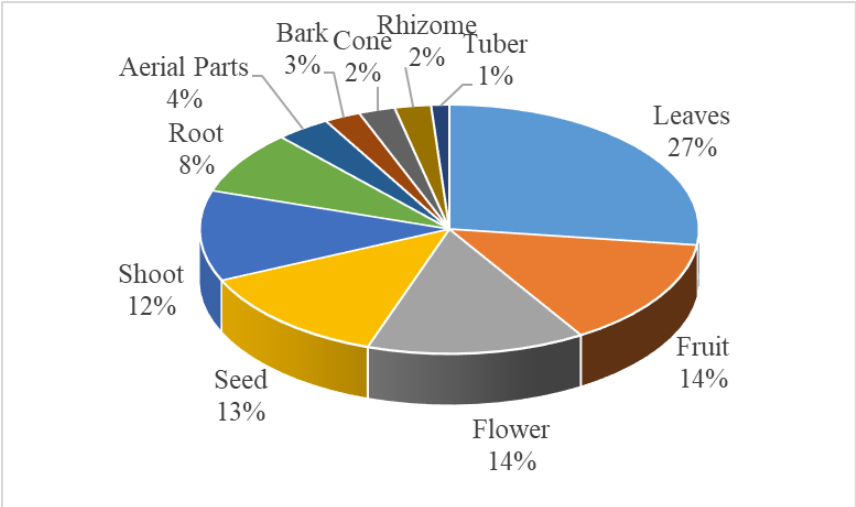

Figure 3. *The percentage of plant parts used*

When the preparation methods were examined, it was determined that the infusion, decoction and powder were the three most commonly used preparation methods. Paste method was used 3 times, oil, bath and raw methods were used 2 times; molasses, smoke, vinegar and marmalade methods were reported only once by customers (*Figure 4*). Totally, 11 different preparation methods were reported by customers.

http://www.aloki.hu ● ISSN 1589 1623 (Print) ● ISSN 1785 0037 (Online)
DOI: http://dx.doi.org/10.15666/aeer/2005_39553976

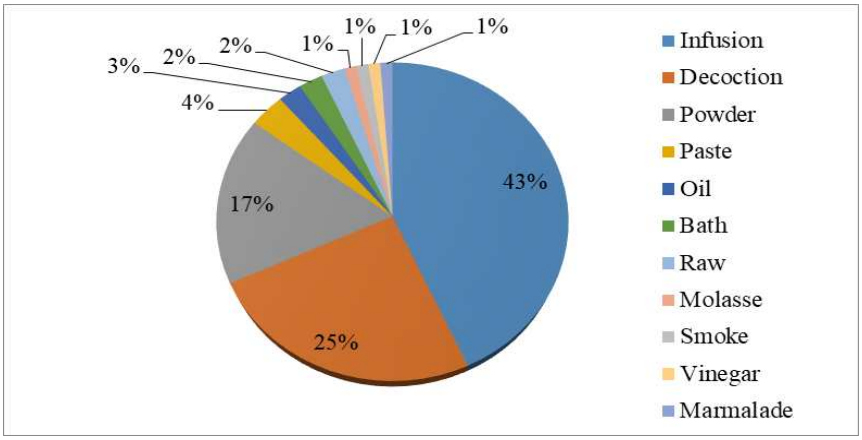

Figure 4. *The percentage of plant parts used*

Salient ailments and indices

The "Anatolian people" living in Anatolia since the Paleolithic Age (50.000-7.000 BC) have constantly benefited from the plants around them (Baytop, 2021). Over time some plants have developed a single medicinal use, whereas some other plants have versatile uses. In the current study, it was determined that 58 plants were used for medicinal purposes and 9 of them showed high versatility in their uses (see bolded taxa in *Table 3*). Plant species with more than 6 use reports include *Urtica dioica*, *Curcuma longa* L., *Achillea arabica* Kotschy, *Mentha* x *piperita*, *Salvia officinalis*, *Thymus* sp., *Peganum harmala* L., *Nigella sativa* L. and *Prunus avium* L.

The plant species that are frequently used against various ailments in the region were determined with the FC value (*Figure 5*). Accordingly, *Mentha* x *piperita* (147), *Thymus* sp. (141), and *Tilia platyphyllos* (132) are the taxa with the highest FC value. Cultural importance index (CI) takes into account not only the prevalence of use (number of informants) for each species, but also its versatility, and it was obtained from the sum of the proportion of informants that mention each species use (Tardio and Pardo-de-Santayana, 2008). Ten plant taxa having the highest CI values are as follows: *Mentha x piperita* (1.43), *Thymus* sp. (0.98), *Salvia officinalis* (0.94), *Tilia platyphyllos* (0.91), *Urtica dioica* (0.72), *Zingiber officinale* (0.72), *Thymbra spicata* L. (0.67), *Orchis* spp. (0.67), *Glycyrrhiza glabra* (0.65), *Rosa canina* L. (0.65).

The RFC can give an indication of the medicinal plants best known or long used by the local people and can represent a source of reliability (Appiah et al., 2017). In this study RFC values ranged from 0.92 to 0.04. *Mentha* x *piperita* has the highest RFC value and *Thymus* sp. (0.88), *Tilia platyphyllos* (0.83), *Salvia officinalis* (0.68) are the other taxa having high RFC values.

The Use Value (UV) index measures the relative importance of species, and UV is important in assessing which herbs are considered most useful for a given group of people and in identifying potential uses of a plant (Zenderland et al., 2019). The UVs of the taxa ranged from 0.03 to 0.86. The taxa having the highest UVs were *Prunus avium* (0.86) followed by *Achillea arabica* (0.55), *Curcuma longa* (0.54), *Papaver rhoeas* L. (0.50). The lowest UVs were recorded for *Tilia platyphyllos* (0.03) and *Glycyrrhiza glabra* (0.03). *Prunus avium* is reported by 7 informants for 6 different pharmacological properties. The UVs of *Tilia platyphyllos* and *Glycyrrhiza glabra* were relatively low because many informants use these taxa often for a few ailments.

http://www.aloki.hu ● ISSN 1589 1623 (Print) ● ISSN 1785 0037 (Online)
DOI: http://dx.doi.org/10.15666/aeer/2005_39553976

Table 3. *Medicinal plants traded in Gaziantep herbal markets*

Botanical Names	Family	Vernacular/ English Names	Parts used	Preparation Form	Uses (FC_{event})	FC	CI	RFC	UV
Equisetum arvense L.	EQUISETACEAE	Boğumlu ot / Horsetail	Stem and Leaves	Infusion, Bath	Diuretic (3), carminative (6), astringent (4), regulates menses (2)	11	0,10	0,07	0,36
Juniperus communis L.	CUPRESSACEAE	Ardıç / Common juniper	Cones	Decoction, oil	Bronchitis (5), halitosis (2), hemorrhoids (7), liniment (3)	13	0,10	0,08	0,31
Juniperus drupacea Lab.	CUPRESSACEAE	Andız / Syrian juniper	Cones	Molasses, Infusion	Asthma (22), bronchitis (18), urinary burning (6), skin diseases (8)	34	0,34	0,21	0,12
Pistacia terebinthus L.	ANACARDIACEAE	Menengiç / Turpentine tree	Fruits, Roots	Powder; Decoction	Diuretic (7), intestinal disorders (15), skin diseases (3)	24	0,37	0,15	0,21
Rhus coriaria L.	ANACARDIACEAE	Sumak / Sumac	Leaves, Fruits	Powder; Decoction	Cold (6), diarrhea (18), astringent (12), stomach and intestinal disorders (22)	17	0,15	0,11	0,18
Anethum graveolens L.	APIACEAE	Dereotu / Dill	Aerial parts, Seeds	Infusion	Halitosis (18), galactagogues (56), appetiser (32), carminative (25)	65	0,52	0,41	0,05
Cuminum cyminum L.	APIACEAE	Kimyon / Cumin	Seeds	Powder	Carminative (9), galactagogues (12), digestive (6)	87	0,63	0,54	0,25
Foeniculum vulgare Mill.	APIACEAE	Rezene / Fennel	Roots, Leaves, Seeds	Decoction, Powder	Galactagogues (38), carminative (35), intestinal problems (22), kidney stones (8)	12	0,18	0,08	0,06
ê*Ilex paraguariensis* A.St.-Hil.	AQUIFOLIACEAE	Mate / Yerba mate	Leaves	Infusion	Anti-fatigue (5), diabetes (3), lose weight and antiobesity (12)	13	0,13	0,08	0,23
***Achillea arabica* Kotschy**	ASTERACEAE	Civan perçemi / Yarrow	Leaves, Flowers	Infusion	Menorrhagia (8), anemia (3), hemorrhoids (1), wounds (2), stomach and intestinal disorders (2)	17	0,16	0,11	0,55
Artemisia absinthium L.	ASTERACEAE	Pelin otuout / Absinth wormwood	Shoots and Leaves	Infusion	Abnormal menstrual cycle (9), diabetes (4), expel worms from digestive tract (2)	11	0,10	0,07	0,27
Carthamus tinctorius L.	ASTERACEAE	Aspir / Safflower	Seeds, Flowers	Infusion	Rheumatism (9), laxative (12)	77	0,58	0,48	0,11

http://www.aloki.hu ● ISSN 1589 1623 (Print) ● ISSN 1785 0037 (Online)
DOI: http://dx.doi.org/10.15666/aeer/2005_39553976

Botanical Names	Family	Vernacular/ English Names	Parts used	Preparation Form	Uses (FC_{event})	FC	CI	RFC	UV
Helichrysum arenarium L.	ASTERACEAE	Ölmez çiçek / Sandy everlasting	Flowers	Infusion	Abnormal menstrual cycle (8), diuretic (3), cholagogue (1)	19	0,14	0,12	0,30
Matricaria chamomilla L.	ASTERACEAE	Mayıs papatyası Chamomile	Flowers	Infusion, Powder, Bath	Insomnia (25), stress (43), sore throat (12), haircare (32)	11	0,09	0,07	0,05
Silybum marianum (L.) Gaertner	ASTERACEAE	Deve dikeni / Milk thistle	Shoots, Seeds	Infusion, Powder	Lung disease (11), kidney stones (8), urinary diseases (7)	10	0,08	0,06	0,18
Saponaria officinalis L.	CARYOPHYLLACEAE	Çöven / Soapwort	Leaves, Roots	Decoction	Expectorant (9), diuretic (4), sedative (2), depurative (8)	16	0,11	0,10	0,25
Erica arborea L.	ERICACEAE	Funda / Tree heath	Shoots, Leaves	Infusion	Urinary problems (12), respiratory disorders (8)	15	0,13	0,09	0,20
Ceratonia siliqua L.	FABACEAE	Keçiboynuzu / Carob tree	Leaves, Shoots, Bark, Fruits	Powder, Decoction	Anemia (32), sexual disorders (35), stomach and intestinal disorders (13)	43	0,44	0,27	0,05
Glycyrrhiza glabra L.	FABACEAE	Meyan / Liquorice	Roots	Decoction	Ulcer (75), laxative (17), stomach ache (55)	90	0,65	0,56	0,03
[ê]*Senna alexandrina* Mill.	FABACEAE	Sinameki / Senna	Leaves	Infusion	Purgative (38), lose weight (32)	64	0,43	0,40	0,05
Hypericum perforatum L.	HYPERICACEAE	Kantoron / St. John's wort	Flowers	Infusion, Oil	Fever (7), skin burns (18), nervous system disorders (16), anxiety (12), canker (7)	21	0,37	0,13	0,24
Juglans regia L.	JUGLANDACEAE	Ceviz / Walnut	Fruits, Leaves	Infusion	Antifungal (3), bronchitis (2), diabetes (6), cholesterol (12)	14	0,15	0,09	0,29
Lavandula stoechas L.	LAMIACEAE	Lavanta / Lavender	Flowers	Infusion	Nervous disorders (2), headache (5), stomach gas (3), stomach ache (1), irregular heart beat (9)	141	0,98	0,88	0,38
Melissa officinalis L.	LAMIACEAE	Oğul out / Lemon balm	Leaves	Infusion	Gas troubles (9), nervous disorders (12), sedative (11), insomnia (7)	108	0,94	0,68	0,22
***Mentha* x *piperita* L.**	LAMIACEAE	Nane / Peppermint	Leaves	Infusion, Decoction	Stomach ache (82), cold (105), nausea (33), halitosis (22), fever (5), influenza (32)	53	0,67	0,33	0,04
Ocimum basilicum L.	LAMIACEAE	Reyhan / Basil	Leaves, Shoots	Infusion	Diabetes (5), cold (4), flu (3), indigestion (9)	45	0,39	0,28	0,24

http://www.aloki.hu ● ISSN 1589 1623 (Print) ● ISSN 1785 0037 (Online)
DOI: http://dx.doi.org/10.15666/aeer/2005_39553976

Botanical Names	Family	Vernacular/ English Names	Parts used	Preparation Form	Uses (FC_{event})	FC	CI	RFC	UV
Rosmarinus officinalis L.	LAMIACEAE	Biberiye / Rosemary	Leaves, Shoots	Infusion	Indigestion (5), diuretic (8), headache (2), nervous disorders (3)	35	0,31	0,22	0,25
***Salvia officinalis* L.**	LAMIACEAE	Adaçayı / Sage	Leaves	Infusion	Antiseptic (22), indigestive (21), tooth (24) and throat inflammation (54), flu (65), fever (8)	13	0,13	0,08	0,06
Sideritis congesta L.	LAMIACEAE	Alanya Çayı / Mountain tea	Shoots	Decoction	Cold (23), appetiser (9), stomach gas (17)	13	0,12	0,08	0,09
Teucrium polium L.	LAMIACEAE	Peryavşan / Felty germander	Aerial parts	Infusion	Appetiser (12), eczema (9), stomach ache (21), indigestive (7), galactagogues (12)	16	0,11	0,10	0,11
Thymbra spicata L.	LAMIACEAE	Zahter / Spiked Thyme	Shoots, Leaves	Infusion	Ulcer (18), expectorant (25), diabetes (23), colds (42)	147	1,43	0,92	0,08
Thymus sp.	LAMIACEAE	Kekik / Thyme	Leaves	Infusion	Stomach ache (33) and headache (13), indigestive (57), cough (72), bronchitis (35), diabetes (27)	18	0,25	0,11	0,04
Vitex agnus-castus L.	LAMIACEAE	Hayıt / Chaste tree	Leaves, Fruits, Seeds	Infusion, Powder	Regulates menses (11), diuretic (5), galactagogue (3)	17	0,14	0,11	0,14
ê*Cinnamomum zeylaniccum* L.	LAURACEAE	Tarçın / Cinnamon	Bark	Powder, Infusion, Decoction	Gas troubles (12), digestive (15), controls blood glucose (17)	64	0,44	0,40	0,06
Laurus nobilis L.	LAURACEAE	Defne / Bay laurel	Leaves, Fruits	Decoction	Diuretic (5), digestive (18), colds (25), appetiser (22)	22	0,28	0,14	0,23
Althaea officinalis L.	MALVACEAE	Hatmi Çiçeği / Marsh mallow	Flowers	Infusion	Cough (10), expectorant (8), purgative (4)	132	0,91	0,83	0,33
ê*Hibiscus sabdariffa* L.	MALVACEAE	Hibiskus / Roselle	Flowers	Infusion	Controls blood pressure (5), diuretic (7), eczema (9), sedative (2)	17	0,18	0,11	0,29
Malva sylvestris L.	MALVACEAE	Ebegümeci Common mallow	Flowers, Leaves	Infusion, Paste	Eczema (2), anti-inflammatory (4), treatment of abscess (8), laxative (9), hemorrhoids (5)	12	0,18	0,08	0,23

http://www.aloki.hu ● ISSN 1589 1623 (Print) ● ISSN 1785 0037 (Online)
DOI: http://dx.doi.org/10.15666/aeer/2005_39553976

Botanical Names	Family	Vernacular/ English Names	Parts used	Preparation Form	Uses (FC_{event})	FC	CI	RFC	UV
Tilia platyphyllos Scop.	MALVACEAE	Ihlamur / Linden	Flowers, Leaves	Decoction	Cold (77), sore throat (29), sedative (33), insomnia (35)	13	0,14	0,08	0,07
ê*Syzygium aromaticum* (L.) Merr. & L.M.Perry	MYRTACEAE	Karanfil / Clove	Flower buds	Raw, Decoction	Antiseptic (9), halitosis (15), toothache (13), canker (7), nausea (6)	22	0,31	0,14	0,27
***Peganum harmala* L.**	NITRARIACEAE	Üzerlik / Wild rue	Seeds, Roots	Infusion, Paste, Smoke	Hemorrhoids (7), eczema (4), stimulant (3), diuretic and urinary system disorders (6), fumigant (28)	33	0,31	0,21	0,04
Olea europaea L.	OLEACEAE	Zeytin / Olive	Leaves	Infusion	Diuretic (2), appetiser (6), diabetes (12), cholesterol (5)	15	0,16	0,09	0,50
Orchis spp.	ORCHIDACEAE	Salep / Sahlep	Tubers	Root powder, Infusion	Cold (27), expectorant (54), aphrodisiac (46)	80	0,67	0,50	0,20
Papaver rhoeas L.	PAPAVERACEAE	Gelincik / Poppy	Flowers	Infusion	Anti-fatigue (5), bronchitis (3), insomnia (6), sedative (5)	8	0,12	0,05	0,18
ê*Piper nigrum* L.	PIPERACEAE	Karabiber / Black pepper	Seeds	Decoction, Powder	Appetiser (7), stomach ache (8), indigestion (15), rheumatism (8)	20	0,23	0,13	0,10
***Nigella sativa* L.**	RANUNCULACEAE	Çörekotu / Black cumin	Seeds	Decoction	Gastrointestinal disorders (27), asthma (5), diabetes (7), indigestion (10), rheumatism (3)	33	0,32	0,21	0,29
Cerasus mahaleb L.	ROSACEAE	Mahlep / Mahaleb	Seeds	Powder	Expectorant (8), asthma (12), aphrodisiac (14), diabetes (22)	96	0,65	0,60	0,86
Crataegus orientalis L.	ROSACEAE	Alıç / Hawthorn	Fruits, Leaves	Vinegar, Infusion	Controls blood pressure (15) and diabetes (5), arrhythmia (12), asthma (2), sedative (3)	55	0,50	0,34	0,04
***Prunus avium* L.**	ROSACEAE	Kiraz / Cherry	Fruits, Fruit stalk	Infusion, Decoction	Cholesterol lowering (7), diuretic (8), purgative, antioxidant (5), bronchitis (3), lose weight (5)	39	0,36	0,24	0,07
Rosa canina L.	ROSACEAE	Kuşburnu / Rosehip	Fruits	Infusion, Marmalade	Cold (52), asthma (18), diabetes (27), anemia (25)	17	0,23	0,11	0,27
Rubus sanctus Schreb.	ROSACEAE	Böğürtlen / Blackberry	Fruits, Roots	Raw, Decoction	Cold (17), anemia (12), haemorrhoid (11), infertility (38)	7	0,17	0,04	0,05

http://www.aloki.hu ● ISSN 1589 1623 (Print) ● ISSN 1785 0037 (Online)
DOI: http://dx.doi.org/10.15666/aeer/2005_39553976

Botanical Names	Family	Vernacular/ English Names	Parts used	Preparation Form	Uses (FC_{event})	FC	CI	RFC	UV
Viscum album L.	SANTALACEAE	Ökse otu, Gövelek out / Mistletoe	Leaves, Shoots, Fruits	Decoction, Infusion, Paste	Anti-allergic (6), purgative (4), control blood pressure (6), anticancer (12)	15	0,19	0,09	0,24
[è]*Capsicum annuum* L.	SOLANACEAE	Pul biber / Red Pepper	Fruit, Seeds	Powder	Cold (37), rheumatism (18), anticancer (26), analgesic (35)	75	0,51	0,47	0,03
[è]*Camellia sinensis* (L.) Kuntze	THEACEAE	Yeşilçay / Green tea	Leaves	Infusion	Diuretic (11), antioxidant (5), increases metabolism (16), lose weight (11)	17	0,27	0,11	0,09
***Urtica dioica* L.**	URTICACEAE	Isırgan / Nettle	Aerial parts	Infusion, Decoction	Asthma (12), hair care (28), diuretic (16), astringent (14), anticancer (78), emmenagogue (8), aphrodisiac (5), purgative (12)	87	0,72	0,54	0,23
[è]***Curcuma longa* L.**	ZINGIBERACEAE	Zerdeçal / Turmeric	Rhizomes	Decoction, Powder	Wound (3), stomach ache (2), digestive (4), cough (8), purgative (6), anemia (2), anticancer (10)	13	0,22	0,08	0,05
[è]*Zingiber officinale* Roscoe	ZINGIBERACEAE	Zencefil / Ginger	Rhizomes	Powder, Decoction	Carminative (31), cough (45), expectorant (25), digestive (13), control blood pressure (18)	97	0,72	0,61	0,54
Tribulus terrestris L.	ZYGOPHYLLACEAE	Deve Çökerten / Puncture Vine	Roots and Shoots	Decoction	Hemorrhoids (3), cough (2), aphrodisiac (3), diuretic (6)	9	0,08	0,06	0,44

[è] exotic plant taxa, not native for the Flora of Turkey
Abbreviations: **FC:** Frequency of citation; **CI:** Cultural importance index; **RFC:** Relative frequency of citation; **UV:** Use value

http://www.aloki.hu ● ISSN 1589 1623 (Print) ● ISSN 1785 0037 (Online)
DOI: http://dx.doi.org/10.15666/aeer/2005_39553976

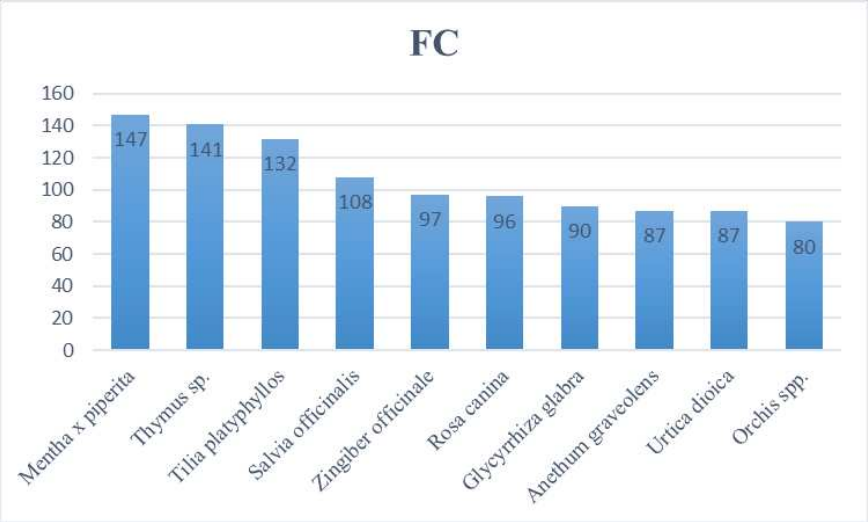

Figure 5. *The percentage of plant parts used*

Discussion

Herbal market characteristics and traditional knowledge

Although the international market for medicinal and aromatic plants and non-timber forest products interest by government, studies on the trade volumes of local herbal markets hardly exist (Bussmann et al., 2016). Increasing interest in medicinal plants day by day ensures that herbal markets become an important source of income for citizens (Wang et al., 2021). The results of the research also confirm the increase in the number of customers, product quality, annual income and the number of herbal markets in the marketplace. It is expected that these markets will grow even more in the near future with the diversification of health problem, human needs and increasing population.

It is estimated that at least 1000 of the native plant species in Turkey are used in various ways and approximately 400 of them are subject to trade (Acıbuca and Bostan Budak, 2018). Globally, approximately 2,500 medicinal plants are traded and worldwide market sales are estimated to reach US$5 trillion by 2050 (Schippmann et al., 2002; Zahoor et al., 2021). As in the whole world, most of the medicinal plants in Turkey are collected from nature, and the number of those grown and traded is very low. However, with the increase in usage areas, the export amounts and trade volume of medicinal plants are increasing day by day. Turkey ranks as the first among exporting countries for products such as thyme, bay leaves and cumin. Today, although the cultivation area of medicinal and aromatic plant has increased by 40% compared to the 2000s, many plants have just been cultivated or studies are still continuing. Cultivation studies should be increased in order to respond to the increasing demand of medicinal plants (Temel et al., 2018). In addition, although some plants are cultivated, people do not want to use the grown ones because they believe that they do not have the same medicinal effect as the ones collected from nature. For this reason, when medicinal plants are cultivated, they should be cultured in places close to natural growing areas, and even in-situ studies should be emphasized. When collecting species from nature, quotas should be determined and excessive consumption should be prevented.

http://www.aloki.hu ● ISSN 1589 1623 (Print) ● ISSN 1785 0037 (Online)
DOI: http://dx.doi.org/10.15666/aeer/2005_39553976

Medicinal plant use preferences

Medicinal plants may contribute to human health through their curative and therapeutic effects. In the present study the families with the highest number of taxa show similarities with other studies conducted in the nearby regions (Güneş et al., 2017; Özer and Türkmen, 2019; Palabaş Uzun and Koca, 2020; Ötnü and Akan, 2020) and even in the other parts of the world (Hanlidou et al., 2004; Ahmed, 2016; Petrakou et al., 2020; Shah et al., 2020). In general, *Lamiaceae* family taxa are widely used and traded as medicinal plants due to the high amounts of essential oils they contain.

The life forms of medicinal plants sold in Gaziantep herbal markets are similar to the other studies; mainly herbs (62.1%), followed by trees (19 %), shrubs (17.2%) and a liana (1.7 %) (Ahmed, 2016; Yeşil and İnal, 2019; Shah et al., 2020; Kızılarslan Hançer et al., 2020). Of the identified taxa 48 (82.8%) are native to Turkey, and 10 (17.2%) are introduced. Unlike the studies conducted in different parts of the world (Hanlidou et al., 2004; Bussmann et al., 2016), the rate of native plants is generally higher. Hanlidou et al. (2004) reported that, while 56.4% of the plants sold in Thessaloniki/Greece plant markets are native species, 43.6% of plants are introduced. In his study conducted in Bolivia, Bussmann et al. (2016) revealed that 61.2% of the plants sold in the plant markets are native and 38.8% are introduced. Since Turkey is a rich country in terms of medicinal and aromatic plant species (Keykubat, 2016) and the people generally learn about the use of these plants from their parents, the sales rates of native and traditional species are higher in herbal markets.

In this study, leaves were the most frequently cited plant part by customers, as in many other studies conducted in different parts of the world (Ahmed, 2016; Petrakou et al., 2020; Zahoor et al., 2021). Conducted studies in different provinces of Turkey also found that leaves, flowers and fruits are the most commonly used plant parts (Akbulut, 2015; Kılıç et al., 2021). The most likely reasons for the frequent use of leaves are that they are easier to access than roots, seeds, flowers and fruits, and they are also active in the production of metabolites (Ghorbani, 2005; Giday et al., 2009), and that removing leaf does not harm plants as much as other plant parts. Although the top-selling plants are similar to the study conducted by Palabaş Uzun and Koca (2020) in Kahramanmaraş, the sales volumes in Gaziantep herbal markets are much higher in terms of quantity. In addition to the large population of the province, the high tourism potential has also an effect on in this.

The amount of use of medicinal plants varies according to the seasons and regions. Generally, taxa such as mint, thyme, sage and nettle have high usage amounts all over the world (Hanlidou et al., 2004; Ahmed, 2016; Nanagulyan et al., 2020; Petrakou et al., 2020; Łuczaj et al., 2021). While reaching similar results in the present study, also licorice is among the taxa with the highest usage amounts. Licorice, which is native in Southern Europe and Asia, has been used in Traditional Chinese Medicine for 1000 years (Jiang et al., 2020). It has also been determined by some other studies that licorice sherbet is consumed a lot in Turkey, especially in the southeastern provinces, during the summer months and during Ramadan, the holy month of Muslims (Palabaş Uzun and Koca, 2020; Ötnü and Akan, 2020). The thirst quenching and stomach-relieving effects of licorice are the reason why it is preferred among people in the region where the summers are very hot. In the region, licorice root is sold in herbal markets as plant material, and is also widely sold in herbal markets, bazaars and streets as sherbet. However, sales of linden increase in autumn and winter due to its sweat-inducing and relaxing effect against

http://www.aloki.hu ● ISSN 1589 1623 (Print) ● ISSN 1785 0037 (Online)
DOI: http://dx.doi.org/10.15666/aeer/2005_39553976

feverish colds and infections. Likewise, green tea sales are increasing for weight loss by increasing metabolic activity in the spring.

When the usage methods are evaluated according to the plant parts, the "infusion" is preferred mostly for the softer plant parts such as leaves, flowers and fruits; "decoction" is preferred for harder plant parts such as roots, bark and shoots. The "powder" is mostly applied to the seeds of plants. In order to benefit from the bioactive compounds of the soft plant parts without crushing too much, they are thrown into boiling water and thus the degradation of phytochemical compounds is prevented. Harder plant parts, on the other hand, are boiled by throwing them into cold water, thus helping to release the bioactive substances (Petrakou et al., 2020).

Quantitative evaluation

To determine the best-known taxa, the frequency of use and the traditional uses of medicinal plants by the local people in Gaziantep herbal markets, some ethnobotanical indices were calculated. Among these indices, the RFC highlights the important taxa, used for many diseases, of the studied region. The fact that the species have high RFC values is very important as it may be an indication that the traditional knowledge about them will reach future generations. Similar to the results of our study, mint, thyme and sage generally have high citation reports, conducted studies in nearby regions (Nanagulyan et al., 2020; Petrakou et al., 2020; Shah et al., 2020).

Indices that record traditional knowledge by measuring current uses (active uses) of plants are noteworthy considerations. At the same time, the information gathered from semi-structured interviews in herbal markets offers a more in-depth analysis about the uses of plants compared to the information collected by the free list method in nature (Tardio and Pardo-de-Santayana, 2008). In the current study, the cultural significance index (CI), calculated according to the citation frequency, records the traditional knowledge and presents the most frequently used plants. Among the plant taxa having the highest CI values, the *Lamiaceae* family has the highest rate compared to other families. Most of the species belonging to the *Lamiaceae* family are aromatic and have essential oils (Lawrence, 1992). In addition, the species of the family are widely used as a spice, especially in the cuisine of Mediterranean countries (Khoury et al., 2016). Mint and thyme are among the most widely used spices in the rich cuisine culture of the region. In addition, they are the most frequently used taxa, especially in colds, stomach ailments, flu and bronchitis. For this reason, they have been the most cited plant taxa by the informant. In addition, most of the taxa with high CI value are among the most-selling taxa by the herbalist. However, *Orchis* spp. taxa draw attention in this list. Since these taxa have been over-harvested from nature for many years, both for food and therapeutic purposes, their populations have declined. Uncontrolled collection of taxa belonging to *Orchidaceae* family from nature is prohibited by the Ministry of Agriculture and Forestry. Today, many taxa belonging to this family are under threat. Salep powder obtained from the tubers of some genera of the *Orchidaceae* family is used by the local people as an aphrodisiac, cold and expectorant, especially in winter. Although the cultivation of some *Orchidaceae* taxa has been achieved in Turkey, it is not yet sufficient to meet the need. For this reason, it is important to increase and encourage the cultivation of the taxa in areas where suitable soil conditions.

http://www.aloki.hu ● ISSN 1589 1623 (Print) ● ISSN 1785 0037 (Online)
DOI: http://dx.doi.org/10.15666/aeer/2005_39553976

Conclusions

Herbal markets are distinctive places for cultures and societies that serve to maintain and illuminate traditional plant uses from different regions and origins, representing the cultural or biological diversity of a particular region on a small scale. With this study, the evaluation of medicinal plants sold in Gaziantep herbal markets was made with the help of some ethnobotanical indices for the first time. In addition, analyze of the herbal market was revealed by evaluating the herbalists both in sales scale and product content and quality scale. In the study, 10 of the 58 medicinal plants sold in herbalists are imported, and some of them (*Zingiber officinale* and *Senna alexandrina*) are among the top-selling plants annually. On the other hand, native plants sold in herbal markets are mostly collected from nature. Among these plants, especially *Glycyrrhiza glabra*, *Ceratonia siliqua* and *Tilia platyphyllos* have very high sales volumes, so the balance of protection and use should be maintained and sales should be controlled.

According to our results the herbal market sector has improved in recent years in terms of customer density, product variety and quality sold, and the number of herbal markets. However, as a result of our observations, it has been determined that herbal markets still do not fully comply with the necessary hygiene and storage conditions. Also, during the field studies, it was observed that herbalists avoided answering some questions about their income due to their professional concerns. Elimination of such concerns will be possible by starting of some professional standards implementation. First of all, some basic training and certificates should be demanded to perform this profession. For herbalists, who are still doing this job, trainings should be organized to support their development, so that they can carry out their work in a well-equipped way and contribute to the transfer of traditional knowledge to future generations in a more accurate way.

As a result, observing the increasing demand for medicinal plants, following the growth of herbal markets and combining those with country's policies will also be a driving force for decision makers.

Conflict of Interests Statement. The authors hereby declare that they have no conflict of interests.

Acknowledgements. This study is based on Master of Science thesis of second author's "Customer Profile and Medicinal Plants Trade in Herbal Shop of Gaziantep Province". The authors would like to thank the local people and the herbalists for their valuable knowledge.

REFERENCES

[1] Acıbuca, V., Bostan Budak, D. (2018): The place and importance of medicinal and aromatic plants in the world and in Turkey. – Çukurova J. Agric. Food Sci. 33(1): 37-44. (in Turkish).

[2] Ahmed, H. M. (2016): Ethnopharmacobotanical study on the medicinal plants used by herbalists in Sulaymaniyah Province, Kurdistan, Iraq. – J. Ethnobiol. Ethnomedicine 12: 8. Doi: 10.1186/s13002-016-0081-3.

[3] Akbulut, S. (2015): Differences in the traditional use of wild plants between rural and urban areas: the sample of Adana. – Stud. Ethno-Med 9: 141-150. Doi: 10.1080/09735070.2015.11905430.

[4] Appiah, K. S., Mardani, H. K., Osivand, A., Kpabitey, S., Amoatey, C. A., Oikawa, Y., Fujii, Y. (2017): Exploring Alternative Use of MedicinalPlants for Sustainable Weed Management. – Sustainability 9(8): 1468. https://doi.org/10.3390/su9081468.

http://www.aloki.hu ● ISSN 1589 1623 (Print) ● ISSN 1785 0037 (Online)
DOI: http://dx.doi.org/10.15666/aeer/2005_39553976

[5] Baytop, T. (2021): Herbal treatment in Turkey in the past and today. – Nobel Tıp Kitapevleri, Üçüncü Baskı (in Turkish).
[6] Bussmann, R. (2002): Ethnobotany and Biodiversity Conservation. – In: Ambasht, R. S., Ambasht, N. K. (eds.) Modern Trends in Applied Terrestrial Ecology. Springer, Boston, MA. https://doi.org/10.1007/978-1-4615-0223-4_18.
[7] Bussmann, R. W., Paniagua Zambrana, N. Y., Moya Huanca, L. A., Hart, L. (2016): Changing markets - medicinal plants in the markets of La Paz and El Alto, Bolivia. – J. Ethnopharmacol 193: 76-95. https://doi.org/10.1016/j.jep.2016.07.074.
[8] Carvalho, A. C. B., Lana, T. N., Perfeito, J. P. S., Silveira, D. (2018): The Brazilian market of herbal medicinal products and the impacts of the new legislation on traditional medicines. – J. Ethnopharmacol 212: 29-35. https://doi.org/10.1016/j.jep.2017.09.040.
[9] Çakır, Ş. (2009): Tahta Köprü Dam and Its Surroundings (Islahiye-Gaziantep) Flora. – Yüzüncüyıl University, Graduate School of Natural and Applied Sciences, Biology, MSc Thesis (in Turkish).
[10] Franco, M. F., Chaw, L. L., Bakar, N., Abas, S. N. H. (2020): Socialising over fruits and vegetables: the biocultural importance of an open-air market in Bandar Seri Begawan. Brunei Darussalam. – J. Ethnobiol. Ethnomedicine 16: 6. https://doi.org/10.1186/s13002-020-0356-6.
[11] Ghorbani, A. (2005): Studies on pharmaceutical ethnobotany in the region of Turkmen Sahra, north of Iran (Part 1): General results. – J. Ethnopharmacol 102: 58-68. https://doi.org/10.1016/j.jep.2005.05.035.
[12] Giday, M., Aswaf, Z., Woldu, Z. (2009): Medicinal plants of the Meinit ethnic group of Ethiopia: An ethnobotanical study. – J. Ethnopharmacol 124: 513-521. https://doi.org/10.1016/j.jep.2009.05.009.
[13] Güllü, E. R. (2009): Gaziantep Armenians from the Ottoman Empire to the Republic. – İstanbul University, Institute of Social Sciences, History, MSc Thesis (in Turkish).
[14] Güneş, S., Savran, A., Paksoy, M. Y., Koşar, M., Çakılcıoğlu, U. (2017): Ethnopharmacological survey of medicinal plants in Karaisalı and its surrounding (Adana-Turkey). – J. Herb. Med 8: 68-75. https://doi.org/10.1016/j.hermed.2017.04.002.
[15] Gürsel, A. (2015): Gaziantep Defense and Şahinbey in the Turkish indepence war. – Int. J. Asian Soc. Sci. 1(1): 52-63. (in Turkish).
[16] Hanlidou, E., Karousou, R., Kleftoyanni, V., Kokkini, S. (2004): The herbal market of Thessaloniki (N Greece) and its relation to the ethnobotanical tradition. – J. Ethnopharmacol. 91(2-3): 281-299. https://doi.org/10.1016/j.jep.2004.01.007.
[17] Heinrich, M., Edwards, S., Moerman, D., Leonti, M. (2009): Ethnopharmacological field studies: A critical assessment of their conceptual basis and methods. – J. Ethnopharmacol. 124: 1-17. https://doi.org/10.1016/j.jep.2009.03.043.
[18] Ji, Y., Fang, Q., Liu, S., Zhang, B., Long, C. (2020): Herbal medicinal markets in China: an ethnobotanical survey. – In: Khasim, S. M., Long, C., Thammasiri, K., Lutken, H. (eds.) Medicinal Plants: Biodiversity, Sustainable Utilization and Conservation. Springer, Singapore. https://doi.org/10.1007/978-981-15-1616-8_24.
[19] Jiang, M., Zhao, S., Yang, S., Lin, X., He, X., Wei, X., Song, Q., Li, R., Fu, C., Zhang, J., Zhang, Z. (2020): An "essential herbal medicine" - licorice: a review of phytochemicals and its effects in combination preparations. – J. Ethnopharmacol. 249: 112439. https://doi.org/10.1016/j.jep.2019.112439.
[20] Jin, B., Liu, Y., Xie, J., Luo, B., Long, C. (2018): Ethnobotanical survey of plant species for herbal tea in a Yao autonomous county (Jianghua, China): results of a 2-year study of traditional medicinal markets on the Dragon Boat Festival. – J. Ethnobiol. Ethnomedicine 14: 58. https://doi.org/10.1186/s13002-018-0257-0.
[21] Keykubat, B. (2016): Medicinal and Aromatic Plants and Good Life. – İzmir Commodity Exchange Report, p. 21.
[22] Khoury, M., Stien, D., Eparvier, V., Ouaini, N., El Beyrouthy, M. (2016): Report on the Medicinal Use of Eleven Lamiaceae Species in Lebanon and Rationalization of Their

http://www.aloki.hu ● ISSN 1589 1623 (Print) ● ISSN 1785 0037 (Online)
DOI: http://dx.doi.org/10.15666/aeer/2005_39553976

Antimicrobial Potential by Examination of the Chemical Composition and Antimicrobial Activity of Their Essential Oils. – eCAM, Article ID: 2547169. https://doi.org/10.1155/2016/2547169.

[23] Kılıç, M., Yıldız, K., Mungan Kılıç, F. (2020): Traditional uses of wild plants in Mardin central district and attached villages (Turkey). – Indian J. Tradit. Knowl. 20(3): 784-798.

[24] Kızılarslan Hançer, Ç., Sevgi, E., Büyükkılıç Altınbaşak, B., Altundağ Çakır, E., Akkaya, M. (2020): Traditional Knowledge of Wild Edible Plants of Biga (Çanakkale), Turkey. – Acta Societatis Botanicorum Poloniae 89(31): 8914. https://doi.org/10.5586/asbp.8914.

[25] Külek, A. (2010): 71 Numaralı Gaziantep Şer'iye Sicili Transkripsiyonu (1-101. Sayfalar-H.1132 / M.1720) [The transcription of the first 101 pages of the 71. Numbered Gaziantep Shar'iyya Registery Book]. – Yüzüncüyıl University, Institute of Social Sciences, History, MSc Thesis, 263p.

[26] Lawrence, B. M. (1992): Chemical components of Labiatae oils and their exploitation. – In: Harley, R. M., Reynolds, T. (eds.) Advances in Labiate Science. Richmond, Royal Botanic Gardens, Kew.

[27] Łuczaj, Ł., Jug-Dujakovic, M., Dolina, K., Jeričević, M., Vitasović-Kosić, I. (2021): Insular Pharmacopoeias: Ethnobotanical Characteristics of Medicinal Plants Used on the Adriatic Islands. – Front. Pharmacol. 12: 623070. https://doi.org/10.3389/fphar.2021.623070.

[28] Łuczaj, Ł., Lamxay, V., Tongchan, K., Xayphakatsa, K., Phimmakong, K., Radavanh, S., Kanyasone, V., Pietras, M., Karbarz, M. (2021): Wild food plants and fungi sold in the markets of Luang Prabang, Lao PDR. – J. Ethnobiol. Ethnomedicine 17: 6. https://doi.org/10.1186/s13002-020-00423-y.

[29] MAF (2021): Republic of Turkey Ministry of Agriculture and Forestry, Noah's ark national biodiversity database. – https://nuhungemisi.tarimorman.gov.tr/public/istatistik (Accessed 10 January 2022).

[30] Mehrnia, M., Akaber, M., Amiri, M. S., Nadaf, M., Emami, S. A. (2021): Ethnopharmacological studies of medicinal plants in central Zagros, Lorestan Province, Iran. – J Ethnopharmacol. 280: 114080. https://doi.org/10.1016/j.jep.2021.114080.

[31] Nanogulyan, S., Zakaryan, N., Kartashyan, N., Piwowarczyk, R., Łuczaj, Ł. (2020): Wild plants and fungi sold in the markets of Yerevan (Armenia). – J. Ethnobiol. Ethnomed. 16: 26. https://doi.org/10.1186/s13002-020-00375-3.

[32] Ötnü, H., Akan, H. (2020): Plants Sold for Phytotheraphy in Pharmacies and Herbalists of Şanlıurfa. – KSU J. Agric Nat 23(4): 947-965. https://doi.org/10.18016/ksutarimdoga.vi.688167.

[33] Özer, H., Türkmen, N. (2019): Investigation of plants with ethnobotanical use in Gaziantep province (Turkey). – GSC Biol. Pharm. Sci. 7(2): 071-078. https://doi.org/10.30574/gscbps.2019.7.2.0076.

[34] Palabaş Uzun, S., Koca, C. (2020): Ethnobotanical survey of medicinal plants traded in herbal markets of Kahramanmaraş. – Plant Divers 42: 443-454. https://doi.org/10.1016/j.pld.2020.12.003.

[35] Petrakou, K., Iatrou, G., Lamari, N. F. (2020): Ethnopharmacological survey of medicinal plants traded in herbal markets in the Peloponnisos, Greece. – J. Herb. Med. 19: 100305. https://doi.org/10.1016/j.hermed.2019.100305.

[36] Prance, G. T. (1991): What is Ethnobotany? – J. Ethnopharmacol. 32: 209-216. https://doi.org/10.1016/0378-8741 (91)90120-3.

[37] Schippmann, U., Leaman, D. J., Cunningham, A. B. (2002): Impact of cultivation and gathering of medicinal plants on biodiversity: global trends and issues, in Biodiversity and the Ecosystem Approach in Agriculture, Forestry and Fisheries. – Ninth Regular Session of the Commission on Genetic Resources for Food and Agriculture, FAO, Rome, Italy.

[38] Shah, S., Khan, S., Sulaiman, S., Muhammad, M., Badshah, L. (2020): Quantative study on medicinal plants traded in selected herbal markets of Khyber Pakhtunkhwa, Pakistan. – Ethnobot. Res. Appl. 20: 57. https://doi.org/10.32859/era.20.57.1-36.

http://www.aloki.hu ● ISSN 1589 1623 (Print) ● ISSN 1785 0037 (Online)
DOI: http://dx.doi.org/10.15666/aeer/2005_39553976

[39] Şahin, Ç. (2011): Evil Eye - Beliefs, Practices and Their Religious-Mythological Origins (Gaziantep Region). – Gaziantep University, Institute of Social Sciences, Turkish language and literature, MSc Thesis (in Turkish).
[40] Tardío, J., Pardo-de-Santayana, M. (2008): Cultural importance indices: a comparative analysis based on the useful wild plants of Southern Cantabria (Northern Spain). – Econ. Bot. 62(1): 24-39. https://doi.org/10.1007/s12231-007-9004-5.
[41] Temel, M., Tınmaz, A. B., Öztürk, M., Gündüz, O. (2018): Production and Trade of Medicinal and Aromatic Plants in the World and Turkey. – KSU J. Agric Nat 21 (Special Issue): 198-214. https://doi.org/10.18016/ksutarimdoga.vi.473036.
[42] Trotter, R. T., Logan, M. H. (1986): Informant consensus: a new approach for identifying potentially effective medicinal plants. – In: Etkin, N. L. (ed.) Plants in Indigenous Medicine and Diet: Biobehavioural Approaches. Redgrave Publishers, Bedford Hills, NY.
[43] TUIK (2018): Technical bulletin, Number 27844. – Turkish Statistical Institute (in Turkish).
[44] TUIK (2020): Turkey's Statistical Yearly Book. – Ankara: TUIK.
[45] Uçuk, C., Kayran, M. F. (2020): Historical Development of Gaziantep Cuisine: Eating and Drinking Activities in The Turkish Independence War. – JOSCAT 3(2): 258-272.
[46] URL-1 (2022): Ethnic structure of Turkey. – Available at: https://upload.wikimedia.org/wikipedia/tr/0/0f/T%C3%BCrkiye_etnik_yap%C4%B1s%C4%B1.png (in Türkish).
[47] Vitalini, S., Iriti, M., Puricelli, C., Ciuchi, D., Segale, A., Fico, G. (2013): Traditional knowledge on medicinal and food plants used in Val San Giacomo (Sondrio, Italy) - an alpine ethnobotanical study. – J. Ethnopharmacol. 145: 517-529. https://doi.org/10.1016/j.jep.2012.11.024.
[48] Wang, Q., Zhao, L., Gao, C., Zhao, J., Ren, Z., Shen, Y., Yao, R., Yin, H. (2021): Ethnobotanical study on herbal market at the Dragon Boat Festival of Chuanqing people in China. – J. Ethnobiol. Ethnomedicine 17: 19. https://doi.org/10.1186/s13002-021-00447-y.
[49] WHO (2013): Traditional Medicine Strategy: 2014-2023. – World Health Organization, Geneva, Switzerland.
[50] Yeşil, Y., İnal, İ. (2019): Traditional knowledge of wild edible plants in Hasankeyf (Batman Province, Turkey). – Acta Societatis Botanicorum Poloniae 88(3): 3633. https://doi.org/10.5586/asbp.3633.
[51] Yüksel, D. (2007): Beliefs and Practices Related to Birth in Gaziantep and Its Surroundings. – Gaziantep University, Institute of Social Sciences, Turkish language and literature, MSc Thesis (in Turkish).
[52] Zahoor, M., Yousaf, Z., Yasin, H., Shinwari, Z. K., Haroon, M. (2021): Ethnobotanicals and commercial trends of herbal markets in Punjab, Pakistan. – J. Herb. Med. 26: 100425. https://doi.org/10.1016/j.hermed.2021.100425.
[53] Zenderland, J., Hart, R., Bussmann, R. W., Zambrana, N. Y. P., Sikharulidze, S., Kikvidze, Z., Kikodze, D., Tchelidze, D., Khutsishvili, M., Batsatsashvili, K. (2019): The use of "Use Value": Quantifying importance in ethnobotany. – Econ Bot 73: 293-303. https://doi.org/10.1007/s12231-019-09480-1.

http://www.aloki.hu ● ISSN 1589 1623 (Print) ● ISSN 1785 0037 (Online)
DOI: http://dx.doi.org/10.15666/aeer/2005_39553976

APPENDIX

APPENDIX I (FOR HERBALIST)

First Part

1. Age of herbalist
2. Gender of herbalist
3. Education level of herbalist
4. How they obtained the knowledge of herbalism
5. Active years at herbal market, number of employees, number of products, annual turnover
6. Monthly earnings of herbalist

Second Part

7. How they buy their products?
8. What are the top-selling plant taxa?
9. Where or from whom they buy the products that they sell?
10. How often they buy medicinal plants?
11. How they get information about plants?
12. Are they aware of the laws regarding the collecting, processing and sale of plants?
13. What are the most important criteria that customers pay attention when purchasing medicinal plants?

APPENDIX II (FOR CUSTOMER)

Date: ---- Informants name:---- Age: ----
Education level:------
1. Local name of plant: ---- 2. Part of plant:---- 3. Diseases being treated:----
5. How to use it (powder, pulp, tea, etc.) ---- Internal □ External □

http://www.aloki.hu ● ISSN 1589 1623 (Print) ● ISSN 1785 0037 (Online)
DOI: http://dx.doi.org/10.15666/aeer/2005_39553976

PREDICTING POTENTIAL DISTRIBUTION OF *STELLERA CHAMAEJASME* UNDER GLOBAL CLIMATE CHANGE IN CHINA

LI, L.[1,2] – ZHANG, B.[1*] – WEN, A. M.[3] – YAO, X. J.[1]

[1]*College of Geographical and Environmental Science, Northwest Normal University, Lanzhou 730070, China*

[2]*Lanzhou Resources & Environment Voc-Tech University, Lanzhou 730021, China*

[3]*State Key Laboratory of Cryosphere Sciences, Northwest Institute of Eco-Environment and Resources, CAS, Lanzhou 730000, China*

[*]*Corresponding author*
e-mail: zhangbo@nwnu.edu.cn; phone: +86-138-9313-6515

(Received 20th March 2022; accepted 11th Jul 2022)

Abstract. The impact and feedback of climate–vegetation interaction on the potential habitat of plants is one of the focuses of terrestrial ecosystem and global climate change research. Based on 246 occurrence records of *S. chamaejasme* and 28 environmental variables (climate, topography and soil), we predicted and analyzed the suitable habitat distributions and shifts of *S. chamaejasme* under current and future (by 2050 and 2070) climate scenarios using the maximum entropy (Maxent) model. The Area Under the receiver operating characteristics Curve (AUC) was used to evaluate the model performance. The key environmental factors were screened by Jackknife tests. The results showed the following: 1) AUC values indicated better performance of MaxEnt modeling. 2) Altitude, annual precipitation, extreme moisture conditions (including precipitation of the wettest and the driest month) and mean temperature of the coldest quarter were the most predominant environmental factors influencing *S. chamaejasme*'s habitat suitability. 3) In the current scenario, *S. chamaejasme* distributed in Qinghai–Tibet plateau, Loess Plateau, Inner Mongolia plateau and Yungui plateau (covering 44.16% of total land of China), especially in Sichuan (37.25%) and Gansu (34.65%) province. 4) With climate change, an increasing trend for the distribution (except in 2050_RCP2.6 and 2050_RCP8.5) had taken place in the area of all suitable classes comparing current and future scenarios overall, while the trends of variation are insignificant. At the same time, the centroid of highly suitable distribution regions shifted to northeast China, and the distribution regions moderately extended to the south. This paper may provide a deep insight for further research and practice management on *S. chamaejasme*.
Keywords: *climate change, Maxent modeling, environmental variables, habitat distribution, S. chamaejasme*

Introduction

The interaction between vegetation and climate change is the focus of many academic fields (in botany, geography, ecology and meteorology) (Zhang et al., 2011). Vegetation and ecosystem change are consistent with the climate variability (Shuman et al., 2019). The most direct reflection of vegetation to climate change is the change of species distribution pattern (Fang et al., 2013; Bradshaw et al., 2016). According to AR6 report, the global surface temperature in the first two decades of the 21st century (2001–2020) is higher than 1850–1900 (IPCC, 2021). The structure and function of terrestrial ecosystems may be altered substantially (Bertrand et al., 2011). Climate change has changed the ecological environment and has a huge impact on the biodiversity and distribution of species that grow on different spatial and temporal

http://www.aloki.hu ● ISSN 1589 1623 (Print) ● ISSN 1785 0037 (Online)
DOI: http://dx.doi.org/10.15666/aeer/2005_39773993

scales and their ecosystems (Rahman et al., 2017; Jiang et al., 2021). More and more attention has been attracted to accurately forecasting the geographical distribution of species and their response to climate change and put forward scientific solutions.

Species habitat is the integration of their living space and biotic factors, including abiotic and biological environments. Species distribution model (SDM) is the main niche model for assessing the response to climate change on species habitat distribution (Georgopoulou et al., 2016), which estimates habitat suitability based on species distribution points and environmental data. Recent years, SDM has been widely used for the study of biodiversity loss in future climate change scenarios (Penner et al., 2017), biological invasion (Wan et al., 2017) and management and conservation of threatened species (Remya et al., 2015; Yi et al., 2016). Currently, SDM models for predicting species distribution are widely used, such as ENFA, GARP, DOMAIN, BIOCLIM, and Maxent (Maximum Entropy) (Wen et al., 2022). Among the above available algorithms, Maxent modeling could predict species' habitat range relatively accurately, based on simplified and constrained species occurrences and environmental variables. It has come into particularly common use (Humphreys et al., 2017; Zhao et al., 2021; Su et al., 2021).

Stellera chamaejasme L. (*S. chamaejasme* for short), a perennial poisonous herbaceous plant widely inhabits China, Russia, Mongolia, North Korea and other countries. Its poisonous nature, high competition and adaptability pose great threat to the growth of healthy vegetation in the degraded grasslands where the ecosystem is extremely fragile, particularly in the farming–pastoral ecotones over China (Liu et al., 2021; Guo et al., 2021). Previous research on *S. chamaejasme* mainly concentrated on biological and pharmacological traits (Grey, 1995; Li et al., 2014), impact on soil physical and chemical properties (An et al., 2016; Wei et al., 2017), spatial association and distribution pattern (Zhao et al., 2010), remote sensing monitoring and detecting in larger scale (Guo et al., 2017) and weed control techniques and uses (Zhang et al., 2011). However, the detailed actual spatial distribution of this weed species in China is unclear. It has been reported that the niches, range and reproduction of *S. chamaejasme* population were greatly affected by climate warming (Zhang et al., 2010), but the responses of climate change on the distribution of the suitable habitat are ignored. Additionally, *S. chamaejasme* have been shown to have notable effect on soil nutrient pools and dynamics, but the soils properties' influence on its habitat distribution is unknown (Yin et al., 2012; Yang et al., 2018). Moreover, it is verified that topography changes have clear response mechanism on spatial association and distribution pattern of *S. chamaejasme*, but only based on point pattern analysis (Gao et al., 2014). So, it became necessary and vital to ascertain the species distribution pattern, habitat suitability, the extent of expansion, and relationship with natural and environmental factors, which also provide bedrock for conservation, restoration and weed control for grassland ecosystem diversity.

This aim of this study include: (1) exploring the key ecological factors and their suitable range of affecting the potential distributions; (2) delineating the potential geographical distribution and shifts of *S. chamaejasme* under current and future climatic scenarios; (3) assessing whether the overall global distribution and habitat suitability expand or contract as a result of climate change.

http://www.aloki.hu ● ISSN 1589 1623 (Print) ● ISSN 1785 0037 (Online)
DOI: http://dx.doi.org/10.15666/aeer/2005_39773993

Materials and methods

Occurrence records

S. chamaejasme's occurrences in China were acquired and collected from the Chinese Virtual Herbarium (CVH, http://www.cvh.ac.cn), the China Species Information Service (CSIS, http://www.chinabiodiversity.com) and extensive literature. Then the presence samples databases of *S. chamaejasme* were deleted and filtered spatially, within 10 km×10 km, to ensure that there are no duplicate points. Finally, in general, 246 samples, representing the total known distribution of this plant in China (*Fig. 1*), were finally saved as .csv file format for further modeling.

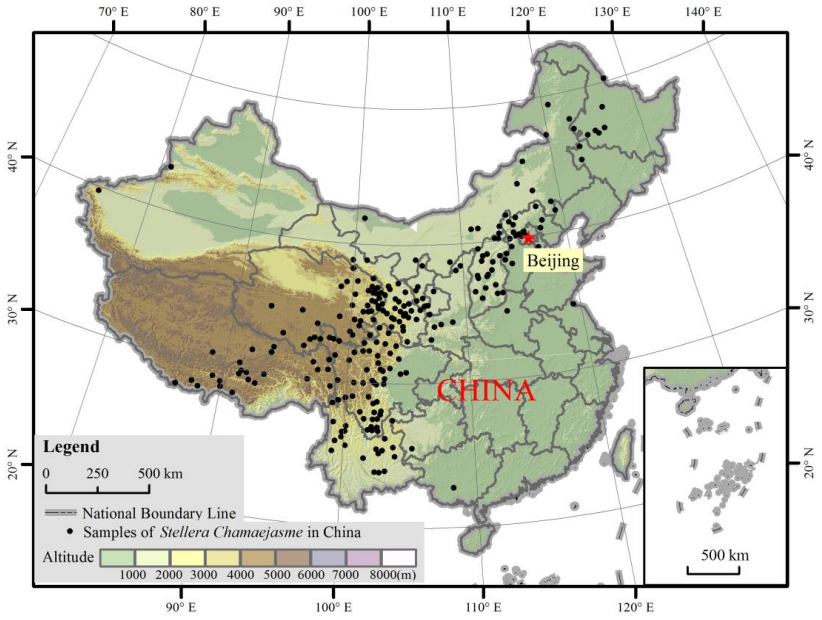

Figure 1. *Presence samples of S. chamaejasme in China*

Environmental variables

Taking into account the biological relevance to habitat distributions and niches of *S. chamaejasme* (Nybom, 2004), 28 environmental variables (climate, topography, soil, *etc*.) were used to predict the potential geographical distribution and shifts of *S. chamaejasme* under current and future (2050s and 2070s) climate scenarios (*Table 1*). 19 bioclimatic variables (bio01–bio19) of present climate condition were collected from the WorldClim database (http://www.worldclim.org/bioclim), which represents seasonality, extremities and annual trends of climate (Hijmans et al., 2005). Additionally, these climate variables under four representative concentration pathway of RCP2.6, RCP4.5, RCP6.0 and RCP8.5 (BCC-CSM1-1) scenarios during 2050s and 2070s released by IPCC Assessments Report 5 (AR5) were downloaded from the Climate Change, Agriculture and Food Security Web site (http://www.ccafs-climate.org); Topographical factors (including elevation, slope and aspect) were generated from DEM data (ca.1 km, http://westdc.westgis. ac.cn) using surface analysis function of ArcGIS 9.3 software; Moreover, five soil variables within topsoil (0–30 cm; t_oc, t_sand, t_clay, t_bden, t_ph and t_gravel) were downloaded from HWSD database

http://www.aloki.hu ● ISSN 1589 1623 (Print) ● ISSN 1785 0037 (Online)
DOI: http://dx.doi.org/10.15666/aeer/2005_39773993

(http://webarchive.iiasa.ac.at) (Nachtergaele et al., 2008; Guo et al., 2015); Geographical base map of China was acquired from http://nfgis.nsdi.gov.cn. All above environmental variables were resampled to 2.5′ longitude/latitude (ca. 5 km at ground spatial resolution) for the study area, and then converted to the ASCII format (.asc) for further Maxent modeling. The projections of all variables were set to WGS 1984 projection.

Table 1. *Contributions of each environmental variable in Maxent modeling*

Code	Environmental variables	Percent contribution	Permutation importance
alt	Altitude	25.3	13.6
bio12	Annual Precipitation	22.3	29.7
bio13	Precipitation of Wettest Month	13.5	4.6
bio14	Precipitation of Driest Month	9.7	1.4
bio11	Mean Temperature of Coldest Quarter	8.8	2.3
t_oc	Topsoil organic carbon	2.0	0.5
bio04	Temperature Seasonality (standard deviation *100)	1.7	8.5
t_sand	Topsoil sand fraction	1.7	4.7
slo	Slope	1.6	1.6
t_clay	Topsoil clay fraction	1.5	0.9
asp	Aspect	1.5	1.4
bio01	Annual Mean Temperature	1.4	0.0
bio03	Isothermality (BIO2/BIO7) (*100)	1.4	2.4
t_bden	Topsoil reference bulk density	1.3	2.1
t_ph	Topsoil pH (H_2O)	1.2	2.2
bio02	Mean Diurnal Range (Mean of monthly (max temp - min temp))	1.0	2.6
t_gravel	Topsoil gravel content	0.8	0.8
bio16	Precipitation of Wettest Quarter	0.7	10.7
bio15	Precipitation Seasonality (Coefficient of Variation)	0.6	1.3
bio07	Temperature Annual Range (BIO5-BIO6)	0.5	0.1
bio19	Precipitation of Coldest Quarter	0.4	5.8
bio05	Max Temperature of Warmest Month	0.3	0.8
bio09	Mean Temperature of Driest Quarter	0.3	0.3
bio06	Min Temperature of Coldest Month	0.2	0.0
bio17	Precipitation of Driest Quarter	0.2	1.0
bio10	Mean Temperature of Warmest Quarter	0.2	0.0
bio08	Mean Temperature of Wettest Quarter	0.2	0.7
bio18	Precipitation of Warmest Quarter	0.0	0.0

Predicting potential distribution

MaxEnt software 3.4.0 k (available at http://www.cs.princeton.edu/*schapire/maxent) was used for habitat suitability simulation, which performed relatively better than other SDMs (Phillips et al., 2006; Elith et al., 2011; Trisurat et al., 2011). Occurrence locations and its related environmental variables were required by Maxent. Of the 246 samples of *S. chamaejasme*, 75% were used for the training, and 25% for testing. The Jacknife analysis, under current condition, was performed in order to evaluate the contribution and response of each environmental variable to potential geographical distribution of *S. chamaejasme*. And the performance of MaxEnt was evaluated by AUC (Area Under the receiver operating characteristics Curve) value,

http://www.aloki.hu ● ISSN 1589 1623 (Print) ● ISSN 1785 0037 (Online)
DOI: http://dx.doi.org/10.15666/aeer/2005_39773993

which ranged from 0.5 (random) to 1.0 (perfect discrimination) (Swets, 1988; Weber, 2011).

The modeling outputs of ASCII format were imported into ArcGIS9.3 for further spatial analysis and statistics. Potential distribution regions were reclassified into five classes by referring to Zhang et al. (2016): (1) unsuitable ($p < 0.1$); (2) marginally suitable ($0.1 \leq p < 0.3$); Low–level suitable ($0.3 \leq p < 0.5$); (4) moderately suitable ($0.5 \leq p < 0.7$); and (5) highly suitable ($p \geq 0.7$).

Results

Model performance

The average AUC data in MaxEnt model for 28 environmental variables under current scenario indicated good performance (*Fig. 2a*) (Swets, 1988). Similarly, the AUC values for the training data and test data of eight future climatic projections (2050s and 2070s) ranged from 0.891 to 0.897, and 0.851 to 0.856, respectively (*Fig. 2b*). These results suggested that Maxent had a high predictive power for the distribution of *S. chamaejasmes* over China.

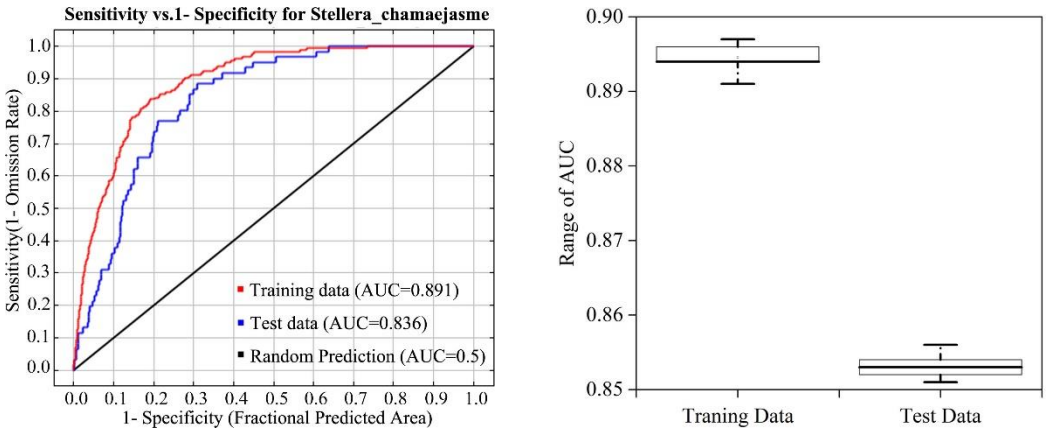

Figure 2. *AUC results of Maxent modeling: Left) AUC curve of current scenario; Right) box plot showing changes in AUC values based on current and eight future climatic projections (2050-RCP2.6, 2050-RCP4.5, 2050-RCP6.0, 2050- RCP8.5, 2070-RCP2.6, and 2070-RCP4.5, 2070-RCP6.0, 2070-RCP8.5)*

Contribution of environmental variables

Jackknife tests gave estimates of contribution percentage and permutation importance of the environmental variables (*Table 1*). Overall, the total contribution of precipitation is 47.4%, topography is 28.4%, temperature is 16% and soil is 8.5%. Among 28 environmental variables, altitude, annual precipitation (bio12), extreme moisture conditions (including precipitation of the wettest and the driest month *i.e.*, bio13 and bio14) and mean temperature of the coldest quarter mainly influenced the geographic distribution and habitat suitability of *S. chamaejasme*. Precipitation had a large influence on the spatial distribution of *S. chamaejasme*. The boxplots of the five suitable habitat type maps also indicated that the annual precipitation of suitable habitat regions is smaller than unsuitable habitat regions. It can be found that *S. chamaejasme* is mainly distributed in regions with 500 mm annual precipitation (*Fig. 3*). Meanwhile,

http://www.aloki.hu ● ISSN 1589 1623 (Print) ● ISSN 1785 0037 (Online)
DOI: http://dx.doi.org/10.15666/aeer/2005_39773993

annual precipitation is strongly correlated with precipitation of the wettest and the driest month. Average altitude of suitable distribution regions extracted and calculated in ArcGIS dedicated that suitable habitat of *S. chamaejasme* distributed from 1400 m in the Inner Mongolia Plateau to 1900 m in the Loess Plateau, 2300 m in the Yungui Plateau, to 3500 m in the Qinghai-Tibet Plateau (*Fig. 4*), and sunny slope. The high contribution of elevation was similarly reported in other papers (Zhang et al., 2016; Tang et al., 2017), for that it closely related to temperature, light and precipitation. Thus, precipitation and temperature were the key factors of influencing potential distributions, colonizing, and growing potentials of *S. chamaejasme*. Importing mean precipitation and temperature data of 12 months into MaxEnt model for further simulating; it was further found that the precipitation in April and May, and average temperature of July and August, had the highest contributions for the potential distribution (*Fig. 5*). Additionally, soil properties in root zone played an important role next to hydrothermal conditions and topographical conditions, but this was not obvious.

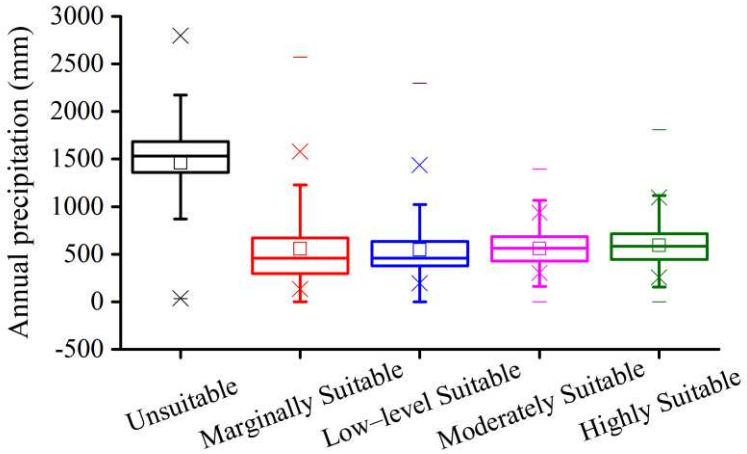

Figure 3. *Box plots showing variation range in occurrence annual precipitation*

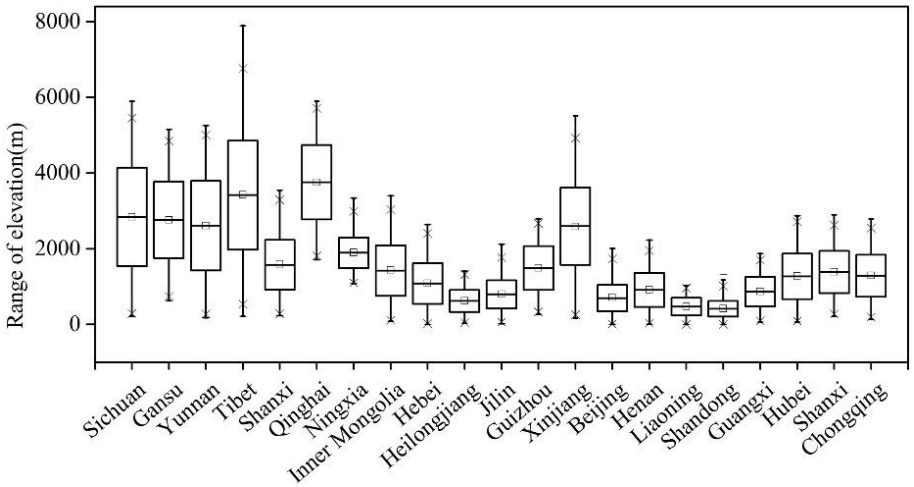

Figure 4. *Box plots showing variation range in occurrence elevation values of S. chamaejasme in different provinces over China*

http://www.aloki.hu ● ISSN 1589 1623 (Print) ● ISSN 1785 0037 (Online)
DOI: http://dx.doi.org/10.15666/aeer/2005_39773993

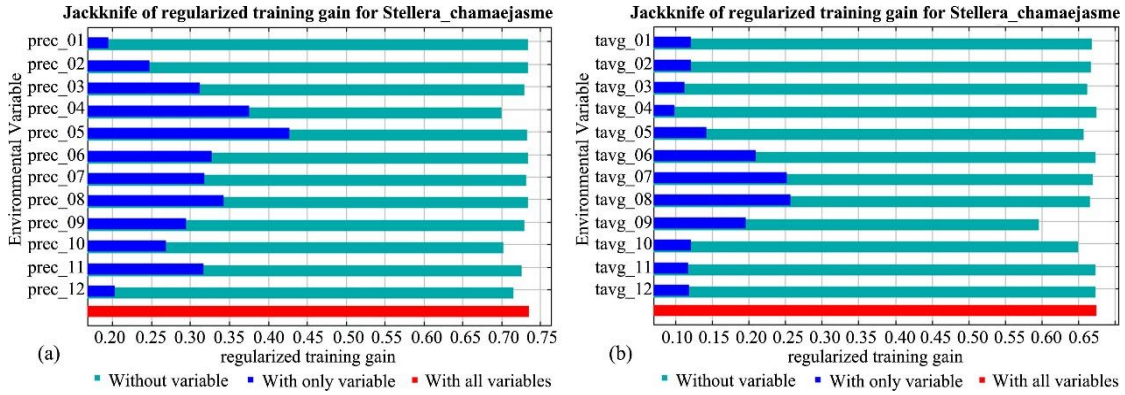

Figure 5. *Jackknife test for variable importance of S. chamaejasme habitat suitability distribution: (a) precipitation; (b) average temperature*

Scatter graphs (*Fig. 6*) further illustrated the climate niches of *S. chamaejasme* in two dimensions for four key bioclimatic variables (bio11_bio13 and bio12_bio14). In the potential distribution regions, this weed species was suitable for the extremely hydro-thermal conditions: -1– -17°C mean temperature of the coldest quarter (even -24.5°C), 80-160 mm precipitation of the wettest month (*Fig. 6a*), 300–750 mm annual precipitation and 0–5 mm precipitation of the driest month respectively (*Fig. 6b*).

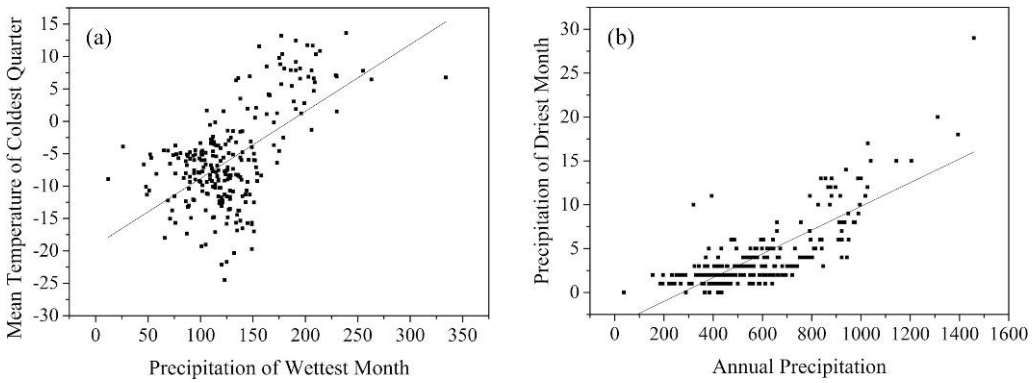

Figure 6. *Scatter graphs for two-dimensional climate niches: (a) precipitation of wettest month (bio13) and mean temperature of coldest quarter (bio11); (b) annual precipitation (bio12) and precipitation of driest month (bio14)*

Predicted current potential distribution

From the MaxEnt modeling result in *Fig. 7* under current climate scenario, the potential distribution regions of *S. Chamaejasme* mainly located in Q–T plateau, loess plateau, Inner Mongolia plateau and Yungui plateau, which extends from the northeast to the southwest (covering 44.16 % of total land of China) along the Hu Line in general.

Cities of moderately and highly suitable habitat were further extracted and conducted. Overall, the core distribution areas were located in the Eastern Monsoon Geo–Eco Region and Q–T Plateau Geo–Eco Region (*Table 2*). The environmental factors in these regions suited the growth and niches of *S. chamaejasme*. Highly suitable regions mainly concentrated in Sichuan (20.62%), Gansu (20.49%), Yunnan (17.83%), Tibet (13.80%), Shanxi (11.28%) and Qinghai (8.09%) province, respectively; and the moderately

http://www.aloki.hu ● ISSN 1589 1623 (Print) ● ISSN 1785 0037 (Online)
DOI: http://dx.doi.org/10.15666/aeer/2005_39773993

suitable areas are mainly in Shanxi (19.35%), Sichuan (16.63%), Tibet (15.80%) and Gansu (14.16%).

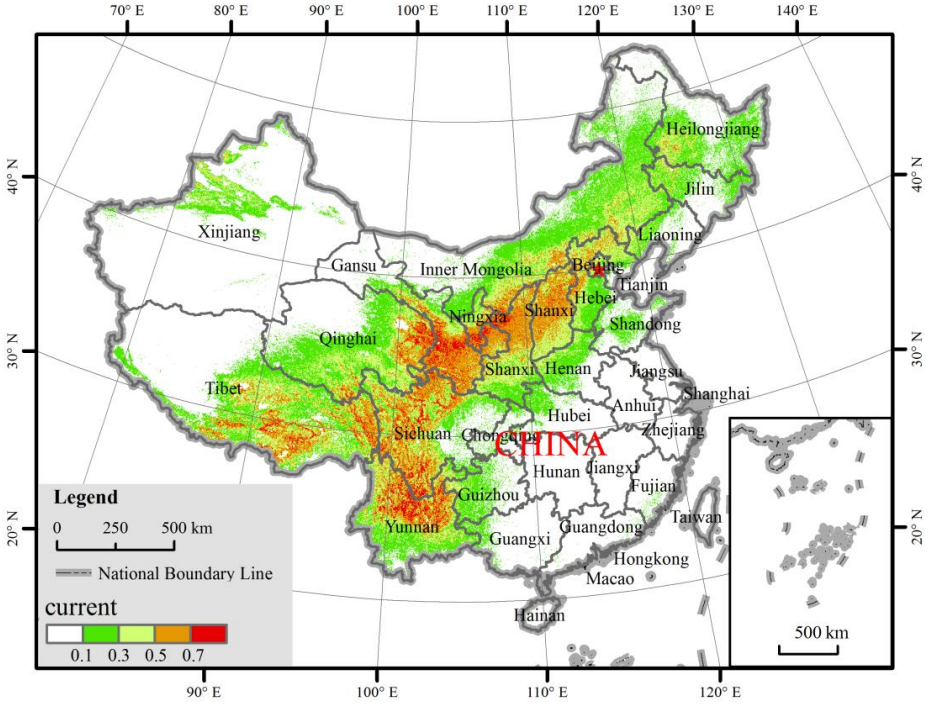

Figure 7. *Potential distribution of S. chamaejasme under current climatic condition*

Table 2. *Analysis of highly and moderately suitable distribution areas of S. chamaejasme under current climatic condition*

Province	Highly suitable			Moderately suitable		
	Area (10^4 km^2)	P/P (%)	P/C (%)	Area (10^4 km^2)	P/P (%)	P/C (%)
Sichuan	3.7292	8.27	20.62	13.6233	30.22	16.63
Gansu	3.7066	8.99	20.49	11.6007	28.13	14.16
Yunnan	3.2257	9.59	17.83	7.7639	23.08	9.48
Tibet	2.4965	2.31	13.80	12.9444	11.96	15.80
Shanxi	2.0399	5.62	11.28	15.8524	43.65	19.35
Qinghai	1.4635	2.18	8.09	6.5347	9.72	7.98
Ningxia	0.6389	12.51	3.53	1.8090	35.42	2.21
Inner Mongolia	0.4583	0.36	2.53	5.5521	4.38	6.78
Hebei	0.1962	1.01	1.08	3.6163	18.67	4.41
Heilongjiang	0.0538	0.10	0.30	0.9392	1.77	1.15
Guizhou	0.0260	0.16	0.14	0.2726	1.73	0.33
Jilin	0.0260	0.12	0.14	0.4253	2.04	0.52
Tibet	0.0156	0.01	0.09	0.5712	0.34	0.70
Beijing	0.0087	0.52	0.05	0.1563	9.31	0.19
Henan	0.0017	0.01	0.01	0.1059	0.66	0.13
Liaoning	0.0017	0.01	0.01	0.1510	1.00	0.18

Note: P/P is percentage of suitable areas of the province; P/C is percentage of suitable areas in China

http://www.aloki.hu ● ISSN 1589 1623 (Print) ● ISSN 1785 0037 (Online)
DOI: http://dx.doi.org/10.15666/aeer/2005_39773993

Spatial pattern changes under global warming scenarios

In order to evaluate the influence of climate warming on the spatial distribution pattern of *S. chamaejasme*, potential distributions under future periods (2050s, 2070s) were predicted and illustrated in *Fig. 8*. In general, slight changes had taken place in the area of all suitable classes for current and future scenarios at large spatial scale, which also were analyzed by spatial analysis and statistics in ArcGIS (*Table 3*). Contrast to current scenario, by 2050s, the total area of suitable regions for RCP2.6 and RCP8.5 reduced and increased for RCP4.5 and RCP6.0, however increased for all RCPs by 2070s. In 2050s, the ratio of highly suitable areas only increased by 0.01% in a stringent mitigation scenario (RCP6.0), and fall in all others (RCP2.6, RCP4.5 and RCP8.5), but moderately suitable class under those three scenarios showed a substantially increasing trend. In 2070s, moderately suitable and high suitable classes increased overall under all RCPs (excepting the highly suitable under RCP2.6). Contrary to the negative effect of global warming on ecosystem, this study verified that the uplift of Qinghai–Tibet Plateau, and climate transformation from warm–dry to warm–humid in northwestern China, accelerated and favored the expansion of *S. chamaejasme*. This competitive advantage could improve invasion capability of *S. chamaejasme* and affect grassland ecosystems functioning and biodiversity in the coming years.

Table 3. *Areas and percentage of suitable habitats distribution of S. chamaejasme under different climate change scenarios*

Climate scenario	Unsuitable		Marginally suitable		Low-level suitable		Moderately suitable		Highly suitable		Total suitable regions
	Area/ $\times10^4$km^2	Ratio /%	Area/ $\times10^4$km^2	Ratio /%	Area/ $\times10^4$km^2	Ratio /%	Area/ $\times10^4$km^2	Ratio /%	Area/ $\times10^4$km^2	Ratio /%	Area /$\times10^4$km^2
Current	504.951	54.36	204.227	21.99	119.663	12.88	81.929	8.82	18.089	1.95	423.908
RCP2.6(2050)	512.047	55.13	197.894	21.31	122.597	13.20	78.597	8.46	17.726	1.91	416.814
RCP2.6(2070)	499.477	53.77	207.326	22.32	118.566	12.76	85.552	9.21	17.939	1.93	429.383
RCP4.5(2050)	497.974	53.61	209.637	22.57	117.616	12.66	86.405	9.30	17.229	1.85	430.887
RCP4.5(2070)	498.635	53.68	207.226	22.31	119.915	12.91	84.835	9.13	18.250	1.96	430.226
RCP6.0(2050)	491.769	52.94	211.639	22.78	121.885	13.12	85.405	9.19	18.163	1.96	437.092
RCP6.0(2070)	490.099	52.76	218.649	23.54	119.628	12.88	81.962	8.82	18.524	1.99	438.763
RCP8.5(2050)	507.060	54.59	200.403	21.58	119.531	12.87	84.288	9.07	17.578	1.89	421.800
RCP8.5(2070)	490.415	52.80	216.823	23.34	120.555	12.98	82.564	8.89	18.505	1.99	438.447

Additionally, in order to reveal the location changes of core potential distribution regions and to indicate recent population expansions of *S. chamaejasme* associated with global climate changes, centroid of geographic distribution was calculated to characterize the position change based on un-regular and un-tidy habitat distribution edges, which was more visual and representative. The analyses for centroid changes of highly suitable and moderately suitable regions are showed in *Fig. 9*. In different RCPs scenarios by 2050s and 2070s, the centroid shifted with a distance of 5.31–5.76 km (longitudinal distances) to the northeast of China against current climate scenario for highly suitable distribution regions (*Fig. 9a*); extended to south (4.01–4.65 km) for moderately suitable regions (*Fig. 9b*), which is generally the same as the view of Zhang et al. (2010). Specifically, the city with the biggest highly suitable distribution area shifted from Sichuan to Gansu, while from Shanxi to Sichuan for moderately suitable region. The south–north parallel valleys and mountain chains would provide an ecological corridor for the immigration of *S. chamaejasme*.

http://www.aloki.hu ● ISSN 1589 1623 (Print) ● ISSN 1785 0037 (Online)
DOI: http://dx.doi.org/10.15666/aeer/2005_39773993

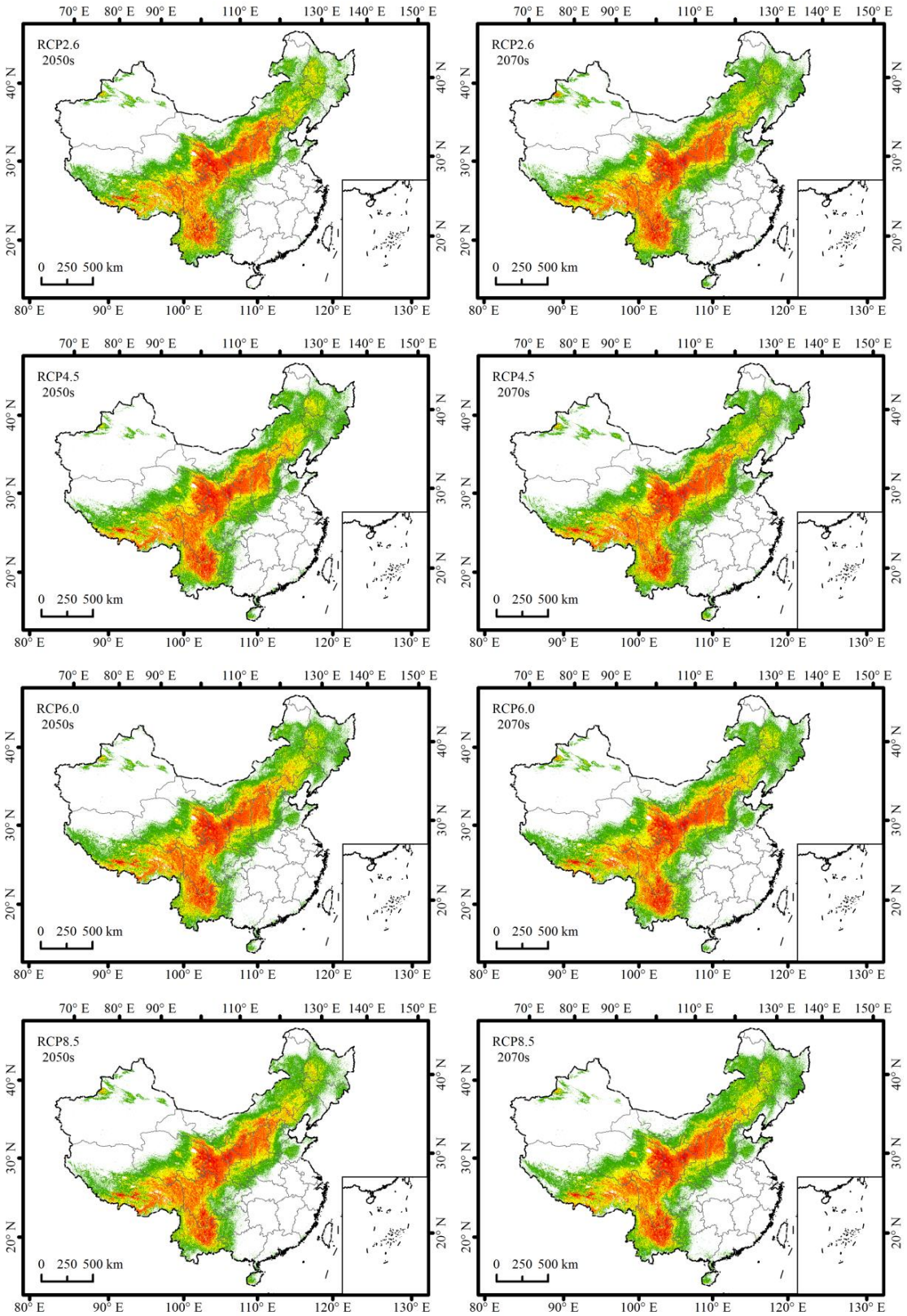

Figure 8. *Future habitat distribution of S. chamaejasme under different RCPs climate change scenarios for 2050s and 2070s based on BCC-CSM1.1*

http://www.aloki.hu ● ISSN 1589 1623 (Print) ● ISSN 1785 0037 (Online)
DOI: http://dx.doi.org/10.15666/aeer/2005_39773993

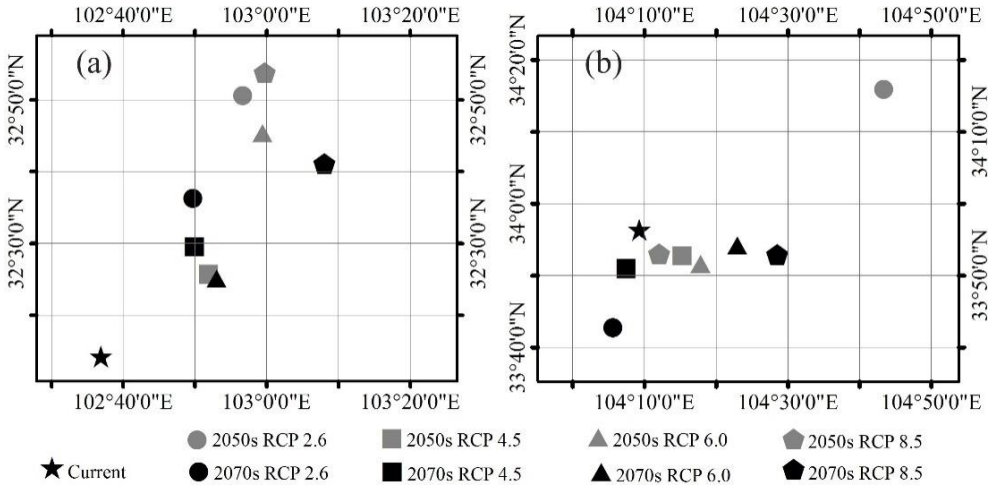

Figure 9. *Centroids distribution under different climate change scenarios: (a) highly suitable distribution areas; (b) moderately suitable distribution areas. (Number beside the mark of centroid represents the longitudinal distances between the mark and current centroid)*

Discussions

Maxent is the most popularized SDMs for analyzing the relationship between climate change and potential geographical distribution of species (Khanum et al., 2013; Qin et al., 2017). AUC was usually utilized for evaluating model accuracy; however, there exist some controversy for the accuracy measurement using AUC in distribution models, even may be misleading, so the test AUC values in this paper only provided a reference to some extent (Lobo et al., 2010). Both sample sizes and environmental variables could influence the accuracy of most SDMs in various degrees. However, distinguished from other SDMs, MaxEnt is little affected by sample sizes, while remains fairly robust for that the simpler models are fitted with smaller samples (Wisz et al., 2008; Ray et al., 2017), while influenced by the quality of occurrence data (West et al., 2016). Additionally, the results of MaxEnt modeling demonstrated that the accuracy of the dataset integrated soil and DEM variables with climate factors was better than that of using climate variables alone, but too many predictor variables may result in poor performance of the model (Barry and Elith, 2006; Vanderwal et al., 2009). Apart from the influence of climatic factors, soil properties and topography, inter-species interactions and the local microclimate also affect species distribution; however existing niche models couldn't well couple the relationships for predicting distribution with high accuracy (Engler et al., 2013). The adaptability of species to environmental factors and specific competition were not considered into Maxent, which may greatly affect the prediction accuracy. Besides, climate change scenarios also influenced the model accuracy, but Maxent model only considered the greenhouse gases emission, and ignored the greenhouse gas feedback.

The area change tendency of potential distribution for S. chamaejasme is 2070 > 2050 > current (Garcia et al., 2013; Chen et al., 2014). Additionally, centroid shifted to northeast for highly suitable distribution regions and extended to the south of China for moderately suitable distribution regions are influenced by global warming and ecosystem shifts with uplift of the Qinghai-Tibet Plateau (Zhang et al., 2010). *S. chamaejasme* will be breeding to places with more suitable "big atmosphere" and "small environment". According to Jackknife results of MaxEnt, climate is the key

http://www.aloki.hu ● ISSN 1589 1623 (Print) ● ISSN 1785 0037 (Online)
DOI: http://dx.doi.org/10.15666/aeer/2005_39773993

environmental factor for species niches and cover at large scale. Vegetation, a link of soil, atmosphere and moisture, acts as an "indicator" in global change. Firstly, climate change determines the dynamics of changes of vegetation types and distribution, vegetation is also actively feedback on climate change (Lambin and Strahler, 1994; Ichii et al., 2002; Pang et al., 2016). The abiotic factors that determine vegetation niches and shifts are hydro-thermal conditions. Thermal condition is the energy source of plant, and hydro condition affect the plant's physiological structure (Yi et al., 2013). Throughout the growing seasons (5–9) of *S. chamaejasme*, our results showed that precipitation in April and May facilitates the grow at the mid of growing season (precipitation has the characteristic of lag), while at the silique mature period, the decline stage, average temperature in July and August plays a leading role. Accordingly, for the response of vegetation to precipitation and temperature a suitable threshold exists (-1–-17℃ for mean temperature of coldest quarter, 80–160 mm for precipitation of wettest month, 300–750 mm annual precipitation and 0–5 mm precipitation of driest month respectively). Thus, temperature and precipitation could both promote and decrease the growth of vegetation. Secondly, the edaphic factors in this paper, including the content of organic carbon, sand, clay, bulk density, pH and gravel within topsoil (0-30 cm), had different attribution for potential distribution of *S. chamaejasme*. Climate warming changes the micro-environmental condition, especially changing soil condition or microclimate, which helps to provide better soil nutrient environment (Gao et al., 2016; Yang et al., 2018).

Much work can be done to refine the use of Maxent for modeling geographic distributions of *S. chamaejasme* in the future. In order to make an adequate prediction, research should further determine the quality and quantity of occurrence data, and screen how much environmental variables will be needed by testing their significance and correlation for avoiding over-fitting and redundancy (Bradie et al., 2017). Additionally, expression of biological factors of *S. chamaejasme* (such as interspecies interactions) in MaxEnt should be replaced by the spatial distribution and density of upper and lower levels in its food chain. AUC method is also necessary to be improved and replaced by PAUC (Slater and Michael, 2012) or AIC index (Riddle and Stratford, 1999). Besides, multiple evaluation techniques, such as remote sensing (RS) technique and field validation should be concerned and integrated in the results assessment of MaxEnt modeling rather than relying on AUC only (Park et al., 2017). Lastly, this paper is the only research to date that have been conducted for predicting potential geographical distribution and shifts of *S. chamaejasme* in response to climate change using MaxEnt model, the results may provide a reference to make a detailed reference for ecological conservation and sustainable management of this plant in the future.

Conclusions

This paper delved the response of *S. chamaejasme* to climate change regarding geographical distributions and habitat suitability based on MaxEnt and GIS in China. Maxent model performance under 9 climate scenarios consistently performed significantly well for *S. chamaejasme*. Average AUC values ranged from 0.851 to 0.897. Predicting performance of MaxEnt was improved by using multiple environmental variables (including climate, soil and topography), but limited likely due to the quantity and quality of sample. The results showed that the distributions of *S. chamaejasme* were largely determined by the hydrothermal conditions: annual precipitation, precipitation

http://www.aloki.hu ● ISSN 1589 1623 (Print) ● ISSN 1785 0037 (Online)
DOI: http://dx.doi.org/10.15666/aeer/2005_39773993

of the wettest and the driest month, and mean temperature of the coldest quarter; precipitation in April and May and average temperature in July and August. Overall, topography, soil and bioclimatic variables are inherently spatially and temporally auto correlated.

Potential distribution region of *S. chamaejasme* mainly distributed in Q-T plateau, loess plateau, Inner Mongolia plateau and Yungui plateau (mainly in Eastern Monsoon Geo-Eco Region and Q–T Plateau Geo–Eco Region) along the Hu line. Specifically, mid-high suitable regions mainly distributed in Sichuan (37.25%) and Gansu (34.65%) province. Maxent logistic predictions for present and future (2050s and 2070s) geographic distribution of suitable habitat of *S. chamaejasme* with climate changing showed that areas of suitable habitats increased (except in 2050_RCP2.6 and 2050_RCP8.5), while not significantly. Results of centroid changes demonstrated that highly suitable distribution regions shifted to northeast China, and moderately suitable distribution regions extended to the south. The results were consistent with global warming, and geographical and ecological alterations that followed the uplift of the Q-T Plateau.

Acknowledgments. This research was funded by the State Key Laboratory of Cryospheric Science (SKLCS 2020-03), the Scientific Research Project of Higher Learning Institution in Gansu Province (2022A-192). We also thank the editors and reviewers for their critical comments and constructive suggestions.

REFERENCES

[1] Barry, S., Elith, J. (2006): Error and uncertainty in habitat models. – Journal of Applied Ecology 43: 413-423.

[2] Bertrand, R., Lenoir, J., Piedallu, C., Riofrío-Dillon, G., Ruffray, P. D., Vidal, C., Pierrat, J-C., Gégout, J-C. (2011): Changes in plant community composition lag behind climate warming in lowland forests. – Nature 479: 517-520.

[3] Bradie, J., Leung, B. (2017): A quantitative synthesis of the importance of variables used in MaxEnt species distribution models. – Journal of Biogeography 44: 1344-1361.

[4] Bradshaw, C. J. A., Leroy, B., Bellard, C., Roiz, D., Albert, C., Fournier, A., Barbet-Massin, M., Salles, J., Simard, F., Courchamp, F. (2016): Massive yet grossly underestimated global costs of invasive insects. – Nature communications 7(1): 1-8.

[5] Chen, B., Zhang, X., Tao, J., Wu, J., Wang, J., Shi, P., Zhang, Y., Yu, C. (2014): The impact of climate change and anthropogenic activities on alpine grassland over the Qinghai-Tibet Plateau. – Agricultural and Forest Meteorology 189: 11-18.

[6] Elith, J., Graham, C. H., Anderson, R. P., Dudík, M., Ferrier, S., Guisan, A., Hijmans, R. J., Huettmann, F., Leathwick, J. H., Lehmann, A., Li, J., Lohmann, L. G., Loiselle, B. A., Manion, G., Moritz, C., Nakamura, M., Nakazawa, Y., Overton, J. M. M., Peterson, A. T., Phillips, S. J., Richardson, K., Scachetti-Pereira, R., Schapire, R. E., Soberón, J., Williams, S., Wisz, M. S., Zimmermannet, N. E. (2006): Novel methods improve prediction of species' distributions from occurrence data. – Ecography 29: 129-151.

[7] Engler, J. O., Rödder, D., Elle, O., Hochkirch, A., Secondiet, J. (2013): Species distribution models contribute to determine the effect of climate and interspecific interactions in moving hybrid zones. – Journal of Evolutionary Biology 26: 2487-2496.

[8] Fang, S., Yan, J., Che, M., Zhu, Y., Liu, Z., Pei, H., Zhang, H., Xu, G., Lin, X. (2013): Climate change and the ecological responses in Xinjiang, China: model simulations and data analyses. – Quaternary International 311: 108-116.

http://www.aloki.hu ● ISSN 1589 1623 (Print) ● ISSN 1785 0037 (Online)
DOI: http://dx.doi.org/10.15666/aeer/2005_39773993

[9] Gao, F. Y., Zao, C. Z., Zhuo Ma, L. C. (2014): Spatial distribution and spatial association of *Stellera chamaejasme* population in the different altitude in degraded alpine grassland. – Acta Ecologica Sinica 33: 605-612. (in Chinese).
[10] Gao, Q., Guo, Y., Xu, H., Ganjurjav, H., Li, Y., Wan, Y., Qin, X., Ma, X., Liu, S. (2016): Climate change and its impacts on vegetation distribution and net primary productivity of the alpine ecosystem in the Qinghai-Tibetan Plateau. – Science of the total Environment 554: 34-41.
[11] Garcia, K., Lasco, R., Ines, A., Lyon, B., Pulhin, F. (2013): Predicting geographic distribution and habitat suitability due to climate change of selected threatened forest tree species in the Philippines. – Applied Geography 44: 12-22.
[12] Georgopoulou, E., Djursvoll, P., Simaiakis, S. M. (2016): Predicting species richness and distribution ranges of centipedes at the northern edge of Europe. – Acta oecologica 74: 1-10.
[13] Grey, W. C. (1995): *Stellera chamaejasme*: an overview. – New Plantsman 2: 43-49.
[14] Guo, H., Cui, H., Jin, H., Yan, Z., Ding, L., Qin, B. (2015): Potential allelochemicals in root zone soils of *Stellera chamaejasme* L. and variations at different geographical growing sites. – Plant Growth Regulation 77: 335-342.
[15] Guo, F., Xiao, J., Fan, J. (2017): Detection and Classification of Grassland with *Stellera chamaejasme* through HJ-1A Hyperspectral Image in Northern Tibet. – 6th International Conference on Energy, Environment and Sustainable Development (ICEESD 2017). Atlantis Press, pp. 453-459.
[16] Guo, L., Zhao, H., Zhai, X., Wang, K., Liu, L., Wang, K., Huang, D. (2021): Study on life history traits of *Stellera chamaejasme* provide insights into its control on degraded typical steppe. – Journal of Environmental Management 291: 112716.
[17] Hijmans, R. J., Cameron, S. E., Parra, J. L., Jones, P. G., Jarvis, A. (2005): Very high resolution interpolated climate surfaces for global land areas. – International Journal of Climatology 25: 1965-1978.
[18] Humphreys, J. M., Elsner, J. B., Jagger, T. H., Pau, S. (2017): A Bayesian geostatistical approach to modeling global distributions of *Lygodium microphyllum* under projected climate warming. – Ecological Modelling 363: 192-206.
[19] Ichii, K., Kawabata, A., Yamaguchi, Y. (2002): Global correlation analysis for NDVI and climatic variables and NDVI trends: 1982-1990. – International Journal of Remote Sensing 23: 3873-3878.
[20] IPCC (2021): Climate Change 2021: The Physical Science Basis. – In Masson-Delmotte, V., Zhai, P., Pirani, A., Connors, S. L., Péan, C., Berger, S., Caud, N., Chen, Y., Goldfarb, L., Gomis, M. I., Huang, M., Leitzell, K., Lonnoy, E., Matthews, J. B. R., Maycock, T. K., Waterfield, T., Yelekçi, O., Yu, R., Zhou, B. (eds.) Contribution of Working Group I to the Sixth Assessment Report of the Intergovernmental Panel on Climate Change. Cambridge University Press, Cambridge, United Kingdom and New York, NY, USA, In press.
[21] Jiang, L., Liu, Y., Wu, S., Yang, C. (2021): Analyzing ecological environment change and associated driving factors in China based on NDVI time series data. – Ecological Indicators 129: 107933.
[22] Khanum, R., Mumtaz, A. S., Kumar, S. (2013): Predicting impacts of climate change on medicinal asclepiads of Pakistan using Maxent modeling. – Acta Oecol 49: 23-31.
[23] Lambin, E. F., Strahler, A. H. (1994): Indicators of land-cover change for change-vector analysis in multitemporal space at coarse spatial scales. – International Journal of Remote Sensing 15: 2099-2119.
[24] Li, J., Zhang, J. J., Pang, X. X., Zhengchen, X., Gan, L. (2014): Biflavanones with anti-proliferative activity against eight human solid tumor cell lines from *Stellera chamaejasme*. – Fitoterapia 93: 163-167.

http://www.aloki.hu ● ISSN 1589 1623 (Print) ● ISSN 1785 0037 (Online)
DOI: http://dx.doi.org/10.15666/aeer/2005_39773993

[25] Liu, Y., Zhao, F., Wang, L., He, W., Liu, J., Long, Y. (2021): Spatial Distribution and Influencing Factors of Soil Fungi in a Degraded Alpine Meadow Invaded by *Stellera chamaejasme*. – Agriculture 11(12): 1280.
[26] Lobo, J. M., Jiménez-Valverde, A., Hortal, J. (2010): The uncertain nature of absences and their importance in species distribution modelling. – Ecography 33: 103-114.
[27] Nachtergaele, F., Velthuizen, H. V., Verelst, L., Verelst, L., Batjes, N., Dijkshoorn, K., Engelen, V. V., Fischer, G., Jones, A., Montanarella, L., Petri, M., Prieler, S., Shi, X., Teixeira, E., Wiberg, D. (2008): Harmonized World Soil Database. – World Congress of Soil Science: Soil Solutions for A Changing World, Brisbane, Australia, 1-6 August 2010. Symposium 1.2.1 Global Soil Spatial Information Systems (pp. 34-37. (Published on DVD)).
[28] Nybom, H. (2004): Comparison of different nuclear DNA markers for estimating intraspecific genetic diversity in plants. – Molecular Ecology 13: 1143-1155.
[29] Pang, G., Wang. X., Yang M. (2016): Using the NDVI to identify variations in, and responses of, vegetation to climate change on the Tibetan plateau from 1982 to 2012. – Quaternary International 44(A): 87-96.
[30] Park, H. C., Lim, J. C., Lee, J. H. (2017): Predicting the potential distributions of invasive species using the Landsat imagery and Maxent: focused on "ambrosia trifida l. var. trifida" in Korean demilitarized zone. – Journal of the Korean Society of Environmental Restoration Technology 20: 1-12.
[31] Penner, J., Rödel, M. O. (2019): Keep it simple? Dispersal abilities can explain why species range sizes differ, the case study of West African amphibians. – Acta Oecologica 94: 41-46.
[32] Phillips, S. J., Anderson, R. P., Schapire, R. E. (2006): Maximum entropy modeling of species geographic distributions. – Ecological Modelling 190: 231-259.
[33] Qin, A., Liu, B., Guo, Q., Bussmann, R. W., Ma, F., Jian, Z., Xu, G., Pei, S. (2017): Maxent modeling for predicting impacts of climate change on the potential distribution of *Thuja sutchuenensis Franch.*, an extremely endangered conifer from southwestern China. – Global Ecology and Conservation 10: 139-146.
[34] Rahman, D. A., Gonzalez, G., Haryono, M., Muhtarom, A. (2017): Factors affecting seasonal habitat use, and predicted range of two tropical deer in Indonesian rainforest. – Acta Oecologica 82: 41-51.
[35] Ray, D., Behera, M. D., Jacob, J. (2017): Evaluating Ecological Niche Models: A Comparison Between Maxent and GARP for Predicting Distribution of *Hevea brasiliensis* in India. – Proceedings of the National Academy of Sciences, India Section B: Biological Sciences 88(4): 1337-1343.
[36] Remya, K., Ramachandran, A., Jayakumar, S. (2015): Predicting the current and future suitable habitat distribution of *Myristica dactyloides, gaertn*. using maxent model in the eastern Ghats, India. – Ecological Engineering 82: 184-188.
[37] Riddle, D. L., Stratford, P. W. (1999): Interpreting validity indexes for diagnostic tests: an illustration using the Berg balance test. – Physical therapy 79: 939-948.
[38] Shuman, B. N., Marsicek, J., Oswald, W. W., Foster, D. R. (2019): Predictable hydrological and ecological responses to Holocene North Atlantic variability. – Proceedings of the National Academy of Sciences of the United States of America 116(13): 5985-5990.
[39] Slater, H., Michael, E. (2012): Predicting the current and future potential distributions of *Lymphatic filariasis* in Africa using maximum entropy ecological niche modelling. – PloS One 7: e32202.
[40] Solomon, S. (2007): Climate change 2007-the physical science basis. – Working group I contribution to the fourth assessment report of the IPCC (Vol. 4). – Cambridge University Press.

http://www.aloki.hu ● ISSN 1589 1623 (Print) ● ISSN 1785 0037 (Online)
DOI: http://dx.doi.org/10.15666/aeer/2005_39773993

[41] Su, H., Bista, M., Li, M. (2021): Mapping habitat suitability for Asiatic black bear and red panda in Makalu Barun National Park of Nepal from Maxent and GARP models. – Scientific Reports 11: 14135.
[42] Swets, J. A. (1988): Measuring the accuracy of diagnostic systems. – Science 240: 1285-1293.
[43] Tang, J., Cheng, Y., Luo, L., Zhang, L., Jiang, X. (2017): Maxent-based prediction of overwintering areas of *Loxostege sticticalis* in china under different climate change scenarios. – Acta Ecologica Sinica 37: 4852-4863. (in Chinese).
[44] Trisurat, Y., Shrestha, R., Kjelgren, R. (2011): Plant species vulnerability to climate change in Peninsular Thailand. – Applied Geography 31: 1106-1114.
[45] Vanderwal, J., Shoo, L. P., Graham, C., Williams, S. E. (2009): Selecting pseudo-absence data for presence-only distribution modeling: how far should you stray from what you know? – Ecological Modelling 220: 589-594.
[46] Wan, J. Z., Wang, C. J., Yu, F. H. (2017): Modeling impacts of human footprint and soil variability on the potential distribution of invasive plant species in different biomes. – Acta Oecol 85: 141-149.
[47] Weber, T. C. (2011): Maximum entropy modeling of mature hardwood forest distribution in four U.S. states. – Forest Ecology and Management 261: 779-788.
[48] Wei, C., Zhong, B., Lian, Y., Geng, S. (2017): Allelopathic effects of root aqueous extract of different age of *Stellera chamaejasme* on four common plants in alpine meadow of Tibet plateau. – Ecological Science (in Chinese).
[49] Wen, A., Wu, T., Zhu, X., Li, R., Wu, X., Chen, J., Qiao, Y., Ni, J., Ma, W., Li, X., Shang, C. (2022): Changes in the spatial distribution of *Bryophytes* on the Qinghai-Tibet Plateau under CMIP6 future projections. – Environmental Earth Sciences 81(1): 1-12.
[50] West, A. M., Kumar, S., Brown, C. S., Stohlgren, T. J., Bromberg, J. (2016): Field validation of an invasive species Maxent model. – Ecological Informatics 36: 126-134.
[51] Wisz, M. S., Hijmans, R. J., Li, J., Peterson, A. T., Graham, C. H., Guisan, A., NCEAS Predicting Species Distributions Working Group (2008): Effects of sample size on the performance of species distribution models. – Diversity & Distributions 14(5): 763-773.
[52] Yang, Z., Zhu, Q., Zhan, W., Xu, Y., Zhu, E., Gao, Y., Li, S., Zheng, Q., Zhu, D., He, Y., Peng, C., Chen, H. (2018): The linkage between vegetation and soil nutrients and their variation under different grazing intensities in an alpine meadow on the eastern Qinghai-Tibetan Plateau. – Ecological Engineering 110: 128-136.
[53] Yi, S., Li, N., Xiang, B., Ye, B., McGuire, A. D. (2013): Representing the effects of alpine grassland vegetation cover on the simulation of soil thermal dynamics by ecosystem models applied to the Qinghai-Tibetan Plateau. – Journal of Geophysical Research: Biogeosciences 118(3): 1186-1199.
[54] Yi, Y. J., Cheng, X., Yang, Z. F., Zhang, S. H. (2016): Maxent modeling for predicting the potential distribution of endangered medicinal plant (H. *riparia Lour*) in Yunnan, China. – Ecological Engineering 92: 260-269.
[55] Yin, H., Chen, Z., Liu, Q. (2012): Effects of experimental warming on soil N transformations of two coniferous species, Eastern Tibetan Plateau, China. – Soil Biology and Biochemistry 50: 77-84.
[56] Zhang, Y. H., Volis, S., Hang, S. (2010): Chloroplast phylogeny and phylogeography of *Stellera chamaejasme* on the Qinghai-Tibet plateau and in adjacent regions. – Molecular Phylogenetics and Evolution 57: 1162-1172.
[57] Zhang, L., Liu, S. R., Sun, P. S. (2011): Comparative evaluation of multiple models of the effects of climate change on the potential distribution of *pinus massoniana*. – Chinese Journal of Plant Ecology 35: 1091-1105. (in Chinese).
[58] Zhang, Z. Q., Zhang, Y. H., Sun, H. (2011): The reproductive biology of *Stellera chamaejasm*e (Thymelaeaceae): A self-incompatible weed with specialized flowers. – Flora-Morphology, Distribution, Functional Ecology of Plants 206: 567-574.

http://www.aloki.hu ● ISSN 1589 1623 (Print) ● ISSN 1785 0037 (Online)
DOI: http://dx.doi.org/10.15666/aeer/2005_39773993

[59] Zhang, L., Cao, B., Bai, C., Li, G., Mao, M. (2016): Predicting suitable cultivation regions of medicinal plants with maxent modeling and fuzzy logics: a case study of *Scutellaria baicalensis*, in China. – Environmental Earth Sciences 75: 361.

[60] Zhang, Y., Sun, H., Zhang, J., Sun, H. (2016): Genetic diversity of the weed species, *Stellera chamaejasme*, in china inferred from amplified fragment length polymorphism analysis, weed biology and management. – Weed Biology and Management 15(4): 165-174.

[61] Zhao, C., Gao, F., Wang, X., Sheng, Y., Shi, F. (2010): Fine-scale spatial patterns of *Stellera chamaejasme* population in degraded alpine grassland in upper reaches of Heihe, China. – Chinese Journal of Plant Ecology 34(11): 1319-1326. (in Chinese).

[62] Zhao, Y., Deng, X., Xiang, W., Chen, L., Ouyang, S. (2021): Predicting potential suitable habitats of Chinese fir under current and future climatic scenarios based on Maxent model. – Ecological Informatics 64: 101393.

http://www.aloki.hu ● ISSN 1589 1623 (Print) ● ISSN 1785 0037 (Online)
DOI: http://dx.doi.org/10.15666/aeer/2005_39773993

MORPHOLOGICAL AND PHYLOGENETIC STUDY OF *OPHIOCORDYCEPS SPHECOCEPHALA* AND *OPHIOCORDYCEPS ASIANA* FROM VIETNAM

MAI, T. N.[1*] – THUY, T. P. D.[1] – HONG, V. N.[2] – TAWAT, T.[3] – SHRESTHA, B.[4]

[1]*Department of Biology, Faculty of Science, Nong Lam University, Linh Trung Ward, Thu Duc District, Ho Chi Minh City, Vietnam*

[2]*Institute of Geography, Vietnam Academy of Science and Technology, A27-No 18, Hoang Quoc Viet street, Cau Giay district, Hanoi, Vietnam*

[3]*RSTDC, Maerim–Samerng Road, Moo 1, Tambol Maeram, Amphur Maerim, Chiang Mai, Thailand*

[4]*Central Department of Biotechnology, Tribhuvan University, Kirtipur, Kathmandu, Nepal*

[*]*Corresponding author*
e-mail: ngtpmai@hcmuaf.edu.vn; phone: +84-287-220-262

(Received 20th Mar 2022; accepted 17th Jul 2022)

Abstract. *Ophiocordyceps* is a megagenus of entomopathogenic fungi belonging to Ophiocordycipitaceae of Hypocreales, Ascomycota. We report here the morphological and phylogenetic analyses of two *Ophiocordyceps* species from Bidoup Nui Ba National Park, Lam Dong Province, southern Vietnam. Our data showed that one of our studied *Ophiocordyceps* is a new intraspecies of *O. sphecocephala* and another is a new record of *O. asiana* from Vietnam.
Keywords: *Bidoup Nui Ba, D1–D2, insect fungi, ITS, species*

Introduction

The genus *Ophiocordyceps* (Hypocreales, Ascomycota) comprises fungal species that exclusively parasitize members of arthropods, kill them and ultimately grow on their cadavers. *Ophiocordyceps sinensis*, growing on moth larvae in the alpine grasslands of Himalayan range and the Tibetan Plateau, is used in traditional oriental medicine to treat kidney diseases, asthma and lung infection (Paterson, 2008). Recent publications have also reported roles of *Ophiocordyceps* species in immunomodulation; cellular apoptosis; anticancer, lung, hepatic and renal support (Paterson, 2008; Zhou et al., 2009; Tuli et al., 2013; Wu et al., 2016). Such properties therefore generate interest in the usage of these fungi as potential sources of bioactive compounds (Shrestha and Sung, 2005; Wang and Yao, 2011; Sasaki et al., 2012; Shrestha et al., 2017; Xiao et al., 2019).

Ophiocordyceps have a worldwide distribution in ecosystem, ranging from sea level up to 5000 m above sea level (Shrestha and Sung, 2005; Li et al., 2011; Araújo et al., 2015; Xiao et al., 2019). The biodiversity of *Ophiocordyceps* is highly endangered due to intensive collection, deforestation and climate change (Hopping et al., 2018; Wei et al., 2021). Hence, study on *Ophiocordyceps* species is essential to provide valuable information for biodiversity monitoring and conservation of these fungi.

Bidoup Nui Ba National Park is located in the northern part of Lam Dong Province, which lies in the Central Highlands of southern Vietnam. In 2005, UNESCO recognized Bidoup Nui Ba as the core zone of Langbiang Biosphere Reserve due to its rich

http://www.aloki.hu ● ISSN 1589 1623 (Print) ● ISSN1785 0037 (Online)
DOI: http://dx.doi.org/10.15666/aeer/2005_39954009

biodiversity. We describe here two species of *Ophiocordyceps* collected in Bidoup Nui Ba National Park, using morphological characteristics and phylogenetic analyses of ribosomal sequences (D1–D2 and ITS).

Materials and methods

Field collection

Specimens of *Ophiocordyceps* species were collected in August 2019 and August 2020 in Bidoup Nui Ba National Park (12°00′00" to 12°52′00" N, 108°17’00" to 108°42′00" E) (*Fig. 1*). The light intensity and relative humidity at the sampling areas were measured using an environmental meter (Extech 45170, Taiwan). All the collected specimens were primarily grouped based on the host insects, one group growing on wasps and the others on bugs. These specimens were either kept in sterile sampling boxes, at 4°C for further analysis or air dried and deposited in the Herbarium of Faculty of Science, Nong Lam University, Ho Chi Minh City, Vietnam (http://sweetgum.nybg.org/, NLU).

Morphological observations

Thirty stromata of each group were observed for morphological measurements. For the microscopic measurements, cross sections of the fertile heads were mounted in sterile distilled water and observed under Olympus CX22 microscope (Olympus, Tokyo, Japan).

DNA extraction and sequencing

DNA was extracted from the specimens using CTAB method (Wu et al., 2001). The D1–D2 region of the 28S rRNA subunit was amplified using NL1/NL4 primer pairs (O'Donnell, 1993). Similarly, the ITS sequence was amplified using ITS1/ITS4 primer pairs (White et al., 1990).

DNA amplification was performed in 35 cycles with a ProFlex PCR System (Thermo Fisher Scientific, MA, USA), each cycle consisting of 3 min at 95°C, 30 sec at 55°C and 2 min at 72°C. High fidelity DNA polymerase (BioFact™ H–Star, Korea) was used for the amplification. The PCR reaction mixture was prepared according to the manufacturer's instruction and the PCR products were kept at 4°C until used further.

The DNA fragments were purified using a PCR purification kit (MEGAquick–spin™ Plus Total Fragment DNA Purification Kit, Intron, MA, USA). The resulted purified fragments were subsequently sequenced using an ABI 3500 genetic analyzer (Thermo Fisher Scientific, MA, USA) with a BigDye® Terminator v3.1 Cycle Sequencing Kit. The sequenced data were deposited in GenBank with accession numbers.

Preliminary species identification was performed using nBLAST against the GenBank nucleotide database (NCBI, Bethesda MD, USA). To evaluate phylogenetic relationships of Vietnamese specimens with closely related *Ophiocordyceps* species (*Table 1*), we conducted multiple sequence alignments using TCoffee (http://tcoffee.crg.cat) with manual corrections using BioEdit (Hall, 1999; Notredame et al., 2000). The alignments were deposited in TreeBASE under accession number ID 28946. Phylogenetic analyses were conducted using RAxML–HPC2 on XSEDE (https://www.phylo.org) (Stamatakis, 2014) with 1000 bootstrap replicates. Default parameters were used under a GTR + G + I model. The tree with the highest likelihood was obtained. The Bayesian inference was performed using MrBayes v.3.2.7a (Ronquist et al., 2012) on XSEDE using default parameters. The outputs were then imported into FigTree v1.4.3 for viewing the phylogenetic trees.

http://www.aloki.hu ● ISSN 1589 1623 (Print) ● ISSN1785 0037 (Online)
DOI: http://dx.doi.org/10.15666/aeer/2005_39954009

Table 1. *List of D1–D2 and ITS sequences used in this phylogenetic analysis. Vietnamese Ophiocordyceps sequences are indicated in bold*

	Accession No.				
Voucher	**D1–D2**	**ITS**	**Country**	***Species***	**Reference**
BCC86880	MW280210	MW285716	Thailand	*O. asiana*	(Khao-ngam et al., 2021)
BCC82789	MW280203	MW285710	Thailand	*O. asiana*	(Khao-ngam et al., 2021)
BCC84229	MW280199	MW285706	Thailand	*O. asiana*	(Khao-ngam et al., 2021)
BCC84230	MW280200	MW285707	Thailand	*O. asiana*	(Khao-ngam et al., 2021)
BCC84234	MW280201	MW285708	Thailand	*O. asiana*	(Khao-ngam et al., 2021)
BCC84235	MW280202	MW285709	Thailand	*O. asiana*	(Khao-ngam et al., 2021)
BCC86436	MW280211	MW285717	Thailand	*O. asiana*	(Khao-ngam et al., 2021)
BCC86440	MW280212	MW285718	Thailand	*O. asiana*	(Khao-ngam et al., 2021)
BCC86875	MW280204	MW285711	Thailand	*O. asiana*	(Khao-ngam et al., 2021)
BCC86876	MW280205	MW285712	Thailand	*O. asiana*	(Khao-ngam et al, 2021)
BCC86878	MW280207	MW285713	Thailand	*O. asiana*	(Khao-ngam et al, 2021)
BCC86879	MW280208	MW285714	Thailand	*O. asiana*	(Khao-ngam et al, 2021)
BCC86880	MW280210	MW285716	Thailand	*O. asiana*	(Khao-ngam et al, 2021)
NLU202011	**MT235757**	**MW684019**	**Vietnam**	***O. asiana***	**This study**
NLU202012	**MT235758**	**MW684020**	**Vietnam**	***O. asiana***	**This study**
NLU202013	**MT235759**	**MZ255516**	**Vietnam**	***O. asiana***	**This study**
NLU202014	**MT235760**	**MW684021**	**Vietnam**	***O. sphecocephala***	**This study**
NLU202015	**MT235761**	**MZ255517**	**Vietnam**	***O. asiana***	**This study**
MY11785	MW280209	MW285715	Thailand	*O. asiana*	(Khao-ngam et al, 2021)
MY11878	MW280213	MW285719	Thailand	*O. asiana*	(Khao-ngam et al, 2021)
MY11884	MW280216	MW285720	Thailand	*O. asiana*	(Khao-ngam et al, 2021)
HUA186097	KC610765		Columbia	*O. australis*	(Sanjuan et al, 2015)
Ophaus1780		KP200888	Columbia	*O. autralis*	(Sanjuan et al, 2015)
MFLU17.1961	NG064484		Thailand	*O. cylindrospora*	GenBank
BCC82256	MH028157		Thailand	*O. granospora*	(Araújo et al, 2020)
BCC82793		MH028141	Thailand	*O. irangiensis*	(Khonsanit et al, 2019)
NBRC101399	JN941425	JN943334	Thailand	*O. irangiensis*	(Sanjuan et al, 2015; Schoch et al, 2012)
NBRC101400	JN941426	JN943335	Thailand	*O. irangiensis*	(Sanjuan et al, 2015; Schoch et al, 2012)
NBRC101401	JN941427	JN943336	Thailand	*O. irangiensis*	(Sanjuan et al, 2015; Schoch et al, 2012)
NHJ10945		GU723767	Thailand	*O. irangiensis*	(Luangsa-Ard et al, 2011)
NHJ3		AJ786566	Thailand	*O. irangiensis*	(Stensrud et al, 2005)
OSC 128579	EF469076		Thailand	*O. irangiensis*	(Sanjuan et al, 2015)
BUO537	MH879600		China	*O. myrmecophila*	(Zihong et al, 2019)
MFLU16.2913	MF372586		Thailand	*O. myrmecophila*	(Xiao et al, 2017)
FMF88		KX197242	Brazil	*O. neonutans*	(Friedrich et al, 2018)
KEL110		KX197240	Brazil	*O. neonutans*	(Friedrich et al, 2018)
KEL113		KX197239	Brazil	*O. neonutans*	(Friedrich et al, 2018)
KEL114		KX197241	Brazil	*O. neonutans*	(Friedrich et al, 2018)
KEL138		KX197243	Brazil	*O. neonutans*	(Friedrich et al, 2018)
03Y3		AB544452	Japan	*O. nutans*	(Sasaki et al, 2012)
06Fuka3		AB544463	Japan	*O. nutans*	(Sasaki et al, 2012)
06Fuka7		AB544467	Japan	*O. nutans*	(Sasaki et al, 2012)

http://www.aloki.hu ● ISSN 1589 1623 (Print) ● ISSN1785 0037 (Online)
DOI: http://dx.doi.org/10.15666/aeer/2005_39954009

Accession No.					
Voucher	**D1–D2**	**ITS**	**Country**	***Species***	**Reference**
06Tank1		AB544473	Japan	*O. nutans*	(Sasaki et al, 2012)
06Tank11		AB544478	Japan	*O. nutans*	(Sasaki et al, 2012)
06Tank21		AB544485	Japan	*O. nutans*	(Sasaki et al, 2012)
06Tank22		AB544486	Japan	*O. nutans*	(Sasaki et al, 2012)
06Yak2		AB544489	Japan	*O. nutans*	(Sasaki et al, 2012)
06Yak3		AB544490	Japan	*O. nutans*	(Sasaki et al, 2012)
06Yaka1		AB544491	Japan	*O. nutans*	(Sasaki et al, 2012)
AUoO113.78		AJ786583	Thailand	*O. nutans*	(Stensrud et al, 2005)
G97035		AJ309367	China	*O. nutans*	(Sasaki et al, 2012)
GDGM20887		JX177484	China	*O. nutans*	GenBank
Iso1		AJ536560	China	*O. nutans*	(Sasaki et al, 2012)
KA12.1247		KR673498	Korea	*O. nutans*	(Kim et al, 2015)
KA12.1340		KR673559	Korea	*O. nutans*	(Kim et al, 2015)
NBRC100944	JN941428		Japan	*O. nutans*	(Ban et al, 2015)
NBRC101749		AB968408	Japan	*O. nutans*	(Sasaki et al, 2012)
Oph994	KJ917567		Columbia	*O. nutans*	(Sanjuan et al, 2015)
OSC110994	DQ518763		n/a	*O. nutans*	(Sanjuan et al, 2015)
T37		AB366634	Japan	*O. nutans*	(Sasaki et al, 2012)
T62		AB366626	Japan	*O. nutans*	(Sasaki et al, 2012)
T70		AB366623	Japan	*O. nutans*	(Sasaki et al, 2012)
MRCIF53		EU573348	Thailand	*O. oxycephala*	(Qu et al, 2018)
Iso6578		AJ536548	China	*O. polyarthra*	(JiaJun et al, 2021)
20877		AJ536550	China	*O. sphecocephala*	(Tian et al, 2010)
MRCIF54		EU573347	Thailand	*O. sphecocephala*	GenBank
NBRC 101416	JN941443		Thailand	*O. sphecocephala*	(Sanjuan et al, 2015)
NBRC 101752	JN941445		Japan	*O. sphecocephala*	(Ban et al, 2015)
NBRC101414	JN941441	JN943443	Thailand	*O. sphecocephala*	(Sanjuan et al, 2015; Schoch et al, 2012)
NBRC101415	JN941442		Thailand	*O. sphecocephala*	(Sanjuan et al, 2015)
NBRC101752	JN941445	JN943351	Japan	*O. sphecocephala*	(Ban et al, 2015; Schoch et al, 2012)
NBRC101753	JN941446	JN943350	Japan	*O. sphecocephala*	(Ban et al., 2015; Schoch et al., 2012)
NHJ4224		GU723778	Thailand	*O. sphecocephala*	(Luangsa-Ard et al., 2011)
OSC 110998	DQ518765		Thailand	*O. sphecocephala*	(Sanjuan et al., 2015)
BCC79226	MW280219	MW285723	Thailand	*O. tessaratomidarum*	(Khao-ngam et al., 2021)
MY10827	MW280217	MW285721	Thailand	*O. tessaratomidarum*	(Khao-ngam et al., 2021)
MY10830	MW280218	MW285722	Thailand	*O. tessaratomidarum*	(Khao-ngam et al., 2021)
MFLU16.2908	MF362990		Thailand	*O. thanathonensis*	(Xiao et al., 2017)
NBRC106968	AB968423		Japan	*O. tricentri*	(Ban et al., 2015)
BCC49498		KF016996	Outgroup	*Aschersonia narathiwatensis*	GenBank
JM0807	HM135162		Outgroup	*Cordyceps militaris*	(Zhong et al., 2010)
BCC55524		KF016995	Outgroup	*Hypocrella sianmensis*	GenBank

http://www.aloki.hu ● ISSN 1589 1623 (Print) ● ISSN1785 0037 (Online)
DOI: http://dx.doi.org/10.15666/aeer/2005_39954009

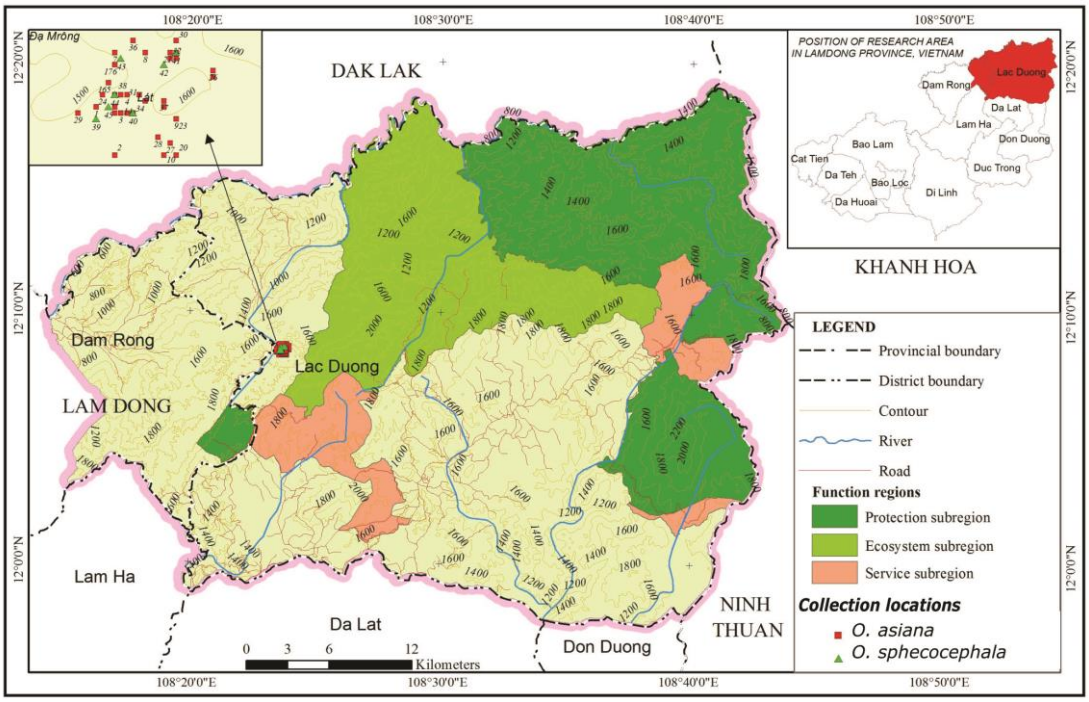

Figure 1. *Collection locations of O. sphecocephala and O. asiana in Bidoup Nui Ba National Park, Lam Dong, Vietnam*

Molecular analyses used the dataset of 101 taxa (including 10 new sequenced data) (*Table 1*). Analysis using the D1–D2 sequences included 45 taxa with a total length of 2200 characters in the final dataset, while the analysis using the ITS sequences included 66 taxa with a total length of 920 characters in the final dataset.

Results and discussion

The analyses of Ophiocordyceps sphecocephala

Ophiocordyceps sphecocephala (Klotzsch ex Berk.) G.H. Sung, J.M. Sung, Hywel-Jones & Spatafora, Stud. Mycol. 2007: 5-59.

MycoBank MB504343.

Taxonomy (*Fig. 2, Table 2*)

The specimens from Vietnam shared the morphological characteristics with the described morphology of *O. sphecocephala* (Sung et al, 2007).

Diagnosis. Stromata solitary or two, thin, creamy yellow, 72–106 mm long, arising from the region between the head and thorax of the host insect. Stipe stout, 0.7–1.0 mm in diam. Fertile head soft when fresh, 10–13 × 1.5–2.0 mm. Perithecia long, oblique in position, thick-walled and immersed in the fertile head, 610–730 × 130–220 µm. Ascospores thread–like and fragmented, 120–260 × 4–6 µm. Part spores fusoid, 7.5-8.5 × 1.5–2.0 µm.

http://www.aloki.hu ● ISSN 1589 1623 (Print) ● ISSN1785 0037 (Online)
DOI: http://dx.doi.org/10.15666/aeer/2005_39954009

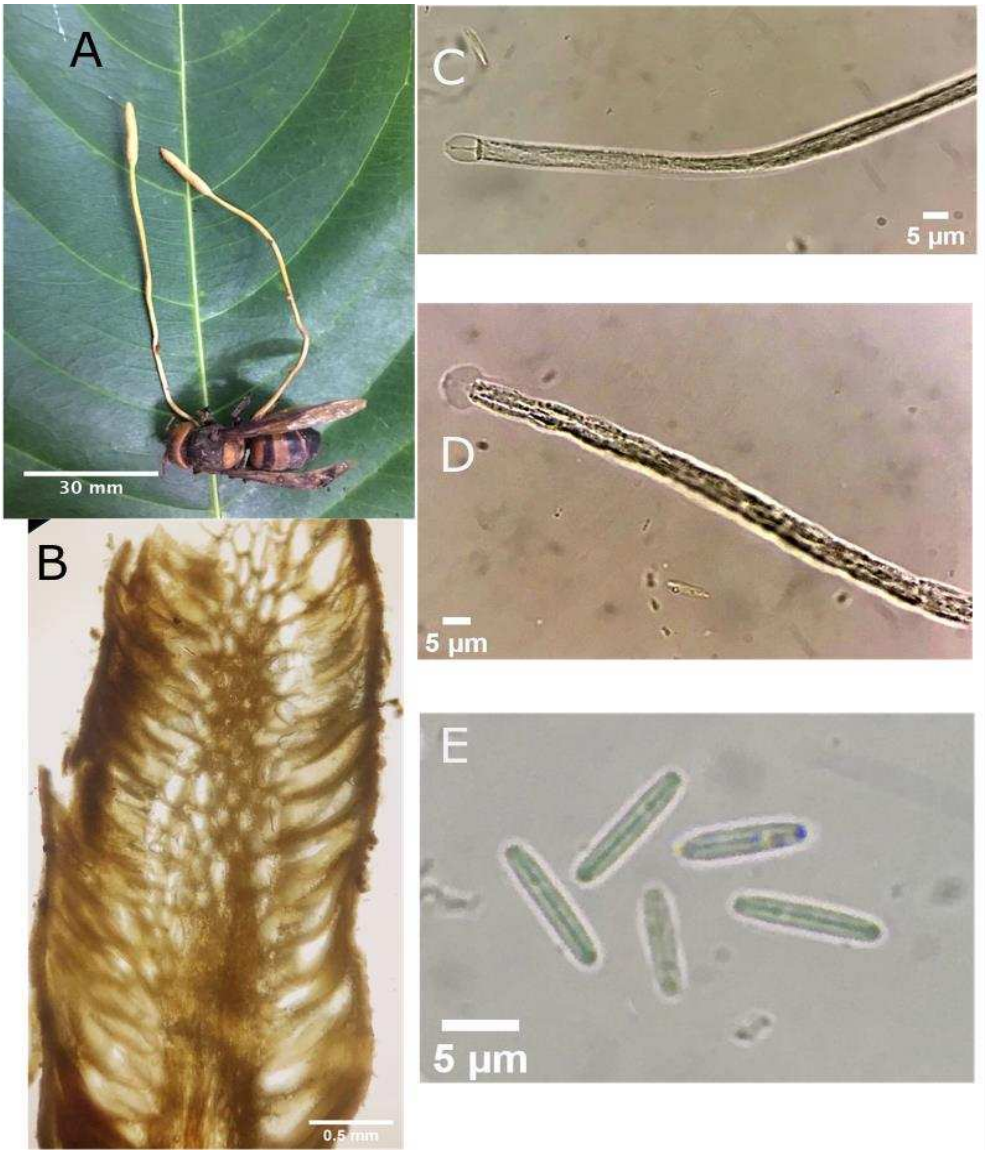

Figure 2. *O. sphecocephala on German wasp (Vespula germanica, Vespidae). A. Stromata and host insect, B. Perithecia, C. immature ascus, D. mature ascus with part spores. E. part spores*

Host insect. The specimens of *O. sphecocephala* were only found on German wasps (*Vespula germanica,* Vespidae). Similar host insect family is reported in Thai *O. sphecocephala* (Hywel-Jones, 1995a).

Locality. Bidoup Nui Ba National Park, Lam Dong province, Vietnam (12°00′00" to 12°52′00" N, 108°17’00" to 108°42′00" E), between 1200 m to 1600 m attitude above sea level, specimens arising from thick layer of decaying leaves on the floor of mixed forest, near the streams at the relative humidity of 62%–68% and less than 200 lx of scattering light.

Remarks. Even though Vietnamese *Ophiocordyceps sphecocephala* shared many characteristics with previous description of *O. sphecocephala*, we observed that Vietnamese *O. sphecocephala* has longer stromata and fertile head while the asci and partspores were smaller (*Table 2*).

http://www.aloki.hu ● ISSN 1589 1623 (Print) ● ISSN1785 0037 (Online)
DOI: http://dx.doi.org/10.15666/aeer/2005_39954009

Table 2. *Morphological characteristics of the collected Ophiocordyceps and the references from Thailand, Japan and Brazil*

Specimen	Host/Voucher	Stroma (mm)	Fertile head (mm)	Peritheticum (mm)	Asci (µm)	Part spore (µm)
O. sphecocephala **(This study)**	On *Vespula germanica,* Vespidae (NLU202014)	72–106 × 0.7–1	10–13×1.5–2.0	610–730 × 130–220	120–260 × 4–6	7.5–8.5 × 1.5–2
O. sphecocephala Thailand (Hywel-Jones, 1995a)		to 45 × 0.15–0.8	2.2–11 × 1.2–1.9	880–1000 × 200–260	700– up × to 7	10–14 × 1.5–2.5
	on *Halyomorpha halys* Pentantomidae (NLU202011)					
	on *Acanthosoma labiduroides* Acanthosomatidae (NLU202012)					
	on *Clavigralla scutellaris* Coreidae (NLU202013)					
	on *Proxys punctulatus* Pentatomidae (NLU202015)					
O. asiana Thailand (Khao-ngam et al, 2021)		30–130 × 1–2	5–20 × 2–3	750–1200 × 200–300	200–600 × 5–6	6–14 × 1.5–2
O. nutans Japan (Type I) (Sasaki et al, 2008)		n/a	n/a	950–970 x 250–260	n/a	n/a
O. nutans Japan (Type II) (Sasaki et al, 2008)		32–112	2.5–14 × 1.5–3.7	610–1170 ×190–560	200–285 × 5–9	3.5–20 × 1–2
O. nutans Thailand (Hywel-Jones, 1995b)		50–90 × 0.4–0.8	6–17 × 3–5	550–800 × 130–300	780 × 7–8	9.3–15 × 1.5–2
O. neonutans Brazil (Friedrich et al, 2018)		23–170 × 1–2	6–19 × 0.9–2.0	550–1200 × 130–360	220–900 × 3–8	6–15 × 1.2–3

http://www.aloki.hu ● ISSN 1589 1623 (Print) ● ISSN1785 0037 (Online)
DOI: http://dx.doi.org/10.15666/aeer/2005_39954009

The BLAST analysis using the D1–D2 sequence of *O. sphecocephala* from Vietnam showed 96.87% identity with *O. sphecocephala* sequence (NBRC 101414) and 96.48% with *O. irangiensis* sequence (NBRC 101399). The phylogenetic analysis using the D1-D2 dataset showed that Vietnamese *O. sphecocephala* formed a monophyletic cluster with high support (95% RAxML, BPP 1.00 and 0.02 pairwise distance) to the group of *O. sphecocephala* (NBRC 101414) and *O. irangiensis* (NBRC101399) from Thailand (*Fig. 3*). It is known that D1–D2 sequences are slowly evolved and the nucleotide substitution values within a species is not higher than 0.01, whereas greater value of nucleotide substitution is recorded in separate biological species (Kurtzman and Robnett, 1997; Raja et al., 2017). In the analysis using the ITS dataset, *O. sphecocephala* again showed its closest relationship to Thai *O. sphecocephala* (NBRC 101414) and *O. irangiensis* (NBRC101399). Even though the support was moderate (79% RAxML, BPP 0.82), the pairwise distances between Vietnamese *O. sphecocephala* and Thai *O. sphecocephala* (NBRC 101414) was 0.09 and the pairwise distance to *O. irangiensis* (NBRC101399) was 0.06 (*Fig. 4*). Chen et al (2004) reported that the ITS sequence distance within a species should be from 0.00 to 0.05. Our results using ITS sequences therefore indicated a genetic variable between Vietnamese *O. sphecocephala* and Thai *O. sphecocephala* (NBRC101414).

It has been known that *O. irangiensis* infects only ants while *O. sphecocephala* grows on wasps only (Hywel-Jones, 1995a; 1996; Araújo et al., 2020). All specimens of *O. sphecocephala* were found on wasps only. Mains (1958) pointed out the presence of longitudinal hyphae at the core of the fertile head as a key character to distinguish *O. sphecocephala* from similar species. Similar descriptions on *O. sphecocephala* were also reported later (Hywel-Jones, 1995a; Sung et al., 2007). Here, we observed the presence of this diagnostic character in Vietnamese *O. sphecocephala* specimens (*Fig. 2*).

So far, data on *O. sphecocephala* were either reported as genetic data or morphological data (Hywel-Jones, 1995a; Sung et al., 2007). There is no morphological description for *O. sphecocephala* (NBRC101414) and many other reported *O. sphecocephala*. Only morphological data of *O. sphecocephala* specimens collected in Thailand is available (Hywel-Jones, 1995a) (*Table 2*), however these specimens are not analyzed phylogenetically. In comparison to the data by Hywel-Jones (1995a), Vietnamese *O. sphecocephala* had longer stromata and fertile heads, while the length of the asci and part spores were smaller (*Table 2*). Our study therefore the first report providing both morphological and genetic data on *O. sphecocephala*.

Our phylogenetic and morphological data consistently showed the differences of Vietnamese *O. sphecocephala* and other reported *O. sphecocephala*. We therefore propose Vietnamese *O. sphecocephala* as a new intraspecies of *O. sphecocephala*.

The analyses of Ophiocordyceps asiana

Ophiocordyceps asiana Mongkolsamrit, Khao-ngam, Himaman, Rungjindamai & Luangsa-Ard, 2021: 341-353.

Mycobank MB838742.

Taxonomy (*Table 2, Fig. 5*)

The specimens of *O. asiana* from Vietnam shared morphological characteristics with recently described characteristics of *O. asiana* from Thailand (Khao-ngam et al., 2021).

Diagnosis. Stromata solitary or up to four, cylindrical, 72–189 mm long, arising from the thorax of adult bugs. Stipe stout, black and wiry, 0.5 to 1.0 mm in diam. Fertile head

http://www.aloki.hu ● ISSN 1589 1623 (Print) ● ISSN1785 0037 (Online)
DOI: http://dx.doi.org/10.15666/aeer/2005_39954009

cylindrical, yellow to reddish orange and soft when fresh, 4.5–31.5 × 0.5–2.5 mm. Perithecia elongated pyriform, thick-walled and immersed in the fertile head, 140-810 × 4–7 µm. Ascospores are thread–like and fragmented. Partspores 7.5-14 × 1.5-3 µm, cylindrical with truncate ends.

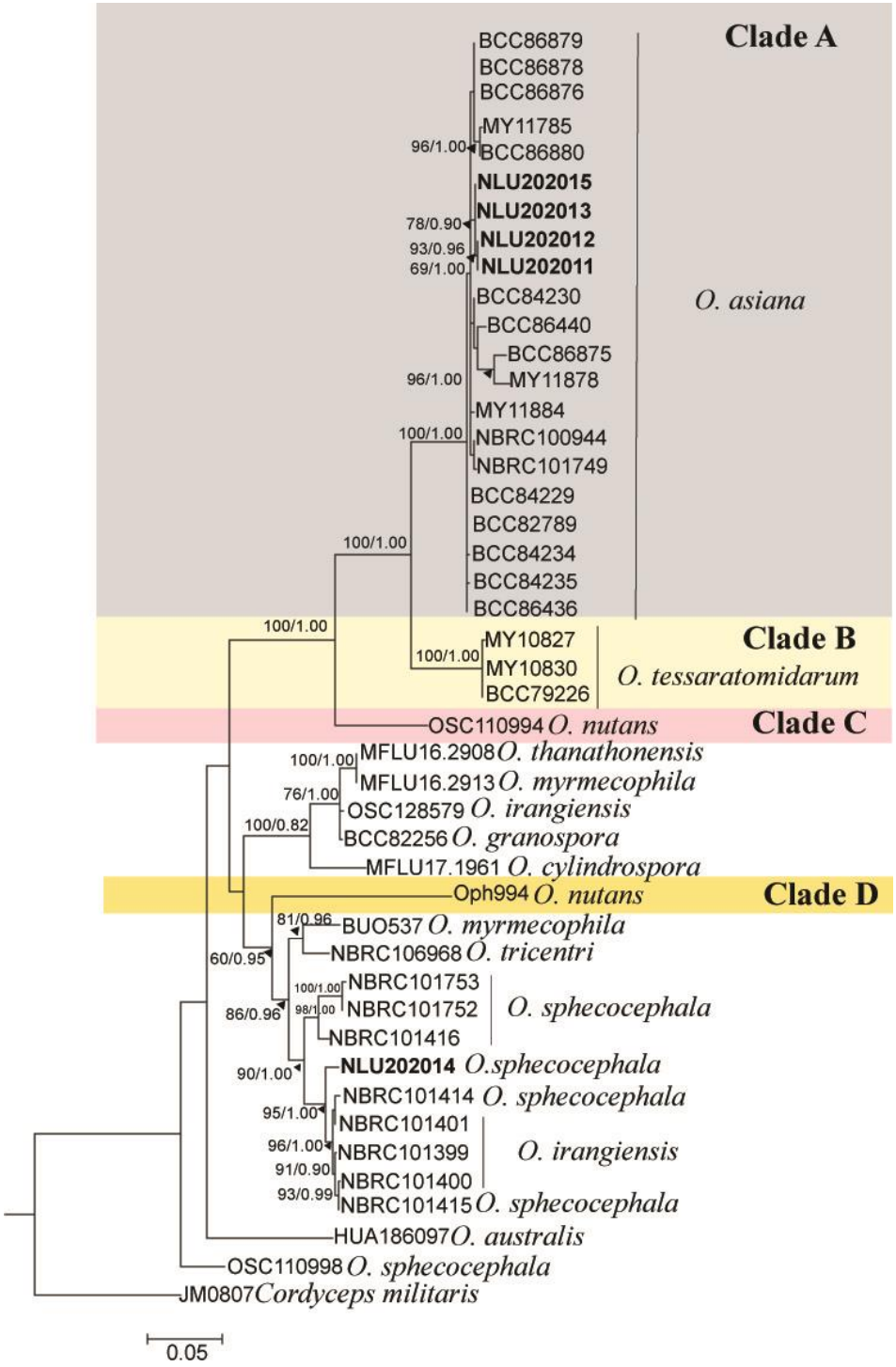

Figure 3. *Phylogenetic tree of the studied O. sphecocephala and O. asiana and the related taxa generated from RAxML analysis using D1–D2 sequences. The RAxML and Bayesian posterior probability values were indicated above the nodes as RAxML/BPP. Vietnamese Ophiocordyceps sequences are indicated in bold*

http://www.aloki.hu ● ISSN 1589 1623 (Print) ● ISSN1785 0037 (Online)
DOI: http://dx.doi.org/10.15666/aeer/2005_39954009

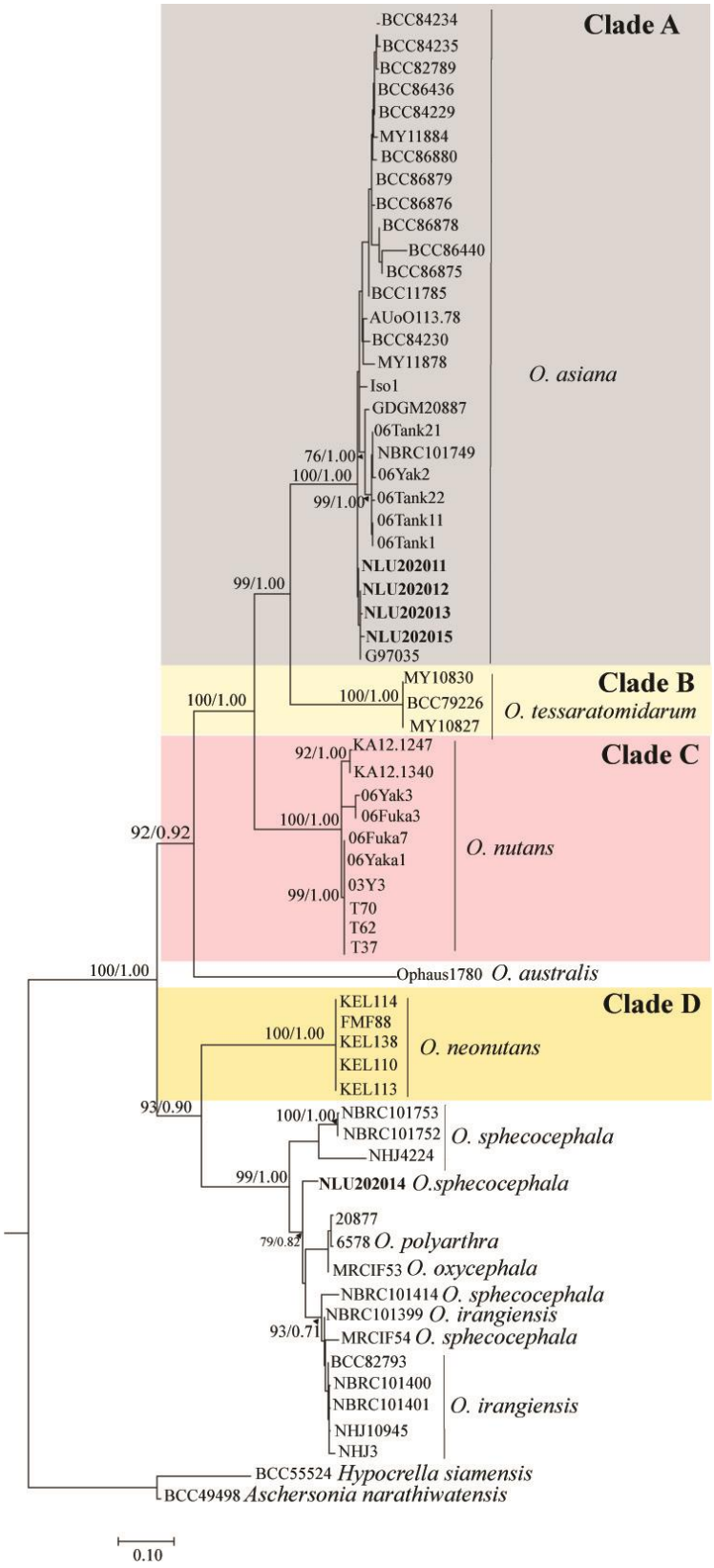

Figure 4. *Phylogenetic tree of the studied O. sphecocephala, O. asiana and the related taxa generated from RAxML analysis using ITS sequences. The RAxML and Bayesian posterior probability values were indicated above the nodes as RAxML/BPP. Vietnamese Ophiocordyceps sequences are indicated in bold*

http://www.aloki.hu ● ISSN 1589 1623 (Print) ● ISSN1785 0037 (Online)
DOI: http://dx.doi.org/10.15666/aeer/2005_39954009

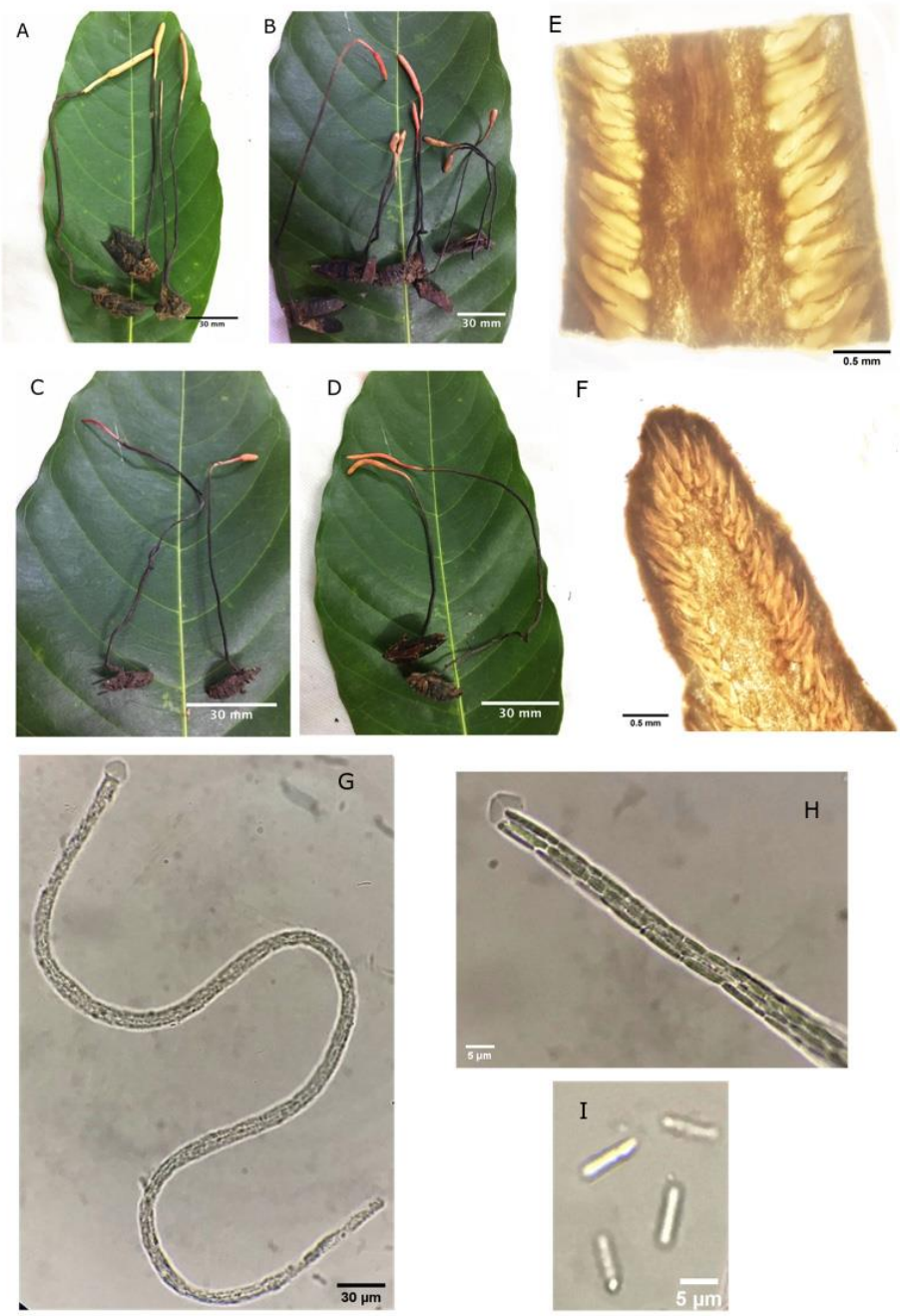

Figure 5. *A–D. Stromata of O. asiana on Halyomorpha halys (Pentatomidae), Acanthosoma labiduroides (Acanthosomatidae), Clavigralla scutellaris (Coreidae), Proxys punctulatus (Pentatomidae), respectively. E, F. Perithecia, G. immature ascus, H. mature ascus with partspores, I. Part spores*

Host insects. The collected specimens were found on a broad range of host insect families. They infected black stinkbug (*Proxys punctulatus,* Pentatomidae), brown marmorated stinkbug (*Halyomorpha halys*, Pentatomidae), scissors turtle bug (*Acanthosoma labiduroides,* Acanthosomatidae) and legume bug (*Clavigralla scutellaris*, Coreidae). Similar results are also reported in *O. asiana* from Thai Lan (Khao-ngam et

http://www.aloki.hu ● ISSN 1589 1623 (Print) ● ISSN1785 0037 (Online)
DOI: http://dx.doi.org/10.15666/aeer/2005_39954009

al., 2021) and *O. nutans* from Japan (Sasaki et al., 2012) while *O. neonutans* is only found in Pentatomidae (Friedrich et al., 2018).

Locality. Bidoup Nui Ba National Park, Lam Dong province, Vietnam (12°00′00" to 12°52′00" N, 108°17’00" to 108°42′00" E) from 1200 m to 1600 m above sea level, near the stream in mixed forest, specimens arising from thick layers of decaying leaves on the forest floor under 62%–68% relative humidity and less than 200 lx of scattering light.

Remarks. Although the specimens from Vietnam of *O. asiana* shared many characteristics with *O. asiana* and *O. nutans* reported from Thailand, Japan and *O. neonutans* reported from Brazil, we observed that the stroma and the fertile head of Vietnamse specimens are longer than those of Thailand, Japan and Brazil (*Table 2*), while the perithecia, asci and partspores are shorter (*Table 2*).

We recorded a broad variation in the morphology of *Ophiocordyceps asiana* infecting different bug species. For example, longer stromata, fertile heads, perithecia and part spores were observed in the specimens infecting *Halyomorpha halys* (Pentatomidae) and *Acanthosoma labiduroides* (Acanthosomatidae) (*Table 2*). Besides, the differences in the stroma color, the sizes of the stromata, fertile head and perithecia were also recorded (*Table 2*).

Four groups of *Ophiocordyceps asiana* from Vietnam had identical D1–D2 and ITS sequences regardless of having different families of host insects (Acanthosomatidae, Coreidae and Pentatomidae).

The nucleotide BLAST analyses using D1–D2 sequences of Vietnamese *O. asiana* specimens revealed more than 99.3% of homology with the sequences of *O. nutans* from Japan (NBRC 101749), Thailand (NBRC 100944) and *O. asiana* from Thailand. The phylogenetic analysis using the D1–D2 sequences showed that Vietnamese *O. asiana* sequences formed a monophyletic group with high support (100% RAxML, BPP 1.00) to the group of *O. asiana* in Clade A reported by Khao-ngam et al. (2021) (*Fig. 2*). This clade includes Thai *O. asiana* (Khao-ngam et al., 2021) and Japanese *O. nutans* type I (Sasaki et al., 2012). In our analysis, the pairwise distance between Vietnamese *O. asiana* and others in clade A was lower than 0.01 (*Fig. 3*).

It is known that D1–D2 sequences are slowly evolved and the nucleotide substitution values of intraspecies is not higher than 0.01, whereas greater value of nucleotide substitution is recorded in separate biological species (Kurtzman and Robnett, 1997; Raja et al., 2017). The results therefore indicated that *O. asiana* from Vietnam belonged to the Clade A of *O. asiana* of Khao-ngam et al. (2021) and *O. nutans* Type I of Sasaki et al. (2012). Since D1–D2 regions are more conserved than ITS regions, we analyzed *O. asiana* at the ITS region to further investigate if there is any genetic variation between Vietnamese *O. asiana* and other *O. asiana* in clade A. Consistent to the analysis results using D1–D2 sequences, the analysis using ITS sequences also showed that Vietnamese *O. asiana* was in Clade A with high support (100% RAxML, BPP 1.00) and low pairwise distance (0.01) (*Fig. 4*). It is therefore confirmed the genetic similarity between Vietnamese *O. asiana*, Thai *O. asiana* and O. *nutans* Type I from Japan.

However, we still noticed that Vietnamese *O. asiana* had longer stroma and fertile heads but shorter perithecia, asci and partspores than those of *O. asiana* from Thailand, of *O. nutans* from Japan and also of *O. neonutans* from Brazil (*Table 2*).

Sasaki et al. (2012) had found that the ITS sequences of *O. nutans* infecting different species of Acanthosomatidae and Pentatomidae are similar. However, the ITS sequences of *O. nutans* infecting Coreidae are different from those on other insect families (Sasaki et al., 2012). Differently, Vietnamese *O. asiana* possessed identical D1–D2 and ITS

http://www.aloki.hu ● ISSN 1589 1623 (Print) ● ISSN1785 0037 (Online)
DOI: http://dx.doi.org/10.15666/aeer/2005_39954009

sequences in all the recorded bug families: Ancanthosomatide, Pentatomidae and also in Coreidae (*Figs. 3,4*).

In the study of *O. nutans* collected in Japan, Sasaki et al. (2008) did not record any significant differences in the morphology of *O. nutans* among the host insect species. In contrast, we noticed a strong impact of the host insect on the morphological diversity of Vietnamese *O. asiana*, which could be observed in the size of the stroma, fertile heads, asci and part spores (*Table 2, Fig. 5*).

Conclusions

The collected specimens of *Ophiocordyceps* on wasps were an intraspecies of *O. sphecocephala* and the specimens on bugs were *O. asiana*.

O. asiana could infect a wide range of host insects and the influence of the host insects on *O. asiana* morphology was also observed, while the host of *O. sphecocephala* was more specific and found only on wasps (Vespidae).

Acknowledgment. The authors acknowledge the financial support from the Ministry of Education and Training, Vietnam (B2020-NLS-01).

Conflict of interests. The authors declare that there is no conflict of interests.

REFERENCES

[1] Araújo, J. P. M., Evans, H. C., Geiser, D. M., Mackay, W. P., Hughes, D. P. (2015): Unravelling the diversity behind the *Ophiocordyceps unilateralis* (Ophiocordycipitaceae) complex: Three new species of zombie-ant fungi from the Brazilian Amazon. – Phytotaxa 220(3): 224-238.

[2] Araújo, J. P. M., Evans, H. C., Fernandes, I. O., Ishler, M. J., Hughes, D. P. (2020): Zombie-ant fungi cross continents: II. Myrmecophilous hymenostilboid species and a novel zombie lineage. – Mycologia 112(6): 1138-1170.

[3] Ban, S., Sakane, T., Nakagiri, A. (2015): Three new species of *Ophiocordyceps* and overview of anamorph types in the genus and the family Ophiocordyceptaceae. – Mycological Progress 14(1): 1017-1030.

[4] Chen, Y. Q., Hu, B., Xu, F., Zhang, W., Zhou, H., Qu, L. H. (2004): Genetic variation of *Cordyceps sinensis*, a fruit-body-producing entomopathogenic species from different geographical regions in China. – FEMS Microbiology Letters 230(1): 153-158.

[5] Friedrich, R. C. S., Shrestha, B., Salvador-Montoya, C. A., Tome, L. M. R., Reck, M., Gues-Neto, A., Drechsler-Santos, E. R. (2018): *Ophiocordyceps neonutans* sp. nov., a new neotropical species from *O. nutans* complex (Ophiocordycipitaceae, Ascomycota). – Phytotaxa 344(3): 215-227.

[6] Hall, T. A. (1999): BioEdit: a user-friendly biological sequence alignment editor and analysis program for Windows 95/98/NT. – Nucleic Acids Symposium Series. London: Information Retrieval Ltd., c1979-c2000; pp. 95-98.

[7] Hopping, K. A., Chignell, S. M., Lambin, E. F. (2018): The demise of caterpillar fungus in the Himalayan region due to climate change and overharvesting. – PNAS 115(45): 11489-11494.

[8] Hywel-Jones, N. (1995a): *Cordyceps sphecocephala* and a *Hymenostilbe* sp. infecting wasps and bees in Thailand. – Mycological Research 99(2): 154-158.

[9] Hywel-Jones, N. (1995b): Notes on *Cordyceps nutans* and its anamorph, a pathogen of hemipteran bugs in Thailand. – Mycological Research 99(6): 724-726.

http://www.aloki.hu ● ISSN 1589 1623 (Print) ● ISSN1785 0037 (Online)
DOI: http://dx.doi.org/10.15666/aeer/2005_39954009

[10] Hywel-Jones, N. (1996): *Cordyceps myrmecophila*-like fungi infecting ants in the leaf litter of tropical forest in Thailand. – Mycological Research 100(5): 613-619.
[11] JiaJun, H., Dan, D., Gui-Ping, Z., Di-Zhe, G., Yong-Lan, T., Gu, R., Zheng-Xiang, Q., Zheng-Hao, Z., Yu, L., Bo, Z. (2021): Morphology and molecular study of three new Cordycipitoid fungi and its related species collected from Jilin Province, Northeast China. – MycoKeys 83: 161-180.
[12] Khao-ngam, S., Mongkolsamrit, S., Rungjindamai, N., Noisripoom, W., Pooissarakul, W., Duangthisan, J., Himaman, W., Luangsa-Ard, J. J. (2021): *Ophiocordyceps asiana* and *Ophiocordyceps tessaratomidarum* (Ophiocordycipitaceae, Hypocreales), two new species on stink bugs from Thailand. – Mycological Progress 20(3): 341-353.
[13] Khonsanit, A., Luangsa-Ard, J. J., Thanakitpipattana, D., Kobmoo, N., Piasai, O. (2019): Cryptic species within *Ophiocordyceps myrmecophila* complex on formicine ants from Thailand. – Mycological Progress 18(1): 147-161.
[14] Kim, C. S., Jo, J. W., Kwag, Y.-N., Sung, G.-H., Lee, S.-G., Kim, S.-Y., Shin, C.-H., Han, S.-K. (2015): Mushroom flora of ulleung-gun and a newly recorded *Bovista* species in the Republic of Korea. – Mycobiology 43(3): 239-257.
[15] Kurtzman, C. P., Robnett, C. J. (1997): Identification of clinically important ascomycetous yeasts based on nucleotide divergence in the 5' end of the large-subunit (26S) ribosomal DNA gene. – Journal of Clinical Microbiology 35(5): 1216-1223.
[16] Li, Y., Wang, X. L., Jiao, L., Jiang, Y., Li, H., Jiang, S. P., Lhosumtseiring, N., Fu, S. Z., Dong, C. H., Zhan, Y., Yao, Y. J. (2011): A survey of the geographic distribution of *Ophiocordyceps sinensis*. – Journal of Microbiology 49(6): 913-996.
[17] Luangsa-Ard, J. J., Ridkaew, R., Tasanathai, K., Thanakitpipattana, D., Hywel-Jones, N. (2011): *Ophiocordyceps halabalaensis*: a new species of *Ophiocordyceps* pathogenic to *Camponotus gigas* in Hala Bala Wildlife Sanctuary, Southern Thailand. – Fungal Biology 115(7): 608-614.
[18] Mains, E. B. (1958): North American entomogenous species of *Cordyceps*. – Mycologia 50(2): 169-222.
[19] Notredame, C., Higgins, D. G., Heringa, J. (2000): T-Coffee: A novel method for fast and accurate multiple sequence alignment. – Journal of Molecular Biology 302(1): 205-217.
[20] O'Donnell, K. (1993): Fusarium and its near relatives. – In: Reynolds, D. R., Taylor, J. W. (eds.) The fungal holomorph: miotic, meiotic and pleomorphic speciation in fungal systematics. Wallingford: CAB International, pp, 225-233.
[21] Paterson, R. R. M. (2008): *Cordyceps*–A traditional Chinese medicine and another fungal therapeutic biofactory? – Phytochemistry 69(7): 1469-1495.
[22] Qu, J. J., Yu, L. A. N., Zhang, J., Han, Y., Xiao, Z. (2018): A new entomopathogenic fungus, *Ophiocordyceps ponerus* sp. nov., from China. – Phytotaxa 343(2): 116-126.
[23] Raja, H. A., Miller, A. N., Pearce, C. J., Oberlies, N. H. (2017): Fungal identification using molecular tools: A primer for the natural products research community. – Journal of Natural Products 80(3): 756-770.
[24] Ronquist, F., Teslenko, M., van der Mark, P., Ayres, D. L., Darling, A., Höhna, S., Larget, B., Liu, L., Suchard, M. A., Huelsenbeck, J. P. (2012): MrBayes 3.2: efficient Bayesian phylogenetic inference and model choice across a large model space. – Systematic Biology 61(3): 539-542.
[25] Sanjuan, T. I., Franco-Molano, A. E., Kepler, R. M., Spatafora, J. W., Tabima, J., Vasco-Palacios, A. M., Restrepo, S. (2015): Five new species of entomopathogenic fungi from the Amazon and evolution of neotropical *Ophiocordyceps*. – Fungal Biology 119(10): 901-916.
[26] Sasaki, F., Miyamoto, T., Yamamoto, A., Tamai, Y., Yajima, T. (2008): Morphological and genetic characteristics of the entomopathogenic fungus *Ophiocordyceps nutans* and its host insects. – Mycological Research 112(10): 1241-1244.
[27] Sasaki, F., Miyamoto, T., Yamamoto, A., Tamai, Y., Yajima, T. (2012): Relationship between intraspecific variations and host insects of *Ophiocordyceps nutans* collected in Japan. – Mycoscience 53(2): 85-91.

http://www.aloki.hu ● ISSN 1589 1623 (Print) ● ISSN1785 0037 (Online)
DOI: http://dx.doi.org/10.15666/aeer/2005_39954009

[28] Schoch, C. L., Seifert, K. A., Huhndorf, S., Robert, V., Spouge, J. L., Levesque, C. A., Chen, W. (2012): Nuclear ribosomal internal transcribed spacer (ITS) region as a universal DNA barcode marker for fungi. – PNAS 109(16): 6241-6246.
[29] Shrestha, B., Sung, J. M. (2005): Notes on *Cordyceps* species collected from the central region of Nepal. – Mycobiology 33(4): 235-239.
[30] Shrestha, B., Tanaka, E., Hyun, M., Han, J., Kim, C., Jo, J., Han, S., Sung, J., Sung, G. H. (2017): Mycosphere Essay 19. *Cordyceps* species parasitizing hymenopteran and hemipteran insects. – Mycosphere, Journal of Fungal Biology 8(9): 1424-1442.
[31] Stamatakis, A. (2014): RAxML version 8: a tool for phylogenetic analysis and post-analysis of large phylogenies. – Bioinformatics 30(9): 1312-1313.
[32] Stensrud, Ø., Hywel-Jones, N. L., Schumacher, T. (2005): Towards a phylogenetic classification of Cordyceps: ITS nrDNA sequence data confirm divergent lineages and paraphyly. – Mycological Research 109(1): 41-56.
[33] Sung, G. H., Hywel-Jones, N. L., Sung, J. M., Luangsa-Ard, J. J., Shrestha, B., Spatafora, J. W. (2007): Phylogenetic classification of Cordyceps and the clavicipitaceous fungi. – Studies in mycology 57(1): 5-59.
[34] Tian, L.-H., Hu, B., Zhou, H., Zhang, W.-M., Qu, L.-H., Chen, Y.-Q. (2010): Molecular phylogeny of the entomopathogenic fungi of the genus *Cordyceps* (Ascomycota: Clavicipitaceae) and its evolutionary implications. – Journal of Systematics and Evolution 48(6): 435-444.
[35] Tuli, H. S., Sharma, A. K., Sandhu, S. S., Kashyap, D. (2013): Cordycepin: a bioactive metabolite with therapeutic potential. – Life Sciences 93(23): 863-869.
[36] Wang, X. L., Yao, Y. J. (2011): Host insect species of *Ophiocordyceps sinensis*: A review. – ZooKeys 127: 43-59.
[37] Wei, Y., Zhang, L., Wang, J., Wang, W., Niyati, N., Guo, Y., Wang, X. (2021): Chinese caterpillar fungus (Ophiocordyceps sinensis) in China: Current distribution, trading, and futures under climate change and overexploitation. – The Science of the total environment 755(Pt 1): 142548-142548.
[38] White, T., Bruns, T., Lee, S., Taylor, J., Innis, M., Gelfand, D., Sninsky, J. (1990): Amplification and Direct Sequencing of Fungal Ribosomal RNA Genes for Phylogenetics. – PCR Protocols: a guide to methods and applications 31. New York: Academic Press. Inc,. pp. 315-322.
[39] Wu, Z. H., Wang, T. H. D., Huang, W., Qu, Y. B. (2001): A simplified method for chromosome DNA preparation from filamentous fungi. – Mycosystema 20(1): 575-577.
[40] Wu, D. T., Lv, G. P., Zheng, J., Li, Q., Ma, S. C., Li, S. P., Zhao, J. (2016): *Cordyceps* collected from Bhutan, an appropriate alternative of *Cordyceps sinensis*. – Scientific Reports 6(1): 376681.
[41] Xiao, Y. P., Wen, T. C., Hongsanan, S., Sun, J., Hyde, K. (2017): Introducing *Ophiocordyceps thanathonensis*, a new species of entomogenous fungi on ants, and a reference specimen for *O. pseudolloydii*. – Phytotaxa 328(2): 115-126.
[42] Xiao, Y. P., Hongsanan, S., Hyde, K. D., Brooks, S., Xie, N., Long, F. Y., Wen, T. C. (2019): Two new entomopathogenic species of *Ophiocordyceps* in Thailand. – MycoKeys 47(1): 53-74.
[43] Zhong, X., Peng, Q., Qi, L., Lei, W., Liu, X. (2010): rDNA-targeted PCR primers and FISH probe in the detection of *Ophiocordyceps sinensis* hyphae and conidia. – Journal of Microbiological Methods 83(2): 188-193.
[44] Zhou, X., Gong, Z., Su, Y., Lin, J., Tang, K. (2009): *Cordyceps* fungi: natural products, pharmacological functions and developmental products. – Journal of Pharmacy and Pharmacology 61(3): 279-291.
[45] Zihong, C., Yuanbing, W., Yongdong, D., Kai, C., Ling, X., Qingcheng, H. (2019): Species diversity and seasonal fluctuation of entomogenous fungi of Ascomycota in Taibaoshan Forest Park in western Yunnan. – Biodiversity Science 27(9): 993-1001.

http://www.aloki.hu ● ISSN 1589 1623 (Print) ● ISSN1785 0037 (Online)
DOI: http://dx.doi.org/10.15666/aeer/2005_39954009

HEAVY METALS DISTRIBUTION AND FRACTIONATION IN MANGROVE SEDIMENTS LINKED TO ORGANIC DEPOSITS VIS-À-VIS ACCUMULATION IN *RHIZOPHORA* SPP. AT TANJUNG PIAI, JOHOR, MALAYSIA

HALIM, N. H. A.[1] – ABDULLAH, R.[2,3*] – KADIR, W. R.[1] – AJENG, A. A.[2] – ZAWAWI, N. Z. B.[2]

[1]*Soil Management Branch, Forest Research Institute Malaysia, Kepong 52109, Selangor Darul Ehsan, Malaysia*

[2]*Institute of Biological Sciences, Faculty of Science, Universiti Malaya, 50603 Kuala Lumpur, Malaysia*

[3]*Centre for Research in Biotechnology for Agriculture (CEBAR), Institute of Biological Sciences, Faculty of Science, Universiti Malaya, 50603 Kuala Lumpur, Malaysia*

**Corresponding author*
e-mail: rosazlin@um.edu.my; phone: +60-37-967-4360

(Received 21st Mar 2022; accepted 11th Jul 2022)

Abstract. Mangrove ecosystems are crucial for ecological processes. However, mangrove forests are currently under peril due to urbanization, aquaculture expansion, and growing pollutant burdens. Marine debris including organic deposits (ODs) is intentionally or unintentionally deposited into the marine environment, which could alter the natural ecology of the ecosystem. ODs from Tanjung Piai, Johor, Malaysia have high concentration of heavy metals (HMs), specially Cd and PB, with respective concentration of 2.45 mg kg^{-}and 82.41 mg kg^{-1}, which surpassed the compost guidelines of the European and United Kingdom. Four sampling sites were established in Tanjung Piai based on ODs levels: T1: without ODs, T2: new ODs, T3 and T4: decomposed ODs 90 m and 150 m from shoreline, respectively. T3 and T4 had the highest Cu and Pb. Modified sequential extraction European Community Bureau of Reference (BCR) reveals that Fe and Mn are highly mobile for mangrove species uptake, with concentrations of these HMs in *Rhizophora* spp. leaves higher than Cd, Pb, and Zn, implying that these species did not meet the criteria for hyperaccumulators due to low metals accumulation, necessitating further research to identify species suited for phytoextraction of HMs.
Keywords: *mangroves, Tanjung Piai, heavy metals, fractionation, Rhizophora spp., phytoextraction*

Introduction

Mangrove ecosystems are among the most significant intertidal wetlands in tropical or subtropical coastal regions. In coastal environments, mangrove sediments can act as sinks for anthropogenic contaminants (especially heavy metal contaminants) due to the anaerobic properties, reductive and rich in sulfides, organic matter and high productivity (Nath et al., 2014). As urbanization and industrialization grow in coastal regions, mangrove ecosystems will play an increasingly important role in controlling heavy metal pollution (Sarath et al., 2021). In order to estimate the toxicity of metallic trace elements in soil, it is necessary to determine not only the total concentration, but also the forms in which heavy metals occur as the implications for the prediction of changes in their solubility that may occur in soil as a result of changes in environmental conditions (Zhang et al., 2010). Several physical properties of particular elements determine their mobility in soil, as well as the properties of the soil.

http://www.aloki.hu ● ISSN 1589 1623 (Print) ● ISSN 1785 0037 (Online)
DOI: http://dx.doi.org/10.15666/aeer/2005_40114030

Generally, heavy metal pollution is usually resistant to environmental factors. Heavy metals have a significant impact on environmental nutrient cycles, as well as the quality of food (Strayer, 2014). Heavy metals may enter the food chain in various ways and accumulate in living organisms (Kumar et al., 2019). Plants typically absorb and accumulate toxic metals from soils, water, or the atmosphere. Among the components of ecosystems, soils are the largest receivers of toxic metals (Kormoker et al., 2021). Anthropogenic sources and soil parent material can affect the total metal concentration in soils. It is important to understand the levels of heavy metals in sediments, in terms of their mobility, their ecological hazards, as well as their availability to plants (Charzyński et al., 2017). Consequently, heavy metals mobility, bioavailability and ecological toxicity to plants are primarily governed by their fractions. The exchangeable forms in these fractions are considered bioavailable, while the bound forms of carbonates, iron, and manganese oxides can also be considered bioavailable (Zhang et al., 2014). However, most residues are not available to plants or microorganisms.

Sequential extraction procedures (SEPs) have been widely used to assess heavy metal speciation in soils (Choleva et al., 2020). By using selective reagents, the heavy metals will be dissolved in different components to provide a more realistic estimation of their environmental impact (Du et al., 2020). The SEPs proposed by the European Community Bureau of Reference (BCR) are widely used for analyzing heavy metals fractions. The BCR sequential extraction method consists of three steps: exchangeable and bound to carbonates; reducible (bound to Fe – Mn oxides); and oxidizable (bound to organic matter and sulfides). In the last step, metals bond with minerals that are soluble in strong acids. With sequential extraction technique, comprehensive information on trace metal origin, availability, mobilization and transportation can be obtained.

Geographically, Tanjung Piai mangrove forest occupies a very unique geographical location. Located at 1°16.00' North, is the southernmost point of mainland Asia, or more precisely, continental Eurasia (Hui et al., 2019). It has been an ongoing battle since Tanjung Piai National Park was established in 1997 to protect its mangrove forest, which has faced serious erosion issues due to intensity of waves generated by thousands of oil tankers that sail by every year, as well as pollution events from oil spills and illegal ballast water dumping (Kunasekaran et al., 2018). The Tanjung Piai mangrove forest is also threatened with marine debris that contains organic deposits which result in the decaying mangrove roots and slowly kills the mangrove trees, due to its acidic composition and high levels of heavy metals (Wan Rasidah et al., 2015). Although quite a number of studies have examined the heavy metal concentration in this area, none have assessed the mobility of heavy metals in Tanjung Piai mangrove forest. Therefore, it is necessary to determine the concentration and distribution of heavy metals in this area to assess the current condition of its ecosystem and to compile baseline data for monitoring in the future. Phytoremediation is a green approach that use several types of plants, known as phytoremediators, to remove heavy metals (HMs) from soil. *Rhizophora apiculata* (*R. apiculata*) is an important mangrove species in Peninsular Malaysia in this regard. Because of its deep root structure, this species is well recognized worldwide for its capacity to enhance water quality by trapping sediments and extracting minerals contained in saltwater (Sarath et al., 2021). However, little study is being done in Malaysia on the phytoextraction potential of several *Rhizophora* spp.

The study aims to investigate the concentration and deposition of selected heavy metals, i.e. Cd, Cu, Fe, Mn, Pb and Zn, in the mangrove sediment around the Tanjung

http://www.aloki.hu ● ISSN 1589 1623 (Print) ● ISSN 1785 0037 (Online)
DOI: http://dx.doi.org/10.15666/aeer/2005_40114030

Piai mangrove forest. The concentration of heavy metals in mangrove sediments and growth of mangrove can be affected by anthropogenic activities such as sewage discharge, waste dumping or shipping activities. Nevertheless, studies on the effects of organic deposits on sediments heavy metals are still lacking. Due to the presents and composition of organic deposits at the study sites were in different composition, therefore heavy metals contents were compared in the sediments not the organic deposit present at the study sites in Tanjung Piai, Johor, Malaysia. This study can enhance the understanding of heavy metal contamination in the Tanjung Piai mangrove forest. The information will contribute to effective monitoring of both environmental quality and sustainable development for decision makers involved in coastal ecosystem management in Malaysia.

Materials and methods

Site description

Tanjung Piai mangrove forest

Tanjung Piai mangrove forest located in Pontian is one of the Ramsar sites in Johor. Ramsar sites are wetlands that have been identified according to the Ramsar Convention on Wetlands based on the representative, rare and unique or the importance of the wetlands to the conservation of biological diversity. Tanjung Piai National Park located 1° 16' 04.2" north latitude and 103° 30' 30.2" east latitude in Johor is the most Southern tip of Peninsular Malaysia which made up mostly of mangrove and mudflats. Located strategically between Malaysia, Singapore and Indonesia, this is the most significant place geographically as the southernmost point of Mainland Asia, which attracted both local and foreign tourists to explore the tip.

Design of the study

The sampling sites were selected at different localities based on the presence and extent of organic deposit (*Figs. 1* and *2*). Three dominant species of *Rhizhophora* spp. in Tanjung Piai mangrove forest have been selected for the leaves sampling. *Table 1* describes the sampling sites for sediments and leaves of *Rhizophora* spp: *Rhizophora stylosa*, *Rhizophora apiculata*, and *Rhizophora mucronata* that had been established in Tanjung Piai mangrove forest.

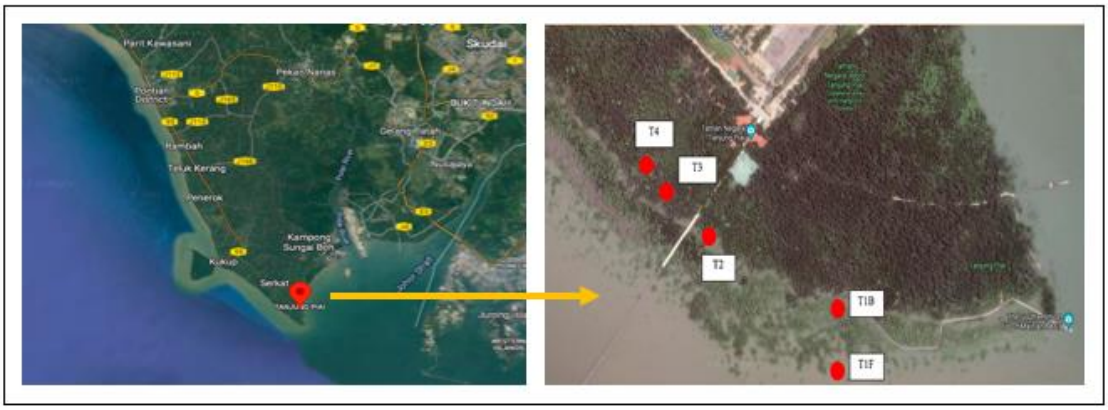

Figure 1. *Map of the study area at Tanjung Piai mangrove forest, Johor*

http://www.aloki.hu ● ISSN 1589 1623 (Print) ● ISSN 1785 0037 (Online)
DOI: http://dx.doi.org/10.15666/aeer/2005_40114030

Figure 2. *Sampling area at Tanjung Piai mangrove forest, Johor, Malaysia*

Table 1. *The description of each plot in Tanjung Piai, Johor*

Plot	Description
T1	Site without organic deposit material • There is no organic material present at this plot • 25 m from shoreline
T2	Site with new organic deposit material • The presence of organic deposit on surface of the sediment • 40 m from shoreline • 1°16'00.2"N 103°30'27.9"E
T3	Site with decomposed organic deposit material • The organic deposit material mixed in the sediment • 90 m from shoreline • 1°16'03.3"N 103°30'25.4"E
T4	Site with decomposed organic deposit material • The organic deposit material mixed in the sediment • 150 m from shoreline • 1°16'03.7"N 103°30'25.0"E

Sediment sampling at T1 were divided into two groups which are:

1. T1F: Sampling site facing sea
2. T1B: Sampling site facing mangrove forest

Organic deposit sampling

Fresh organic deposit was collected around the T2 study sites. Samples were collected in June 2016. Organic deposit samples were collected on top of the soil using stainless steel shovel. Samples were kept in a zip lock plastic bag and transferred directly to the laboratory for analysis. Samples were dried in the oven at temperature to constant weight (60 °C for 48 to 72 h), and ground in an agate mortar.

Organic deposit heavy metal analysis

The heavy metals content of the organic deposit was measured as follows: A crucible holding 0.5 g of organic deposit sample was weighed and heated for 5–6 h in a furnace

http://www.aloki.hu ● ISSN 1589 1623 (Print) ● ISSN 1785 0037 (Online)
DOI: http://dx.doi.org/10.15666/aeer/2005_40114030

at 500 °C. Three drops of pure water were poured to each crucible, followed by 2 mL of strong hydrochloric acid (HCl). The crucible was then placed in the sand bath to dry off the HCl solution. The Agilent 725 ICP-OES was used to determine the elements. 10 ml of 20% nitric acid was pipetted into the crucible and heated on the sand bath for 30 min to 1 h, or until only 3 to 4 mL of nitric acid remained. The materials were filtered into a 25 ml volumetric flask, the crucible was washed, and the solution was brought up to volume. The heavy metal content was determined using an Agilent 725 ICP-OES.

Sediment and leaves sampling

A total of 10 sediments samples (0 – 10 cm and 10 – 30 cm, triplicates for each sample) from sampling plots were collected using sediment Augers. Samples were kept in a zip lock plastic bag and transferred directly to the laboratory for analysis. All sediments samples were dried in the oven at temperature not exceeding 40 °C. The samples were then ground and sieved after completely dried. Random 10 *Rhizophora* spp. trees were selected for leaves analysis. Leaves sampling were collected and placed in separetd container according to the three species of *Rhizophora* spp. within the same study plot for heavy metals content analysis. Random leaf position were collected (upper, middle and basal leaves). Samples were dried to constant weight (60 °C for 48 to 72 h), and ground in an agate mortar. Portions of the sample were kept in a zip lock plastic prior to chemical analysis.

Heavy metal content in sediment at Tanjung Piai mangrove forest

The concentrations of heavy metals Cd, Cu, Fe, Mn, Pb, and Zn were measured using the Agilent 725 ICP – OES and the Aqua Regia extraction technique. 0.5 g of sediment samples were digested with 2 ml hydrochloric acid and 1 ml nitric acid in the digestion tube. The final digested mixture was filtered and heavy metals concentration was determined using an Agilent 725 ICP-OES.

Fractionation of heavy metals in sediment at Tanjung Piai mangrove forest

A four-stage BCR (European Community Bureau of Reference) sequential extraction was followed according to the procedure described fully in Rauret et al. (2000). The extraction process was divided into four stages was performed in triplicate.

Acid soluble and exchangeable portion (F1)

In a 100 mL centrifuge tube with 40 mL of 0.11 M acetic acid, one gramme of material was sonicated for 7 min at 22 ± 5 °C. After that, the mixture was centrifuged at 3000 g for 20 min using Eppendorf Centrifuge 5810. The extract was separated for analysis. After sonicating the residue for 5 min with 20 mL of deionized water, it was centrifuged for 20 min at 3000 g. The water was discarded.

Reducible fraction, bound to Fe/Mn oxides (F2)

The residue from the first step was added with 40 mL of fresh 0.5 M hydroxylamine hydrochloride solution, pH 1.5, and sonicated for 7 min at temperature 22 ± 5 °C. the mixture was then centrifuged at 3000 g for 20 min. For the reducible fraction analysis, the extract was separated. Similarly, to the first stage, the residue was washed with deionized water.

http://www.aloki.hu ● ISSN 1589 1623 (Print) ● ISSN 1785 0037 (Online)
DOI: http://dx.doi.org/10.15666/aeer/2005_40114030

Oxidizable fraction, bound to organic matter (F3)

Residue from the second step was added with 20 mL of 30% hydrogen peroxide and sonicated for 2 min at temperature 22 ± 5 °C. Then, reduced the volume of H_2O_2 around 1 mL using water bath. The moist residue was added with 50 mL of 1 M ammonium acetate and sonicated for 6 min at 22 ± 5 °C. The mixture was then centrifuged at 3000 *g* for 20 min. For analysis, the extract was separated. Similarly, to the previous processes, the residue was washed with deionized water.

Residual fraction (F4)

The third-step residue was extracted with concentrated HNO_3 with addition of 30% H_2O_2. It was heated for 30 min at 80 °C before being left overnight. 20 mL distilled water was added to the mixture, which was then mixed using vortex mixture. It was then filtered and made up to volume in a 100 mL volumetric flask. The fractionation of heavy metals at each step content was determined by Agilent 725 ICP-OES.

Heavy metals content in Rhizophora spp. leaves

0.5 g of each dried sample was weighed into a porcelain crucible and dry-ashed in a muffle furnace (Thermolyne Type 30400 furnace) at 500 °C for five to 6 h. The residue was dissolved with 2 mL HCl on the sand bath until the HCl solution was completely dry. 10 mL of 20% nitric acid was added and heated for 30 min to 1 h on the sand bath, until roughly three to four mL of nitric acid remained inside the crucible. The samples were filtered into 25 mL volumetric flask, the crucible was rinsed, and the solution was prepared to the required volume. Agilent 725 ICP-OES was used to determine the heavy metals content.

Statistical analysis

IBM SPSS version 24 was used to analyze the statistical data (IBM Inc., Armonk, NY, USA). The data was given as mean ± standard deviation of the mean. One-way analysis of variance (ANOVA) and Tukey's Test were used to find the mean difference of data between the variables. When $P \leq 0.05$ was used, the differences were considered statistically significant, and different letters in the same column or row were used to indicate them.

Results

Heavy metals content of organic deposits

The heavy metal content in the organic deposit samples is shown in *Table 2*. The heavy metals value of this study was compared with European countries (EU) and the United Kingdom (UK) for the limit established for compost, as well as a prior study done by Wan Rasidah et al. (2015), for the organic deposit discovered in Tanjung Piai, Johor where the sample of organic deposit were collected in 2013. The sampling site for organic deposit both of this study were at same location which is at T2 (1°16'00.2"N 103°30'27.9"E). The concentrations of Pb and Zn in the organic deposit were greater in the current research in Tanjung Piai than in prior studies and other sample locations. The Zn concentration was seven times higher than in the prior study, but it was still below the

http://www.aloki.hu ● ISSN 1589 1623 (Print) ● ISSN 1785 0037 (Online)
DOI: http://dx.doi.org/10.15666/aeer/2005_40114030

EU and UK maximum ranges. Pb content was greater at bit than in earlier studies, with 82.41 mg kg^{-1}, but it above the EU and UK regulatory range. Despite the fact that the Cd value was lower than in the prior study, it surpassed the EU and UK compost limit. Tanjung Piai Cu content was 21.50 mg kg^{-1}, which was lower than the previous study's result of 27.6 mg kg^{-1}. The concentration of Cd and Cu in the current research is lower than the prior study. However, concentration of Cd were exceed the EU and UK limit range. Cu content were still below the EU and UK maximum range for compost.

Table 2. *Comparison of heavy metal contained in organic deposit with previous study in Tanjung Piai, EU, UK compost limits*

Heavy metal	EU limit range[a]	UK limit range[b]	Previous study[c]	Tanjung Piai[d] (current study)
			Tanjung Piai (2015)	
Cd	0.7	1.5	5.02	2.45 ± 0.30b
Cu	70	200	27.6	21.50 ± 0.10a
Fe	-	-	-	2.61 ± 0.30b
Mn	-	-	-	0.053 ± 0.01b
Pb	45	50	67.2	82.41 ± 0.52a
Zn	200	200	17.5	133.12 ± 1.53a

Means ± standard error of mean value followed by different letters in row are significantly different using repeated measures ANOVA
[ab]Limits set for compost applied in European countries and United Kingdom (Saveyn and Eder, 2014)
[c]Results of heavy metal content in organic deposit from previous study in Tanjung Piai
[d]Mean of heavy metal content in organic deposit from the study

Heavy metals content in sediment

Tables 3–8 demonstrate the concentrations of heavy metals in sediment at all research plots in Tanjung Piai mangrove forest over a one-year period for both depths of 0 to 10 cm and 10 to 30 cm. Zn > Pb > Cu > Fe > Cd > Mn was the sequence in which the mean heavy metal content in the sediment declined.

Table 3. *Cd content in sediments at each study plots*

Site	Cd (mg kg^{-1})				
	Month 1	Month 3	Month 6	Month 9	Month 12
Sediment depth 0 to 10 cm					
T1F	1.96 ± 0.98b	3.19 ± 0.22ab	2.42 ± 0.14a	2.72 ± 0.31a	1.96 ± 0.14abc
T1B	3.12 ± 0.22a	2.44 ± 0.26c	2.31 ± 0.21a	2.36 ± 0.07a	1.84 ± 0.26bc
T2	1.67 ± 0.28b	1.13 ± 0.19d	1.26 ± 0.18b	1.45 ± 0.30b	1.36 ± 0.28c
T3	3.46 ± 0.28a	3.72 ± 0.24a	2.64 ± 0.13a	2.72 ± 0.21a	2.55 ± 0.05a
T4	3.38 ± 0.42a	2.66 ± 0.13bc	2.48 ± 0.42a	2.58 ± 0.63a	2.39 ± 0.19ab
Sediment depth 10 to 30 cm					
T1F	2.38 ± 0.36b	3.43 ± 0.32a	2.64 ± 0.11a	2.42 ± 0.24bc	1.63 ± 0.06c
T1B	3.43 ± 0.32a	3.59 ± 0.21a	2.72 ± 0.24a	2.65 ± 0.16b	1.34 ± 0.12c
T2	1.28 ± 0.23c	2.79 ± 0.18b	1.49 ± 0.17b	1.65 ± 0.42c	1.28 ± 0.22c
T3	3.12 ± 0.09a	3.22 ± a0.12b	2.48 ± 0.37a	3.80 ± 0.20a	3.31 ± 0.20a
T4	2.14 ± 0.37a	2.67 ± 0.05c	2.16 ± a0.40b	2.49 ± 0.37b	2.33 ± 0.36b

Means ± standard error of mean value followed by different letters in column are significantly different using repeated measures ANOVA

http://www.aloki.hu ● ISSN 1589 1623 (Print) ● ISSN 1785 0037 (Online)
DOI: http://dx.doi.org/10.15666/aeer/2005_40114030

Table 4. *Cu concentration in sediments at each study plots*

Site	Cu (mg kg^{-1})				
	Month 1	**Month 3**	**Month 6**	**Month 9**	**Month 12**
Sediment depth 0 to 10 cm					
T1F	12.44 ± 0.49c	12.20 ± 0.52c	12.54 ± 0.28c	7.26 ± 0.13d	9.44 ± 0.36c
T1B	11.66 ± 0.62cd	10.29 ± 0.49d	12.32 ± 0.20c	8.66 ± 0.20c	9.54 ± 0.24c
T2	10.11 ± 0.72c	8.11 ± 0.80d	8.30 ± 0.81d	4.56 ± 0.42d	7.32 ± 0.38d
T3	24.43 ± 1.36a	26.01 ± 0.67a	21.75 ± 0.64a	14.80 ± 0.38a	20.31 ± 0.22a
T4	16.84 ± 0.16b	18.97 ± 0.56b	19.12 ± 0.53b	12.57 ± 0.06b	18.48 ± 0.22b
Sediment depth 10 to 30 cm					
T1F	12.37 ± 0.30c	12.54 ± 0.84c	7.35 ± 0.28c	10.45 ± 0.21c	8.44 ± 0.34c
T1B	9.53 ± 0.26d	12.32 ± 0.28c	7.55 ± 0.14c	11.04 ± 0.13c	8.49 ± 0.42c
T2	10.45 ± 0.26cd	8.29 ± 0.41d	4.10 ± 0.40d	7.45 ± 0.33d	7.69 ± 0.36c
T3	23.69 ± 0.67a	21.76 ± 0.62a	16.95 ± 0.17a	18.35 ± 0.30a	22.56 ± 0.34a
T4	18.61 ± 0.59b	19.12 ± 0.31b	12.97 ± 0.45b	16.40 ± 0.48b	18.85 ± 0.12b

Means ± standard error of mean value followed by different letters in column are significantly different using repeated measures ANOVA

Table 5. *Fe content in sediments at each study plot*

Site	Fe (mg kg^{-1})				
	Month 1	**Month 3**	**Month 6**	**Month 9**	**Month 12**
Sediment depth 0 to 10 cm					
T1F	3.42 ± 0.14c	2.91 ± 0.05ab	2.03 ± 0.10a	3.48 ± 0.10a	2.97 ± 0.02a
T1B	3.35 ± 0.20c	2.18 ± 0.24c	2.03 ± 0.04a	3.07 ± 0.05a	2.95 ± 0.17a
T2	2.19 ± 0.18d	1.39 ± 0.46d	1.23 ± 0.24b	1.39 ± 0.22b	1.58 ± 0.32b
T3	5.15 ± 0.27a	3.46 ± 0.09a	2.13 ± 0.08a	3.53 ± 0.29a	3.39 ± 0.37a
T4	4.45 ± 2.23b	2.36 ± b0.06c	2.01 ± 0.23a	3.57 ± 0.26a	3.06 ± 0.06a
Sediment depth 10 to 30 cm					
T1F	3.36 ± 0.28bc	2.98 ± 0.09a	2.13 ± 0.10a	3.17 ± 0.24b	2.72 ± 0.20a
T1B	2.54 ± 0.02cd	1.48 ± 0.45d	2.26 ± 0.02a	3.35 ± 0.06b	2.69 ± 0.19a
T2	2.38 ± 0.32d	2.33 ± 0.21b	1.30 ± 0.12b	2.25 ± 0.39c	1.44 ± 0.46b
T3	4.42 ± 0.35a	2.38 ± 0.17ab	2.07 ± 0.26a	4.71 ± 0.23a	3.16 ± 0.19a
T4	3.56 ± 0.49bc	2.49 ± 0.02bc	1.90 ± 0.26a	3.18 ± 0.36b	2.52 ± 0.12a

Means ± standard error of mean value followed by different letters in column are significantly different using repeated measures ANOVA

Table 3 shows the results of cadmium (Cd) content in sediments for both sediment depths. T3 > T4 > T1B > T1F > T4 > T2 was the decreasing order of Cd concentration in the sediments from 0 to 10 cm, and T3 > T1B > T1F > T4 > T2 was the decreasing order of Cd concentration in the sediments from 10 to 30 cm. T3 had the greatest Cd concentration in the sediments throughout the measurement periods at both depths, 0 to 10 cm and 10 to 30 cm, whereas T2 had the lowest Cd concentration. Cd concentrations vary from 1.28 mg kg^{-1} to 3.80 mg kg^{-1} across all plots.

http://www.aloki.hu ● ISSN 1589 1623 (Print) ● ISSN 1785 0037 (Online)
DOI: http://dx.doi.org/10.15666/aeer/2005_40114030

The concentration of Cu in the sediments of Tanjung Piai mangrove forest is shown in *Table 4*. The maximum concentration was found at T3 for both the 0 to 10 cm and 10 to 30 cm sediment depths. The greatest concentration is 26.01 mg kg^{-1} at 0 to 10 cm, and 23.69 mg kg^{-1} at 10 to 30 cm. Cu concentrations are lowest in month 6 at T2, with 4.10 mg kg^{-1} at 10 to 30 cm.

Table 6. *Mn concentrations in sediments at each study plots*

Site	Mn (mg kg^{-1})				
	Month 1	**Month 3**	**Month 6**	**Month 9**	**Month 12**
Sediment depth 0 to 10 cm					
T1F	0.08 ± 0.01a	0.07 ± 0.01a	0.04 ± 0.01a	0.07 ± 0.01a	0.06 ± 0.01a
T1B	0.07 ± 0.01a	0.07 ± 0.00a	0.04 ± 0.00a	0.05 ± 0.01b	0.06 ± 0.01b
T2	0.03 ± 0.00b	0.03 ± 0.01b	0.02 ± 0.01b	0.02 ± 0.00c	0.03 ± 0.01b
T3	0.01 ± 0.01c	0.01 ± 0.00c	0.02 ± 0.00b	0.01 ± 0.01c	0.02 ± 0.01b
T4	0.02 ± 0.01b	0.01 ± 0.1c	0.01 ± 0.01b	0.01 ± 0.01c	0.02 ± 0.01b
Sediment depth 10 to 30					
T1F	0.10 ± 0.00a	0.13 ± 0.01a	0.06 ± 0.00a	0.06 ± 0.01a	0.05 ± 0.01a
T1B	0.06 ± 0.01b	0.08 ± 0.01b	0.05 ± 0.01a	0.07 ± 0.00a	0.05 ± 0.01a
T2	0.03 ± 0.01c	0.06 ± 0.01b	0.02 ± 0.01b	0.03 ± 0.01b	0.03 ± 0.01b
T3	0.01 ± 0.01d	0.01 ± 0.00c	0.01 ± 0.00c	0.02 ± 0.01b	0.01 ± 0.01c
T4	0.01 ± 0.01d	0.01 ± 0.01b	0.01 ± 0.00c	0.01 ± 0.01b	0.02 ± 0.01bc

Means ± standard error of mean value followed by different letters in column are significantly different using repeated measures ANOVA

Table 7. *Pb concentration in sediments at each study plots*

Site	Pb (mg kg^{-1})				
	Month 1	**Month 3**	**Month 6**	**Month 9**	**Month 12**
Sediment depth 0 to 10 cm					
T1F	25.64 ± 2.61c	86.06 ± 2.54b	26.29 ± 1.70c	34.18 ± 2.73b	26.44 ± 1.62b
T1B	25.08 ± 0.64c	64.56 ± 3.97c	23.86 ± 2.51cd	26.13 ± 1.02c	26.52 ± 1.86b
T2	26.12 ± 1.08c	24.21 ± 2.71d	13.86 ± 3.52d	16.16 ± 3.97d	17.64 ± 3.27c
T3	69.23 ± 3.89a	117.31 ± 5.58a	51.24 ± 6.82a	56.67 ± 2.34a	21.23 ± 0.75bc
T4	48.19 ± 1.67b	78.69 ± 5.05b	28.63 ± 1.35b	34.8 ± 2.91b	42.97 ± 1.82a
Sediment depth 10 to 30 cm					
T1F	30.03 ± 1.19c	86.59 ± 1.80ab	24.74 ± 0.23b	26.25 ± 1.05c	26.031.25ab
T1B	27.39 ± 2.04c	44.18 ± 3.12d	27.40 ± 1.20b	26.83 ± 1.37c	25.27 ± 1.54b
T2	24.24 ± 1.59c	65.46 ± 3.56c	18.91 ± 1.29c	23.54 ± 1.77c	22.81 ± 2.85b
T3	67.07 ± 5.72a	88.54 ± 3.39a	34.26 ± 1.84a	59.36 ± 1.18a	27.86 ± 0.78a
T4	52.36 ± 2.57b	78.39 ± 3.23b	37.71 ± 3.55a	45.28 ± 1.64b	16.75 ± 0.83c

Means ± standard error of mean value followed by different letters in column are significantly different using repeated measures ANOVA

Table 5 shows the Fe content in the sediments of all plots in the Tanjung Piai mangrove forest. T3 has the greatest Fe concentrations at depths of 0 to 10 cm and 10 to

http://www.aloki.hu ● ISSN 1589 1623 (Print) ● ISSN 1785 0037 (Online)
DOI: http://dx.doi.org/10.15666/aeer/2005_40114030

30 cm, respectively, with 5.15 mg kg^{-1} and 4.17 mg kg^{-1}. At depths of 0 to 10 cm, there is no significant difference between plot T1F, T1B, T3 and T4 during month 6, month 9, and month 12 measurements. Among the other heavy metals tested in the sediment samples, Mn had the lowest concentration (*Table 7*). At T1F, the greatest Mn content is 0.13 mg kg^{-1}. Mn concentrations are lowest at T3 and T4, ranging from 0.01 to 0.02 at both depths. The second greatest concentration of Pb was found in the sediments, as reported in *Table 7*. Pb concentrations were greatest in all plots during M3, compared to other months in this research. From month 1 to month 3, the concentration increased, then decreased during month 6. T3 has the greatest concentration, 117.31 mg kg^{-1}. At T2, the lowest value of Pb was 16.16 mg kg^{-1}. *Table 8* shows the Zn concentrations at all research plots. The highest concentrations of Zn were identified in T1F and T1B, whereas the lowest concentrations were observed in T2. Save for T2, which had the greatest concentration of Zn in month 3 for both depths, 0 to 10 cm and 10 to 30 cm, the maximum concentration of Zn was detected in month 6 in all plots except T2.

Table 8. *Zn concentration in sediments at each study plots*

Site	Zn (mg kg^{-1})				
	Month 1	**Month 3**	**Month 6**	**Month 9**	**Month 12**
Sediment depth 0 to 10 cm					
T1F	82.54 ± 2.35a	87.45 ± 0.44b	110.17 ± 2.52a	94.88 ± 3.67a	93.73 ± 2.81a
T1B	86.24 ± 1.18a	89.37 ± 2.35b	112.35 ± 0.52a	81.60 ± 3.69b	96.18 ± 2.68a
T2	44.01 ± 2.52c	126.35 ± 3.62a	82.24 ± 1.88b	34.55 ± 2.02d	53.02 ± 0.74c
T3	43.63 ± 1.65c	50.22 ± 5.44d	97.63 ± 5.34ab	67.07 ± 2.90c	72.35 ± 1.67b
T4	64.87 ± 2.88b	64.88 ± 2.49c	119.02 ± 4.35a	72.42 ± 4.24c	69.40 ± 3.26b
Sediment depth 10 to 30 cm					
T1F	88.43 ± 1.97a	90.01 ± 3.51a	115.86 ± 3.23a	95.23 ± 2.53a	94.98 ± 0.83a
T1B	65.59 ± 3.20b	88.84 ± 5.01a	116.86 ± 2.49a	88.29 ± 0.78b	83.87 ± 3.47b
T2	35.58 ± 3.14d	73.31 ± 1.07b	68.53 ± 3.95c	47.00 ± 0.21d	65.67 ± 3.92c
T3	57.61 ± 1.18bc	67.39 ± 3.70b	124.65 ± 0.69a	69.03 ± 0.13c	76.36 ± 3.47b
T4	52.93 ± 4.90c	82.62 ± 1.18a	91.26 ± 3.83b	73.16 ± 4.04c	56.72 ± 1.74c

Means ± standard error of mean value followed by different letters in column are significantly different using repeated measures ANOVA

Heavy metals content in Rhizophora spp. leaves

For this study, heavy metals were analyzed in the leaves of three different mangrove species. Heavy metal concentrations in plant leaves of *R. stylosa*, *R. apiculata*, and *R. mucronata* at four research plots in Tanjung Piai mangrove forest are shown in *Table 9*. Mn > Fe > Pb > Cu > Zn > Cd is the average concentration of heavy metals in the leaves, from highest to lowest. The greatest concentration detected in *Rhizophora* spp. leaves is Mn, which has a concentration of 657.60 mg kg^{-1} in *R. apiculata* leaves at T1. *R. stylosa* and *R. mucronata* had the highest Mn concentrations at T1 in the four-study plot, with 489.87 mg kg^{-1} and 374.12 mg kg^{-1}, respectively. Others with reading of Mn concentration more than 200 mg kg^{-1} are *R. stylosa* at T2, *R. apiculata* at T4 and *R. mucronata* at T3.

Second highest concentration of heavy metals in *Rhizophora* spp. leaves is Fe with 469.99 mg kg^{-1} in *R. mucronata* at T3, 303.05 at T4 and 226.84 at T1. *R. stylosa* in T3

http://www.aloki.hu ● ISSN 1589 1623 (Print) ● ISSN 1785 0037 (Online)
DOI: http://dx.doi.org/10.15666/aeer/2005_40114030

and T4 also have high concentration of Fe with 346.59 mg kg^{-1} and 350.00 mg kg^{-1} followed by T1 with 283.57 mg kg^{-1}. *R. apiculata* leaves samples at T1, T3 and T4 also recorded Fe concentration with more than 200 mg kg^{-1}. All *Rhizophora* spp. leaves at T2 have the Fe concentration below than 200 mg kg^{-1} but more than 100 mg kg^{-1}.

Table 9. *Heavy metal content in Rhizophora spp. leaves*

Site	mg kg^{-1}					
	Cd	**Cu**	**Fe**	**Mn**	**Pb**	**Zn**
Rhizophora stylosa						
T1	nd	nd	283.57 ± 2.79b	489.87 ± 2.28a	0.73 ± 0.09c	nd
T2	nd	0.48 ± 0.05b	164.79 ± 2.43c	207.19 ± 1.06b	2.22 ± 0.04a	nd
T3	0.05 ± 0.01b	0.43 ± 0.02b	346.59 ± 5.48a	196.17 ± 0.94b	1.63 ± 0.07b	nd
T4	0.53 ± 0.03a	2.64 ± 0.13a	350.00 ± 1.50a	162.43 ± 6.18c	1.56 ± 0.04b	nd
Rhizophora apiculata						
T1	nd	nd	216.08 ± 2.17c	657.60 ± 2.98a	1.30 ± 0.04d	0.62 ± 0.04a
T2	nd	0.39 ± 0.33b	176.25 ± 1.04d	186.66 ± 2.33c	2.83 ± 0.07a	nd
T3	nd	1.63 ± 0.14a	276.71 ± 1.68a	189.53 ± 1.514c	2.29 ± 0.04b	nd
T4	nd	0.75 ± 0.07b	248.19 ± 0.93b	248.28 ± 2.09b	1.73 ± 0.04c	nd
Rhizophora mucronata						
T1	nd	0.06 ± 0.01b	226.84 ± 2.56c	374.13 ± 0.85a	1.57 ± 0.29b	0.05 ± 0.35a
T2	nd	nd	135.36 ± 1.59d	167.91 ± 1.74c	2.92 ± 0.10a	nd
T3	nd	1.51 ± 0.06a	469.99 ± 3.99a	224.93 ± 1.97b	1.17 ± 1.14b	nd
T4	nd	1.49 ± 0.08a	303.05 ± 1.23b	163.10 ± 2.05d	1.20 ± 0.05b	nd

Means ± standard error of mean value followed by different letters in column are significantly different using repeated measures ANOVA. Note: nd = not detectable

However, the maximum Pb content was detected in *Rhizophora* spp. leaves at T2. 2.92 mg kg^{-1} *for R. mucronata*, 2.83 mg kg^{-1} for *R. apiculata*, and 2.22 mg kg^{-1} for *R. stylosa*. Except for *R. stylosa* at T1, which had 0.73 mg kg^{-1}, all Pb values were over 1 mg kg^{-1}. Cu concentration was found to be greatest in *R. stylosa* at T4 with 2.64 mg kg^{-1}, followed by *R. mucronata* at T3 and T4 as well as *R. apiculata* at T3 with 1.51, 1.49, and 1.63 mg kg^{-1}, respectively. *R. mucronata* had the lowest Cu concentration of 0.06 mg kg^{-1} at T1 and is not detectable at T1 for both *R. stylosa* and *R. mucronata* and T2 for *R. mucronata*. The Zn concentrations were only measurable at T1 for *R. apiculata* and *R. mucronata* and others were not detectable. The concentration for *R. apiculata* is 0.62 mg kg^{-1} and only 0.05 mg kg^{-1} detected for *R. mucronata*. Same as Cd concentration, most of the *Rhizophora* spp. leaves were not detectable for this study but only found in *R. stylosa* at T3 and T4 with concentration less than 1 mg kg^{-1}. Heavy metal concentration of Cu, Fe, Mn, Pb and Zn were found to be significantly different ($p < 0.05$) between *Rhizophora stylosa* species over the study plots, while the concentration of Cd was not significantly different. In *Rhizophora apiculata*, the concentration of Cu, Fe, Mn, Pb and Zn were found to be significantly different ($p < 0.05$) between each treatment plots. Next for *Rhizophora mucronata*, the heavy metals except for Cd were found to be significantly different over treatment plots in Tanjung Piai mangrove forest.

http://www.aloki.hu ● ISSN 1589 1623 (Print) ● ISSN 1785 0037 (Online)
DOI: http://dx.doi.org/10.15666/aeer/2005_40114030

Fractionation of heavy metals content of mangrove sediment at different localities in Tanjung Piai mangrove forest

Fractionation of Cd

Figures 3 and *4* visually illustrate the average proportion of metals in fractionation at each research location at both depths; 0 to 10 cm and 10 to 30 cm respectively. The fractionation of heavy metals (Cd, Cu, Fe, Mn, Pb, and Zn) in the extracted solutions was conducted by Agilent 725 ICP-OES. The availability of heavy metals is the sum of residual and oxidizable fraction (F1 + F2). The mobility of heavy metals may be calculated by adding the residual fraction, oxidizable fraction, and reducible fraction (F1 + F2 + F3).

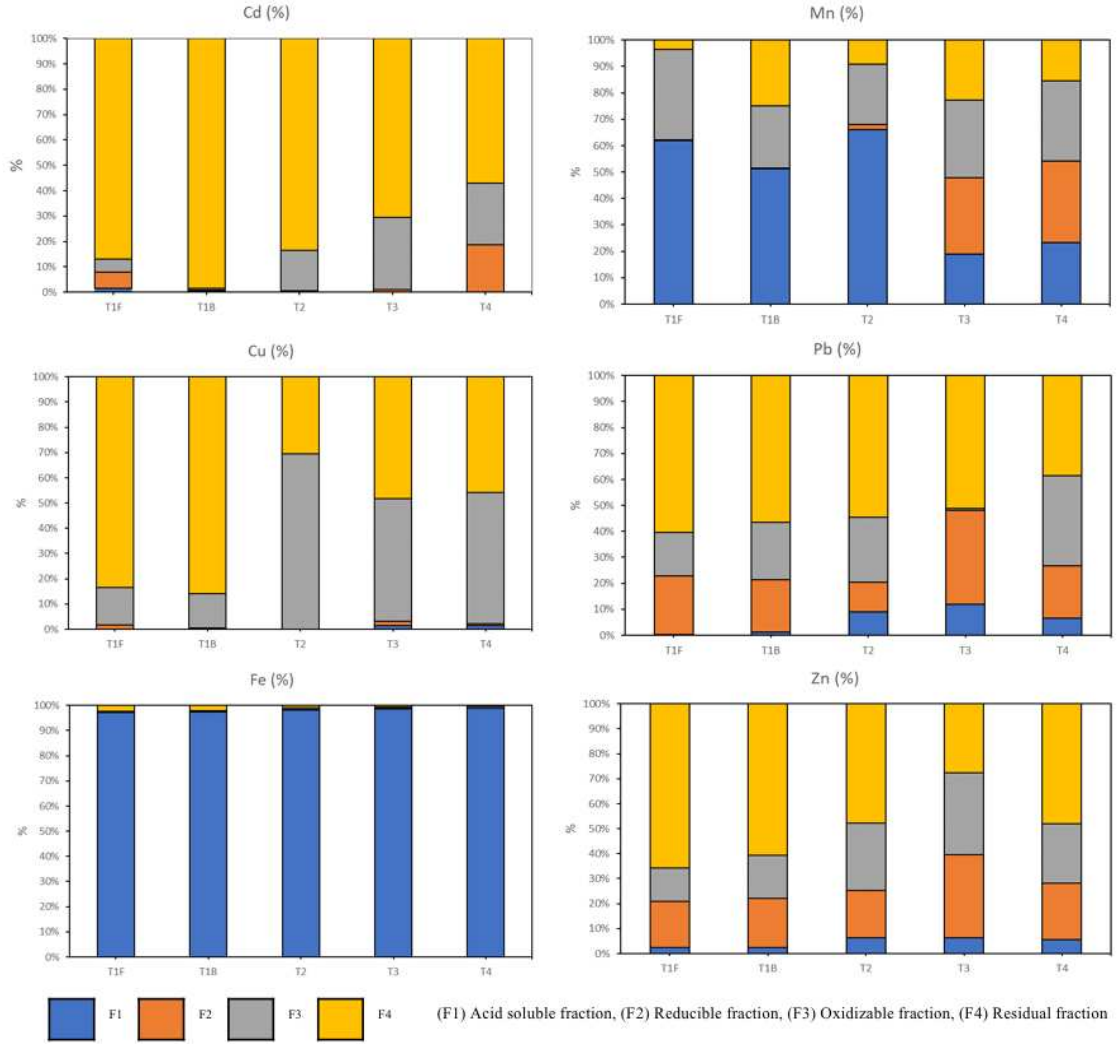

Figure 3. *Fractionation of heavy metals at 10 cm at all study plots in Tanjung Piai, Johor*

Cd fractionation was in the following sequence at both depths, 0 to 10 cm and 10 to 30 cm: Acid soluble fraction > Residual fraction > Oxidizable fraction > Reducible fraction. T1B has the largest percentage of residual fraction (F4) in the 0 to 10 cm depth range, with 98.56%, followed by T1F with 86.94%. T4 had the lowest residual fraction percentage, at only 57.05%. At a depth of 0 to 10 cm, the mobility and availability of

http://www.aloki.hu ● ISSN 1589 1623 (Print) ● ISSN 1785 0037 (Online)
DOI: http://dx.doi.org/10.15666/aeer/2005_40114030

Cd decreases in the following order: T4 (42.95%) > T3 (29.59%) > T2 (16.46%) > T1F (13.55%) > T1B (1.44%) Cd mobility and availability were as follows between 10 and 30 cm: T2 (39.65%) > T3 (39.38%) > T4 (12.21%) > T1B (11.62%) > T1F (11.62%) (11.54%). At both sediment depths, Cd mobility and availability were not the same. When compared to 0 to 10 cm, Cd was more mobile and available at T4, but less mobile and available from 10 to 30 cm. However, in comparison to others, the proportion of Cd mobility and availability was low at T1F and T1B, at both sediment depths.

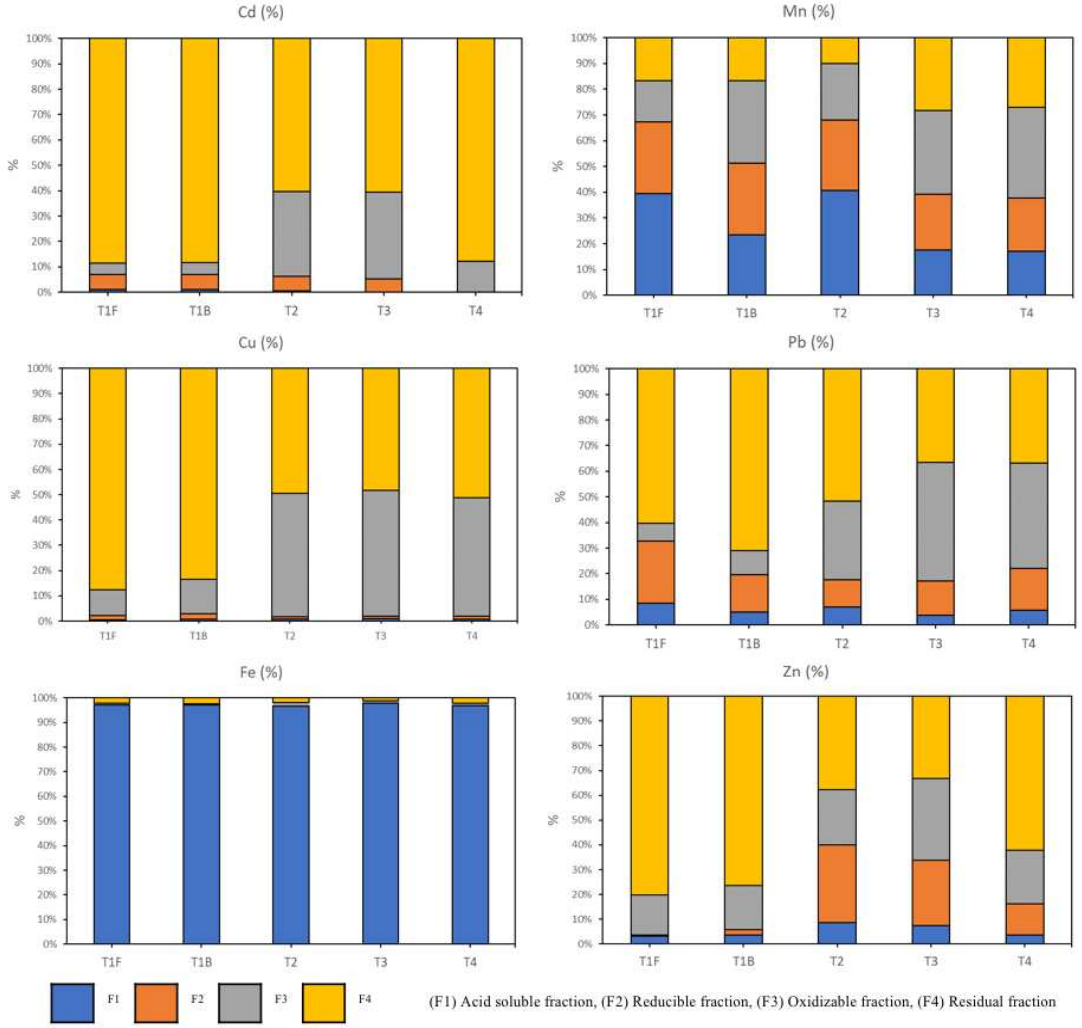

Figure 4. *Fractionation of heavy metals at 30 cm at all study plots in Tanjung Piai, Johor*

The largest percentages of oxidizable fraction (F3) are found at T3 (28.57%) and T4 (24.16%), whereas the percentage of oxidizable fraction is less than 20% at the other three plots. At T4, the reducible fraction (F2) accounted for 18.79%, while T1F accounted for 6.34%. Cd percentage for residual fraction (T4) was high at 10 to 30 cm depth at T1F, T1B, and T4, with 88.46%, 88.37%t, and 87.79%, respectively. T3 and T2 contain substantial percentages of oxidizable fraction at this level, with 34.20% and 33.33%, respectively. Both the acid soluble fraction (F1) and the reducible fraction (F2) had percentages of less than 10%. The acid soluble fraction ranges from 0.00% to 1.16%, whereas the reducible fraction ranges from 0.00% to 5.18%.

http://www.aloki.hu ● ISSN 1589 1623 (Print) ● ISSN 1785 0037 (Online)
DOI: http://dx.doi.org/10.15666/aeer/2005_40114030

Fractionation of copper (Cu)

Cu is divided into fractions. The following orders were followed at both depths: Acid soluble fraction > Residual fraction > Oxidizable fraction > Reducible fraction Cd fractionation was also substantial from 0 to 10 cm, with 83.42%at T1F and 86.00% at T1B, similar to Cd. The residual proportion in the other three research plots was less than 50%. The oxidizable fraction was greatest at T2, with 69.52%, followed by T4 with 52.06%, and T3 with 48.62%. The oxidizable percentage was only 14.80% and 13.62% at T1F and T1B, respectively. At all research sites, the percentage of acid soluble fraction and reducible fraction was less than 3%. At each research plot, the mobility and availability of Cu at 0 to 10 cm deep were in the following order: T2 (69.52%) > T4 (54.27%) > T3 (51.80%) > T1F (16.59%) > T1B (16.59%) (14.00%). Cu mobility and availability were in the following order between 10 and 30 cm: T3 (51.62%) > T2 (50.54%) > T4 (48.76%) > T1B (16.5%) > T1F (12.4%). T1F and T1B had larger residual fractionation from 10 to 30 cm, with 87.5% and 83.50%, respectively.

T2, T3, and T4 had nearly identical percentages of residual and oxidizable fractions, with 48.93% (F3) and 49.46% (F4) at T2, 49.60% (F3) and 48.38% (T4) at T3, and 46.88% (F3) and 51.24% (F4) at T4. The range for acid soluble and reducible fractionation at all study site is in between 0.57% to 2.17%.

Fractionation of iron (Fe)

At both depths, the fractionation of Fe decreases in the following order: Residual fraction > Oxidizable fraction > Reducible fraction > Acid soluble fraction. Acid soluble and exchangeable fractionation (F1) was more than 95% at both depths, with values ranging from 97.24 to 98.74% from 0 to 10 cm and 96.54 to 97.77% at 10 to 30 cm. As a result, Fe mobility at all researched locations was extremely high at both depths. Other fractionations for Fe were less than 3%. Heavy metals' mobility and toxicity in sediment are primarily determined by their binding structures. Bioavailable substances are those that are exchangeable (F1) or bonded to carbonates (F2). Plants and microorganisms may be able to use the oxidizable fractions (F3), but the residual fraction is largely unavailable to them.

Fractionation of manganese (Mg)

The following was the order of Mn fractionation from 0 to 10 cm depth: Oxidizable fraction > Residual fraction > Reducible fraction > Acid soluble fraction At 0 to 10 cm depth, T2 has the largest proportion of acid soluble (F1) with 66.03%, followed by T1F with 61.97%. The reducible fraction (F2) at T3 and T4 was high, at 28.96% and 30.94%, respectively, compared to the other three locations, where residual fraction ranged from 0.13% to 1.92%. Even though F2 fractionation was less than 2% at T1F, T1B, and T1, Mn availability was substantial due to the strong F1 fractionation at these three locations. Mn's movement was in the following order: T1F > T2 > T4 > T3 > T1B.

Mn fractionation was in the following sequence at 10 to 30 cm: Reducible fraction > Acid soluble fraction > Residual fraction > Oxidizable fraction Reduced fraction (F2) at T1F, T1B, and T2 were high at 10 to 30 cm depth as compared to 0 to 10 cm depth. Mn was more accessible from 10 to 30 cm at T1F and T2, with a percentage of availability of more than 65%. With 89%, 82%, and 81%, Mn mobility is high at T2, T1B, and T1F, respectively.

http://www.aloki.hu ● ISSN 1589 1623 (Print) ● ISSN 1785 0037 (Online)
DOI: http://dx.doi.org/10.15666/aeer/2005_40114030

Fractionation of lead (Pb)

Pb fractionation decreased from 0 to 10 cm depth in the following order: Acid soluble fraction > Residual fraction > Reducible fraction > Oxidizable fraction Pb fractionation is done in the following order at 10 to 30 cm: residual fraction > oxidizable fraction > reducible fraction > acid soluble fraction. In comparison to other fractions, the residual fraction (F4) was large at both depths. T1F has the largest percentage of F4 from 0 to 10 cm, with 66.35%. Pb has a low acid soluble fraction (F1) when compared to Mn and Fe. At 0 to 10 cm, the F1 fraction ranges from 0.24% to 8.95%. Pb availability was poor at depths of 0 to 10 cm, with the total of acid soluble and reducible fractions at all four locations falling below 38%. The mobility of Pb is likewise poor, since the sum of three fractions (F1 + F2 + F3) is less than 50%, with the exception of T4, where the mobility of Pb is 61.43%. T1B has the largest proportion of residual fraction (70.96%) at 10 to 30 cm, followed by T1F with 60.31%. Pb availability was equally poor at this level, with mobility percentages ranging from 17.04% to 32.77%. At T3 and T4, Pb mobility was high, with percentages of mobility of 63.49% and 63.17%, respectively. The proportion of Pb mobility was less than 50% at the other three research sites.

Fractionation of zinc (Zn)

Zn fractionation decreased in the following sequence at both depths: Acid soluble fraction > Residual fraction > Oxidizable fraction > Reducible fraction > Study sites T1F and T1B exhibit the largest residual fraction (F4) at both depths, with 65.81% and 60.62% respectively from 0 to 10 cm and 80.27% and 76.45% at 10 to 30 cm. This also suggests that Zn is not readily accessible or mobile in plants.

At T2, both depths show modest acid soluble fractionation, with less than 10%. At T2, the residual proportion of 0 to 10 cm was greater than that of 10 to 30 cm. It has a limited availability but is simple to transport since the mobility percentage at both depths is more than 50%. Next, when compared to other research sites, the oxidizable percentage at T3 was high at both depths. With 32.66% in the 0-10 cm range and 32.98% in the 10-30 cm range. This also suggests that Zn was easily transportable from the sediment to the plant at T3. With 48.13% residual (F4) at 0 to 10 cm and 62.20% at 10 to 30 cm, T4 has the largest proportion of residual (F4). At T4, Zn mobility is low at 10 to 30 cm and high at 0 to 10 cm. The availability of Zn at T3 and T4 at both depths was poor since the total of F1 and F2 was less than 40% at this research location. Even though it is easily movable, there is not much of it in the sediment.

Discussion

The mobility and immobility of heavy metals along with their availability in sediment largely depend on their types of binding forms. The mobility and availability of the metals decrease in order of acid soluble fraction > reducible fraction > oxidizable fraction > residual forms (Zimmerman and Weindorf, 2010). The first two fractions, acid soluble and reducible fractions constitute a more available form of the metals. The last two fractions, oxidizable fraction and residual fraction form a less available pool (Alvarez et al., 2002). According to Rauret (1998), the concentration of the first three fractions (acid soluble + reducible + oxidizable) are mobile fractions.

http://www.aloki.hu ● ISSN 1589 1623 (Print) ● ISSN 1785 0037 (Online)
DOI: http://dx.doi.org/10.15666/aeer/2005_40114030

Cd, Pb, and Zn are prevalent in the residual fractions of all samples. Cd, Pb, and Zn were abundant in the residual phase but not in the other geochemical phases, indicating that these metals were more stable in this environment than the other metals. In T2 and T3, the Cu fraction is found to be more bound to organic matter than the other elements. Because of the high formation of organic – Cu compounds, copper can easily complex with organic matters (Fagbote and Olanipekun, 2010). The presence of a high concentration of acid-soluble Fe and Mn indicated that the metal exited in the reduced form (Tessier et al., 1979). The fractional distribution of cadmium indicates that the majority is bound to the residual fraction at all of the Tanjung Piai mangrove forest sites. Only a negligible amount of Cd (1.44% to 42.95%) was released from the non-residual fraction and 57.05% to 98.56% was released from the residual fraction. The high concentration of metal present in the inert phase (residual) is of lattice and detrital origin and can be attributed to natural sources (Singh et al., 2003).

A higher proportion of heavy metals in the non-residual fraction indicates a greater proclivity to become bioavailable. The higher percentages of Fe and Mn in the bioavailable non-residual fraction indicated that their bioavailability and mobility in Tanjung Piai mangrove forest sediments were high. As a result, the potential hazards of Fe and Mn were greater than those of Cd, Pb, and Zn, which were mostly found in the residual fraction. Heavy metal contamination can result in increased heavy metal concentrations in the non-residual fraction, which reflects the degree of anthropogenic influence (McLaren et al., 2004). High mobility and greater availability of Fe and Mn in this study indicate environmental pollution and can pose a critical toxicity risk in plant production areas over time.

The results of heavy metal content in *Rhizophora* spp. leaves show high concentrations of Fe and Mn, which support the fractionation results of Fe and Mn at each plot where their mobility percentage is high, according to *Table 9*. Heavy metal mobility and plant uptake progress through the solution phase. Plant heavy metal uptake is determined not only by its activity in solution, but also by the relationship that exists between solid-phase ions and solution ions (Violante et al., 2010). Mn was found in significant amounts in the reducible fraction; this Mn exists as oxides and may be released if the sediment is subjected to more reducing conditions (Panda et al., 1995). According to Peng et al. (2004), a significant amount of Mn may be released into the environment (reducible fraction) if conditions become more acidic.

Heavy metals like iron, copper, vanadium, and manganese occur naturally in the environment and, depending on their concentration, might function as plant nutrients. Some, such as mercury, lead, cadmium, and chromium, may be dispersed indirectly as a result of human activities and may be harmful even at low concentrations (Khosropour et al., 2019). *Table 9* illustrates the heavy metal concentrations in *Rhizophora* spp. leaves, with Mn having the greatest concentration relative to the other heavy metals. Mn plays an important role in a variety of photosynthetic activities (Ariyanto et al., 2019). Plants with low Mn levels have fewer chloroplasts, reduced chlorophyll content, poorer net photosynthetic efficiency, and are more susceptible to pathogen infections (Alejandro et al., 2017). However, high Mn concentrations may be toxic to the plant. The toxic concentration of Mn is highly dependent on plant species and genotype (Fernando and Lynch, 2015). Excess Mn can inhibit the uptake and translocation of essential elements like Ca, Fe, P, and Mg (Yamaji et al., 2013), cause a decrease in photosynthetic rate (Lambers et al., 2015), and inhibit chlorophyll biosynthesis (Blamey et al., 2015).

http://www.aloki.hu ● ISSN 1589 1623 (Print) ● ISSN 1785 0037 (Online)
DOI: http://dx.doi.org/10.15666/aeer/2005_40114030

Fe is the second most abundant metal found in *Rhizophora* spp. leaves after Mn. Fe, like Mn, is involved in chlorophyll synthesis, and the cause of chlorosis (yellowing) at the leaf surface is associated with Fe deficiency (Yoneyama, 2021). Competition from other cations in the soil, such as calcium and manganese, may cause a lack of Fe uptake (Kathpalia and Bhatla, 2018). Because of the low redox potential of waterlogged soils, the concentration of soluble iron can increase by several orders of magnitude. Excessive Fe uptake is potentially toxic and can promote the formation of reactive oxygen-based radicals, which can damage vital cellular constituents via lipid peroxidation (Mezzaroba et al., 2019). According to Karimian et al. (2018), an increase in the concentration of available Fe in acidic or flooded soils can result in excessive Fe adsorption, often reaching toxic levels. Aside from that, the presence of organic matter, such as organic deposits, can increase Fe availability, presumably by supplying soluble complexing agents that interfere with fixation (Vardhan et al., 2019).

Among the heavy metals found in the sediments, Zn had the highest concentration. Zn is essential for cellular metabolism and can be regulated by organisms in their bodies (Chaiyara et al., 2013). Because of its environmental persistence, toxicity, and ability to be incorporated into food chains, zinc is regarded as a serious pollutant in aquatic ecosystems (Kishe and Machiwa, 2003). Mangrove plants were also known to absorb and accumulate heavy metals in tissues, with Zn mostly accumulating in the roots and less so in the leaves and stems (Kumar et al., 2010). This explains why zinc was mostly undetectable in the leaves of *Rhizophora* spp. in *Table 9*.

Conclusion

The chemical composition of organic deposits in this study have high concentration of Pb and Zn compared to the pervious study. The content of Pb and Cd in Tanjung Piai's organic deposit are higher than the European and American bio-waste limits. Zn > Pb > Cu > Fe > Cd > Mn were the heavy metal concentrations in the sediments in decreasing order. Fe and Mn fractionation show that these two metals are the most mobile and have the greatest availability. Both metals had high concentrations in leaf samples, indicating that they are easily transportable from sediment to plant. As a result, more research into ecological risk and human health risk assessment is needed to measure human and terrestrial animal exposure in the proximity of the mangrove forest.

Acknowledgements. The authors would like to acknowledge financial support from Forest Research Institute Malaysia (FRIM) for the financial support (GA016-2021).

REFERENCES

[1] Alejandro, S., Cailliatte, R., Alcon, C., Dirick, L., Domergue, F., Correia, D., Curie, C. (2017): Intracellular distribution of manganese by the trans-Golgi network transporter NRAMP2 is critical for photosynthesis and cellular redox homeostasis. – The Plant Cell 29(12): 3068-3084.

[2] Alvarez, E. A., Mochón, M. C., Sanchez, J., Rodríguez, M. T. (2002): Heavy metal extractable forms in sludge from wastewater treatment plants. – Chemosphere 47(7): 765-775.

http://www.aloki.hu ● ISSN 1589 1623 (Print) ● ISSN 1785 0037 (Online)
DOI: http://dx.doi.org/10.15666/aeer/2005_40114030

[3] Ariyanto, D., Gunawan, H., Puspitasari, D., Ningsih, S. S., Jayanegara, A., Hamim, H. (2019): The differences of the elements content in Rhizophora mucronata leaves from asahan regency, North Sumatra, Indonesia. – Polish J. Nat. Sci 34(4): 481-491.
[4] Blamey, F. P. C., Hernandez-Soriano, M. C., Cheng, M., Tang, C., Paterson, D. J., Lombi, E., ... Kopittke, P. M. (2015): Synchrotron-based techniques shed light on mechanisms of plant sensitivity and tolerance to high manganese in the root environment. – Plant Physiology 169(3): 2006-2020.
[5] Chaiyara, R., Ngoendee, M., Krautrachue, M. (2013): Accumulation of Cd, Cu, Pb and Zn in water, sediments, and mangrove crabs (Sesarma mederi) in the upper Gulf of Thailand. – Science Asia 39: 376-383.
[6] Charzyński, P., Plak, A., Hanaka, A. (2017): Influence of the soil sealing on the geoaccumulation index of heavy metals and various pollution factors. – Environmental Science and Pollution Research 24(5): 4801-4811.
[7] Choleva, T. G., Tsogas, G. Z., Vlessidis, A. G., Giokas, D. L. (2020): Development of a sequential extraction and speciation procedure for assessing the mobility and fractionation of metal nanoparticles in soils. – Environmental Pollution 263: 114407.
[8] Du, X., Gao, L., Xun, Y., Feng, L. (2020): Comparison of different sequential extraction procedures to identify and estimate bioavailability of arsenic fractions in soil. – Journal of Soils and Sediments 20(10): 3656-3668.
[9] Fagbote, E. O., Olanipekun, E. O. (2010): Speciation of heavy metals in soil of bitumen deposit impacted area of Western Nigeria. – Eur. J. Sci. Res. 47: 265-277.
[10] Fernando, D. R., Lynch, J. P. (2015): Manganese phytotoxicity: new light on an old problem. – Annals of Botany 116(3): 313-319.
[11] Hui, N. Y., Mohamed, M., Othman, M. N. A., Tokiman, L. (2019): Diversity and behaviour of mudskippers of Tanjung Piai, Pontian, Johor. – IOP Conference Series: Earth and Environmental Science 269(1): 012037.
[12] Karimian, N., Johnston, S. G., Burton, E. D. (2018): Iron and sulfur cycling in acid sulfate soil wetlands under dynamic redox conditions: a review. – Chemosphere 197: 803-816.
[13] Kathpalia, R., Bhatla, S. C. (2018): Plant Mineral Nutrition. – In: Bhatla, S. C., Lal, M. A. (eds.) Plant Physiology, Development and Metabolism. Springer, Singapore, pp. 37-81.
[14] Khosropour, E., Attarod, P., Shirvany, A., Pypker, T. G., Bayramzadeh, V., Hakimi, L., Moeinaddini, M. (2019): Response of Platanus orientalis leaves to urban pollution by heavy metals. – Journal of Forestry Research 30(4): 1437-1445.
[15] Kishe, M. A., Machiwa, J. F. (2003): Distribution of heavy metals in sediments of Mwanza Gulf of Lake Victoria, Tanzania. – Environment International 28: 619-625.
[16] Kormoker, T., Proshad, R., Islam, S., Ahmed, S., Chandra, K., Uddin, M., Rahman, M. (2021): Toxic metals in agricultural soils near the industrial areas of Bangladesh: ecological and human health risk assessment. – Toxin Reviews 40(4): 1135-1154.
[17] Kumar, J. I. N., Sajish, P. R., Kumar, R. N., George, B., Viyol, S. (2010): An assessment of the accumulation potential of lead (Pb), zinc (Zn) and cadmium (Cd) by Avicennia marina (Forssk.) Vierh. in Vamleshwar Mangroves near Narmada Estuary, West Coast of Gujarat, India. – World Journal of Fish and Marine Sciences 2(5): 450-454.
[18] Kumar, S., Prasad, S., Yadav, K. K., Shrivastava, M., Gupta, N., Nagar, S., ... Malav, L. C. (2019): Hazardous heavy metals contamination of vegetables and food chain: role of sustainable remediation approaches. A review. – Environmental Research 179: 108792.
[19] Kunasekaran, P., Rozak, N. I. N., Adam, S. M., Shuib, A. (2018): Perception of local communities on the indicators of governance in Tanjung Piai National Park. – International Journal of Business and Society 19(S1): 79-87.
[20] Lambers, H., Hayes, P. E., Laliberte, E., Oliveira, R. S., Turner, B. L. (2015): Leaf manganese accumulation and phosphorus-acquisition efficiency. – Trends in Plant Science 20(2): 83-90.

http://www.aloki.hu ● ISSN 1589 1623 (Print) ● ISSN 1785 0037 (Online)
DOI: http://dx.doi.org/10.15666/aeer/2005_40114030

[21] McLaren. R. G., Kanjanapa. K., Navasumrit, P., Gooneratne. S. R. and Ruchirawat, M. (2004): Cadmium in the water and sediments of the Chao Phraya River and associated waterways, Bangkok, Thailand. – Water, Air, Soil Pollut. 154: 385-398.
[22] Mezzaroba, L., Alfieri, D. F., Simão, A. N. C., Reiche, E. M. V. (2019): The role of zinc, copper, manganese and iron in neurodegenerative diseases. – Neurotoxicology 74: 230-241.
[23] Namieśnik, J., Rabajczyk, A. (2010): The speciation and physico-chemical forms of metals in surface waters and sediments. – Chemical Speciation & Bioavailability 22(1): 1-24.
[24] Nath, B., Chaudhuri, P., Birch, G. (2014): Assessment of biotic response to heavy metal contamination in Avicennia marina mangrove ecosystems in Sydney Estuary, Australia. – Ecotoxicology and Environmental Safety 107: 284-290.
[25] Onrizal, O., Amelia, R., Amri, K., Sulistiyono, N., Mansor, M. (2019): Stand structure and diversity of restored mangroves at abandoned pond in eastern coast of North Sumatra. – IOP Conference Series: Earth and Environmental Science 305(1): 012050.
[26] Panda, D., Subramanian, V., Panigrahy, R. C. (1995): Geochemical fractionation of heavy metals in Chilka Lake (east coast of India)—a tropical coastal lagoon. – Environmental Geology 26(4): 199-210.
[27] Peng, S. H., Wang, W. X., Li, X., Yen, Y. F. (2004): Metal partitioning in river sediments measured by sequential extraction and biomimetic approaches. – Chemosphere 57(8): 839-851.
[28] Rauret, G. (1998): Extraction procedures for the determination of heavy metals in contaminated soil and sediment. – Talanta 46(3): 449-455.
[29] Sarath, N. G., Puthur, J. T. (2021): Heavy metal pollution assessment in a mangrove ecosystem scheduled as a community reserve. – Wetlands Ecology and Management 29(5): 719-730.
[30] Saveyn, H., Eder, P. (2014): End-of-Waste Criteria for Biodegradable Waste Subjected to Biological Treatment (Compost & Digestate): Technical Proposals. – Publications Office of the European Union, Luxembourg.
[31] Singh, M., Müller, G., Singh, I. B. (2003): Geogenic distribution and baseline concentration of heavy metals in sediments of the Ganges River, India. – Journal of Geochemical Exploration 80(1): 1-17.
[32] Strayer, D. L. (2014): Understanding how nutrient cycles and freshwater mussels (Unionoida) affect one another. – Hydrobiologia 735(1): 277-292.
[33] Tessier, A., Campbell, P. G., Bisson, M., (1979): Sequential extraction procedure for the speciation of particulate trace metals. – Anal. Chem. 51(7): 844-851.
[34] Vardhan, K. H., Kumar, P. S., Panda, R. C. (2019): A review on heavy metal pollution, toxicity and remedial measures: current trends and future perspectives. – Journal of Molecular Liquids 290: 111197.
[35] Violante, A., Cozzolino, V., Perelomov, L., Caporale, A. G., Pigna, M. (2010): Mobility and bioavailability of heavy metals and metalloids in soil environments. – Journal of Soil Science and Plant Nutrition 10(3): 268-292.
[36] Wan Rasidah, K., Mohd Zaki, M. I., Mohd Fakhri, I. (2015): Muddy Substrates of Malaysia Coast. – Institut Penyelidikan Perhutanan Malaysia, Kepong.
[37] Yamaji, N., Sasaki, A., Xia, J. X., Yokosho, K., Ma, J. F. (2013): A node-based switch for preferential distribution of manganese in rice. – Nature Communications 4(1): 1-11.
[38] Yoneyama, T. (2021): Iron delivery to the growing leaves associated with leaf chlorosis in mugineic acid family phytosiderophores-generating graminaceous crops. – Soil Science and Plant Nutrition 1-12.
[39] Zhang, M. K., Liu, Z. Y., Wang, H. (2010): Use of single extraction methods to predict bioavailability of heavy metals in polluted soils to rice. – Communications in Soil Science and Plant Analysis 41(7): 820-831.

http://www.aloki.hu ● ISSN 1589 1623 (Print) ● ISSN 1785 0037 (Online)
DOI: http://dx.doi.org/10.15666/aeer/2005_40114030

[40] Zhang, C., Yu, Z. G., Zeng, G. M., Jiang, M., Yang, Z. Z., Cui, F., ... Hu, L. (2014): Effects of sediment geochemical properties on heavy metal bioavailability. – Environment International 73: 270-281.
[41] Zimmerman, A. J., Weindorf, D. C. (2010): Heavy metal and trace metal analysis in soil by sequential extraction: a review of procedures. – Int. J. Analyt. Chem. 1-8. DOI: 10.1155/2010/387803.

http://www.aloki.hu ● ISSN 1589 1623 (Print) ● ISSN 1785 0037 (Online)
DOI: http://dx.doi.org/10.15666/aeer/2005_40114030

A NEW VARIANT OF *bla*SHV HAS BEEN REVEALED IN *KLEBSIELLA PNEUMONIA* IN SULAIMANI/IRAQ

HAMA SOOR, T. A.

College of Health and Medical Technology, Sulaimani Polytechnic University, Sulaimani, Iraq (e-mail: taib.ahmed@spu.edu.iq)

Medical Laboratory Analysis, Cihan University-Sulaimaniya, Sulaimani, Iraq

(Received 22nd Mar 2022; accepted 11th Jul 2022)

Abstract. In recent years, a large number of multidrug-resistant *Klebsiella pneumonia* has been revealed bearing different variants of *bla*SHV. In the current study, antibiotic sensitivity test and the rate and molecular characterization of three common beta-lactam resistance genes, *bla*SHV, *bla*OXA, and *bla*CTX were investigated in *K. pneumonia* isolated from layer chickens in Sulaimani city/Iraq. Furthermore, the molecular characterization of *bla*SHV was studied. The highest rate of resistance was to ceftazidime (92.9%) and cefotaxime (82.3%), while the lowest rate was found against meropenem (4.7) and imipenem (8.2%). Among 85 isolates of *K. pneumonia,* 33 isolates (33.8%) had CTX gene which is the highest rate among the three resistance genes. The second most common resistance gene was SHV gene, 22.3%, and OXA gene showed the lowest rate 11.7%. After PCR amplification and sequencing, it was revealed that a novel variant of *bla*SHV, SHV-Suly213 was recovered from *K. pneumonia* and it exists in the studied area. The new variant contains a hybrid mutation which is composed of a mixture of nucleotide sequence of previously known *bla*SHV, SHV-1 and SHV-213. Phylogenetic tree shows that the novel SHV is more closely related to SHV-213; therefore, it was named SHV-Suly213. The bacteria were resistant to ceftriaxone and cefotaxime, but meropenem was still active against the bacteria. In conclusion, the current study discovered a new variant of *bla*SHV, SHV-Suly213. The resistance gene compromised of mixed sequences (hybrid) of both SHV-1 and SHV-2113 that contain three nucleotide mutations in comparison to them. The bacteria are resistant to many beta-lactam antibiotics such as ceftriaxone and cefotaxime, but not meropenem.
Keywords: *bacteria, beta-lactamase resistance genes, antibiotic sensitivity, blaSHV, novel mutation*

Introduction

Beta-lactam antibiotics are counted as a first line of antibiotics against gram negative bacteria, but recently broad-spectrum resistances have developed against them due to beta-lactamase resistance genes. In the last decades, diverse types of beta-lactamases have been spotted, and they are different in their response to different classes of beta lactam antibiotics; therefore, new classification is required for the new types of beta lactamases (Ambler, 1980; Liakopoulos et al., 2016).

The *bla*SHV is one member of beta-lactamase resistance genes and it is mostly found in *Klebsiella pneumonia* and sometimes in *Escherichia coli* (*E. coli*). There are various types of SHV beta-lactamases, and they are different in their responses to beta-lactam antibiotics due to amino acid mutations and replacement in their structures. SHV1 is a beta-lactamase enzyme that was discovered in *E. coli* for the first time in 1972 (Pitton, 1972) and it has been found recently that it is mostly distributed in *K. pneumonia* and other members of Enterobacteria (Rahim et al., 2020; Shaikh et al., 2014). SHV1 is resistant against different types of Penicillin antibiotics including ampicillin and pipercillins (Livermore, 1995; Matthew et al., 1979).

http://www.aloki.hu ● ISSN 1589 1623 (Print) ● ISSN 1785 0037 (Online)
DOI: http://dx.doi.org/10.15666/aeer/2005_40314038

It is believed that the ancestor of SHV1 is more likely expressed from chromosomal gene that is isolated from *Klebsiella pneumonia* in feces of neonate (Hæggman et al., 1997) and its then diffused to bacterial plasmid and distributed among Enterobacteriaseae (Barthélémy et al., 1988; Shaikh et al., 2014).

Materials and methods

Sample collection and bacterial isolation

Eighty-five samples were taken and analyzed from layer chicken viscera from local slaughter houses delivered form different poultry farms of Sulaimani city in November 2019. The samples were cultured on differential media (MacConkey agar, and Eosin methylene blue) (Accumedia LAB, Neogene Culture Media, Heywood, UK), and then incubated at 37 °C for 16 h. The isolates of *Klebsiella* were further identified and confirmed through biochemical tests, such as IMViC test (Harley and Prescott, 2002) and the final confirmation was done by amplification of 16S-23S ITS (130 bp) gene using a set of primer specific to *K. pneumonia.*

Antimicrobial susceptibility testing

Antimicrobial susceptibility testing was performed for the isolates by disc diffusion test as defined by the Clinical Laboratory Standard Institute (CLSI) guidelines for the following beta lactam antibiotics, amoxicillin (AX 25 μg), amoxicillin-clavulanic acid (AMC 30 μg), oxacillin (OX 1 μg), meropenem (MEM 10 μg), ceftriaxone (CRO 30 μg) and cefotaxime (CTX 30 μg), Imipenem (IMP10 μg), Cefixime (FX 5 μg), ceftazidime (CAZ 30 μg) (Bioanalyse, Ankara, Turkey).

Molecular identification of beta-lactamase genes, SHV, CTX, and OXA

Crude DNA of bacteria was extracted by boiling fresh colony of bacteria in 100 ul of distilled water for 15 min. *bla*SHV (800 bp), *bla*OXA (610 bp), and *bla*CTX (550 bp) genes were PCR amplified using specific primers according to the procedure and protocol described by (Ahmed et al., 2007, 2009). The PCR DNA product was then visualized under blue light, cut and gel purified after resolving on 1.5% DNA agarose gel using SmartDoc 2.0 Imaging System (Accuris, NJ, USA).

Sequence analysis

*bla*SHV gene from ten bacterial isolates were sequenced. The isolates were chosen from different poultry farms and we avoided using many repetition of the same poultry farm. The amplicons of different isolates of *Kleibsella* were sequenced through Sanger sequencing on ABI-3730XL capillary machine (Macrogen Inc., South Korea). One of the gene sequences was deposited in to GenBank National Center for Biotechnology Information (NCBI) through Bankit (Benson et al., 2015) with the accession number of OK376493.

NCBI BLASTn search tool (http://www.ncbi.nlm.nih.gov/) was used to blast the sequences and find the diversity of the gene. The multi-sequence alignment was carried out by ClustalW multi alignment tool. A phylogenic tree was built for the sequences and retrieved sequences of NCBI by the neighbor-joining (NJ) program (Phylogeny.fr) (Dereeper et al., 2010).

http://www.aloki.hu ● ISSN 1589 1623 (Print) ● ISSN 1785 0037 (Online)
DOI: http://dx.doi.org/10.15666/aeer/2005_40314038

Results

Isolation of klebsiella and antibiotic sensitivity testing

Eighty-five isolates of *K. pneumonia* were taken from viscera of layer chicken after slaughtering originated from the same local farm. The samples were taken by bacteriological swabs and streaked out on MacCkonkey and Eosin methylene blue agar. Then the bacteria were further identified by catalase, oxidase and common test for Enterobacteriaseae bacteria, IMViC (Indole test, Methyl red test, Voges-Proskauer test, and Citrate utilization test). The final confirmation was done by amplification of 16S-23S ITS gene using a set of primer specific to *K. pneumonia* (*Fig. 2*).

K. pneumonia isolates were analyzed to determine their antibiotic resistance pattern against nine types of beta-lactam antimicrobials. The highest rate of resistance was to ceftazidime (92.9%) and cefotaxime (82.3%), while the lowest rate was found against meropenem (4.7%) and imepenem (8.2%) (*Fig. 1A*).

The isolates that harbored SHV gene containing new mutations were resistant to oxacillin, amoxicillin, cefotaxime, and ceftriaxone, but they were sensitive to amoxicillin-clavulanic acid, cefixime, imipenem and meropenem.

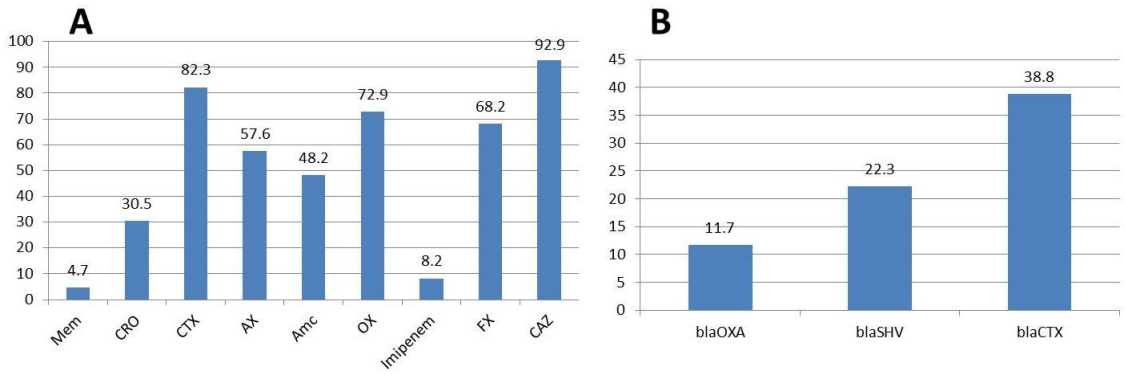

Figure 1. *Antibiotic resistance pattern and the rate of beta-lactam resistance genes in K. pneumonia isolates in different samples of layer chickens. (A) The percentage of resistant K. pneumonia isolates against nine beta-lactam antibiotics. (B) The rate of different beta-lactam resistance genes in K. pneumonia isolates*

Investigation of resistance gene, blaSHV, blaOXA and blaCTX

To investigate the variants of *bla*SHV, *bla*OXA and *bla*CTX, specific primers were used to amplify each of the resistance genes using conventional PCR techniques (*Fig. 2B*). Among 85 isolates of *K. pneumonia,* 33 isolates (33.8%) had CTX gene which is the highest rate among the three resistance genes. The second most common resistance gene was SHV gene which was found in 19 isolates (22.3%) and OXA gene showed the lowest rate which was discovered in 10 samples (11.7%) (*Fig. 1B*).

Ten of SHV genes were sequenced using Sanger sequencing. The sequences of the resulted genes were blasted and aligned to the available sequences on the website, NCBI. The results showed that the sequence of all studied *bla*SHV contain three nucleotide mutations in comparison to two previously found *bla*SHV, SHV1 and SHV-213. During investigation the *bla*SHV gene via sequencing and phylogenetic tree, a novel allele was discovered (*Figs. 3* and *4*) and named as *bla*SHV-Suly213 and the sequence was deposited into NCBI with accession number (OK376493).

http://www.aloki.hu ● ISSN 1589 1623 (Print) ● ISSN 1785 0037 (Online)
DOI: http://dx.doi.org/10.15666/aeer/2005_40314038

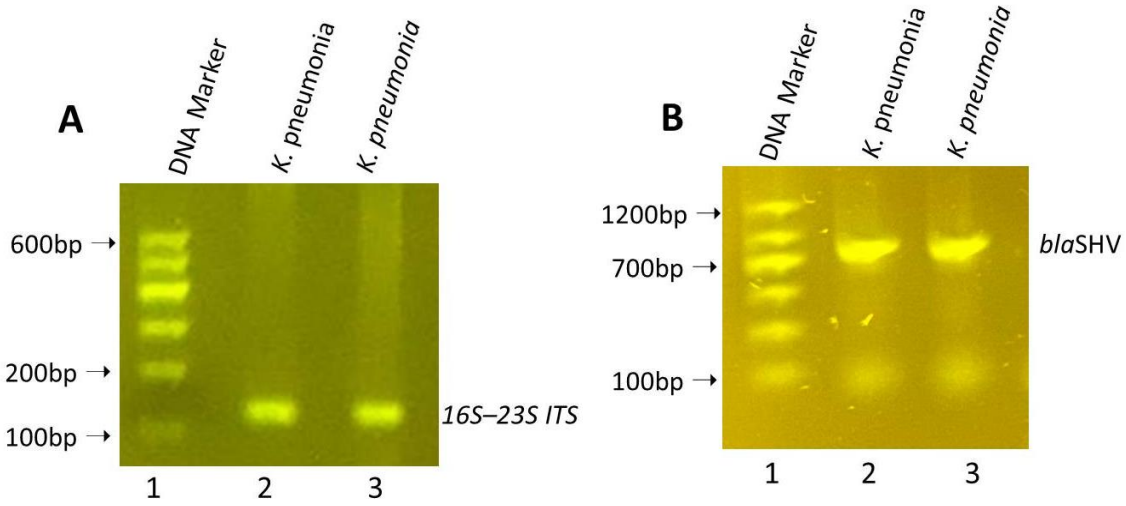

Figure 2. *PCR amplification of 16S-23S ITS and blaSHV gene of K. pneumonia. (A) PCR confirmation of K. pneumonia using specific primer to amplify16S-23S ITS gene. (B) PCR amplification of beta-lactamase resistance genes, blaSHV are shown in lane 2 and 3 that recovered from nineteen isolates of Kleibsella*

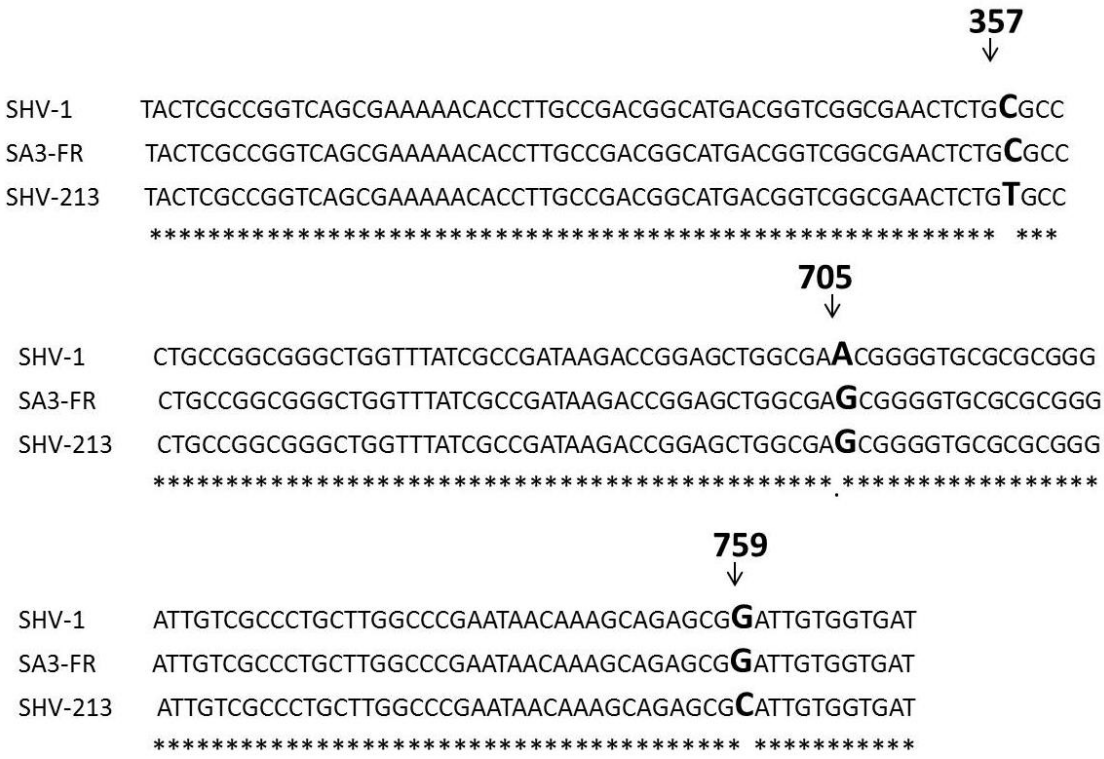

Figure 3. *Multiple sequence alignment of blaSHV gene recovered from K. pneumonia. SHV gene in K. pneumonia isolated from layer chicken in Sulaimaniyah in comparison with published SHV-1 and SHV-213 from GenBank*

In comparison to SHV-213, the gene of the current study contains two mutations which are located at the nucleotide number 357 starting from the starting codon and at position number 759 from the starting codon where guanine replaced by cytosine. In

http://www.aloki.hu ● ISSN 1589 1623 (Print) ● ISSN 1785 0037 (Online)
DOI: http://dx.doi.org/10.15666/aeer/2005_40314038

comparison to SHV1, it contains a mutation at locations number 705 where guanine replaced by adenine (*Fig. 3*). The diversity of the gene was compared to different related sequences available online. 11 gene sequences of SHV enzyme were taken and put into a phylogenetic tree to find the diversity of the gene found in this study (*Fig. 4*).

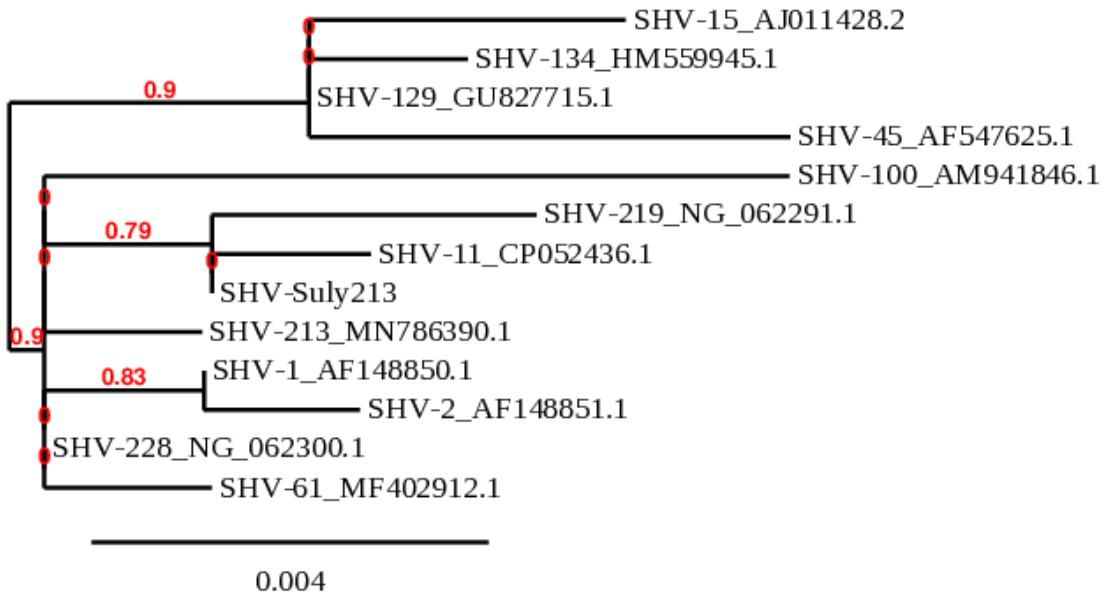

Figure 4. *Phylogenic analysis of SHV-Suly213. Phylogenetic tree was built to the sequence of SHV-Suly213 in comparison to very closely related sequences and 11 available sequences retrieved from NCBI Blast*

Discussion

Antibiotics are strong agents still used to treat bacterial infections in human and animals and beta-lactam antibiotic is known as frontline protection antimicrobials against bacterial infection (Bradford, 2001). On the other hand, bacterial resistance to common antibiotics causes difficulties in treatment and high morbidity and mortality in animal and poultry (Grover et al., 2013). Local and wild birds bearing resistant bacteria may spread these bacteria into the environment and to human (Peirano et al., 2011; Alaa et al., 2020). Therefore, antibiotic resistance phenotype of *K. pneumonia* to nine common beta-lactam antibiotics was tested including amoxicillin-clavulanic acid, amoxicillin, oxacillin, ceftriaxone, meropenem, ceftazidim, and cefotaxime. The highest rate of resistance was to ceftazidime and cefotaxime, while the lowest rate was found against meropenem and imepenem. Therefore, imipenem and merpenem remains as the most active antibiotic against *K. pneumonia*, but the bacteria was resistant to most antibiotics at an alarming level. The distribution of resistant *K. pneumonia* to beta-lactam antibiotics is similarly highly distributed in different countries. The result of our studies agrees with the study in Egypt where highly resistant bacteria is recorded against beta-lactam antibiotics (Abdel-Rhman SH, 2020) and similar result was also recorded in Turkey (Aktas et al., 2002).

Resistance genes were found in most of the isolates in high rates. Among 85 isolates of *K. pneumonia,* 33 isolates (33.8%) had CTX gene which is the highest rate among

http://www.aloki.hu ● ISSN 1589 1623 (Print) ● ISSN 1785 0037 (Online)
DOI: http://dx.doi.org/10.15666/aeer/2005_40314038

three resistance genes. The second most common resistance gene was SHV gene which was found in 19 isolates (22.3%) and the lowest rate was OXA gene which was discovered in 10 samples (11.7%) (*Fig. 1B*). This indicates that bacteria harboring resistance gene are endemic, and they are circulating in the hosts of the study area. The high rate of beta-lactamase genes in *K. pneumonia* is not recorded only in this studied area, but also in other countries such as in Brazil (Ferreira et al., 2019). The isolates harboring SHV genes containing new mutations were highly resistant to oxacillin, amoxicillin, cefotaxime, and ceftriaxone, but they were sensitive to amoxicillin-clavulanic acid. Meropenem and imipenem are still the most active antibiotics against *K. pneumonia* and the bacteria were completely sensitive to the latter antibiotic.

Finally, the interesting result of this study, other than antibacterial resistance pattern of *K. pneumonia* is finding the novel *bla*SHV gene variant which is different from all previously discovered variants of *bla*SHV. The bacteria containing new SHV gene variants recovered from ten isolates of *K. pneumonia* harboring SHV genes. The bacteria were isolated from the viscera of layer chicken after slaughtering in local slaughterhouses. The novel allele was named *bla*SHV-Suly213 because it is more closely related to *bla*SHV213 variant (Aung et al., 2021) (*Fig. 3*). The new variants contain three nucleotide mutations in comparison to both SHV-1 (CP052436.1) and SHV-213 (*Fig. 2*). In comparison to SHV-213, the new gene contains two mutations which are located at the nucleotide number 357 starting from the starting codon sequence and at position number 759 from the starting codon sequence where guanine is replaced by cytosine. In comparison to SHV1, it contains one mutation at locations number 705 where guanine is replaced by adenine (*Fig. 2*). The diversity of the gene was compared to different related sequences available online. 11 different gene sequences of SHV enzyme were taken and put into a phylogenetic tree to find the diversity of the gene found in this study and it was revealed that the novel allele is more closely related to SHV-213 and SHV-1 (*Fig. 3*).

Interestingly, all three mutations are silent mutations. The nucleotide number 357 thymine was changed to cytosine (TGT/TGC) and both codons translate to the same amino acid, cysteine. The second mutation at the position number 705 where adenine is replaced by guanine (GAA/GAG) and both codons generate the same amino acid, glutamate. The third mutation, cytosine is replaced by guanine at position number 759 (CGC/CGG) and both codons make arginine. Nucleotides have been mutated but the amino acid sequence and open reading frame remained intact. Therefore, the mutations may not be advantageous for the bacteria, but the strategy of the bacteria to have these mutations and the reason of changing these nucleotides remains unclear.

Conclusion

In summary, the current study analyzed the molecular study of antibiotic resistance of clinical isolates, *K. pneumonia* originated from layer chicken in Sulaimani city. The data discovered a new variant of *bla*SHV, SHV-Suly213. The resistance gene compromised mixed sequences (hybrid) of both SHV-1 and SHV-213 that contain three nucleotide mutations. The bacteria are resistant to ceftriaxone, and cefotaxime, but not meropenem. These findings show the genetic diversity of beta lactamase gene, *bla*SHV and generation of new variants of SHV genes in bacteria generated through periodic mutations.

http://www.aloki.hu ● ISSN 1589 1623 (Print) ● ISSN 1785 0037 (Online)
DOI: http://dx.doi.org/10.15666/aeer/2005_40314038

REFERENCES

[1] Abdel-Rhman S. H. (2020): Characterization of β-lactam resistance in K. pneumoniae associated with ready-to-eat processed meat in Egypt. – PLoS ONE 15(9): e0238747. https://doi.org/10.1371.

[2] Ahmed, A. M., Motoi, Y., Sato, M., Maruyama, A., Watanabe, H., Fukumoto, Y., Shimamoto, T. (2007): Zoo animals as reservoirs of gram-negative bacteria harboring integrons and antimicrobial resistance genes. – Applied and Environmental Microbiology 73(20): 6686-6690.

[3] Ahmed, A. M., Shimabukuro, H., Shimamoto, T. (2009): Isolation and molecular characterization of multidrug-resistant strains of *Escherichia coli* and salmonella from retail chicken meat in Japan. – Journal of Food Science 74(7): 405-410.

[4] Aktas E., Yigit N., Yazgi H., Ayyildiz A. (2002): Detection of Antimicrobial Resistance and Extended-spectrum β-Lactamase Production in Klebsiella Pneumoniae Strains from Infected Neonates. – The Journal of International Medical Research 30: 445 – 448.

[5] Alaa et al. (2020): The antibiotic resistance pattern and molecular characterization of bla CTX and bla TEM genes of *E. Coli* isolated from different hosts based on the rate of antibiotic consumption in Sulaymaniyah/Iraq. – Applied Ecology and Environmental Research 18(5): 6025-6040.

[6] Ambler, R. P. (1980): The structure of beta-lactamases. – Philosophical Transactions of the Royal Society of London. Series B, Biological Sciences 289(1036): 321-331.

[7] Aung, M. S., Win, N. C., San, N., Hlaing, M. S., Myint, Y. Y., Thu, P. P., Aung, M. T., et al. (2021): Prevalence of extended-spectrum beta-lactamase/carbapenemase genes and quinolone-resistance determinants in *Klebsiella pneumoniae* clinical isolates from respiratory infections in Myanmar. – Microbial Drug Resistance 27(1): 36-43.

[8] Barthélémy, M., Peduzzi, J., Labia, R. (1988): Complete amino acid sequence of p453-plasmid-mediated PIT-2 beta-lactamase (SHV-1). – The Biochemical Journal 251(1): 73-79.

[9] Benson, D. A., Clark, K., Karsch-Mizrachi, I., Lipman, D. J., Ostell, J., Sayers, E. W. (2015): GenBank. – Nucleic Acids Research 43(database issue): D30-5.

[10] Bradford, P. A. (2001): Extended-spectrum lactamases in the 21st century: characterization, epidemiology, and detection of this important resistance threat. – Clinical Microbiology Reviews14(4): 933-951.

[11] Dereeper, A., Audic, S., Claverie, J. M., Blanc, G. (2010): BLAST-EXPLORER helps you building datasets for phylogenetic analysis. – BMC Evolutionary Biology 10(1): 8-13.

[12] Ferreira H., Ribeiro A., Silva R., Cavaco-Paulo A., Pharm. J. (2019): High prevalence of multidrug-resistant Klebsiella pneumoniae harboring several virulence and b-lactamase encoding genes in a Brazilian intensive care unit. – Drug Delivery Res. 4: 1000139.

[13] Grover, N., Sahni, A. K., Bhattacharya, S. (2013): Therapeutic challenges of ESBLS and Ampc beta-lactamase producers in a tertiary care center. – Medical Journal Armed Forces India 69(1): 4-10.

[14] Hæggman, S., Löfdahl, S., Burman, L. G. (1997): An allelic variant of the chromosomal gene for class A β-lactamase K2, specific for *Klebsiella pneumoniae*, is the ancestor of SHV-1. – Antimicrobial Agents and Chemotherapy 41(12): 2705-2709.

[15] Harley, J. P., Prescott, L. M. (2002): Laboratory Exercises in Microbiology. 5th Ed. – McGraw-Hill Publishers, Boston, MA.

[16] Liakopoulos, A., Mevius, D., Ceccarelli, D. (2016): A review of SHV extended-spectrum β-lactamases: neglected yet ubiquitous. – Frontiers in Microbiology 7(Sep). https://doi.org/10.3389/fmicb.2016.01374.

[17] Livermore, D. M. (1995): beta-Lactamases in laboratory and clinical resistance. – Clin Microbiol Rev 8(4): 557-584.

http://www.aloki.hu ● ISSN 1589 1623 (Print) ● ISSN 1785 0037 (Online)
DOI: http://dx.doi.org/10.15666/aeer/2005_40314038

[18] Matthew, M., Hedges, R. W., Smith, J. T. (1979): Types of β-lactamase determined by plasmids in gram-negative bacteria. – Journal of Bacteriology 138(3): 657-662.
[19] Peirano, G., Asensi, M. D., Pitondo-Silva, A., Pitout, J. D. D. (2011): Molecular characteristics of extended-spectrum β-lactamase-producing *Escherichia coli* from Rio de Janeiro, Brazil. – Clinical Microbiology and Infection 17(7): 1039-1043.
[20] Pitton, J. S. (1972): Mechanisms of bacterial resistance to antibiotics. Ergebnisse der Physiologie Review of Physiology 65: 15-93. Doi: 10.1007/3-540-05814-1_2.
[21] Rahim, A., Ahmadissa, S., Muhamad, L., Hama Soor, T. (2020): Antibiotic resistance: current global issue and future challenges. – Microbial Biosystems 5(2): 29-68.
[22] Shaikh, S., Fatima, J., Shakil, S., Mohd, S., Rizvi, D., Kamal, M. A. (2014): Antibiotic Resistance and extended spectrum beta-lactamases: types, epidemiology and treatment. – Saudi Journal of Biological Sciences, King Saud University. https://doi.org/10.1016/j.sjbs.2014.08.002.

http://www.aloki.hu ● ISSN 1589 1623 (Print) ● ISSN 1785 0037 (Online)
DOI: http://dx.doi.org/10.15666/aeer/2005_40314038

NUTRIENT RESPONSES OF *CAREX SCHMIDTII* TO CONSECUTIVE DROUGHT AND RE-FLOODING EPISODES IN SEMI-ARID WETLANDS: IMPLICATIONS FOR TUSSOCK RESTORATION

ZHANG, D. J.[1*] – XIA, J. B.[1] – SUN, J. K.[1] – MA, J. Z.[1] – ZHAO, D. D.[1] – DUAN, D. X.[1] – WANG, X. H.[2] – TONG, S. Z.[3*]

[1]*Shandong Key Laboratory of Eco-Environmental Science for the Yellow River Delta, Binzhou University, Binzhou 256603, Shandong Province, China*

[2]*The Institute for Advanced Study of Coastal Ecology, Key Laboratory of Ecological Restoration and Conservation of Coastsal Wetlands in Universities of Shandong, Ludong University, Yanta, 264025, Shandong Province, China*

[3]*Northeast Institute of Geography and Agroecology, Chinese Academy of Sciences, Changchun 130102, Jilin Province, China*

**Corresponding authors*
e-mail: zhangdongjie14@mails.ucas.ac.cn; tongshouzheng@iga.ac.cn

(Received 26th Mar 2022; accepted 11th Jul 2022)

Abstract. The regulation mechanism of wetland plants in response to consecutive drought (D) and re-flooding (RT) events can be identified via nutrient responses. Nutrient responses of *Carex schmidtii* were tested using a simulation experiment with five treatments: D, wetting (W) and RT resulted in *C. schmidtii* being re-flooded after 30, 40 and 60 days of drought. D and RT treatments partly affected nutrient stoichiometry of *C. schmidtii*. Plant nutrient stoichiometry experienced a shift of adaption from drought to flooding and making part or full recoveries after RT with reference to D and W treatments. Plant P concentration had a negative relationship with N:K ratio. D and RT effects on plant trade-offs and scaling exponents of *C. schmidtii* were profound; the scaling exponent of P~N increased with initial re-flooding time, while that of K~N decreased. Although nutrient trade-offs in D gradually differed from W and RT over time, the nutrient trade-offs of RT recovered with reference to W. The D and RT were recorded to contribute to nutrient flexibility of *C. schmidtii*; however, strong internal stability of stoichiometric relationships effectively relieved changes in plant nutrient stoichiometry. The findings aid our understanding of nutrient responses of *C. schmidtii* to D and RT.
Keywords: *nutrient trade-offs, hydrological changes, Carex schmidtii tussocks, Momoge wetland, wetland restoration, semi-arid environments*

Introduction

Nutrient homeostasis or flexibility focused on nutrient stoichiometry and stoichiometric relationships can reveal the internal mechanisms of wetland plants in response to environmental fluctuations (Elser et al., 2000; Güsewell et al., 2003; Sistla and Schimel, 2012; Julian et al., 2020). Nutrient homeostatic or flexibility are closely associated with plant growth strategy and adaption, by which plants regulate the underlying physiological processes and biochemical allocations in response to environmental fluctuations (Yu et al., 2015; Hu et al., 2018; Li et al., 2018). Nutrient trade-offs are the dynamic equilibrium of nutrients and their ratios in organisms, regulating their nutrient stoichiometry and stoichiometric relationship, thereby affecting nutrient homeostasis or flexibility (Sistla and Schimel, 2012; Corrales-Carvajal et al., 2016; Zhang et al., 2021). As nutrient trade-offs

http://www.aloki.hu ● ISSN 1589 1623 (Print) ● ISSN 1785 0037 (Online)
DOI: http://dx.doi.org/10.15666/aeer/2005_40394060

are a response to the degree of coupling effects of multi nutrient stoichiometry and their environment on plant growth and eco-physiological processes (Wright et al., 2004; Yan et al., 2019), nutrient homeostasis or flexibility relying on nutrient trade-offs are therefore widely applied to solve related problems in ecological systems. However, whether nutrient homeostasis and flexibility together regulate plant growth and nutrient responses by nutrient trade-offs is currently unclear.

Nutrient stoichiometry and responses of wetland plants with respect to nutrient trade-offs and homeostasis or flexibility are important factors regulating the adaptability of plants to hydrological fluctuation (Sistla and Schimel, 2012; Rong et al., 2015; Mariotte et al., 2017). Nitrogen (N), phosphorus (P) and potassium (K) are the abundant essential elements in higher plants; these nutrients are also common nutrients supporting plant growth, having a strong relationship to individual performance (Wright et al., 2011; Chiwa et al., 2019). N and P are also important sources for the synthesis of photosynthetic pigments, proteins and nuclei (Wan et al., 2020; Huang et a., 2021; Zhang et al., 2019a). K plays a vital role in the production, transportation and storage processes of carbohydrates, it promotes protein synthesis and activates certain enzymes or coenzymes (Chiwa et al., 2019; Gierth and Mäser, 2007; Liu et al., 2021). Additionally, ratios of N, P and K are proxies for stoichiometric relationships regulating plant nutrient acquisition, transportation and availability, as well as being used to indicate nutrient limitation of species and ecosystems (Güsewell et al., 2003; Pan et al., 2020; Zhang et al., 2021). Whether nutrients and their ratios vary within a certain range is closely related to nutrient homeostasis or flexibility (Sistla and Schimel, 2012; Julian et al., 2020). Previous studies indicated a general pattern of nutrient stoichiometry under multi environments, highlighting that nutrient homeostasis relieved environmental fluctuation effects on plants (Reich et al., 2010; Tian et al., 2018; Hu et al., 2021). Therefore, examining nutrient stoichiometry and responses is an effective method to help understand the adaption of plant functional trait adaptation under environmental fluctuations. However, the majority of studies have only focused on nutrient performance across species on global or zonal scales, few investigations have been undertaken on the nutrient response of wetland plants at a single species level.

In a wetland system, hydrological fluctuations with changes in flooding depth, frequency and duration are master factors controlling plant growth and eco-physiological processes (Casanova and Brock, 2000; Zhang et al., 2019a). Extreme hydrological fluctuations due to changes from consecutive drought episodes to flooding events have complex effects on plant growth and nutrient trade-offs. These effects influence community structure and vegetation patterns in wetlands around the world, especially in semi-arid zones (Li et al., 2017b; Wen et al., 2017; Zhang et al., 2019b). Although it has been previously shown that initial flooding results in a decrease of plant N, P and K concentrations in plant leaves, flooding events also result in an increase of nutrient concentration in roots (Chen et al., 2005). Concentration of N and P in plant shoots of submersed macrophytes significantly decreased along a water depth gradient, while the N:P ratio increased (Li et al., 2015). Chen et al. (2020) reported species-specific responses of leaf N and P stoichiometry to flooding duration at the intra-species level, other than at the inter-species level. Additionally, leaf N and P concentrations of wetland plants significantly increased with flooding duration, while their ratio decreased (Chen et al., 2020). Recently, Zhang et al. (2021) recorded hydrological fluctuations to have complex effects on the dynamic of nutrient response and stoichiometric relationships of wetland plants. However, the majority of studies focused on plant

http://www.aloki.hu ● ISSN 1589 1623 (Print) ● ISSN 1785 0037 (Online)
DOI: http://dx.doi.org/10.15666/aeer/2005_40394060

growth performance under hydrological fluctuations (Hamdan et al., 2010; Garssen et al., 2015; Yuan et al., 2019); few investigations have examined nutrient response and trade-offs of wetland plants to hydrological fluctuations, especially re-flooding conditions after consecutive drought episodes.

Carex schmidtii is a native tussock-forming species with hydrological fluctuation tolerance, contributing to the wide distribution of tussocks in riparian wetlands and mountainous marshes in north temperate climates (Qi et al., 2021a; Zhang et al., 2019a). *C. schmidtii* tussocks have an abundant root system, facilitated to absorb and conserve nutrients in biomass and the hummocks (Lawrence et al., 2013; Wang et al., 2019a). Due to climate changes and anthropogenic activities, *C. schmidtii* tussocks have suffered serious degradation and death over the last few decades (Pan et al., 2006; Qi et al., 2021b). The effects of hydrological gradient and fluctuations on plant growth and eco-physiological responses of *C. schmidtii* have been previous reported, indicating that this plant relies on final or dynamic performance (Yan et al., 2015; Zhang et al., 2019a, b). However, despite the importance of nutrient stoichiometry for the ecological adaptation of wetland species, few investigations have focused on nutrient responses of *C. schmidtii* to consecutive drought and re-flooding episodes from the perspective of nutrient trade-off and recovery.

As there is a substantial information gap relating to nutrient trade-offs regarding hydrological fluctuations and plant growth recovering in wetland ecosystems, we examine in detail the role of nutrient homeostasis or flexibility with respect to ecological responses (Julian et al., 2020; Chen et al., 2020; Zhang et al., 2021). Nutrient responses of *C. schmidtii* in a simulation experiment were tested under various hydrological treatments, including consecutive drought, wetting and re-flooding treatments. The aims of this study are: (1) to examine the effects of consecutive drought and re-flooding on nutrient stoichiometry of *C. schmidtii* at each growth stage;(2) to identify the responses of nutrient trade-offs and their scaling exponents to re-flooding; and (3) to evaluate the nutrient recovery effect of *C. schmidtii*. We hypothesized that (1) consecutive drought episodes and re-flooding significantly affected plant nutrient stoichiometry and their trade-offs, (2) and re-flooding effectively recovered plant nutrients in *C. schmidtii*. We also hypothesized that consecutive drought and re-flooding promoted nutrient flexibility of *C. schmidtii*, and nutrient homeostasis and flexibility together regulate plant nutrient responses. Findings from this investigation will aid in understanding the response of nutrient stoichiometry and trade-offs of *C. schmidtii* to consecutive drought and re-flooding treatments, providing information about nutrient recovery of *C. schmidtii* in semi-arid zones.

Materials and methods

Experimental process

In May 2018, hummocks of *C. schmidtii* tussocks and soil were collected from a riparian wetland situated along the Nenjiang River in Momoge Wetland Nature Reserve, Northeast China. Hummocks and soil were transported to a greenhouse (Northeast Institute of Geography and Agroecology, Chinese Academy of Sciences) within 12 h of collection. Hummocks without above-biomass were cut into uniform pieces (20 cm in height and 15 cm in diameter). The bottom 30 cm of each plastic container (cubes with a side length of 50 cm) was filled with mixed soil, in which hummocks were individually planted; the top half of the section was left uncovered.

http://www.aloki.hu ● ISSN 1589 1623 (Print) ● ISSN 1785 0037 (Online)
DOI: http://dx.doi.org/10.15666/aeer/2005_40394060

The experimental culture and equipment used in this simulation can be found in Zhang et al. (2019b, 2020). Plant rhizomes were successfully sprouted from the hummocks and were cultivated for 18 days with a soil water content of 36.32 ± 1.46%. Physicochemical properties of tap water and soil used in this experiment are the same as those highlighted in Zhang et al. (2019b). The soil has a total nitrogen content of 4.27 ± 0.67 $mg \cdot g^{-1}$, total phosphorus content of 0.52 ± 0.07 $mg \cdot g^{-1}$. During the experimental period, the air temperature and relative humidity in the greenhouse ranged from 25 to 38 ℃ and 36 to 58%, respectively.

In June 2018, 30 *C. schmidtii* tussocks with a similar plant size (a height of 52.98 ± 1.19 cm and biomass of 0.12 ± 0.02 g) were selected for our experiment. Five treatments were undertaken in this analysis: wet treatment (W), consecutive drought treatment (D) and re-flooding treatments (RT: DF30, DF40 and DF60). Each treatment had six duplicates. A soil water content ranging from 37.11 to 41.62% was maintained in treatment W by replenishing the water every two or three days (keep the soil surface moist); treatment D naturally reduced the soil water content over time; and treatments RT resulted in *C. schmidtii* tussocks being re-flooded about 5 cm after 30 days (DF30), 40 days (DF40) and 60 days (DF60) of drought, respectively. The changes in soil water content under D and W treatment can be found in Zhang et al. (2019b). Plants were flooded after RT so as to simulate submergence events caused by irregular heavy rainfall in July and August. Notably, *C. schmidtii* tussocks naturally reduced the soil water content over time before re-flooding, and then the treatments maintained a 5 cm flooding depth above the soil surface. Plants from the independent tussocks were then randomly analyzed for each treatment every ten days. The experiment lasted for 110 days (from June 1 to September 18, 2018), covering the entire growth stage of *C. schmidtii* (Zhang et al., 2019b).

Sampling and analysis

In order to evaluate the effects of consecutive drought episodes and re-flooding on nutrient stoichiometry and trade-offs of *C. schmidtii*, plants were randomly selected from each treatment at different growth stage (Day 0, 10, 20, 30, 40, 50, 60,70, 80, 90, 100, 110, respectively) and dried for 2 h at 120 ℃ before being dried at 65 ℃ until a constant weight was recorded, Samples were then ground into powder and sieved through a 0.25 mm sieve. Sulfuric acid ($\omega = 98\%$; $\rho = 1.84$) and hydrogen peroxide ($\omega = 30\%$; $\rho = 1.13$) were added to the plant samples before they were digested at 375 ℃ using a muffle furnace until the liquid was clear. Before analysis, the clear liquid was cooled to room temperature and made up to a volume of 500 mL. Plant N and P concentrations were determined using Kjeldahlanalysis and the Molybdenum-Antimony-Spectropho-Tometric Method with an automatic chemistry analyzer (Smartchem 300, Advanced Monolithic Systems, Graz, Italy), respectively. Plant K concentrations were determined by atomic emission spectrometer (ICPS-7500, Shimadzu, Japan). All N:P, N:K and K:P ratios for every treatment were calculated as mass ratios (Zhang et al., 2021).

Statistical analysis

Statistical analyses were performed using SPSS 20, Origin 9.2 and R v4.0.1 (R Development Core Team 2021). Plant N, P, K concentrations and their ratios in different growth stages were checked for normality and homogeneity before further analyses. To meet the assumptions of homoscedasticity, some variables were log-

http://www.aloki.hu ● ISSN 1589 1623 (Print) ● ISSN 1785 0037 (Online)
DOI: http://dx.doi.org/10.15666/aeer/2005_40394060

transformed. One-way analysis of variance (ANOVA) was used to determine the effects of consecutive drought and re-flooding on plant nutrients and their ratios of *C. schmidtii*. Multiple comparisons of means were undertaken using Duncan's test at the 0.05 significance level. Correlations between plant nutrients and their ratios were performed using "PerformanceAnalytics" package (https://CRAN.R-project.org/package=PerformanceAnalytics) in R. Strong correlations between plant nutrients and their ratios were expressed by the power function as *Equation 1:*

$$\mathrm{Lg}i = \alpha \times \mathrm{Lg}j + \beta \quad \text{(Eq.1)}$$

where α and β indicate the slope (i.e. the scaling exponent) and 'elevation' or Y-intercept (i.e. normalization constant; Reich et al., 2010; Tian et al., 2018); *i* and *j* indicate N, P, K and their ratios of *C. schmidtii*, respectively.

Fittings were performed to describe plant nutrient trade-offs in each treatment based on data collected from the entire *C. schmidtii* growth stage (Day 0~110) and data collected after re-flooding treatments, respectively. Ordinary least square (OLS) regression was used to determine the *i~j* scaling relationship under different treatments using package "lmodel2" in R (https://CRAN.R-project.org/package=lmodel2). Principal component analysis (PCA) of plant nutrients and their ratios of *C. schmidtii* in different growth stages were performed using "FactomineR" (https://CRAN.R-project.org/package=FactoMineR) and "factoextra" (https://CRAN.R-project.org/package=factoextra) packages.

Results

Effects of consecutive drought and re-flooding events on nutrients and their ratios of C. schmidtii

Consecutive drought and re-flooding treatments had complex effects on N, P and K concentrations of *C. schmidtii* (*Figs. 1* and *A1*). Fluctuation curves of plant N concentrations were observed in D and W treatments, with significant differences being identified on the Day 10 (*Fig. 1* and *Table 1*). The highest plant N concentration was recorded in the W treatment recorded as 29.26% higher than the value in the D treatment. However, plant N concentrations in D and W treatments decreased to 13.68 $mg \cdot g^{-1}$ and 13.91 $mg \cdot g^{-1}$ by the Day 30, respectively. From Day 40 to Day 70, plant N concentrations in the W treatment increased with time; N concentration in the D treatment decreased from 17.29 $mg \cdot g^{-1}$ to 15.43 $mg \cdot g^{-1}$ in the same time period (*Fig. A1*). Compared to the D and W treatments, plant N concentrations recorded partial or full recoveries under re-flooding treatments (DF30, DF40 and DF60) due to a shift of adaptation from drought to flooding. Plant P concentrations in the D treatment increased from 0.73 $mg \cdot g^{-1}$ to 1.04 $mg \cdot g^{-1}$ before decreasing to 0.41 $mg \cdot g^{-1}$ with time (*Fig. 1b*). Significant differences in plant P concentration were identified between D and W treatments on Day 20 (*Fig. 1a*). From Day 40 to Day 70, plant P concentrations in the W treatment were significantly higher than those in the D treatment. No significant differences in plant P concentrations were recorded among W and RT (DF30, DF40 and DF60) during the late growth stage. Plant K concentrations changes with time in the D treatment (Day 0 ~Day 70); across the entire growth stage, K concentrations recorded a decreasing tend in the W treatment. Although plant K concentration recorded a decrease at the early stage of re-flooding treatments, concentrations in DF40 and DF60 treatments recorded full recoveries compared to the W treatment.

http://www.aloki.hu ● ISSN 1589 1623 (Print) ● ISSN 1785 0037 (Online)
DOI: http://dx.doi.org/10.15666/aeer/2005_40394060

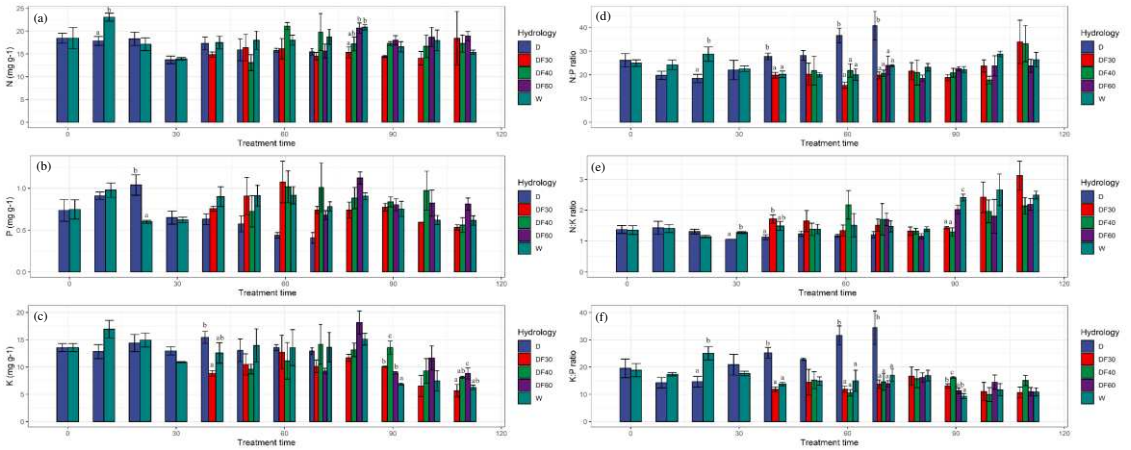

Figure 1. *Effects of consecutive drought and re-flooding episodes on N concentrations (a), P concentrations (b), K concentrations (c), N:P ratios (d), N:K ratios (e) and K:P ratios (f) of Carex schmidtii. W is the wet treatment; D is the consecutive drought treatment; DF30, DF40 and DF60 refer to re-flooding after 30, 40 and 60 days of consecutive drought, respectively. Different letters stand for significant differences at the 0.05 significance level in treatments in the same growth stage and there are no significant differences among treatments without any letters*

Table 1. *One-way ANOVAs results (F and p values) for the effects of consecutive drought and re-flooding treatments on N, P, K concentrations and their ratios for Carex schmidtii at each growth stage*

Nutrient	Day 0		Day 10		Day 20		Day 30		Day 40		Day 50	
	F	***p***	***F***	***p***	***F***	***p***	***F***	***p***	***F***	***p***	***F***	***p***
N	0.000	1.000	**14.868**	**0.008**	0.253	0.630	0.061	0.818	1.531	0.248	0.780	0.527
P	0.005	0.948	0.328	0.588	**6.090**	**0.043**	0.111	0.756	2.895	0.086	0.960	0.443
K	0.000	0.993	3.159	0.126	0.051	0.828	7.172	0.055	**6.537**	**0.009**	0.940	0.452
N:P	0.136	0.731	2.304	0.180	**10.282**	**0.015**	0.011	0.920	**11.026**	**0.001**	0.931	0.456
N:K	0.008	0.933	0.011	0.921	1.850	0.216	**44.143**	**0.003**	**5.881**	**0.013**	0.640	0.604
K:P	0.025	0.881	3.697	0.103	**10.128**	**0.015**	0.684	0.455	**29.907**	**0.000**	1.883	0.186
Nutrient	**Day 60**		**Day 70**		**Day 80**		**Day 90**		**Day 100**		**Day 110**	
	F	***p***	***F***	***p***	***F***	***p***	***F***	***p***	***F***	***p***	***F***	***p***
N	3.337	0.077	1.291	0.315	**5.549**	**0.023**	3.767	0.059	0.921	0.473	0.505	0.687
P	3.059	0.092	2.565	0.078	3.100	0.089	0.282	0.837	1.595	0.265	2.852	0.086
K	0.164	0.917	1.141	0.373	3.991	0.052	**20.759**	**0.000**	1.173	0.379	**4.312**	**0.031**
N:P	**13.557**	**0.002**	**7.115**	**0.002**	0.330	0.804	1.573	0.270	2.860	0.104	0.764	0.537
N:K	1.973	0.197	0.550	0.702	0.996	0.443	**20.437**	**0.000**	0.672	0.593	2.811	0.089
K:P	**12.768**	**0.002**	**7.532**	**0.001**	0.037	0.990	**13.463**	**0.002**	0.510	0.686	1.236	0.343

In treatment D, the N:P ratio decreased from 26.11 to 18.40 before increased to 40.73; in the W treatment, moderate fluctuations were recorded between 20.01 and 28.79 (*Figs. 1* and *A1*). Similar N:P recovery patterns were also recorded among DF30, DF40 and DF60 treatments. The N:P ratio decreased at the early stage of RT and then recovered to a higher value (>16) by the end of the experiment. The N:K ratio recorded a variation under D treatment, with values < 1.2 between Day 30 to Day 60 (except for

http://www.aloki.hu ● ISSN 1589 1623 (Print) ● ISSN 1785 0037 (Online)
DOI: http://dx.doi.org/10.15666/aeer/2005_40394060

Day 50). N:K ratio, however, recorded a significant increase under W and RT treatments, especially during the late growth stage (*Fig. 1e*). Under treatment D, the K:P ratio decreased before increasing, under the W treatment it recorded an increase before decreasing in W treatment (*Fig. 1f*). Significant differences in K:P ratios were identified on the Day 20, Day 40, Day 60~70 and Day 90. On the Day 20, the highest value of the K:P ratio was recorded in the W treatment, this being 1.71 times of the value in D treatment. However, the K:P ratio in the D treatment was significantly higher than W treatment between the Day 40 ~ Day 70. Re-flooding treatments effectively relieved the negative effects of the D treatment, recorded full recovery of the K:P ratio with reference to the W treatment.

Effects of consecutive drought and re-flooding on nutrient trade-offs of C. schmidtii

Positive relationships were identified among N, P and K concentrations of *C. schmidtii* using correlations analysis. Divergent pairwise correlations among the N:P, N:K and K:P ratios were recorded. The N:P ratio was positively related to N:K and K:P ratios for *C. schmidtii*, and the N:K ratio was negatively related to the K:P ratio. Plant P concentrations exhibited relatively moderate and negative relationships with the N:K ratio (*Fig. 2*).

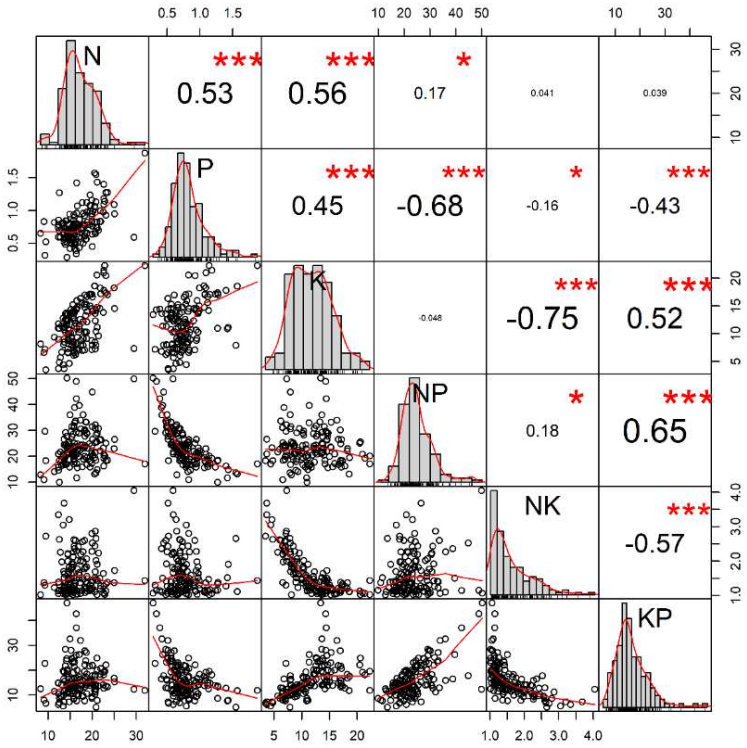

Figure 2. *Correlation analysis of N, P, K concentrations and their ratios of Carex schmidtii*

Consecutive drought and re-flooding had profound effects on the trade-offs among N, P and K concentrations of *C. schmidtii* (*Fig. A2; Table 2*). The P~N scaling exponent in treatment D was 1.201, 21.68% higher than that recorded in the W treatment (0.987). The P~N scaling exponents in re-flooding treatments increased with the order of DF30

http://www.aloki.hu ● ISSN 1589 1623 (Print) ● ISSN 1785 0037 (Online)
DOI: http://dx.doi.org/10.15666/aeer/2005_40394060

(0.464) < DF40 (0.684) < DF60 (0.999); the scaling exponent in treatment DF60 was much similar to that recorded in treatment W. K~N scaling exponents in D and W treatments were 0.733 and 1.708, respectively; scaling exponents in re-flooding treatments decreased with the order of DF30 (0.833) > DF40 (0.707) > DF60 (0.564). K~P scaling exponents in treatments D, DF60, DF40, DF30 and W were 0.136, 0.214, 0.347, 0.500 and 1.036, respectively. However, trade-offs between N:P ratio~K, N:K ratio~N and K:P ratio~N were not clear under consecutive drought and re-flooding treatments (*Table A1*). Trade-offs of K~P based on nutrient performance after re-flooding were significant and their scaling exponent had the order of DF30 (0.540) < DF40 (0.606) < DF60 (0.981; *Table A2*). Based on data for the entire growth stage of *C. schmidtii*, these results were contrary to those for the K~P scaling exponent (*Table 2*).

Table 2. *Summary of fitting results between N, P and K concentrations of Carex schmidtii under consecutive drought and re-flooding conditions. Fittings in D, W, DF30, DF40 and DF60 were based on nutrient data collected from the entire growth stage of C. schmidtii. α Scaling exponents, CI Confidence interval*

Lg *i*~ Lg *j*	Treatments	Fittings	α (95%CI)	R^2	p
Lg P~ Lg N	W	Y = 0.987X-1.350	0.987 (0.678~1.297)	0.484	< 0.001
	D	Y = 1.201X-1.655	1.201 (0.554~1.848)	0.324	< 0.001
	DF30	Y = 0.464X-0.668	0.464 (0.101~0.828)	0.133	< 0.05
	DF40	Y = 0.684X-947	0.684 (0.256~1.113)	0.199	< 0.01
	DF60	Y = 0.999X-1.368	0.999 (0.557~1.441)	0.331	< 0.001
Lg K~ Lg N	W	Y = 1.708X-1.088	1.708 (1.218~2.198)	0.529	< 0.001
	D	Y = 0.733X + 0.240	0.733 (0.440~1.026)	0.465	< 0.001
	DF30	Y = 0.833X + 0.016	0.833 (0.385~1.281)	0.246	< 0.001
	DF40	Y = 0.707X + 0.211	0.707 (0.282~1.132)	0.211	< 0.01
	DF60	Y = 0.564X + 0.400	0.564 (0.133~0.996)	0.142	< 0.05
Lg K~ Lg P	W	Y = 1.036X + 1.167	1.306 (0.644~1.429)	0.391	< 0.001
	D	Y = 0.136X + 1.158	0.136 (-0.046~0.319)	0.072	0.138
	DF30	Y = 0.500X + 1.067	0.500 (0.124~0.876)	0.143	< 0.05
	DF40	Y = 0.347X + 1.117	0.347 (0.056~0.640)	0.121	< 0.05
	DF60	Y = 0.214X + 1.124	0.214 (-0.046~0.474)	0.062	0.104

Nutrient recovery of C. schmidtii under consecutive drought and re-flooding conditions

PCA results of nutrients and their ratios revealed two PCs explaining 78.6% ~87.7% of the total variation in the seven growth stages (Day 0~110; *Figs. 3* and *A3*). Between Day 0~10, plant N, P, K concentrations and their ratios in D and W treatments were similar (*Fig. 3a*). Significant differences in nutrient balance between D and other treatments (W, DF30, DF40 and DF60) were identified along PC1 as they occupied unique positions in the four growth stages from Day 20~70. DF30, DF40 and DF60 treatments recorded similar nutrient balance results as that in treatment W in the entire re-flooding stage (Day 40~110). Additionally, DF30 recorded significant differences in

http://www.aloki.hu ● ISSN 1589 1623 (Print) ● ISSN 1785 0037 (Online)
DOI: http://dx.doi.org/10.15666/aeer/2005_40394060

the nutrient balance along PC1 with DF40 between Day 80~90, and with DF60 from Day 100~110. The nutrient balance in DF60 was much more convergent than that in other treatments in the early re-flooding stage (Day 70). Additionally, PCA of nutrients and their ratios revealed two PCs explaining 77.1% and 77.8% of total variation based on the nutrient data collected after re-flooding (*Fig. A4 a* and *b*) and the entire growth stages (*Fig. A4 c* and *d*), respectively. Nutrient trade-offs in treatment D recorded significant differences along PC1 and PC2 due to their unique positions (*Fig. A4 b*). Interestingly, nutrient trade-offs developed to the negative direction along PC1 with the order of D, DF60, DF40, DF30 (*Fig. A4 d*).

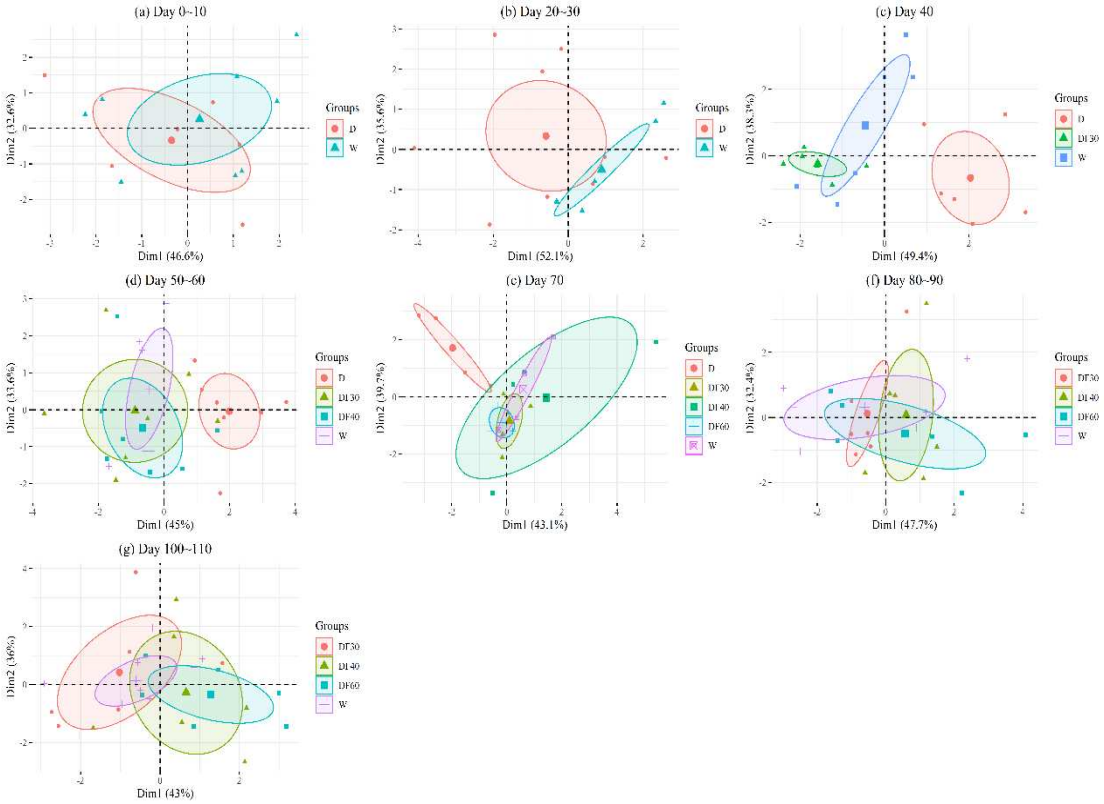

Figure 3. *The PCA plot showing the locations of nutrients in Carex schmidtii under consecutive drought and re-flooding conditions based on nutrient data collected from the entire growth stage. (a) Day 0~10, (b) Day 20~30, (c) Day 40, (d) Day 50~60, (e) Day 70, (f) Day 80~90 and (h) Day 100~110. Markers represent individual sample locations, while ellipses represent the 95% confidence zone for each treatment*

The coupling relationship of biomass nutrients and their ratios in Carex schmidtii

The pathway analysis model explained 48.33%, 81.43% and 36.00% of plant N, P, K concentrations, respectively (*Fig. 4*). Due to the strong internal stability of plant nutrient stoichiometry, results indicated that consecutive drought and re-flooding conditions had no significant contribution and path flux to plant nutrient and their ratios. Treatment time had negative effects on plant K concentration, N:P ratio and K:P ratio. Plant P and K concentrations, N:P ratio and treatment time had positive effects on plant N concentration. Additionally, plant K concentration has a high contribution to plant P concentration.

http://www.aloki.hu ● ISSN 1589 1623 (Print) ● ISSN 1785 0037 (Online)
DOI: http://dx.doi.org/10.15666/aeer/2005_40394060

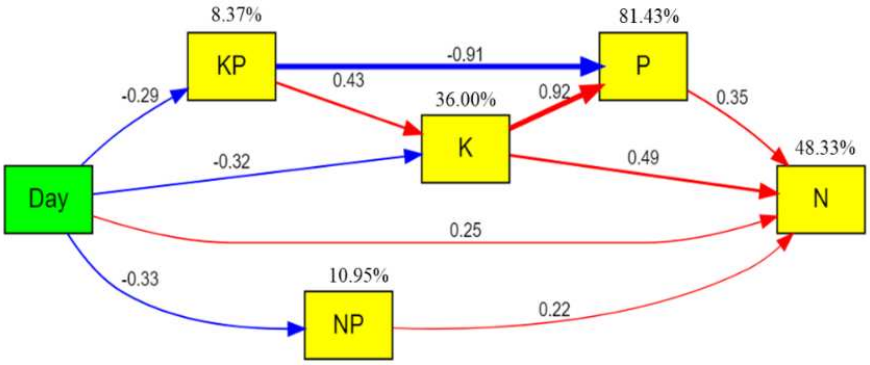

Figure 4. *Structural equation modeling (SEM) of treatment time, plant N, P, K concentrations and their ratios (χ^2 = 1.647, Df = 5, p = 0.895, GFI = 0.996, RMSEA = 0). Red and blue solid arrows indicate significant positive and negative pathways, respectively. Numbers in the arrows indicate the path coefficients. Percentage values close to the variables refer to the proportion of explained variance (R^2) by the model. Day, treatment time; NP, N:P ratio; KP, K:P ratio*

Discussion

Nutrient homeostasis or flexibility are recognized as the middle ground of ecological stoichiometry, affecting the stoichiometric relationships of terrestrial vegetation (Sistla et al., 2015; Gu et al., 2017; Mariotte et al., 2017). In previous studies, most plants displayed clear homeostatic behavior between the plant-soil system under conditions where nutrients were added (Wang et al., 2018; Yang et al., 2019). Additionally, the majority of previous studies focused on nutrient homeostasis of wetland plants regarding multi species on a global or zonal scale (Yu et al., 2015; Li et al., 2018; Hu et al., 2018). However, it is also controversial that nutrient homeostasis or flexibility regulate the ecological, physiological and biochemical processes of plants in response to environmental fluctuations (Sistla and Schimel, 2012; Julian et al., 2020). Therefore, debates regarding to nutrient homeostasis or flexibility have highlighted the significance of understanding nutrient responses of wetland plants to hydrological fluctuations. In semi-arid zones, the hydrological management using re-flooding to relieve drought is a common method to relieve the effects of consecutive drought episodes on plant growth performance (Li et al., 2017b; Zhang et al., 2019b; Qi et al., 2021a). Whether nutrient homeostasis or flexibility together regulate nutrient responses of *C. schmidtii*, and what is the degree of re-flooding treatments effect on *C. schmidtii*, are interesting and meaningful ecological questions.

Inconsistent with our hypothesis, consecutive drought and re-flooding treatments have complex effects on nutrient stoichiometry of *C. schmidtii* at each growth stage. Flooding condition promoted plant N concentration compared to consecutive drought treatment (Day10). This finding is consistent with that of Li et al. (2017a), who found that increasing soil water content promoted foliar nutrient concentrations of *Carex brevicuspis*. Additionally, short-term drought contributed to an increase in plant P concentrations and the decrease of N:P and K:P ratios (Day 20) by enhancing P-related physiological processes under an aerobic environment. However, a sharp decrease in nutrients occurred in D and W treatments on Day 30. This result may be related to 1) the dilution effects of nutrients due to the rapid growth of wetland plants, and 2) the protective strategy of plants by transferring nutrients to root systems in response to a

http://www.aloki.hu ● ISSN 1589 1623 (Print) ● ISSN 1785 0037 (Online)
DOI: http://dx.doi.org/10.15666/aeer/2005_40394060

sharp increase temperature stress. Additionally, as our study paid close attention to the dynamic process of nutrient performance in wetland plants within a certain time period and on key hydrological transition nodes, and we found that re-flooding after varying degrees of drought resulted in complex wetland plant responses. The growth and nutrient responses of wetland plants are influenced by the transition order, duration and frequency of drought-flooding (Li et al., 2017a; Yuan et al., 2019; Lan et al., 2021). In this study, re-flooding after drought (one form of alternating flooding-drought conditions) contributed to an increase of plant P concentrations and a decrease in the N:P ratio compared to consecutive drought events. Zhang et al. (2019a) reported that plant N and P concentrations decreased under alternating flooding-drought conditions; the ratio of N:P increased compared to those under consecutive flooding treatments. Previous studies have also revealed that hydrological fluctuations have significant effects on the dynamic of plant N and K concentrations, and their ratios in *C. schmidtii* (Zhang et al., 2021). These results indicate that suitable water conditions are conducive to nutrient absorption and storage in wetland plants. Significant differences in some nutrient stoichiometry among the treatments recorded nutrient flexibility of wetland plants. However, no significant differences of plant nutrients were recorded despite hydrological changes, finding that strongly support the regulation of nutrient homeostasis in plant response processes (Sistla and Schimel, 2012; Gu and Grogan, 2017).

Alternating flooding-drought conditions is an effective water-saving method to recover plant growth and nutrient stoichiometry of wetland plants in a semi-arid zone (Li et al., 2017b; Yang et al., 2020). Hydrological management in this zone with respect to alternating flooding-drought conditions effectively restores typical wetland plants including *Phragmites australis* and *C. schmidtii* (Wen et al., 2017; Zhang et al., 2019a). However, only a few studies have reported nutrient responses and trade-offs of wetland plants to re-flooding despite the significance for understanding the recovery dynamic and mechanism of plants under alternating flooding-drought conditions. In this study, re-flooding effectively alleviated drought effects on plant nutrient stoichiometry, except for K concentrations. However, plant P and K concentrations and their ratio recorded full recoveries; plant N concentration, N:P and N:K ratios recovered to a certain ratio of that in treatment W. P is closely associated with nucleus and eco-physiological processes in plants (Ghimire et al., 2017). Consecutive drought events exerted negative effects on P absorption, transportation and conservation, limiting the synthesis of ATP and phospholipid, resulting in withering of plants and death (Elser et al., 2000; Mariotte et al., 2020). Additionally, a significant fluctuation of plant nutrient stoichiometry occurred during the early stage of re-flooding after drought, indicating that plants experienced a shift from drought-adaption to flooding-adaption (Zhang et al., 2019b). The recovery dynamic of nutrients and their ratios are also influenced by initial re-flooding time, affecting drought duration and plant growth (Baldwin et al., 2006; Wang et al., 2015). Re-flooding in the early growth stage facilitated rapid and successful plant growth recovery (Zhang et al., 2019a, b). However, the recovery of plant nutrient concentrations increased with an increase in initial re-flooding time after Day 70. Although wetland plants have strong plastic deformation in the early growth stage (Bizet et al., 2015; Yao et al., 2021), re-flooding in the late growth stage can affect nutrient stoichiometry, increase plant vitality and extend the phenology period of plants (Feng et al., 2021; Zhang et al., 2021).

http://www.aloki.hu ● ISSN 1589 1623 (Print) ● ISSN 1785 0037 (Online)
DOI: http://dx.doi.org/10.15666/aeer/2005_40394060

Nutrient responses to consecutive drought and re-flooding plays vital roles in the ecological adaption of wetland species. Taking into account the growth of *C. schmidtii* in this experiment (Zhang et al., 2019b), we can more intuitively understand the regulation of nutrients on plant ecological and physiological adaptation. Both D and RT had positive or negative interactive effects on the growth and photosynthesis of *C. schmidtii*. D treatment decreased plant height, specific leaf area, chlorophyll content in the middle growth stage. Although RT were found to successfully recovery plant mass, chlorophyll content and photosynthesis of *C. schmidtii*, flooding condition inhibited plant performance in the late growth stage (Zhang et al., 2019b). This is closely related to the recovery dynamic of plant nutrients. Nutrient responses to consecutive drought and re-flooding are synergistic with plant physiological and ecological traits.

Nutrient trade-off and stoichiometric relationships are important proxies for nutrient homeostasis and flexibility (Sistla and Schimel, 2012; Corrales-Carvajal et al., 2016; Jeyasingh et al., 2017). Robust stoichiometric relationships of P~N and K~N under various hydrological conditions provided strong evidence for nutrient homeostasis (Tian et al., 2018; Zhang et al., 2021). Scaling exponents (SE) were undertaken on data collected during the entire growth stage of *C. schmidtii*, resulting in comparable SE results among the five treatments. SE of P~N increased with an increase of initial re-flooding time, and SE of P~N in DF60 was almost the same as that in treatment W. This result indicated that the relationship of P~N in DF60 recovered in relation to that in treatment W. However, due to consecutive drought events promoting the reduction of N and P, maintaining their robust stoichiometric relationships, the highest SE of P~N were recorded in treatment D. SE of K~N decreased with an increase of initial re-flooding time, results that were similar to those for treatment D. Under hydrological fluctuations, the stoichiometric relationship of K~N changed, except for that under treatment W. With consideration of nutrient stoichiometric relationships of K~P, N:P ratio~K, N:K ratio~P and K:P ratio~N, nutrient flexibility was much more common, a finding that supported the responses of internal nutrient relationships to hydrological fluctuations. Additionally, based on the data collected after re-flooding, the majority of SE in RT were absent, a finding that indicates nutrient flexibility. PCA results indicated that nutrient trade-offs of RT were also similar to W, however, they gradually separated with those in treatment D (*Figs. 3* and *A4*). Differences in area and position of confidence ellipses revealed nutrient flexibility, and the overlapping of confidence ellipses supported nutrient homeostasis despite hydrological fluctuations (Zhang et al., 2021). SEM analysis indicated a strong relationship between nutrients and their ratios, ignoring hydrological changes. Although consecutive drought and re-flooding conditions contributed to nutrient flexibility of *C. schmidtii*, strong internal stability of stoichiometric relationships effectively relieved changes in plant nutrient stoichiometry. Therefore, nutrient homeostasis and flexibility together regulate plant growth and nutrient responses.

In semi-arid zones, water scarcity limited plant growth and wetland development (Pan et al., 2006; Wang et al., 2019b). A key ecological question for wetland restoration and management in these areas is how to effectively recovery plant growth utilizing a water-saving methods (Li et al., 2017b; Zhang et al., 2019a, b; Yang et al., 2020). Although wetland restoration and conservation have been strengthened in this zone recently, hydrological management methods suitable for specific wetland species are still being explored (Qi et al., 2021a). Thus, comprehensive and deepening of wetland

http://www.aloki.hu ● ISSN 1589 1623 (Print) ● ISSN 1785 0037 (Online)
DOI: http://dx.doi.org/10.15666/aeer/2005_40394060

restoration and protection for tussock wetlands require further development (Guo et al., 2016; Zhang et al., 2019a; Qi et al., 2021c). Recovery technologies based on techniques utilizing seedbanks, transplanting rhizomes, and creating microtopography have been conducted to restore tussocks in wetlands, especially in semi-arid zones (Wang et al., 2020; Qi et al., 2021c). Additionally, hydrological management and regulation has been applied to restore tussock wetlands (Zhang et al., 2019a, b). Although previous studies examining hydrological fluctuations paid close attention to plant growth and physiological characteristics (Yan et al., 2015; Guo et al., 2016; Zhang et al., 2019a), few studies have evaluated the effects of consecutive drought and re-flooding events on nutrient responses of *C. schmidtii*. In this study, DF30, DF40 and DF60 were effectively found to alleviate consecutive drought effects on plant nutrients; the final performance of *C. schmidtii* after re-flooding increased with an increase in initial re-flooding time. By considering results from previous investigations with the aim of recovering plant growth, we recommend flexible alternating flooding-drought conditions to restore *C. schmidtii* wetlands in semi-arid zones (Zhang et al., 2019a, b; Wang et al., 2019b; Qi et al., 2021c). Reasonable irrigation according to the available water can guarantee the survival and development of tussocks.

Conclusion

Consecutive drought and re-flooding treatments had complex effects on nutrient stoichiometry of *C. schmidtii* at each growth stage. With reference to drought (D) and wetting (W) treatments, plant nutrient stoichiometry recorded partial or full recoveries under re-flooding treatments (RT: DF30, DF40 and DF60) by experiencing a shift of adaption from drought to flooding. Positive relationships were identified among N, P and K concentrations of *C. schmidtii*, and plant P concentration exhibited a relatively moderate and negative relationship with the N:K ratio. Consecutive drought and re-flooding treatments profoundly affected the trade-offs among N, P and K of *C. schmidtii*. Significant stoichiometric relationships of P~N and K~N were quantified using the empirical equation model, and the scaling exponent of P~N increased with the order of DF30 < DF40 < DF60, while that of K~N decreased. With an increase in treatment time, nutrient trade-offs in treatment D gradually differed from W and re-flooding treatments, however nutrient trade-offs of re-flooding treatments recovered in comparison to W. Although consecutive drought and re-flooding conditions contributed to nutrient flexibility of *C. schmidtii* to a certain degree, strong internal stability of nutrient stoichiometric relationships of *C. schmidtii* regulated nutrient trade-offs and effectively relieved changes in plant nutrient stoichiometry due to treatment time and hydrological conditions. Nutrient homeostasis and flexibility together regulate plant growth. Efficient evaluation of nutrient recovery aids our understanding of nutrient responses of *C. schmidtii* to consecutive drought and re-flooding treatments. Simultaneously, our findings provide valuable information for hydrological management and restoration of *C. schmidtii* tussocks in semi-arid zones.

Acknowledgements. This research was supported by the National Natural Science Foundation of China (No. 42101111 and 41871101); the Shandong Provincial Natural Science Foundation (No. ZR2021QD101); the PhD research startup foundation of Binzhou University (No. 2021Y14); the Youth Innovation and Technology Program in Colleges and Universities of Shandong Province (2021KJ081).

http://www.aloki.hu ● ISSN 1589 1623 (Print) ● ISSN 1785 0037 (Online)
DOI: http://dx.doi.org/10.15666/aeer/2005_40394060

REFERENCES

[1] Baldwin, D. S., Rees, G. N., Mitchell, A. M., Watson, G., Williams, J. (2006): The short-term effects of salinization on anaerobic nutrient cycling and microbial community structure in sediment from a freshwater wetland. – Wetlands 26(2): 455-464. https://doi.org/10.1672/0277-5212(2006)26[455:TSEOSO]2.0.CO;2.

[2] Bizet, F., Bogeat-Triboulot, M. B., Montpied, P., Christophe, A., Ningre, N., Cohen, D., Hummel, I. (2015): Phenotypic plasticity toward water regime: response of leaf growth and underlying candidate genes in Populus. – Physiologia Plantarum 154(1): 39-53. https://doi.org/10.1111/ppl.12271.

[3] Casanova, M. T., Brock, M. A. (2000): How do depth, duration and frequency of flooding influence the establishment of wetland plant communities? – Plant Ecology 147: 237–250. https://doi.org/10.1023/A:1009875226637.

[4] Chen, H., Qualls, R. G., Blank, R. R. (2005): Effect of soil flooding on photosynthesis, carbohydrate partitioning and nutrient uptake in the invasive exotic *Lepidium latifolium*. – Aquatic Botany 82(4): 250-268. https://doi.org/10.1016/j.aquabot.2005.02.013.

[5] Chen, Y., Stagg, C. L., Cai, Y., Lü, X., Wang, X., Shen, R., Lan, Z. (2020): Scaling responses of leaf nutrient stoichiometry to the lakeshore flooding duration gradient across different organizational levels. – Science of the Total Environment 740: 139740. https://doi.org/10.1016/j.scitotenv.2020.139740.

[6] Chiwa, M., Sheppard, L. J., Leith, I. D., Leeson, S. R., Tang, Y. S., Cape, J. N. (2019): P and K additions enhance canopy N retention and accelerate the associated leaching. – Biogeochemistry 142(3): 413-423. https://doi.org/10.1007/s10533-019-00543-y.

[7] Corrales-Carvajal, V. M., Faisal, A. A., Ribeiro, C. (2016): Internal states drive nutrient homeostasis by modulating exploration-exploitation trade-off. – Elife 5: e19920. http://dx.doi.org/10.1101/070086.

[8] Elser, J. J., Fagan, W. F., Denno, R. F., Dobberfuhl, D. R., Folarin, A., Huberty, A., Interlandi, S., Kilham, S. S., McCauley, E., Schulz, K. L., Siemann, E. H., Sterner, R. W. (2000): Nutritional constraints in terrestrial and freshwater food webs. – Nature 408: 578-580. https://doi.org/10.1038/35046058.

[9] Feng, S. L., Sikdar, A., Wang, J. X., Memon, M., Li, B. Y., Ma, H. F., Lv, G. L. (2021): Response of *Amorpha fruticosa* seedlings to drought and rewatering in arid and semi-arid environment. – Pakistan Journal of Botany 53(2): 419-424. http://dx.doi.org/10.30848/PJB2021-2(22).

[10] Garssen, A. G., Baattrup-Pedersen, A., Voesenek, L. A., Verhoeven, J. T., &Soons, M. B. (2015): Riparian plant community responses to increased flooding: a meta-analysis. – Global Change Biology 21(8): 2881-2890. https://doi.org/10.1111/gcb.12921.

[11] Ghimire, B., Riley, W. J., Koven, C. D., Kattge, J., Rogers, A., Reich, P. B., Wright, I. J. (2017): A global trait-based approach to estimate leaf nitrogen functional allocation from observations. – Ecological Applications 27(5): 1421-1434. https://doi.org/10.1002/eap.1542.

[12] Gierth, M., &Mäser, P. (2007): Potassium transporters in plants–involvement in K^+ acquisition, redistribution and homeostasis. – FEBS Letters 581(12): 2348-2356. https://doi.org/10.1016/j.febslet.2007.03.035.

[13] Gu, Q., Zamin, T. J., Grogan, P. (2017): Stoichiometric homeostasis: a test to predict tundra vascular plant species and community-level responses to climate change. – Arctic Science 3(2): 320-333. https://doi.org/10.1139/as-2016-0032.

[14] Guo, J., Jiang, H., Bian, H., He, C., Gao, Y. (2016): Effects of hydrologic mediation and plantation of *Carex schmidtii* Meinsh on peatland restoration in China's Changbai Mountain region. – Ecological Engineering 96: 187-193. https://doi.org/10.1016/j.ecoleng.2016.01.015.

http://www.aloki.hu ● ISSN 1589 1623 (Print) ● ISSN 1785 0037 (Online)
DOI: http://dx.doi.org/10.15666/aeer/2005_40394060

[15] Güsewell, S., Koerselman, W., Verhoeven, J. T. (2003): Biomass N:P ratios as indicators of nutrient limitation for plant populations in wetlands. – Ecological Applications 13(2): 372-384. https://doi.org/10.1890/1051-0761(2003)013[0372:BNRAIO]2.0.CO;2.
[16] Hamdan, M. A., Asada, T., Hassan, F. M., Warner, B. G., Douabul, A., Al-Hilli, M. R., Alwan, A. A. (2010): Vegetation response to re-flooding in the Mesopotamian wetlands, Southern Iraq. – Wetlands 30(2): 177-188. https://doi.org/10.1007/s13157-010-0035-9.
[17] Hu, M., Peñuelas, J., Sardans, J., Sun, Z., Wilson, B. J., Huang, J., Zhu, Q., Tong, C. (2018): Stoichiometry patterns of plant organ N and P in coastal herbaceous wetlands along the East China Sea: implications for biogeochemical niche. – Plant and Soil 431(1): 273-288. https://doi.org/10.1007/s11104-018-3759-6.
[18] Hu, Y. K., Liu, X. Y., He, N. P., Pan, X., Long, S. Y., Li, W., Zhang, M. Y., Cui, L. J. (2021): Global patterns in leaf stoichiometry across coastal wetlands. – Global Ecology and Biogeography 30(4): 852-869. https://doi.org/10.1111/geb.13254.
[19] Huang, Y., Lou, C., Luo, L., Wang, X. C. (2021): Insight into nitrogen and phosphorus coupling effects on mixotrophic *Chlorella vulgaris* growth under stably controlled nutrient conditions. – Science of the Total Environment 752: 141747. https://doi.org/10.1016/j.scitotenv.2020.141747.
[20] Jeyasingh, P. D., Goos, J. M., Thompson, S. K., Godwin, C. M., &Cotner, J. B. (2017): Ecological stoichiometry beyond redfield: an ionomic perspective on elemental homeostasis. – Frontiers in Microbiology 8: 722. https://doi.org/10.3389/fmicb.2017.00722.
[21] Julian, P., Gerber, S., Bhomia, R. K., King, J., Osborne, T. Z., Wright, A. L. (2020): Understanding stoichiometric mechanisms of nutrient retention in wetland macrophytes: stoichiometric homeostasis along a nutrient gradient in a subtropical wetland. – Oecologia 193(4): 969-980. https://doi.org/10.1007/s00442-020-04722-9.
[22] Lan, Z., Chen, Y., Shen, R., Cai, Y., Luo, H., Jin, B., Chen, J. (2021): Effects of flooding duration on wetland plant biomass: the importance of soil nutrients and season. – Freshwater Biology 66(2): 211-222. https://doi.org/10.1111/fwb.13630.
[23] Lawrence, B. A., Fahey, T. J., Zedler, J. B. (2013): Root dynamics of *Carex stricta*-dominated tussock meadows. – Plant and Soil 364: 325-339. https://doi.org/10.1007/s11104-012-1360-y.
[24] Li, W., Cao, T., Ni, L., Zhu, G., Zhang, X., Fu, H., Song, X., Xie, P. (2015): Size-dependent C, N and P stoichiometry of three submersed macrophytes along water depth gradients. – Environmental Earth Sciences 74(5): 3733-3738. https://doi.org/10.1007/s12665-015-4295-9.
[25] Li, F., Hu, J. Y., Xie, Y. H., Yang, G. S., Hu, C., Chen, X. S., Deng, Z. M. (2017a): Foliar stoichiometry of carbon, nitrogen, and phosphorus in wetland sedge *Carex brevicuspis* along a small-scale elevation gradient. – Ecological Indicators 92: 322-329. https://doi.org/10.1016/j.ecolind.2017.04.059.
[26] Li, X., Wen, B., Yang, F., Hartley, A., Li, X. (2017b): Effects of alternate flooding–drought conditions on degenerated *Phragmites australis* salt marsh in Northeast China. – Restoration Ecology 25(5): 810-819. https://doi.org/10.1111/rec.12500.
[27] Li, W., Li, Y., Zhong, J., Fu, H., Tu, J., Fan, H. (2018): Submerged macrophytes exhibit different phosphorus stoichiometric homeostasis. – Frontiers in Plant Science 9: 1207. https://doi.org/10.3389/fpls.2018.01207.
[28] Liu, Y., Bachofen, C., Lou, Y., Ding, Z., Jiang, M., Lü, X., Buchmann, N. (2021): The effect of temperature changes and K supply on the reproduction and growth of *Bolboschoenus planiculmis*. – Journal of Plant Ecology 14(2): 337-347. https://doi.org/10.1093/jpe/rtaa091.
[29] Mariotte, P., Canarini, A., Dijkstra, F. A. (2017): Stoichiometric N:P flexibility and mycorrhizal symbiosis favour plant resistance against drought. – Journal of Ecology 105(4): 958-967. https://doi.org/10.1111/1365-2745.12731.

http://www.aloki.hu ● ISSN 1589 1623 (Print) ● ISSN 1785 0037 (Online)
DOI: http://dx.doi.org/10.15666/aeer/2005_40394060

[30] Mariotte, P., Cresswell, T., Johansen, M. P., Harrison, J. J., Keitel, C., Dijkstra, F. A. (2020): Plant uptake of nitrogen and phosphorus among grassland species affected by drought along a soil available phosphorus gradient. – Plant and Soil 448: 121-132. https://doi.org/10.1007/s11104-019-04407-0.

[31] Pan, X., Zhang, D., Quan, L. (2006): Interactive factors leading to dying-off *Carex* tato in Momoge wetland polluted by crude oil, Western Jilin, China. – Chemosphere 65(10): 1772-1777. https://doi.org/10.1016/j.chemosphere.2006.04.063.

[32] Pan, Y., Cieraad, E., Armstrong, J., Armstrong, W., Clarkson, B. R., Colmer, T. D., Pedersen, O., Visser, E. J. W., Voesenek, L. A. C. J., van Bodegom, P. M. (2020): Global patterns of the leaf economics spectrum in wetlands. – Nature Communications 11(1): 1-9. https://doi.org/10.1038/s41467-020-18354-3.

[33] Qi, Q., Zhang, D. J., Zhang, M. Y., Tong, S. Z., An, Y., Wang, X. H., Zhu, G. L. (2021a): Hydrological and microtopographic effects on community ecological characteristics of *Carex schmidtii* tussock wetland. – Science of The Total Environment 780: 146630. https://doi.org/10.1016/j.scitotenv.2021.146630.

[34] Qi, Q., Zhang, D., Zhang, M., Tong, S., Wang, W., An, Y. (2021b): Spatial distribution of soil organic carbon and total nitrogen in disturbed *Carex* tussock wetland. – Ecological Indicators 120: 106930. https://doi.org/10.1016/j.ecolind.2020.106930.

[35] Qi, Q., Zhang, D., Tong, S., Zhang, M., Wang, X., An, Y., &Lu, X. (2021c): The driving mechanisms for community expansion in a restored *Carex* tussock wetland. – Ecological Indicators 121: 107040. https://doi.org/10.1016/j.ecolind.2020.107040.

[36] Reich, P. B., Oleksyn, J., Wright, I. J., Niklas, K. J., Hedin, L., Elser, J. J. (2010): Evidence of a general 2/3-power law of scaling leaf nitrogen to phosphorus among major plant groups and biomes. – Proceedings of the Royal Society B: Biological Sciences 277(1683): 877-883. https://doi.org/10.1098/rspb.2009.1818.

[37] Rong, Q., Liu, J., Cai, Y., Lu, Z., Zhao, Z., Yue, W., Xia, J. (2015): Leaf carbon, nitrogen and phosphorus stoichiometry of *Tamarix chinensis* Lour. in the Laizhou Bay coastal wetland, China. – Ecological Engineering 76: 57-65. https://doi.org/10.1016/j.ecoleng.2014.03.002.

[38] Sistla, S. A., Schimel, J. P. (2012): Stoichiometric flexibility as a regulator of carbon and nutrient cycling in terrestrial ecosystems under change. – New Phytologist 196(1): 68-78. https://doi.org/10.1111/j.1469-8137.2012.04234.x.

[39] Sistla, S. A., Appling, A. P., Lewandowska, A. M., Taylor, B. N., Wolf, A. A. (2015): Stoichiometric flexibility in response to fertilization along gradients of environmental and organismal nutrient richness. – Oikos 124: 949-959. https://doi.org/10.1111/oik.02385.

[40] Tian, D., Yan, Z., Niklas, K., Han, W., Kattge, J., Reich, P., Luo, Y., Chen, Y., Tang, Z., Hu, H., Wright, I., Schmid, B., Fang, J. Y. (2018): Global leaf nitrogen and phosphorus stoichiometry and their scaling exponent. – National Science Review 5(5): 728-739. https://doi.org/10.1093/nsr/nwx142.

[41] Wan, S. Z., Yang, G. S., Mao, R. (2020): Responses of leaf nitrogen and phosphorus allocation patterns to nutrient additions in a temperate freshwater wetland. – Ecological Indicators 110: 105949. https://doi.org/10.1016/j.ecolind.2019.105949.

[42] Wang, W. Q., Sardans, J., Wang, C., Zeng, C. S., Tong, C., Asensio, D., Penuelas, J. (2015): Ecological stoichiometry of C, N, and P of invasive Phragmites australis and native *Cyperus malaccensis* species in the Minjiang River tidal estuarine wetlands of China. – Plant ecology 216(6): 809-822. https://doi.org/10.1007/s11258-015-0469-5.

[43] Wang, J., Wang, J., Guo, W., Li, Y., Wang, G. G., Wu, T. (2018): Stoichiometric homeostasis, physiology, and growth responses of three tree species to nitrogen and phosphorus addition. – Trees 32(5): 1377-1386.https://doi.org/10.1007/s00468-018-1719-7.

[44] Wang, M., Wang, S., Wang, G., Jiang, M. (2019a): Importance of tussocks in supporting plant diversity in *Carex schmidtii* Meinsh. wetlands. – Marine and Freshwater Research 70(6): 807-815. https://doi.org/10.1071/MF18237.

http://www.aloki.hu ● ISSN 1589 1623 (Print) ● ISSN 1785 0037 (Online)
DOI: http://dx.doi.org/10.15666/aeer/2005_40394060

[45] Wang, X., Zhang, D., Qi, Q., Tong, S., An, Y., Lu, X., Liu, Y. (2019b): The restoration feasibility of degraded *Carex* Tussock in soda-salinization area in arid region. – Ecological Indicators 98: 131-136.https://doi.org/10.1016/j.ecolind.2018.08.066.
[46] Wang, M., Wang, S., Wang, G., Jiang, M. (2020): Soil seed banks and restoration potential of tussock sedge meadows after farming in Changbai Mountain, China. – Marine and Freshwater Research 71(9): 1099-1106. https://doi.org/10.1071/MF19025.
[47] Wen, B., Li, X., Yang, F., Lu, X., Li, X., Yang, F. (2017): Growth and physiology responses of *Phragmites australis* to combined drought-flooding condition in inland saline-alkaline marsh, Northeast China. – Ecological Engineering 108: 234-239. https://doi.org/10.1016/j.ecoleng.2017.08.036.
[48] Wright, I. J., Reich, P. B., Westoby, M., Ackerly, D. D., Baruch, Z., Bongers, F., Cavender-Bares, J., Chapin, T., Cornelissen, J. H. C., Diemer, M., Flexas, J., Garnier, E., Groom, P. K., Gulias, J., Hikosaka, K., Lamont, B. B., Lee, T., Lee, W., Lusk, C., Midgley, J. J., Navas, Marie-Laure, Niinemets, Ü., Oleksyn, Ja., Osada, N., Poorter, H., Poot, P., Prior, L., Pyankov, V. I., Roumet, C., Thomas, S. C., Tjoelker, M. G., Veneklaas, E. J., Villar, R. (2004): The worldwide leaf economics spectrum. – Nature 428(6985): 821-827. https://doi.org/10.1038/nature02403.
[49] Wright, S. J., Yavitt, J. B., Wurzburger, N., Turner, B. L., Tanner, E. V. J., Sayer, E. J., Santiago, L. S., Kaspari, M., Hedin, L. O., Harms, K. E., Garcia, M. N., Corre, M. D. (2011): Potassium, phosphorus or nitrogen limit root allocation, tree growth, or litter production in a lowland tropical forest. – Ecology 92(8): 1616-1625. https://doi.org/10.1890/10-1558.1.
[50] Yan, H., Liu, R., Liu, Z., Wang, X., Luo, W., Sheng, L. (2015): Growth and physiological responses to water depths in *Carex schmidtii* Meinsh. – PloS one 10(5): e0128176. https://doi.org/10.1371/journal.pone.0128176.
[51] Yan, Z., Hou, X., Han, W., Ma, S., Shen, H., Guo, Y., Fang, J. (2019): Effects of nitrogen and phosphorus supply on stoichiometry of six elements in leaves of *Arabidopsis thaliana*. – Annals of Botany 123(3): 441-450. https://doi.org/10.1093/aob/mcy169.
[52] Yang, D., Song, L., &Jin, G. (2019): The soil C:N:P stoichiometry is more sensitive than the leaf C:N:P stoichiometry to nitrogen addition: a four-year nitrogen addition experiment in a *Pinus koraiensis* plantation. – Plant and Soil 442(1): 183-198. https://doi.org/10.1007/s11104-019-04165-z.
[53] Yang, Y., Mou, X., Wen, B., Liu, X. (2020): Soil carbon, nitrogen and phosphorus concentrations and stoichiometries across a chronosequence of restored inland soda saline-alkali wetlands, Western Songnen Plain, Northeast China. – Chinese Geographical Science 30(5): 934-946. https://doi.org/10.1007/s11769-020-1155-7.
[54] Yao, X., Cao, Y., Zheng, G., Devlin, A. T., Li, X., Li, M., Tang, S., Xu, L. (2021): Ecological adaptability and population growth tolerance characteristics of *Carex cinerascens* in response to water level changes in Poyang Lake, China. – Scientific Reports 11(1): 1-15. https://doi.org/10.1038/s41598-021-84282-x.
[55] Yu, Q., Wilcox, K., Pierre, K. L., Knapp, A. K., Han, X., Smith, M. D. (2015): Stoichiometric homeostasis predicts plant species dominance, temporal stability, and responses to global change. – Ecology 96(9): 2328-2335. https://doi.org/10.1890/14-1897.1.
[56] Yuan, S., Yang, Z., Liu, X., Wang, H. (2019): Water level requirements of a *Carex* hygrophyte in Yangtze floodplain lakes. – Ecological Engineering 129: 29-37. https://doi.org/10.1016/j.ecoleng.2019.01.006.
[57] Zhang, D., Qi, Q., Wang, X., Tong, S., Lv, X., An, Y., Zhu, X. (2019a): Physiological responses of *Carex schmidtii* Meinsh to alternating flooding-drought conditions in the Momoge wetland, northeast China. – Aquatic Botany 153: 33-39. https://doi.org/10.1016/j.aquabot.2018.11.010.
[58] Zhang, D., Tong, S., Qi, Q., Zhang, M., An, Y., Wang, X., Lu, X. (2019b): Effects of drought and re-flooding on growth and photosynthesis of *Carex schmidtii* Meinsh:

http://www.aloki.hu ● ISSN 1589 1623 (Print) ● ISSN 1785 0037 (Online)
DOI: http://dx.doi.org/10.15666/aeer/2005_40394060

implication for tussock restoration. – Ecological Indicators 103: 134-144. https://doi.org/10.1016/j.ecolind.2019.04.005.

[59] Zhang, D. J., Zhang, M. Y., Tong, S. Z., Qi, Q., Wang, X. H., Lu, X. (2020): Growth and physiological responses of *Carex schmidtii* to water-level fluctuation. – Hydrobiologia 847(3): 967-981. https://doi.org/10.1007/s10750-019-04159-z.

[60] Zhang, D. J., Qi, Q., Tong, S. Z., Wang, J., Zhang, M. Y., Zhu, G. L., Lu, X. G. (2021): Effect of hydrological fluctuation on nutrient stoichiometry and trade-offs of *Carex schmidtii*. – Ecological Indicators 120: 106924. https://doi.org/10.1016/j.ecolind.2020.106924.

APPENDIX

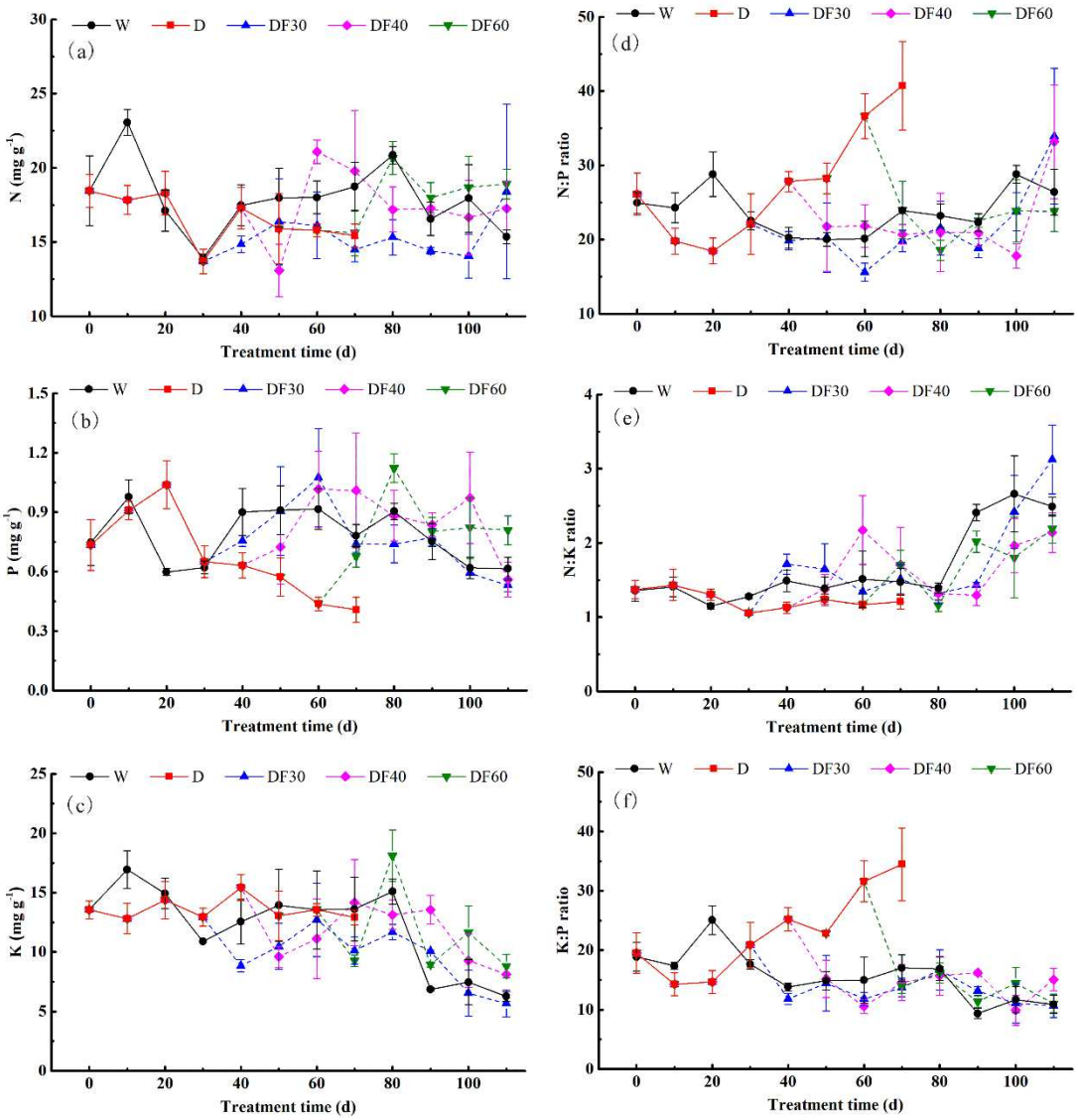

Figure A1. *Effects of consecutive drought and re-flooding episodes on N concentrations (a), P concentrations (b), K concentrations (c), N:P ratios (d), N:K ratios (e) and K:P ratios (f) of Carex schmidtii. Dotted lines show the changes in nutrients and their ratios of Carex schmidtii after re-flooding. W is the wet treatment; D is the consecutive drought treatment; DF30, DF40 and DF60 refer to re-flooding after 30, 40 and 60 days of consecutive drought, respectively*

http://www.aloki.hu ● ISSN 1589 1623 (Print) ● ISSN 1785 0037 (Online)
DOI: http://dx.doi.org/10.15666/aeer/2005_40394060

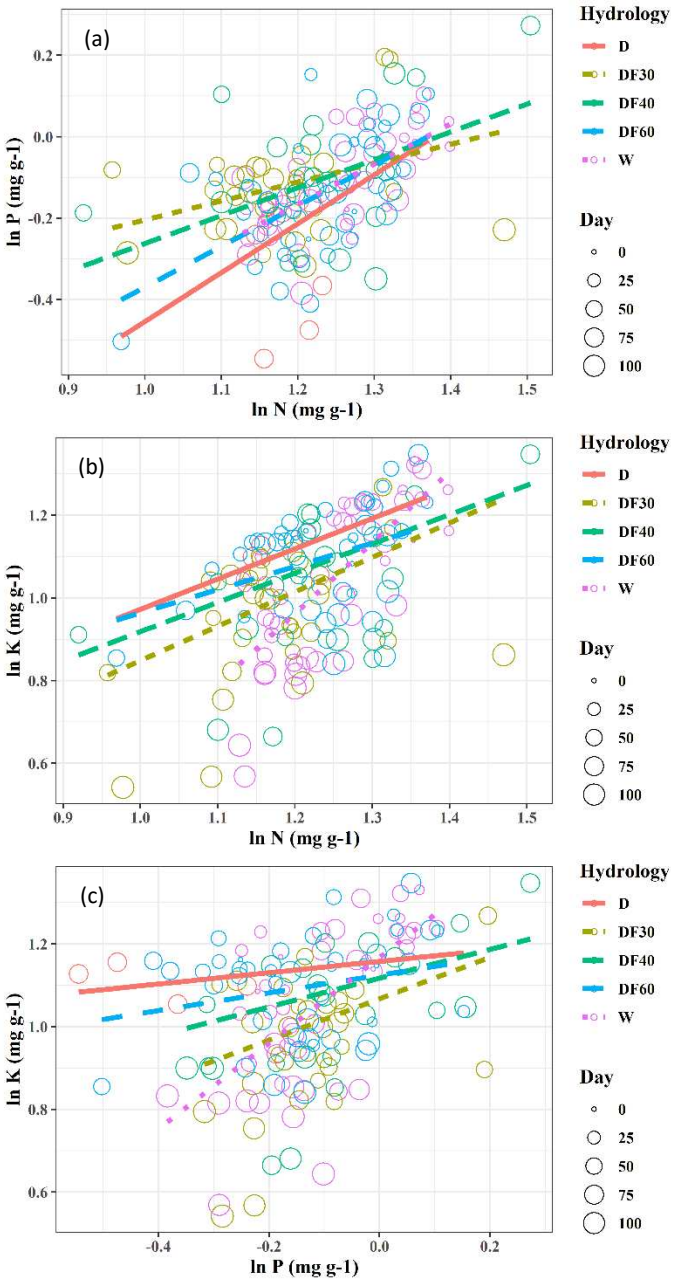

Figure A2. *Relationships between N, P and K concentrations of Carex schmidtii under consecutive drought and re-flooding conditions. (a) ln P = α ln N + β. (b) ln K = α ln N + β. (c) ln K = α ln P + β. α Scaling exponents, β elevation. Fittings in D, W, DF30, DF40 and DF60 were based on nutrient data collected from the entire growth stage of C. schmidtii. W is the wet treatment; D is the consecutive drought treatment; DF30, DF40 and DF60 refer to re-flooding after 30, 40 and 60 days of consecutive drought, respectively*

http://www.aloki.hu ● ISSN 1589 1623 (Print) ● ISSN 1785 0037 (Online)
DOI: http://dx.doi.org/10.15666/aeer/2005_40394060

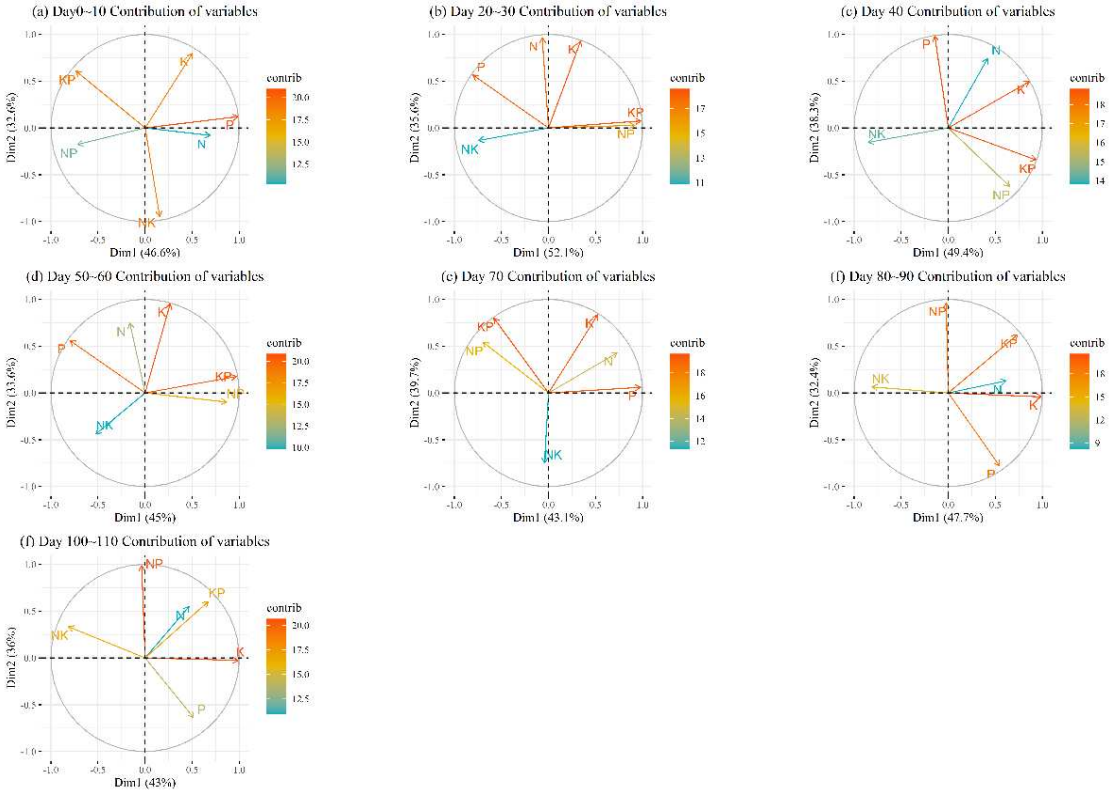

Figure A3. *PCA plot showing the contribution of nutrients and their ratios of Carex schmidtii under consecutive drought and re-flooding conditions based on nutrient data collected from each growth stage of C. schmidtii. Markers represent individual sample locations, while ellipses represent 95% confidence zone for each treatment*

http://www.aloki.hu ● ISSN 1589 1623 (Print) ● ISSN 1785 0037 (Online)
DOI: http://dx.doi.org/10.15666/aeer/2005_40394060

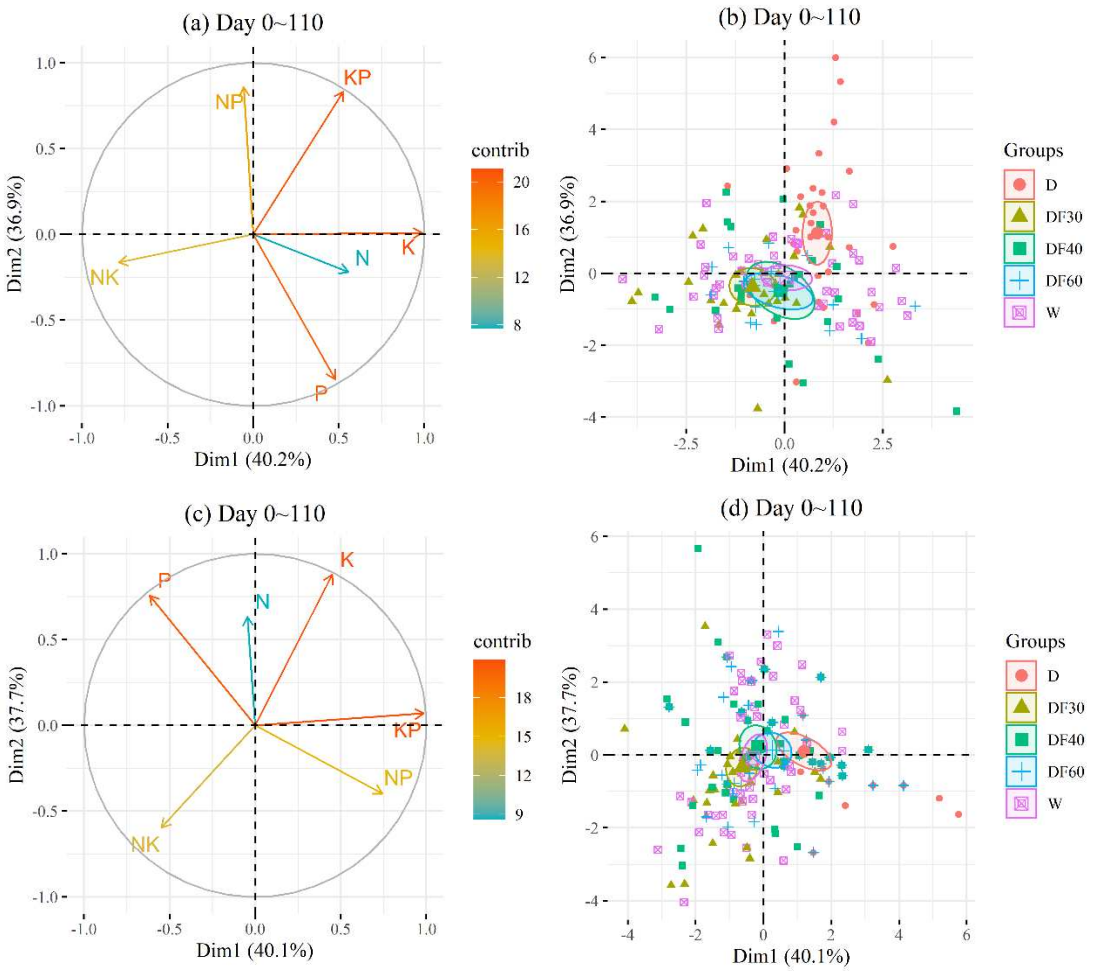

Figure A4. *PCA plot showing the locations of nutrients and their ratios of Carex schmidtii under consecutive drought and re-flooding conditions (Day 0~110). Figure A4 a and b were based on nutrient data of C. schmidtii collected after re-flooding. Figure A4 c and d were based on nutrient data of C. schmidtii collected from the entire growth stage. Markers represent individual sample locations, while ellipses represent 95% confidence zone for each treatment*

http://www.aloki.hu ● ISSN 1589 1623 (Print) ● ISSN 1785 0037 (Online)
DOI: http://dx.doi.org/10.15666/aeer/2005_40394060

Table A1. *Summary of fitting results between nutrients and their ratios of Carex schmidtii under consecutive drought and re-flooding conditions. Fittings in D, W, DF30, DF40 and DF60 were based on nutrient data collected from the entire growth stage of C. schmidtii. α Scaling exponents, CI Confidence interval*

Lg Y~ Lg X	Treatments	Fittings	α (95%CI)	R^2	p
Lg K:P ratio~ Lg N	W	Y = 0.721X + 0.263	0.721 (0.209~1.234)	0.155	< 0.01
	D	Y = -0.469X + 1.895	-0.469 (-1.230~0.233)	0.050	0.218
	DF30	Y = 0.368X + 0.684	0.368 (-0.135~0.872)	0.048	0.147
	DF40	Y = 0.022X + 1.158	0.022 (-0.524~0.569)	0.000	0.934
	DF60	Y = -0.435 X + 1.768	-0.435 (-1.040~0.170)	0.048	0.154
Lg N:K ratio~ Lg P	W	Y = -0.546X + 0.139	-0.546 (-0.885~-0.207)	0.193	< 0.01
	D	Y = 0.133X + 0.111	0.133 (-0.005~0.271)	0.114	0.058
	DF30	Y = -0.213X + 0.160	-0.213 (-0.561~0.136)	0.034	0.225
	DF40	Y = -0.058X + 0.142	-0.058 (-0.340~0.335)	0.004	0.682
	DF60	Y = 0.117X + 0.154	0.117(-0.140~0.375)	0.020	0.363
Lg N:P ratio~ Lg K	W	Y = -0.068X + 1.438	-0.068 (-0.198~0.062)	0.025	0.296
	D	Y = 0.108X + 1.288	0.108 (-0.497~0.713)	0.004	0.718
	DF30	Y = 0.009X + 1.300	0.009 (-0.229~0.247)	0.000	0.941
	DF40	Y = -0.048X + 1.386	-0.048 (-0.334~0.237)	0.003	0.735
	DF60	Y = -0.036X + 1.409	-0.036 (-0.332~0.259)	0.001	0.807

Table A2. *Summary of fitting results between nutrients and their ratios of Carex schmidtii after re-flooding. Fittings in DF30, DF40 and DF60 were based on nutrient data collected after re-flooding. α Scaling exponents, CI Confidence interval*

Lg Y~ Lg X	Treatments	Fittings	α (95%CI)	R^2	p
Lg P~ Lg N	DF30	Y = 0.283X-0.464	0.283 (-0.152~0.717)	0.060	0.194
	DF40	Y = 0.573X-0.800	0.573 (-0.022~1.168)	0.160	0.058
	DF60	Y = 0.520X-0.742	0.520 (-0.217~1.257)	0.140	0.152
Lg K~ Lg N	DF30	Y = 0.644X + 0.195	0.644 (0.079~1.209)	0.163	< 0.05
	DF40	Y = 0.730X + 0.129	0.730 (0.122~1.338)	0.229	< 0.05
	DF60	Y = 0.616X + 0.255	0.616 (-0.428~1.659)	0.103	0.226
Lg K~ Lg P	DF30	Y = 0.540X + 1.024	0.540 (0.049~1.031)	0.153	< 0.05
	DF40	Y = 0.606X + 1.082	0.606 (0.209~1.004)	0.324	< 0.01
	DF60	Y = 0.981X + 1.114	0.981 (0.420~1.542)	0.501	< 0.01
Lg K:P ratio~ Lg N	DF30	Y = 0.362X + 0.660	0.362 (-0.226~0.950)	0.054	0.218
	DF40	Y = 0.157X + 0.928	0.157 (-0.463~0.777)	0.013	0.604
	DF60	Y = 0.095X + 0.996	0.095 (-0.681~0.871)	0.005	0.796
Lg N:K ratio~ Lg P	DF30	Y = -0.329X + 0.180	-0.329 (-0.815~0.157)	0.064	0.176
	DF40	Y = -0.326X + 0.171	-0.326 (-0.734~0.080)	0.117	0.110
	DF60	Y = -0.711X + 0.164	-0.711 (-1.363~-0.058)	0.281	< 0.05
Lg N:P ratio~ Lg K	DF30	Y = -0.031X + 1.338	-0.031 (-0.354~0.292)	0.001	0.845
	DF40	Y = -0.220X + 1.548	-0.220 (-0.618~0.178)	0.059	0.263
	DF60	Y = -0.344X + 1.697	-0.344 (-0.703~0.014)	0.232	0.058

http://www.aloki.hu ● ISSN 1589 1623 (Print) ● ISSN 1785 0037 (Online)
DOI: http://dx.doi.org/10.15666/aeer/2005_40394060

TRANSCRIPTOME SEQUENCING AND ANALYSIS OF ATRAZINE STRESS ON *SUAEDA SALSA*

LU, H. B. – WEI, H. F.*

Dalian Ocean University, Dalian, China
(e-mail: 15293557967@163.com – H. B. Lu)

**Corresponding author*
e-mail: weihaifeng@dlou.edu.cn

(Received 1st Apr 2022; accepted 26th Jul 2022)

Abstract. Pesticides are an indispensable part of agricultural production, and herbicides are more widely used in agriculture. Through the hydroponic experiment, it was found that atrazine would affect the growth of *Suaeda salsa*. High throughput sequencing was used to analyze its transcriptome in order to explain the growth pathway of atrazine on *Suaeda salsa* at molecular level. A total of 78.92 g data were obtained by transcriptome sequencing of *Suaeda salsa*, 443515 transcripts with an average length of 998 BP were obtained, and 261694 unigenes with an average length of 864 BP were obtained by splicing. All unigenes were annotated with seven databases, and 195917 unigenes were annotated successfully in at least one of the above seven databases, accounting for 74.86% of the total unigenes. The results of differential analysis were analyzed by KEGG pathway enrichment analysis. The results showed that the processes of significant enrichment of high, medium and low atrazine concentrations compared with the control group were ribosome, phagosome and oxidative phosphorylation. The transcription and translation related genes of elongation factor in ribosomes and SecY membrane protein related genes producing protein membrane channels were up-regulated, the F-actin and V-ATPase related genes involved in transport in phagocytes were up-regulated, and the f-atpase and V-ATPase related genes producing ATP during oxidative phosphorylation were up-regulated, indicating that the above related genes were involved in the corresponding response to atrazine stress.
Keywords: *Suaeda salsa, transcriptional response, atrazine stress, molecular level*

Introduction

Atrazine is a triazine herbicide with low production cost and good herbicidal effect (Ge et al., 2021; Yan et al., 2015). However, the structural stability and non-degradable nature of atrazine can cause it to stay in the soil for a long time. Therefore, atrazine can be toxic to sensitive crops (Mali et al., 2021). In addition, atrazine has water-soluble properties. Therefore, atrazine present in the soil that cannot be decomposed in a short time is easily dissolved in rainwater and agricultural irrigation water, or seeps into the ground or sinks into rivers. Eventually, it causes pollution and damage to the ecosystem (Bachetti et al., 2021). In summary, it is reasonable to speculate that atrazine affects chemical and biological processes in the soil environmental system. It was found (Zhang et al., 2017; Rohr, 2021) that atrazine affects the normal growth and development of crops, the structural composition of soil microbial communities and the transformation of substances in the soil, ultimately causing pollution of the environment.

Atrazine mainly enters the plant body through the roots and leaves of root plants and the cell surface of unicellular plants. Atrazine blocks the binding of D1 protein to plastoquinone by acting as an inhibitor of plastoquinone binding, thereby blocking electron transfer in photosynthetic system II. This blockage would lead to chlorophyll destruction and termination of carbohydrate synthesis, thus inhibiting photosynthesis

http://www.aloki.hu ● ISSN 1589 1623 (Print) ● ISSN 1785 0037 (Online)
DOI: http://dx.doi.org/10.15666/aeer/2005_40614077

(Karim et al., 2021). At the same time, the oxidative stress and free radical production caused by the blockage of electron transfer can cause massive and rapid cellular damage, which can lead to plant decay and death (Kumari et al., 2021; James and Kumar, 2021). Current studies have shown that higher concentrations of atrazine have a strong toxic effect on aquatic vascular plants (Li et al., 2008). In addition, when the concentration of atrazine was above 0.1 mg/L, it significantly affected the photosynthesis and chlorophyll content of aquatic plants (Alberto et al., 2016). The effects of atrazine on chlorophyll content, antioxidant enzyme activity and chlorophyll content of reed were investigated by hydroponic experiments. The results showed that southern reed was tolerant when the atrazine concentration was less than or equal to 8 mgL-1, but the growth of southern reed was stopped after 2 weeks of stress (Qi et al., 2014). Liu et al. (2011) investigated the response of the symbiotic system of the bush mycorrhizal fungus Cannon to atrazine stress. The results showed that atrazine stress inhibited the growth and development of plantain. Atrazine stress reduced photosynthetic rate, transpiration and stomatal conductance of plantain roots. Thus, this stress caused damage to the cellular and subcellular structure and also led to the occurrence of intracellular antioxidant stress responses, which in turn affected the growth and photosynthesis of plantain.

Suaeda salsa is an annual herb belonging to the genus Suaeda in the family Lycidae. It grows in coastal, lakeside, desert and other saline alkali land. It is a pioneer plant developing from land to coast and is also a typical saline alkali indicator plant (Su et al., 2018). *Suaeda salsa* is 20-90 cm in height, with red stems and leaves which are slightly fleshy, elongated (Kang et al., 2021). However, with the influence of human activities in recent years, *Suaeda salsa* has died in a large area in Panjin red beach, Liaoning Province, in China. After extensive preliminary research, it was found that atrazine does exist in the seawater and in the soil of Panjin Red Beach (Liu et al., 2020). In conclusion, atrazine has a toxic effect on *Suaeda salsa*, but the effect of atrazine on the gene expression of *Suaeda salsa* is still unclear. Therefore, this study analyzed the transcriptomic response of *Suaeda salsa* to atrazine stress. The differences in gene expression of *Suaeda salsa* at different atrazine concentrations were analyzed. The aim of this paper is to find a theoretical basis for the mass mortality of Panjin Red Beach and to provide a reference for the ecological restoration of Panjin Red Beach.

Materials and methods

Plant material and culture

Suaeda salsa seeds were purchased from Panjin City, Liaoning Province. The herbicide atrazine was produced by Jiangsu Ruibang Pesticide Factory Co., Ltd. (the content of effective components was 90%, and the dosage form was water dispersible granule).

The experiment was carried out in Liaoning Key Laboratory of coastal marine environmental science and technology, Dalian Ocean University. In the experiment, *Suaeda salsa* seedlings with the same growth time and similar plant height were cleaned in the form of hydroponics. The roots were washed with deionized water. The cleaned *Suaeda salsa* seedlings were put into a beaker containing Hogland nutrient solution. The beaker was placed in a light incubator. The light cycle was 12 h, the temperature was controlled at 20 °C, and the light intensity was 6480 lux, stable for 3 days. The consumed nutrient solution was supplemented every day.

http://www.aloki.hu ● ISSN 1589 1623 (Print) ● ISSN 1785 0037 (Online)
DOI: http://dx.doi.org/10.15666/aeer/2005_40614077

Three days later, atrazine solution was prepared with Hogland nutrient solution. By reviewing the relevant literature and the results of field monitoring of atrazine, three concentrations were determined: high, medium and low, respectively, for the control group (C, 0 mg/L), low concentration group (L, 0.1 mg/L), medium concentration group (M, 0.4 mg/L) and high concentration group (H, 1 mg/L). Stable *Suaeda salsa* seedlings were put into atrazine solutions with different concentrations. About 20 seedlings were placed in each concentration. Three seedlings were placed in each experimental group in parallel. The nutrient solution was changed every 4 days to keep atrazine concentration unchanged. The experimental period was 6 days. The control group and three concentration gradient samples are represented by C, l, m and h, respectively. Due to the existence of parallel experiments, the results are represented as C-1, C-2, C-3, L-1, L-2, L-3, M-1, M-2, M-3, H-1, H-2 and H-3, with a total of 12 samples. The samples were frozen in liquid nitrogen for sequencing analysis. Immediately after collection, the samples were placed in precooled RNAiso, then refrigerated in dry ice and sent to Novo Zhiyuan for RNA extraction and sequencing.

Sample collection and RNA extraction

RNA was extracted using a Trizol kit (Invitrogen, CS, USA) according to standard procedures. RNA degradation and contamination was monitored on 1% agarose gels. The purity and integrity of RNA were detected by Nanodrop and Agilent 2100 respectively. RNA concentration was measured using Qubit® RNA Assay Kit in Qubit® 2.0 Flurometer (Life Technologies, CA, USA).

Library preparation and sequencing

The transcriptome library was prepared according to the procedure described in the previous report (Kang et al., 2020). The library building starting RNA was total RNA, and mRNA with polyA tails was first enriched by Oligo (dT) magnetic beads, followed by random interruption of the obtained mRNA with divalent cations in Fragmentation Buffer. Using the fragmented mRNA as a template and random oligonucleotides as primers, the first strand of cDNA was synthesized in the M-MuLV reverse transcriptase system, followed by degradation of the RNA strand with RNaseH and synthesis of the second strand of cDNA with dNTPs under the DNA polymerase I system. The purified double-stranded cDNA was end-repaired, A-tailed and connected to the sequencing junction, and the cDNA of about 370~420 bp was screened with AMPure XP beads, PCR amplified, and the PCR products were purified again with AMPure XP beads to finally obtain the library. After the library was constructed, the library was initially quantified using a Qubit 2.0 Fluorometer and diluted to 1.5 ng/ul, and then the insert size of the library was detected using an Agilent 2100 bioanalyzer, and after the insert size was as expected, the effective concentration of the library was accurately quantified by qRT-PCR. After the insert size met the expectation, qRT-PCR was performed to accurately quantify the effective concentration of the library (effective library concentration above 2 nM) to ensure its quality.

After passing the library test, different libraries are pooled according to the effective concentration and the target downstream data volume and then sequenced by Illumina, and 150 bp paired-end reads are generated. The basic principle of sequencing is Sequencing by Synthesis.

http://www.aloki.hu ● ISSN 1589 1623 (Print) ● ISSN 1785 0037 (Online)
DOI: http://dx.doi.org/10.15666/aeer/2005_40614077

Transcriptome assembly and gene functional annotation

The raw image data files obtained by high-throughput sequencing were converted into sequenced reads (raw reads) by the CASAVA Base Calling analysis. After the raw reads were obtained, the sequencing error rate was first evaluated by Qphred (Q20 and Q30 respectively indicate that the base correct recognition rate is 99%, 99.9%); in addition, the presence or absence of the AT and GC separation phenomenon was detected by the GC content distribution. Clean reads were obtained from raw reads by removing reads containing adapter, N > 10% (N indicates the base could not be determined) and low-quality reads. After obtaining clean reads, the clean reads were spliced by Trinity. The transcript sequence obtained by splicing was used as reference sequence for subsequent analysis.

Gene function annotations for transcript were performed based on seven databases, including: Nr, Nt, Pfam, KOG/COG, Swiss-prot, KEGG, GO. Among them, NR, KOG/COG and Swiss-Prot were annotated with software diamond; NT, KEGG, Pfam, GO were annotated by software NCBI blast, KAAS, hmmscan and Blast 2 GO respectively.

Differential expression analysis

Gene expression analysis was performed by RSEM. Using software Bowtie2 with parameter mismatch 0 (default). Prior to differential gene expression analysis, for each sequenced library, the read counts data obtained from gene expression analysis were adjusted by edgeR program package through one scaling normalized factor as described in the previous report (Mevy et al., 2020). Differential expression analysis of two samples was performed using the DEGseq (2010) R package, and $P < 0.005$ & $|\log2 (\text{Fold Change})| > 1$ was set as the threshold for significantly differential expression. GO enrichment of differentially expressed genes was performed on GOseq with the parameter $P < 0.05$ (Chakrapani et al., 2016). KEGG enrichment was performed on differentially expressed genes using KOBAS with the parameter $P < 0.05$ (Li et al., 2019).

Results

RNA-seq, data preprocessing and sequence assembly

The raw data of control group C and experimental group L, M and H were sequenced. Raw reads of 12 samples ranged from 20.969 million to 23.919 million. The number of high-quality clean reads obtained by filtration ranged from 20.642 million to 23.436 million. The total number of clean bases in 12 groups reached 78.92 G. The error rate was 0.02% except for C-3 and M-3, which were 0.03%; The contents of Q20, Q30 and GC are shown in *Table 1*.

After processing by Trinaty software, a total of 443,515 transcripts were obtained, with an average length of 998 bp and a maximum length of 15,773 bp for N50 and N90. Among them, the number of transcripts between 300-500 bp was 175,499. Finally, after double-end information assembly, the longest transcript of each gene was selected as a single gene, and a total of 261,694 single genes were obtained, with an average length of 864 bp and a maximum length of 15,773 bp. the number of single genes between 300 and 500 bp was 110,356, and N50 and N90 were 1,117 bp and 404 bp, respectively. The frequency distribution of splice length and splice distribution of the lengths are shown in *Tables 2* and *3*.

http://www.aloki.hu ● ISSN 1589 1623 (Print) ● ISSN 1785 0037 (Online)
DOI: http://dx.doi.org/10.15666/aeer/2005_40614077

Table 1. *Sequencing data quality*

Sample	Raw reads	Clean reads	Clean bases	Error (%)	Q20 (%)	Q30 (%)	GC (%)
C_1	21921679	21385313	6.42G	0.02	98.24	94.58	42.53
C_2	21865080	21336345	6.4G	0.02	98.32	94.82	42.31
C_3	22549184	22000121	6.6G	0.03	97.8	93.54	42.3
L_1	22050991	21370452	6.41G	0.02	98.2	94.53	43.32
L_2	22967081	22421164	6.73G	0.02	98.25	94.67	43.99
L_3	23513368	23076060	6.92G	0.02	98.34	94.84	42.74
M_1	23919239	23435778	7.03G	0.02	98.21	94.53	42.43
M_2	22607574	22048616	6.61G	0.02	98.15	94.39	42.73
M_3	21423335	21101407	6.33G	0.03	98.04	94.12	42.12
H_1	23473927	23056249	6.92G	0.02	98.35	94.92	47.51
H_2	21570548	21200975	6.36G	0.02	98.25	94.67	45.53
H_3	20969253	20642107	6.19G	0.02	98.19	94.45	42.64

Clean bases: the number of sequenced sequences multiplied by the length of sequenced sequences, and converted to the unit of G; Error (%): sequencing base error rate; Q20, 30 (%): the percentage of bases with phred values greater than 20 and 30 in total bases; GC content (%): the percentage of the total number of bases g and C in the total number of bases

Table 2. *Splicing length frequency distribution*

Transcript length interval	300-500 bp	500-1 kbp	1 k-2 k bp	>2 k bp	Total
Number of transcripts	175499	128559	85922	53535	443515
Number of unigenes	110356	88052	42487	20799	261694

Table 3. *Splicing length distribution*

	Min length	Mean length	Median length	Max length	N50	N90	Total nucleotides
Transcripts	301	998	615	15773	1485	418	442633466
Unigenes	301	864	562	15773	1117	404	226195038

N50, N90: the spliced transcripts are sorted according to the length from large to small, and the length of the spliced transcripts is accumulated to the length of no less than 50%/90% of the total length, which is N50/N90

Gene function annotation

Since there is no genome-wide background of *Suaeda salsa*, we compared 261694 single genes with known public databases NR, NT, Swiss, Protein, Pfam, KEGG, COG and counted the number of single genes annotated in each database by BLASTN and BLASTX to complete the annotation of *Suaeda salsa* genes and prediction of function. By comparing with the above seven databases, 147,649, 89,782, 74,786, 129,562, 137,391, 137,383 and 80,756 unigenes were able to obtain homology comparison information, accounting for 56.42%, 34.3%, 28.57%, 49.5%, 52.5%, 52.49% and 30.85%, respectively. And at least one of the above seven databases successfully annotated 195917 single genes, accounting for 74.86% of the total number of single genes (*Table 4*).

http://www.aloki.hu ● ISSN 1589 1623 (Print) ● ISSN 1785 0037 (Online)
DOI: http://dx.doi.org/10.15666/aeer/2005_40614077

Table 4. *Gene annotation success rate statistics*

	Number of Unigenes	**Percentage (%)**
Annotated in NR	147649	56.42
Annotated in NT	89782	34.3
Annotated in KO	74786	28.57
Annotated in SwissProt	129562	49.5
Annotated in PFAM	137391	52.5
Annotated in GO	137383	52.49
Annotated in KOG	80756	30.85
Annotated in all Databases	27840	10.63
Annotated in at least one Database	195917	74.86
Total Unigenes	261694	100

Gene differential expression analysis

Compared with the control group, a total of 33,907 differential genes were generated in experimental group H, of which 33,370 were up-regulated and 537 were down-regulated; a total of 8,450 differential genes were generated in experimental group M, of which 7,303 were up-regulated and 1,147 were down-regulated; a total of 15,832 differential genes were generated in experimental group L, of which 14,791 were up-regulated and 1041 genes were down-regulated (*Fig. 1*).

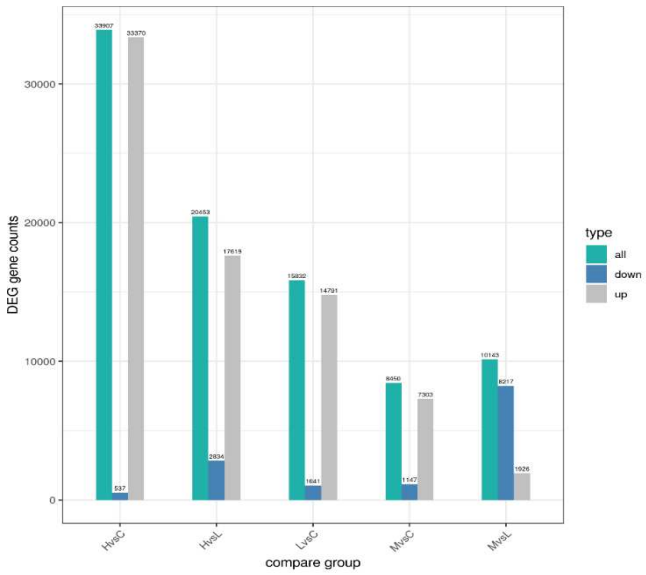

Figure 1. *Number of differential genes*

Differentially expressed transcripts in the three experimental groups were found to increase with increasing concentrations of atrazine (*Fig. 2*). There were 10216 differentially expressed transcripts in the group L, 2183 differentially expressed transcripts in the group M and 26691 differentially expressed transcripts in the group H. This indicates that the *Suaeda salsa* transcriptional responds more to the stress of high concentration of atrazine.

http://www.aloki.hu ● ISSN 1589 1623 (Print) ● ISSN 1785 0037 (Online)
DOI: http://dx.doi.org/10.15666/aeer/2005_40614077

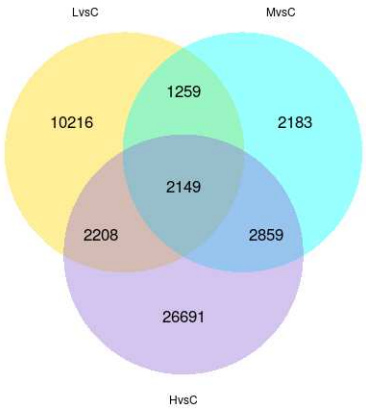

Figure 2. *Venn of differentially expressed transcripts. The sum of the numbers in each circle represents the number of differentially expressed transcripts in a group, the intersecting part represents the differentially expressed transcripts contained in each group, and the non intersecting part is the unique differentially expressed transcripts of the group*

GO enrichment analysis of differentially expressed genes

Differential transcriptome expression under high concentration of atrazine stress (group H, *Fig. 3a*). The most up-regulated differential genes occurred in cellular and cellular fractions, both with 7077, followed by intracellular fraction and intracellular with 6644 and 6678, respectively; under the classification of biological processes, the most up-regulated differential genes occurred in biosynthetic processes and organic matter biosynthesis, with 6264 and 6040, respectively; under the classification of molecular functions, the largest number of differential genes were found in oxidoreductase activity, structural activity and structural components of ribosomes, with 2193, 2035 and 1676 differential genes, respectively.

Differential transcriptome expression under medium concentration of atrazine stress (group M, Fig. 3b)

Under the cellular component the most differential genes with upregulation occurred in the cell and cellular fraction, both with 1944, followed by the intracellular fraction and intracellular with 1839 and 1847, respectively; under the biological process classification, the most differential genes with upregulation occurred in the biosynthetic process and organic matter biosynthesis with 1699 and 1651, respectively; under the molecular function classification, structural molecular activity and under the classification of molecular functions, the largest number of differential genes were found in the structural molecular activity and structural components of ribosomes, with 776 and 678 differential genes, respectively.

Differential transcriptome expression under stress of low concentration of atrazine (group L, Fig. 3c)

Under the cellular composition classification, the most differential genes were up-regulated in cells and cellular fractions, both with 3960; in the biological processes metabolic processes were up-regulated with 6698, followed by nitrogen compound metabolic processes and cellular nitrogen compound metabolic processes with 4135 and 2469, respectively; under the molecular function classification, the most differential genes were up-regulated in catalytic activity with 5438.

http://www.aloki.hu ● ISSN 1589 1623 (Print) ● ISSN 1785 0037 (Online)
DOI: http://dx.doi.org/10.15666/aeer/2005_40614077

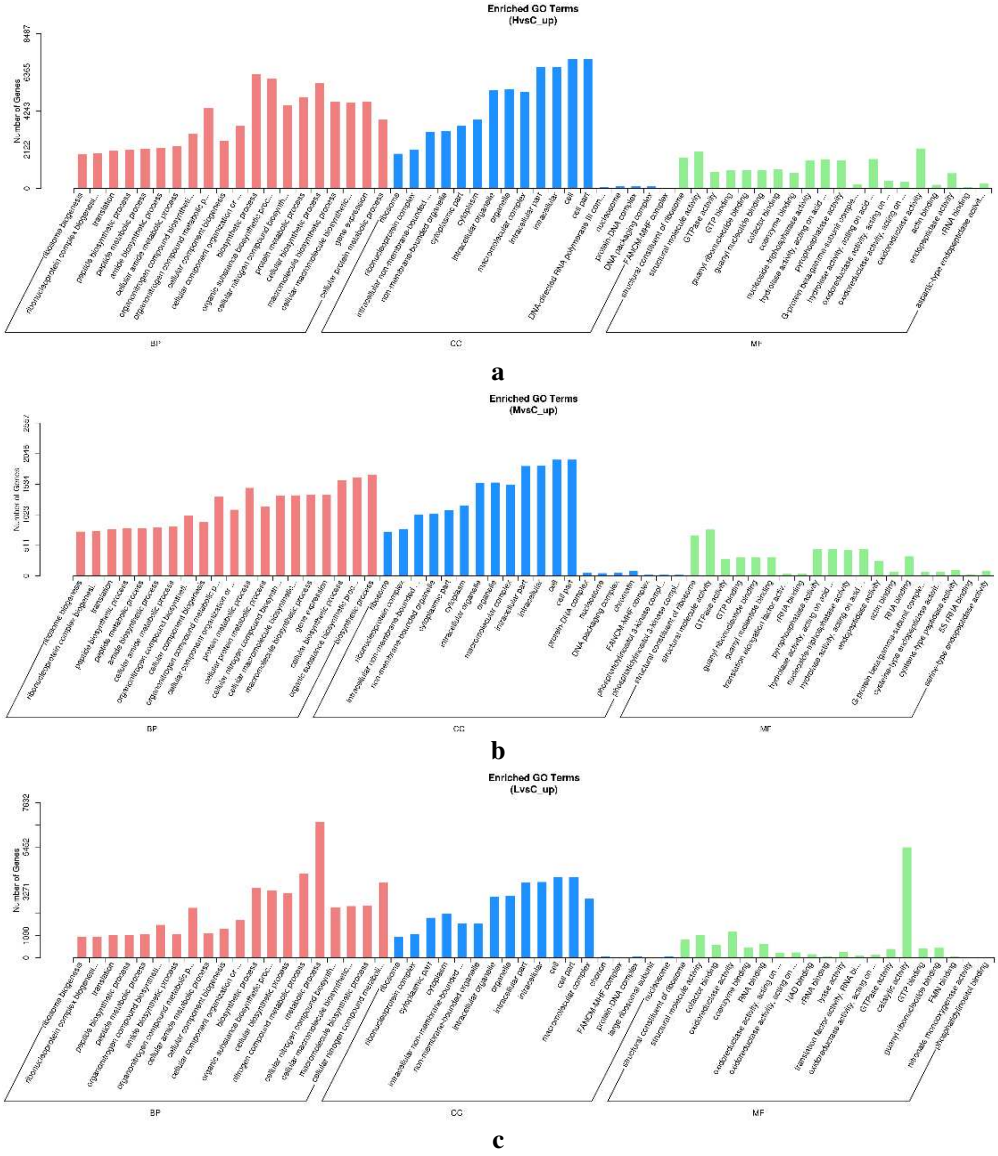

Figure 3*. The GO enrichment analysis result for (a) group H, (b) group M and (c) group L*

KEGG enrichment analysis of differentially expressed genes

The results of the difference analysis were subjected to KEGG PATHWAY enrichment analysis, and it was found that the processes that were significantly enriched at high, medium and low atrazine concentrations compared to the control were (*Fig. 4a, b, c*): oxidative phosphorylation, steroid biosynthesis, photosynthesis and protein processing in endoplasmic reticulum.

Ribosomal pathway

Among the main KEGG enrichment pathways, ribosome was significantly enriched in the three atrazine concentrations. As shown in *Figure 5,* through KEGG annotation, 142 unigenes in the transcriptome of *Suaeda salsa* were annotated into the KEGG pathway of ribosome under group H. Most of the genes were up-regulated including EF-Tu protein and SecY protein.

http://www.aloki.hu ● ISSN 1589 1623 (Print) ● ISSN 1785 0037 (Online)
DOI: http://dx.doi.org/10.15666/aeer/2005_40614077

Phagosome pathway

Through KEGG annotation, 73 unigenes were annotated into the KEGG pathway of phagosome under group H. As shown in *Figure 6,* 15 genes are up-regulated including V-ATPase, F-actin, F-actin, tuba protein.

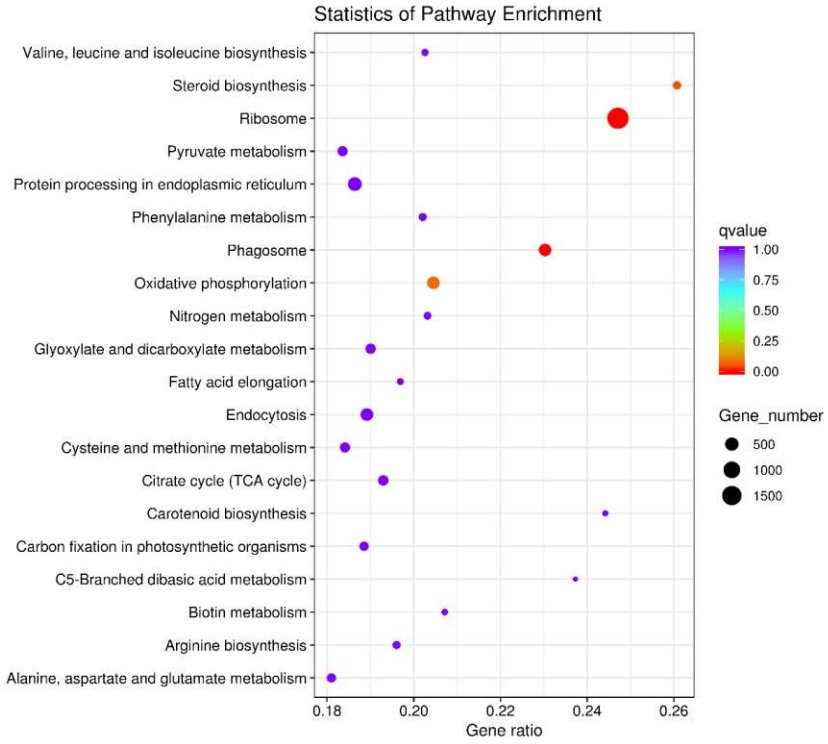

a

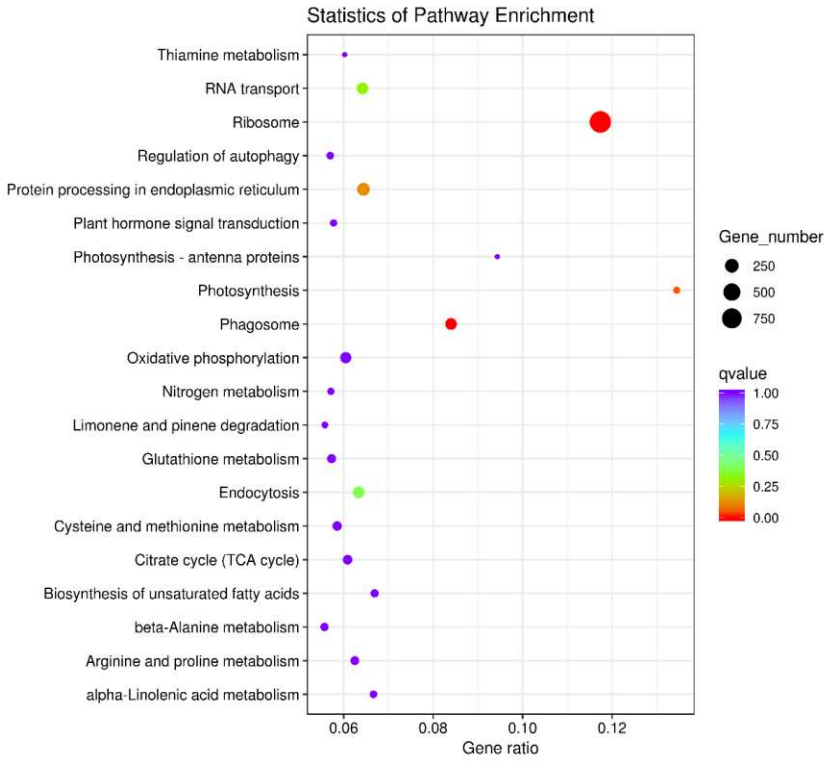

b

http://www.aloki.hu ● ISSN 1589 1623 (Print) ● ISSN 1785 0037 (Online)
DOI: http://dx.doi.org/10.15666/aeer/2005_40614077

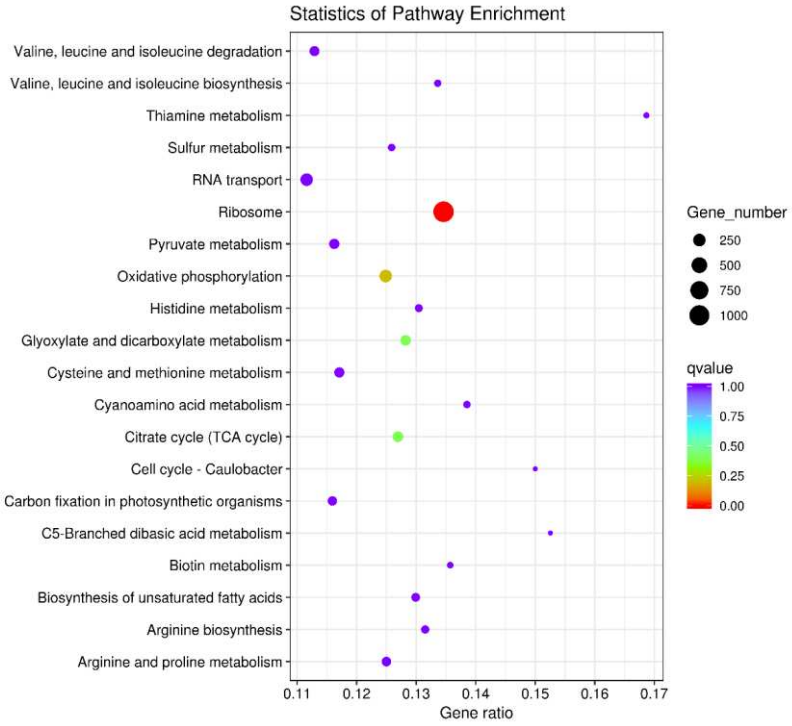

c

Figure 4. *The KEGG enrichment analysis result for (a) group H, (b) group M and (c) group L*

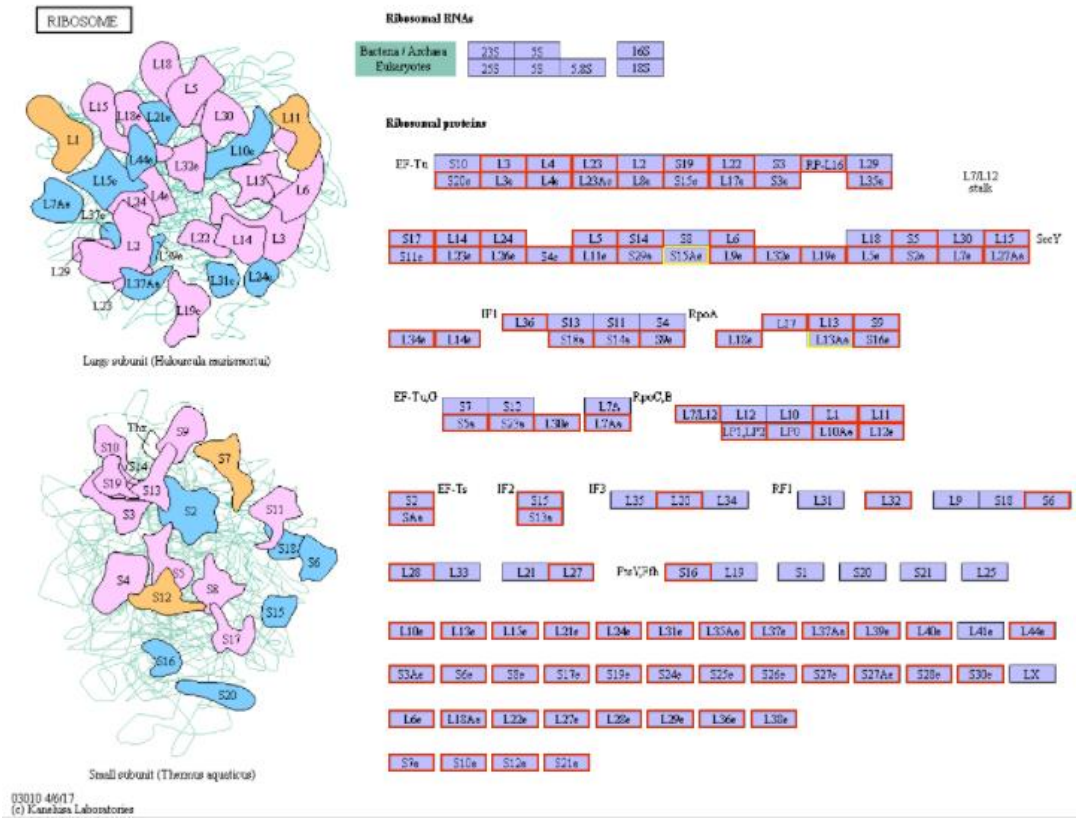

Figure 5. *The ribosomal pathway of differential genes at group H*

http://www.aloki.hu ● ISSN 1589 1623 (Print) ● ISSN 1785 0037 (Online)
DOI: http://dx.doi.org/10.15666/aeer/2005_40614077

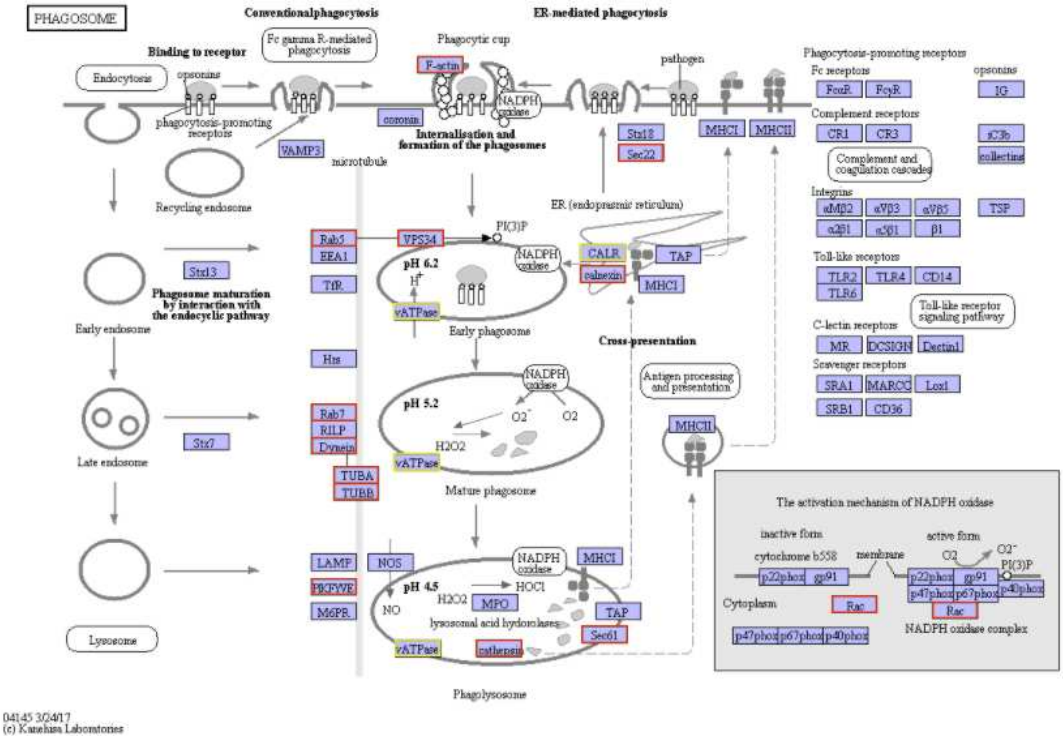

Figure 6. *Differential gene phagosome pathway at group H*

Oxidative phosphorylation

Through KEGG annotation, we found that 192 unigenes were annotated into KEGG pathway of oxidative phosphorylation under group H. As shown in *Figure 7,* 62 genes are up-regulated, including NADH dehydrogenase, F-ATPase, V-ATPase.

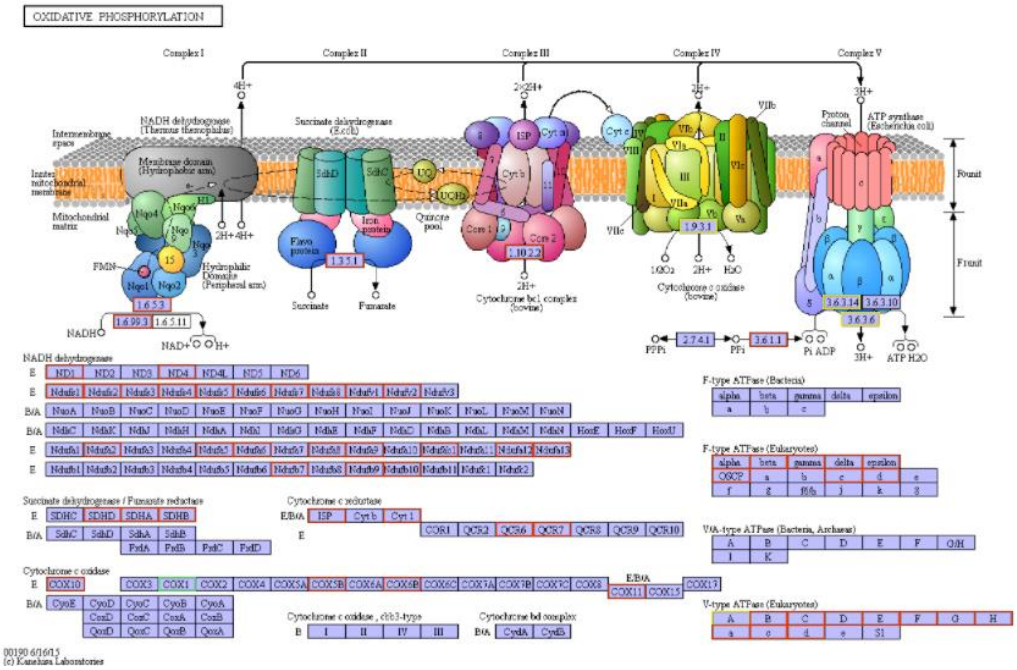

Figure 7. *Pathways of oxidative phosphorylation of differential genes at group H*

http://www.aloki.hu ● ISSN 1589 1623 (Print) ● ISSN 1785 0037 (Online)
DOI: http://dx.doi.org/10.15666/aeer/2005_40614077

Discussion

In this study, the effects of different concentrations of atrazine on the growth of *Suaeda salsa* under hydroponic conditions were studied, and the whole transcriptome of *Suaeda salsa* under the action of different concentrations of atrazine was sequenced by high-throughput sequencing technology. The results of differential analysis were enriched by KEGG path. The molecular regulation mechanism of atrazine in *Suaeda salsa* was studied from the level of metabolic pathway.

Ribosomal pathway regulation

Elongation factor EF-Tu protein is an important protein involved in protein translation and extension (Cai et al., 2022). They promote and control protein synthesis by catalyzing the extension of amino acid chain on ribosome (Aviner, 2020; Wang et al., 2013). It is found that EF-Tu is the protein with the highest content among the proteins related to translation mechanism in cells (DeLey Cox et al., 2019). In addition, it also plays a very important role in growth signal transduction, heat resistance, drought resistance and disease resistance (Zhang et al., 2022; Fu et al., 2012). EF-Tu protein brings aminoacyl transfer RNA (tRNA) into ribosome in the extension stage of translation. EF-Tu • guanosine triphosphate (GTP) has high affinity with tRNA to form a ternary complex EF-Tu • GTP • tRNA. EF-Tu can recognize the common characteristics of tRNA and also recognize that tRNA is aminoacylated (Hughes, 2013). It is speculated that Suaeda Heteroptera has its own stress response under atrazine stress, resulting in the up regulation of EF-Tu protein related differential genes.

SecY is a membrane protein involved in the protein transport of cell membrane (Ma et al., 2019). The Sec system is the main pathway responsible for the export of proteins across the plasma membrane and the insertion of proteins into the plasma membrane. The Sec system is composed of membrane proteins SecY, sece and SecG, which form a channel on the cytoplasmic membrane for protein transport; Intracellular protein SecA mediates the transport of presecretory proteins into the channel through the energy of adenosine triphosphate (ATP) hydrolysis (Ma et al., 2019). Kakizawa et al. (2001) cloned SecA, SecY and sece genes from phytoplasma onion yellowing, and confirmed the existence of secretory protein transport system in phytoplasma. It is speculated that when atrazine stresses Suaeda Heteroptera, the stress response of self-protection produced by the body leads to the increase of EF-Tu protein in ribosome, which increases the SecY of transport protein and the up regulation of SecY related genes.

Phagosome pathway regulation

A universal mechanism of V-ATPase is reversible decomposition (Hooper et al., 2022). Cells decompose in the absence of glucose, a mechanism for preserving cellular ATP during starvation. Recombination occurs rapidly after glucose recovery (McGuire and Forgac, 2018). However, experiments show that in some mammalian cells, V-ATPase assembly actually occurs under low sugar conditions and low amino acid availability conditions, which may be a mean to promote the circulation of biochemical building blocks through autophagy (Jaskolka and Kane, 2020; Eaton et al., 2021; Harvey, 1992). During the maturation of dendritic cells of the immune system, the assembly of V-ATPase on lysosomal membrane increases to stimulate antigen processing, which depends on the activity of protease, and it is the most effective at low pH (Stransky and Forgac, 2015). Studies have shown that in yeast, V-

http://www.aloki.hu ● ISSN 1589 1623 (Print) ● ISSN 1785 0037 (Online)
DOI: http://dx.doi.org/10.15666/aeer/2005_40614077

atpases on vacuoles will increase under high extracellular pH or osmotic stress, which need to increase the transport of protons into vacuoles (Vasanthakumar and Rubinstein, 2020; Banerjee and Kane, 2020). F-Actin is an important cytoskeleton component in dendritic filamentous feet and processes, and it is involved in regulating the morphogenesis and synaptic plasticity of processes (Kim, 2009). In cells, the spiny end of F-actin faces the cell membrane, and the tip is fixed deep in the F-actin network. There, actin steps on a large scale, polymerizes directly below the membrane and depolymerizes at the rear of the F-actin network, thus providing power for membrane protrusions (Galkin et al., 2010; Ma and Tymanskyj, 2020). TUBA protein is a new scaffold protein. Its function is to bind dynein and actin regulatory protein together. It selectively binds dynein through four N-terminal SRC homology-3 (SH3) regions. TUBA protein binds to a variety of actins through the C-terminal SH3 domain. Forcibly targeting the C-terminal SH3 domain to the mitochondrial surface can promote the accumulation of F-actin around mitochondria (Wagh et al., 2015; Salazar et al., 2003).

Oxidative phosphorylation

Oxidative phosphorylation is the coupling reaction of ADP and inorganic phosphoric acid to synthesize ATP. NADH dehydrogenase is a protein composed of 42 subunits, of which 7 subunits are encoded by the mitochondrial genome (Ludwig et al., 2020; Burstein et al., 2000). NADH dehydrogenase is located in mitochondria and is called complex I during oxidative phosphorylation. Its main function is to transfer a pair of electrons to CoQ and 4 H^+ to the membrane gap. When protons return to the mitochondrial matrix, it drives ATP synthase to synthesize ATP (Braun, 2020; Manoj, 2018; Piccoli et al., 2008). NADH dehydrogenase subunit is located on the inner mitochondrial membrane, and its expression change can change the permeability of the inner mitochondrial membrane, thus changing the state of cytochrome c on the mitochondrial membrane, thus affecting the regulation of mitochondria on apoptosis (Manoj et al., 2020; Chen et al., 2009). Type F-ATPase is an ATPase/synthase that exists in bacterial plasma membrane, mitochondrial inner membrane (oxidative phosphorylation, which is called complex V there) and chloroplast thylakoid membrane. It uses a proton gradient to drive ATP synthesis, allows the passive flux of protons to pass through the membrane along its electrochemical gradient, and uses the energy released by the transport reaction to release the newly formed ATP from the active site of F-ATPase. Like V-ATPase and A-ATPase, F-ATPase belongs to the superfamily of related rotating ATPases (Chen et al., 2021; Kühlbrandt, 2019). F-ATPase mainly acts as ATP synthase and takes ADP and inorganic phosphate as substrates. It exists on the plasma membrane of eubacteria, the inner membrane of mitochondria and the thylakoid membrane of chloroplast. V-ATPase only acts as an ion pump driven by ATP hydrolysis and exists in various intracellular and interventricular membranes, such as chromatin granules, lysosomes, endosomes, synaptic vesicles, Golgi derived vesicles, yeast vesicles and plant vacuolar plastids. They are involved in many intracellular and intercellular processes, including receptor-mediated endocytosis, protein transport, pH maintenance and neurotransmitter release (Fan, 2009). The results of differential analysis were analyzed by KEGG pathway enrichment analysis. The results showed that the processes of significant enrichment of high, medium and low atrazine concentrations compared with the control group was oxidative phosphorylation. The

http://www.aloki.hu ● ISSN 1589 1623 (Print) ● ISSN 1785 0037 (Online)
DOI: http://dx.doi.org/10.15666/aeer/2005_40614077

transcription and translation related genes of elongation factor in ribosomes and SecY membrane protein related genes producing protein membrane channels were up-regulated, the F-Actin and V-ATPase related genes involved in transport in phagocytes were up-regulated, and the F-ATPase and V-ATPase related genes producing ATP during oxidative phosphorylation were up-regulated, indicating that the above related genes were involved in the corresponding response to atrazine stress. The stress response of Suaeda Heteroptera to atrazine stress is an energy consuming process. In this process, the expression of genes related to respiratory chain producing ATPase increases, the content of transcription and translation proteins of elongation factor in ribosome increases, and the expression of F-Actin and V-ATPase in phagosome increases. It is speculated that due to stress, a large number of body related proteins are transcribed and translated by elongation factors in ribosomes, and then proteins are transported through SecY membrane proteins, which are transported by phagocytes with the support of F-Actin and the catalysis of V-ATPase. At the same time, F-ATPase and V-ATPase supply a large amount of ATP during oxidative phosphorylation. NADH dehydrogenase affects the regulation of mitochondria on cell apoptosis guaranteeing the maintenance of system balance.

Conclusion

The results of the difference analysis were subjected to KEGG PATHWAY enrichment analysis, and it was found that the processes that were significantly enriched at high, medium and low atrazine concentrations compared to the control were mainly: steroid biosynthesis, photosynthesis, protein processing in endoplasmic reticulum and oxidative phosphorylation. The genes related to F-actin and V-ATPase involved in transport in phagosome were up-regulated, and the genes related to F-ATPase and V-ATPase involved in ATP production in oxidative phosphorylation were up-regulated, indicating that all the above related process genes were involved in the corresponding response to atrazine stress. The stress response to atrazine stress is an energy-consuming process in which the expression of respiratory chain-related ATPase-generating genes increases, while the content of transcriptionally translated proteins of elongation factors in the ribosomes increases, and the expression of F-actin and V-ATPase both increase in the phagosomes. SecY membrane proteins produce channels in the membrane for protein transport, supported by F-actin and catalyzed by V-ATPase by phagosomes, while the oxidative phosphorylation process F-ATPase and V-ATPase supply large amounts of ATP, and NADH dehydrogenase affects the regulation of apoptosis by mitochondria to ensure the maintenance of system homeostasis.

A certain concentration of herbicides was found in the Panjin Red Beach wetland through monitoring, which originated from herbicides in the surrounding agricultural fields; it may have led to the degradation and even death of winged alkali ponies, so this study helps to further analyze the causes of its degradation.

Declaration of competing interests. The authors declare that they have no known competing financial interests or personal relationships that could have appeared to influence the work reported in this paper.

http://www.aloki.hu ● ISSN 1589 1623 (Print) ● ISSN 1785 0037 (Online)
DOI: http://dx.doi.org/10.15666/aeer/2005_40614077

REFERENCES

[1] Alberto, D., Serra, A.-A., Sulmon, C., Gouesbet, G., Couée, I. (2016): Herbicide-related signaling in plants reveals novel insights for herbicide use strategies, environmental risk assessment and global change assessment challenges. – Science of the Total Environment 569-570:1618-1628.

[2] Aviner, R. (2020): The Science of puromycin: from studies of ribosome function to applications in biotechnology. – Computational and Structural Biotechnology Journal 18: 1074-1083.

[3] Bachetti, R. A., Urseler, N., Morgante, V., Damilano, G., Porporatto, C., Agostini, E., Morgante, C. (2021): Monitoring of atrazine pollution and its spatial-seasonal variation on surface water sources of an agricultural river basin. – Bulletin of Environmental Contamination and Toxicology 106: 929-935.

[4] Banerjee, S., Kane, P. M. (2020): Regulation of V-ATPase activity and organelle pH by phosphatidylinositol phosphate lipids. – Frontiers in Cell and Developmental Biology, 8:510

[5] Braun, H.-P. (2020): The oxidative phosphorylation system of the mitochondria in plants. – Mitochondrion 53(2020): 66-75.

[6] Burstein, S. H., Rossetti, R. G., Yagen, B., Zurier, R. B. (2000): Oxidative metabolism of anandamide. – Prostaglandins Other Lipid Mediat 61(1-2): 29-41.

[7] Cai, L., Liu, Z., Cai, L., Yan, X., Hu, Y., Hao, B., Xu, Z., Tian, Y., …, Wan, J. (2022): Nuclear encoded elongation factor EF-Tu is required for chloroplast development in rice grown under low-temperature conditions. – Journal of Genetics and Genomics 5: 502-505.

[8] Chakrapani, V., Patra, S. K., Mohapatra, S. D., Rasal, K. D., Deshpande, U., Nayak, S.,…, Barman, H. K. (2016): Comparative transcriptomic profiling of larvae and post-larvae of macrobrachium rosenbergii in response to metamorphosis and salinity exposure. – Genes & Genomics 38(11): 1061-1076.

[9] Chen, B., Liu, X. G., Zheng, H. L., Liang, J. Y., Liang, N. C. (2009): Protein kinase CK2α'Screening of interacting protein NADH dehydrogenase 4. – Chinese Tropical Medicine 9(8): 1427-1428.

[10] Chen, X. X., Ding, Y. L., Yang, Y. Q., Song, C. P., Wang, B. S., Yang, S. H., Guo, Y., Gong, Z. Z. (2021): Protein kinases in plant responses to drought, salt, and cold stress. – Journal of Integrative Plant Biology 63(1):53-78.

[11] DeLey Cox, V. E., Cole, M. F., Gaucher, E. A. (2019): Incorporation of modified amino acids by engineered elongation factors with expanded substrate capabilities. – ACS Synthetic Biology 8(2): 287–296.

[12] Eaton, A. F., Merkulova, M., Brown, D. (2021): The H(+)ATPase (v-ATPase): from proton pump to signaling complex in health and disease. – American Journal of Physiology 320(3):392-414.

[13] Fan, H. (2009): Retroviruses. – Encyclopedia of Microbiology (Elsevier) 47: 519-534.

[14] Fu, J. M., Momčilović, I., Vara Prasad, P. V. (2012): Roles of protein synthesis elongation factor EF-Tu in heat tolerance in plants. – Journal of Botany 2012(Article ID 835836):8.

[15] Galkin, V. E., Orlova, Al., Schröder, G. F., Egelman, E. H. (2010): Structural polymorphism in F-actin. – Nature Structural & Molecular Biology 17(11):1318-1323.

[16] Ge, J. Y., Liu, J., Wang, T. W., Huang, D., Li, J. W., Zhang, S., …, Zhao, L. J. (2021): Prolonged exposure to the herbicide atrazine suppresses immune cell functions by inducing spleen cell apoptosis in rats. – Ecotoxicology and Environmental Safety 220:112386.

[17] Harvey, W. R. (1992): Physiology of V-ATPases. – Journal of Experimental Biology 172(1): 1-17.

http://www.aloki.hu ● ISSN 1589 1623 (Print) ● ISSN 1785 0037 (Online)
DOI: http://dx.doi.org/10.15666/aeer/2005_40614077

[18] Hooper, K. M., Jacquin, E., Li, T., Goodwin, J. M., Brumell, J. H., Durgan, J., Florey, O. (2022): V-ATPase is a universal regulator of LC3-associated phagocytosis and non-canonical autophagy. – The Journal of Cell Biology 6.
[19] Hughes, D. (2013): Elongation Factors: Translation. – Brenner's Encyclopedia of Genetics (Second Edition), 466-468.
[20] James, A., Kumar, S. D. (2021): Atrazine detoxification by intracellular crude enzyme extracts derived from epiphytic root bacteria associated with emergent hydrophytes. – Journal of Environmental Science and Health, Part B 6.
[21] Jaskolka, M. C., Kane, P. M. (2020): Interaction between the yeast RAVE complex and Vph1-containing Vo sectors is a central glucose-sensitive interaction required for V-ATPase reassembly. – Journal of Biological Chemistry 295(8):2259-2269.
[22] Kakizawa, S., Oshima, K., Kuboyama, T., Namba, S. (2001): Cloning and expression analysis of phytoplasma protein translocation genes. – Molecular Plant-Microbe Interactions (MPMI) 14(9):1043-1050.
[23] Kang, J., Ma, G. B., Yuan, L., Fu, Y. B., Li, F., Peng, C. S. (2021): Habitat suitability analysis of Suaeda heteroptera in coastal beach - Taking Caozhuang sea area of Xingcheng as an example. – Marine Environmental Science 2: 207-214.
[24] Kang, W. J., Jiang, Z. H., Chen, Y. G., …, Zhang, X. X. (2020): Plant transcriptome analysis reveals specific molecular interactions between alfalfa and its rhizobial symbionts below the species level. – BMC Plant Biology 20(1):293.
[25] Karim, R., Reading, L., Dawes, L., Dahan, O., Orr, G. (2021): Transport of photosystem II (PS II)–inhibiting herbicides through the vadose zone under sugarcane in the Wet Tropics, Australia. – Catena 206:105527.
[26] Kim, E. (2009): Postsynaptic development: Neuronal Molecular Scaffolds. – In: Binder, M. D. et al. (eds.) Encyclopedia of Neuroscience. Springer, Berlin, pp. 817-824.
[27] Kühlbrandt, W. (2019): Structure and mechanisms of F-type ATP synthases. – Annual Review of Biochemistry 88(1):515-549.
[28] Kumari, U., Banerjee, T., Singh, N. (2021): Evaluating ash and biochar mixed biomixtures for atrazine and fipronil degradation. – Environmental Technology & Innovation 23:101745.
[29] Li, F. C., Cao, W. R., Wang, S. B., Cheng, H. Q., Zhao, C., Guan, M. (2008): Toxic effects of herbicide atrazine on Scenedesmus obliquus population. – Anhui Agricultural Science 17:7427-7428.
[30] Li, J., Yu, X., Liu, Q., Ou, S., Xu, R. (2019): Screening of important lncRNAs associated with the prognosis of lung adenocarcinoma, based on integrated bioinformatics analysis. – Molecular Medicine Reports 19(5): 4067-4080.
[31] Liu, S., Wei, H. F., Liu, C. F., Zhang, M. L., He, J., Gao, J., Zhao, Y. M. (2020): On site ecological restoration of Suaeda Heteroptera in Panjin red beach. – China wild plant resources 6: 1-4.
[32] Liu, Y., Song, C. W., Li, Y., Liu, Y., Song, J. M. (2011): The distribution of organochlorine pesticides (OCPS) in surface sediments of Bohai Sea Bay, China. – Environmental Monitoring & Assessment 184(4): 1921-1927.
[33] Ludwig, N., Yerneni, S. S., Menshikova, E. V., Gillespie, D. G., Jackson, E. K., Whiteside, T. L. (2020): Author correction: simultaneous inhibition of glycolysis and oxidative phosphorylation triggers a multi-fold increase in secretion of exosomes: possible role of 2',3'-cAMP. – Scientific Reports 10:6948.
[34] Ma, C., Wu, X., Sun, D., Park, E., Catipovic, M. A., …, Li, L. (2019): Structure of the substrate-engaged SecA-SecY protein translocation machine. – Nature Communications 10(1):1-9.
[35] Ma, L., Tymanskyj, S. R. (2020): Axon Growth and Branching. – Cellular Migration and Formation of Axons and Dendrites (Second Edition):57-58.

http://www.aloki.hu ● ISSN 1589 1623 (Print) ● ISSN 1785 0037 (Online)
DOI: http://dx.doi.org/10.15666/aeer/2005_40614077

[36] Mali, G. R., Verma, A., Malunjker, B. D. (2021): Effect of different post-emergence herbicides tank mix with atrazine on nutrient uptake and chlorophyll content in maize (*Zea mays* L.). – Current Journal of Applied Science and Technology 40(46):1-8.
[37] Manoj, K. M. (2018): Aerobic respiration: criticism of the proton-centric explanation involving rotary adenosine triphosphate synthesis, chemiosmosis principle, proton pumps and electron transport chain. – Biochemistry Insights 11:1-23.
[38] Manoj, K. M., Gideon, D. A., Parashar, A. (2020): What is the role of lipid membrane-embedded quinones in mitochondria and chloroplasts chemiosmotic Q-cycle versus murburn reaction perspective. – Cell Biochemistry and Biophysics 79(38):1-8.
[39] McGuire, C. M., Forgac, M. (2018): Glucose starvation increases V-ATPase assembly and activity in mammalian cells through AMP kinase and phosphatidylinositide 3-kinase/Akt signaling. – The Journal of Biological Chemistry 293(23):9113-9123.
[40] Mevy, J. P., Loriod, B., Liu, X., Corre, E., Torres, M., Büttner, M.,…, Gauquelin, T. (2020): Response of downy oak (Quercus pubescens Willd.) to climate change: transcriptome assembly, differential gene analysis and targeted metabolomics. – Plants 9(9):1149.
[41] Piccoli, C., Ripoli, M., Quarato, G., Scrima, R. (2008): Coexistence of mutations in pink1 and mitochondrial DNA in early onset parkinsonism. – Journal of medical genetics 45(9): 596.
[42] Qi, W., Müller, B., Pernet-Coudrier, B., Singer, H., Liu, H., Qu, J., Berg, M. (2014): Organic micropollutants in the Yangtze River: seasonal occurrence and annual loads. – Science of the Total Environment 472: 789-799.
[43] Rohr, J. R. (2021): The atrazine saga and its importance to the future of toxicology, science, and environmental and human health. – Environmental Toxicology and Chemistry 40(6):1544-1558.
[44] Salazar, M. A., Kwiatkowski, A. V., Pellegrini, L. Cestra, G., Butler, M. H., Rossman, K. L.,…. De Camilli, P. (2003): Tuba, a novel protein containing bin/amphiphysin/Rvs and Dbl homology domains, links dynamin to regulation of the actin cytoskeleton. – Journal of Biological Chemistry 278(49):49031-43.
[45] Stransky, L. A., Forgac, M. (2015): Amino acid availability modulates vacuolar H+-ATPase assembly. – The Journal of Biological Chemistry 290(45):27360-27369.
[46] Guo J., Chen Y. Y, Lu P. Z.,et al.(2021).Roles of endophytic bacteria in Suaeda salsa grown in coastal wetlands: Plant growth characteristics and salt tolerance mechanisms. Environmental Pollution 287:117641.
[47] Vasanthakumar, T., Rubinstein, J. L. (2020): Structure and roles of V-type ATPases. – Trends in Biochemical Sciences 45(4):295-307.
[48] Wagh, D., Terry-Lorenzo, R., Waites, C. L., …, Garner, C. C. (2015): Piccolo directs activity dependent F-actin assembly from presynaptic active zones via Daam1. – PloS ONE 10(4):e0120093.
[49] Wang, Z. M., Niu, Y., Xu, J. Q., Sun, Z. J., Ding, Z. Q., Yang, X. Q. (2013): Cloning and sequence analysis of pollen protein elongation factor gene of heading cabbage. – Journal of Horticulture 10: 1990-1998.
[50] Yan, Q. X., Zhao, P., Li, X., Zhang, M. H., Jiang, Y. J. (2015): Development trend and countermeasures of atrazine. – Pesticides 54(12): 933-936.
[51] Zhang, H. Y., Hou, Z. H., Zhang, Y. L., Zhi, Y., Chen, J., Zhou, Y. B., Xu, Z. S. (2022): A soybean EF-Tu family protein GmEF8, an interactor of GmCBL1, enhances drought and heat tolerance in transgenic Arabidopsis and soybean. – International journal of Biological Macromolecules (Elsevier) 205:462-472.
[52] Zhang, Y., Cao, B., Jiang, Z., Zhang, X. Y., Wang, Z. Y., Li, R. X. (2017): Effects of atrazine on enzyme activity and microbial diversity in black soil. – Journal of Northeast Agricultural University 48(3): 48-53.

http://www.aloki.hu ● ISSN 1589 1623 (Print) ● ISSN 1785 0037 (Online)
DOI: http://dx.doi.org/10.15666/aeer/2005_40614077

TEMPORAL AND SPATIAL ANALYSIS OF PM_{10} AND SO_2 CONCENTRATION WITH THE USE OF GIS IN SOUTHEASTERN ANATOLIA REGION CITIES OF TURKEY (2010-2020)

DOGAN RASTGELDI, T.* – ATBINICI, M.

Department of Environmental Engineering, Faculty of Engineering, Harran University, 63200 Sanliurfa, Turkey

**Corresponding author*
e-mail: trastgeldi@harran.edu.tr; phone: +90-414-318-3000 / 1162; fax: +90-414-318-3799
ORCID: https://orcid.org/0000-0002-8246-388X

(Received 7th Apr 2022; accepted 11th Jul 2022)

Abstract. This study aims to determine the effect of the mandatory use of natural gas for heating to prevent air pollution in 2020 in 9 provinces in the Southeast Anatolian Region (SAR), the fastest developing region of Turkey, that were using coal for heating in 2010. Monthly PM_{10} and SO_2 concentrations of SAR provinces in 2010 and 2020 were analysed and evaluated by means of GIS-IDW mapping method. As a result of the 12-month evaluation, it was determined that the use of natural gas, especially in the winter months, reduced the PM_{10} and SO_2, while it didn't reduce the amount of SO_2 in provinces with high population growth and increased number of vehicles (an increase of 288% in vehicles in Kilis and an increase of 35% in population in Sanliurfa). Regarding Turkey's SAR border provinces, it was determined that PM was transported atmospherically from the Sahara, Syrian and Arabian Peninsula desert in the spring and autumn months both in 2010 and 2020, and therefore an increase was found in PM_{10} by the HYSPLIT model. The countries are recommended to measure the PM_{10} and SO_2 daily, which directly affect human health, create maps and develop policies to reduce the values.
Keywords: *air pollutants, particulate matter (PM), Hybrid Single-Particle Lagrangian Integrated Trajectory (HYSPLIT) model, Southeast Anatolian Region (SAR)*

Introduction

Clean air is one of the fundamental prerequisites of human health. However, in the age of economic development, air pollution has been and continues to be a serious threat to health around the globe. The causes of air pollution include economic development, urbanization, energy consumption, transportation, and motorization (Chen and Kan, 2008).

Air pollution problem has recently been one of the biggest problems in most of the developed and developing countries (Gorai et al., 2018). The main environmental pollutants that cause diseases and deaths worldwide are particulate matter (PM), ozone (O_3), nitrogen dioxide (NO_2), sulfur dioxide (SO_2) and carbon monoxide (CO), respectively (Zhu et al., 2019; Fischer et al., 2020). PM is considered as an important component of ambient air, as it plays a vital role in human health and air quality. PM with aerodynamic diameters less than 10 $\mu g/m^3$ is called PM_{10} (Talbi et al., 2018). Particulate matter (PM_{10} and $PM_{2.5}$) is the most harmful and dangerous part of aerosol pollutants because of inhalation risks (Zeydan, 2021). In urban areas, airborne PM is considered a strong air pollutant. Industries, coal and biomass incineration, vehicles, and oil sources are among the largest sources of PM_{10} (Li et al., 2018). Like most pollutants, SO_2 has both natural and anthropogenic sources (Ray and Kim, 2014). On a global scale, SO_2 emissions from anthropogenic activities are about ten times higher than emissions from natural sources (Qiao et al., 2018). SO_2 is discharged into the atmosphere at a rate of 73%

http://www.aloki.hu ● ISSN 1589 1623 (Print) ● ISSN 1785 0037 (Online)
DOI: http://dx.doi.org/10.15666/aeer/2005_40794093

from power plants and 20% from other industrial facilities by burning fossil fuels containing sulfur, as well as 7% from natural resources (Hosseiniebalam and Ghaffarpasand, 2015; Sari and Esen, 2021).

Many pollutants are among the main causes of diseases among humans. PM, which is among the pollutants with various sizes, enters the body through inhalation and causes dysfunctions in the central nervous system, cancer, cardiovascular diseases and damage to the reproductive system (Manisalidis et al., 2020). It has been stated that individuals suffer tom asthma and related disorders such inflammation of lungs, oxidative stress, increased respiratory symptoms, and poor lung function due to being exposed to PM_{10} and SO_2 for short or long periods of time (US EPA, 2017; Huang et al., 2019). Such adverse health effects of pollutants result in increased respiratory morbidity, respiratory mortality, emergency room visits or hospitalization in individuals (Rajak and Chattopadhyay, 2019).

The seasonal variation of air pollution is associated with the seasonal variation that leads to the formation of summer and winter periods, also known as the "warming" season, and the specificity of certain months. The occurrence of higher air pollution values in different months of the year is associated with the type of climate and resulting different atmospheric conditions in certain months, changing weather conditions on a given day, and anthropogenic activity. The emergence of these conditions results in different levels of air pollution for a given period (Cichowicz et al., 2017).

The problem of air pollution can only be solved by determining the present situation. With the advances in technology, both developed and developing countries can evaluate the size of air pollution through measurement stations. However, $PM_{2.5}$ is still not measured at many stations, as there is not yet a regulatory limit for the atmospheric concentration of this pollutant, while PM_{10} is measured at all stations in Turkey (UCTEA, 2017).

According to the studies carried out by the World Health Organization (WHO), the air quality limit values are exceeded in the areas where 91% of the world population live, and 4.2 million individuals die due to air pollution every year (WHO, 2020; Zeydan, 2021). Therefore, the air quality directive 2008/50/EC sets legal limit values for particulate matter (PM_{10}) concentrations in ambient air, which is 50 $\mu g/m^3$ for the daily average. Continuous monitoring of PM_{10} and SO_2 levels is required to improve air quality in an area (Caselli et al., 2009; Ceylan and Bulkan, 2018). Therefore, there are many studies in the literature on future predictions of atmospheric SO_2 and PM_{10} concentrations (Schornobay-Lui et al., 2019; Gündogdu, 2020). Sengupta et al. (1996) identified the population and risky areas that are exposed to air pollution through GIS. Fiala et al. (2001) determined the sulfur accumulation in the atmosphere using annual SO_2 concentration and precipitation data. Elbir (2004) studied on a GIS-based decision support system for the forecasting, mapping and analysis of air pollution in many metropolitan cities in Turkey.

Air pollution caused by PM is currently a major problem in all countries of the world and is a very important issue in Turkey. Accordingly, research on this subject is increasing regarding various specific regions and cities. It was reported by Karaca (2012) that the regions with the highest PM_{10} levels in Turkey are the eastern region of the Black Sea, the eastern part of Turkey, the northeastern part of the Central Anatolian region and the western part of the Northeastern Anatolia (Toros et al., 2013) examined 16 metropolitan cities in terms of PM_{10} to evaluate the overall air quality of Turkey. It is clearly stated that 75% of these cities exceed the daily average PM values. The average daily total PM_{10}

http://www.aloki.hu ● ISSN 1589 1623 (Print) ● ISSN 1785 0037 (Online)
DOI: http://dx.doi.org/10.15666/aeer/2005_40794093

concentration in the Central Anatolian Region of Turkey was reported to be 148 μg/m^3 by Ozel and Çakmakyapan (2015) using Poisson processes (Cekim, 2020).

One of the crucial factors affecting the air quality in Turkey is urbanization. Significant attempts have been made in recent years, such as transition from coal to natural gas, which aim to minimize air pollution levels in Turkey. In many metropolitan cities, natural gas pipeline systems have been installed for residential heating and industrial use. Thus, it has been reported that the air quality of some cities has improved and there have been changes in air pollution rates in Turkey (Deniz and Durmusoglu, 2008; Karaca, 2012b). However, since there seems to be no study on this matter in the related literature, the purpose in this study is to fill the gap in literature.

The aim of this study is to determine, analyze and map monthly changes in daily concentrations of SO_2 and PM_{10}, which are among the most threatening health pollutants, between 2010 and 2020 in 9 provinces located in the southeast region of Turkey (SAR). As a result of the comparison over the last 10 years: (a) the effect of the transition from coal use for heating purposes in 2010 to natural gas in 2020 was determined, (b) the impact of the atmospheric particulate matter transport on the provinces bordering the deserts (Sanliurfa, Mardin, Gaziantep, Kilis, Sirnak) was determined by the HYSPLIT model, (c) the relationship between population growth and PM_{10} and SO_2 increase was analyzed, and (d) the effect of the increase in motor vehicles on PM_{10} and SO_2 was determined. This study is significant in terms of determining the air quality of Turkey's SAR provinces on a monthly basis and revealing the outcomes of the measurements, monitoring and evaluation policy for the improvement of air quality in a 10-year period.

Material and Methods

Study field and data collection

The Southeastern Anatolia Region of Turkey, selected as the study area, consists of 9 provinces (Sanliurfa, Mardin, Sirnak, Kilis, Batman, Diyarbakir, Adiyaman, Gaziantep, Siirt) located on an area of 76.327 km^2 (*Table 1, Fig. 1*).

Table 1. *The location of monitoring stations*

States	Stations	Latitude (N)	Longitude (E)
Adiyaman	Adiyaman Meteorological Service	37.755	38.279
Batman	Batman Provincial Directorate of Environment, Urbanization and Climate Change	37.872	41.171
Diyarbakir	Diyarbakir Provincial Directorate of Environment, Urbanization and Climate Change	37.909	40.212
Gaziantep	Gaziantep Provincial Directorate of Environment, Urbanization and Climate Change	37.058	37.351
Kilis	Kilis Provincial Directorate of Environment, Urbanization and Climate Change	36.709	37.112
Mardin	Mardin Provincial Directorate of Environment, Urbanization and Climate Change	37.313	40.738
Siirt	Siirt Meteorological Service	37.931	41.935
Sanliurfa	Sanliurfa Meteorological Service	37.159	38.796
Sirnak	Sirnak Provincial Directorate of Environment, Urbanization and Climate Change	37.522	42.456

http://www.aloki.hu ● ISSN 1589 1623 (Print) ● ISSN 1785 0037 (Online)
DOI: http://dx.doi.org/10.15666/aeer/2005_40794093

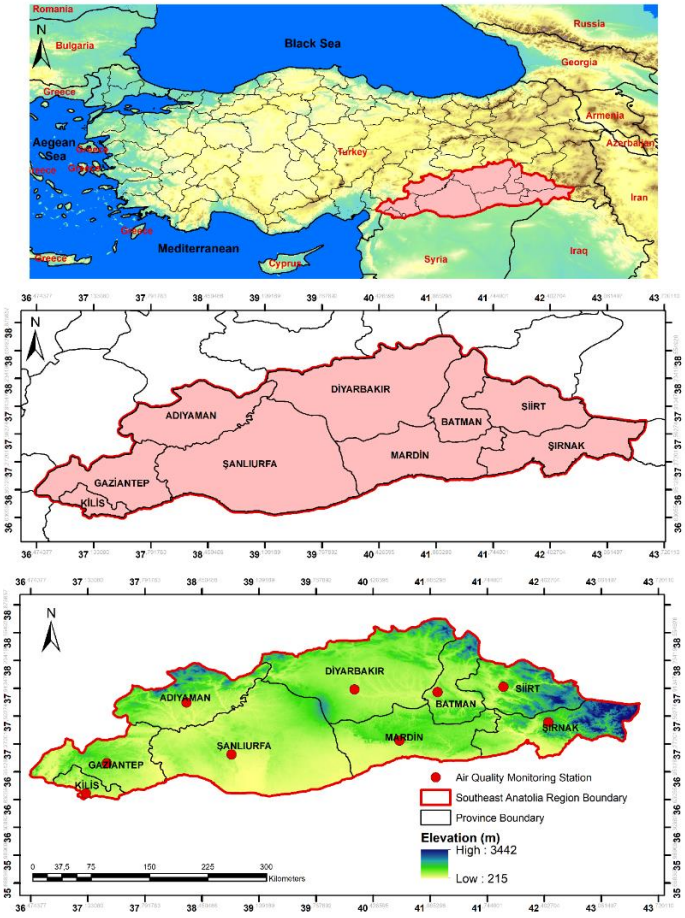

Figure 1. *The study area of the provinces of the SAR of Turkey showing the stations with PM_{10} and SO_2 concentrations*

When SAR provinces are examined as in (*Table 2*), negative effects on air quality are estimated due to rapid population growth and an increase in motor vehicles. However, the transition to natural gas over time (for the last five years) and to using natural gas for heating in all provinces in 2020 is important, while coal was used in 2010 for heating.

Table 2. *Information of SAR Provinces in 2010 and 2020 (TSI, 2021)*

Provinces	Population (n)			Area (km^2)	Number of vehicles (n)		
	2010	2020	Percentage		2010	2020	Percentage
Adiyaman	590,935	632,459	7,003	7,337	64,962	110,433	6,9
Batman	510,200	620,278	21,575	4,477	34,381	45,916	33,5
Diyarbakir	1,528,958	1,783,431	16,643	15,272	320,032	540,397	68,8
Gaziantep	1,700,763	2,101,157	23,542	6,803	96,272	124,672	29,5
Kilis	123,135	142,792	15,963	1,412	28,457	110,430	288,05
Mardin	744,606	854,716	14,787	8,779	51,921	76,605	47,5
Siirt	300,695	331,070	10,101	5,718	13,596	20,394	50
Sanliurfa	1,663,371	2,115,256	27,166	19,451	194,193	255,664	31,6
Sirnak	430,109	537,762	25,029	7,078	28,475	29,145	2,3

http://www.aloki.hu ● ISSN 1589 1623 (Print) ● ISSN 1785 0037 (Online)
DOI: http://dx.doi.org/10.15666/aeer/2005_40794093

In order to accurately measure air pollution, the Turkish Ministry of Environment and Urbanization established the National Air Quality Monitoring Network throughout Turkey. The air pollutant parameters (SO_2 and PM_{10}), monitored from the established air pollution measurement stations, can be measured automatically. The collected data at the measurement stations are transferred to the Environment Reference Laboratory Data Processing Center of the Ministry via this network (VPN) by means of GSM Modems, are monitored and broadcast simultaneously. However, the fact that the data from this station has not been revealed with respect to the effect of air pollution for many years is a significant gap in the literature. For this reason, the 24-hour average values of PM_{10} and SO_2 of the 9 provinces located in SAR were obtained from the database of the Ministry of Environment Urbanization and Climate Change (MEUCC) (www.havaizleme.gov.tr) for the analysis of air pollution between the periods of 2010 (January 1, 2010-December 31, 2010) and 2020 (January 1, 2020-December 31, 2020) and were evaluated on a monthly basis (TR_MEUCC, 2019).

One-fifth of the earth is covered by deserts. PM in micrometer size that form the deserts is easily lifted by the effect of cyclones, pressure, and winds, and is suspended in the air and carried many kilometers away. Desert dust consisting of atmospheric particulate matter is transported from the Sahara Desert, the Arabian Peninsula and the Syrian desert to the border provinces of the SAR (Sanliurfa, Gaziantep, Kilis, Mardin, Sirnak). This has serious influences on air quality. To determine desert dust transport to these provinces, backward trajectories of the Hybrid Single-Particle Lagrangian Integrated Trajectory (HYSPLIT) model were used in order to determine the direction of the inflow of air masses (Stein et al., 2015). The HYSPLIT model has so far been successfully used in analysis of the inflow and conditions of both anthropogenic dispersions, i.e., PM, SO_2, NO (Lee et al., 2013), radionuclides (Draxler et al., 2015), as well as natural air pollution, i.e., volcanic dust and forest fires (Palarz and Celińskı-Mysław, 2017).

Method

The IDW (Inverse Distance Weighted) interpolation method in the Spatial Analyst module of ArcGIS 10.2 software was used to generate the spatial distribution maps that show the monthly averages of PM_{10} and SO_2 values for the years 2010 and 2020 of the 9 provinces in the study area.

Inverse distance weighted (IDW) interpolation method

This interpolation method estimates cell values by means of the mean values of sample data points located around each cell. IDW prefers data or point value closer to each other. The assumption is that distance reduces the local influence of the measured points, the more relative are the points to the target region, the higher weight they have (Gómez-Losada et al., 2019; Shukla et al., 2020). That is, the high weight value is given to the sample points with closest distance to the cell. Moving away from the estimation location reduces the effects of the points. In cases when any point is in an area different from the estimation location, considering a very distant point may not be suitable in this method. Considering a sufficient number of points and creating a surface for small areas can solve this problem. The amount, distribution and surface character of the sample points may determine the number of points (Esri, 2014). The basis of this method is the calculation of distances from the desired point to data points, and the linear weighting of the effect of data points on the value at the desired point using an inverse function (Loyd, 2010).

http://www.aloki.hu ● ISSN 1589 1623 (Print) ● ISSN 1785 0037 (Online)
DOI: http://dx.doi.org/10.15666/aeer/2005_40794093

$$Z\,(Xo) = \frac{\sum_{i=1}^{n} Z\,(Xi).\,d_{i0}^{-r}}{\sum_{i=1}^{n} d_{i0}^{-r}} \qquad \text{(Eq.1)}$$

Here (*Eq.1*), the predictions are conducted in the Xo position, which is a function of adjacent measurements, n [Z (Xi) and i = 1, 2, …, n,]. r refers to the exponential number determining the assigned weight of each observation, and d is the distance between the observation position (Xi) and the estimated position (Xo).

The assigned weight of observations at a given distance from the estimation location becomes smaller depending on how large the exponent is. Increases in exponents indicates that the estimations are very similar to the closest observations (Aksu and Hepdeniz, 2016).

Results and Discussion

Evaluation of PM_{10} concentration

PM_{10} concentrations values measured daily by air quality measurement station in SAR provinces were calculated as monthly average values. The monthly average PM_{10} exposure according to the 24-hour average values within the scope of the air quality standards determined by the WHO is 50 μg/m^3 and this has been compared with the average PM_{10} concentrations of the SAR provinces (WHO, 2006).

Considering monthly average, the PM_{10} concentrations in 2010 given in *Fig. 2*, it was determined that the WHO limit value of 50 μg/m^3 was exceeded in 9 provinces in November, December, January, February, March, and April, and the air quality was at levels to threaten health. In May and June 2010, PM_{10} concentration was measured as 5 and 10 μg/m^3, respectively, and below the WHO standard only in Gaziantep. In 2020, PM values decreased considerably in 9 provinces in January, February, March, and April and remained below the WHO limit value. PM_{10} concentration was high in Kilis during February and March in 2020 with values of 202 and 96 μg/m^3. As a consequence of a forest fire in Sirnak in May 2020, the PM_{10} concentration increased to 557 μg/m^3, which was the highest value creating threats to health. In 2010, PM_{10} concentration was measured quite low in summer months (June, July, August) compared to winter months. This was mainly a consequence of not using coal for heating. As a result, PM_{10} values were lower in summer months and higher in winter months. Due to the use of coal in 2010, the values exceeded the WHO standard, but in 2020, it remained below the WHO value, except for a few provinces, and it was determined that natural gas use had a positive effect on air quality.

Palarz and Celiński-Mysław reported in the study conducted in small towns located in the basins of the Polish Carpathians, i.e. Jaslo, Zakopane, and Zywiec that the use of poor quality coal increased the amount of PM_{10} and SO_2, despite the fact that towns were small. The highest concentrations of PM_{10}, SO_2 and NO_2 were observed during the winter season, which seems to have stemmed from decreases in solar radiation, lower temperatures, and increased air pollutant emissions due to furnaces home furnaces (Palarz and Celiński-Mysław, 2017).

Due to the insufficient air quality monitoring stations in Malaysia, reliable mapping was developed with IDV and the maximum and minimum values were determined as 76 μg/m^3 and 42 μg/m^3 in the PM_{10} thematic map produced by IDW (Tella and Balogun, 2021).

http://www.aloki.hu ● ISSN 1589 1623 (Print) ● ISSN 1785 0037 (Online)
DOI: http://dx.doi.org/10.15666/aeer/2005_40794093

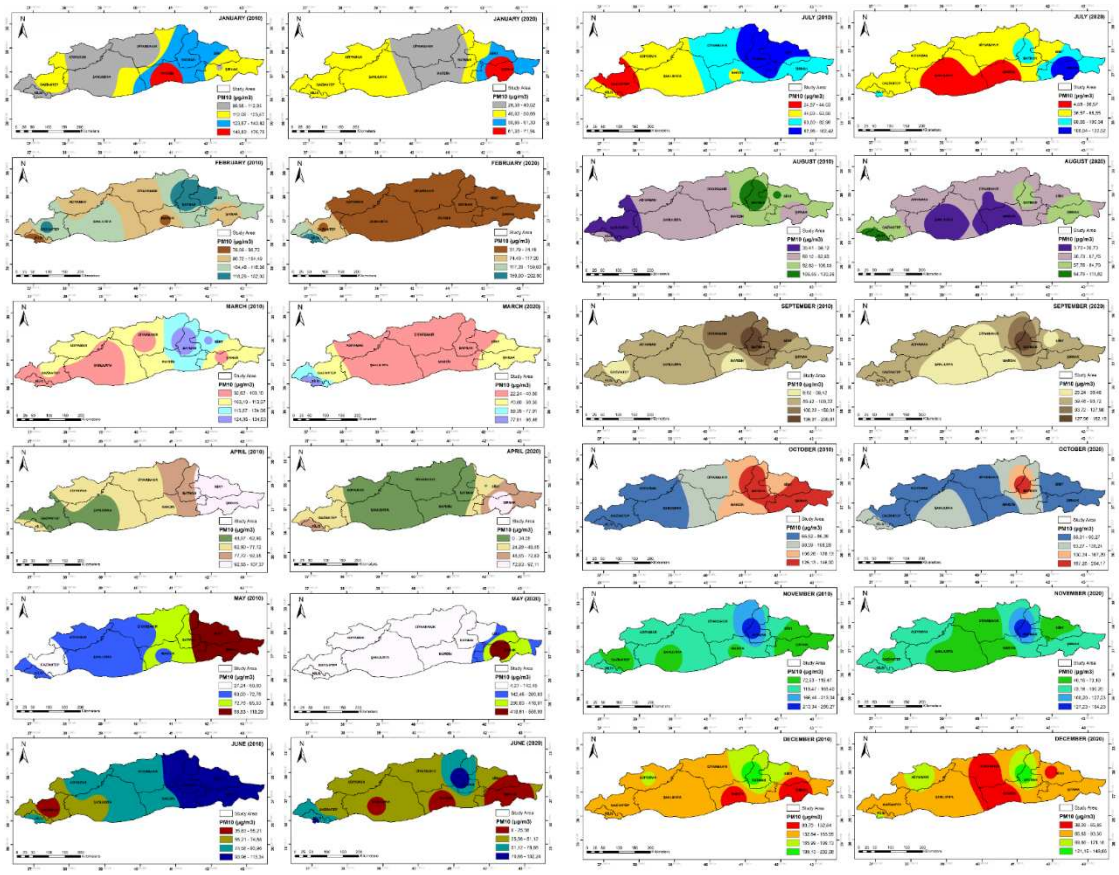

Figure 2. *Spatial distributions of PM10 in 9 provinces of the SAR in 2010 and 2020 (12 months)*

Atmospheric particulate matter transport from deserts and the HYSPLIT model

Many studies in the literature have reported that the amount of PM_{10} increases especially because of the use of coal for heating purposes during winter months. However, in our study, it was observed that PM_{10} concentration increased in border provinces, especially in the spring and autumn months. One-fifth of the earth is covered with deserts. These deserts consist of particulate matter with different sizes. These particulate matters constitute atmospheric particles that are transported many kilometers away by meteorological phenomena and pressure.

In *Fig. 2*, the PM_{10} concentration in March (spring) 2010 was determined as follows for the the SAR provinces: Sanliurfa 92.62 μg/m^3, Diyarbakır 98.73 μg/m^3, Sirnak 99.76 μg/m^3, Kilis 100.29 μg/ m^3, Gaziantep 103.65 μg/m^3, Adiyaman 107.06 μg/m^3, Mardin 112.54 μg/m^3, Siirt 125.16 μg/m^3 and Batman 134.53 μg/m^3. As a result of the measurement, the values were found to exceed the WHO standards.

Atmospheric particles (PM_{10} and smaller particles) have received increasing attention in recent years due to a vital role they play in altering air quality, human health, and climate change (Gray, 2015; Sakhamuri and Cummings, 2019). One of the most common natural sources of particulate matter is desert dust since one-fifth of the earth is covered with arid and semi-arid regions. Dusts from these sources are suspended fine particles that can be transported and deposited in the downwind side due to atmospheric transport. A study conducted by NASA researchers has shown that an average of 182 million tons

http://www.aloki.hu ● ISSN 1589 1623 (Print) ● ISSN 1785 0037 (Online)
DOI: http://dx.doi.org/10.15666/aeer/2005_40794093

of dust is transported each year from desert areas (Gray, 2015). The Sahara is the largest hot desert in the world, covering around 10 million square kilometers, about the size of the United States (Goudarzi et al., 2015). It expands across the following eleven countries: Algeria, Chad, Egypt, Libya, Mali, Mauritania, Morocco, Niger, Western Sahara, Sudan and Tunisia. The content of the dust originating from the Saharan desert may change based on the agricultural and industrial practices of the people living in these countries. Particulate matter transported from the Saharan Desert can reach not only to countries in the vicinity (such as Turkey) but also North and South America as well as Caribbean region. border provinces (Sanliurfa, Kilis, Gaziantep, Mardin and Sirnak) is under the influence of Sahara Desert, which is the largest desert in the world, Syria desert and the Arabian Peninsula together with Simoom, Khamsin and Sirocco winds. Therefore, the city is exposed to particulate matters from these regions as a result of atmospheric transport. With the developments in technology, we are now able to determine which desert source affects a particular region by giving coordinates through HYSPLIT model program at different height levels (500, 1000, 1500 m). When we look at the daily examinations in 2020, Sanliurfa province has been affected by particulate matter from the deserts of Syria and the Arabian Peninsula on many days of the year, especially in Spring (March-April-May) and Autumn months (September-October-November) as it is neighbor to Syria and in the direction of Sahara air flow (Dogan et al., 2021). This atmospheric desert transport leaves the city only when it rains. However, rainfall may not occur during spring. In this case, dust can remain suspended in the air for 3 days and sometimes weeks. Since the PM is inhalable, the environment, including many living and non-living organisms especially children and the elderly, is affected. Also, the dust reduces the range of sight and there can be accidents and problems in transportation as a result. In the case of precipitation containing dust, traditionally known as muddy rain, also pollutes the city.

When the PM_{10} concentration in Sanliurfa province was examined at 500-1000-1500 meters by means of the HYSPLIT model as shown in *Fig. 3a*, it was determined that the increase in the PM_{10} concentration was caused by transport from Syria, the Arabian Peninsula and the Sahara deserts with the effect of the winds on 10-11-12 March, 2010 (*Fig. 3a*). It was reported by Dogan et al. in their study that atmospheric dust particles are transported to Sanliurfa in spring and autumn, leading to a 4.57% decrease in the efficiency of solar panels (Dogan et al., 2020). In addition, PM_{10} concentration values in October, the autumn month of 2020, were measured as follows: 69.48 $\mu g/m^3$ in Mardin, 76.96 $\mu g/m^3$ in Sirnak, 81.31 $\mu g/m^3$ in Gaziantep, 103.91 $\mu g/m^3$ in Sanliurfa, 107.15 $\mu g/m^3$ in Kilis, which were all above the WHO standards in all SAR provinces. When the province of Sanliurfa, which had the highest score, was examined with the HYSPLIT model, it was determined that the reason for the PM_{10} concentration values during 26.27 $\mu g/m^3$ and 28 October, 2020 to be above the standards, especially in the border provinces with a maximum level, was the increase in desert dusts during autumn months (*Fig. 3b*).

Evaluation of SO_2 concentration

The sources of air pollutants are mainly combustion processes, various technological processes, as well as vehicle traffic (Lelieveld et al., 2015). It should also be noted that pollutants are emitted from low-emission sources mostly during the heating season, and remote systems do this in varying intensities all year round (Lin et al., 2011).

http://www.aloki.hu ● ISSN 1589 1623 (Print) ● ISSN 1785 0037 (Online)
DOI: http://dx.doi.org/10.15666/aeer/2005_40794093

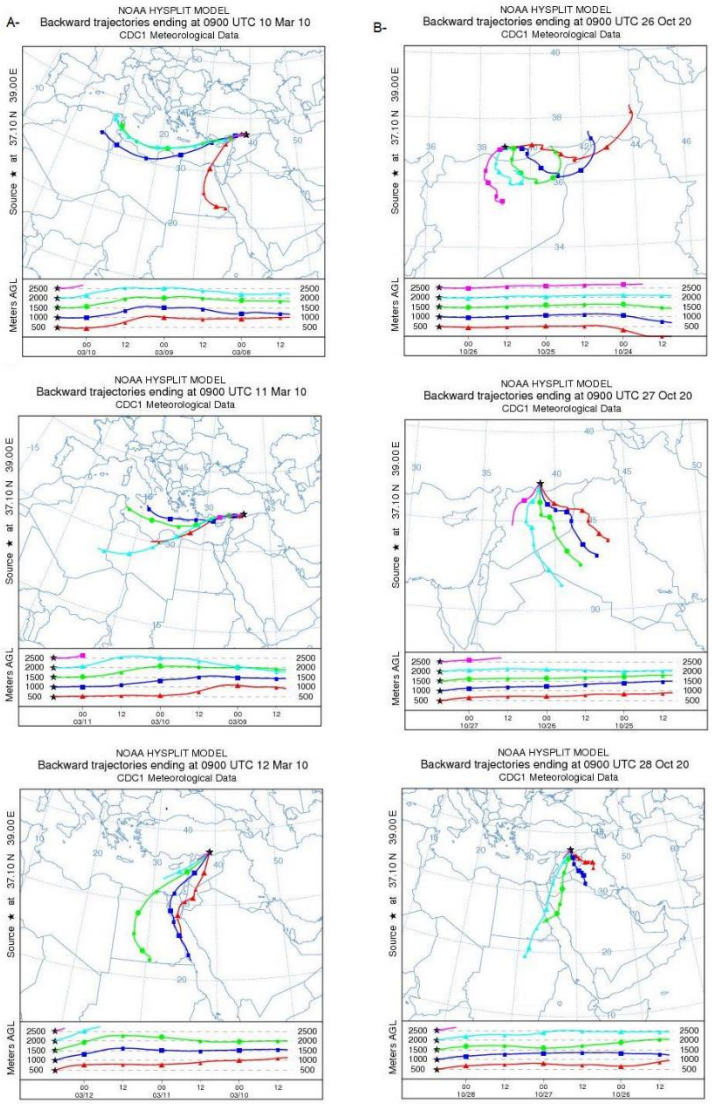

Figure 3. a. *HYSPLIT model of Sanliurfa province on 10-12 March 2010,* ***b.*** *HYSPLIT model of Sanliurfa province on 26-28 October 2020*

It is known that the anthropogenic source of SO_2 in the atmosphere is the burning of coal. SO_2 is considered the most common pollution that threatens the environment and human health and may lead to the increase in the number of cardiovascular and respiratory diseases (Landim et al., 2018).

In the study conducted over a seven-year period (2009–2015) in eastern Wielkopolska, Poland, PM_{10} was associated with sulfur dioxide, higher pollution levels in winter and PM_{10} concentrations exceeding the limit values. In addition, it was stated that the levels of pollutants such as sulfur dioxide, nitrogen dioxide and carbon monoxide increase in winter, but do not exceed the limit values (Cichowicz et al., 2017).

SO_2 concentrations values measured daily by air quality measurement station in SAR provinces were calculated as monthly average values. The monthly average SO_2 exposure according to the 24-hour average values within the scope of the air quality standards determined by the WHO is 20 $\mu g/m^3$ and this has been compared with the average SO_2 concentrations of the SAR provinces (WHO, 2006).

http://www.aloki.hu ● ISSN 1589 1623 (Print) ● ISSN 1785 0037 (Online)
DOI: http://dx.doi.org/10.15666/aeer/2005_40794093

As can be seen in *Fig. 4*, the SO_2 concentration exceeded the WHO standards in Sirnak, one of the coldest provinces of the SAR, with values of November (102.58 μg/m^3), December (283.64 μg/m^3), January (326.05 μg/m^3), February (234.77 μg/m^3), March (116.90 μg/m^3) and April (63.87 μg/m^3) during 2010. Since the SO_2 concentration does not exceed the WHO standard during spring and summer in Sirnak, it can be understood that this high rate of SO_2 resulted from the use of poor-quality coal due to the lack of natural gas systems. Natural gas started to be used in Sirnak, except for the suburban areas, in 2020. SO_2 values measured in Sirnak for the year 2020 were November (57.11 μg/m^3), December (98.13 μg/m^3), January (104.01 μg/m^3), February (77.29 μg/m^3), March (38.25 μg/m^3) and April (22.32 μg/m^3). As seen in *Table 1*, although the population of Sirnak increased by 25.02% and the number of vehicles by 2.3% over a 10-year period, the decrease in SO_2 concentration was found to be the result of natural gas use.

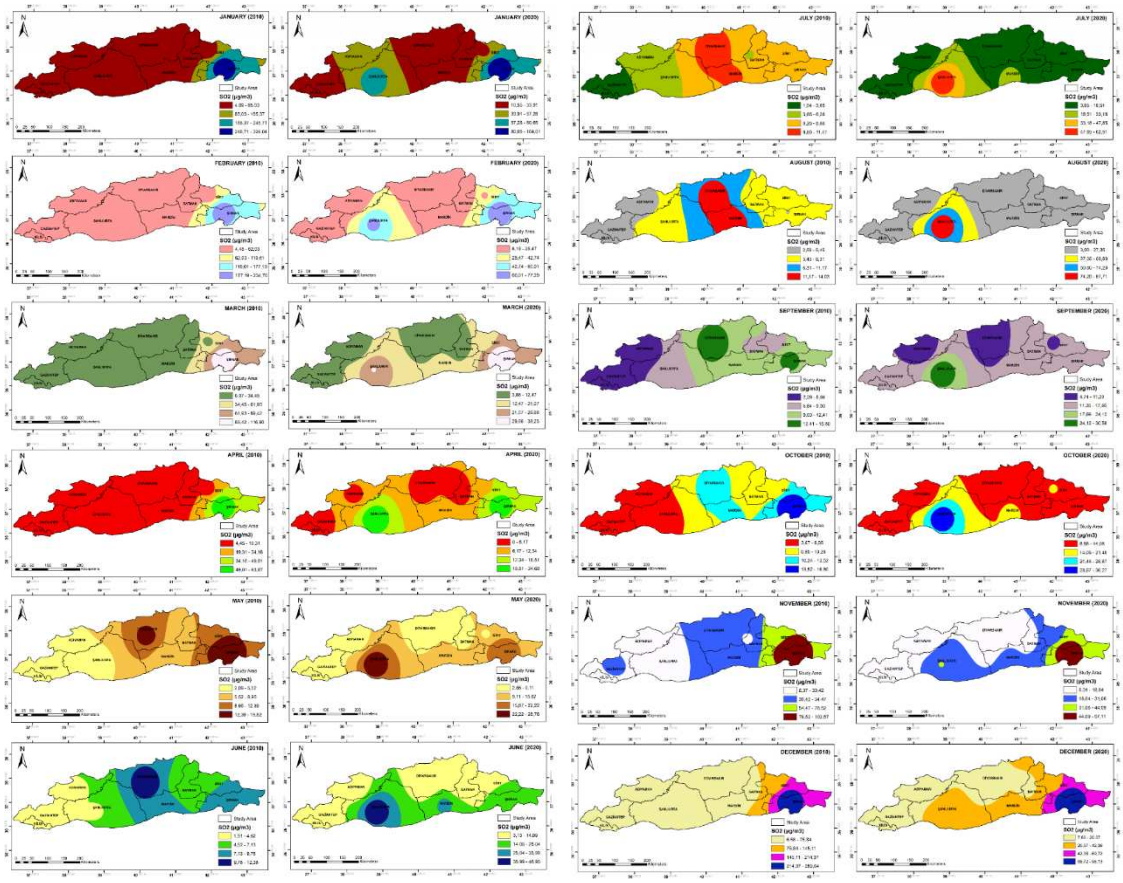

Figure 4. *Spatial distributions of SO_2 in 9 provinces of the SAR in 2010 and 2020 (12 months)*

Use of vehicles is increasing dramatically. This increase has a tremendous impact on the environment, including air pollution, particularly due to private vehicle users (Boedisantoso et al., 2019). In this study, when we examine the province of Kilis as in *Table 2*, while there were 28.457 motor vehicles in 2010, it was 110.430 in 2020 with an increase by 288.05%.

Coal is not burned for heating purposes in spring (March, April, May) and summer in Turkey, and natural gas is used instead of coal in 2020. However, when the spring and

http://www.aloki.hu ● ISSN 1589 1623 (Print) ● ISSN 1785 0037 (Online)
DOI: http://dx.doi.org/10.15666/aeer/2005_40794093

summer months of 2010 and 2020 in Kilis were considered as in *Fig. 4*, an increase in SO_2 concentration was found in April, May, June, July, August, September, and October. It is estimated that the only main source of this was the 288% increase in the number of vehicles.

Batman Oil Refinery, Turkey's first refinery, causes a significant decrease in the air quality of the province. As a result of the burning of fuels such as fuel oil and refinery gas in processes in refineries, emissions such as hydrocarbons, sulfur oxide, carbon dioxide, CO, dust, H_2S, VOC, heavy metals and nitrogen oxides occur (Batan, 2013). Waste gas emissions from the refinery cause air pollution on a local, regional, and global scale after being released into the atmosphere from the refinery. The main problem observed at the local scale is the deterioration of air quality due to SO and PM and its impact on public health (Zeydan, 2019). Batman province had the highest PM_{10} value in 2010 and 2020, which is considered to have resulted from waste gas emissions from the oil refineries.

Conclusions

Considerable differences in air quality were found among the SAR provinces over a 10-year period, which are among the fastest developing regions of Turkey in terms of both industry and population. In 2010, PM_{10} level was found to be high due to the burning of coal especially in winter (December-January-February) and autumn (September-October-November). Transition to natural gas as an alternative to burning coal for heating in 2020 has had a positive impact on the air quality of SAR provinces. However, in border provinces (Sanliurfa, Gaziantep, Mardin, Kilis, Sirnak), the amount of PM_{10} was found to be high in the spring (March-April-May) and autumn (September-October-November) both in 2010 and 2020. The reason for this was determined, using the HYSPLIT model, to be the transport of atmospheric aerosols from the deserts of Sahara, Syria, and Arabian Peninsula. Dogan et al. reported in their study conducted in Sanliurfa in 2020 that the maximum PM_{10} and $PM_{2.5}$ concentrations during the spring and autumn months were 150 and 250 $\mu g/m^3$, respectively (Dogan et al., 2020).

The highest SO_2 concentration was 326.05 $\mu g/m^3$ in January 2010 in Sirnak province. With the transition to natural gas in 2020, the positive consequences of not using coal for heating have been observed in Sirnak, and both PM_{10} and SO_2 concentrations have considerably decreased.

Exhaust gases from vehicles are known to be a serious SO_2 source. The highest increase in the number of vehicles between 2010 and 2020 (28.457 in 2010, 110.430 in 2020 with an increase by 288.05%) was in Kilis. While the SO_2 value was low in 2010 despite using coal for heating purposes, this value increased despite the use of natural gas for heating purposes in 2020. The reason for this increase can be attributed to the vehicles as the SO_2 value increased especially in the spring (March-April-May) and summer (June-July-August).

Batman was the province with the highest concentration of PM_{10} and had the lowest air quality in 2010 and 2020. This can be due to waste gas emissions from oil refineries. In SAR provinces, the highest value of PM_{10} was measured in Batman in November, 2010 as 260.28 $\mu g/m^3$ while the lowest value was measured in Mardin in September as 9.62 $\mu g/m^3$. On the other hand, the SO_2 concentration was measured at the maximum level of 326.05 $\mu g/m^3$ in Sirnak in January and at a minimum level of 1.04 $\mu g/m^3$ in Kilis in July. In 2020, PM_{10} concentration increased to a maximum level of 557 $\mu g/m^3$ in Sirnak

http://www.aloki.hu ● ISSN 1589 1623 (Print) ● ISSN 1785 0037 (Online)
DOI: http://dx.doi.org/10.15666/aeer/2005_40794093

in May and at a minimum level of 3.70 μg/m^3 in Mardin in August. The SO_2 concentration was measured at a max level of 104.01 μg/m^3 in Sirnak in January and at a minimum level of 2.55 μg/m^3 in Diyarbakır in May.

In conclusion, the transition from coal use for heating purposes to natural gas has decreased the PM_{10} concentration in all provinces during the winter months (December-January-February) in the 10-year period between 2010 and 2020. In 2020, the main source of air pollution in SAR provinces was the increase in the number of vehicles, the secondary reason was the increase in population, and the third reason was atmospheric aerosols transported from the deserts (Syria, Arabian Peninsula, Sahara). The concentrations of other gases (nitrous oxide, carbon dioxide, etc.) should be measured daily to maintain human health at the stations that automatically measure the air quality of the provinces. People should be warned not to go outside and to open windows on dates when PM_{10} and SO_2 concentrations are high. In order to prevent global warming in the world and for people to breathe cleaner air, the use of coal for heating should be abandoned, and transition to renewable energy sources should be the policy and goal of all countries.

Acknowledgements. We thank the Ministry of Environment, Urbanization and Climate Change of the Republic of Turkey for permission to use PM_{10} and SO_2 concentrations.

Data availability. NOAA-HYSPLIT trajectory and PM_{10} and SO_2 data are freely accessible from the data providers mentioned in "Material and methods" of the manuscript; NOAA-HYSPLIT: https://www.ready.noaa.gov/HYSPLIT_traj.php; PM_{10} and SO_2 data: www.havaizleme.gov.tr.

REFERENCES

[1] Aksu, H. H., Hepdeniz, K. (2016): Mapping with the aid of Geographic Information System and analysis of annual and monthly average maximum air temperature distribution in Burdur. – Mak. Er. U. Fen. Bil. Ens. Derg. 7: 202-214.

[2] Batan, M. (2013): A Research on Effect to the Warming the Air Pollution Causing of Polluting Emissions in Batman City. – Batman University Journal of Life Sciences 3(2): 90-104.

[3] Boedisantoso, R., Ciptaningayu, T. N., Syafei, A. D., Assomadi, A. F., Slamet, A., Hermana, J. (2019): Reduction of CO, NOx and SO_2 emissions from the transfer of private vehicles to public transportation: a case study of Surabaya. – In IOP Conference Series: Earth and Environmental Science 239: 012041. IOP Publishing. https://doi.org/10.1088/1755-1315/239/1/012041.

[4] Caselli, M., Trizio, L., Gennaro, D. G., Ielpo, P. (2009): A simple feedforward neural network for the PM_{10} forecasting: Comparison with a radial basis function network and a multivariate linear regression model. – Water, Air, and Soil Pollution 201: 365-377. https://doi.org/10.1007/s11270-008-9950-2.

[5] Cekim, H. O. (2020): Forecasting PM_{10} concentrations using time series models: a case of the most polluted cities in Turkey. – Environmental Science and Pollution Research 27(20): 25612-25624. https://doi.org/10.1007/s11356-020-08164-x.

[6] Ceylan, Z., Bulkan, S. (2018): Forecasting PM_{10} levels using ANN and MLR: A case study for Sakarya City. – Global Nest Journal 20(2): 281-290. https://doi.org/10.30955/gnj.002522.

[7] Chen, B., Kan, H. (2008): Air pollution and population health: a global challenge. – Environmental Health and Preventive Medicine 13: 94-101. https://doi.org/10.1007/s12199-007-0018-5.

http://www.aloki.hu ● ISSN 1589 1623 (Print) ● ISSN 1785 0037 (Online)
DOI: http://dx.doi.org/10.15666/aeer/2005_40794093

[8] Cichowicz, R., Wielgosiński, G., Fetter, W. (2017): Dispersion of atmospheric air pollution in summer and winter season. – Environmental monitoring and assessment 189(12): 1-10. https://doi.org/10.1007/s10661-017-6319-2.

[9] Deniz, C., Durmuşoğlu, Y. (2008): Estimating shipping emissions in the region of the Sea of Marmara, Turkey. – Science of the total environment 390: 255-261. https://doi.org/10.1016/j.scitotenv.2007.09.033.

[10] Dogan, T. R., Beşli, N., Aktacir, M. A., Dinç, M. N., İlkhan, M. A., Öztürk, F., Yıldız, M. (2020): Seasonal effects of atmospheric particulate matter on performance of different types of photovoltaic modules in sanliurfa, Turkey. – Atmospheric Pollution Research 11(12): 2173-2181. https://doi.org/10.1016/j.apr.2020.06.009.

[11] Dogan, T. R., Yilmaz, D., Yalcin, S. (2021): Gamma ray characterization of the albedo of atmospheric dust from Southeast Anatolia, Turkey. – Instrum. Sci. Technol 49(6): 604-615. https://doi.org/10.1080/10739149.2021.1915797.

[12] Draxler, R., Arnold, D., Chino, M., Galmarini, S., Hort, M., Jones, A., Leadbetter, S., Malo, A., Maurer, Ch., Rolph, G., Saito, K., Servranck, R., Shimbori, T., Solazzo, E., Wotawa, G. (2015): World Meteorological Organization's model simulations of the radionuclide dispersion and deposition from the Fukushima Daiichi nuclear power plant accident. – Journal of Environmental Radioactivity 139: 172-184. https://doi.org/10.1016/j.jenvrad.2013.09.014.

[13] Elbir, T. (2004): A GIS based decision support system for estimation, visualization and analysis of air pollution for large Turkish cities. – Atmospheric Environment 38: 4509-4517. https://doi.org/10.1016/j.atmosenv.2004.05.033.

[14] Esri (2014): Desktop spatial analysis for ArcGIS. – Esri Information Systems Engineering and Education Ltd. Sti. 1st Edition, Ankara.

[15] Fiala, J., Reider, M., Duarakova, M., Lvorova, H. (2001): Trends in the Atmospheric and Hydrological Cycle of Sulphur at Catchments in the Czech Republic. – Atmospheric Environment 35: 52-55. https://doi.org/10.1016/S1352-2310(00)00516-1.

[16] Fischer, P. H., Marra, M., Ameling, C. B., Velders, G. J., Hoogerbrugge, R., de Vries, W., Houthuijs, D. (2020): Particulate air pollution from different sources and mortality in 7.5 million adults - The Dutch Environmental Longitudinal Study (DUELS). – Science of the Total Environment 705: 135778. https://doi.org/10.1016/j.scitotenv.2019.135778.

[17] Gómez-Losada, Á., Santos, F. M., Gibert, K., Pires, J. C. (2019): A data science approach for spatiotemporal modelling of low and resident air pollution in Madrid (Spain): implications for epidemiological studies. – Computers, Environment and Urban Systems 75: 1-11. https://doi.org/10.1016/j.compenvurbsys.2018.12.005.

[18] Gorai, A. K., Tchounwou, P. B., Biswal, S. S., Tuluri, F. (2018): Spatio-temporal variation of particulate matter ($PM_{2.5}$) concentrations and its health impacts in a mega city, Delhi in India. – Environmental health insights 12: 1178630218792861. https://doi.org/10.1177/1178630218792861.

[19] Goudarzi, G., Geravandi, S., Foruozandeh, H., Babaei, A. A., Alavi, N., Niri, M. V., Mohammadi, M. J. (2015): Cardiovascular and respiratory mortality attributed to ground-level ozone in Ahvaz, Iran. – Environmental monitoring and assessment 187(8): 487. https://doi.org/10.1007/s10661-015-4674-4.

[20] Gray, E. (2015): NASA Satellite Reveals How Much Saharan Dust Feeds Amazon's Plants. – https://www.nasa.gov/content/goddard/nasa-satellite-reveals-how-much-saharan-dust-feeds-amazon-s-plants. (Accessed January 5, 2022).

[21] Gündoğdu, S. (2020): Comparison of static MLP and dynamic NARX neural networks for forecasting of atmospheric PM_{10} and SO_2 concentrations in an industrial site of Turkey. – Environmental Forensics 21(3-4): 363-374. https://doi.org/10.1080/15275922.2020.1771637.

[22] Hosseiniebalam, F., Ghaffarpasand, O. (2015): The effects of emission sources and meteorological factors on sulphur dioxide concentration of Great Isfahan, Iran. – Atmospheric Environment 100: 94-101. https://doi.org/10.1016/j.atmosenv.2014.10.012.

http://www.aloki.hu ● ISSN 1589 1623 (Print) ● ISSN 1785 0037 (Online)
DOI: http://dx.doi.org/10.15666/aeer/2005_40794093

[23] Huang, K., Shi, C. M., Min, J. Q., Li, L., Zhu, T., Yu, H., Deng, H. (2019): Study on the mechanism of curcumin regulating lung injury induced by outdoor fine particulate matter (PM2.5). – Mediators of Inflammation 9: 8613523. https://doi.org/10.1155/2019/8613523.
[24] Karaca, F. (2012): Determination of air quality zones in Turkey. – Journal of the Air & Waste Management Association 62: 408-419. https://doi.org/10.1080/10473289.2012.655883.
[25] Landim, A. A., Teixeira, E. C., Agudelo-Castañeda, D., Schneider, I., Silva, L. F., Wiegand, F., Kumar, P. (2018): Spatio-temporal variations of sulfur dioxide concentrations in industrial and urban area via a new statistical approach. – Air Quality, Atmosphere & Health 11(7): 801-813.
[26] Lee, S., Ho, Ch., Lee, Y. G., Choi, H., Song, Ch. (2013): Influence of transboundary air pollutants from China on the high PM10 episode in Seoul, Korea for the period October 16-20, 2008. – Atmos. Environ. 77: 430-439. https://doi.org/10.1016/j.atmosenv.2013.05.006.
[27] Lelieveld, J., Evans, J. S., Fnais, M., Giannadaki, D., Pozzer, A. (2015): The contribution of outdoor air pollution sources to premature mortality on a global scale. – Nature 525: 367-371. https://doi.org/10.1038/nature15371.
[28] Li, J., Chen, B., de la Campa, A. M. S., Alastuey, A., Querol, X., de la Rosa, J. D. (2018): 2005–2014 trends of PM10 source contributions in an industrialized area of southern Spain. – Environmental Pollution 236: 570-579. https://doi.org/10.1016/j.envpol.2018.01.101.
[29] Lin, W., Xu, X., Ge, B., Liu, X. (2011): Gaseous pollutants in Beijing urban area during the heating period 2007–2008: variability, sources, meteorological, and chemical impacts. – Atmospheric Chemistry and Physics 11: 8157-8170. https://doi.org/10.5194/acp-11-8157-2011.
[30] Loyd, C. D. (2010): Local Models for Spatial Analysis. – 2nd ed. ISBN 9780367864934, Temple University, Philadelphia, PA, USA., 98p.
[31] Manisalidis, I., Stavropoulou, E., Stavropoulos, A., Bezirtzoglou, E. (2020): Environmental and health impacts of air pollution: a review. – Frontiers in public health 8(14). https://doi.org/10.3389/fpubh.2020.00014.
[32] Ozel, G., Cakmakyapan, S. (2015): A new approach to the prediction of PM10 concentrations in Central Anatolia Region, Turkey. – Atmos Pollut Res. 6: 735-741. https://doi.org/10.5094/APR.2015.082.
[33] Palarz, A., Celiński-Mysław, P. (2017): The effect of temperature inversions on the particulate matter PM10 and sulfur dioxide concentrations in selected basins in the Polish Carpathians. – Carpathian Journal of Earth and Environmental Sciences 12(2): 629-640.
[34] Qiao, X., Du, J., Kota, S. H., Ying, Q., Xiao, W., Tang, Y. (2018): Wet deposition of sulfur and nitrogen in Jiuzhaigou National Nature Reserve, Sichuan, China during 2015–2016: Possible effects from regional emission reduction and local tourist activities. – Environmental Pollution 233: 267-277. https://doi.org/10.1016/j.envpol.2017.08.041.
[35] Rajak, R., Chattopadhyay, A. (2019): Short and long-term exposure to ambient air pollution and impact on health in India: a systematic review. – International Journal of Environmental Health Research 30(6): 593-617. https://doi.org/10.1080/09603123.2019.1612042.
[36] Ray, S., Kim, K. H. (2014): The pollution status of sulfur dioxide in major urban areas of Korea between 1989 and 2010. – Atmospheric Research 147(148): 101-110. https://doi.org/10.1016/j.atmosres.2014.05.011.
[37] Sakhamuri, S., Cummings, S. (2019): Increasing trans-Atlantic intrusion of Sahara dust: a cause of concern. – The Lancet Planetary Health 3(6): 242-243. https://doi.org/10.1016/S2542-5196(19)30088-9.
[38] Sari, M. F., Esen, F. (2021): Effect of COVID-19 on PM_{10} and SO_2 concentrations in Turkey. – Environmental Forensics. https://doi.org/10.1080/15275922.2021.1907818.

http://www.aloki.hu ● ISSN 1589 1623 (Print) ● ISSN 1785 0037 (Online)
DOI: http://dx.doi.org/10.15666/aeer/2005_40794093

[39] Schornobay-Lui, E., Hanisch, W. S., Corrêa, E. M., Corrêa, N. A. (2019): Prediction of short and medium term PM_{10} concentration using artificial neural networks. – Management of Environmental Quality: An International Journal 30(2): 414-436. https://doi.org/10.1108/MEQ-03-2018-0055.
[40] Sengupta, S., Patil, R. S., Venkatachalam, P. (1996): Assessment of population exposure and risk zone due to air pollution using the GIS, Comput. – Environment and Urban Systems 20(3): 191-199. https://doi.org/10.1016/S0198-9715(96)00014-2.
[41] Shukla, K., Kumar, P., Mann, G. S., Khare, M. (2020): Mapping spatial distribution of particulate matter using Kriging and Inverse Distance Weighting at supersites of megacity Delhi. – Sustainable cities and society 54: 101997. https://doi.org/10.1016/j.scs.2019.101997.
[42] Stein, A. F., Draxler, R. R., Rolph, G. D., Stunder, B. J. B., Cohen, M. D., Ngan, F. (2015): NOAA'S HYSPLIT atmospheric transport and dispersion modelling system. – Bulletin of the American Meteorological Society 96: 2059-2077. https://doi.org/10.1175/BAMS-D-14-00110.1.
[43] Talbi, A., Kerchich, Y., Kerbachi, R., Boughedaoui, M. (2018): Assessment of annual air pollution levels with PM1, PM2.5, PM_{10} and associated heavy metals in Algiers, Algeria. – Environmental Pollution (Barking, Essex: 1987) 232: 252-263. https://doi.org/10.1016/j.envpol.2017.09.041.
[44] Tella, A., Balogun, A. L. (2021): Prediction of ambient PM_{10} concentration in Malaysian cities using geostatistical analyses. – Journal of Advanced Geospatial Science & Technology 1(1): 115-127.
[45] Toros, H., Erdun, H., Çapraz, Ö., Özer, B., Daylan, B. E., Öztürk, A. İ. (2013): Air pollution and quality levels in metropolitans of Turkey for sustainable life. – European Journal of Science and Technology 1(1): 12-18.
[46] TR Ministry of Environment, Urbanization and Climate Change (2019): https://www.havaizleme.gov.tr. (Accessed January, 5, 2022).
[47] TSI (Turkish Statistical Institute) (2020): The ınformation source of Turkey. – https://www.tuik.gov.tr. (Accessed January 5, 2022).
[48] UCTEA (Union of Chambers of Turkish Engineers and Architects) Chamber of Environmental Engineers (2017): The Air Pollution Report 2017. – http://cmo.org.tr/resimler/ekler/2145efce8f89f52_ek.pdf. (Accessed January 5, 2022).
[49] United States Environmental Protection Agency (US EPA) (2017): Integrated science assessment for sulfur oxides – health criteria. – https://www.epa.gov/isa/integrated-science-assessment-isa-sulfur-oxides-health-criteria. (Accessed January 5, 2022).
[50] WHO (World Health Organization) (2006): WHO Air Quality Guidelines for Particulate Matter, Ozone, Nitrogen Dioxide and Sulfur Dioxide. – Global Update 2005-Summary of Risk Assessment, 2006. WHO, Geneva.
[51] WHO (World Health Organization) (2020): Air Pollution. – https://www.who.int/health-topics/air-pollution#tab=tab_2. (Accessed January 5, 2022).
[52] Zeydan, O. (2021): Assessment of Particulate Matter (PM_{10}) Pollution in Turkey in 2019. – Journal of the Institute of Science and Technology 11(1): 106-118. https://doi.org/10.21597/jist.745539.
[53] Zhu, F., Ding, R., Lei, R., Cheng, H., Liu, J., Shen, C., Cao, J. (2019): The short-term effects of air pollution on respiratory diseases and lung cancer mortality in Hefei: A time-series analysis. – Respiratory medicine 146: 57-65. https://doi.org/10.1016/j.rmed.2018.11.019.

http://www.aloki.hu ● ISSN 1589 1623 (Print) ● ISSN 1785 0037 (Online)
DOI: http://dx.doi.org/10.15666/aeer/2005_40794093

RESPONSE OF KERNEL STRUCTURE-RELATED TRAITS TO PLANTING DENSITY AND CULTIVAR IN DIFFERENT PARTS OF THE WAXY CORN EAR

XUE, J. F.[1,2*] – CUI, W. H.[1,2] – LIU, C. B.[1,2] – LIU, K. K.[1,2] – ZHAO, X. H.[3] – GAO, Z. Q.[1,2]

[1]*College of Agriculture, Shanxi Agricultural University, Taigu County, Shanxi Province, 03l0801, China*

[2]*State Key Laboratory of Integrative Sustainable Dryland Agriculture (in preparation), Taiyuan 030031, China*

[3]*College of Life Sciences, Shanxi Agricultural University, Taigu 030800, China*

**Corresponding author*
e-mail: fudange95@163.com

(Received 16th Apr 2022; accepted 11th Jul 2022)

Abstract. Kernel structure-related traits are important factors that affect the yield and ear appearance of waxy corn (*Zea mays* L. var. ceratina), regulated together by genetic factors and cultivation practices. Two planting densities, 52500 plants/ha and 67500 plants/ha, were established in this study for three major cultivars that are promoted in the local region: Jinnuo 18# (JN18), Jinnuo 20# (JN20), and Jindannuo 41# (JdN41). We measured how the kernel length, width, thickness, volume, 100-kernel weight, and kernel weight of different parts of the waxy corn ear changed with planting density and cultivar. The results showed that planting density did not significantly affect the structure-related traits of kernels in different parts of the waxy corn ear. Most of the kernel structure-related traits in the middle and basal parts were significantly higher than those in the apical part of the waxy corn ear. Compared with planting density, cultivar had a greater influence on kernel structure-related traits in waxy corn. Comparison between different cultivars showed that the kernel structure-related traits in JN18 were better than those in JdN41.

Keywords: *kernel size, kernel shape, kernel volume, traits of kernel structure, kernel morphological traits*

Introduction

Waxy corn (*Zea mays* L. var. ceratina) is commonly consumed in most Asian countries, particularly China, Korea, Tailand, and Vietnam (Lim and Yi, 2019; ÖZata, 2021; Kim et al., 2022). With the fast growth of the economy in China, the average household income is rising rapidly and the quality of life is also improved greatly. Consequently, food consumption patterns rapidly transitioned from one in which grains and vegetables dominated to one having more animal products and more diversification in China (Yuan et al., 2019). Increasingly more people have begun to emphasize healthy eating and nutritional balance. Waxy corn is rich in various amino acids, vitamins, and minerals, giving it extremely high nutrition values and making it favored by many consumers (Xiao et al., 2022). Currently, the planting area of fresh corn has reached 1.34 million hectares, and which has become the largest consumers and producers of fresh corn in the world (Huang et al., 2022; Xiao et al., 2022). Taste is among the important parameters used to evaluate the eating quality of waxy corn. The kernel structure traits (kernel length, width, thickness, and volume) have a major influence not only on the yield but also the taste of waxy corn (Jung et al., 2005). In recent years,

http://www.aloki.hu ● ISSN 1589 1623 (Print) ● ISSN 1785 0037 (Online)
DOI: http://dx.doi.org/10.15666/aeer/2005_40954108

kernel structure-related traits have become the target of selection by breeders to obtain a higher yield of common corn (Yang et al., 2016; Li et al., 2019, 2022; Qu et al., 2022).

Kernels of corn ear have different shape-related traits due to the influences of genetic factors (Li et al., 2009, 2022; Liu et al., 2020; Pang et al., 2021; Qu et al., 2022) and cultivation practices (Abdelghany et al., 2019; Zhang et al., 2021). Generally, kernel abortion can appear in the apical kernels (Otegui et al., 1995; Shen et al., 2005), causing an increased barren tip length and a decrease in the quality of physical appearance. Furthermore, kernels that develop in different parts of the ear exhibited large differences. In some studies, kernels are divided into apical, middle, and basal sets based on their positions on the ear. The results have shown that the basal kernels exhibited the greatest 100-kernel weight, followed by that of the middle kernels, and the apical kernels had the lowest 100-kernel weight (Zhang, 2010; Xu et al., 2013a, 2015). Moreover, the moisture content of kernels in the apical part of the ear were lower than those in the middle and basal parts during the middle and late stages (Li et al., 2020). Currently, most studies on the kernel structure-related traits at different positions of the ear have been conducted in common corn and have focused more on kernel weight, overlooking kernel length, width, thickness, and volume. Better understanding the differences in kernel structure-related traits between different parts of the corn ear will help improve the eating quality of waxy corn ears.

Currently, kernel structure-related traits have not been widely studied, and such studies are mostly concentrated on common corn with breeding-related purposes, while the impact of cultivation practice has rarely been studied. With the increase in planting density, the 100-kernel weight, kernel length, and kernel width decreased, while the kernel thickness had no significant changes (Wang, 2016). The kernel volume also decreased with the increase in planting density, but the degree of decrease was different in different cultivars for common corn (Xu et al., 2013b). However, there has been little research on the impact of cultivar and planting density on kernel structure-related traits in waxy corn. Currently, the majority of common corn are compact-types of plant with higher planting density (>67500 plants/ha), however, most of waxy corn are flat-type of plant with lower planting density (<52500 plants/ha). Otherwise, there are great difference in kernel morphological characteristics between common corn and waxy corn. Those would result in the difference in kernel formation and its structure-related traits. Elucidating the influences of planting density and cultivar on kernel structure-related traits in waxy corn is important for increasing the yield of fresh waxy corn and improving the eating quality of kernels.

In this study, we analyzed the differences in kernel structure-related traits, including 100-kernel weight, kernel length, width, thickness, and volume, in different parts of the ear of waxy corn of different cultivars at different planting densities. Our goal was to provide a theoretical reference for improving the eating quality of waxy corn ears.

Materials and methods

Experimental site

The experiment was conducted in Luojiazhuang Village, Qingyuan Town, Qingxu County, Taiyuan, Shanxi (37°58’ N, 112°36’ E), which was located in the Eastern Loess plateau. It has a temperate continental climate, with four distinct seasons. The mean annual sunshine duration is 2577.5 h. The mean annual temperature is approximately 9.9 ℃. The mean annual precipitation is approximately 462 mm. The

http://www.aloki.hu ● ISSN 1589 1623 (Print) ● ISSN 1785 0037 (Online)
DOI: http://dx.doi.org/10.15666/aeer/2005_40954108

mean annual frost-free period is 183 days. The preceding crop at the test site was common corn. Organic matter in the 0-20 cm soil layer was 15.20 g/kg, with alkali-hydrolyzale nitrogen 59.06 mg/kg, available phosphorus 33.76 mg/kg, and available potassium 209.32 mg/kg.

Experimental design

This study used a two-factor randomized block design, three waxy corn cultivars (Jinnuo 18# (JN18, white), Jinnuo 20# (JN20, black), and Jindannuo 41# (JdN41, yellow)), and two planting densities (52500 plants/ha (PD_{52500}, conventional density) and 67500 plants/ha (PD_{67500}, high density)). Each treatment had three replicates in a total of 18 plots, each plot had an area of 50 m^2 (10 m × 5 m). In early April, the test site was watered with flood irrigation. Before sowing, each plot was fertilized with a compound fertilizer (N:P:K = 23:12:5) as the base fertilizer at 600 kg/ha. After rotary tillage, waxy corn were planted with 50 cm of row distance in all plots. The plant distance within a row were 41.67 cm and 32.35 cm in density of 52500 plants/ha and 67500 plants/ha, respectively. Urea was applied at 337.5 kg/ha through ditches at the jointing stage. Seeds were sown on May 17. On May 26 and July 4, a mixture of cypermethrin, chlorpyrifos-phoxim EC, and chlorpyrifos was applied twice to kill pests. At the flowering stage, plants were bagged, and hand pollination was conducted to prevent crossing. The optimal harvest time was different for different waxy corn cultivars. JdN41 and JN18 were harvested on August 21, and JN20 was harvested on August 29.

Kernel structure-related traits in different parts of the ear

At the optimal harvest time, 10 ears were randomly selected from each plot. Here, we divided the ear of waxy corn into three equal parts depending on the length of the ear, including apical (the upper third of the ear), middle (the middle third of the ear), and basal (the lower third of the ear) parts from the top to bottom of the ear. From each ear, kernels were removed and weighed. The kernel weight (g) in each part was recorded. One hundred kernels were randomly selected to measure the 100-kernel weight (g).

Among the kernel samples, 10 kernels were randomly selected from each of the apical, middle, and basal parts. The kernel size parameters such as length, width, and thickness (mm) were measured using a Vernier caliper. The length/width, length/thickness, and width/thickness ratios of each kernel were calculated for the evaluation of kernel shape. In addition, 10 apical, 10 middle, and 10 basal kernels were randomly selected from each plot and placed individually in a 20-mL graduated cylinder with 10 mL distilled water. The cylinder was shaken until the kernels were completely submerged in water. The changes in water volume were taken to be the kernel volume (mL) and converted to single-kernel volume (cm^3). The measurement was repeated 10 times for each plot.

Data analysis

WPS Office 2019 was used for data sorting and graphing. SPSS 16.0 was used for statistical analysis of the data. Duncan's multiple range test was conducted to analyze the differences among different planting densities and cultivars. Pearson correlation analysis of different parameters was conducted in SPSS 16.0, and R 4.0.3 software (R Core Team, 2020) was used to graph the correlation coefficients.

http://www.aloki.hu ● ISSN 1589 1623 (Print) ● ISSN 1785 0037 (Online)
DOI: http://dx.doi.org/10.15666/aeer/2005_40954108

Results

The cultivars of waxy corn had a significant effect on most of kernel structure-related traits, e.g., kernel length, width, thickness, kernel length/thickness and width/thickness ratios (*Table 1*). Planting density of waxy corn had no effect on kernel structure-related traits in different ear parts in the study.

Table 1. *Analysis of variance for kernel structure-related traits in different ear parts*

Source of variation	KL			KW			KT		
	Apical	**Middle**	**Basal**	**Apical**	**Middle**	**Basal**	**Apical**	**Middle**	**Basal**
WCC	*	*	*	ns	*	*	**	**	ns
PD	ns	ns	ns	ns	ns	ns	ns	ns	ns
WCC × PD	ns	ns	ns	ns	ns	ns	ns	ns	ns
Source of variation	**KL/WR**			**KL/TR**			**KW/TR**		
	Apical	**Middle**	**Basal**	**Apical**	**Middle**	**Basal**	**Apical**	**Middle**	**Basal**
WCC	*	ns	ns	*	**	*	*	**	**
PD	ns	ns	ns	ns	ns	ns	ns	ns	ns
WCC × PD	ns	ns	*	ns	ns	ns	ns	ns	ns
Source of variation	**KV**			**100-KW**			**KWE**		
	Apical	**Middle**	**Basal**	**Apical**	**Middle**	**Basal**	**Apical**	**Middle**	**Basal**
WCC	ns	ns	ns	ns	ns	ns	ns	ns	ns
PD	ns	ns	ns	ns	ns	ns	ns	ns	ns
WCC × PD	ns	ns	ns	ns	ns	ns	ns	ns	*

WCC is waxy corn cultivars, PD is planting density, KL is kernel length, KW is kernel width, KT is kernel thickness, KL/WR is kernel length/width ratios, KL/TR is kernel length/thickness ratios, KW/TR is kernel width/thickness ratios, KV is kernel volume, 100-KW is 100-kernel weight, KWE is kernel weight per ear. * and ** indicate significance at the 5% and 1% levels, respectively

Kernel size

Under two planting densities, the average kernel length, width, and thickness in different parts of the ear was 9.56-10.12 mm, 8.53-8.95 mm, and 4.43-4.99 mm, respectively (*Fig. 1 I, III, V*). The apical, middle, and basal kernels of the waxy corn ear were not significantly different in length, width, or thickness under two planting densities. Analyzing kernel structure-related traits in different parts of the ear revealed that the average length and width of apical kernels were 4.7% and 2.4% less than those of middle kernels, respectively, and 2.8% and 4.4% less than those of basal kernels ($p < 0.05$). Middle kernels were significantly longer by 1.9% than basal kernels, while the average width of middle kernels was significantly lower by 2.1% than that of basal kernels ($p < 0.05$). The average thicknesses of apical and basal kernels were not significantly different, however, they were significantly greater than that of middle kernels, by 4.5% and 6.4%, respectively ($p < 0.05$).

Comparison of kernel structure-related traits among different cultivars showed that the lengths of the apical, middle, and basal kernels followed the order of JN18 > JN20 > JdN41 ($p < 0.05$), with significant differences between cultivars, and that the kernel lengths in JN18 were 4.9-16.4% longer than those in other cultivars (*Fig. 1 II, IV, VI*). The apical, middle, and basal kernels of JN18 were significantly wider than those of JN20 by 5.7-6.7% and JdN41 by 5.4-8.9% ($p < 0.05$), respectively,

http://www.aloki.hu ● ISSN 1589 1623 (Print) ● ISSN 1785 0037 (Online)
DOI: http://dx.doi.org/10.15666/aeer/2005_40954108

while the difference in kernel width between the latter two cultivars was not significant. The kernel thicknesses were significantly lower in JN18 than those in JdN41 and JN20, by 9.2-15.3% and 9.3-17.9% ($p < 0.05$), respectively, and which were inconsistent in different ear parts of the latter two cultivars.

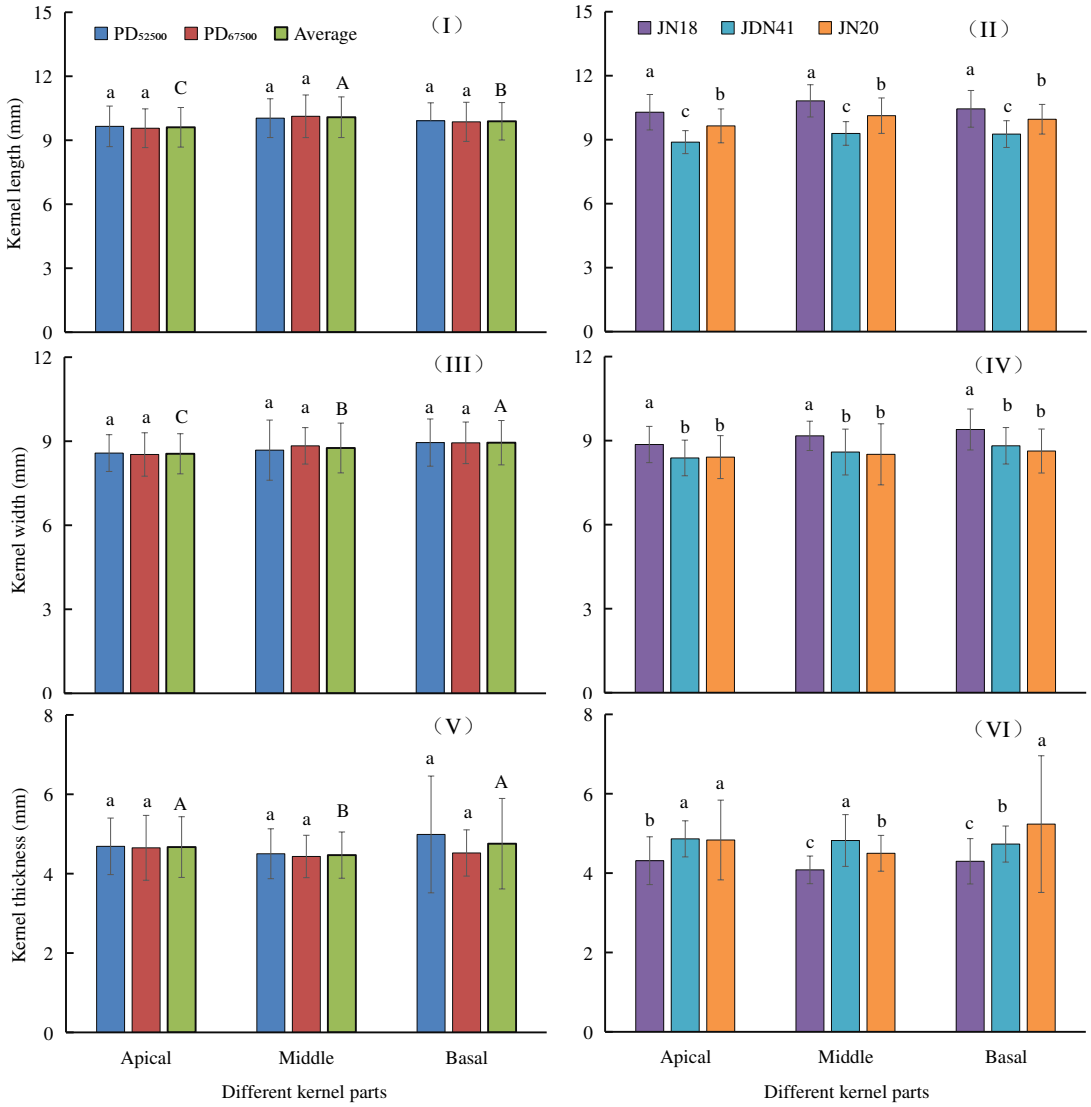

Figure 1. *Effects of planting density and variety on length, width and thickness in different parts of waxy corn ear. The lowercase letters indicate statistical difference among different planting density or cultivars in the same sample position at $p < 0.05$. The capital letters in (I), (III), and (V) indicate statistical difference among different parts of waxy corn ear, which are the average value under two planting densities*

Kernel shape

The average kernel length/width, length/thickness, and width/thickness ratios in different parts of the ear under two planting densities were 1.11-1.19, 2.10-2.32, and 1.87-2.02, respectively; there was no significant difference between the two planting densities (*Fig. 2 I, III, V*). Compared with the apical and basal kernels, the middle kernels had a significantly higher average length/width ratio (by 3.7-5.3%) and

http://www.aloki.hu ● ISSN 1589 1623 (Print) ● ISSN 1785 0037 (Online)
DOI: http://dx.doi.org/10.15666/aeer/2005_40954108

length/thickness ratio (by 6.2-9.0%) ($p < 0.05$). The apical kernels were significantly lower in the width/thickness ratio (by 6.0% and 4.3%, respectively) than the middle and basal kernels ($p < 0.05$); there was no significant difference between the latter two. A comparison between different cultivars showed that compared with JN20, the kernel length/width ratio in the three ear parts of JdN41 was significantly lower by 8.4-12.8% (*Fig. 2 II, IV, VI*, $p < 0.05$). The length/thickness ratio in the three parts of JN18 was significantly higher than those of the other two cultivars ($p < 0.05$). In addition, the length/thickness ratios of the apical and middle kernels were significantly lower in JdN41 than in JN20, however, the length/thickness ratio of the basal kernels was not significantly different between the two cultivars. JN18 had a significantly higher kernel width/thickness ratio in the three parts of the ear than JdN41 and JN20 (by 18.4-25.6%) ($p < 0.05$), while the latter two cultivars had no significant difference.

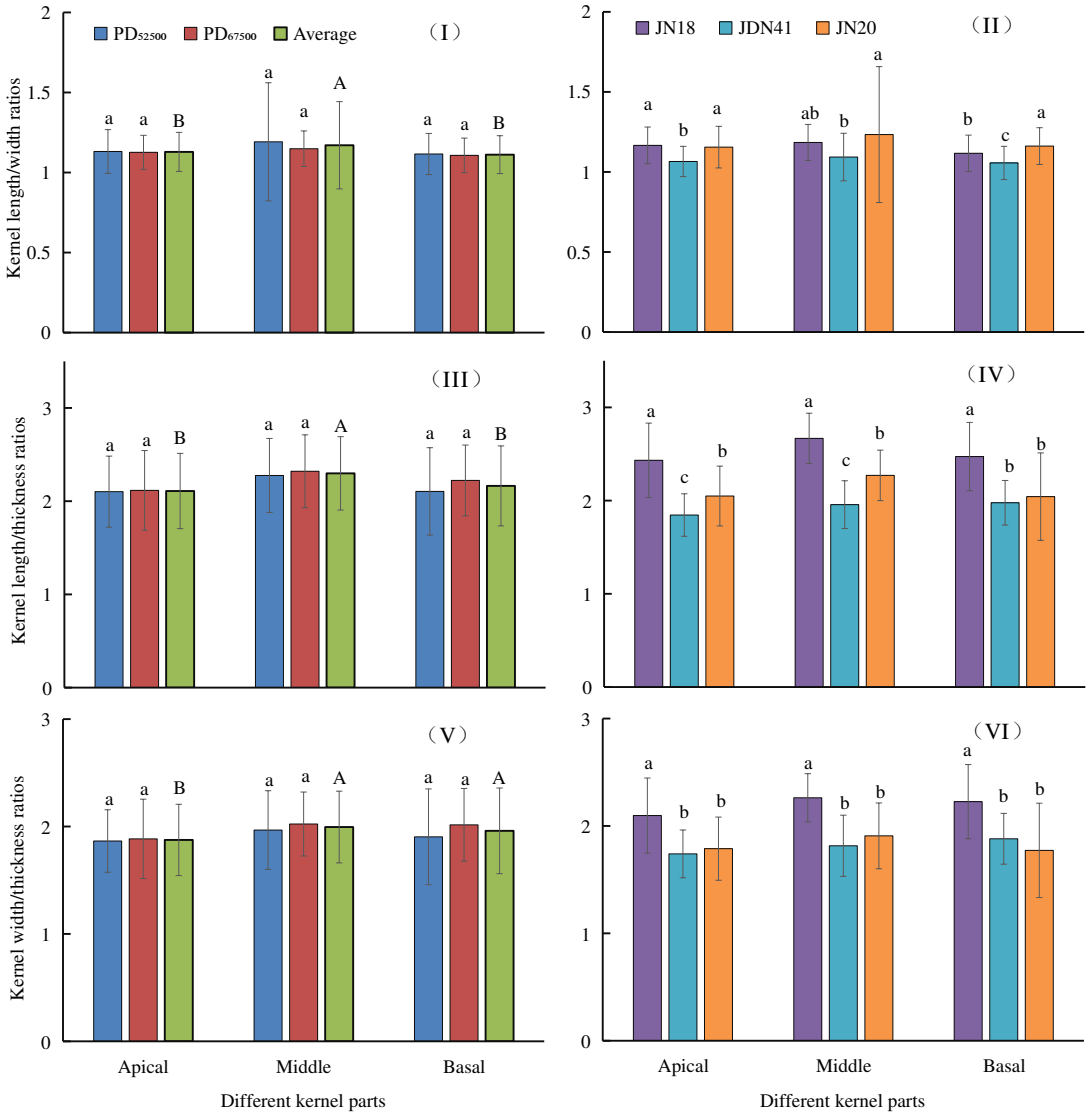

Figure 2. *Effects of planting density and variety on kernel shape in different parts of waxy corn ear. The lowercase letters indicate statistical difference among different planting density or cultivars in the same sample position at $p < 0.05$. The capital letters in (I), (III), and (V) indicate statistical difference among different parts of waxy corn ear, which are the average value under two planting densities*

http://www.aloki.hu ● ISSN 1589 1623 (Print) ● ISSN 1785 0037 (Online)
DOI: http://dx.doi.org/10.15666/aeer/2005_40954108

Kernel volume

The single-kernel volume in the apical, middle, and basal parts of the waxy corn ear were 0.28-0.30 cm^3, and there was no significant difference between the two planting densities (*Fig. 3 I*). Single-kernel volume in the apical part was significantly lower by 6.1% and 7.6% than those in the middle and basal parts, respectively ($p < 0.05$). There was no significant difference in kernel volume in the apical part between cultivars (*Fig. 3 II*). The kernel volumes in the middle and basal parts of JN18 were significantly higher by 7.9% and 4.3% than those of JdN41 ($p < 0.05$), respectively, however, which were not significantly different from those of JN20.

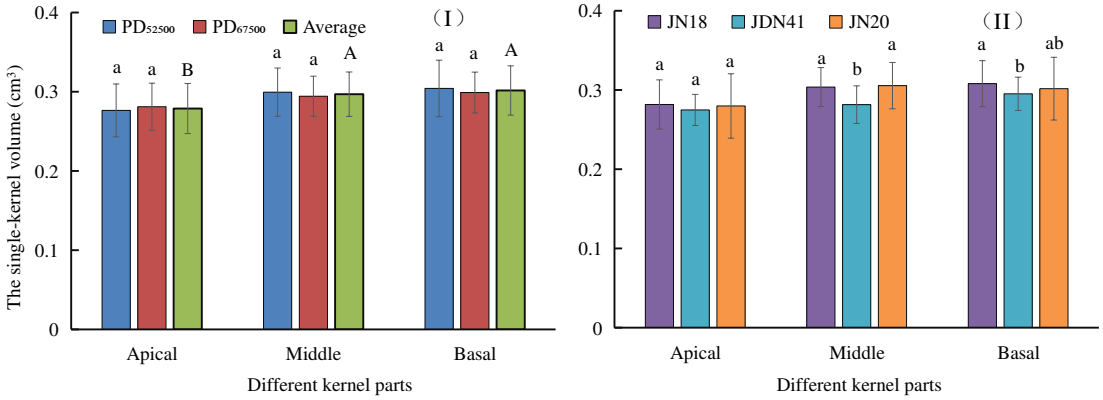

Figure 3. *Effects of planting density and variety on kernel volume in different parts of waxy corn ear. The lowercase letters indicate statistical difference among different planting density or cultivars in the same sample position at $p < 0.05$. The capital letters in (I) indicate statistical difference among different parts of waxy corn ear, which are the average value under two planting densities*

100-kernel weight

The average 100-kernel weight in the apical, middle, and basal parts of waxy corn ears ranged from 29.90 to 34.31 g, with no significant difference between the two planting densities (*Fig. 4 I*). The 100-kernel weight in the apical part was significantly lower by 10.0% and 10.1% than those in the middle and basal parts, respectively ($p < 0.05$). Comparing the different cultivars (*Fig. 4 II*), the 100-kernel weights of kernels in the apical and middle ear of JdN41 were significantly lower by 1.6% and 4.5% than those of JN20, respectively ($p < 0.05$), however, which exhibited no significant difference in the 100-kernel weight in the basal part. In addition, the 100-kernel weights of kernels in the middle and basal parts of JN18 were both significantly higher than those of JdN41 ($p < 0.05$).

Kernel weight per ear

The apical, middle, and basal kernels of waxy corn ears weighed 50.38-69.89 g, and there was no significant difference between the two planting densities (*Fig. 5 I*). Kernel weight in different parts of the ear followed the order of basal > middle > apical; the differences between each part were significant (*Fig. 5 I*, $p < 0.05$). Compared with JN18 (*Fig. 5 II*), JdN41 and JN20 were significantly lower by 12.6-16.9% and 15.3-18.2% in kernel weight in the apical and middle parts of the ear, respectively ($p < 0.05$), while the

http://www.aloki.hu ● ISSN 1589 1623 (Print) ● ISSN 1785 0037 (Online)
DOI: http://dx.doi.org/10.15666/aeer/2005_40954108

differences between the latter two cultivars were not significant. There was no significant difference in kernel weight in the basal part of the ear between JN18 and JN20, however, they were both significantly higher than that in JdN41 ($p < 0.05$).

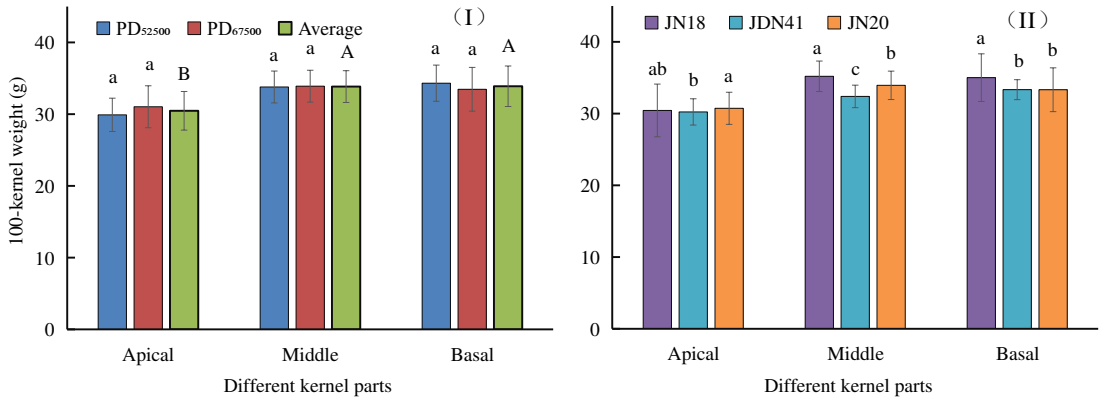

Figure 4. *Effects of planting density and variety on hundred-grain weight of waxy corn in different parts of ear. The lowercase letters indicate statistical difference among different planting density or cultivars in the same sample position at $p < 0.05$. The capital letters in (I) indicate statistical difference among different parts of waxy corn ear, which are the average value under two planting densities*

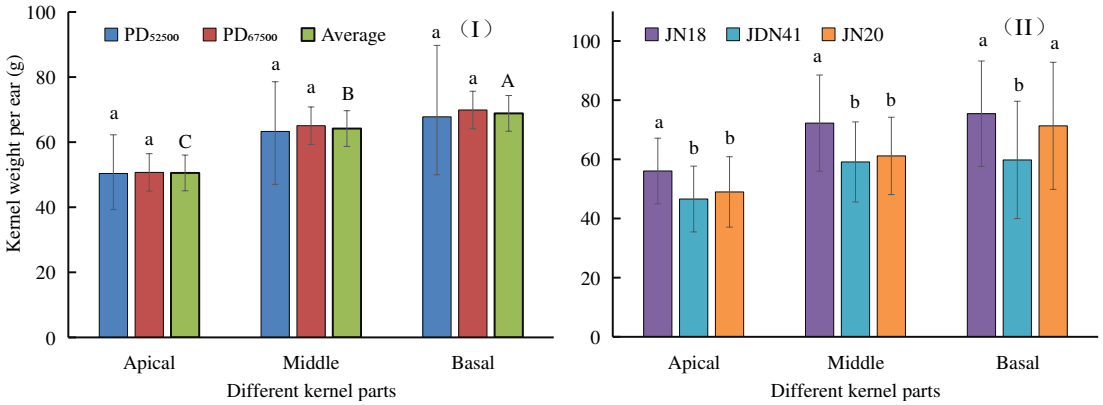

Figure 5. *Effects of planting density and variety on weight of grain per ear of waxy corn. The lowercase letters indicate statistical difference among different planting density or cultivars in the same sample position at $p < 0.05$. The capital letters in (I) indicate statistical difference among different parts of waxy corn ear, which are the average value under two planting densities*

The correlation among kernel structure-related traits

The correlation among kernel structure-related traits of waxy corn were shown in *Figure 6*. Positive correlation between kernel length and kernel width were presented ($p < 0.001$). However, negative correlation between kernel thickness and kernel length ($p < 0.001$) was observed, similar trend was showed between kernel thickness and kernel width ($p < 0.01$). Moreover, there were positive effects of kernel length and kernel width on 100-kernel weight and kernel weight per ear ($p < 0.001$), while on

http://www.aloki.hu ● ISSN 1589 1623 (Print) ● ISSN 1785 0037 (Online)
DOI: http://dx.doi.org/10.15666/aeer/2005_40954108

which were negative effects of kernel thickness. In addition, kernel length/thickness and width/thickness ratios had significant positive effects on kernel volume, 100-kernel weight and kernel weight per ear.

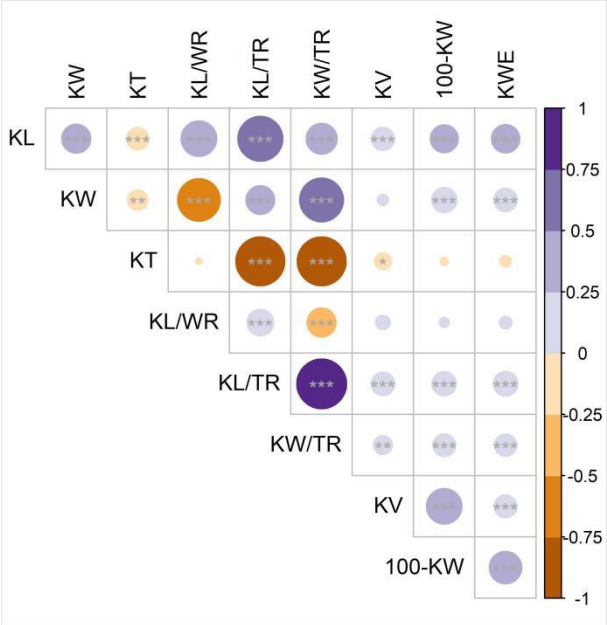

Figure 6. *The correlation coefficient plot among kernel structure-related traits. Significant correlation at *0.05, **0.01, and ***0.001 levels. KL is kernel length, KW is kernel width, KT is kernel thickness, KL/WR is kernel length/width ratios, KL/TR is kernel length/thickness ratios, KW/TR is kernel width/thickness ratios, KV is kernel volume, 100-KW is 100-kernel weight, KWE is kernel weight per ear*

Discussion

Analysis of kernel structure-related traits in different parts of the waxy corn ear

The differences in the development of kernels in different parts of the ear could lead to differences in kernel structure-related traits. So far, researches on kernel structure-related traits in different parts of the ear have mostly concentrated on common corn and on studying kernel weight (Wei et al., 2019; Yin et al., 2021), however, which in waxy corn are rarely studied. Most studies have shown that the 100-kernel weight in different parts of the ear follows the order of basal > middle > apical (Zhang, 2010; Xu et al., 2013a), while some studies showed that the distribution of ^{14}C-assimilates followed the order of middle > basal > apical (Xu et al., 2015). In this study, we found that kernel length, width, volume, 100-kernel weight, and kernel weight in the apical part of the ear were all significantly lower than those in the middle and basal parts. Moreover, the length/width and length/thickness ratios in the apical part of the ear were significantly lower than those in the middle part of the ear. Generally, floret development, silking, and pollination occur earlier in the middle and basal parts of the ear than in the apical part, which could inhibit the growth of florets in the apical part (Cárcova et al., 2000). Thus, compared with the kernels in the middle and basal parts, kernels in the apical part exhibit worse grain-filling and lower kernel weight and therefore are inferior kernels (Zhang, 2010). The volume and size of kernels in the apical part is also inhibited to a certain extent. Focusing on the breeding of a cultivar with good kernel shape in the

http://www.aloki.hu ● ISSN 1589 1623 (Print) ● ISSN 1785 0037 (Online)
DOI: http://dx.doi.org/10.15666/aeer/2005_40954108

apical part of the ear is necessary for increasing waxy corn yield and improving its physical appearance.

In recent years, kernel structure-related traits in corn have gradually become the target of selection by breeders (Li et al., 2009). Some results showed that kernel length exhibits a high positive correlation with yield in common corn (Li et al., 2009; Veldboom et al., 1994; Veldboom et al., 1996), however, relevant information in waxy corn is scarce. Moreover, the correlation between kernel structure-related traits and yield in waxy corn has not been reported. There has been very little study of the relationship between kernel structure-related traits and yield components. The correlation analysis conducted in this study found that the kernel weight and 100-kernel weight in waxy corn exhibited positive correlations with kernel length, width, and volume (*Fig. 6*).

The mechanism of the interaction between kernel weight and kernel structure-related traits remains unclear. Some researchers used common corn and synchronous hand pollination to eliminate the influence of the timing of pollination on floret development in different parts of the ear. The kernels in the top 3-13 kernel rings of the ear were apical kernels, and the kernels in the middle and basal 23-33 rings were middle and basal kernels. These studies showed that kernel weight, number of endosperm cells, sucrose, and total sugar in the middle and basal kernels of the ear were higher than those in the apical kernels. The difference in the assimilate-holding capacity of kernels and the imbalance of the supply of assimilates may be one reason for the differences in kernels between different parts of the ear (Shen et al., 2005; Zhang et al., 2010). Differences in kernel structure-related traits in different parts of the ear could also be related to the type and cultivar of the corn and how different parts of the ear are divided (Xu et al., 2015).

Impact of planting density on kernel structure-related traits in waxy corn

As a consumer product, waxy corn is usually sold as single ears; increasing planting density is important for boosting profits. Kernel structure-related traits in waxy corn are closely related to its taste and its marketability. Studies on kernel structure-related traits have mostly focused on common corn and rarely on waxy corn. Some studies showed that as the planting density increased, the 100-kernel weight, kernel volume, length, and width decreased, while the kernel thickness had no clear pattern of change (Wang, 2016; Peng et al., 2011). Kernel structure-related traits in corn, including 100-kernel weight, kernel length, and kernel width, are not easily influenced by the external environment (Yang et al., 2016; Zhang et al., 2006). In this study, kernel size, shape, volume, 100-kernel weight, and kernel weight in different parts of the ear in waxy corn exhibited no significant difference between the two planting densities. Proper close planting is one of the best ways to increase yield and economic benefits of waxy corn. If the planting density is too low, population spatial structure becomes inappropriate, which would lead to inappropriate soil utilization and a waste of light energy. Too high of a planting density will lead to shading between individuals and competition over resources, including water, fertilizer, air, and heat (Cárcova et al., 2000; Wang et al., 2017) resulting in a yield reduction and worsened quality of physical appearance and edibility. In a literature review, we found that the planting density in recent studies on different waxy corn cultivars was 37,500-75,000 plants/ha (Cao et al., 2018; Tan et al., 2019; Doebley et al., 2006; Borrás and Otegui, 2001). In farmers' actual practice, it is generally 52,500 plants/ha. In this study, the 100-kernel weight, kernel length, and

http://www.aloki.hu ● ISSN 1589 1623 (Print) ● ISSN 1785 0037 (Online)
DOI: http://dx.doi.org/10.15666/aeer/2005_40954108

kernel width in waxy corn exhibited no significant difference after the planting density was increased to 67,500 plants/ha. This indicated that increasing planting density in waxy corn is feasible to a certain extent. However, it will be influenced by soil fertility and management technologies. Differences in the results may be related to the differences in the gradient of established planting densities, corn type and cultivar, field management, climate conditions, and soil type in different studies. A multiyear, multilocation, comprehensive experiment is needed to study this matter in greater depth.

Impact of cultivar on kernel structure-related traits in waxy corn

Genetic makeup is one of the most important factors that affect kernel structure-related traits in waxy corn. In this study, we found that kernel structure-related traits, including kernel size and shape, exhibited significant differences between different waxy corn cultivars and that cultivar a greater influence than planting density. This also indicated that kernel structure-related traits are influenced more by genetic factors in waxy corn. Particularly, the kernel weight, 100-kernel weight, kernel length, width, length/width ratio, length/thickness ratio, width/thickness ratio in JN18 were significantly higher than those in JdN41 but were similar to those in JN20. JdN41 was approved by the Shanxi Crop Cultivar Approval Committee in 2001, and JN18 and JN20 were approved in 2018 and 2019, respectively. The promotion of JdN41 application in production was earlier, while JN18 and JN20 are newly bred and approved cultivars that may have more advantages in adapting to social needs and might better satisfy consumers' needs.

Kernel structure-related traits in waxy corn and taste

Currently, consumers' demand for waxy corn is increasing, and the requirement for the quality of physical appearance and palatability continues to rise. The yield and the physical appearance of waxy corn are closely related to kernel weight and kernel structure-related traits (Doebley et al., 2006). The 100-kernel weight is one of the major yield components, while kernel volume, size, and shape are related to its physical appearance and palatability. We believe that suitable length, width, and thickness could impact the experience of biting and chewing the kernels. Too long (or short), too wide (or narrow), or too thick (or thin) kernels could cause an uncomfortable eating experience. A brief survey showed that during corn consumption, the taste of kernels in the apical part of the corn was worse than that of kernels in the middle and basal parts. However, there is no available scientific evidence on this topic. In our upcoming work, we are going to evaluate the relationship between taste and different kernel structure-related traits through sensory analysis. In addition, the physical appearance and kernel arrangement may be other important factors that influence consumers' selection of waxy corn, and these factors also need more in-depth investigation. These aspects will provide new ideas and directions for waxy corn breeding, such as using kernel structure-related traits (100-kernel weight, volume, and size) to select waxy corn cultivars (Li et al., 2009).

Limitations

The comparisons and analyses of the samples in this study allow for preliminary but clear conclusions. However, only a one-year field experiment was conducted in one locale in this study. Because of factors such as climate conditions, the reproducibility of

http://www.aloki.hu ● ISSN 1589 1623 (Print) ● ISSN 1785 0037 (Online)
DOI: http://dx.doi.org/10.15666/aeer/2005_40954108

our results needs to be tested via multiyear, multilocation experiments. Second, this study selected three waxy corn cultivars for comparison, including JN18 (white), JN20 (yellow), and JdN41 (yellow). These three cultivars are promoted well at the local market and are thus representative waxy corn cultivars in the local region. In this study, one representative cultivar was selected from among the waxy corns of each color for comparison. Next, we will increase the number of waxy corn cultivars that have the same color and thoroughly analyze their kernel structure-related traits. Third, we think that kernel structure-related traits in waxy corn are closely related to the eating experience, but there is a lack of in-depth study on this aspect, a subject of our future work. We will also evaluate the consumers' preferences from the perspectives of kernel arrangement, color, and size. Our goal is to provide new directions for the breeding of waxy corn. Moreover, we compared kernel structure-related traits of waxy corn between two planting densities in current study, including the conventional density of 52500 plants/ha and higher density of 67500 plants/ha. We mainly observed the difference in structure-related traits under higher densities than conventional density, not trying to obtain the optimum density. In future studies, we will set up 4~6 more densities to obtain the optimal planting density.

Conclusions

Kernel structure-related traits in different parts of the waxy corn ear exhibited significant differences, these traits being significantly inferior in the apical part compared to the middle and basal parts. Strengthening the breeding of cultivars with better kernel structure-related traits in the apical part has practical significance. In the current study, planting density had no significant impact on kernel structure-related traits in different parts of the waxy corn ear. In contrast, cultivar had a significant impact on kernel structure-related traits.

Acknowledgements. This research was funded by Scientific and Technological Innovation Fund of Shanxi Agricultural University (2017YJ25) and Research Program Sponsored by State Key Laboratory of Integrative Sustainable Dryland Agriculture (in preparation), Shanxi Agricultural University (202105D121008-3-1).

REFERENCES

[1] Abdelghany, M., Liu, X., Hao, L., Gao, C., Kou, S., Su, E., Zhou, Y., Wang, R., Zhang, D., Li, Y., Li, C., Song, Y., Shi, Y., Wang, T., Li, Y. (2019): QTL analysis for yield-related traits under different water regimes in maize. – Maydica 64(2): 1-10.

[2] Borrás, L., Otegui, M. E. (2001): Maize kernel weight response to postflowering source–sink ratio. – Crop Science 41: 1816-1822.

[3] Cao, Q. J., Jiang, X. L., Yang, F. T., Mao, G., Wang, F. G., Cao, X. X., Kong, F. L., Li, G. (2018): Effect of planting density on grain yield and quality of fresh sweet corn and waxy corn. – Journal of Maize Sciences 26: 94-98.

[4] Cárcova, J., Uribelarrea, M., Borrás, L., Otegui, M. E., Westgate, M. E. (2000): Synchronous pollination within and between ears improves kernel set in maize. – Crop Science 40: 1056-1061.

[5] Doebley, J. F., Gaut, B. S., Smith, B. D. (2006): The molecular genetics of crop domestication. – Cell 127: 1309-1321.

http://www.aloki.hu ● ISSN 1589 1623 (Print) ● ISSN 1785 0037 (Online)
DOI: http://dx.doi.org/10.15666/aeer/2005_40954108

[6] Huang, C., Zhang, W., Wang, H., Gao, Y., Ma, S., Qin, A., Liu, Z., Zhao, B., Ning, D., Zheng, H., Liu, Z. (2022): Effects of waterlogging at different stages on growth and ear quality of waxy maize. – Agricultural Water Management 266: 107603.
[7] Jun, T. W., Kim, S. L., Moon, H. G., Son, B. Y., Kim, S. J., Kim, S. K. (2005): Major characteristics related on eating quality and classification of inbred lines of waxy corn. – Korean Journal of Crop Science 50(S): 161-166.
[8] Kim, J., Chung, I., Kim, M., Lee, J., Son, B., Bae, H., Go, Y. S., Kim, S., Baek, S., Kim, S., Yi, G. (2022): Comparison of antioxidant activity assays in fresh purple waxy corn (*Zea mays* L.) during grain filling. – Applied Biological Chemistry 65: 1.
[9] Li, Y. X., Wang, Y., Shi, Y. S., Song, Y. C., Wang, T. Y., Li, Y. (2009): Correlation analysis and QTL mapping for traits of kernel structure and yield components in maize. – Acta Agronomica Sinica 42: 408-418.
[10] Li, P., Wei, J., Wang, H., Fang, Y., Yin, S., Xu, Y., Liu, J., Yang, Z., Xu, C. (2019): Natural variation and domestication selection of *ZmPGP1* affects plant architecture and yield-related traits in maize. – Genes 10(9): 664.
[11] Li, H., Y., Li, L. L., Wang, Y. H., Zhao, R. L., Zhang, W. J., Ming, B., Wang, K. R., Xie, R. Z., Hou, P., Zhang, W. X., Liu, W. M., Xue, J., Li, S. K. (2020): Study on dynamic difference of kernel moisture content in different parts of maize ears. – Journal of Maize Sciences 28(5): 102-109.
[12] Li, T., Wang, Y. P., Dong, Y., Guo, R. S., Li, D. M., Tang, Y. L., Zhang, X. H., Xue, J. Q., Xu, S. T. (2022): Dissecting the genetic basis of kernel size related traits and their combining ability based on a hybrid population in maize. – Acta Agronomica Sinica https://kns.cnki.net/kcms/detail/11.1809.S.20220321.1827.002.html.
[13] Lim, S., Yi, G. (2019): Investigating seed mineral composition in Korean lan-drace maize (*Zea mays* L.) and its kernel texture specificity. – Journal of Integrative Agriculture 18(9): 1996-2005.
[14] Liu, M., Tan, X., Yang, Y., Liu, P., Zhang, X., Zhang, Y., Wang, L., Hu, Y., Ma, L., Li, Z., Zhang, Y., Zou, C., Lin, H., Gao, S., Lee, M., Lübberstedt, T., Pan, G., Shen, Y. (2020): Analysis of the genetic architecture of maize kernel size traits by combined linkage and association mapping. – Plant Biotechnology Journal 18: 207-221.
[15] Otegui, M. E., Andrade, F. H., Suero, E. E. (1995): Growth, water use, and kernel abortion of maize subjected to drought at silking. – Field Crops Research 40: 87-94.
[16] ÖZata, E. (2021): Yield and quality stabilities of waxy maize genotypes using biplot analysis. – International Journal of Life Sciences and Biotechnology 4(1): 61-89.
[17] Pang, J., Fu, J., Zong, N., Wang, J., Song, D., Zhang, X., He, C., Fang, T., Zhang, H., Fan, Y., Wang, G., Zhao, J. (2019): Kernel size-related genes revealed by an integrated eQTL analysis during early maize kernel development. – The Plant Journal 98: 19-32.
[18] Peng, B., Li, Y., Wang, Y., Liu, C., Liu, Z., Tan, W., Zhang, Y., Wang, D., Shi, Y., Sun, B., Song, Y., Wang, T., Li, Y. (2011): QTL analysis for yield components and kernel-related traits in maize across multi-environments. – Theoretical and Applied Genetics 122: 1305-1320.
[19] Qu, J. Z., Feng, W. H., Zhang, X. H., Xu, S. T., Xue, J. Q. (2022): Dissecting the genetic architecture of maize kernel size based on genome-wide association study. – Acta Agronomica Sinica 48(2): 304-319.
[20] R Core Team (2020): language and environment for statistical computing. – R Foundation for Statistical Computing, Vienna. https://www.R-project.org/.
[21] Shen, L. X., Wang, P., Zhang, F. S., Yi, Z. X. (2005): Effect of nitrogen supply on grain filling at different ear position in summer maize. – Acta Agronomica Sinica 31: 532-534.
[22] Tan, H. P., Zhao, F. C., Bao, F., Han, H. L., Wang, G. Y. (2019): Effects of densities on plant traits, SPAD value of functional leaves and ears of waxy maize. – Journal of Zhejiang Agricultural Sciences 60: 2319-2320, 2323.

http://www.aloki.hu ● ISSN 1589 1623 (Print) ● ISSN 1785 0037 (Online)
DOI: http://dx.doi.org/10.15666/aeer/2005_40954108

[23] Veldboom, L. R., Lee, M. (1994): Molecular marker-facilitated studies of morphological traits in maize. II: Determination of QTLs for grain yield and yield components. – Theoretical and Applied Genetics 89: 451-458.
[24] Veldboom, L. R., Lee, M. (1996): Genetic mapping of quantitative trait loci in maize in stress and nonstress environment: grain yield and yield components. – Crop Science 36: 1310-1319.
[25] Wang, H. (2016): QTL mapping for ear architectural and kernel traits in maize under three plant densities. – MA thesis, Chinese Academy of Agricultural Sciences, Beijing.
[26] Wang, G. Y., Shao, M. H., Tan, H. P., Bao, F., Han, H. L., Zhao, F. C. (2017): Analysis of yield and agronomic traits of waxy corn under different density level. – Molecular Plant Breeding 15: 377-383.
[27] Wei, S., Wang, X., Li, G., Qin, Y., Jiang, D., Dong, S. (2019): Plant density and nitrogen supply affect the grain-filling parameters of maize kernels located in different ear positions. – Frontiers in Plant Science 10: 180.
[28] Xiao, Y. N., Yu, Y. T., Xie, L. H., Qi, X. T., Li, C. Y., Wen, T. X., Li, G. K., Hu, J. G. (2022): Genetic diversity analysis of Chinese fresh corn hybrids using SNP Chips. – Acta Agronomica Sinica 48(6): 1301-1311.
[29] Xu, Y. J., Gu, D. J., Zhang, B. B., Zhang, H., Wang, Z. Q., Yang, J. C. (2013a): Hormone contents in kernels at different positions on an ear and their relationship with endosperm development and kernel filling in maize. – Acta Agronomica Sinica 39: 1452-1461.
[30] Xu, Y. R., Sun, M. Y., Zhong, Y., Hou, Z. Y., Liu, X. E., Jiao, R. H. (2013b): Effect of planting density on the commodity quality of maize. – Journal of Jilin Agricultural Sciences 38: 1-3.
[31] Xu, Y. J., Gu, D. J., Qin, H., Zhang, H., Wang, Z. Q., Yang, J. (2015): Changes in carbohydrate accumulation and activities of enzymes Involved in starch synthesis in maize kernels at different positions on an ear during grain filling. – Acta Agronomica Sinica 41: 297-307.
[32] Yang, C., Zhang, L., Jia, A., Rong, T. (2016): Identification of QTL for maize grain yield and kernel-related traits. – Journal of Genetics 95(2): 239-247.
[33] Yin, X. B., Hou, J. F., Ming, B., Zhang, Y., Guo, X. Y., Gao, S., Wang, K. R., Hou, P., Li, S. K., Xie, R. Z. (2021): Kernel position effects of grain morphological characteristics by X-ray micro-computed tomography (μCT). – International Journal of Agricultural and Biological Engineering 14(2): 159-166.
[34] Yuan, M., Seale Jr, J. L., Wahl, T., Bai, J. (2019): The changing dietary patterns and health issues in China. – China Agricultural Economic Review 11(1): 143-159.
[35] Zhang, H. Y. (2010): Study on kernel position effects during kernel development in maize. – Journal of Maize Sciences 18: 93-95.
[36] Zhang, F. L., Jiang, Y. L., Zhao, G. S., Zhang, J. H. (2006): Relationship between distribution of 14C-assimilates and kernel abortion in maize. – Acta Agronomica Sinica 32: 1104-1106.
[37] Zhang, L., Xie, X., Tang, H., Sun, B., Liu, C. (2021): Maize grain configuration characters: relationship with yield and drought resistance. – XinJiang Agricultural Sciences 58(10): 1784-1790.

http://www.aloki.hu ● ISSN 1589 1623 (Print) ● ISSN 1785 0037 (Online)
DOI: http://dx.doi.org/10.15666/aeer/2005_40954108

AN ETHNOVETERINARY STUDY ON MEDICINAL PLANTS USED FOR ANIMAL DISEASES IN RIZE (TURKEY)

AKBULUT, S.* – ÖZKAN, Z. C.

Department of Forest Engineering, Faculty of Forestry, Karadeniz Technical University, 61080 Trabzon, Turkey

**Corresponding author*
e-mail: sakbulut@ktu.edu.tr; phone: +90-462-377-2841

(Received 18th Apr 2022; accepted 11th Jul 2022)

Abstract. Medicinal plants used in the treatment of animals in Rize province in northeast of Türkiye were recorded through semi-structured interviews with farmers and shepherds. The collected data were analyzed using the quantitative indices informant consensus factor (FIC) and fidelity level (FL). It was identified that a total of 38 plants belonging to 30 families were found used in ethnoveterinary. The most cited families were Fabaceae and Asteraceae. The highest FIC was recorded for digestive system diseases (0.93), followed by skin diseases (0.88) and milk production (0.85). The high FL values were *Datisca cannabina* L. for varroa, *Malva sylvestris* L. for wound healing, and *Sambucus ebulus* L. for external parasite (respectively 100%). Ethnoveterinary uses of *Datisca cannabina* L., *Caltha palustris* L., *Bryum schleicheri* Schwägr., *Adiantum capillus-veneris* L., *Solidago virgaurea* L. were recorded for the first time.

Keywords: *ethnoveterinary knowledge, folk remedies, informant consensus factor, livestock ailments, traditional practices*

Introduction

Plants have been a natural resource for humans and their pets to stay healthy. The best way to detect plants used in animal diseases is ethnoveterinary and ethnobotanical studies (Erarslan and Kültür, 2019). About 70000 of the plants on earth are used for therapeutic purposes. A large part of the world's population continues to trust folk medicine in the treatment of animals as well as their private health (WHO, 2021).

Ethnoveterinary medicine is a traditional treatment method applied by local people to protect the health of livestock and pets according to their traditions and cultures (McCorkle, 1986). Ethnoveterinary apps, which are unlike medical veterinary apps, are practiced and developed by farmers and shepherds and are handed down from generation to generation (Pande et al., 2007). This information, which usually does not have a written record, is in danger of being lost over time.

Traditional treatment methods for animals in Türkiye are limited to ethnobotanical studies. There are few resources available for ethnoveterinary knowledge (Sinmez and Aslım, 2017; Sinmez and Yaşar, 2017; Yıpel et al., 2017; Sinmez et al., 2018; Güler et al., 2021; Akbulut, 2022; Babacan et al., 2022). For this reason, recording traditional information in Türkiye will contribute to the development of animal husbandry. It was a decrease in the presence of cattle and a significant increase in bees and small cattle in the last 20 years in Rize. The cattle population, which was over one hundred thousand before, has decreased to 29,522 today. There are 6,908 sheep, 10,855 goats, 173 odd-toed ungulates, 2,425 cats and dogs, and 7,259 poultry. In Rize, the culture breed is Jersey, and there are few Brown Swiss and Holstein breeds. Beekeeping activities have gained momentum in recent years. The number of old type hives (black hives) is 4.159,

http://www.aloki.hu ● ISSN 1589 1623 (Print) ● ISSN 1785 0037 (Online)
DOI: http://dx.doi.org/10.15666/aeer/2005_41094119

and new type hives are 62,952, totaling 67,111. The number of villages dealing with beekeeping is 303. Annual honey production; is 638.250 kg, and wax production; is 22.400 kg. The number of registered farmers is over 10.000. (TR Ministry of Agriculture and Forestry, 2021). The study aims to record the plant taxa used in the ethnoveterinary, their preparation, and application methods used by local farmers and shepherds in treating different animal diseases in Rize and to contribute to animal medicine in this context.

Materials and methods

Study area

Rize is located in the Eastern Black Sea Region of Türkiye (*Fig. 1*). It is adjacent to the Black Sea in the north, Trabzon in the west, Artvin in the east, Bayburt in the southwest, and Erzurum in the south, and located between 40°-21' and 41°-25' east longitudes and 40°-33' and 41°-20' north latitudes. Rize is located in the Euro-Siberian flora region and the A8 squares according to the grid system by Davis (Davis, 1965). It has a significant plant diversity with approximately 1430 plant taxa, 110 of which are endemic (Güner et al., 2000). The region was mentioned for the first time in written records in the 8th century BC. Since then, it has hosted many civilizations covering Urartu, Pontus, Roman, Byzantine, and Ottoman (TR Ministry of Culture and Tourism, 2021). The most significant source of income of the region is tea agriculture. Due to the mountainous terrain, animal husbandry is usually ranched in the plateaus of Rize.

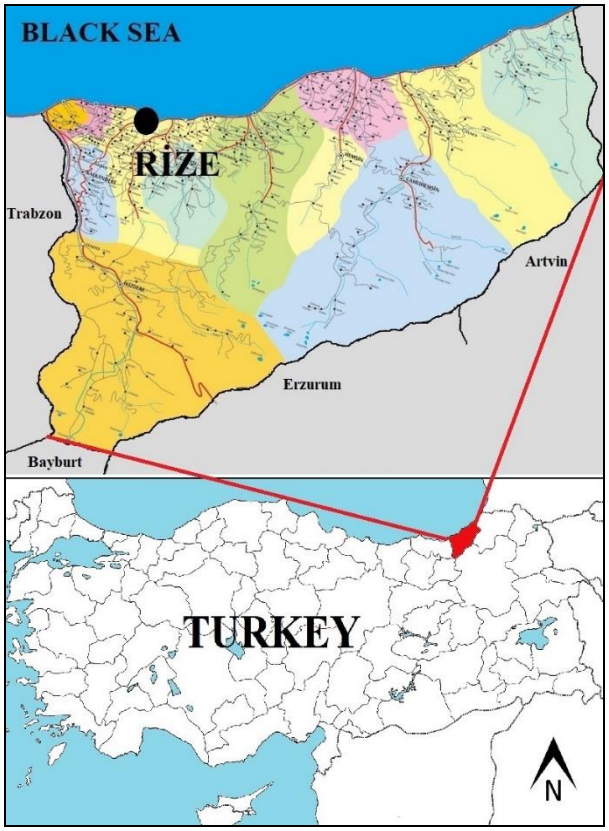

Figure 1. *The geographical location of Rize province*

http://www.aloki.hu ● ISSN 1589 1623 (Print) ● ISSN 1785 0037 (Online)
DOI: http://dx.doi.org/10.15666/aeer/2005_41094119

Data collection

The study was performed in the villages and highlands of Rize province between March and November 2021. Semi-structured interviews were carried out by 83 locals. Locals were chosen among the farmers and shepherds in the region. A survey was managed to the locals through face-to-face interviews. The demographic characteristics of the informants were noted. In the second part of the survey, the traditional methods related to the treatment of animals, plant species used, and the plant parts were recorded. Prior Informed Consent was taken orally before beginning each survey. Ethical directives considered the Code of Ethics of the International Society for Ethnobiology (ISE, 2008). Plant taxa were identified and named according to the Flora of Turkey (Davis, 1965-1985; Güner et al., 1987; Davis et al., 1988) and World Flora Online (WFO, 2021).

Data analysis

Ethnoveterinary information obtained from the surveys with farmers and shepherds was evaluated using quantitative methods (informant consensus factor and fidelity level).

The informant consensus factor (FIC) was calculated for each disease group to determine the informants' agreement on the noted treatment (Andrade-Cetto, 2009). The FIC formula was (*Eq. 1*):

$$FIC = (Nur - Nt)/(Nur - 1) \quad \text{(Eq.1)}$$

Nur: Total citation in each disease group. Nt: The number of use taxa.

Fidelity level (FL) refers to the specificity of the plants of choice for the diseases most frequently cited by locals (Friedman et al., 1986). The FL formula was (*Eq. 2*):

$$FL(\%) = \frac{Ip}{Iu} \times 100 \quad \text{(Eq.2)}$$

Ip: The number of people recommending utilizes of a plant for a specific disease. Iu: The total people who cited that a taxon is used to treat any disease.

Results

The study results showed that farmers and shepherds in Rize province use various ethnoveterinary methods for the health of their animals.

Ethnoveterinary records were compiled from face-to-face interviews with 83 locals. The informant ages ranged from 33 to 82, and the average was 52 (*Table 1*). The results showed that besides using the plants medicinally were used for milk yield and egg production (*Table 2*).

Ethnoveterinary medicine was usually used in cattle and small cattle. This is followed by bees, poultry, and horses. In the current study, a total of 38 plant taxa from 30 families used by farmers and shepherds for animal health were identified (*Table 2*). Plants were commonly used in the treatment of diseases such as wounds, cough, varroa, external parasites, and diarrhea. The most dominant family in terms of the number of species in the region was Fabaceae (4 taxa) and Asteraceae (3 taxa), and the remaining families had one or two taxa (*Fig. 2*). Leaves (15 taxa) and aerial parts (12 taxa) were used more for therapeutic effects, followed by flowers (6), fruits (3), and roots (2), respectively (*Fig. 3*).

http://www.aloki.hu ● ISSN 1589 1623 (Print) ● ISSN 1785 0037 (Online)
DOI: http://dx.doi.org/10.15666/aeer/2005_41094119

Table 1. *Demographic features of informants*

Indicator		Number of informants	Percentage (%)
Gender	Male	31	37.35
	Female	52	62.65
Educational level	Elementary school	6	7.23
	Secondary school	24	28.92
	High school	43	51.81
	University	10	12.05
Age groups	30-40	19	22.89
	41-50	33	39.76
	> 50	31	37.35

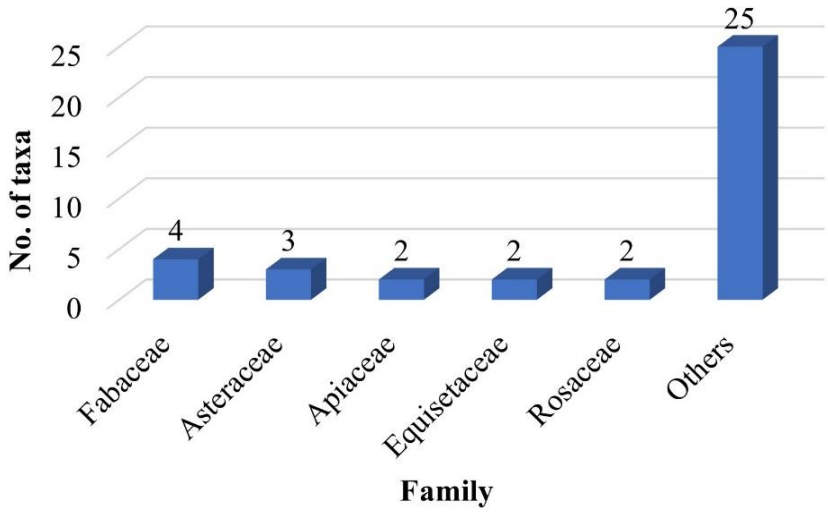

Figure 2. *The most frequently used plant families*

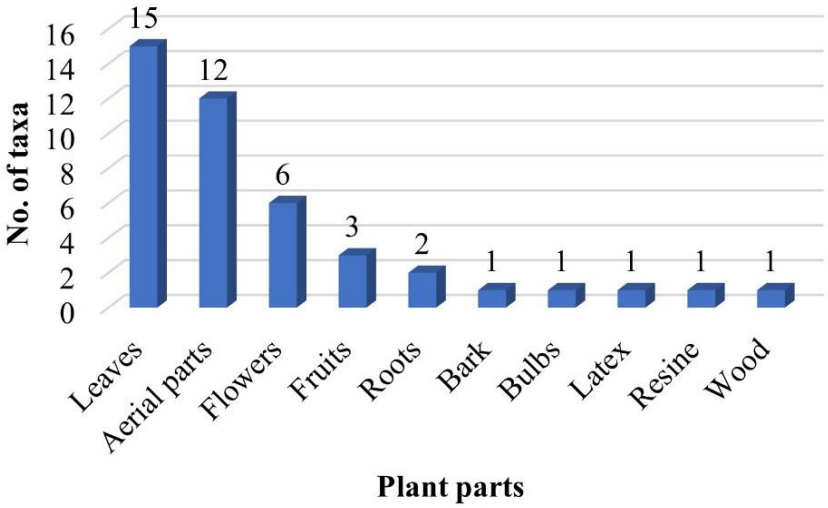

Figure 3. *Plant parts used*

http://www.aloki.hu ● ISSN 1589 1623 (Print) ● ISSN 1785 0037 (Online)
DOI: http://dx.doi.org/10.15666/aeer/2005_41094119

Table 2. *Ethnoveterinary uses of plant taxa in Rize (Türkiye)*

Scientific name	Family	Vernacular name	Parts used	Preparation	Route	Ethnoveterinary uses/therapeutic effect
Sambucus ebulus L.	Adoxaceae	Livor	Aerial parts	Decoction	Dermal	External parasites
Chenopodium polyspermum L.	Amaranthaceae	Sirken, Düdülü otu	Aerial parts	Fresh (fodder)	Oral	Increasing milk secretion
Allium sativum L.	Amaryllidaceae	Sarımsak	Bulb	Fresh	Dermal	Wound healing
				Cooking	Oral	Abdominal distension
Rhus coriaria L.	Anacardiaceae	Sumak	Fruits	Decoction	Dermal	Wound healing
Ferula szowitziana DC.	Apiaeae	Çakşır	Roots (dried)	Powder	Oral	Muscle pain (The powder is added to the water the animal will drink.)
Sanicula europaea L.	Apiaceae	Kadra	Aerial parts	Dried (fodder)	Oral	Boosting the immune system (for chicks)
Hedera helix L.	Araliaceae	Sarmaşık	Leaves	Decoction	Oral	Wound healing
Achillea millefolium L.	Asteraceae	Mayasıl otu	Leaves, flowers	Crushing	Dermal	Wound healing (for cat and dog)
Helichrysum plicatum DC.	Asteraceae	Altınotu, İspir çiçeği	Flowers	Decoction	Dermal	Wound healing
Solidago virgaurea L.	Asteraceae	Altınbaşak	Leaves (dried)	Powder	Oral	Burn wounds
Anchusa azurea Mill.	Boraginaceae	Sığırotu, Goriz	Leaves	Fresh	Oral	Poisoning
Bryum schleicheri Schwägr.	Bryaceae	Yosun	Leaves	Decoction	Oral	Sore mouth
Cannabis sativa L.	Cannabaceae	Kenevir	Leaves	Set on fire (dried)	Dermal	Varroa
Colchicum speciosum Steven	Colchicaceae	Göçkovan	Flowers	Decoction	Dermal	Cleaning cow udders
Juniperus communis L.	Cupressaceae	Ardıç	Bark	Set on fire	Dermal	Varroa
Datisca cannabina L.	Datiscaceae	Renkotu	Aerial parts	Set on fire (dried)	Dermal	Varroa
Equisetum arvense L.	Equisetaceae	Atkuyruğu	Aerial parts	Crushing	Dermal	Wound healing
Equisetum fluviatile L.	Equisetaceae	Atkuyruğu	Aerial parts	Crushing	Dermal	Wound healing
Euphorbia djimilensis Boiss.	Euphorbiaceae	Sütleğen	Aerial parts	Fresh	Oral	Snake poisoning (for goat)
Astracantha microcephala (Willd.) Podlech	Fabaceae	Geven	Leaves, roots	Decoction	Oral	Increasing milk secretion
				Poultice	Dermal	Swollen leg and foot
Medicago sativa L.	Fabaceae	Yonca	Aerial parts	Fresh (fodder)	Oral	Increasing milk secretion
Onobrychis viciifolia Scop.	Fabaceae	Korunga, Alapur	Aerial parts	Decoction	Oral	Increasing milk secretion
				Dried	Oral	Antitussive
Trifolium pratense L.	Fabaceae	Yonca	Leaves	Fresh (fodder)	Oral	Increasing milk secretion
				Poultice	Dermal	Wound healing
Populus tremula L.	Fagaceae	Kavak, Çençi	Wood	Wooden ash	Oral	Fungal infection (on the face of cattle)
Hypericum perforatum L.	Hypericaceae	Kantaron	Flowers	Centaury oil	Dermal	Wound healing, burn wound
Rosmarinus officinalis L.	Lamiaceae	Biberiye	Aerial parts	Crushing	Dermal	Cleaning up fleas
Malva sylvestris L.	Malvaceae	Ebegümeci	Leaves	Crushing	Dermal	Wound healing
Ficus carica L.	Moraceae	İncir	Latex	Fresh	Dermal	Warts (on cow udder)
Epilobium angustifolium L.	Onagraceae	Yakıotu	Leaves	Decoction	Dermal	Wound healing
				Crushing	Dermal	Wound healing, hemostasis
Picea orientalis (L.) Peterm.	Pinaceae	Karaçam	Resine	Cooking	Dermal	Wound healing (with olive oil)
Plantago major L.	Plantaginaceae	Çıbanotu, Damarotu	Leaves	Fresh	Oral	Antitussive, diarrhea
Triticum aestivum L.	Poaceae	Buğday	Leaves Fruits	Crushing	Oral	Antitussive
				Grind	Oral	Increasing egg production in chickens

http://www.aloki.hu ● ISSN 1589 1623 (Print) ● ISSN 1785 0037 (Online)
DOI: http://dx.doi.org/10.15666/aeer/2005_41094119

Adiantum capillus-veneris L.	Pteridaceae	Baldırıkara	Leaves	Poultice	Oral	Increasing milk secretion
					Dermal	Sprains and swelling
Caltha palustris L.	Ranunculaceae	Gongoros	Aerial parts	Decoction	Dermal	Foot pain
Alchemilla sericea Willd.	Rosaceae	Kapara otu, Tifilica	Leaves, flowers	Dried (fodder)	Oral	Antitussive (for horses)
Alchemilla speciosa Buser	Rosaceae	Kapara otu, Tifilica	Leaves, flowers	Dried (fodder)	Oral	Antitussive (for horses)
Viscum album subsp. *austriacum* (Wiesb.) Vollm.	Santalaceae	Çabu	Fruits	Crushing	Dermal	Wound healing
Urtica dioica L.	Urticaceae	Sığran, Erengiç	Aerial parts	Dried	Oral	Enterozoa
				Cooking	Oral	Eclampsia

The decoction was the most preparation method in traditional remedies (10 taxa), followed by fresh (8 taxa), crushing (7 taxa), and dried (7 taxa) (*Fig. 4*). Two routes of administration, dermal and oral, were used in the treatments. Both were equally cited.

Ethnoveterinary data were collected in 8 main categories in the FIC evaluation. In the current study, the FIC value ranged from 0.67 to 0.93 (*Table 3*). The medicinal plants are mostly used for skin diseases and wound healing, followed by digestive system diseases, milk production, and respiratory system diseases. Digestive system diseases have the highest FIC value (0.93). Skin diseases have the second-highest FIC value (0.88), milk production has the 3rd highest FIC value (0.85). The lowest FIC value with 0.67 corresponds to internal system diseases.

Table 3. *Informant consensus factor (FIC) for each disease category*

Disease categories	Diseases	Nt	Nur	FIC
Digestive system diseases	Enterozoa, diarrhea, stomach ailments, dyspepsia	3	30	0.93
Skin diseases	External parasites, skin inflammation, flea, varroa	9	66	0.88
Milk production	Milk production	5	27	0.85
Respiratory system diseases	Cough	4	18	0.82
Wound healing	Wound, burn, fungus, tomies	14	65	080
Poisonings	Poisonings	2	5	0.75
Orthopedics and traumatology	Sprains and strains, mouse, foot pain, muscle pain	4	12	0.73
Internal system diseases	Eclampsia, tonic	2	4	0.67

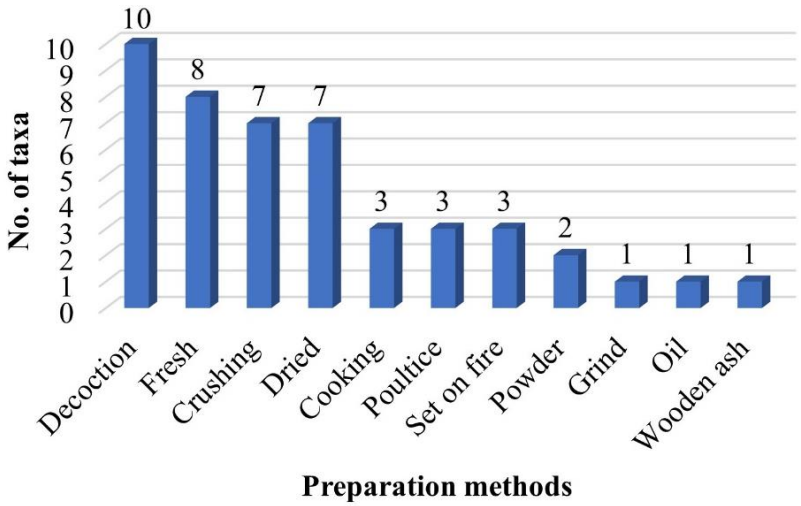

Figure 4. *Usage preferences in traditional remedies*

http://www.aloki.hu ● ISSN 1589 1623 (Print) ● ISSN 1785 0037 (Online)
DOI: http://dx.doi.org/10.15666/aeer/2005_41094119

An evaluation had made of the FL values of the cited plants. These values were found for the six most frequently cited plants, and their ranks ranged from 47.8 to 100 (*Table 4*). High FL was *Datisca cannabina* for varroa, *Malva sylvestris* for wound healing, and *Sambucus ebulus* for external parasite (respectively 100%).

Table 4. *Fidelity level (FL) index for the most cited medicinal plants*

Scientific name	Disease	Ip	Iu	FL value (%)
Datisca cannabina L.	Varroa	15	15	100
Malva sylvestris L.	Wound healing	11	11	100
Sambucus ebulus L.	External parasite	16	16	100
Hypericum perforatum L.	Wound healing	18	26	69.2
Allium sativum L.	Wound healing	8	13	61.5
Plantago major L.	Cough	12	23	52.2
Plantago major L.	Diarrhea	11	23	47.8

Discussion

In the current study, locals used mostly the leaves for treatment. Similarly, it was reported that leaves were the most preferred plant part in ethnobiology studies, especially in ethnoveterinary medicine in Türkiye (Erarslan and Kültür, 2019). Difference from those, aerial parts took place in the first place in the study conducted in Trabzon, which is adjacent to the research area (Akbulut, 2022).

The decoction was the most frequently used method for treatment in the study area that was like the various research from Northeast and Eastern Anatolia (Güler et al., 2021; Akbulut, 2022; Babacan et al., 2022). In the studies carried out in Central Anatolia and the Mediterranean, different preparation methods took the first place (Yaşar et al., 2015; Sinmez and Aslım, 2017; Yıpel et al., 2017; Sinmez et al., 2018).

Ethnoveterinary uses of *Datisca cannabina, Caltha palustris, Bryum schleicheri, Adiantum capillus-veneris, Solidago virgaurea* were recorded for the first time in Türkiye. Different usage areas of *Populus tremula, Astracantha microcephala, Cannabis sativa, Juniperus communis* were reported.

Beekeeping is so common and is a significant source of income in the region. Various measures are taken for varroa disease, which is effective in honey yield. The "set on fire" method, which is applied using various plants to protect bees from varroa disease, has not been included in the records before. In this method, especially *Datisca cannabina*, *Cannabis sativa*, and *Juniperus communis* are fired and the bees are exposed to smoke.

The majority of recorded plants are in general use for the treatment of all animals. Some plant species are used specifically to treat animals in different categories, as in beekeeping. The main groups and the plants used in the treatment resume in *Table 5*.

Some studies have shown that *Adiantum capillus-veneris* extract has been used on animals in clinical studies (Yadegari et al., 2019). It was reported that *Adiantum capillus-veneris* was used for increasing milk secretion, sprains, and swelling. The use of the plant in our study area was different from the world and it was reported that it was used for diarrhea and birth (Benítez et al., 2012; Shoaib et al., 2021). It was recorded that different species of *Adiantum* were used for different purposes such as skin diseases (Prakash et al., 2021) and abdominal pain (Abbasi et al., 2013).

http://www.aloki.hu ● ISSN 1589 1623 (Print) ● ISSN 1785 0037 (Online)
DOI: http://dx.doi.org/10.15666/aeer/2005_41094119

Table 5. *Main animal groups and plants used in their treatment*

Main groups	Plants used especially and diseases
Cattle-raising	*Colchicum speciosum* - Cleaning cow udders *Populus tremula* - Fungal infection *Ficus carica* - Warts
Sheep and goat breeding	*Euphorbia djimilensis* - Snake poisoning
Poultry farming	*Sanicula europaea* - Boosting the immune system *Triticum aestivum* - Increasing egg production
Odd-toed ungulates	*Alchemilla sericea* - Antitussive *Alchemilla speciose* - Antitussive
Domestic animals	*Achillea millefolium* - Wound healing
Beekeeping	*Datisca cannabina* - Varroa *Cannabis sativa* - Varroa *Juniperus communis* - Varroa

In the research area, it was recorded that the aerial parts of *Caltha palustris* were used in the treatment of foot pain. Extracts from this plant are known to have immunomodulatory properties (Suszko et al., 2012). The plant was reported to be used in skin diseases in China (Shen et al., 2010) and the treatment of worm-infested wounds and broken horns in India (Pande et al., 2007). With this study, the use of the plant for foot pain has also been added to the world literature.

Bryum schleicheri is a species from the bryophyte flora of the region. The plant, a type of moss, was recorded for the first time in ethnoveterinary folk medicine in Türkiye and the world. The decoction prepared from the leaves is given to animals for treatment of mouth sores.

Solidago virgaurea was included in the list of folk medicine for the first time in Türkiye and the world as a species used in the treatment of burns. The use of the plant for different purposes has been reported in the literature, such as antitoxic and abscess (Pande et al., 2007; Carrió et al., 2012). It has already been reported that the active ingredients of *Solidago virgaurea* are used in veterinary homeopathy in clinical signs (EMEA, 2000). Ajaib et al. (2021) stated in their study in Pakistan that *Solidago lacustralis* was used for ethnobotanical purposes in the treatment of burns in human medicine.

High FIC values document the use of herbs by many informants to treat a particular disease (Heinrich et al., 1998). In the current study, the highest FIC value of 0.93 belongs to digestive system diseases. In similar studies from Türkiye, the FIC value of dermatological ailments is generally higher (Erarslan and Kültür, 2019; Güler et al., 2021; Akbulut, 2022). In other countries, different disease groups come to the fore in high FIC values. It has the highest FIC values for respiratory disorders in China (Xiong and Long, 2020), gastrointestinal diseases in Lebanon (Arnold-Apostolides et al., 2020), dermatological and gastrointestinal diseases in Pakistan (Ahmad et al., 2015; Sharma and Manhas, 2015), and digestion in Indonesia (Pratama et al., 2021).

Plants with high FL are more preferred by local people compared to plants in the same category. High FL values have *Sambucus ebulus* for parasites and *Malva sylvestris* for wounds in the current study. It was also similar using methods and diseases in the various research from Türkiye and the world (Akerreta et al., 2010; Yıpel et al., 2017; Güler et al., 2021; Pascual and Herrero, 2021; Akbulut, 2022). *Datisca cannabina* has been accepted as the species used in traditional treatment methods for varroa disease in beekeeping.

http://www.aloki.hu ● ISSN 1589 1623 (Print) ● ISSN 1785 0037 (Online)
DOI: http://dx.doi.org/10.15666/aeer/2005_41094119

Conclusion

Traditional treatment methods are significant for livestock activities in mountainous terrains and rural areas. It has been determined that the local people dealing with animal diseases in Rize province use 38 plants in ethnoveterinary practices. Each study adds new plants used in treatment to the literature. In this study, it was determined that *Datisca cannabina, Caltha palustris, Bryum schleicheri, Adiantum capillus-veneris, Solidago virgaurea* species were used in the treatment of diseases. It is thought that such determinations can be a source for medical and veterinary research.

Acknowledgments. The authors thank Rize locals and informants for their contributions to the study.

REFERENCES

[1] Abbasi, A. M., Khan, S. M., Ahmad, M., Khan, M. A., Quave, C. L., Pieroni, A. (2013): Botanical ethnoveterinary therapies in three districts of the Lesser Himalayas of Pakistan. – Journal of Ethnobiology and Ethnomedicine 9: 84.

[2] Ahmad, K., Ahmad, M., Weckerlec, C. (2015): Ethnoveterinary medicinal plant knowledge and practice among the tribal communities of Thakht-e-Sulaiman hills, West Pakistan. – Journal of Ethnopharmacology 170: 275-283.

[3] Ajaib, M., Ishtiaq, M., Bhatti, K. H., Hussain, I., Maqbool, M., Hussain, T., Mushtaq, W., Ghani, A., Azem, M., Khan, S. M. R., Thind, S., Bashir, R. (2021): Inventorization of traditional ethnobotanical uses of wild plants of Dawarian and Ratti Gali areas of District Neelum, Azad Jammu and Kashmir Pakistan. – PLoS One 16(7): e0255010.

[4] Akbulut, S. (2022): An ethnoveterinary study on therapeutic plants used for livestock ailments in the province of Trabzon (Turkey). – Fresenius Environmental Bulletin 31(2): 2276-2284.

[5] Akerreta, S., Calvo, M. I., Cavero, R. Y. (2010): Ethnoveterinary knowledge in Navarra (Iberian Peninsula). – Journal of Ethnopharmacology 130: 369-378.

[6] Andrade-Cetto, A. (2009): Ethnobotanical study of the medicinal plants from Tlanchinol, Hidalgo, Mexico. – Journal of Ethnopharmacology 122: 163-171.

[7] Arnold-Apostolides, N., Nasser, H., Baydoun, S. (2020): Medicinal plants and traditional ethnoveterinary practices by rural community of Lebanon. – Acta Horticulturae 1287: 93-102.

[8] Babacan, E. Y., Polat, R., Güler, O., Moyan, A., Paksoy, M. Y., Çakılcıoğlu, U. (2022): An ethno-veterinary study on plants used for the treatment of livestock diseases in Genç (Bingöl-Turkey). – Indian Journal of Traditional Knowledge 21(1): 81-88.

[9] Benítez, G., González-Tejero, M. R., Molero-Mesa, J. (2012): Knowledge of ethnoveterinary medicine in the province of Granada, Andalusia, Spain. – Journal of Ethnopharmacology 139: 429-439.

[10] Carrió, E., Rigat, M., Garnatje, T., Mayans, M., Parada, M., Vallés, J. (2012): Plant ethnoveterinary practices in two Pyrenean territories of Catalonia (Iberian Peninsula) and in two areas of the Balearic Islands and comparison with ethnobotanical uses in human medicine. – Evidence-Based Complementary and Alternative Medicine 896295.

[11] Davis, P. H. (1965): Flora of Turkey and the East Aegean Islands. Vol. 1. – Edinburgh University Press, Edinburg.

[12] Davis, P. H. (1965-1985): Flora of Turkey and the East Aegean Islands. Vol. 1-9. – Edinburgh University Press, Edinburg.

[13] Davis, P. H., Mill, R. R., Tan, K. (1988): Flora of Turkey and the East Aegean Islands. Vol. 10. – Edinburgh University Press, Edinburg.

http://www.aloki.hu ● ISSN 1589 1623 (Print) ● ISSN 1785 0037 (Online)
DOI: http://dx.doi.org/10.15666/aeer/2005_41094119

[14] EMEA (2000): Committee for veterinary medicinal products: Solidago virgaurea, summary report. – The European Agency for the Evaluation of Medicinal Products Veterinary Medicines Evaluation Unit. chrome-extension://efaidnbmnnnibpcajpcglclefindmkaj/https://www.ema.europa.eu/en/documents/mrl-report/solidago-virgaurea-summary-report-committee-veterinary-medicinal-products_en.pdf, (Accessed date: 26.06.2022).
[15] Erarslan, Z. B., Kültür, Ş. (2019): Ethnoveterinary medicine in Turkey: a comprehensive review. – Turkish Journal of Veterinary and Animal Sciences 43: 555-582.
[16] Friedman, J., Yaniv, Z., Dafni, A., Palewitch, D. (1986): A preliminary classification of the healing potential of medicinal plants, based on a rational analysis of an ethnopharmacological field survey among Bedouins in the Negev Desert, Israel. – Journal of Ethnopharmacology 16(2-3): 275-287.
[17] Güler, O., Polat, R., Karaköse, M., Çakılcıoğlu, U., Akbulut, S. (2021): An ethnoveterinary study on plants used for the treatment of livestock diseases in the province of Giresun (Turkey). – South African Journal of Botany 142: 53-62.
[18] Güner, A., Vural, M., Sorkun, K. (1987): Rize flora, vegetation and pollen analysis of local honey. – TÜBİTAK TBAG, Project No: 650, Ankara.
[19] Güner, A., Özhatay, N., Ekim, T., Başer, K. H. C. (2000): Flora of Turkey and the East Aegean Islands, Vol. 11. – Edinburgh University Press, Edinburg.
[20] Heinrich, M., Ankli, A., Frei, B., Weimann, C., Sticher, O. (1998): Medicinal plants in Mexico: healers' consensus and cultural importance. – Social Science and Medicine 47: 1859-1871.
[21] ISE (2008): International society of ethnobiology (ISE) code of ethics. – http://ethnobiology.net/code-of-ethics (accessed date: 22.03.2021).
[22] McCorkle, C. M. (1986): An introduction to ethnoveterinary research and development. – Journal of Ethnobiology 6(1): 129-149.
[23] Pande, P. C., Tiwari, L., Pande, H. C. (2007): Ethnoveterinary plants of Uttaranchal - A review. – Indian Journal of Traditional Knowledge 6(3): 444-458.
[24] Pascual, J. C., Herrero, B. (2021): Plants for veterinary use in the Montaña Palentina region (Palencia, Spain). – Journal of Medicinal Plants Research 15(2): 73-85.
[25] Prakash, P., Radha, P. P., Kumar, M., Pundir, A., Puri, S., Prakash, S., Kumari, N., Thakur, M., Rathour, S., Jamwal, R., Janjua, S., Ali, M., Bangar, S. P., Singh, C., Chandran, D., Rajalingam, S., Senapathy, M., Dhumal, S., Singh, S., Samota, M. K., Damale, R. D., Changan, S., Natta, S., Alblihed, M., El-kott, A. F., Abdel-Daim, M. M. (2021): Documentation of commonly used ethnoveterinary medicines from wild plants of the high mountains in Shimla district, Himachal Pradesh, India. – Horticulturae 7(10): 351.
[26] Pratama, A. M., Herawati, O., Nabila, A. N., Belinda, T. A., Wijayanti, A. (2021): Ethnoveterinary study of medicinal plants used for cattle treatment in Bojonegoro District, East Java, Indonesia. – Biodiversitas 22(10): 4236-4245.
[27] Sharma, R., Manhas, R. K. (2015): Ethnoveterinary plants for the treatment of camels in Shiwalik regions of Kathua district of Jammu & Kashmir, India. – Journal of Ethnopharmacology 169: 170-175.
[28] Shen, S., Qian, J., Ren, J. (2010): Ethnoveterinary plant remedies used by Nu people in NW Yunnan of China. – Journal of Ethnobiology and Ethnomedicine 6: 24.
[29] Shoaib, G., Shah, G. M., Shad, N., Dogan, Y., Siddique, Z., Shah, A. H., Farooq, M., Khan, K. R., Nedelcheva, A. (2021): Traditional practices of the ethnoveterinary plants in the Kaghan valley, Western Himalayas-Pakistan. – Revista de Biologia Tropical 69(1): 1-11.
[30] Sinmez, Ç. Ç., Aslım, G. (2017): An ethnoveterinary remedies used in the treatment of diseases of Aksaray Malaklısı shepherd dogs. – Erciyes University Faculty of Veterinary Medicine 14(3): 191-200.

http://www.aloki.hu ● ISSN 1589 1623 (Print) ● ISSN 1785 0037 (Online)
DOI: http://dx.doi.org/10.15666/aeer/2005_41094119

[31] Sinmez, Ç. Ç., Yaşar, A. (2017): The use of herbal drugs in organic animal production: the case of ethnoveterinary medicine in Central Anatolia region. – Turkish Journal of Agriculture - Food Science and Technology 5(13): 1690-1695.
[32] Sinmez, Ç. Ç., Aslım, G., Yaşar, A. (2018): An ethnoveterinary study on plants used in the treatment of dermatological diseases in Central Anatolia, Turkey. – Journal of Complementary Medicine Research 8(2): 71-84.
[33] Suszko, A., Szczypka, M., Lis, M., Kuduk-Jaworska, J., Obminska-Mrukowicz, B. (2012): Influence of polysaccharide fraction C isolated from Caltha palustris L. on T and B lymphocyte subsets in mice. – Central European Journal of Immunology 37(3): 193-199.
[34] TR Ministry of Agriculture and Forestry (2021): TR ministry of agriculture and forestry strategy development department agricultural investor advisory office Rize, agricultural investment guide. – chrome-extension://efaidnbmnnnibpcajpcglclefindmkaj/viewer.html?pdfurl=https%3A%2F%2Fwww.tarimorman.gov.tr%2FSGB%2FTARYAT%2FBelgeler%2Fil_yatirim_rehberleri%2Frize.pdf&clen=1126088 (accessed date: 10.11.2021).
[35] TR Ministry of Culture and Tourism (2021): Rize provincial directorate of culture, history. – https://rize.ktb.gov.tr/TR-55291/tarihce.html (accessed date: 10.11.2021).
[36] WFO (2021): World Flora Online. An online flora of all known plants. – http://www.worldfloraonline.org/ (accessed date: 12.12.2021).
[37] WHO (2021): General guidelines for methodologies in research and evaluation of traditional medicine. – World Health Organization, Geneva, Switzerland. https://apps.who.int/iris/handle/10665/66783, (accessed date: 10.11.2021).
[38] Xiong, Y., Long, C. (2020): An ethnoveterinary study on medicinal plants used by the Buyi people in Southwest Guizhou, China. – Journal of Ethnobiology and Ethnomedicine 16: 46.
[39] Yadegari, M., Sellami, M., Riahy, S., Mirdar, S., Hamidian, G., Saeidi, A., Abderrahman, A. B., Hackney, A. C., Zouhal, H. (2019): Supplementation of Adiantum capillus-veneris modulates alveolar apoptosis under hypoxia condition in Wistar Rats exposed to exercise. – Medicina 55: 401.
[40] Yaşar, A., Sinmez, Ç. Ç., Aslım, G. (2015): Ruminant parasitic diseases and treatment methods at folklore of Konya area in Central Anatolia region. – Kafkas Universitesi Veteriner Fakultesi Dergisi 21(1): 1-7.
[41] Yıpel, M., Yipel, F. A., Tekeli, I. O., Güzel, Y. (2017): Ethnoveterinary uses of medicinal plants in Mediterranean district, Turkey. – Revista de Chimie 68(2): 411-416.

http://www.aloki.hu ● ISSN 1589 1623 (Print) ● ISSN 1785 0037 (Online)
DOI: http://dx.doi.org/10.15666/aeer/2005_41094119

RESPONSES OF ROOT GROWTH AND FINE ROOT BIOMASS OF *ABIES GEORGEI* VAR. *SMITHII* SEEDLINGS OF DIFFERENT AGE LEVELS TO ENVIRONMENT IN SOUTHEAST TIBET

ZHANG, X. S. – LU, J.* – ZHOU, C. N. – ZHANG, M. – YU, D. S.

Institute of Tibet Plateau Ecology, Tibet Agricultural & Animal Husbandry University, Nyingchi, Tibet 860000, China

Key Laboratory of Forest Ecology in Tibet Plateau (Tibet Agricultural & Animal Husbandry University), Ministry of Education, Nyingchi, Tibet 860000, China

Linzhi National Forest Ecosystem Observation & Research Station of Tibet, Nyingchi, Tibet 860000, China

Key Laboratory of Alpine Vegetation Ecological Security in Tibet, Nyingchi, Tibet 86000, China

**Corresponding author*
e-mail: tibetlj@163.com

(Received 19th Apr 2022; accepted 11th Jul 2022)

Abstract. The root distribution of most plants at high elevations in the soil is vague because studying roots at different elevations is time consuming and methodologically challenging. The purpose of this study is to understand the growth characteristics of the seedling roots of different age groups of *Abies georgei* var. *smithii* along the elevation bands in Southeast Tibet, as well as the influence of environmental factors on the growth of seedling roots. In July 2021, the roots of seedlings of five age classes were collected from six elevation bands (3800, 3900, 4000, 4100, 4200, and 4300 m) on the western slope of Sejila Mountain in southeastern Tibet. Rhizosphere soil sampling and analysis were conducted to assess the influence of elevation on the distribution characteristics of seedling root growth and fine root biomass (FRB), and the correlations of these characteristics with various soil factors were studied. Results showed that no significant differences in root length and FRB were observed among different elevation bands ($p > 0.05$), but significant differences among different age groups were noted ($p < 0.05$). Root length and FRB remarkably increased with increasing age class. Ammonium nitrogen and particulate organic carbon were the main soil factors affecting the root growth of seedlings, and available phosphorus was the major contributor to the FRB. In summary, soil factors play an important role in *A. georgei* var. *Smithii* seedlings' root growth at high elevation areas.
Keywords: *root distribution, age level, elevation, soil properties, seedling*

Introduction

In the gradient study of plant adaptation to environmental characteristics, elevation gradient gradually replaced latitudinal gradient as the model template (Rahbek, 2005). Elevation and environmental changes related to elevation (climate, soil factors, etc.) can induce plants to produce corresponding traits, thus directly or indirectly controlling local ecosystem processes (Violle et al., 2007; Paillex et al., 2013). Studies have shown that the growth of species at high elevation is limited by climate severity and resource availability (Lomolino, 2010). Among them, soil nutrients, as important resources for plant growth and development, vary significantly at different elevations (Wilcox and Nichols, 2008). Consequently, elevation gradient is a suitable natural platform for exploring the effects of environmental factors on plant roots (Dunne et al., 2004; Malhiet al., 2010).

http://www.aloki.hu ● ISSN 1589 1623 (Print) ● ISSN 1785 0037 (Online)
DOI: http://dx.doi.org/10.15666/aeer/2005_41214143

As a part of the natural ecosystem, the root system not only participates in numerous ecological processes (Jackson et al., 1990; Eissenstat, 1992; Norby et al., 2000; Bardgett et al., 2014) but also provides various ecological benefits for the underground and above-ground environments (Thevathasan and Gordon, 2004; Jose, 2009; Ramachandran et al., 2009). Root distribution refers to the distribution and growth pattern of roots in soil, which can be divided into horizontal roots distribution and vertical roots distribution (Qi, 2020). Information on the distribution of plant roots is the basis for understanding the underground ecological processes of plants (Mandy et al., 2011). Because of the spatial heterogeneity of environmental factors at different scales, root distributions are largely influenced by environmental factors, such as topography, climate, and soil (Schenk and Jackson, 2005), and their response to environmental factors is plastic (Simpson et al., 2020; Gonzalez-Ollauri et al., 2021). Previous studies attempted to analyze the relationship between root distribution and environmental factors, and results showed that, compared with other factors, root distribution is mostly determined by soil factors and tree age (Chang et al., 2012; Zhang et al., 2018).

The underground biomass, including coarse and fine roots, is an important component of the total biomass of woodland ecosystems (Qi et al., 2019); by comparison, fine roots (diameter < 2 mm) play an important role in the dynamics of water, nutrients, and carbon in the ecosystem (Zhang et al., 2018). Therefore, temporal and spatial changes in fine root biomass (FRB) and its distribution patterns have been extensively studied (Ronald and Hendrick, 1993; Yuan and Chen, 2010; Li et al., 2019; Xu et al., 2019). The growth of fine roots is relatively independent of stem growth, and spatiotemporal changes in root growth largely depend on soil conditions (Makkonen and Helmisaari, 2001). Earlier studies revealed that the biomass of fine roots along elevation gradient is generally determined by soil temperature and humidity (Foster et al., 2020) and increases with tree age (Makkonen and Helmisaari, 2001). Previous research on plant root biomass in high-elevation areas in China mainly focused on the Loess Plateau, Inner Mongolia Plateau, and Qinghai-Tibet Plateau; studies on the FRB at a certain elevation have also been conducted (Qi et al., 2020; Ma et al., 2008; Wang et al., 2007). Unfortunately, changes in FRB with the elevation gradient and tree age have not been explored.

Studies have shown that both root distribution and root biomass belong to the category of root traits (Li et al., 2016; King, 2021). Although some researchers have found that root traits played an important role in competition dynamics and stress tolerance (Leger et al., 2019; Bristiel et al., 2019; Kramer-Walter et al., 2016; Markesteijn and Poorter, 2009), but so far, most studies just focused on aboveground. Until recently, studies have linked root traits to seedling establishment and survival. For example, changes in seedling root length explained most of the changes in seedling survival (Harrison and LaForgia, 2019) and were the best predictors of seedling survival in wild sites (Leger et al., 2019). Root mass ratio was correlated with seedling competitiveness (Ferguson et al., 2015; Leger and Goergen, 2017); There was a trade-off between root dry matter content and growth rate (Larson et al., 2020). Other studies have found that some characteristics of roots were closely related to soil nutrients and water content (Kramer-Walter et al., 2016; Bristiel et al., 2019; Hanslin et al., 2019). However, these studies did not pay attention to the effects of elevation, age grade and soil factors on root traits. Under the background of ecological security stress on the Qinghai-Tibet Plateau, it is urgent to study the effects of environment (elevation, soil and other factors) on plant survival and the ecological strategies of plants.

http://www.aloki.hu ● ISSN 1589 1623 (Print) ● ISSN 1785 0037 (Online)
DOI: http://dx.doi.org/10.15666/aeer/2005_41214143

Sejila Mountain in Southeast Tibet is well known for its extensive forest coverage and pivotal role as an ecological security barrier (Kato et al., 2006). The mountain coverage is mainly composed of dark coniferous forest, in which *Abies georgei* var. *smithii* is the dominant species. Research on the seedlings of *A. georgei* var. *smithii* in Sejila Mountain mainly focus on their spatial pattern and natural regeneration (Luo, 2010; Xie et al., 2015; Wang et al., 2018); however, the elevation distribution of the root growth of these seedlings and its relationship with soil factors remains unclear. Therefore, in this study, we selected different ages of *A. georgei* var. *smithii* seedlings to explore the growth and distribution characteristics of their root system along elevation bands, as well as their relationships with environmental factors. The results of this work will provide theoretical support and basic data for the protection of subalpine forest resources on the Qinghai–Tibet Plateau and boost the subalpine forest system play an excellent ecological security barrier function. The objectives of the present study were as follows: (i) investigate the distribution characteristics of horizontal root lengths (HRL), vertical root lengths(VRL), fine root biomass (FRB) of Abies georgei var. smithii seedlings along different elevations; (ii) investigate the variation of horizontal root lengths (HRL), vertical root lengths (VRL), fine root biomass (FRB) of Abies georgei var. smithii seedlings at different age levels; (iii) explore the individual effect and interaction of elevation and age level on root length and FRB; (iv) sort out the main soil influencing factors of root length and FRB.

Materials and methods

Study area

The study site is located in Sejila Mountain (93°12′–95°35′ E, 29°10′–30°15′ N) in Nyingchi City, Tibet Autonomous Region of China (*Fig. 1*). Sejila Mountain is close to the branch of the Yarlung Zangbo River (Niyang River basin), with an elevation of 2100–5300 m, and is part of the Nyenqing Tanggula mountain range (Zhou et al., 2015). This region is characterized by typical warm temperate and temperate mountain climates, with dry and wet seasons. The annual temperature ranges from −13.98 ℃ to 9.23 ℃, and the annual average temperature is −0.73 ℃ (Wang et al., 2019). Most of the rainfall occurs from June to September, and the precipitation could exceed 1000 mm, accounting for 80% of the total precipitation received by the area annually. The frost period is as long as 6 months, the total sunshine duration is as long as 1151 h, and the humidity is between 60% and 80% (Duan et al., 2020).

Sample collection

In July 2017, a 50 m × 50 m plot were established at elevations of 3800, 3900, 4000, 4100, 4200, and 4300 m. The plot was not connected to each other at different elevations, and a total of 6 plots were established. The basic information of plots at each elevation are shown in *Table 1*.

The whole excavation method (Williams et al., 2019) was used to collect all seedlings of *A. georgei* var. *smithii* in each plot. The collected seedlings were divided into five age grades: 1–2 years old, 3–4 years old, 5–6 years old, 7–8 years old, and 9–10 years old; here, 5 seedlings of each age grade were collected from each plot. Seedling age was determined by branch color, lenticels, and bud scale marks (Parent et al., 2003). The age of the seedlings was determined according to the following method. Starting from the top

http://www.aloki.hu ● ISSN 1589 1623 (Print) ● ISSN 1785 0037 (Online)
DOI: http://dx.doi.org/10.15666/aeer/2005_41214143

of the branches and extending to the base of the seedlings, the branches of the current year can be identified as the 1-year-old branches; then downwards, according to the bud scale marks and the color of the branches, 2-10 years old branches were determined. At last, the number of annual rings at the base of the branches were used to verify the age levels (Deng et al., 2018). During excavation, roots were gently dipped along the lateral root extension direction by using tools such as a spatula and brush until the end of the root system was obtained. This method could help avoid measurement errors due to the interference of other plants' roots and seedling root damage.

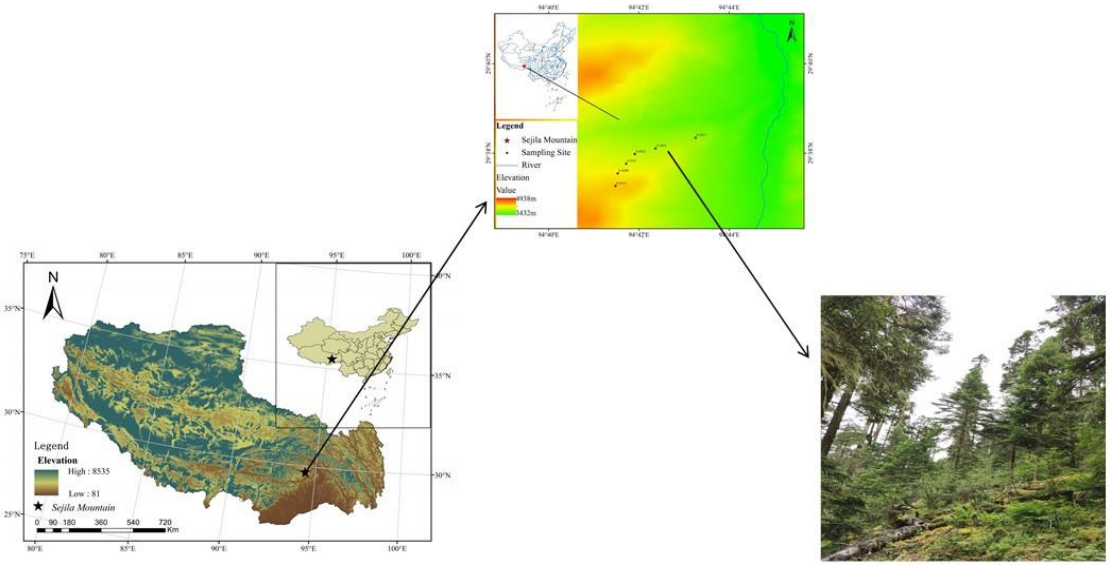

Figure 1. *Study area, sampling sites and habitats*

At the same time of root collection, soil near seedling roots was also collected, and three soil samples (100–300 g) were collected from each plot (a total of 18 soil samples). The soil profile near the seedling root was dug, and three samples of 0–20 cm of undisturbed soil was collected with cutting ring (100 cm^3) from each plot (a total of 18 cutting ring samples). The collected soil samples were stored in plastic bags at a low temperature and promptly sent to the laboratory for processing. Soil temperature (ST) were measured by a portable soil hygrograph (KM-WSD01, Jingmai Instruments Inc, China). Please refer to *Table A1* in the supplementary document for soil index data.

Table 1. *Basic situation of the sample site*

Elevation (m)	Longitude (°E)	Latitude (°N)	Slope angle (°)	Slope aspect	Average coverage	Average crown density	Main species
3837	94.7212	29.6432	24	South	0.91 ± 0.03	0.61 ± 0.02	*LoniceraInconspicua;* *Abies georgei var. smithii*
3953	94.7142	29.6413	36	South	0.78 ± 0.02	0.67 ± 0.02	*LoniceraInconspicua;* *Abies georgei var. smithii*
4021	94.7105	29.6403	39	South	0.95 ± 0.02	0.51 ± 0.02	Bryophyte; *Abies georgei var. smithii*
4111	94.7090	29.6385	36	South	0.87 ± 0.02	0.45 ± 0.04	Bryophyte; *Abies georgei var. smithii*
4206	94.7074	29.6369	36	South	0.93 ± 0.03	0.65 ± 0.04	*Rhododendron pingianum* Fan; *Abies georgei var. smithii*
4333	94.7071	29.6346	28	South	0.71 ± 0.03	0.41 ± 0.02	*Rhododendron pingianum* Fan; *Abies georgei var. smithii*

http://www.aloki.hu ● ISSN 1589 1623 (Print) ● ISSN 1785 0037 (Online)
DOI: http://dx.doi.org/10.15666/aeer/2005_41214143

Index measurements

The collected seedlings were divided into above- and underground parts, and the plant height, aboveground diameter, horizontal root length (HRL), and vertical root length (VRL) of underground parts were measured. When measuring underground parts, the root system was gently shaken to dislodge the soil adhered to the roots. The remaining soil attached to the root surface was flushed with distilled water to maintain the natural growth condition of the root system. The roots were then spread on clean filter paper to absorb the excess water. A Vernier caliper was used to measure HRL and VRL. Here, HRL was defined as the horizontal spread of roots and VRL was defined as the vertical extension of roots. After HRL and VRL were measured, the root samples were scanned by the WinRHIZO Root Analysis System (WinRHIZO TRON 2009, Regent Instruments Inc., Canada) to analyze the average length and diameter of fine roots and other indicators. After scanning, fine roots were separated from taproots according to the criteria fine roots: diameter < 2 mm and thick roots: diameter ≥ 2 mm (Qi et al., 2020). The separated fine roots were placed in an envelope, dried in the oven at 80 °C to a constant weight, and then weighed (dry weight, g). The characteristics of seedlings of different age groups are shown in *Table 2*.

The physical and chemical properties of the soil samples were determined after air drying. After removing stones and visible plant roots, the soil samples were passed through a 0.25 mm screen. Soil water content (SWC) was measured by the drying method (Chang et al., 2012). Total organic carbon (TOC) was determined by the dry combustion method at 500 °C (Storer et al., 1984). Total nitrogen (TN) and total phosphorus (TP) were determined by the Kjeldahl and NaOH alkali fusion–molybdenum-antimony anti-colorimetric methods (Sparks et al., 1996), respectively. Total potassium (TK) and available potassium (AK) were determined by NaOH melt-flame photometry and 1 mol/L ammonium acetate extraction-flame photometry (Gammon, 1951), respectively. Available phosphorus (AP) was determined via an offline extraction column (Jakmunee and Junsomboon, 2009). Nitrate nitrogen (NO_3^--N) was determined by the phenol disulfonic acid colorimetry method (Haby, 1989). Ammonium nitrogen (NH_4^+-N) was extracted with 1.2 mol/L KCl via the indophenol blue colorimetric method (Dorich and Nelson, 1983). Particulate organic carbon (POC) was assayed according to the method of Garten et al. (1999). Easily oxidized organic carbon (EOC) was assessed according to the determination method of Chen et al. (2017). Dissolved organic carbon (DOC) was determined according to Fang et al. (2014).

Statistical analysis

The normality of the variances was tested using raw data via the Kolmogorov–Smirnov test ($p = 0.05$), and the homogeneity of these variances was tested using Levene's test ($p > 0.05$). These calculations were conducted using SPSS 26.0 (IBM, USA). One-way ANOVA and Tukey's HSD test were used to determine differences in statistical parameters (e.g., root distribution parameters and soil physical and chemical properties) across the root distributions and FRBs of seedlings at different elevations and ages ($p \leq 0.05$). In addition, we used two-factor ANOVA to analyze the effects of elevation, stand age and elevation × stand age on seedling root indexes. Statistical analyses (i.e., mean ± standard deviation) were conducted using Excel 2013 (Microsoft, USA) and SPSS 26.0. ((IBM Corp., Armonk, NY, United States)). All charts depicting

http://www.aloki.hu ● ISSN 1589 1623 (Print) ● ISSN 1785 0037 (Online)
DOI: http://dx.doi.org/10.15666/aeer/2005_41214143

variations in parameters were generated using Origin 2021 (OriginLab, Northampton, MA, USA). Redundancy analysis (RDA) was performed using Canoco 5.0 (Microcomputer Power, USA) to evaluate the effects of environmental factors on the root distributions and FRBs of different seedling age groups. Prior to RDA, the significance of the effect of each variable was assessed using a Monte Carlo permutation test.

Table 2. *Characteristics of Abies georgei var. smithii seedlings of different age levels*

Elevation (m)	Age groups	Average plant height (cm)	Mean ground diameter (mm)	Mean diameter of fine roots (mm)	Mean length of fine roots (cm)
3837	1-2	4.17 ± 1.33 Ba	0.57 ± 0.16 Ba	0.27 ± 0.09 Ba	0.46 ± 0.3 Ca
	3-4	4.53 ± 1.45 Bcd	0.64 ± 0.08 Bb	0.27 ± 0.02 Bbc	0.78 ± 0.09 Cbc
	5-6	10.87 ± 2.32 Aa	2.65 ± 0.73 Aa	0.67 ± 0.07 Aa	3.07 ± 1.39 Ba
	7-8	11.93 ± 3.7 Aa	2.53 ± 1.1 Aa	0.73 ± 0.12 Aa	3.44 ± 0.83 Bab
	9-10	16.53 ± 2.9 Aa	4.15 ± 0.79 Aa	0.84 ± 0.16 Aab	5.89 ± 0.45 Aa
3953	1-2	3.83 ± 0.49 Ca	0.63 ± 0.11 Ca	0.2 ± 0.13 Ba	0.31 ± 0.2 A a
	3-4	8.9 ± 1.75 ABCab	1.56 ± 0.56 BCa	0.42 ± 0.03 Aa	2.19 ± 0.92 Aa
	5-6	7.33 ± 1.92 BCa	2.21 ± 0.39 BCa	0.44 ± 0.04 Ab	1.19 ± 0.75 Aa
	7-8	11.2 ± 2.5 ABa	2.88 ± 0.52 ABa	0.43 ± 0.09 Aab	1.17 ± 0.19 Ab
	9-10	14.63 ± 3.67 Aa	4.54 ± 1.6 Aa	0.53 ± 0.04 Ab	5.18 ± 4.57 Aa
4021	1-2	2.12 ± 0.32 Ca	0.56 ± 0.03 Ba	0.2 ± 0.06 Da	0.44 ± 0.43 Ba
	3-4	3.86 ± 0.55 BCd	0.66 ± 0.11 Bb	0.22 ± 0.04 CDc	0.32 ± 0.16 Bc
	5-6	10.1 ± 2.1 ABCa	1.79 ± 0.96 Ba	0.37 ± 0.04 BCb	1.98 ± 0.76 ABa
	7-8	10.93 ± 1.94 ABa	3.07 ± 0.58 ABa	0.44 ± 0.1 ABab	2.74 ± 1.3 ABab
	9-10	17.97 ± 6.52 Aa	4.61 ± 1.9 Aa	0.57 ± 0.04 Aab	4.8 ± 2.23 Aa
4111	1-2	4.1 ± 0.78 Ca	0.79 ± 0.03 Ca	0.18 ± 0.06 Ba	0.49 ± 0.08 Ba
	3-4	10.4 ± 0.56 AaB	1.87 ± 0.23 BCa	0.35 ± 0.07 ABab	1.85 ± 0.13ABab
	5-6	8.93 ± 0.81 Ba	2.35 ± 0.19 BCa	0.33 ± 0.05 ABb	1.91 ± 1.11 ABa
	7-8	10.6 ± 1.93 ABa	3.2 ± 0.77 Ba	0.33 ± 0.06 ABb	2 ± 1.04 ABab
	9-10	14.47 ± 2.5 Aa	5.54 ± 1.01 Aa	0.5 ± 0.08 Ab	3.18 ± 1.19 Aa
4206	1-2	3.73 ± 0.72 Ca	0.65 ± 0.13 Da	0.23 ± 0.02ABCa	0.32 ± 0.1 Cabc
	3-4	7 ± 0.53 BCbc	1.54 ± 0.27 CDa	0.22 ± 0.04 BCc	1.53 ± 0.17 BCa
	5-6	10.13 ± 0.81 BCa	2.15 ± 0.63Ca	0.16 ± 0.04 Cc	1.78 ± 1.15 BCa
	7-8	11.7 ± 3.91 ABa	3.19 ± 0.14Ba	0.51 ± 0.24 ABab	4.49 ± 1.2 Aa
	9-10	18.8 ± 5.11 Aa	4.73 ± 0.26Aa	0.53 ± 0.07 Ab	2.74 ± 0.42 ABa
4333	1-2	4.2 ± 1.22 Ca	0.89 ± 0.36Ca	0.38 ± 0.03 Ba	0.62 ± 0.61 Aa
	3-4	9.4 ± 1.01 Bab	1.72 ± 0.32Ca	0.42 ± 0.04 Ba	1.25 ± 0.76Aabc
	5-6	9.27 ± 1.25 Ba	1.75 ± 0.38Ca	0.33 ± 0.07 Bb	2.32 ± 0.87 Aa
	7-8	13.17 ± 3.52 ABa	3.67 ± 0.3Ba	0.63 ± 0.04 ABab	3.08 ± 1.69 Aab
	9-10	15.1 ± 0.78 Aa	4.74 ± 0.52Aa	1.07 ± 0.41 Aa	6.32 ± 5.04 Aa

Different capital letters indicate significant differences among seedlings of different age groups at the same elevation *($p < 0.05$).* Different lowercase letters indicate significant differences among seedlings of the same age group at different elevations *($p < 0.05$)*

http://www.aloki.hu ● ISSN 1589 1623 (Print) ● ISSN 1785 0037 (Online)
DOI: http://dx.doi.org/10.15666/aeer/2005_41214143

Results

Distribution characteristics of the horizontal and vertical root lengths of seedlings as a function of elevation

The average HRL of the five age grades of seedlings ranged from 0.83 ± 0.53 cm to 15.90 ± 7.19 cm (*Table A2*), but no significant difference in HRL was observed at all seedling age levels ($p > 0.05$) except at 3–4 years (*Fig. 2; Table A2*). The average VRL of the seedlings ranged from 2.66 ± 1.29 cm to 13.55 ± 4.99 cm (*Table A2*), and no significant difference among elevation bands was noted ($p > 0.05$; *Fig. 2; Table A2*). The HRL of seedlings growing at the same elevation significantly differed among the different age groups ($p < 0.05$). However, no significant difference in VRL between different age groups was observed at 4300 m ($p > 0.05$). Significant differences in VRL among different age groups were observed at the five other elevations ($p < 0.05$).

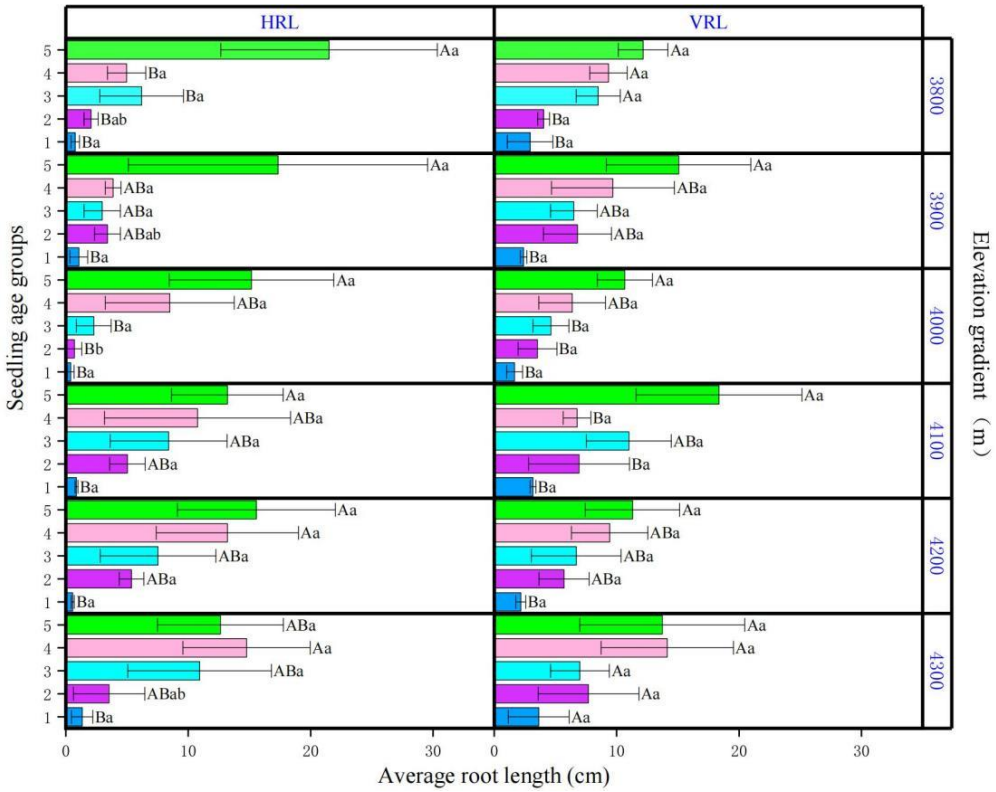

Figure 2. *Root distribution characteristics of seedlings of different age levels as a function of elevation. Error bars represent one SD (std. deviation). HRL: Horizontal root length; VRL: Vertical root length. 1: 1–2-year-old seedlings; 2: 3–4-year-old seedlings; 3: 5–6-year-old seedlings; 4: 7–8-year-old seedlings; 5: 9–10-year-old seedlings. Different capital letters indicate significant differences among seedlings of different age groups at the same elevation ($p < 0.05$). Different lowercase letters indicate significant differences among seedlings of the same age level at different elevations ($p < 0.05$)*

Distribution characteristics of the fine root biomass of seedlings of different age levels as a function elevation

The FRB of seedlings of different age levels ranged from 0.01 ± 0.01 g to 0.90 ± 0.53 g (*Table A2*). The FRB of 9–10-year-old seedlings at 4100 m was larger

http://www.aloki.hu ● ISSN 1589 1623 (Print) ● ISSN 1785 0037 (Online)
DOI: http://dx.doi.org/10.15666/aeer/2005_41214143

than the FRBs of all other seedling age levels. The FRB of the first four age grades (1–2 years, 3–4 years, 5–6 years, and 7–8 years) decreased with the elevation. Except for 3–4- and 5–6-year-old seedlings, no significant difference in FRB was observed among other age levels (1–2 years, 7–8 years, 9–10 years) as a function at the same elevation ($p > 0.05$) (*Fig. 3; Table A2*). At the same elevation, the FRB of 9–10-year-old seedlings was significantly higher than that of the four other age grades ($p < 0.05$).

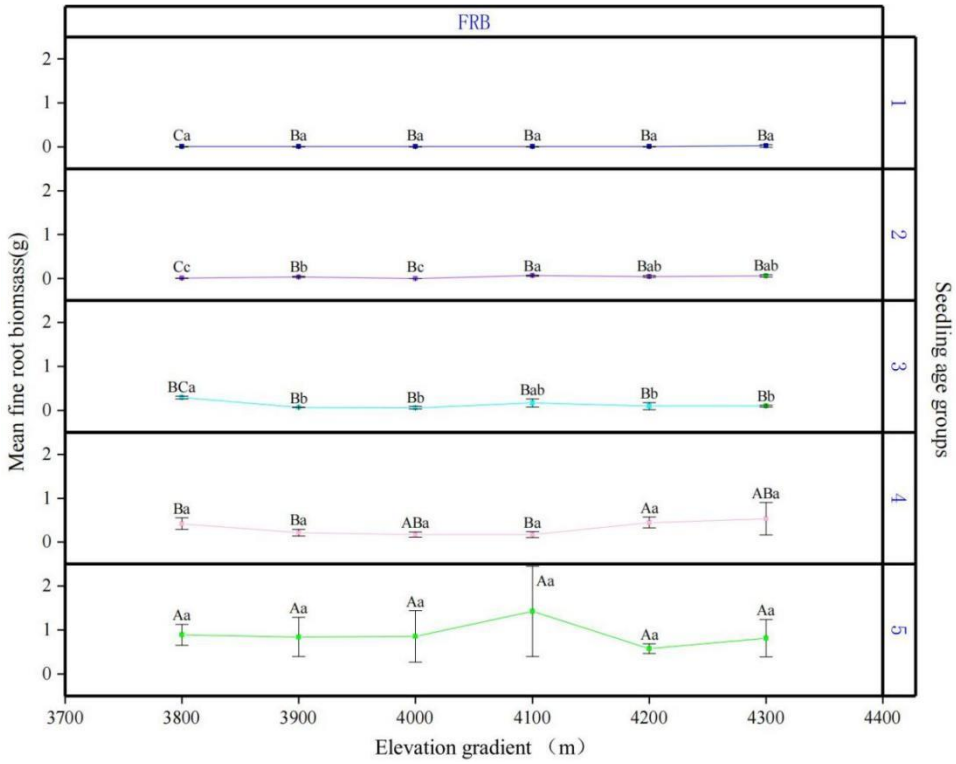

Figure 3. *Fine root biomass of seedlings of different age levels as function of elevation. Error bars represent one SD (std. deviation). FRB: Fine root biomass. 1: 1–2-year-old seedlings; 2: 3–4-year-old seedlings; 3: 5–6-year-old seedlings; 4: 7–8-year-old seedlings; 5: 9–10-year-old seedlings. Different capital letters indicate significant differences among seedlings of different age groups at the same elevation ($p < 0.05$). Different lowercase letters indicate significant differences among seedlings of the same age level at different elevations ($p < 0.05$)*

Effects of elevation and age level on the root length growth and FRB of Abies georgei var. smithii seedlings

HRLs decreased in the order of 4300 m > 4200 m > 4100 m > 3800 m > 3900 m > 4000 m; VRLs decreased in the order of 4100 m > 4300 m > 3900 m > 3800 m > 4200 m > 4000 m; and FRB decreased in the order of 4100 m > 3800 m > 4300 m > 3900 m > 4200 m > 4000 m. The HRL, VRL and FRB of *A. georgei* var. *smithii* seedlings were lowest at 4000 m and increased with increasing age level (*Table A2*). The results of two-factor ANOVA showed (*Table 3*) that elevation had no significant effect on HRL, VRL and FRB of *Abies georgei* var. *Smithii* seedlings ($p > 0.05$), while age groups had extremely significant effect on them ($p < 0.001$). The combined effect of elevation and age groups also showed no significant effect ($p > 0.05$). Regression analysis was conducted on the relationship

http://www.aloki.hu ● ISSN 1589 1623 (Print) ● ISSN 1785 0037 (Online)
DOI: http://dx.doi.org/10.15666/aeer/2005_41214143

between stand age and seedling root indexes (*Table 3*). The results showed that HRL, VRL and FRB at different elevations showed a binomial growth trend with the increase of forest age, and the regression equation had a high fitting degree. At different elevations, HRL, VRL and FRB were significantly correlated with stand age ($p < 0.05$).

Table 3. *Analysis of variance of HD, VD, FRB were performed on the Abies Georgei var. smithii seedlings, and linear regression analysis of root index and stand age of seedlings at different elevations*

ANOVA	**HRL**			**VRL**			**FRB**		
EL	0.551ns			1.344ns			0.297ns		
AL	27.443***			25.031***			36.159***		
EL x AL	1.252ns			0.905ns			1.049ns		
Residuals	22.021			10.814			0.06789		
Elevation/m	**Regression equation**	**R^2**	***p-value***	**Regression equation**	**R^2**	***p-value***	**Regression equation**	**R^2**	***p-value***
3837	y = 4.43x - 6.21	0.546	$P < 0.001$	y = 2.37x + 0.26	0.819	$p < 0.001$	y = 0.219x - 0.334	0.822	$p < 0.001$
3953	y = 3.30x - 4.17	0.348	$P < 0.05$	y = 2.82x - 0.37	0.556	$p < 0.001$	y = 0.185x - 0.324	0.552	$p < 0.01$
4021	y = 3.73x - 5.79	0.630	$p < 0.001$	y = 2.08x - 0.87	0.723	$p < 0.001$	y = 0.188x - 0.345	0.468	$p < 0.01$
4111	y = 3.04x - 1.46	0.533	$p < 0.01$	y = 3.02x + 0.17	0.453	$p < 0.01$	y = 0.295x - 0.520	0.409	$p < 0.05$
4206	y = 3.78x - 2.90	0.652	$p < 0.001$	y = 2.20x + 0.46	0.593	$p < 0.001$	y = 0.154x - 0.229	0.819	$p < 0.001$
4333	y = 3.38x - 1.51	0.530	$p < 0.01$	y = 2.66x + 1.25	0.425	$p < 0.01$	y = 0.205x - 0.312	0.601	$p < 0.001$

HRL: horizontal root length; VRL: vertical root length; FRB: fine root biomass; EL: elevation; AL: age level
***P < 0.001; **P < 0.01; *P < 0.05; ns: no significance

Effects of soil properties on the root growth and FRB of Abies georgei var. smithii seedlings

According to the results of the Monte Carlo permutation test, all soil factors (i.e., AP, AK, NH_4^+-N, NO_3^--N, TP, TK, TN, TOC, SWC, ST, EOC, DOC, POC) explained 83.2% of the variation in root length of seedlings of all age levels (HRL1, HRL2, HRL3, HRL4, HRL5, VRL1, VRL2, VRL3, VRL4, VRL4, and VRL5). The cumulative percentage of species–environment relationships between axes 1 and 2 was 65.14%, and Axis 1 accounted for 40.27% of the interpretation ratio, which means seedling root growth and soil factors are highly correlated and could well reflect the influence of dominant factors on seedling root growth (*Fig. 4A*). Among the 13 soil factors, NH_4^+-N and POC had the largest contribution value and significant influence on the root growth of seedlings ($P < 0.05$), indicating that NH4 + -N and POC were the main soil factors affecting the root growth of seedlings (*Table 4*).

According to the results of the Monte Carlo permutation test, all soil factors (i.e., AP, AK, NH_4^+-N, NO_3^--N, TP, TK, TN, TOC, SWC, ST, EOC, DOC, POC) explained 72.7% of the variation in FRB (FRB1, FRB2, FRB3, FRB4, and FRB5) of seedlings of all levels The cumulative percentage of species–environment relationships between axes 1 and 2 was 97.43%, and Axis 1 accounted for 86.48% of the interpretation ratio, which indicates that FRB is highly correlated with soil factors and could well reflect the influence of leading factors on seedling root growth (*Fig. 4B*). Among the 13 soil factors studied, AP contributed the most to FRB ($p < 0.05$), which indicates that AP is the main soil factor affecting the FRB of *A. georgei* var. *smithii* seedlings (*Table 4*).

http://www.aloki.hu ● ISSN 1589 1623 (Print) ● ISSN 1785 0037 (Online)
DOI: http://dx.doi.org/10.15666/aeer/2005_41214143

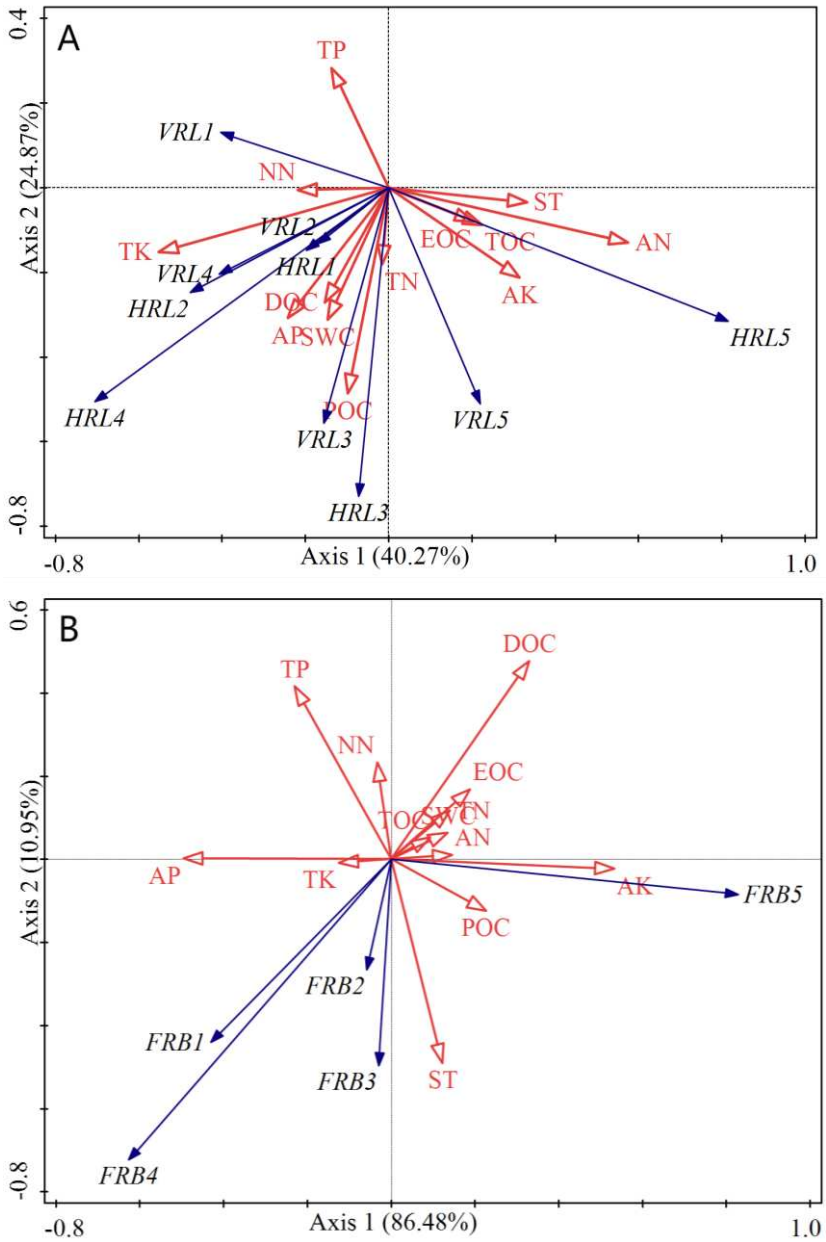

Figure 4. *Relationships between soil properties and root distributions. (A) RDA double sequence diagrams of HRL, VRL and soil factors at different ages; (B) RDA double sequence diagrams of FRB and soil factors at different ages. Red arrows: root indexes; Blue arrows: soil factors. HRL: Horizontal root length; VRL: Vertical root length; FRB: Fine root biomass. AN: NH_4^+-N; NN: NO_3^--N. 1: 1–2-year-old seedlings; 2: 3–4-year-old seedlings; 3: 5–6-year-old seedlings; 4: 7–8-year-old seedlings; 5: 9–10-year-old seedlings. ST: Soil temperature; SWC: Soil water content; TOC: Total organic carbon; TN: Total nitrogen; TP: Total phosphorus; TK: Total potassium; AK: available potassium; AP: Available phosphorus; NO_3^-–N: Nitrate nitrogen; NH_4^+–N: Ammonium nitrogen; POC: Particulate organic carbon; EOC: Easily oxidized organic carbon; DOC: Dissolved organic carbon*

The results of RDA (*Tables A3, A4,* and *A5*) showed that 13 soil factors have different effects on the HRL, VRL and FRB of *A. georgei* var. *smithii* seedlings at different age levels. The main soil factors affecting HRL were ST and AK (1–2 years);

http://www.aloki.hu ● ISSN 1589 1623 (Print) ● ISSN 1785 0037 (Online)
DOI: http://dx.doi.org/10.15666/aeer/2005_41214143

NO_3^--N (3–4 years); AP (5–6 years); TK and NO_3^-N (7–8 years); and NH_4^+-N and SWC (9–10 years). The main soil factors affecting the VRL of *A. georgei* var. *smithii* seedlings were NH_4^+-N (1–2 years); NO_3^--N, TK, and TP (3–4 years); TP (5–6 years); DOC (7–8 years); and ST and DOC (9–10 years). The main soil factors affecting FRB were TK, SWC, and NO_3^--N (1–2 years); TK (3–4 years); ST (5–6 years); TK and DOC (7–8 years); and AP (9–10 years). Figure 4 clearly shows the correlation between soil factors and root growth, FRB of seedlings of different age groups. As can be seen from *Figure 4A,* VRL1 were located in the upper left corner of the RDA plot and positively correlated with NO_3^--N (NN) and TP but negatively correlated with NH_4^+-N (AN) and AK. HRL1, HRL2, HRL3, HRL4, VRL2, VRL3 and VRL4 were located at the left end of RDA axis 1 and positively correlated with TK, SWC, POC, and AC. HRL5 and VRL5 were located at the lower right corner of the sequence diagram. NH_4^+-N (AN), AK, and TOC were positively correlated with HRL5 and VRL5, but negatively correlated with TP. *Figure 4B* shows that FRB1, FRB2, FRB3 and FRB4 are located at the left end of RDA axis 1, and are positively correlated with TK, AP and ST, but negatively correlated with DOC, TP and AK. FRB5 is located at the lower right corner of the sorting diagram, and is positively correlated with AK and POC, while negatively correlated with TK and AP.

Table 4. *Contribution rates and P values of soil factors to the RD and FRB of Abies georgei var. smithii seedlings*

RD			FRB		
Name	**Contribution %**	***p*-value**	**Name**	**Contribution %**	***p*-value**
POC	15	0.022	AP	28.5	0.034
NH_4^+-N	15	0.046	DOC	15	0.074
DOC	8	0.244	AK	24.7	0.086
ST	9.6	0.122	ST	5.3	0.334
TK	8.8	0.124	NO_3^--N	4.6	0.362
TP	6.8	0.262	TK	4.7	0.372
SWC	7.3	0.21	NH_4^+-N	1.2	0.73
AP	6.2	0.286	TN	3.8	0.462
EOC	3.2	0.706	SWC	2.4	0.606
TOC	6.5	0.3	POC	2.8	0.572
NO_3^--N	3.6	0.64	TP	1.7	0.73
AK	6.9	0.24	TOC	2.8	0.636
TN	3.4	0.594	EOC	2.5	0.672

RD: Root distribution; FRB: Fine root biomass; ST: Soil temperature; SWC: Soil water content; TOC: Total organic carbon; TN: Total nitrogen; TP: Total phosphorus; TK: Total potassium; AK: available potassium; AP: Available phosphorus; NO_3^-–N: Nitrate nitrogen; NH_4^+–N: Ammonium nitrogen; POC: Particulate organic carbon; EOC: Easily oxidized organic carbon; DOC: Dissolved organic carbon

Discussion

Distribution characteristics of the root growth and fine root biomass of Abies georgei var. smithii seedlings as a function of elevation

Plant growth and development are largely affected by the environment, and harsh environments tend to inhibit the development of plant organs (Bryndís, 2017; Du et al.,

http://www.aloki.hu ● ISSN 1589 1623 (Print) ● ISSN 1785 0037 (Online)
DOI: http://dx.doi.org/10.15666/aeer/2005_41214143

2012; Guadalupe et al., 2013). In the seedling stage, plants obtain water and nutrients from the soil layer through the horizontal and vertical extension of roots (Grill and Hubertl, 1998; Mulumba and Lal, 2008). Our results showed that the vertical roots of *A. georgei* var. *smithii* seedlings are mainly distributed in the 0–20 cm soil layer; moreover, the roots of the species extend horizontally over a distance of 0–25 cm. Both HRL and VRL increased with increasing seedling age level (*Fig. 2*), and significant differences were observed among different age classes ($p < 0.001$) (*Table 3*). These findings are consistent with a previous study involving Norwegian forests, which found that tree age has a significant effect on spruce root distribution ($p < 0.05$; Isabella et al., 2008). Some researchers have also found that the root length of *Quercus wutaishansea* seedlings in the Loess Plateau region of China increases from 3.34 ± 0.56 cm to 5.15 ± 0.67 cm with increasing age grade (Xia et al., 2012).

In previous studies, physiological characteristics of seedlings at different elevation bands were different (Reinhardt et al., 2011), and elevation has been shown to influence plant growth strongly (Takahashi, 2010; Pickering and Green, 2009). This parameter mainly controls plant traits and ecosystem functions by indirectly changing other driving factors, such as soil properties and species diversity (Fu et al., 2020; Case et al., 2005). In this study, we found no significant difference between the HRL and VRL of seedlings of different age levels along the elevation bands ($p > 0.05$) (*Table 3*), which contradicts the results of previous research (Marcora et al., 2016). Thus, our hypothesis (1) is rejected. This finding may be explained by that fact that, as the dominant population in Sejila Mountain, *A. georgei* var. *smithii* is well adapted to the climate of high elevation areas; thus, the physiological characteristics of its seedlings are minimally affected by elevations in the range of 3800–4100 m. Only when the elevation exceeds 4400 m do the physiological indices of the species change drastically under the influence of elevation (Liu et al., 2017). In this study, because only seedlings grown in the elevation range of 3800–4300 m were collected, minimal differences in root distribution were observed along the elevation bands.

Studying the distribution of underground root biomass is more challenging than studying the aboveground biomass of plants because the former requires more work and resources (Vogt et al., 1995; Hu et al., 2005; Hendricks et al., 2006; Metcalfe et al., 2007). Studies have shown that FRB increases with increasing forest age (Makkonen and Helmisaari, 2001). FRB and biomass-related morphological characteristics follow the same trend as the time series (Isabella et al., 2008). Our study confirmed that FRB significantly differs among different age grades ($p < 0.001$) (*Table 3*) and gradually increases with increasing age of *A. georgei* var. *smithii* seedlings (*Fig. 3*). We further studied the effect of elevation on FRB and found no difference in seedling FRB among different elevation bands ($p > 0.05$) (*Table 3*). Studies have demonstrated that the FRB of spruce forests in Northern Europe, Central Europe, and the European Alps increases significantly with elevation and that the greatest FRB is nearly twice that of the lowest stand (Hertel and Schling, 2011). In the Peruvian Andes, Girardin et al. findings fine root biomass gradually increased along the elevation bands (194-3020 m) and reached the maximum at 2020 m (Girardin et al., 2010). In the Changbai Mountain Nature Reserve, China, the FRB decreases significantly with elevation (Zhou et al., 2013), which is inconsistent with the results of our research. Such a finding indicates that elevation is not the main factor affecting the root growth of *A. georgei* var. *smithii* seedlings in high-elevation areas (Liu et al., 2017). This is consistent with Ji et al. findings that fine root biomass is not affected by elevation in southwest China (Ji et al., 2019).

http://www.aloki.hu ● ISSN 1589 1623 (Print) ● ISSN 1785 0037 (Online)
DOI: http://dx.doi.org/10.15666/aeer/2005_41214143

However, other studies on the FRB of adult *A. georgei* var. *smithii* in Sejila Mountain found high FRBs at 3900 m and 4200 m; specifically, the FRB is highest at 3900 m (Xin et al., 2017), and significant differences in FRB between these elevations could be observed ($p < 0.01$). These results indicate that the roots of *A. georgei* var. *smithii* in the alpine regions of Southeast Asia do not yet show differentiation characteristics with elevation at the seedling stage.

Effects of soil factors on the root growth and FRB of Abies georgei var. smithii seedlings

Studies have found that environmental heterogeneity, such as that due to temperature, water, light, and soil, caused by elevation lead to changes in the root distribution and physiological and ecological characteristics of alpine plants (Pan et al., 2009). For example, it has been found that soil temperature may be responsible for limiting the growth performance of high-elevation conifer seedlings in British Columbia (Balisky and Burton, 1997). Of course, studies in different regions will have different results. In our study area, our results reveal that the environmental response of roots of *A. georgei* var. *smithii* seedlings from Sejila Mountain in Tibet is mainly reflected in the influence of soil factors and that the heterogeneity of soil properties is indirectly caused by changes among the elevation bands (Soethe et al., 2006). We found that NH_4^+-N and POC greatly influence the root growth of *A. georgei* var. *smithii* seedlings ($p < 0.05$) (*Table 4*). A sufficient N supply could change the process of root growth and development, thereby increasing root weight and diameter (Mackiedaw Son et al., 1995). NH_4^+-N could directly affect the root length and root dry matter accumulation of seedlings (Viciedo and Dilier, 2017). SOC is a key factor affecting plant root growth and development (Vogel et al., 2005; Ruess et al., 2003; Dam et al., 1997), while POC, a component of persistent soil active organic carbon, is involved in the growth and development of various plant components (Witzgall et al., 2021).

Establishing the relationship between root biomass and its limiting factors is especially important in alpine ecosystems because the distribution and degradation of permafrost and uncertain environmental factors may affect FRB (Chang et al., 2012; Li et al., 2011). Studies have shown that soil factors strongly affect FRB, yield, and turnover in boreal forests (Pechackova et al., 1999; Yuan and Chen, 2010). The present study found that AP is the major contributor to FRB at different seedling age levels, consistent with the previous finding that AP affects the FRB in northern Queensland rainforests (Maycock and Congdon, 2000). In addition, studies have found that nutrient turnover in fine roots decreases with elevation at high elevation (Garkoti, 2012), but subalpine *A. georgei* var. *Smithii* have a unique nutrient acquisition strategy, with greater input of biomass and more active metabolism as the reason for *A. georgei* var. *Smithii* to absorb more soil nutrients (Ugawa et al., 2010). It is not difficult to understand that the fine root biomass of *A. georgei* var. *Smithii* seedlings is less affected by elevation. Therefore, soil factors, rather than elevation, are the most important factors affecting the growth of *A. georgei* var. *Smithii* seedlings.

Conclusions

The root growth and FRB of *A. georgei* var. *smithii* seedlings increased with their age level. While no difference in the characteristics of *A. georgei* var. *smithii* roots as a function of elevation were observed at the seedling stage, changes in soil properties

http://www.aloki.hu ● ISSN 1589 1623 (Print) ● ISSN 1785 0037 (Online)
DOI: http://dx.doi.org/10.15666/aeer/2005_41214143

caused by the elevation significantly affected the root growth and FRB of the seedlings. Our results revealed variations in the root growth and FRB of *A. georgei* var. *smithii* seedlings as a function of elevation and age level, as well as their correlation with soil factors. Our findings enrich the knowledge on underground ecosystems of natural forests in high-elevation areas and provide data support for the regeneration and conservation of dominant species in subalpine forest ecosystems. However, this study presents some limitations because we did not evaluate elemental differences between seedling roots of different age levels (Cao et al., 2020) or fully explore environmental factors, such as soil microbial diversity, at different elevations in the study area. Therefore, we encourage future researchers to explore, in detail, the effects of environmental factors on the chemical elements of seedling roots and exert efforts to reveal the complete growth characteristics and influencing mechanisms of *A. georgei* var. *smithii* seedlings in southeast Tibet.

Acknowledgments. This work was supported by the National Natural Science Foundation of China (31960256), Graduate Innovation Program of Key Laboratory of Forest Ecology in Tibet Plateau, Ministry of Education (XZA-JYBSYS-2021-Y13) and the Independent Research Project of Science and Technology Innovation Base in Tibet Autonomous Region (XZ2022JR0007G).

REFERENCES

[1] Balisky, A. C., Burton, P. (1997): Planted conifer seedling growth under two soil thermal regimes in high-elevation forest openings in interior British Columbia. – New Forests 14(1): 63-82. DOI: 10.1023/A:1006592705104.

[2] Bardgett, R. D., Mommer, L., De Vries, F. T. (2014): Going underground: root traits as drivers of ecosystem processes. – Trends Ecol. Evol. 29(12): 692-699. DOI: 10.1016/j.tree.2014.10.006.

[3] Bristiel, P., Roumet, C., Violle, C., Volaire, F. (2019): Coping with drought: root trait variability within the perennial grass Dactylis glomerata captures a trade-off between dehydration avoidance and dehydration tolerance. – Plant Soil 434: 327-342. DOI: 10.1007/s11104-018-3854-8.

[4] Bryndís, M. (2014): Seed rain and seed bank reveal that seed limitation strongly influences plant community assembly in grasslands. – PLoS ONE 9(7): 1-7. DOI: 10.1371/journal.pone.0103352.

[5] Cao, Y., Li, Y., Zhang, G., Zhang, J., Chen, M. (2020): Fine root C:N:P stoichiometry and its driving factors across forest ecosystems in northwestern China. – Science of the Total Environment 737: 140299. DOI: 10.1016/j.scitotenv.2020.140299.

[6] Case, M. J., Peterson, D. L. (2005): Fine-scale variability in growth-climate relationships of Douglas-fir, north cascade range, Washington. – Can. J. For. Res. 35: 2743-2755. DOI: 10.1139/x05-191.

[7] Chang, R., Fu, B., Liu, G., Yao, X., Shuai, W. (2012): Effects of soil physicochemical properties and stand age on fine root biomass and vertical distribution of plantation forests in the loess plateau of China. – Ecological Research 27(4): 827-836. DOI: 10.1007/s11284-012-0958-0.

[8] Chen, X., Yang, Q., Chen, Z., Xuexiao, Y. U., Yang, Q., Lei, J. (2017): Distribution of soil easily oxidized organic carbon and its response to soil factors in the tropical coastal forest of Hainan Island, China. – Journal of Central South University of Forestry & Technology 37(11): 140-145 (in Chinese).

http://www.aloki.hu ● ISSN 1589 1623 (Print) ● ISSN 1785 0037 (Online)
DOI: http://dx.doi.org/10.15666/aeer/2005_41214143

[9] Dam, D. V., Breemen, N. V., Veldkamp, E. (1997): Soil organic carbon dynamics: variability with depth in forested and deforested soils under pasture in costa rica. – Biogeochemistry 39(3): 343-375. DOI: 10.1023/A:1005880031579.
[10] Deng, L., Guan, J. H., Zhang, W. H. (2018): Response of root morphological characteristics of *Quercus liaotungensis* seedlings to environmental gradients. – Acta Ecologica Sinica 38(16): 5739-5749 (in Chinese).
[11] Dorich, R. A., Nelson, D. W. (1983): Direct colorimetric measurement of ammonium in potassium chloride extracts of soils. – Soil Science Society of America Journal 47(4): 833-836. DOI: 10.2136/ sssaj1983.03615995004700040042x.
[12] Du, Y. J., Mi, X. C., Liu, X. J., Ma, K. (2012): The effects of ice storm on seed rain and seed limitation in an evergreen broad-leaved forest in east China. – Acta Oecologica 39: 87-93. DOI: 10. 1016/j.actao.2012.01.006.
[13] Duan, F., Fang, J. P., Zhou, C. N. (2020): Study on the relationship between the release characteristics of organic carbon from litters and soil organic carbon pool in Tibetan primitive dark coniferous forest. – Journal of Soil and Water Conservation 34(03): 349-355 (in Chinese).
[14] Dunne, J. A., Saleska, S. R., Fischer, M. L., Harte, J. (2004): Integrating experimental and gradient methods in ecological climate change research. – Ecology 85: 904-916. DOI: 10.1890/03-8003.
[15] Eissenstat, D. M. (1992): Costs and benefits of constructing roots of small diameter. – J. Plant Nutr 15(6-7): 763-782. DOI: 10.1080/01904169209364361.
[16] Fang, H. J., Cheng, S. L., Yu, G. R., Xu, M. J., Wang, Y. S. (2014): Experimental nitrogen deposition alters the quantity and quality of soil dissolved organic carbon in an alpine meadow on the Qinghai-Tibetan plateau. – Applied Soil Ecology 81: 1-11. DOI: 10.1016/j.apsoil.2014.04.007.
[17] Ferguson, S. D., Leger, E. A., Li, J., Nowak, R. S. (2015): Natural selection favors root investment in native grasses during restoration of invaded fields. – J Arid Environ 116: 11-17. DOI: 10.1016/j.jaridenv.2015.01.009.
[18] Foster, A. C., Martin, P. H., Redmond, M. D. (2020): Soil moisture strongly limits Douglas-fir seedling establishment near its upper elevational limit in the southern Rocky Mountains. – Canadian Journal of Forest Research 50: 1-22. DOI: 10.1139/cjfr-2019-0296.
[19] Fu, H., Yuan, G., Ge, D., Li, W., Jeppesen, E. (2020): Cascading effects of elevation, soil moisture and soil nutrients on plant traits and ecosystem multi-functioning in Poyang Lake wetland, China. – Aquatic Sciences 82(34): 1-10. DOI: 10.1007/s00027-020-0711-7.
[20] Gammon, N. (1951): Determination of total potassium and sodium in sandy soils by flame photometer. – Soil Science 71(3): 211-214. DOI: 10.1021/ac60051a025.
[21] Garkoti, S. C. (2012): Dynamics of fine root N, P and K in high elevation forests of central Himalaya. – Forestry Studies in China 14: 1. DOI: 10.1007/s11632-012-0203-5.
[22] Garten, C. T., Post, W. M., Hanson, P. J., Cooper, L. W. (1999): Forest soil carbon inventories and dynamics along an elevation gradient in the southern Appalachian Mountains. – Biogeochemis Try 1999: 45(2): 115-145. DOI: 10.1023/A:1006121511680.
[23] Girardin, C., Malhi, Y., Leoc Aragão, Mamani, M., Huasco, W. H., Durand, L., et al. (2010): Net primary productivity allocation and cycling of carbon along a tropical forest elevational transect in the Peruvian Andes. – Global Change Biology 16(12): 3176-3192. DOI: 10.1111/j.1365-2486.
[24] Gonzalez-Ollauri, A., Hudek, C., Mickovski, S. B., Viglietti, D., Freppaz, M. (2021): Describing the vertical root distribution of alpine plants with simple climate, soil, and plant attributes. – Catena 203(1): 105305. DOI: 10.1016/j.catena.2021.105305.
[25] Grill, E., Hubert, Z. (1998): A plant's dilemma. – Science 282: 252-253. DOI: 10.1126/science.282 5387.252.

http://www.aloki.hu ● ISSN 1589 1623 (Print) ● ISSN 1785 0037 (Online)
DOI: http://dx.doi.org/10.15666/aeer/2005_41214143

[26] Guadalupe, G., Pablo, O. B., Scopel, A. L., Hutchings, M. J. (2013): The dynamics of three shrub species in a fire-prone temperate savanna: the interplay between the seed bank, seed rain and fire regime. – Plant Ecology 214(1): 75-86. DOI: 10.1007/s11258-012-0147-9.
[27] Haby, V. A. (1989): Soil no3-n analysis in ca(oh)2 extracts by the chromotropic acid method. – Soil Science Society of America Journal 53(1): 308-310. DOI: 10.2136/sssaj1989. 03615995005300010 059x.
[28] Hanslin, H. M., Bischoff, A., Hovstad, K. A. (2019): Root growth plasticity to drought in seedlings of perennial grasses. – Plant Soil 440: 551-568. DOI: 10.1007/s11104-019-04117-7.
[29] Harrison, S., LaForgia, M. (2019): Seedling traits predict drought-induced mortality linked to diversity loss. – Proc Natl Acad Sci 116: 5576-5581. DOI: 10.1073/pnas.1818543116.
[30] Hendricks, J. J., Hendrick, R. L., Wilson, C. A., Mitchell, R. J., Pecot, S. D., Guo, D. (2006): Assessing the patterns and controls of fine root dynamics: an empirical test and methodological review. – Journal of Ecology 94(1): 40-57. DOI: 10.1111/j.1365-2745.2005.01067.x.
[31] Hertel, D., Schling, D. (2011): Below-ground response of Norway spruce to climate conditions at Mt. Brocken (Germany)—a re-assessment of central Europe's northernmost treeline. – Flora 206(2): 127-135. DOI: 10.1016/j.flora.2010.05.001.
[32] Hu, Z. M., Fan, J. W., Zhong, H. P., Han, B. (2005): Progress on grassland underground biomass researches in China. – Chinese Journal of Ecology. l24(9): 1095-1101 (in Chinese).
[33] Isabella, B., De, W. H. A., Arne, S., Hooshang, M. (2008): Stand age and fine root biomass, distribution and morphology in a Norway spruce chronosequence in Southeast Norway. – Tree Physiology 28(5): 773-784. DOI: 10.1093/treephys/28.5.773.
[34] Jackson, R., Manwaring, J., Caldwell, M. (1990): Rapid physiological adjustment of roots to localized soil enrichment. – Nature 344(6261): 58-60. DOI: 10.1038/344058a0.
[35] Jakmunee, J., Junsomboon, J. (2009): Determination of available phosphorus in soils by using a new extraction procedure and a flow injection amperometric system. – Talanta 79(4): 1076-1080. DOI: 10.1016/j.talanta.2009.01.028.
[36] Ji, Z., Zhao, Y., Wang, Y. (2019): The trade-off between growth and reproduction in an alpine herbaceous plant along an elevation gradient. – Pakistan Journal of Botany 51(3): 1075-1080. DOI: 10.30848/PJB2019-3(41).
[37] Jose, S. (2009): Agroforestry for ecosystem services and environmental benefits: an overview. – Agroforestry Systems 76(1): 1-10. DOI: 10.1007/s10457-009-9229-7.
[38] Kato, T., Tang, Y., Song, G. U., Hirota, M., Zhao, X. (2006): Temperature and biomass influences on interannual changes in CO2 exchange in an alpine meadow on the Qinghai-Tibetan Plateau. – Global Change Biology 12(7): 1285-1298. DOI: 10.1111/j.1365-2486.2006.01153.x.
[39] King, J. S. (2021): Root biomass distribution and soil physical properties of short-rotation coppice American sycamore (Platanus occidentalis L.) grown at different planting densities. – Forests 12. DOI: 10.3390/f12121806.
[40] Kramer-Walter, K. R., Bellingham, P. J., Millar, T. R., Smissen, R. D., Richardson, S. J., Laughlin, D. C. (2016): Root traits are multidimensional: specific root length is independent from root tissue density and the plant economic spectrum. – J Ecol 104: 1299-1310. DOI: 10.1111/1365-2745.12562.
[41] Larson, J. E., Anacker, B. L., Wanous, S., Funk, J. L. (2020): Ecological strategies begin at germination: traits, plasticity and survival in the first 4 days of plant life. – Funct Ecol 34: 968-979. DOI: 10.1111/1365-2435.13543.
[42] Leger, E. A., Atwater, D. Z., James, J. J. (2019): Seed and seedling traits have strong impacts on establishment of a perennial bunch-grass in invaded semi-arid systems. – Journal of Applied Ecology 97: 311-325. DOI: 10.1111/1365-2664.13367.

http://www.aloki.hu ● ISSN 1589 1623 (Print) ● ISSN 1785 0037 (Online)
DOI: http://dx.doi.org/10.15666/aeer/2005_41214143

[43] Leger, E. A., Goergen, E. M. (2017): Invasive Bromus tectorum alters natural selection in arid systems. – J Ecol 105: 1509-1520.DOI: 10.1111/1365-2745.12852.
[44] Li, F., Xie, Y., Yang, G., Zhu, L., Hu, C., Chen, X., et al. (2016): Interactive influence of water level, sediment heterogeneity, and plant density on the growth performance and root characteristics of Carex brevicuspis. – Limnologica 62: 111-117. DOI: 10.1016/j.limno.2016.11.007.
[45] Li, X., Minick, K. J., Luff, J., Noormets, A., King, J. S. (2019): Effects of microtopography on absorptive and transport fine root biomass, necromass, production, mortality and decomposition in a coastal freshwater forested wetland, southeastern USA. – Ecosystems 23: 1294-1308. DOI: 10.1007/ s10021-019-00470-x.
[46] Li, X., Zhang, X., Wu, J., Shen, Z., Wei, Y. (2011): Root biomass distribution in alpine ecosystems of the northern Tibetan Plateau. – Environmental Earth Sciences 64(7): 1911-1919. DOI: 10.1007/s 12665-011-1004-1.
[47] Liu, J. M., Xing, F. M., Yang, X. L., Zhao, K. T., Jia, L. M. (2017): Basic characteristics and physiological index changes of *Abies georgei* var. *smithii* seedlings at different altitudes of Shergyla Mountain. – Journal of Zhejiang University (Agric. & Life Sci.) 43(05): 623-630(in Chinese).
[48] Lomolino, M. V. (2010): Elevation gradients of species-density: historical and prospective views. – Glob Ecol Biogeogr 10: 3-13. DOI: 10.1046/j.1466-822x.2001.00229.x.
[49] Luo, D. (2010): Fruiting characteristics of *Abies georgei* var. *smithii* forest on the eastern slope of the Sejila Mountain in Tibet. – Scientia Silvae Sinicae 4398(1): 738901-18. DOI: DOI: 10.1117/ 12.835932.
[50] Ma, W. H., Yang, Y. H., He, J. S., Zeng, H., Fang, J. Y. (2008): Above- and belowground biomass in relation to environmental factors in temperate grasslands, Inner Mongolia. – Science in China Series C Life Sciences 51(3): 263-279. DOI: 10.1007/s11427-008-0029-5.
[51] Mackiedawson, L. A., Millard, Proe, M. F. (1995): The effect of nitrogen supply on root-growth and development in sycamore and Sitka spruce trees. – Forestry 68(2): 107-114. DOI: 10.1093/ forestry/68.2.107.
[52] Makkonen, H. S., Helmisaari. (2001): Fine root biomass and production in Scots pine stands in relation to stand age. – Tree physiology 21: 193-198. DOI: 10.1093/treephys/21.2-3.193.
[53] Malhi, Y., Silman, M., Salinas, N., Bush, M., Meir, P., Saatchi, S. (2010): Introduction: elevation gradients in the tropics: laboratories for ecosystem ecology and global change research. – Global Change Biol 16: 3171-3175. DOI: 10.1111/j.1365-2486.2010.02323.x.
[54] Marcora, P. I., Tecco, P. A., Zeballos, S. R., Hensen, I. (2016): Influence of altitude on local adaptation in upland tree species from Central Argentina. – Plant Biology 19(2): 123-131. DOI: 10.1111/plb.12513.
[55] Markesteijn, L., Poorter, L. (2009): Seedling root morphology and biomass allocation of 62 tropical tree species in relation to drought- and shade-tolerance. – J Ecol 97: 311-325. DOI: 10.1111/j.1365-2745.2008.01466.x.
[56] Maycock, C. R. , Congdon, R. A. (2000): Fine root biomass and soil N and P in north Queensland rain forests. – Biotropica 32(1): 185-190. DOI: 10.1111/j.1744-7429.2000.tb00460.x.
[57] Metcalfe, D. B., Williams, M., Aragão, L. E. O. C., da Costa, A. C. L., de Almeida, S. S., Braga, A. P., et al. (2007): A method for extracting plant roots from soil which facilitates rapid sample processing without compromising measurement accuracy. – New Phytol 174(3): 697-703. DOI: 10.1111/j.1469-8137.2007.02032.x.
[58] Mulumba, L. N., Lal, R. (2008): Mulching effects on selected soil physical properties. – Soil & Tillage Research 98(1): 106-111. DOI: 10.1016/j.still.2007.10.011.

http://www.aloki.hu ● ISSN 1589 1623 (Print) ● ISSN 1785 0037 (Online)
DOI: http://dx.doi.org/10.15666/aeer/2005_41214143

[59] Norby, R. J., Jackson, R. B. (2000): Root dynamics and global change: seeking an ecosystem perspective. – New Phytol 147: 3-12. DOI: 10.1046/j.1469-8137.2000.00676.x.
[60] Paillex, A., Dolédec, S., Castella, E. (2013): Functional diversity in a large river floodplain: anticipating the response of native and alien mac-roin vertebrates to the restoration of hydrological connectivity. – J Appl Ecol 50: 97-106. DOI: 10.1111/1365-2664.12018.
[61] Pan, H. L., Li, M. H., Cai, X. H., Wu, J., Du, Z., Liu, X. L. (2009): Responses of growth and ecophsiology of plants to altitude. – Ecology and Environmental Sciences 18(02): 722-730 (in Chinese).
[62] Parent, S., Simard, M. J., Morin, H., Messier, C. (2003): Establishment and dynamics of the balsam fir seedling bank in old forests of northeastern Quebec. – Canadian Journal of Forest Research 33(4): 597-603. DOI: 10.1139/x02-194.
[63] Pechackova, S., During, H. J., Rydlova, V., Herben, T. (1999): Species-specific spatial pattern of below-ground plant parts in a montane grassland community. – Journal of Ecology 87: 569-582. DOI: 10.1046/j.1365-2745.1999.00375.x.
[64] Pickering, C. M., Green, K. (2009): Vascular plant distribution in relation to topography, soils and micro-climate at five gloria sites in the snowy mountains, Australia. – Australian Journal of Botany 57(3): 189-199. DOI: 10.1023/A:1014419309885.
[65] Qi, Y. L. (2020): Influences of soil preparation measures on root distribution characteristics and ecological effect of plant communities on the loess plateau. – Forestry College, Northwest A&F University July, 2020. DOI: 10.27409/d.cnki.gxbnu.2020.001444.
[66] Qi, Y., Wei, W., Chen, C., Chen, L. (2019): Plant root-shoot biomass allocation over diverse biomes: a global synthesis. – Global Ecology and Conservation 18: e00606. DOI: 10.1016/j.gecco. 2019.e00606.
[67] Qi, Y., Wei, W., Li, J., Chen, C., Huang, Y. (2020): Effects of terracing on root distribution of Pinus tabulaeformis carr. forest and soil properties in the Loess Plateau of China. – Science of the Total Environment 721: 137506. DOI: 10.1016/j.scitotenv.2020.137506.
[68] Rahbek, C. (2005): The role of spatial scale and the perception of large-scale species-richness patterns. – Ecol Lett 8: 224-239. DOI: 10.1111/j.1461-0248.2004.00701.x.
[69] Ramachandran Nair, P., Mohan Kumar, B., Nair, V. D. (2009): Agroforestry as a strategy for carbon sequestration. – Journal of Plant Nutrition and Soil Science 172(1): 10-23. DOI: 10.1002/ jpln.200800030.
[70] Reinhardt, K., Castanha, C., Germino, M. J., Kueppers, L. M. (2011): Ecophysiological variation in two provenances of Pinus flexilis seedlings across an elevation gradient from forest to alpine. – Tree Physiology 31(6): 615-625. DOI: 10.1093/treephys/tpr055.
[71] Ronald, L., Hendrick, P. (1993): The dynamics of fine root length, biomass, and nitrogen content in two northern hardwood ecosystems. – Canadian Journal of Forest Research 23(12): 2507-2520. DOI: 10.1021/ja00817a061.
[72] Ruess, R. W., Hendrick, R. L., Burton, A. J., Pregitzer, K. S., Maurer, G. E. (2003): Coupling fine root dynamics with ecosystem carbon cycling in black spruce forests of interior Alaska. – Ecological Monographs 73(4): 643-662. DOI: 10.1890/02-4032.
[73] Schenk, H. J., Jackson, R. B. (2005): Mapping the global distribution of deep roots in relation to climate and soil characteristics. – Geoderma 126(1-2): 129-140. DOI: 10.1016/j.geoderma.2004.11. 018.
[74] Simpson, C. R., Gonzales, J., Enciso, J., Nelson, S. D., Sétamou, M. (2020): Root distribution and seasonal fluctuations under different grove floor management systems in citrus. – Scientia Horticulturae 272: 109364. DOI: 10.1016/j.scienta.2020.109364.
[75] Soethe, N., Lehmann, J., Engels, C. (2006): The vertical pattern of rooting and nutrient uptake at different altitudes of a South Ecuadorian montane forest. – Plant & Soil 286(1-2): 287-299. DOI: 10.1007/s11104-006-9044-0.

http://www.aloki.hu ● ISSN 1589 1623 (Print) ● ISSN 1785 0037 (Online)
DOI: http://dx.doi.org/10.15666/aeer/2005_41214143

[76] Sparks, D. L., Page, A., Helmke, P., Loeppert, R., Soltanpour, P., Tabatabai, M., et al. (1996): Methods of Soil Analysis. Part 3. Chemical Methods. – Soil Science Society of America Inc., Madison, WI (No. 631.417/S736 V. 3).
[77] Storer, D. A. (1984): A simple high sample volume ashing procedure for determination of soil organic matter. – Communications in Soil Science and Plant Analysis 15(7): 759-772. DOI: 10.1080/00103628 409367515.
[78] Takahashi, K. (2010): Effects of altitude and competition on growth and mortality of the conifer Abies sachalinensis. – Ecological Research 25(4): 801-812. DOI: 10.1007/s11284-010-0710-6.
[79] Thevathasan, N., Gordon, A. (2004): Ecology of tree intercropping systems in the North temperate region: experiences from southern Ontario, Canada. – Agroforestry Systems 61-62(1): 257-268. DOI: 10.1023/B:AGFO.0000029003.00933.6d.
[80] Ugawa, S., Miura, S., Iwamoto, K., Kaneko, S., Fukuda, K. (2010): Vertical patterns of fine root biomass, morphology and nitrogen concentration in a subalpine fir-wave forest. – Plant & Soil 335(1-2): 469-478. DOI: 10.1007/s11104-010-0434-y.
[81] Viciedo, O., Dilier. (2017): Response of radish seedlings (Raphanus sativus, L.) to different concentrations of ammoniacal nitrogen in absence and presence of silicon. – Agronomía Colombiana 35: 198-204. DOI: 10.15446/agron.colomb.v35n2.62772.
[82] Violle, C., Navas, M. L., Vile, D., Kazakou, E., Fortunel, C., Hummel, I., Garnier, E. (2007): Let the concept of trait be functional! – Oikos 116: 882-892. DOI: 10.2307/40235131.
[83] Vogel, J. G., Valentine, D. W., Ruess, R. W. (2005): Soil and root respiration in mature Alaskan black spruce forests that vary in soil organic matter decomposition rates. – Canadian Journal of Forest Research 35(1): 161-174. DOI: 10.1139/x04-159.
[84] Vogt, K. A., Vogt, D. J., Palmiotto, P. A., Boon, P., O'Hara, J., Asbjornsen, H. (1995): Review of root dynamics in forest ecosystems grouped byclimate, climatic forest type and species. – Plant Soil 187: 195-219. DOI: 10.1007/BF00017088.
[85] Wang, C. T., Cao, G. M., Wang, Q. L., Jing, Z. C., Ding, L. M., Long, R. J. (2007): Species composition of plant community in alpine meadow and biomass change along environmental gradient in Tibetan Plateau. – Sci China (Ser C) Life Sci 37(5): 585-592. DOI: 10.3969/j.issn.1674-7232.2007.05.014.
[86] Wang, R. H., Li, J. R., Pan, G. (2018): Natural regeneration factors of *Abies georgei* var. *smithii* on Sejila Mountain. – Journal of Zhejiang A & F University (in Chinese).
[87] Wang, W., Xu, W., Collett, J. L., Liu, D., Liu, X. (2019): Chemical compositions of fog and precipitation at Sejila Mountain in the southeast Tibetan Plateau, China. – Environmental Pollution 253: 560-568. DOI: 10.1016/j.envpol.2019.07.055.
[88] Wilcox, D. A., Nichols, S. J. (2008): The effects of water-level fluctuations on vegetation in a Lake Huron wetland. – Wetlands 28: 487-501. DOI: 10.1672/07-129.1.
[89] Williams, A., George, S., Birt, H., Daws, M. I., Tibbett, M. (2019): Sensitivity of seedling growth to phosphorus supply in six tree species of the Australian great western woodlands. – Australian Journal of Botany 67: 1-30. DOI: 10.1071/BT18247.
[90] Witzgall, K., Vidal, A., Schubert, D. I., Hschen, C., Mueller, C. W. (2021): Particulate organic matter as a functional soil component for persistent soil organic carbon. – Nature Communications 12(1): 4115. DOI: 10.1038/s41467-021-24192-8.
[91] Xia, F., Wang, X. A., Guo, H., Wang, S. X., Li, H. W., Fan, W. Y. (2012): Effects of Root Morphology on Seedling Growth of Quercus liaotungensis in Different Age Classes on Loess Plateau. – Chinese Agricultural Science Bulletin 28(10): 32-36 (in Chinese).
[92] Xie, C. Q., Tian, M. X., Zhao, Z. R., Zheng, W. L., Wang, G. Y. (2015): Spatial point pattern analysis of *Abies georgei* var. *smithii* in forest of Sygera Mountains in Southeast Tibet, China. – Chinese Journal of Applied Ecology 26(6): 1617-1624 (in Chinese).
[93] Xin, F. M., Liu, J. M., Yang, X. L., Zhao, K. T. (2017): Variation in leaf and fine root traits with altitude in *Abies georgei* var. *smithii* in Mt. Shergyla. – Acta Ecologica Sinica 37(8): 2719-2728. DOI: 10.5846/stxb201511162322.

http://www.aloki.hu ● ISSN 1589 1623 (Print) ● ISSN 1785 0037 (Online)
DOI: http://dx.doi.org/10.15666/aeer/2005_41214143

[94] Xu, Y., Zhang, Y., Li, W., Liu, W., Gu, X., Guan, Z., et al. (2019): Effects of tree functional diversity and environmental gradients on belowground biomass in a natural old-growth forest ecosystem. – Canadian Journal of Forest Research 49(12): 1623-1632. DOI: 10.1139/cjfr-2019-0254.

[95] Yuan, Z. Y., Chen, H. (2010): Fine root biomass, production, turnover rates, and nutrient contents in boreal forest ecosystems in relation to species, climate, fertility, and stand age: literature review and meta-analyses. – Critical Reviews in Plant Sciences 29(4): 204-221. DOI: 10.1080/07352689 2010.483579.

[96] Zhang, Z., Huang, M., Zhang, Y. (2018): Vertical distribution of fine-root area in relation to stand age and environmental factors in black locust (Robinia pseudoacacia) forests of the Chinese Loess Plateau. – Canadian Journal of Forest Research 48: 1-34. DOI: 10.1139/cjfr-2018-0149.

[97] Zhou, C. N., Ren, Y. H., Ma, H. P., Guo, Q. Q. (2015): Research on soil organic carbon pool of typical natural dark coniferous forests in Sygara Mountains in Tibet. – Environmental Science & Technology 38(06): 1-7 (in Chinese).

[98] Zhou, Y., Su, J. Q., Janssens, I. A., Zhou, G. S., Xiao, C. W. (2013): Fine root and litterfall dynamics of three Korean pine (Pinus koraiensis) forests along an altitudinal gradient. – Plant and Soil 374(1): 19-32. DOI: 10.1007/s11104-013-1816-8.

APPENDIX

Table A1. *F and p values of Abies georgei var. smithii seedling characteristics*

		Average plant height (cm)		**Mean ground diameter (mm)**		**Mean diameter of fine roots (mm)**		**Mean length of fine roots (cm)**	
		***F*-values**	***p*-values**	***F*-values**	***p*-values**	***F*-values**	***p*-values**	***F*-values**	***p*-values**
Variance analysis of different age groups at the same elevation	3815–3882 m	13.188	$p < 0.001$	14.328	$p < 0.001$	19.586	$p < 0.001$	25.165	$p < 0.001$
	3921–3992 m	9.251	$p = 0.002$	9.826	$p < 0.001$	7.403	$p = 0.004$	2.398	$p = 0.119$
	4009–4089 m	11.668	$p < 0.001$	9.080	$p = 0.002$	21.146	$p < 0.001$	6.894	$p = 0.006$
	4113–4194 m	18.161	$p < 0.001$	28.100	$p < 0.001$	8.764	$p = 0.002$	3.624	$p = 0.044$
	4207–4283 m	11.229	$p < 0.001$	64.428	$p < 0.001$	7.117	$p = 0.005$	12.163	$p < 0.001$
	4311–4379 m	15.432	$p < 0.001$	51.747	$p < 0.001$	7.868	$p = 0.003$	2.481	$p = 0.111$
Analysis of variance of the same age groups at different elevations	1	2.391	$p = 0.100$	1.662	$p = 0.218$	2.761	$p = 0.069$	0.398	$p = 0.885$
	2	18.389	$p < 0.001$	9.442	$p < 0.001$	13.148	$p < 0.001$	5.713	$p = 0.006$
	3	1.685	$p = 0.212$	0.956	$p = 0.480$	30.384	$p < 0.001$	1.104	$p = 0.407$
	4	0.273	$p = 0.919$	1.021	$p = 0.447$	4.100	$p = 0.021$	3.050	$p = 0.052$
	5	0.615	$p = 0.690$	0.462	$p = 0.796$	4.515	$p = 0.015$	0.706	$p = 0.629$

http://www.aloki.hu ● ISSN 1589 1623 (Print) ● ISSN 1785 0037 (Online)
DOI: http://dx.doi.org/10.15666/aeer/2005_41214143

Table A2. *Mean ± SD value, F-value and P-value of root indexes of Abies georgei var. smithii seedlings*

		HRL /cm		VRL/cm		FRB/g	
Mean ± SD	Elevation /m (EL)						
	3815–3882	7.10 ± 8.54a		7.39 ± 3.81a		0.32 ± 0.35a	
	3921–3992	5.73 ± 7.68a		8.09 ± 5.39a		0.23 ± 0.37a	
	4009–4089	5.41 ± 6.74a		5.37 ± 3.54a		0.22 ± 0.40a	
	4113–4194	7.65 ± 5.91a		9.25 ± 6.30a		0.37 ± 0.68a	
	4207–4283	8.45 ± 6.73a		7.06 ± 4.08a		0.23 ± 0.25a	
	4311–4379	8.64 ± 6.60a		9.24 ± 5.71a		0.31 ± 0.39a	
	Age levels (AL)						
	1	0.83 ± 0.53d		2.66 ± 1.29d		0.01 ± 0.01c	
	2	3.35 ± 2.08cd		5.78 ± 2.87cd		0.04 ± 0.03c	
	3	6.39 ± 4.57bc		7.39 ± 2.97bc		0.13 ± 0.09bc	
	4	9.34 ± 5.87b		9.29 ± 3.96b		0.33 ± 0.21b	
	5	15.90 ± 7.19a		13.55 ± 4.99a		0.90 ± 0.53a	
		F-values	*p*-values	*F*-values	*p*-values	*F*-values	*p*-values
Variance analysis of different age groups at the same elevation	3815–3882	11.234	$p < 0.001$	16.543	$p < 0.001$	27.509	$p < 0.001$
	3921–3992	4.217	$p = 0.029$	4.608	$p = 0.022$	9.015	$p = 0.002$
	4009–4089	8.043	$p = 0.003$	9.958	$p = 0.002$	5.797	$p = 0.011$
	4113–4194	3.401	$p = 0.052$	6.639	$p = 0.007$	5.022	$p = 0.017$
	4207–4283	5.541	$p = 0.012$	4.385	$p = 0.026$	29.630	$p < 0.001$
	4311–4379	5.333	$p = 0.014$	3.004	$p = 0.072$	5.833	$p = 0.010$
Analysis of variance of the same age groups at different elevations	1	1.359	$p = 0.305$	0.897	$p = 0.513$	0.929	$p = 0.495$
	2	4.179	$p = 0.019$	1.049	$p = 0.433$	9.214	$p < 0.001$
	3	2.059	$p = 0.147$	2.084	$p = 0.137$	8.222	$p = 0.002$
	4	2.321	$p = 0.107$	1.846	$p = 0.178$	2.474	$p = 0.092$
	5	0.517	$p = 0.758$	0.978	$p = 0.469$	0.779	$p = 0.583$

HRL: Horizontal root length; VRL: Vertical root length; FRB: Fine root biomass. 1: 1–2-year-old seedlings; 2: 3–4-year-old seedlings; 3: 5–6-year-old seedlings; 4: 7–8-year-old seedlings; 5: 9–10-year-old seedlings

Different lowercase letters indicate significant differences among different elevations or age levels ($p < 0.05$)

http://www.aloki.hu ● ISSN 1589 1623 (Print) ● ISSN 1785 0037 (Online)
DOI: http://dx.doi.org/10.15666/aeer/2005_41214143

Table A3. *Contribution rate and P value of soil factors to HRL of Abies Georgei var. smithiit seedlings at different age groups*

HRL1			HRL2			HRL3			HRL4			HRL5		
Name	**Contribution %**	**P**	**Name**	**Contribution %**	**P**	**Name**	**Contribution %**	**P**	**Name**	**Contribution %**	**P**	**Name**	**Contribution %**	**P**
ST	32.5	0.018	NO_3^--N	19.5	0.048	AP	36.4	0.02	TK	19.7	0.046	NH_4^+-N	36.3	0.018
AK	13.9	0.042	TOC	7.3	0.37	POC	17.5	0.066	NO_3^--N	17.8	0.042	SWC	22.7	0.024
TOC	17.9	0.052	POC	17.2	0.144	NH_4^+-N	7.6	0.174	TP	11.6	12.9	POC	9	0.182
EOC	9.4	0.062	AK	7.7	0.31	ST	4.9	0.306	AP	4.9	0.302	TP	7.3	0.252
DOC	8.2	0.054	SWC	9.8	0.242	SWC	7.9	0.178	AK	4.3	0.326	TN	4.3	0.288
TK	11	0.206	TK	9.3	0.262	TOC	9	0.13	TOC	9.9	0.154	TOC	4.7	0.298
AP	4.6	0.24	ST	4.6	0.39	DOC	3.9	0.304	TN	9.4	0.108	ST	5.5	0.258
SWC	1.3	0.372	NH_4^+-N	2.6	0.558	TK	5.2	0.24	DOC	3	0.4	AP	6.1	0.2
NO_3^--N	0.4	0.62	EOC	0.9	0.734	AK	2.1	0.484	SWC	7.9	0.12	EOC	2	0.494
POC	0.4	0.658	TN	1	0.726	EOC	2.2	0.438	EOC	5	0.194	AK	1.5	0.57
TN	0.3	0.744	TP	0	0	TP	2.1	0.492	NH_4^+-N	2.3	0.322	TK	0.4	0.736
TP	< 0.1	0.876	AP	0	0	NO_3^--N	0.5	0.734	POC	2.5	0.342	DOC	< 0.1	0.992
NH_4^+-N	< 0.1	0.978	DOC	0	0	TN	0.8	0.702	ST	0	0	NO_3^--N	0	0

HRL: Horizontal root length.1:1-2-year-old seedlings; 2. 3-4 years old seedlings; 3:5-6 years old seedlings; 4:7-8 years old seedlings; 5:9-10 years old seedlings

Table A4. *Contribution rate and P value of soil factors to VRL of Abies Georgei var. smithiit seedlings at different age groups*

VRL1			VRL2			VRL3			VRL4			VRL5		
Name	**Contribution %**	**P**	**Name**	**Contribution %**	**P**	**Name**	**Contribution %**	**P**	**Name**	**Contribution %**	**P**	**Name**	**Contribution %**	**P**
NO_3^--N	20	0.082	TK	35.3	0.02	TP	29	0.042	DOC	39.5	0.016	DOC	28.5	0.05
NH_4^+-N	11.5	0.026	NO_3^--N	29.2	0.014	TK	13.4	0.132	TK	9.6	0.184	NH_4^+-N	20.5	0.082
TN	16.3	0.062	TP	13.2	0.046	DOC	4.2	0.422	NO_3^--N	13.7	0.2	ST	20.5	0.036
TK	17	0.112	ST	6.2	0.122	ST	11.3	0.152	POC	3.3	0.454	POC	7.8	0.168
EOC	9.3	0.126	DOC	4.9	0.186	EOC	8.1	0.252	SWC	2.9	0.468	TN	4.5	0.246
DOC	8.3	0.202	NH_4^+-N	5.2	0.152	TOC	11.6	0.13	TOC	1	0.7	TP	5.8	0.264
AP	4.7	0.336	EOC	2.3	0.272	SWC	3.7	0.37	AK	0.5	0.794	AK	2.9	0.384
TP	4	0.368	TOC	1.7	0.424	NO_3^--N	3.8	0.314	ST	0.2	0.876	TK	2.6	0.48
AK	4	0.406	AK	0.9	0.544	AK	4.8	0.32	TN	0.2	0.896	SWC	1.1	0.62
SWC	1.9	0.346	AP	0.6	0.612	TN	4	0.318	TP	0	0	EOC	0.8	0.662
TOC	2.7	0.282	TN	0.3	0.748	AP	1.2	0.606	AP	0	0	NO_3^--N	4.1	0.412
ST	0.3	0.698	POC	0.2	0.86	NH_4^+-N	1.5	0.58	EOC	0	0	TOC	0.4	0.776
POC	0	0	SWC	< 0.1	0.896	POC	3.4	0.458	NH_4^+-N	0	0	AP	0	0

VRL: Vertical root length.1:1-2-year-old seedlings; 2. 3-4 years old seedlings; 3:5-6 years old seedlings; 4:7-8 years old seedlings; 5:9-10 years old seedlings

http://www.aloki.hu ● ISSN 1589 1623 (Print) ● ISSN 1785 0037 (Online)
DOI: http://dx.doi.org/10.15666/aeer/2005_41214143

Table A5. *Contribution rate and P value of soil factors to FRB of Abies Georgei var. smithiit seedlings at different age groups*

FRB1			FRB2			FRB3			FRB4			FRB5		
Name	**Contribution %**	**P**	**Name**	**Contribution %**	**P**	**Name**	**Contribution %**	**P**	**Name**	**Contribution %**	**P**	**Name**	**Contribution %**	**P**
TK	24.3	0.026	TK	52.9	0.008	ST	79.6	0.002	DOC	29.7	0.024	AP	32.8	0.032
SWC	8.3	0.09	ST	11	0.104	EOC	7.8	0.068	TK	24.6	0.014	AK	28.1	0.088
NO_3^--N	17.5	0.028	DOC	6.7	0.214	AP	4.5	0.15	AK	8.6	0.118	DOC	10.8	0.178
AK	20.7	0.086	NH_4^+-N	4.8	0.26	DOC	1.1	0.46	AP	6.5	0.152	TP	3.7	0.42
DOC	10.9	0.22	AK	7.2	0.154	TOC	1.5	0.388	TP	5.9	0.152	NO_3^--N	2.1	0.544
EOC	3.4	0.256	POC	3.9	0.334	TN	0.2	0.744	TOC	7	0.14	POC	0.6	0.778
AP	3.7	0.2	TP	3.2	0.312	POC	0.5	0.692	EOC	3.9	0.212	TN	2.8	0.502
TOC	2.1	0.41	EOC	2.6	0.416	NO_3^--N	0.3	0.754	NO_3^--N	3.1	0.22	SWC	2.2	0.596
NH_4^+-N	5.1	0.16	TOC	4.2	0.304	NH_4^+-N	0.4	0.726	SWC	3.2	0.232	NH_4^+-N	2.5	0.604
TN	2.7	0.292	AP	1.8	0.514	TP	< 0.1	0.882	POC	6.2	0.078	EOC	0.6	0.816
ST	0.9	0.534	NO_3^--N	0.9	0.648	SWC	< 0.1	0.89	ST	0.9	0.462	TOC	1.7	0.702
TP	0.2	0.78	TN	0.4	0.78	TK	0	0	TN	0.4	0.624	TK	0.4	0.86
POC	0.3	0.764	SWC	0	0	AK	0	0	NH_4^+-N	0	0	ST	0	0

FRB: Fine root biomass.1:1-2-year-old seedlings; 2. 3-4 years old seedlings; 3:5-6 years old seedlings; 4:7-8 years old seedlings; 5:9-10 years old seedlings

Table A6. *Mean ± SD value, F-value and p-value of soil factors at each elevation*

	3815–3882m	**3815–3882m**	**3815–3882m**	**3815–3882m**	**3815–3882m**	**3815–3882m**	***F*-values**	***p*-values**
AP	1.84 ± 0.48a	1.39 ± 0.24a	1.55 ± 0.77a	1.54 ± 0.21a	2.18 ± 0.37a	2.06 ± 0.5a	1.377	$p = 0.299$
AK	0.09 ± 0.02a	0.06 ± 0.01a	0.07 ± 0.01a	0.07 ± 0.02a	0.07 ± 0.01a	0.08 ± 0.04a	0.496	$p = 0.773$
NH_4^+-N	7.17 ± 0.73a	6.49 ± 0.78a	5.11 ± 0.43a	3.99 ± 1.83a	6.73 ± 1.76a	5.1 ± 2.81a	1.707	$p = 0.207$
NO_3^--N	0.97 ± 0.64c	2.47 ± 0.77bc	2.71 ± 0.13ab	2.23 ± 0.77bc	4.13 ± 0.29a	2.24 ± 0.64bc	8.884	$p = 0.002$
TP	0.42 ± 0.08b	0.73 ± 0.07a	0.59 ± 0.03ab	0.52 ± 0.02b	0.72 ± 0.11a	0.59 ± 0.05ab	8.564	$p = 0.002$
TK	5.53 ± 0.45b	8.13 ± 0.53a	7.97 ± 0.54a	8.46 ± 0.6a	8.82 ± 0.71a	9.19 ± 1.02a	11.244	$p < 0.001$
TN	2.21 ± 0.45a	3.56 ± 0.84a	2.79 ± 0.18a	2.73 ± 0.87a	4.08 ± 0.14a	3.97 ± 2.14a	1.626	$p = 0.226$
TOC	45.83 ± 7.5a	52.86 ± 9.26a	38.38 ± 3.19a	34.52 ± 5.59a	45.68 ± 3.09a	53.07 ± 23.29a	1.378	$p = 0.299$
SWC	0.31 ± 0.04b	0.39 ± 0.01ab	0.37 ± 0.02ab	0.37 ± 0.01ab	0.4 ± 0.01ab	0.43 ± 0.07a	3.711	$p = 0.029$
ST	14.6 ± 0.5a	9.5 ± 0.4cd	9.5 ± 0.6cd	10.87 ± 0.57b	8.83 ± 0.12d	10.53 ± 0.35bc	63.241	$p < 0.001$
EOC	15.06 ± 3.46a	23.27 ± 4.61a	14.35 ± 1.77a	12.92 ± 3.69a	16.97 ± 1.48a	22.1 ± 13.35a	1.431	$p = 0.282$
DOC	48.29 ± 8.57b	186.77 ± 41.99a	190.51 ± 44.37a	235.17 ± 49.43a	146.46 ± 17.66ab	147.4 ± 42.5ab	8.654	$p = 0.002$
POC	18.68 ± 2.85a	17.05 ± 6.62a	10.99 ± 3.57a	19.7 ± 12.97a	27.84 ± 5.99a	47.63 ± 35.36a	1.982	$p = 0.153$

Different lowercase letters indicate significant differences among different elevations ($p < 0.05$)

http://www.aloki.hu ● ISSN 1589 1623 (Print) ● ISSN 1785 0037 (Online)
DOI: http://dx.doi.org/10.15666/aeer/2005_41214143

THE POTENTIAL APPLICABILITY OF NATURAL MINERALS AS FILTER MEDIA FOR MODULATING WATER QUALITY IN AQUATIC ECOSYSTEMS

ÖZ, M.[1] – ŞAHIN, D.[2*] – YILMAZ, E.[3] – ÖZ, Ü.[4]

[1]*Department of Aquaculture, Fisheries Faculty, Sinop University, 57000 Sinop, Turkey*

[2]*Vocational School, Sinop University, 57000 Sinop, Turkey*

[3]*Fatsa Faculty of Marine Sciences, Ordu University, 52400 Fatsa, Ordu, Turkey*

[4]*Department of Hydrobiology, Fisheries Faculty, Sinop University, 57000 Sinop, Turkey*

**Corresponding author*
e-mail: dsahin@sinop.edu.tr; phone: +90-533-483-4093

(Received 19th Apr 2022; accepted 11th Jul 2022)

Abstract. The optimal water quality requirement varies among species, and natural filtration materials can be used in aquatic systems to provide and maintain species-specific water quality parameters. Ammonia is one of the nitrogenous compounds originating from the metabolic wastes of aquatic organisms in aquatic ecosystems. Toxic substances and ammonia can be controlled in various ways by ion exchange and adsorption. In this study, the effects of natural clinoptilolite and diatomite on fresh water parameters were determined. This investigation was conducted by trial groups with 3 replicates for 16 days in two experimental systems. For the first experimental group, 3 g of raw zeolite (Z) was directly placed in a 500 ml freshwater aquarium, and the second experimental group was arranged with 3 g of raw diatomite (D) under the same conditions. The third experimental group was described as the control group (C) without zeolite and diatomite. Water parameters (such as pH and ammonium) were determined daily during the experiment period (8 days). After experiment 1, when zeolite and diatomite reached saturation, a desorption system was created with 3 groups containing 3 replicates, and this period was named experiment 2. During the 8-day period, water parameters were determined 7 times. At the end of the study, it was found that the NH_4^+-N concentrations different statistically ($P < 0.05$). pH, temperature and oxygen values did not vary among the experimental groups ($P > 0.05$). The results suggested that zeolite and diatomite have good adsorption performance for NH_4^+-N removal from the aqueous environment.
Keywords: *zeolite, diatomite, aquatic environment, ammonium, adsorption, freshwater*

Introduction

Optimum water quality parameters should always be constant to ensure the growth and health of fish in aquaculture. Ensuring optimum water quality is a critical factor, especially in aquarium conditions (Devi et al., 2017). In aquaculture systems, water quality parameters tend to deviate from a suitable range due to the metabolic waste of live animals and waste materials originating from uneaten feed (Hlordzi et al., 2020). In fish culture systems, it is known that the main wastes are excessive fish feed and feces. Various studies have reported that the amount of waste resulting from feces and unconsumed feed in intensive culture is approximately 10-30% (Kibria et al., 1997). In the ammonium adsorption process, water temperature and pH are efficient water quality parameters in fresh water. In sustainable aquaculture, pH values are slightly acidic for some species, while some species live in more alkaline waters. The water temperature values vary between 10-23 °C for warm water fish and 23-28 °C for tropical fish species. Freshwater culture medium and ambient conditions thought to be suitable for

http://www.aloki.hu ● ISSN 1589 1623 (Print) ● ISSN 1785 0037 (Online)
DOI: http://dx.doi.org/10.15666/aeer/2005_41454155

ammonia removal by natural adsorbents were created in this study. To maintain aquarium water conditions, proper filtration techniques and materials must be used (Öz et al., 2016).

Biological and chemical treatment is one of the methods used to remove ammonia. Materials such as marine and freshwater sand, shellfish, and activated carbon are used to prepare a substrate in the bacterial ammonia removal process (Aly et al., 2016). Ion exchange is a reversible chemical reaction in which an ion bound to a solid is exchanged for an ion in solution. While the ions on the solid surface pass into the solution, the ions in the solution are bound to the surface of the solid by electrostatic forces. This exchange process continues until the concentrations of the two types of ions on the surface and in the solution reach an equilibrium (Zain et al., 2018; Aly et al., 2016).

Natural adsorbent materials, such as zeolite, bentonite, and diatomite, can be used as filtration materials in aquarium filtration systems or as substrate materials on aquarium floors (Öz et al., 2021). Determining the application properties of these natural materials as filtration, decoration and plant ground materials in aquariums will make a multifaceted contribution to the regulation of aquarium ecosystems. Especially for recirculatory systems for intensive cultivation, these natural materials have some advantages to ensure and maintain the necessary balance between water parameters and aquatic species. These are economy, physico-chemical properties, easy availability, increasing efficiency by processing, sizing, not causing dispersion or turbidity in water, and use with different decoration features (Eroğlu et al., 2017; AbuKhadra et al., 2020).

Zeolite is a naturally occurring rock that has a fairly unique structure with large internal cavities and entry channels that are easily filled with water, air, and other molecules. They have strong capacities to adsorb and desorb molecules that allow for rapid uptake and loss of charged particles. Zeolite is relevant to aquaculture (Ramesh et al., 2011; Aly et al., 2016).

Clinoptilolite has a limited capacity to adsorb ammonia, and when it reaches saturation, it can be made ready for reuse by soaking in a suitable solution. This process can be repeated several times (Aly et al., 2016).

Diatomite is a low-cost silica material of soft sedimentary rock that is abundantly available. It is a porous material with low density and constitutes mainly silicon dioxide. Although diatomite has a unique combination of physical and chemical properties, its use as an adsorbent in wastewater treatment has not been extensively investigated (Ahmad et al., 2019; Bakr, 2010). As a result, diatomite is nontoxic and odorless, present naturally in large quantities with high purities, and subsequently available at low cost (Bello et al., 2014). In this study, which will be one of the first studies made with diatomite in aquaculture, primarily a study on ammonia originating from fish feed was planned. This research aimed to determine the potential applicability of natural adsorbents in aquaculture environment conditions by examining the effects of natural adsorbents [zeolite (clinoptilolite) and diatomite] on important parameters, such as ammonium, pH and dissolved oxygen.

Materials and methods

Adsorbent materials

Raw (no preconditioning was applied) zeolite and diatomite were tested for their capability of adsorbing ammonia or effects on dissolved oxygen and pH in a freshwater

http://www.aloki.hu ● ISSN 1589 1623 (Print) ● ISSN 1785 0037 (Online)
DOI: http://dx.doi.org/10.15666/aeer/2005_41454155

aquarium. Zeolite (Clinoptilolite) and diatomite were provided by the Gordes Mining Company, Manisa, Turkey and Nanotech inşaat Kimya Maden ve Lojistic San. Tic. A.Ş., respectively. In this study, Anatolian zeolite (clinoptilolite) and diatomite were used, and their chemical compositions are shown in *Table 1*. The clinoptilolite and diatomite used in the experiment were characterized by SEM/XRF/BET (*Fig. 1*). These analyses were performed in the Kastamonu University Central Research Laboratory. pH values were calculated according to Tokat (2019) and Güneş (2017).

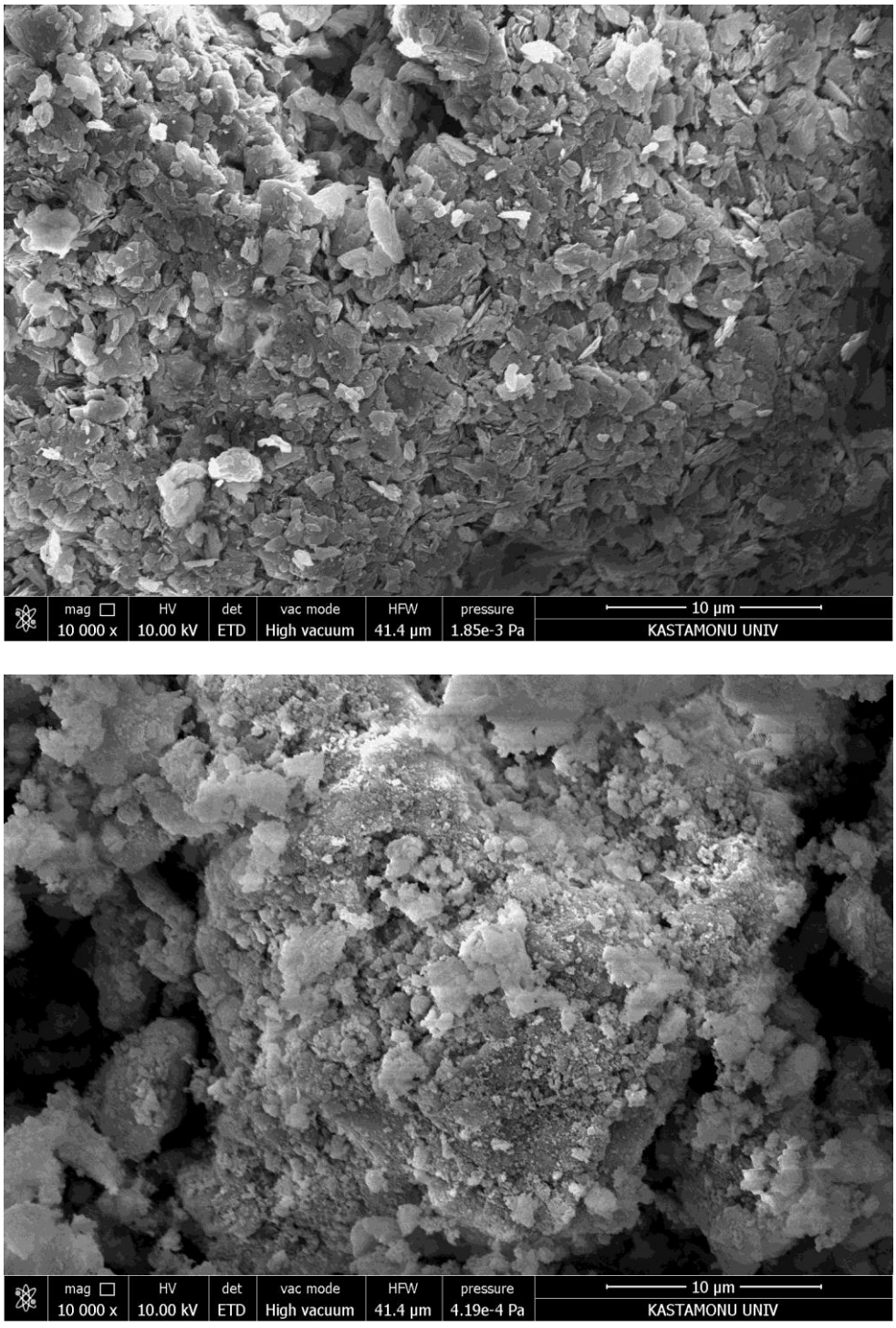

Figure 1. *SEM analysis of clinoptilolite (a) and diatomite (b)*

http://www.aloki.hu ● ISSN 1589 1623 (Print) ● ISSN 1785 0037 (Online)
DOI: http://dx.doi.org/10.15666/aeer/2005_41454155

Table 1. *XRF values of clinoptilolite and diatomite*

	Clinoptilolite composition	**Diatomite composition**
SiO_2 (%)	78.41	81.66
Al_2O_3 (%)	13.83	10.02
MgO (%)	1.646	3.839
K_2O (%)	2.372	0.99
CaO (%)	3.885	2.041
Na_2O (%)	1.042	1.261
Fe_2O_3 (%)	1.414	2.291
P_2O_5 (%)	0.058	0.243
SiO_2/Al_2O_3	5.67	8.149
BET Surface Area	34.316 m^2/g	174.698 m^2/g
pH	8.31	7.06

Experiment period 1

The main sources of ammonia in aquaculture are fish metabolic wastes and unconsumed feed. In this study, unconsumed feed was used as a source of ammonia. Tap water with the same characteristics was used in all groups. Experiments were conducted in plastic aquariums with 500 ml of water, 0.5 g fish feed (47.5% crude protein, 6.5% crude fat, 2% cellulose and 6% moisture 6%), and 3 g natural adsorbent. The experiment was carried out in 3 groups. Zeolite at 3 g/500 ml water was placed in the experimental aquariums for the first group (Z), while for the second group (D), diatomite was placed in the experimental aquariums at 3 g/500 ml water. Zeolite and diatomite were not used in the third group (control, C). The experiment was designed in triplicate (Zain et al., 2018) for each group without any fish or aeration. Water parameters values were determined in the beginning of this study, and all water parameter values were determined each day during the first experiment period.

Experiment period 2

After experiment 1, where zeolite and diatomite had reached saturation, a desorption system was created, and 3 groups were formed with 3 replicates; this period was named experiment 2. During this 8-day period, water parameters were determined 7 times. Saturated zeolite (3 g) and diatomite (3 g) in the first period were placed inside 500 ml tap water for the SZ (saturated zeolite) and SD (saturated diatomite) groups. Zeolite and diatomite were not used in the third group (control, C), and in experiment 2, a control group without feed was formed, and no further application was made until the end of the 2nd experiment (*Fig. 2*).

The physico-chemical quality of the water in the experimental aquariums was monitored at the same time daily. Experimental data were determined using the multi-parameter YSI Professional Instrument.

During the study, NH_3 and TAN (total ammonia nitrogen) ($TAN = NH_3 + NH_4$) levels were calculated using NH_4^+, pH and water temperature values were also determined (Purwono et al., 2017).

The water parameters were statistically checked with one-way analysis of variance (ANOVA) and the means were compared at 5% ($p < 0.05$) significance level using the Tukey test. The results were analyzed statistically with the "Minitab Release 17 for Windows" software (Nanda et al., 2021).

http://www.aloki.hu ● ISSN 1589 1623 (Print) ● ISSN 1785 0037 (Online)
DOI: http://dx.doi.org/10.15666/aeer/2005_41454155

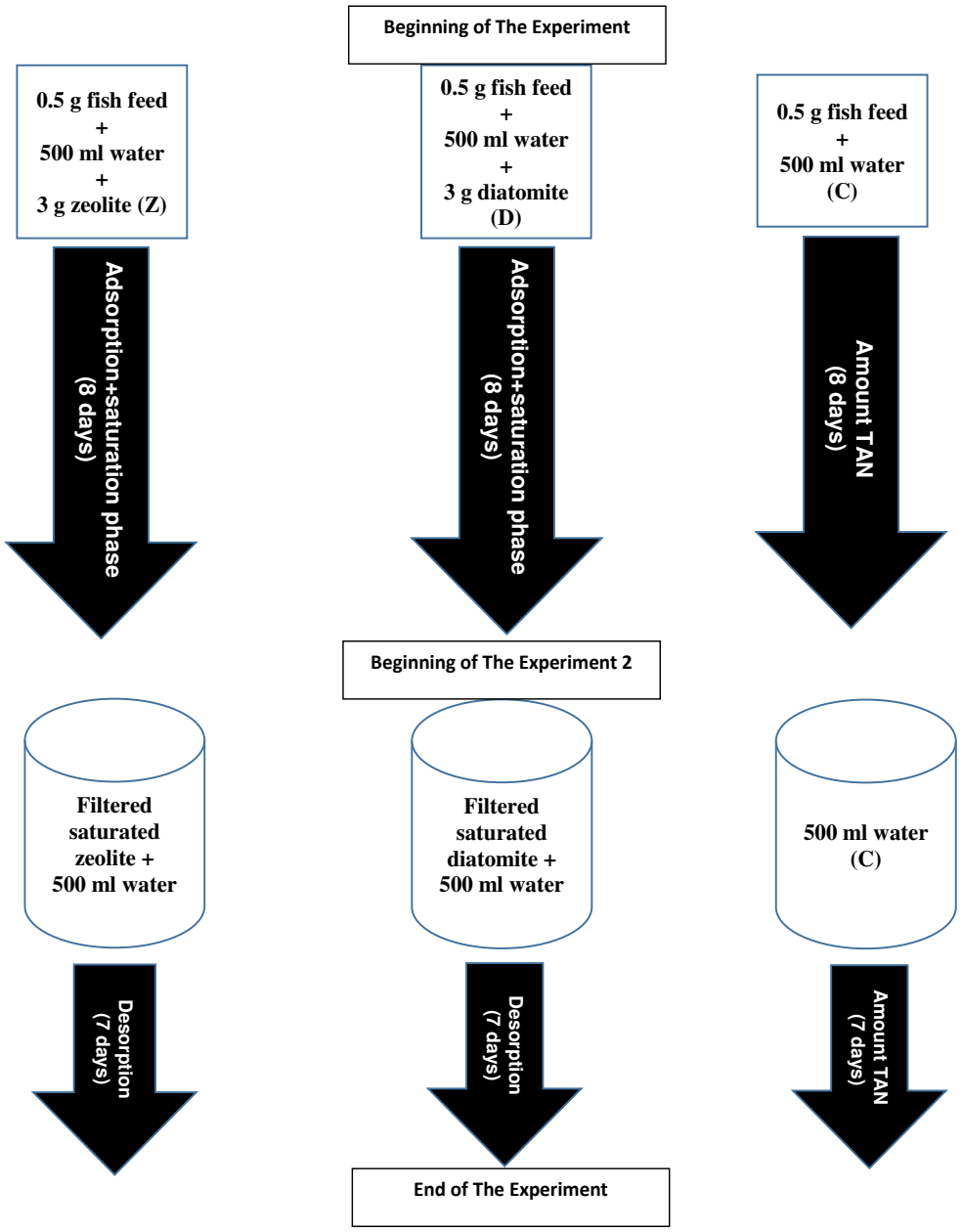

Figure 2. *Flowchart detailing experimental design*

Results

Tap water with the same characteristics was used in all groups. At the beginning of the study, water temperature, dissolved oxygen, pH and ammonium were determined to be 21.7 ± 0.01 °C, 2.84 ± 0.01 mg/l, 8.20 ± 0.01 and 0.4 ± 0.01 mg/l, respectively, in all groups.

The water quality parameters determined at the end of experiment 1 are summarized in *Table 2*. At the end of the first experiment, although the differences between groups (Z, D, C) regarding water temperature, pH and dissolved oxygen were statistically insignificant ($p > 0.05$), there was a difference among groups in values of NH_4^+-N levels (Z, C) ($p < 0.05$).

http://www.aloki.hu ● ISSN 1589 1623 (Print) ● ISSN 1785 0037 (Online)
DOI: http://dx.doi.org/10.15666/aeer/2005_41454155

Table 2. *Water parameters at the end of the first experimental period (adsorption) (mean ± SE)*

Experimental groups*	Temperature (°C)	Dissolved Oxygen (mg/l)	pH	NH_3 (mg/l)	NH_4^+-N (mg/l)	TAN (mg/l)
Z (Zeolite)	20.26 ± 0.28	0.44 ± 0.15	7.67 ± 0.07	0.22 ± 0.05	8.60 ± 1.50^{b}	8.83 ± 1.55^{b}
D (Diatomite)	20.08 ± 0.26	0.47 ± 0.15	7.70 ± 0.07	0.34 ± 0.09	11.73 ± 2.46^{ab}	12.07 ± 2.55^{b}
C (Control)	20.17 ± 0.25	0.47 ± 0.16	7.66 ± 0.08	0.44 ± 0.12	18.53 ± 3.58^{a}	18.97 ± 3.68^{b}

*Superscript letters in a column indicate significant ($p < 0.05$) differences between experimental groups. Means were tested by ANOVA and ranked by Tukey's multiple range test

At the end of the first experiment, TAN values in water were determined to be 8.83 ± 1.55, 12.07 ± 2.55 and 18.97 ± 3.68 for the Z, D, and C groups, respectively. When these values were examined statistically, it was found that the two groups were different ($p < 0.05$) compared to the control group. Likewise, using TAN data obtained from the three experimental groups, TAN concentrations decreased by 57.57 ± 0.41% in the Z group and 27.21 ± 3.34% in the D group compared to the control group. At the beginning of experiment 2, water temperature, dissolved oxygen, pH and ammonium were determined to be 19.2 ± 0.01 °C, 2.79 ± 0.01 mg/l, 8.60 ± 0.01 and 0.2 ± 0.01 mg/l, respectively, in all groups. The water quality parameters determined at the end of the second experiment are presented in *Table 3*. At the end of the second experiment, TAN values in water were determined to be 3.21 ± 0.30, 3.90 ± 0.29 and 0.30 ± 0.01 for the Z, D, and C groups, respectively. When these values were examined statistically, it was found that the two groups were different ($p < 0.05$) compared to the control group.

Table 3. *Water parameters at the end of the second experimental period (desorption) (mean ± SE)*

Experimental groups*	Temperature (°C)	Dissolved Oxygen (mg/l)	pH	NH_3 (mg/l)	NH_4^+-N (mg/l)	TAN (mg/l)
Z (Zeolite)	20.18 ± 0.21	0.55 ± 0.03	8.48 ± 0.02	0.37 ± 0.04^{a}	2.84 ± 0.26^{a}	3.21 ± 0.10^{a}
D (Diatomite)	19.87 ± 0.22	0.57 ± 0.03	8.47 ± 0.02	0.42 ± 0.04^{a}	3.48 ± 0.26^{a}	3.90 ± 0.29^{a}
C (Control)	19.75 ± 0.22	0.63 ± 0.03	8.52 ± 0.02	0.03 ± 0.00^{b}	0.24 ± 0.01^{b}	0.30 ± 0.01^{b}

*Superscript letters in a column indicate significant ($p < 0.05$) differences between experimental groups. Means were tested by ANOVA and ranked by Tukey's multiple range test

When the 1st and 2nd experiments were evaluated together, the ammonia concentration started to differ between the groups on and after the 4th day, and the adsorbent groups had lower concentrations than the control group. With the saturation of adsorbents on the 8th day of study, the 2nd trial period started, and when zeolite and diatomite, which reached saturation at the end of experiment 1, were taken into the fresh water in experiment 2, it was determined that some of the NH_3 adsorbed was released to the water as 0.51 and 0.49 mg/l, respectively (*Fig. 3*). The base ANOVA tables were given in *Table 4* for experiment 1 and 2.

http://www.aloki.hu ● ISSN 1589 1623 (Print) ● ISSN 1785 0037 (Online)
DOI: http://dx.doi.org/10.15666/aeer/2005_41454155

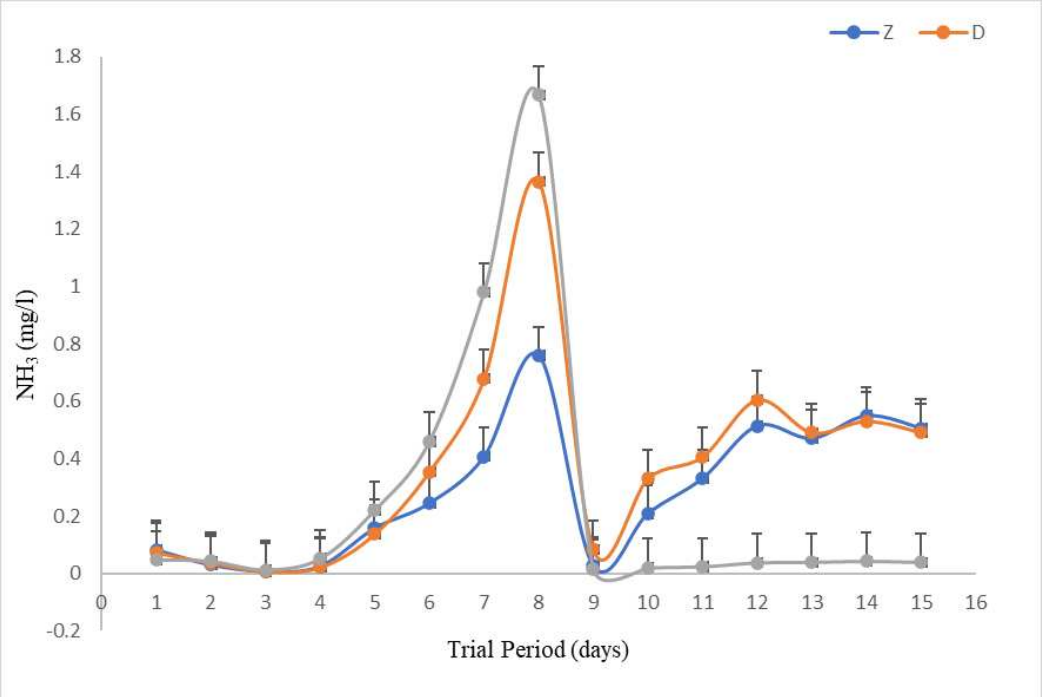

Figure 3. *NH_3 exchange during the experimental period (15 days)*

Table 4. *The base ANOVA tables for the first (adsorption) and second experimental period (desorption)*

Experimental groups*	Df	Adj SS	Adj MS	F	P
First experiment	2	1234	617.2	3.66	0.03
Second experiment	2	123.57	61.78	64.83	0.01

Discussion

This study focused on testing two different natural adsorbents, zeolite and diatomite, and their efficiency in removing ammonium cations from freshwater environments. TAN is the sum of NH_3 and NH_4. NH_3 values are important for fisheries. Therefore, in this study, TAN, which shows the total values, and NH_3 values, which are important for fisheries, were examined.

Metabolic wastes of aquatic organisms and unconsumed feeds are among the most important factors affecting water quality in aquaculture (Boyd, 1990).

The potential to use natural zeolite mineral, which is used as a filtration material, has increased rapidly in recent years due to a natural, economical and effective ammonia removal. Many studies have been conducted on the use of natural zeolite mineral in water treatment (Jorgersen and Weatherley, 2003; Mazeikiene et al., 2008; Öz et al., 2017).

Diatomite is a low-cost silica material of soft sedimentary rock that is abundantly available. It is a porous material with low density and constitutes mainly silicon dioxide. There are studies conducted on hydrogen sulfide (Ahmad et al., 2019), heavy metal (Şenol and Şimşek, 2020; ElSayed, 2018) or ammonium (Luo et al., 2011; Khadra et al., 2020) retention by raw or processed diatomite.

http://www.aloki.hu ● ISSN 1589 1623 (Print) ● ISSN 1785 0037 (Online)
DOI: http://dx.doi.org/10.15666/aeer/2005_41454155

Ammonium adsorption of natural adsorbents changes with the amount, pore size, surface area, and mining area of minerals, initial concentration, pH, temperature, and presence of other cations in the solution (Huang et al., 2017).

Many factors are effective in ammonia removal using natural adsorbents, such as zeolite and diatomite. These factors include the amount of adsorbent, its size, preliminary applications, and the temperature of the environment, pH, other competitor ions or the concentration of the substance to be removed. At the end of the first experiment (adsorption), groups containing raw zeolite (Z) and raw diatomite (D) had lower ammonia values (8.6 ± 1.50 and 11.73 ± 2.46 mg/l, respectively), whereas the control group had a higher ammonia value (18.53 ± 3.58 mg/l). The final of the second trial period (desorption), the Z and D groups had higher ammonia values of 2.84 ± 0.26 mg/l and 3.48 ± 0.26 mg/l, respectively. The control group contained the lowest ammonia value (0.24 ± 0.01 mg/l) compared to the adsorbent-added groups.

In this study, the TAN removal percentages of crude zeolite and crude diatomite were found to be $57.57 \pm 0.41\%$ and $27.21 \pm 3.34\%$, respectively, compared to the control group. Similar to our study, Zhou and Boyd (2014) found a TAN removal percentage of 43% in zeolite. Clinoptilolite and diatomite exchange ions in their structures with ammonium ions in the aquatic environment. Thus, it reduces the amount of ammonia in the water and prevents it from rising to harmful levels (Ghiasi and Jasour, 2012; Khadra et al., 2020).

One of the most important water parameters affecting production in aquaculture is total ammonia nitrogen. In closed or circulating aquaculture systems, among the main causes of diseases and fish deaths, nitrogenous compounds produced by the deterioration of feces and uneaten fish feed (El-Gendy et al., 2015). It has been determined that the harmful efficients of ammonia (NH_3) for short-term effect is generally between 0.6 and 2.0 mg/L for aquaculture, and non-lethal effects can occur between 0.1 and 0.3 mg/L. It has been suggested that the tolerable ammonia limit for aquaculture should be lower than 0.2 mg/L (Bhatnagar and Devi, 2013). In general, it was determined that ammonium in the water was adsorbed by the adsorbents in the 1st experiment and that ammonia retained by the adsorbents was released into the water in the 2nd experiment. In this study, on the 5th day, the NH_3 level was approximately 0.1 mg/l in the zeolite and diatomite groups, while this value was found to be 0.2 mg/l in the control group. From the 6th day, the NH_3 values of the diatomite group were higher than those of the zeolite group but remained at lower levels than those of the control group. On the 8th day, it was determined that the adsorbents reached saturation and the adsorption efficiency decreased. In the second period, it was ascertained that diatomite and clinoptilolite could release some of the adsorbed NH_3, and this result was similar to the results of Henstrom and Amofah (2008) and Öz et al. (2017).

Conclusion

Controlling the data in the study revealed that when the zeolite and diatomite reached saturation, they desorbed as dramatically as the amount of ammonium they retained. As soon as clinoptilolite and diatomite reach saturation, they can be used again by keeping them in salt water and similar solutions. In intensive aquaculture systems or aquarium conditions, based on the present results, zeolite and diatomite should be used after being processed for the required period and ready for readsorption.

http://www.aloki.hu ● ISSN 1589 1623 (Print) ● ISSN 1785 0037 (Online)
DOI: http://dx.doi.org/10.15666/aeer/2005_41454155

It has been reported that zeolite can be used effectively for ammonia removal in aquaculture for a long time, studies on ammonia removal with diatomite are more recent, with limited information available. Even the number of studies related to aquaculture is deficient. In this regard, the results of this study indicated that diatomite can be used effectively in ammonia removal, especially for aquaculture. In future research, application processes, such as preconditioning or the use of mixed adsorbents, can be investigated to increase the efficiency of both zeolite and diatomite in conditions with ammonia, pH and water temperature suitable for aquaculture.

Acknowledgment. We would like to express our appreciation to the company, Gordes Mining Company, and Nanotech İnşaat Kimya Maden ve Lojistic San. Tic. A.Ş for providing us with the zeolite and diatomite trial materials.

REFERENCES

[1] AbuKhadra, M. R., Eid, M. H., Allam, A. A., Ajarem, J. S., Almalki, A. M., Salama, Y. (2020): Evaluation of different forms of Egyptian diatomite for the removal of ammonium ions from Lake Qarun: a realistic study to avoid eutrophication. – Environmental Pollution 266: 115277. https://doi.org/10.1016/j.envpol.2020.115277.

[2] Ahmad, W., Sethupathi, S., Noraini, M. S. N., Bashir, M. J. K., Chun, C. Y. (2019): Hydrogen sulfide removal using diatomite. – 6th International Conference on Environment (ICENV2018) AIP Conf Proc 2124: 020005-1-020005-8; https://doi.org/10.1063/1.5117065.

[3] Aly, H. A., Abdel Rahim, M. M., Lotfy, A. M., Abdelaty, B. S., Sallam, G. R. (2016): The Applicability of Activated Carbon, Natural Zeolites, and Probiotics and Its Effects on Ammonia Removal Efficiency and Fry Performance of European Seabass *Dicentrarchus labrax*. – Journal of Aquaculture Research and Development 7(11): 8. https://doi.org/10.4172/2155-9546.1000459.

[4] Bakr, H. E. G. M. M. (2010): Diatomite: Its Characterization, Modifications and Applications. – Asian Journal of Material Science 2(3): 121-136. ISSN 1996-3394.

[5] Bello, O. S., Adegoke, K. A., Oyewole, R. O. (2014): Insights into the Adsorption of Heavy Metals from Wastewater using Diatomaceous Earth. – Separation Science and Technology 49: 1787-1806.

[6] Bhatnagar, A., Devi, P. (2013): Water quality guidelines for the management of pond fish culture. – International Journal of Environmental Science 3(6): 1980-2009.

[7] Boyd, C. E. (1990): Water Quality in Ponds for Aquaculture. – Auburn University, Alabama Agricultural Experiment Station, Auburn, AL, Pres. 482 (taken from: Boyd, C. E. (1997): Practical Aspects of Chemistry in Pond Aquaculture. The Progressive Fish Culturist 59: 85-93).

[8] Devi, P. A., Padmavathy, P., Aanand, S., Aruljothi, K. (2017): Review on water quality parameters in freshwater cage fish culture. – International Journal of Applied Research 3(5): 114-120.

[9] El-Gendy, M., Gouda, A., Shehab El-Din, M. (2015): Effect of zeolite on feeding rates and growth performance for nile tilapia (*Oreochromis niloticus*). – International Journal of Scientific Research in Agricultural Sciences 2: 18-24.

[10] ElSayed, S. B. (2018): Natural diatomite as an effective adsorbent for heavy metals in water and wastewater treatment (a batch study) – Water Science 32: 32-43. https://doi.org/10.1016/j.wsj.2018.02.001.

http://www.aloki.hu ● ISSN 1589 1623 (Print) ● ISSN 1785 0037 (Online)
DOI: http://dx.doi.org/10.15666/aeer/2005_41454155

[11] Eroglu, N., Emekci, M., Athanassiouc, C. G. (2017): Applications of natural zeolites on agriculture and food production. – Journal of Science and Food Agriculture. https://doi.org/10.1002/jsfa.8312.
[12] Ghiasi, F., Jasour, M. (2012): Effects of natural Zeolite (Clinoptilolte) on water quality, growth performance and nutritional parameters of fresh water aquarium fish, angel (*Pterophyllum scalare*). – International Journal of Research in Fisheries and Aquaculture 2(3): 22-25.
[13] Güneş, Ö. (2017): Determination of usage characteristics of Isparta-Keçiborlu Amorphous silica deposits in the field of agricultural technologies (Isparta-keçiborlu amorf silis yataklarının tarım teknolojileri alanında kullanım özelliklerinin belirlenmesi). – Master Thesis, Süleyman Demirel University Institute of Science (in Turkish).
[14] Hedstrom, A., Amofah, L. R. (2008): Adsorption and desorption of ammonium by clinoptilolite adsorbent in municipal wastewater treatment systems. – Journal of Environmental Engineering and Science 7: 53-61.
[15] Hlordzi, V., Kuebutornye, F. K. A., Afriyie, G., Abarike, E. D., Lu, Y., Chi, S., Anokyewaa, M. A. (2020): The use of Bacillus species in maintenance of water quality in aquaculture: a review. – Aquaculture Reports 18: 100503. https://doi.org/10.1016/j.aqrep.2020.100503.
[16] Huang, J., Kankanamge, N. R., Chow, C., Welsh, D. T., Li, T., Teasdale, P. R. (2017): Removing ammonium from water and wastewater using cost-effective adsorbents: a review. – Journal of Environmental Sciences 63: 174-197.
[17] Jorgersen, T. C., Weatherley, L. R. (2003): Ammonia removal from wastewater by ion exchange in the presence of organic contaminants. – Water Research 37(8): 1723-1728. https://doi.org/10.1016/S0043-1354(02)00571-7.
[18] Khadra, M. R. A., Eid, M. H., Allam, A. A., Ajarem, J. S., Almalki, A. M., Salama, Y. (2020): Evaluation of different forms of Egyptian diatomite for the removal of ammonium ions from Lake Qarun: a realistic study to avoid eutrophication. – Environmental Pollution 266(2): 1-14. https://doi.org/10.1016/j.envpol.2020.115277.
[19] Kibria, G., Nugegoda, D., Fairclough, R., Lam, P. (1997): The nutrient content and the release of nutrients from fish food and faeces. – Hydrobiologia 357: 165-171.
[20] Luo, Z., Yuan, X., Yuan, D., Chen, L. (2011): A study on modified diatomite treatment the wastewater of ammonia nitrogen. – IEEE Xplore 978-1-4244-9171-1/11.
[21] Mazeikiene, A., Valentukeviciene, M., Rimeika, M., Matuzevicius, A. B., Dauknys, R. (2008): Removal of nitrates and ammonium ions from water using natural sorbent: Zeolites (clinoptilolite). – Journal of Environmental Engineering and Landscape Management 16(1): 38-44. https://doi.org/10.3846/1648-6897.2008.16.38-44.
[22] Nanda, A., Mohapatra, B. B., Mahapatra, A. P. K., Mahapatra, A. P. K., Mahapatra, A. P. K. (2021): Multiple comparison test by Tukey's honestly significant difference (HSD): do the confident level control type I error. – International Journal of Statistics and Applied Mathematics 6(1): 59-65. https://doi.org/10.22271/maths.2021.v6.i1a.636.
[23] Öz, M., Şahin, D., Aral, O. (2016): The effect of natural zeolite clinoptilolite on aquarium water conditions. – Hacettepe Journal of Biology and Chemistry 44(2): 205-208.
[24] Öz, M., Şahin, D., Öz, Ü., Karslı, Z., Aral, O. (2017): Investigation of ammonium saturation and desorption conditions of clinoptilolite type zeolite in aquarium conditions. – Turkish Journal of Agriculture-Food Science and Technology 5(12): 1590-1594. https://doi.org/10.24925/turjaf.v5i12.1590-1594.1670.
[25] Öz, M., Şahin, D., Karslı, Z., Aral, O., Bahtiyar, M. (2021): Investigation of the Use of Zeolite (Clinoptilolite) As aquarium filtration material for electric blue hap (*Sciaenochromis ahli*). – Marine Science and Technology Bulletin 10(2): 207-212. https://doi.org/10.33714/masteb.895198.
[26] Purwono, Rezagama, A., Hibbaan, M., Budihardjo, M. A. (2017): Ammonia-nitrogen (NH_3-N) and ammonium-nitrogen (NH_4^+-N) equilibrium on the process of removing

http://www.aloki.hu ● ISSN 1589 1623 (Print) ● ISSN 1785 0037 (Online)
DOI: http://dx.doi.org/10.15666/aeer/2005_41454155

nitrogen by using tubular plastic media. – Journal of Materials and Environmental Science 8(S): 4915-4922.

[27] Ramesh, K., Biswas, A. K., Rao, A. S. (2011:) Zeolites and their potential uses in agriculture. – Advances in Agronomy 113:215-236. https://doi.org/10.1016/B978-0-12-386473-4.00009-9.

[28] Şenol, Z. M., Şimşek, Ş. (2020): Removal of Pb2+ ions from aqueous medium by using chitosan- diatomite composite: equilibrium, kinetic, and thermodynamic studies. – JOTCSA 7(1): 307-318. https://doi.org/10.18596/jotcsa. 634590.

[29] Tokat, S. (2019): Determination of Chemical Components of Zeolite Quarries in Gördes (Manisa) by Xrf Spectrometric Method (Gördes (Manisa) zeolit ocaklarının kimyasal bileşenlerinin xrf spektrometrik yöntem ile belirlenmesi). – Kastamonu University Institute of Science, Kastamonu (in Turkish).

[30] Zain, R. A. M. M., Shaari, N. F. I., Amin, M. F. M., Jani, M. (2018): Effects of different dose of zeolite (clinoptilolite) in improving water quality and growth performance of red hybrid tilapia (*Oreochromis* sp.). – ARPN Journal of Engineering and Applied Sciences 13(24): 9421-9426.

[31] Zhou, L., Boyd, C. E. (2014): Total ammonia nitrogen removal from aqueous solutions by the natural zeolite, mordenite: a laboratory test and experimental study. – Aquaculture 432: 252-257. https://doi.org/10.1016/j.aquaculture.2014.05.019.

http://www.aloki.hu ● ISSN 1589 1623 (Print) ● ISSN 1785 0037 (Online)
DOI: http://dx.doi.org/10.15666/aeer/2005_41454155

GGE BI-PLOT ANALYSIS OF HIGH-ZINC RICE (*ORYZA SATIVA* L.) GENOTYPES UNDER MULTIPLE ENVIRONMENTS FOR GRAIN YIELD

BEHERA, P. P.[1,2] – SINGH, S. K.[1] – MAJHI, P. K.[3*] – SARMA, R. N.[2] – SIVASANKARREDDY, K.[2] – PATRA, B.[4] – BORAH, N.[5] – SAHARIA, N.[2] –AHAMAD, A.[6]

[1]*Department of Genetics and Plant Breeding, Institute of Agricultural science, Banaras Hindu University, Varanasi 221005, Uttar Pradesh, India*
(e-mail: shravanbhu1964@gmail.com (Singh, S. K.))

[2]*Department of Plant Breeding and Genetics, Assam agricultural University, Jorhat 785013, Assam, India*
(e-mail: parthapratimbehera44@gmail.com, ORCID: https://orcid.org/0000-0001-5050-5400 (Behera, P. P.); ramendra.sarma@aau.ac.in (Sarma, R. N.); sivagpb@gmail.com (Sivasankarreddy, K.); niharikasaharia10@gmail.com (Saharia, N.))

[3]*Department of Plant Breeding and Genetics, Regional Research and Technology Transfer Station, Odisha University of Agriculture and Technology, Keonjhar 758002, Odisha, India*
(e-mail: prasantakumarmajhi53@gmail.com, ORCID: https://orcid.org/0000-0001-6412-6452 (Majhi, P. K.))

[4]*Center for Biotechnology, Siksha 'O' Anusandhan Deemed to be University, Bhubaneswar 751003, Odisha, India*
(e-mail: patrabiswaranjan37@gmail.com)

[5]*Assam Don Bosco University, Guwahati 782402, Assam, India*
(e-mail: bora.nayanmoni54@gmail.com)

[6]*Nuclear Agriculture and Biotechnology Division, Bhabha Atomic Research Centre (BARC), Mumbai 400094, Maharashtra, India*
(e-mail: ayazahamad2013@gmail.com)

[*]*Corresponding author*
e-mail: prasantakumarmajhi53@gmail.com; phone: +91-890-803-3010
ORCID: https://orcid.org/0000-0001-6412-6452

(Received 24th Apr 2022; accepted 11th Jul 2022)

Abstract. Bi-plot analysis has been a popular method for determining the magnitude of the genotype-environment (G × E) interaction in plant breeding and agricultural research. The 21 high-zinc rice genotypes for grain yield per plant (GYP) and grain zinc content (GZC) were evaluated in a complete randomized block design with three replications in Uttar Pradesh, India to identify the winning genotype through multi environmental trials (MET) using GGE bi-plot analysis. The first principal component (PC1) and the second principal component (PC2) each showed 61.56% and 17.25% of the variance, respectively, and together they explained 78.81% of the overall variance. Using GGE bi-plot polygon views, GYP and GZC might each have two feasible mega-environments. In E1 and E2, the genetic information for GYP and GZC was highly correlated and comparable. The genotype V13 (BRRI dhan 72) had the greatest mean GYP and was the most stable, while V8 (IR 96248-16-3-3-2-B) was highly unstable and V17 (IR 64) yielded the least. The greatest GZC and most stable genotypes were found in V1 (IR 95044:8-B-5-22-19-GBS), whereas the highest GZC and most unstable genotypes were found in V19 (Sambamahsuri). For GYP, V20 (Swarna) won only in E3, while V13 (BRRI dhan 72) won in the other environments; for GZC, V3 (IR 99704-24-2-1) won only in E3, while V1 (IR 95044:8-B-5-22-19-GBS) won in the other environments. As

http://www.aloki.hu ● ISSN 1589 1623 (Print) ● ISSN1785 0037 (Online)
DOI: http://dx.doi.org/10.15666/aeer/2005_41574172

a conclusion, in future breeding programmes, the V13 (BRRI dhan 72) for GYP and V1 (IR 95044:8-B-5-22-19-GBS) for GZC might be suggested for cultivar selection and zinc bio-fortification.
Keywords: *genotype-environment (G × E) interaction, grain Zinc content, multi environmental trial, stable genotypes, winner genotypes*

Introduction

Rice (*Oryza sativa* L.) is considered an essential food for humans and it is cultivated all over the world. Rice is consumed by about half of the world's population (Suman et al., 2021). Asia produces about 80% of the world's rice. Despite having the world's largest rice crop area (44.1 million hectares) and a production of 165.3 million tonnes, India's productivity per hectare (3.78 tonnes) is low (Kesh et al., 2021). Zinc concentration in rice is also important. More than 30% of the world's soils are Zinc (Zn) deficient. Legumes are more vulnerable to Zn deficiency, affecting grain production and nutritional quality (Impa et al., 2013). Rice grown on soils lacking in Zn leads to lower yields and nutritional quality. For example, poor plant-accessible Zn soils reduced grain Zn concentration by 80%. Reduced human bioavailability owing to decreasing Zn concentration in grain has increased Zn deficiency in vulnerable areas (Cakmak, 2008a). Agronomic Zn bio-fortification of rice grains is a promising and cost-effective strategy (Zaman et al., 2018). As a result, in the present day, sufficient sustainable production of healthy, safe foods production is challenging task. Demands for higher productivity with micronutrients availability have become a serious concern all over the world.

As a consequence, producing enough nutritious, safe meals in a sustainable manner is a challenging job in today's world. Micronutrient availability has become a key issue globally as productivity demands grow. Rice production has been hampered by a lack of better varieties (early maturing, biotic and abiotic stress resistant and high-yielding genotypes), inadequate soil fertility, and genotype-environment interactions (GEI) that hinder the selection process for several crops, including rice. GEIs for quantitative characteristics like seed yield may lead genotypes to behave differently in different situations (Gurmu et al., 2009). For this purpose, plant breeders use multi-environment trials (MET) to evaluate genotype performance and assess genotype adaptability and stability. Stable genotypes must be able to perform well in ideal conditions and yield well in less favourable environments. Rice cultivars need to be bred in order to measure how well they can adapt and stay stable. While MET collects data on several variables, it generally focuses on only one (usually yield), ignoring data on other features. Even though the observed yield is a result of the influence of genotype (G), environment (E), and genotype environment interaction (GEI), only G and GE matter (GE). Bi-plot analysis is a vital statistical tool in plant breeding and agricultural research. Genotype-by-environment data, defined as noise or a confounding factor, is frequently confined to genotype evaluation based on genotype main effect (G). Some practitioners, such as breeders, biometricians, and quantitative geneticists, still disagree on how GE should be judged. The term "GGE bi-plot" was recently coined, and numerous bi-plot visualisation methodologies were developed to address specific GGE data difficulties (Kaplan et al., 2017).

Diverse studies have validated and then used the GGE bi-plot methodology to analyse data from multi-environment trials, showing the method's effectiveness for selecting optimum stable genotypes. The first two symmetrically scaled principal components, PC1 and PC2, are formed through the singular value decomposition of environment-centered multi-environment trial (MET) data. The GGE biplot graphically displays a MET's G plus

http://www.aloki.hu ● ISSN 1589 1623 (Print) ● ISSN1785 0037 (Online)
DOI: http://dx.doi.org/10.15666/aeer/2005_41574172

GE for easy visual cultivar evaluation and mega-environment identification. In addition, GGE biplot analysis can visually answer most inquiries given to a genotype by an environment table (Yan and Tinker, 2005, 2006). It enables accurate genotype evaluation as well as a full understanding of the target and test environments. An understanding of the target environment as a whole, i.e., whether it is made up of one or several mega-environments, may help determine if GE can be used or avoided. Bi-plot analysis may help evaluate if test conditions within a single mega-environment are informative, representative, and genotype discriminative. Simultaneously, bi-plot analysis may examine genotypes' mean performance as well as their environmental stability. Short-and long-term difficulties may be addressed using GGE biplot analysis of genotype by environment data. The GGE biplot has been used to analyse durum (Kendal and Sener, 2015), maize (Oyekunle et al., 2017), barley (Solonechnyi et al., 2018), sorghum (Gasura et al., 2016), lentil (Karimizadeh et al., 2013), sweet-potato (Mustamu et al., 2018) and Bambara groundnut (Tena et al., 2019; Olanrewaju et al., 2021). So, GGE Bi-plot analysis was used in this study to find the best genotypes and environments based on both average performance and stability for both grain yield per plant and grain zinc content.

Materials and methods

Plant materials

Twenty-one genotypes used in the present study were mentioned in *Table 1*. These genotypes were locally collected from IRRI South Asia Hub, Hyderabad, India and the experiment was conducted at five different locations (*Table 2*) in Uttar Pradesh, India during *Kharif*-2017.

Table 1. *List of high zinc rice genotypes used for the experiment (Source: IRRI South Asia Hub, Hyderabad, India)*

Entry No.	Entry Name	Grain Zinc Content (ppm)	Entry No.	Entry Name	Grain Zinc Content (ppm)
1	IR 95044:8-B-5-22-19-GBS	20.6	12	BRRI dhan 64	24.97
2	IR 84847-RIL 195-1-1-1-1	21.8	13	BRRI dhan 72	20.7
3	IR 99704-24-2-1	14.67	14	DRR Dhan 45	18.13
4	IR 99647-109-1-1	23.7	15	DRR Dhan 48	19.2
5	IR 97443-11-2-1-1-1-1 -B	14.45	16	DRR Dhan 49	17.63
6	IR 97443-11-2-1-1-1-3 -B	23.47	17	IR 64	23.57
7	IR 82475-110-2-2-1-2	24.73	18	MTU1010	21.70
8	IR 96248-16-3-3-2-B	27.18	19	Samba Mahsuri	24.47
9	R-RHZ-7	26.61	20	Swarna	18.89
10	CGZR-1	24.43	21	Local check (HUR3022)	16.9
11	BRRI dhan 62	23.33			

Experimental design

The experiment was laid out in a completely randomized block design with three replications. The weather conditions during the evaluations period from June 2017 to November 2017 were almost normal and favorable for crop growth. All the experiments

http://www.aloki.hu ● ISSN 1589 1623 (Print) ● ISSN1785 0037 (Online)
DOI: http://dx.doi.org/10.15666/aeer/2005_41574172

of five different locations were carried out at irrigated ecosystem and medium upland with transplanted nursery establishment.

Table 2. *Five different environments used for the experiment*

Environment Code	Location Name	Latitude	Longitude	Altitude	Land Type	Avg. Temp. (°C)	Avg. Rainfall (mm)
E1	BHU Agriculture Research farm –I	25.18° N	80.30° E	81M	Up land	27.51	181.4
E2	BHU Agriculture Research farm –II	25.18° N	80.30° E	81M	Low land	27.5	181.5
E3	Bhikaripur	25.26° N	82.83° E	87M	Low land	28.32	187.4
E4	Karsada	25.22° N	82.90° E	85M	Up land	28.88	167.2
E5	Rampur	25.23°N	82.89°E	80M	Up land	29.39	155.8

Cultural practices

The single seedling was transplanted at a 15 cm × 20 cm distance. All the standard recommended cultural practices were followed. Fertilizers were applied as 120 kg N, 60 kg $P_2O_5$and 60 kg K_2O per hectare.

Quantitative and qualitative traits data observations

For all yield and yield attribution variables except days to first flowering, 50% flowering, and maturity, five competing plants were randomly chosen from each row of each genotype in each replication. The performance of the cultivars was assessed using the parameters listed (Grain yield per plant and Grain zinc content) in *Table 3* and *Table 4*. The quantitative features were shown and evaluated as indicated by Biodiversity International (IPGRI and WARDA, 2007).

Table 3. *Mean Grain Yield per Plant (gm) of 21 high zinc rice genotypes in five different environments*

Genotypes	Name of the genotype	E1	E2	E3	E4	E5	Mean
V1	IR 95044:8-B-5-22-19-GBS	10.86	12.92	13.05	7.68	6.01	10.11
V2	IR 84847-RIL 195-1-1-1-1	11.50	13.66	13.74	7.99	6.57	10.69
V3	IR 99704-24-2-1	13.12	15.58	14.33	9.96	8.39	12.27
V4	IR 99647-109-1-1	10.79	12.77	15.28	5.35	5.12	9.86
V5	IR 97443-11-2-1-1-1-1 -B	14.90	17.62	18.01	9.10	9.31	13.79
V6	IR 97443-11-2-1-1-1-3 -B	15.39	18.15	20.30	7.59	9.10	14.11
V7	IR 82475-110-2-2-1-2	12.91	15.30	15.61	8.35	7.66	11.97
V8	IR 96248-16-3-3-2-B	12.22	14.42	17.81	5.09	6.01	11.11
V9	R-RHZ-7	11.25	13.33	15.49	5.88	5.63	10.31
V10	CGZR-1	10.96	13.03	13.57	7.33	5.96	10.17
V11	BRRI dhan 62	10.76	12.76	14.95	5.65	5.21	9.86
V12	BRRI dhan 64	12.73	15.01	18.73	4.98	6.32	11.56
V13	BRRI dhan 72	15.92	18.78	20.36	8.38	9.75	14.64
V14	DRR Dhan 45	12.99	15.33	18.31	5.81	6.80	11.85
V15	DRR Dhan 48	11.52	13.69	13.69	8.07	6.61	10.72
V16	DRR Dhan 49	14.34	16.95	18.11	8.13	8.58	13.22
V17	IR 64	9.63	11.46	12.84	5.96	4.54	8.89
V18	MTU1010	13.67	16.14	18.63	6.56	7.54	12.51
V19	Samba Mahsuri	11.91	14.12	15.11	7.28	6.59	11.00
V20	Swarna	13.85	16.29	21.02	4.47	6.91	12.51
V21	Local check(HUR3022)	13.95	16.49	18.11	7.52	8.09	12.83

http://www.aloki.hu ● ISSN 1589 1623 (Print) ● ISSN1785 0037 (Online)
DOI: http://dx.doi.org/10.15666/aeer/2005_41574172

Table 4. *Mean Grain Zinc content (ppm) of 21 high zinc rice genotypes in five different environments*

Genotypes	Name of the genotype	E1	E2	E3	E4	E5	Mean
V1	IR 95044:8-B-5-22-19-GBS	29.63	27.25	29.00	15.61	32.54	26.81
V2	IR 84847-RIL 195-1-1-1-1	27.63	25.67	28.67	17.62	29.66	25.85
V3	IR 99704-24-2-1	25.23	23.66	27.28	18.43	26.64	24.25
V4	IR 99647-109-1-1	28.79	26.41	27.47	14.22	31.93	25.76
V5	IR 97443-11-2-1-1-1-1 –B	19.61	18.12	17.47	9.84	22.43	17.49
V6	IR 97443-11-2-1-1-1-3 –B	19.88	18.73	20.66	14.60	21.46	19.07
V7	IR 82475-110-2-2-1-2	29.14	26.68	27.40	13.65	32.50	25.87
V8	IR 96248-16-3-3-2-B	27.34	25.16	26.32	14.22	30.25	24.66
V9	R-RHZ-7	25.92	23.95	25.35	14.45	28.54	23.64
V10	CGZR-1	26.57	24.77	27.93	17.77	28.39	25.09
V11	BRRI dhan 62	24.67	22.99	25.32	15.99	26.66	23.13
V12	BRRI dhan 64	26.26	24.24	25.56	14.36	28.96	23.88
V13	BRRI dhan 72	18.26	17.14	17.91	12.26	20.21	17.16
V14	DRR Dhan 45	24.05	22.24	23.20	13.38	26.65	21.90
V15	DRR Dhan 48	21.88	20.48	22.40	14.86	23.72	20.67
V16	DRR Dhan 49	22.13	20.37	20.04	10.76	25.12	19.68
V17	IR 64	24.22	22.40	23.38	13.45	26.82	22.05
V18	MTU1010	22.97	21.24	21.78	12.49	25.63	20.82
V19	Samba Mahsuri	20.07	19.13	22.71	17.63	20.86	20.08
V20	Swarna	17.32	16.37	17.55	12.87	18.94	16.61
V21	Local check(HUR3022)	23.53	21.61	21.36	11.11	26.65	20.85

Nutritional traits data estimation

Grain Zinc content of samples was estimated by Atomic Absorption Spectrophotometer (Thermo Scientific, Model: iCE 3500, Double beam optics, Acetylene flame) in Indian Institute of Rice Research (IIRR), Hyderabad as followed the protocol suggested by the Sahrawat et al. (2002).

Statistical analysis

Multivariate Analysis was carried out in using R (4.0.5) software packages and R studio (Team R, 2019). Multi-trait multi-environment analysis including GGE bi-plot analysis for grain yield per plant (GYP) and grain zinc content (GZC) were analyzed using METAN packages (Olivoto and Lúcio, 2020). The ggplot2 packages were used to create the GGE bi-plot display (Wickham et al., 2016). A mixed ANOVA was performed using genotypes and environmental factors as fixed and random factors, respectively. Based on the singular value decomposition (SVD) of the first two main components, a GGE biplot (Yan et al., 2000) model is:

$$Y_{ij} = \mu + \beta_i + \sum_{n=1}^{K} \lambda_n \xi_{in} \gamma_{jn} + \varepsilon_{ij} \quad \text{(Eq.1)}$$

$$Y_{ij} = \mu + \beta_j + \sum_{n=1}^{k} \lambda_n \xi_{in} \eta_{in} + \varepsilon_{ij} \quad \text{(Eq.2)}$$

http://www.aloki.hu ● ISSN 1589 1623 (Print) ● ISSN1785 0037 (Online)
DOI: http://dx.doi.org/10.15666/aeer/2005_41574172

where Y_{ij} is the mean of genotype *i* in environment *j*; μ is the grand mean; β_i is the environment *j* main effect; *n* is the singular value; λ_n, ξ_{in} and are, respectively, singular value, genotype eigenvectors, and environment eigenvectors for n^{th} interaction principal component; and ε_{ij} is the residual effect.

Grain yield and zinc content were modelled using a mixed linear model (site). The GGE bi-plot study used mean grain yield and zinc content as two-way table data. For ATC, polygon, and vector views, GGE bi-plots employed the first two symmetrically scaled PCs (to visualise the correlations among environments or genotypes). The GGE bi-plots utilised the mean GYP and GZC performances of 21 high zinc rice genotypes (*Table 3*, *Table 4*, *Figure 1*and *Figure 2*). We compared genotypes to ideal environments and environments to ideal genotypes. The "which-won-where" option identified mega-environments and winning genotypes.

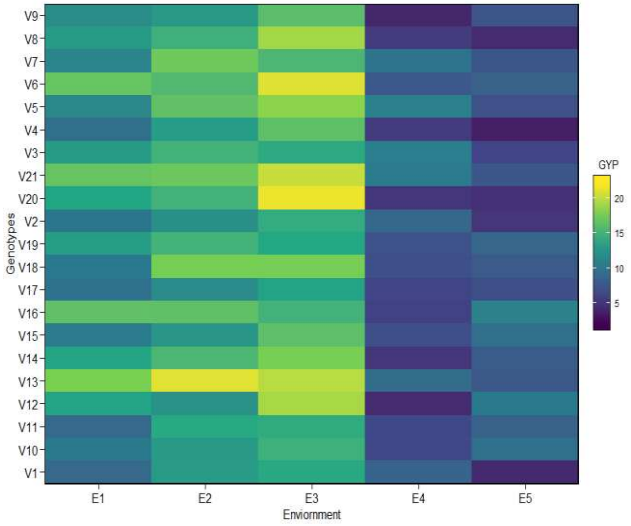

Figure 1. *Heat map showing which genotype win in which environment based on GYP mean performance*

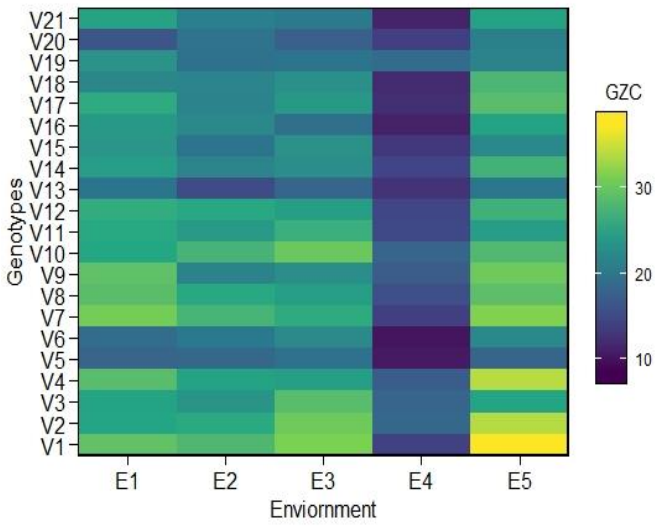

Figure 2. *Heat map showing which genotype win in which environment based on GZC mean performance*

http://www.aloki.hu ● ISSN 1589 1623 (Print) ● ISSN1785 0037 (Online)
DOI: http://dx.doi.org/10.15666/aeer/2005_41574172

Results and discussion

Evaluation of environments using GGE bi-plots for GYP and GZC

Relationships among test environments

The GGE bi-vector plot's view summarises the environment. Variability in the bi-plot between two environments is a good indicator. The length of an environmental vector may be used to assess its discriminating power (Yan et al., 2007). This study revealed that the first and second principal components (PC1) explained 61.56 and 17.25% of the variation, respectively (*Figure 3*). It can detect environmental correlations. This is seen in *Figure 3A* and *Table 3*, while *Figure 4A* and *Table 4* exhibit GZC data. An environment-centered (centering = 2) G by E bi-plot with no scaling (scaling = 0). This bi-plot explained 78% of the environmental G by E variation. These lines can be thought of as environment vectors in the GGE bi-plot shown in *Figure 3A*. In GYP, the acute angle between E1, E2, E3, and E5 suggests a good connection between the environments. When E3 and E4 form an obtuse angle, the two have a negative correlation. The absence of a straight angle between the two environments indicates no relationship. Large negative correlations (obtuse angles) suggest a substantial crossover GE. The greatest angle between E3 and E4 is more than 90°, indicating a larger GE here. The distance between two habitats reveals their genetic similarities (Yan and Tinker, 2006). The cosine of the angle between two environments indicates their resemblance (covariance). Fewer testing contexts (E1 and E2) provide the same genetic information, cutting testing expenses. One of two test conditions may be eliminated without impacting genetic information. For GZC, all environments form an acute angle. E1 and E2 have similar GZC genetic information, but E5 and E4 are considerably distinct.

Discriminativeness and representativeness of test environments

An ideal environment is one that is descriptive and has the greatest ability to discriminate (Yan and Tinker, 2006). The ideal environment is positioned in the first concentric circle of the GGE bi-plot, and the desirable environments are those that are close to the ideal environment. In the bi-plot, each environment's standard deviation shows its discriminating ability. E3 was the most discriminating (informative) environment for GYP, whereas E5 was the least (*Fig. 3A*). Non-discriminating (non-informative) test environments provide minimum genetic information and should not be used. GZC found E5 to be the most discriminatory, whereas E2 was the least (*Fig. 4A*). *Figure 3B* depicts the average-environment axis (AEA). AEA connects the average coordinates of all test environments to the bi-plot origin. As in *Figure 3B*, the AEA for GYP represents numerous test situations. So E2 represents the most and E4 the least. Good test environments for choosing generic genotypes are discriminating and representative (e.g. E2). Discriminating but non-representative test environments (E4 and E3) may be used to select genotypes that are perfectly matched to target environments through removing the unstable genotypes. Non-discriminating test environments E1 (with short vectors) is less beneficial since it gives minimal genotype discrimination in GZC, E1 is the most representative, while E4 is the least representative (*Figure 4B*). Similar kinds of results were reported in hybrid rice by Akter et al. (2015) and high zinc rice by Inabangan-Asilo et al. (2021).

http://www.aloki.hu ● ISSN 1589 1623 (Print) ● ISSN1785 0037 (Online)
DOI: http://dx.doi.org/10.15666/aeer/2005_41574172

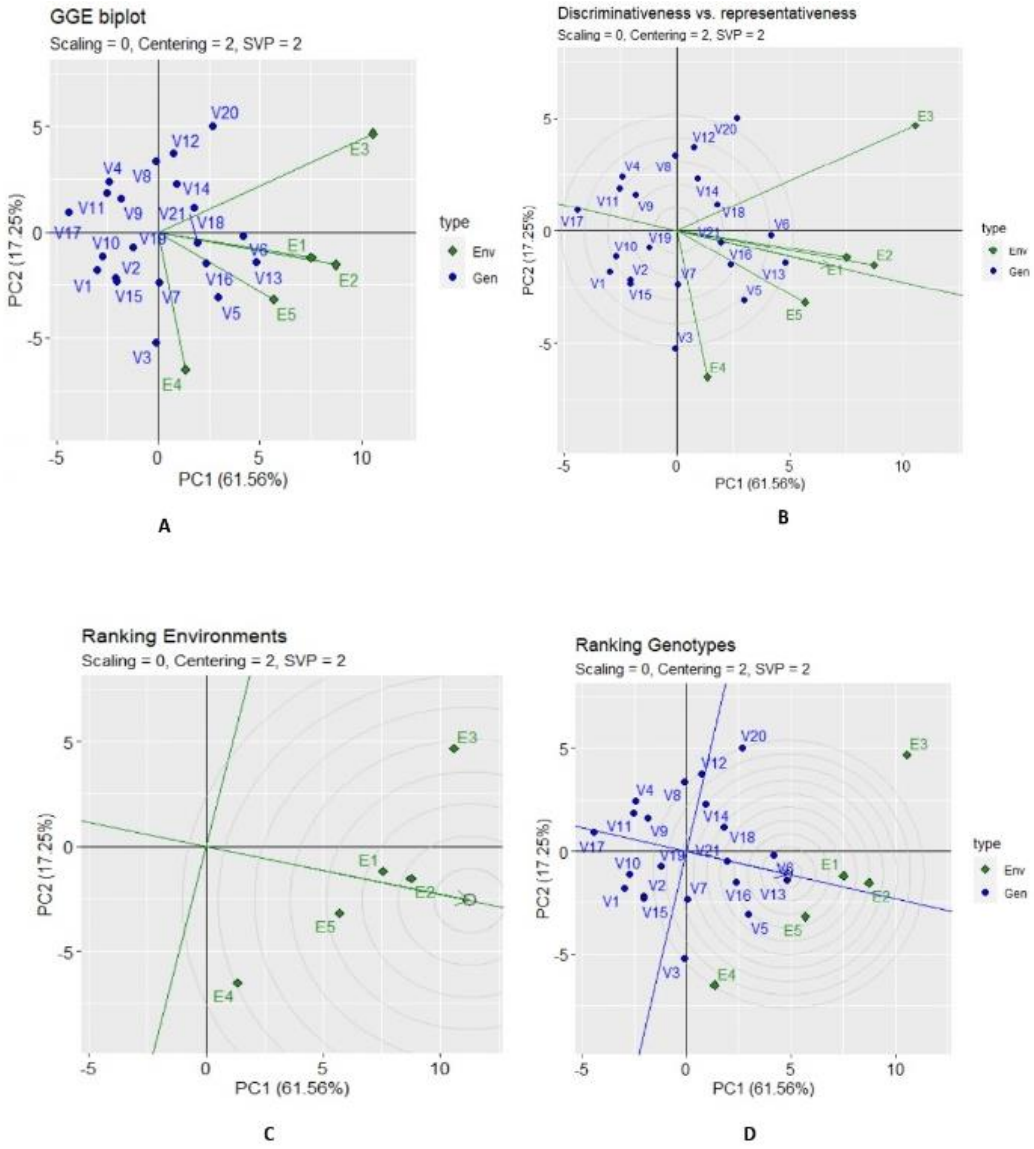

Figure 3. *GGE Biplots of GYP A) Relationship among test environments in discriminating the genotypes B) Discrimitiveness vs. representativenss of test environments C) Ranking environments relative to an ideal test environment based on both discriminating ability and representativeness D) Ranking genotypes based on performance of each genotype in each environment*

Ideal test environments for selecting generally adapted genotypes

The ideal test environment inside a mega-environment is discriminating (informative) and reflective of the intended environment. The concentric rings in *Figure 3C* and *Figure 4C* constitute an "ideal test environment". It is a positive point on the AEA ("most representative") with a distance from the bi-plot origin equal to the longest vector of all environments ("most informative"). For GYP, E2 is the best, while E4 and E3 were worse for choosing cultivars suitable for the whole area (*Fig. 3C*). Regarding GZC, E3 was the best choice for picking cultivars suited to the whole area, whereas E4 and E5 were the worst (*Fig. 4C*). A similar kind of experiment was conducted by Sincik et al. (2021) in canola, where she used E8 and E6 as the target environments in canola.

http://www.aloki.hu ● ISSN 1589 1623 (Print) ● ISSN1785 0037 (Online)
DOI: http://dx.doi.org/10.15666/aeer/2005_41574172

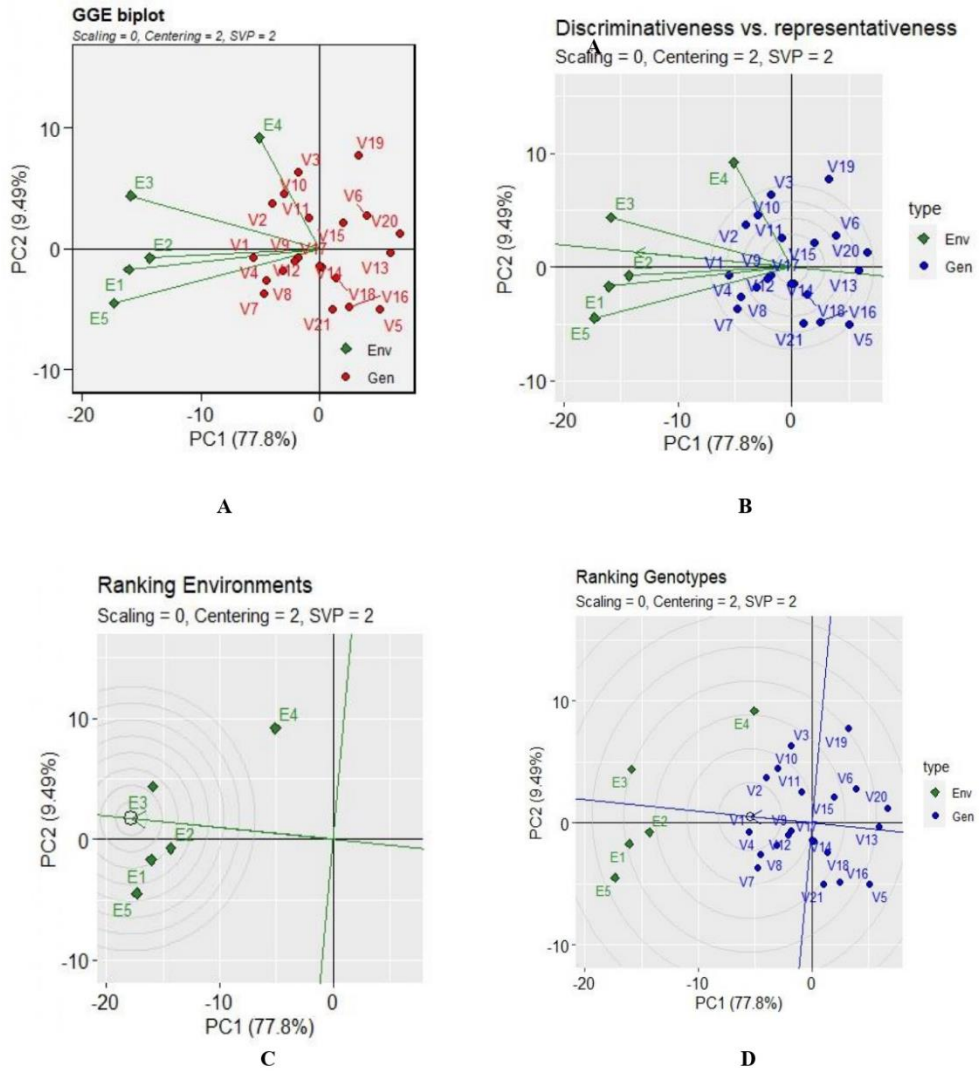

Figure 4. *GGE Biplots of GZC A) Relationship among test environments in discriminating the genotypes B) Discrimitiveness vs. representativenss of test environments C) Ranking environments relative to an ideal test environment based on both discriminating ability and representativeness D) Ranking genotypes based on performance of each genotype in each environment*

Evaluation of genotypes using GGE bi-plots for GYP and GZC

Performance of the genotypes in specific environments

Figure 3D depicts the relationships between genotypes and environments (i.e., genotype performance in each environment). A genotype's performance in an environment is better than average if the angle between its vector and the environment's vector is less than 90° (Yan and Tinker, 2006). While, V4, V9, V11, and V17 were below average in all environments (obtuse angles) in the current experiment for GYP, V21, V6, V13, V16, and V5 were above average in all contexts (acute angles). In all environments, V5, V13, and V20 were below average, but V1, V4, V9, and V2 were above average. In E2, V14 is the same as the average GZC, while V21 is closer to the average (right angle). The interaction's amplitude is determined by the cosine (angle) and length (vector length)

http://www.aloki.hu ● ISSN 1589 1623 (Print) ● ISSN1785 0037 (Online)
DOI: http://dx.doi.org/10.15666/aeer/2005_41574172

of the interaction. The performance of a genotype in different situations can be used to figure out where it ranks, as can the performance of the places where it lives.

Ranking genotypes based on performance in best environment

A line is formed between the bi-plot origin and the environment to rank the genotypes in the best environment (E2). This is the axis for this environment, and it ranks the genotypes (Yan and Tinker, 2006). The genotypes are ranked in *Figure 5*. A based on their performance in E2 for GYP. V17, V4, V11, V1, V10, V9, V2, V15, V19, and V8 yielded less than average, while V12, V7, and V14 yielded near-average and the others yielded more than average. V13 had the greatest yield in E2, followed by V6 and V17, which had the lowest output. *Figure 6A* ranks the genotypes in GZC depending on their performance in E2. GZC was lower than normal in the V5, V20, V13, V16, V6, V21, V18, and V15 genotypes, but near average in the V19 genotype. In E2, the genotypes with the greatest GZC were V2 and V1, followed by V10, and the genotype with the lowest GZC was V5. Similar kinds of findings were reported by Khan et al. (2021) in Bambara groundnut.

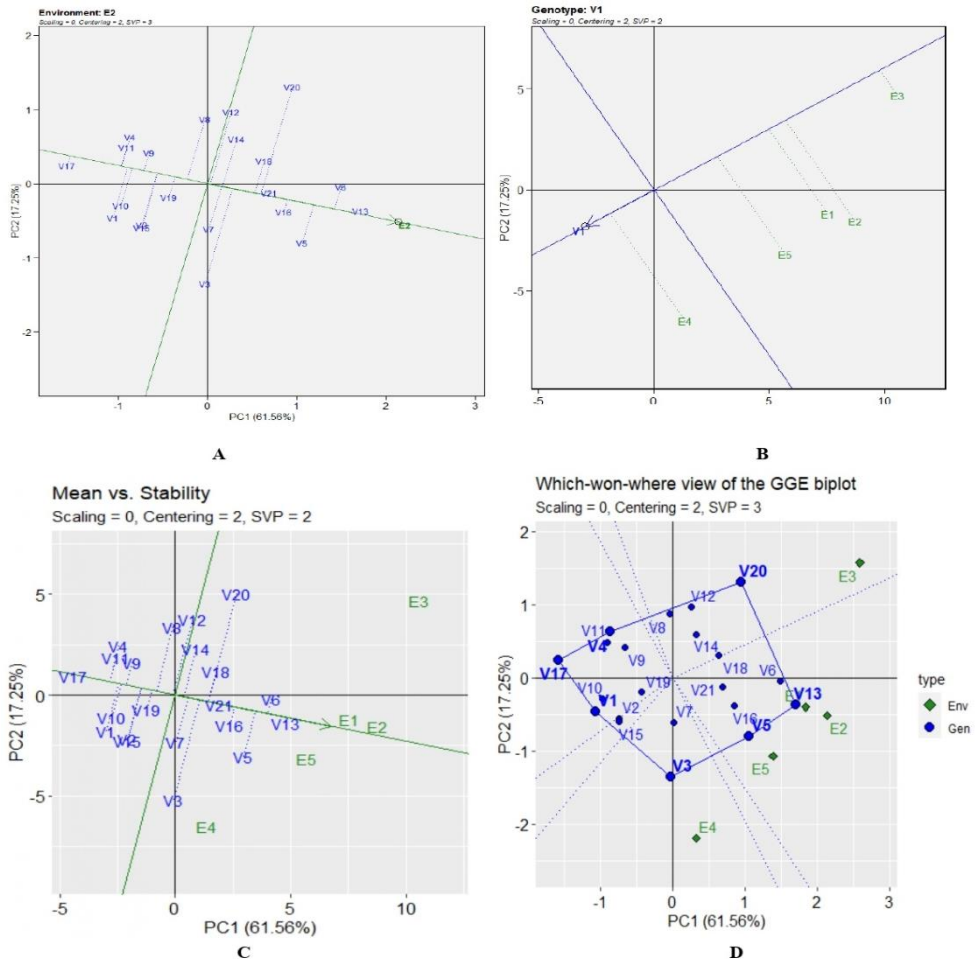

Figure 5. *GGE Biplots of GYP A) Ranking genotypes based on their performance in one environment E2 B) Ranking test environments in terms of the relative performance of a genotype V1 C) The average-environment coordination (AEC) view to rank genotypes based on both mean and stability D) The which-won-where polygon view of the GGE biplot to show which genotype performed bests in which environment*

http://www.aloki.hu ● ISSN 1589 1623 (Print) ● ISSN1785 0037 (Online)
DOI: http://dx.doi.org/10.15666/aeer/2005_41574172

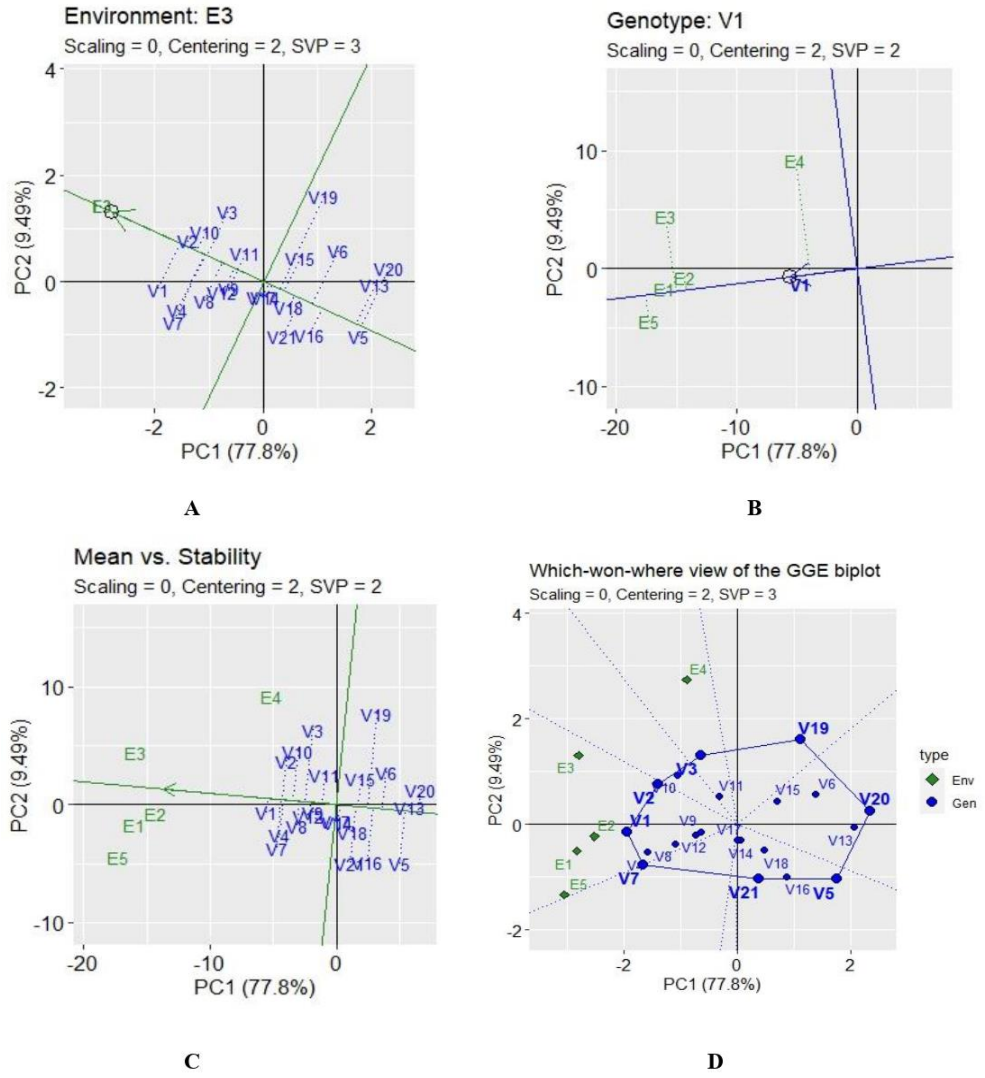

Figure 6. *GGE Biplots of GZC A) Ranking genotypes based on their performance in one environment E2 B) Ranking test environments in terms of the relative performance of a genotype V1 C) The average-environment coordination (AEC) view to rank genotypes based on both mean and stability D) The which-won-where polygon view of the GGE biplot to show which genotype performed bests in which environment*

Ranking environments based on the performance of a genotype

A line is drawn from the bi-plot origin to the genotype to rate the genotype's relative performance in each environment. The axis of this genotype is a line that ranks the environments (Yan and Tinker, 2006). *Figure 5B* ranks the test environments based on the genotype V1's relative performance. Environment E4 had the highest average yield, whereas other environments yielded lower average yields. In *Figure 6B*, V1 had a greater GZC than the average in the environment E5, as seen in the figure.

Mean performance and stability of the genotypes

All genotypes in a single mega-environment must be evaluated on mean performance and environmental stability. *Figure 5C* displays the GGE bi-plot from an AEC viewpoint.

http://www.aloki.hu ● ISSN 1589 1623 (Print) ● ISSN1785 0037 (Online)
DOI: http://dx.doi.org/10.15666/aeer/2005_41574172

The single-arrowed line is the (AEA), which leads to increased mean yield across environments (SVP =1) (Yan and Tinker, 2006). The highest mean yield was V13, followed by V6, V5, V16, and V21; the grand mean was V12; and the lowest, V17. The AEC ordinate is a double-red line that denotes poor stability. Due to the excellent stability of V13, it may be used as a genotype reference. Given that the bi-plot only addresses a small fraction of the entire variance, certain genotypes that seem stable may not be stable at all. Unlike other rice genotypes, V8 was very unstable, yielding less in E3 and E4, but more in E5, and was less appealing than other rice genotypes. Its E1 and E2 yields were precisely anticipated by its total yield. For example, in *Figure 6B*, V1 had the greatest GZC, followed by 4, 2, 7, 10, 8, and 11, with a mean close to the grand mean, and V20 the lowest. V19 was a very unstable genotype, while V1 was a stable one. In 2017, Haider et al. (2017) found similar findings.

Ranking genotypes relative to the ideal genotype

To maximize yield, genotypes should have a high PC1 (high yielding ability) and a low (absolute) PC2 score (high stability). However, an "ideal" genotype's vector length is equal to the longest genotype's vector ("highest mean performance"). Thus, closer genotypes to the "ideal genotype" are desired (Rakshit et al., 2012). In spite of the greater average yield, V16 beat V5 in the case of GYP. Of course, V17 was the worst, and V13 was the greatest. *Figure 3D* shows "Stability." The best stability is combined with ordinary performance. 1. D shows V17 as "stable." Inconsistency in V17's performance does not make it good. V17 outperformed V20 and V3 in several situations. Similarly, for GZC, on average, V20 was the worst genotype in *Figure 4D*, whereas V1 was the best. Searching for "stability" genes might be deceptive. Only genotypes with high mean performances are considered "stable".

Comparison among all genotypes

The GGE bi-plot in *Fig. 3B* for GYP can also give clear cut differences among the genotypes. The distance between two genotypes approximates the Euclidean distance between them, which is a measure of their total dissimilarity. V20 and V3 are distinct genotypes, although V2 and V15 are extremely similar. For each setting, the bi-plot origin represents a “virtual” genotype. This “average” genotype contributes nothing to G or GE. A genotype's distance from the bi-plot origin assesses its contribution to G, GE, or both. Thus, genotypes near the bi-plot origin contribute little to both G and GE, whereas genotypes with longer vectors contribute much to either G or GE (Yan and Tinker, 2006). Thus, the best (V13), worst (V17), or most unstable (V3 and V20) genotypes have the longest vectors. The angle between a genotype's vector and the AEA divides its length into G and GE components. For example, an obtuse or acute angle suggests the contribution is mostly to G, resulting in lower-than-average mean performance; while a right angle means the contribution is mostly to GE, resulting in higher-than-average mean performance. The angle between two genotypes reveals their environmental similarity. For example, an acute angle (V11 vs. V4) suggests the two genotypes behaved similarly and the difference was proportionate in all settings. Obtuse angles (e.g., V20 vs. V3) indicate that the two genotypes behaved inversely, with the first genotype outperforming the second. For each genotype (for example, V6 and V12), the environments for GZC are in *Figure 4B*, V19, and V5 have quite distinct genotypes, although V2 and V10 are fairly close. An acute angle between V1 and V2 shows similarity in response to GZC contexts, but an obtuse angle between V7 and V19 implies the opposite response. Inabangan-Asilo

http://www.aloki.hu ● ISSN 1589 1623 (Print) ● ISSN1785 0037 (Online)
DOI: http://dx.doi.org/10.15666/aeer/2005_41574172

et al. (2019) found that by looking at genotype-environment interaction (G × E) and stable genotypes from multiple locations, they could help find lines that could be released as new varieties.

Which-won-where

In multi-location yield trials, the GGE-bi-plot analysis polygon perspective helps discover cross-over and non-crossover genotype-by-environment interactions and helps identify mega environments (Yan et al., 2007). A GGE bi-plot may display the which-won-where pattern of a genotype by environment dataset for GYP (*Figure 5D*). That it visually handles essential themes like crossover GE, mega-environment differentiation, particular adaptation, etc. The GGE bi-plot's "which-won-where" function extends the previous “pair-wise comparison” function. First, a polygon was created on the genotypes farthest from the bi-plot origin, including all other genotypes. The environments were in two sectors, whereas the genotypes were in all four. The genotypes in the sector's vertices are the most beneficial (Yan and Tinker, 2006). Then, starting from the bi-plot origin, draw perpendicular lines to each side of the polygon. The GGE bi-plot polygon views revealed one probable mega habitat for both GYP and GZC. The first mega environment for GYP was made up of four environments (E1, E2, E4 and E5), and the second mega environment was made up of one environment (E3), whereas the first mega environment for GZC was made up of four environments (E1, E2, E3 and E5), and the second mega environment was made up of one environment (E3) (E4). In one or more situations, the genotypes placed at the polygon's vertices (V17, V20, V13, and V3) fared best or worse. The perpendicular lines on the polygon are equality lines that allow for visual comparison of neighbouring genotypes. According to the equality line between V20 and V13, V20 was better in just E3, but V13 was better in all other environments, too. As shown by the equality line between the two, V20 was better than V11 in all situations. V12 and V8 are connected to V20 and V11 via a line. This indicates that in all environments, the order V20 > V12 > V4 > V11 was true. In E1 and E2, V13 was the best, while in E5 and E4, V5 and V3 were the greatest. Only E3 saw V20 emerge victorious, while the other environments witnessed V13 succeed. In *Fig. 6D*, the same goes for GZC. In one or more situations, V1, V2, V3, V19, V20, V5, V21, and V7 were the best or worse. The equality line between V2 and V3 suggests that V3 was superior in just one environment, E4, while V2 was superior in all others. According to the equality line between V2 and V3, V2 was superior to V3 in all environments. In all contexts, the genotype hierarchy for GZC was V3 > V19 > V20. V1 had the greatest success in E2 and E1, while V7 had the greatest success in E5, and V2 had the greatest success in E3. Only E3 had a winner, whereas the other settings had V1 as the winner. The findings suggest that the environment and GEI have a role in yield trait expression (Gedif et al., 2014; Bhartiya et al., 2017).

Conclusion

The results of the present study revealed that the first principal component (PC1) and the second (PC2) explained 61.66% and 17.25% of the variation separately, and combined they explained 78% of the variance. Bi-plot analysis has been a vital tool in the fields of crop improvement and agricultural research throughout the years. The GGE bi-plot analysis solves a long-standing problem of genotype by environment data analysis for plant breeders, geneticists, and agronomists. The GGE bi-plot's polygon views revealed two feasible mega environments for both GYP and GZC. The discriminativeness

http://www.aloki.hu ● ISSN 1589 1623 (Print) ● ISSN1785 0037 (Online)
DOI: http://dx.doi.org/10.15666/aeer/2005_41574172

vs. representativeness concept has proved useful in evaluating test environments. For GYP, there was a positive correlation among the environments (E1, E2, E3 and E5) and a negative correlation between E3 and E4 for GYP; whereas for GZC, all environments were positively correlated among themselves. There were close associations among the test environments (E1 and E2) having similar kinds of genotype information for GYP and GZC. For GYP, E5 was the most discriminating and E2 was the least discriminating of the tested high zinc rice genotypes. For GZC, E5 was the most discriminating and E2 was the least discriminating. was the most representative and E3 the least representative, whereas for GZC, E1 was the most representative and E3 the least representative. The highest GYP and GZC test environments were E3 and E5, respectively. E2 was the best or ideal test environment for selecting generally adapted genotypes for GYP, whereas for GZC, E3 was the ideal test environment. The genotypes with codes V21, V6, V13, V16, and V5 for GYP and V1, V4, V9, and V2 for GZC were above average in all the environments. The genotype V13 had the highest mean grain yield and the most stable genotypes, while V8 was highly unstable and V17 was the lowest yielder. V1 had the highest GZC and the most stable genotypes, whereas, V19 was highly unstable. For GYP, V3 was the winner in only E3, whereas V13 was the winner in the other environments. For GZC, V3 was the winner in only E3, whereas V1 was the winner in the other environments. As a result, the V13 (BRRI dhan 72) for grain yield and the V1 (IR 95044:8-B-5-22-19-GBS) for grain zinc content could be recommended for future breeding programmes for cultivar selection and zinc bio-fortification.

REFERENCES

[1] Akter, A., Hasan, M. J., Kulsum, U., Rahman, M. H., Khatun, M., Islam, M. R. (2015): GGE biplot analysis for yield stability in multi-environment trials of promising hybrid rice (*Oryza sativa* L.). – Bangladesh Rice Journal 19(1): 1-8. https://doi.org/10.3329/brj.v19i1.25213.

[2] Bhartiya, A., Aditya, J. P., Singh, K., Purwar, J. P., Agarwal, A. (2017): AMMI & GGE biplot analysis of multi environment yield trial of soybean in North Western Himalayan state Uttarakhand of India. – Legume Research-An International Journal 40(2): 306-312.

[3] Cakmak, I., Pfeiffer, W. H., McClafferty, B. (2010): Biofortification of durum wheat with zinc and iron. – Cereal Chemistry 87(1): 10-20. https://doi.org/10.1094/CCHEM-87-1-0010.

[4] Gasura, E., Setimela, P. S., Souta, C. M. (2015): Evaluation of the performance of sorghum genotypes using GGE biplot. – Canadian Journal of Plant Science 95(6): 1205-1214. https://doi.org/10.4141/cjps-2015-119.

[5] Gedif, M., Yigzaw, D., Tsige, G. (2014): Genotype-environment interaction and correlation of some stability parameters of total starch yield in potato in Amhara region, Ethiopia. – Journal of Plant Breeding and Crop Science 6(3): 31-40. https://doi.org/10.5897/JPBCS2013.0426.

[6] Gurmu, F., Mohammed, H., Alemaw, G. (2009): Genotype x environment interactions and stability of soybean for grain yield and nutrition quality. – African crop science journal 17(2). https://doi.org/10.4314/acsj.v17i2.54202.

[7] Haider, Z., Akhter, M., Mahmood, A., Khan, R. A. R. (2017): Comparison of GGE biplot and AMMI analysis of multi-environment trial (MET) data to assess adaptability and stability of rice genotypes. – African Journal of Agricultural Research 12(51): 3542-3548. https://doi.org/10.5897/AJAR2017.12528.

[8] Impa, S. M., Morete, M. J., Ismail, A. M., Schulin, R., Johnson-Beebout, S. E. (2013): Zn uptake, translocation and grain Zn loading in rice (*Oryza sativa* L.) genotypes selected for

http://www.aloki.hu ● ISSN 1589 1623 (Print) ● ISSN1785 0037 (Online)
DOI: http://dx.doi.org/10.15666/aeer/2005_41574172

Zn deficiency tolerance and high grain Zn. – Journal of Experimental Botany 64(10): 2739-2751. https://doi.org/10.1093/jxb/ert118.

[9] Inabangan-Asilo, M. A., Mallikarjuna-Swamy, B. P., Amparado, A. F., Descalsota-Empleo, G. I. L., Arocena, E. C., Reinke, R. (2019): Stability and G × E analysis of zinc-biofortified rice genotypes evaluated in diverse environments. – Euphytica 215(3): 1-17. https://doi.org/10.1007/s10681-019-2384.

[10] International Plant Genetic Resources Institute, & West Africa Rice Development Association. (2007): Descriptors for Wild and Cultivated Rice (*Oryza Spp*.). – Bioversity International.

[11] Kaplan, M., Kokten, K., Akcura, M. (2017): Assessment of Genotype× Trait× Environment interactions of silage maize genotypes through GGE Biplot. – Chilean Journal of Agricultural Research 77(3): 212-217.

[12] Karimizadeh, R., Mohammadi, M., Sabaghni, N., Mahmoodi, A. A., Roustami, B., Seyyedi, F., Akbari, F. (2013): GGE biplot analysis of yield stability in multi-environment trials of lentil genotypes under rainfed condition. – Notulae Scientia Biologicae 5(2): 256-262. https://doi.org/10.15835/nsb529067.

[13] Kendal, E., Sener, O. (2015): Examination of genotype × environment interactions by GGE biplot analysis in spring durum wheat. – Indian Journal of Genetics and Plant Breeding 75(3): 341-348.

[14] Kesh, H., Kharb, R., Ram, K., Munjal, R., Kaushik, P., Kumar, D. (2021): Adaptability and AMMI biplot analysis for yield and agronomical traits in scented rice genotypes under diverse production environments. – Indian Journal of Traditional Knowledge 20(2): 550-562.

[15] Khan, M. M. H., Rafii, M. Y., Ramlee, S. I., Jusoh, M., Al Mamun, M. (2021): AMMI and GGE biplot analysis for yield performance and stability assessment of selected Bambara groundnut (*Vigna subterranea* L. Verdc.) genotypes under the multi-environmental trails (METs). – Scientific Reports 11(1): 1-17. https://doi.org/10.1038/s41598-021-01411-2.

[16] Mustamu, Y. A., Tjintokohadi, K., Grüneberg, W. J., Karuniawan, A., Ruswandi, D. (2018): Selection of superior genotype of sweet-potato in Indonesia based on stability and adaptability. – Chilean Journal of Agricultural Research 78(4): 461-469.

[17] Olanrewaju, O. S., Oyatomi, O., Babalola, O. O., Abberton, M. (2021): GGE Biplot Analysis of Genotype× Environment Interaction and Yield Stability in Bambara Groundnut. – Agronomy 11(9): 1839. https://doi.org/10.3390/agronomy11091839.

[18] Olivoto, T., Lúcio, A. D. C. (2020): metan: An R package for multi-environment trial analysis. – Methods in Ecology and Evolution 11(6): 783-789. https://doi.org/10.1111/2041-210X.13384.

[19] Oyekunle, M., Haruna, A., Badu-Apraku, B., Usman, I. S., Mani, H., Ado, S. G., Ahmed, H. O. (2017): Assessment of early-maturing maize hybrids and testing sites using GGE biplot analysis. – Crop Science 57: 1-9. https://doi.org/10.2135/cropsci2016.12.1014.

[20] Sahrawat, K. L., Kumar, G. R., Murthy, K. V. S. (2002): Sulfuric acid–selenium digestion for multi-element analysis in a single plant digest. – Communications in Soil Science and Plant Analysis 33(19-20): 3757-3765. https://doi.org/10.1081/CSS-120015920.

[21] Sincik, M., Goksoy, A. T., Senyigit, E., Ulusoy, Y., Acar, M., Gizlenci, S., Suzer, S. (2021): Response and yield stability of canola (*Brassica napus* L.) genotypes to multi-environments using GGE biplot analysis. – Bioagro 33(2): 105-114. https://doi.org/10.51372/bioagro332.4.

[22] Solonechnyi, P., Kozachenko, M., Vasko, N., Gudzenko, V., Ishenko, V., Kozelets, G., Vinyukov, A. (2018): AMMI and GGE biplot analysis of yield performance of spring barley (*Hordeum vulgare* L.) varieties in multi environment trials. – Poljoprivreda i Sumarstvo 64(1): 121-132.

[23] Suman, K., Neeraja, C. N., Madhubabu, P., Rathod, S., Bej, S., Jadhav, K. P., Voleti, S. R. (2021): Identification of Promising RILs for High Grain Zinc Through Genotype×

http://www.aloki.hu ● ISSN 1589 1623 (Print) ● ISSN1785 0037 (Online)
DOI: http://dx.doi.org/10.15666/aeer/2005_41574172

Environment Analysis and Stable Grain Zinc QTL Using SSRs and SNPs in Rice (*Oryza sativa* L.). – Frontiers in Plant Science 22. https://doi.org/10.3389/fpls.2021.587482.

[24] Team, R. C. (2019): R: A language and environment for statistical computing. – Vienna, Austria: R Foundation for Statistical Computing; 2019. URL www.R-project.org.

[25] Tena, E., Goshu, F., Mohamad, H., Tesfa, M., Tesfaye, D., Seife, A. (2019): Genotype× environment interaction by AMMI and GGE-biplot analysis for sugar yield in three crop cycles of sugarcane (*Saccharum officinirum* L.) clones in Ethiopia. – Cogent Food & Agriculture 5(1): 1651925. https://doi.org/10.1080/23311932.2019.1651925.

[26] Wickham, H., Chang, W., Wickham, M. H. (2016): Package 'ggplot2'. Create elegant data visualisations using the grammar of graphics. – Version 2(1): 1-189.

[27] Yan, W., Tinker, N. A. (2005): An integrated biplot analysis system for displaying, interpreting, and exploring genotype-byenvironment interactions. – Crop Science 45: 1004-1016. https://doi.org/10.2135/cropsci2004.0076.

[28] Yan, W., Tinker, N. A. (2006): Biplot analysis of multi-environment trial data: Principles and applications. – Canadian Journal of Plant Science 86(3): 623-645. https://doi.org/10.4141/P05-169.

[29] Yan, W., Kang, M. S., Ma, B., Woods, S., Cornelius, P. L. (2007): GGE biplot vs. AMMI analysis of genotype-by-environment data. – Crop Science 47(2): 643-653. https://doi.org/10.2135/cropsci2006.06.0374.

[30] Zaman, Q. U., Aslam, Z., Yaseen, M., Ihsan, M. Z., Khaliq, A., Fahad, S., Naeem, M. (2018): Zinc biofortification in rice: leveraging agriculture to moderate hidden hunger in developing countries. – Archives of Agronomy and Soil Science 64(2): 147-161. https://doi.org/10.1080/03650340.2017.1338343.

http://www.aloki.hu ● ISSN 1589 1623 (Print) ● ISSN1785 0037 (Online)
DOI: http://dx.doi.org/10.15666/aeer/2005_41574172

THE IMPACT OF DIFFERENT IRRIGATION INTERVALS AND LEVELS ON YIELD AND QUALITY OF DRIP-IRRIGATED CORN SILAGE (*ZEA MAYS* L.) UNDER ARID CLIMATE

TARI, A. F.

Department of Agricultural Structures and Irrigation, Agricultural Faculty, Harran University, Şanlıurfa, Turkey
(e-mail: aftari@hotmail.com)

(Received 29th Apr 2022; accepted 11th Jul 2022)

Abstract. Soil moisture availability exerts significant impacts on the yield and productivity of crop plants. Moisture availability becomes more critical in arid climates, as irrigation is the single source to fulfill the moisture requirements of the plants. Therefore, the level of applied irrigation water and time interval between two irrigations significantly alter the yield and quality of produce. This two-year study determined the effects of different irrigation levels and intervals on yield, quality and water use efficiency of silage maize. The experiment was laid out according to randomized complete block design with split plot arrangements. The main plots consisted of irrigation intervals (3 and 6 days), whereas sub-plots included four irrigation levels (125%, 100%, 75% and 50% of Class-A pan evaporation) based on class A pan evaporation. Drip irrigation method was used to supply the required amount of the water according to the treatments. The annual water consumption rate (ETc) varied between 397 and 725 mm, and between 402 and 759 mm in different study years. The silage yield (FY) during the first year ranged between 36.44 and 81.69 t ha^{-1}, and between 38.31 and 78.96 t ha^{-1} during the second year. The FY was significantly altered by different irrigation intervals ($p \leq 0.05$) and irrigation levels ($p \leq 0.01$). The dry matter ratio (DMR) (a yield component) was not altered by irrigation intervals and irrigation levels. However, the other yield components such as amount of dry matter yield (DMY) and plant height were significantly ($p \leq 0.01$) affected by irrigation levels. Crude protein (CP) content significantly differed ($p \leq 0.05$) among irrigation intervals and irrigation levels ($p \leq 0.01$). However, the remaining quality parameters, i.e., acid detergent fiber (ADF), neutral detergent fiber (NDF) and crude fiber were only affected by irrigation levels. The pH remained unaffected by irrigation levels and intervals. Leaf area index (LAI) gradually increased after sowing and reached to the highest values at 70-80 days after sowing. Water productivity (WP) and irrigation water productivity (IWP) did not differ among applied irrigation levels and irrigation intervals. It is concluded that frequent irrigations increased silage yield of corn with drip irrigation under arid climatic conditions. However, low water application during the whole growing season caused significant decreases in silage yield.
Keywords: *drip irrigation, irrigation levels, water productivity, leaf area index, corn silage*

Introduction

The ever increasing urban and industrial water demands along with the contamination of available water resources are decreasing the amount of water devoted to agriculture. Furthermore, water scarcity and frequent droughts because of ongoing global climate changes are seriously threatening plant production in almost all parts of the world (Katerji et al., 2008). Currently, >40% of the global human population is being adversely affected by water scarcity (Steduto et al., 2012). In Turkey, only 19% of agricultural lands can be irrigated due to the inadequate availability of water resources (DSI, 2022), and problems related to water availability will be worsened in the future. Therefore, the farmers should protect the limited water resources for their sustainable use (Cai et al., 2002; Bekele and Tilahun, 2007).

The agricultural lands in the Mediterranean basin are located in the arid and semi-arid climate zones, where summer crops cannot be grown without irrigation. The

http://www.aloki.hu ● ISSN 1589 1623 (Print) ● ISSN 1785 0037 (Online)
DOI: http://dx.doi.org/10.15666/aeer/2005_41734191

Southeastern Anatolia region is dominated by Mediterranean climate in Turkey, and it is the most important region in terms of agricultural production in the country. Moreover, it is the hottest and driest region of the country; thus, summer crops must be irrigated for obtaining optimum yield. The crops in the region are irrigated by furrow irrigation method, which results in significant water losses. Hence, expansion and use of modern irrigation systems is the only way to effectively utilize limited available water resources in the country/region. Water savings and water efficiency can be increased by adopting modern irrigation methods, which would increase irrigation efficiency and farmers' income (Gonçalves et al., 2011; Pereira, et al., 2012). The most appropriate solution is the use of a high-efficiency irrigation system, i.e., drip irrigation (Cai et al., 2002). Drip irrigation is a highly efficient technology as it allows better timing and more precise water applications (Keller and Bliesner, 1990; Goorahoo et al., 2011).

Increasing industrialization and urbanization is decreasing agricultural areas, whereas the number of people to be fed from exiting areas is increasing rapidly. Accordingly, the demands for plant and animal products are rapidly increasing. Corn (*Zea mays* L.) is one of the most widely cultivated crops to fulfill these demands. Corn plant can provide cheap and high-quality feed (Geren et al., 2003). Corn is widely grown in all continents of the world and ranks second after wheat in terms of area production among cereal crops. Due to its high productivity, it ranks first in terms of production (FAO, 2020). The main reasons for the global preference of corn as a silage crop are production of high fresh biomass per unit area, easy harvesting, delicious and highly prefered by animals (Kaplan, 2005), suitability for silage production and high nutritional value (Miller, 1979; Kılıç, 1986; McDonald et al., 1991; Meeske et al., 1993). In addition, it requires less labor and machinery than many other forage crops (Roth et al., 1995), which is another reason for the preference of corn for silage making or ensiling.

Corn is a high-water requiring forage crop (Musick and Dusek, 1980; Stone et al., 1996; Karam et al., 2003; Payero et al., 2006; Farre and Faci, 2009). It requires ~500 to 800 mm water during the growing season (Brouwer and Heibloem, 1986). Several studies have reported adverse effects of water stress on biomass production, pollen viability and grain count in corn having tropical and temperate genetic characteristics (Herrero and Johnson, 1981; Edreira et al., 2011). Water stress decreases plant height, leaf area, DMY, FY, and quality of corn silage (NeSmith and Ricthie, 1992; Cox et al., 1998).

Low and erratically distributed precipitation in arid and semi-arid climatic regions is a major hurdle in optimum plant growth of corn. Therefore, irrigation is the most important agricultural practice which would significantly alter FY in such regions (Büyüktaş, et al., 2020). Hence, producers should opt the techniques/methods with high water productivity (WP) through efficient use of limited available irrigation water (IW). Meanwhile, the opted techniques/methods should result in higher quality and quantity of silage since quality of silage is extremely important for animal production besides quantity. Several researchers around the world have investigated the effects of different irrigation practices on WP, FY, and its quality (ADF, NDF, CP, pH etc.) in different climatic regions (Islam et al., 2012; Rusere et al., 2012; Bouazzama et al., 2012; Yolcu et al., 2016; Gheysari et al., 2017; Nilahyane et al., 2020; Büyüktaş et al., 2020). However, the researchers have reported contrasting findings regarding quality and quantity of corn silage.

The extensive literature search revealed that insufficient studies have been conducted to evaluate the combined effect of different irrigation intervals and irrigation levels on

http://www.aloki.hu ● ISSN 1589 1623 (Print) ● ISSN 1785 0037 (Online)
DOI: http://dx.doi.org/10.15666/aeer/2005_41734191

corn silage grown as a second crop under arid climate conditions. The main aim of the current study was to investigate the impact of different irrigation intervals and levels on growth, yield, quality, and the water use efficiency of drip irrigated corn silage in an arid region. It was hypothesized that growth, yield, quality, and the water use efficiency of drip irrigated corn silage will significantly differ among tested irrigation intervals and levels. The results would help to find the optimum irrigation level and irrigation interval for higher silage yield with high quality under arid climates.

Materials and methods

Experimental site climatic conditions

This current study was conducted in the Harran Plain (37°10'N, 39°59'E, and 499 m above sea level) in Şanlıurfa, Turkey, where second crop corn is intensively grown during 2017 and 2018 growing seasons.

Harran Plain is situated in the hottest region of Turkey and dominated by arid climatic. The summer months are extremely hot and dry, whereas winter months are cold and rainy. The June, July, August, and September are the hottest months, while December and January are the coldest months. The daily maximum temperature during July and August often exceeds 40 °C, while minimum temperatures drop below 0 °C during winter. According to long-term (1920-2021) climate, the annual total precipitation in Harran Plain is 340 mm, and evaporation from the open water surface is 1850 mm. The weather data of the experimental years was similar to long-term average data of the experimental site. Out of the total rainfall, only 4% is received during the vegetation period of the second crop corn.

The experimental soil was clay textured (USSL, 1954), having low salt contents and slightly alkaline. The experimental site has a deep profile and useful water holding capacity of 0-90 cm depth was 102.5 mm (*Table 1*). The electrical conductivity of the IW used in the study was 0.358 dS m^{-1} and it belonged to C_2S_1 class according to the water quality diagram of the US Salinity Laboratory.

Table 1. *Physical and chemical properties of the experimental soil*

Soil layers (cm)	Texture	Field capacity (g g^{-1})	Wilting point (g g^{-1})	Bulk density (g cm^{-3})	EC (dS m^{-1})	pH	Lime %
0-30	C	0.286	0.205	1.36	0.582	7.4	8.1
30-60	C	0.298	0.213	1.37	0.654	7.4	8.7
60-90	C	0.301	0.217	1.37	0.703	7.5	9.3

EC: electrical conductivity

Agronomic practices

Seedbed preparation, sowing and harvesting: The experimental site was ploughed in June immediately after wheat harvest, and prepared for corn planting with combi plough and cultivator. The corn was planted with a pneumatic seeder on 21 June and 23 June 2018 by keeping row-to-row distance of 70 cm. The 'May Hido' corn variety belonging to FAO 700 maturity group was used in the study. The experimental units were 6.00 m long and 4.20 m (6 rows) wide covering a total area of 25.60 m^2. However, at harvest,

http://www.aloki.hu ● ISSN 1589 1623 (Print) ● ISSN 1785 0037 (Online)
DOI: http://dx.doi.org/10.15666/aeer/2005_41734191

0.5 m from the edges two border rows were left to avoid edge effect; thus, remaining plants in 14 m^2 area were manually harvested.

Plant protection and fertilization: Hoeing was done twice to control the weeds after the emergence of corn by using a manual hoeing machine. Thinning and earthing up were done with second hoeing to maintain plant-to-plant distance of 15-20 cm. A total 80 kg ha^{-1} P_2O_5 and 240 kg ha^{-1} N were applied. While the whole amount of P_2O_5 and 80 kg ha^{-1} N was applied at sowing using 20-20-0 fertilizer, the remaining N was applied with fertigation in three equal splits. The insect pests were controlled by using chemical control as needed during the corn growth period.

Experimental treatments and design

Experimental treatments: The experiment was carried out according to randomized complete block design with split plot arrangements. The irrigation intervals were kept in main plots, whereas irrigation levels based on coefficients of Class a Pan were randomized in sub plots. Eight different irrigation programs were applied during the field study. The experimental treatments are summarized in *Table 2*.

Table 2. *Different irrigation level and irrigation interval treatments used in the study*

Main plots (different irrigation intervals)	**Subplots (irrigation levels)**
D_1 (irrigation every 3rd day) D_2 (irrigation every 6th day)	I_1 = 125% (Kp_1 = 1.25) I_2 = 100% (Kp_2 = 1.00) I_3 = 75% (Kp_3 = 0.75) I_4 = 50% (Kp_4 = 0.50)

Irrigation system and irrigation water

Drip irrigation system was used to provide the desired amount of IW according to the treatments. The IW was taken from a deep well situated in the trial area. The IW taken from the well was first filtered in the control unit. The control unit consisted of sand gravel filter, screen filter, pressure regulator, manometers, fertilizer tank and water clock. The filtered water was conveyed to the experimental site with 75 mm polyethylene pipes and then distributed to the experimental units with 50 mm polyethylene pipes. A lateral line was laid for each row; thus, lateral spacing was 0.70 m (Sl = 0.70 m). The lateral pipes were 16 mm, and the drippers were spaced 0.30 m apart (Sd = 0.30 m). The drippers had a flow rate of 4 l/h. The selection of the drippers was based on soil characteristics as described by Keller and Bliesner (1990). All experimental units were irrigated with same amount of IW by using sprinkler irrigation immediately after sowing to ensure homogeneous plant germination and development. The second hoeing and earthing up were done once the plants reached 25-30 cm height, afterwards drip irrigation system was installed in the experimental field.

Measurement of IW

The amount of IW to be applied in different treatments was determined by multiplying the evaporation amount from Class A Pan evaporation pan present in the trial area with different crop-pan coefficients (Kp). The amount of evaporation between

http://www.aloki.hu ● ISSN 1589 1623 (Print) ● ISSN 1785 0037 (Online)
DOI: http://dx.doi.org/10.15666/aeer/2005_41734191

two irrigation intervals (3 and 6 days) was multiplied by the Kp and cover percentage (P) to determine the amount of IW. The percentage of cover used in the computations was determined by measuring the plant canopy before each irrigation. The first irrigation was given when 50% of the available water in 0-60 cm soil profile was consumed. Gravimetric method was used to determine the soil available moisture in 0-60 and 0-90 cm soil depth.

All experimental units were irrigated to field capacity during first irrigation, and then calculated amount of IW was applied according to the treatment. The applied amount of IW amounts was controlled by water clocks in each experimental unit. The precipitation amount was taken from the meteorology station located next to the experimental area. The following equation was used to calculate the amount of IW amount (Ünlü et al., 2011):

$$IW = A \times E_{pan} \times K_p \times P_c \quad \text{(Eq.1)}$$

Here, IW: is the amount of irrigation water (mm), Epan is the cumulative evaporation for irrigation interval (mm), Kp is the crop-pan coefficient, and Pc is plant cover (%). Free surface water evaporation was measured with a screened Class A pan located at the meteorological station near the experimental field.

Soil moisture monitoring

Soil moisture in all experimental plots was monitored at soil depth of 0-120 cm with gravimetric method. The water budget equation was used for the calculation of ETc (James, 1988):

$$ETc = I + P + D_p \pm R_{off} \pm \Delta S \quad \text{(Eq.2)}$$

Here, ET is evapotranspiration (mm), I is the irrigation water (mm), P is the rainfall (mm), D_p is the deep percolation (mm), R_{off} is the runoff (mm) and ΔS is the change of moisture content in the 0-90 cm root depth (mm).

Irrigation water use efficiency (IWP) and water use efficiency (WP) were determined in order to assess the effects of irrigation treatments (Howell et al., 1990). The equations are as follows:

$$WP = \frac{Y}{ET} \quad \text{(Eq.3)}$$

$$IWP = \frac{Y}{IW} \quad \text{(Eq.4)}$$

where Y is yield (kg ha^{-1}), ET is the seasonal evapotranspiration (mm), and IW is the amount of seasonal irrigation water (mm).

Leaf area index

Plant samples were taken to score the leaf area index (LAI) throughout the growing season at intervals of 10 days. Five plants were randomly selected for sample collection.

http://www.aloki.hu ● ISSN 1589 1623 (Print) ● ISSN 1785 0037 (Online)
DOI: http://dx.doi.org/10.15666/aeer/2005_41734191

Leaf area was measured with leaf area meter (LI-COR 3100): Leaf area index was the computed by dividing leaf area with ground area.

Ensiling procedure and chemical analyses

For analyzing silage quality, silage material was taken from each experimental unit and placed in 1 L airtight jars. The jars were opened after 60 days of fermentation. Extracts of fermented materials were prepared by homogenizing 25 g wet material with 100 mL water in a blender. The content was then filtered through two layers of cheesecloth and pH was determined. Silage samples were ground after drying at 65 °C. Afterwards, dry matter (DM) and CP were analyzed by following the procedure of AQAC (1984). The NDF and ADF contents were determined according to the procedure of Goering and Van Soest (1970). Crude fibers were analyzed according to method described by Crampton and Maynard (1938).

Statistical analysis

The results of the study were evaluated using Minitab 18 statistics software. Firstly, analysis of variance (ANOVA) was used to evaluate the effects of different irrigation treatments on the yield and quality of corn silage. Tukey's post-hoc test was used for comparing and ranking the treatment means.

Results and discussion

The ETc amounts from different experimental units were determined by considering soil moisture content at the effective root depth, rainfall, and the amount of applied IW. The seasonal water consumption of the treatments and the amount of irrigation water applied in the experimental treatments are given in *Table 3*.

Table 3. *Amount of irrigation water (IW) and evapotranspiration (ETc) in different irrigation treatments used in the current study*

Treatments		2017				2018			
		Rainfall mm	ΔS mm	IW mm	ETc mm	Rainfall mm	ΔS mm	IW mm	ETc mm
D_1	I_1	0	3.1	705.3	708.4	5.7	-3.9	737.3	739.1
	I_2	0	13.9	585.4	599.3	5.7	15.3	609.1	630.1
	I_3	0	36.3	465.6	501.9	5.7	22.7	480.8	509.2
	I_4	0	51.6	345.7	397.3	5.7	43.8	352.5	402.0
D_2	I_1	0	13.4	712.0	725.4	5.7	9.5	743.9	759.1
	I_2	0	28.0	590.8	618.8	5.7	11.6	614.3	631.6
	I_3	0	46.1	469.6	515.7	5.7	38.3	484.7	528.7
	I_4	0	58.7	348.4	407.1	5.7	58.4	355.1	419.2

ΔS: The change of moisture content in the 0-90 cm root depth, IW: irrigation water, ET_c: crop evapotranspiration

Harran Plain receives almost no precipitation during the growing period of corn. No precipitation was recorded during the first year of study, whereas only 5.7 mm was received during the second year. Therefore, plants obtained a significant part of required

http://www.aloki.hu ● ISSN 1589 1623 (Print) ● ISSN 1785 0037 (Online)
DOI: http://dx.doi.org/10.15666/aeer/2005_41734191

water from IW and a small amount from the water stored in the soil from early spring precipitation. The utilization of water retained in the soil was higher in treatments receiving less IW.

Since wheat was the winter crop in the experimental area, the land prepared for corn planting immediately after wheat harvest was irrigated with sprinkler irrigation to prepare seedbed. After emergence, fixed irrigation was applied twice in every year until the initiation of irrigation treatments. In the fixed irrigations, 62- and 57-mm water was applied during first and second year, respectively. The irrigation treatments were imposed once the plants attained 30 cm height. The irrigation treatments were initiated on 27 July and terminated on 25 September during 1st year. During the 2nd year, irrigation treatments were initiated and terminated on 30 July and 27 September, respectively.

The amount of IW applied to different irrigation treatments differed depending on the crop-pan coefficient and plant canopy. The amount of IW applied in I_1 treatment (full irrigation) was 705.3- and 712.0-mm during the first year, whereas IW was slightly higher in the second year due to prevailing climatic conditions.

The treatments differed for ETc depending on the amount of IW applied. While the ETc of the treatments where high amount of IW was applied were close to the total IW applied, the difference between the amount of IW and ETc increased with decreasing amount of applied IW. The ETc values for full irrigation treatment (I_1) were 708.4- and 725.4-mm during 1st year, while the values were 739.1- and 759.1 mm during 2nd year. Since the experiment was carried out in arid conditions, it increased in the amount of ETc. In the earlier studies ETc has been reported to vary from 474 to 605 mm by Kanber et al. (1990), from 494 to 644 mm by Kateji (1996), from 465 to 802 mm by Howell (1998), from 641 to 668 mm by Pandey (2000), from 366 to 625 mm by Payero et al. (2006), from 947 to 1003 mm by Simşek et al. (2011) from 184 to 425 mm by Ors et al. (2015), from 568 to 580 mm by Gheysari (2017), and from 708 to 759 mm by Büyüktaş et al. (2020). It can be concluded that genotypic differences, farming techniques, climatic conditions, soil texture, irrigation systems and IW amount significantly affect ETc (Igbadun et al., 2008).

When the corn grains reach the pulping stage (BBCH 83), plants were harvested manually, and FY and yield components were recorded and presented in *Table 4*.

The data analysis of FY revealed that D_1 recorded higher yield compared to D_2 ($p \leq 0.05$). This reveals that maintain soil moisture at a specific level through frequent irrigation exerted positive impact on FY. The FY was also significantly ($p \leq 0.01$) affected by the amount of IW in addition to irrigation intervals. The reduction in the amount of IW significantly reduced FY. The 51% reduction in IW reduced FY by 53%. Similar results were obtained for the rest of the reductions in the amount of IW. In other words, the decrease in FY was closer to reduction in IW. Statistical analysis revealed that irrigation interval by irrigation level interaction had non-significant effect on FY. The highest FY was noted for D1-I1 treatment.

Statistical analysis of FY data for the second year revealed similar findings as of first year. The individual effects of irrigation intervals ($p \leq 0.05$) and irrigation levels ($p \leq 0.01$) significantly altered FY. However, interactive effect of irrigation intervals and irrigation levels remained non-significant for FY. A 7.5% decrease in FY was recorded when irrigation interval was increased to 6 days from 3 days. Similarly, 17%, 35% and 52% reduction in IW reduced FY yield by 7%, 22% and 49%, respectively. The adverse effects of water stress became more severe with increased reduction in IW.

http://www.aloki.hu ● ISSN 1589 1623 (Print) ● ISSN 1785 0037 (Online)
DOI: http://dx.doi.org/10.15666/aeer/2005_41734191

Örs et al. (2015) reported that frequent irrigation increased FY, while Yazar et al. (2002) reported that irrigations performed with 3- or 6-days intervals had no effect on FA. In addition, several researchers reported that ET and FY are positively correlated, and the highest FY was obtained with full irrigation (Lizaso, 2001; Yazar et al., 2002; Payero et al., 2006; Bekele and Tilahun, 2007; Lauer, 2007; Montgomory, 2009; Rusere et al., 2012; Islam et al., 2012; Örs et al., 2015; Nihalyane et al., 2020; Büyüktaş et al., 2020).

Table 4. *Means and statistical groups for silage yield and yield component of corn grown under different irrigation intervals and irrigation levels (n = 3)*

Treatments	FY t ha^{-1}		*DMR* %		DMY t ha^{-1}		Plant height m	
	2017	**2018**	**2017**	**2018**	***2017***	***2018***	***2017***	***2018***
D_1	61.50a	64.26a	27.51	28.59	16.80	18.28a	2.59	2.69
D_2	57.39b	59.47b	28.18	27.59	16.07	16.35b	2.57	2.60
P (Factor A)	*	*	*ns*	*ns*	ns	*	*ns*	*ns*
I_1	78.64a	77.03a	27.06	27.89	21.27a	21.51a	2.92a	3.04a
I_2	66.70b	71.64a	27.34	27.48	18.22b	19.70ab	2.75b	2.84b
I_3	55.54c	59.73b	28.02	27.82	15.57c	16.65b	2.48c	2.53c
I_4	36.89d	39.05c	28.96	29.16	10.68d	11.40c	2.16d	2.18d
P (Factor B)	**	**	*ns*	*ns*	**	**	**	**
D_1-I_1	81.69	78.96	26.78	27.91	21.87	22.09	2.95	3.07
D_1-I_2	70.40	75.62	26.95	28.40	18.98	21.44	2.76	2.89
D_1-I_3	56.59	62.68	27.86	28.20	15.74	17.69	2.45	2.58
D_1-I_4	37.34	39.79	28.45	29.84	10.63	11.88	2.18	2.22
D_2-I_1	75.59	75.01	27.34	27.87	20.67	20.93	2.88	3.01
D_2-I_2	63.00	67.66	27.73	26.56	17.47	17.95	2.73	2.79
D_2-I_3	54.50	56.79	28.18	27.44	15.39	15.60	2.51	2.47
D_2-I_4	36.44	38.31	29.47	28.47	10.74	10.92	2.14	2.14
P (A*B)	ns	ns	ns	ns	*ns*	*ns*	*ns*	*ns*

FY: The silage yield, DMR: The dry matter ratio, DMY: the dry matter yield, ^{ns} = non-significant, ^{a}The treatment means followed by the same letter are statistically non-significant at 95% probability level by Tukey's test

The fresh silage samples harvested from different experimental units were dried to determine matter ratio (DMR) and the amount of DMY produced. The DMRs of different irrigation treatments increased numerically with increasing water stress and the highest DMR was noted for I_4. However, the differences among treatments were non-significant according to ANOVA. The earlier studies have reported contrasting results for DMRs. Some studies reported that DMR was not affected by IW (Baran, 2015), whereas the others reported that DMR decreased with increasing amount of IW (Makela et al., 2005; Kruse et al., 2008; Setter and Parra, 2010; Bulut, 2015). In contrast to these results, İslam et al. (2012) reported a significant increase in DMR with increasing amount of IW. These differences can be explained with varieties used in different studies, agricultural techniques opted and time of silage making stage.

http://www.aloki.hu ● ISSN 1589 1623 (Print) ● ISSN 1785 0037 (Online)
DOI: http://dx.doi.org/10.15666/aeer/2005_41734191

In parallel with FY, the amount of DMY differed among applied irrigation treatments. Different irrigation intervals had non-significant effect on DMY. However, IW significantly affected ($p \leq 0.01$) DMY. The DMY was linearly increased with increasing amount of IW. Each irrigation level was placed in different grouped according to Tukey's post-hoc test. The ANOVA revealed significant effect of irrigation intervals ($p \leq 0.05$) and irrigation levels ($p \leq 0.01$) on DMY production during second year. The DMY in corn was increased with frequent irrigation. Similarly, DMY was also increased with increasing amount of IW and reached to 21.51 t ha^{-1} with full irrigation. The earlier studies have also reported similar results as of current study (Lizaso et al., 2001; Schmaher et al., 2003; Greysari et al., 2009; Islam et al., 2012; Ferreria, 2015).

Plant height is an important yield-related parameter of corn silage. In the current study irrigation intervals had non-significant effect on plant height during both years, whereas irrigation levels significantly ($p \leq 0.01$) altered plant height. Each irrigation level was ranked in different group according to Tukey's test. The plants receiving full irrigation (I_1) reached 2.92 m height during first year, and plant height significantly reduced with decreasing amount of IW. The 34% reduction in IW decreased plant height by 44 cm, while 51% reduction in IW decreased plant height by 76 cm. Similar results were obtained for plant height during second year of the study. The treatments receiving lower amount of IW resulted in lower plant height, whereas increase in plant height was recorded with increasing amount of IW. Several earlier studies have reported similar results as obtained in the current study (Otegui et al., 1995; İstanbulluoğlu et al., 2002; Bozkurt et al., 2006; Soler et al., 2007; Kızıloğlu et al., 2009; Greysari et al., 2009; Bulut, 2015).

Silage samples were taken from each experimental unit and quality traits were determined to assess the impact of irrigation treatments on silage quality. The quality traits of silage maize recorded during the current study are summarized in *Table 5*.

Silage quality is of great importance in in addition to high silage yield. The CP, ADF, NDF crude fiber ratios and pH values are used to assess silage quality. High CP contents are desired in high quality silage. The CP contents were significantly altered by irrigation interval ($p \leq 0.05$) and the irrigation levels ($p \leq 0.01$) during 2017. The treatments which were frequently irrigated had higher CP contents. The amount of IW applied also affected CP content and increasing amount of IW increased CP contents. The highest CP contents were recorded for the treatment receiving the highest amount of IW. The least water receiving two treatments did not differ statistically. Similar CP contents as of first year were noted during the second year of the study. The CP contents were significantly affected by irrigation intervals ($p \leq 0.01$) and irrigation levels ($p \leq 0.01$). However, in contrast to the first year, the CP contents were lower in frequently irrigated treatments. The treatments receiving the highest amount of water resulted in the highest CP contents during second year, whereas the lowest CP contents were noted for the treatment facing higher drought stress. The interactive effect of irrigation intervals and irrigation levels remained non-significant for CP contents during both years of the study. The earlier studies have reported contrasting correlations between IW and CP contents. For example, Pelleschi et al. (1997), Yosef et al. (2009) and Şimşek et al. (2011) reported that CP contents increased with increasing amount of IW, whereas some other studies reported non-significant effect of IW on CP contents (Oweis et al., 1999; Hargreaves et al., 2009; Islam et al., 2012; Liu et al., 2013; Seif et al., 2016). In contrast, Montgomory (2019) and Nihalyane et al. (2020) reported a negative correlation between IW and CP contents.

http://www.aloki.hu ● ISSN 1589 1623 (Print) ● ISSN 1785 0037 (Online)
DOI: http://dx.doi.org/10.15666/aeer/2005_41734191

Table 5. *Means and statistical groups for some silage quality characteristics of treatments*

Treatments	*CP* %		*ADF* %		*NDF* %		*Crude fiber* %		*pH*	
	2017	**2018**	**2017**	**2018**	**2017**	**2018**	**2017**	**2018**	**2017**	**2018**
D_1	8.01a	7.54b	30.27	30.28	43.70	41.29	16.22b	16.73	3.56	3.71
D_2	7.85b	7.68a	29.52	29.85	44.01	41.89	16.77a	16.35	3.53	3.64
P (Factor A)	*	*	*ns*	*ns*	*ns*	*ns*	*	*ns*	*ns*	*ns*
I_1	8.39a	8.00a	31.40a	31.39a	46.37a	42.82	17.66a	17.40ab	3.58	3.62
I_2	8.03b	7.65b	31.39a	31.75a	44.99ab	42.22	17.20ab	17.74a	3.54	3.62
I_3	7.64c	7.60b	28.77ab	29.54ab	42.34bc	41.28	16.32b	16.15bc	3.49	3.75
I_4	7.66c	7.20c	28.00b	27.40b	41.78c	40.05	14.80c	14.88c	3.57	3.71
P (Factor B)	**	**	**	*	**	*ns*	**	**	*ns*	*ns*
D_1-I_1	8.44	7.95	32.86	31.40	45.80	42.74	17.12	17.16	3.57	3.65
D_1-I_2	8.15	7.52	31.73	32.44	44.15	40.91	17.14	18.12	3.55	3.61
D_1-I_3	7.74	7.64	28.23	29.21	42.13	41.68	16.05	16.31	3.51	3.79
D_1-I_4	7.70	7.04	28.26	28.07	42.73	39.85	14.58	15.33	3.59	3.77
D_2-I_1	8.33	8.04	29.95	31.37	46.95	42.90	18.21	17.63	3.58	3.59
D_2-I_2	7.91	7.78	31.06	31.06	45.82	43.53	17.26	17.36	3.53	3.62
D_2-I_3	7.54	7.55	29.32	29.86	42.56	40.88	16.58	15.98	3.47	3.70
D_2-I_4	7.62	7.36	27.75	26.73	40.84	40.25	15.03	14.44	3.54	3.64
P (A*B)	*ns*	*ns*	*ns*	*ns*	*ns*	*ns*	*ns*	*ns*	*ns*	*ns*

CP: The crude protein, ADF: the acid detergent fiber, ND: the neutral detergent fiber, ^{ns} = non-significant, $^{a:}$ The treatment means followed by same letters are statistically non-significant at 95% probability level by Tukey's test

The ADF is a good indicator of feed digestibility and energy intake of the animals (Goering and Van Soest, 1970, 1994). Assefa and Ledin (2001) reported that lower ADF contents in silage represent high quality. The ADF values ranged between 27.75 and 32.86% during first year and were not affected by irrigation intervals. However, irrigation levels had significant ($p \leq 0.01$) effect on ADF. There were no significant differences among high IW receiving treatments (I_1 and I_2). However, increasing water stress significantly reduced ADF ratio. Similar results for ADF were obtained during 2018. Irrigation with 3-day or 6-day intervals did not affect ADF content; however, ADF ratio significantly ($p \leq 0.05$) increased with increasing amount of IW. Irrigation interval had non-significant effect on ADF in the current study. Ors et al. (2015) also reported that ADF was not affected by irrigation intervals. However, some previous studies indicated that ADF ratio increased with increasing amount of IW (Şimşek et al., 2011; Kuchenmeister et al., 2013; Kaplan, 2016). In contrast to these findings, Montgomory (2019), İslam et al. (2012), Seif (2016), Nihalyane (2020) and Shahrabian and Soleymani (2011) reported that increasing IW decreased ADF ratio. Besides some other studies reported that ADF content was not affected by IW (Islam et al., 2012; Işık et al., 2012; Ors et al., 2005). It is thought that the differences in the effects of IW on ADF content in current study are related to the applied agricultural techniques, crop variety and harvest time.

The NDF content is also an important quality criterion in corn silage and should not be high (Dawyer, 1998). In the study, irrigation intervals did not affect NDF ratio

http://www.aloki.hu ● ISSN 1589 1623 (Print) ● ISSN 1785 0037 (Online)
DOI: http://dx.doi.org/10.15666/aeer/2005_41734191

during both years. However, the increase in the amount of IW applied affected the NDF ratios ($p \leq 0.01$) in the first year, while had no effect during the second year. Previous studies have reported conflicting results on the effect of IW on NDF contents. Like the findings of current study, several studies reported NDF ratio increases with increase in the amount of IW (Islam et al., 2012; Şimşek et al., 2011; Shahrabian and Soleymani, 2011; Ferreria, 2015). Contrastingly, numerous studies also reported decrease in NDF content with increasing IW application (Montgomory, 2009; Seif et al., 2016; Nihalyane et al., 2020). Besides, Işık (2012) reported that NDF was not affected by IW.

The pH values of the silages obtained from different experimental units varied between 3.47-3.59 and 3.59-3.79 in 2017 and 2018, respectively. Although the pH value, which was 3.54 in the first year, increased to 3.67 during second year, different irrigation day intervals or irrigation levels had non-significant effect on the pH of silage. The pH values of the treatments were like optimum pH levels corn silage reported by Kolver et al. (2001). Mould et al. (1983) and Bates (2009) reported that pH values decreased with increasing amount of IW. Contrastingly, İslam et al. (2012) and Kaplan (2016) reported an increase in pH value with increasing amount of IW.

Crude fiber ratio is an important quality criterion affecting the digestibility of silage. Irrigation intervals ($p \leq 0.05$) and irrigation levels ($p \leq 0.01$) had significant effect on the crude fiber content during first year; however, their interaction was non-significant. The crude fiber content increased with increase in irrigation interval, and the treatments irrigated at 6-day interval recorded higher crude fiber contents. On the other hand, crude fiber ratios increased as the amount of IW increased. According to the results of the Tukey test, each irrigation level was in a separate group, while the first group contained I_1. Irrigation interval did not affect crude fiber content during second year; however, irrigation levels significantly ($p \leq 0.01$) affected crude fiber content first year. The highest crude fiber content was recorded for I_2, while the lowest ratio was recorded for the treatment receiving the least amount of IW. Baran (2015) also reported similar results that decrease in IW lowered crude fiber content. Corn silage should have a crude fiber content of 14-18% and this ratio should not exceed 20% for feeding to dairy cattle (Yüksel et al., 2000; Aydınoğlu, 2005). The crude fiber content were between these limits in the current study; thus, meet the desired ratios for dairy cattle.

Leaf area index and water use efficiencies

Leaf development is associated with photosynthesis and evapotranspiration (ET), and leaf area is used in the evaluation of most agronomic and physiological studies as well as plant growth (Guo and Sun, 2001).

LAI varies depending on leaf size and number of leaves per plant. It is negatively affected by water stress and nutrient deficiency (Longnecker, 1994). The LAI values recorded from different treatments in the current study are presented in *Figure 1*.

A sigmoidal relationship was recorded between LAI and time in the current study during both years. The LAI started to increase from plants' emergence and reached the maximum level at 0-80 days from planting. Although LAI continuously increased in all treatments, the values differed among various irrigation treatments. Negative effects of water stress on LAI became evident 48 DAS 48 (*Fig. 1*). The LAI started declining after reaching the peak values. The decrease in LAI was more pronounced in the treatments receiving lower amount of IW (I_3 and I_4), and the treatments irrigated with higher amount of IW (I_1 and I_2) observed less decrease in LAI. The highest LAI value was

http://www.aloki.hu ● ISSN 1589 1623 (Print) ● ISSN 1785 0037 (Online)
DOI: http://dx.doi.org/10.15666/aeer/2005_41734191

noted from fully irrigated plants D_1-I_1 and D_2-I_1, and the values were 4.83 and 4.71 and 5.12 and 5.01 during 1st and 2nd year, respectively.

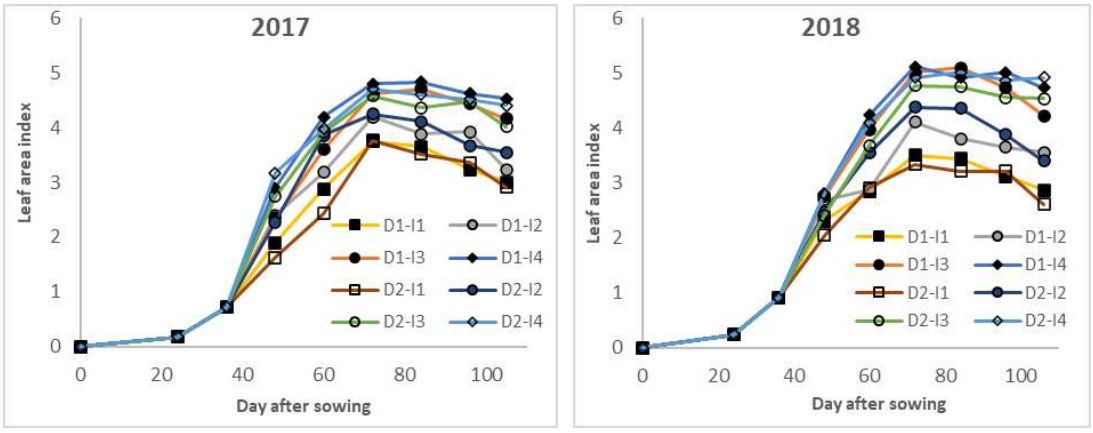

Figure 1. *Temporal changes in leaf area index of corn silage grown under different irrigation treatments (DAS = days after sowing)*

Although differences were noted among different irrigation treatments, the LAI values of the treatments with high IW application (full irrigation) in this study were consistent with the results of previous studies (Stone et al., 2001; Yazar et al., 2002; Karam et al., 2006; Sampathkumar et al., 2013). The highest LAI value was obtained from full irrigation treatment. However, differences were noted among treatments for time to reach the highest LAI in the current study. Agricultural practices, environment and variety exert significant effects on LAI.

Silage yield increased depending on the increase in the amount of IW and ETc. *Figure 2a* shows the correlation among ETc and yield. In addition, yield response factor (Ky) applied to evaluate the relation between water consumption and yield is shown in *Figure 2b*.

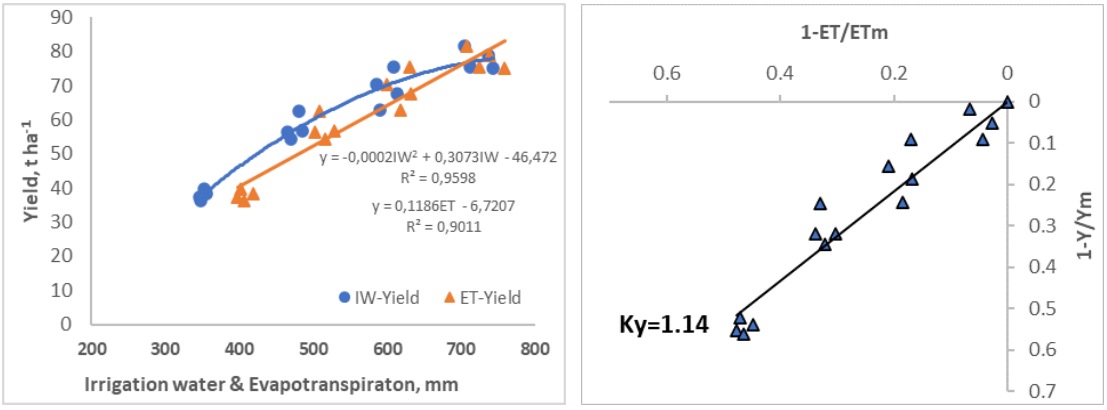

Figure 2. *The relationship between fresh yield and irrigation water and evapotranspiration (a) and relationship between relative evapotranspiration deficit and relative yield reduction (b)*

Silage yield witnessed an increase with increasing ETc values. A significant ($p \leq 0.01$) linear relationship was noted between ETc and yield with two years' average

http://www.aloki.hu ● ISSN 1589 1623 (Print) ● ISSN 1785 0037 (Online)
DOI: http://dx.doi.org/10.15666/aeer/2005_41734191

data. Several researchers in earlier studies reported a linear relationship between ET and yield (Howell et al., 1998; Kızıloğlu et al., 2009; Şimşek et al., 2011; Okursoy, 2009). A second order significant sigmoidal ($p \leq 0.01$) relationship was recorded between IW and yield. Silage yield increased with increasing amount of IW. However, as the amount of seasonal IW increased, the positive effect of IW on yield decreased. While some researchers reported a sigmoidal relationship between IW and FY in previous studies on corn silage (Bozkurt et al., 2006; Ors et al., 2015), the others reported a linear relationship (Yazar et al., 2002; Okursoy, 2009).

The slopes of the relationships between relative yield reduction and relative evapotranspiration deficit termed the "yield response factor" by Doorenbos and Kassam (1979) were 1.14. The Ky value ≥ 1.0 indicate that the plant is highly sensitive to water stress. The results of this study indicated that that corn silage is highly sensitive to water stress in arid climates. The earlier studies have also reported similar results. Doorenbos and Kassam (1979), reported that seasonal Ky factor of corn grown in deep and medium textured soils was 1.25. Şimşek et al. (2011) reported the Ky factor of 1.13 for drip irrigated corn. Howell et al. (1997) reported that the ky factor was 1.47 in Bushland, Texas.

Water use efficiency is an important criterion considered in determining the most appropriate irrigation program in limited irrigation research. The two-year average IWP and WP values calculated for the applied treatments in this study are shown in *Figure 3*.

There was no precipitation during corn growing season in the first year, and only a little precipitation was received in the second year. Therefore, almost all ETc was obtained from the IW. For this reason, the WP and IWP values of the treatments where more IW was applied were close to each other. Since the treatments with low IW application benefited more from the available moisture in the soil, significant differences were noted between the WP and IWP values of these treatments. The IWP values of applied treatments ranged between 10.6 and 12.6 kg m^{-3}, with the lowest IWP values noted for D_2-I_4 and D_2-I_2 treatments irrigated at 6-day interval. The IWP values of D_1 treatment were higher than D_2 at all irrigation levels. This is because the silage yield in D_1 was higher than D_2. These results indicate that frequent irrigation increases IW productivity of corn silage.

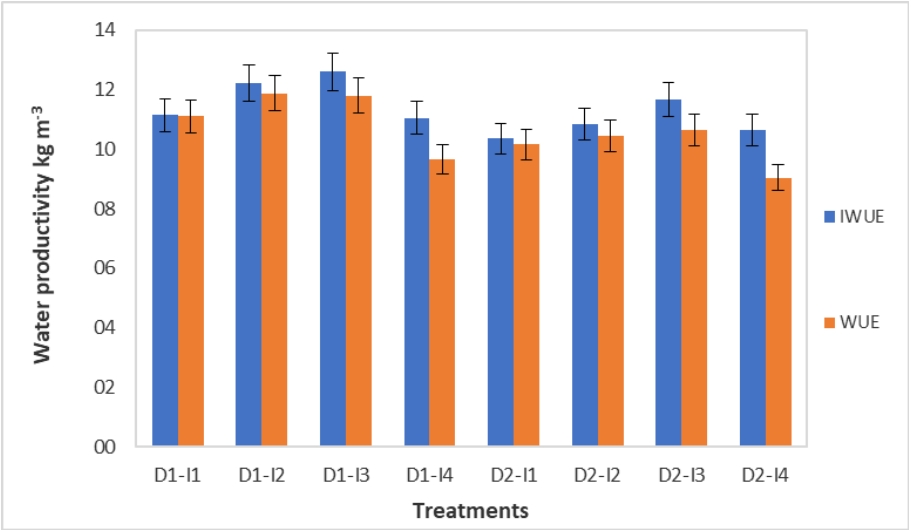

Figure 3. *Water productivity and irrigation water production for various irrigation treatments used in the current study*

http://www.aloki.hu ● ISSN 1589 1623 (Print) ● ISSN 1785 0037 (Online)
DOI: http://dx.doi.org/10.15666/aeer/2005_41734191

The WP values were also like IWP values. The D_1 interval had higher WP values than D_2 with all irrigation levels. In other words, maintaining the root zone at a certain moisture level with frequent irrigation increased WP in corn. While the WP values of the treatments where more water was applied were close to each other, the WP of the least applied IW (I_4) was lower than the rest of the treatments.

No precipitation is received during the growing season of corn silage in arid regions and ETc in such regions is higher than other climatic regions. This reduces WP and IWP values of irrigations in arid regions. Several earlier studies indicated that low water availability reduced WP (Farre and Faci, 2006; Igbadun et al., 2008; Payero et al., 2006; Kızıloğlu, 2009; Yazar, 2009; Şimşek, 2011 Bauzzama, 2012), whereas some studies reported contrasting findings that low water availability increased WP (Rusere, 2012; Mostafa, 2013). Howell (1998) reported no significant change in WP in response to water shortage. The IWP values obtained in previous studies also differed from each other. Farre (2006) reported that IWP increased with an increase in the amount of IW, while on the contrary some studies reported that IWP decreased as the amount of IW increased (Payero et al., 2006; Yenesew and Tilahun, 2009). These different results regarding the effect of IW on IWP are linked to climatic conditions and irrigation method used to grow corn silage.

Conclusion

Frequent irrigations increased silage yield of corn with drip irrigation under arid climatic conditions. However, low water application during the whole growing season caused significant decreases in silage yield. For this reason, if irrigation water needs to be reduced in corn silage cultivation, it should be applied when the plant is less sensitive to water stress. Irrigation frequency had no effect on silage quality characteristics; however, the amount of IW exerted significant impacts. Contrary to the negative effect of water shortage on yield, it improved quality of silage.

Acknowledgments. This work was financially supported by the Harran University Application and Research Center for Science and Technology (Project number: 17240).

REFERENCES

[1] Assefa, G., Ledin, I. (2001): Effect of variety, soil type and fertilizer on the establishment, growth, forage yield, quality and voluntary intake by cattle of oats and vetches cultivated in pure stands and mixtures. – Anim Feed Sci Technol. 92: 95-111. DOI: 10.1016/S0377-8401(01)00242-5.

[2] Aydınoğlu, B. (2005): Effects of different cutting stages on forage yield and chemical composition of sorghum (Sorghum bicolor L. Moench). – PhD Thesis, Akdeniz University, Department of Field Crops, Antalya.

[3] Bates, G. (2009): SP434D Corn Silage. – The University of Tennessee Agricultural Extension Service, SP434D-5M-9/98 E12-2015-00-082-99. http://trace.tennessee.edu/utk_agexfora/6.

[4] Bekelei, S., Tilahun, K. (2007): Regulated deficit irrigation scheduling of onion in a semiarid region of Ethiopia. – Agric. Water Management 89: 148-152. DOI: 10.1016/j.agwat.2007.01.002.

http://www.aloki.hu ● ISSN 1589 1623 (Print) ● ISSN 1785 0037 (Online)
DOI: http://dx.doi.org/10.15666/aeer/2005_41734191

[5] Bouazzama, B., Xanthoulis, D., Bouaziz, A. (2012): Effect of water stress on growth, water consumption and yield of silage maize under flood irrigation in a semi-arid climate of Tadla (Morocco). – Biotechnol. Agron. Soc Env. 16(4): 468-477.
[6] Bozkurt, Y., Yazar, A., Gencel, B., Sezen, M. S. (2006): Optimum lateral spacing for drip-irrigated corn in the Mediterranean Region of Turkey. – Agr. Water Management 85: 113-120.
[7] Brouwer, C., Heibloem, M. (1986): Irrigation water management: irrigation water needs. – Training Manual No: 3. FAO, Rome.
[8] Bulut, M. E. (2015): Effect of irrigation methods and irrigation levels on yield and yield component of second crops silage corn (Zea mays L.). – Master Thesis, Field Crops Main Discipline, Iğdır University.
[9] Buyuktas, D., Bastug, R., Ozen, N., Aydinsakir, K., Karaca, C., Curek M., Erdal, S. (2020): Evapotranspiration, yield and silage quality characteristics of three maize hybrids grown under Mediterranean conditions. – Archives of Agronomy and Soil Science 67(10): 1341-1358.
[10] Cai, H., Shao, G., Zhang, Z. (2002): Lateral layout of drip irrigation under plastic mulch for cotton. – Trans CSAE 18(1): 45-48.
[11] Cox, W. J., Cherney, D. R., Hanchar, J. J. (1998): Row spacing, hybrid, and plant density effects on corn silage yield and quality. – J. Prod. Agric. 11: 128-134.
[12] Crampton, E. W., Maynard, L. A. (1938): The relation of cellulose and lignin content to the nutritive value of animal feeds. – J. Nutr. 15: 383.
[13] Doorenbos, J., Kassam, A. H. (1979): Yield Response to Water. – FAO Irrigation and Drainage Paper No. 33, FAO, UN, Rome.
[14] DSI (2022): https://www.dsi.gov.tr/Sayfa/Detay/720. – Access date: 1 April 2022.
[15] Edreira, J. R., Carpici, E. B., Sammarro, D., Otegui, M. (2011): Heat stress effects around flowering on kernel set of temperate and tropical maize hybrids. – Field Crop. Res. 123: 62-73.
[16] FAO (2020): The State of Food and Agriculture 2020. – Overcoming water challenges in agriculture. Rome. DOI: https://doi.org/10.4060/cb1447en.
[17] Farré, I., Faci, J. M. (2006): Comparative response of maize (*Zea mays* L.) and sorghum (*Sorghum bicolor* L Moench) to deficit irrigation in a Mediterranean environment. – Agr. Water Management 83(1): 135-143. DOI: 10.1016/j.agwat.2005.11.001.
[18] Farré, I., Faci, J. M. (2009): Deficit irrigation in maize for reducing agricultural water use in a Mediterranean environment. – Agric. Water Management 96: 383-394.
[19] Ferreira, G. (2015): Understanding the effects of drought stress on corn silage yield and quality. – Tri-State Dairy Nutrition Conference, April 20-22, 2015, Virginia, ABD.
[20] Geren, H., Avcıoğlu, R., Kır, B., Demircioğlu, G., Yılmaz, M., Cevheri, A. C. (2003): Effect of different sowing dates on the yield and quality characteristics of some maize cultivars grown as second crop for silage. – Journal of Agriculture Faculty of Ege University 40(3): 57-64.
[21] Gheysari, M., Mirlatifi, S. M., Bannayan, M., Homaee, M., Hoogenboom, G. (2009): Interaction of water and nitrogen on maize grown for silage. – Agr. Water Manage. 96: 809-821.
[22] Gheysari M., Sadeghi, S. H., Loescher, H. W., Amiri, S., Zareian, M. J., Majidi, M. M., Asgarinia, P., Payero, J. O. (2017): Comparison of deficit irrigation management strategies on root, plant growth and biomass productivity of silage maize. – Agr. Water Management 182: 126-138.
[23] Goering, H. K., Van Soest, P. J. (1970): Forage Fiber Analysis. Agricultural Handbook. – Department of Agriculture 379.
[24] Goncalves, J. M., Muga, A. P., Horst, M. G., Pereira, L. S. (2011): Furrow irrigation design with multicriteria analysis. – Biosystems Engineering 109(4): 266-275.
[25] Goorahoo, D., Sharma, F. C., Adhikari, D. D., Benes, S. E. (2011): Irrigation. 6th Ed. – Irrigation Association, Fairfax, VA.

http://www.aloki.hu ● ISSN 1589 1623 (Print) ● ISSN 1785 0037 (Online)
DOI: http://dx.doi.org/10.15666/aeer/2005_41734191

[26] Guo, D. P., Sun, Y. Z. (2001): Estimation of leaf area of stem lettuce (Lactuca sativa var angustana) from linear measurements. – Indian Journal of Agric. Science 71(7): 483-486.
[27] Hargreaves, A., Hill, J., Leaver, J. D. (2009): Effect of stage of growth on the chemical composition and nutritive value and ensilability of whole-crop barley. – Anim. Feed Sci. Technol. 152: 50-61.
[28] Herrero, M. P., Johnson, R. (1981): Drought stress and its effects on maize reproductive systems 1. – Crop Science 21: 105-110.
[29] Howell, T. A., Cuenca, R. H., Solomon, K. H. (1990): Crop Yield Response. – In: Hoffman, G. J., Howell, T. A., Solomon, K. H. (eds.) Management of Farm Irrigation Systems. An ASAE Monograph, St. Joseph, MI, pp. 93-116, Chapter 5.
[30] Howell, T. A., Schneider, A. D., Evett, S. R. (1997): Subsurface and surface microirrigation of corn Southern High Plains. – Trans. ASAE 40(3): 635-641.
[31] Howell, T. A., Tolk, J. A., Arland, D. S., Evertt, R. (1998): Evapotranspiration, yield and water use efficiency of corn hybrids differing in maturity. – Agron. J. 90: 3-9.
[32] Igbadun, H. E., Salim, B. A., Tarimo, A. K. P. R., Mahoo, H. F. (2008): Effect of deficit irrigation scheduling on yields and soil water balance of irrigated maize. – Irrig Sci. 27: 11-23. DOI: 10.1007/s00271-008-0117-0.
[33] Isik, S., Aydogan, S., Gunes, A., Ozcan, G., Tezel, M., Aksoyak, S., Aktas, A. H., Mulayim, A., Tamkoc, A., Acar, R., Tari, A. F., Ates, S. (2012): Artificial pasture determining the impact on quality of irrigation level. – Research Journal of Agricultural Sciences 5(2): 148-150.
[34] Islam, M. R., Garcia, S. C., Horadagoda, A. (2012): Effects of irrigation and rates and timing of nitrogen fertilizer on dry matter yield, proportions of plant fractions of maize and nutritive value and in vitro gas production characteristics of whole crop maize silage. – Anim Feed Sci Tech. 172: 125-135. DOI: 10.1016/j.anifeedsci.2011.11.013.
[35] Istanbulluoglu, A., Kocaman, I., Konukcu, F. (2002): Water use-production relationship of maize under Tekirdag conditions in Turkey. – Pak J Biol Sci. 5(3): 287-291. DOI: 10.3923/pjbs.2002.287.291.
[36] James, L. G. (1988): Principles of Farm Irrigation Systems Design. – John Wiley and Sons Inc, New York.
[37] Kanber, R., Yazar, A., Eylen, M. (1990): The Water-Yield Relationship of Corn, the Second Crop After Wheat, in Çukurova Conditions. – Institute of Tarsus Topraksu Res., Gen. Pub. No: 173/108, Tarsus.
[38] Kaplan, M. (2005): Effects of different intra and inter row spacing on yield and yield components of second crop silage maize (Zea mays L.) under Kahramanmaraş conditions. – MSc thesis, Institute of Natural and Applied Science Department of Field Crops, University of Kahramanmaraş.
[39] Kaplan, M., Baran, O., Unlukara, A., Kale, H., Arslan, M., Kara, K., Buyukkilic Beyzi, S., Konca, Y., Ulas, A. (2016): The effects of different nitrogen doses and irrigation levels on yield, nutritive value, fermentation and gas production of corn silage. – Turk J Field Crops 21(1): 101-109.
[40] Karam, F., Breidy, J., Stepan, C., Rouphael, Y. (2003): Evapotranspiration, yield and water use efficiency of drip irrigated corn in the Bekaa Valley of Lebanon. – Agric. Water Management 63: 125-137.
[41] Katerji, N., Hoorn, J. W., Hamdy, A., Karam, F., Mastrorilli, M. (1996): Effect of salinity on water stress, growth and yield of maize and sunflower. – Ag. Water Manag. 30: 237-249.
[42] Katerji, N., Mastrorilli, M., Rana, G. (2008): Water use efficiency of crops cultivated in the Mediterranean region: review and analysis. – European Journal of Agronomy 28(4): 493-507. https://doi.org/10.1016/j.eja.2007.12.003.
[43] Keller, J., Bliesner, R. D. (1990): Sprinkle and Trickle Irrigation. – Chapman and Hall, New York.

http://www.aloki.hu ● ISSN 1589 1623 (Print) ● ISSN 1785 0037 (Online)
DOI: http://dx.doi.org/10.15666/aeer/2005_41734191

[44] Kılıç, A. (1986): Silo Feed (Teaching, Learning and Practice Advice). – Bilgehan Press, İzmir.
[45] Kiziloglu, M. F., Sahin, U., Kuslu, Y., Tunc, T. (2009): Determining water-yield relationship, water use efficiency, crop and pan coefficients for silage maize in a semiarid region. – Irrigation Science 27: 129-137. DOI: 10.1007/s00271-008-0127-y.
[46] Kolver, E. S., Roche, J. R., Miller, D., Densley, R. (2001): Maize silage for dairy cows. – Proc New Zealand Grasslands Asso. 63: 195-201.
[47] Kruse, S., Hermann, A., Kornher, A., Taube, F. (2008): Evaluation of genotype and environmental variation in fiber content of silage maize using a model-assisted approach. – Eur. J. Agron. 8: 210-223.
[48] Kuchenmeister, K., Kuchenmeister, F., Kayser, M., WrageMonnig, N., Isselstein, J. (2013): Influence of drought stress on nutritive value of perennial forage legumes. – Int J Plant Prod. 7: 693-710.
[49] Lauer, J. (2007): Drought stress reduces corn silage yield more than quality. – Agronomy advice, University of Wisconsin, Agronomy Department.
[50] Liu, L., Maier, A., Klocke, N., Yan, S., Rogers, D., Tesso, T., Wang, D. (2013): Impact of deficit irrigation on sorghum physical and chemical properties and ethanol yield. – American Society of Agricultural and Biological Engineers 56(4): 1541-1549.
[51] Lizaso, J. I., Melendez, L. M., Ramirez, R. (2001): Early flooding of two cultivars of tropical maize. – I. Shoot and root growth. J. Plant Nutr. 24: 979-995.
[52] Longnecker, N. (1994): Nutrient Deficiencies and Vegetative Growth. – In: Basra, A. S. (ed.) Mechanisms of Plant Growth and Improved Productivity: Modern Approaches and Perspectives. Marcel Dekker, New York, pp. 137-172.
[53] Makela, P., McLaughlin, J. E., Boyer, J. S. (2005): Imaging and quantifying carbohydrate transport to the developing ovaries of maize. – Ann. Bot. 96: 75-86.
[54] McDonald, P., Henderson, A. R., Heron, S. J. E. (1991): The Biochemistry of Silage. 2nd Ed. – Chalcombe Publication, Marlow, pp.81-151.
[55] Meeske, R., Ashbell, G., Weinberg, Z. G., Kipnis, T. (1993): Ensiling forage sorghum at two stages of maturity with the addition of lactic acid bacterial inoculants. – Anim. Feed Sci. Technol. 43: 165-175.
[56] Miller, W. J. (1979): Dairy Cattle Feeding and Nutrition. – Academic Press, New York.
[57] Montgomery, R. (2009): Influence of corn hybrids and water stress on yield and nutritive value. – MS Thesis, Texas Tech University.
[58] Mostafa, H., Derbala, A. (2013): Performance of supplementary irrigation systems for corn silage in the sub-humid areas. – Agricultural Engineering International: The CIGR Journal of Scientific Research and Development 15(4): 9-15.
[59] Mould, F. L., Ørskov, E. R. (1983): Manipulation of rumen fluid pH and its influence on celluloslysis *in sacco*, dry matter degradation and the rumen microflora of sheep offered either hay or concentrate. – Anim. Feed Sci. Technol. 10: 1-14.
[60] Musick, J. T., Dusek, D. A. (1980): Irrigated corn yield response to water. – Trans. ASAE 23: 92-98.
[61] NeSmith, D. S., Ritchie, J. T. (1992): Short and long-term responses of corn to a preanthesis soil water deficit. – Argon. Journal 84: 107-113.
[62] Nilahyane, A., Islam, M. A., Mesbah, A. O., Herbert, S. K., Axel Garcia, Y., Garcia, A. G. (2020): Growth, water productivity, nutritive value, and physiology responses of silage corn to water stress. – Agronomy Journal 112: 1625-1635. DOI: https://doi.org/10.1002/agj2.20015.
[63] Okursoy, H. (2009): Determination of water production functions of secondary crop maize under different irrigation methods in Trakya conditions. – PhD thesis, Graduate School of Natural and Applied Sciences, Namık Kemal University.
[64] Ors, S., Sahin, U., Kiziloglu, F. M. (2015): Yield, quality and irrigation water use of drip-irrigated silage maize with different irrigation techniques. – Pak J Agric Science 52(3): 595-607.

http://www.aloki.hu ● ISSN 1589 1623 (Print) ● ISSN 1785 0037 (Online)
DOI: http://dx.doi.org/10.15666/aeer/2005_41734191

[65] Otegui, M. E., Andrade, F. H., Suero, E. E. (1995): Growth, water use, and kernel abortion of maize subjected to drought at silking. – Field Crop Resource 40(2): 87-94.
[66] Oweis, T., Pala, M., Ryan, J. (1999): Management alternatives for improved durum wheat production under supplemental irrigation in Syria. – Eur. J. Agron. 11(3): 255-266. DOI: 10.1016/S1161-0301(99)00036-2.
[67] Pandey, R. K., Maranville, J. W., Chetima, M. M. (2000): Deficit irrigation and nitrogen effects on maize in a Sahelian environment: II. Shoot growth, nitrogen uptake and water extraction. – Agricultural Water Management 46(1): 15-27.
[68] Payero, J. O., Melvin, S. R., Irmak, S., Tarkalson, D. (2006): Yield response of corn to deficit irrigation in a semiarid climate. – Agricultural Water Management 84: 101-112. DOI: 10.1016/j.agwat.2006.01.009.
[69] Pelleschi, S., Rocher, J. P., Prioul, J. L. (1997): Effect of water restriction on carbohydrate metabolism and photosynthesis in mature maize leaves. – Plant Cell Environmental 20: 493-503.
[70] Pereira, L. S., Cordery, I., Iacovides, I. (2012): Improved indicators of water use performance and productivity for sustainable water conservation and saving. – Agricultural Water Management 108: 39-51. DOI: https://doi.org/10.1016/j.agwat.2011.08.022.
[71] Roth, G., Undersander, D., Allen, M., Ford, S., Harrison, J., Hunt. C. (1995): Corn Silage Production, Management, and Feeding. – NCR574. ASA, Madison, WI.
[72] Rusere, F., Soropa, G., Gwatibaya, S., Moyo, D., Ndeketeya, A., Mavima, G. A. (2012): Effects of deficit irrigation on winter silage maize production in Zimbabwe. – International Research Journal of Plant Science 3(9): 188-192.
[73] Sampathkumar, T., Pandian, B. J., Rangaswamy, M. V., Manickasundaram, P., Jeyakumar, P. (2013): Influence of deficit irrigation on growth, yield and yield parameters of cotton–maize cropping sequence. – Agricultural Water Management 130: 90-102.
[74] Schmaler, K., Kruger, U., Richert, H. (2003): Ertrag und Qualität von Silomais in Abhängigkeit vom Wasserangebot. – Archives of Agronomy and Soil Science 49(4): 357-374.
[75] Seif, F., Paknejad, F., Azizi, F., Kashani, A., Shahabifar, M. (2016): Effect of different irrigation regimes and zeolite application on yield and quality of silage corn hybrids. – Journal of Experimental Biology and Agricultural Sciences 4: 721-729. DOI: 10.18006/2016.4(VIS).721.729.
[76] Setter, T. L., Parra, R. (2010): Relationship of carbohydrate and abscisic acid levels to kernel set in maize under postpollination water deficit. – Crop Science 50: 980-988.
[77] Shahrabian, E., Soleymani, A. (2011): Influence of silage maize (*Zea mays* L.) cultivars and different water level on nutritive value. – Journal of Food Agriculture and Environment 9(3): 336-339.
[78] Şimşek, M., Can, A., Denek, N., Tonkaz, T. (2011): The effects of different irrigation regimes on yield and silage quality of corn under semi-arid conditions. – African Journal of Biotechnology 10(3): 5689-5877. DOI: 10.5897/AJB11.259.
[79] Soler, C. M. T., Hoogenboom, G., Sentelhas, P. C., Duarte, A. P. (2007): Impact of water stress on maize grown off-season in a subtropical environment. – Journal of Agronomy and Crop Science 193(4): 247-61. DOI: 10.1111/j. 1439-037X.2007.00265.x.
[80] Steduto, P., Faurès, J. M., Hoogeveen, J., Winpenny, J., Burke, J. (2012): Coping with Water Scarcity: An Action Framework for Agriculture and Food Security. – Food and Agriculture Organization of the United Nations, Rome.
[81] Stewart, J. L., Cuenca, R. H., Pruit, W. O., Hagen, R. M., Tosso, J. (1977): Determination and Utilization of Water Production Functions for Principal California Crops. (California Contrib. Project Reports, w-67). – University of California, Davis.

http://www.aloki.hu ● ISSN 1589 1623 (Print) ● ISSN 1785 0037 (Online)
DOI: http://dx.doi.org/10.15666/aeer/2005_41734191

[82] Stone, L. R., Schlege, A. J., Gwin, R. E., Khan, A. H. (1996): Response of corn, grain sorghum, and sunflower to irrigation in the High Plains of Kansas. – Agricultural Water Management 30: 251-259.
[83] Stone, P. J., Wilson, D. R., Reid, J. B., Gillespie, R. N. (2001): Water deficit effects on sweet corn. I: Water use, radiation use efficiency, growth, and yield. – Australian Journal of Agricultural Research 52(1): 103-113. DOI: 10.1071/AR99146.
[84] Ünlü, M., Kanber, R., Koç, D. L., Tekin, S., Kapur, B. (2011): Effects of deficit irrigation on the yield and yield components of drip irrigated cotton in a Mediterranean environment. – Agricultural Water Management 98(4): 597-605. https://doi.org/10.1016/j.agwat.2010.10.020.
[85] USSL (1954): Diagnosis and improvement of saline and alkaline soils. – Soil Sci Soc Am J. 18(3): 348.
[86] Yazar, A., Gokçel, F., Sezen, M. S. (2009): Corn yield response to partial rootzone drying and deficit irrigation strategies applied with drip system. – Plant Soil Environ. 55: 494-503. DOI: https://doi.org/10.17221/96/2009-PSE.
[87] Yazar, A., Sezen, S. M., Gencel, B. (2002): Drip irrigation of corn in the Southeast Anatolia Project (GAP) area in Turkey. – Irrig. And Drainage 51: 293-300.
[88] Yenesew, M., Tilahun, K. (2009): Yield and water use efficiency of deficit-irrigated maize in a semi-arid region of Ethiopia. – Afr. J. Food Agr. Nutr. Develop. 9: 1635-1651.
[89] Yolcu, R., Üzen, N., Çetin, Ö. (2016): Irrigation and nitrogen fertigation strategies providing the maximum net return and water productivity for second crop silage corn. – Soil Water Journal 5(2): 59-64. DOI: https://doi.org/10.21657/topraksu.269369.
[90] Yosef, E., Carmi, A., Nikbachat, M., Zenou, A., Umiel, N., Miron, J. (2009): Characteristics of tall versus short-type varieties of forage sorghum grown under two irrigation levels, for summer and subsequent fall harvests, and digestibility by sheep of their silages. – Animal Feed Science and Technology 152(1): 1-11. DOI: 10.1016/j.anifeedsci.2009.01.018.
[91] Yüksel, A. N., Kocaman, İ., Soysal, M. İ., Soysal, S. İ. (2000): Dairy Cattle Basic Book. – Hasat Publishing, İstanbul.

http://www.aloki.hu ● ISSN 1589 1623 (Print) ● ISSN 1785 0037 (Online)
DOI: http://dx.doi.org/10.15666/aeer/2005_41734191

EFFECT OF ALLELOCHEMICALS PRESENT IN LEAF LITTER OF *BOMBAX CEIBA* L. AND *POPULUS DELTOIDES* L. TREE SPECIES ON WHEAT IN AGROFORESTRY SYSTEM

IQBAL, W.[1] – SIDDIQUI, T.[1] – AHMAD, I.[1] – FAROOQ, M.[2]

[1]*Department of Forestry and Range Management, University of Agriculture, Faisalabad, Pakistan*

[2]*Department of Agronomy, University of Agriculture, Faisalabad. Pakistan*

**Corresponding author*
e-mail: Waqas1168@yahoo.com phone: +92-333-838-4438

(Received 1st Jul 2022; accepted 23rd Aug 2022)

Abstract. The study was organized to analyze the allelopathic influence of leaf litter of *Populus deltoides* (poplar) and *Bombax ceiba* (simal) tree species under the agroforestry system during December 2018-2019 in the research area of the Department of Forestry and Range Management, University of Agriculture, Faisalabad. The allelopathic interference of both tree species was determined on the germination, radicle and plumule length plant height, number of productive tillers, spike length, spikelets per spike, grains per spike 00-grains weight, leaf area index, leaf area duration, grain yield, biological yield and harvest index were recorded. Biochemical analysis of leaf proline, chlorophyll contents, and leaf malondialdehyde contents was also carried out. Water-related attributes were also examined as osmotic potential, water potential and pressure potential of wheat. In the present study, the wheat was grown in pots and screened to analyze the allelopathic potential of *Bombax ceiba* L. and *Populus deltoides* L. by using four different leaf powder concentrations of 0 g/pot 30 g/pot, 60 g/pot and 90 g/pot of both tree species separately. There were observed significant inhibitory effects of *Populus deltoides* L. on wheat as compared to *Bombax ceiba* L. as the concentration of leaf litter of both tree species was increased.
Keywords: *allelopathy, wheat, germination, radicle, plumule, allelochemicals, agroforestry*

Introduction

Agroforestry is a very sustainable practice for sustainable production and livelihood improvement globally. It also plays very vital role in degradation of environmental hazards and socio-economic advantages but some trees emit phytotoxic elements to the soil that have a detrimental effect on the germination and yield of understory crops (Zubay et al., 2021), In agroforestry, allelopathic experiences in tree crop associations have a direct effect on crop production. The release of allelochemicals by a number of trees has adverse effect on the production of understory crops. Allelopathic influence of *Bombax ceiba* L., *Populus deltoides*, *Eucalyptus camaldulesis*, *Acacia nilotica* and *Cassia siamea* species have been reported by Hassan (2018), Xaxa et al. (2018), Singh et al. (2021) and Siregar et al. (2021).

Agroforestry system is also very common in Pakistan like other agricultural countries but it is being declined due to the allelopathic influence of trees on agricultural crops. *Populus deltoides* (poplar) and *Bombax ceiba* (simal) are multipurpose, fast-growing, valuable timber species and are considered very significant and major agrisilviculture tree species in Pakistan. Many other crop rotations used in Pakistan are not as commercially feasible or sustainable as poplar and simal-based agroforestry system is preferred. In the agroforestry system, farmers use a variety of tree-crop combinations including poplar and simal. Poplar and simal creates a lot of biomass in a shorter period

http://www.aloki.hu ● ISSN 1589 1623 (Print) ● ISSN 1785 0037 (Online)
DOI: http://dx.doi.org/10.15666/aeer/2005_41934209

of time and recycles soil nutrients by introducing leaf litter from its leaf shed during the winter season. Farmers prefer to grow these tree species alongwith wheat due to their smaller rotation and suitable climatic and ecological conditions in the country (Baig et al., 2021; Abbas et al., 2021). Wheat is a staple crop and it is cultivated on a large area (8.8 million hectares) and has more importance than any other kind of crop in Pakistan. It is abundant in vitamins, nutrients, carbohydrates, fats, oils, and protein in their natural state. Wheat is the most commonly planted crop in the interspaces of poplar during the winter season in Pakistan.

Even though agroforestry system has the ability to improve production but it also competes with food crops. Allelochemicals are found in leaf powder, and their toxic effects differ by species (Lebedev et al., 2019; Bakhshayeshan et al., 2020). Before proposing any tree species for an agroforestry program, comprehensive studies on the impact of allelochemicals present in tree species and their negative influence on seed emergence, growth and metabolism of crop plants must be known. Over the last two decades, allelopathy is imparting in serious reduction of growth and yield of major crops and this is an emerging problem which needs to be overcome. There was not any major work is being done in Faisalabad especially regarding poplar and simal agroforestry system. It needs to be studied further. As a result, the current research focuses on determining the allelopathic effect of *Populus deltoides* L. and *Bombax ceiba* L. on the germination and growth characteristics of the wheat crop.

Materials and methods

The research was directed to investigate the allelopathic potential of Poplar tree species on wheat in the research experimental area of the department of Forestry and Range Management, University of Agriculture, Faisalabad. This study was carried out in semi-arid climatic conditions with extremely hot and humid summers followed by cool and dry winters. The average temperature range was a maximum of 40.5 °C (104.9 °F) and a minimum of 26.9 °C (80.4 °F) in June while in January the average temperature range was a maximum of 19.4 °C (66.9 °F) and a minimum 4.1 °C (39.4 °F).

In the present experimental study, leaves of poplar and simal tree species were collected from Punjab Forest Research Institute, Gatwala, Faisalabad. Then leaves of both tree species were sundried for 72 h and grinded in an electric grinder separately. There were given four different treatments including control with four replications for each tree species. The powder of leaves of both tree species was collected and mixed with the sandy clay loam soil separately at different concentration levels of 0 g/pot (control), 30 g/pot, 60 g/pot and 90 g/pot. After mixing the leaf litter the pots were filled with 7 kg soil with the similar mixed soil. Wheat variety was grown in the pots filled with sandy clay loam soil. The cultivar used for sowing was Ujala 2014. Twenty seeds were planted in each pot on Nov 15, 2017, and harvested on April 25, 2018.

On the seventh day after sowing, germination was inscribed and data recorded for 15 days. The number of germinated seeds was used to determine germination rate (%) while a ruler was used to measure the length (cm) of the radicle and plumule of the germinated crop. Plant height (cm) was measured at maturity stage with a meter rod. The number of productive tillers was counted by counting the tillers bearing spikes. Spike length (cm) was measured from the base to the uppermost tip of the spikelet with a measuring scale. Spikelets per spike were counted the spikelets from each experimental unit and the average was calculated. Grains per spike were calculated by

http://www.aloki.hu ● ISSN 1589 1623 (Print) ● ISSN 1785 0037 (Online)
DOI: http://dx.doi.org/10.15666/aeer/2005_41934209

counting the grains of each experimental unit and the average was calculated. 100-grains weight (g) was calculated for each experimental unit was obtained by using an electric weighing balance. Leaf area was measured with a leaf area meter (CT-202, CID Inc. USA) and leaf area index was computed as the ratio of leaf area to land area followed by Ploschuk et al. (2021). Leaf area duration (LAD) was determined using following Hunt's formula as exhibited by Mubeen et al. (2021).

$$LAD = \frac{(LAI1 + LAI2) \times (t2 - t1)}{2}$$

LAI_1 and LAI_2 are respectively indices at time's t_1 and t_2.

Wheat was thrashed manually grain yield (g) biological yield (gm $^{-2}$) and total dry matter (gm $^{-2}$) was calculated with a measuring scale and harvest index (%) was computed. Water-related attributes were examined, in which relative water contents were calculated by following Barr and Weatherley's method described by Sapes et al. (2021). Osmotic potential was followed by Wenkert (1980), while water potential was calculated by following Scholander et al. (1964). The leaf chlorophyll contents were determined using Arnon methodology as expressed by Ahmad et al. (2022). Further leaf proline contents were examined by following the approach of Bates et al. (1973). Leaf malondialdehyde contents were examined by following the methodology of Hnilickova et al. (2021) and Leng et al. (2021).

Soil was collected from 3-6 ft depth and soil samples were taken before adding the leaf powder of *P. deltoides* and *B. ceiba* and also at harvest (from pots) for soil analysis. Soil texture was analyzed using bouyoucos hydro-meter mechanism presented by Acevedo et al. (2021). Soil organic matter was examined by following the Walkley and Black method as expressed by Xing et al. (2021). Soil available nitrogen (N) (Akaline-$KMno_4$ method), phosphorus (P) (P-Olsen method) and potassium K (Flame photometric method) were measured as exhibited by Mukherjee et al. (2021), Eberhardt et al. (2021) and Chen et al. (2021) respectively. PH of the soil was assessed by using PH-meter (HORIBA D-54) as revealed by Zeng et al. (2021). Electrical conductivity (EC) of the soil was explored by using Hanna EC-meter, Romania (Stanek et al., 2021). Soil saturation was estimated with gravimetric method exposed by Duarte et al. (2021). Total soluble phenolic (TSP) contents were investigated by following the methodology of Akomeng et al. (2021).

This study was statically analyzed using a two-way ANOVA to test the species (S) effects, treatments (T) effects and their interaction effect (S × T). Significant differences between all the treatments were respectively compared to controlled treatments using Dunnett's test. All tests were taken significantly at $p < 0.05$. The software (Statistica 12.5, Maisons-Alfort, France) was used to run all the tests.

Results

Wheat germination, growth and yield parameters

The order of reduction in all parameters under treatments for both species (leaf powder) was T4 (90 g leaf powder) > T3 (60 g leaf powder) > T2 (30 g leaf powder) > T1 (control). However, poplar leaf powder showed greater inhibitory effects and reduction as compared to simal leaf powder for all parameters. The allelopathic interaction of poplar and Simal tree species on wheat germination and growth parameters is demonstrated in

http://www.aloki.hu ● ISSN 1589 1623 (Print) ● ISSN 1785 0037 (Online)
DOI: http://dx.doi.org/10.15666/aeer/2005_41934209

the following *Table 1*. Poplar leaf powder showed a higher inhibitory effect on wheat as compared to simal. The leaf powder of *Populus deltoides* distinctly inhibited wheat seed germination. The highest reduction in germination rate was found in the T_4 group of *Populus deltoides* L. tree species obtained 90 g leaf powder. The ratio of seed germination decreased as the concentration of leaf powder increased for both tree species, with the lowest germination (73.45%) recorded in leaf powder of *Populus deltoides* L. with treatment T_4 (40 percent powder concentration).

Wheat crop radicle and plumule lengths were measured and compared to control plants. Application of leaf powder delayed the development of both radicle and plumule (*Table 1*). The effect of leaf powder of *Bombax ceiba* L. and *Populus deltoides* on growth parameters decreased as the concentration of leaf powder increased but higher inhibitory effect of leaf powder of *Populus deltoides* L. was observed as compared to the leaf powder of the *Bombax ceiba* L. on wheat. The maximum radicle length (4.20 cm) and plumule length (3.18) were documented in T_1 (control) treatment of *Bombax ceiba* L. as compare to *Populus deltoides* L. while the maximum reduction was determined in radicle length (2.49 cm) and plumule length (1.68 cm) in T_4 (40% conc) treatment of leaf powder of *Populus deltoides* L. as compared to *Bombax ceiba* L.

The highest mean values of plant height were measured (76.08 cm for simal and 74.34 cm for poplar) in control (T1), followed by T2 (30 g leaf powder): 70.82 cm and 68.62 cm for simal and poplar respectively. The lowest plant height was observed for T4 (90 g leaf powder) for simal and poplar tree species 14.95% and 20.74% respectively as compared to control. The maximum productive tillers (9.87 and 9.69) were recorded for T1 (control) for both species. It reduced gradually with the increase of leaf powder concentration of both species. The smallest number of productive tillers (6.97) was calculated for T4 i.e. 90 g leaf powder of poplar. The maximum spike length was measured (11.74 cm for simal and 11.53 cm for poplar) in control (T1), followed by T2 (30 g leaf powder): 10.85 cm and 10.20 cm for simal and poplar respectively. For T3 (60 g leaf powder), spike length reduced by 15.84% for simal and 16.39% for poplar as compared to control. The minimum spike length was measured for T4 (90 g leaf powder) for both simal and poplar tree species18.64% and 19.16% respectively as compared to control. The maximum mean value of spikelets (15.88 and 15.74) was recorded for T1 (control). It reduced gradually with the increased concentration of leaf powder for both species. The minimum mean value of spikelets per spike (13.54) was calculated for T4 (90 g leaf powder) for poplar and was 2.54% lower than the mean value of spikelets at 90 g leaf powder of simal.

The maximum number of grains was noted (36.52 for simal and 36.46 for poplar) in control (T1), followed by T2 (30 g leaf powder): 33.72 and 32.50 for simal and poplar respectively. For T3 (60 g leaf powder), the number of grains per spike reduced by 13.6% for simal and 22.35% for poplar as compared to control. The minimum grains per spike was measured for T4 (90 g leaf powder) simal and poplar tree species was 23.63% and 32.66% respectively as compared to control. The maximum grain yield was recorded (8.72 g/pot for simal and 8.68 g/pot for poplar) in control (T1), followed by T2 (30 g leaf powder): 8.28 g/pot and 7.88 g/pot for simal and poplar respectively. For T3 (60 g leaf powder), the grain yield reduced by 13.3% for simal and 20.9% for poplar as compared to control. The minimum grain yield was measured for T4 (90 g leaf powder) for simal and poplar tree species was 16.51% and 29.03% respectively as compared to control. Harves index was also declined in both tree species but higher reduction was noticed under poplar as compared to simal as described in *Table 1*.

http://www.aloki.hu ● ISSN 1589 1623 (Print) ● ISSN 1785 0037 (Online)
DOI: http://dx.doi.org/10.15666/aeer/2005_41934209

Table 1. *Effect of allelochemicals present in leaf litter powder of P. deltoides L. and B. ceiba L. on germination and growth parameters of wheat crop. A two-way ANOVA was used to test for species effect (S-effects), treatment effect (T-effects), and interaction effect (S × T). Significant differences between treatments within each species tested using the Dunnett's test are denoted by small letters. At $p < 0.05$, all tests were considered significant*

Treatments	Germination (%)		Radicle length (cm)		Plumule length (cm)		Plant height (cm)		No. of productive tillers		Spike length (cm)		Spikelets per spike		Grains per spike		100 grains weight (g)		Leaf area index		Leaf area duration (Days)		Grain yield (g/pot)		Biological yield (gm^{-2})		Harvest index (%)	
	B. ceiba	*P. deltoides*	*B. ceiba*	*P. deltoides*	*B. ceiba*	*P. deltoides*	*B. ceiba*	*P. deltoides*	*B. ceiba*	*P. deltoides*	*B. ceiba*	*P. deltoides*	*B. ceiba*	*P. deltoides*	*B. ceiba*	*P. deltoides*	*B. ceiba*	*P. deltoides*	*B. ceiba*	*P. deltoides*	*B. ceiba*	*P. deltoides*	*B. ceiba*	*P. deltoides*	*B. ceiba*	*P. deltoides*	*B. ceiba*	*P. deltoides*
0 g/pot leaf powder (Control) (T_1)	91.4d	90.8b	4.2e	4.15c	3.18b	3.17c	76.08f	74.34a	9.87b	9.696c	11.74a	11.53a	15.886c	15.744d	36.522b	36.46a	5.12d	4.89e	5.772a	5.73c	240a	236f	8.70 a	8.59f	24.78b	24.46b	26.1a	25.9e
30 g/pot leaf powder (T_2)	86.4c	78.6d	3.91e	3.72c	2.92a	2.78b	70.82e	68.62b	8.86e	7.906d	10.85d	10.206a	15.32a	15.07b	33.724b	35.502c	4.75b	4.35f	5.446a	5.334b	233c	228e	8.08 e	7.56f	22.98c	21.8a	24.5c	23.6f
60 g/pot leaf powder (T_3)	80.8b	73.6a	3.48f	3.22d	2.34c	2.12d	67.28a	60.98c	7.514g	7.154e	9.882c	9.648b	14.456e	14.156g	31.558a	28.314e	4.06a	3.46a	5.23b	5.062a	221d	217a	7.21 d	6.72a	19.57a	18.1b	21.4d	20.2a
90 g/pot leaf powder (T_4)	70a	61.8e	2.95d	2.49b	1.89f	1.68a	64.6b	58.92c	7.036f	6.97a	9.558b	9.32c	13.894e	13.548a	27.862d	24.664f	3.15f	2.67d	4.756d	4.614d	212a	205c	6.72 c	5.95c	16.23 d	15.3c	19.2b	17.7c
S-effect	0.53**		0.28**		0.31**		0.47**		0.34**		0.32**		0.41**		0.48**		0.51**		0.08**		1.58**		0.52**		0.70**		1.44**	
T-effect	1.02**		0.52**		0.66**		1.05**		0.56**		0.61**		0.63**		0.68**		0.73**		0.080**		2.30**		0.79**		1.05**		2.11**	
(S×T) ($p \leq 0.05$)	1.25**		0.63*		1.16**		1.33**		0.89*		0.81**		0.92**		1.17**		1.09*		0.19**		2.67*		1.14*		1.22**		3.01**	

http://www.aloki.hu ● ISSN 1589 1623 (Print) ● ISSN 1785 0037 (Online)
DOI: http://dx.doi.org/10.15666/aeer/2005_41934209

The maximum leaf area was computed for control and it gradually decreased with increasing the concentration of leaf powder. The highest leaf area was calculated (5.72 for simal and 5.73 for poplar) in control while the lowest leaf area was estimated for T4 (90 g leaf powder) for simal and poplar tree species was 17.13% and 19.54% respectively as compared to control. The maximum leaf area duration (240 and 236 days) was recorded for T1 (control) for both species. It was reduced gradually for different concentrations of leaf powder for both species. The lowest leaf area duration (205 days) was calculated for T4 (90 g leaf powder) for poplar and was 3.30% lower than the leaf area duration at 90 g leaf powder of simal as compared to control.

Water-related attributes

Osmotic potential

The osmotic potential showed significant variation under different concentrations of leaf powder of both tree species. The higher osmotic potential was computed for control and it gradually decreased with increasing the concentration of leaf powder. The maximum measured osmotic potential was (0.169 for simal and 0.096 for poplar) in control (T1), followed by T2 (30 g leaf powder): 0.155 and 0.087 for simal and poplar respectively. The minimum osmotic potential was measured for T4 (90 g leaf powder) for both tree species as described in *Figure 1*.

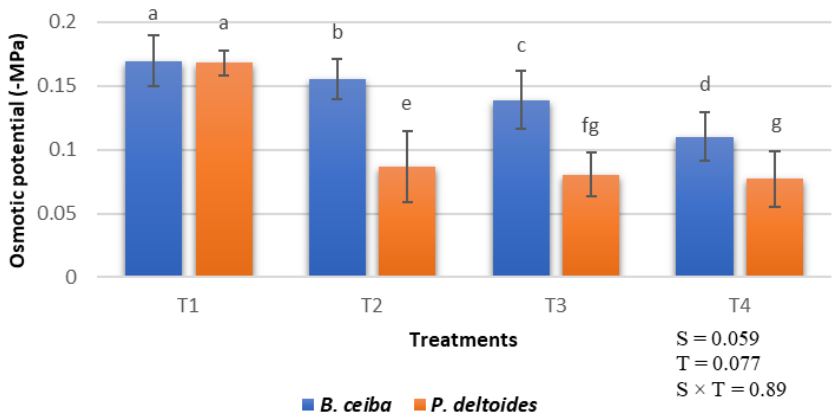

Figure 1. *Effect of P. deltoides and B. ceiba leaf powder on osmotic potential of wheat*

Water potential

It was noted that different concentrations of leaf powder of both tree species have shown significant variation regarding water potential (*Fig. 2*). The maximum water potential was computed for T4 (90 g leaf powder) and it gradually decreased for the lower level of leaf powder concentration. The highest mean value of water potential was measured 1.44 for simal in (T4), followed by T3 (60 g leaf powder): 1.36 and 1.31 for simal and poplar respectively. The reduction in water potential under control treatment was 28.47% for simal and 30.21% for poplar respectively as compared to T4.

Pressure potential

It was recorded that different concentrations of leaf powder of both tree species have shown significant variation for pressure potential. The maximum pressure potential was

http://www.aloki.hu ● ISSN 1589 1623 (Print) ● ISSN 1785 0037 (Online)
DOI: http://dx.doi.org/10.15666/aeer/2005_41934209

computed for T4 (90 g leaf powder) and it gradually decreased for the lower level of leaf powder. The highest mean value of pressure potential was measured (1.33 for simal in T4 (90 g leaf powder) followed by T3 (30 g leaf powder 60 g leaf powder): 1.22 and 1.16 for simal and poplar respectively as demonstrated in *Figure 3*. The lowest pressure potential was observed for control (0 g leaf powder) for both tree species.

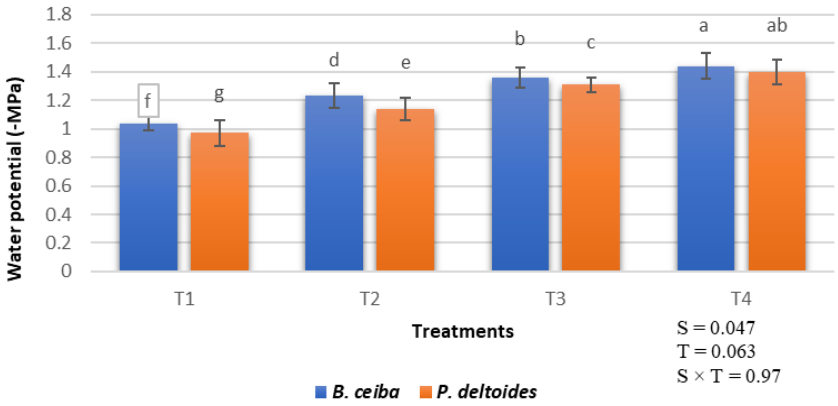

Figure 2. *Effect of P. deltoides and B. ceiba leaf powder on water potential of wheat*

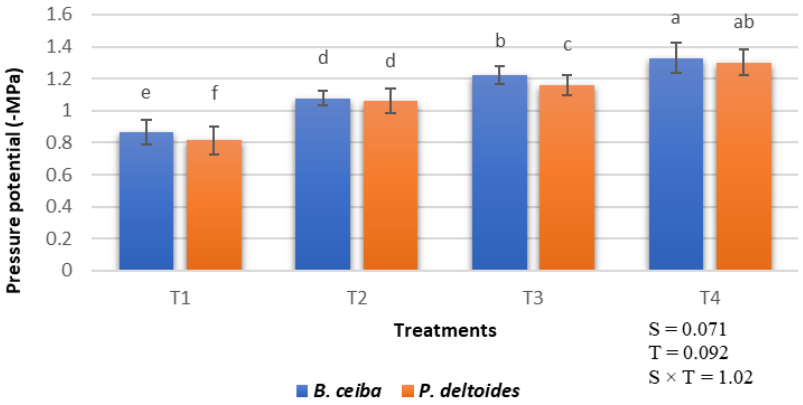

Figure 3. *Effect of P. deltoides and B. ceiba leaf powder on pressure potential of wheat. A two-way ANOVA was used to test for species effect (S-effects), treatment effect (T-effects), and interaction effect (S × T) regarding Figures 1, 2 and 3. Significant differences between treatments within each species tested using the Dunnett's test are denoted by small letters. At $p < 0.05$, all tests were considered significant*

Biochemical attributes

Chlorophyll a

It was found that the chlorophyll a content decreased gradually with the increase of concentration of tree leaf powder, however, this reduction was greater for poplar leaf powder as compared to simal (*Fig. 4*). The maximum chlorophyll a (0.292 µg g^{-1} and 0.288 µg g^{-1}) was recorded for T1 (control) for both species. The minimum chlorophyll a content (0.236 µg g^{-1}) was calculated for T4 (90 g leaf powder) for poplar and was 3.67% lower than the chlorophyll content a, at 90 g leaf powder of simal.

http://www.aloki.hu ● ISSN 1589 1623 (Print) ● ISSN 1785 0037 (Online)
DOI: http://dx.doi.org/10.15666/aeer/2005_41934209

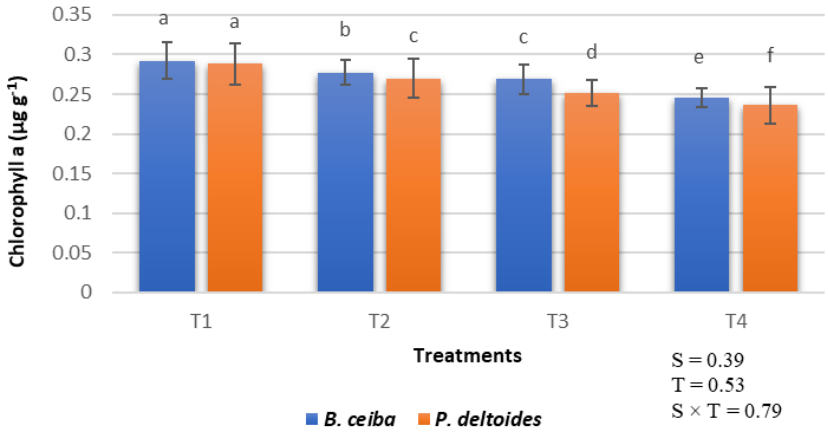

Figure 4. *Effect of P. deltoides and B. ceiba leaf powder on chlorophyll a of wheat*

Chlorophyll b

It was observed that the chlorophyll b decreased gradually with the increase of concentration of tree leaf powder concentration, however, this reduction was greater for poplar leaf powder as compared to simal as shown in *Figure 5*. The maximum chlorophyll b (0.223 µg g^{-1} and 0.202 µg g^{-1}) was recorded for T1 (control) for both species. The minimum chlorophyll b content (0.151 µg g^{-1}) was calculated for T4 (90 g leaf powder) for poplar and was 4.43% lower than the chlorophyll b, at 90 g leaf powder of simal.

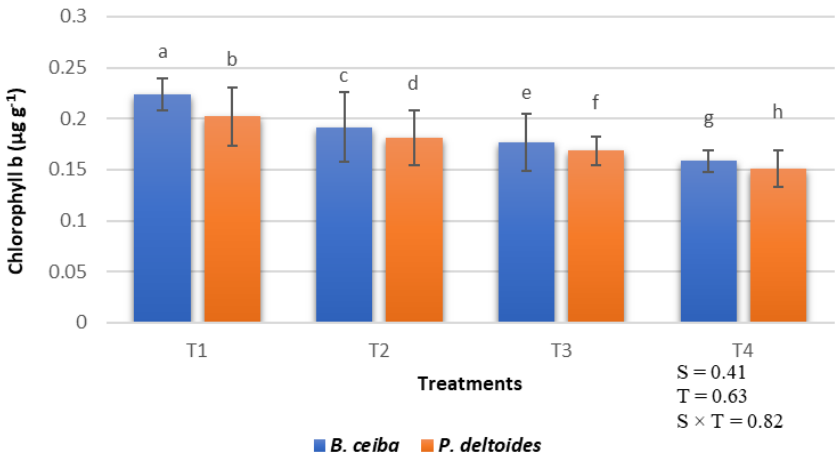

Figure 5. *Effect of P. deltoides and B. ceiba leaf powder on chlorophyll b of wheat*

Leaf proline

It was observed that different concentrations of leaf powder of both tree species have shown significant variation in proline content. The maximum proline content was computed for T4 (90 g leaf powder) and it gradually decreased for the lower level of leaf powder as revealed in *Figure 6*. The highest mean value of proline content was measured (0.41 µmol g^{-1} for simal in T4 (90 g leaf powder), followed by T3 (60 g leaf powder): 0.36 µmol g^{-1} and 0.35 µmol g^{-1} for simal and poplar respectively. The lowest proline content was observed for control (0 g leaf powder) for simal and poplar was 29.26% and 31.57% respectively as compared to T4 for both species.

http://www.aloki.hu ● ISSN 1589 1623 (Print) ● ISSN 1785 0037 (Online)
DOI: http://dx.doi.org/10.15666/aeer/2005_41934209

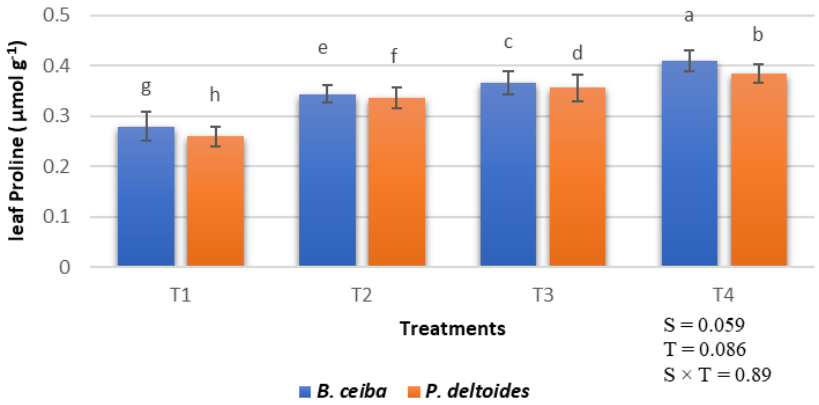

Figure 6. *Effect of P. deltoides and B. ceiba leaf powder on leaf proline of wheat*

Malondialdehyde (MDA)

It was recorded that different levels of leaf powder of both tree species have shown significant variation in MDA content. The maximum MDA was computed for control and it gradually decreased with increasing the concentration of leaf powder as expressed in *Figure 7*. The highest leaf MDA was calculated (5.41 µmol g^{-1} for simal and 5.33 µmol g^{-1} for poplar) in control (T1), followed by T2 (30 g leaf powder): 4.82 µmol g^{-1} and 4.27 µmol g^{-1} for simal and poplar respectively. The lowest mean MDA value was estimated for T4 (90 g leaf powder) of simal and poplar was 37.15% and 45.40% respectively as compared to control.

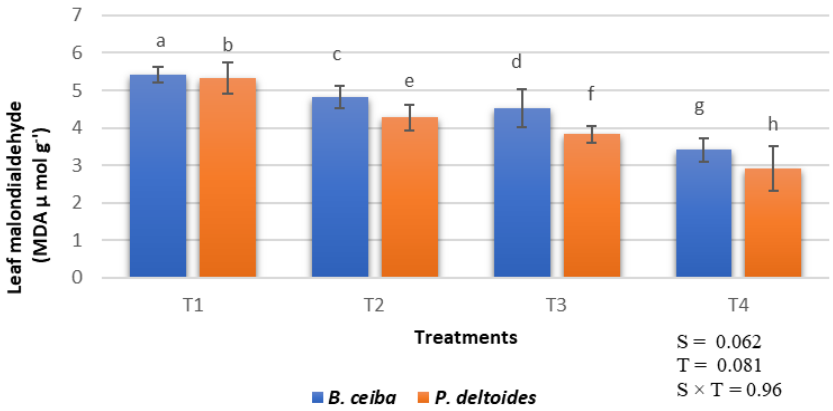

Figure 7. *Effect of P. deltoides and B. ceiba leaf powder on leaf malondialdehyde (MDA) of wheat. A two-way ANOVA was used to test for species effect (S-effects), treatment effect (T-effects), and interaction effect (S × T) regarding Figures 4, 5, 6 and 7. Significant differences between treatments within each species tested using the Dunnett's test are denoted by small letters. At $p < 0.05$, all tests were considered significant*

Effect on soil properties

The results regarding soil showed the phytotoxic impact on the soil properties in both tree species but highest reduction was recorded in *P. deltoides* as compared to *B. ceiba* tree species as expressed in *Table 2*. The resulted indicated that soil orgaic matter,

http://www.aloki.hu ● ISSN 1589 1623 (Print) ● ISSN 1785 0037 (Online)
DOI: http://dx.doi.org/10.15666/aeer/2005_41934209

N,P,K was significantly declined in *P. deltoides* while PH and EC of the soil was noted higher in *P. deltoides* as compared to *B. ceiba as* demonstrated in *Table 2*. The saturation of the soil was remained same in both tree species. Total soluble phenolics also showed the significant elevation under *P. deltoides* (8.55 mg g^{-1}) as compared to *B. ceiba* (7.03 mg g^{-1}).

Table 2. *Phytotoxic effect on soil properties under agroforestry system based on Populus deltoides L. (poplar) and B. ceiba L. (simal) tree species along with wheat crop*

Serial No.	Parameters	Values (at sowing without leaf powder of *P. deltoides* and *B. ceiba*)	Values (at harvest)	
			Wheat along with *P. deltoides* L.	Wheat along with *B. ceiba* L.
1	Soil texture	Sand 36%, Silt 43%, Clay 19% (Loam)	Sand 36%, Silt 43%, Clay 19% (Loam)	Sand 36%, Silt 43%, Clay 19% (Loam)
2	Organic matter (%)	1.06	1.02	1.09
3	Available nitrogen (N) (%)	0.055	0.051	0.058
4	Available phosphorus (P)(ppm)	12.7	13.1	13.6
5	Available potassium (K) (ppm)	125	129	136
6	PH	7.4	7.4	7.2
7	EC (dSm-1)	0.89	0.88	0.82
8	Soil saturation (%)	36	35	35
9	Total soluble phenolic (TSP) (mg g^{-1})	6.12	8.55	7.03

Discussion

The current findings back up a previous study by Tahir et al. (2019), which found that leachate from the leaves, roots and tubers of *Pistacia atlantica* tree species inhibited the germination and growth of food crops. In addition, Khalid et al. (2020), Adhikari et al. (2020) and Kumar et al. (2021) revealed that the inhibitory effects of different tree species included *Dalbergia sissoo*, *Populus deltoides* L. and *Bombax ceiba* L. leaf powder on germination on the wheat crop was proportional to the powder concentration. Moreover, Elbouzidi et al. (2021) found that as the concentration of leaf leachates of *Matricaria chamomilla* L. was increased, the reduction in germination, radicle and plumule length of wheat was observed. Alazzam et al. (2021) also found that leaf powder of *Rumex vesicarius* L. and *Zygophyllum coccineum* L. is similarly noxious to *T. aestivum* germination, plumule, and radicle formation. Correspondingly, Hachani et al. (2019) found that the *Populus nigra* and *Casuarina glauca* inhibited the plumule duration and radicle length of *T. aestivum*. Ahmad et al. (2020) have observed that the agroforestry trees *J. regia, M. azedarach,* and *A. altissima* had an allelopathic impact on wheat seed germination and development. Leachates had concentration-dependent effects on wheat crops.

The application of leaf powder of both selected tree species in the present study also showed inhibitory effects on the leaf area index, duration and crop growth rate of the wheat crop. This reduction was higher at greater concentration levels of leaf powder of poplar has greater inhibitory effects on leaf area index, duration, crop growth rate and dry matter accumulation as compared to simal leaf powder. It was also found that the

http://www.aloki.hu ● ISSN 1589 1623 (Print) ● ISSN 1785 0037 (Online)
DOI: http://dx.doi.org/10.15666/aeer/2005_41934209

leaf area index, duration and crop growth rate decreased substantially at 90 g poplar leaf powder application as compared to simal. Similar results were reported by Ibáñez et al. (2019) in crops and invasive species while Hussain et al. (2020) revealed the phytotoxic influence of *Acacia melanoxylon* on *Lactuca sativa*; Kato-Naguchi and Hisashi (2021) for agricultural crops.

The findings of this study are also concur with the results reported by Ayalew et al. (2020), Lalremsang et al. (2020) and Hussain et al. (2021) who reported the allelopathic effect of tree species: *E. camaldulensis*, *G. Robusta, C. equisetifolia, P. deltoides, A. indica* and *M. azedarach* on various crops including Maize, Wheat cowpeas and rice. Seed germination and survival of germinated seedlings were also inhibited by Eucalyptus tree species. Allelopathic plants greatly affected the growth parameters such as plant height, spike length, grain and biological yield. The allelopathic influence of leaf powder of *Juglans nigra* showed the maximum effect on all the growth and yield parameters of *T. aestivum* and *O. sativa* (Ochekwu et al., 2020). Our results are in agreement with Vasishth et al. (2020) who described the effect of allelochemicals compounds secreted by different tree species *Boehmeria rugulosa*, *Ougeinia oojeinensis* and *Zanthoxylum armatumand* which reduce the growth and yield of wheat and other agricultural crop.

Biochemical-related attributes findings are in agreement with the findings of de Sousa et al. (2020) described the reduction in biochemical attributes under the higher concentrations of leaf powder as compared to control. Similar inhibitory results for Eucalyptus and some other allelopathic trees including *P. deltoides* and *B. ceiba* were observed in wheat crop (Tahir et al., 2018; Guo et al., 2020; Gao et al., 2021; Tian et al., 2022). The allelochemicals actuated oxidative stress in the objective plant tissues and hinder the cell reinforcement component (Alqarawi et al., 2018; Ladhari et al., 2020; Šoln et al., 2022). It appears to be that phytotoxic extracts of *Descurainia sophia, Galium tricorne,* wild oat, and *sativa* caused oxidative stress by invigorating lipid peroxidation in *T. aestivum* and higher MDA contents were recorded higher in each treatment except for control (Shao et al., 2018). Comparable inhibitory consequences of poplar and some other allelopathic trees were seen in wheat yield (Ghafarizadeh et al., 2018; Šućur et al., 2021). Decline in the water-related attributes is in agreement with the results of Shah et al. (2020). Similar allelopathic inhibitory findings were reported for *E. camaldulensis* and some other tree species in *T. aestivum* and some other major crops (Bali et al., 2019; Rizvi et al., 2020; Heile et al., 2021; Hassanisaadi et al., 2022).

Trees have the abilities to affect the soil properties (Bargali et al., 2019; Tajik et al., 2019; Ahirwal et al., 2020). The results of this research are comprising with the findings of Mantino et al. (2019), Dibala et al. (2021) and Seyfried et al. (2021). They documented that agroforestry trees including poplar-based agroforestry system influenced the different soil properties including organic matter, PH, soil nutrients and as well as texture of the soil. N, P, K of the soil were reduced significantly under *P. deltoides* and *B. ceiba* trees in the current study. However, the reduction was higher under *P. deltoides* as compared to *B. ceiba*. Similar outcomes relating with soil nutrients decline due to trees interference were portrayed by Sauvadet et al. (2019), Wang et al. (2021) and Woś et al. (2021). Further studies have been depicted that *A. pseudoplatanus, A. platanoides, A. alba, B. pendula, C. betulus, F. sylvatica, P. sylvestris, Q. robur, T. cordata* and many other tree species are involved in affecting the soil chemical properties and soil nutrient including PH and electrical conductivity due to their phytotoxic litter which is in agreement with the present study (Álvarez et al.,

http://www.aloki.hu ● ISSN 1589 1623 (Print) ● ISSN 1785 0037 (Online)
DOI: http://dx.doi.org/10.15666/aeer/2005_41934209

2021; Stefanowicz et al., 2021; Amorim et al., 2022; Cesarz et al., 2022). The effect on soil properties and decreasing nutrient ultimately cause the negative influence on the crop growth, yield and soil fertility (Castro-Díez et al., 2019; Puttaso et al., 2020; Gillespie et al., 2021; Yates et al., 2021). The findings related to total soluble phenolic contents are inclined with the results of Yaseen et al. (2020) and Irshad et al. (2021) there is clearly indicated that moringa and *J. Curcus* trees increased the TSP contents.

Conclusion

Allelopathy is the release of chemicals from a plant that inhibits the growth of neighboring plant. *Populus deltoides* L. and *Bombax ceiba* L. both tree species have allelopathic ability to decline the wheat crop production according to this study report. Allelochemicals present in both tree species suppressed the wheat crop germination, radicle, and plumule length according to recorded data but it was also noticed that the concentration of leaf powder of *Populus deltoides* L. has higher adverse effects to inhibit the germination and growth parameters of the wheat crop as compared to *Bombax ceiba* L. The findings of this study also revealed that phytotoxicity of *P. deltoides* and *B. ceiba* caused negative impacts on the soil properties and it also varies from species-species dependent on releasing phytotoxic compounds at different leaves. Regarding these findings, it is being confirmed that allelopathy is a concentration-dependent process, in which the adverse effects of leaf litter of both tree species on receptor plants escalate as the concentration of leaf litter rises.

REFERENCES

[1] Abbas, G., Ali, A., Khan, M., Mahmood, H. Z., Wahab, S. A., Amir-ud-Din, R. (2021): The transition from arid farming systems to agroforestry systems in Pakistan: a comparison of monetary returns. – Small-Scale Forestry 20(3): 325-350.

[2] Acevedo, S. E., Contreras, C. P., Ávila, C. J., Bonilla, C. A. (2021): Testing the integral suspension pressure method for soil particle size analysis across a range of soil organic matter contents. – International Agrophysics 35(4): 357-363.

[3] Adhikari, B., Lodhiyal, N., Lodhiyal, L. S. (2020): Assessment of crop yield, productivity and carbon sequestration in agroforestry systems in Central Himalaya, India. – Agroforestry Systems 94(1): 281-296.

[4] Ahirwal, J., Kumar, A., Maiti, S. K. (2020): Effect of fast-growing trees on soil properties and carbon storage in an afforested coal mine land (India). – Minerals 10(10): 840.

[5] Ahmad, Z., Khan, K. R., Farooq, M., Shah, A. H., Mehmood, A., Jabeen, T., Zohra, L. (2020): Evaluation of allelopathic potential of agricultural land associated trees on germination attributes of wheat (*Triticum aestivum* L.). – Proceedings of the International Academy of Ecology and Environmental Sciences 10(2): 38-44.

[6] Ahmad, A., Aslam, Javed, T., Hussain, S., Raza, A., Shabbir, R., Mora-Poblete, F., Saeed, T., Zulfiqar, F., Ali, M., Nawaz, M. (2022): Screening of wheat (*Triticum aestivum*) genotypes for drought tolerance through agronomic and physiological response. – Agronomy 12(2): 287.

[7] Akomeng, N., Adusei, S. (2021): Organic solvent extraction and spectrophotometric quantification of total phenolic content of soil. – Heliyon 7(11): e08388.

[8] Alazzam, S. A., Sharqi, M. M., Almehemdi, A. F. (2021): Allelochemicals analysis of *Rumex vesicarius* L. and *Zygophyllum coccineum* L., and their effect on seed germination and seedling growth of wheat, *Triticum aestivum* L. – IOP Conference Series: Earth and Environmental Science 761(1): 012077.

http://www.aloki.hu ● ISSN 1589 1623 (Print) ● ISSN 1785 0037 (Online)
DOI: http://dx.doi.org/10.15666/aeer/2005_41934209

[9] Alqarawi, A. A., Hashem, A., Kumar, A., Al-Arjani, A. F., Allah, E. F. A., Dar, B. A., Wirth, S., Davranov, K., Egamberdieva, D. (2018): Allelopathic effects of the aqueous extract of *Rhazya stricta* on growth and metabolism of *Salsola villosa*. – Plant Biosystems - An International Journal Dealing with all Aspects of Plant Biology 152(6): 1263-1273.
[10] Álvarez, F., Casanoves, F., Suárez, J. C. (2021): Influence of scattered trees in grazing areas on soil properties in the Piedmont region of the Colombian Amazon. – PloS ONE 16(12): e0261612.
[11] Amorim, H. C. S., Ashworth, A. J., Zinn, Y. L., Sauer, T. J. (2022): Soil organic carbon and nutrients affected by tree species and poultry litter in a 17-year agroforestry site. – Agronomy 12(3): 641.
[12] Ayalew, A., Asfaw, Z. (2020): Allelophatic Effects of Gravellia Robusta, *Eucalyptus Camaldulensis* and *Casuarina Equisetifolia* on germination and root length of maize and wheat. – Inte J Rese Stud Agric Sci (IJRSAS) 6: 15-20.
[13] Baig, M. B., Burgess, P. J., Fike, J. H. (2021): Agroforestry for healthy ecosystems: constraints, improvement strategies and extension in Pakistan. – Agroforestry Systems 95(5): 995-1013.
[14] Bakhshayeshan-Agdam, H., Salehi-Lisar, S. Y. (2020): Agronomic Crops Response and Tolerance to Allelopathic Stress. – In: Hasanuzzaman, M. (ed.) Agronomic Crops. Springer, Singapore, pp. 313-348.
[15] Bali, A. S., Sidhu, G. P. S. (2019): Abiotic Stress-Induced Oxidative Stress in Wheat. – In: Hasanuzzaman, M. et al. (eds.) Wheat Production in Changing Environments. Springer, Singapore, pp. 225-239.
[16] Bargali, S. S., Padalia, K., Bargali, K. (2019): Effects of tree fostering on soil health and microbial biomass under different land use systems in the Central Himalayas. – Land Degradation & Development 30(16): 1984-1998.
[17] Bates, L. S., Waldren, R. P., Teare, I. D. (1973): Rapid determination of free proline for water-stress studies. – Plant and Soil 39(1): 205-207.
[18] Castro-Díez, P., Alonso, Á., Romero-Blanco, A. (2019): Effects of litter mixing on litter decomposition and soil properties along simulated invasion gradients of non-native trees. – Plant and Soil 442(1): 79-96.
[19] Cesarz, S., Craven, D., Auge, H., Bruelheide, H., Castagneyrol, B., Gutknecht, J., Hector, A. et al. (2022): Tree diversity effects on soil microbial biomass and respiration are context dependent across forest diversity experiments. – Global Ecology and Biogeography 31(5): 872-885.
[20] Chen, J., Guo, Z., Chen, H., Yang, X., Geng, J. (2021): Effects of different potassium fertilizer types and dosages on cotton yield, soil available potassium and leaf photosynthesis. – Archives of Agronomy and Soil Science 67(2): 275-287.
[21] de Sousa, G. O., de Jesus Matos Viégas, I., Galvão, J. R., Conceição, S. S., Yakuwa, T. K. M., Pacheco, M. J. B., Viana, T. C. (2021): Biochemical modulations in açaí palm (*Euterpe oleracea* Mart.) under vegetative stages in an agroforestry system of the Amazon. – Journal of Plant Nutrition and Soil Science 184(1): 76-87.
[22] Dibala, R., Jose, S., Gold, M., Hall, J. S., Kallenbach, R., Knapp, B. (2021): Tree density effects on soil, herbage mass and nutritive value of understory Megathyrsus maximus in a seasonally dry tropical silvopasture in Panama. – Agroforestry Systems 95(4): 741-753.
[23] Duarte, T. F., da Silva, T. J. A., Bonfim-Silva, E. M., Koetz, M. (2021): Using Arduino sensors to monitor vacuum gauge and soil water moisture. – Dyna 88(219): 190-196.
[24] Eberhardt, D., Marchão, R., Quiquampoix, H., Le Guernevé, C., Ramaroson, V., Sauvadet, M., Muraoka, T., Becquer, T. (2021): Effects of companion crops and tillage on soil phosphorus in a Brazilian oxisol: a chemical and 31P NMR spectroscopy study. – Journal of Soils and Sediments 21(2): 1024-1037.
[25] Elbouzidi, A., Bencheikh, N., Seddoqi, S., Bouhrim, M., Bouramdane, Y., Addi, M. (2021): Investigation of the allelopathic effect of *Matricaria chamomilla* L. parts'

http://www.aloki.hu ● ISSN 1589 1623 (Print) ● ISSN 1785 0037 (Online)
DOI: http://dx.doi.org/10.15666/aeer/2005_41934209

aqueous extracts on germination and seedling growth of two moroccan varieties of durum wheat. – International Journal of Agronomy. https://doi.org/10.1155/2021/4451181.

[26] Gao, X., Li, M. E. I., Gao, Z., Li, C., Sun, Z. (2009): Allelopathic effects of *Hemistepta lyrata* on the germination and growth of wheat, sorghum, cucumber, rape, and radish seeds. – Weed Biology and Management 9(3): 243-249.

[27] Gao, Y., Chang, J., Wang, Y., Li, F., Li, H. (2021): Allelopathic effects of *Stellera chamaejasme* on seed germination and growth of three crops. – Acta Prataculturae Sinica 30(10): 83.

[28] Ghafarizadeh, A., Nejad, S. M. S., Vafaei, M., Gilani, A., Saboora, A. (2018): A study on the allelopathic effect of olive fruit pomace (*Olea europaea* L.) on some physiological parameters and yield of three wheat cultivars in climatic conditions of Khuzestan. – Journal of Iranian Plant Ecophysiological Research 13(51): 31-50.

[29] Gillespie, L. M., Hättenschwiler, S., Milcu, A., Wambsganss, J., Shihan, A., Fromin, N. (2021): Tree species mixing affects soil microbial functioning indirectly via root and litter traits and soil parameters in European forests. – Functional Ecology 35(10): 2190-2204.

[30] Guo, Y., Lv, J., Zhao, Q., Dong, Y., Dong, K. (2020): Cinnamic acid increased the incidence of Fusarium wilt by increasing the pathogenicity of *Fusarium oxysporum* and reducing the physiological and biochemical resistance of faba bean, which was alleviated by intercropping with wheat. – Frontiers in Plant Science 11: 608389.

[31] Hachani, C., Abassi, M., Lazhar, C., Lamhamedi, M. S., Béjaoui, Z. (2019): Allelopathic effects of leachates of *Casuarina glauca* Sieb. Ex Spreng. and *Populus nigra* L. on germination and seedling growth of *Triticum durum* Desf. under laboratory conditions. – Agroforestry Systems 93(5): 1973-1983.

[32] Hassan, M. O. (2018): Leaf litter of *Bombax ceiba* L. threatens plant cover and floristic diversity in a new urban ecosystem. – Flora 242: 22-30.

[33] Hassanisaadi, M., Barani, M., Rahdar, A., Heidary, M., Thysiadou, A., Kyzas, G. Z. (2022): Role of agrochemical-based nanomaterials in plants: biotic and abiotic stress with germination improvement of seeds. – Plant Growth Regulation 97: 375-418.

[34] Heile, A. O., Zaman, Q. U., Aslam, Z., Hussain, A., Aslam, M., Saleem, M. H., Abualreesh, M. H., Alatawi, A., Ali, S. (2021): Alleviation of cadmium phytotoxicity using silicon fertilization in wheat by altering antioxidant metabolism and osmotic adjustment. – Sustainability 13(20): 11317.

[35] Hnilickova, H., Kraus, K., Vachova, P., Hnilicka, F. (2021): Salinity stress affects photosynthesis, malondialdehyde formation, and proline content in *Portulaca oleracea* L. – Plants 10(5): 845.

[36] Hussain, M. I., El-Sheikh, M. A., Reigosa, M. J. (2020): Allelopathic potential of aqueous extract from *Acacia melanoxylon* R. Br. on *Lactuca sativa*. – Plants 9(9): 1228.

[37] Hussain, I., Khan, E. A., Nazir, J. (2021): Inhibitory impact of white cedar (*Melia azedarache*) leaves litter on wheat (*Triticum aestivum*) seedlings. – Pakistan Journal of Weed Science Research 27(2).

[38] Ibáñez, M. D., Blázquez, M. A. (2019): Phytotoxic effects of commercial *Eucalyptus citriodora*, *Lavandula angustifolia*, and *Pinus sylvestris* essential oils on weeds, crops, and invasive species. – Molecules 24(15): 2847.

[39] Irshad, M., Ullah, F., Fahad, S., Mehmood, S., Khan, A. U., Brtnicky, M., Kintl, A. et al. (2021): Evaluation of *Jatropha curcas* L. leaves mulching on wheat growth and biochemical attributes under water stress. – BMC Plant Biology 21(1): 1-12.

[40] Kato-Noguchi, H. (2021): Phytotoxic substances involved in teak allelopathy and agroforestry. – Applied Sciences 11(8): 3314.

[41] Khalid, S., Naseem, M., Sajjad, M., Riaz, S., Ibrahim, U., Shumail, H., Haq, S. I. U. (2020): 17. The allelopathic effects of *Rumex dentatus* and *Dalbergia sissoo* on growth and germination of *Brassica campestris* L. – Pure and Applied Biology (PAB) 10(1): 199-208.

http://www.aloki.hu ● ISSN 1589 1623 (Print) ● ISSN 1785 0037 (Online)
DOI: http://dx.doi.org/10.15666/aeer/2005_41934209

[42] Kumar, P., Sirohi, C., Kumari, S., Dhillon, R. S., Redhu, I. (2021): Performance of wheat cultivars under different spacing of poplar (*Populus deltoides* Bartr. Ex Marsh.) based agroforestry system in semi-arid ecosystem of Northern India. – Annals of Horticulture 14(1): 61-67.
[43] Ladhari, A., Andolfi, A., DellaGreca, M. (2020): Physiological and oxidative stress responses of lettuce to Cleomside A: a thiohydroximate, as a new allelochemical from *Cleome arabica* L. – Molecules 25(19): 4461.
[44] Lalremsang, P., Gopichand, B., Upadhyaya, K., Remlalpeka, C., Lungmuana, S., Singh, B. P. (2020): Allelopathic effects of *Flemingia semialata* Roxb. on seedling growth of maize (*Zea mays* L.) and rice (*Oryza sativa* L.). – Allelopath. J 50: 173-183.
[45] Lebedev, V. G., Krutovsky, K.V., Shestibratov, K. A. (2019): Fell Upas Sits, the Hydra-Tree of Death, or the Phytotoxicity of Trees. – Molecules 24(8): 1636.
[46] Leng, Y., Li, Y., Ma, Y., He, L., Li, S. (2021): Abscisic acid modulates differential physiological and biochemical responses of roots, stems, and leaves in mung bean seedlings to cadmium stress. – Environmental Science and Pollution Research 28(5): 6030-6043.
[47] Mantino, A., Volpi, I., Micci, M., Pecchioni, G., Bosco, S., Dragoni, F., Mele, M., Ragaglini, G. (2019): Effect of tree presence and soil characteristics on soybean yield and quality in an innovative alley-cropping system. – Agronomy 10(1): 52.
[48] Mirmoeini, T., Pishkar, L., Kahrizi, D., Barzin, G., Karimi, N. (2021): Phytotoxicity of green synthesized silver nanoparticles on *Camelina sativa* L. – Physiology and Molecular Biology of Plants 27(2): 417-427.
[49] Morugán-Coronado, A., Linares, C., Gómez-López, M. D., Faz, A., Zornoza, R. (2020): The impact of intercropping, tillage and fertilizer type on soil and crop yield in fruit orchards under Mediterranean conditions: a meta-analysis of field studies. – Agricultural Systems 178: 102736.
[50] Mubeen, M., Bano, A., Ali, B., Islam, Z. U., Ahmad, A., Hussain, S., Fahad, S., Nasim, W. (2021): Effect of plant growth promoting bacteria and drought on spring maize (*Zea mays* L.). – Pak. J. Bot 53(2): 731-739.
[51] Mukherjee, S., Saha, N., Sarkar, B., Sengupta, S., Ghosh, S., Dey, P. (2021): Assessing methods for estimating potentially mineralisable nitrogen under organic production system in new alluvial soils of lower Gangetic plain. – Journal of Soil Science and Plant Nutrition 21(2): 1030-1040.
[52] Ochekwu, E. B., Uzoma, M. C. (2020): Allelopathic effects of *Juglans nigra* on wheat and rice. – Int. J. Innov. Agric. Biol. Res 8: 15-23.
[53] Ploschuk, R. A., Miralles, D. J., Striker, G. G. (2021): Early-And late-waterlogging differentially affect the yield of wheat, barley, oilseed rape and field pea through changes in leaf area index, radiation interception and radiation use efficiency. – Journal of Agronomy and Crop Science 207(3): 504-520.
[54] Puttaso, P., Namanusart, W., Thumanu, K., Kamolmanit, B., Brauman, A., Lawongsa, P. (2020): Assessing the effect of rubber (*Hevea brasiliensis* (Willd. ex A. Juss.) Muell. Arg.) leaf chemical composition on some soil properties of differently aged rubber tree plantations. – Agronomy 10(12): 1871.
[55] Rizvi, A., Zaidi, A., Ameen, F., Ahmed, B., AlKahtani, M. D. F., Khan, M. S. (2020): Heavy metal induced stress on wheat: phytotoxicity and microbiological management. – RSC Advances 10(63): 38379-38403.
[56] Sapes, G., Sala, A. (2021): Relative water content consistently predicts drought mortality risk in seedling populations with different morphology, physiology and times to death. – Plant, Cell & Environment 44(10): 3322-3335.
[57] Saud, S., Fahad, S., Cui, G., Yajun, C., Anwar, S. (2020): Determining nitrogen isotopes discrimination under drought stress on enzymatic activities, nitrogen isotope abundance and water contents of Kentucky bluegrass. – Scientific Reports 10(1): 1-16.

http://www.aloki.hu ● ISSN 1589 1623 (Print) ● ISSN 1785 0037 (Online)
DOI: http://dx.doi.org/10.15666/aeer/2005_41934209

[58] Sauvadet, M., Van den Meersche, K., Allinne, C., Gay, F., de Melo, E., Filho, V., Chauvat, M., Becquer, T., Tixier, P., Harmand, J. (2019): Shade trees have higher impact on soil nutrient availability and food web in organic than conventional coffee agroforestry. – Science of the Total Environment 649: 1065-1074.
[59] Scholander, P. F., Hammel, H. T., Hemmingsen, E. A., Bradstreet, E. D. (1964): Hydrostatic pressure and osmotic potential in leaves of mangroves and some other plants. – Proceedings of the National Academy of Sciences 52(1): 119-125.
[60] Seyfried, G. S., Canham, C. D., Dalling, J. W., Yang, W. H. (2021): The effects of tree-mycorrhizal type on soil organic matter properties from neighborhood to watershed scales. – Soil Biology and Biochemistry 161: 108385.
[61] Shah, A., Smith, D. L. (2020): Flavonoids in agriculture: chemistry and roles in, biotic and abiotic stress responses, and microbial associations. – Agronomy 10(8): 1209.
[62] Shao, Q., Li, W., Yan, S., Zhang, C., Huang, S., Ren, L. (2019): Allelopathic effects of different weed extracts on seed germination and seedling growth of wheat. – Pakistan Journal of Botany 51(6): 2159-2167.
[63] Singh, R., Upadhyay, S. K., Singh, B. J., Verma, R., Sharma, I., Sharma, P., Rani, A., Singh, C. (2021): Allelopathic effect of eucalyptus (*Eucalyptus camaldulensis* Dehnh) on the growth of Aloe vera. – Plant Cell Biotechnology and Molecular Biology 22(21-22): 94-100.
[64] Siregar, M., Purnomo, D. W., Iryadi, R. (2021): Impact of invasive alien species - *Acacia nilotica* on the remnant dry deciduous forest of Palu Valley, Central Sulawesi, Indonesia. – Annual Research & Review in Biology. DOI: 10.9734/arrb/2021/v36i730403.
[65] Šoln, K., Klemenčič, M., Koce, J. D. (2022): Plant cell responses to allelopathy: from oxidative stress to programmed cell death. – Protoplasma. DOI: 10.1007/s00709-021-01729-8.
[66] Stanek-Tarkowska, J., Szostek, M., Rybak, M. (2021): Effect of different doses of ash from biomass combustion on the development of diatom assemblages on podzolic soil under oilseed rape cultivation. – Agronomy 11(12): 2422.
[67] Stefanowicz, A. M., Rożek, K., Stanek, M., Rola, K., Zubek, S. (2021): Moderate effects of tree species identity on soil microbial communities and soil chemical properties in a common garden experiment. – Forest Ecology and Management 482: 118799.
[68] Šućur, J., Konstantinović, B., Crnković, J., Bursić, V., Samardžić, N., Malenčić, D., Prvulović, D., Popov, M., Vuković, G. (2021): Chemical composition of *Ambrosia trifida* L. and its allelopathic influence on crops. – Plants 10(10): 2222.
[69] Tahir, N. A., Qader, K. O., Azeez, H. A., Rashid, J. S. (2018): Inhibitory allelopathic effects of *Moringa oleifera* Lamk plant extracts on wheat and *Sinapis arvensis* L. – Allelopathy Journal 44(1): 35-48.
[70] Tahir, N., Azeez, H., Hama-Amin, H., Rashid, J., Omer, D. (2019): Antibacterial activity and allelopathic effects of powder from leaf, stem and bark of Mt. Atlas mastic tree (*Pistacia atlantica* subsp kurdica) on crops and weeds. – Allelopathy J. 46: 121-132.
[71] Tajik, S., Ayoubi, S., Khajehali, J., Shataee, S. (2019): Effects of tree species composition on soil properties and invertebrates in a deciduous forest. – Arabian Journal of Geosciences 12(11): 1-11.
[72] Tian, M., Li, Q., Zhao, W., Qiao, B., Shi, S., Yu, M., Li, X., Li, C., Zhao, C. (2022): Potential allelopathic interference of Abutilon theophrasti Medik. powder/extract on Seed germination, seedling growth and root system activity of maize, wheat and soybean. – Agronomy 12(4): 844.
[73] Vasishth, A., Kokliyal, N., Joshi, R., Dhanai, C. S. (2020): Allelopathic effects of tree species on germination and seedling growth of traditional agricultural crops of Garhwal Himalayas. – Indian Journal of Agroforestry 22(2).
[74] Wang, Q., Xiao, J., Ding, J., Zou, T., Zhang, Z., Liu, Q., Yin, H. (2021): Differences in root exudate inputs and rhizosphere effects on soil N transformation between deciduous and evergreen trees. – Plant and Soil 458(1): 277-289.

http://www.aloki.hu ● ISSN 1589 1623 (Print) ● ISSN 1785 0037 (Online)
DOI: http://dx.doi.org/10.15666/aeer/2005_41934209

[75] Wenkert, W. (1980): Measurement of tissue osmotic pressure. – Plant Physiology 65(4): 614-617.
[76] Woś, B., Józefowska, A., Likus-Cieślik, J., Chodak, M., Pietrzykowski, M. (2021): Effect of tree species and soil texture on the carbon stock, macronutrient content, and physicochemical properties of regenerated postfire forest soils. – Land Degradation & Development 32(18): 5227-5240.
[77] Xaxa, S. S., Daniel, S., Srinivas, K., Suren, A. (2018): Effect of aqueous leaf extracts of poplar (*Populus deltoides* L.) on germination and seedling growth of wheat varieties (*Triticum aestivum* L.). – Journal of Pharmacognosy and Phytochemistry 7(4): 2332-2334.
[78] Xing, Z., Du, C., Shen, Y., Ma, F., Zhou, J. (2021): A method combining FTIR-ATR and Raman spectroscopy to determine soil organic matter: improvement of prediction accuracy using competitive adaptive reweighted sampling (CARS). – Computers and Electronics in Agriculture 191): 106549.
[79] Yaseen, A., Hájos, M. T. (2020): Study on moringa tree (*Moringa oleifera* Lam.) leaf extract in organic vegetable production: a review. – Research on Crops 21(2).
[80] Yates, C. F., Guo, J., Bell, T. B., Fleishman, S. M., Bock, H. W., Trexler, R. V., Eissenstat, D. M., Centinari, M. (2021): Tree-induced alterations to soil properties and rhizoplane-associated bacteria following 23 years in a common garden. – Plant and Soil 461(1): 591-602.
[81] Zeng, L.-L., Bian, X., Zhao, L., Wang, Y., Hong. Z. (2021): Effect of phosphogypsum on physiochemical and mechanical behaviour of cement stabilized dredged soil from Fuzhou, China. – Geomechanics for Energy and the Environment 25: 100195.
[82] Zubay, P., Kunzelmann, J., Ittzés, A., Zámboriné, É. N., Szabó, K. (2021): Allelopathic effects of leachates of *Juglans regia* L., *Populus tremula* L. and juglone on germination of temperate zone cultivated medicinal and aromatic plants. – Agroforestry Systems 95(2): 431-442.

http://www.aloki.hu ● ISSN 1589 1623 (Print) ● ISSN 1785 0037 (Online)
DOI: http://dx.doi.org/10.15666/aeer/2005_41934209

THE RELATIONSHIP BETWEEN WILD PLANTS AND GRAZING LIVESTOCK BEHAVIOR - REVIEW

AL-HARBI, N. A.

Biology Department, University College of Tayma, University of Tabuk, Tabuk, Saudi Arabia (e-mail: nalharbi@ut.edu.sa)

(Received 25th Jun 2021; accepted 22nd Dec 2021)

Abstract. The region of the Arab peninsula has a diversity of plants and animals. Grazing on natural rangeland plants may have a neutral, positive, or negative impact on both animals and plants as well depending on several factors. Grazing environmental forces includes herbivory, physical impact, and deposition. When animals graze on plants, they show a hierarchy that leads to understanding instinctive responses and behavioral activities. Mouth anatomy of goats gives them the merit of capability of selecting plants in the range, while that of sheep enables them to graze quite near the ground. Preference is a behavioral trait that includes the proportional selection of plant species from a group of two or more. Animal behavioral preference in governed by abundance of a plant species, its morphological features, the animal species in question and the variety of species available. Animals have two distinct acquired behaviors (i.e. evolutionary and field acquired). Forage quality and quantity were inversely proportional to the ratio of spent time to graze in group to the region taken in the landscape, to be concluded that wild plants affect grazing animals by modifying their behaviors to adapt the current situation in the range.
Keywords: *overgrazing, herbivory force, physical impact, deposition*

Introduction

Grazing perturbation trample plants, divides soil surfaces, mixes the seed into the soil and compacts soil via hoof activity, pawing and wallowing. The deposition of urines or dung high in nitrogen can make contribute to the food web by helping grazing animals promoting nutrient cycling.

The ecological dynamics of ungulate pasture - herbivory, physical impacts and deposition - have formed natural habitats throughout the planet. Grassing habitats have developed depending on herbivores, strong hooves, nitrogen deposits and massive migrating ungulates' carcasses. These pressures could change the biological communities and the function of ecosystems if they were introduced to ecosystems which did not evolve with regular pasture and this affects on livestock behavior.

Accordingly, this article reviews the relationship between wild plants and grazing livestock behavior.

Literature review

The term "wild plants" refers to plant species that grow spontaneously without human interference (Chatterji and Fauquet, 2000) in self- maintained natural or semi-natural ecosystems. They are in opposite to plant species "cultivate" or "domesticated" that have arisen because of human activity such as selection or breeding and those depend on their continued existence (FAO, 1999).

There are several geographic regions within the Arab peninsula each with a diversity of plants and animals adapted to their specific habitats (Al-Sodany et al., 2011). These habitats include the country vast mountains, deserts, highlands, steppes, hills and valleys. There are nearly 3,500 plant species in the country, with nearly 1,000 known

http://www.aloki.hu ● ISSN 1589 1623 (Print) ● ISSN 1785 0037 (Online)
DOI: http://dx.doi.org/10.15666/aeer/2005_42114220

plant species from southwest Asir which is an area with higher rainfall (Anthony et al., 2004).

If these plants are suitable for grazing animals, they are called range plants or wild grazing plants (Shaheen et al., 2019). However, the majority of plants in wild life are perennials, grazing on natural rangeland plants may have a neutral, positive, or negative impact on both animals and plants depending on several factors, grazing and browsing livestock and wildlife get their nutrients from rangeland plants, which include proteins, carbohydrates, and sugars made by plant photosynthesis (Lyons and Hanselka, 2001). Since photosynthesis occurs only in green plant tissue, primarily the leaves, animals destroy the leaves (defoliation) during grazing and browsing leading to a reduction plant ability to produce food, at least temporarily (Soder et al., 2007).

Both individual plants and plant populations are affected by grazing and browsing, indicators show which plants are at risk of excessive animal herbivory (Diogo et al., 2016). Drought, flood, burning, and grazing have all harmed rangeland habitats. To a certain degree, depending on time, intensity and disturbance frequency, all disturbances affect the plants directly or indirectly, generally, the more diverse the vegetation, the more disturbed the rangeland (Moller et al., 2020). However, knowing the factors that affect these plants and the available management options allow a better decision on the best actions for a specific site as well as appropriate time to take action (Schueller et al., 2020).

Grazing environmental forces

Such forces include:

Herbivory force: The plant leaves, stalks, flowers, seeds and sometimes roots eaten by herbivores. Herbivorous patterns greatly influence the composition, structure and productivity of the plant community.

Physical impact: Pasting animals crush plants, break up the surfaces of the soil and mix the seed into the earth and tiny soils via hooves, paving and wallowing.

Deposition: The deposition of nitrogen-rich urine and dung by grazing animals contributes to nutrient cycling, and their carcasses can play a significant part in food web.

Animal behavior

When animals graze on plants, they show a hierarchy that leads to understand instinctive responses and behavioral activities (Kuhlmann and Ribeiro, 2016). Animals keep fit through feeding to consume energy and/or other nutrients in the highest possible amount. However, these mechanisms can be traced back to the evolution of species (Callaway et al., 2005).

When animals are born, they possess inherited distinct physiological requirements and legacy capabilities. Such requirements and capacity differ greatly depending on age, species, race, sex, physiological condition, and experience and knowing how such features affect dietary selection, can greatly help to elucidate animal behavior in ranges, animal behaviors can be formed through dietary selection experiences (Burritt and Frost, 2006).

Grazers, such as cattle and horses, feed mostly on grass. Cattle are better suited to grazing than browsing due to their overall size and mouth design (Huang et al., 2016).

http://www.aloki.hu ● ISSN 1589 1623 (Print) ● ISSN 1785 0037 (Online)
DOI: http://dx.doi.org/10.15666/aeer/2005_42114220

Bovines mainly feed on grass as they have a relatively low digestive ability to process significant amounts of feedstuff (Burritt and Frost, 2006). Due to their big lips, muzzle, and tongue, which they use as a prehensile foraging weapon, cattle consume large amounts of forages (Palmer et al., 2003). These big muzzles, however, restrict their forage selection ability (both for the 9 plant as well as plant different parts).

On the other hand, sheep, considered as intermediate grazers since thy have relatively big rumen compared to body mass which gives them the merit of having the ability to select plants in the range (Bergman et al., 2001). Sheep also have a small mouth, so they can graze near the ground. They make little bites, for example, to choose certain portions of a plant (i.e. as small leaves or buds) (Dias-Silva and Filho, 2021). Sheep are used to control several weedy forbs. They were successfully used for controlling weeds (Tu et al., 2001). If grasses are abundant or other forage sources are limited, sheep can readily eat grass-dominated diets. As forbs supply increases, sheep prefer to eat more forbs. They find tall dense stands of forage hard to graze than small thick groves, compared to cattle. In addition, sheep are tiny, agile, and well-suited to traversing difficult terrain (Glienke et al., 2016). It is steeper than most livestock that sheep graze and tends to avoid marshy wetlands.

Goats are browsers by nature. They are ideally suited to chew branches and extracting individual leaves from woody stems due to their tiny, muscular mouth and dexterous tongue (Burritt and Frost, 2006). Because of their tiny jaws, goats can eat only the best leaves and stems, resulting in higher-quality meals (Pauler et al., 2020). Goats have larger livers than cattle or sheep in terms of body weight, allowing them to deal with plants that produce secondary compounds such as terpenes or tannins more efficiently. That could give a reason for why goats eat more leafy-spurge than cattle or sheep, which includes a variety of plant-defense compounds (Nielsen et al., 2015). Therefore, preference is a behavioral trait that includes the proportional selection of one plant species from a group of two or more. Indeed, the abundance of a plant species, its morpho/phenological features, the animal species in question and the variety of species available all play a role in its preference status (Amdam and Hovland, 2011). As abiotic influences (such as season and weather conditions) change the essence of the plant population, preferences shift. Some organisms are only chosen under specific circumstances (Dominguez, 2002; Wong and Candolin, 2015). Animal selectivity is a complex, situation-specific operation, so broad generalizations about species selection and preference should be tempered. Recent research, (Akre et al., 2009; Beyer et al., 2010; Amdam and Hovland, 2011) has shown that preference can be quantified for an animal species as well as selection order can be predicted using the relative rank order of absolute preference values. The idea that specialized or concentrated grazing on some plant species may be related to its relative preference rating at the time of active growth is implicit in these findings.

Foraging behaviors of animals

Each animal has a different way of finding food, whether by smelling, seeing, or detecting it chemically (Danchin, et al., 2008), individually and in groups, animals seek food. The available plant species, their spatial arrangement, and structural configuration, (for example, a grassland community with scattered trees less than 1 m in height versus a shrub land with dense shrubs over 3 m high with some grassland filling

http://www.aloki.hu ● ISSN 1589 1623 (Print) ● ISSN 1785 0037 (Online)
DOI: http://dx.doi.org/10.15666/aeer/2005_42114220

the interspaces), are all examples of habitats. Habitats may be divided into patches, containing a more homogeneous community of organisms (Spiesman et al., 2018).

Animals learn how to forage. Learning is a behavioral change based on previous experiences, or a behavioral modification (Raine and Chittka, 2008). One way to learn is to 'forge innovation' - an animal that consumes new food or uses a new foraging technology in response to its dynamic living environment (Dugatkin, 2004). Foraging is divided into two main types. The first is solo foraging when animals drink by themselves. The other is group foraging (Pyke, 2019). Group food consumption includes two cases: when this activity is beneficial for the animals (aggregation economy), and when it has adverse effects on them (dispersion economy). After orienting itself in a habitat, the animal must determine when to lower its head and set up a feeding station along its grazing path. The animal must choose which plant species and parts to consume inside the feeding station (Searle and Shipley, 2008). As a result, there are two main levels to the diet selection process that must be distinguished: spatial choice and species choice. They look for the most energy efficient forage sources based on established water sources (Luca et al., 2010). The optimal grazing area is roughly defined as a circle with a radius of less than 0.8 kilometers from the water source. The overall external boundary for a flock of cattle or flock of sheep to balance their needs of water and forage is around 1.6 kilometers (Stephenson, 2010). However, as the forage supply decreases during a drought, the successful grazing area is increased. The amount of time spent grazing per day is determined by the quality of the forage, the thermal balance, and the short-term reliability of the forage supply. As the digestibility of accessible forage decreases as well as the retention time of ingesta rises, animals reduce their daily grazing time (Hummel, et al., 2006). Forage quality and quantity were inversely proportional to the time spent grazing in the group to the region taken in the landscape (Menajovsky et al., 2018). Compared to other communities available to the animal, the higher the density of high-quality food organisms, the slower the grazing velocity and thus the greater residence time and the intake level is attained (Menajovsky et al., 2018). Site choice is amplified when these populations are located near critical water and thermal foci.

Following the establishment of a grazing area, an animal's familiarity with the accessible forage is used in a species-to-species plant assessment and selection method. This is a mechanism that is unique to each animal species. Herbivores have evolved a preference for plant species (Kempel et al., 2015) from one or more of their primary food classes, grasses, forbs, and browse. As a result, a plant's grazing value is determined by the animal species in question. It is critical to distinguish between the palatability of a plant and the preference for that plant at this stage (Khan and Hussain, 2012).

Based on the abundance of highly profitable species, one might hypothesize that animals would be drawn to plant communities during rapid growth cycles while studying grazing strategies over time. Animals can minimize species selectivity as phenologies of plant populations become more mixed, focusing their attention on communities that provide the highest harvest rates of green foliage, regardless of species. Once the herbage has gone dormant, the animal's only choice is to graze on more plentiful plant material, regardless of its greenness.

http://www.aloki.hu ● ISSN 1589 1623 (Print) ● ISSN 1785 0037 (Online)
DOI: http://dx.doi.org/10.15666/aeer/2005_42114220

Impact of plants

Plants are divided into five groups based on their selectivity (preferred, proportional, forced, detrimental, and non-consumable) (Panter et al., 2011). Preferred or favored organisms are those selected in more significant amounts, as a percentage of the diet, than those present in the landscape (as a percentage of composition). Unless they dominate the population, in most cases, particular plant species are not dominant in the diet. Preferable animals, on the other hand, improve the nutritional value of the diet, resulting in better animal output rather than normal. Such species are highly handled by animals and/or have low floristic composition but high nutrient concentrations. The more plentiful species are commonly eaten in proportion to their available abundance and are known as proportional or desired species. Generally, the percentage of species not readily consumed by animals is less than that of the vegetation. This is known as by-consumption and as conditions change, it is believed to react to animal sampling from the environment. No matter the abundance or presence of the associated species, specific plant species are preferred; the preferred species are generally higher in succession.

Some species are consumed in a manner that is highly commensurate with availability and consumption. Another group is the third across all selection divisions, the utilization of which adjusts as weed mass declines from avoidance to preference. These plant species are known as species of variable or secondary preference and generally have morphologic constraints on animal consumption. Lastly, the final group of averted species are selected under their accessibility. Avoided species' selection rates are poorly linked to their inherent abundance. These species generally have unwanted nutritional characteristics.

Generally, there is no consumption other than specific adverse conditions (Attia-Ismail, 2015, 2016). Pods or fruiting bodies may be exempts. These species typically only have an indirect effect on the animal by decreasing the total pasture amplitude but may have a beneficial impact on food (Benvenutti et al., 2009). Shrubs have a primary herbicide-like impact when they produce microclimates for some species which maintain the verdant ingredients or are nutritionally richer state for a cold or dry period of the year, which is particularly the case with shrubbing. Finally, harmful or toxic species are present. When most favorites in the landscape are reduced, the diet is devastated by toxic species. An example of this problem is cyclical toxic plant problems in arid regions (Laca, 2009). Plant species with the highest volume of green leaf density at the highest concentration of nutrients and the lowest secondary content are most likely to be grazed. In general, the drilling quality of the landscape appears to be high with the consequences of increasing time in search, decreasing bite rates and increasing bite size, which can be highly profitable by non-ungulates (Pontes-Prates et al., 2020).

The morphology of plants also influences the likelihood of weeding. When grasses produce an early selective response, selective pressure increases with relative abundance change or phenologies (Carvalho and Stobbs, 2013). Therefore, in the early growing season, municipalities with a high proportion of the forage are more likely to be grazed if environmental conditions favor plant growth.

In grasses, the physical presence of the green blade in relation to the pattern of senescence and culms development appears as morphological features (Larson-Praplan et al., 2015). Grasses with a speed of climax growth and strong, midrib leaf structures are less frequently chosen if long-term, shrunk leaf material is allowed to develop. Sheath development and growth angle by tillers affect the height and position of the

http://www.aloki.hu ● ISSN 1589 1623 (Print) ● ISSN 1785 0037 (Online)
DOI: http://dx.doi.org/10.15666/aeer/2005_42114220

blade material in relation to the soil surface so that the selection by cattle of short or declining species is a much harder one than the selection by sheep (Nunes et al., 2019).

Forbs are distinguished by two temporal presentations: ephemeral and perennial. Ephemeral annual forbs are fast growing and their life cycle is rapidly ending. Therefore, ungulates have a unique problem with them: in the annual production cycle of the animal, forbs have a high value for short periods. Most forbs have nutrient concentrations exceeds ungulates' nutritional requirements. Thus, their distribution in the landscape and standing crops in various communities, together with the bite size, affect animal food tactics from one country to another, while they are a favorite group (Semmartin and Oesterheld, 2001).

Perennial forbs are more resource-based than annual forbs and therefore create greater quality difference between plant parts. Moreover, as shrubby strolls, they generally do not accumulate growth in previous years. As they are present throughout the pasture season, by forbidding non-ungulates, they are especially vulnerable to overuse. This overuse decreases the relative acceptability of plant parts, which makes the plant more attractive to the animal. This eventually, reduces the processing time and increases bite size/quality (Ungar, 2019).

Browse takes many forms: deciduous or always green, spineless, single leaves or compound leaves, short or large, single or multi-stemmed, etc. Selective pressure on this food group again relies on the animal species community associated with it (Aruwayo and Adeleke, 2019). Prehensile and digestive organs were adapted to suit levels where height, spininess and secondary compounds were the principal plant characteristics, which affected the selective pressure in the navy species (concentrates and intermediate feeders; Clauss and Hummel, 2017). In general, selective pressure on evergreen species by using secondary compounds plays a major role. Spininess, leaf size, and secondary compounds, to a lesser extent, are the significant morphological and physiological attributes of feedback species that affect the selection response. The relative significance also depends on the attributes of each animal species.

Conclusion

The review is concluded that wild plants affect grazing animals by making them modify their behaviors to adapt to the current situation in their range. However, to understand solo or group foraging behavior requires a game theory approach. Animals have to find and use resources to succeed and do extraordinary work to achieve this (modifying their behavior, for instance to adapt to the present forages). Animals have two distinct acquired behaviors (i.e. evolutionary and field acquired).

This review recommends, future research in this area should therefore maintain the theoretic approach but recognize the distinction between evolutionarily and behaviorally stable strategies, and focus on the behavioral and cognitive mechanisms involved. In this way, we should understand what group foraging animals do, how they do it and why they behave in this way.

http://www.aloki.hu ● ISSN 1589 1623 (Print) ● ISSN 1785 0037 (Online)
DOI: http://dx.doi.org/10.15666/aeer/2005_42114220

REFERENCES

[1] Akre, A. K., Bakken, M., Hovland, A. L. (2009): Social preferences in farmed silver fox females (Vulpes vulpes): does it change with age? – Applied Animal Behaviour Science 120: 186-191. https://doi.org/10.1016/j.applanim.2009.06.008.

[2] Al-Sodany, Y. M., Mosallam, H. A., Bazaid, S. A. (2011): Vegetation analysis of Mahazat Al-Sayd protected area: the second largest fenced nature reserve in the world. – World Applied Sciences Journal 15(8): 1144-1156.

[3] Amdam, G. V., Hovland, A. L. (2011): Measuring animal preferences and choice behavior. – Nature Education Knowledge 3(10): 74.

[4] Anthony, H., Brekhus, S. M., Andrew, M. (2004): Saudi Arabia. – Lonely Planet, Fort Mill, pp. 41-42.

[5] Aruwayo, A., Adeleke, R. A. (2019): A review of browse plants' use in the tropics and their chemical constituents. – FRsCS 1(3).

[6] Attia-Ismail, S. A. (2015): Plant Secondary Metabolites of Halophytes and Salt Tolerant Plants. Plant Secondary metabolites: Deleterious Effects, Remediation (Special Reference to Forage). – Springer, Dordrecht, pp. 169-178. DOI: 10.1007/978-94-017-7194-8. https://doi.org/10.1201/b19862-11.

[7] Attia-Ismail, S. A. (2016): Plant Secondary Metabolites of Halophytes and Salt Tolerant Plants. – In: El Shaer, H. M., Squires, V. R. (eds.) Halophytic and Salt-Tolerant Feedstuffs Impacts on Nutrition, Physiology and Reproduction of Livestock. CRC Press Taylor & Francis Group, Boca Raton, FL, pp. 348-357.

[8] Benvenutti, M. A., Cangiano, C. A. (2011): Características de las Pasturas y su Relación con el Comportamiento Ingestivo y Consumo en Pastoreo. – In: Cangiano, C. A., Brizuela, M. A. (eds.) Producción Animal en Pastoreo. Ediciones INTA, Buenos Aires, pp. 259-290.

[9] Bergman, C. M., Fryxell, J. M., Gates, C. C., Fortin, D. (2001): Ungulates foraging strategies: energy maximizing or time maximizing? – J. Anim. Ecol. 70: 289-300. https://doi.org/10.1046/j.1365-2656.2001.00496.x.

[10] Beyer, H. L., Haydon, D. T., Morales, J. M., Frair, J. L., Hebblewhite, M., Mitchell, M., Matthiopoulo, J. (2010): The interpretation of habitat preference metrics under use-availability designs. – Phil. Trans. R. Soc. B 365: 2245-2254. https://doi.org/10.1098/rstb.2010.0083.

[11] Burritt, E., Frost, R. (2006): Animal Behavior: Principles and Practices. 22-31. – In: Launchbaugh, K. (ed.) Targeted Grazing: A Natural Approach to Vegetation Management and Landscape Enhancement. American Sheep Industry Association Cottrell Printing, Centennial, Colo.

[12] Callaway, R. M., Kikodze, D., Chiboshvili, M., Khetsuriani, L. (2005): Unpalatable plants protect neighbors from grazing and increase plant community diversity. – Ecology 86: 1856-1862. https://doi.org/10.1890/04-0784.

[13] Carvalho, P. C. F., Stobbs, H. (2013): Memorial lecture: can grazing behavior support innovations in grassland management? – Trop. Grassl. 1: 137-155. https://doi.org/10.17138/TGFT(1)137-155.

[14] Chatterji, N., Fauquet, C. M. (2000): Ecology of Plant Viruses, with Special Reference to Whitefly-Transmitted Geminiviruses (WTGs). – In: Hurst, C. J. Viral Ecology. Academic Press, Cambridge, MA., pp. 321-351. https://doi.org/10.1016/B978-012362675-2/50009-4.

[15] Clauss, M., Hummel, J. (2017): Physiological adaptations of ruminants and their potential relevance for production systems. – R. Bras. Zootec. 46(7). https://doi.org/10.1590/s1806-92902017000700008.

[16] Danchin, E., Giraldeau, L., Cezilly, F. (2008): Behavioural Ecology. – Oxford University Press, New York.

http://www.aloki.hu ● ISSN 1589 1623 (Print) ● ISSN 1785 0037 (Online)
DOI: http://dx.doi.org/10.15666/aeer/2005_42114220

[17] Dias-Silva, T. P., Filho, A. L. A. (2021): Sheep and goat feeding behavior profile in grazing systems. – Acta Scientiarum. Animal Sciences 43: e51265. https://doi.org/10.4025/actascianimsci.v43i1.51265.
[18] Diogo, I. J. S., Martins, F. R., Verola, C. F., Costa, I. R. d. (2016): Variation in plant-animal interactions along an elevational gradient of moist forest in a semiarid area of Brazil. – Acta Botanica Brasilica 30: 27-34. https://doi.org/10.1590/0102-33062015abb0198.
[19] Dominguez, J. (2002): Biotic and abiotic factors affecting the feeding behavior of the black-tailed godwit. – International Journal of Waterbird Biology 25(4): 393-400. https://doi.org/10.1675/1524-4695(2002)025[0393:BAAFAT]2.0.CO;2.
[20] Dugatkin, L. A. (2004): Principles of Animal Behavior. – University of Chicago Press, Chicago, IL.
[21] FAO (1999): Use and potential of wild plants in farm households. –FAO, Rome. http://www.fao.org/3/W8801E/w8801e00.htm#toc_00.
[22] Glienke, C. L., Rocha, M. G., Pötter, L., Roso, D., Montagner, D. B., Oliveira Neto, R. A. (2016): Canopy structure, ingestive behavior and displacement patterns of beef heifers grazing warm-season pastures. – Arquivo Brasileiro de Medicina Veterinária e Zootecnia 68(2): 457-465. https://doi.org/10.1590/1678-4162-8230.
[23] Huang, Y., Wang, L., Wang, D. et al. (2016): How does the foraging behavior of large herbivores cause different associational plant defenses? – Sci Rep 6: 20561. https://doi.org/10.1038/srep20561.
[24] Hummel, J., Südekum, K. H., Streich, W. J., Clauss, M. (2006), Forage fermentation patterns and their implications for herbivore ingesta retention times. – Functional Ecology 20: 989-1002. https://doi.org/10.1111/j.1365-2435.2006.01206.x.
[25] Kempel, A., Razanajatovo, M., Stein, C., Unsicker, S. B., Auge, H., Weisser, W. W., Fischer, M., Prati, D. (2015): Herbivore preference drives plant community composition. – Ecology 96(11): 2923-2934. https://doi.org/10.1890/14-2125.1.
[26] Khan, M., Hussain, F. (2012): Palatability and animal preferences of plants in Tehsil Takht-e-Nasrati, District Karak, Pakistan. – African Journal of Agricultural Research 7(44). https://doi.org/10.5897/AJAR12.2095.
[27] Kuhlmann, M., Ribeiro, J. F. (2016): Evolution of seed dispersal in the Cerrado biome: ecological and phylogenetic considerations. – Acta Botanica Brasilica 30: 271-282. https://doi.org/10.1590/0102-33062015abb0331.
[28] Laca, E. A. (2009): New approaches and tools for grazing management. – Rangel. Ecol. Manag. 62: 407-417. https://doi.org/10.2111/08-104.1.
[29] Larson-Praplan, S., George, M. R., Buckhouse, J. C., Laca, E. A. (2015): Spatial and temporal domains of scale of grazing cattle. – Anim. Prod. Sci. 55: 284-297. https://doi.org/10.1071/AN14641.
[30] Luca, F., Perry, G. H., Di Rienzo, A. (2010): Evolutionary adaptations to dietary changes. – Annu Rev Nutr. 21(30): 291-314. https://doi.org/10.1146/annurev-nutr-080508-141048.
[31] Lyons, R. K., Hanselka, C. W. (2001): Grazing and browsing: how plants are affected. – https://agrilifeextension.tamu.edu/library/ranching/grazing-and-browsing-how-plants-are-affected/.
[32] Menajovsky, S. B., Walpole, C. E., DeVries, T. J., Schwartzkopf-Genswein, K. S., Walpole, M. E., Penner, G. B. (2018): The effect of the forage-to-concentrate ratio of the partial mixed ration and the quantity of concentrate in an automatic milking system for lactating Holstein cows. – Journal of Dairy Science 101(11): 9941-9953. https://doi.org/10.3168/jds.2018-14665.
[33] Moller, J., van de Velde, R. N., Merten, L., Puschmann, C. (2020): Explaining online news engagement based on browsing behavior: creatures of habit? – Social Science Computer Review 38(5): 616-632. https://doi.org/10.1177/0894439319828012.

http://www.aloki.hu ● ISSN 1589 1623 (Print) ● ISSN 1785 0037 (Online)
DOI: http://dx.doi.org/10.15666/aeer/2005_42114220

[34] Nielsen, B. L., Rampin, O., Meunier, N., Bombail, V. (2015): Behavioral responses to odors from other species: introducing a complementary model of allelochemics involving vertebrates. – Front Neurosci. 9: 226. https://doi.org/10.3389/fnins.2015.00226.
[35] Nunes, P. A. D. A., Bredemeier, C., Bremm, C., Caetano, L. A. M., de Almeida, G. M., de Souza Filho, W., Anghinoni, I., Carvalho, P. C. D. F. (2019): Grazing intensity determines pasture spatial heterogeneity and productivity in an integrated crop-livestock system. – Grassl. Sci. 65: 49-59. https://doi.org/10.1111/grs.12209.
[36] Palmer, S. C. F., Hester, A. J., Elston, D. A., Gordon, I. J., Hartley, S. E. (2003): The perils of having tasty neighbours: grazing impacts of large herbivores at vegetation boundaries. – Ecology 84: 2877-2890. https://doi.org/10.1890/02-0245.
[37] Panter, K. E., Ralphs, M. H., Pfister, J. A., Gardner, D. R., Stegelmeier, B. L., Lee, S. T., Welch, K. D., Green, B. T., Davis, T. Z., Cook, D. (2011): Plants Poisonous to Livestock in the Western States. – Agriculture Bulletin No. 415. U.S. Department of Agriculture, Washington, DC.
[38] Pauler, C. M., Isselstein, J., Berard, J., Braunbeck, T., Schneider, M. K. (2020): Grazing allometry: anatomy, movement, and foraging behavior of three cattle breeds of different productivity. – Front. Vet. Sci. 14. https://doi.org/10.3389/fvets.2020.00494.
[39] Pontes-Prates, A., de Faccio Carvalho, P. C., Laca, E. A. (2020): Mechanisms of grazing management in heterogeneous swards. – Sustainability 12: 8676. https://doi.org/10.3390/su12208676.
[40] Pyke, G. H. (2019): Optimal Foraging Theory: The Basic Foundations. – Encyclopedia of Animal Behavior. 2nd Ed. https://doi.org/10.1016/B978-0-12-809633-8.01156-0.
[41] Raine, N. E., Chittka, L. (2008): The correlation of learning speed and natural foraging success in bumble-bees. – Proceedings of the Royal Society B: Biological Sciences. 275(1636): 803-808. https://doi.org/10.1098/rspb.2007.1652.
[42] Schueller, S. M., Steakley-Freeman, D. M., Mohr, D. C., Yom-Tov, E. (2020): Understanding perceived barriers to treatment from web browsing behavior. – Journal of Affective Disorders 267: 63-66. https://doi.org/10.1016/j.jad.2020.01.131.
[43] Searle, K. R., Shipley, L. A. (2008): The Comparative Feeding Behaviour of Large Browsing and Grazing Herbivores. – In: Gordon, I. J., Prins, H. H. T. (eds.) The Ecology of Browsing and Grazing. Ecological Studies. Springer, Berlin. https://doi.org/10.1007/978-3-540-72422-3_5.
[44] Semmartin, M., Oesterheld, M. (2001): Effects of grazing pattern and nitrogen availability on primary productivity. – Oecologia 126: 225-230. https://doi.org/10.1007/s004420000508.
[45] Shaheen, H., Qureshi, R., Qaseem, M. F., Bruschi, P. (2019): The fodder grass resources for ruminants: an indigenous treasure of local communities of Thal desert Punjab, Pakistan. – PLoS ONE. https://doi.org/10.1101/796227.
[46] Soder, K. J., Rook, A. J., Sanderson, M. A., Goslee, S. C. (2007): Interaction of plant species diversity on grazing behavior and performance of livestock grazing temperate region pastures. – Crop Sci. 47: 416-425. https://doi.org/10.2135/cropsci2006.01.0061.
[47] Spiesman, B. J., Stapper, A. P., Inouye, B. D. (2018): Patch size, isolation, and matrix effects on biodiversity and ecosystem functioning in a landscape microcosm. – Ecosphere 9(3): e02173. 10.1002/ecs2.2173. https://doi.org/10.1002/ecs2.2173.
[48] Stephenson, M. B. (2010): Effect of grazing system on livestock performance, botanical composition, and standing crop in the Nebraska Sandhills. – Theses, Dissertations, and Student Research in Agronomy and Horticulture 7. https://digitalcommons.unl.edu/agronhortdiss/7.
[49] Tu, M., Hurd, C., Randall, J. M. (2001): Chapter 2: Grazing. – In: Tu, M. et al. (eds.) Weed Control Methods Handbook. The Nature Conservancy, Arlington, VA. http://tncweeds.ucdavis.edu.

http://www.aloki.hu ● ISSN 1589 1623 (Print) ● ISSN 1785 0037 (Online)
DOI: http://dx.doi.org/10.15666/aeer/2005_42114220

[50] Ungar, E. D. (2019): Perspectives on the concept of rangeland carrying capacity, and their exploration by means of Noy-Meir's two-function model. – Agric. Syst. 173: 403-413. https://doi.org/10.1016/j.agsy.2019.03.023.
[51] Wong, B. B. M., Candolin, U. (2015): Behavioral responses to changing environments. – Behavioral Ecology 26(3): 665-673. https://doi.org/10.1093/beheco/aru183.

http://www.aloki.hu ● ISSN 1589 1623 (Print) ● ISSN 1785 0037 (Online)
DOI: http://dx.doi.org/10.15666/aeer/2005_42114220

ANTHELMINTIC DRUG ALBENDAZOLE TREATED SHEEP URINATION INFLUENCES SOIL NITROGEN TRANSFORMATIONS AND NITROUS OXIDE EMISSIONS FROM GRASSLANDS

REN, J. F. – HOU, F. J. – BOWATTE, S.*

State Key Laboratory of Grassland Agro-ecosystems; Key Laboratory of Grassland Livestock Industry Innovation Ministry of Agriculture and Rural Affairs; College of Pastoral Agriculture Science and Technology, Lanzhou University, Lanzhou 730020, Gansu Province, China

*Corresponding author
e-mail: samanbowatte@lzu.edu.cn*

(Received 1st Jan 2022; accepted 11th Jul 2022)

Abstract. This study investigated the deposition of the anthelmintic drug albendazole through sheep urine and how it affects soil nitrogen transformations and nitrous oxide (N_2O) emissions in grazed grasslands. Three one-year-old Tibetan rams were dosed with fast-acting albendazole capsules at 11 mg per kg body weight to measure the concentration of albendazole and its metabolites in each sheep's urine. Three rams were used as a control group. Albendazole, albendazole sulfoxide and albendazole sulfone were all excreted with urine, but albendazole sulfoxide was the main metabolite. The effect of albendazole or its metabolites' excretion in urine on soil nitrogen transformations and nitrous oxide emissions were investigated at an alpine grassland site. Greater nitrification activity was observed in soils where urine from albendazole-dosed rams had been applied. The mean total N_2O emissions over the six-week measurement period for albendazole-dosed sheep urine, control urine and no urine were 0.94 ± 0.34, 0.18 ± 0.11 and 0.02 ± 0.05 g N_2O-N m^{-2}, respectively. These results suggest that N_2O pollution from animal urine patches can be potentially exacerbated through anthelmintic drug administration to grazed animals.
Keywords: *ammonium, nitrate, sheep urine, urine patches, greenhouse gas*

Introduction

Gastrointestinal parasite infection is a major issue in livestock farming throughout the world. Recently, this issue has become a serious concern in the global livestock industry as the number of animals raised on livestock farms has substantially increased due to the increase in demand for meat and milk products. Since the use of anthelmintic drugs is a common practice for controlling internal parasites, there has been a significant worldwide effort into the research and development (Zhang et al., 2019), and applications (Han et al., 2017) of anthelmintics. While anthelmintic drugs are beneficial for overcoming animal health issues, studies have increasingly identified some unintended consequences, as anthelmintics given to ruminants can enter the environment through faeces or urine (Beynon, 2012). Anthelmintics may enter the environment through excreta as the parent active ingredient, metabolites or a combination of both, and the proportions of different anthelmintics excreted in faeces or urine can vary (Wu et al., 2009). Potential environmental impacts of some of these anthelmintic products or their breakdown metabolites on non-target organisms are well documented (Oh et al., 2009; Beynon, 2012; Wagil et al., 2015; Prchal et al., 2016). Among the existing literature, substantial research papers report the potential environmental impacts of the anthelmintic products on aquatic systems (Oh et al., 2006; Belew et al., 2021; Mooney et al., 2021) and contamination

http://www.aloki.hu ● ISSN 1589 1623 (Print) ● ISSN1785 0037 (Online)
DOI: http://dx.doi.org/10.15666/aeer/2005_42214235

through faeces (McKellar, 1997). Surprisingly, information on how animal-grazed grasslands are ecologically impacted through animal urine excretion is lacking.

This study aimed to investigate the impacts of urine from sheep fed the anthelmintic drug albendazole on soil microbial processes, with a particular focus on the soil nitrogen (N) cycle in grazed grasslands. The microbial-driven soil N transformations in animal urine patches are important in animal-grazed grasslands as they influence plant productivity as well as environmental pollution via nitrate leaching and nitrous oxide (N_2O) emissions to the atmosphere (Haynes and Williams, 1993). Grazing animals harvest N from across the grasslands, and then deposit it through urine in small patches with a high N load. The high N load deposited to soil exceeds plant uptake ability, so it becomes subject to soil microbial-driven N transformations, including N_2O production. The production of N_2O in soils occurs primarily via the biological pathways of nitrification and denitrification. Nitrification in soils produces nitrate (NO_3^-) from ammonium (NH_4^+), while also producing some N_2O. The NO_3^--N produced by nitrification can be taken up by plants, leached or transformed to N_2O production by denitrification (Giles et al., 2012).

Albendazole is a broad-spectrum anthelmintic drug that is widely used to control gastrointestinal parasite infections in sheep and cattle. Single-dose fast-acting albendazole tablets are commonly used in countries including China, while long-lasting slow-release albendazole capsules are generally used in countries such as Australia and New Zealand (Fisher and Van Sittert, 2013). After oral ingestion by animals, albendazole is metabolised into anthelmintically active albendazole sulfoxide, which is then oxidized to the less anthelmintically active albendazole sulphone (Prchal et al., 2016). Pope (2009) reported that albendazole and its metabolites are mainly excreted with animal urine. Several previous studies have indicated that anthelmintics excreted with animal faeces have significant effects on soil organisms such as earthworms, soil bacteria (Sun et al., 2005), soil fungi (Wang et al., 2021) and soil fauna (Madsen et al., 1990). In this study, we hypothesize that the composition of the urine of albendazole-dosed animals would be different from non-dosed animals, and the albendazole and its metabolites excreted with sheep urine would impact soil microbial activity related to the N cycle. We conducted two separate experiments to answer the following specific science questions: 1) What quantities of albendazole and its metabolites are excreted to grazed grasslands through sheep urine? 2) What are the effects of albendazole-treated sheep urine on soil N transformations and soil N_2O emissions?

Materials and methods

Ethics statement

The animal management were in accordance with the rules and regulations of experimental field management protocols (file No: 2010-1 and 2010-2), which were approved by Lanzhou University.

Detection of albendazole and its metabolites' excretion in sheep urine

Experimental setup

This experiment was carried out at Linze Grassland Agriculture Research Station of Lanzhou University in Linze County, Gansu Province, China (latitude 39.24°N, longitude 100.06°E, altitude 1390 m), in June 2018. Six one-year-old Hu sheep × thin-tail Han

http://www.aloki.hu ● ISSN 1589 1623 (Print) ● ISSN1785 0037 (Online)
DOI: http://dx.doi.org/10.15666/aeer/2005_42214235

crossbred rams with an average body weight of 39.04 ± 4.67 kg were used in the experiment. Three sheep received the anthelmintic dose and three sheep were used as a control group. The sheep were placed in individual metabolic cages (*Fig. 1*). The cages were made of steel with a wooden floor that had a gap for faeces and urine drainage, which was collected in a nylon mesh and tilted plastic cloth beneath the wooden floor. Three sheep received albendazole tablets (Jixing Animal Pharmaceutical Co., Ltd., Sichuan, China) at a dose recommended by the manufacturer of 11 mg per kg body weight, the animals were treated with the albendazole only once. During the experiment period, the sheep were fed oat hay purchased from a local forage feed supplier and alfalfa hay produced at a university farm, mixed at the ratio of 9:1, compositions of mixed forage see *Table 1*. All the sheep had free access to sufficient water.

Figure 1. *Individual metabolic cages used for urine collection at Linze research station*

Table 1. *Chemical composition of forage fed to sheep during urine collection*

Nutrient indexes*	Linze forage	Maqu forage
OM, g/kg DM	906	897
CP, g/kg DM	148	79
NDF, g/kg DM	463	599
ADF, g/kg DM	348	326
Ether extract, g/kg DM	21	32

*OM, organic matter; CP, crude protein; NDF, neutral detergent fiber; ADF, acid detergent fiber; DM, dry matter

Urine collection

The sheep were managed in metabolic cages for one week to adapt to the conditions before the albendazole tablets were fed to them. Urine from dosed sheep was collected at 6, 11, 24 h and 3, 4, 5, 6 and 14 days after feeding the albendazole tablets. Urine from control sheep was collected only at 6 and 72 h and 14 days. The urine samples collected up to 72 h were the total urine excretions between sampling times. For example, the

http://www.aloki.hu ● ISSN 1589 1623 (Print) ● ISSN1785 0037 (Online)
DOI: http://dx.doi.org/10.15666/aeer/2005_42214235

sample at 6 h included urine excreted during the 0 to 6 h period and the sample at 11 h included urine excreted during the 6 to 11 h period. The samples collected at day 6 and day 14 were urine excreted just on that day. Urine collected in the bucket was thoroughly mixed and filtered through a clean gauze. A sub-sample of 50 ml urine was stored in a 50 ml centrifuge tube at −20 °C until further analysis.

Analysis of albendazole and its metabolites

Albendazole and its metabolites, albendazole sulfoxide and albendazole sulfone, were analysed at a commercial laboratory at Sci-tech Innovation Quality Testing Co., Ltd., Qingdao, China, using a liquid chromatograph mass spectrometer (Thermo SHISEIDO SP-TSQ Quantum Ultra, USA). The protocol adapted by the laboratory was briefly: weigh approximately 2 g of urine sample into a 50 ml centrifuge tube, add 15 ml of ethyl acetate solution and 100 µl of 2 M NaOH solution, vortex for 15 min, centrifuge at 6000 rpm for 5 min, collect the supernatant and transfer it to a 100 ml chicken heart bottle, rotary-evaporate at 40 °C to dryness, add 1 ml methanol-aqueous solution (4:6, V/V) to ultrasonic for 1 min to dissolve the residue, transfer the solution from the chicken heart bottle to a 10 ml centrifuge tube, add 2 ml of N-hexane and vortex for 2 min to centrifuge at 6000 rpm for 5 min, take the water phase solution through a 0.22 µm filter membrane and test it on the liquid chromatograph mass spectrometer.

Field experiment to investigate the effects of albendazole-fed sheep urination on soil nitrogen transformations and N_2O emissions

Experimental site

The experiment was conducted at Maqu Grassland Agriculture Research Station of Lanzhou University in Maqu County, Gansu province, China (latitude 35.97°N, longitude 101.88°E, altitude, 3750 m), in August 2018 (*Fig. 2*). The research site is located in the northeast portion of the Qinghai Tibetan Plateau. The climate is continentally cold/humid. The average annual temperature at the site is about 1.2 °C and the average annual rainfall is about 620 mm. The vegetation at the site is botanically diverse, consisting of typical alpine meadow plant species such as *Kobresia* (*K. graminifolia*, *K. capillifolia*, *K. humilis*, *K. Tibetica*), *Elymus* (*E. nutans*), *Potentilla* (*P. anserina*), *Stipa* (*S. aliena*), *Festuca* (*F. ovina*) and various other species. The alpine meadows at the site were subjected to year-round free-grazing by yak. The soil at the site is classified as alpine meadow soil. Site soil properties at 0–10 cm depth were: total C, 70.33 ± 3.66 g kg^{-1}; total N, 4.16 ± 0.15 g kg^{-1}; total P, 492.55 ± 32.4 mg kg^{-1}; and pH 6.23 (1:2.5, soil: water).

Urine collection

Six one-year-old Tibetan rams of the Oula breed with body weight 25.98 ± 3.34 kg were used to collect the urine for this experiment. Sheep were randomly allocated to two groups: the albendazole-dose group and the control group. Sheep were fed with forage cut from the mixed pasture at the site. The chemical composition of forage is shown in *Table 1*. The dose group sheep received albendazole capsules at a dose of 11 mg per kg body weight (Jixing Animal Pharmaceutical Co., Ltd., Sichuan, China), the animals were treated with the albendazole only once. All sheep were supplied with free access to sufficient water. The sheep were placed in individual metabolic cages. The cages and urine collection process were as described earlier. We used cumulative urine collected up to 48 h for the field experiment, as the previous experiment identified that the maximum

http://www.aloki.hu ● ISSN 1589 1623 (Print) ● ISSN1785 0037 (Online)
DOI: http://dx.doi.org/10.15666/aeer/2005_42214235

amount of albendazole and its metabolites' residues would excrete within 48 h. The dose group urine and control group urine were separately stored at −20 °C before use.

Figure 2. *Nitrous oxide emissions measurement using static chamber method at Maqu Grassland Agriculture Research Station of Lanzhou University, China*

The experimental design and urine application

The experimental plots were established within a 6 × 8 m area that was fenced to exclude grazing. There were three treatments – albendazole-dosed sheep urine, control sheep urine and no urine control treatment – with five replicates. The treatment plots (gas chamber bases) were arranged according to row and column design. The urine treatments were applied at a rate of 3 L m^{-2}, within a standard sheep urine patch as reported by Haynes and Williams (1993). The N concentration of the applied urine was unknown at the time of application. The N concentration of the urine stored at 4 °C for eight weeks was later detected by the direct distillation method (Hoogendoorn et al., 2010). Urine was slowly poured from a height of 30 cm to inside the chamber base area (0.4 x 0.4 m). No treatments were added to the control plots.

Gas sampling

Nitrous oxide emissions after urine treatment applications were measured by the static chamber method (de Klein et al., 2003). The cubic chambers (0.4 × 0.4 × 0.4 m) were constructed from stainless steel. The stainless-steel chamber was covered with a silver adiabatic material to reduce the impact of direct radiative heating during sampling. The top of the chamber had two holes plugged with rubber septa, which were used to insert a temperature probe and a sampling port connected to a three-way stopcock. For a gas seal at the soil surface, the bottom edge of each chamber was seated into a Y-shaped, water-filled stainless-steel channel, with the lower arm of the 'Y' penetrating the soil to approximately 0.1 m depth. The Y-shaped chamber bases were installed one week before treatment application. The day before the treatment application, herbage was cut to 5 cm above the ground. Gas samples were taken two days before urine application, four days

http://www.aloki.hu ● ISSN 1589 1623 (Print) ● ISSN1785 0037 (Online)
DOI: http://dx.doi.org/10.15666/aeer/2005_42214235

during the first week, two days during weeks two to four, and then one sample per week until emissions reached the baseline by six weeks.

On each occasion, gas samples were taken between 10 am and 12 pm local time. The chamber was placed on the chamber base channel, which was filled with water to give an airtight seal. Two headspace gas samples were taken during a cover period of 30 min at times 0 and 30 min. Headspace gas samples were taken using a 60 ml polypropylene syringe and injected into pre-evacuated 500 ml aluminum foil gas-collecting bags (China Dalian Gas Packing Co., Ltd). The N_2O concentration of the gas samples was analysed by gas chromatography (GC-2014 Shimadzu corporation, Japan). The hourly N_2O emission fluxes were calculated for each chamber from the linear increase in headspace N_2O concentrations over the sampling time (de Klein et al., 2003). Hourly N_2O emissions (mg N m^{-2} h^{-1}) were calculated as follows:

$$N_2Oflux = \frac{\delta N_2O}{\delta t} \cdot \frac{M}{v_m} \cdot \frac{v}{A} \quad \text{(Eq.1)}$$

where N_2O flux is hourly N_2O emission (mg N_2O-N m^{-2} hr^{-1}), δN_2O is the increase in headspace N_2O during the enclosure period (µl L^{-1}), δt is the enclosure period (h), M is the molar weight of N in N_2O (g mol^{-1}), Vm is the molar volume of gas at the sampling temperature (L mol^{-1}), V is the headspace volume (m^3) and A is the area covered (m^2). Hourly emissions were integrated over time for each chamber to estimate total emissions. The emission factor (EF3) was calculated as the cumulative total amount of N_2O-N emitted as a percentage of urine N applied.

Soil mineral nitrogen measurements

Soil mineral nitrogen changes were measured using the ion exchange resin membranes (IEM) method (Bowatte et al., 2008). Membrane sheets (50 x 10 mm; VWR International Ltd, Poole, England) were fixed to plastic plant labels (100 x 15 mm) and inserted in the soil in the centre of the chamber base to leave the top of the sheet at the soil surface so that the effective depth sampled was 50 mm; the IEM probes were changed weekly. After removal, the IEM were washed with distilled water, extracted with 25 ml of 2 M KCl, filtered with Whatman #42 filter paper, and the nitrate (NO_3^--N) and ammonium (NH_4^+-N) contents were analysed using a FIAstar 5000 flow injection analyser (Foss Tecator, Hoganas, Sweden).

Statistical analysis

The amounts of albendazole and its metabolites excreted in urine over time for both dosed and control animals are presented for individual sheep. The mean and the standard error of the mean is presented to indicate the variability of the values among individual sheep.

The effect of urine treatments, time and their interactions on IEM-absorbed N and N_2O flux were tested by analysis of variance (ANOVA) using SPSS 20.0 statistical analysis software. All data were checked for assumptions of normality by the Kolmogorov–Smirnov test and log-transformed where necessary. The statistical significance of treatment means was tested by the Duncan method at the $P<0.05$ level.

http://www.aloki.hu ● ISSN 1589 1623 (Print) ● ISSN1785 0037 (Online)
DOI: http://dx.doi.org/10.15666/aeer/2005_42214235

Results

Albendazole and its metabolites' excretion in sheep urine

The amounts of albendazole, albendazole sulfoxide and albendazole sulfone detected in urine samples of six sheep are shown in *Table 2*. Albendazole and its metabolites were detected in both treated and untreated sheep urine samples, albeit at mostly trace amounts in untreated sheep urine. The highest amount of albendazole and its metabolite excretion, and the time when the highest amount appeared, varied between individual sheep. The maximum amount of albendazole was detected by the 24–36 h period from sheep 1 and 3, whereas it was by 6 h from sheep 2. The maximum amount of albendazole sulfoxide was detected from sheep 1 by the 24–36 h period, sheep 2 by 6 h and sheep 3 by 6–11 h. The maximum amount of albendazole sulfone was detected from sheep 1 by the 24–36 h period, sheep 2 by the 36–48 h period and sheep 3 by 6–11 h. The amount of albendazole sulfoxide excretion was substantially higher than albendazole or albendazole sulfone. By 72 h after the sheep were dosed with albendazole, the average total amounts of albendazole, albendazole sulfone and albendazole sulfoxide excreted with urine were 458.71 ± 106.12, 679.49 ± 575.98, 2341.31 ± 879.59 μg, respectively. After 48 h of dosing, low levels of albendazole and its metabolites were observed.

Effects of albendazole-fed sheep urination on soil nitrogen transformations and N_2O emissions

The changes in soil NO_3^- content after urine application are shown in *Fig. 3A*. The NO_3^- content in soil increased after the urine application in both urine treatment plots, indicating nitrification was occurring. Higher soil NO_3^- content was found in urine treatment soils compared with no urine control plots up to four weeks after urine application. The soil NO_3^- content was generally higher in albendazole-fed sheep urine treatment plots, where significant differences (P<0.05) in soil NO_3^- content between urine treatments were observed at 32 and 50 days after urine application.

The changes in soil NH_4^+ content after urine application are shown in *Fig. 3B*. The NH_4^+ content in soil increased after the urine application in both urine treatment plots compared with the no urine control plots, and the increase was significantly greater (P<0.05) in albendazole-fed sheep urine-treated plots at 7 days. The NH_4^+ content in soil then decreased with time in both urine treatment plots and by 40 days reached the level found in no urine control plots. Significant differences in soil NH_4^+ content between urine treatments were found only in the first week after urine application.

The changes in soil N_2O fluxes after urine application are shown in *Fig. 3C*. Two weeks after urine application, higher N_2O emissions were observed from urine treatment plots compared with no urine control plots. The N_2O emissions were significantly higher (P<0.05) from the albendazole-fed sheep urine-treated plots than the control urine plots at 21, 24 and 32 days. The mean total N_2O emissions over the six-week measurement period were significantly different (P<0.05) among the treatments: 0.94 ± 0.34, 0.18 ± 0.11 and 0.02 ± 0.05 g N_2O-N m^{-2} for albendazole-dosed sheep urine, control urine and no urine, respectively (*Fig. 4*). The N_2O-N emitted as a percentage of urine N applied (emission factor, EF3) was significantly different between urine treatments (P<0.05): 1.88 ± 0.72 in albendazole-fed sheep urine-treated plots compared with 0.41 ± 0.27 in control urine-treated plots (*Fig. 5*).

http://www.aloki.hu ● ISSN 1589 1623 (Print) ● ISSN1785 0037 (Online)
DOI: http://dx.doi.org/10.15666/aeer/2005_42214235

Table 2. *Amount of albendazole and its metabolites (μg) in sheep urine at different times, after a single dose of albendazole was administered*

Metabolite	Treatment	Sheep ID		Urine collection period (hours after dosing)								
				0-6	**6-11**	**11-24**	**24-36**	**36-48**	**48-60**	**60-72**	**6 d**	**14d**
albendazole	Dosed		1	8.79	11.09	0.23	627.95	13.27	0.19	0.4	0.14	0.44
			2	240.59	9.56	0.13	0.08	52.71	0.78	0.19	0.44	0.45
			3	60.99	7.52	3.44	321.43	16.69	0.02	0.07	0.37	0.37
		mean		**103.46**	**9.39**	**1.27**	**316.49**	**27.56**	**0.33**	**0.22**	**0.32**	**0.42**
		sem		**70.2**	**1.03**	**1.09**	**181.27**	**12.62**	**0.23**	**0.1**	**0.09**	**0.03**
	No dose		4	0.09							0.12	0.07
			5	0.07							0.13	0.27
			6	0.06							0.74	0.38
		mean		**0.07**							**0.33**	**0.24**
		sem		**0.02**							**0.36**	**0.16**
albendazole sulfone	Dosed											
			1	1.44	1.43	1.96	70.37	5.08	0.83	2.32	1.35	6.42
			2	43.1	3.49	3.44	0.35	66.22	3.09	4.15	3.11	3.15
			3	10.85	1739.91	1.03	76.01	3.34	0.07	0	2.21	2.33
		mean		**18.46**	**581.61**	**2.14**	**48.91**	**24.88**	**1.33**	**2.16**	**2.22**	**3.97**
		sem		**12.61**	**579.15**	**0.7**	**24.33**	**20.68**	**0.91**	**1.2**	**0.51**	**1.25**
	No dose		4	0							0	0
			5	0.55							0	0
			6	0							5.04	0
		mean		**0.18**							**1.68**	**0**
		sem		**0.18**							**1.68**	**0**
albendazole sulfoxide	Dosed											
			1	11.11	14.39	11.53	1094.93	22.36	2.13	8.8	2.58	11.3
			2	1014.81	15.63	10.68	0.51	702.2	25.83	26.66	12.19	3.75
			3	228.92	3358.27	9.12	452.12	13.28	0.08	0.56	11.08	7.74
		mean		**418.28**	**1129.43**	**10.44**	**515.85**	**245.95**	**9.35**	**12.01**	**8.62**	**7.6**
		sem		**304.82**	**1114.42**	**0.71**	**317.53**	**228.14**	**8.26**	**7.7**	**3.04**	**2.18**
	No dose		4	1.17							0.95	0.43
			5	2.07							0.58	1.84
			6	0.71							13.73	2.51
		mean		**1.32**							**5.09**	**1.59**
		sem		**0.4**							**4.32**	**0.61**

http://www.aloki.hu ● ISSN 1589 1623 (Print) ● ISSN1785 0037 (Online)
DOI: http://dx.doi.org/10.15666/aeer/2005_42214235

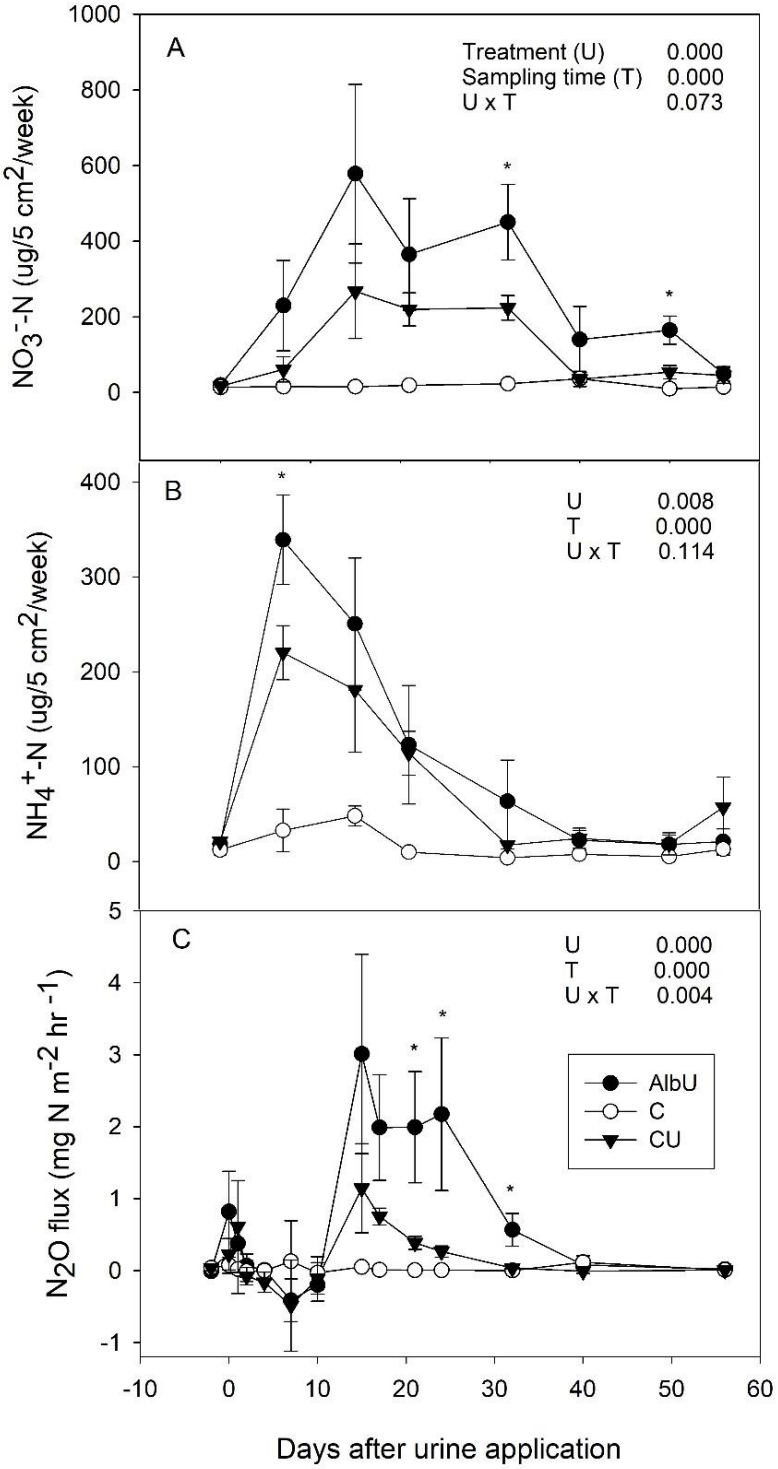

Figure 3. *Resin adsorbed soil NO_3^--N (A), NH_4^+-N (B) and nitrous oxide fluxes (C) after the application of urine from sheep treated with an albendazole (AlbU) or untreated (CU) and a non-urine control (C) to soil. Values are means (n=5) and error bars indicate standard error of mean. The statistical significances (P value) of treatment (U), sampling time (T) and their interaction (U×T) are shown on the top right of each figure. * indicate significant differences (P<0.05) between the AlbU treatment and CU treatment*

http://www.aloki.hu ● ISSN 1589 1623 (Print) ● ISSN1785 0037 (Online)
DOI: http://dx.doi.org/10.15666/aeer/2005_42214235

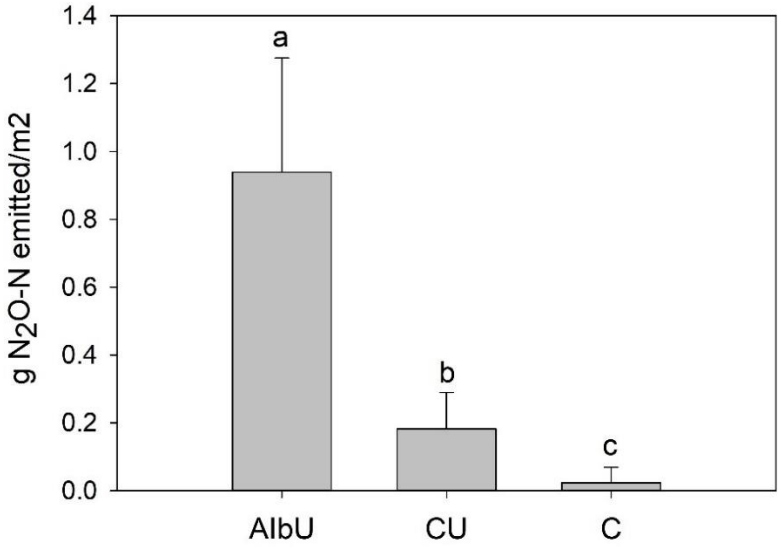

Figure 4. *The total N_2O emissions over the six-week measurement period from sheep treated with an albendazole (AlbU) or untreated (CU) and a non-urine control (C). Values are means ± SE, n=5. Different lowercase letters indicate significant difference at P<0.05*

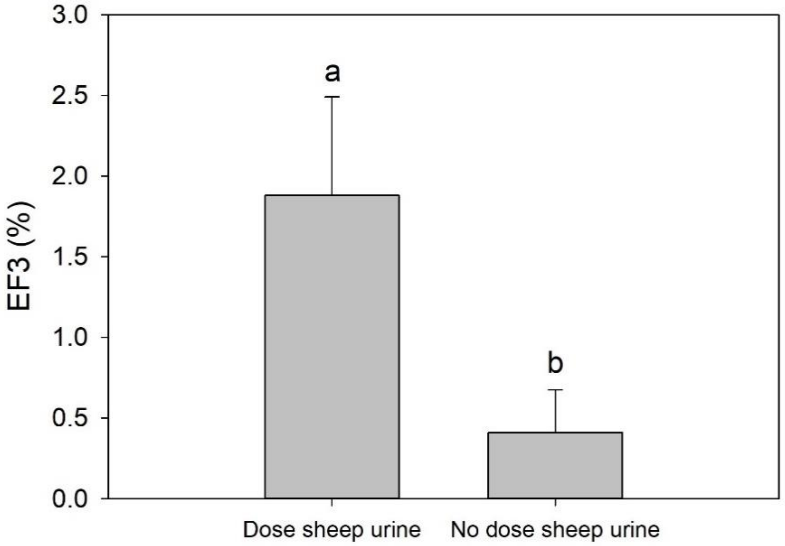

Figure 5. *N_2O emissions as a percentage of applied urine N (EF3). Values are means ± SE, n=5. Different lowercase letters indicate significant difference at P<0.05*

Discussion

We observed rapid and substantial excretion of albendazole and its metabolites in urine, indicating that animal urine deposition to grasslands is an important pathway for anthelmintic drugs to enter the environment. We found that albendazole sulfoxide excretion in urine was markedly greater than albendazole or albendazole sulfone. Gyurik et al. (1981) similarly found most metabolites in the urine of albendazole-fed cattle, sheep, rats and mice were sulfoxide and sulfone. In their study, unchanged albendazole was found in minor amounts, but we observed reasonable amounts of unchanged albendazole

http://www.aloki.hu ● ISSN 1589 1623 (Print) ● ISSN1785 0037 (Online)
DOI: http://dx.doi.org/10.15666/aeer/2005_42214235

in urine by 72 h (mean 458.71 ± 106.12 μg, n=3). The amount of albendazole and its metabolites excreted after oral administration with time, as well as the time of peak excretion, appeared to vary between individual sheep (*Table 2*), indicating the significant influence of differences in animal physiology on anthelmintic metabolism and excretion with urine. Interestingly, albendazole and its metabolites were also detected in the untreated sheep group, indicating some albendazole and its metabolites may be already present in the environment.

Our study showed that, once these chemicals enter the grassland environment, they can influence important ecosystem processes. Several previous studies have discussed anthelmintic drug resistance as a potential consequence of anthelmintic drug entry into the environment (Han et al., 2017), while others have focused on the impacts on non-target soil organisms (Beynon, 2012). Our study demonstrated a previously unrecognised important consequence of anthelmintic drug release to grazed grasslands, and the influence on soil microbial processes that drive the soil nitrogen cycle. Our observation of higher N_2O emissions from albendazole-dosed sheep urination has a greater significance. Nitrous oxide is the third most important greenhouse gas, after methane and carbon dioxide (Blunden and Arndt, 2013). Atmospheric N_2O has risen steadily since the mid-twentieth century, from approximately 290 ppb in 1940 to 330 ppb in 2017 (Thompson et al., 2019) and grazed grasslands contribute a significant proportion of this increase (Oenema et al., 2010). In grazed grasslands, the biggest source of N_2O is animal urine (Selbie et al., 2015). Our results suggest that N_2O pollution from animal urine patches can be potentially exacerbated through anthelmintic drug administration to grazed animals.

One reason for the greater N_2O emissions observed in albendazole-dosed sheep urine-deposited soils compared with control urine-deposited soils in our study may be due to N loading differences. We were unable to test the N concentration of urine before the treatment application as the laboratory facilities were not available at the remote field site. However, we analysed the N concentration of the urine after the field experiment and found the N concentration of albendazole-dosed sheep urine (15 g L^{-1}) was greater than control sheep urine (10 g L^{-1}). There have been no previous studies in the literature reporting N excretion differences in urine after feeding albendazole or other anthelmintics, but Zhong et al. (2016) have reported enhanced feed intake by Small-tailed Han and Ujumqin ewes after anthelmintic drug administration. Greater feed intake can result in higher urinary N (Jardstedt et al., 2017). We did not monitor feed or water intake in our study, but higher feed intake or lower water intake could also potentially increase the N concentration in urine. Future studies investigating feed and water intake differences after anthelmintic drug administration and potential consequences for N excretion in urine are clearly warranted.

The urine treatments in our experiment maintained the same urine volume per unit area within the range of standard sheep urinations (Haynes and Williams, 1993). The N concentration difference between two urine treatments resulted in a higher N load in albendazole-dosed sheep urine treatment plots. We found greater ion exchange resin adsorption of NH_4^+, indicating higher NH_4^+ in soils of albendazole-dosed sheep urine treatment plots. This difference could possibly be due to the higher N load deposited in the dosed sheep urine treatment plots. The ion exchange resin adsorption of NO_3^- increased with time in both urine treatment plots, indicating that transformation of NH_4^+ to NO_3^- by nitrification was occurring. There was greater ion exchange resin adsorption of NO_3^- in albendazole-dosed sheep urine plots. This observation indicates that soil

http://www.aloki.hu ● ISSN 1589 1623 (Print) ● ISSN1785 0037 (Online)
DOI: http://dx.doi.org/10.15666/aeer/2005_42214235

nitrification activity was greater in albendazole-dosed sheep urine plots and therefore higher NO_3^- content was available for soil denitrification. These differences in soil N transformations in albendazole-dosed sheep urine treatment plots may have contributed to greater N_2O emissions (*Fig. 3C*) as both nitrification and denitrification contribute to N_2O production. Greater N_2O emissions from albendazole-dosed sheep urine treatment may be due to higher N load deposition (de Klein et al., 2014) but the estimation of the emissions from the same amount of N application (N_2O emissions as a percentage of applied urine N; EF3) was still higher in the albendazole-dosed sheep urine treatment compared with the control urine treatment (*Fig. 5*). This may suggest that the higher emissions in dosed sheep urine treatment plots could have resulted from factors other than greater N deposition to the soil. This conclusion is in agreement with van Groenigen et al. (2005), who did not observe a significant effect of the amount of urine N on emission percentage and highlighted that the most important controlling factors in their study that affected the emission factor were urine volume and C availability rather than the amount of N.

The other possible reason that stimulatory soil nitrogen transformations, and thereby N_2O emissions, were observed from albendazole-dosed sheep urine-treated plots could potentially be due to the direct effects of urine composition changes by albendazole or its metabolites on microbes responsible for soil nitrification and denitrification. Nevertheless, to the best of our knowledge, no such studies have been reported in the literature. However, there is evidence that N_2O can be formed through a process called co-denitrification (Spott and Florian Stange, 2011) where an N–N-linkage can occur between the amino group of an amine species and an N compound of the denitrification pathway (e.g., NO_2^-), which then results in excess N_2O or N_2 gas production. Recently, several studies have shown evidence for N_2O production via co-denitrification under simulated ruminant urine patch conditions (Clough et al., 2017; Rex et al., 2019). Albendazole undergoes rapid metabolism inside the animal gastrointestinal tract and transforms into multiple metabolites. Gyurik et al. (1981) identified nine metabolites of albendazole in the urine of cattle, sheep, rats and mice that had been orally fed albendazole. Stuchlíková et al. (2020) reported that albendazole can metabolise into 21 metabolites in alfalfa plants. Several of these metabolites consist of amine ($-NH_2$) and nitroso (-N=O) groups in their chemical structure, so there is the potential for these metabolites to take part in co-denitrification and produce excess N_2O. Future studies are therefore necessary to confirm the role of albendazole metabolites in co-denitrification.

This study was carried out using single-dose administration of fast-acting albendazole to sheep and N_2O measurements at a single grassland site during one season, hence similar studies with other forms of anthelmintics, including long-lasting slow-releasing capsule feeding in wider grassland environmental settings, are required to confirm its findings.

Conclusion

This study provided evidence of the rapid metabolism of orally ingested fast-acting albendazole capsules by sheep and the deposition of a substantial amount of albendazole, albendazole sulfoxide and albendazole sulfone to grazed grasslands through urine. Furthermore, the albendazole-fed sheep urine depositions altered the N transformations occurring in soil, resulting in greater N_2O emissions. The results of this study suggest that N_2O pollution from animal urine patches can be potentially exacerbated through anthelmintic drug administration to grazed animals. Further studies in multiple anthelmintic forms in wider environmental settings are warranted.

http://www.aloki.hu ● ISSN 1589 1623 (Print) ● ISSN1785 0037 (Online)
DOI: http://dx.doi.org/10.15666/aeer/2005_42214235

Acknowledgments. This work was supported by the Project of the Second Tibetan Plateau Scientific Expedition (2019QZKK0302), Strategic Priority Research Program of Chinese Academy of Sciences (XDA2010010203), Program for Changjiang Scholars and Innovative Research Team in University (IRT17R50).

REFERENCES

[1] Belew, S., Suleman, S., Wynendaele, E., Duchateau, L., De Spiegeleer, B. (2021): Environmental risk assessment of the anthelmintic albendazole in Eastern Africa, based on a systematic review. – Environmental Pollution 269: 116106.
[2] Beynon, S. A. (2012): Potential environmental consequences of administration of anthelmintics to sheep. – Veterinary Parasitology 189(1): 113-124.
[3] Blunden, J., Arndt, D. S. (2013): State of the Climate in 2012. – Bulletin of the American Meteorological Society 94(8): S75-S78.
[4] Bowatte, S., Tillman, R., Carran, A., Gillingham, A., Scotter, D. (2008): In situ ion exchange resin membrane (IEM) technique to measure soil mineral nitrogen dynamics in grazed pastures. – Biology and Fertility of Soils 44(6): 805-813.
[5] Clough, T. J., Lanigan, G. J., De Klein, C. A., Samad, M. S., Morales, S. E., Rex, D., Bakken, L. R., Johns, C., Condron, L. M., Grant, J., Richards, K. G. (2017): Influence of soil moisture on codenitrification fluxes from a urea-affected pasture soil. – Scientific reports 7(1): 1-12.
[6] de Klein, C. A., Barton, L., Sherlock, R. R., Li, Z., Littlejohn, R. P. (2003): Estimating a nitrous oxide emission factor for animal urine from some New Zealand pastoral soils. – Soil Research 41(3): 381-399.
[7] de Klein, C. A., Luo, J., Woodward, K. B., Styles, T., Wise, B., Lindsey, S., Cox, N. (2014): The effect of nitrogen concentration in synthetic cattle urine on nitrous oxide emissions. – Agriculture, Ecosystems and Environment 188: 85-92.
[8] Fisher, A. D., Van Sittert, S. J. (2013): The efficacy of a slow-release albendazole capsule against Haemonchus contortus with known resistance to albendazole. – Journal of the South African Veterinary Association 84(1): 1-5.
[9] Giles, M. E., Morley, N. J., Baggs, E. M., Daniell, T. J. (2012): Soil nitrate reducing processes–drivers, mechanisms for spatial variation, and significance for nitrous oxide production. – Frontiers in Microbiology 3: 407.
[10] Gyurik, R. J., Chow, A. W., Zaber, B., Brunner, E. L., Miller, A. J., Villani, A. J., Petka, L. A., Parish, R. C. (1981): Metabolism of albendazole in cattle, sheep, rats and mice. – Drug Metabolism and Disposition 9(6): 503-508.
[11] Han, T., Wang, M., Zhang, G., Han, D., Li, X., Liu, G., Li, X., Wang, Z. (2017): Gastrointestinal nematodes infections and anthelmintic resistance in grazing sheep in the Eastern Inner Mongolia in China. – Acta Parasitol 62(4): 815-822.
[12] Haynes, R. J., Williams, P. H. (1993): Nutrient Cycling and Soil Fertility in the Grazed Pasture Ecosystem. – In: Donald, L.S. (ed.) Advances in Agronomy, Academic press, New Zealand
[13] Hoogendoorn, C., Betteridge, K., Costall, D., Ledgard, S. (2010): Nitrogen concentration in the urine of cattle, sheep and deer grazing a common ryegrass/cocksfoot/white clover pasture. – New Zealand Journal of Agricultural Research 53(3): 235-243.
[14] Jardstedt, M., Hessle, A., Nørgaard, P., Richardt, W., Nadeau, E. (2017): Feed intake and urinary excretion of nitrogen and purine derivatives in pregnant suckler cows fed alternative roughage-based diets. – Livestock Science 202: 82-88.
[15] Madsen, M., Nielsen, B. O., Holter, P., Pedersen, O., Jespersen, J. B., Jensen, K.-M. V., Nansen, P., Gronvold, J. (1990): Treating cattle with Ivermectin: effects on the fauna and decompsition of dung pats. – Journal of Applied Ecology 27(1): 1-15.

http://www.aloki.hu ● ISSN 1589 1623 (Print) ● ISSN1785 0037 (Online)
DOI: http://dx.doi.org/10.15666/aeer/2005_42214235

[16] McKellar, Q. (1997): Ecotoxicology and residues of anthelmintic compounds. – Veterinary Parasitology 72(3-4): 413-435.
[17] Mooney, D., Richards, K. G., Danaher, M., Grant, J., Gill, L., Mellander, P. E., Coxon, C. E. (2021): An analysis of the spatio-temporal occurrence of anthelmintic veterinary drug residues in groundwater. – Science of the total Environment 769: 144804.
[18] Oenema, J., Burgers, S., Verloop, K., Hooijboer, A., Boumans, L., Berge, H. T. (2010): Multiscale effects of management, environmental conditions, and land use on nitrate leaching in dairy farms. – Journal of Environmental Quality 39(6): 2016-2028.
[19] Oh, S. J., Park, J., Lee, M. J., Park, S. Y., Lee, J. H., Choi, K. (2006): Ecological hazard assessment of major veterinary benzimidazoles: acute and chronic toxicities to aquatic microbes and invertebrates. – Environmental Toxicology and Chemistry 25(8): 2221-2226.
[20] Oh, J.-H., Kwon, C.-H., Jeon, J.-S., Choi, D.-M. (2009): Management of veterinary drug residues in food. – Korean Journal of Environmental Agriculture 28(3): 310-325.
[21] Pope, L. J. (2009): Fate and effects of parasiticides in the pasture environment. – Ph.D. thesis, University of York, Heslington.
[22] Prchal, L., Podlipna, R., Lamka, J., Dedkova, T., Skalova, L., Vokral, I., Lecova, L., Vanek, T., Szotakova, B. (2016): Albendazole in environment: faecal concentrations in lambs and impact on lower development stages of helminths and seed germination. – Environmental Science and Pollution Research 23(13): 13015-13022.
[23] Rex, D., Clough, T. J., Richards, K. G., Condron, L. M., De Klein, C. A., Morales, S. E., Lanigan, G. J. (2019): Impact of nitrogen compounds on fungal and bacterial contributions to codenitrification in a pasture soil. – Scientific Reports 9(1): 1-10.
[24] Selbie, D. R., Buckthought, L. E., Shepherd, M. A. (2015): The Challenge of the Urine Patch for Managing Nitrogen in Grazed Pasture Systems. – In: Donald, L.S. (ed.) Advances in Agronomy, Academic press, New Zealand
[25] Spott, O., Florian Stange, C. (2011): Formation of hybrid N_2O in a suspended soil due to co-denitrification of NH_2OH. – Journal of Plant Nutrition and Soil Science 174(4): 554-567.
[26] Stuchlíková, L.R., Navrátilová, M., Langhansová, L., Moťková, K., Podlipná, R., Szotáková, B., Skálová, L. (2020): The identification of metabolites and effects of albendazole in alfalfa (*Medicago sativa*). – International Journal of Molecular Sciences 21(16): 5943.
[27] Sun, Y., Diao, X., Shen, J. (2005): Effects of avermectin B1a on soil microorganism and earthworm (*Eisenia fetida*). – The Journal of Applied Ecology 16(11): 2140-2143.
[28] Thompson, R. L., Lassaletta, L., Patra, P. K., Wilson, C., Wells, K. C., Gressent, A., Koffi, E. E., Chipperfield, M. P., Winiwarter, W., Davidson, E. A., Tian, H., Canadell, J. G. (2019): Acceleration of global N_2O emissions seen from two decades of atmospheric inversion. – Nature Climate Change 9(12): 993-998.
[29] van Groenigen, J. W., Kuikman, P. J., de Groot, W. J. M., Velthof, G. L. (2005): Nitrous oxide emission from urine-treated soil as influenced by urine composition and soil physical conditions. – Soil Biology and Biochemistry 37(3): 463-473.
[30] Wagil, M., Bialk-Bielinska, A., Puckowski, A., Wychodnik, K., Maszkowska, J., Mulkiewicz, E., Kumirska, J., Stepnowski, P., Stolte, S. (2015): Toxicity of anthelmintic drugs (fenbendazole and flubendazole) to aquatic organisms. – Environmental Science and Pollution Research 22(4): 2566-2573.
[31] Wang, B., Zhang, N., Gong, P., Li, J., Wang, X., Li, X., Wang, F., Cai, K., Zhang, X. (2021): *In vitro* assays on the susceptibility of four species of nematophagous fungi to anthelmintics and chemical fungicides/antifungal drug. – Letters in Applied Microbiology 73(2): 124-131.
[32] Wu, Z., Tucker, I. G., Razzak, M., Medlicott, N. J. (2009): Stability of ricobendazole in aqueous solutions. – Journal of Pharmaceutical & Biomedical Analysis 49(5): 1282-1286.
[33] Zhang, H., Liu, C., Zheng, Q. (2019): Development and application of anthelminthic drugs in China. – Acta Tropica 200: 105181.

http://www.aloki.hu ● ISSN 1589 1623 (Print) ● ISSN1785 0037 (Online)
DOI: http://dx.doi.org/10.15666/aeer/2005_42214235

[34] Zhong, R. Z., Cheng, L., Wang, Y. Q., Sun, X. Z., Luo, D. W., Fang, Y., Bush, R. D., Zhou, D. W. (2016): Effects of anthelmintic treatment on ewe feed intake, digestion, milk production and lamb growth. – The Journal of Agricultural Science 155(2): 326-333.

http://www.aloki.hu ● ISSN 1589 1623 (Print) ● ISSN1785 0037 (Online)
DOI: http://dx.doi.org/10.15666/aeer/2005_42214235

EFFECTS OF DIFFERENT EXOGENOUS SELENIUM ON ENZYME ACTIVITIES AND MICROORGANISMS IN ARSENIC-CONTAMINATED SOIL

HU, L.[1] – ZHANG, B. J.[2*] – WU, D. S.[3*] – LIU, Y.[4] – GAO, G. Q.[1] – WANG, X. L.[1] – HU, S. M.[1] – FAN, H. B.[1] – FANG, H. Y.[1]

[1]*Jiangxi Provincial Key Laboratory for Restoration of Degraded Ecosystems & Watershed Ecohydrology, Nanchang Institute of Technology, Nanchang 330099, China*

[2]*School of Public Health, Jiangxi Provincial Key Laboratory of Preventive Medicine, Nanchang University, Nanchang 330006, China*

[3]*School of Materials and Chemical Engineering, Pingxiang University,Pingxiang 337000，China*

[4]*Jiangxi Biotech Vocational College, Nanchang 330200, China*

**Corresponding authors*
e-mail/phone: zhangbaoj04@163.com/+86-137-6799-0214;
daishewuprof@163.com/+86-189-7009-2386

(Received 2nd Mar 2022; accepted 13th Jul 2022)

Abstract. The environmental behavior of arsenic (As) in soil is closely related to the composition of the soil microbial community and soil enzyme activity. In this paper, the effects of inorganic selenium (Se(IV), Se(VI)) and organic Se (Se-Cys, Se-Met) on enzyme activity and microbial community composition in As-contaminated soil were studied by a pot experiment under greenhouse conditions. The results showed that the application of inorganic Se and organic Se can significantly affect the activities of urease, catalase, invertase, fluorescein diacetate (FDA) hydrolase and dehydrogenase in As-contaminated soil. The total phospholipid fatty acid (PLFA) microbial content in the soil with organic Se treatments was higher than that in the control group (CK), while the inorganic Se treatments was opposite. Organic Se promoted the growth of microorganisms in the soil, while the inorganic Se treatments was opposite. From the perspective of the distribution and community structure of microorganisms, organic Se treatment enriches the microbial diversity and increases the content of gram-positive bacteria (G^+), gram-negative bacteria (G^-), and fungi, while the inorganic Se treatment group shows the opposite trend. This study can provide a reference for in-depth exploration of the mechanism of Se and microbial metabolism of As and its application in the treatment of As pollution.
Keywords: *Se, As, Soil enzyme, Microbial community structure*

Introduction

Arsenic (As) pollution in farmland soil poses a serious threat to the sustainable development of modern agriculture and the quality and safety of agricultural products, and it can spread to the human body through the food chain, thereby posing a serious threat to human health. The restoration and safe use of As-contaminated farmland soil has become a key issue that urgently needs to be solved in agricultural and environmental fields around the world (Dong et al., 2020). Soil enzymes are the general term for a class of protein compounds in the soil that can catalyze biologically exclusive organisms. They participate in various biochemical processes in the soil and are an important part of the soil ecosystem. These enzymes play a role in biocatalysis in the soil, promote the metabolism of organic matter, provide nutrients to plants, and play a pivotal role in the soil ecosystem. Soil enzyme activity roughly reflects the relative

http://www.aloki.hu ● ISSN 1589 1623 (Print) ● ISSN 1785 0037 (Online)
DOI: http://dx.doi.org/10.15666/aeer/2005_42374255

intensity of soil biochemical processes (Moscatelli et al., 2018) and can be used as one of the early warning indicators to distinguish the degradation of soil ecosystems under stressful environments (Moscatelli et al., 2018). To date, approximately 60 kinds of enzymes have been identified. Among them, urease, dehydrogenase, fluorescein diacetate (FDA) hydrolase, invertase, phosphatase, etc. are usually used as indicators of the impact of Se and As on soil quality (Bhattacharyya et al., 2008). For example, Wang et al. (2016) simulated the effects of As pollution and long-term As pollution in mining areas on soil enzyme activities and confirmed that soil enzymes were more sensitive and accurate pollution evaluation indicators. Research has shown that enzymatic activity is very effective for understanding the negative effects of heavy metals on soil. By measuring the activity of dehydrogenase and catalase, they were considered indicators of soil overall and respiration activity, and valuable information about soil fertility status can be obtained (Samuel et al., 2012). Lyubun et al. (2013) conducted studies on the effects of As on soil enzyme activities and the bioavailability of As extracted from five field crops. The results showed that plant growth increased the activity of soil dehydrogenase by 2.4 times and 2.5 times, respectively, by 3 times for ryegrass and sudangrass, and 5.2 times by spring oilseed relative to the contaminated but unplanted control soil. The activity of soil peroxidase increased by 33% with the increase in ryegrass and rape, while the activity of soil phosphatase was directly related to residual As. Mondal et al. (2015) carried out the seasonal variation characteristics of soil enzymes (amylase, invertase, cellulase, urease) in As-contaminated areas, and the study of soil enzyme activity was helpful to evaluate the impact of As on soil biochemical quality.

Microorganisms in the soil play an important role in the migration and transformation of As. The quantity, population and activity intensity of soil microorganisms change with changes in soil quality and environment. The use of the number of microorganisms and the composition of the community structure was one of the important ways to identify the quality and fertility of the soil. Soil microbial community composition and soil enzyme activity affect the bioavailability of soil As, which is a research hotspot in soil As pollution control methods. The microorganisms in the soil ecosystem are divided according to their morphological characteristics and are mainly divided into three groups: actinomycetes, fungi and bacteria (Lin et al., 2012). Studies have shown that As is the main driving factor for the reduction of soil functional gene diversity, and rhizosphere bacteria play an important role in the process of centipede grass absorption and hyperaccumulation of soil As (Xiong et al., 2010). As pollution reduces metabolic diversity, there was a strong correlation between the level of As pollution in rhizosphere soil and the distribution of functional genes. It was reported that the metabolic potential and diversity of microorganisms along the depth in As-contaminated soil were significantly reduced, and the community structure was significantly different (Xiong et al., 2012). Polymerase chain reaction (PCR) and denaturing gradient gel electrophoresis (DGGE) showed that the bacterial community composition of As-contaminated soil was different from that of control soil. Soil fungi and Proteobacteria showed tolerance to As, while the tolerance of other flora decreased (Lorenz et al., 2006). Turpeinen et al. (2004) suggested that microorganisms can respond to soil metal pollution and maintain metabolic activity by changing the community structure and resistance selection.

Selenium (Se) is one of the essential trace elements for the human body. It has important biological functions and can prevent diseases and improve health. In

http://www.aloki.hu ● ISSN 1589 1623 (Print) ● ISSN 1785 0037 (Online)
DOI: http://dx.doi.org/10.15666/aeer/2005_42374255

agriculture, applying the appropriate amount of Se fertilizer can improve soil quality and increase crop yield and stress resistance (Ramkissoon et al., 2019; Tremblay et al., 2014).

At present, there are few reports on the influence of exogenous Se, especially organic Se, on soil microorganisms. In addition to physical and chemical processes, microorganisms also play an important role in the regulation and transformation of Se and As and can metabolize Se through a variety of methods and pathways (Michael et al., 2020). It was reported that the metabolism of Se by microorganisms mainly includes the transport, reduction, oxidation, assimilation and methylation of Se (Michael et al., 2020). Microorganisms can convert inorganic Se into nano-Se (Lampis et al., 2014), reduce it to selenoprotein through assimilation, and convert it into Se methyl selenide through methylation (Lampis et al., 2014). It was reported that the metabolic mechanism of As by microorganisms was mainly divided into the following three types: As methylation, As reduction and As oxidation (Sodhi et al., 2019). Owing to Se antagonism to As (Feng et al., 2021), so exploring the metabolic mechanism of microorganisms to As is extremely important for the treatment of As pollution due to Se antagonism to As. Research on the regulation of Se on enzyme activity and microbial community composition in As-contaminated soil is lacking. The aim of this study was to carry out a comparative study on the effect of inorganic Se and organic Se on the enzyme activity and microbial community in As-contaminated soil. The findings in this study could provide novel understanding about the microbial regulation of Se on As and could provide a research basis for the treatment of As-contaminated soil.

Materials and methods

Soil cultivation test

The test soil was collected from a vegetable field in the suburbs of Nanchang City in China, A multi-point sampling method was used to collect soil samples from a depth of 0–20 cm. After the samples air dried, they were passed through a 2 mm sieve. The tested soil had the following physical and chemical properties: the pH (soil:water = 1:2.5) was 4.9; the organic matter content was 16.22 g kg^{-1}; the alkaline hydrolysable nitrogen (N) was 137.83 mg kg^{-1}; the available phosphorus (P) was 5.61 mg kg^{-1}; the available potassium (K) was 67.32 mg kg^{-1}; the As content was 11.32 mg kg^{-1}; and the Se content was 0.53 mg kg^{-1}. The soil cultivation experiment was carried out in a greenhouse according to a previously published method (Hu et al., 2020). In short, 30 mg As kg^{-1} with sodium arsenite was added to each pot in the soil to simulate As-contaminated soil. The pot was 21 cm in diameter and 18 cm in height. The exogenous inorganic Se added to the soil was sodium selenite and sodium selenate, and the exogenous organic Se added was yeast selenium (Se-Y) and malt selenium (Se-M). The detailed test treatment was as follows: (1) 30 mg As kg^{-1} (control group [CK]); (2) 30 mg As kg^{-1} + 1 mg Se kg^{-1} (1Se(IV)); (3) 30 mg As kg^{-1} + 3 mg Se kg^{-1} (3 Se(IV)); (4) 30 mg As kg^{-1} + 6 mg Se kg^{-1} (6Se(IV)); (5) 30 mg As kg^{-1} + 12 mg Se kg^{-1} (12Se(IV)); (6) 30 mg As kg^{-1} + 24 mg Se kg^{-1} (24Se(IV)); (7) 30 mg As kg^{-1} + 1 mg Se kg^{-1} (1Se(VI)); (8) 30 mg As kg^{-1} + 3 mg Se kg^{-1} (3Se(VI)); (9) 30 mg As kg^{-1} + 6 mg Se kg^{-1} (6Se(VI)); (10) 30 mg As kg^{-1} + 12 mg Se kg^{-1} (12Se(VI)); (11) 30 mg As kg^{-1} + 24 mg Se kg^{-1} (24Se(VI)); (12) 30 mg As kg^{-1} + 1 mg Se kg^{-1} (1Se-Y); (13) 30 mg As kg^{-1} + 3 mg Se kg^{-1} (3Se-Y); (14) 30 mg As kg^{-1} + 6 mg Se kg^{-1} (6Se-Y); (15) 30 mg As kg^{-1} + 12 mg Se kg^{-1} (12Se-Y); (16) 30 mg As kg^{-1} + 24 mg Se kg^{-1} (24Se-Y); (17)

http://www.aloki.hu ● ISSN 1589 1623 (Print) ● ISSN 1785 0037 (Online)
DOI: http://dx.doi.org/10.15666/aeer/2005_42374255

30 mg As kg^{-1} + 1 mg Se kg^{-1} (1Se-M); (18) 30 mg As kg^{-1} + 3 mg Se kg^{-1} (3Se-M); (19) 30 mg As kg^{-1} + 6 mg Se kg^{-1} (6Se-M); (20) 30 mg As kg^{-1} + 12 mg Se kg^{-1} (12Se-M) and (21) 30 mg As kg^{-1} + 24 mg Se kg^{-1} (24Se-M). Each treatment was replicated three times and the treatments were arranged in random blocks. The indoor temperature was set to 23 °C during the day and 18 °C at night. The soil moisture content was maintained at 60–80% of the maximum value. After 50 days of equilibration, 100 g of topsoil in the pot was taken for experimental determination. Among them, 50 g of fresh soil was used for soil enzyme analysis, and the other 50 g of soil was freeze-dried for determination of soil PLFA. sodium selenite, sodium selenate, sodium arsenite were analytically pure from Sinopharm Reagent Company (China). Se-Y (containing 2,000 mg kg^{-1} Se) and Se-M (containing 1,600 mg Se kg^{-1}), which have been analyzed and verified, were purchased from Nanchang Industrial Biotechnology Co., LTD in Nanchang, China.

Determination of soil enzymes

The activities of urease, catalase, sucrase, FDA hydrolase and dehydrogenase were measured according to the procedures presented in Zhang et al. (2015b). The soil urease activity was determined by the phenol active sodium-sodium hypochlorite colorimetric method, while sucrase activity was determined by the 3,5-dinitrosalicylic acid colorimetric method. The urease and sucrase activities were expressed as mg g^{-1} d^{-1} and mg glucose g^{-1} d^{-1}, respectively. Catalase (ml g^{-1} h^{-1}) activity was determined by potassium permanganate titration, while FDA hydrolase (μg g^{-1} h^{-1}) activity was determined by fluorescein colorimetry. The dehydrogenase (μg g^{-1} h^{-1}) activity was measured by the TTC colorimetric method.

Determination of phospholipid fatty acids

The determination and calculation of phospholipid fatty acid (PLFA) in soil were completely determined by the method described by Shen et al. (2019). In brief, after phospholipid extraction, SPE extraction, fatty acid separation, methylation and cleaning, the samples were identified by gas chromatography (7890A, Agilent Technologies, USA) fitted with a MIDI Sherlocks Microbial Identification System (Version 4.5, MIDI, USA). The different PLFA microbial components are shown below. The sum of 16:0 10-methyl, 17:0 10-methyl and 18:0 10-methyl represented the actinomycetes, and the sum of 18:2 w6c, 16:1 w5c, 18:3 w6c and 20:4 w6c was identified as the fungus. The sum of 14:0 iso, 15:0 iso, 15:0 anteiso, 16:0 iso, 17:0 iso and 17:0 anteiso were identified as gram-positive bacteria, and the sum of 16:1 w7c, 17:0 cyclo w7c, 18:1 w7c and 19:0 cyclo w7c represented gram-negative bacteria.

Statistical analysis

All data are expressed as the mean and standard deviation (SD) with three repetitions, and diagrams were made using Origin 9.1 (OriginLab, USA). Statistical analysis and correlation analysis were carried out using SPSS 19.0 (IBM, USA). Two-sided p values < 0.05 were considered statistically significant. A normal distribution test and a homogeneity of variance test were performed prior to one-way analysis of variance (ANOVA), which was used to assess the variability of the data sets and validity of the results. The Shapiro–Wilks method was used for the normal distribution test.

http://www.aloki.hu ● ISSN 1589 1623 (Print) ● ISSN 1785 0037 (Online)
DOI: http://dx.doi.org/10.15666/aeer/2005_42374255

Results and discussion

Activity characteristics of soil enzymes

Urease is an amidase that promotes the hydrolysis of enzymatic bonds in organic molecules (Javadi et al., 2018) and is closely related to the action of organic matter and microorganisms in the soil. The activity of urease in the soil is shown in *Figure 1A*. Compared with the CK, the soil enzyme activity of the Se(IV) and Se(VI) treatment groups both showed a slight increase and then a decrease. The application of the two kinds of organic Se significantly activated urease activity, the overall trend was increasing, and the urease activity of each Se application level was higher than that of the corresponding CK and inorganic Se treatment groups. At the levels of 3Se, 6Se and 12Se, the urease activity of the Se-M group was higher than that of the Se-Y group, while at the 24Se level, the urease activity of the Se-Y group was higher than that of the Se-M group, reaching the highest value among all treatment groups. Catalase can promote the decomposition of excessive hydrogen peroxide in organisms, thereby preventing damage and poisoning. Its activity is related to the content of soil organic matter and the number of microorganisms (Xiong et al., 2013).

In this study, the inorganic Se treatment group showed a significant inhibitory effect on catalase, and each Se level group was lower than the CK ($P < 0.05$) (*Figure 1B*). The catalase activity of the Se-Y and Se-M treatment groups at the 24Se level was higher than that of the CK group, and other Se levels were lower than that of the CK group ($P < 0.05$). With the increase in the Se level, the catalase activity of the inorganic Se group and the organic Se group showed a trend of first decreasing and then increasing. Sucrase is called invertase because its enzymatic substrate is sucrose, which can characterize soil fertility and microbial activity (Zhang et al., 2015a). The sucrase activity of each treatment group was not the same (*Figure 1C*). Both the Se(IV) and Se(VI) treatment groups showed a tendency to increase first and then decrease, while the Se-Y and Se-M treatment groups both showed a gradually increasing trend. This may be due to the complex biochemical interaction with As and other substances in the soil under the cumulative effect of this Se level, causing the sudden activation of enzyme activity. It has been reported that the complex biochemical interaction from was caused by complexing agents, which can act as carriers for trace elements in soil solution (Violante et al., 2010). So, the toxicity of metals can be reduced by complexation. The interaction between as and se is a key factor to understand their transport, environmental fate and related toxicological effects in soil plant systems (Ali et al., 2021). As and Se induce cytotoxicity and genotoxicity through the generation of reactive oxygen species (ROS). In this study, the four Se sources have different chemical compositions and have their own chemical properties, they produce different results.

Soil FDA hydrolase can be hydrolyzed by soil microorganisms, such as fungi, bacteria, algae, etc., resulting in changes in enzyme activity (Tao et al., 2021). As shown in *Figure 1D,* the FDA hydrolase activity of the Se(IV) and Se(VI) (except for the 24Se level) treatment groups was lower than that of the CK. The enzyme activities of the Se-Y and Se-M groups at high Se levels (6Se, 12Se and 24Se) were significantly higher than those of the CK group ($P < 0.05$) and showed a trend of gradual increase. It was reported in the literature that As-contaminated soil can reduce the activity of FDA hydrolase (Ghosh et al., 2004). In this study, after applying exogenous Se to As-contaminated soil, it interacted with As and aroused changes in soil microorganisms, increasing the activity of FDA hydrolase.

http://www.aloki.hu ● ISSN 1589 1623 (Print) ● ISSN 1785 0037 (Online)
DOI: http://dx.doi.org/10.15666/aeer/2005_42374255

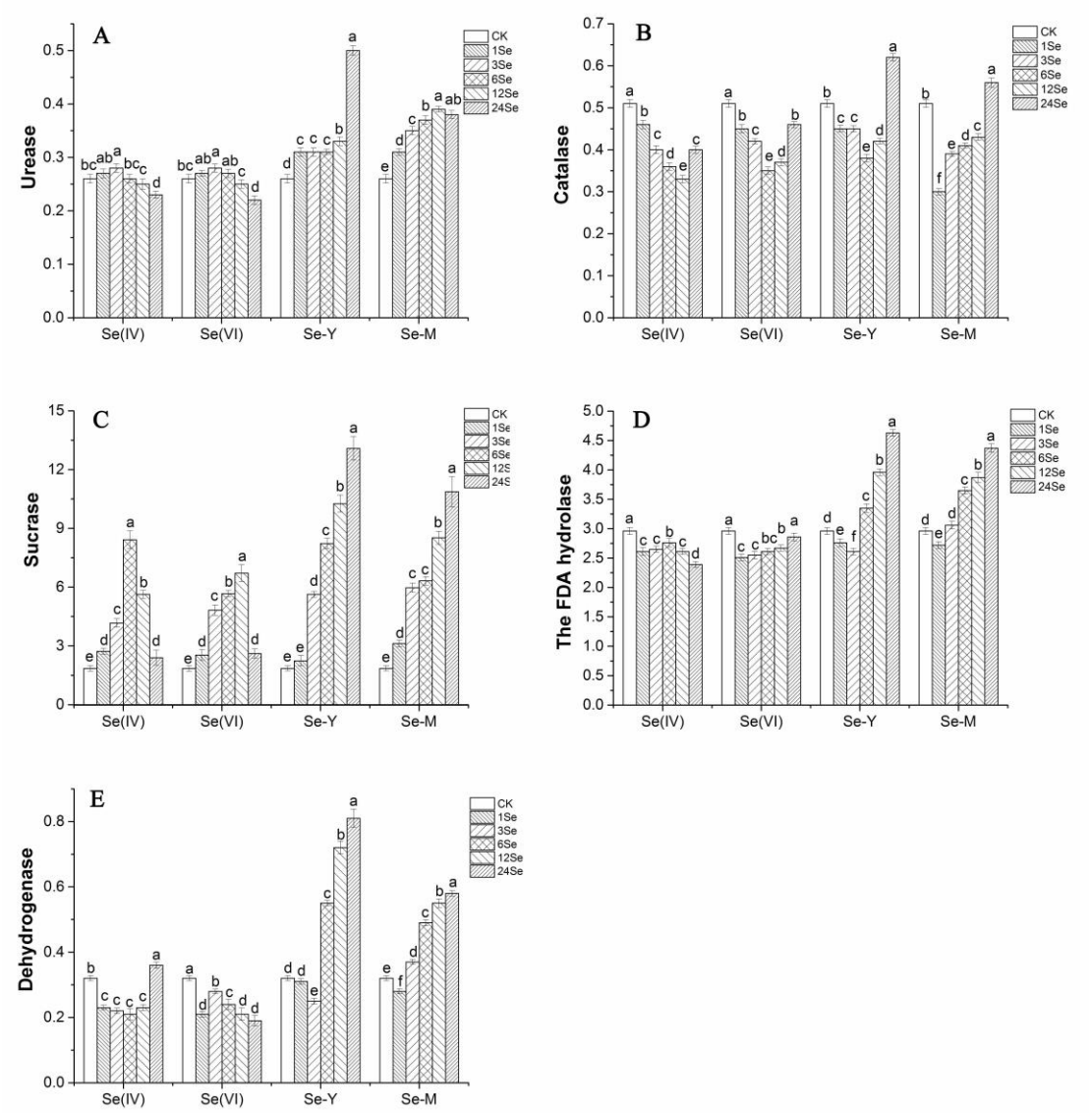

Figure 1. *Enzyme activity in soil after adding different Se. (A) urease (mg g^{-1} d^{-1}). (B) catalase (ml g^{-1} h^{-1}), (C) sucrase (mg g^{-1} d^{-1}). (D) the FDA hydrolase (μg g^{-1} h^{-1}). (E) dehydrogenase (μg g^{-1} h^{-1}). All data are expressed as mean ± SD (n = 3); the letters in each column indicate the significant differences at a level of 0.05*

Dehydrogenase is an enzyme that can promote the oxidation–reduction reaction of organic substances. It belongs to the oxidoreductase system and can reflect the metabolism of soil microorganisms. As shown in *Figure 1E,* the 24Se level of soil dehydrogenase after applying Se(IV) was significantly higher than that of the CK ($P < 0.05$), and other Se levels were significantly lower than the CK ($P < 0.05$). After applying Se(VI), the dehydrogenase activity of each treatment level was significantly lower than that of the CK ($P < 0.05$). When the 3Se level reached a maximum value, it showed a trend of increasing first and then decreasing. The dehydrogenase activity of the Se-Y group showed a trend of first decreasing and then increasing, while the Se-M group showed a gradually increasing trend. The two organic Se treatment groups had significantly higher high Se levels than the CK group ($P < 0.05$).

http://www.aloki.hu ● ISSN 1589 1623 (Print) ● ISSN 1785 0037 (Online)
DOI: http://dx.doi.org/10.15666/aeer/2005_42374255

Studies have shown that the dehydrogenase activity of soil polluted by As-containing tailings was related to total As and total water-soluble As (As(III) + As(V)), which could be used to evaluate the effect of tailings dispersion on the influence of soil microbial oxidation ability (Fernández et al., 2005). The results of this study showed that, compared with the CK, the effects of organic or inorganic Se treatment on dehydrogenase were the opposite. Inorganic Se treatments had a certain inhibitory effect on soil dehydrogenase, while organic Se treatment had a certain stimulating effect on soil dehydrogenase. This may be due to the different properties of inorganic Se and organic Se, which has been reported that the bioavailability of Se in soil was determined by the form of Se and soil organic components (Li, et al., 2017). So Se has different effects on As and microbes in soil, leading to different enzyme responses. Under the action of organic Se, soil microorganisms may enhance their metabolic activities, resulting in an increase in soil microbial biomass and enhancing the repair of biofilms. This in turn causes changes in enzyme activity. The activity of various soil enzymes is an important manifestation of the biological properties of soil. There have been many studies on the effect of exogenous Se addition on the activity of soil enzymes. For example, Wu et al. (2010) and Fan et al. (2015) studied the effects of exogenous inorganic Se on soil enzyme activities. Shi et al. (2018) studied the dynamic response of soil enzymes to exogenous organic Se and inorganic Se. The effect of Se on soil enzyme activity varies according to the type of enzyme. For example, Yang et al. (2010) found that soil catalase and urease were more sensitive to Se, while amylase was not sensitive to Se. Similarly, Yang et al. (2017) studied the effects of Se on the soil urease, invertase and acid phosphatase activities of different varieties of tea plants. However, when soil Se was contaminated, it had a certain inhibitory effect on the activities of soil catalase and urease. Since urease was most inhibited by Se and there was a significant correlation between its inhibition rate and soil Se content, the urease inhibition rate can often be used as a biological indicator of Se ecological risk assessment (Lin et al., 2005). Studies have shown that low concentrations of Se have varying degrees of activation effects on the activities of soil catalase, dehydrogenase, urease and alkaline phosphatase, while high concentrations of Se have a certain inhibitory effect on the activities of four soil enzymes (Wu et al., 2010). Inorganic Se of different valences has different responses to soil enzyme activities. Wu et al. (2010) found that there was a significant negative correlation between the concentration of exogenous Se(VI) and Se(IV) and soil urease activity ($P < 0.01$). Through correlation analysis and stepwise regression analysis, it was found that Se(VI) and Se(IV) have inhibitory effects on soil invertase activity and urease activity, and the two valences of Se applied to the soil were mainly manifested in water-soluble Se on soil enzyme activity. In addition, compared with inorganic Se, organic Se was more conducive to the growth of soil microorganisms, improved soil enzyme activity and promoted the circulation of N, P and C nutrients in the soil ecosystem (Shi et al., 2018). This was consistent with our study results. In our study, compared with Se(IV) and Se(VI), both Se-Y and Se-M increased the activities of urease and dehydrogenase to varying degrees. The role of Se in plant antioxidant stress showed that Se induces a mechanism to protect photosynthesis from damage by slightly changing the sensitivity of photosynthetic cell membranes. Generally, the antioxidant effect of Se is related to an increase in glutathione peroxidase (GSH-Px) activity (Pilarczyk et al., 2001), thereby increasing the scavenging ability of hydrogen peroxide and improving the ability of plants to resist stress. In addition, reports

http://www.aloki.hu ● ISSN 1589 1623 (Print) ● ISSN 1785 0037 (Online)
DOI: http://dx.doi.org/10.15666/aeer/2005_42374255

indicated that added exogenous Se can promote the maintenance of antioxidant capacity by inducing more glutathione and nonprotein thiols (Srivastava et al., 2009). As an inducer, low concentrations of Se can upregulate defense and stress resistance genes and downregulate related growth genes. Exogenous pollutants in the soil, such as heavy metals, As and Se, may have different mechanisms for soil enzymes: binding with enzyme-substrate complexes; binding with enzyme active centres; and chemical reactions with substrates (Karaca et al., 2010).

Community structure characteristics of soil microorganisms

Phospholipid fatty acid (PLFA) composition monomer type statistics

As shown in *Table 1,* a total of 33 PLFA monomers were detected in the control soil. After the addition of Se(IV), the number of PLFA monomers detected in the soil at each Se application level was lower than that of the CK, showing a decreasing trend. Twenty-eight and 27 types of PLFAs were detected in the soil with 12Se and 24Se levels, respectively, which indicates that the addition of sulphite can inhibit the types of microorganisms in the soil. After the application of Se(VI), the number of monomers detected in the low-Se level soil was lower than that of the CK. In the 24Se high Se level group, 50 PLFA monomers were detected, which increased sharply. It can be seen from the data that the number of microorganisms has an increasing trend.

After the application of Se-Y, the number of monomers in the Se treatments was higher than that in the CK. Compared with the Se(VI) group, except for the 24Se level, the number of monomers at the other Se levels was higher than that in the Se(VI) group. After adding Se-M, the number of PLFA monomers detected in the soil was significantly higher than that of the CK. Under the 6Se level, a total of 51 monomers were detected, reaching the highest level of all treatments. From the above analysis, it is evident that the application of organic Se is more beneficial to increase the types of PLFAs in the soil than the application of inorganic Se. Se-M was significantly richer than the PLFA species in the Se-Y and inorganic Se groups.

Total PLFA was the sum of the individual numbers of various microorganisms (n = 3). By analyzing the PLFAs that have been detected in the soil, we found that gram-positive bacteria (G^+) and gram-negative bacteria (G^-) were the most distributed PLFAs in the soil. The sum of the two accounts for more than 63% of the total phospholipid fat, and the species were more abundant than other types. One species of arbuscular mycorrhizal fungus (16:1 w5c) and another species (18:2 w6c) were detected in all soils. Arbuscular mycorrhizal fungi can form a mutually beneficial symbiosis with plants, help plants resist adverse stress and have important ecological research significance. This probably suggested that when Se and As were added to the soil, they affected the composition and structure of microorganisms in the soil. The addition of different forms of Se to As-contaminated soil resulted in different numbers and communities of microorganisms in the soil.

Total PLFA content and microbial community distribution characteristics

PLFAs have the exclusive specificity of microorganisms and can be used as characteristic fatty acids of microorganisms. Therefore, PLFAs can be used to characterize soil microbial biomass and its diversity. The soil microorganisms identified in the soil in this study were divided into G^+, G^-, actinomycetes, fungi and anaerobic microorganisms. Among them, G^+, G^-, actinomycetes and fungi were detected in

http://www.aloki.hu ● ISSN 1589 1623 (Print) ● ISSN 1785 0037 (Online)
DOI: http://dx.doi.org/10.15666/aeer/2005_42374255

different Se-treated soils and control soils. According to reference reports (Shen et al., 2019; Liu et al., 2016) experimental results in this article, the following PLFAs were selected as specific microbial markers. Among them, there were three kinds of actinomycetes, six kinds of G^+, four kinds of G^-, four kinds of fungi and a total of 17 kinds of PLFA monomers.

Table 1. *The number of PLFA species detected in the soil after adding different exogenous Se*

Treatment	Se levels	Actinomycetes	G^+	G^-	Fungus	Anaerophyte	Total PLFA
CK	0Se	5	11	10	7	0	33
Se(IV)	1Se	5	10	8	4	0	27
	3Se	5	12	9	6	0	32
	6Se	5	10	8	4	0	27
	12Se	5	11	8	4	0	28
	24Se	5	10	8	4	0	27
Se(VI)	1Se	5	10	9	4	0	28
	3Se	5	9	8	4	0	26
	6Se	5	10	10	5	0	30
	12Se	4	12	9	4	0	29
	24Se	7	17	16	7	3	50
Se-Y	1Se	5	12	9	6	0	32
	3Se	5	12	11	7	0	35
	6Se	6	11	10	4	2	33
	12Se	5	12	11	9	0	37
	24Se	6	14	10	10	1	41
Se-M	1Se	6	14	11	8	2	41
	3Se	5	12	14	6	1	38
	6Se	5	15	20	10	1	51
	12Se	5	15	12	9	3	44
	24Se	6	15	17	8	2	48

As shown in *Figure 2,* the total PLFA content in the control soil was 28.82 nmol g^{-1}. In the Se(IV) treatments, the total PLFA content in the soil was lower than that in the CK. In the 6Se, 12Se and 24Se treatments, the PLFA contents were 19.88, 16.17 and 13.09 nmol g^{-1}, respectively, showing a significant decrease. The PLFA content of the Se treatment group showed a gradual increase in Se(VI) treatments, but they were all lower than the CK. When the Se concentration was 24 mg kg^{-1}, the PLFA microbial content rose to 25.77 nmol g^{-1}. The PLFA content in the soil showed a gradually increasing trend in the Se-Y treatments. It was lower than the CK in the 1Se, 3Se and 6Se treatments, and higher than the CK in the 12Se and 24Se treatments. The PLFA contents were 39.31 and 48.32 nmol g^{-1}, respectively. The PLFA content showed a gradual increase in the Se-M treatment. The PLFA contents in the 1Se and 3Se treatments were 19.18 and 26.84 nmol g^{-1}, respectively, which were lower than that in the CK. The levels of PLFAs at the 6Se, 12Se and 24Se levels were higher than those of the CK, and their contents were 29.46, 34.44 and 40.19 nmol g^{-1}, respectively. It can be

http://www.aloki.hu ● ISSN 1589 1623 (Print) ● ISSN 1785 0037 (Online)
DOI: http://dx.doi.org/10.15666/aeer/2005_42374255

seen from the above results that the addition of inorganic Se sources reduces the total PLFA microbial content in the soil, and the addition of organic Se sources increases the total PLFA microbial content in the soil.

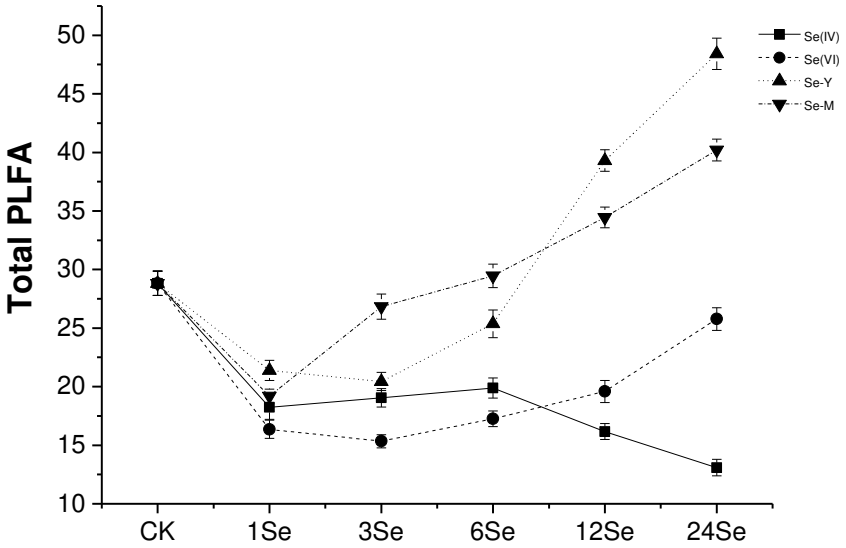

Figure 2. *Total PLFAs content in soil after adding different Se sources (nmol g^{-1}). All data are expressed as mean ± SD, n = 3); variance bars represent significant differences ($p < 0.05$)*

As shown in *Figure 3,* the G^+ content of the soil in the CK was 5.95 nmol g^{-1}. In the Se(IV) and Se(VI) treatments, the G^+ content in the soil was lower than that of the CK. The addition of inorganic Se sources reduces the G^+ content in the soil. With the increase in the concentration of Se(IV), the G^+ content of each Se treatment showed a decreasing trend, while the Se(VI) group showed an increasing trend. In the Se-Y and Se-M treatments, the G^+ content in the soil showed an increasing trend as the Se level increased. In the low-Se group, the G^+ content was lower than that in the CK group, and in the high-Se group, the G^+ content was higher than that in the control. In the 24Se treatment, the soil G^+ after adding Se-Y and Se-M was 8.56 and 7.80 nmol g^{-1}, respectively. This shows that the application of organic Se increases the number and communities of microorganisms that produce resistance to As stress in the soil, and the ecosystem is readjusted to adapt to the environment and gain stress resistance. The G^- content of the soil in the CK was 6.76 nmol g^{-1}. After the addition of inorganic Se, its value was lower than that of the CK, and its size and G^+ content were consistent. In the Se(IV) treatment group, the Se level gradually decreased with the addition of Se, while in the Se(VI) group, the opposite was true. In the low Se group (1Se, 3Se, 6Se), the Se(IV) group was higher than the Se(VI) group, and in the high Se group (12Se, 24Se), the opposite was true.

The soil G^- content in the organic Se group showed inconsistent results with that in the inorganic Se group. In the Se-Y and Se-M groups, the soil G^- level was lower than the CK at low Se application and higher than the CK at high Se application, and both showed an increasing trend with the increase of Se level. Under the Se levels of 1Se, 3Se, 6Se, 12Se and 24Se, the soil G contents of the Se-Y group and the Se-M group were 3.48, 4.18, 5.58, 10.84 and 12.62 nmol g^{-1} and 3.49, 5.93 and 6.99, respectively, and 8.51 and 8.95

http://www.aloki.hu ● ISSN 1589 1623 (Print) ● ISSN 1785 0037 (Online)
DOI: http://dx.doi.org/10.15666/aeer/2005_42374255

nmol g^{-1}. It can be seen from the above that the G^- content in Se-Y at the low Se level is lower than that in Se-M, while at the high Se level, the opposite was true.

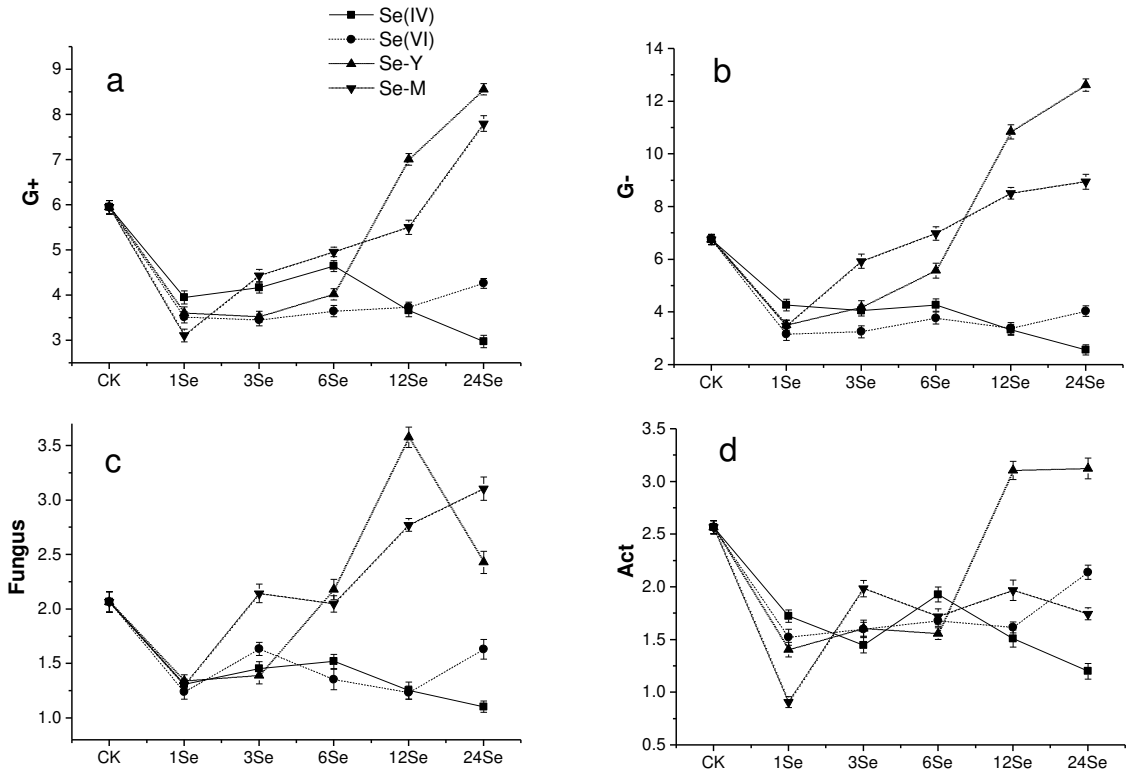

Figure 3. *The contents of different microbial communities in soil after adding different Se sources (nmol g^{-1}). All data are expressed as mean ± SD, n = 3); variance bars represent significant differences ($p < 0.05$)*

The fungal content in the soil of the CK was 2.07 nmol g^{-1}. The content of fungi in the soil in the inorganic Se group was lower than that in the CK group. In the organic Se group, the content of fungi with high Se levels was higher than that in the CK. As the organic Se level increased, the microbial content in the soil increased.

The content of actinomycetes in the soil of the CK was 2.57 nmol g^{-1}. After applying inorganic Se and Se-M, the content of soil actinomycetes at each Se level was lower than that of the CK. The addition of Se reduces the content of actinomycetes in the soil, and the response of actinomycetes to Se is more obvious. After applying Se-Y, the level of Se applied at 1, 3, 6Se was significantly lower than that of the CK, and the level of Se applied at 12 and 24Se was significantly higher than that of the CK. The contents of actinomycetes were 3.11 and 3.12 nmol g^{-1}, respectively.

The G^+/G^- value of the soil in the CK was 0.880, and the G^+/G^- value of the inorganic Se treatment group was higher than that of the CK. As shown in *Figure 4,* the F/B value in the CK was 0.163. The average F/B values of the Se(IV), Se(VI), Se-Y and Se-M treatment groups were 0.177, 0.197, 0.183 and 0.192, respectively, which were higher than those of the CK.

http://www.aloki.hu ● ISSN 1589 1623 (Print) ● ISSN 1785 0037 (Online)
DOI: http://dx.doi.org/10.15666/aeer/2005_42374255

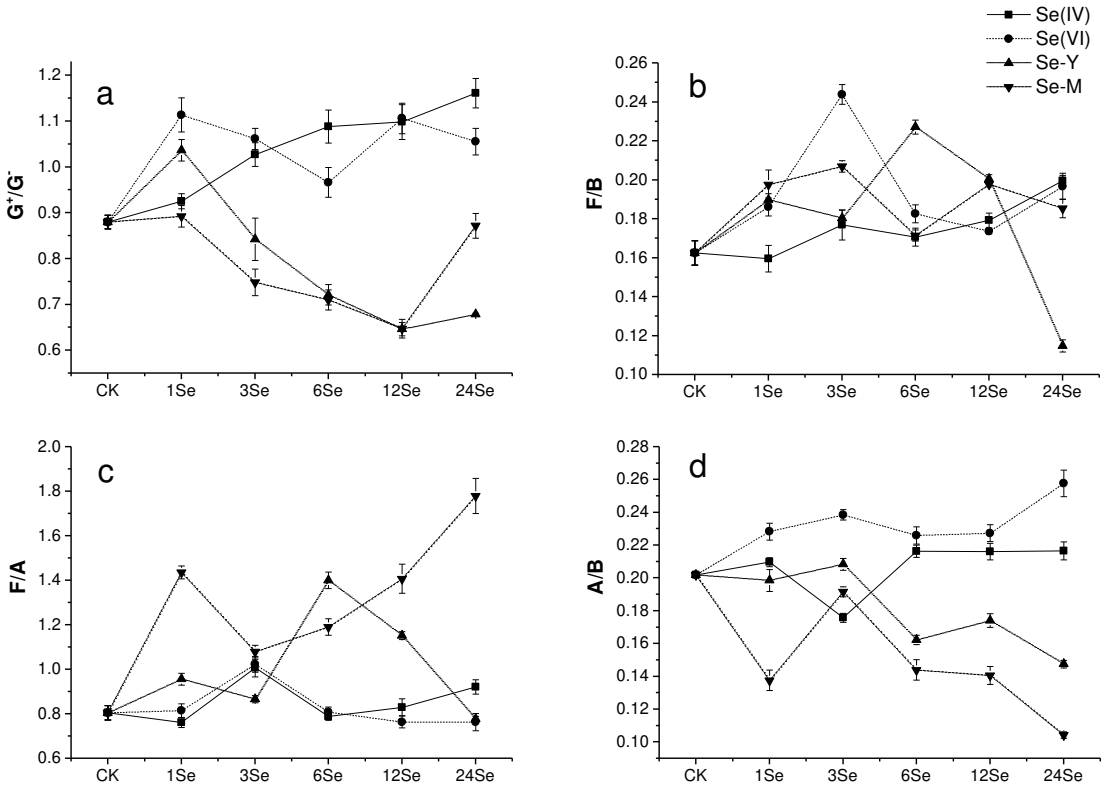

Figure 4. *The ratio of F/B, G^+/G^-, A/B, F/A in soil after adding different Se sources. All data are expressed as mean ± SD, n = 3); variance bars represent significant differences ($p < 0.05$)*

The addition of exogenous Se will increase the F/B value in the soil. With increasing Se application level, the F/B value of the Se(IV) treatment showed a gradually increasing trend, and the F/B value of the other three Se treatments showed a trend of first increasing and then decreasing. The F/A value in the CK was 0.805, and the average F/A values of the Se(IV), Se(VI), Se-Y and Se-M treatment groups were 0.861, 0.834, 1.030 and 1.379, respectively, all of which were higher than that of CK. This indicates that the application of exogenous Se can increase the F/A value of the soil.

The A/B value in the CK was 0.202, and the average A/B values of the Se(IV), Se(VI), Se-Y and Se-M treatment groups were 0.207, 0.236, 0.178 and 0.144, respectively. The A/B value of the inorganic Se group was greater than that of the CK, while the A/B value of the organic Se group was smaller than that of the CK.

Soil microorganisms are involved in various biochemical processes in the soil and have a positive effect on the conversion of soil organic matter and nutrients and the formation of soil fertility. The quantity distribution and structural characteristics of soil microorganisms are not only related to the ecological conditions of the soil but also affected by exogenous soil pollutants. This may be due to heavy metal pollutants or exogenous substances (such as As and Se) entering the soil and plants; they will participate in related biochemical actions with microorganisms, causing changes in soil enzyme activity (Wang et al., 2020), changing soil microbial biomass and communities (Turpeinen et al., 2014) and stimulating changes in antioxidant enzymes in the plant, thereby changing the environmental quality of the soil and the growth and yield of crops.

http://www.aloki.hu ● ISSN 1589 1623 (Print) ● ISSN 1785 0037 (Online)
DOI: http://dx.doi.org/10.15666/aeer/2005_42374255

Other studies have shown that as the level of Se application increases (1-30 mg kg^{-1}), the number of bacteria and fungi and actinomycetes in the soil shows a trend of first increasing and then decreasing (Fan et al., 2015). However, under different Se treatment conditions, the levels of the maximum number of various microorganisms are not the same (Fan et al., 2015). Research has suggested that the application of an appropriate concentration (5-10 mg kg^{-1}) of inorganic Se fertilizer can promote an increase in soil bacteria and fungi and actinomycetes. High concentrations (30 mg kg^{-1} or higher) of Se reduce the number of bacteria and fungi and actinomycetes in the soil (Fan et al., 2015). It was reported that microorganisms can change the form of As in the soil and that bacteria in the soil can promote the conversion of As(V) to As(III) (Jomova et al., 2011). Inorganic As may be methylated into less toxic organic forms of As, such as monomethylarsonic acid (MMA) and dimethylarsinic acid (DMA) (Jomova et al., 2011). Zhang et al. (2018) used *Trichoderma aculeatus* (SM-12F1) and ferrihydrite to repair As-contaminated soil. The results showed that compared with the CK, the total PLFA, G^+, G^-, actinomycetes, bacteria and fungi PLFAs in the repaired soil increased by 114%, 68%, 276%, 292%, 133% and 626%, respectively. Sun et al. (2015) studied the distribution characteristics of microbial diversity in As-contaminated soil in a realgar mining area, and the results showed that the content of each fungus was in the order of bacteria > fungi > actinomycetes. Among them, bacteria accounted for 71.54%-80.66% of the total microorganisms. In our study, the changes in the number of microorganisms under different Se treatments were different. Organic Se can increase G^+ and G^- in the soil, while inorganic Se can reduce G^+ and G^- in the soil.

Correlation analysis

There was a significant positive correlation between soil enzyme activity and most microorganisms, which indicates that the two have good consistency in response to exogenous Se (*Tables 2, 3, 4* and *5*). In the inorganic Se and organic Se treatment groups, FDA hydrolase was also significantly positively correlated with G^- and G^+, which was consistent with the results of other studies (Ma et al., 2010). The above results show that the application of Se to As-contaminated soil significantly affects the activity of soil enzymes and the changes in the structure of the microbial community. It was reported in the literature (Pal et al., 2009) that urease activity was significantly related to the level of As pollution in the soil, and the number of microorganisms and soil enzymes can reflect the characteristic level of soil As pollution.

Through the biochemical action of microorganisms on Se-containing soil, the absorption of Se by plants can be strengthened, which is conducive to the production of Se-rich food (Paulraj and Kumar, 2016). Fan et al. (2015) studied the relationship between the application amount of exogenous Se in different valences and the soil enzyme activity and the number of microorganisms in tobacco-growing soil and found that the amount of Se(VI) and the soil invertase activity, urease activity, catalase activity and fungi. They found that there was a negative correlation between the number and the number of actinomycetes and a positive correlation with the soil neutral phosphatase activity and the number of bacteria. The amount of Se(IV) was negatively correlated with soil invertase activity, urease activity, neutral phosphatase activity and the number of bacteria and fungi and positively correlated with soil catalase activity and the number of actinomycetes. The regression analysis between soil enzyme activity and the number of soil microorganisms also showed that the number of soil microorganisms

http://www.aloki.hu ● ISSN 1589 1623 (Print) ● ISSN 1785 0037 (Online)
DOI: http://dx.doi.org/10.15666/aeer/2005_42374255

was negatively correlated with soil neutral phosphatase activity, urease activity and catalase activity but had no significant effect on soil invertase activity (Fan et al., 2015).

Table 2. *Correlation among soil As, soil enzymes and microorganisms after selenite addition (n = 15)*

	Urease	Sucrase	Catalase	Dehydrogenase	The FDA hydrolase	Actinomyces	G^+	G^-	Fungus
Urease	1								
Sucrase	.173	1							
Catalase	.341	-.662**	1						
Dehydrogenase	-.703**	-.570*	.168	1					
The FDA hydrolase	.744**	.761**	-.163	-.804**	1				
Actinomyces	.504*	.678**	-.014	-.731**	.830**	1			
G^+	.720**	.713**	-.085	-.849**	.911**	.847**	1		
G^-	.858**	.414	.254	-.829**	.831**	.824**	.915**	1	
Fungus	.754**	.670**	-.069	-.760**	.886**	.710**	.951**	.862**	1

**Significant correlation at the 0.01 level. *Significant correlation at the 0.05 level

Table 3. *Correlation among soil As, soil enzymes and microorganisms after selenate addition (n = 15)*

	Urease	Sucrase	Catalase	Dehydrogenase	The FDA hydrolase	Actinomyces	G^+	G^-	Fungus
Urease	1								
Sucrase	.304	1							
Catalase	-.296	-.884**	1						
Dehydrogenase	.804**	.383	-.248	1					
The FDA hydrolase	-.763**	-.105	.224	-.417	1				
Actinomyces	-.769**	-.358	.390	-.398	.934**	1			
G^+	-.834**	-.270	.325	-.563*	.919**	.914**	1		
G^-	-.548*	-.092	.025	-.291	.733**	.780**	.831**	1	
Fungus	-.220	-.295	.427	.282	.370	.561*	.418	.489*	1

**Significant correlation at the 0.01 level. *Significant correlation at the 0.05 level

In this study, there was a significant positive correlation between soil microorganisms and urease activity in the Se(IV) treatments (*Table 2*). In the Se(VI) treatments, soil microorganisms were also negatively correlated with urease activity and positively correlated with catalase (*Table 3*). After adding two kinds of organic Se, there was a significant positive correlation between soil microorganisms and most enzymes. Many studies have analyzed and summarized the effects of heavy metals on the community structure of soil microorganisms, the physiological and biochemical effects of soil microorganisms, different levels of heavy metal pollution, heavy metal compound pollution and the combined effects of soil physical and chemical properties and heavy metals on soil enzyme activities (Subrahmanyam et al., 2016; Xian et al., 2015). However, there are few studies on the relationship between soil enzyme activity and microorganisms at present, and the mechanism or mechanisms of its action are not very clear. The addition amount of the four kinds of exogenous Se showed a good curve fitting relationship with the soil PLFA microbial biomass (*Figure 5*), and the correlation coefficient was above 0.95. As the amount of Se in the Se(IV) treatment group

http://www.aloki.hu ● ISSN 1589 1623 (Print) ● ISSN 1785 0037 (Online)
DOI: http://dx.doi.org/10.15666/aeer/2005_42374255

increased, the microbial biomass in the soil showed a trend of first increasing and then decreasing, while the other three Se sources all showed a gradual increase in microbial biomass with the increase in the Se application rate. This shows that compared with other types of exogenous Se, inorganic selenite has a significant inhibitory effect on soil microorganisms. This may be due to the inconsistent chemical and biological functions of different types of exogenous Se, resulting in different effects on soil microorganisms (Guo et al., 2021).

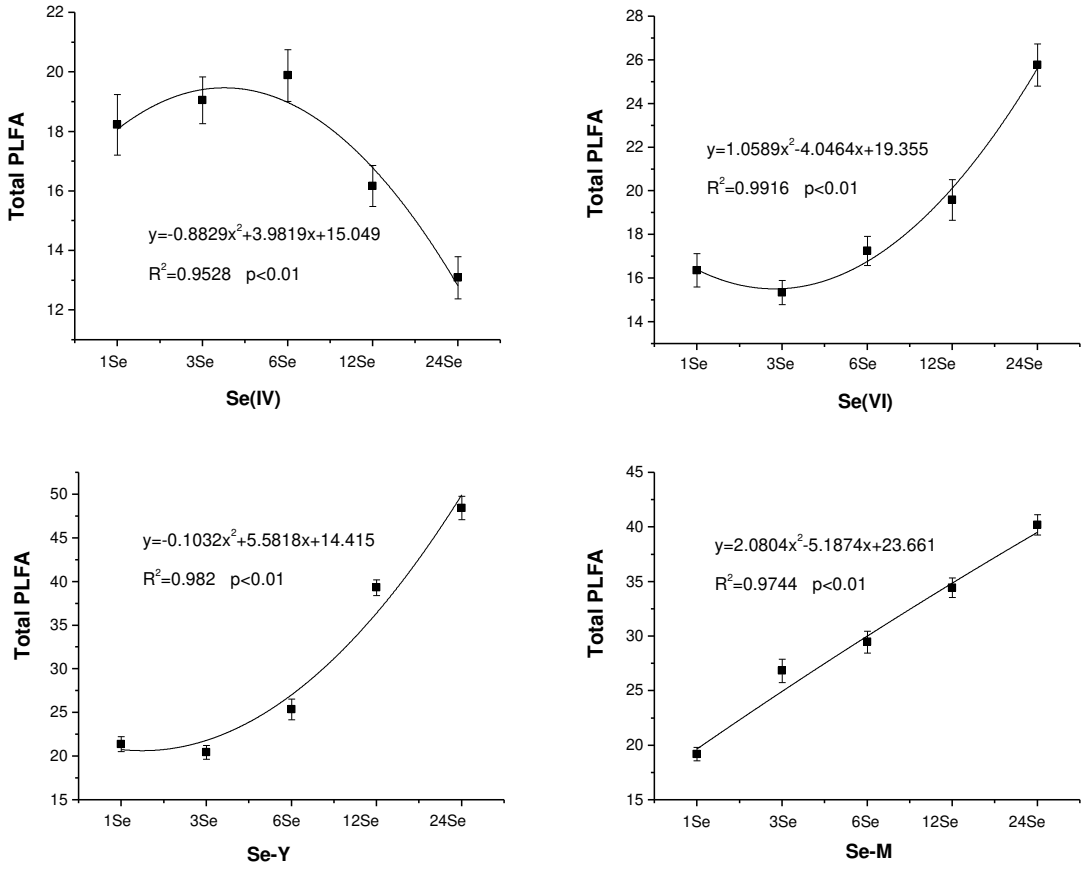

Figure 5. *Relationship between the amount of different Se sources and the microbial content of PLFA*

Table 4. *Correlation among soil As, soil enzymes and microorganisms after Se-Y addition (n = 15)*

	Urease	Sucrase	Catalase	Dehydrogenase	The FDA hydrolase	Actinomyces	G^+	G^-	Fungus
Urease	1								
Sucrase	.745**	1							
Catalase	.941**	.516*	1						
Dehydrogenase	.702**	.922**	.452*	1					
The FDA hydrolase	.826**	.928**	.619**	.978**	1				
Actinomyces	.693**	.857**	.551*	.878**	.901**	1			
G^+	.841**	.887**	.698**	.919**	.965**	.965**	1		
G^-	.780**	.928**	.603**	.945**	.969**	.977**	.988**	1	
Fungus	.249	.728**	.004	.822**	.730**	.824**	.716**	.793**	1

**Significant correlation at the 0.01 level. *Significant correlation at the 0.05 level

http://www.aloki.hu ● ISSN 1589 1623 (Print) ● ISSN 1785 0037 (Online)
DOI: http://dx.doi.org/10.15666/aeer/2005_42374255

Table 5. *Correlation among soil As, soil enzymes and microorganisms after Se-M addition (n = 15)*

	Urease	Sucrase	Catalase	Dehydrogenase	The FDA hydrolase	Actinomyces	G^+	G^-	Fungus
Urease	1								
Sucrase	.867**	1							
Catalase	.778**	.967**	1						
Dehydrogenase	.946**	.927**	.880**	1					
The FDA hydrolase	.881**	.957**	.940**	.974**	1				
Actinomyces	.812**	.642**	.572*	.651**	.553*	1			
G^+	.778**	.971**	.996**	.893**	.954**	.534*	1		
G^-	.962**	.953**	.896**	.978**	.956**	.753**	.898**	1	
Fungus	.892**	.986**	.931**	.916**	.922**	.727**	.932**	.963**	1

**Significant correlation at the 0.01 level. *Significant correlation at the 0.05 level

Conclusions

This research carried out the regulation of Se on microbial and enzyme activities in As-contaminated soil. Research has shown that the application of inorganic Se and organic Se can significantly affect the activities of dehydrogenase, urease, FDA hydrolase, invertase and catalase in As-contaminated soil. The application of organic Se could increase the total amount of microorganisms in As-contaminated soil and enrich the microbial community structure, while inorganic Se could have the opposite effect. There was a significant positive correlation between various microorganisms and enzyme activities in the soil. This study also showed that the regulation of As in soil by Se was closely related to soil microorganisms and enzyme activities. Follow-up work should be conducted to study the mechanism of Se and microorganisms in the treatment of soil As pollution.

List containing the detected species and their classification

Soil enzymes: urease, catalase, sucrase, FDA hydrolase and dehydrogenase.

Soil microorganisms: actinomycetes, fungus, gram-positive bacteria (G^+), gram-negative bacteria (G^-).

Acknowledgements. This work was financially supported by the National Key Research and Development Program of China (2017YFD0800900); the Natural Science Foundation Project of Jiangxi Provincial Department of Science and Technology (20212BAB204042), National Natural Science Foundation of China (42162023, 31960308), the Jiangxi Provincial Key Scientific Research Plan (20203BBGL73220); Research Foundation of Education Bureau of Jiangxi Province, China (GJJ201904); Water Science and Technology Fund of Jiangxi Province in China (202124ZDKT15).

REFERENCES

[1] Ali, W., Zhang, H., Junaid, M., Mao, K., Xu, N., Chang, C. Y., Rasool, A., Aslam, M. W., Ali, J., Yang, Z. G. (2021): Insights into the mechanisms of arsenic-selenium interactions and the associated toxicity in plants, animals, and humans: a critical review. – Crit Rev Env Sci Tec 51(7): 704-750.

[2] Bhattacharyya, P., Tripathy, S., Kim, K., Kim, S. H. (2008): Arsenic fractions and enzyme activities in arsenic-contaminated soils by groundwater irrigation in West Bengal. – Ecotoxicol Environ Saf 71(1): 149-156.

http://www.aloki.hu ● ISSN 1589 1623 (Print) ● ISSN 1785 0037 (Online)
DOI: http://dx.doi.org/10.15666/aeer/2005_42374255

[3] Cullen, W. R. (2014): Chemical mechanism of arsenic biomethylation. – Chem Res Toxicol 27(4): 457-461.
[4] Dong, Y., Gao, M., Liu, X., Qiu, W. (2020): The mechanism of polystyrene microplastics to affect arsenic volatilization in arsenic-contaminated paddy soils. – J Hazard Mater 398: 122896.
[5] Fan, J., Wang, R., Hu, H. Q., Ye, X. J., Xia, P. L., Deng, J. Q. (2015): Effects of exogenous selenium with different valences on se forms, enzyme activities and microbial quantity of soil. – J Soil Water Conserv (5): 137-141.
[6] Feng, R., W., Zhao, P. P., Zhu, Y. M. (2021): Application of inorganic selenium to reduce accumulation and toxicity of metals and metalloids in plants: the main mechanisms, concerns, and risks. – Sci Total Environ 771(6): 144776.
[7] Fernández, P., Sommer, I., Cram, S., Rosas, I., Gutiérrez, M. (2005): The influence of water-soluble As(III) and As(V) on dehydrogenase activity in soils affected by mine tailings. – Sci Total Environ 348(1-3): 231-243.
[8] Ghosh, A. K., Bhattacharyya, P., Pal, R. (2004): Effect of arsenic contamination on microbial biomass and its activities in arsenic contaminated soils of Gangetic West Bengal, India. – Environ Interna 30(4): 491-499.
[9] Guo, Y., Mao, K., Cao, H. (2021): Exogenous selenium (cadmium) inhibits the absorption and transportation of cadmium (selenium) in rice. – Environ Pollut 268: 115829.
[10] Hu, L., Fan, H. B., Wu, D. S. (2020): Effects of selenium on antioxidant enzyme activity and bioaccessibility of arsenic in arsenic-stressed radish. – Ecotoxicol Environ Saf 200: 110768.
[11] Javadi, N., Khodadadi, H., Hamdan, N. (2018): EICP treatment of soil by using urease enzyme extracted from watermelon seeds. – IFCEE 20: 115-124.
[12] Jomova, K., Jenisova, Z., Feszterova, M. (2011): Arsenic: toxicity, oxidative stress and human disease. – J Appl Toxicol 31(2): 95-107.
[13] Karaca, A., Cetin, S. C., Turgay, O. C., Kizilkaya, R. (2010): Effects of heavy metals on soil enzyme activities. – Soil Heavy Metals 19: 237-262.
[14] Lampis, S., Zonaro, E., Bertolini, C., Bernardi, P., Butler, C. S., Vallini, G. (2014): Delayed formation of zero-valent selenium nanoparticles by Bacillus mycoides SeITE01 as a consequence of selenite reduction under aerobic conditions. – Microbial cell factories 13(1): 35.
[15] Li, Z., Liang, D., Peng, Q. (2017): Interaction between selenium and soil organic matter and its impact on soil selenium bioavailability: a review. – Geoderma 295: 69-79.
[16] Lin, K., F., Xu, X. Q., Jin, X., Xiang, J. L. (2005): Eco-toxicology effects of soil selenium pollution on soil enzyme. – China Environ Sci 25(S1): 94-97.
[17] Lin, X., Cao, L., Jian, X., Zhang, R. (2012): Interactions of denitrifying bacteria, actinomycetes, and fungi on nitrate removal in mix-culturing systems. – Water Air Soil Pollut 223(6): 2995-3007.
[18] Liu, H. Y., Wei, T. X., Wang, X. (2016): Soil microbial community structure and functional diversity in typical plantations marked by PLFA in hilly loess region. – J Beijing Forestry University 38(01): 28-35.
[19] Lorenz, N., Hintemann, T., Kramarewa, T., Katayama, A., Kandeler, E. (2006): Response of microbial activity and microbial community composition in soils to long-term arsenic and cadmium exposure. – Soil Biol Biochem 38(6): 1430-1437.
[20] Lyubun, Y. V., Pleshakova, E. V., Mkandawire, M., Turkovskaya, O. V. (2013): Diverse effects of arsenic on selected enzyme activities in soil–plant–microbe interactions. – J Hazard Mater 262(22): 685-690.
[21] Ma, X. Z. (2010): Activity of soil fluorescein diacetate (FDA) hydrolase under long-term fertilization. – J of Zhejiang University (Agriculture and Life Sciences) 36(4): 451-455.
[22] Michael, W., Stolz, J. F. (2020): Microbial selenium metabolism: a brief history, biogeochemistry and ecophysiology. – FEMS Microbiol Ecol (12): 12-20.

http://www.aloki.hu ● ISSN 1589 1623 (Print) ● ISSN 1785 0037 (Online)
DOI: http://dx.doi.org/10.15666/aeer/2005_42374255

[23] Mondal, N. K., Dey, U., Ghosh, S., Datta, J. K. (2015): Soil enzyme activity under arsenic-stressed area of Purbasthali, West Bengal, India. – Arch Agron Soil Sci 61(1): 73-87.
[24] Moscatelli, M. C., Secondi, L., Marabottini, R., Papp, R., Stazi, S. R., Mania, E., Marinari, S. (2018): Assessment of soil microbial functional diversity: land use and soil properties affect CLPP-MicroResp and enzymes responses. – Pedobiologia 66: 36-42.
[25] Pal, P., Bhattacharyay, D., Mukhopadhyay, A., Sarkar, P. (2009): The detection of mercury, cadmium, and arsenic by the deactivation of urease on rhodinized carbon. – Environ Eng Sci 26(1): 25-32.
[26] Pilarczyk, B., Jankowiak, D., Tomza-Marciniak, A. (2012): Selenium concentration and glutathione peroxidase (GSH-Px) activity in serum of cows at different stages of lactation. – Biol Trace Elem Res 147(1): 91-96.
[27] Ramkissoon, C., Degryse, F., Silva, R., Baird, R., Mclaughlin, M. J. (2019): Improving the efficacy of selenium fertilizers for wheat biofortification. – Sci Rep 9(1): 19520.
[28] Samuel, A. D., Felix, B. C., Domuţa, C., Şandor, M., Vuşcan, A., Borza, I., Brejea, R. (2012): Influence of heavy metal contamination on soil enzyme activities. – Natural Resources and Sustainable 9: 1-10.
[29] Shen, F. F., Wu, J. P., Fan, H. B., Liu, W. F., Guo, X. M., Duan, H. L., Wei, X. H. (2019): Soil N/P and C/P ratio regulate the responses of soil microbial community composition and enzyme activities in a long-term nitrogen loaded Chinese fir forest. – Plant soil 436(1): 91-107.
[30] Shi, Y. J., Shi, Y. J., Wang, Y. L., Li, T. C., Zhou, B. C., Xie, Y., Xu, F. Y., Liang, R. Y. (2018): Dynamic responses of soil enzymes to exogenous sodium selenite and selenomethionine. – Acta Scientiae Circumstantiae 38(3): 1189-1196.
[31] Paulraj, S., Kumar, M. S. (2016): Selenium Bioavailability through Microbes. – In: Singh, U., Praharaj, C. S., Singh, S. S., Singh, N. P. (eds.) Biofortification of Food Crops. – Springer, New Delhi, pp. 303-316.
[32] Sodhi, K. K., Kumar, M., Agrawal, P. K. (2019): Perspectives on arsenic toxicity, carcinogenicity and its systemic remediation strategies. – Environ Tech Innova 16: 100462.
[33] Srivastava, M., Ma, L. Q., Rathinasabapathi, B., Srivastava, P. (2009): Effects of selenium on arsenic uptake in arsenic hyperaccumulator Pteris vittata L. – Bioresour Technol 100(3): 1115-1121.
[34] Subrahmanyam, G., Shen, J. P., Liu, Y. R., Archana, G., Zhang, L. M. (2016): Effect of long-term industrial waste effluent pollution on soil enzyme activities and bacterial community composition. – Environmental Monitoring & Assessment 188(2): 112-125.
[35] Sun, Y. Q., Zhang, C., Wu, Z. X., Wu, S. L., Hu, Y. J., Xing, Y., Chen, B. D. (2015): Soil microbial community structure and carbon source metabolic diversity in the Realgar mining area. – Acta Scientiae Circumstantiae 35(11): 10-16.
[36] Tao, K., Tian, H., Fan, J. (2021): Kinetics and catalytic efficiency of soil fluorescein diacetate hydrolase under the pesticide parathion stress. – Sci Total Environ 771: 144835.
[37] Tremblay, G. F., Bélanger, G., Lajeunesse, J., Chouinard, Y. (2014): Timothy response toincreasing rates of selenium fertilizer in eastern Canada. – Agron J 107(1): 211-220.
[38] Turpeinen, R., Kairesalo, T., HÄGgblom, M. M. (2004): Microbial community structure and activity in arsenic, chromium and copper contaminated soils. – FEMS Microbiol Ecol 47(1): 39-50.
[39] Violante, A., Cozzolino, V., Perelomov, L. (2010): Mobility and bioavailability of heavy metals and metalloids in soil environments. – J Soil Sci Plant Nutr10(3): 268-292.
[40] Wang, Z. Q., Li, Y. B., Tan, X. P., He, W. X., Wei, G. H. (2016): Effect of arsenate contamination on free, immobilized and soil alkaline phosphatases: activity, kinetics and thermodynamics. – European Journal of Soil Science 68(1): 126-135.

http://www.aloki.hu ● ISSN 1589 1623 (Print) ● ISSN 1785 0037 (Online)
DOI: http://dx.doi.org/10.15666/aeer/2005_42374255

[41] Wang, Z., Tian, H., Lei, M., Megharaj, M., He, W. (2020): Soil enzyme kinetics indicate ecotoxicity of long-term arsenic pollution in the soil at field scale. – Ecotoxicol Environ Saf 191: 110215.
[42] Wu, X. P., Wu, T. X., Fu, D. D., Duan, M. L., Wei, W., Liang, D. L. (2010): Effects of selenate and selenite pollution on soil enzymes activity. – J Agro-Environ Sci. 29(8): 1526-1533.
[43] Xian, Y., Wang, M., Chen, W. (2015): Quantitative assessment on soil enzyme activities of heavy metal contaminated soils with various soil properties. – Chemosphere 139(11): 604-608.
[44] Xiong, J., Wu, L., Tu, S., Nostrand, J. V., He, Z., Zhou, J., Wang, G. (2010): Microbial communities and functional genes associated with soil arsenic contamination and the rhizosphere of the arsenic-hyperaccumulating plant Pteris vittata L. – Appl Environ Microbiol 76(21): 7277-7284.
[45] Xiong, J., He, Z., Van Nostrand, J. D., Luo, G., Tu, S., Zhou, J., Wang, G., Gilbert, J. A. (2012): Assessing the microbial community and functional genes in a vertical soil profile with long-term arsenic contamination. – Plos One 7(11): e50507.
[46] Xiong, D., Gao, Z., Fu, B., Sun, H., Tian, S., Xiao, Y., Qin, Z. (2013): Effect of pyrimorph on soil enzymatic activities and respiration. – Eur J Soil Biol 56: 44-48.
[47] Xue, T., Hartikainen, H., Piironen, V. (2001): Antioxidative and growth-promoting effect of selenium on senescing lettuce. – Plant and Soil 237(1): 55-61.
[48] Yang, L. F., Qin, E. H., Wan, Z. X., Wei, L. (2010): Effects of selenium addition and incubation time on soil enzyme activities. – Chinese J Soil Sci 41(05): 1064-1068.
[49] Yang, H., Ze, X. U., Sheng, Z., Xiu, H., Deng, M. (2017): Effects of selenium on soil enzyme activity and selenium content of tea varieties. – Ecolo Environ Sci. 26(11): 1872-1877.
[50] Zhang, H., Zeng, X., Bai, L., Shan, H., Wang, Y., Wu, C., Duan, R., Su, S. (2018): Reduced arsenic availability and plant uptake and improved soil microbial diversity through combined addition of ferrihydrite and Trichoderma asperellum SM-12F1. – Environ Sci Pollu Res 25(11): 24125-24134.
[51] Zhang, X. X., Liu, Z. W., Luc, N. T., Liang, X., Liu, X. B. (2015a): Dynamics of the biological properties of soil and the nutrient release of Amorpha fruticosa L. litter in soil polluted by crude oil. – Environ Sci Pollu Res. 22: 16749-16757.
[52] Zhang, Y. L., Chen, L. J., Chen, X. H. (2015b): Response of soil enzyme activity to long-term restoration of desertified land. – Catena 133: 64-70.

http://www.aloki.hu ● ISSN 1589 1623 (Print) ● ISSN 1785 0037 (Online)
DOI: http://dx.doi.org/10.15666/aeer/2005_42374255

CHANGES IN THE BACTERIAL COMMUNITY STRUCTURE AND DIVERSITY OF CHAGAN LAKE SEDIMENTS, NORTHEASTERN CHINA

DU, X.[1,2#] – LI, M. S.[3#] – SONG, D.[1,2] – YANG, J. S.[4] – LIU, H.[1,2] – SUI, X.[5] – HUO, T. B.[1,2*]

[1]*Heilongjiang River Fisheries Research Institute, Chinese Academy of Fishery Sciences, 150076 Harbin, PR China*

[2]*Heilongjiang River Basin Fishery Ecological Environment Monitoring Center, Ministry of Agriculture and Rural Affairs, 150076 Harbin, PR China*

[3]*Institute of Nature and Ecology, Heilongjiang Academy of Sciences, 150040 Harbin, PR China*

[4]*Jilin Chagan Lake National Nature Reserve Administration, 138099 Songyuan, PR China*

[5]*School of Life Sciences, Heilongjiang University, Harbin, PR China*

[#]*Xue Du and Mengsha Li contributed equally to this work*

[*]*Corresponding author*
e-mail: tbhuo@163.com

(Received 16th Mar 2022; accepted 26th Jul 2022)

Abstract. This study employed Illumina MiSeq high-throughput sequencing to explore the composition of the bacterial community of Chagan Lake sediments and its response to soil physicochemical properties. Our findings indicated that bacterial abundance and diversity are significantly correlated with water depth. Particularly, the bacterial alpha diversity and phyla relative abundance increased with water depth. Furthermore, the five dominant bacterial phyla in the bacterial community according to all plots were Proteobacteria, Chloroflexi, Acidobacteriota, and Actinobacteriota. Moreover, our findings indicated that electrical conductivity (EC), pH, and total carbon (TC) in sediments are important factors that affect the bacterial community structure and diversity of sediments. In summary, the bacterial community structure and diversity varied significantly in different plot sediments of Chagan Lake, which were regulated by soil nutrients and physical properties. The results of this study can be used to further explore the potential relationship between bacterial communities and the environment, and provide a scientific basis for the prediction of ecosystem structure and function of alpine inland wetlands.
Keywords: *soil environmental factors, soil physicochemical properties, bacterial composition, water depth, functional prediction*

Introduction

Microbial community and diversity in sediments are crucial for lake ecosystems. Particularly, sediment microbes drive the morphological transformation and geochemical cycle of most bioactive elements, regulate the environmental quality of water bodies, and contribute to water purification (Wan et al., 2017; Li et al., 2017). Furthermore, the distribution of sediment microbial communities is also affected by environmental factors such as temperature, pH, dissolved oxygen, electrical conductivity and nutrients (Chen et al., 2010; Fermani et al., 2013; Shao et al., 2013; Zhang et al., 2019). Therefore, studying the diversity, community composition, and environmental factors that shape sediment microbial communities is critical for the conservation of lake ecosystems.

http://www.aloki.hu ● ISSN 1589 1623 (Print) ● ISSN1785 0037 (Online)
DOI: http://dx.doi.org/10.15666/aeer/2005_42574270

Bacteria are a major component of lake microbial communities and are the main decomposers of organic compounds. Several studies have evaluated the microbial community structure of lake sediments and have reported that the microbial community composition of sediments varies depending on location, season, and sediment depth. Huang et al. (2015) studied the composition of bacterial communities in the sediments of Meiliang Bay, Xuhu Lake, and East Taihu Lake in summer, and found that the dominant bacterial phyla in different lake areas varied depending on the region. Chen et al. (2010) found that the composition of eukaryotic microbial communities in Meiliang Bay and the lake center of Taihu Lake exhibited obvious seasonal changes, and different lake areas responded differently to environmental factors. Meiliang Bay and the lake center were affected by total phosphorus (TP), total nitrogen (TN), and electrical conductivity (EC). However, Wan et al. (2017) found that, rather than lake location, season was the most important determinant of microbial community structure in sediments. Ye et al. (2009) found that although the vertical distribution of bacterial communities in the sediments of Meiliang Bay in Taihu Lake was similar, the composition of archaeal communities varied significantly depending on water depth.

Chagan Lake is the largest inland lake in Jilin Province and is located within a large water network between the Nenjiang and the Huolin rivers. It is an important fishery base in Jilin Province and the largest lake in the Songliao Plain. Research on Chagan Lake has largely focused on characterizing the levels of organic matter in its sediments (Qu et al., 2021), its benthic community structure (Du et al., 2020), and the elemental composition of its sediments (Bu et al., 2009). However, very few studies have explored the microbial community composition of Chagan Lake sediments. Therefore, our study collected sediments from a 10–15 cm depth in the coastal areas of Chagan Lake and the center of the lake in 2017. The bacterial community structure of the sediments was then characterized via high-throughput sequencing technology to explore its relationship with different sediment properties. Collectively, our findings provide insights into the formation mechanism of sediment bacterial communities in Chagan Lake, which can serve as a theoretical basis for maintaining the stability of the Chagan Lake ecosystem.

Material and Methods

Research area

Chagan Lake (124°03'–124°34', 45°09'–45°30') is located in the boundary of the northwestern Jilin Province, Inner Mongolia Autonomous Region, Heilongjiang Province, and Jilin Province in China, and acts as a weir at the end of the Huolin River. Sai Lake is among the top ten freshwater lakes in China, the largest natural lake, and the largest fishery production base in Jilin Province at the confluence of the Songhua River, the southern source of Songhua River, and the Nen River (*Figure 1*). The lake has an area of 420 km^2 and an average water depth of 2.5 m. Furthermore, the lake integrates with the Xindianpao and Mayingpao lakes when the water level reaches 130 m. Chagan Lake is primarily replenished through natural precipitation, water diversion from the Songhua River, and return water from irrigation areas. The lake is surrounded by farmlands and is therefore severely affected by agricultural non-point source pollution. Saline-alkali land and sandy terrain are widely distributed around the lake and serve as a runoff collection area. Furthermore, the rapid development of tourism and catering services in the surrounding area threatens the water quality of Chagan Lake. In this study, nine sampling points were established across Chagan Lake based on its habitat

http://www.aloki.hu ● ISSN 1589 1623 (Print) ● ISSN1785 0037 (Online)
DOI: http://dx.doi.org/10.15666/aeer/2005_42574270

characteristics (*Figure 1*). According the water depth, we divided 9 soil point into three categories: low water depth (S7 and S9) ≤ 2 m, medium water depthe (S1 and S8) between 2 m and 3 m and high water depth (S2, S3, S4, S5 and S6) ≥ 3 m.

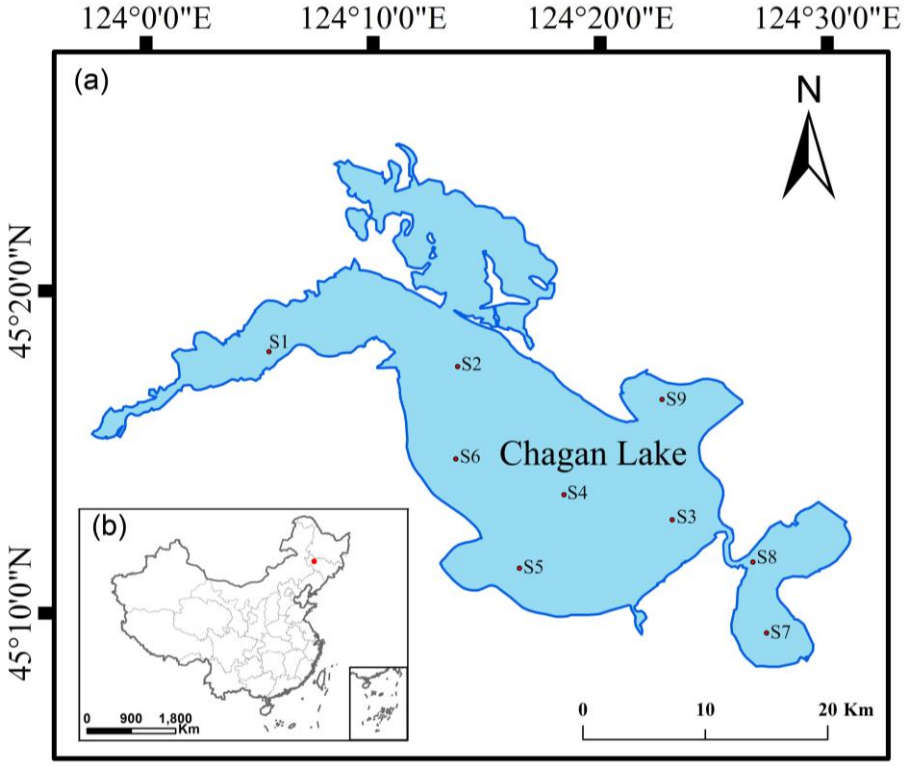

Figure 1. *Distribution of sampling sites in Chagan Lake. (a) the map of China and the red point is the research site; (b) research site and S1-S9 indicated the locations of sediment samples taken*

Sediment samples

On October 10, 2017, sediment samples were collected from a 10–15 cm depth from the surface of the lake bottom using a stainless steel grab. In each plot, the five sediment soils (each sediment soil were ~100 g) were taken and then mixed one sediment soil. The samples were then placed in sterilized self-sealing bags, stored at 4 °C, and quickly transported to the laboratory. Microbial DNA was immediately extracted from a portion of the fresh sediment samples, whereas the other portion was freeze-dried, ground, passed through a 125 μm sieve, and stored at -20 ℃ to characterize the physicochemical properties of the sediment samples within one week.

Analysis of physical and chemical indicators

The soil-water pH ratio of the sediment (1:2.5) was determined using a pH meter, the EC value of the sediment was determined using a soil EC value tester, and the total carbon (TC), total nitrogen (TN), and total phosphorus (TP) in the sediment were determined via ammonium molybdate spectrophotometry.

http://www.aloki.hu ● ISSN 1589 1623 (Print) ● ISSN1785 0037 (Online)
DOI: http://dx.doi.org/10.15666/aeer/2005_42574270

DNA extraction and sequencing of sediment microorganisms

The total DNA of the microorganisms in the sediment samples was extracted using the FastDNA SPIN kit (MP Biomedical, USA). PCR amplification was performed on the V3-V4 region of the 16S rRNA of the DNA samples using the 338F (5′- ACT CCT ACG GGA GGC AGC AG-3′) and 806R (5′- GGA CTA CHV GGG TWT CTA AT-3′) primer pair. Each 30 μl reaction contained 100 ng of template DNA, 15 μl 2x EasyTaq PCR SuperMix, and 10 μM of primers. All reactions were conducted in triplicate in a Veriti 96-well fast thermocycler (ABI, USA) and the reagents used in our experiments were purchased from Beijing Quanshijin Company. The PCR amplification conditions were the following: pre-denaturation at 95 °C for 2 min, followed by 30 cycles of denaturation at 95 °C for 20 s, annealing at 52 °C for 60 s, extension at 72 °C for 60 s, and a final extension at 72 °C for 10 min.

Bioinformatics and statistical analyses

The purified sediment PCR products were sequenced on the Illumina MiSeq platform (Illumina, USA) (2 × 300 bp paired-end sequencing). Quality control measures were taken to ensure the quality of the reads, and the original sequences were filtered and spliced, after which chimeric sequences were removed using the QIIME2 software (Bolyen et al., 2019) and the sequence length was screened. The clean reads were then assigned to different operational taxonomic units (OTUs) at a 97% similarity threshold using QIIME. Annotation of taxonomic information from the phylum to genus level was performed by aligning the sequences with those in the SILVA database using RDP Classifier. The OTUs were analyzed based on abundance and diversity indices, including the Chao1 and ACE indices of community richness, as well as the Shannon and Simpson indices of community evenness.

Multiple comparisons between groups were conducted through one-way analysis of variance (ANOVA) using the SPSS 26.0 software and differences were considered statistically significant at $P<0.05$. Pearson correlation was used to analyze the correlation between the physicochemical properties of the sediment and the alpha diversity of the sediment, and correlations were considered statistically significant at $P<0.05$ and $P<0.01$. The top 50 bacterial phyla with the highest abundances and soil physicochemical properties were visualized in heatmaps using the ‘vegan’ package in R (R Development Core Team, 2017). Canonical association analysis was performed using Canoco5.0. Principal co-ordinates analysis (PCoA) was also conducted based on OTU-level composition profiles using the ‘vegan’ package in R. Dilution profiles were also analyzed using the ‘vegan’ package. Functional predictive analysis (Functional Annotation of Prokaryotic Taxa, FAPROTAX) was used to predict the microbial functions in the sediments. Permutational Multivariate Analysis of Variance (PERMANOVA) performed by R software using the ‘vegan’ package.

Results

Analysis of physicochemical properties of the bottom sediments in Chagan Lake

As summarized in *Table 1*, the water depths of the nine points in Chagan Lake ranged from 1.4 m (S7) to 3.6 m (S6). Soil TP in sediments ranged from 0.34 to 1.07 g/kg, TC ranged from 3.23 to 47.96 g/kg, TN ranged from 0.26 to 3.03 g/kg, pH ranged from 8.2 to 9.0, conductivity ranged from 519 to 1082, and the C/N variation

http://www.aloki.hu ● ISSN 1589 1623 (Print) ● ISSN1785 0037 (Online)
DOI: http://dx.doi.org/10.15666/aeer/2005_42574270

ranged from 0.4 to 6.69. Among the sampling points, S4 had the highest TP, TC, TN, and EC, reaching values of 1.07 g/kg, 47.96 g/kg, 3.03 g/kg, and 1082, respectively. In contrast, S1 had the lowest TP and TN levels (0.34 and 0.71 g/kg, respectively).

Table 1. *Soil physicochemical properties at different points across Chagan Lake*

Plots	TP	TC	TN	C/N	pH	EC	Water depth	Categories
S1	0.34	9.46	0.71	0.55	8.62	1049	2.3	medium
S2	0.83	33.81	1.97	0.44	8.83	1002	3.6	high
S3	0.18	3.23	0.26	0.48	8.86	1069	3	high
S4	1.07	47.96	3.03	0.57	8.7	1082	3.5	high
S5	0.50	15.02	0.86	0.54	8.84	980	3.1	high
S6	0.82	29.71	1.67	0.4	9.00	1030	3.6	high
S7	0.65	26.60	1.75	0.58	8.27	552	1.4	low
S8	0.39	10.20	0.76	6.69	8.84	985	2.1	medium
S9	0.62	36.03	2.4	6.13	8.2	519	1.9	low

Rarefaction curve of bacterial communities in the bottom sediment of Chagan Lake

The rarefaction curve reflects the sampling depth of the sample and can be used to evaluate whether the sequencing volume is sufficient to cover all taxa. *Figure 2* illustrates the rarefaction curve of all samples in this experiment under a 97% similarity threshold. As illustrated in *Figure 2*, the dilution curves of all soil samples tended to be flat, indicating that the read numbers were high enough to accurately reflect the bacterial community structure of the soil samples.

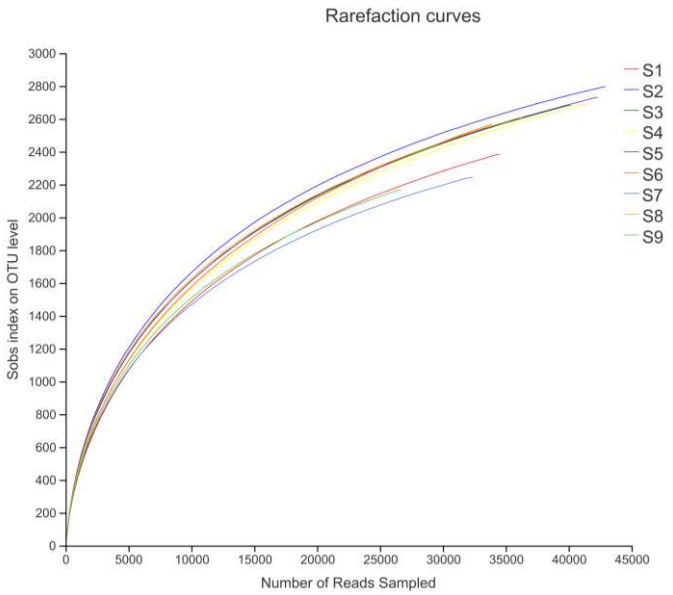

Figure 2. *Rarefaction curves of different sample points in Chagan Lake*

Alpha diversity of the bacterial community of Chagan Lake sediment

As summarized in *Table 2*, the coverage of each sample library ranged from 97% to 98%, indicating that the sequencing results accurately reflected the structure of the bacterial communities in the sediments. The abundance of bacterial communities

http://www.aloki.hu ● ISSN 1589 1623 (Print) ● ISSN1785 0037 (Online)
DOI: http://dx.doi.org/10.15666/aeer/2005_42574270

reflected by the Chao1 and Ace indices exhibited the same order: low water depth (S7 and S9) < medium water depth (S1 and S8) < high water depth (S2, S3, S4, S5, S6). In other words, the water level increased proportionally with flooding degree, and bacterial abundance was affected by the water level. Bacterial abundance was highest at the S2, S3, and S4 sample points (where the water level was high), but the results at low water depths did not change significantly (P<0.05). In contrast, the bacterial Shannon indices at medium water depths were significantly different but exhibited no consistent trend (P<0.05). Therefore, these findings demonstrated that the water depth significantly affected the bacterial abundance in the sediments, but the difference in the uniformity was not significant.

Table 2. *Bacterial alpha diversity in Chagan Lake sediments*

Plots	Sobs	Shannon	Simpson	Ace	Chao1	Coverage (%)	PD
S1	2384.00	6.05	0.01	3129.86	3063.26	98	238.59
S2	2797.00	6.46	0.00	3483.69	3473.16	98	276.22
S3	2683.00	6.36	0.00	3451.95	3470.29	98	258.66
S4	2688.00	6.30	0.01	3524.26	3466.48	98	262.85
S5	2731.00	6.41	0.00	3497.31	3481.71	98	269.15
S6	2567.00	6.06	0.01	3528.15	3510.47	97	257.76
S7	2243.00	6.11	0.01	2864.26	2854.29	98	217.81
S8	2607.00	6.35	0.01	3405.81	3398.09	98	250.17
S9	2165.00	6.11	0.01	2832.75	2850.00	97	211.01
One-way ANOVA (Water depth)	P<0.05	P<0.05	P>0.05	P<0.05	P<0.05	P>0.05	P<0.05

Beta diversity of the bacterial community in Chagan Lake sediment

According to the principal coordinate analysis of the Pearson distance algorithm at the OTU level, the correlations and differences of the bacterial communities in the sediments of the nine sampling points were compared. As shown in *Figure 3*, the cumulative explained variation of the first axis and the second axis reached 41.93% and 21.42%, respectively. The bacterial communities at different sampling points in Chagan Lake did not overlap significantly with each other and could thus be easily distinguished. From the perspective of bacterial community similarity, there were similarities in the bacterial community structure of the subsoil of the S7 and S9, S1, S5, and S2, and S1, S3, S6, and S8 sampling points, and therefore these sampling sites formed three distinct clusters (*Figure 3*). Overall, the community structure of bacteria in the sediments of different water depths was significantly different (PERMANOVA P<0.05), which indicated that the water depths had a significant effect on the bacterial community structure of the sediments.

Analysis of bacterial community structure in Chagan Lake sediments

A total of 5,362 OTUs were identified in the nine sampling points using high-throughput sequencing, which encompassed 60 bacterial phyla (*Figure 4(a)*) and 1,077 bacterial genera (*Figure 4(b)*). As illustrated in *Figure 4(a)*, the main phyla in the soil samples included Proteobacteria (26%), Chloroflexi (14%), Acidobacteriota (10%), Actinobacteriota (9%), Desulfobacterota (8%), Bacteroidota (8%), and Cyanobacteria (7%).

http://www.aloki.hu ● ISSN 1589 1623 (Print) ● ISSN1785 0037 (Online)
DOI: http://dx.doi.org/10.15666/aeer/2005_42574270

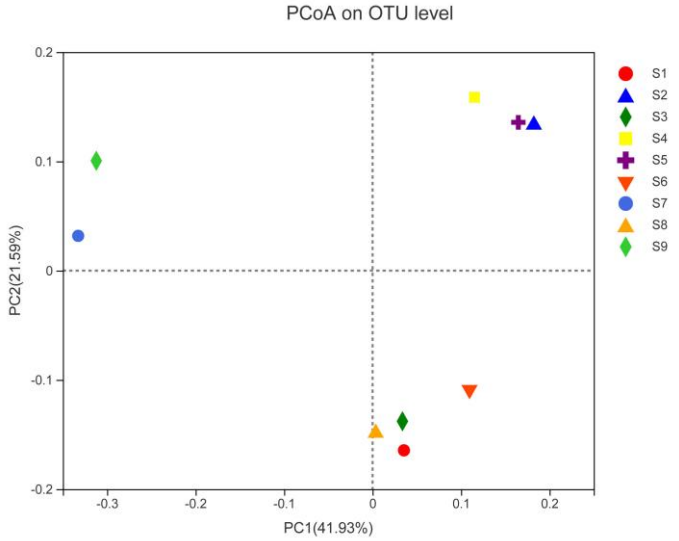

Figure 3. *Bacterial beta diversity in the sediments of Chagan Lake*

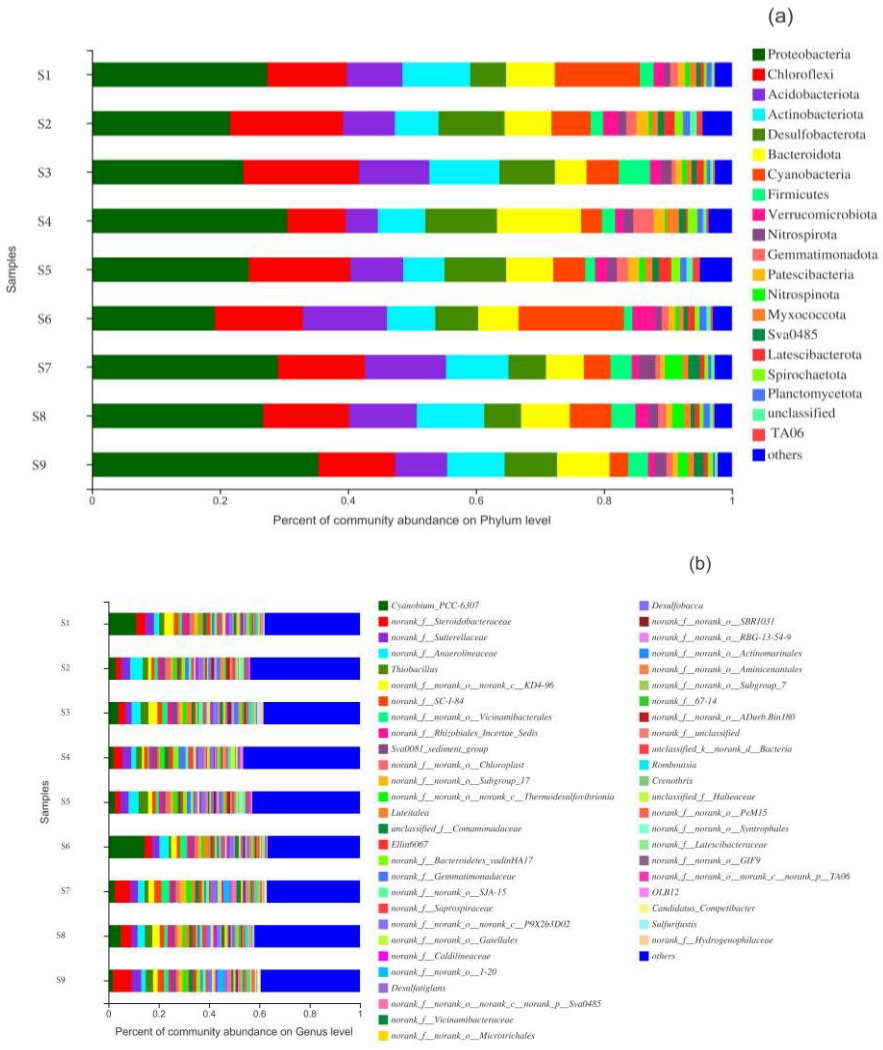

Figure 4. *Bacterial phyla (a) and genera (b) level classification in sediments of Chagan Lake*

http://www.aloki.hu ● ISSN 1589 1623 (Print) ● ISSN1785 0037 (Online)
DOI: http://dx.doi.org/10.15666/aeer/2005_42574270

Redundancy analysis of bacterial community and physicochemical properties in sediments of Chagan Lake

The key environmental factors affecting the sediment bacterial community of Chagan Lake were further analyzed, and the soil fungal community structure and soil physicochemical properties were explored via redundancy analysis (*Fig. 5*). Our findings indicated that the cumulative explained variation of the two axes reached 47.07%, and could thus reflect nearly 50% of the variation characteristics of soil bacterial communities and their influencing factors. Particularly, pH was the key environmental factor that dominated the bacterial community changes (R^2 = 0.75, P = 0.01).

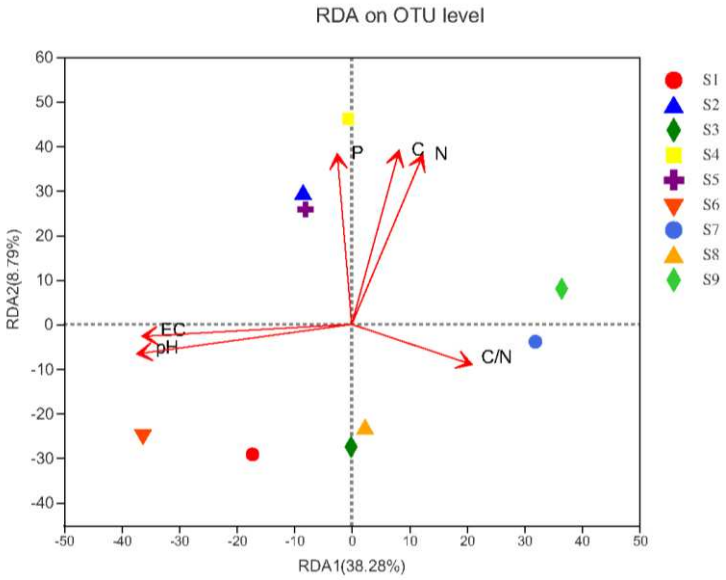

Figure 5. *Redundancy analysis of bacterial community and physicochemical properties in sediments of Chagan Lake*

The key environmental factors affecting the abundance of soil bacteria in the bottom of Chagan Lake were further analyzed, and the correlation between the horizontal abundance of soil fungi and soil physicochemical properties was determined (*Fig. 6*). Our findings indicated that the abundance of different bacterial phyla was affected by different environmental factors, among which WS4, WOR-1, Elusimicrobiota, Verrucomicrobiota, and Proteobacteria were significantly correlated with soil pH; Nitrospinota was significantly correlated with soil EC; Proteobacteria, Chloroflexi, Nitrospinta, MBNT15, WS2, Sumerlaeota, Caldisericota, Elusimicrobes, and Fibrobacteria were significantly correlated with C/N; Spirochaetota was significantly correlated with C, N, P; and Actinobacteriota was significantly correlated with soil C and P.

Relationships between soil physicochemical properties and soil bacterial alpha diversity

As summarized in *Table 3*, the correlation analysis between soil physicochemical properties and the alpha diversity of soil bacteria in the sediments indicated that the

http://www.aloki.hu ● ISSN 1589 1623 (Print) ● ISSN1785 0037 (Online)
DOI: http://dx.doi.org/10.15666/aeer/2005_42574270

Sobs index, Shannon index, Ace index, and Chao1 index were significantly positively correlated with the soil organic carbon in the sediments (P<0.05). However, there was no significant correlation between other indices and the physicochemical properties of the sediment.

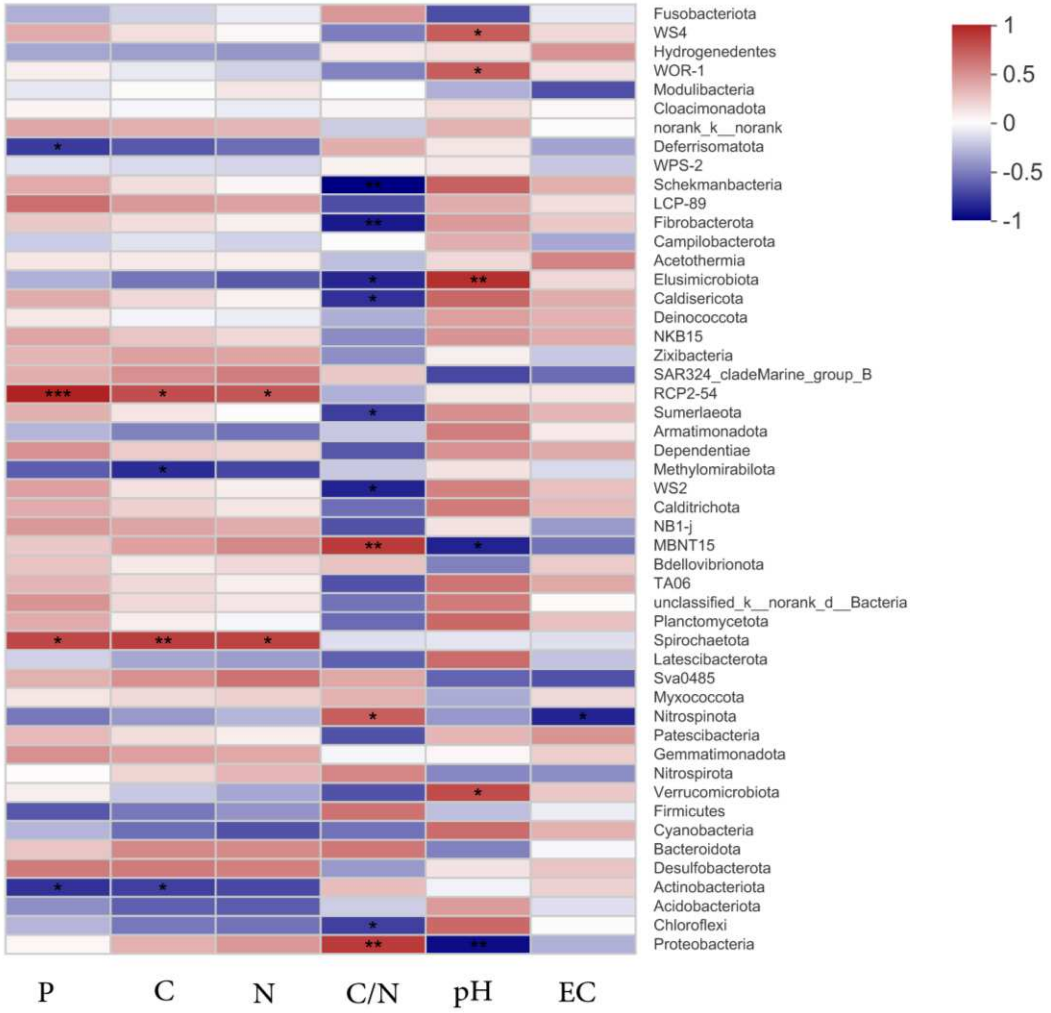

Figure 6. *Correlation heatmap between soil physicochemical properties and soil bacterial phyla. Asterisk indicates significantly different at P <0.05 and P<0.01*

Table 3. *Correlation coefficients between the soil physicochemical properties and soil bacterial α-diversity*

Alpha diversity	TP	TC	TN	C/N	pH	EC
Sobs	0.441	0.985**	0.119	-0.090	-0.175	-0.371
Shannon	0.563	0.720*	-0.030	-0.108	-0.148	-0.037
Simpson	-0.378	-0.630	0.259	0.313	0.380	0.384
Ace	0.242	0.955**	0.165	-0.065	-0.155	-0.347
Chao1	0.212	0.948**	0.134	-0.085	-0.176	-0.310

*P<0.05; **P<0.01

http://www.aloki.hu ● ISSN 1589 1623 (Print) ● ISSN1785 0037 (Online)
DOI: http://dx.doi.org/10.15666/aeer/2005_42574270

Functional annotation space of sediment bacteria

Different types of sediment bacterial communities were predicted and analyzed by the FAPROTAX function prediction software to analyze the changes in the microbial function of the subsoil as shown in *Figure 7*. A total of 48 types of metabolic function-related pathways were identified in all samples, among which 18 types of sediment bacteria were the main functional microorganisms in the nine sampling points (the relative abundance of functional gene sequences was >1%). As shown in *Fig. 7*, the functions with abundance rates greater than 10% among all samples included chemoheterotrophy, phototrophy, cyanobacteria, oxygenic_photoautotrophy, and photoautotrophy. Additionally, the functional structures of S1 and S8, S7 and S9, and S2, S3, S5, and S6 were similar.

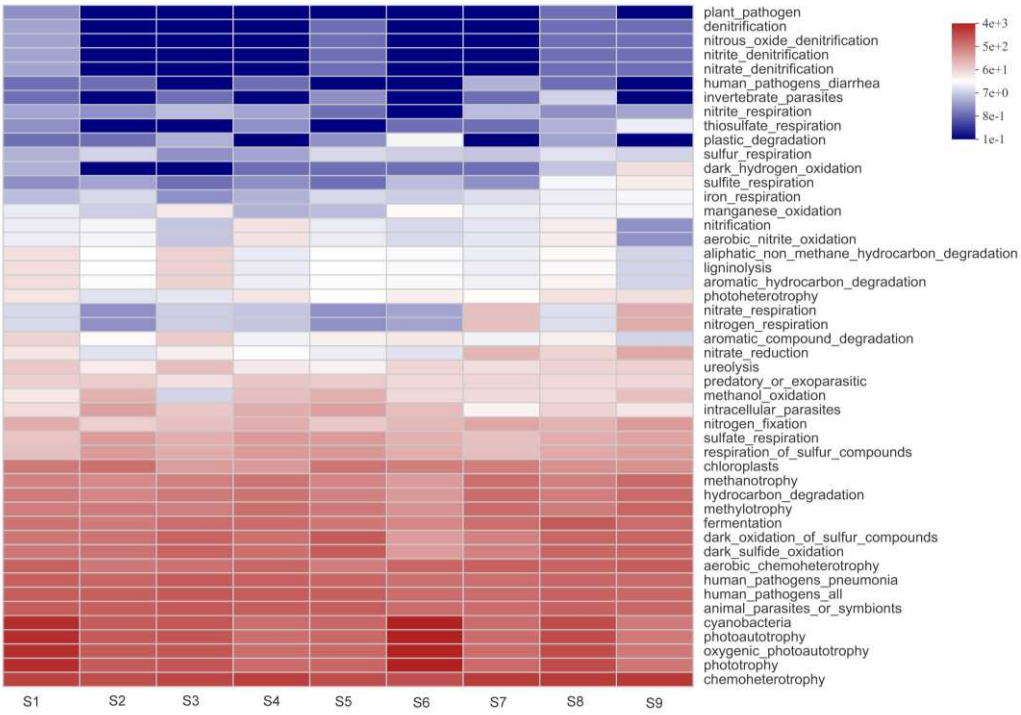

Figure 7. *Prediction of FAPROTAX functions of soil bacteria in sediments of Chagan Lake at different locations*

Discussion

Lake sediment is a unique biological environment that is characterized by the participation of various microorganisms, frequent exchange of substances, and high biological activity (Yang et al., 2018). Soil microbes possess complex metabolisms and reproduce rapidly and are thus considered a key component of soil ecology. However, these microbial communities are highly sensitive to external environmental disturbances. Water depth is a key factor affecting the ecological processes of lakes (Gutknecht et al., 2006), and many studies have demonstrated that changes in flooding degree can significantly affect soil microbial communities (Rees et al., 2006; Mentzer et al., 2006). Wang Peng et al. studied the characteristics of soil bacterial communities in the vegetation zone of Poyang Lake with different water levels and found that the soil

http://www.aloki.hu ● ISSN 1589 1623 (Print) ● ISSN1785 0037 (Online)
DOI: http://dx.doi.org/10.15666/aeer/2005_42574270

under the medium water level had a higher bacterial community abundance. Through the study of soil microorganisms in coastal reed wetlands under different flooding conditions, Zhang et al. (2017) reported that soil archaea and bacterial diversity were higher under flooding conditions. Zhang et al. (2016) studied the bacterial diversity in plant roots at different water level depths and found that the bacterial diversity in the plant roots decreased as water depth increased. Liu (2017) also demonstrated that water depth has a significant effect on bacterial community structures. Our findings indicated that different water depths had a significant impact on the bacterial community diversity in the sediment, which was consistent with the findings of Zhang et al. (2017) and Wang et al. (2016a). In this study, the bacterial diversity in the bottom sediment of Chagan Lake exhibited the following order: low water depth < medium water depth < high water depth. In other words, bacterial diversity was higher in deeper waters. The potential mechanisms that drive this phenomenon will be described below.

Changes in water level conditions can directly change the living environment of the bacterial community in the sediment. Our findings indicated that the soil TP, TC, and TN contents in the deeper sampling points were significantly higher than those in the low- and medium-water levels. High nutrient conditions provide abundant carbon and nitrogen sources, thus promoting microorganism growth. From the perspective of the beta diversity of sediment bacteria, the bacterial community structure of sediments at different water levels was also significantly different. The bacterial community structure in the sediments of the S7 and S9, S1, S5, and S2, and S1, S3, S6, and S8 samples was similar. This was consistent with our bacterial alpha diversity results. That is, the soil richness, uniformity, and community structure of different sample sites varied significantly depending on the water level. Our findings demonstrated that the changes in microbial community abundance, diversity, and community structure composition in response to different water level conditions were largely the same. Deeper waters were associated with greater bacterial community abundance and diversity indices, and therefore water depth could be used as a predictor of bacterial diversity and abundance in Chagan Lake. Understanding the environmental changes caused by different water depths and submerged periods would provide a basis for the development of better management practices for the conservation of Chagan Lake.

As the most important inland lake in Jilin Province, Chagan Lake is the largest lake in the Songliao Plain and an important fishery base in Jilin Province. The water quality of Chagan Lake is directly affected by the quality of its recharge sources (particularly the recharge water in the Qianguo Irrigation Area), as well as the water dynamics in the Songnen Plain and the lake area (Sun et al., 2011). The water quality of Chagan Lake has been steadily deteriorating each year, with decreases in dissolved oxygen concentrations and increases in pH and pollutant concentrations including nitrogen and phosphorus (Du et al., 2020). Recent studies have demonstrated that the water quality of Chagan Lake is close to the Class III standard and is in a state of mild eutrophication (Du et al., 2020). Water pollution leads to increased nutrient fluxes in river waters, destroys water ecosystems, and affects bacterial community compositions (Xue et al., 2018). This study showed that the abundance of Proteobacteria in the bottom sediments of Lake Chagan was the highest (26%), followed by Chloroflexi (14%) and Actinobacteria (10%). This is consistent with a study by Wang et al. (2016b), where sediment bacteria from the bottom of the Hunhe river was dominated by Proteobacteria, as well as other bacterial taxa including Cyanobacteria and Bacteroidetes. Zhang et al. (2016) reported similar results in a study of lake sediments in Finland. Many studies

http://www.aloki.hu ● ISSN 1589 1623 (Print) ● ISSN1785 0037 (Online)
DOI: http://dx.doi.org/10.15666/aeer/2005_42574270

have shown that Proteobacteria have a high proportion in lake sediments (Yu et al., 2020; Hu et al., 2021), and also have strong tolerance to polluted soils, so they are the dominant bacterial community in different lake sediments. Addition, there are a large number of aerobic or facultative bacteria in Proteobacteria, and the lake sediment has been in a state of high water level for a long time, and the relative abundance of Proteobacteria is less under the high water level conditions (*Figure 4a*); Chloroflexi is another dominant bacterial phylum, and the response of Chloroflexi to different water level conditions presents the characteristics of diversity. In our study, it was found that the largest abundance appeared at low water level (*Figure 4a*), this is due to the Chloroflexi are facultative anaerobic bacteria, relying on light energy for photosynthesis and anaerobic respiration under anaerobic conditions (Yu et al., 2020), so under low water level, the environment is more suitable for the growth of Chloroflexi. Actinobacteria is also one of the phyla with higher distribution in this study (*Figure 4a*). The reason may be the surface source pollution in Chagan Lake. Because Actinomycetes belong to Saprophytic bacteria can exist in polluted environments, so we speculate that the increase of Actinomycetes may be due to the influence of farmland and human activities around Chagan Lake, and a large amount of agricultural sewage and pesticides injected into the water body. Particularly, the sediments were mainly dominated by Proteobacteria, as well as Acidobacteria and Actinobacteria. However, different sites can have specific bacterial compositions. In this study, Desulfobacterota and Bacteroidota in S9 were more abundant than in other sampling points. S9 is located at the confluence of Chagan Lake and the Nenjiang River. The research site is seriously polluted by agricultural non-point sources and it is close to the saline-alkali area in western Heilongjiang. Therefore, the study area is affected by high saline-alkali water and water eutrophication, which might explain the high abundance of Desulfobacterota and Bacteroidota at this site. Different soil physicochemical properties can affect the bacterial community structure in sediments (Wang et al., 2016a). Our study demonstrated that EC, TC, and TN, as well as pH and C/N, were the main environmental factors that shaped the bacterial community structure of the Chagan Lake sediments at the phylum level (*Figure 6*). Wang et al. (2017) and Wang et al. (2018) studied the Poyang Lake estuary and found that the main environmental factor of microbial community structure was also pH. Previous studies of lake sediments in the United Kingdom (Wang et al., 2016b) and Qiantang River sediments in China (Liu et al., 2015) also reported that pH was the main factor that influenced bacterial community structure. Xue et al. (2021) also found that soil SOC, TN, and pH were the main factors affecting soil bacterial communities in Jialing River sediments. However, additional studies are needed to comprehensively explore the structure and diversity of bacterial communities at the genus level. Our study identified significant differences in the bacterial community structure of sediments depending on the sampling locations, suggesting that the structure of these bacterial assemblages responds to the environmental pressures of each location.

Conclusion

This study evaluated the variations in the bacterial community structure and diversity of Chagan Lake sediments collected at different points. Our findings indicated that the bacterial community diversity in the sediments of different points of Chagan Lake varied depending on the water depth, with higher diversity occurring in deeper sites.

http://www.aloki.hu ● ISSN 1589 1623 (Print) ● ISSN1785 0037 (Online)
DOI: http://dx.doi.org/10.15666/aeer/2005_42574270

The five dominant phyla in the sediment samples were Proteobacteria, Chloroflexi, Acidobacteriota, Actinobacteriota, and Actinobacteriota. However, the proportions of these and other phyla varied depending on the sampling site, thus demonstrating the influence of environmental characteristics on bacterial communities. Among these environmental factors, EC, pH, and TC had the most significant effects on bacterial community composition and diversity. Taken together, our findings provide key insights into the response of sediment bacterial communities to environmental factors and how these responses affect the functions of lake ecosystems, which is of great significance for the rational utilization of water and biological resources.

Acknowledgements. This work was financially supported by the National Key Research and Development Program of China (2019YFD0900602 and 2019YFD0900605), National Natural Science Foundation of China (No. 31802298) and the Finance Special Fund of Ministry of Agriculture and Rural Affairs (Fisheries Resources and Environment Survey in the Key Water Areas of Northeast China). We also thank Scientific Paper Edit Co. Ltd for linguistic editing.

REFERENCES

[1] Bolyen, E., Rideout, J. R., Dillon, M. R., Bokulich, N. A., Abnet, C. C., Al-Ghalith, G. A., Caporaso, J. G. (2019): Reproducible, interactive, scalable and extensible microbiome data science using QIIME 2. – Nat Biotechnol 37(8): 852-857.

[2] Bu, X. J., Chai, S. L., Zhang, Q. W., Xu, X. C. (2009): The spatial distributions of elements in sediments of lake Chagan in west Jilin Province. – J. Arid Land Resour. Environ 23: 179-184.

[3] Chen, M., Chen, F., Zhao, B., Wu, Q. L., Kong, F. (2010): Seasonal variation of microbial eukaryotic community composition in the large, shallow, subtropical Taihu Lake, China. – Aqua Ecol 44(1): 1-12.

[4] Du, X., Yang, J. S., Song, D., Wang, H. B., Jin, X., Liu, H., Wang, L., Huo, T. B. (2020): Community structure of macroinvertebrate and its relationship with environmental factors in chagan lake. – Chin J Fish 33(6): 61-67.

[5] Fermani, P., Diovisalvi, N., Torremorell, A., Lagomarsino, L., Zagarese, H. E., Unrein, F. (2013): The microbial food web structure of a hypertrophic warm-temperate shallow lake, as affected by contrasting zooplankton assemblages. – Hydrobiologia 714(1): 115-130.

[6] Gutknecht, J. L., Goodman, R. M., Balser, T. C. (2006): Linking soil process and microbial ecology in freshwater wetland ecosystems. – Plant Soil 289(1): 17-34.

[7] Hu, H., Li, D. L., Wang, Y. N., Liu, Y. G., Wang, Y. (2021): Response of bacterial community structure and diversity in sediment of arsenic-rich lakeside wetland to water level change. – Environ Chem 40(5): 1452-1463.

[8] Huang, R., Zhao, D., Jiang, C., Wang, M. (2015): Heterogeneity of bacterial community compositions in surface sediments of three Lake zones in Lake Taihu. – Proceedings of the National Academy of Sciences, India Section B: Biological Sciences 85(2): 465-474.

[9] Li, F., Li, M., Shi, W., Li, H., Sun, Z., Gao, Z. (2017): Distinct distribution patterns of proteobacterial nirK-and nirS-type denitrifiers in the Yellow River estuary, China. – Can J Microbiol 63(8): 708-718.

[10] Liu, S., Ren, H., Shen, L., Lou, L., Hu, B. (2015): pH levels drive bacterial community structure in sediments of the Qiantang River as determined by 454 pyrosequencing. – Front Microbiol 6: 285.

[11] Liu, Y. J. (2017): Response of soil microbial community structure and function to water condition change in Wetland. – Nanchang: Nanchang Univer.

[12] Mentzer, J. L., Goodman, R. M., Balser, T. C. (2006): Microbial response over time to hydrologic and fertilization treatments in a simulated wet prairie. – Plant Soil 284(1): 85-100.

http://www.aloki.hu ● ISSN 1589 1623 (Print) ● ISSN1785 0037 (Online)
DOI: http://dx.doi.org/10.15666/aeer/2005_42574270

[13] R Development Core Team (2017): R: A Language and Environment for Statistical Computing. – R Foundation for Statistical Computing: Vienna, Austria, 2017. Available online: http://www.R-project.org/.
[14] Rees, G. N., Watson, G. O., Baldwin, D. S., Mitchell, A. M. (2006): Variability in sediment microbial communities in a semipermanent stream: impact of drought. – J N Am Benthol Soc 25(2): 370-378.
[15] Shao, K., Gao, G., Wang, Y., Tang, X., Qin, B. (2013): Vertical diversity of sediment bacterial communities in two different trophic states of the eutrophic Lake Taihu, China. – J Environ Sci 25(6): 1186-1194.
[16] Sun, X., Wang, Z., Zhao, C., Xu, L., Dong, Y. (2011): Impact assessment of saline-sodic agricultural drainage on water quality in vented area of Chagan Lake. – Trans Chin Society Agricultu Eng 27(9): 214-219.
[17] Wan, Y., Bai, Y., He, J., Zhang, Y., Li, R., Ruan, X. (2017): Temporal and spatial variations of aquatic environmental characteristics and sediment bacterial community in five regions of Lake Taihu. – Aqua Ecol 51(3): 343-358.
[18] Wang, N. F., Zhang, T., Yang, X., Wang, S., Yu, Y., Dong, L. L., Guo, Y. D., Ma, Y. X., Zang, J. Y. (2016a): Diversity and composition of bacterial community in soils and lake sediments from an arctic lake area. – Front. Microbiol 7. doi: 10.3389/fmicb.2016.01170.
[19] Wang, J., Peng, J., Song, Y., Yuan, L., Shi, G. (2016b): Seasonal changes of microbial community distribution in sediments of hunhe river. – Res Environ Sci 29(2): 202-210.
[20] Wang, P., Chen, B., Zhang, H. (2017): High throughput sequencing analysis of bacterial communities in soils of a typical Poyang lake wetland. – Acta Ecologica Sin 37(5): 1650-1658.
[21] Wang, P., Xiao, H. Y., Zhang, H., Liu, J. Z. (2018): Bacterial communities in the estuarine sediment of Poyang Lake. – China Environ Sci 38(4): 1481-1489.
[22] Xue, Y., Liu, F., Jiang, X., Geng, J., Teng, J., Xie, W., Chen, X. Y. (2018): The diversity of bacterial communities in the sediment of different lake zones of Lake Taihu in winter. – China Environ. Sci 38(2): 719-728.
[23] Xue, Y. Q., Xu, F., Liu, K. H., Wang, J. Y., Zhu, L. P., Zhu, Z. H., Zhang, T. (2021): Non-point Source Pollution (NPSP) Induces Structural and Functional Variation of Bacterial Communities in Sediments of Jialing River. – Environ Sci. 43(5): 2595-2605.
[24] Yang, H., Zhang, G. Z., Yang, X. N., Jian, L. I., Song, X. S., Wang, B. S. (2018): Microbial community of sediment in cellar water and its correlation with environmental factors. – J Lanzhou Jiaotong Univer. 37(3): 110-115.
[25] Ye, W., Liu, X., Lin, S., Tan, J., Pan, J., Li, D., Yang, H. (2009): The vertical distribution of bacterial and archaeal communities in the water and sediment of Lake Taihu. – FEMS Microbiol Ecol 70(2): 263-276.
[26] Yu, X., Zhang, P., Zhang, J., Chen, F., Yang, Y. (2020): Characteristics of distribution patterns of microbial biomass and community structures in the sediments from urban river. – Acta Sci. Circumstantiae 40: 585-596.
[27] Zhang, X. (2016): Microbial community characteristics and microbial indicators evaluation study in fresh water sediment. – Shanghai: Shanghai Univer.
[28] Zhang, Q. Q., Huang, X. R., Guo, X. Y. (2016): Analysis of the characteristics of rhizosphere bacterial diversity from plants with different water level gradients based on T-RFLP. – Acta Ecologica Sin 36: 4518-4530.
[29] Zhang, H. X., Zheng, S. L., Wei, W. C., Wang, B. C., Wang, O. M., Liu, F. H. (2017): Effects of water conditions on the diversity of soil microbial communities in the coastal reed wetlands. – Marine Sci 41(5): 144-152.
[30] Zhang, L., Zhao, T., Shen, T., Gao, G. (2019): Seasonal and spatial variation in the sediment bacterial community and diversity of Lake Bosten, China. – J Basic Microbiol 59(2): 224-233.

http://www.aloki.hu ● ISSN 1589 1623 (Print) ● ISSN1785 0037 (Online)
DOI: http://dx.doi.org/10.15666/aeer/2005_42574270

ORGANIC FERTILIZER INCREASES SOIL ORGANIC CARBON AND CROP YIELD IN FOUR-YEAR TILLAGE AND CROP ROTATIONS ON THE LOESS PLATEAU, CHINA

LIU, Q. [1,2] – YU, Z. Y.[1*] – WANG, X. M.[1] – ZHAO, S. L.[1]

[1]*College of Resources and Environmental Engineering, Tianshui Normal University, Tianshui 741000, China*

[2]*State Key Laboratory of Soil Erosion and Dryland Farming on Loess Plateau, Institute of Soil and Water Conservation, Chinese Academy of Sciences and Ministry of Water Resources, Yangling 712100, China*

**Corresponding author*
e-mail: 448354326@qq.com

(Received 23rd Mar 2022; accepted 11th Jul 2022)

Abstract. To define the role of organic or inorganic fertilizers in the stability and sustainability of soil organic carbon (SOC) and crop yield, we examined changes in SOC and crop yield, as well as their correlation, in nine different fertilization treatments (sheep manure [M], sheep manure and urea [MN], sheep manure and diammonium phosphate [MP], sheep manure, urea, and diammonium phosphate [MNP], urea and diammonium phosphate [NP], urea and potassium sulfate [NK], diammonium phosphate and potassium sulfate [PK], diammonium phosphate, urea, and potassium sulfate [NPK], no fertilizer [CK]) from 2015 to 2018 on the Loess Plateau. The organic carbon content was higher in organic fertilizer (M, MNP, MP, MN) than in inorganic fertilizer treatments (NP, NPK, NK, PK) and the control. Crop yield was higher for organic than for inorganic fertilizers, whereas that of the control was always lower than those in the fertilization treatments. The highest crop yield was obtained in MNP. Crop yield and soil organic matter quality score correlated positively, with correlation coefficients ranging from 0.5994 to 0.7151. Our results provide a theoretical basis for organic and inorganic fertilizer application in dry farming areas on the Loess Plateau and aid the long-term healthy development of soil in cultivated areas.
Keywords: *different fertilization treatments, dry land, farmland soils, SOC content, food crops*

Introduction

Increasing the content of organic carbon in soil is not only conducive to the development of agriculture but also plays a vital role in ecosystems globally (Blair et al., 2006). However, the overexploitation of farmland has caused a continuous decrease in the soil organic carbon (SOC) content and soil degradation, ultimately affecting the development of agriculture and challenging the sustainable use of soil (Adams et al., 2020; Akoto-Danso et al., 2019). Soil organic carbon is an important basis for soil fertility (Beza et al., 2016) and regulates physical, chemical, and biological processes in soil, and is a prerequisite for the sustainable utilization of land and high and stable crop yields (Arunrat et al., 2020; Bhatt et al., 2020; Bibi et al., 2019). In addition to being influenced by local climate and soil properties, the SOC content is determined by the fertilization method (Bista et al., 2019; Cai et al., 2016). Fertilization has become a common farmland management measure for improving crop yield, an important factor affecting the conversion rate and accumulation of SOC, and the primary factor in the evolution of soil fertility (Cenini et al., 2016; Van Groenigen et al., 2017). Fertilization mainly affects the organic carbon content and soil dynamics by increasing the bio-yield

http://www.aloki.hu ● ISSN 1589 1623 (Print) ● ISSN 1785 0037 (Online)
DOI: http://dx.doi.org/10.15666/aeer/2005_42714282

of crops and the input of organic residues to the soil, as well as by affecting the number and activity of soil microorganisms and thereby the biodegradation of organic matter (Chen et al., 2015). The effect of fertilization on increasing SOC contents also depends on climatic conditions (Choudhary et al., 2019; Dong et al., 2015). A variety of fertilizers have been widely used in agricultural production to provide sufficient nutrients for plant growth and increase aboveground biomass production (Espinoza et al., 2017). Increased plant biomass, as an important source of SOC, increases the supply of soil carbon sources and the amount of organic carbon in soil (Frossard et al., 2016). Fertilizer application slowly changes the physical and chemical characteristics of the soil, affecting microbial and root activity in the soil and indirectly the SOC reservoir (Gao et al., 2015; Gelaw et al., 2015).

The rapid development of the fertilizer industry has decreased the dependence of agriculture on organic fertilizers, leading to a decreased amount of organic matter in farmland soils and an altered balance of SOC (Gwon et al., 2019). The application of fertilizer, especially when unbalanced, has a negative effect on the SOC content, the accumulation of SOC, as well as the content of SOC components (Han et al., 2020). The application of organic fertilizer has the opposite effect (He et al., 2015a). Organic fertilizer is rich in elements and organic nutrients needed for plant growth, meets the nutrient needs of different long-term crops, improves soil structure as well as physical and chemical properties, directly affects the level of the comprehensive soil fertility index, and renders crop yields stable and sustainable (He et al., 2015b). Increasing the application of organic fertilizer as a substitute for inorganic fertilizers is an effective way to solve problems related to the application of inorganic fertilizers (Horak et al., 2020). To this end, many studies have been carried out to elucidate changes in the SOC content after soil fertilization and the relationship between crop yield and the SOC content (Hwang et al., 2020). Li et al. (2015) and others found that the SOC content was significantly increased after long-term application of organic fertilizer and a combined application of organic and inorganic fertilizer. Liu et al. (2018) reported that long-term application of organic fertilizer was positively linearly correlated with the total organic carbon and nitrogen content of farmland. After entering the soil, organic fertilizer effectively improves soil physical and chemical characteristics in the tillage layer, and successfully regulates the content of soil nitrogen, phosphorus, and potassium, increasing the SOC content (Iqbal et al., 2019; Jalal et al., 2020). The large amount of carbon and nitrogen sources provided by organic fertilizer increase the microbial biomass, thus promoting root–microbial interactions (Kolbe et al., 2015).

The Loess Plateau region is a typical rain-fed agricultural area. For a long time, agricultural production was mainly focused on cultivation of food crops due to prevalent drought conditions and low precipitation, soil erosion and degradation, as well as wind and sand hazards. The SOC content is only approximately 1%, rarely reaching 1.5%. In the past 20 years, with the increase in the farmers' investment in land, the input of inorganic fertilizers has increased, neglecting the use of organic fertilizer, a practice that has resulted in reduced soil quality. Therefore, the effect of fertilization on crop yield and SOC in the Loess Plateau needs to be studied to develop a sustainable agriculture, improve the quality of cultivated land, increase agricultural production and income, and reduce greenhouse gas emissions. Several studies have been conducted to assess the impact of the combined use of inorganic fertilizers and organic materials on crop yield and soil nutrients. However, such research has hardly been conducted in the Loess Plateau region. Therefore, the purpose of this study was to assess the stability and

http://www.aloki.hu ● ISSN 1589 1623 (Print) ● ISSN 1785 0037 (Online)
DOI: http://dx.doi.org/10.15666/aeer/2005_42714282

sustainability of increasing SOC and crop yield using long-term experiments. We show that the use of only organic fertilizer or a combination of inorganic and organic fertilizers increases the SOC content and ultimately increases crop yield.

Materials and methods

Study sites

The field experiment was conducted in 2015 and 2018 at a study site located in the middle of the Loess Plateau (36°51′N, 109°18′E). The site is located 1068 m above sea level (*Fig. 1*); it has a mean annual temperature of 8.8 °C and an annual precipitation level of 500.0 mm in the last 10 years. The recorded annual precipitation was 381.2 mm in 2015 and 492.1 mm in 2016. The recorded annual precipitation was 557.6 mm in 2017 and 536.3 mm in 2018. The precipitation during the growth period (between March and September) was 240.5 mm in 2015, accounting for 63% of the total annual precipitation, 417.9 mm in 2016, accounting for 79.47% of the total annual precipitation, 443.1 mm in 2017, accounting for 79.47% of the total annual precipitation; and 503.1 mm in 2018, accounting for 93.8% of the total annual precipitation 2018 (*Table 1*). The soil type in the study site was loess soil; basic soil physical and chemical properties were measured at the depth of 0–20 cm before fertilization (*Table 2*).

Figure 1. *Test field*

Table 1. *Precipitation in the study area from 2015 to 2018 (mm)*

Year	Annual precipitation	Growth period precipitation
2015	381.2 mm	240.5 mm
2016	492.1 mm	417.9 mm
2017	557.6 mm	443.1 mm
2018	536.3 mm	503.1 mm
Average precipitation in the last 10 years	500.0 mm	427.2 mm

http://www.aloki.hu ● ISSN 1589 1623 (Print) ● ISSN 1785 0037 (Online)
DOI: http://dx.doi.org/10.15666/aeer/2005_42714282

Table 2. *Basic physical and chemical properties of the soil before fertilization*

Soil depth (cm)	Bulk density	SOM	TN	TP	pH
20 cm	1.387	8.053	0.382	0.588	8.42

SOM, soil organic matter. TN, soil total nitrogen. TP, soil total phosphorus, all in ($g \cdot kg^{-1}$)

Experimental design

Organic and inorganic fertilizers were used. The nitrogen fertilizers (N) were urea and diammonium phosphate, the phosphate fertilizer (P) was diammonium phosphate, the potassium fertilizer (K) was potassium chloride, and the organic fertilizer (M) was sheep manure. Organic fertilizer treatments were the following: M, MN, MP, and MNP. Inorganic fertilizer treatments were NP, NK, PK, and NPK. In addition, a no-fertilizer treatment was used as the control (CK). The fertilizers were spread evenly on the soil surface before sowing. The nine fertilization practices are shown in *Table 3*.

Table 3. *Experimental fertilization levels*

Treatment	Illustration
M	Sheep manure (0.75 kg/m^2)
MN	Sheep manure (0.75 kg/m^2) + Urea 0.021 kg/m^2
MP	Sheep manure (0.75 kg/m^2) + Diammonium phosphate (0.017 kg/m^2)
MNP	Sheep manure (0.75 kg/m^2) + Urea (0.021 kg/m^2) + Diammonium phosphate (0.017 kg/m^2)
NP	Urea 0.021 kg/m^2 + Diammonium phosphate (0.017 kg/m^2)
NK	Urea (0.021 kg/m^2) + Potassium sulfate (0.012 kg/m^2)
PK	Diammonium phosphate (0.017 kg/m^2) + Potassium sulfate (0.012 kg/m^2)
NPK	Diammonium phosphate (0.017 kg/m^2) + Urea (0.021 kg/m^2) + Potassium sulfate (0.012 kg/m^2)
CK	No fertilizer

Local heat and moisture conditions dictate that crops are only grown once a year. Millet was planted in 2015, and the millet cultivar was Changsheng 7. Broomcorn millet was planted in 2016, and the broomcorn millet cultivar was BaiRuanmei. Millet was planted in 2017, and the millet cultivar was Changsheng 7. Soybeans were planted in 2018, and the soybean variety planted was Zhonghuang 35. Each of the nine treatments contained 4 plots, yielding a total of 36 plots. Each plot was 3.5 m long and 8.57 m wide (plot area of 30 m^2). The soil fertility and environmental conditions in all plots were uniform. Organic fertilizer, potash fertilizer, and phosphate fertilizer were each applied once, urea fertilizer was applied at a rate of 136 g per plot, and the remaining 500 g of nitrogen fertilizer were applied during the flowering period. The millet was fertilized with urea on April 24th, 2015, and supplementary nitrogen fertilizer was added on July 1rd. The broomcorn millet was fertilized with urea on April 26th, 2016, and supplementary nitrogen fertilizer was added on July 16th. The millet was fertilized with urea on April 27th, 2017, and supplementary nitrogen fertilizer was added on July 3rd. Urea fertilizer was added to soybeans on April 28th, 2018, and supplementary nitrogen fertilizer was added on July 26th. The experimental design of the different fertilization experiments is shown in *Table 4*.

http://www.aloki.hu ● ISSN 1589 1623 (Print) ● ISSN 1785 0037 (Online)
DOI: http://dx.doi.org/10.15666/aeer/2005_42714282

Table 4. *Experimental design of the different fertilization experiments*

Experimental plots								
1	2	3	4	5	6	7	8	9
MN	M	NPK	PK	NK	NP	CK	MNP	MP
10	11	12	13	14	15	16	17	18
MP	MN	PK	NK	CK	NPK	NK	M	MNP
19	20	21	22	23	24	25	26	27
MNP	MP	CK	NK	NP	PK	NPK	MN	M
28	29	30	31	32	33	34	35	36
M	MNP	NP	CK	NPK	NK	PK	MP	MN

M, organic fertilizer; MN, organic fertilizer combined with nitrogen fertilizer; MP, organic fertilizer combined with phosphate fertilizer; MNP, organic fertilizer combined with nitrogen and phosphate fertilizer; NP, nitrogen fertilizer combined with phosphate fertilizer; NK, nitrogen fertilizer combined with potassium fertilizer; PK, phosphorus combined with potassium fertilizer; NPK, nitrogen combined with phosphate and potassium fertilizer; CK, no-fertilizer control. Consecutive integers (1, 2... 27) indicate the plot number

Soil sampling and crop harvesting

Soil sample collection method: taking each plot as a unit, the soil sampling point was more than 1 m away from the boundary of the sample plot. Sampling points were randomly selected with an S shape. Surface debris was then removed and soil samples were collected. All soil samples from the same sampling point were combined and then passed through a 2-mm sieve. Samples were stored and labelled after the relevant sampling information had been recorded. The soil samples were transported to the laboratory, air-dried naturally, plant roots and other impurities removed, and the SOM content measured. SOM was analyzed using the dichromate oxidation method. The 2015 millet was harvested on October 10th. The 2016 broomcorn millet was harvested on October 4th. The 2017 millet was harvested on October 12th. The 2018 soybean crop was harvested on October 4th. In 2017, SOM was measured on October 12th. In 2016, SOM was measured on October 6th. In 2017, SOM was measured on October 13th. In 2018, SOM was measured on October 5th. At the end of the growing season, three quadrats (1 m × 1 m) were harvested in each plot by cutting at the soil surface level; the harvested plants were dried in an oven (75 °C, 24 h), weighed, and the value was converted to plot yield. The final crop yield was obtained by harvesting four replicates of each treatment.

Calculations and statistics

The productivity of the cropping system was determined using the sustainable yield index. The sustainable yield index (*SYI*) developed by Singh was used for assessment (Zhou et al., 2019):

$$SYI = \bar{Y} - \sigma_{n-1}/Y_{max}$$

where $\overline{Y}$ is the mean yield, σ_{n-1} is the standard deviation, and Y_{max} is the maximum yield data obtained from the treatment in any year.

One-way ANOVA was used to examine the effects of fertilization treatment on SOC, crop yield, and the sustainable yield index (SYI; $P < 0.05$). Before the analysis, we

http://www.aloki.hu ● ISSN 1589 1623 (Print) ● ISSN 1785 0037 (Online)
DOI: http://dx.doi.org/10.15666/aeer/2005_42714282

performed a normality and homogeneity test of the data. Linear regression analysis was used to show the relationship between crop yield and SOC. All statistical analyses were performed using the software package IBM SPSS Statistics (version 26.0). The differences between the treatments were calculated using the least significance difference test at a 0.05 probability level. Figures were prepared using Origin 9.0.

Results

Soil organic carbon

To evaluate the impact of various fertilization treatments on crop yield, we analyzed the effects of MP, MN, PK, NP, CK, NPK, NK, and MMNP fertilization. We studied the effects of long-term application of inorganic fertilizers (N, P), organic fertilizer, and combined application of inorganic and organic fertilizers on SOC dynamics. The variation trend of SOC in different treatments was similar over time. The increase in soil SOC by organic fertilizer treatment, especially in combination with inorganic fertilizer, was significant in comparison to that observed by inorganic fertilizer treatment and no fertilizer application ($P < 0.05$).

Overall, higher SOC contents were recorded after fertilization. In 2015, the SOC content of the M, MN, MP, MNP, NP, NK, PK, and NPK plots was greater by 80%, 78%, 85%, 94%, 18%, 13%, 9%, and 16% compared with the CK treatment, respectively. In 2016, the SOC content of the M, MN, MP, MNP, NP, NK, PK, and NPK plots was higher than that of the CK plots by 77%, 80%, 82%, 83%, 23%, 12%, 5%, and 22%, respectively. In 2017, the SOC content of the M, MN, MP, MNP, NP, NK, PK, and NPK plots was greater by 74%, 90%, 91%, 93%, 17%, 8%, 4%, and 17% compared with the CK treatment, respectively. In 2018, the SOC content of the M, MN, MP, MNP, NP, NK, PK, and NPK plots was higher than that of the CK plots by 74%, 86%, 86%, 101%, 25%, 4%, 1%, and 22%, respectively (*Fig. 2*).

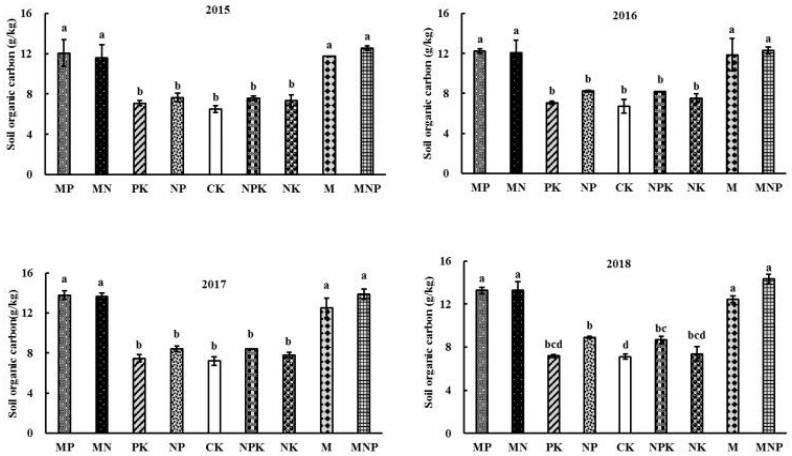

Figure 2. *Soil organic carbon content (mean ± standard error) at different fertilization from 2015 to 2018. Note: Values in the same column and the same year followed by different letters indicate significant differences (Duncan P < 0.05). The error bar is the standard deviation. M, organic fertilizer; MN, organic fertilizer combined with nitrogen fertilizer; MP, organic fertilizer combined with phosphate fertilizer; MNP, organic fertilizer combined with nitrogen and phosphate fertilizer; NP, nitrogen fertilizer combined with phosphate fertilizer; NK, nitrogen fertilizer combined with potassium fertilizer; PK, phosphorus combined with potassium fertilizer; NPK, nitrogen combined with phosphate and potassium fertilizer*

http://www.aloki.hu ● ISSN 1589 1623 (Print) ● ISSN 1785 0037 (Online)
DOI: http://dx.doi.org/10.15666/aeer/2005_42714282

Crop yield

The average yield for the period 2015–2018 was used to evaluate the long-term effects of different fertilization practices. Organic fertilizer treatments increased crop yield significantly more than inorganic fertilizer and no fertilizer treatments ($P < 0.05$). Overall, higher crop yield was recorded after fertilization. In 2015, the crop yield of the M, MN, MP, MNP, NP, NK, PK, and NPK plots was greater by 22%, 2%, 25%, 81%, 1%, 48%, 42%, and 42% compared with the CK treatment, respectively. In 2016, the crop yield of the M, MN, MP, MNP, NP, NK, PK, and NPK plots was higher than that of the CK plots by 279%, 316%, 198%, 337%, 271%, 28%, 28%, and 177%, respectively. In 2017, the crop yield of the M, MN, MP, MNP, NP, NK, PK, and NPK plots was greater by 266%, 317%, 121%, 320%, 295%, 177%, 101%, and 205% compared with the CK treatment, respectively. In 2018, the crop yield of the M, MN, MP, MNP, NP, NK, PK, and NPK plots was higher than that of the CK plots by 118%, 171%, 189%, 239%, 119%, 120%, 146%, and 165%, respectively (*Fig. 3*).

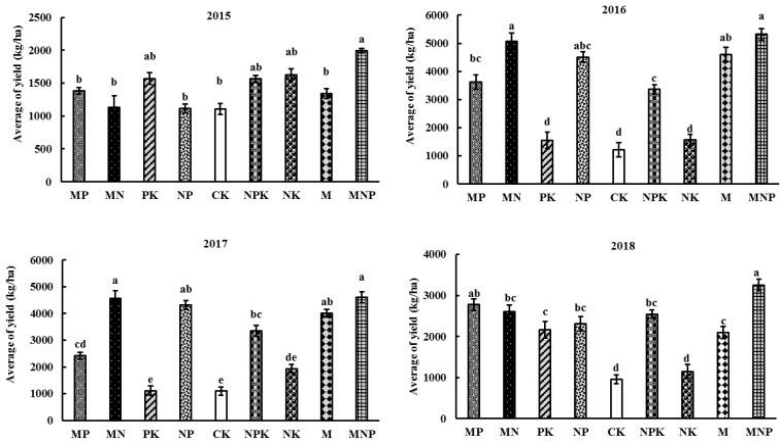

Figure 3. *Average yield (mean ± standard error) at different fertilization treatments in 2015, 2016, 2017, and 2018. Note: Values in the same column and the same year followed by different letters indicate significant differences (Duncan $P < 0.05$). The error bar is the standard deviation. M, organic fertilizer; MN, organic fertilizer combined with nitrogen fertilizer; MP, organic fertilizer combined with phosphate fertilizer; MNP, organic fertilizer combined with nitrogen and phosphate fertilizer; NP, nitrogen fertilizer combined with phosphate fertilizer; NK, nitrogen fertilizer combined with potassium fertilizer; PK, phosphorus combined with potassium fertilizer; NPK, nitrogen combined with phosphate and potassium fertilizer; CK, no-fertilizer control*

Correlation among different parameters and SYI

Using Pearson correlation analysis (*Fig. 4*), we found a significant correlation between crop yield and SOC in 2015, 2016, 2017, and 2018 ($P < 0.05$). The SYI value for the for yield in organic fertilizer treatments was greater than that in the other treatments, indicating that application of organic fertilizer increases crop yield as compared to the other fertilization treatments (*Table 5*). The SYI value was the highest in the MNP treatment, while the lowest SYI value was in the CK treatment. The SYI values in the other organic fertilizer treatments (MP, MN, M) were similar to that of the MNP treatment. These results indicate that organic fertilizer has the potential to maintain a sustainable crop yield.

http://www.aloki.hu ● ISSN 1589 1623 (Print) ● ISSN 1785 0037 (Online)
DOI: http://dx.doi.org/10.15666/aeer/2005_42714282

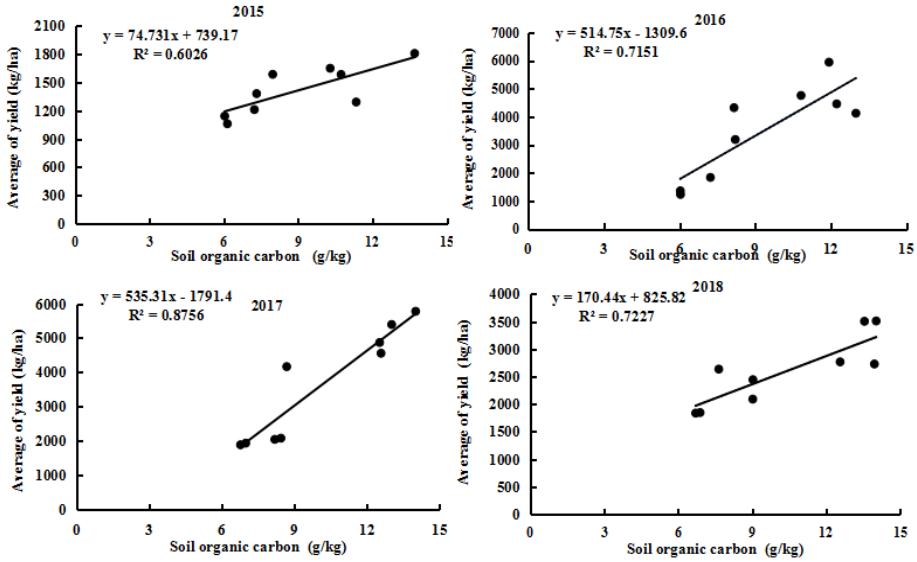

Figure 4. *Correlation of SOC and crop yields in 2015, 2016, 2017, and 2018. Note: Values in the same column and the same year followed by different letters indicate significant differences (Duncan P < 0.05). M, organic fertilizer; MN, organic fertilizer combined with nitrogen fertilizer; MP, organic fertilizer combined with phosphate fertilizer; MNP, organic fertilizer combined with nitrogen and phosphate fertilizer; NP, nitrogen fertilizer combined with phosphate fertilizer; NK, nitrogen fertilizer combined with potassium fertilizer; PK, phosphorus combined with potassium fertilizer; NPK, nitrogen combined with phosphate and potassium fertilizer; CK, no-fertilizer control*

Table 5. *Sustainable yield index (SYI) values for the four years of growing influenced by different fertilization treatments*

Years	MP	MN	PK	NP	CK	NPK	NK	M	MNP
SYI_{2015}	0.60ab	0.62a	0.49b	0.48b	0.30c	0.50b	0.50b	0.57ab	0.69a
SYI_{2016}	0.57ab	0.61a	0.47b	0.47b	0.31c	0.48b	0.49b	0.54ab	0.67a
SYI_{2017}	0.58ab	0.61a	0.46b	0.45b	0.29c	0.51b	0.48b	0.55ab	0.68a
SYI_{2018}	0.59ab	0.60a	0.51b	0.49b	0.30c	0.48b	0.48b	0.58ab	0.70a

Values in the same column and the same year followed by different letters indicate significant differences (Duncan P < 0.05)

Discussion

Organic fertilizers significantly increased the SOC content and crop yield compared with non-organic fertilizers and no fertilizer application. Different fertilization models significantly increased the SOC content. Their application increased crop growth, which in turn increased the amount of crop residues. As crop residues are decomposed, they are converted into organic carbon, thereby increasing the SOC content (Zhao et al., 2019; Jalal et al., 2020). The applied inorganic fertilizers were not as effective as the organic fertilizers in increasing the SOC content, mainly because inorganic fertilizer application increased the activity of soil microorganisms and thus the consumption of SOC (Zanatta et al., 2019). The total organic carbon reservoir in the soil originated from decomposition in the soil (Yu et al., 2020; Yang et al., 2019). Consequently, SOC

http://www.aloki.hu ● ISSN 1589 1623 (Print) ● ISSN 1785 0037 (Online)
DOI: http://dx.doi.org/10.15666/aeer/2005_42714282

accumulation was greater than its consumption. The application of inorganic fertilizer increased the SOC content, although the increase was lower than in the soil amended with organic fertilizers. These results were consistent with those of other studies (Yusuf et al., 2015).

The organic carbon content of the soil amended with organic fertilizer was greater than that of the soil treated with inorganic fertilizers and the control. The SOC accumulation rate in the NPK, NK, and PK treatments during the four years of crop rotation was small because of the relatively small rate of organic carbon formation, which is mainly due to plant residues, root residues, and root secretions. There was no input of exogenous organic carbon. In the present study, the crop yield in the CK treatment was significantly lower than that in the treatments with fertilizers, confirming that fertilization affected the crop yield. The highest crop yield obtained in the MNP treatment is attributed to N and P, which were directly supplemented to the soil, while mineral fertilizer regulates the release intensity and rate of inorganic nutrients in the soil. The crop thus has a continuous access to nutrients, the nutrient demands are met at all stages of plant growth, and consequently crop yield is improved (Yan et al., 2020; Yadav et al., 2020). Besides the application of organic fertilizers, decomposition in soil is another process that produces organic acids, promotes soil nutrient cycling, improves soil efficiency, and increases crop yield, which has been reported in various other studies (Xu et al., 2015, 2020; Wild et al., 2017).

We observed a positive correlation ($P < 0.05$) among SOC, crop, and crop yield in all growing seasons. The results indicated that crop yield increased with increasing SOC. There was a significant difference in crop yield and the SYI under different long-term fertilization protocols. The highest SYI was obtained after application of organic fertilizer, it was lower in treatments with inorganic fertilizers, and the lowest in the control. Mineral nutrients provided by inorganic fertilizers were immediately released into the soil and absorbed and utilized by the crops (Wang et al., 2015, 2020); therefore, soil fertility was short-lived and the SYI was low. Only a tiny fraction of mineral nutrients was immediately released from organic manure, and most of the nutrients were released slowly; the process was longer and thus could meet the nutrient demand of the crops throughout the whole season (Villamil et al., 2015). This reduces the reliance on chemical fertilizers, maintains the stability and sustainability of crop production, and preserves a high SYI.

Conclusions

Long-term fertilization can significantly improve the SOC content. The SOC content in treatments with organic fertilizers was higher than that in treatments with inorganic fertilizers and in the control. Application of organic fertilizer accelerated the accumulation of SOC, nitrogen, and other nutrients as compared to the application of inorganic fertilizer or no fertilizer application. Long-term fertilization also significantly improved crop yield. The highest crop yield was obtained with MNP fertilization, indicating that organic fertilizer combined with N and P fertilizer can effectively improve crop yields by directly supplementing soil nutrients while regulating the release of nutrients to meet the needs of the crops. The crop yield dependence on fertilizer is thus reduced. The combination of organic and inorganic fertilizers in the soil of the dry farming area on the Loess Plateau can promote the long-term healthy development of soil in this cultivated area.

http://www.aloki.hu ● ISSN 1589 1623 (Print) ● ISSN 1785 0037 (Online)
DOI: http://dx.doi.org/10.15666/aeer/2005_42714282

Funding. This research was supported by the National Science Foundation of China (42077075).

Acknowledgments. Many thanks to Yuan Gao for their technical assistance in the laboratory work. We would like to thank Pei Ge and Ruixi Liu for providing statistics assistance.

Conflict of interests. The authors declare no conflict of interests.

REFERENCES

[1] Adams, A. M., Gillespie, A. W., Dhillon, G. S., Kar, G., Minielly, C., Koala, S., Ouattara, B., Kimaro, A. A., Bationo, A., Schoenau, J. J. (2020): Long-term effects of integrated soil fertility management practices on soil chemical properties in the Sahel. – Geoderma 366.

[2] Akoto-Danso, E. K., Manka'Abusi, D., Steiner, C., Werner, S., Haering, V., Nyarko, G., Marschner, B., Drechsel, P., Buerkert, A. (2019): Agronomic effects of biochar and wastewater irrigation in urban crop production of Tamale, northern Ghana. – Nutr Cycl Agroecosys 115: 231-247.

[3] Arunrat, N., Pumijumnong, N., Sereenonchai, S., Chareonwong, U. (2020): Factors Controlling soil organic carbon sequestration of highland agricultural areas in the Mae Chaem Basin, Northern Thailand. – Agronomy-Basel 10.

[4] Beza, S. A., Assen, M. A. (2016): Soil carbon and nitrogen changes under a long period of sugarcane monoculture in the semi-arid East African Rift Valley, Ethiopia. – J Arid Environ 132: 34-41.

[5] Bhatt, M. K., Raverkar, K. P., Chandra, R., Pareek, N., Labanya, R., Kumar, V., Kaushik, S., Singh, D. K. (2020): Effect of long-term balanced and imbalanced inorganic fertilizer and FYM application on chemical fraction of DTPA-extractable micronutrients and yields under rice-wheat cropping system in mollisols. – Soil Use Manage 36: 261-273.

[6] Bibi, Z., Ding, W., Jilani, G., Khan, N. U., Saleem, H. (2019): Organic and mineral fertilizers sway the nitrogen availability to plants via microbial diversity - a long-term impact. – Pak J Bot 51: 1517-1522.

[7] Bista, P., Ghimire, R., Machado, S., Pritchett, L. (2019): Biochar effects on soil properties and wheat biomass vary with fertility management. – Agronomy-Basel 9.

[8] Blair, N., Faulkner, R. D., Till, A. R., Crocker, G. J. (2006): Long-term management impacts on soil C, N and physical fertility - Part III: Tamworth crop rotation experiment. – Soil Till Res 91: 48-56.

[9] Cai, J., Wu, Q., Zhong, X., Hu, J., Hu, Q. (2016): Soil organic carbon and total nitrogen in reclaimed paddy fields vary with reclamation duration in Poyang Lake region. – Shengtaixue Zazhi 35: 2009-2013.

[10] Cenini, V. L., Fornara, D. A., McMullan, G., Ternan, N., Carolan, R., Crawley, M. J., Clement, J., Lavorel, S. (2016): Linkages between extracellular enzyme activities and the carbon and nitrogen content of grassland soils. – Soil Biol Biochem 96: 198-206.

[11] Chen, L., He, Z., Du, J., Yang, J., Zhu, X. (2015): Patterns and controls of soil organic carbon and nitrogen in alpine forests of northwestern China. – Forest Sci 61: 1033-1040.

[12] Choudhary, A., Yadav, S. R., Parewa, H. P. (2019): Effect of wool waste in combination with farm yard manure and fertilizer on soil properties in aridisol of Bikaner, Rajasthan, India. – J Environ Biol 40: 1067-1072.

[13] Dong, W., Zhang, X., Wang, H., Dai, X., Sun, X., Qiu, W., Yang, F. (2012): Effect of different fertilizer application on the soil fertility of paddy soils in red soil region of southern China. – Plos One 7.

[14] Espinoza, Y., Lozano, Z., Malpica, L. (2017): Effect of the tillage system on the structure and fractions of carbon and nitrogen in the soil and its impact on the development of corn. – Rev Fac Agron Luz 34: 448-476.

http://www.aloki.hu ● ISSN 1589 1623 (Print) ● ISSN 1785 0037 (Online)
DOI: http://dx.doi.org/10.15666/aeer/2005_42714282

[15] Frossard, E., Buchmann, N., Biinemann, E. K., Kiba, D. I., Lompo, F., Oberson, A., Tamburini, F., Traore, O. Y. A. (2016): Soil properties and not inputs control carbon : nitrogen : phosphorus ratios in cropped soils in the long term. – Soil 2: 83-99.
[16] Gao, W., Yang, J., Ren, S., Liu, H. (2015): The trend of soil organic carbon, total nitrogen, and wheat and maize productivity under different long-term fertilizations in the upland fluvo-aquic soil of North China. – Nutr Cycl Agroecosys 103: 255.
[17] Gelaw, A. M., Singh, B. R., Lal, R. (2015): Organic carbon and nitrogen associated with soil aggregates and particle sizes under different land uses in Tigray, Northern Ethiopia. – Land Degrad Dev 26: 690-700.
[18] Gwon, H. S., Khan, M. I., Yoon, Y. E., Lee, Y. B., Kim, P. J., Hwang, H. Y. (2019): Unexpected higher decomposition of soil organic matter during cold fallow season in temperate rice paddy. – Soil Till Res 192: 250-257.
[19] Han, X., Hu, C., Chen, Y., Qiao, Y., Liu, D., Fan, J., Li, S., Zhang, Z. (2020): Crop yield stability and sustainability in a rice-wheat cropping system based on 34-year field experiment. – Eur J Agron 113.
[20] He, H., Yang, X., Wang, D., Sun, Y., Yin, C., Li, T., Li, Y., Zhou, G., Zhang, L., Liu, Q. (2015a): Ecological stoichiometric characteristics of soil carbon, nitrogen and phosphorus of Sibiraea angustata shrub in eastern Qinghai-Tibetan Plateau. – Chinese Journal of Applied and Environmental Biology 21: 1128-1135.
[21] He, Y. T., Zhang, W. J., Xu, M. G., Tong, X. G., Sun, F. X., Wang, J. Z., Huang, S. M., Zhu, P., He, X. H. (2015b): Long-term combined chemical and manure fertilizations increase soil organic carbon and total nitrogen in aggregate fractions at three typical cropland soils in China. – Sci Total Environ 532: 635-644.
[22] Horak, J., Simansky, V., Aydin, E. (2020): Benefits of biochar and its combination with nitrogen fertilization for soil quality and grain yields of barley, wheat and corn. – J Elementol 25: 443-458.
[23] Hwang, H. Y., Cuello, J., Kim, S. Y., Lee, J. G., Kim, P. J. (2020): Green manure application accelerates soil organic carbon stock loss under plastic film mulching. – Nutr Cycl Agroecosys 116: 257-269.
[24] Iqbal, A., He, L., Khan, A., Wei, S., Akhtar, K., Ali, I., Ullah, S., Munsif, F., Zhao, Q., Jiang, L. (2019): Organic manure coupled with inorganic fertilizer: an approach for the sustainable production of rice by improving soil properties and nitrogen use efficiency. – Agronomy-Basel 9.
[25] Jalal, F., Arif, M., Akhtar, K., Khan, A., Naz, M., Said, F., Zaheer, S., Hussain, S., Imtiaz, M., Khan, M. A., et al. (2020): Biochar integration with legume crops in summer gape synergizes nitrogen use efficiency and enhance maize yield. – Agronomy-Basel 10.
[26] Kolbe, S. E., Townsend-Small, A., Miller, A. I., Culley, T. M., Cameron, G. N. (2015): Effect of Lonicera maackii on soil carbon and nitrogen in southwestern Ohio forests. – Invas Plant Sci Mana 8: 375-384.
[27] Li, S., Su, J., Liu, W., Lang, X., Huang, X., Jia, C., Tong, Q., Tang, H. (2015): Changes in Soil organic carbon and nitrogen stocks in Pinus kesiya var. langbiannesis plantation. – Forest Research 28: 810-817.
[28] Liu, C., Nie, Y., Zhang, Y., Tang, J., Siddique, K. H. M. (2018): Introduction of a leguminous shrub to a rubber plantation changed the soil carbon and nitrogen fractions and ameliorated soil environments. – Sci Rep-Uk 8.
[29] Van Groenigen, J. W., Van Kessel, C., Hungate, B. A., Oenema, O., Powlson, D. S., Van Groenigen, K. J. (2017): Response to the letter to the editor regarding our viewpoint "Sequestering soil organic carbon: a nitrogen dilemma". – Environ Sci Technol 51: 11503-11504.
[30] Villamil, M. B., Nafziger, E. D. (2015): Corn residue, tillage, and nitrogen rate effects on soil carbon and nutrient stocks in Illinois. – Geoderma 253: 61-66.
[31] Wang, X., Zhou, W., Liang, G., Song, D., Zhang, X. (2015): Characteristics of maize biochar with different pyrolysis temperatures and its effects on organic carbon, nitrogen

http://www.aloki.hu ● ISSN 1589 1623 (Print) ● ISSN 1785 0037 (Online)
DOI: http://dx.doi.org/10.15666/aeer/2005_42714282

and enzymatic activities after addition to fluvo-aquic soil. – Sci Total Environ 538: 137-144.

[32] Wang, K., Li, F., Dong, Y. (2020): Methane emission related to enzyme activities and organic carbon fractions in paddy soil of South China under different irrigation and nitrogen management. – J Soil Sci Plant Nut 20: 1397-1410.

[33] Wild, B., Alaei, S., Bengtson, P., Bode, S., Boeckx, P., Schnecker, J., Mayerhofer, W., Rutting, T. (2017): Short-term carbon input increases microbial nitrogen demand, but not microbial nitrogen mining, in a set of boreal forest soils. – Biogeochemistry 136: 261-278.

[34] Xu, X., Hui, D., King, A. W., Song, X., Thornton, P. E., Zhang, L. (2015): Convergence of microbial assimilations of soil carbon, nitrogen, phosphorus, and sulfur in terrestrial ecosystems. – Sci Rep-Uk 5.

[35] Xu, H., Liu, K., Zhang, W., Rui, Y., Zhang, J., Wu, L., Colinet, G., Huang, Q., Chen, X., Xu, M. (2020): Long-term fertilization and intensive cropping enhance carbon and nitrogen accumulated in soil clay-sized particles of red soil in South China. – J Soil Sediment 20: 1824-1833.

[36] Yadav, S. S., Guzman, J. G., Meena, R. S., Lal, R., Yadav, G. S. (2020): Long term crop management effects on soil organic carbon, structure, and water retention in a cropland soil in central Ohio, USA. – J Plant Nutr Soil Sc 183: 200-207.

[37] Yan, W., Jiang, W., Han, X., Hua, W., Yang, J., Luo, P. (2020): Simulating and predicting crop yield and soil fertility under climate change with fertilizer management in Northeast China based on the decision support system for agrotechnology transfer model. – Sustainability-Basel 12.

[38] Yang, B., Ma, Y., Zhang, C., Jia, Y., Li, B., Zheng, X. (2019): Cleaner production technologies increased economic benefits and greenhouse gas intensity in an eco-rice system in China. – Sustainability-Basel 11.

[39] Yu, Q., Hu, X., Ma, J., Ye, J., Sun, W., Wang, Q., Lin, H. (2020): Effects of long-term organic material applications on soil carbon and nitrogen fractions in paddy fields. – Soil Till Res 196.

[40] Yusuf, H. M., Treydte, A. C., Sauerborn, J. (2015): Managing semi-arid rangelands for carbon storage: grazing and woody encroachment effects on soil carbon and nitrogen. – Plos One 10.

[41] Zanatta, J. A., Beber Vieira, F. C., Briedis, C., Dieckow, J., Bayer, C. (2019): Carbon indices to assess quality of management systems in a Subtropical Acrisol. – Sci Agr 76: 501-508.

[42] Zhang, Q., Laanbroek, H. J. (2018): The effects of condensed tannins derived from senescing Rhizophora mangle leaves on carbon, nitrogen and phosphorus mineralization in a Distichlis spicata salt marsh soil. – Plant Soil 433: 37-53.

[43] Zhang, Z., Zhang, X., Mahamood, M., Zhang, S., Huang, S., Liang, W. (2016): Effect of long-term combined application of organic and inorganic fertilizers on soil nematode communities within aggregates. – Sci Rep-Uk 6.

[44] Zhao, H., Song, J., Zhao, G., Xiang, Y., Liu, Y. (2019): Novel semi-IPN nanocomposites with functions of both nutrient slow-release and water retention. 2. Effects on soil fertility and tomato quality. – J Agr Food Chem 67: 7598-7608.

[45] Zhou, X., Lu, Y., Liao, Y., Zhu, Q., Cheng, H., Nie, X., Cao, W., Nie, J. (2019): Substitution of chemical fertilizer by Chinese milk vetch improves the sustainability of yield and accumulation of soil organic carbon in a double-rice cropping system. – J Integr Agr 18: 2381-2392.

http://www.aloki.hu ● ISSN 1589 1623 (Print) ● ISSN 1785 0037 (Online)
DOI: http://dx.doi.org/10.15666/aeer/2005_42714282

ASSESSMENT OF FUNCTIONAL FEEDING GROUPS OF AQUATIC INSECT COMMUNITIES IN THE MOHLAPITSI RIVER, SOUTH AFRICA

ADDO-BEDIAKO, A.

Department of Biodiversity, University of Limpopo, Private Bag X1106, Sovenga 0727, South Africa (e-mail: abe.addo-bediako@ul.ac.za; phone: +27-15-268-3145; ORCID: 0000-0002-5055-8315)

(Received 25th Mar 2022; accepted 11th Jul 2022)

Abstract. The changes occurring in the catchment of the Mohlapitsi River in South Africa as a result of anthropogenic activities are affecting the integrity of the river and may subsequently alter the composition and functional structure of aquatic insect assemblages. The aim of this study was to assess aquatic insect composition and richness of the functional feeding groups at different sites along the river. The insect structural composition differed among sites and seasons. The number of taxa and the diversity of insects remained relatively high across the river, especially in the downstream. The highest abundance of aquatic insects was recorded at the downstream sites, S5 and S6. Taxa richness and abundance were higher during the dry season than during the wet season. Collector-gatherer was the dominant functional feeding group in abundance and the predator was the dominant group in taxa (family) richness. The spatial and temporal functional composition were related to the environmental variables in the river. These relationships suggest that the physicochemical variables have influence on the distribution, abundance, and diversity of functional groups. However, the low abundance and taxa richness in the midstream suggest that the activities along the river are gradually impacting the river. It is important to implement proper measures to reduce agricultural and domestic discharges into the river in order to maintain its integrity and conserve the aquatic biota.
Keywords: *bioindicators, functional structure, land use changes, macroinvertebrates, water quality*

Introduction

Many freshwater ecosystems are being polluted due to discharges from mining, industrial, agricultural, and domestic activities (Li et al., 2018; Chen et al., 2019). Furthermore, land use changes have caused destruction of riparian vegetation and loss of habitats, which have affected both the integrity of freshwater bodies and the aquatic biota. The community structure of many aquatic organisms, specifically aquatic insects, represents a high degree of spatial variation along rivers and therefore serves as good indicators of water quality (Keke et al., 2017; Sor et al., 2017; Addo-Bediako, 2021). The spatial variation in their composition may be influenced by physicochemical variables (Al-Shami et al., 2013; Cortes et al., 2013; Kumar and Khan, 2013) and trophic factors (Nicola et al., 2010; Cai et al., 2012).

Many metrics such as abundance, taxa richness and diversity of macroinvertebrates have been used in monitoring freshwater ecosystems. Recently, a functional approach based on macroinvertebrate functional feeding groups (FFG) is being used as indicator of ecosystem attributes and to assess the ecological health of rivers/streams (Merritt et al. 2005; Fierro et al., 2017). Functional feeding group is an important tool for establishing trophic relationships and community dynamics (Vannote et al., 1980; Cummins et al., 2005; Fu et al., 2016).

The classification of FFG considers the morphological and behavioural characteristics used in food acquisition (Ramirez and Gutiérrez-Fonseca, 2014). Macroinvertebrates can be classified into five groups based on consumption of diverse food resources and feeding

http://www.aloki.hu ● ISSN 1589 1623 (Print) ● ISSN 1785 0037 (Online)
DOI: http://dx.doi.org/10.15666/aeer/2005_42834294

strategies: shredders, collector-gatherers, collector-filterers, predators and scrapers. Shredders feed on living or dead parts of plants and therefore, perform an important role in the transformation of coarse particulate organic matter (CPOM) to fine particulate organic matter (FPOM) in rivers; collector-gatherers feed on smaller particulate organic matter deposited on substrates; collector-filterers filter organic particles directly from the water column; predators feed on other live animals, whole or part of them; and scrapers feed on organic matter, algae and other associated organisms (periphyton), that usually form a matrix on the surface of substrates, such as rocks and submerged plant material. Thus, the food sources and availability influence significantly the distribution of FFGs (Allan and Castillo, 2007). Generally, shredders and scrapers are more sensitive to disturbances that might change the availability of certain food or habitat, while collectors (filterers and gatherers) are more tolerant, so they can potentially be used to assess aquatic ecosystem health (Bhawsar et al., 2015; Meira et al., 2021).

The Mohlapitsi River is an important tributary of the Olifants River Basin and it has long been known to provide the basin with water of good quality. However, due to the increasing agriculture, sand mining activities, together with human settlements in the catchment, the river is being degraded. Little is known about the ecological impact of the activities on the river and aquatic biota such as insects. There is a need therefore to study the spatial community structure of organisms and their relation to environmental factors in the river. The objective of the study was to assess the spatial and temporal differences in FFG of aquatic insects and relate these to differences in ecosystem attributes. It was hypothesized that there is a change in the FFG structural composition from upstream to downstream of the river in relation to changes in energy flow as predicted by the River Continuum Concept (RCC).

Materials and methods

Study area

The Mohlapitsi River in South Africa is an important tributary of the Olifants River, as it supplies the latter with water of good quality. The river takes its source in a protected Wolkberg Wilderness area, then flows downstream passing through various agricultural fields and human settlements before joining the Olifants River. The communities in the area depend on the river for domestic use, irrigation and livestock. Six sampling sites were selected along the river (*Fig. 1*); Site S1 (24.1650044S; 30.1043448E) was in the Wolkberg Wilderness area; it is surrounded by vegetation, comprising trees, shrubs and ferns, with little bank erosion. Site S2 (24.1738869S; 30.1027902E) was adjacent to a small human settlement, with a very little disturbance and there are big trees which provide shade to a greater part of the site. Site S3 (24.1806804S; 30.0975124E) was below a weir, with less vegetation around, though there are reeds and shrubs, with a few fig trees adjacent to the river. Site S4 (24.2367189S; 30.0778399E) was adjacent to a settlement (Ga Mafefe village), sand mining, washing of clothes occur at this site and also serves as source of drinking water for some of the communities and livestock. Site S5 (24.2370664S; 30.0785938E) was near a cattle grazing area, though it was in the downstream, the site is surrounded by trees, especially wild fig trees, which provide shade to a greater part of this section of the river. Site S6 (24.2371333S; 30.0781493E) was at the confluence of the Mohlapitsi River and the Olifants River. The area is mostly surrounded by shrubs and grasses. The sites were selected to cover upstream (S1 and S2), midstream (S3 and S4), and downstream (S5 and S6).

http://www.aloki.hu ● ISSN 1589 1623 (Print) ● ISSN 1785 0037 (Online)
DOI: http://dx.doi.org/10.15666/aeer/2005_42834294

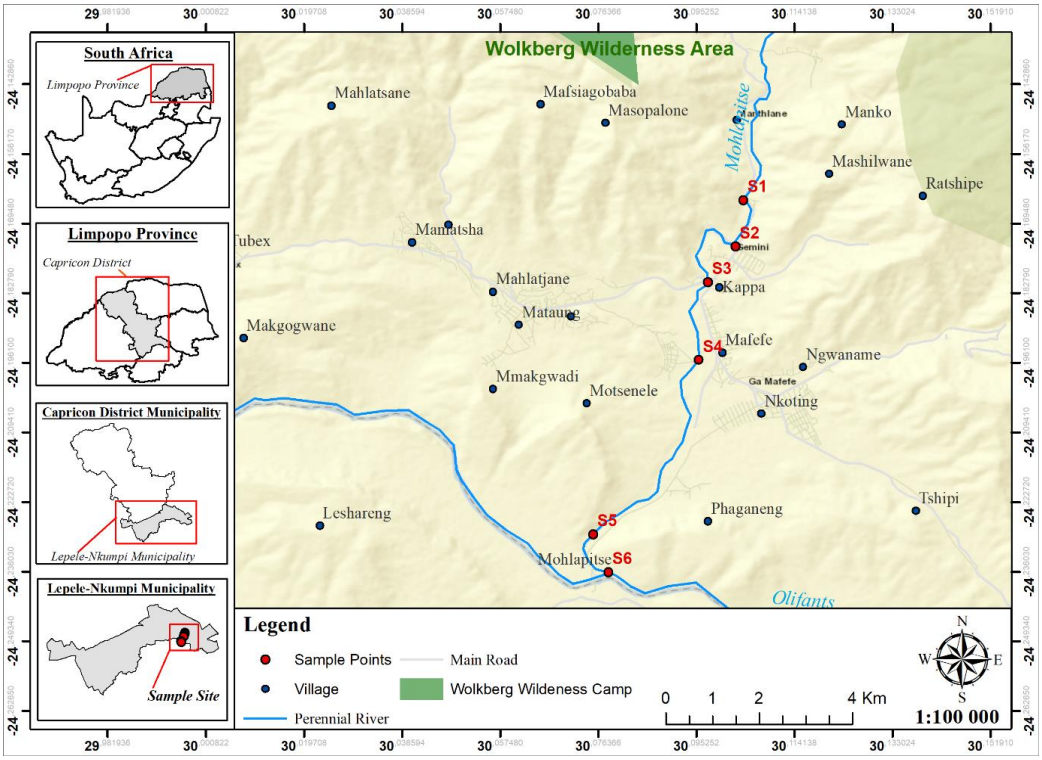

Figure 1. *The selected sampling sites of the Mohlapitsi River of the Olifants River Basin*

Water sampling

Water samples were collected at the six sites of the Mohlapitsi River in March (autumn), June (winter), October (spring) and December (summer), 2019. The water samples were collected in 1000 ml acid pre-treated polyethylene bottles. The water was stored at 4°C prior to chemical analysis. The pH, water temperature, dissolved oxygen, total dissolved solids (TDS), electrical conductivity and salinity were recorded *in situ* at sampling sites using the YSI Model 554^{TM} Datalogger multiprobe (YSI Inc., Yellow Springs, Ohio). The water samples were analyzed for nutrients (nitrate, nitrite, total nitrogen, ammonia and phosphate), and turbidity in the laboratory (Waterlab) using a spectrophotometer (Spectroquant Pharo 100, Merck, Germany). Flow velocity was measured using a Flo-mate portable flowmeter Model 2000 (Marsh McBirney, Maryland, US). The width and water depth were measured using a measuring tape and graduated measuring rod, respectively.

Sampling of aquatic insects

Aquatic insects were collected at the selected sites using a standard net of 300 mm x 300 mm with the mesh size of approximately 500 µm. The kick sampling method described by Dickens and Graham (2002) was used. The substrate was disturbed by kicking with the feet while sweeping the net in a zig-zag manner to free insects. At each site, approximately 6 min was spent sampling all aquatic habitats (i.e. riffles, pools and vegetated margins) and were combined to form one composite sample. The insect samples collected were identified to the family level in the field using an Invertebrate Field Guide Manual (Gerber and Gabriel 2002), with the aid of magnifying glass. However, those insects which could not be identified in the field were preserved in 70% ethanol in a litre polypropylene containers and transported to the laboratory for further

http://www.aloki.hu ● ISSN 1589 1623 (Print) ● ISSN 1785 0037 (Online)
DOI: http://dx.doi.org/10.15666/aeer/2005_42834294

identification using a stereomicroscope (Leica EZ4). The insects were then classified into functional feeding groups (FFGs): Shredders (Sh), Collector-gatherers (CG), Collector-filterers (CF), Scrapers (Sc) and Predators (P), using the criteria of Merrit and Cummins (1996), Cummins et al. (2005) and Cummins (2016).

Data analysis

The mean and standard deviation of the physicochemical parameters were calculated. One-way ANOVA was used to compare means of physicochemical variables of water and insect distribution across the sites, after data was checked for normality (Shapiro–Wilk test) and homogeneity of variance (Levene's test) and log transformations where necessary, using Statistica Version 10. The percentage contribution of each FFG to the different communities was determined to find out the relative contribution of each group. The influence of physicochemical variables on macroinvertebrate communities and functional feeding groups were determined by canonical correspondence analysis (CCA) using CANOCO version 5.1 software (Ter Braak and Smilauer, 2002).

Results

Physicochemical parameters

The measured physicochemical parameters are shown in *Table 1*. There were no significant differences in the physicochemical variables among the sampling sites ($p < 0.05$), however, DO and conductivity showed significant differences among the sites ($F = 3.979$, $p = .013$ and $F = 2.822$, $p = 0.047$ respectively). The upstream site, S1 had the lowest mean values for all parameters except DO. The highest mean water temperature and salinity levels were recorded at S3 and the highest pH, conductivity and TDS were recorded at S6. Generally, nutrient levels were very low at all sites. Ortho-phosphate was below detection level at all sites. The highest nitrate and total nitrogen concentrations were recorded at S5. The highest mean ammonium concentration was at S2 and the concentration of nitrite was the same at all sites except S2.

Table 1. *Mean water physicochemical variables (± standard deviation) recorded across the six sites of the Mohlapitsi River*

Physicochemical parameters	S1	S2	S3	S4	S5	S6	Guideline values
Velocity (ms^{-1})	0.47 ± 0.2	0.66 ± 0.3	0.84 ± 0.7	0.80 ± 0.3	0.42 ± 0.1	0.50 ± 0.5	
Depth (m)	0.46 ± 0.1	0.31 ± 0.1	0.51 ± 0.2	0.57 ± 0.1	0.47 ± 0.2	0.64 ± 0.8	
Width (m)	6.12 ± 0.9	7.40 ± 1.0	6.80 ± 1.7	8.15 ± 0.8	10.2 ± 2.1	15.8 ± 0.3	
pH	7.6-7.9	7.7-8.0	7.9-8.4	7.9-8.4	7.8-8.2	7.9-8.5	6.5.0-9.0[1]
Temperature (°C)	18.1 ± 2.5	19.5 ± 2.4	20.4 ± 2.0	20.2 ± 1.5	19.6 ± 1.7	20.0 ± 1.2	
Conductivity (µS/cm)	140.3 ± 32	231.6 ± 67	234.0 ± 67	234.5 ± 67	266.3 ± 61	275.1 ± 68	1700[1]
TDS (mg/l)	104.6 ± 20	165.8 ± 45	166.7 ± 45	165.7 ± 45	194.7 ± 44	296.8 ± 224	1200[1]
DO (mgl)	10.5 ± 1.7	9.7 ± 1.1	9.3 ± 0.8	8.7 ± 0.8	8.4 ± 0.6	7.6 ± 0.7	-
Salinity (ppt)	0.07 ± 0.02	0.11 ± 0.3	0.34 ± 0.4	0.12 ± 0.03	0.16 ± 0.02	0.2 ± 0.14	0.5[1]
Nitrate (mg/l)	0.15 ± 0.06	0.2 ± 0.01	0.15 ± 0.1	0.15 ± 0.06	0.25 ± 0.17	0.2 ± 0.14	< 11.0[1], 13[2]
Nitrite (mg/l)	0.05 ± 0.01	0.03 ± 0.01	0.05 ± 0.0	0.05 ± 0.00	0.05 ± 0.01	0.05 ± 0.1	< 0.9[1], 0.6[2]
Ammonium (mg/l)	0.07 ± 0.6	0.63 ± 0.4	0.45 ± 0.4	0.45 ± 0.1	0.61 ± 0.4	0.6 ± 0.4	< 0.01[1]
Total Nitrogen (mg/l)	0.31 ± 0.05	0.25 ± 0.03	0.2 ± 0.1	0.2 ± 0.06	0.39 ± 0.1	0.25 ± 0.13	< 0.5 (oligotrophic)
Ortho-Phosphate (mg/l)	< 0.1	< 0.1	< 0.1	< 0.1	< 0.1	< 0.1	

[1]DWAF (1996)
[2]CCME (2012)

http://www.aloki.hu ● ISSN 1589 1623 (Print) ● ISSN 1785 0037 (Online)
DOI: http://dx.doi.org/10.15666/aeer/2005_42834294

Insect community structure

The abundance of the insect taxa and functional feeding groups (FFG) assigned are shown in *Table 2*. A total of 6 386 individual insects belonging to 51 families and seven orders were recorded. Diptera had the highest taxa (11), followed by Odonata (10), Tricoptera (9), Hemipteran (8), Ephemeroptera (6), Coleoptera (6), and then Plecoptera (1). The most abundant family was Baetidae (2527), followed by Hydropsychidae (700) and then Gomphidae (587). The highest abundance of insects was recorded at S5, followed by S6, S1, S2, S4 and the least abundance at S3.

Table 2. *Functional feeding groups of aquatic insects recorded at different sites of the Mohlapitsi River*

Order	Family		S1	S2	S3	S4	S5	S6	Total	FFG
Plecoptera	Perlidae	Perl	17	1	2	0	0	4	24	P
Ephemeroptera	Baetidae	Baet	541	477	91	158	658	602	2527	CG
	Caenidae	Caen	25	0	0	0	0	0	25	CG
	Ephemeridae	Ephem	0	0	0	0	17	0	17	CG
	Heptageniidae	Hept	9	19	0	17	1	41	87	SC
	Oligoneuridae	OligoN	0	0	0	8	0	0	8	CF
	Tricorythidae	Tric	0	11	3	5	0	0	19	CG
Odonata	Calopterygidae	Calo	0	7	14	0	78	6	105	P
	Chlorocyphidae	Chlo	1	0	0	0	33	6	40	P
	Syntestidae	Synt	0	0	0	0	95	0	95	P
	Coenagrionidae	Coen	9	8	5	7	57	6	92	P
	Lestidae	Lest	3	0	0	18	0	12	33	P
	Platycnemidae	Plat	0	0	12	0	0	0	12	P
	Aeshnidae	Aesh	51	16	12	12	27	4	122	P
	Corduliidae	Cord	0	0	7	12	16	0	35	P
	Gomphidae	Gomp	101	143	57	64	114	108	587	P
	Libelliludae	Libe	20	1	6	4	17	1	49	P
Hemiptera	Nacauridae	Naca	0	9	4	3	5	0	21	P
	Notonectidae	Noto	0	2	0	0	0	0	2	P
	Belostomatidae	Belo	1	0	0	0	13	6	20	P
	Gerridae	Gerr	3	1	16	0	0	0	20	P
	Hydrometridae	HydroM	0	1	0	2	0	0	3	P
	Corixidae	Cori	0	3	0	0	0	0	3	P
	Veliidae	Veli	0	16	2	35	0	0	53	P
	Nepidae	Nepi	6	8	1	0	27	0	42	P
Tricoptera	Dipseudopsidae	Dips	74	0	0	0	0	0	74	CF
	Ecnomidae	Ecno	65	16	31	0	43	106	261	CF
	Hydropsychidae	HydroP	294	90	23	8	135	150	700	CF
	Philopotamidae	Philo	3	27	0	0	0	78	108	CF
	Polycentropodidae	PolyC	4	0	5	0	9	0	18	CF
	Psychomyiidae	Psyc	0	12	0	0	74	50	136	CG
	Hydroptilidae	Hydropt	0	0	0	5	6	10	21	CG
	Lepidostomatidae	LepiDM	1	9	0	6	16	11	43	SH
	Leptoceridae	LepTC	0	9	0	0	11	0	20	SH
Coleoptera	Dystiscidae	Dyst	2	0	0	0	0	0	2	P
	Gyrinidae	Gyri	0	2	0	4	0	0	6	P
	Elmidae	Elmi	3	8	22	13	43	19	108	SC
	Helodidae	Helo	0	0	0	0	8	0	8	SH
	Psephenidae	Psep	10	10	27	87	85	41	260	SC
	Hydrophilidae	Hydroph	0	0	0	0	0	59	59	CG

http://www.aloki.hu ● ISSN 1589 1623 (Print) ● ISSN 1785 0037 (Online)
DOI: http://dx.doi.org/10.15666/aeer/2005_42834294

	Athericidae	Ather	23	11	8	4	1	5	52	P
	Ceratopogonidae	Cerat	28	35	61	31	32	0	187	P
	Chironomidae	Chiro	3	0	0	11	11	0	25	CG
	Culicidae	Culi	1	0	0	3	0	3	7	CF
	Dixidae	Dix	0	0	1	0	0	6	7	CF
Diptera	Ephydridae	Ephy	0	0	4	0	0	0	4	SH
	Muscidae	Musc	0	0	0	0	5	4	9	P
	Psychodidae	Psycho	5	2	23	15	15	0	60	CG
	Syrphidae	Syrp	0	0	4	15	0	0	19	CG
	Simulidae	Simu	0	2	0	3	5	16	26	CF
	Tabanidae	Taba	34	19	11	2	44	15	125	P
Total			1337	975	452	552	1701	1369	6386	

Functional organization

In terms of the functional feeding group (FFG) abundance, collector-gatherer was the dominant group (45.5%), followed by predator (27.2%), collector-filterer (18.9%), scraper (7.1%), and then shredder (1.2%). There were differences in abundance and proportion of the functional feeding groups among sites (*Table 3*), but there were no significant differences ($p > 0.05$). The highest abundance of the collector-filterers was at S1, and collector-gatherers, predators, scrapers and shredders at S5 (*Fig. 2*). Predators, collector-gatherers, collector-filterers, shredders and scrapers comprised 25, 10, nine, four and three families respectively. In the CCA analysis, axis 1 was positively correlated with high DO and associated with S1, and the site was characterized by CF and CG. The second axis was associated with S3 and S4, and correlated with velocity, depth and NO_2, and the sites were characterized by scrapers. Sites S2 and S5 were characterized by shredders and were associated with TDS and width of the river (*Fig. 3*). The first three CCA axes accounted for 98.2% variation, with the first and second axes contributing 92.4% of the total variation (Monte Carlo test; $P < 0.05$) (*Table 4*).

Table 3. *Abundance of functional feeding groups of the various sites in the Mohlapitsi River*

Site	S1	S2	S3	S4	S5	S6
CF	441	135	60	22	192	359
CG	574	502	121	209	781	721
P	299	283	218	198	564	177
Sc	22	37	49	117	129	101
Sh	1	18	4	6	35	11
Total	1337	975	452	552	1701	1369

Table 4. *The CCA results which indicate correlation between physicochemical variables and the aquatic insects of the Mohlapitsi River*

Axes	1	2	3	4	Total inertia
Eigenvalues	0.020	0.010	0.001	0.000	
Taxa-environment correlations	1.000	1.000	1.000	1.000	
% cumulative variance of taxa-environment	67.1	92.4	98.2	100	
Sum of eigenvalues					0.025

http://www.aloki.hu ● ISSN 1589 1623 (Print) ● ISSN 1785 0037 (Online)
DOI: http://dx.doi.org/10.15666/aeer/2005_42834294

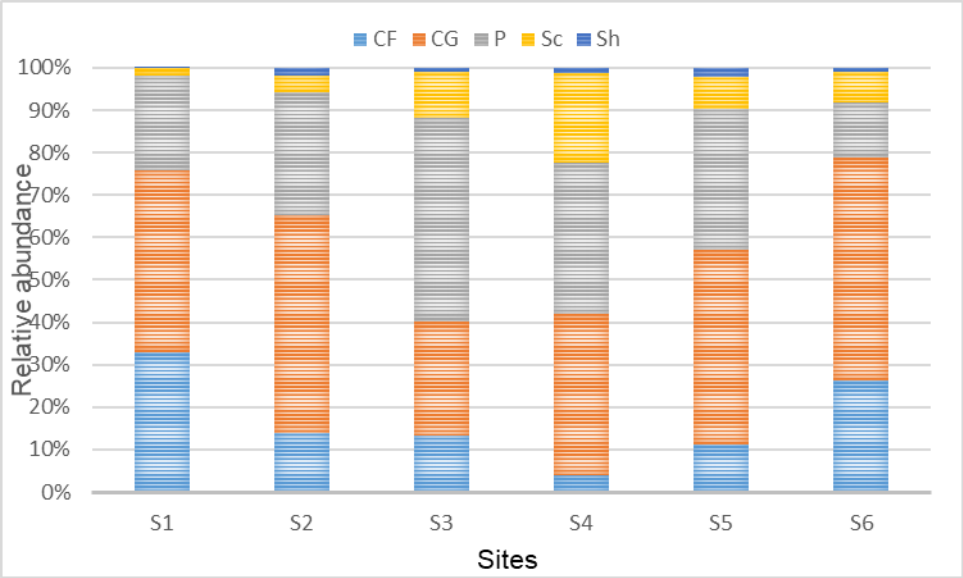

Figure 2. *Relative abundance of the functional feeding groups at studied sites of the Mohlapitsi River (CF = collector filterers, CG = collector gatherers, P = predators, Sc = scrapers, Sh = shredders)*

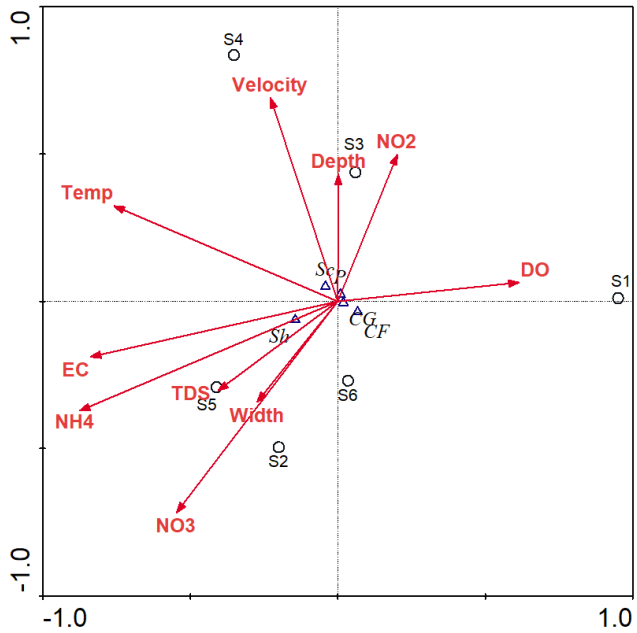

Figure 3. *Canonical correspondence analysis (CCA) showing the relationship between environmental variables and macroinvertebrate functional feeding groups*

Seasonally, the highest abundance was in autumn (2057), followed by winter (2051), spring (1607) and then summer (671). The highest number of taxa was during autumn (38), followed by winter (37), spring (35) and then summer (21) (*Table 5*). Collector-gatherers, collector-filterers were numerically dominant during autumn, predators and

http://www.aloki.hu ● ISSN 1589 1623 (Print) ● ISSN 1785 0037 (Online)
DOI: http://dx.doi.org/10.15666/aeer/2005_42834294

shredders were dominant in winter (*Fig. 4*). However, there were no significant variations in terms of distribution of the FFGs among seasons ($p > 0.05$).

Table 5. *Seasonal abundance of functional feeding groups in the Mohlapitsi River*

	Summer	Autumn	Winter	Spring	Total
CF	67	450	389	303	1209
CG	366	941	940	661	2908
P	183	446	564	546	1739
Sc	51	202	112	90	455
Sh	4	18	46	7	75
Total	671	2057	2051	1607	6386

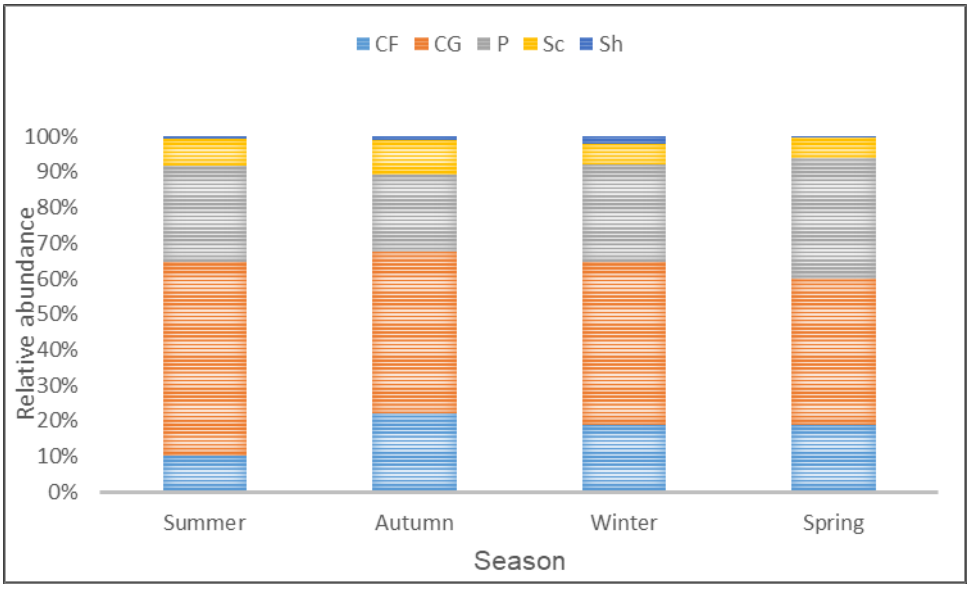

Figure 4. *Relative abundances of the functional feeding groups of insects at different seasons (CF = collector filterers, CG = collector gatherers, P = predators, Sc = scrapers, Sh = shredders)*

Discussion

Physicochemical parameters

Most of the physicochemical parameters and nutrients measured were within the standard guideline values. Thus, the human disturbances such as runoff, mainly from agricultural areas and the discharge of domestic waste waters have not significantly impacted the river. However, there was increasing concentration of TDS, electrical conductivity and turbidity from upstream to downstream. The nutrient levels were generally lower in the upstream but higher at the midstream and downstream sites due to increasing flow discharge and flooding from upstream and midstream of the river (Magoale et al., 2022). This is an indication that human activities are gradually having impact on the river. The most visible disturbances observed during this study were road construction near S3, which has resulted in the removal of most of the riparian vegetation and causing erosion of stream banks and sand mining at S4. These have

http://www.aloki.hu ● ISSN 1589 1623 (Print) ● ISSN 1785 0037 (Online)
DOI: http://dx.doi.org/10.15666/aeer/2005_42834294

contributed to the sediment loads entering the river and may reduce available microhabitats for the biota (Addo-Bediako, 2021).

Insect community structure

The high abundance and taxa richness of the Mohlapitsi River could be attributed to the presence of riparian vegetation along most parts of the river which may provide food and breeding sites for many insect taxa. The high numbers of Ephemeroptera, Tricoptera and Odonata is attributed to clear water and a high level of dissolved oxygen in the river (Dobson et al., 2002). The high richness and abundance of insects at tsites, S5 and S6 might be attributed to the large width and depth of the river, these conditions promote different microhabitats and high nutrient and sediment load (Al-Shami et al., 2013). In addition, the high nutrient and high temperature recorded in the downstream of the river may provide ideal conditions for phytoplanktons (Vannote et al., 1980), and subsequently increase the abundance and richness of zooplanktons including some insect larvae and nymphs (Cai et al., 2012).

Functional organization

The collector-gatherers were the dominant group at all sites of the river, but the highest abundance was at the downstream sites, S5 and S6. The collector-filterers were also well represented at all the sites. The high abundance of the collectors could be due to the fact that they can feed on a broad range of food materials (Merritt et al., 2002; Addo-Bediako, 2021). The predators were well represented at all the sites. The high abundance and taxa richness of predators along the whole longitudinal gradient of the river may be due to availability of food (prey) and less competition (Ono et al., 2020). The predator distribution was almost similar at all sites, in support of the fact that they usually have similar proportion throughout the length of a stream channel, according to the river continuum concept (Vannote et al., 1980). The low number of shredders recorded is not unique to this river, such pattern has also been reported in many tropical and sub-tropical rivers and does not support the RCC model (e.g., Oliveira and Nessimian, 2010; Masese et al., 2014; Brasil et al., 2014; Doong et al., 2021, Makgoale et al. 2022). The significance of shredders in decomposition of organic material tends to decrease with low latitude (Gonçalves et al., 2006), instead there is a faster microbial decomposition due to the higher temperatures (Kaboré et al., 2016; Madomguia et al., 2016). Furthermore, the presence of secondary compounds in leaves of tropical trees reduce the palatability and nutrient content (Wantzen et al., 2002).

The CCA analysis indicated a significant relationship between the environmental factors and the functional groups in the axis 1 and axis 2 ($p < 0.05$). Shredders were mainly found at S2 and S5 and scrapers were mainly found at S4, where it is exposed to more sunlight, which promotes better growth of periphyton. However, collector-gatherers, collector-filterers and predators were well distributed throughout the sites, an indication that there was abundant food for these groups.

Seasonal influence was noted in the structural and functional organization of the aquatic insects due to seasonal differences in water quality and habitat characteristics. The abundance of most taxa was considerably lower in the hot and wet summer season than in the cold and dry seasons. This was also observed in other studies of tropical rivers, where abundance increased during the dry season (Tumwesigye et al., 2000; Arimoro et al., 2012). Flow reduction during the dry season contributes to seasonal

http://www.aloki.hu ● ISSN 1589 1623 (Print) ● ISSN 1785 0037 (Online)
DOI: http://dx.doi.org/10.15666/aeer/2005_42834294

variability in physicochemical conditions that could influence aquatic insect community structure. In this study, the increase in the number of insects and taxa during winter and autumn (relatively dry seasons) was probably related to a better water quality and increased algal availability as a result of reduced turbidity. Thus, algal food sources for scrapers probably were limited during the wet season. Whiles the increase in shredder abundance during the dry seasons could be due to more food (fallen leaves from the riparian vegetation). However, in other studies of tropical rivers, abundance decreased during the dry season (Masese et al., 2009, 2014).

Conclusion

The abundance and relative proportion of the functional feeding group showed variation across sites. In general, collector-gathers and predators were the dominant groups at all sites. The variation in functional feeding group distribution across sites may have significant implications in understanding the spatial changes in aquatic insect community structure. The shredder and collector co-dominance in the headwaters was not observed as predicted by RCC. Though, the collector-gatherers dominated the downstream of the rivers, which supports the prediction of the RCC. The fact that changing environmental conditions influenced the FFG pattern confirms that FFG is an effective tool to assess ecological integrity of rivers. The spatial patterns of FFG insect community structure in the Mohlapitsi River were affected by resource availability, habitat heterogeneity and human alterations. Seasonal changes played a major role determining the distribution of aquatic insect taxa. The results suggest that policies governing changes in land use occurring in the Mohlapitsi River catchment should take into consideration the impact on biodiversity.

Acknowledgements. The author is grateful to the Flemish Inter-University Council (VLIR-UOS), Belgium for the financial support and postgraduate students in the water lab for their assistance in the data collection.

Data availability. Data will be made available on request.

Conflict of interests. The author reports no conflict of interests.

REFERENCES

[1] Addo-Bediako, A. (2021): Spatio-temporal distribution patterns of functional feeding groups of benthic macroinvertebrates in Blyde River, South Africa. – Applied Ecology and Environmental Research 19(3): 2241-2257.

[2] Allan, J. D., Castillo, M. M. (2007): Stream Ecology: Structure and Function of Running Waters. – Springer, Dordrecht.

[3] Al-Shami, S., Che Salmah, M. R., Hassan, A. A., Madrus, M. R. (2013): Biodiversity of stream insects in the Malaysian Peninsula: spatial patterns and environmental constraints. – Ecological Entomology 38: 238-249.

[4] Arimoro, F. O., Obi-Iyeke, G. E., Obukeni, P. J. O. (2012): Spatiotemporal variation of macroinvertebrates in relation to canopy cover and other environmental factors in Eriora River, Niger Delta, Nigeria. – Environment Monitoring and Assessment 184: 6449-6461.

[5] Bhawsar, A., Bhat, M. A., Vyas, V. (2015): Distribution and composition of macroinvertebrates functional feeding groups with reference to catchment area in Barna

http://www.aloki.hu ● ISSN 1589 1623 (Print) ● ISSN 1785 0037 (Online)
DOI: http://dx.doi.org/10.15666/aeer/2005_42834294

Sub-Basin of Narmada River Basin. – International Journal of Scientific Research and Engineering Studies 3(11): 385-393.

[6] Brasil, S., Juen, L., Batista, J. D., Pavan, M. G., Cabette, H. S. R. (2014): Longitudinal distribution of the functional feeding groups of aquatic insects in streams of the Brazilian Cerrado Savanna. – – Neotropical Entomology 43: 421-428.

[7] Cai, Y., Gong, Z., Qin, B. (2012): Benthic macroinvertebrate community structure in Lake Taihu, China: effects of trophic status, wind-induced disturbance and habitat complexity. – Journal of Great Lakes Research 38: 39-48.

[8] CCME (Canadian Council of Ministers of the Environment). 2012: Canadian water quality guidelines for the protection of aquatic life and sediment quality guidelines for the protection of aquatic life.in. – Canadian Council of Ministers of the Environment, Gatinaeu, QC, Canada.

[9] Chen, N., Chen, L., Ma, Y., Chen, A. (2019): Regional disaster risk assessment of China based on self-organizing map: clustering, visualization and ranking. – – International Journal of Disaster and Risk Reduction 33: 196-206.

[10] Cortes, R. M. V., Hughes, S. J., Pereira, V. R., Varandas, S. D. G. P. (2013): Tools for bioindicator assessment in rivers: the importance of spatial scale, land use patterns and biotic integration. – Ecological Indicators 34: 460-477.

[11] Cummins, K. W. (2016): Combining taxonomy and function in the study of stream macroinvertebrates. – Journal of Limnology 75: 235-241.

[12] Cummins, K. W., Merritt, R. W., Andrade, P. (2005): The use of invertebrate functional groups to characterize ecosystem attributes in selected streams and rivers in southeast Brazil. – Studies of Neotropical Fauna and Environment 40: 69-89.

[13] Dobson, M., Magana, A., Mathooko, J. M., Ndegwa, F. K. (2002): Detritivores in Kenya highland streams: more evidence for the paucity of shredders in the tropics? – Freshwater Biology 47: 909-919.

[14] Doong, M. K. T., Anticamara, J. A., Magbanua, F. S. (2021): Spatial variations in the distribution of benthic macroinvertebrate functional feeding groups in tropical rivers. – Indonesian Journal of Limnology 2(1): 35-52.

[15] DWAF (Department of Water Affairs and Forestry). (1996): South African Water Quality Guidelines. Vol. 7: Aquatic Ecosystems. 2nd Ed. – DWAF, Pretoria, South Africa.

[16] Fierro, P., Bertrán, C., Tapia, J., Hauenstein, E., Peña-Cortés, F., Vergara, V., Cerna, C., Vargas-Chacoff, L. (2017): Effects of local land-use on riparian vegetation, water quality, and the functional organization of macroinvertebrate assemblages. – Science of the Total Environment 609: 724-734.

[17] Fu, L., Jiang, Y., Ding, J., Liu, Q., Peng, Q. Z., Kang, M. Y. (2016): Impacts of land use and environmental factors on macroinvertebrate functional feeding groups in the Dongjiang River basin, southeast China. – Journal of Freshwater Ecology 31(1): 21-35.

[18] Gonçalves, J. F., Graça, M. A. S., Callisto, M. (2006): Leaf-litter breakdown in 3 streams in temperate, Mediterranean, and tropical Cerrado climates. – Journal of the North American Benthological Society 25: 344-355.

[19] Kaboré, I., Moog, O., Alp, M., Guenda, W., Koblinger, T., Mano, K., Ouéda, A., Ouédraogo, R., Trauner, D., Melcher, A. H. (2016): Using macroinvertebrates for ecosystem health assessment in semi-arid streams of Burkina Faso. – Hydrobiologia 766: 57-74.

[20] Keke, U. N., Arimoro, F. O., Auta, Y. I., Ayanwale, A. V. (2017): Temporal and spatial variability in macroinvertebrate community structure in relation to environmental variables in Gbako River, Niger State, Nigeria. – Tropical Ecology 58: 1-14.

[21] Kumar, P. S., Khan, A. B. (2013): The distribution and diversity of benthic macroinvertebrate fauna in Pondicherry mangroves, India. – Aquatic Biosystems 9: 1-18.

[22] Li, H., You, S., Zhang, H., Zheng, W., Zou, L. (2018): Investigating the environmental quality deterioration and human health hazard caused by heating emissions. – Science of the Total Environment 628: 1209-1222.

http://www.aloki.hu ● ISSN 1589 1623 (Print) ● ISSN 1785 0037 (Online)
DOI: http://dx.doi.org/10.15666/aeer/2005_42834294

[23] Madomguia, D., Zebaze, T. S. H., Fomena, A. (2016): Macro invertebrates functional feeding groups, Hilsenhoff biotic index, percentage of tolerant taxa and intolerant taxa as major indices of biological assessment in ephemeral stream in Sudano-Sahelian zone (Far-North, Cameroon). – International Journal of Current Microbiology and Applied Sciences 5: 792-806.
[24] Makgoale, M. M., Addo-Bediako, A., Ayisi, K. K. (2022): Distribution pattern of macroinvertebrate functional feeding groups in the Steelpoort River, South Africa. – Applied Ecology and Environmental Research 20(1): 189-206.
[25] Masese, F. O., Raburu, P. O., Muchiri. M. (2009): A preliminary benthic macroinvertebrate index of biotic integrity (B-IBI) for monitoring the Moiben River, Lake Victoria Ba-sin, Kenya. – Africa Journal of Aquatic Science 34: 1-14.
[26] Masese, F. O., Nzula-Kitaka, N., Kipkembo, J., Gettel, G. M., Irvine, K., McClain, M. E. (2014): Macroinvertebrate functional feeding groups in Kenyan highland streams: evidence for a diverse shredder guild. – Freshwater Science 33(2): 435-450.
[27] Meira, B. R., Progênio, M., Leite, E. C., Lansac-Tôha, F. M., Durán, C. L. G., Jati, S., Rodrigues, L. C., Lansac-Tôha, F. A., Velho, L. F. M. (2021): Functional feeding groups of Protist Ciliates (Protist: Ciliophora) on a neotropical flood plain. – Annales de Limnologie - International Journal of Limnology 57: 13.
[28] Merritt, R. W., Cummins, K. W. (1996): An Introduction to the Aquatic Insects of North America. 3th Ed. – Hunt Publishing Company, Kendall.
[29] Merritt, R. W., Cummins, K. W., Berg, M. B., Novak, J. A., Higgins, M. J., Wessel, K. J., Lessard, J. L. (2002): Development and application of a macroinvertebrate functional-group approach in the bioassessment of remnant river oxbows in southwest Florida. – Journal of the North American Benthological Society 21(2): 290-310.
[30] Merritt, R. W., Cummins, K. W., Andrade, P. C. N. (2005): The use of invertebrate functional groups to characterize ecosystem attributes in selected streams and rivers in southeast Brazil. – Studies of Neotropical Fauna and Environment 40: 71-90.
[31] Nicola, G. G., Almodvar, A., Elvira, B. (2010): Effects of environmental factors and predation on benthic communities in headwater streams. – Aquatic Science 72: 419-429.
[32] Oliveira, A. L. H., Nessimian. J. L. (2010): Spatial distribution and functional feeding groups of aquatic insect communities in Serra da Bocaina streams, southeastern Brazil. – Acta Limnologica Brasiliensia 22(4): 424-441.
[33] Ono, E. R., Manoel, P. S., Melo, A. L. U., Uieda, V. S. (2020): Effects of riparian vegetation removal on the functional feeding group structure of benthic macroinvertebrate assemblages. – Community Ecology 21: 145-157.
[34] Ramirez, A., Gutiérrez-Fonseca, P. E. (2014): Functional feeding groups of aquatic insect families in Latin America: a critical analysis and review of existing literature. – Revista de Biología Tropical 62: 155-167.
[35] Sor, R., Pieter Boets, P., Ratha Chea, R., Goethals, P. L. M., Lek, S. (2017): Spatial organization of macroinvertebrate assemblages in the Lower Mekong Basin. – Limnologica 64: 20-30.
[36] Ter Braak, C. J. F., Verdonschot, P. F. M. (1995): Canonical correspondence analysis and related multivariate methods in aquatic ecology. – Aquatic Science 57: 255-289.
[37] Tumwesigye, C., Yusuf, S. K., Makanga, B. (2000): Structure and composition of benthic macroinvertebrates of a tropical forest stream, River Nyamweru, western Uganda. – Africa Journal of Ecology 38: 72-77.
[38] Vannote, R. L., Minshall, G. W., Cummins, K. W., Sedell, J. R., Cushing, C. E. (1980): The river continuum concept. – Canadian Journal of Fisheries and Aquatic Sciences 37: 130-137.
[39] Wantzen, K. M., Wagner, R. (2006): Detritus processing by invertebrate shredders: a neotropical-temperate comparison. – Journal of the North American Benthological Society 25: 216-232.

http://www.aloki.hu ● ISSN 1589 1623 (Print) ● ISSN 1785 0037 (Online)
DOI: http://dx.doi.org/10.15666/aeer/2005_42834294

EXOGENOUSLY APPLIED GLYCINEBETAINE ALLEVIATES CHROMIUM TOXICITY IN PEA BY REDUCING CR UPTAKE AND IMPROVING ANTIOXIDANT DEFENSE SYSTEM

FAISAL, M.[1] – IMRAN, K.[2] – MUHAMMAD, B. C.[3] – RIZWAN, M.[2] – ATHAR, M.[2] – RASHID, W. K.[4] – ARBAB, J.[5] – HAIFA, A. S. A.[6] – SABRY, H.[7] – SAJID, U.[8] – MUHAMMAD, U. H.[9] – SAMEER, H. Q.[10*]

[1]Department of Environmental Sciences & Engineering, Government College University, Faisalabad, Pakistan

[2]Department of Agronomy, University of Agriculture, Faisalabad 38040, Pakistan

[3]Department of Agronomy, Faculty of Agricultural Sciences, University of the Punjab Lahore, Lahore 54590, Pakistan

[4]Insititute of Horticultural Sciences, University of Agriculture, Faisalabad 38040, Pakistan

[5]Agronomy (Forage Production) Section, Ayub Agricultural Research Institute, Faisalabad, Pakistan

[6]Biology Department, College of Science, Jouf University, Sakaka 2014, Saudi Arabia

[7]Department of Biology, College of Science, Taif University, P.O. Box 11099, Taif 21944, Saudi Arabia

[8]Insititute Soil and Environmental Sciences, University of Agriculture, Faisalabad 38040, Pakistan

[9]Research Center on Ecological Sciences, Jiangxi Agricultural University, Nanchang 330045, China

[10]Department of Biology, Al-Jumum University College, Umm Al-Qura University, Makkah 21955, Saudi Arabia

**Corresponding author*
e-mail: shqari@uqu.edu.sa

(Received 27th Mar 2022; accepted 26th Jul 2022)

Abstract. Soils with chromium (Cr) pollution are significantly increasing globally. Therefore, proper measures should be opted for to restrict its entry into food crops. *Glycinebetaine* (GB)-induced tolerance in plants against different abiotic stresses has been well documented, but still little evidence is available concerning its potential to increase the tolerance of pea against Cr stress. Therefore, this study determined the impact of GB application in increasing Cr tolerance in pea (*Pisum sativum*). The experiment was comprised of three concentrations of Cr (0 mM, 0.25 mM, and 0.50 mM) and two levels of foliar-applied GB (0 and 50 mM). Chromium stress led to a significant reduction in growth, biomass production, and photosynthetic pigments however, Cr stress increased reactive oxygen species (ROS) production. Exogenously applied GB reduced the deleterious impacts of Cr stress on pea and increased growth, biomass production, and photosynthetic pigments. Moreover, GB reduced ROS production and Cr accumulation in plant roots and shoots by increasing the activities of antioxidant enzymes (APX, CAT, POD and SOD) and consequently increased growth and plant biomass production. In conclusion, beneficial effects of GB under Cr stress were attributed to reduced Cr uptake, enhanced photosynthetic pigment and enzymatic activities and less ROS production.
Keywords: *chromium, glycinebetaine, growth, photosynthetic pigments, ROS*

http://www.aloki.hu ● ISSN 1589 1623 (Print) ● ISSN 1785 0037 (Online)
DOI: http://dx.doi.org/10.15666/aeer/2005_42954307

Introduction

Chromium magnification in agricultural soils has become a serious concern worldwide owing to its non-degradable nature and unfavorable consequences for plant development and productivity (Singh and Gautam, 2013). Cr is considered as a non-essential element for plants and exposure of plants to Cr stress cause significant reduction in plant growth (Samantaray et al., 2015; El-Baz et al., 2021). It enters into the soil through different sources i.e., bed rocks, volcanoes, human activities, agricultural use of domestic and municipal wastewaters, electro-plating, tanning and mining (Ali et al., 2015; Medda and Mondal, 2017; Hassan et al., 2021). The pernicious consequences of Cr stress on plants have been widely documented by many researchers (Hayat et al., 2012; Ahmad et al., 2020). Chromium toxicity in plants decreased germination, growth, synthesis of photosynthetic pigments and biomass production, induced chlorosis, altered enzymatic activities, and caused ultra-structural changes in the plant cell membrane and chloroplasts (Ghani and Ghani, 2011; Yin et al., 2021). Moreover, Cr toxicity in plants also alters mineral nutrition and reduces the process of photosynthesis, and thereby leads to serious reduction in crop yield (Mushtaq et al., 2021). Additionally, Cr also induced ROS production in plants, which reduced the plant's performance by the oxidation of important molecules i.e., proteins and lipids (Pandey et al., 2012). Plants possess excellent antioxidant system consisting of antioxidants including ascorbate peroxidase (APX), catalase (CAT), superoxide dismutase (SOD), and peroxidase (POD) in order to get protection from oxidative stress (Sofo et al., 2015). The response of antioxidants in plants depends upon plant species and stress faced by the plants. Nonetheless, Cr stress reduced the activity of different antioxidant enzymes and led to a serious reduction in crops productivity (Adrees et al., 2015; Gautam et al., 2020).

The current increase in global population demands a substantial increase in the crop in the scenarios of rapid climate change and different abiotic stress (Hassan et al., 2017, 2020a, b; Rasheed et al., 2020). Pea (*Pisum sativum* L.) is an imperative legume crop of tropics and subtropics and is an imperious source of protein, minerals, carbohydrates, vitamins, and antioxidants (Dahl et al., 2012). In Pakistan, pea crop is cultivated in the winter season and is used as food and fodder crop. Pakistan is facing severe problems of decreasing agricultural land due to the increasing human population, and it is estimated that Pakistan's population would double by 2040 (Anjum et al., 2020). Therefore, it is necessary to increase crop production to meet the demands of the booming population. Phytoextraction of Cr using hyper-accumulator plant species is not a viable option for the remediation of Cr contaminated soils, especially for countries like Pakistan which is already facing population and food pressures. Thereby, the productive soils must be used for the cultivation of food crops to meet the needs of the population, whilst alternative measures should be adopted to reduce Cr toxicity and its accumulation in food crops.

Glycinebetaine (GB) is a non-toxic, water-soluble, and environmentally friendly agent. Elevated concentrations of GB have been reported to accumulate in plants under different stress conditions (Hassan et al., 2019; Ahmad et al., 2020). Nonetheless, GB accumulated by plants under various stresses is not enough to protect them from stresses. Surprisingly, exogenously applied GB has the potential to reduce harmful effects of these stresses on the plant (Hossain et al., 2010). Likewise, foliar-applied GB improved the drought and salinity stress tolerance in wheat (*Triticum aestivum*), rice (*Oryza sativa*) and maize (*Zea mays*) by increasing antioxidant activities, photosynthetic

http://www.aloki.hu ● ISSN 1589 1623 (Print) ● ISSN 1785 0037 (Online)
DOI: http://dx.doi.org/10.15666/aeer/2005_42954307

efficiency and decreasing oxidative stress through ROS scavenging (Sofy et al., 2020; Dustgeer et al., 2021). Exogenously applied GB increased wheat growth, photosynthetic pigments and decreased Cr toxicity and its accumulation by improving antioxidant activities (Ali et al., 2015). Likewise, in another study, Jabeen et al. (2016) noticed that GB application enhanced the Cr tolerance in mungbean (*Vigna radiata*) by reducing its uptake and enhancing antioxidant enzyme activities. However, no study has been performed where the significance of GB regarding the alleviation of Cr toxicity in pea has been reported. Therefore, we postulated that exogenously applied GB can reduce the Cr toxicity in pea plants by reducing Cr uptake and improving the activity of different antioxidant enzymes. This study investigated the beneficial role of exogenously applied GB on pea growth, morphology, photosynthetic pigments, Cr uptake and antioxidant activities grown in Cr stress conditions.

Materials and methods

Experimental site

The pot study was performed in the greenhouse area of the Faculty of Agriculture, University of Agriculture, Faisalabad in 2017. The soil was collected from the horticultural farm area from a depth of 0-20 cm and analyzed to determine the different physio-chemical properties. The pots with a diameter of 28 cm and a depth of 31 cm were filled with 8 kg of soil and 5 seeds of pea (Pea-2009) were sown in each pot. The soil physicochemical analysis revealed that the soil had sandy loam texture with organic matter (OM) 0.81%, pH, 7.7, nitrogen (N) 0.03%, phosphorus (P) 6.30 mg kg^{-1} and potassium (K) 177 mg kg^{-1}.

Experimental details

Three different levels of Cr stress i.e., 0 mM, 0.25 mM, and 0.50 mM were applied via utilizing $K_2Cr_2O_7$, while two levels of foliar-applied GB i.e., 0 and 50 mM were applied via dissolving GB in 0.1% tween-20 solutions. These levels of treatment were chosen after conducting a series of experiments to determine the toxic levels of Cr and to optimize the best level of GB application. $K_2Cr_2O_7$ were purchased from local market of Faisalabad. Chromium stress was applied with irrigation water after 20 days of plant emergence. Later, foliar application of GB was applied using a handheld sprayer according to treatments after 7 days of Cr stress. Moreover, a completely randomized design with factorial arrangements having three replications was used to perform the study. Experimental pots were regularly visited and carefully watered as per crop requirements. The pots were once fertilized with 160 mg of N and 240 mg of each P and K in the form of urea (46% N), single superphosphate (21% P) and sulfate of potash (50% K). The weeds grown in pots were manually uprooted and no attack of insects and diseases was noted during the study.

Observations

Growth parameters

Three plants were marked and manually uprooted from pots 10 days post GB application their roots and shoots were separated and their lengths were measured and averaged. Likewise, harvested plant roots and shoots were weighed separately on the

http://www.aloki.hu ● ISSN 1589 1623 (Print) ● ISSN 1785 0037 (Online)
DOI: http://dx.doi.org/10.15666/aeer/2005_42954307

balance to determine the root and shoot fresh weights. The cumulative length of roots was taken for the determination of root length. Moreover, three plants were selected in each pot and leaves were counted and plant height was measured.

Estimation of photosynthetic pigments

For the measurements of chlorophyll and carotenoid contents, plant samples were homogenized in an 80% solution of acetone and absorbance was noted with a spectrophotometer (PerkinElmer AAnalyst™ 800) at three different wavelengths (663, 645 and 480 nm) and chlorophyll and carotenoid contents were determined by the methods of Arnon (1949).

Appraisal of the antioxidant enzyme activities

Peroxidase (POD) activities were determined by the standard procedures of Zhang (1992). Plant samples (0.5 g) were homogenized in 5 ml of potassium buffer (50 mM) and centrifuged at 15,000 rpm and 4 °C and absorbance was noted at 470 nm. For SOD determination the 1 mL reaction mixture constituted 10 mM pyrogallol, 50 mL extract of the enzyme, 10 mM EDTA, and 50 mM sodium-phosphate buffer having a pH of 7.8. SOD activity in the reaction mixture was measured at 420 nm (Roth and Gilbert, 1984). Catalase (CAT) and ascorbate peroxidase (APX) activities were determined by the standard methods of Aebi (1984) and Nakano and Asada (1981). For CAT determination, we took 3 mL assay mixture that contained 100 µL of enzyme extract, 100 µL H_2O_2 (300 mM), 2.8 mL phosphate buffer (50 mM) with 2 mM CA having a 7.0 pH, afterwards CAT activity was noted at 240 nm. For APX determination the mixture consisted of 100 µL enzyme extracts, 100 µL ascorbate (7.5 mM), 100 µL H_2O_2 (300 mM), and 2.7 mL potassium buffer (25 mM) 2 mM CA having a 7.0 pH. The activities of APX enzyme were measured with variations in wavelength at 290 nm.

Assessment of H_2O_2 and MDA contents

Hydrogen peroxide (H_2O_2) and malondialdehyde (MDA) were determined by the standard methods of Velikova et al. (2000) and Dhindsa et al. (1981). For H_2O_2 determination, 0.5 g of plant samples were taken and homogenized on an ice bath in 1 mL of 0.1% TCA. After this supernatant (0.5 mL) was reacted with 0.5 mL of 50 mM PP buffer (pH = 7.5) and 1 mL potassium iodide (IM). The spectrophotometer was used to measure the absorbance at 390 nm wavelength. For MDA determination 1 g of plant sample was taken and homogenized in 10%, 8 ml trichloroacetic acid and centrifuged for 20 min at 4000 rpm. After that 2 ml of thiobutaric acid (60%) were mixed in the plant extracts and heated for 20 min at 100 °C and then cooled quickly with ice cubes for 20 min and centrifuged for 10 min at 10,000 ×*g*. Then the spectrometer was used to measure the absorbance at different wavelengths (450, 532, 600 nm).

Determination of Cr concentrations in shoots and roots of pea plant

Root and shoot samples were initially air-dried and stored and later oven dried. After oven drying, 0.5 g of each plant part was digested on hot plate by adding a mixture of HNO_3 and $HClO_4$ in 2:1 ratio (Jones and Case, 1990). Afterwards Cr concentration in plant parts was determined by atomic absorption spectrometer.

http://www.aloki.hu ● ISSN 1589 1623 (Print) ● ISSN 1785 0037 (Online)
DOI: http://dx.doi.org/10.15666/aeer/2005_42954307

Statistical analysis

Fisher's analysis of variance was done for all the recorded data using CoStat6.2 (Monterey, USA) to analyze the date and least significant difference (LSD) test was utilized for comparing significant differences among the treatment means at $p \leq 0.05$ (Steel et al., 1996).

Results

Growth attributes

Chromium stress had deleterious effects on the growth and morphological traits of pea. Plant height and number of leaves were significantly decreased with increasing Cr concentrations. However, foliar-applied GB (50 mM) considerably increased the plant height and the number of leaves in normal as well as Cr stressed plants (*Table 1*). A considerable reduction in leaf length, leaf width, and root length was observed in pea plants under Cr stress. Foliar spray of GB increased the leaf length by 17%, leaf width 30%, and root length 11% under Cr stress (50 mM), compared to control. The results depicted that Cr considerably decreased the root and shoot fresh weights as compared to control treatment. However, in the case of foliar-applied GB, we noted a significant increase in root (67%, 56%) and shoot fresh weight (36%, 37%) under Cr stress (25 mM, 50 mM) as compared to control (*Table 1*).

Table 1. *Effect of GB application on plant height, leaf length, leaf width, fresh weight of shoot and root, number of leaves and root length of pea under different levels of Cr stress*

Cr stress (mM)	GB (mM)	Plant height (cm)	Leaf length (cm)	Leaf width (cm)	Shoot FW (g)	Root FW (g)	Leaves per plant	Root length (cm)
0	0	36.3 ± 12.1b	5.80 ± 1.90b	2.90 ± 1.67cd	7.63 ± 2.54b	0.34 ± 0.11b	35.0 ± 0.4c	27.0 ± 9.01b
	50	42.6 ± 0.40a	6.30 ± 0.08a	4.10 ± 2.36a	7.91 ± 0.01a	0.58 ± 0.01a	63.3 ± 1.2 a	31.3 ± 1.22a
25	0	26.3 ± 1.20c	2.60 ± 7.50e	1.63 ± 0.94e	3.27 ± 7.24e	0.19 ± 8.26e	32.6 ± 2.3cd	20.0 ± 1.85d
	50	35.0 ± 1.63b	4.36 ± 0.12c	2.43 ± 1.40d	5.43 ± 0.01c	0.26 ± 0.01c	35.0 ± 0.4c	23.3 ± 0.4 c
50	0	23.0 ± 9.01c	2.13 ± 15.9 f	2.60 ± 1.50cd	3.21 ± 15.5e	0.16 ± 16.6e	29.3 ± 7.2e	17.0 ± 11.1e
	50	27.0 ± 0.81c	3.50 ± 0.04d	3.40 ± 1.96b	5.02 ± 0.01d	0.22 ± 0.01d	31.0 ± 0.4de	19.0 ± 0.81ed
LSD ≤ 0.05 P		4.47	0.222	0.415	0.101	0.209	2.54	2.17

FW: Fresh weight, GB: glycinebetaine, Cr: chromium, different letters showing the significant differences at 0.05 P level according to LSD test

Photosynthetic pigments

Chromium stress significantly reduced the photosynthetic pigments as compared to control (*Fig. 1*). However, chlorophyll (a, b and a/b) and carotenoid contents were significantly increased under normal and Cr stressed conditions with GB application as compared to Cr stress without foliar-applied GB. The maximum chlorophyll and carotenoid contents were recorded in normal conditions (no Cr stress) with foliar application of GB (50 mM) and minimum chlorophyll and carotenoid contents were recorded in Cd stress (50 mM) without GB application (*Fig. 1*).

MDA and H_2O_2 contents

Higher concentrations of H_2O_2 and MDA were recorded in pea plants subjected to higher Cr concentrations (*Fig. 2*). Foliar application of GB (50 mM) significantly

http://www.aloki.hu ● ISSN 1589 1623 (Print) ● ISSN 1785 0037 (Online)
DOI: http://dx.doi.org/10.15666/aeer/2005_42954307

reduced the H_2O_2 by 51% and 18% at 25- and 50-mM Cr stress whereas foliar applied GB (50 mM) reduced MDA contents by 42% and 23% under Cr stress of 25 and 50 mM, compared to control (*Fig. 2*).

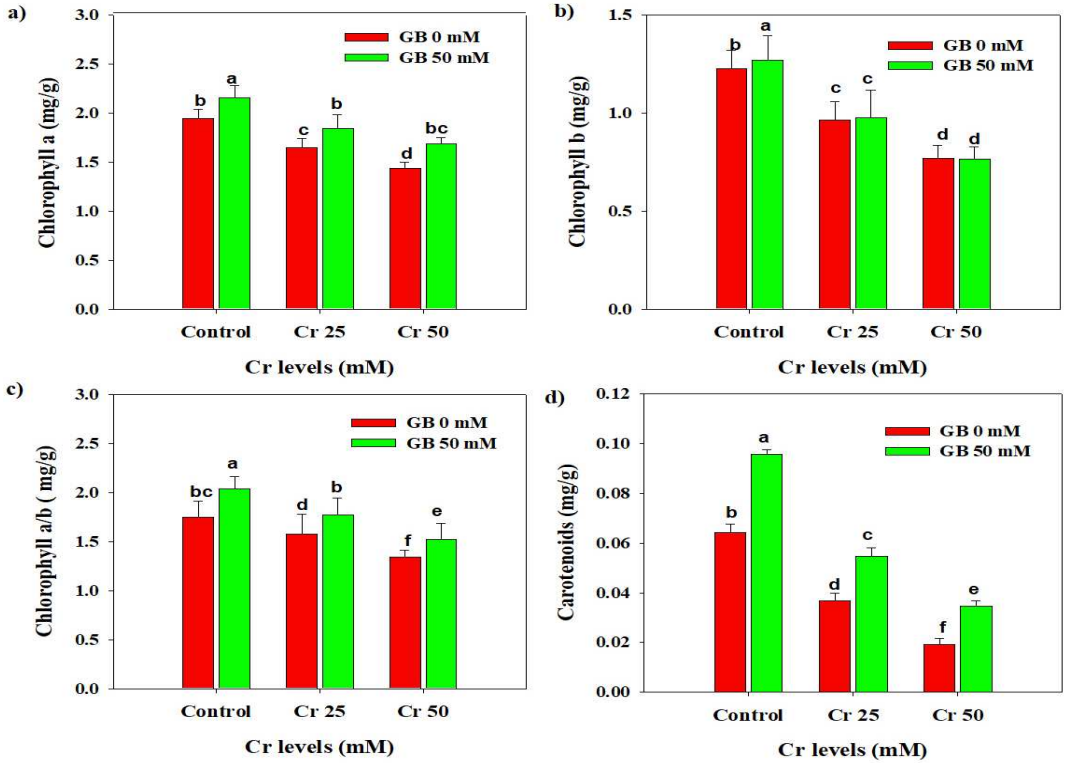

Figure 1. *Chlorophyll (a, b, a/b) and carotenoid contents in pea leaves grown in different concentrations of Cr stress with and without exogenously applied GB. Vertical bars are three replicates mean have ± S.E. and different letters indicate significant difference at 0.05 P level according to LSD test*

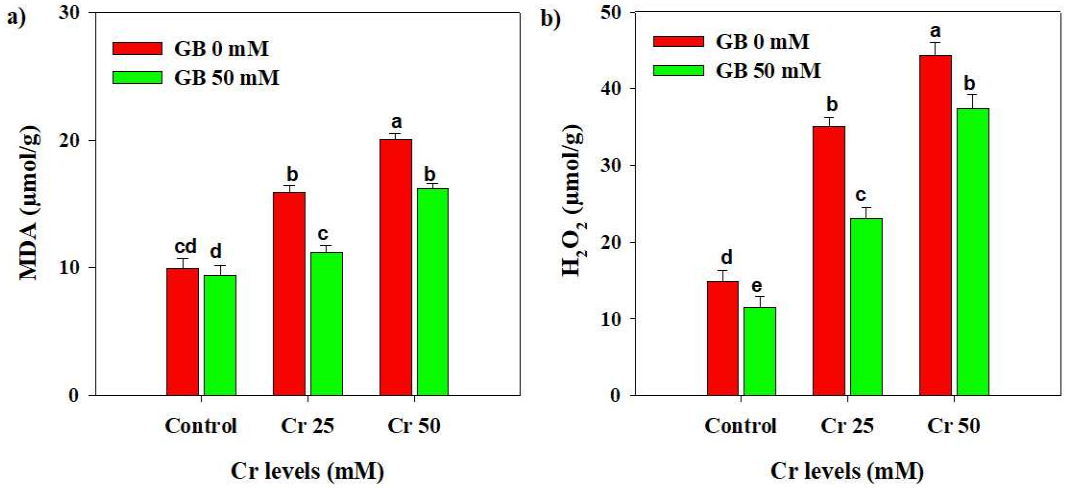

Figure 2. *The contents* ***of*** *MDA and H_2O_2 in pea leaves grown in different concentrations of Cr stress with and without exogenously applied GB. Vertical bars are three replicates mean have ± S.E. and different letters indicate significant difference at 0.05 P level according to LSD test*

http://www.aloki.hu ● ISSN 1589 1623 (Print) ● ISSN 1785 0037 (Online)
DOI: http://dx.doi.org/10.15666/aeer/2005_42954307

Antioxidant enzymes

Antioxidant activities were significantly increased in lower and higher Cr stress conditions as compared to no Cr stress. Moreover, foliar application of GB has further increased in activities of APX and CAT under both levels of Cr stress and control. Likewise, POD and SOD activities were also increased under Cr stress which gives clear evidence that antioxidant activities considerably increased under Cr stress conditions. Moreover, GB has a positive effect on the activities of POD and SOD both under Cr stress and control (no Cr stress) conditions. However, the maximum improvement in POD and SOD activity was recorded under Cr stress (50 mM) with foliar application of GB (50 mM) as compared to control (no Cr stress) (*Fig. 3*).

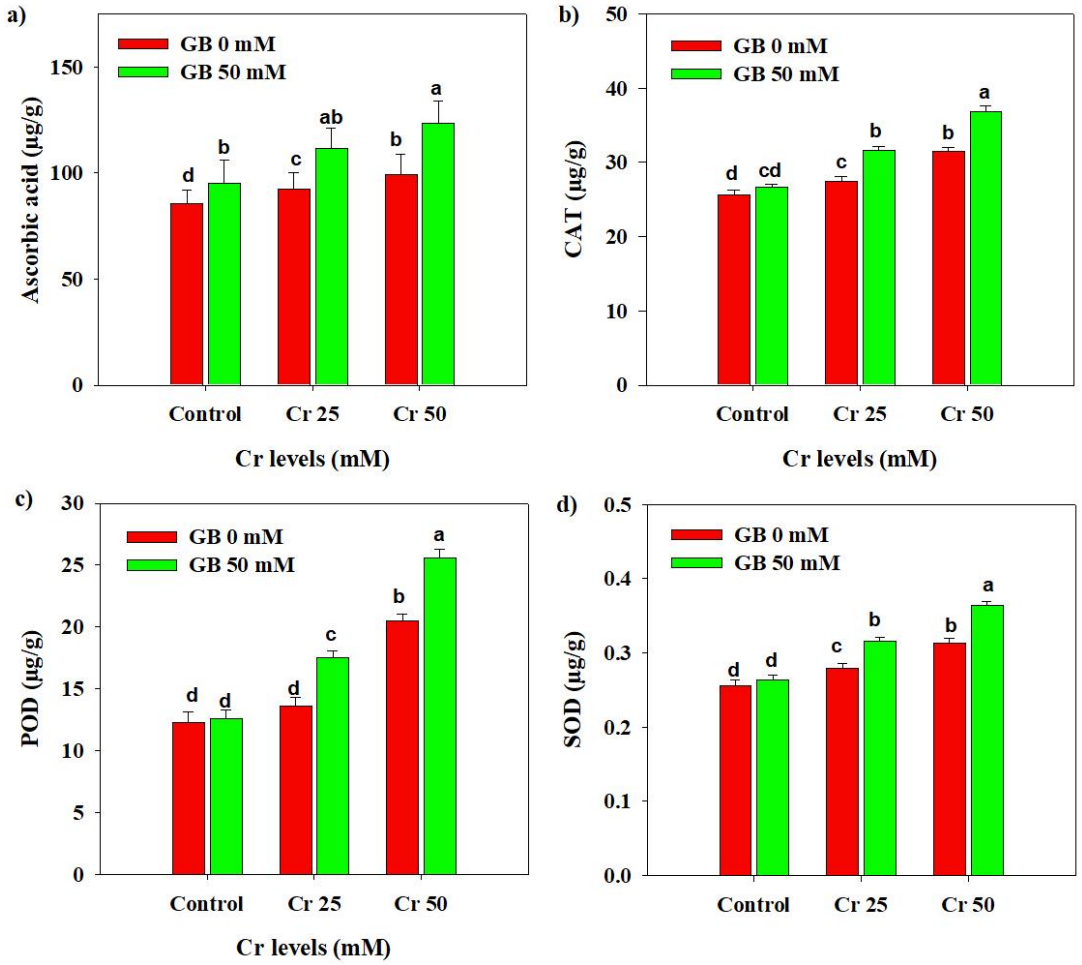

Figure 3. *Ascorbic acid contents, CAT, POD, and SOD activities in pea leaves grown in different concentrations of Cr stress with and without exogenously applied GB. Vertical bars are three replicates mean have ± S.E. and different letters indicate significant difference at 0.05 P level according to LSD test*

Chromium concentration in plant parts

The results indicated that Cr concentration in plant parts was increased under Cr stress conditions, however, it was dose-dependent; increase in Cr concentration in growing media significantly increased the Cr in plant root and shoot. The maximum Cr

http://www.aloki.hu ● ISSN 1589 1623 (Print) ● ISSN 1785 0037 (Online)
DOI: http://dx.doi.org/10.15666/aeer/2005_42954307

concentration was recorded in plant roots as compared to shoots (*Fig. 4*). Nonetheless, foliar-applied GB (50 mM) significantly reduced the Cr concentration in roots and shoots (*Fig. 4*).

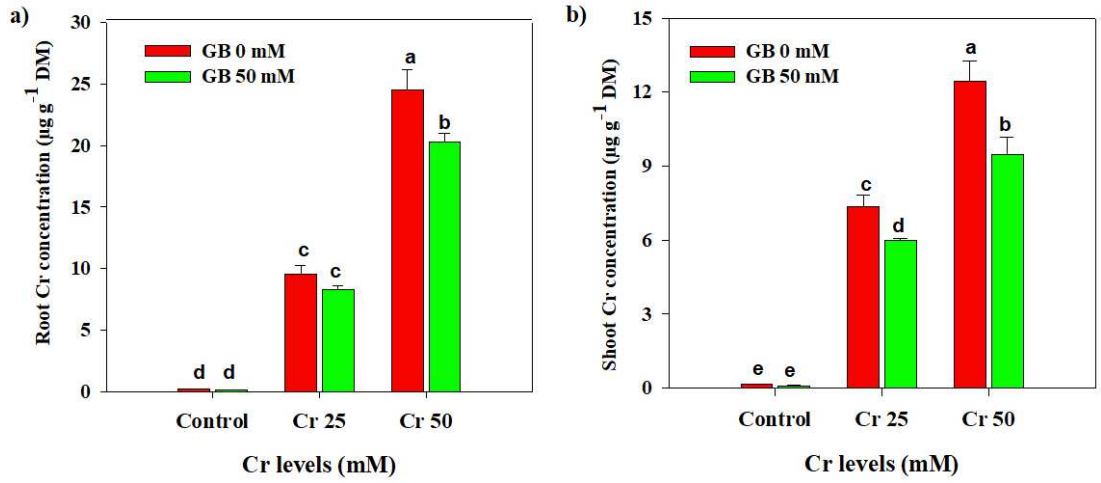

Figure 4. *The concentrations of Cr in roots and shoots of pea grown in different concentrations of Cr stress with and without exogenously applied GB. Vertical bars are three replicates mean have ± S.E. and different letters indicate significant difference at 0.05 P level according to LSD test*

Discussion

Chromium toxicity in soils has been continuously increasing and posing a serious threat to food production. We tested the impact of Cr stress on growth, physiological traits, and antioxidant enzymes and role of the GB in alleviating the deleterious impacts of Cr stress. We noticed that Cr stress had negative effects on plant growth and morphology and an increase in Cr concentration had more deleterious effects on plant growth and morphological characteristics (*Table 1*).

Reduction in plant growth due to Cr has been widely documented by different authors (Ali et al., 2013; Wakeel and Xu, 2020). Reduction in growth attributes might be due to a restricted supply of important nutrients (Aamer et al., 2018; Majhi and Samantaray, 2020) as Cr interferes with different nutrients and reduced their uptake and availability and therefore reduced plant growth (Guo et al., 2020). Cr stress reduced root length which can be due to Cr accumulation in pea roots or mutilation of root tip cells due to Cr stress (Gill et al., 2015).

Foliar applied GB featured a remarkable improvement in the growth and biomass production of pea plants. *Glycinebetaine* improves nutrient uptake and leaf gas exchange qualities and therefore, leads to a substantial increase in the growth and morphology under stress conditions (Shahbaz et al., 2012; Aamer et al., 2018). Moreover, GB-mediated improvement in plant growth was due to positive effect of GB on photosynthetic and transpiration rates and sub-stomatal CO_2 concentration (Jan et al., 2020). *Glycinebetaine* also increased gene expression for scavenging of ROS which, therefore, protects photosynthetic machinery, photosynthetic enzymes (rubisco and rubisco activase) and major molecules (proteins, DNA) from damaging effects of oxidative stress and therefore, increased the growth under stress conditions (Chen and Murata, 2011).

http://www.aloki.hu ● ISSN 1589 1623 (Print) ● ISSN 1785 0037 (Online)
DOI: http://dx.doi.org/10.15666/aeer/2005_42954307

Chromium stress also induced a significant reduction in chlorophyll (a,b and a/b) and carotenoids and increase in Cr concentration linearly deceased the photosynthetic pigments (*Fig. 1*). Cr stress decreased the photosynthetic pigments owing to alterations in chloroplast structures and reduction in synthesis of photosynthestic pigments and carotenoids due to substantial increase in activities of chlorophyllase (Hegedüs et al., 2001) and production of Cr induced ROS (Zewail et al., 2020). A significant increase in photosynthetic pigments was observed with GB application under control and Cr stress conditions (*Fig. 1*). Accumulation of GB under stress conditions protects the chlorophyll structure and improves the photosynthetic efficiency and stomatal conductance and therefore leads to significant improvement in chlorophyll and carotenoid contents under stress conditions (Wang et al., 2010). GB also reduced the Cr uptake and increased the antioxidant activities (*Fig. 3*) which in turn increased the concentration of photosynthetic pigments under stress conditions (Wang et al., 2010).

It was noticed Cr stress induced a significant increase in H_2O_2 production and MDA contents (*Fig. 2*), interestingly activities of the antioxidant enzymes were significantly increased under both levels of Cr stress (*Fig. 3*). The increase in activities of antioxidant under stress conditions has been reported in spinach and maize (Aamer et al., 2018; Dustgeer et al., 2021). The increase in activities of antioxidant enzymes gives evidence about the role of antioxidants in scavenging ROS and providing protection to plants under stress. In current investigation, foliar-applied GB considerably improved antioxidant activities under Cr stress. Glycinebetaine-induced increase in antioxidant activities reduced the Cr uptake and ROS production. Therefore, exogenous GB contributes toward the detoxification of ROS and leads to significant improvement in plant tolerance against the Cr stress (Ali et al., 2015). Exogenously applied GB also reduced the H_2O_2 and MDA contents under stress conditions owing to a marked increase in activities of antioxidant enzymes (*Fig. 3*) (Bharwana et al., 2014; Jabeen et al., 2016).

Chromium concentration was increased in plant roots and shoots under Cr contaminated soil (*Fig. 4*). Likewise, Ali et al. (2015) also noticed a significant increase in Cr accumulation plant parts with increasing Cr concentration. Nonetheless, in this study, foliar-applied GB remarkably reduced the Cr in plant roots and shoots (*Fig. 4*). GB protected the cell membranes and reduced Cr entrance in the cytoplasm and consequently lead to a reduction in Cr uptake and accumulation in plant parts (Giri, 2011; Daud et al., 2021). Another possible reason for the reduction in Cr uptake by foliar-applied GB might be due to Cr competition with other nutrients, as exogenously applied GB increased the uptake of nutrients that compete with the Cr and therefore reduce Cr uptake (Shahbaz and Zia, 2011; Castro-Duque et al., 2020).

Conclusions

In conclusion, chromium stress significantly reduced plant growth, photosynthetic pigments, and antioxidant activities, while enhanced Cr accumulation in different plant parts. However, exogenous applied GB alleviated the detrimental effects of Cr toxicity and increased plant growth, production of biomass and concentration of photosynthetic pigments. The GB-induced alleviation of Cr toxicity in pea was associated with improved antioxidant activities and reduced Cr uptake. However, further studies should be conducted to understand the molecular and cellular mechanisms of alleviation of Cr toxicity by exogenously applied GB.

http://www.aloki.hu ● ISSN 1589 1623 (Print) ● ISSN 1785 0037 (Online)
DOI: http://dx.doi.org/10.15666/aeer/2005_42954307

REFERENCES

[1] Aamer, M., Muhammad, U. H., Li, Z., Abid, A., Su, Q., Liu, Y., Huang, G. (2018): Foliar application of glycinebetaine (gb) alleviates the cadmium (cd) toxicity in spinach through reducing cd uptake and improving the activity of anti-oxidant system. – Applied Ecology Environment Research 16: 7575-7583.

[2] Adrees, M., Ali, S., Rizwan, M., Ibrahim, M., Abbas, M., Farid, M., Bharwana, S. A. (2015): The effect of excess copper on growth and physiology of important food crops: a review. – Environmental Science and Pollution Research 22: 8148-8162.

[3] Aebi, H: (1984): Catalase in vitro. – Methods in Enzymology 105: 121-126.

[4] Ahmad, R., Ali, S., Abid, M., Rizwan, M., Ali, B., Tanveer, A., Ghani, M. A. (2020): Glycinebetaine alleviates the chromium toxicity in *Brassica oleracea* L. by suppressing oxidative stress and modulating the plant morphology and photosynthetic attributes. – Environmental Science and Pollution Research 27: 1101-1111.

[5] Ali, S., Farooq, M. A., Yasmeen, T., Hussain, S., Arif, M. S., Zhang, G. (2013): The influence of silicon on barley growth, photosynthesis and ultra-structure under chromium stress. – Ecotoxicology and Environmental Safety 89: 66-72.

[6] Ali, S., Chaudhary, A., Rizwan, M., Anwar, H. T., Adrees, M., Farid, M., Anjum, S. A. (2015): Alleviation of chromium toxicity by glycinebetaine is related to elevated antioxidant enzymes and suppressed chromium uptake and oxidative stress in wheat (*Triticum aestivum* L.). – Environmental Science and Pollution Research 22: 10669-10678.

[7] Anjum, Q. S., Amjad, M., Ziaf, K., Habib, A. (2020): Seed treatment with salicylic acid improves growth, biochemical attributes and quality seed production of pea. – Pakistan Journal of Agricultural Science 57: 1370-1379.

[8] Arnon, D. (1949): Copper enzymes in isolated chloroplasts. Polyphenoloxidase in Beta vulgaris. – Plant Physiology 24: 1.

[9] Bharwana, S. A., Ali, S., Farooq, M. A., Iqbal, N., Hameed, A., Abbas, F., Ahmad, M. S. A. (2014): Glycine betaine-induced lead toxicity tolerance related to elevated photosynthesis, antioxidant enzymes suppressed lead uptake and oxidative stress in cotton. – Turkish Journal of Botany 38: 281-292.

[10] Castro-Duque, N. E., Chávez-Arias, C. C., Restrepo-Díaz, H. (2020): Foliar glycine betaine or hydrogen peroxide sprays ameliorate waterlogging stress in cape gooseberry. – Plant 9: 644.

[11] Chen, T. H. H., Murata, N. (2011): Glycinebetaine protects plants against abiotic stress: mechanisms and biotechnological applications. – Plant Cell Environment 34: 1-20.

[12] Dahl, W. J., Foster, L. M., Tyler, R. T. (2012): Review of the health benefits of peas (*Pisum sativum* L.). – The British Journal of Nutrition 108: 3-10.

[13] Daud, M. K., Ali, S., Variath, M. T., Khan, M., Jamil, M., Ahmad, M., Zhu, S. J. (2021): Chromium (VI)-Induced leaf-based differential physiological, metabolic and microstructural changes in two transgenic cotton cultivars (J208, Z905) and their hybrid line (ZD14). – Journal of Plant Growth Regulation 1-13.

[14] Dhindsa, R. S., Plumb-Dhindsa, P., Thorpe, T. A. (1981): Leaf senescence: correlated with increased levels of membrane permeability and lipid peroxidation, and decreased levels of superoxide dismutase and catalase. – Journal of Experimental Botany 32: 93-101.

[15] Dustgeer, Z., Seleiman, M. F., Imran, K., Chattha, M. U., Alhammad, B. A., Hassan, M. U. (2021): Glycine-betaine induced salinity tolerance in maize by regulating the physiological attributes, antioxidant defense system and ionic homeostasis. – Notulae Botanicae Horti Agrobotanici Cluj-Napoca 49: 12248-12248.

[16] El-Baz, A. A., Hendy, I., Dohdoh, A. M., Srour, M. I. (2021): Adsorption of high chromium concentrations from industrial wastewater using different agricultural residuals. – Journal of Environmental Treatment Techniques 9: 122-138.

http://www.aloki.hu ● ISSN 1589 1623 (Print) ● ISSN 1785 0037 (Online)
DOI: http://dx.doi.org/10.15666/aeer/2005_42954307

[17] Gautam, V., Sharma, P., Bakshi, P., Arora, S., Bhardwaj, R., Paray, B. A., Ahmad, P. (2020): Effect of Rhododendron arboreum leaf extract on the antioxidant defense system against chromium (VI) stress in *Vigna radiata* plants. – Plant 9: 164.
[18] Ghani, A., Ghani, A. (2011): Effect of chromium toxicity on growth, chlorophyll and some mineral nutrients of *Brassica juncea* L. – Egyptian Academic Journal of Biological Sciences 2: 9-15.
[19] Gill, R. A., Zang, L., Ali, B., Farooq, M. A., Cui, P., Yang, S., Ali, S., Zhou, W. (2015): Chromium-induced physio-chemical and ultrastructural changes in four cultivars of *Brassica napus* L. – Chemosphere 120: 154-164.
[20] Giri, J. (2011): Glycinebetaine and abiotic stress tolerance in plants. – Plant Signaling and Behavior 6: 1746-1751.
[21] Guo, X., Ji, Q., Rizwan, M., Li, H., Li, D., Chen, G. (2020): Effects of biochar and foliar application of selenium on the uptake and subcellular distribution of chromium in *Ipomoea aquatica* in chromium-polluted soils. – Ecotoxicology Environment Safety 206: 111184.
[22] Hassan, M. U., Aamer, M., Chattha, M. U., Ullah, M. A., Sulaman, S., Guoqin, H. (2017): The role of potassium in plants under drought stress: mini review. – Journal of Basic & Applied Sciences 13: 268-271.
[23] Hassan, M. U., Chattha, M. U., Khan, I., Chattha, M. B., Aamer, M., Khan, T. A. (2019): Nickel toxicity in plants: reasons, toxic effects, tolerance mechanisms, and remediation possibilities-a review. – Environmental Science and Pollution Research 26: 12673-12688.
[24] Hassan, U., Aamer, M., Chattha, M. U., Haiying, T., Shahzad, B., Guoqin, H. (2020a): The critical role of zinc in plants facing the drought stress. – Agriculture 10: 396.
[25] Hassan, M. U., Chattha, M. U., Khan, I., Chattha, M. B., Barbanti, L., Aslam, M. T. (2020b): Heat stress in cultivated plants: nature, impact, mechanisms, and mitigation strategies-a review. – Plant Biosystems 155: 211-234.
[26] Hassan, M. U., Aamer, M., Chattha, M. U., Haiying, T., Khan, I., Afzal, A. (2021): Sugarcane distillery spent wash (DSW) as a bio-nutrient supplement: a win-win option for sustainable crop production. – Agronomy 11: 183.
[27] Hayat, S., Khalique, G., Irfan, M., Wani, A. S., Tripathi, B. N., Ahmad, A. (2012): Physiological changes induced by chromium stress in plants: an overview. – Protoplasma 249: 599-611.
[28] Hegedüs, A., Erdei, S., Horváth, G (2001): Comparative studies of H_2O_2 detoxifying enzymes in green and greening barley seedlings under cadmium stress. – Plant Science 160: 1085-1093.
[29] Hossain, M. A., Hasanuzzaman, M., Fujita, M. (2010): Up-regulation of antioxidant and glyoxalase systems by exogenous glycinebetaine and proline in mung bean confer tolerance to cadmium stress. – Physiology and Molecular Biology of Plant 16: 259-272.
[30] Jabeen, N., Abbas, Z., Iqbal, M., Rizwan, M., Jabbar, A., Abbas, F. (2016): Glycinebetaine mediates chromium tolerance in mung bean through lowering of Cr uptake and improved antioxidant system. – Archives of Agronomy and Soil Science 62: 648-662.
[31] Jan, S., Noman, A., Kaya, C., Ashraf, M., Alyemeni, M. N., Ahmad, P. (2020): 24-Epibrassinolide alleviates the injurious effects of Cr (VI) toxicity in tomato plants: insights into growth, physio-biochemical attributes, antioxidant activity and regulation of Ascorbate–glutathione and Glyoxalase cycles. – Journal of Plant Growth Regulation 39: 1587-1604.
[32] Jones, J. B., Case, W. W. (1990): Sampling, handling and analyzing plant tissue samples. – Sampling Handling and Analyzing Plant Tissue Samples 1990: 389-427.
[33] Majhi, P., Samantaray, S. M. (2020): Effect of hexavalent chromium on paddy crops (Oryza sativa). – Journal of Pharmacognosy Phytochemistry 9: 1301-1305.

http://www.aloki.hu ● ISSN 1589 1623 (Print) ● ISSN 1785 0037 (Online)
DOI: http://dx.doi.org/10.15666/aeer/2005_42954307

[34] Medda, S., Mondal, K. K. (2017): Chromium toxicity and ultrastructural deformation of *Cicer arietinum* with special reference of root elongation and coleoptile growth. – Annals of Agrarian Science 15: 396-401.
[35] Mushtaq, Z., Asghar, H. N., Zahir, Z. A. (2021): Comparative growth analysis of okra (*Abelmoschus esculentus*) in the presence of PGPR and press mud in chromium contaminated soil. – Chemosphere 262: 127865.
[36] Nakano, Y., Asada, E. (1981): Hydrogen peroxide is scavenged by ascorbate-specific peroxidase in spinach chloroplasts. – Plant cell Physiology 22: 867-880.
[37] Pandey, V., Dixit, V., Shyam, R. (2009): Chromium effect on ROS generation and detoxification in pea (*Pisum sativum*) leaf chloroplasts. – Protoplasma 236: 85-95.
[38] Rasheed, A., Hassan, M. U., Aamer, M., Batool, M., Sheng, F., Ziming, W., Huijie, L (2020): A critical review on the improvement of drought stress tolerance in rice (*Oryza sativa* L.). – Notulae Botanicae Horti Agrobotanici Cluj-Napoca 48: 1756-1788.
[39] Roth, E. F., Gilbert, P. S. (1984): The pyrogallol assay for superoxide dismutase: absence of a glutathione artifact. – Annuals of Biochemistry 137: 50-53.
[40] Samantaray, S., Das, S., Mohanty, R. C., Mohanty, M., Pradhan, C. (2015): Altered germination index and chlorophyll biosynthesis in seedlings of wild rice cultivars in response to hexavalent chromium stress. – Discovery 27: 27-35.
[41] Shahbaz, M., Zia, B. (2011): Does exogenous application of glycinebetaine through rooting medium alter rice (*Oryza sativa* L.) mineral nutrient status under saline conditions. – Journal of Applied Botany and Food Quality 84: 54-60.
[42] Shahbaz, M., Masood, Y., Perveen, S., Ashraf, M. (2012): Is foliar-applied glycinebetaine effective in mitigating the adverse effects of drought stress on wheat (*Triticum aestivum* L.). – Journal of Applied Botany and Food Quality 84: 192-198.
[43] Singh, P. K., Gautam, S. (2013): Role of salicylic acid on physiological and biochemical mechanism of salinity stress tolerance in plants. – Acta Physiologiae Plant 35: 2345-2353.
[44] Sofo, A., Scopa, A., Nuzzaci, M., Vitti, A. (2015): Ascorbate peroxidase and catalase activities and their genetic regulation in plants subjected to drought and salinity stresses. – International Journal of Molecular Sciences 16: 13561-13578.
[45] Sofy, M. R., Elhawat, N., Alshaal, T (2020): Glycine betaine counters salinity stress by maintaining high K+/Na+ ratio and antioxidant defense via limiting Na+ uptake in common bean (*Phaseolus vulgaris* L.). – Ecotoxicology Environmental Safety 200: 110732.
[46] Steel, R. G. D., Torrie, J. H., Dickey, D. A. (1996): Principles and Procedures of Statistics: A Biometric Approach. 3rd Ed. – McGraw-Hill Book Company, Inc., New York.
[47] Velikova, V. I., Yordanov, A., Edreva, A (2000): Oxidative stress and some antioxidant systems in acid rain-treated bean plants: protective role of exogenous polyamines. – Plant Science 151: 59-66.
[48] Wakeel, A., Xu, M. (2020): Chromium morpho-phytotoxicity. – Plant 9: 564.
[49] Wang, G. P., Li, J., Zhang, M. R., Zhao, Z., Hui, W., Wang, W. (2010): Overaccumulation of glycine betaine enhances tolerance of the photosynthetic apparatus to drought and heat stress in wheat. – Photosynthetica 48: 30-41.
[50] Yin, J., Wang, L., Wang, L., Huang, T., Zhang, X. (2021): Pretreatment with selenium prevented the accumulation of hexavalent chromium in rainbow trout (*Oncorhynchus mykiss*) and reduced the potential health risk of fish consumption. – Food Control 122: 107817.
[51] Zewail, R. M., El-Desoukey, H. S., Islam, K. R. (2020): Chromium stress alleviation by salicylic acid in Malabar spinach (*Basella alba*). – Journal of Plant Nutrition 43: 1268-1285.

http://www.aloki.hu ● ISSN 1589 1623 (Print) ● ISSN 1785 0037 (Online)
DOI: http://dx.doi.org/10.15666/aeer/2005_42954307

[52] Zhang, X. Z. (1992): The measurement and mechanism of lipid peroxidation and SOD, POD and CAT activities in biological system. – Research Methodology Crop Physiology Agriculture Press Beijing 208-211.

http://www.aloki.hu ● ISSN 1589 1623 (Print) ● ISSN 1785 0037 (Online)
DOI: http://dx.doi.org/10.15666/aeer/2005_42954307

EFFECTS OF REPLACEMENT CONTROL WITH *HUMULUS SCANDENS* ON THE RHIZOSPHERE MICROBIAL COMMUNITY DIVERSITY OF THE INVASIVE PLANT, *ALTERNANTHERA PHILOXEROIDES*

GONG, Z. F.[1] – DAI, Y. Y.[1] – ZHANG, Z.[1,2*] – MU, J.[1] – HE, M. Y.[1]

[1]*School of Resources and Environment, Anhui Agricultural University, Hefei, Anhui 230036, China*

[2]*State Key Laboratory of Vegetation and Environmental Change, Beijing 100093, China*

[*]*Corresponding author*
e-mail: xjzhangzhen@163.com

(Received 3rd Apr 2022; accepted 26th Jul 2022)

Abstract. The impacts of invasive plants are known to be mediated by plant-microbial interactions. Many ecologists are interested in the variance of the microbial community structure of invasive plants and native plants in the rhizosphere soils. In order to clarify the interaction mechanism between native plants and invasive plants, we reported the characteristics of soil microbial communities in invasive plants under different degrees of replacement plant. *Alternanthera philoxeroides* (Mart.) Griseb. is a serious invasive weed in many regions. Rhizospheric soils of *A. philoxeroides* with different degrees of substitution by *Humulus scandens* (Lour.) Merr. (unreplacement, low degree, high degree, replacement and CK using its coverage in the invaded ecosystems) were collected. pH, soil electrical conductance, available phosphorous and available potassium were major factors to alter the microbial community structure of *A. philoxeroides* in the rhizosphere. Plant replacement significantly reduced the abundance of *Acidobacteria* and *Verrucomicrobia*, but not *Chloroflexi* and *Actinobacteria*. Low and high degrees of *H. scandens* increased the richness of soil fungal community. Overall, the results suggested that rhizosphere microbes were changed by replacement plant of this invader in the novel environment, which provided a theoretical basis for the control of *A. philoxeroides*.
Keyword: *microbial communities, replacement control, invasive species, native species, rhizosphere microorganisms*

Introduction

Biological invasion has become one of the global environmental problems (Sala et al., 2000), and invasive species can disrupt native mutualism, cause population declines, reduce biodiversity, and alter ecosystem function (Claudia and Florens, 2011). At present, the methods to control invasive plants are focused on mechanical control, chemical control, biological control and ecological control. Among the available weed control methods, mechanical control is considered as a type of physical disturbance, which can be time, energy and financially consuming. Meanwhile it cannot last for a long time (Jia et al., 2009). Due to the increasing health concerns of chemical control (Lin et al., 2016) and the possible non-target effects of biological control (Liu et al., 2015), as the main technology of ecological control methods, replacement control has been raised more and more attention (Li et al., 2015). In the study of the replacement control of invasive plants, previous students found that microorganisms living in the rhizosphere, where soil is surrounded and affected by plant roots, have long been recognized to have significant effect on plant nutrition and health (Moreau et al., 2015). Most organisms are directly or indirectly associated with mutualistic partner, just like plants interact with soil

http://www.aloki.hu ● ISSN 1589 1623 (Print) ● ISSN1785 0037 (Online)
DOI: http://dx.doi.org/10.15666/aeer/2005_43094320

microorganisms by positive feedback or negative feedback (Wagg et al., 2011). Meanwhile, the decomposers provide the plants with available nutrients by degrading plant residues which is commonly considered as one of the main drivers of plant-microbe interactions (Yu et al., 2011; Shen et al., 2016). Root-associated organisms and their consumers influence the quality, direction, and flow of energy and nutrients between plants and decomposers (Ehrenfeld and Scott, 2001; Bever, 2002; Wardle et al., 2004). It suggests that the research on replacement control of invasive plants is also more inclined to change the relationship between native plants, invasive plants and soil microorganisms.

Alternanthera philoxeroides (Mart.) Griseb. (Amaranthaceae) originated in the Parana River region of South America and is considered a serious weed in the United States, China, Australia, New Zealand, Indonesia, India and Thailand (Julien et al., 1995). The control of the invasive plant is difficult because mechanical, chemical and biological control methods are not effective on sustained reduction in biomass (Jia et al., 2009; Reeves, 2017). We observed that *Humulus scandens* (Lour.) Merr. (Moraceae) often coexist with *A. philoxeroides* in the same habitats in field and significantly affect the growth of the later species. which is a climbing therophyte vine and vegetative growth, usually cluster together with strong ability to adapt to the cold and drought and found cohabiting with *A. philoxeroides* currently. It has various positive uses. For example, it can be harvested for medicinal use (Chen et al., 2012), material of industry (Gargiullo, 2005) and soil and water conservation (Li et al., 2014).

To test these hypotheses, we conducted field investigations of the microbiome interactions between *H. scandens* and *A. philoxeroides*, addressing three questions: (1) How do soil nutrient contents change? (2) How has the soil microbial community structure changed in the change of substitution degree? (3) What is the relationship between soil nutrients and soil microorganisms?

Materials and Methods

Site description

Samples were obtained from Anhui agricultural university in Hefei, China (31°86'N, 117°25'E). The study area has a Subtropical monsoon humid climate, with an annual mean temperature of approximately 15.7 ℃ and an annual precipitation of approximately 1000 mm. The type of vegetation of these samples are: *H. scandens*(Humulus), *A. philoxeroides* (Amaranthaceae), *Digitaria sanguinalis* (Poaceae), *Echinochloa crusgalli* (Poaceae), *Setaria viridis* (Poaceae).

Experimental design

In August 2016, rhizospheric soil samples with different degrees of *A. philoxeroides* and *H. scandens* invasion were collected from the chosen area, i.e., unreplacement (0%, A), low degree (<35%, A+H), high degree (>75%, H+A) , replacement(100%, H), and CK (no *A. philoxeroides* and *H. scandens*) using the coverage of *H. scandens* in the replacement ecosystem in spring 2015. Three soil samples within an approximately 20 cm radius of *H. scandens* and *A. philoxeroides* rhizosphere from each replacement degree in each site were collected. The rhizosphere soil collection was used to refer to the Inderjit method (Inderjit, 1997) and the soil of 1cm around the root of the plant was interrhizosphere soil. A total of fifteen treatment combinations were obtained: 3 sample areas × 5 replacement degrees. The soil samples were passed through a 2 mm sieve to

http://www.aloki.hu ● ISSN 1589 1623 (Print) ● ISSN1785 0037 (Online)
DOI: http://dx.doi.org/10.15666/aeer/2005_43094320

remove leaves, plant roots, and gravel. All soil samples from one site were homogenized by thorough mixing and then stored for further processing. Soil samples can be divided into two parts, the part is used for the determination of soil physicochemical properties, the other part into sealed sterile bags, put in ice packs back to lab, to -80 ℃ cryopreservation for DNA extraction.

Determination of soil physicochemical properties

Soil pH values were measured using a glass electrode (1:2.5 soil–water ratios) after shaking the samples for approximately 30 min to equilibrate. Soil organic matter was analyzed using the method of $K_2Cr_2O_7$–H_2SO_4 oxidation. Soil nitrogen (N) concentration was determined by the Semimicro-Kjeldahl method. Soil phosphorus (P) concentration was determined using the Mo-Sb antispetrophotography method. Soil potassium (K) concentration was determined with the NaOH-melt method.

Determination of structure and diversity in soil microbial communities

Genomic DNA was isolated from the 15 samples using a PowerSoil DNA isolation kit (MO Bio Laboratories, Inc. Carlsbad, CA) following the manufacturer's instructions. The internal transcribed spacer (ITS) egion was amplified using fungal-specific primers: ITS3F(5'-GCATCGATGAA GAACGCAGC-3'), ITS4R(5'-TCCTCCGCTTATTGATATGC-3'). Bacterial 16s rRNA gene amplicons were amplified using primers 515F(5'-GTGCCAGCMGCCGCGGTAA-3'), 907R (5'-CCGTCAATTCMTTTRAGTTT-3'). DNA regions were amplified using the HotStarTaq Plus Master Kit (Qiagen, Valencia, CA). Amplicons from different samples were mixed in equal concentrations and purified using Agencourt Ampure beads (Agencourt Bioscience Corporation, USA). Paired-end 2 × 250 bp sequencing was performed on an Illumina MiSeq instrument (Illumina Inc., San Diego, CA, USA).

Statistical analyses

OTU richness and diversity indices (richness, Shannon, inverse Simpson and Pielou's evenness), together with accumulation curves were calculated using the QIIME (http://qiime.org/index.html) (Vishnu et al., 2021). Cluster analysis was performed using the UPGMA method. Canoco 4.5 was used to perform the RDA (Abbas et al., 2021). R statistical software 3.2.5 was used to perform OUT and heatmap.

All data were checked for deviations from normality and homogeneity of variance before analysis. The effects of the degree of *H. scandens* on soil microbial communities of *A. philoxeroides* in the rhizosphere and Shannon–Wiener diversity and evenness indices of soil microorganisms were determined by analysis of variances (ANOVA) with site considered as a block effect using IBM SPSS 20.0. LSD was used at 0.05 of probability for comparing the differences between different treatment means.

Results

Soil physicochemical properties

Soil pH value increased by 1.1% to 6.5% as the replacement degree of increased (*Table 1*, $P < 0.05$) whereas high degrees had no significant effect on soil pH value (*Table 1*, $P > 0.05$). High degrees of increased soil electrical conductance; the difference between the effects of low, high and none degrees of replacement on soil electrical

http://www.aloki.hu ● ISSN 1589 1623 (Print) ● ISSN1785 0037 (Online)
DOI: http://dx.doi.org/10.15666/aeer/2005_43094320

conductance was not significant (*Table 1*, P > 0.05). Soil available phosphorous concentration under low and high degrees of replacement was significantly higher than that under none degrees (*Table 1*, P < 0.05), which is the same as soil available potassium (*Table 1*, P < 0.05). Both none, low and high degrees did not significantly change soil organic matter, total nitrogen, total phosphorous, total potassium concentrations (*Table 1*, P > 0.05).

Table 1. *Physicochemical properties of the soil samples in five replacement situation*

Treatment	Soil pH	EC×10^{3}us/cm	TN g/kg	TK g/kg	TP g/kg	AP mg/kg	AK mg/kg	Organic matter g/kg
H	7.68±0.26ab	0.11±0.017ab	2.81±0.39a	12.73±1.64a	0.27±0.071a	5.4±1.25a	195.67±15.044a	11.56±2.67a
H+A	7.98±0.20a	0.16±0.02a	2.62±0.12a	12.42±0.86a	0.41±0.19a	6.35±1.37a	196.33±25.58a	11.22±3.72a
A+H	7.57±0.168b	0.14±0.026ab	2.31±1.18a	12.84±0.94a	0.42±0.11a	5.01±0.59a	197.67±18.56a	8.67±1.46a
A	7.49±0.07b	0.11±0.00b	2.28±0.46a	14.11±1.75a	0.25±0.03a	0.68±0.49b	148.33±3.79b	9.4±0.75a
CK	7.75±0.05ab	0.14±0.058ab	3±0.42a	11.9±1.07a	0.39±0.16a	6.89±1.29a	212.33±10.50a	8.92±1.92a

The values in the table represent means of the values of the three replicates with the same replacement degree of *H. scandens*. Data with different superscript letters in a vertical row indicate significant difference (P < 0.05).H: replacement (100%), H+A: high degree of replacement (>75%), A+H: low degree of replacement (<35%), A: none degrees of replacement (0%), CK (no A. philoxeroides and *H. scandens*

Structure of soil microbial communities

Analyzing the microbial communities associated with the rhizospheres of *A. philoxeroides*, we obtained 151,757 and 648,340 total seqs, which resulted in 20,184 and 9,411 OTUs for bacteria and fungi, respectively (*Table 2*). The levels of bacteria diversity (chao1, Shannon, Simpson,) of *A. philoxeroides* in the rhizosphere tended to be higher in the high degrees than in the other samples (*Table 2*). However, the levels of fungi diversity of *A. philoxeroides* in the rhizosphere tended to be higher in the low degrees than in the other samples (*Table 2*).

Table 2. *Shannon–Wiener diversity(H'), Simpson, chao1 index and average genetic diversity of bacteria and fungi in five replacement situation*

	Replacement situation	No. of seqs	No. of OTUs	chao1	Observed species	Simpson	Shannon
Bacteria	CK	10289	1232	1713.026	1000	0.9786	7.6742
	H+A	8180	1394	2004.943	1260	0.9917	8.6321
	H	11296	1319	1676.083	1035	0.9821	7.9177
	A	9512	1457	1995.713	1223	0.9832	8.2654
	A+H	11308	1326	1711.178	1034	0.9831	7.9260
Fungi	CK	41204	682	836.716	593	0.7212	3.7890
	H+A	49296	514	672.494	416	0.6697	2.9415
	H	48606	673	796.176	547	0.9106	4.8395
	A	33288	512	699.756	470	0.4695	2.4016
	A+H	43720	756	900.246	631	0.9165	5.0244

Statistics of No. of seqs for each sample: sum the values of each column, that is, the total number of sequences for each sample. Statistics of No. of OTUs for each sample: in each column of values, all values greater than 0 are recorded as 1 and summed, that is, the total number of OTUs for each sample

http://www.aloki.hu ● ISSN 1589 1623 (Print) ● ISSN1785 0037 (Online)
DOI: http://dx.doi.org/10.15666/aeer/2005_43094320

A total of 30 distinct bacterial phyla (relative abundance>1%) were detected across all samples. The most abundant sequences of every degree of *H. scandens* were affiliated with the phylum *Acidobacteria* (33.4-18.7% of total relative abundance), followed by *Proteobacteria* (23.5-16.7%), *Chloroflexi* (30.3-12.9%), *Actinobacteria* (12.7-3.4%), *Verrucomicrobia* (7.5-5.3%), *Gemmatimonadetes* (5.8-2.6%), *Bacteroidetes* (2.8%-1.1%), *Nitrospirae* (2.5-1.2%) (*Figure 1a*). The abundant sequences of *Acidobacteria* and *Verrucomicrobia* decreased with the increase of substitution, but increasing degrees of *H. scandens* increased the abundance of *Chloroflexi* and *Actinobacteria* of soil bacterial community in rhizosphere of *A. philoxeroides*.

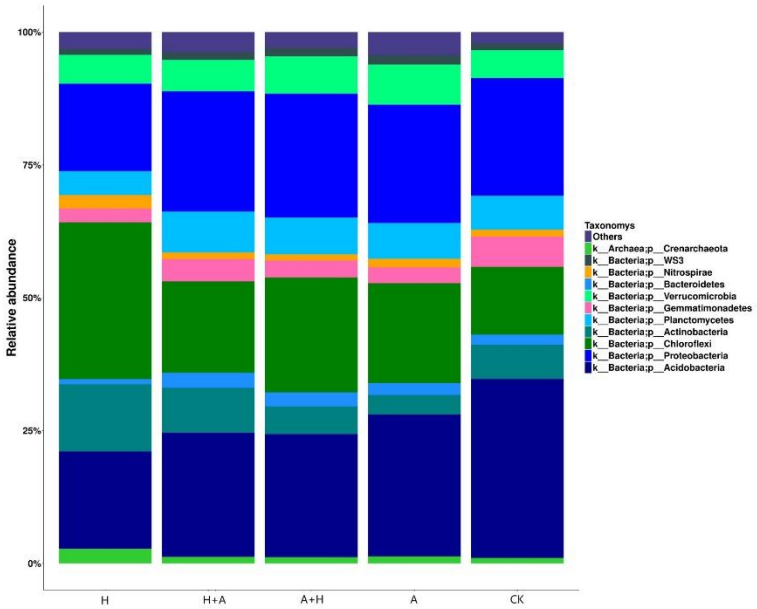

(a)

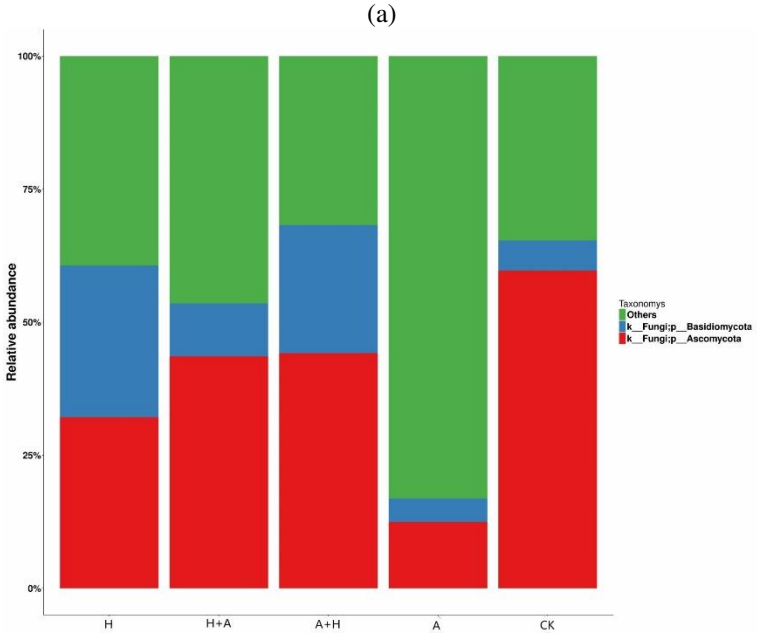

(b)

Figure 1. *Mean relative abundances of taxa (phylum levels) (a) bacterial and (b) fungal communities within each degree. The group 'Other' encompasses unclassified sequences together with phylums representing ≤0.5% of total sequences*

http://www.aloki.hu ● ISSN 1589 1623 (Print) ● ISSN1785 0037 (Online)
DOI: http://dx.doi.org/10.15666/aeer/2005_43094320

Fungal communities were dominated by the phylum *Ascomycota* (59.7-12.6%) and *Basidiomycota* (57.3-10.1%). Compared with the rhizosphere microorganism in the unsubstituted region, *Ascomycota* in other samples were significantly reduced (*Figure 1b*).

Correlation analysis between microorganisms and soil physicochemical

Results showed that the different classes of bacteria and fungi were significantly correlated with these soil parameters (*Table 3*). Factors such as pH and nutrient status are the main drivers controlling composition and diversity of soil microbial communities. *Acidobacteria* had significant negative (r=-0.592, p=0.02) relationships with soil electrical conductance. *Proteobacteria* and *Nitrospirae* had significant positive relationships with pH (r=0.545, p=0.027) (r=0.692, p=0.004) and soil electrical conductance (r=0.607, p=0.006) (r=0.682, p=0.005). *Gemmatimonadetes* had positive relationship with available phosphorous (r=0.532, p=0.034), available potassium (r=0675, p=0.002) and total phosphorous (r=0.515, p=0.035). *Ascomycota* had positive relationship with available phosphorous (r=0.662, p=0.002) and available potassium (r=0.672, p=0.002). *Basidiomycota* and *Glomeromycota* had significant positive relationships with pH (r=0.683, p=0.002) (r=0.815, p=0.000053), soil electrical conductance (r=0.684, p=0.005) (r=0.604, p=0.006) and available phosphorous (r=0.655, p=0.005) (r=0.701, p=0.003). *Chytridiomycota* had positive (r=0.775, p=0.001) relationship with soil organic matter.

Table 3. *Correlation between soil properties and the different bacterial and fungal phylums*

	Phyla	**Soil pH**	**EC**	**TN**	**AP**	**AK**	**TK**	**TP**	**Organic matter**
Bacteria	Acidobacteria	-0.283	-0.592*	0.244	0.067	0.131	-0.063	-0.328	0.136
	Proteobacteria	0.545*	0.607*	0.258	0.278	0.073	-0.359	0.254	-0.385
	Chloroflexi	-0.275	0.038	-0.366	-0.371	-0.257	0.417	0.24	0.059
	Actinobacteria	-0.216	0.161	-0.027	-0.138	-0.169	0.067	-0.092	-0.497
	Planctomycetes	-0.216	-0.097	0.214	-0.148	-0.07	0.037	0.053	-0.165
	Verrucomicrobia	-0.49	-0.162	0.278	0.349	0.347	-0.318	-0.169	-0.341
	Gemmatimonadetes	-0.09	0.211	0.114	0.532*	0.675**	-0.377	0.515*	-0.069
	Bacteroidetes	-0.222	-0.241	-0.101	0.044	0.18	0.066	0.256	0.08
	Nitrospirae	0.692**	0.682**	0.235	0.401	0.269	-0.193	0.293	0.279
Fungi	Ascomycota	0.181	-0.039	0.307	0.662**	0.672**	-0.384	0.122	0.164
	Basidiomycota	0.683**	0.684**	0.252	0.655**	0.495	-0.426	0.402	0.032
	Zygomycota	0.094	-0.299	0.411	0.372	0.26	-0.143	-0.212	0.262
	Glomeromycota	0.815**	0.604*	0.258	0.701**	0.513	-0.235	0.446	0.42
	Chytridiomycota	-0.17	-0.124	0.093	-0.105	0.079	0.201	0.03	0.775**

* indicates significant differences at the 0.05 probability level. ** indicates significant differences at the 0.01 probability level

Redundancy analysis was conducted to quantify the relative influence of the selected variables on microbial community composition (*Figure 2a*), which showed the relationship between the bacteria and soil chemistry parameters (*Figure 2b*). The first axi and the second axi explained 36.32% and 11.53%. Notably, the first axi had relationship with soil electrical conductance (r=-0.6278) and available potassium (r= 0.62059); the

http://www.aloki.hu ● ISSN 1589 1623 (Print) ● ISSN1785 0037 (Online)
DOI: http://dx.doi.org/10.15666/aeer/2005_43094320

second axi had relationship with total nitrogen (r= -0.562422) and pH (r= -0.519036). The result of relative between fungus and soil properties showed that the first axi and the second axi explained 25.89% and 13.43% (*Figure 2b*). The first axi had relationship with soil electrical conductance (r=-0.72508); the second axi had relationship with total nitrogen (r=0.7949).

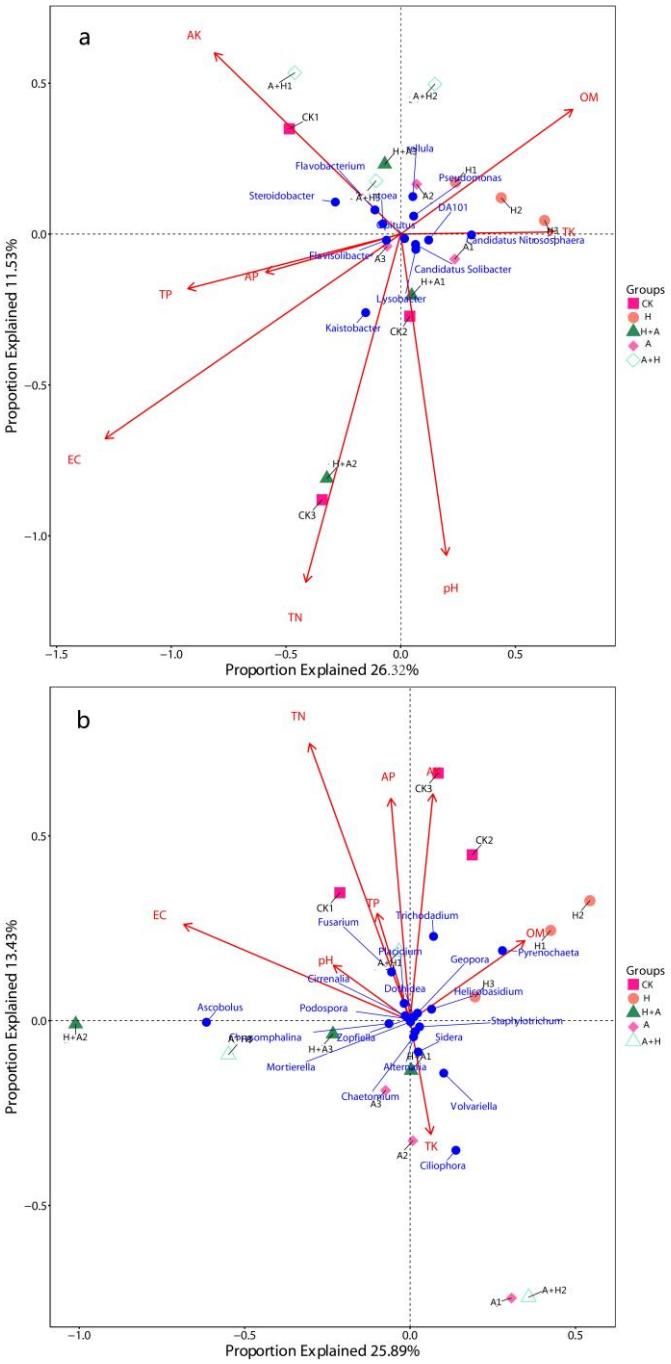

Figure 2. *Distance-based redundancy analysis (db-RDA) biplot of (a) bacterial and (b) fungal communities. Only the environmental variables that significantly (P < 0.05) explained variability in microbial community structure are shown (arrows). The direction of the arrows indicates the direction of maximum change of that variable, whereas the length of the arrow is proportional to the rate of change*

http://www.aloki.hu ● ISSN 1589 1623 (Print) ● ISSN1785 0037 (Online)
DOI: http://dx.doi.org/10.15666/aeer/2005_43094320

Surprisingly, environmental variables of pH, soil electrical conductance, available potassium, available phosphorous appeared to exert an important effect on the reference soils community composition.

Discussion

Currently, there are many studies on the impact of alternative control of invasive plants on soil physicochemical properties and microbial community structure (Lankau, 2010). However, few studies have used *A. philoxeroides* with *H. scandens* as alternative controls (Cao et al., 2013). This study suggested that soil physicochemical, including pH, soil electrical conductance, total nitrogen, available phosphorous and available potassium, had positive relationship with different degrees of replacement. Meanwhile, there were significant differences in the microbial diversity of *A. philoxeroides* in the rhizosphere at different degrees. Plant root exudates mostly are inorganic salts, soluble sugar, organic acid and other active substances, which can change the soil physicochemical properties and provide nitrogen source and carbon source for the growth of microorganisms, thereby changing the composition of soil microorganisms (de Vries et al., 2012).

Previous studies have shown that plant replacement significantly reduced the abundance of *Acidobacteria* and *Verrucomicrobia*, but not *Chloroflexi* and *Actinobacteria*. This result may be attributed mainly to the fact that *Acidobacteria* and *Verrucomicrobia* belong to the oligotrophic bacteria that are sensitive to soil nutrient content and decrease with the increase of soil nutrient content (Ramirez et al., 2012). Ramirez found that nitrogen application reduced the relative abundance of *Acidobacteria* and *Verrucomicrobia* (Ramirez et al., 2012). *Actinobacteria* are potent plant polysaccharide degrading microbes that play an important role in plant biomass degradation by producing a variety of lignocellulolytic enzymes and amylolytic enzymes in soil and various other environments (Kanokratana et al., 2011). Low and high degrees of invasion increased the richness of the soil fungal community and low degree was elevated significantly, which was the same as the results of *Wedelia trilobata* (Si et al., 2013). That roots of native plant proliferate sufficiently impedes the nutrient uptake of invasive species, which correlate strongly with the mycorrhizal dependence of species encountered in the invaded range (Stinson et al., 2006).

The correlation analysis between dominant population and soil physicochemical properties showed that pH, soil electrical conductance, total nitrogen, available phosphorous and available potassium were the main soil factors affecting microbial community diversity (Saggar et al., 1999; Liu et al., 2015). Redundancy analysis indicated that the bacteria community composition was most strongly affected by total nitrogen content followed by pH, soil electrical conductance and available potassium. The previous study showed that there was a significant negative correlation between *Acidobacteria* and pH (Campbell et al., 2010). In contrast, there was no correlation between *Acidobacteria* and pH in this study. Soil inorganic salts, organic matter and plants are other factors that alter *Acidobacteria* abundance (Liu et al., 2014). *Proteobacteria* and *Nitrospirae* had significant positive correlation with pH and soil electrical conductance, and nitrogen content was reported to be the factor that changed pH (Noah et al., 2012). Meanwhile, both *Proteobacteria* and *Nitrospirae* are active in the nitrogen cycle (Janssen, 2006). *Gemmatimonadetes* had significant correlation with nitrogen and phosphorus content., and recently, one of its few representatives, Gemmatimonas phototrophica, was found to contain purple bacterial photosynthetic

http://www.aloki.hu ● ISSN 1589 1623 (Print) ● ISSN1785 0037 (Online)
DOI: http://dx.doi.org/10.15666/aeer/2005_43094320

reaction centers , which appear to favour soil and wastewater treatment-associated habitats (Zeng et al., 2016). The results of PE Mortimer also indicated that soil electrical conductance and total nitrogen were the main soil factors of soil fungal community diversity (Mortimer et al., 2008). The main dominant species of *Ascomycota* and *Basidiomycota* are mainly pathogens. Studies have shown that some pathogenic fungi, such as *Fusarium* (Tan et al., 2002), *Nimbya* (Pomella et al., 2007) and *Alternaria* can infect *A. philoxeroides*.

By leaching and secretion activity in the alternative control process of *A. philoxeroides* changed soil physicochemical properties (Coleman et al., 2000), which also indirectly changed the soil microbial community structure (Saggar et al., 1999), making the resources conducive to the growth of *H. scandens*. The previous studies showed that replacement plants can alter soil physicochemical properties by changing the soil microbial community (which is closely related to plant growth and development), thus changing the invasion process (Yan et al., 2011). After the intercropping of *Lolium Perenne* and *Trifolium repens*, *T. repens* also changed the rhizosphere microbial community structure of Triticale (Hiddink et al., 2005), the reason of which may be that plants changed the soil microbial community through rhizosphere exudates and facilitate replacement plant growth (Bending and Lincoln, 1999; Smolinska and Horbowicz, 2010). However, elucidating the effects of single species of soil biota outside of the context of the entire soil community may not accurately describe the interactions that occur in nature (Reinhart and Callaway, 2006). The development of prevention and control of *A. philoxeroides* may be focus on the species interaction mechanism (*Acidobacteria*, *verrucomicrobia Chloroflexi*, *Actinobacteria* and fungi of *Ascomycota* and *Basidiomycota*), and the synergistic effects of the entire below-ground community may be particularly useful in determining the effects of soil biota on plants in their native and nonnative ranges.

Conclusion

In the current study, we provided evidence that pH, soil electrical conductance, available phosphorous and available potassium were major factors to alter the rhizosphere microbial community structure of *A. philoxeroides.* Plant replacement significantly reduced the abundance of *Acidobacteria* and *Verrucomicrobia*, but not *Chloroflexi* and *Actinobacteria*. Low and high degrees of *H. scandens* increased the richness of soil fungal community. Overall, the results suggested that rhizosphere microbes were changed by replacement plant of this invader in the novel environment, which provided a theoretical basis for the control of *A. philoxeroides*.

Acknowledgements. This study was supported by State Key Laboratory of Vegetation and Environmental Change (LVEC-2022kf01) and the National Natural Science Foundation of China (31772235).

Author Contributions. Z Zhang, ZF Gong, and MY He designed the research. Z Zhang, YY Dai wrote the manuscript. YY Dai and J Mu performed research, and collected the datasets and conducted the data pre-processing. Z Zhang supervised the project and commented on the contents of the manuscript. All authors reviewed the manuscript.

Additional Information. The authors declare no competing financial interests.

http://www.aloki.hu ● ISSN 1589 1623 (Print) ● ISSN1785 0037 (Online)
DOI: http://dx.doi.org/10.15666/aeer/2005_43094320

REFERENCES

[1] Abbas, A. M., Ayed, F. A. A., Sheded, M. G., Alrumman, S. A., Radwan, T. A. A., Badry, M. O. (2021): Vegetation analysis and environmental relationships of riverain plants in the Aswan Reservoir, Egypt. – Plants 10: 2712.
[2] Bending, G. D., Lincoln, S. D. (1999): Characterisation of volatile sulphur-containing compounds produced during decomposition of brassica juncea tissues in soil. – Soil Biology & Biochemistry 31: 695-703.
[3] Bever, J. D. (2002): Host-specificity of am fungal population growth rates can generate feedback on plant growth. – Plant and Soil 244: 281-290.
[4] Campbell, B. J., Polson, S. W., Hanson, T. E., Mack, M. C., Schuur, E. A. G. (2010): The effect of nutrient deposition on bacterial communities in arctic tundra soil. – Environmental Microbiology 12: 1842-1854.
[5] Cao, Y., Wang, T., Xiao, Y., Zhou, B. (2013): The interspecific competition between *Humulus scandens* and *Alternanthera philoxeroides*. – Journal of Plant Interactions 9: 194-199.
[6] Chen, Z., Meng, S., Yang, J., Nie, H. G., Jiang, H., Hu, H. Y., Meng, F. H. (2012): *Humulus scandens* chemical constituents determination and pharmacological action research. – Medicinal Chemistry 2: 29-32.
[7] Cláudia, B., Florens, F. B. V. (2011): Control of invasive alien weeds averts imminent plant extinction. – Biological Invasions 13: 2641-2646.
[8] Coleman, M. D., Dickson, R. E., Isebrands, J. G. (2000): Contrasting fine-root production, survival and soil CO_2 efflux in pine and poplar plantations. – Plant and Soil 225: 129-139.
[9] de Vries, F. T., Manning, P., Tallowin, J. R. B., Mortimer, S. R., Pilgrim, E. S., Harrison, K. A., Hobbs, P. J., Quirk, H., Shipley, B., Cornelissen, J. H. C., Kattge, J., Bardgett, R. D. (2012): Abiotic drivers and plant traits explain landscape-scale patterns in soil microbial communities. – Ecology Letters 10: 1230-1239.
[10] Ehrenfeld, J. G., Scott, N. (2001): Invasive species and the soil: effects on organisms and ecosystem processes. – Ecological Applications 11: 1259-1260.
[11] Fagan, W. F., Lewis, M. A., Neubert, M. G., Driessche, P. V. D. (2010): Invasion theory and biological control. – Ecology Letters 5: 148-157.
[12] Gargaret, M. B. (2004): Invasive plants of Asian origin established in the United States and their natural enemies, Volume 1. – The Journal of the Torrey Botanical Society 132: 375.
[13] Hiddink, G. A., Termorshuizen, A. J., Raaijmakers, J. M., Van Bruggen, A. H. C. (2005): Effect of mixed and single crops on disease suppressiveness of soils. – Phytopathology 95: 1325-1332.
[14] Inderjit, A. U. M. (1997): Effect of phenolic compounds on selected soil properties. – Forest Ecology & Management 92: 11-18.
[15] Janssen, P. H. (2006): Identifying the dominant soil bacterial taxa in libraries of 16s rRNA and 16s RNA genes. – Applied & Environmental Microbiology 72: 1719-28.
[16] Jia, X., Pan, X. Y., Li, B., Chen, J. K., Yang, X. Z. (2009): Allometric growth, disturbance regime, and dilemmas of controlling invasive plants: a model analysis. – Biological Invasions 11: 743-752.
[17] Julien, M. H., Skarratt, B., Maywald, G. F. (1995): Potential geographical distribution of alligator weed and its biological control by *Agasicles hygrophila*. – Journal of Aquatic Plant Management 33: 55-60.
[18] Kanokratana, P., Uengwetwanit, T., Rattanachomsri, U., Bunterngsook, B., Nimchua, T., Tangphatsornruang, S., Plengvidhya, V., Champreda, V., Eurwilaichitr, L. (2011): Insights into the phylogeny and metabolic potential of a primary tropical peat swamp forest microbial community by metagenomic analysis. – Microbial Ecology 61: 518-528.
[19] Lankau, R. (2010): Soil microbial communities alter allelopathic competition between *Alliaria petiolata* and a native species. – Biological Invasions 12: 2059-2068.

http://www.aloki.hu ● ISSN 1589 1623 (Print) ● ISSN1785 0037 (Online)
DOI: http://dx.doi.org/10.15666/aeer/2005_43094320

[20] Li, Q. S., Wang, D. M., Xin, Z. B. (2014): Root system characteristics of herbaceous plants at different sites of aquatic-terrestrial ecotone of Lijiang river. – Bulletin of Soil & Water Conservation 34: 236-241.
[21] Li, W., Luo, J. N., Tian, X. S., Soon Chow, W., Sun, Z., Zhang, T., Peng, S. L., Peng, C. L. (2015): A new strategy for controlling invasive weeds: selecting valuable native plants to defeat them. – Scientific Reports 5: 1-11.
[22] Lin, L., Cao, A. C., Yu, D. Z., Zhu, W. D., Yan, D. D., Ouyang, C. B. (2016): Effect of *Brassica napus* L. on replacement control of *Eupatorium adenophorum* Spreng. – Chinese Journal of Oil Crop Sciences 38: 513-517.
[23] Liu, J., Sui, Y., Yu, Z., Shi, Y., Chu, H. Y., Jin, J., Liu, X. B., Wang, G. H. (2014): High throughput sequencing analysis of biogeographical distribution of bacterial communities in the black soils of northeast China. – Soil Biology and Biochemistry 70: 113-122.
[24] Liu, J., Wisniewski, M., Droby, S., Tian, S., Hershkovitz, V., Tworkoski, T. (2015): Effect of heat shock treatment on stress tolerance and biocontrol efficacy of *Metschnikowia fructicola*. – FEMS Microbiology Ecology 76: 145-155.
[25] Liu, J., Sui, Y. Y., Yu, Z. H., Shi, Y., Chu, H. Y., Jin, J., Liu, X. B., Wang, G. G. (2015): Soil carbon content drives the biogeographical distribution of fungal communities in the black soil zone of northeast China. – Soil Biology and Biochemistry 83: 29-39.
[26] Moreau, D., Pivato, B., Bru, D., Busset, H., Deau, F., Faivre, C. L., Matejicek, A., Strbik, F., Philippot, L., Mougel, C. (2015): Plant traits related to nitrogen uptake influence plant-microbe competition. – Ecology 96: 2300-2310.
[27] Mortimer, P. E., Pérez-Fernández, M. A., Valentine, A. J. (2008): The role of arbuscular mycorrhizal colonization in the carbon and nutrient economy of the tripartite symbiosis with nodulated *Phaseolus vulgaris*. – Soil Biology & Biochemistry 40: 1019-1027.
[28] Noah, F., Christian, L. L., Kelly, S. R., Jesse, Z., Mark, A. B., Rob, K. (2012): Comparative metagenomic, phylogenetic and physiological analyses of soil microbial communities across nitrogen gradients. – The ISME Journal 6: 1007-1017.
[29] Pomella, A. W. V., Barreto, R. W., Charudattan, R. (2007): *Nimbya alternantherae* a potential biocontrol agent for alligatorweed, *Alternanthera philoxeroides*. – Biocontrol 52: 271-288.
[30] Ramirez, K. S., Craine, J. M., Fierer, N. (2012): Consistent effects of nitrogen amendments on soil microbial communities and processes across biomes. – Global Change Biology 18: 1918-1927.
[31] Reeves, J. L. (2017): Climate change effects on biological control of invasive plants by insects. – CAB Reviews 12: 1-8.
[32] Reinhart, K. O., Callaway, R. M. (2006): Soil biota and invasive plants. – New Phytologist 170: 445-457.
[33] Saggar, S., Mcintosh, P. D., Hedley, C. B., Knicker, H. (1999): Changes in soil microbial biomass, metabolic quotient, and organic matter turnover under *Hieracium* (*H. pilosella* L.). – Biology and Fertility of Soils 30: 232-238.
[34] Sala, O. E., Chapin, F. S., Armesto, J. J., Berlow, E., Bloomfield, J., Dirzo, R., HuberSanwald, E., Huenneke, L. F., Jackson, R. B., Kinzig, A., Leemans, R., Lodge, D. M., Mooney, H. A., Oesterheld, M., Poff, N. L., Sykes, M. T., Walker, B. H., Walker, M., Wall, D. H. (2000): Global biodiversity scenarios for the year 2100. – Science 287: 1770-1774.
[35] Shen, S., Xu, G. F., Clements, D. R., Jin, G. M., Liu, S. F., Yang, Y. X., Chen, A. D., Zhang, F. D., Noguchi, H. K. (2016): Suppression of reproductive characteristics of the invasive plant *Mikania micrantha* by sweet potato competition. – BMC Ecology 16: 1-9.
[36] Si, C., Liu, X. Y., Wang, C. Y., Wang, L., Dai, Z. C., Qi, S. S., Du, D. L. (2013): Different degrees of plant invasion significantly affect the richness of the soil fungal community. – Plos One 8: 1-9.

http://www.aloki.hu ● ISSN 1589 1623 (Print) ● ISSN1785 0037 (Online)
DOI: http://dx.doi.org/10.15666/aeer/2005_43094320

[37] Smolinska, U., Horbowicz, M. (2010): Fungicidal activity of volatiles from selected cruciferous plants against resting propagules of soil-borne fungal pathogens. – Journal of Phytopathology 147: 119-124.
[38] Stinson, K. A., Campbell, S. A., Powell, J. R., Wolfe, B. E., Callaway, R. M, Thelen, G. C., Hallett, S. G., Prati, D., Klironomos, J. N. (2006): Invasive plant suppresses the growth of native tree seedlings by disrupting belowground mutualisms. – Plos Biology 4: 727-731.
[39] Tan, W. Z., Li, Q. J., Qing, L. (2002): Biological control of alligatorweed (*Alternanthera philoxeroides*) with a *Fusarium* sp. – BioControl 47: 463-479.
[40] Vishnu, R. V., Karthikeyan, S., Maharaja, S., Rajkumar, J., Panneerselvam, A., Thajuddin, N., Dhanasekaran, D. (2021): Metagenomic analysis of lichen-associated bacterial community profling in *Roccella montagnei*. – Archives of Microbiology 204: 54.
[41] Wagg, C., Jansa, J., Stadler, M., Schmid, B., van der Heijden, M. G. A. (2011): Mycorrhizal fungal identity and diversity relaxes plant–plant competition. – Ecology 92: 1303-1313.
[42] Wardle, D. A., Bardgett, R. D., Klironomos, J. N., Setala, H., Putten, W. H., Wall, D. H. (2004): Ecological linkages between aboveground and belowground biota. – Science 304: 1629-1633.
[43] Yan, S. L., Huangfu, C. H., Li, G., Zuo, Z. J., Ma, J., Yang, D. L. (2011): Effects of replacement control with four forage species on bacterial diversity of soil invaded by *Flaveria bidentis*. – Chinese Journal of Plant Ecology 35: 45-55.
[44] Yu, H., Liu, J., He, W. M., Miao, S. L., Dong, M. (2011): *Cuscuta australis* restrains three exotic invasive plants and benefits native species. – Biological Invasions 13: 747-756.
[45] Zeng, Y., Baumbach, J., Barbosa, E. G. V., Azevedo, V., Zhang, C., Koblizek, M. (2016): Metagenomic evidence for the presence of phototrophic Gemmatimonadetes bacteria in diverse environments. – Environmental Microbiology Reports 8: 139-149.

http://www.aloki.hu ● ISSN 1589 1623 (Print) ● ISSN1785 0037 (Online)
DOI: http://dx.doi.org/10.15666/aeer/2005_43094320

DETERMINATION OF THE CRITICAL PERIOD OF WEED CONTROL (CPWC) TO INCREASE THE YIELD OF BARLEY (*HORDEUM VULGARE* L.) CROP IN EGYPT

FARAHAT, E. A.[1] – AL-YASI, H. M.[2] – AL-BAKRE, D. A.[3] – EL-MIDANY, M. M.[1] – HASSAN, L. M.[1] – GALAL, T. M.[2*]

[1]*Botany and Microbiology Department, Faculty of Science, Helwan University, Cairo 11790, Egypt*

[2]*Department of Biology, College of Sciences, Taif University, P.O. Box 11099, Taif 21944, Saudi Arabia*

[3]*Department of Biology, College of Science, University of Tabuk, Saudi Arabia*

[*]*Corresponding author*
e-mail: tarekhelwan@yahoo.com; phone: 00966570159791; ORCID: 0000-0001-9847-1051

(Received 10th Apr 2022; accepted 11th Jul 2022)

Abstract. The purpose of this study was to determine the effect of different weed competition periods on the growth and yield of an Egyptian barley crop under field conditions, as well as to estimate the critical period of weed control (CPWC) in barley. The treatments were arranged in a randomized complete block design with three replications (i.e., plots 4 × 4 m each) and consisted of a quantitative series of both increasing duration of weed interference and length of weed-free periods. The measured morphological parameters of barley plants were greater in non-weedy barley fields than in weedy barley fields. The shoot height of non-weedy barley plants was significantly ($P < 0.05$) higher than that of weedy plants. After 75 DAE (Days After Emergence) of weed infestation, the maximum height and plant density were obtained. The biomass of barley plants and their associated weeds was gradually increased until 45 DAE, when barley biomass continued to increase, while weed biomass decreased. The maximum barley yield in the weed-free plots was 3.2 t ha^{-1} after 90 DAE, while it was 2.2 t ha^{-1} in the weed-infested plots after 75 DAE. Based on a 10% yield loss, the CPWC fell between 63 and 79 DAE, while a 5% yield loss fell between 41 and 102 DAE. Weed presence prior to and after the CPWC is not expected to reduce crop yield. As a result, weed removal at the CPWC is critical to allow plants to grow to their full potential without being hampered by competition and, hence, crop yield loss.
Keywords: *Barley, weed management, logistic model, yield loss, experimental design*

Introduction

Weeds compete with crops for moisture, nutrients, light, and space, resulting in significant yield losses, increased production costs, and crop quality degradation (Kalaitzandonakes et al., 2015). They compete with the crop plant throughout its life cycle, but weeds are more aggressive in a specific period during the crop cycle, when they can cause the greatest yield losses (Zafar et al., 2010; Menalled et al., 2020). Different crops necessitate different management activities, which can disrupt weed life cycles and prevent weed dominance (Bagheri et al., 2020). The timing of weed emergence and the duration of weed competition have a significant impact on crop yield, and studies have shown that just a few days of early crop growth relative to weeds can significantly shift the competitive balance in favor of the crop (Otto et al., 2009). Weeds have the greatest impact on crop growth during the critical period of weed control (CPWC); however, weed interference outside of this period had no effect on crop yield (Johnson et

http://www.aloki.hu ● ISSN 1589 1623 (Print) ● ISSN1785 0037 (Online)
DOI: http://dx.doi.org/10.15666/aeer/2005_43214338

al., 2004). Furthermore, weeds that grow alongside crops deplete significant amounts of nutrients and soil moisture, resulting in poor crop growth (Shah, 2013).

The optimum plant population, which is determined by the cultivar, cropping system, planting date, and environmental conditions, may be used to achieve the goal of maximum yield and improved quality (Khan et al., 2021). Crop cultivation, floristic composition, and weed distribution, as well as biological traits of the crop such as growth rate and development during the growing season, maximum plant height, and leaf cover, all have a significant impact on crop competitiveness against weeds (Uremis et al., 2010). Furthermore, plant density makes the crop more competitive against weeds, while herbicides can be applied at lower rates (Simić et al., 2012). Integrated weed management (IWM) strategies are a method of reducing herbicide use in agricultural practices (Swanton et al., 2010; Seyyedi et al., 2016). The CPWC is a key component of IWM programs (Knezevic et al., 2002), and identifying it is the first step in designing a successful IWM in major crops; thus, the use of the critical period threshold model will aid in crop yield improvement (Tursun et al., 2016).

The concept of CPWC can be defined as a period during the crop growing season during which weeds should be removed to prevent crop yield loss due to weed competition (Jhala et al., 2014). However, Zimdahl (1993) defined it as the time between seeding or emergence when weed competition does not reduce crop yield and the time when weed competition no longer reduces crop yield. The CPWC is regarded as an important factor in developing an alternative weed management strategy (Ahmadvand et al., 2009). It is calculated by calculating the time interval between two independently measured crop-weed competition components: the critical duration of weed interference and the critical weed-free period (Tursun et al., 2016). CPWC studies are typically conducted by keeping the crop free of weeds until a predetermined period and then allowing the weeds to emerge, or by growing weeds with the crop for a predetermined period and then removing all weeds until the end of the growing season (Ahmadvand et al., 2009).

Farmers' primary goal in their pursuit of economically efficient agricultural production is to maximize crop yield (Al-Gaadi et al., 2016). Weed-crop competition studies can provide farmers and land managers with valuable information about the best time to apply weed-control practices to protect crop yield (Swanton et al., 2015). As a result, the current study aims to investigate the effect of different weed competition periods on barley crop growth and yield under field conditions, as well as to estimate the critical period of weed control in barley. The information gathered can be used to improve weed management and increase barley crop yield.

Materials and methods

Study crop

Barley (*Hordeum vulgare* L.) is a Poaceae family annual cereal crop plant that is the fourth most important cereal crop in the world after wheat, maize, and rice, as well as the most widely distributed crop geographically (Al-Abdallat et al., 2017; Ay et al., 2018). The optimum temperature for germination of barley seeds is around 20°C, though germination can occur at temperatures as low as 3°C. Furthermore, optimal plant growth occurs in areas with 500 to 1000 mm of annual rainfall, but it can withstand drought conditions with 200 mm of annual rainfall. Barley is more resistant to saline and alkaline soils than other cereals, but it cannot tolerate impermeable, compacted soils or excessive

http://www.aloki.hu ● ISSN 1589 1623 (Print) ● ISSN1785 0037 (Online)
DOI: http://dx.doi.org/10.15666/aeer/2005_43214338

humidity (Van Gaelen, 2014). The growth period of barley is about 90 to 120 days for spring varieties, and 180 to 240 days for winter varieties (El-Midany, 2020). In 2021/2022, the global average barley yield was 2.98 tons per hectare (USDA, 2022). It is grown to produce non-alcoholic beverages, as well as for animal feed and medicinal purposes (Naeem et al., 2021). Its straw can also be used to build traditional huts and grain stores (Asfaw, 2000). Because barley is a competitive crop, selecting barley cultivars with highly competitive abilities is critical for effective weed management (Watson et al., 2006). Weeds, like other cereals, compete for resources, resulting in significant yield losses (Naeem et al., 2021b). However, while barley crops can grow quickly, suppress weed pressure, and provide a high dry weight yield, they have a low protein content for forage (Houshyar, 2017).

Experimental design

A field experiment was laid out as a factorial design with the treatments arranged in a randomized complete block design with three replications, during the period from November 2017 till April 2018, in the agricultural farm at Helwan University (29° 52.11′ 66″N - 31° 18.57′ 48″E), South Cairo Governorate, Egypt. Soil preparation was conducted according to the local practices for barley production. The soil of the study site had a pH of 7.5 with loamy sand texture. The experimental factors consisted of a quantitative series of both increasing duration of weed interference and length of weed-free periods. Four cultivated plots (4 × 4 m each) were assigned for this experiment, where each plot was consisted of 9 rows spaced at 25 cm between rows, and barley grains (genotype $Giza_{126}$) were sown with a density of 270 grain m^{-2} (optimum density for barley grains production: El-Midany, 2020) (*Fig. 1*). No pre-emergence or pre-plant herbicides were used. In the first plot, nine sampling times including six initial weed-free periods: 0 (WF0), 15 (WF15), 30 (WF30), 45 (WF45), 60 (WF60) and 75 (WF75) days after crop emergence (DAE), in which the cultivated plot was kept manually free of weeds. After that, weeds were allowed to grow until harvest time (120 DAE). In the second plot, nine sampling times including six initial weed infested periods: 0 (W0), 15 (W15), 30 (W30), 45 (W45), 60 (W60) and 75(W75), in which weeds were left without removing, after that the plot was kept free of weeds until harvest. The remaining plots were used as control, where the third one was kept free of weeds, and the fourth was left without removing weeds for the period from the emergence until harvest of barley at 120 DAE. The plots were irrigated regularly according to the indigenous agricultural practices in Egypt. Barley irrigated with 200 to 300 mm water 2 to 3 irrigation during the whole cultivation. Application of nitrogen, potassium and phosphate fertilizers and pest and disease control were carried out according to the recommended agronomic practices in the region. The climate of the study area during the growing season of barley was characterized by an average temperature of 20°C and an annual rain fall of 12.7 mm (El-Midany, 2014).

Weed and crop measurements

A natural and mixed weed species population were utilized to determine the CPWC for general weed interference. Weeds began to emerge 10 days after barley planting; these weeds included *Cyperus rotundus, Bidens pillosa, Anagallis arvensis, Avena fatua, Chenopodium murale, Sonchus oleraceus* and *Melilotus indicus* with two other common associated species (*Medicago polymorpha* and *Euphorbia peplus*). Measurements of weed traits were exclusive to the latter two common associated weeds since both were present in significant higher cover compared to other weed species. Weed infestations

http://www.aloki.hu ● ISSN 1589 1623 (Print) ● ISSN1785 0037 (Online)
DOI: http://dx.doi.org/10.15666/aeer/2005_43214338

were evaluated at the end of each treatment using three 0.5 m × 0.5 m quadrats/plot. In each quadrat, the number of barley tillers and the number of individuals of each common associated weed were counted to calculate their densities (i.e., number of individuals / unit area). Then, the whole plant individuals of barley plants and its associated weeds within each quadrat were harvested and transferred to the laboratory in polyethelene bags. In the laboratory, plant species were separated and some morphological measurements including culm (stem without sheath) diameter, root length, number of leaves, leaf length and width, sheath length, spike length and number of spikelets per each spike were measured for barley as well as shoot height for barley and its common associated weeds. The leaf area of barley plants (single sided) was measured using the equation (Kemp, 1960): $A = 0{\cdot}905\ LB$, *where* L = length of leaf; B = breadth at a point midway along the length; A = area. After the morphological measurements, the sampled shoots of barley and its associated weeds were oven-dried at 70°C till constant weight, and then the average dry weights of the shoots were calculated to estimate the aboveground biomass (DM gm^{-2}). The total biomass of all weedy species was also calculated. In addition, the grains of barley were harvested from each quadrat and weighed to calculate the yield per unit area of barley in each treatment. All measurements were carried out in three replicates.

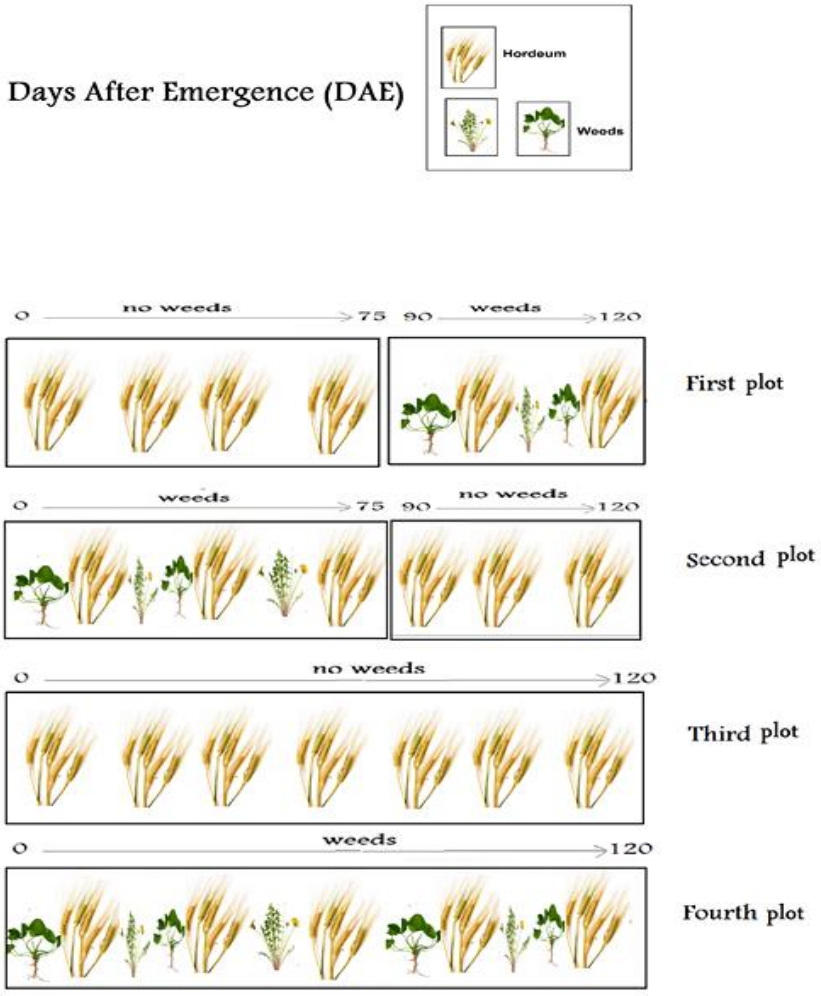

Figure 1. *Schematic diagram showing the design of the critical period of weed control experiment*

http://www.aloki.hu ● ISSN 1589 1623 (Print) ● ISSN1785 0037 (Online)
DOI: http://dx.doi.org/10.15666/aeer/2005_43214338

Plant analysis

After 75 DAE, three composite plant samples were taken from the above-ground shoots (stem and leaves) of barley plants in weed-free and weed-infested plots. Samples were oven-dried before being homogenized in a metal-free plastic mill and passing through a 2 mm mesh sieve. A 1 g ground sample was digested in 20 ml of a tri-acid mixture of $H2SO_4$:$HClO_4$:HF (1:1:2 V:V:V). The Kjeldahl method was used to determine total nitrogen (N). P, Mg, Ca, K, and Na concentrations were determined using an Agilent 4210 MP-AES (Agilent, USA). These procedures were recommended by Allen (1989). The instrument settings and operational procedures were adjusted in accordance with the user manual provided by the manufacturer.

Soil analysis

At the end of the barley growing season, three composite soil samples were collected from each sampling plot's profile (0-50 cm depth). Soil samples were brought to the laboratory in plastic bags as soon as they were collected; they were air dried, passed through a 2 mm sieve to remove debris, and then packed in paper bags for mechanical and chemical analysis. Soil pH (measured with a pH meter Model 9107 BN, ORION type, Thermo Scientific, USA) and electrical conductivity were determined using 1:5 w/v soil-water extracts (conductivity meter 60 Sensor Operating Instruction Corning, USA). Bicarbonates were determined by titration against 0.01N HCl, chlorides by direct titration against silver nitrate solution with 5 percent (w/v) potassium chromate as an indicator, and sulphates by turbidimetric determination as barium sulphate at 500 nm. Phosphorus was measured with a spectrophotometer (CECIL CE 1021, Cecil Instruments Limited, Corston, UK) using molybdenum blue methods (Allen, 1989). Titration against 0.01N versenate solution with meroxide and erichrome black T as indicators yielded calcium and magnesium concentrations. A flame photometer was used to measure sodium and potassium. Allen (1989) outlines all these procedures.

Data analysis

Sigma Plot 10.0 was used to fit the curves for calculating the CPWC. The Gompertz equation was used to model the effect of weed-free period on barley grain yield during both years, while the logistic equation was used to model the effect of weed duration on yield. The Gompertz model has been shown to provide an adequate fit to yield as the length of the weed-free period increases (Hall et al., 1992; Knezevic et al., 2002). The model has the following form (*Equation 1*):

$$Y = \mathrm{A} \times \exp\{-\mathrm{B} \times \exp(-\mathrm{K} \times \mathrm{T})\} \qquad \text{(Eq.1)}$$

where Y is the relative yield (measured as a percentage of the season-long weed-free period), A is the relative yield asymptote, B and K are constants, and T is the length of the weed-free period after emergence in days (DAE). Moreover, a three-parameter logistic equation was used to describe the effect of increasing duration of weeds infestation on relative yield of barley (*Equation 2*). The parameters of nonlinear regression were estimated using Sigma Plot 10.0, in line with the procedure suggested by Knezevic et al. (2002) as follow (*Equation 2*):

$$Y = ((1/(\exp(\mathrm{K} * (\mathrm{T} - \mathrm{X})) + \mathrm{F})) + ((\mathrm{F} - 1)/\mathrm{F})) * 100 \qquad \text{(Eq.2)}$$

http://www.aloki.hu ● ISSN 1589 1623 (Print) ● ISSN1785 0037 (Online)
DOI: http://dx.doi.org/10.15666/aeer/2005_43214338

where Y is the relative barley grain yield (% season-long weed-free control), T is the length of the weedy period after emergence in days (DAE), X is the point of inflection, and K and F are constants. The determination of the CPWC in this study was carried out based on the arbitrarily chosen yield loss levels of 5% and 10%, which was judged to be acceptable, considering the present economics of weed control (Ahmadvand et al., 2009).

Statistical analysis

Using a paired-sample t-test, the differences in soil characteristics, morphological traits, and biomass of barley between weedy and weed-free treatments were determined (SPSS, 2012).

Results

Soil properties

The soil of the cultivated barley in the experimental farm of Helwan University showed no significant differences in the investigated variables, except soil pH and K, between weedy and weed-free cultivated plots (*Table 1*). The soils of the weedy and weed-free plots were alkaline (pH: 7.20 and 7.75) with high salinity (8.61 and 8.56 µs cm^{-1}), respectively. The nutrients of the soil were characterized by high content of K, followed by Ca, Mg and P.

Table 1. *Soil characteristics (mean ± standard deviation) of the weedy and weed-free cultivated plots of barley in the experimental farms of Helwan University*

Soil variable		Sampling plot		T-value
		Weedy	Weed-free	
pH		7.20±1.02	7.75±0.89	2.47*
EC (µs cm^{-1})		8.61±0.93	8.54±0.90	1.23
Cl^-	**(mg kg^{-1})**	2.64±0.62	2.72±0.44	0.98
HCO_3^-		2.66±0.12	2.70±1.01	1.06
SO_4^{2-}		1.75±0.09	1.54±0.84	2.10
P		44.60±8.35	45.49±6.34	1.34
K		290.08±38.76	229.50±27.64	2.53*
Ca		62.00±13.42	66.00±11.23	1.86
Mg		50.00±14.63	57.20±8.46	1.04
Na		3.82±1.02	4.48±1.06	0.98

*Significance at $p < 0.05$

Growth measurements

The growth measurements of barley in the experiment indicated the significant impact of weed interference on the growth properties of barley plants (*Table 2*). It was found that the growth measurements of barley in the weed-free periods were higher than those in the weed-infested periods. In the weedy plot, some growth criteria were significantly ($P < 0.05$) increased from the weed infestation to the weed-free period. For example, crop plant density (467.5 to 772.7 tillers m^{-2}), shoot length (46.6 to 71.1 cm), sheath length (6.4 to 6.9 cm), leaf area (13.7 to 18.2 cm^2) and the plant biomass (256.5 to 627.1 g DM

http://www.aloki.hu ● ISSN 1589 1623 (Print) ● ISSN1785 0037 (Online)
DOI: http://dx.doi.org/10.15666/aeer/2005_43214338

m^{-2}). In the same context, the plots that start without weed infestation showed slight increase in the growth parameters of the barley plants. Whereas, the plant density was significantly increased from 605.5 to 731.3 tillers m^{-2}, while the shoot length ranged between 45.7 and 72.9 cm, the sheath length between 6.5 and 9.5 cm, and the plant biomass had a range from 224.3 to 551.5 DM gm^{-2}, before and after change weed presence, respectively.

Table 2. *Growth characteristics (mean ± standard deviation) of barley plants in weedy and weed-free plots before and after change from weedy to weed free and vice versa*

Parameters	Weedy plots			Weed-free plots		
	Before change	After change	T-test	Before change	After change	T-test
No. of tillers m^{-2}	467.5±241.8	772.7±55.0	4.2**	605.5±228.4	731.3±194.3	3.3*
Shoot length (cm)	46.6±19.6	71.1±4.7	6.2**	45.7±15.4	72.9±9.9	15.0***
Culm diameter (cm)	0.3±0.1	0.3±0.1	1.3	0.4±0.5	0.3±0.1	0.7
Root length (cm)	6.0±2.2	7.6±2.1	1.2	5.5±3.0	6.6±1.5	0.6
No. of leaves/individual	4.3±1.0	4.7±0.5	0.8	4.1±1.0	3.7±0.4	1.1
Leaf length (cm)	18.9±4.4	20.1±2.0	0.4	18.6±4.0	17.9±3.5	1.3
Sheath length (cm)	6.4±1.8	9.6±1.6	4.2**	6.5±1.3	9.2±0.8	8.4***
Leaf width (cm)	0.8±0.3	1.0±0.3	1.1	0.7±0.2	0.7±0.2	1.2
Leaf area (cm^2)	13.7±1.2	18.2±3.6	2.4*	11.8±1.3	11.3±1.7	1.1
Shoot biomass (g DM m^{-2})	248.0±82.2	622.3±102.4	7.4**	218.5±77.2	540.8±123.4	8.8***
Root biomass (g DM m^{-2})	8.5±2.8	4.7±1.5	1.6	5.9±4.7	10.7±3.2	2.2
Total biomass (g DM m^{-2})	256.5.±66.1	627.1±102.3	7.2**	224.3±75.6	551.5±125.4	9.0***

*: $p < 0.05$, **: $p < 0.01$, ***: $p < 0.001$

Impact of weed infestation on the functional traits of barley

Shoot length

The shoot length of barley and its common associated weeds indicated that the barley plant continues to increase in height until reach its maximum (72.9 cm) at the end of weed infestation period (75 DAE), while *Medicago polymorpha* reached its maximum height (19.7 cm) after 60 DAE, and then decreased to 18.0 cm at the end of the weedy period (*Fig. 2*). In addition, the maximum height of *Euphorbia peplus* (7 cm) was recorded after 75 DAE. These results indicated that *M. polymorpha* was affected by the highly competitive effectiveness more than *E. peplus*.

Plant density

The impact of weeds infestation on the plant density showed that the average plant density (599.5 tillers m^{-2}) in the weed-free plot was significantly higher than 497.5 tillers m^{-2} in the weed-infested plots with a reduction percentage of 17.0% (*Table 3*). In the weed-free plot, the plant density increased with increasing the time till reaches its maximum (824.0 tillers m^{-2}) after 90 DAE, and then decreased to reach its minimum (344.0 tillers m^{-2}) at the harvest time (120 DAE) due to weed infestation. On the other hand, the barley in the weedy plot showed slight increase in density until reaches its maximum (644.0 tillers m^{-2}) after 75 DAE, and then gradually decreases to reach

http://www.aloki.hu ● ISSN 1589 1623 (Print) ● ISSN1785 0037 (Online)
DOI: http://dx.doi.org/10.15666/aeer/2005_43214338

240.0 tillers m^{-2} at the harvest time. It is worth to note that the highest reduction percentage (32.0%) was observed after 90 DAE, while the lowest value (5.0%) was recorded after 105 DAE.

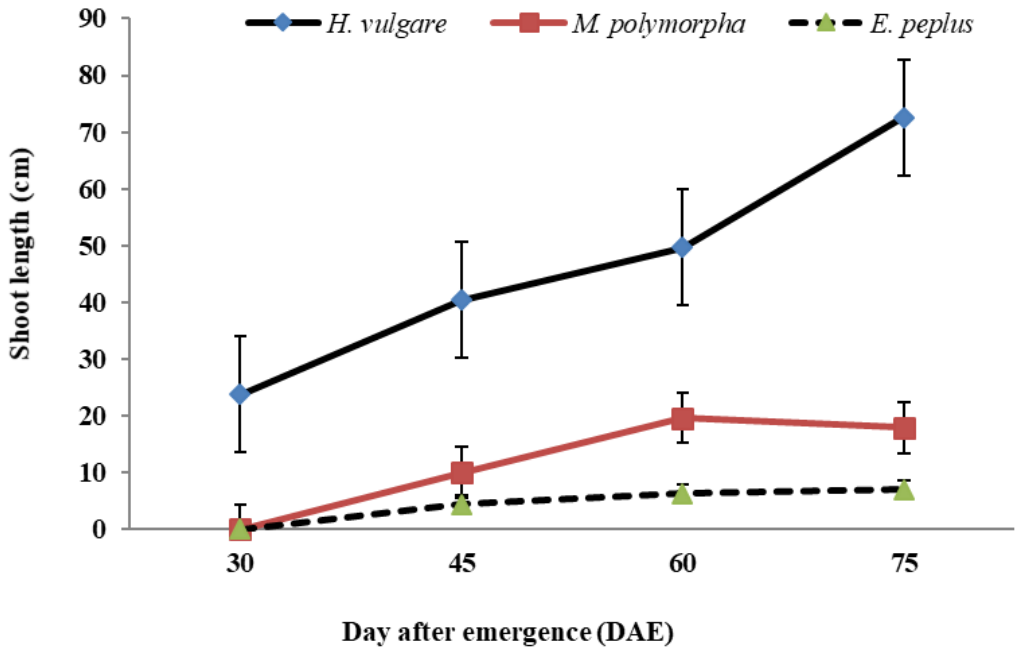

Figure 2. *Shoot length (cm) of barley and its common associated species in the weed-infested plots. H. vulgare: Hordeum vulgare, M. polymorpha: Medicago polymorpha, E. peplus: Euphorbia peplus. Vertical bars are the standard errors*

Table 3. *Plant density (tillers m^{-2}) of barley grown in weedy and weed-free plots, and the calculated reduction % in barely density in weedy plots compared to the weed-free plots*

Days after emergence (DAE)	Plant density (tillers m^{-2})		
	Weed-free plot	Weedy plot	Reduction (%)
15	528	424	20
30	560	456	19
45	568	496	13
60	712	588	17
75	656	644	2
90	824	560	32
105	604	572	5
120	344	240	30
Mean ± standard deviation	599.5± 140	497.5± 126	17± 8
T-test	3.8**		

The barley plants had a high competitiveness compared with its common associated weeds including *M. polymorpha* and *E. peplus* (*Fig. 3*). The plant density curve of barley plants in presence of the two common weeds was sigmoid, where it was gradually increased till 30 DAE, and then showed sharp increase until it reached its maximum

http://www.aloki.hu ● ISSN 1589 1623 (Print) ● ISSN1785 0037 (Online)
DOI: http://dx.doi.org/10.15666/aeer/2005_43214338

(652.0 tillers m^{-2}) after 60 DAE and after that it exhibited slight increase until reached 666.0 tillers m^{-2} at the end of weed infestation period (75 DAE). However, *M. polymorpha* and *E. peplus* started to emerge after 45 DAE with density of 4.0 and 10.0 individuals m^{-2}, respectively, and then reached their maximum (12.0 and 20.0 individuals m^{-2}) after 60 DAE corresponding to the maximum barley density, which then started to increase gradually in response to declining weed density.

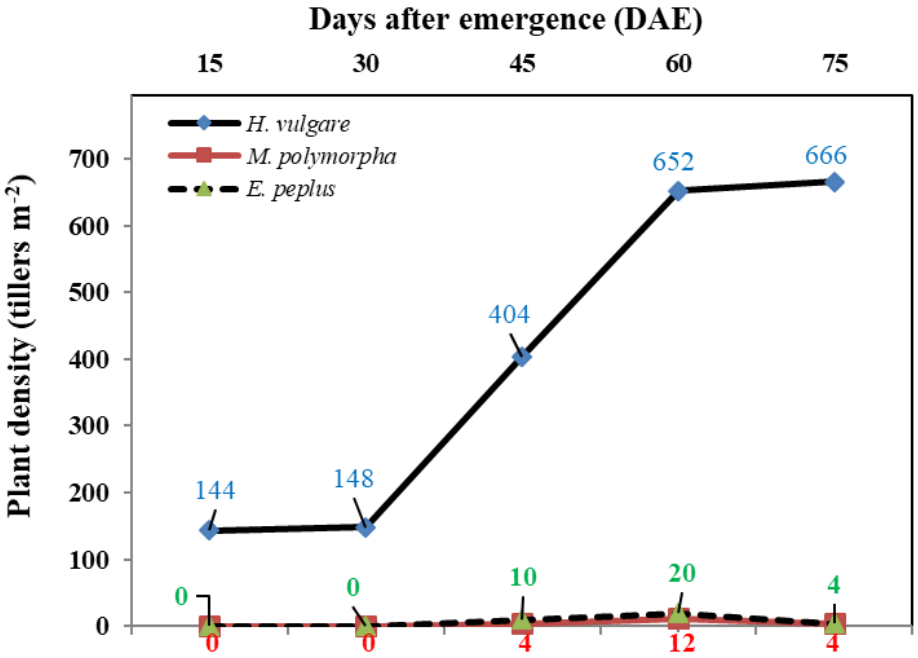

Figure 3. *Plant density of barley (tillers m^{-2}) and its common associated species (individuals m^{-2}). H. vulgare: Hordeum vulgare, M. polymorpha: Medicago polymorpha, E. peplus: Euphorbia peplus. Vertical bars are the standard errors*

Plant biomass

The data of shoot and total biomass of barley plant and its common associated weeds showed great competitive potential of barley compared to the other weeds (*Fig. 4*). The aboveground biomass of barley showed gradual increase until reached 83.0 g DM m^{-2} after 45 DAE, and then showed exponential increase to 539.4 g DM m^{-2} at the end of the weed infestation period. Meanwhile, the biomass of *M. polymorpha* and *E. peplus* had its maximum (14.8 and 15.4 g DM m^{-2}, respectively) after 45 DAE, and then started to decrease by increasing the biomass of barley, Comparing the average total biomass, including above- and below-ground parts, of barley with that of all associated weeds in the weed-infested plots showed that the biomass of both barley and associated weeds gradually increased until 45 DAE (*Fig. 5*). After that the biomass of barley continued to increase, while the biomass of weeds declined and then increased at the end of infestation period.

http://www.aloki.hu ● ISSN 1589 1623 (Print) ● ISSN1785 0037 (Online)
DOI: http://dx.doi.org/10.15666/aeer/2005_43214338

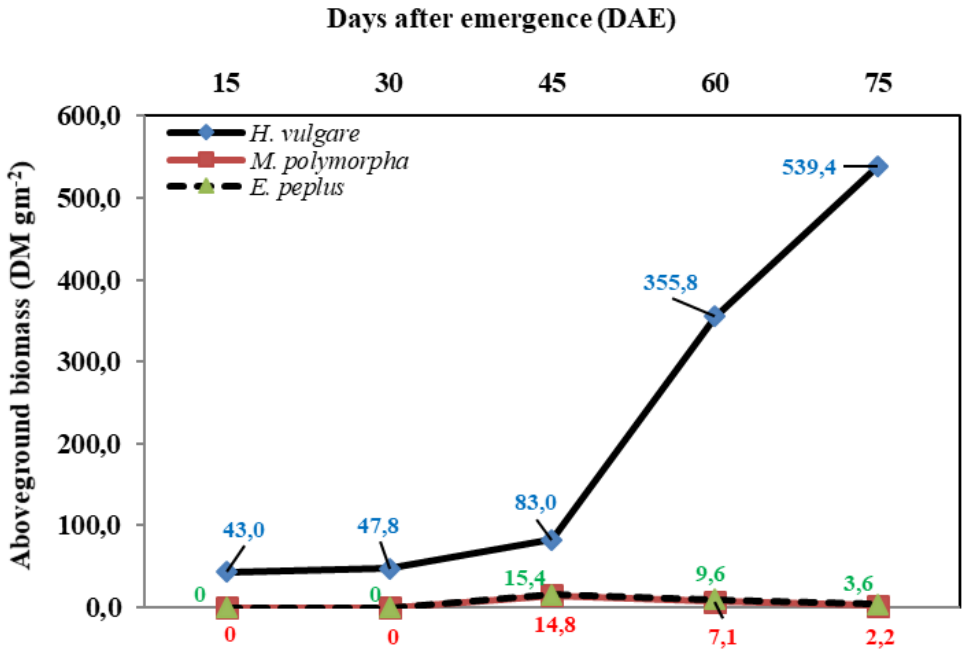

Figure 4. *Aboveground biomass (g DM m^{-2}) of barley and its common associated species. H. vulgare: Hordeum vulgare, M. polymorpha: Medicago polymorpha, E. peplus: Euphorbia peplus*

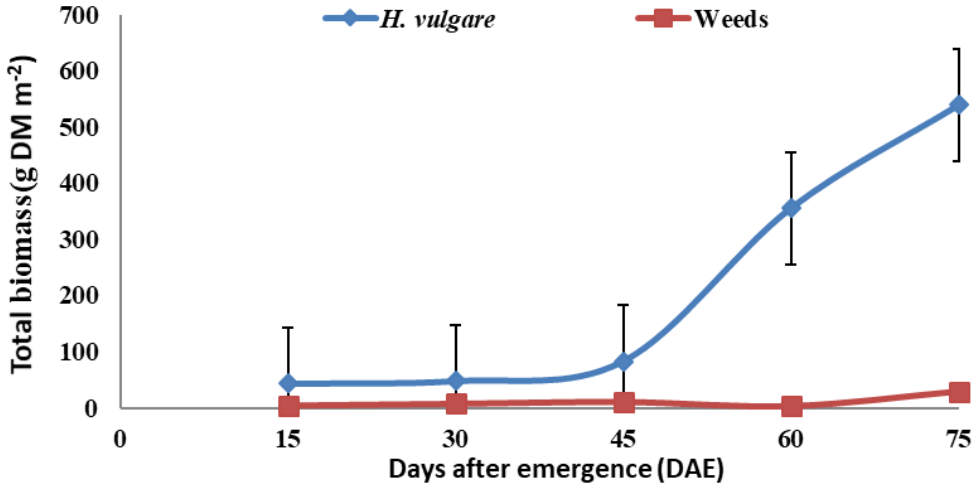

Figure 5. *Total biomass (g DM m^{-2}) of barley and all recorded associated weed species in the experimental farm at Helwan University. Vertical bars are the standard errors*

Plant nutrients

The nutrients content of the barley shoots indicated significant differences ($P < 0.05$) for all nutrients (except P and K) between weed-infested and weed-free plants (*Table 4*). It was found that the total N, Ca, Mg and Na contents (1.87, 0.16, 0.41 and 0.58%) of barley from weed-free plot were significantly higher than that recorded for plants from weed-infested plot (1.79, 0.12, 0.31 and 0.43%, respectively). On the other hand, the

http://www.aloki.hu ● ISSN 1589 1623 (Print) ● ISSN1785 0037 (Online)
DOI: http://dx.doi.org/10.15666/aeer/2005_43214338

contents of most nutrients (except P and Na) of the barley grains from weed-free plots were significantly higher than those of the grains collected from weed-infested barley.

Table 4. *Impact of weed interference on nutrients concentration (mean ± standard deviation) of the shoots and grains of barley cultivated in weed-infested and weed-free plots*

Nutrient (%)	Shoot			Grains		
	Weedy	Weed-Free	T-test	Weedy	Weed-Free	T-test
N	1.79±0.10	1.87±0.15	2.4*	1.31±0.26	1.58±0.22	2.4*
P	0.16±0.02	0.13±0.02	2.6*	0.43±0.01	0.40±0.03	0.35
K	1.35±0.17	1.39±0.19	1.34	1.20±0.16	1.53±0.19	7.8**
Ca	0.12±0.01	0.16±0.06	3.1*	0.05±0.02	1.08±0.06	44.3***
Mg	0.31±0.05	0.41±0.07	3.4*	0.29±0.18	0.36±0.02	7.6**
Na	0.43±0.24	0.58±0.27	4.1*	0.04±0.01	0.04±0.02	0.5

Yield responses to weed control

The present study recorded that the beginning of CPWC based on 10% yield loss occurred at 63 DAE, while the end of CPWC occurred at 79 DAE (*Fig. 6*). According to 5% yield loss, the beginning of the CPWC occurred by 41 DAE, while the end occurred by 102 DAE. The onset of the CPWC became earlier and it ended later as the predetermined acceptable yield loss level decreased from 10% to 5%. Moreover, it was found that in the weed free plots the barley yield increased with duration until it reached its maximum value (3.2 t ha^{-1}) by 90 DAE, and then decreased gradually under weed infestation (*Table 5*). On the other side, the barley yield of the weed-infested plot had its maximum value (2.2 t ha^{-1}) after 75 DAE, and then fluctuated by removing weeds.

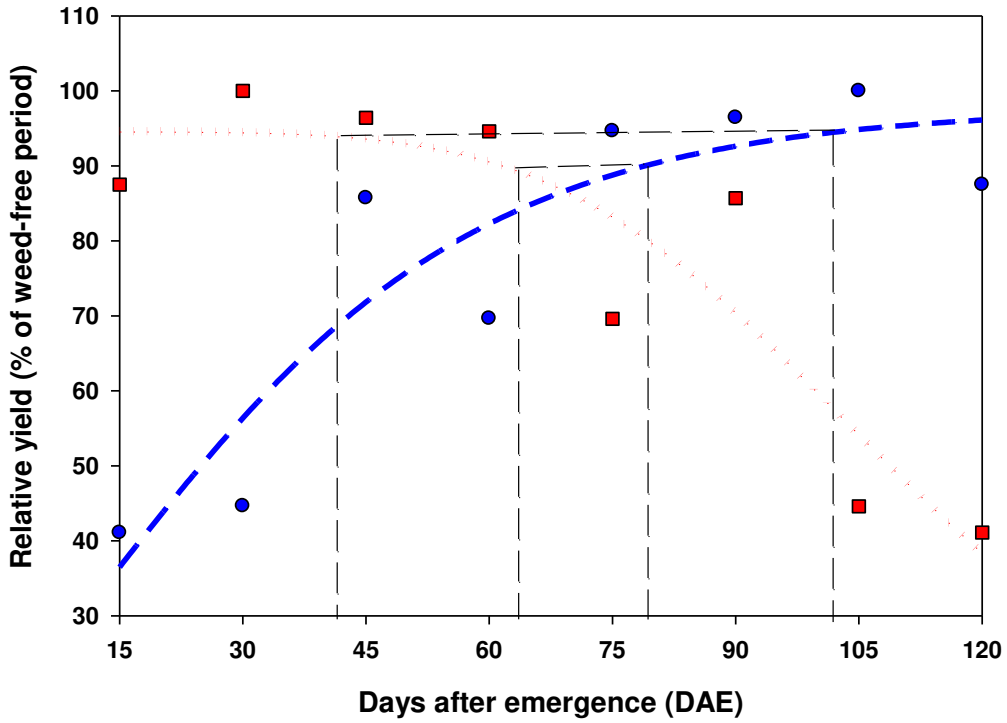

Figure 6. *Effects of increasing duration of weed interference (squares) and weed-free periods (circles) from crop planting on barley yield*

http://www.aloki.hu ● ISSN 1589 1623 (Print) ● ISSN1785 0037 (Online)
DOI: http://dx.doi.org/10.15666/aeer/2005_43214338

Table 5. *Impact of weeds on the yield (t ha^{-1}) of barley crop cultivated in weed-free and weedy plots*

Days after emergence (DAE)	Plant yield (t ha^{-1})		
	Weed-free plot	**Weedy plot**	**Reduction (%)**
15	2.0	1.5	25.0
30	2.2	1.6	27.3
45	2.2	1.8	18.2
60	2.7	2.1	22.2
75	2.5	2.3	8.0
90	3.2	2.0	37.5
105	2.3	2.0	13.0
120	1.3	0.9	30.8
Mean ± standard deviation	2.3± 0.5	1.8 ± 0.5	22.8 ± 8.5
T-test	5.2***		

Discussion

In recent years, the areas occupied by barley have decreased due to a variety of economic, climatic, and other factors, and thus maintaining high yields requires optimizing all processes in cultivation technology and taking climate change into account (Georgiev and Delchev, 2016). Furthermore, if weed species are not adequately controlled, it can result in significant economic losses (Soltani et al., 2014). The experimental barley fields in the current study had a low weed abundance, which could be attributed to its reported allelopathic activity (Schuster et al., 2020). The measured morphological parameters of barley plants were found to be higher in non-weedy barley fields than in weedy barley fields. Non-weedy barley plants had higher shoot heights than weedy plants. *M. polymorpha* and *E. peplus* reached their maximum heights after 60 and 75 DAE, respectively, and then decreased to the minimum at the end of the weedy period, whereas barley plants continued to grow until reaching their maximum at the end of the weedy period (75 DAE). These findings indicated that *M. polymorpha* was more influenced by barley's highly competitive effectiveness than *E. peplus*. Belete et al. (2018) attributed the increased plant height in the weedy plot to intense competition among plants, which causes them to elongate in search of light and lack abundant growth, allowing the plants to grow taller. Furthermore, Vandeleur and Gill (2004) reported that taller barley cultivars were typically better weed tolerators and suppressors of weed growth. Similar findings have been reported for rice plants, where their height is significantly reduced when rice competes with weeds for 70 days or longer, and rice plant height is inversely proportional to weed competition length (Micheal et al., 2013).

The current study observed that barley growth measurements in weed-free periods were higher than those in weed-infested periods, with the leaf area increasing significantly ($P < 0.05$) from the weed infestation to the weed-free period. According to Chowdhury et al. (2015), weed competition for growth factors with crop plants was absent or negligible in weed-free crops, resulting in increased shoot length. Furthermore, the decrease in barley leaf dimensions with increased weeds was caused by increased weed biomass or weed competition with crop, which may have reduced the availability of environmental resources to crop plants, and hampered crop canopy establishment (Zafar

http://www.aloki.hu ● ISSN 1589 1623 (Print) ● ISSN1785 0037 (Online)
DOI: http://dx.doi.org/10.15666/aeer/2005_43214338

et al., 2010). Therefore, removal of weeds at early crop growth stages helped plants to make full use of growth factors without facing any competition effect.

Weed density appears to be important in determining when the CPWC begins (Kumar et al., 2020). In the weedy plot, barley density increased gradually until it reached its maximum after 75 DAE, then decreased gradually until it reached its minimum at harvest time. However, in the presence of the two common weeds, the plant density curve of barley plants was sigmoid, with a gradual increase until 30 DAE, then a sharp increase until it reached its maximum after 60 DAE, and then a slight increase until the end of the weed infestation period (75 DAE). *M. polymorpha* and *E. peplus* appear after 45 DAE, reach a peak after 60 DAE, and then decline sharply. According to Swanton et al. (2015), after weed emergence time, weed density is the second most important variable, as there is clearly a relationship between weed density and duration of interference. They hypothesized that weeds that emerge with or before the crop are by far the most competitive and cause the most yield loss, whereas weeds that emerge later than the crop are much less competitive in terms of crop yield loss. Furthermore, Bagheri et al. (2020) attributed this trend of weed density suppression to an increase in barley plants' competition ability against weeds at higher crop density. When compared to its common associated weeds, such as *M. polymorpha* and *E. peplus*, barley plants had a high competitiveness. It was discovered that having a larger number of tillers increases the crop stand's shading ability (Hoad et al., 2006). Seavers and Wright (1999) demonstrated this in a study of wheat, barley, and oat cultivars, where cultivars with greater tiller economy had a superior suppressive ability against weeds due to a cultivar's ability to maintain high levels of light interception.

Crop variety, sowing rate, weed species and density, and crop emergence time relative to the weed can all influence weed competition (El-Midany, 2020). With a reduction percentage of 17.0 percent, the average barley density in the weed-free plot was higher than that in the weed-infested plot until harvest. This result agreed with Singh et al. (2017), who found that weed-free treatments had the highest number of effective tillers, while weedy check treatments had a significantly lower number due to higher weed density and biomass. Furthermore, Chowdhury et al. (2015) reported that the low number of tillers in the weedy plot was due to increased competition between crop plants and weeds for nutrients, air space, light, and water. According to Belete et al. (2018), the production of more total tillers in weed-free plots may be attributed to better access to space, nutrients, water, and light, which allowed plants to produce more tillers m^{-2}, whereas the reduction in tiller number m^{-2} may be due to increased weed population and continuous competition reduced access to different resources.

The biomass of barley plants and their associated weeds increased gradually until 45 DAE, when the biomass of barley continued to increase while that of weeds declined and then increased again at the end of the infestation period. Micheal et al. (2013) discovered that the lowest weed dry weight was recorded in plots that were weed-free for more than 45 days during the rice crop season. Hugo et al. (2014) discovered that the highest biomass of naked crabgrass (*Digitaria nuda*) was recorded at 78 DAE, which corresponded with corn plant tasseling. According to Kumar et al. (2020) and Mondani et al. (2011), weed biomass increased with increasing weed infestation duration and decreased with increasing weed free period duration. Furthermore, weed control after 20 DAE reduces weed density and dry weight by up to 76 and 95%, respectively, and increases grain yield by up to 34% (Ali et al., 2014).

http://www.aloki.hu ● ISSN 1589 1623 (Print) ● ISSN1785 0037 (Online)
DOI: http://dx.doi.org/10.15666/aeer/2005_43214338

Crops and weeds' competitive ability for nutrient uptake in agricultural ecosystems will be primarily determined by their intrinsic nutrient requirements and uptake efficiencies (Swanton et al., 2015). The total N, Ca, Mg, and Na contents of barley shoots from weed-free plot were significantly higher than those found in weed-infested plot plants. Furthermore, the contents of most nutrients (except P and Na) in barley grains from weed-free plots were significantly higher than those in weed-infested barley grains. The lower nutrients contents of barley in the weedy plots may be due to the high accumulation potential of the associated weeds to these nutrients (Galal and Shehata, 2015).

The barley yield increased with duration in the weed-free plot until it reached its maximum value (3.2 t ha^{-1}) by 90 DAE, and then decreased gradually under weed infestation. The weed-infested plot's barley yield, on the other hand, peaked at (2.2 t ha^{-1}) after 75 DAE and then fluctuated as weeds were removed. According to Belete et al. (2018), the maximum weed control enhanced the production of effective tillers, which subsequently contributed towards the increase in wheat yield. In addition, Singh et al. (2017) reported that the presence of weeds throughout the growing season resulted in a 24 percent reduction in grain yield when compared to weed-free conditions. At harvest, the yield of barley in the weed-free plot was higher than the yield of barley in the weed-infested plot. Singh et al. (2017) discovered similar results in a barley crop. According to Walters and Craig (2017), a significant part of the effect of weed competition on barley yield was due to a decrease in the number of grain-bearing ears per plant, which affected yield. Furthermore, weeds can reduce barley yield, so integrated weed management practices should be used to control weeds in barley crops (GRDC, 2016). Weeds were discovered to reduce yields, lower crop market value by reducing quality, and raise harvesting, drying, and cleaning costs (Galal and Shehata, 2015).

In the current study, the biomass of *M. polymorpha* and *E. peplus* peaked at 45 DAE and then began to decline as the biomass and density of the barley plant increased. This result was consistent with the findings of Dhima and Eleftherohorinos (2001), who found that increasing crop density resulted in a significant reduction in weed biomass. In a similar study, Belete et al. (2018) attributed the higher wheat grain yield to lower weed dry weight and efficient resource utilization, while the lower yield was attributed to weed infestation, accumulation of high dry matter in weeds, and the presence of different weed species in weedy plots. Similar results were reported by Ud Din et al. (2016) for maize and Latif et al. (2021) for broccoli, and Simarmata et al. (2018) for sweet corn.

Knowing the critical periods for weed control helps growers decide whether to pursue additional weed control measures to protect crop yield (Swanton et al., 2015). To determine the predicted and observed barley yield as affected by the duration of the weed-infested or weed-free periods, the Gompertz and logistic equations were used. According to the current study, the start of CPWC based on a 10% yield loss occurred at 63 DAE, and the end of CPWC occurred at 79 DAE. However, based on a 5% yield loss, the start of the CPWC occurred 41 DAE earlier, while the end occurred 102 DAE later. Bukun (2004) discovered that weeds must be controlled from 15 to 84 DAE for efficient yield in a similar study on Turkish cotton, whereas Mondani et al. (2011) and Baziramakenga and Leroux (1994) recorded CPWC of 20–60 DAE and 15–68 DAE, respectively, for the minimum potato yield loss. Furthermore, when yield losses exceeded 5%, the CPWC of corn production ranged between 12 and 44 DAE (Hugo et al., 2014), while acceptable yield loss levels of 5% and 10% were 20 and 9 days (Ghanizadeh et al.,

http://www.aloki.hu ● ISSN 1589 1623 (Print) ● ISSN1785 0037 (Online)
DOI: http://dx.doi.org/10.15666/aeer/2005_43214338

2009) and 48 and 35 days, respectively (Tursun et al., 2016). Furthermore, the estimated CPWC for a 10% acceptable rice yield loss was 17–53 DAE (Micheal et al., 2013).

Conclusion

According to the current study, the start of CPWC based on a 10% yield loss occurred at 63 DAE, and the end of CPWC occurred at 78 DAE. However, based on a 5% yield loss, the start of the CPWC occurred 41 DAE earlier, while the end occurred 102 DAE later. As a result, weed removal at the CPWC is urgently needed to assist plants in making full use of growth factors without competition, resulting in crop yield loss. Non-weedy barley fields had higher measured morphological parameters of barley plants, such as plant height and leaf area, than weedy barley fields. The average barley density and biomass, as well as the inorganic nutrient content, were higher in the weed-free plots than in the weed-infested plots. Finally, the current study concluded that barley plants were highly competitive when compared to their commonly associated weed species.

Competing interests. The authors declare that they have no competing interests.

Acknowledgments. The authors extend their appreciation to the deanship of scientific research for funding this article by Taif University Research Supporting Project number (TURSP-2020/199), Taif University, Taif, Saudi Arabia.

REFERENCES

[1] Ahmadvand, G., Mondani, F., Golzardi, F. (2009): Effect of crop plant density on critical weed competition in potato. – Sci Hortic 121: 249-254.
[2] Al-Abdallat, A. M., Karadsheh, A., Hadadd, N. I., Akash, M. W., Ceccarelli, S., Baum, M., Hasan, M., Jighly, A., Abu Elenein, J. M. (2017): Assessment of genetic diversity and yield performance in Jordanian barley (*Hordeum vulgare* L.) landraces grown under Rainfed conditions. – BMC Plant Biol 17: 191.
[3] Al-Gaadi, K. A., Hassaballa, A. A., Tola, E., Kayad, A. G., Madugundu, R., Alblewi, B., Assiri, F. (2016): Prediction of potato crop yield using precision agriculture techniques. – Plos One 11(9): e0162219.
[4] Ali, H., Tahir, M., Nadeem, M. A. (2014): Determining critical period of weed competition in wheat under different tillage systems. – Pak J life Soc Sci 12(2): 74-79.
[5] Allen, S. E. (1989): Chemical analysis of ecological materials. – Blackwell Scientific Publications, London.
[6] Asfaw, Z. (2000): The barleys of Ethiopia. – In: Brush, S. D. (ed.) Genes in the field: On-Farm Conservation of Crop Diversity. Lewis Publisher, Florida, USA. pp. 77-108.
[7] Ay, H., Aykanat, S., Anay, A., Akkaya, M. R., Zeybek, A. (2018): Agronomic and quality evaluation of rainfed barley (*Hordeum vulgare* L.) in eastern Mediterranean condition. – Fresen Environ Bull 27(10): 6532-6546.
[8] Bagheri, A., Sohrabi, N., Mondani, F., Nosratti, I. (2021): Weed infestation is affected by chickpea farmer demographics and agronomic practices. – Weed Res 61: 45-54.
[9] Baziramakenga, R., Leroux, G. D. (1994): Critical period of quackgrass (Elytrigia repens) removal in potatoes (Solanum tuberosum). – Weed Sci 42: 528-533.
[10] Belete, B., Dalga, D., Sorsa, Z. (2018): Effect of weed management on yield components and yield of bread wheat (*Triticum aestivum* L.) at Wolaita Sodo in Southern Ethiopia. – Int J Res Agri Forest 5(10): 34-43.

http://www.aloki.hu ● ISSN 1589 1623 (Print) ● ISSN1785 0037 (Online)
DOI: http://dx.doi.org/10.15666/aeer/2005_43214338

[11] Bukun, B. (2004): Critical period for weed control in cotton in Turkey. – Weed Res 44: 404-412.
[12] Chowdhury, I. F., Ali, M. H., Karim, M. F., Masum, S. M., Rahman, A. (2015): Weed control strategies affecting yield potential of aromatic rice. – Pak. J. Weed Sci Res 21(4): 453-466.
[13] Dhima, K. V., Eleftherohorinos, I. G. (2001): Influence of nitrogen on competition between winter cereals and sterile oat. – Weed Sci 49: 77-82.
[14] El-Midany, M. M. (2014): Population dynamics of Calotropis procera (Ait.) Ait. f. in Cairo Province. – MSc. Thesis, Faculty of Sciences, Helwan University, 166p.
[15] El-Midany, M. M. (2020): Weed-crop interaction and allelopathic effects on *Hordeum vulgare* L. in Egypt. – Ph.D. Thesis, Faculty of Sciences, Helwan University, 155p.
[16] Galal, T. M., Shehata, H. S. (2015): Impact of nutrients and heavy metals capture by weeds on the growth and production of rice (*Oryza sativa* L.) irrigated with different water sources. – Ecol Indic 54: 108-115.
[17] Georgiev, M., Delchev, G. (2016): Achievements and Problems in the weed control in barley (*Hordeum vulgare* L.). – J Agron LIX: 294-297.
[18] Ghanizadeh, H., Lorzadeh, S., Ariannia, N. (2009): Critical period for weed control in corn in the south-west of Iran. – Asian J Agri Res 4: 80-86.
[19] GRDC (2016): Barley: Southern Region. – Grains Research and Development Corporation, Australia.
[20] Hall, A. J., Rebella, C. M., Ghersa, C. M., Culot, P. M. (1992): Field crop systems of the Pampas. – In: Pearson, C. J. (ed.) Ecosystems of the World. Field Crop Ecosystems. Elsevier, New York, pp. 413-450.
[21] Hoad, S. P., Davies, D. H. K., Topp, C. F. E. (2006): How to select varieties for organic farming: science and practice. – In: Atkins, C., Ball, B., Davies, D. H. K., Rees, R., Russell, G., Stockdale, E. A., Watson, C. A., Walker, R., Younie, D. (eds.) What will organic farming deliver? Aspects of Applied Biology. Association of Applied Biologists, Warwick, UK, Vol. 79, pp. 117-120.
[22] Houshyar, E. (2017): Environmental impacts of irrigated and rain-fed barley production in Iran using life cycle assessment (LCA). – Spanish J Agri Res 15(2): e0204.
[23] Hugo, E., Morey, L., Saayman-du Toit, A. E. J., Reinhardt, C. F. (2014): Critical periods of weed control for naked crabgrass (Digitaria Nuda), a grass weed in corn in South Africa. – Weed Sci 62(4): 647-656.
[24] Jhala, A. J., Sandell, L. D., Rana, N., Kruger, G. R., Knezevic, S. Z. (2014): Confirmation and control of triazine and 4-hydroxyphenyl pyruvate dioxygenase–inhibiting herbicide resistant Palmer amaranth (Amaranthus palmeri) in Nebraska. – Weed Technol 28: 28-38.
[25] Johnson, D. E., Wopereis, M. C. S., Mbodj, D., Diallo, S., Powers, S., Haefele, S. M. (2004): Timing of weed management and yield losses due to weeds in irrigated rice in the Sahel. – Field Crops Res 85: 31-42.
[26] Kalaitzandonakes, N., Kruse, J., Gouse, M. (2015): The potential economic impacts of herbicide-tolerant maize in developing countries: a case study. – AgBioForum 18(2): 221-238.
[27] Kemp, C. D. (1960): Methods of estimating the leaf area of grasses from linear measurements. – Ann Bot Oxford 24: 491-499.
[28] Khan, B., Ishfaq, M., Murtza, K., Batool, Z., Ali, N., Aslam, M. S., Khan, I., Anjum, S. A. (2021): Effect of varying planting density on weed infestation, crop phenology, yield, and fiber quality of cotton under different sowing methods. – Pure Appl Biol 10(3): 676-690.
[29] Knezevic, S. Z., Evans, S. P., Blankenship, E. E., Van Acker, R. C., Lindquist, J. L. (2002): Critical period of weed control: the concept and data analysis. – Weed Sci 50: 773-786.
[30] Kumar, V., Mahajan, G., Dahiya, S., Chauhan, B. S. (2020): Challenges and opportunities for weed management in No-till farming systems. – In: No-till Farming Systems for Sustainable Agriculture. Springer, pp. 107-125.

http://www.aloki.hu ● ISSN 1589 1623 (Print) ● ISSN1785 0037 (Online)
DOI: http://dx.doi.org/10.15666/aeer/2005_43214338

[31] Latif, A., Jilani, M. S., Baloch, M. S., Hashimc, M. M., Khakwani, A., Khand, Q. U., Saeed, A., Mamoon-ur-Rashid, M. (2021): Evaluation of critical period for weed crop competition in growing broccoli crop. – Sci Horticult 287: 110270.
[32] Menalled, U. D., Bybee-Finley, K. A., Smith, R. G., Ditommaso, A., Pethybridge, S. J., Ryan, M. R. (2020): Soil-mediated effects on weed-crop competition: elucidating the role of annual and perennial intercrop diversity legacies. – Agron 10: 1373.
[33] Micheal, J. S. A., Juraimi, A. S., Selamat, A., Man, A., Anwar, P., Uddin, K. (2013): Critical period of weed control in aerobic rice system. – Aust J Crop Sci 7(5): 665-673.
[34] Mondani, F., Golzardi, F., Ahmadvand, G., Ghorbani, R., Moradi, R. (2011): Influence of weed competition on potato growth, production and radiation use efficiency. – Not Sci Biol 3(3): 42-52.
[35] Naeem, M., Hussain, M., Farooq, M., Farooq, S. (2021a): Weed flora composition of different barley-based cropping systems under conventional and conservation tillage practices. – Phytoparasit 49: 751-769.
[36] Naeem, M., Mehboob, N., Farooq, M., Farooq, S., Hussain, S., Ali, H. M., Hussain, M. (2021b): Impact of different barley-based cropping systems on soil physicochemical properties and barley growth under conventional and conservation tillage systems. – Agron 11: 8.
[37] Otto, S., Masin, R., Casari, G., Zanin, G. (2009): Weed-corn competition parameters in late-winter sowing in northern Italy. – Weed Sci 57(2): 194-201.
[38] Schuster, M. Z., Gastal, F., Doisy, D., Charrier, X., De Moraes, A., Médiène, S., Barbu, C. M. (2020): Weed regulation by crop and grassland competition: critical biomass level and persistence rate. – Europ J Agron 113: 125963.
[39] Seavers, G. P., Wright, K. J. (1999): Crop canopy development and structure influence weed suppression. – Weed Res 39: 319-328.
[40] Seyyedi, S. M., Moghaddam, P. R., Mahallati, M. N. (2016): Weed competition periods affect grain yield and nutrient uptake of black seed (*Nigella Sativa* L.). – Horticult Plant J 2(3): 172-180.
[41] Shah, P. (2013): Weeds associated with tillage, mulching and nitrogen in wheat and their effect on yield: a review. – Int J Geol Agri Environ Sci 1(1): 20-25.
[42] Simarmata, M., Nurjanah, U., Setyowati, N. (2016): Determination of the critical period for weed control of sweet corn under tropical organic farming system. – Asian J Agri Biol 6(4): 447-454.
[43] Simić, M., Srdic, J., Videnovic, Z., Dolijanovic, Z., Uludag, A., Kovacevic, D. (2012): Sweet maize (*Zea mays* L. saccharata) weeds infestation, yield and yield quality affected by different crop densities. – Bulg J Agric Sci 18: 668-674.
[44] Singh, B., Kumar, M., Dhaka, A. K., Lamba, R. A. S. (2017): Efficacy of pinoxaden alone and in combination with metsulfuron-methyl and carfentrazone-ethyl against complex weed flora in barley (*Hordeum vulgare* L.). – Int J Curr Microbiol Appl Sci 6(4): 134-143.
[45] Soltani, N., Brown, L. R., Cowan, T., Sikkema, P. H. (2014): Weed management in spring seeded barley, oats, and wheat with prosulfuron. – Int J Agron ID: 950923. https://doi.org/10.1155/2014/950923.
[46] SPSS (2012): SPSS Version 20.0. – SPSS Inc., 233 S. Wacker Drive, Chicago, Illinois.
[47] Swanton, C. J., O'Sullivan, J., Robinson, D. E. (2010): The critical weed-free period in carrot. – Weed Sci 58: 229-233.
[48] Swanton, C. J., Nkoa, R., Blackshaw, R. E. (2015): Experimental methods for crop–weed competition studies. – Weed Sci 63: 2-11.
[49] Tursun, N., Datta, A., Sami, M., Kantarci, Z., Knezevic, S. Z., Singh, B. (2016): The critical period for weed control in three corn (*Zea mays* L.) types. – Crop Protec 90: 59-65.
[50] Ud Din, W., Naveed, K., Iqbal, S., Ali, A., Khan, S. M. (2016): Effect of different weeding intervals and methods on the yield and yield components of hybrid (PIONEER 3025). – ARPN J Agri Biol Sci 11(3): 100-106.

http://www.aloki.hu ● ISSN 1589 1623 (Print) ● ISSN1785 0037 (Online)
DOI: http://dx.doi.org/10.15666/aeer/2005_43214338

[51] Uremis, I., Uludag, A., Ulger, A. C., Cakir, B. (2010): Determination of critical period for weed control in the second crop corn under Mediterranean conditions. – Afri J Biotechnol 8: 4475-4480.
[52] USDA (United States Department of Agriculture) (2022): World Agricultural Production. – Foreign Agricultural Service/USDA, Global Market Analysis, FAS, USDA, 41p.
[53] Van Gaelen, H. (2014): Simulating yield response of barley to weed infestation in AquaCrop: case study Tigray, Northern Ethiopia. – M.Sc. Thesis, Faculteit Bio-ingenieurswetenschappen, Katholieke Universiteit Leuven, Ethiopia, 110p.
[54] Vandeleur, R. K., Gill, G. S. (2004): The impact of plant breeding on the grain yield and competitive ability of wheat in Australia. – Aust J Agri Res 55: 855-861.
[55] Walters, L., Craig, S. (2017): Increasing weed competition with competitive barley cultivars. – Proceedings of the 18th Australian Society of Agronomy Conference, Ballarat, Australia.
[56] Watson, P. R., Derksen, D. A., Van Acker, R. C. (2006): The ability of 29 barley cultivars to compete and withstand competition. – Weed Sci 54: 783-792.
[57] Zafar, M., Tanveer, A., Cheema, Z. A., Ashraf, M. (2010): Weed-crop competition effects on growth and yield of sugarcane planted using two methods. – Pak J Bot 42(2): 815-823.
[58] Zimdahl, R. L. (1993): Fundamentals of weed science. – Academic Press, New York.

http://www.aloki.hu ● ISSN 1589 1623 (Print) ● ISSN1785 0037 (Online)
DOI: http://dx.doi.org/10.15666/aeer/2005_43214338

THE EFFECT OF SOME HEAVY METAL COMBINATIONS ON GROWTH AND CHEMICAL COMPOSITION OF SOME ORNAMENTAL SHRUBS COMMON IN EGYPT Nº1. – HOP BUSH (*DODONAEA VISCASA* L.)

NOFAL, E. M. S.[1] – SHAHIN, S. M.[2*] – EL-TARAWY, A. M. A.[1] – OMAR, S. H. M.[2]

[1]*Hort. Dept., Fac. Agric., Kafrelsheikh Univ., Kafrelsheikh, Egypt*

[2]*Botanical Gards. Res. Dept., Hort. Res. Inst., ARC, Giza, Egypt*

[*]*Corresponding author*
e-mail: sayedshaheen551@gmail.com

(Received 16th Apr 2022; accepted 26th Jul 2022)

Abstract. A study was undertaken during 2019/20 and 2020/21 seasons to reveal the impact of lead (Pb), cadmium (Cd), and nickel (Ni) in combinations at various concentrations on the survival, growth, and chemical composition of *Dodonaea viscasa* L. seedlings after two periods of growth (PG): 6- and 18-months from planting. The interaction effect was also studied. The results indicated that survival % was 100% under the different sole or combined treatments, but the mean values of vegetative and root growth traits were gradually decreased with few exceptions as the concentrations of heavy metals were increased to reach minimum by the T4 combination. Elongating growth period up to 18 months significantly improved growth relative to that measured after 6 months. Hence, combining between planting in either unpolluted or polluted mixture with T1 combination and a growing period of 18 months gave the best growth. The gradual increment in HMs concentrations was accompanied by a gradual decrement in pollution resistance index (PRI) percentages, which were higher than 66% at the highest HMs concentrations indicating its high ability to withstand HMs toxicity. Different responses were observed regarding the chemical composition of the leaves and roots. Accordingly, *Dodonaea viscosa* L. plant can be used as a good phytoremediator.
Keywords: *survival, root length, Dodonaea viscasa* L.*, lead, cadmium, nickel, chemical composition*

Introduction

Hop bush (*Dodonaea viscasa* L.) which belongs to the Sapindaceae to Fam., is a very widespread tropical and subtropical bush, used in gardens for hedges and as a solitary specimen on turf. Its height reaches up to 4.5-5 m, has usually sticky shoots and simple, undivided, oblongish alternate leaves up to 7-10 cm long and about 2.5-3.0 cm wide. The flowers are greenish, in short terminal or axillary racemes. The fruits are 3-winged, notched at the apex, and red or purple in colour. It is propagated easily by seeds (Huxley et al., 1992).

Soils polluted with heavy metals (HMs) are still one of the most growing problems facing vegetative in all countries (Adrees et al., 2015). Among various HMs, lead (Pb), cadmium (Cd) and nickel (Ni) are the most serious ones due to their high mobility and toxicity, causing acute biological effects on plant growth and productivity with dangerous disorders to human health (Keller et al., 2015). They are more persistent and not degradable naturally like other organic pollutants, so accumulate in the soils and the different organs of plants (Khudhur et al., 2016). Thus, it is urgent to find out an effective and reasonable way to overcome this problem with the least cost through phytoremediation technology, in which some ornamentals (as non-food chain plants) can be used for remediation of contaminated soils with more cost-effective and fewer side

http://www.aloki.hu ● ISSN 1589 1623 (Print) ● ISSN1785 0037 (Online)
DOI: http://dx.doi.org/10.15666/aeer/2005_43394350

effects as well than chemical and physical methods (Tauqeer et al., 2016). Among ornamentals that may serve in this approach *Dodonaea viscasa* as a good bioindicator for pollution in industrial areas due to its high ability to absorb higher concentrations of Fe, Zn, As, Pb, Ni, and Co heavy metals resulting from steel factories irrespective of the lower concentration of chlorophyll a, b, total chlorophyll, carotenoids and total protein contents (Salih and Aziz, 2019). Among *Dodonaea viscasa* L., *Myrtus communis, Platycladus orientalis,* and *Ficus benjamina* ornamentals, Mamand et al. (2020) reported that *Dodonaea viscasa* L., is the most effective phytoremediator.

On other ornamental plants, similar reports were mentioned by Ma et al. (2018) on *Taxoidium* hybrid "Zhong shanshan", Omar (2018) on *Sambucus nigra* and *Bauhinia purpurea*, Eisa (2019) on *Populus nigra* and *Salix mueronata*, and Ouf and Gaber (2019) on *Salix mucronata*. Likewise, were those results of Dinu et al. (2021) on *Mentha piperita* and Khan et al. (2021) on some wild plants (*Digitaria sanguinalis*, *Hordeum leporinum,* and *Achantherum hymenoides*).

This study, however, aims to reveal the ability of *Dodonaea viscasa* seedlings to withstand the toxicity of Pb, Cd, and Ni heavy metals when applied in combination at ascending concentrations.

Materials and Methods

An experiment was carried out in the open field at Orman Botanical Garden, Giza, Egypt during the two successive seasons of 2019/2020 and 2020/2021 to examine the long-term impact of lead (Pb), cadmium (Cd), and nickel (Ni) in combinations at various concentrations for each metal on survival, growth and chemical composition of hop bush (*Dodonaea viscasa* L.) seedlings.

So, homogenous seedlings of such plant species at a height of about 12.3 cm, with one branch carrying about 12.0 leaves were planted on April, 15th for every season in 20-cm-diameter polyethylene black bags (one seedling/bag) filled with about 3 kg/bag of sand and clay mixture at equal volume parts (1:1, v/v). The physical and chemical properties of the sand and clay used in the two seasons were determined and shown in (*Table 1*).

Table 1. *The physical and chemical properties of the sand and clay used in 2019/20 and 2020/21 seasons*

Soil texture	Seasons	Particle size distribution (%)				S.P.	E.C. (dS/m)	pH	Cations (meq/L)				Anions (Meq/L)		
		Coarse sand	Fine sand	Silt	Clay				Ca^{++}	Mg^{++}	Na^{+}	K^{+}	HCO_3^{-}	Cl^{-}	SO_4^{--}
Sand	2019/20	18.72	71.28	4.76	5.34	21.83	1.58	8.20	2.65	2.48	21.87	0.78	3.85	13.00	10.93
	2020/21	79.76	9.30	2.50	8.44	23.10	1.76	7.90	19.42	8.33	7.20	0.75	1.60	7.80	26.30
Clay	2019/20	7.46	16.75	34.53	40.89	41.67	2.10	8.33	16.93	9.33	20.44	0.37	3.82	1.46	41.79
	2020/21	7.64	22.50	30.15	39.71	53.36	2.23	7.92	7.50	2.21	15.49	0.75	6.28	8.12	11.05

Thawing salts of Pb, Cd, and Ni (acetates), manufactured by Aldrich Chemical Co., Inc., Wisconsin 53233, USA were mixed well in combinations through the particles of the used soil mixture before filling the plastic bags at concentrations of 0.00 ppm for each metal as a control, 500 ppm Pb + 50 ppm Cd + 25 ppm Ni for treatment number one (T_1)

http://www.aloki.hu ● ISSN 1589 1623 (Print) ● ISSN1785 0037 (Online)
DOI: http://dx.doi.org/10.15666/aeer/2005_43394350

and 2-, 3- and 4- fold of these concentrations for treatments number two (T2), three (T3) and four (T4), respectively.

Immediately after planting, the plastic holeless bags were irrigated with 300 ml of fresh water/bag, but afterward the irrigation was done once day by day with only 250 ml of water/bag during the summer months, while during winter ones the plants were irrigated once every 3 or 4 days to keep the roots from decay. The usual agricultural practices required for such plantation were done whenever needed. The plants were set out for every season in a complete randomized design and replicated thrice with five plants per replicate (Mead et al., 1993).

Data of the current study were recorded after two periods of growth; the first after 6 months from planting (on October, 15th for every season) and the second after one year (12 months) from the first one (on the next October, 15th) and then expressed in the tables as other factor besides the factor of heavy metals combinations. These data were: survival percentage, plant height (cm), stem diameter at the base (cm), number of branches/plant, number of leaves/plant, means root length (cm), as well as fresh and dry weights of aerial parts and roots (g). Besides, the pollution resistance index as a percentage (PRI %) was calculated from the equation proposed by Wilkins (1957) as follows:

$$\text{PRI \%} = \text{Mean root length of the polluted plants (cm)/mean root length of control x 100} \quad \text{(Eq.1)}$$

In fresh leaf samples were taken from the middle parts of the plants, photosynthetic pigments (chlorophyll a, b and carotenoids, mg/g f.w.) and the percent of total soluble sugars were determined according to the methods of Sumantha et al. (2014) and Dubois et al. (1966), respectively, whereas in dry ones, the percentages of nitrogen, phosphorus, and potassium were measured by the methods explained by Chapman and Pratt (1975). Moreover, concentrations of Pb, Cd, and Ni as mg/100 g d.w. in dry samples of both leaves and roots were assessed using a Perkin Elmer 403 atomic absorption spectrophotometer (Jackson, 1973). All chemical analyses were evaluated in the second season only.

Data were then tabulated and subjected to analysis of variance using the program of SAS Institute (2009), followed by Duncan`s new multiple range t-test (Steel and Torrie, 1980) to detect the significance level among heavy metals combinations, growth periods, and their interactions.

Results and Discussion

Effect of lead (Pb), cadmium (Cd), and nickel (Ni) combinations on:

1- Survival percentage and vegetative and root growth traits

As shown in *Table 2*, survival of plants was 100% under the different treatments used in this study although the mean values of their vegetative and root growth parameters were greatly reduced by growing them in polluted soil, especially at the high concentrations of heavy metals (T3 and T4). This may indicate the high ability of plants to tolerate heavy metals toxicity due to their root type, which is fibrous and has a large surface area to cover and absorb more soil metals over time without damaging and affecting any of its tissues (Mamand et al., 2020).

http://www.aloki.hu ● ISSN 1589 1623 (Print) ● ISSN1785 0037 (Online)
DOI: http://dx.doi.org/10.15666/aeer/2005_43394350

Table 2. *Effect of heavy metals combinations, growth period, and their interactions on survival, plant height, and stem diameter of Dodonaea viscosa L. plants during 2019/20 and 2020/21 seasons*

Growth period (G.P.) / Pollution treatments	Survival (%)			Plant height (cm)			Stem diameter (cm)		
	1st G.P.	2nd G.P.	Mean	1st G.P.	2nd G.P.	Mean	1st G.P.	2nd G.P.	Mean
	First season; 2019/2020								
Control	100.00a	100.00a	100.00A	23.33e	88.33a	55.83A	0.287b	0.640a	0.464A
T1	100.00a	100.00a	100.00A	22.33ef	88.03a	55.18A	0.273b	0.633a	0.453A
T2	100.00a	100.00a	100.00A	20.30f	85.57b	52.94B	0.233b	0.600a	0.417A
T3	100.00a	100.00a	100.00A	15.63g	76.67c	46.15C	0.173b	0.633a	0.403A
T4	100.00a	100.00a	100.00A	14.50g	56.67d	35.59D	0.167b	0.533a	0.350B
Mean	100.00A	100.00A		19.22B	79.05A		0.227B	0.608A	
	Second season; 2020/2021								
Control	100.00a	100.00a	100.00A	25.70e	95.90a	60.80A	0.320d	1.113a	0.717A
T1	100.00a	100.00a	100.00A	24.50ef	95.97a	60.23A	0.303d	0.967b	0.635A
T2	100.00a	100.00a	100.00A	22.37f	91.03b	56.70B	0.260d	0.783c	0.522B
T3	100.00a	100.00a	100.00A	17.40g	85.13c	51.27C	0.207d	0.800c	0.504B
T4	100.00a	100.00a	100.00A	16.03g	64.03d	40.03D	0.193d	0.747c	0.470B
Mean	100.00A	100.00A		21.20B	86.41A		0.257B	0.882A	

Control: 0.00 ppm for Pb, Cd and Ni, T1: 500 ppm Pb + 50 ppm Cd + 25 ppm Ni; T2: 1000 ppm Pb + 100 ppm Cd + 50 ppm Ni; T3: 1500 ppm Pb + 150 ppm Cd + 75 ppm Ni and T4: 2000 ppm Pb + 200 ppm Cd + 100 ppm Ni. Means followed by the same latter in a column or row are not differ significantly according to Duncan's New Multiple Range t-Test at 5 % level

On the other hand, data averaged in *Tables 2, 3, 4, 5, and 6* indicate that means of various growth traits, expressed as: plant height (cm), stem diameter (cm), No. branches and leaves/plant, leaf area (cm^2), root length (cm), No root branches/plant, as well as fresh and dry weights of top growth and roots (g) were gradually decreased with increasing HMs concentrations to reach the minimal values by T4 combination, comparing with records of either control or any other metal combinations in the two seasons. This may be due to the higher accumulation of toxic metals in the leaves and roots (as indicated in *Table 7*), which always leads to depression of vital processes and metabolism, such as photosynthesis, inhibition of some enzymatic systems and blocking the formation of proteins and chlorophylls (Adrees et al., 2015). In this regard, a reduction in glutathione reductase activity in relation to Cd and Pb stress was observed by Chauhan and Mathur (2020) in *Helianthus annuus*. Furthermore, Ma et al. (2018) suggested that the common consequence of heavy metals toxicity is the excessive accumulation of reactive oxygen species (ROS) and methyl glyoxal (MG), both of them can cause peroxidation of lipids, oxidation of protein, inactivation of enzymes, DNA damage and/or interact with other vital constituents of plant cells. These hazardous effects were documented by Lajayer et al. (2019) who mentioned that heavy metals may inhibit plant metabolic processes such as water uptake, N assimilation, respiration, photosynthesis and transcription, and may retard the different enzymatic activities via binding to sulfhydryl (SH-) groups and intensifying reactive oxygen species (ROS) production leading to oxidative stress. Besides, Mamand et al. (2020) stated that lead can negatively affect the structure of mitochondria through decreasing mitochondrial cristae and in turn lowering the capability of oxidative phosphorylation.

http://www.aloki.hu ● ISSN 1589 1623 (Print) ● ISSN1785 0037 (Online)
DOI: http://dx.doi.org/10.15666/aeer/2005_43394350

Table 3. *Effect of heavy metals combinations, growth period, and their interactions on No. branches; No. leaves and leaf area of Dodonaea viscasa L. plants during 2019/20 and 2020/21 seasons*

Growth period (G.P.) / Pollution treatments	No. branches/plant			No. leaves/plant			Leaf area (cm2)		
	1st G.P.	2nd G.P.	Mean	1st G.P.	2nd G.P.	Mean	1st G.P.	2nd G.P.	Mean
	First season; 2019/2020								
Control	1.00f	4.00a	2.50A	43.33f	481.70a	262.52A	14.57b	14.62b	14.60A
T1	1.00f	3.67b	2.34B	29.67g	453.30c	241.58B	14.47b	14.98a	14.73A
T2	1.00f	3.33c	2.17C	25.67h	450.30b	237.99B	12.90d	14.00c	13.45B
T3	1.00f	3.00d	2.00D	18.67i	385.70d	202.19C	11.83e	13.00d	12.42C
T4	1.00f	2.67e	1.84E	15.33j	280.00e	147.67D	9.87f	12.10e	10.99D
Mean	1.00B	3.33A		26.53B	409.90A		12.83B	13.74A	
	Second season; 2020/2021								
Control	1.00f	4.90a	2.95A	49.10e	438.00a	243.55A	15.00d	16.20b	15.60A
T1	1.00f	4.23b	2.62B	32.83f	436.00a	234.42B	14.77de	16.53a	15.65A
T2	1.00f	4.00c	2.500B	29.27g	410.30b	219.79C	13.70f	15.47c	14.58B
T3	1.00f	3.50d	2.25C	21.33h	360.00c	190.67D	12.63h	14.63e	13.63C
T4	1.00f	2.97e	1.99D	18.03i	295.90d	156.97E	11.03i	13.37g	12.20D
Mean	1.00B	3.92A		30.11B	388.04A		13.43B	15.24A	

Control: 0.00 ppm for Pb, Cd and Ni, T1: 500 ppm Pb + 50 ppm Cd + 25 ppm Ni; T2: 1000 ppm Pb + 100 ppm Cd + 50 ppm Ni; T3: 1500 ppm Pb + 150 ppm Cd + 75 ppm Ni and T4: 2000 ppm Pb + 200 ppm Cd + 100 ppm Ni. Means followed by the same latter in a column or row are not differ significantly according to Duncan's New Multiple Range t-Test at 5 % level

Table 4. *Effect of heavy metal combinations, growth period, and their interactions on root length; No. root branches and PRI of Dodonaea viscosa L. plants during 2019/20 and 2020/21 seasons*

Growth period (G.P.) / Pollution treatments	Root length			No. root branches/plant			Pollution resistance Index (PRI %)		
	1st G.P.	2nd G.P.	Mean	1st G.P.	2nd G.P.	Mean	1st G.P.	2nd G.P.	Mean
	First season; 2019/2020								
Control	29.33d	38.33a	33.83A	14.23b	16.67a	15.45A	100.00a	100.00a	100.00A
T1	25.83f	34.33b	30.08B	11.67e	17.00a	14.34B	88.33c	90.00b	89.17B
T2	23.20g	33.00c	28.10C	10.67f	13.33c	12.00C	79.17f	86.43e	82.80C
T3	19.57h	33.33c	26.45D	10.17g	12.67d	11.42D	66.63h	87.13d	76.88D
T4	18.43i	26.67e	22.55E	10.00g	11.67e	10.84E	62.83i	69.63g	66.23E
Mean	23.27B	33.13A		11.35B	14.27A		79.39B	86.64A	
	Second season; 2020/2021								
Control	32.33e	30.50a	35.92A	12.83c	15.07ab	13.95A	100.00a	100.00a	100.00A
T1	28.77g	37.77b	33.27B	10.63e	15.30a	12.97B	89.17e	95.70b	92.44B
T2	26.37h	35.67d	31.05C	9.60f	14.73b	12.17C	81.63f	90.37d	86.00C
T3	21.87i	36.70c	29.29D	9.33f	11.43d	10.38D	67.57h	92.87c	80.22D
T4	20.87j	29.63f	25.25E	9.17f	10.43e	9.80E	64.53i	75.00g	69.77E
Mean	26.04B	35.85A		10.31B	13.39A		80.58B	90.79A	

Control: 0.00 ppm for Pb, Cd and Ni, T1: 500 ppm Pb + 50 ppm Cd + 25 ppm Ni; T2: 1000 ppm Pb + 100 ppm Cd + 50 ppm Ni; T3: 1500 ppm Pb + 150 ppm Cd + 75 ppm Ni and T4: 2000 ppm Pb + 200 ppm Cd + 100 ppm Ni. Means followed by the same latter in a column or row are not differ significantly according to Duncan's New Multiple Range t-Test at 5 % level

http://www.aloki.hu ● ISSN 1589 1623 (Print) ● ISSN1785 0037 (Online)
DOI: http://dx.doi.org/10.15666/aeer/2005_43394350

Table 5. *Effect of heavy metals combinations, growth period, and their interactions on top growth fresh and dry weights of Dodonaea viscosa L. plants during 2019/20 and 2020/21 seasons*

Growth period (G.P.) / Pollution treatments	Top growth fresh weight (g)			Top growth dry weight (g)		
	1st G.P.	2nd G.B.	Mean	1st G.P.	2nd G.B.	Mean
	First season; 2019/2020					
Control	5.02f	99.70a	52.36A	1.75f	35.26a	18.50A
T1	3.46fg	84.70c	44.08C	1.23f	30.26c	15.75B
T2	2.99fg	90.27b	46.63B	1.06f	31.43b	16.25B
T3	2.25g	73.67d	37.96D	0.82f	26.03d	13.42C
T4	1.81g	65.83e	33.82E	0.65f	23.37e	12.01D
Mean	3.11B	82.83A		1.10B	29.27A	
	Second season; 2020/2021					
Control	6.04f	109.40a	57.72A	2.18f	38.77a	20.48A
T1	4.22fg	93.57b	48.90B	1.54fg	32.97b	17.25B
T2	3.78fg	84.97c	44.38C	1.38fg	29.23c	15.31C
T3	3.09g	70.40d	36.75D	1.13g	24.83d	12.98D
T4	2.43g	64.70e	33.57E	0.90g	22.60e	11.75E
Mean	3.91B	84.61A		1.43B	29.68A	

Control: 0.00 ppm for Pb, Cd and Ni, T1: 500 ppm Pb + 50 ppm Cd + 25 ppm Ni; T2: 1000 ppm Pb + 100 ppm Cd + 50 ppm Ni; T3: 1500 ppm Pb + 150 ppm Cd + 75 ppm Ni and T4: 2000 ppm Pb + 200 ppm Cd + 100 ppm Ni. Means followed by the same latter in a column or row are not differ significantly according to Duncan's New Multiple Range t-Test at 5 % level

Table 6. *Effect of heavy metals combinations, growth period, and their interactions on roots fresh and dry weights of Dodonaea viscosa L. plants during 2019/20 and 2020/21 seasons*

Growth period (G.P.) / Pollution treatments	Roots fresh weight (g)			Roots dry weight (g)		
	1st G.P.	2nd G.P.	Mean	1st G.P.	2nd G.P.	Mean
	First season; 2019/2020					
Control	1.60f	19.53a	10.57A	1.09e	8.03a	4.56A
T1	1.45f	17.50b	9.48B	0.99ef	7.40b	4.20B
T2	1.32fg	15.03c	8.18C	0.90e-g	6.33c	3.61C
T3	1.11g	14.43d	7.77D	0.76fg	6.17c	3.46C
T4	1.02g	12.60e	6.81E	0.69g	5.33d	3.01D
Mean	1.30B	15.82A		0.88B	6.65A	
	Second season; 2020/2021					
Control	2.01f	19.71a	10.86A	1.30f	9.93a	5.62A
T1	1.76g	18.10b	9.93B	1.16fg	9.03b	5.10B
T2	1.60g	14.81c	8.21C	1.03fg	7.37c	4.20C
T3	1.37h	13.57d	7.47D	0.92g	6.80d	3.86D
T4	1.40h	12.53e	6.97E	0.87g	6.27e	3.57E
Mean	1.63B	15.75A		1.06B	7.88A	

Control: 0.00 ppm for Pb, Cd and Ni, T1: 500 ppm Pb + 50 ppm Cd + 25 ppm Ni; T2: 1000 ppm Pb + 100 ppm Cd + 50 ppm Ni; T3: 1500 ppm Pb + 150 ppm Cd + 75 ppm Ni and T4: 2000 ppm Pb + 200 ppm Cd + 100 ppm Ni. Means followed by the same latter in a column or row are not differ significantly according to Duncan's New Multiple Range t-Test at 5 % level

http://www.aloki.hu ● ISSN 1589 1623 (Print) ● ISSN1785 0037 (Online)
DOI: http://dx.doi.org/10.15666/aeer/2005_43394350

Table 7. *Effect of heavy metals combinations, growth period, and their interactions on pigments and total soluble sugars concentrations in Dodonaea viscosa L. leaves during 2020/21 season*

Growth period (G.P.) / Pollution treatments	Chlorophyll (a) (mg/g f.w.)			Chlorophyll (b) (mg/g f.w.)			Carotenoids (mg/g f.w.)			Total soluble sugars (%)		
	1st G.P.	2nd G.P.	Mean	1st G.P.	2nd G.P.	Mean	1st G.P.	2nd G.P.	Mean	1st G.P.	2nd G.P.	Mean
Control	1.388b	1.345b	1.367B	0.335a	0.368a	0.352A	0.326a	0.363a	0.345A	27.16a	16.10b	21.63A
T1	1.466a	1.446a	1.456A	0.359a	0.344a	0.352A	0.350a	0.315b	0.333A	25.67a	16.81b	21.24A
T2	1.304b	1.403a	1.354B	0.227c	0.328a	0.278B	0.208c	0.303b	0.256C	15.50c	15.78c	15.64B
T3	1.217c	1.363b	1.290C	0.199c	0.301b	0.250B	0.239c	0.340a	0.290B	14.81c	15.18c	15.00B
T4	1.194c	1.309b	1.252C	0.176c	0.298b	0.237C	0.194c	0.338a	0.266C	9.76d	16.89b	13.33C
Mean	1.314A	1.373A		0.259B	0.328A		0.264B	0.332A		18.58A	16.15B	

Control: 0.00 ppm for Pb, Cd and Ni, T1: 500 ppm Pb + 50 ppm Cd + 25 ppm Ni; T2: 1000 ppm Pb + 100 ppm Cd + 50 ppm Ni; T3: 1500 ppm Pb + 150 ppm Cd + 75 ppm Ni and T4: 2000 ppm Pb + 200 ppm Cd + 100 ppm Ni. Means followed by the same latter in a column or row are not differ significantly according to Duncan's New Multiple Range t-Test at 5 % level

The previous results, however are in agreement with those detected by Ma et al. (2018) on two *Taxodium* clones (T.118 and T.406), Eisa (2019) on *Populus nigra* and *Salix mucronata* and Chauhan and Mathur (2020) who found that the different concentrations of Pb, Cd, Cu and As caused morphological irregularities and hampered shoot and root lengths, fresh weight of shoot/root and leaf area of both varieties PBH and DRSF-108 of *Helianthus annuus.* The maximum shoot and root lengths were observed in control plants, while the minimum was recorded by PBH variety plants.

The only exception noticed in such work is that some HMs combinations, especially T1 caused either a slight improvement or reduction in some growth traits with non-significant differences relative to control in some cases of the two seasons. This may be referred to that some heavy metals, such as Cd at low concentration may act as co-factor for some metabolic enzymes. In this concern, Tauqeer et al. (2016) reported that the activity of superoxide dismutase (SOD), peroxidase (POD), catalase (CAT), and ascorbate peroxidase (APX) in *Alternanthera bettzickiana* plant tissues increased under lower levels of Cd and Pb (0.5 and 1.0 mM), but decreased at higher ones (2.0 mM). On willow (*Salix mucronata*), Ouf and Gaber (2019) revealed that the HMs-contaminated soil obtained from the Sabaghy El-Baida district in Kafr El-Dawar City was superior than the non-contaminated soil (control) in improving growth parameters (plant height, stem diameter, leaf area, No. leaves, root length, fresh and dry weights of leaves, shoots, and roots) and wood properties (specific gravity and fiber length).

Data in the aforementioned tables indicate also that elongating growth period up to 18 months significantly improved the mean values of the different measured growth characters compared to their means recorded after only 6 months of growth. This may be reasonable because the plants took enough time for good growth and alter their growth behavior to cope with pollution stress. Furthermore, dodonaea plant is considered one of the quick-growing shrubs with high biomass production that can both tolerate and accumulate pollutants. It has also a great ability to restore its growth after pruning or any stress. In this respect, Ouf and Gaber (2019) found that various growth traits of *Salix mucronata* plants potted in MHs-contaminated soil were progressively improved with prolonging growth period from 6- to either 12- or 18 months.

http://www.aloki.hu ● ISSN 1589 1623 (Print) ● ISSN1785 0037 (Online)
DOI: http://dx.doi.org/10.15666/aeer/2005_43394350

Accordingly, the best growth of plants under conditions of this trial was attained by combining between planting in either unpolluted soil mixture or T1 polluted one and 18 months growing period, as these two combined treatments gave the highest growth means, which were statistically at par with each other in most cases of both seasons.

These results could be documented by those of Salih and Aziz (2019) who stated that *Dodonaea viscasa* is a good bioindicator for pollution and has a high accumulation ability rendering it suitable for removing HMs from soil and atmosphere. Similarly, Mamand et al. (2020) mentioned that *Dodonaea viscosa* is the most effective phytoremediator among *F. benjamina*, *Myrtus communis,* and *Platycladus orientalis* because of its root type which is fibrous and has a large surface area to cover and absorb more HMs by time without injury. On *Salix mucronata*, Ouf and Gaber (2019) noticed that plant height, stem diameter, leaf area, No. leaves and fresh and dry weights of leaves and shoots mean values were progressively increased with time spanned up to the end of the experiment (18 months).

2- Pollution resistance index as a percentage (PRI %)

Data averaged in *Table 4* exhibit that PRI of control plants was 100% in the two seasons. However, the gradual increase in HMs concentrations was accompanied by a gradual decrease in the percentages of this index to be minimum by the highest concentrations of such metals (T4 combination), which reduced its means to 66.23% in the 1st season and to 69.77% in the 2nd one. Reduction of PRI to a percent higher than 66% in both seasons plus 100% survival under the highest concentrations of toxic metals clearly show that dodonaea plants are good tolerant for toxicity of Pb, Cd, and Ni metals under the conditions of such work. This may be ascribed to the good distribution of dodonaea fibrous roots in the polluted soil mixture without damage (Mamand et al., 2020). In this respect, Eisa (2019) suggested that *Populus nigra* and *Salix mucronata* are good candidates for remediation of Cd, Cu and Pb contaminated soil due to their high tolerance index. Likewise, Ouf and Gaber (2019) pointed out that growing *Salix mucronata* in HMs-contaminated soil linearly increased their root length with increasing growth period from 6 to either 12 or 18 months, increasing its tolerance to HMs toxicity over time.

The mean values of PRI registered in the second growth period (after 18 months from planting) were higher than those recorded in the first one because the plants gave longer roots in the 2nd growth period than those attained in the 1st one (*Table 4*). So, the highest % of PRI in the two seasons was achieved by combining between planting in soil mixture free from HMs and either of growth period, followed directly by connecting between planting in soil mixture of T1 combination and the longer growth period (18 months). These gains are in harmony with those of Mamand et al. (2020) on *Dodonaea viscasa*, Eisa (2019) on *Populus nigra* and *Salix mucronata*.

3- The chemical composition of leaves and roots

It is obvious from data presented in *Table 7* that chlorophyll a, b, and carotenoids concentrations (mg/g. f.w.) were significantly decreased by T2, T3, and T4 HMs combinations with the inferiority of T4 one that scored the least concentrations, whereas control and T1 combination recorded values closely near together with non-significant differences among themselves, except for T1 combination that raised chlorophyll-a concentration to the highest value, even over control value. Plants also acquired higher concentrations of the three pigments at a growth period of 18 months than those recorded

http://www.aloki.hu ● ISSN 1589 1623 (Print) ● ISSN1785 0037 (Online)
DOI: http://dx.doi.org/10.15666/aeer/2005_43394350

at 6 months one. Generally, combining between planting in T1-polluted soil mixture and either 6- or 18-month growth period gave the utmost high concentration of chlorophyll a, while that was true for both chlorophyll b and carotenoids by interacting between planting in either control or T1-polluted soil mixture and either growth period.

The harmful effect of HMs on the photosystem may be referred to as the disturbances caused by the metals in Calvin cycle reactions and down-regulation or even feedback inhibition of electron transport by the excessive amounts of ATP and NADPH (Krupa et al., 1993). Besides, Droppa et al. (1996) found that Cd in greening leaves interferes with chlorophyll biosynthesis, and acts mainly by inhibiting the LHC synthesis into stable complexes required for normal functional photosynthesis activity.

Data presented in *Table 8* exhibit that N % in the leaves was progressively decreased with increasing HMs concentrations. The opposite was the right regarding P and K percentages, as their concentrations have fluctuated with non-significant differences in between, except for P %, which was reduced to the minimum (0.285%) by T2 combination, and K %, which was the least (1.63%) by control (zero HMs). In addition, the percentages of N and P measured after the long period growth was significantly higher than those measured after the short one. Thus, the highest concentration of N was achieved by interacting between planting in unpolluted soil mixture and the 18-months growth period, but that was true for P % by combining between planting in either T1 or T4 polluted soil and 18-months growth period. The highest K %, however was attained by most interaction treatments, especially after the short growth period (6 months).

Table 8. *Effect of heavy metals combinations, growth period, and their interactions on nitrogen, phosphorus, and potassium in Dodonaea viscosa L. leaves during 2020/21 season*

Growth period (G.P.) / Pollution treatments	N (%)			P (%)			K (%)		
	1st G.P.	2nd G.P.	Mean	1st G.P.	2nd G.P.	Mean	1st G.P.	2nd G.P.	Mean
Control	1.991b	2.857a	2.424A	0.259c	0.363b	0.311AB	1.47c	1.78b	1.63B
T1	2.213b	1.993b	2.103B	0.257c	0.451a	0.354A	1.93a	2.07a	2.00A
T2	1.337d	1.659c	1.448C	0.233c	0.337b	0.285C	2.13a	1.88b	2.01A
T3	1.116e	1.327d	1.222D	0.264c	0.418a	0.341A	1.98a	2.04a	2.01A
T4	0.996e	1.548c	1.272D	0.168d	0.452a	0.310AB	2.10a	1.79b	1.95A
Mean	1.531B	1.877A		0.236B	0.404A		1.92A	1.91A	

Control: 0.00 ppm for Pb, Cd and Ni, T1: 500 ppm Pb + 50 ppm Cd + 25 ppm Ni; T2: 1000 ppm Pb + 100 ppm Cd + 50 ppm Ni; T3: 1500 ppm Pb + 150 ppm Cd + 75 ppm Ni and T4: 2000 ppm Pb + 200 ppm Cd + 100 ppm Ni. Means followed by the same latter in a column or row are not differ significantly according to Duncan's New Multiple Range t-Test at 5 % level

As for Pb, Cd, and Ni concentrations (mg/100 g d.w.), data presented in *Table 9* show that their mean values were gradually increased in the leaves and roots as a result of increasing their levels in the contaminated soil mixture to reach the maximum by T4 HMs-combination, except for Pb concentration that was maximum in the roots by T3 HMs-combination. On the other side, elongating the growth period to 18 months increased only Cd and Ni concentrations in the leaves over those scored in the 6 months one, and the opposite was the correct in the matter of Pb concentration. In the roots, however that was true for only Cd concentration which was 114.142 mg/100 g. d.w. after 18 months from planting against 99.725 mg/100 g d.w. after only 6 months of growth.

http://www.aloki.hu ● ISSN 1589 1623 (Print) ● ISSN1785 0037 (Online)
DOI: http://dx.doi.org/10.15666/aeer/2005_43394350

Hence, combining between planting in T4 polluted soil mixture and growth period of 6 months gave the highest Pb concentration in the leaves, but for the highest Cd and Ni concentration in the leaves, it was attained by connecting between planting in T4 polluted soil and growth period of 18 months. In the roots, however the highest Pb concentration was obtained by planting in T3 polluted soil in the first growth period, while the highest Cd concentration was recorded by planting in T4 polluted soil in the second growth period, and that of Ni concentration was found due to planting in T4 polluted soil in the first growth period. In general, concentrations of Pb, Cd, and Ni in the roots were higher than those in the leaves, with few exceptions.

Table 9. *Effect of heavy metals combinations, growth period, and their interactions on lead, cadmium, and nickel concentrations in Dodonaea viscosa L. leaves and roots during 2020/21 season*

Growth period (G.P.) / Pollution treatments	Pb (mg/100 g d.w.)			Cd (mg/100 g d.w.)			Ni (mg/100 g d.w.)		
	1st G.P.	2nd G.P.	Mean	1st G.P.	2nd G.P.	Mean	1st G.P.	2nd G.P.	Mean
	In the leaves								
Control	39.341e	26.500h	32.921E	31.143i	73.535f	52.339E	14.187e	13.246e	13.717D
T1	47.635d	27.876h	37.756D	35.256h	80.333e	57.795D	17.146d	16.725d	16.936C
T2	56.495c	30.583g	43.539C	52.951g	91.675d	72.313C	18.500d	18.705d	18.603C
T3	62.138b	36.676f	49.407B	82.075e	120.310b	101.193B	21.893c	26.459b	24.176B
T4	73.663a	36.798f	55.231A	104.640c	152.923a	128.782A	26.376b	29.591a	27.984A
Mean	55.855A	31.687B		61.213B	103.755A		19.621B	20.945A	
	In the roots								
Control	74.548e	11.465h	43.007E	61.548h	74.665g	68.107E	23.290f	25.299e	24.295D
T1	83.436d	13.501h	48.469D	73.860g	87.740f	80.800D	26.795e	23.967f	25.381D
T2	91.742c	16.239g	53.991C	97.399e	115.036d	106.218C	28.932d	25.983e	27.458C
T3	116.501a	33.510f	75.006A	130.807c	139.768b	135.2088B	43.500c	30.786d	37.143B
T4	110.400b	35.102f	72.751B	135.012b	153.500a	144.256A	52.099a	46.179b	49.139A
Mean	95.326A	21.963B		99.725B	114.142A		34.923A	30.443B	

Control: 0.00 ppm for Pb, Cd and Ni, T1: 500 ppm Pb + 50 ppm Cd + 25 ppm Ni; T2: 1000 ppm Pb + 100 ppm Cd + 50 ppm Ni; T3: 1500 ppm Pb + 150 ppm Cd + 75 ppm Ni and T4: 2000 ppm Pb + 200 ppm Cd + 100 ppm Ni. Means followed by the same latter in a column or row are not differ significantly according to Duncan's New Multiple Range t-Test at 5 % level

Absorption of metals by roots of plants grown in HMs-polluted soil may be necessary for these stressed plants to keep the equilibrium between their concentrations in soil solution and nutrient content in plant tissues. In this respect, Salih and Aziz (2019) observed that higher concentrations of Fe, Zn, As, Pb, Cd, and Co were recorded in the leaves of *Dodonaea viscosa* grown in the garden inside the steel factory (polluted site), which was accompanied with lower concentrations of Ni, chlorophyll a and b, total chlorophyll (a + b), carotenoids and protein. Similarly, Mamand et al. (2020) indicated that the highest bioaccumulation factor (BF) of Pb (39.15) was observed in *Dodonaea viscasa*. So, the maximum values of total Pb (1084.96 mg/kg) were detected in this garden plant. On *Mentha piperita*, Dinu et al. (2021) showed that Cd, Ni, and Pb were accumulated in the different parts of the plant, except for As.

In a biomonitoring study for HMs accumulation in some wild plants, Khan et al. (2021) revealed that the highest Co, Cu, Zn, Fe, and Mn contents were observed in *Digitaria*

http://www.aloki.hu ● ISSN 1589 1623 (Print) ● ISSN1785 0037 (Online)
DOI: http://dx.doi.org/10.15666/aeer/2005_43394350

sanguinalis (0.3 mg/kg), *Hordeum leporinum* (15.7 mg/kg), *H. leporinum* (36.5 mg/kg), *Achnatherum hymenoides* (26.1 mg/kg) and *H. Leporinum* (28.3 mg/kg), respectively. One of the maximum dangerous impacts of HMs is the slow disappearance of chlorophyll and yellowing of leaves, which can be associated with a reduction in the photosynthesis potential (Ma et al., 2018).

Conclusion

From the previous results, it can be advised to use Hop bush plants as a good phytoremediator for toxic HMs.

REFERENCES

[1] Chapman, H. D., Pratt, R. E. (1975): Methods of Analysis for Soil, Plant and Water. – California Univ., Division of Agric. Sci., pp. 172-173.
[2] Chauhan, P., Mathur, J. (2020): Phytoremediation efficiency of *Helianthus annuus* L. for reclamation of heavy metals-contaminated industrial soil. – Environ. Sci. & Pollut. Res. 27: 29954-29966.
[3] Dinu, C., Gheorghe, S., Tenea, A. G., Stoica, C., Vesile, G., Popescu, R. L., Serban, E. A., Pascu, L. F. (2021): Toxic metals (As, Cd, Ni, Pb) impact in the most common medicinal plant (Mentha piperita). – Inter. J. Environ. Res. and Public Health 18: 3904-3924.
[4] Droppa, M., Oravecz, A., Boddi, B., Horvath, G. (1996): Heavy metals inhibition of photosynthetic membrane. – Proc. 1st Egypt-Hung. Hort. Conf., Kofrelgholkh 1: 13-18.
[5] Dubois, M., Smith, F., Illes, K. A., Hamilton, J. K., Rebers, P. A. (1966): Colorimetric method for determination of sugars and related substances. – Ann. Chem. 28(3): 350-356.
[6] Eisa, E. A. T. (2019): Phytoremediation of heavy metals contaminated soil by plantation of *Populus nigra* L. and *Salix mucronata* L. transplants. – Ph.D. Thesis, Hort. Dept. (Floriculture), Fac. Agric., Kafrelsheikh Univ.
[7] Huxley, A., Griffiths, M., Levy, M. (1992): The New Royal Hort. Soci. Dict. of Gardening. – The Stockton Press, Ltd., New York, 257 Park Avenue South, N. Y. New York, N.Y. 10010, USA, vol. 2, 747p.
[8] Jackson, M. H. (1973): Soil Chemical Analysis. – Prentice-Hall of India Private Limited M-97, New Delhi, India, 498p.
[9] Keller, C., Rizwan, M., Davidian, J. C., Pokrovsky, O. S., Bovet, N., Chaurand, P., Meunier, J. D. (2015): Effect of silicon on wheat seedlings grown in hydroponics under Cu stress. – Planta 241: 847-860.
[10] Khan, Z. I., Ugulu, I., Zafar, A., Mehmood, N., Bashir, H., Ahmad, K., Sana, M. (2021): Biomonitoring of heavy metals accumulation in wild plants growing at Soon valley, Khushab, Pakistan. – Pak. J. Bot. 53(1): 1-6.
[11] Khudhur, N. S., Khudhur, S. M., Ameen, N. O. H. (2016): A study on soil bacterial population in steel Co. and some related area in Erbil city in relation to heavy metal pollution. – ZANCO J. Pure and Appl. Sci. 28(5): 101-116.
[12] Krupa, Z., Siedlecka, A., Maksymiec, W., Baszynski, T. (1993): *In vivo* response of photosynthetic apparatus of *Phaseolus vulgaris* L. to nickel toxicity. – J. Plant Physiol. 142(6): 664-668.
[13] Lajayer, B. A., Moghadam, N. K., Maghsoodi, M. R., Ghorbanpour, M., Kariman, K. (2019): Phytoextraction of heavy metals from contaminated soil, water and atmosphere using ornamental plants: mechanisms and efficiency improvement strategies. – Environ. Sci & Pollu. Res. 26: 8468-8484.

http://www.aloki.hu ● ISSN 1589 1623 (Print) ● ISSN1785 0037 (Online)
DOI: http://dx.doi.org/10.15666/aeer/2005_43394350

[14] Ma, Y., Wang, H., Wang, P., Yu, C., Luo, S., Zhang, Y., Xie, Y. (2018): Effects of cadmium stress on the antioxidant system and chlorophyll characteristics of two *Taxodium* clones. – Plant Cell Reports 37: 1547-1555.
[15] Mamand, S. F., Khudhur, N. S., Darweh, D. A. (2020): Phytoremediation efficiency of some evergreen plant genera for lead polluted soil. – ZANCO J. Pure and Appl. Sci. 35(5): 174-178.
[16] Mead, R., Curnow, R. N., Harted, A. M. (1993): Statistical Methods in Agriculture and Experimental Biology. – 2nd ed., Chapman & Hall Ltd., London, 335p.
[17] Omar, S. H. M. (2018): Studies on tolerance of some ornamental plants to soil pollution with some combinations of heavy metals. – M.Sc. Thesis, Hort. Dept. (Floriculture), Fac. Agric., Kafrelsheikh Univ.
[18] Ouf, A. A., Gaber, M. K. (2019): Determination of heavy metals absorption and accumulation by willow plants as a phytoremediator to soil contaminants. – Middle East J. Agric. Res. 8(2): 400-410.
[19] Salih, Z., Aziz, F. (2019): Heavy metals accumulation in leaves of five plant species as a bioindicator of steel factory pollution and their effects on pigment content. – Poll. J. Environ. Stud. 28(6): 4351-4358.
[20] SAS Institute. (2009): SAS/STAT User`s Guides Statistics. – Vers. 6.04, 4th ed., SAS Institute Inc. Cary, N.C., USA.
[21] Steel, R. G. D., Torrie, J. H. (1980): Principles and Procedures of Statistics. – McGrow Hill Book Co., Inc., New York, pp. 377-400.
[22] Sumantha, N., Haque, C. I., Nishika, J., Suprakash, R. (2014): Spectrophotometric Analysis of chlorophyllous and carotenoids from commonly grown Fern species by using various extracting solvents. – Res. J. Chem. Sci. 4(9): 63-69.
[23] Tauqeer, H. M., Ali, S., Rizwan, M., Ali, Q., Saeed, R., Iftikhar, U., Ahmad, R., Farid, M., Abbasi, G. H. (2016): Phytoremediation of heavy metals by *Alternanthera bettzickiana*: growth and physiological response. – Ecotoxicol. and Environ. Saf. 126: 138-146.
[24] Wilkins, D. A. (1957): A technique for the measurement of lead tolerance in plants. – Nature 180: 73-78.

http://www.aloki.hu ● ISSN 1589 1623 (Print) ● ISSN1785 0037 (Online)
DOI: http://dx.doi.org/10.15666/aeer/2005_43394350

LONG-TERM EFFECT OF SOME HEAVY METAL COMBINATIONS ON GROWTH AND CHEMICAL COMPOSITION OF SOME ORNAMENTAL SHRUBS COMMON IN EGYPT Nº2. – COMMON OLEANDER (*NERIUM OLEANDER* L.)

NOFAL, E. M. S.[1] – SHAHIN, S. M.[2*] – EL-TARAWY, A. M. A.[1] – OMAR, S. H. M.[2]

[1]*Hort. Dept., Fac. Agric., Kafrelsheikh Univ., Kafrelsheikh, Egypt*

[2]*Botanical Gards. Res. Dept., Hort. Res. Inst., ARC, Giza, Egypt*

[*]*Corresponding author*
e-mail: sayedshaheen551@gmail.com

(Received 16th Apr 2022; accepted 26th Jul 2022)

Abstract. An experiment was carried out at Orman Botanical Garden, Giza, Egypt during 2019/20 and 2020/21 seasons to reveal the response of *Nerium oleander* L. transplants to Pb, Cd, and Ni in combinations at various concentrations after short and long growth periods. Pollution treatments and growth periods were combined factorially to study the effect of interactions. The results showed that survival % was 100% by the various applied treatments. Plant height, stem diameter, and leaf area traits were improved by heavy metal combinations, whereas No. branches and leaves/plant, root length and top growth, and roots fresh and dry weights were negatively affected. Elongating growth period up to 18 months significantly increased means of the different vegetative and root growth traits compared to 6-months period. So, combining between planting in either control or first treatment combination mixture and the longer growth period significantly improved most of the growth parameters. The percent of pollution resistance index took a similar trend, and it was higher than 88% in the two seasons by fourth treatment combination indicating a high tolerance to HMs toxicity. Thus, *N. oleander* plants can be successfully used for landscaping HMs-polluted sites due to their high survival and tolerance potential.
Keywords: *Nerium oleander L., heavy metals pollution, PRI, survival, growth traits*

Introduction

Nowadays, phytoremediation is one of the most important, cheap, and effective tool to remove different contaminants from the soil and air (Ibrahim and El-Afandi, 2020). Ornamental plants specifically are important bioindicators for environmental pollution, as they are not food-chain crops and remove a considerable amount of pollutants from the soil atmosphere, and water. They act as sink and living filters to minimize environmental pollution by various ways like HMs absorption, adsorption, accumulation, or detoxification, besides their role in improving the air quality by releasing O_2 into the atmosphere and absorb CO_2 (Salih et al., 2017). Among them, *Nerium oleander* may be valid in this concern.

In this regard, Seaward and Mashhour (1991) found that homogenous seedlings of *N. oleander* have a great ability in collecting HMs on the surface of their leaves, mainly from aerial sources and controlled by substratum. This is due to that its leaves characterize by their lanceolate form with a high cuticle thickness (Akosy and Oztürk, 1997). This fact was documented by Houdaji et al. (2010) who reported that it has been known that *N. oleander* assumes an essential role in reducing heavy metals in nature because of its morphological and physic-compound attributes that make it has lanceolate leaves with high cuticle skin thickness. Similar responses were also observed on *N. oleander* by Salih

http://www.aloki.hu ● ISSN 1589 1623 (Print) ● ISSN1785 0037 (Online)
DOI: http://dx.doi.org/10.15666/aeer/2005_43514361

et al. (2017), Safari et al. (2018), Salih and Aziz (2019), and Ibrahim and El-Afandi (2020).

On the same line, were those results obtained by Ma et al. (2018) on *Taxodium* hybrid "Zhongshaushan", Omar (2018) on *Sambucus nigra* and *Bauhinia purpurea*, Eisa (2019) on *Populus nigra* and *Salix mucronata*, Ouf and Gaber (2019) on *Salix mucronata* and Chauhan and Mathur (2020) who found that industrially contaminated soil caused a great reduction in shoot length, root length, fresh weight of shoot/root and leaf area of *Helianthus annuus* vars. PBH and DRSF-108. Chlorophyll a, b and total chlorophyll (a + b) concentrations were decreased, while accumulation of Pb, Cd, Zn, Cu, Fe and as was increased at different range (0.62-158.29, 0.8-59.6, 0.81-166.5, 0.09-101.89, 2.06-53.25 and 0.002-2.55 mg/kg, respectively. Similarly, were those findings of Eid et al. (2020) on four aquatic macrophytes (*Eichhornia crassipes*, *Ludwigia stolonifera*, *Echinochloa stagnina,* and *Phragmites australis*).

However, this work was set out to investigate the effect of Pb, Cd, and Ni heavy metals in combinations at different concentrations on growth performance and chemical composition of common oleander transplants at two different growth periods. This ornamental shrub (*Nerium oleander* L., Fam. Apocynaceae) is an evergreen, erect shrub of 4-4.45 m height; leaves linear to oblong-lanceolate to 20-25 cm long, entire, dark dull green; blooms in summer, showy flowers in terminal branching cymes, yellowish to rose-pink, red-purple or white, sometimes scented; native to Mediterranean region to Japan (Bailey, 1976).

Oleanders are generally grown outdoors in mild climates. They require little attention and are very drought resistant. In cold regions, they are favorite as pot or tub plants, and should be cut back and rested after flowering, then potted in a mixture of loam and rotted manure. It is of easy culture and is well adapted to city conditions. Propagated easily by good-sized cuttings of mature firm wood, sometimes in water. All parts are very poisonous if eaten (Huxley et al., 1992).

Materials and Methods

This investigation was conducted at Orman Botanical Garden, Giza, Egypt under the full sun throughout 2019/20 and 2020/21 consecutive seasons to study the long-term effect of lead (Pb), cadmium (Cd), and nickel (Ni) when applied together at gradual concentrations on survival, growth and chemical composition of *Nerium oleander* L. transplants, as a strong growing ornamental shrub widely used for various landscape purposes in Egypt.

Thus, uniform transplants at a length of about 30-31.5 cm, with two branches carrying about 25-27 leaves were planted on April, 15th for every season in 20-cm-diameter polyethylene black bags (one transplant/bag) filled with about 3 kg/bag of sand and clay mixture at equal volume parts (1:1, v/v). The physical and chemical properties of the sand and clay used in the two seasons were determined and shown in *Table 1*.

Acetate quick thawing salts of Pb, Cd, and Ni, produced by Aldrich Chemical Co., USA were mixed well in combinations through the particles of the used soil mixture before filling the plastic bags at concentrations of 0.00 ppm for each metal as a control, 500 ppm Pb + 50 ppm Cd + 25 ppm Ni for treatment number one (T_1) and 2-, 3- and 4-fold of these concentrations for treatments number two (T2), three (T3) and four (T4), respectively.

http://www.aloki.hu ● ISSN 1589 1623 (Print) ● ISSN1785 0037 (Online)
DOI: http://dx.doi.org/10.15666/aeer/2005_43514361

Table 1. *The physical and chemical properties of the sand and clay used in 2019/20 and 2020/21 seasons*

Soil texture	Seasons	Particle size distribution (%)				S.P.	E.C. (dS/m)	pH	Cations (meq/L)				Anions (Meq/L)		
		Coarse sand	Fine sand	Silt	Clay				Ca^{++}	Mg^{++}	Na^{+}	K^{+}	HCO_3^{-}	Cl^{-}	SO_4^{--}
Sand	2019/20	18.72	71.28	4.76	5.34	21.83	1.58	8.20	2.65	2.48	21.87	0.78	3.85	13.00	10.93
	2020/21	79.76	9.30	2.50	8.44	23.10	1.76	7.90	19.42	8.33	7.20	0.75	1.60	7.80	26.30
Clay	2019/20	7.46	16.75	34.53	40.89	41.67	2.10	8.33	16.93	9.33	20.44	0.37	3.82	1.46	41.79
	2020/21	7.64	22.50	30.15	39.71	53.36	2.23	7.92	7.50	2.21	15.49	0.75	6.28	8.12	11.05

Immediately after planting, the plastic holeless bags were irrigated with 300 ml of fresh water/bag, but afterward the irrigation was done once day by day with only 250 ml of water/bag during the summer months, while during winter ones the plants were irrigated once every 3 or 4 days to keep the roots from decay. The usual agricultural practices required were done whenever needed. The plants were set out for every season in a complete randomized design and replicated thrice with five plants per replicate (Mead et al., 1993).

Data of the current study were recorded after two periods of growth; the first after 6 months (on October, 15th for every season) and the second after one year (12 months) from the first one (on the next October, 15th) and then expressed in the tables as other factor beside the factor of heavy metals combinations. The recorded data were: survival percentage, plant height (cm), stem diameter at the base (cm), number of branches/plant, number of leaves/ plant, means of root length (cm), as well as fresh and dry weights of top growth and roots (g). Besides, the pollution resistance index as a percentage (PRI %) was calculated from the equation proposed by Wilkins (1957) as follows:

$$\text{PRI \%} = \text{Mean root length of the polluted plants (cm)/mean root length of control x 100} \quad \text{(Eq.1)}$$

In fresh leaf samples taken from the middle parts of the plants, photosynthetic pigments (chlorophyll a, b and carotenoids, mg/g f.w.) and the percent of total soluble sugars were determined according to the methods of Sumantha et al. (2014) and Dubois et al. (1966), respectively, whereas in dry ones, the percentages of nitrogen, phosphorus, and potassium were measured by the methods explained by Chapman and Pratt (1975). Moreover, concentrations of Pb, Cd, and Ni as mg/100 g d.w. in dry samples of both leaves and roots were assessed using a Perkin Elmer 403 atomic absorption spectrophotometer (Jackson, 1973). All chemical analyses were evaluated in the second season only.

Data were then tabulated and subjected to analysis of variance using the program of SAS Institute (2009), followed by Duncan`s new multiple range t-test (Steel and Torrie, 1980) to detect the significance level among heavy metals combinations, growth periods, and their interactions.

http://www.aloki.hu ● ISSN 1589 1623 (Print) ● ISSN1785 0037 (Online)
DOI: http://dx.doi.org/10.15666/aeer/2005_43514361

Results and Discussion

Effect of heavy metal combinations, growth period, and their interactions on:

1- Survival percentage and vegetative and root growth traits

It can be seen from data averaged in *Table 2* that the survival percentage was 100% by the different sole and combined treatments employed in this trial indicating the ability of common oleander plants to withstand the toxicity of HMs, even at high concentrations and with prolonging growth period. however, some growth parameters were not negatively affected by the pollution treatments, where plant height (cm) was significantly improved by HMs combinations compared to control in the two seasons (*Table 2*), with the prevalence of T2 combination in the first season and T1 combination in the second one. Likewise, results of stem diameter reached maximum by T1 combination in both seasons (*Table 2*).

Table 2. *Effect of heavy metal combinations, growth period, and their interactions on survival %, height, and stem diameter of Nerium oleander L. plants during 2019/20 and 2020/21*

Growth period (G.P.) / Pollution treatments	Survival %			Plant height (cm)			Stem diameter (cm)		
	1st G.P.	2nd G.P.	Mean	1st G.P.	2nd G.P.	Mean	1st G.P.	2nd G.P.	Mean
	First season; 2019/2020								
Control	100.00a	100.00a	100.00A	44.63f	105.70d	75.17C	0.53e	1.24b	0.89C
T1	100.00a	100.00a	100.00A	51.10w	113.00bc	82.05B	0.70c	1.39a	1.05A
T2	100.00a	100.00a	100.00A	51.67e	118.30a	84.99A	0.63cd	1.27b	0.95BC
T3	100.00a	100.00a	100.00A	48.83e	116.00ab	82.42B	0.60de	1.28b	0.94BC
T4	100.00a	100.00a	100.00A	50.03e	112.00c	81.02B	0.63cd	1.28b	0.96B
Mean	100.00A	100.00A		49.25B	113.00A		0.62B	1.29A	
	Second season; 2020/2021								
Control	100.00a	100.00a	100.00A	49.23e	110.00c	79.62C	0.63e	1.37b	1.00C
T1	100.00a	100.00a	100.00A	56.17d	118.10a	87.14A	0.83c	1.53a	1.18A
T2	100.00a	100.00a	100.00A	56.90d	113.20b	85.05AB	0.73d	1.41b	1.07B
T3	100.00a	100.00a	100.00A	51.13e	114.80b	82.97B	0.70de	1.40b	1.05BC
T4	100.00a	100.00a	100.00A	49.07e	108.60c	78.84C	0.70de	1.38b	1.04BC
Mean	100.00A	100.00A		52.50B	112.94A		0.72B	1.42A	

Control: 0.00 ppm for Pb, Cd and Ni, T1: 500 ppm Pb + 50 ppm Cd + 25 ppm Ni; T2: 1000 ppm Pb + 100 ppm Cd + 50 ppm Ni; T3: 1500 ppm Pb + 150 ppm Cd + 75 ppm Ni and T4: 2000 ppm Pb + 200 ppm Cd + 100 ppm Ni. Means followed by the same latter in a column or row are not differ significantly according to Duncan's new multiple range t-test at 5 % level

The leaf area (cm^2) was also improved (*Table 3*), where T2, T3, and T4 combinations gave the highest records with non-significant differences among themselves in the two seasons. The other growth parameters were however negatively affected by HMs combinations, especially by T2, T3, and T4 combinations with few exceptions in both seasons (*Tables, 3, 4, 5, and 6*). On the other side, prolonging growth period up to 18 months significantly increased mean values of the different vegetative and root growth attributes measured in the two seasons compared with those measured after only 6

http://www.aloki.hu ● ISSN 1589 1623 (Print) ● ISSN1785 0037 (Online)
DOI: http://dx.doi.org/10.15666/aeer/2005_43514361

months. Besides, the interactions of the two factors exerted also a significant effect on various growth criteria, where interacting between planting in either control or T1 combination and the longer growth period (18 months) attained the highest means in most growth characters in the two seasons. However, combining between planting in soil mixture polluted with T3 and T4 combinations and the short period of growth (6 months) achieved the least records with inferiority of planting in T4-polluted soil + 6 months growth treatment which gave the minimal values relative to all the other combinations in both seasons.

Table 3. *Effect of heavy metal combinations, growth period, and their interactions on No. branches, No. leaves and leaf area of Nerium oleander L. plants during 2019/20 and 2020/21 seasons*

Growth period (G.P.) / Pollution treatments	No. branches/plant			No. leaves/plant			Leaf area (cm^2)		
	1st G.P.	2nd G.P.	Mean	1st G.P.	2nd G.P.	Mean	1st G.P.	2nd G.P.	Mean
	First season; 2019/2020								
Control	2.00c	3.27a	2.63A	30.00ef	67.00a	48.50A	35.20d	44.90b	40.05B
T1	2.00c	3.43a	2.72A	33.00d	56.00b	44.50B	37.77c	44.37b	41.07B
T2	1.67d	2.67b	2.17B	31.33de	50.33c	40.83C	39.70c	47.83a	43.77A
T3	1.67d	2.67v	2.17B	28.33f	56.00b	42.17C	37.83c	47.40a	42.62A
T4	1.67d	2.77b	2.22B	27.67f	56.67b	42.17C	39.17c	46.37ab	42.77A
Mean	1.80B	2.96A		30.07B	57.20A		37.93B	46.17A	
	Second season; 2020/2021								
Control	2.33d	3.60b	2.97A	33.70de	71.00a	52.35A	35.93c	45.33a	40.63B
T1	2.40d	3.836a	3.12A	35.53d	62.26bc	48.89B	38.50b	44.97a	41.74AB
T2	2.20d	2.93c	2.57B	34.60d	57.17c	45.89BC	40.23b	46.20a	43.22A
T3	2.20d	2.93c	2.57B	31.63ef	59.20bc	45.42C	38.70b	46.37ab	42.54A
T4	2.17d	2.93c	2.55B	29.60f	59.87b	44.74C	39.57b	45.03a	42.30A
Mean	2.26B	3.25A		33.01B	61.89A		38.59B	45.58A	

Control: 0.00 ppm for Pb, Cd and Ni, T1: 500 ppm Pb + 50 ppm Cd + 25 ppm Ni; T2: 1000 ppm Pb + 100 ppm Cd + 50 ppm Ni; T3: 1500 ppm Pb + 150 ppm Cd + 75 ppm Ni and T4: 2000 ppm Pb + 200 ppm Cd + 100 ppm Ni. Means followed by the same latter in a column or row are not differ significantly according to Duncan's new multiple range t-test at 5 % level

Similar results were obtained by Salih et al. (2017) who stated that *Nerium oleander* and neem are found to be more tolerant to air pollution than date palm or Conocarpus. Similarly, Safari et al. (2018) reported that *N. oleander* was found to have the highest absorption capacity for Ni, Pb, Co, and V-metals from the air and soil than *Bugainvillea spectabilis* and *Hibiscus rosa-sinensis* and so, it is a very suitable tool for managing air and soil pollution in highly industrialized area. Furthermore, Ibrahim and El-Afanid (2020) declared that *N. oleander* plants are able to stabilize HMs (Pb, Cd, and Zn) in the soil making them the less available from the soil.

A parallel trend was also revealed in other ornamental plants by Ma et al. (2018) on *Taxodium* hybrid (T118 and T406), Eisa (2019) on *Populus nigra* and *Salix mucronata,* and Chauhan and Mathur (2020) who found that industrially contaminated soil had a significant impeding on *Helianthus annuus* plantlets by reducing shoot and root lengths, leaf area and fresh weight of shoot and root.

http://www.aloki.hu ● ISSN 1589 1623 (Print) ● ISSN1785 0037 (Online)
DOI: http://dx.doi.org/10.15666/aeer/2005_43514361

Table 4. *Effect of heavy metal combinations, growth period, and their interactions on root length, No. root branches and PRI of Nerium oleander L. plants during 2019/20 and 2020/21 seasons*

Growth period (G.P.) / Pollution treatments	Root length (cm)			No. root branches/plant			Pollution resistance Index (PRI %)		
	1st G.P.	2nd G.P.	Mean	1st G.P.	2nd G.P.	Mean	1st G.P.	2nd G.P.	Mean
	First season; 2019/2020								
Control	33.67d	40.17c	36.92B	12.33g	25.67a	19.00C	100.00cd	100.00cd	100.00B
T1	33.90d	46.37b	40.14A	17.33e	24.17b	20.75A	101.90c	115.40b	108.65A
T2	30.10e	50.33a	40.22A	16.00f	22.83c	19.42B	89.80e	127.30a	108.55A
T3	26.33f	45.57b	35.95B	10.67i	18.97d	14.82D	78.57f	115.90b	97.24B
T4	28.33ef	38.60c	33.47C	11.33h	18.43d	14.88D	85.23cd	96.23d	90.73C
Mean	30.47B	44.21A		13.53B	22.01A		91.10B	110.97A	
	Second season; 2020/2021								
Control	37.03c	43.63a	40.33A	11.10h	22.63b	16.87C	100.00a	100.00a	100.00A
T1	37.20c	45.03a	41.12A	14.60f	23.27a	18.94A	101.60a	103.50a	102.55A
T2	33.20d	44.17a	38.69B	13.77g	21.03c	17.40B	90.07b	101.50a	95.79B
T3	31.17d	43.50a	37.34B	9.77i	17.30d	13.54D	85.17c	99.80a	92.49C
T4	31.13d	40.07b	35.60C	9.60i	16.60e	13.10E	85.17c	91.93b	88.55D
Mean	33.95B	43.28A		11.77B	20.17A		92.40B	99.35A	

Control: 0.00 ppm for Pb, Cd and Ni, T1: 500 ppm Pb + 50 ppm Cd + 25 ppm Ni; T2: 1000 ppm Pb + 100 ppm Cd + 50 ppm Ni; T3: 1500 ppm Pb + 150 ppm Cd + 75 ppm Ni and T4: 2000 ppm Pb + 200 ppm Cd + 100 ppm Ni. Means followed by the same latter in a column or row are not differ significantly according to Duncan's new multiple range t-test at 5 % level

Table 5. *Effect of heavy metals combinations, growth period, and their interactions on top growth fresh and dry weights of Nerium oleander L. plants during 2019/20 and 2020/21 seasons*

Growth period (G.P.) / Pollution treatments	Top growth fresh weight (g)			Top growth dry weight (g)		
	1st G.P.	2nd G.P.	Mean	1st G.P.	2nd G.P.	Mean
	First season; 2019/2020					
Control	37.70e	142.40a	90.05A	9.23de	48.90c	29.07BC
T1	42.93d	129.80b	86.37BC	10.40d	51.33b	30.87A
T2	35.43e	140.20a	87.82AB	8.70de	55.23a	31.97A
T3	34.83e	124.60c	79.72D	8.17ef	49.00c	28.58C
T4	36.93e	131.90b	84.42C	9.13def	52.17b	30.65B
Mean	37.56B	133.78A		9.13B	51.33A	
	Second season; 2020/2021					
Control	41.50e	134.60c	88.05B	9.77e	52.70c	31.24B
T1	45.00e	142.10b	93.55A	10.43e	55.77b	33.10A
T2	38.97f	147.10a	93.04A	9.40e	57.53a	33.47A
T3	38.30f	129.90d	84.10C	9.27e	50.83d	30.05C
T4	37.57f	131.70cd	84.64C	9.00e	51.27d	30.14C
Mean	40.27B	137.08A		9.57B	53.62A	

Control: 0.00 ppm for Pb, Cd and Ni, T1: 500 ppm Pb + 50 ppm Cd + 25 ppm Ni; T2: 1000 ppm Pb + 100 ppm Cd + 50 ppm Ni; T3: 1500 ppm Pb + 150 ppm Cd + 75 ppm Ni and T4: 2000 ppm Pb + 200 ppm Cd + 100 ppm Ni. Means followed by the same latter in a column or row are not differ significantly according to Duncan's new multiple range t-test at 5 % level

http://www.aloki.hu ● ISSN 1589 1623 (Print) ● ISSN1785 0037 (Online)
DOI: http://dx.doi.org/10.15666/aeer/2005_43514361

Table 6. *Effect of heavy metals combinations, growth period, and their interactions on roots fresh and dry weights of Nerium oleander L. plants during 2019/20 and 2020/21*

Growth period (G.P.) / Pollution treatments	Roots fresh weight (g)			Roots dry weight (g)		
	1st G.P.	2nd G.P.	Mean	1st G.P.	2nd G.P.	Mean
	First season; 2019/2020					
Control	6.33c	59.57a	32.95A	1.58d	23.70bc	12.64BC
T1	7.20c	60.27a	33.74A	1.99d	24.60b	13.30B
T2	6.73c	61.60a	34.17A	2.07d	26.47a	14.27A
T3	5.87c	58.43a	32.15A	1.57d	24.77b	13.17B
T4	6.30c	51.77b	29.03B	1.74d	22.87c	12.31C
Mean	6.49B	58.33A		1.79B	24.48A	
	Second season; 2020/2021					
Control	6.63e	65.37a	36.00A	1.65e	25.80a	13.73AB
T1	7.43e	65.00a	36.22A	1.96e	26.13a	14.05A
T2	6.93e	60.13b	33.53B	1.88e	24.67b	13.28A
T3	6.13e	56.33c	31.23BC	1.59e	23.50c	12.55C
T4	6.37e	52.33d	29.35C	1.66e	22.13d	11.90D
Mean	6.70B	59.83A		1.75B	24.45A	

Control: 0.00 ppm for Pb, Cd and Ni, T1: 500 ppm Pb + 50 ppm Cd + 25 ppm Ni; T2: 1000 ppm Pb + 100 ppm Cd + 50 ppm Ni; T3: 1500 ppm Pb + 150 ppm Cd + 75 ppm Ni and T4: 2000 ppm Pb + 200 ppm Cd + 100 ppm Ni. Means followed by the same latter in a column or row are not differ significantly according to Duncan's new multiple range t-test at 5 % level

2- Pollution resistance index as a percentage (PRI %)

As shown in *Table 4*, the percentages of PRI of control plants in both seasons were 100% and significantly increased in the first season to 108.65 and 108.55% by T1 and T2 HMs-combinations, respectively, while in the 2nd one raised only to 102.55% by T1 combination with non-significant differences relative to control. Increasing HMs concentrations afterwards in T3 and T4 in the 1st season and in T2, T3, and T4 in the 2nd one significantly decreased the means of such index to percents slightly higher than 90% in both seasons by T4 (which contains the highest concentrations of Pb, Cd, and Ni). This may clearly indicate the high ability of *N. oleander* in tolerating HMs toxicity. In this connection, Salih et al. (2017) found that air pollution tolerance index tends to increase in *Azadirachta indica* and *Nerium oleander* plants grown in the polluted site near Bahrain Oil Refinery. Similarly, Safari et al. (2018) observed that the highest comprehensive bioconcentration index (CBCI) was found in leaf (0.37) and bark (0.12) of *N. oleander*, whereas the maximum metal accumulation index (MAI) was found in leaf of *N. oleander* (1.58) and bark of *H. rose-sinensis* (1.95).

In relation to the effect of growth period, it was noticed that determination of PRI after 18 months from planting significantly recorded higher percentages than those determined after only 6 months of growth in the two seasons as prolonging growth period was accompanied by longer roots irrespective of pollution treatment. Thus, combining between planting in soil mixture polluted with T1, T2, and T3 HMs-combinations and 18-months growth period gave the highest mean values of this index over all the other combinations in the first season, but that was true in the second one by interacting between planting in soil mixture polluted with T1 and T2 HMs combinations and 18-months growth period.

http://www.aloki.hu ● ISSN 1589 1623 (Print) ● ISSN1785 0037 (Online)
DOI: http://dx.doi.org/10.15666/aeer/2005_43514361

The forgoing results are in accordance with those postulated by Salih et al. (2017) and Safari et al. (2018) on *N. oleander* and Omar (2018) who cited that PRI % of *Sambucus nigra* grown in contaminated soil with Pb, Cd, and Ni was slightly improved by the low concentrations of HMs, while decreased by the medium and high levels of such metals to be more than 50-55 % by the highest levels showing the ability of *S. nigra* to withstand the high levels of the 3 toxic metals when applied in combinations.

3- The chemical composition of leaves and roots

Data listed in *Table 7* exhibit that, concentrations of chlorophyll a, b, and carotenoids (mg/g f. w.), as well as the percentage of total soluble sugars in the leaves were non-constant in response to either HMs combinations or growth periods, as the variations among treatments were narrow in most instances. The effect of interaction treatments took a similar trend.

Table 7. *Effect of heavy metals combinations, growth period, and their interactions on pigments and total soluble sugars concentrations in Nerium oleander L. leaves during 2020/21 season*

Growth period (G.P.) / Pollution treatments	Chlorophyll a (mg/g. f. w.)			Chlorophyll b (mg/g. f. w.)			Carotenoids (mg/g. f. w.)			Total soluble sugars (%)		
	1st G.P.	2nd G.P.	Mean	1st G.P.	2nd G.P.	Mean	1st G.P.	2nd G.P.	Mean	1st G.P.	2nd G.P.	Mean
Control	0.596a	0.597a	0.597A	0.312b	0.236c	0.274B	0.240b	0.234b	0.237A	17.55d	18.06c	17.81C
T1	0.597a	0.519c	0.558B	0.367a	0.248c	0.308A	0.263a	0.240b	0.252A	21.50a	18.45c	19.98A
T2	0.583a	0.503c	0.543B	0.303b	0.231c	0.267C	0.229b	0.231b	0.230B	19.50b	16.56e	18.03B
T3	0.577a	0.561b	0.569A	0.372a	0.210d	0.291B	0.263a	0.218c	0.241A	16.90d	18.50c	17.70C
T4	0.560b	0.598a	0.579A	0.410a	0.238c	0.324A	0.268a	0.236b	0.252A	14.76f	16.58e	15.67D
Mean	0.583A	0.556A		0.353A	0.233B		0.253A	0.232A		18.04A	17.63B	

Control: 0.00 ppm for Pb, Cd and Ni, T1: 500 ppm Pb + 50 ppm Cd + 25 ppm Ni; T2: 1000 ppm Pb + 100 ppm Cd + 50 ppm Ni; T3: 1500 ppm Pb + 150 ppm Cd + 75 ppm Ni and T4: 2000 ppm Pb + 200 ppm Cd + 100 ppm Ni. Means followed by the same latter in a column or row are not differ significantly according to Duncan's new multiple range t-test at 5 % level

On the other hand, the percentages of N, P, and K were the highest in control plants but were decreased by HMs combinations with various significance levels compared to those of control treatment (*Table 8*). The concentration of N and P was significantly improved by prolonging growth period (after 18 months) relative to the short growth period (6 months), while the opposite was the right regarding K percentage. In general, combining between planting in non-polluted (control) soil mixture and either short or long growth period scored the utmost high N and K concentrations, whereas interacting between planting in soil mixture polluted with either T1 or T4 HMs combinations and the longer growth period acquired the highest P concentration.

As for Pb, Cd, and Ni concentrations in the leaves and roots (mg/100 g d. w.), data averaged in (*Table 9*) show that a progressive increase in concentrations of these three metals was accompanied to their gradual increment in the polluted soil mixture to reach maximum by T4 combination either in the leaves or in roots. However, Pb concentration in the leaves was significantly decreased with prolonging growth period to 18 months, but the opposite was occurred regarding Cd concentration. In the roots, however concentrations of the three metals were significantly decreased by prolonging growth

http://www.aloki.hu ● ISSN 1589 1623 (Print) ● ISSN1785 0037 (Online)
DOI: http://dx.doi.org/10.15666/aeer/2005_43514361

period. In addition, the connecting between planting in soil mixture treated with either T3 or T4 HMs combinations and short growth period attained the highest concentration of Pb in the leaves, but that was true for Cd and Ni concentrations by connecting between planting in T4 combination treated-soil mixture and the longer growth period. In the roots, however combining between planting in soil mixture polluted with T4 HMs combination and the short growth period increased the three metals content to the utmost high concentrations over all the other combinations.

Table 8. *Effect of heavy metals combinations, growth period, and their interactions on nitrogen, phosphorus, and potassium concentrations in Nerium oleander L. leaves during 2020/21 season*

Growth period (G.P.) / Pollution treatments	N (%)			P (%)			K (%)		
	1st G.P.	2nd G.P.	Mean	1st G.P.	2nd G.P.	Mean	1st G.P.	2nd G.P.	Mean
Control	2.213a	2.310a	2.262A	0.438c	0.535b	0.487A	2.04a	2.18a	2.11A
T1	1.327c	1.576b	1.452C	0.347d	0.601a	0.474A	1.87b	1.55c	1.71B
T2	1.547b	1.653b	1.601B	0.361d	0.526b	0.444B	1.87b	1.37d	1.62B
T3	1.565b	1.671b	1.618B	0.238e	0.579b	0.409C	1.64c	1.35d	1.50C
T4	1.548b	1.550b	1.549C	0.179f	0.703a	0.441B	1.63c	1.72b	1.68B
Mean	1.640B	1.752A		0.313B	0.589A		1.81A	1.64B	

Control: 0.00 ppm for Pb, Cd and Ni, T1: 500 ppm Pb + 50 ppm Cd + 25 ppm Ni; T2: 1000 ppm Pb + 100 ppm Cd + 50 ppm Ni; T3: 1500 ppm Pb + 150 ppm Cd + 75 ppm Ni and T4: 2000 ppm Pb + 200 ppm Cd + 100 ppm Ni. Means followed by the same latter in a column or row are not differ significantly according to Duncan's new multiple range t-test at 5 % level

Table 9. *Effect of heavy metals combinations, growth period, and their interactions on lead, cadmium, and nickel concentrations in Nerium oleander L. leaves and roots during 2020/21 season*

Growth period (G.P.) / Pollution treatments	Pb (mg/100 g d. w.)			Cd (mg/100 g d. w.)			Ni (mg/100 g d. w.)		
	1st G.P.	2nd G.P.	Mean	1st G.P.	2nd G.P.	Mean	1st G.P.	2nd G.P.	Mean
	In the leaves								
Control	15.517e	11.833f	13.675E	37.551g	54.366e	45.959E	16.003d	8.676f	12.340E
T1	18.633d	13.654e	16.144D	37.978g	68.763d	53.371D	16.886d	11.258e	14.072D
T2	32.689b	26.879c	29.784C	45.600f	137.315c	91.458C	18.500d	16.950d	17.725C
T3	37.245a	28.600c	32.923B	68.403d	204.150b	136.277B	23.210c	25.431c	24.321B
T4	36.583a	32.901b	34.742A	67.526d	235.648a	151.587A	28.086b	38.939a	33.513A
Mean	28.134A	22.774B		51.412B	140.043A		20.537A	20.251A	
	In the roots								
Control	17.690g	23.952f	20.821E	210.0841f	178.243h	194.164D	28.310f	21.129g	24.720D
T1	19.219g	28.389e	23.804D	243.179d	195.984g	219.582C	32.403d	30.956e	31.680C
T2	30.256d	31.240d	30.748C	259.875b	214.500e	237.188B	33.796d	30.967e	32.368C
T3	43.950b	35.000c	39.475B	263.733a	250.130c	256.932A	41.948b	33.598d	37.773B
T4	58.257a	40.756b	49.507A	261.500a	256.431b	258.966A	44.977a	35.736c	40.357A
Mean	33.875A	31.868B		247.674A	219.058B		36.287A	30.477B	

Control: 0.00 ppm for Pb, Cd and Ni, T1: 500 ppm Pb + 50 ppm Cd + 25 ppm Ni; T2: 1000 ppm Pb + 100 ppm Cd + 50 ppm Ni; T3: 1500 ppm Pb + 150 ppm Cd + 75 ppm Ni and T4: 2000 ppm Pb + 200 ppm Cd + 100 ppm Ni. Means followed by the same latter in a column or row are not differ significantly according to Duncan's new multiple range t-test at 5 % level

http://www.aloki.hu ● ISSN 1589 1623 (Print) ● ISSN1785 0037 (Online)
DOI: http://dx.doi.org/10.15666/aeer/2005_43514361

The previous results could be supported by those reported by Salih et al. (2017) who found that *Nerium oleander* grown near Bahrain oil refinery accumulated more Cu, Cr, Mn, Mo, and Fe than Neem, Conocarpus, and date palm, but chlorophyll content was decreased. Because oleander plants remove significant amounts of toxic metals from the environment, it is considered an excellent phytoremediator. Likewise, Safari et al. (2018) declared that *N. oleander* absorbed higher amounts of Ni, Pb, Co, V from the air and soil than *Bougainvillea spectabilis* and *H. rosa-sinensis*. So, it is very suitable tool for remediating HMs pollution in highly industrialized areas. Besides, Salih and Aziz (2019) found that pigments and protein contents in leaves of *N. oleander* plants grown near steel factories were lower than those in leaves of plants far away from the factory. Ibrahim and El-Afandi (2020) concluded that Pb was accumulated in the roots, while Cd and Zn were concentrated in the aerial parts of *N.* oleander plants grown in El-Dakhlia (industrial zone), Alexandria, Egypt.

Identical responses were also obtained by Eisa (2019) on *Populus nigra* and *Salix mucronata* and Ouf and Gaber (2019) who revealed that the highest accumulation of Cd, Pb, Zn, N, P and K elements was found in different parts of willow plants grown in polluted soil at different growth periods (16, 12 and 18 months). Chauhan and Mathur (2020) stated that *Helianthus annuus* plantlets grown in industrially contaminated soil accumulated different concentrations of Pb, Cd, Zn, Cu, Fe, and As. Similarly, Eid et al. (2020) cited that *Phragmites australis* accumulated the highest concentrations of Cd and Ni, while *Eichhornia crassipes*, accumulated the highest concentration of Pb in its tissues.

From foregone, it is obvious that common oleander (*Nerium oleander* L.) plants can tolerate Pb, Cd, and Ni metals when applied to the soil in combination at high concentrations without mortality, but with little adverse effects on some growth characters. Because of its higher concentrations uptake from these toxic metals, it can be used as a good phytoremediator for the HMs-polluted soil.

Conclusion

It can be advised to use *Nerium oleander* shrub for beautification and landscaping contaminated areas with toxic or heavy metals.

REFERENCES

[1] Akosy, A., Oztürk, E. (1997): *Nerium oleander* L. as biomonitor of lead and other heavy metals pollution in Mediterranean. – Sci. Total Environ. 205: 2-3.

[2] Bailey, L. H. (1976): Hortus Third. – Macmillan Publishing Co., Inc., 866 Third Avenue, New York, N.Y. 10022.1290p.

[3] Chapman, H. D., Pratt, R. E. (1975): Methods of Analysis for Soil, Plant and Water. – California Univ., Division of Agric. Sci., pp. 172-173.

[4] Chauhan, P., Mathur, J. (2020): Phytoremediation efficiency of *Helianthus annuus* L. for reclamation of heavy metals-contaminated industrial soil. – Environ. Sci. & Pollut. Res. 27: 29954-29966.

[5] Dubois, M., Smith, F., Illes, K. A., Hamilton, J. K., Rebers, P. A. (1966): Colorimetric method for determination of sugars and related substances. – An. Chem. 28(3): 350-356.

[6] Eid, E. M., Galal, T. M., Sewelam, N. A., Talha, N. I., Abdallah, S. M. (2020): Phytoremediation of heavy metals by four aquatic macrophytes and their potential use as contamination indicators: a comparative assessment. – Environ. Sci. & Poll. Res. 27: 12138-12151.

http://www.aloki.hu ● ISSN 1589 1623 (Print) ● ISSN1785 0037 (Online)
DOI: http://dx.doi.org/10.15666/aeer/2005_43514361

[7] Eisa, E. A. T. (2019): Phytoremediation of heavy metals contaminated soil by plantation of *Populus nigra* L. and *Salix mucronata* L. transplants. – Ph.D. Thesis, Hort. Dept. (Floriculture), Fac. Agric., Kafrelsheikh Univ.
[8] Haudaji, M., Ataabadi, M., Najafi, P. (2010): Biomonitoring of Air Borne Heavy Metals Contamination. – Air Pollution Monitoring, Modeling, Health and Control, 3rd ed., 221p.
[9] Huxley, A., Griffiths, M., Levy, M. (1992): The New Royal Hort. Society Dictionary of Gardening. – The Stockton Press, New York, N. Y. 10010, USA, vol. 3, 790p.
[10] Ibrahim, N., El-Afandi, G. (2020): Phytoremediation uptake model of heavy metals (Pb, Cd and Zn) in soil using *Nerium oleander*. – Heliyon 6(7): e04445.
[11] Jackson, M. H. (1973): Soil Chemical Analysis. – Prentice-Hall of India Private Limited M-97, New Delhi, India, 498p.
[12] Ma, Y., Wang, H., Wang, P., Yu, C., Luo, S., Zhang, Y., Xie, Y. (2018): Effects of cadmium stress on the antioxidant system and chlorophyll characteristics of two *Taxodium* clones. – Plant Cell Reports 37: 1547-1555.
[13] Mead, R., Curnow, R. N., Harted, A. M. (1993): Statistical Methods in Agriculture and Experimental Biology. – 2nd ed., Chapman & Hall Ltd., London, 335p.
[14] Omar, S. H. M. (2018): Studies on tolerance of some ornamental plants to soil pollution with some combinations of heavy metals. – M.Sc. Thesis, Hort. Dept. (Floriculture), Fac. Agric., Kafrelsheikh Univ.
[15] Ouf, A. A., Gaber, M. K. (2019): Determination of heavy metals absorption and accumulation by willow plants as a phytoremediator to soil contaminants. – Middle East J. Agric. Res. 8(2): 400-410.
[16] Safari, M., Ramavandi, B., Sanati, A. M., Sorial, G. A., Hashemi, S., Tahmasebr, S. (2018): Potential of trees leaf/bark to control atmospheric metals in a gas and petrochemical zone. – J. Environ. Management 222: 12-20.
[17] Salih, A. A., Mohamed, A. A., Abohussain, A. A., Tashtoosh, F. (2017): Use of some trees to mitigate air and soil pollution around oil refinery, Kingdom of Bahrain. – J. Environ. Sci., & Pollut. Res. 3(2): 167-170.
[18] Salih, Z., Aziz, F. (2019): Heavy metals accumulation in leaves of five plant species as a bioindicator of steel factory pollution and their effects on pigment content. – Poll. J. Environ. Stud. 28(6): 4351-4358.
[19] SAS Institute (2009): SAS/STAT User`s Guides Statistics. – Vers. 6.04, 4th ed., SAS Institute Inc. Cary, N.C., USA.
[20] Seaward, M. R., Mashhour, M. A. (1991): Oleander (*Nerium oleander* L.) as a Monitor of Heavy Metal Pollution. – Urban Ecology, Izmir (Turkey), Ege Univ. Press, pp. 48-61.
[21] Steel, R. G. D., Torrie, J. H. (1980): Principles and Procedures of Statistics. – McGrow Hill Book Co., Inc., New York, pp. 377-400.
[22] Sumantha, N., Haque, C. I., Nishika, J., Suprakash, R. (2014): Spectrophotometric Analysis of chlorophyllous and carotenoids from commonly grown Fern species by using various extracting solvents. – Res. J. Chem. Sci. 4(9): 63-69.
[23] Wilkins, D. A. (1957): A technique for the measurement of lead tolerance in plants. – Nature 180: 73-78.

http://www.aloki.hu ● ISSN 1589 1623 (Print) ● ISSN1785 0037 (Online)
DOI: http://dx.doi.org/10.15666/aeer/2005_43514361

IMPACT OF ROOTSTOCKS ON FRUIT QUALITY, MINERAL NUTRITION AND LEAF PHYSIOLOGY OF 'RED GLOBE' IN THE EAST MEDITERRANEAN REGION

KAMILOĞLU, Ö.

Hatay Mustafa Kemal University, Faculty of Agriculture, Department of Horticulture, Antakya, Turkey
e-mail: okoglu@gmail.com; phone: +90-3262-213-317 ext. 11042

(Received 18th Apr 2022; accepted 26th July 2022)

Abstract. Red Globe is a table grape variety with commercial importance, preferred in terms of cultivation. This variety is new to our country and the Mediterranean Region. The objective of the present study was to determine phenological periods, fruit quality, cluster properties, berry characteristics, chlorophyll content, photosynthetic rate and nutrient status of 'Red Globe' on 41 B, SO 4, and 1103 P rootstocks. This grape variety ripened during both years in the first week of August. It was determined that effective heat summation (EHS), required from bud burst until ripeness, was 1600-1700 degree days (d.d). SO4 rootstock yielded the highest value in terms of cluster and berry weights, Total Soluble solids (TSS)/acidity, and pH, and it was followed by 1103 P rootstock. The effect of rootstock on chlorophyll content was found to be similar. Likewise, it was identified that the effect of rootstocks on photosynthetic and transpiration rates was not significant. Effects of rootstocks on leaf mineral matter intake were found to be significant in terms of certain elements. P, K, Ca and Mg macro nutrient element contents were found to be higher in 1103 P rootstock than the other two rootstocks. Rootstocks showed similarity in terms of the intake of micronutrient elements (other than Fe).
Keywords: *grapevine, rootstock, fruit quality, chlorophyll, photosynthesis*

Introduction

Table grape exhibits a strong growth throughout the world. In the recent years, China and Turkey have shown an increasing trend affected by different dynamics (Seccia et al., 2015). According to 2018 data, Turkey ranks the 2nd in table grape production with 7% (1.9 mt) (OIV, 2019).

The Mediterranean region has an important place in Turkish viticulture in terms of area and production. Table grapes occupy 76.8% of the production under grape cultivation in this region (TUIK, 2019).

Red Globe is a variety appreciated by consumers due to its characteristics as a table grape, which has a potential for increased cultivation in vineyards in terms of producer preferences. As a matter of fact, Red Globe grape variety, cultivated in an area of 165.000 ha, is the second most commonly cultivated table grape variety worldwide (OIV, 2017).

Phylloxera, which is a root-feeding aphid, can kill grapevines of the species *Vitis vinifera* (Cousins, 2005). There is no way to eradicate phylloxera from an infested vineyard. The only sure way to prevent phylloxera damage to grapevines is to plant vines grafted to phylloxera-tolerant rootstocks of American origin (Skinkis et al., 2009; Gautier et al., 2020). Rootstocks have recently gained great importance in the only consistently effective and successful strategy in major viticultural countries worldwide (Rizk-Alla et al., 2011). Grapevine rootstocks can significantly affect the performance of grafted vines (Sivilotti et al., 2007; Li et al., 2019). For this reason, rootstock selection is a critical decision when establishing a vineyard (Jogaiah et al., 2013).

http://www.aloki.hu ● ISSN 1589 1623 (Print) ● ISSN1785 0037 (Online)
DOI: http://dx.doi.org/10.15666/aeer/2005_43634376

Grapevine rootstocks are known to affect various aspects of scion performance, such as growth (Satisha et al., 2010; Rizk-Alla et al., 2011; Ibacache et al., 2016), nutrient uptake (Ibacache and Sierra, 2009; Wooldridge et al., 2010; Ibacache et al., 2020), quality (Valenzuela-Ruiz et al., 2005; Satisha et al., 2010; Ghule et al., 2021), and some physiological and biochemical parameters (Koblet et al., 1995; Cox et al., 2012; Jogaiah et al., 2013; Ghule et al., 2021). A rootstock, found to be beneficial for one cultivar, may not be universally advantageous for others, as the interaction of stock and scion influences the vine performance more than the stock or scion alone (Satisha et al., 2010). Any commercial grape cultivar must be cultivated as composite plants by grafting it onto the recommended rootstock (Verma et al., 2010). In viticulture, it is possible to come across many studies (Gu, 2003; Valenzuela-Ruiz et al., 2005; Ibacache and Sierra, 2009; Rizk-Alla et al., 2011; Corso et al., 2016; Klimek et al., 2022) about the appropriate rootstock selection for grape varieties. In the Eastern Mediterranean region, there are a limited number of studies conducted in this regard. In the regional grape trade, it is common to grow Horoz Karası, Hatun Parmağı and Pafı varieties on the rootstock of Rupestris du lot with the goblet training system.

This study used three rootstocks with different genetic characteristics, which are commonly used in Turkey. The aim of this investigation was evaluating the effects of 41 B, 1103 P and SO4 on fruit quality, photosynthesis, chlorophyll content and nutrient status of 'Red Globe' cultivar.

Material and Methods

This study was conducted in the Hatay Mustafa Kemal University, Agriculture Faculty in Turkey, during two consecutive seasons. Study parcel is located at 81 m elevation at 36°18'32"N and 36°13'60"E coordinates in Amik plain in Hatay province, which has a Mediterranean climate. Soil texture is loamy (51% sand, 32% silt and %17 clay), with a pH of 7.97 and an electrical conductivity of 0.78 mmhos/cm. Temperature and precipitation long-term average of Hatay are shown in *Figure 1*. Average temperature was 18.3°C, temperatures in the coldest month were 8.1°C, temperatures in the hottest month were 27.9°C, and average amounts of precipitation were 1161.5 mm by annual.

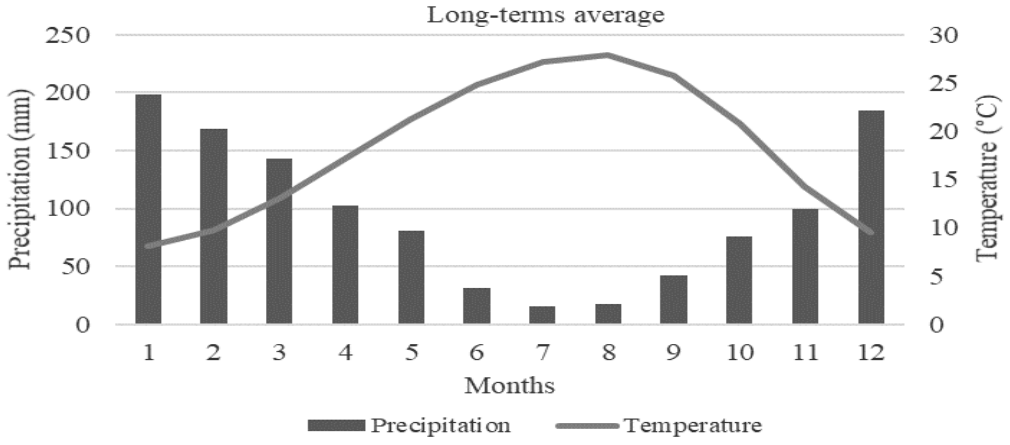

Figure 1. *Monthly precipitation and average temperature change over long-terms*Hatay meteorology general directorate (Anonymous, 2022)*

http://www.aloki.hu ● ISSN 1589 1623 (Print) ● ISSN1785 0037 (Online)
DOI: http://dx.doi.org/10.15666/aeer/2005_43634376

In the trial area, ungrafted rootstock (41B, SO4, 1103P) saplings were planted in a completely randomized block design, in three rows at a spacing of 3.0 m x 2.0 m (row x vine). Each row had 27 vines consisting of 9 on each of three rootstocks. 'Red Globe' cultivar was grafted on rootstocks by cleft grafting method. The 4-year-old vines were trellised by one-armed pergolas system and irrigated by drip irrigation system. Rows were planted in an East-West orientation. Pests and diseases control and other vineyard management practices were applied in accordance with conventional vineyard practice (*Figure 2*).

Figure 2. *A photograph of the research area, infloresence and maturity time*

In the trial, 4 vines were selected and marked for each repetition. Phenological variables, such as determination of bud-break, full bloom, veraison and ripening were collected from each grapevine (Ağaoğlu, 2002; OIV, 2009). In consideration of phenological development dates, EHS (dd) by periods was determined with the following formula as follows (*Eq. 1*) (Winkler et al., 1974).

$$EHS = \sum(T1 - T2) \qquad \text{(Eq.1)}$$

where T_1= Daily average temperature (^oC), T_2= Equal temperature (10^oC).

20 berry samples were picked up in three-day intervals, 5 periods, and each repetition during the period before harvesting in both years of the study with the aim of observing the effect of rootstocks on the progress of ripeness of grapes. TSS, pH, acidity, and ripeness index were analyzed in obtained grape samples. Harvest was made on August 5 in the first year and on August 1 in the second year. Pomological variables in fruits [cluster weight (g), cluster length (cm), cluster width (cm), berry weight (g), berry length (mm), berry width (mm), TSS (%), pH, acidity (%) and TSS/acidity] were measured in the study. Cluster characteristics were identified using 20 clusters during each repeat. 50 berries were used during each repeat for berry characteristics and must properties. TSS content (%) in the juice was determined using hand refractometer (Atago, Manual, made in Japon) and juice pH was determined by pH meter (pH330

http://www.aloki.hu ● ISSN 1589 1623 (Print) ● ISSN1785 0037 (Online)
DOI: http://dx.doi.org/10.15666/aeer/2005_43634376

WTW, made in Germany). Acidity was measured using potentiometric method, while prepared juice was titrated with 0.1 N NaOH solution until 8.1 value was read on the pH meter and results were calculated in percentage of tartaric acid. SUNDOO SH-100 Model Digital Force Gauge device was used for measurement berry removal force (N).

Physiological measurements, recently fully expanded two leaves, which were selected randomly from every vine stock, were marked. 8 leaves were used for the measurements of photosynthesis and chlorophyll during each repetition. Photosynthetic rate ($\mu molm^{-2}s^{-1}$) and transpiration rate ($mmolm^{-2}s^{-1}$) of the leaves were measured, from 09.00 am to 13.00 pm, using a portable photosynthesis system (model LCA-4, ADC Bioscientific Ltd., Hoddesdon, UK). Chlorophyll content (measured SPAD value) was identified on the same leaves using a portable chlorophyll meter (SPAD 502, Minolta Co. Ltd. Japan). In chlorophyll measurements, three readings were made in different directions of each leaf. Additionally, the same leaves were also used for the determination of leaf area and the chlorophyll contents (Chlorophyll a, Chlorophyll b, total Chlorophyll), under laboratory conditions. Chlorophyll was extracted with 80% acetone from leaf discs. Chlorophyll a and chlorophyll b contents, and total chlorophyll content, were measured according to the method of Arnon (1949). Measurements were conducted on May 24 in the first year, and May 18 in the second year.

When the plants were in full bloom, the leaves across the first cluster of primary shoots, which were selected randomly, were collected, and brought to the laboratory in an icebox. 20 leaf blades, collected for each repetition, were washed and dried in the drying oven (65-70°C). Samples, ground in porcelain mortars, were burned in muffle furnace according to dry ashing method. N content was determined according to Kjeldahl method. Total P, K, Ca, Mg, Mn, Fe, Cu ve Zn concentrations of dissolved samples were determined by ICP-OES (Kacar and İnal, 2008). Macro elements were determined as %, and micro elements were determined as ppm.

Statistical analysis

The data was analyzed as a completely randomized block design by the analysis of variance using SAS software. The mean separations were carried out by the least significant difference (LSD) method at a 5% significance level.

Results and Discussion

In Red Globe grape variety, effects of different rootstocks on phenological periods were found to be similar on the basis of years. Upon analysis of monthly average temperature values by years, it was determined that the values for the second year were higher than the first year (*Table 1*); thus, full bloom occurred 9-10 days, veraison occurred 7-8 days and ripening occurred 4 days earlier (*Table 2*). As a matter of fact, according to Winkler index method; EHS during both bud break-harvest and flowering-harvest times were higher in the second year (*Table 3*). Steel and Greer (2008) also reported in their study with the same variety that they did not observe difference in phenological stages (bud break, flowering, and harvest time) between rootstocks. Similarly, it was observed that rootstocks were not effective on phenological periods in Red Globe variety grafted on Harmony and Freedom rootstocks (Valenzuela-Ruiz et al., 2005). Santibáñez et al. (2014) reported that EHS (dd) requirements of late season cultivars such as Red Globe and Crimson Seedless, to complete fruit maturity from full flower, were 1100 to 1500 dd. In the study, EHS requirement in Red Globe variety

http://www.aloki.hu ● ISSN 1589 1623 (Print) ● ISSN1785 0037 (Online)
DOI: http://dx.doi.org/10.15666/aeer/2005_43634376

(1268.2-1371.7) was found to be between limit values indicated by the researchers. In other studies; EHS (full flower- maturity) value of the same cultivar was determined as 1133.0 dd in Sakarya (Cangi and Altun, 2015) and 1447.0 dd in Antalya (Aktürk and Uzun, 2019). In ecologies, the period from bud break until ripeness is systematically reduced due to increased temperature. In other terms, ripeness can be achieved 1 to 2 months earlier in hotter regions than colder regions (Santibáñez et al., 2014). In this study conducted within Mediterranean ecology, the period between flowering and harvest were determined as 79 to 85 days.

Table 1. *Monthly precipitation and average temperature change by years**

Year	Month	I	II	III	IV	V	VI	VII	VIII	IX	X	XI	XII
1st	Temp. (ºC)	8.1	9.2	12.2	16.0	20.5	25.2	28.0	28.8	26.2	18.7	9.4	6.6
	Pcpn.(mm)	70.4	75.8	56.8	53.4	26.2	11.4	0.0	0.0	0.6	63.5	42.8	132.8
2nd	Temp. (ºC)	6.7	8.2	12.2	18.1	21.5	26.8	28.9	29.6	27	20.2	14.6	9.4
	Pcpn.(mm)	279.7	0.0	19.6	24.3	30.8	2.0	0.0	0.0	0.0	61.2	158	280.5

*Hatay Meydan meteorology station

Table 2. *The effects of rootstocks on phenological development dates (days.month) for Red Globe grapes grown in the East Mediterranean region*

Rootstock	Bud break		Full bloom		Veraison		Ripening	
	1st year	2nd year	1st year	2nd year	1st year	2nd year	1st year	2nd year
41B	03.04	03.04	19.05	10.05	20.07	12.07	05.08	01.08
SO4	04.04	04.04	20.05	10.05	20.07	12.07	05.08	01.08
1103P	03.04	04.04	20.05	10.05	19.07	12.07	05.08	01.08

Table 3. *The values of EHS according to phenological periods*

Fenological Stages	Heat summation above 10 °C (degree days/total days)	
	1st year	2nd year
Bud burst-Full bloom	334.1/46 days	329.4/37 days
Full bloom- Veraison	966.9/63 days	979.6/64 days
Veraison- Ripening	301.3/16 days	392.1/20 days
Bud burst-Ripening	1602.3/125 days	1701.1/121 days

In non-climacteric fruits likes grape, TSS and acidity play on major role at the time of maturity (Chanana and Gill, 2008). Therefore, TSS, pH, acidity and TSS/acidity changes in berries, collected periodically during the period close to ripeness in Red Globe variety, were analyzed in the study (*Figure 3*). In general, the highest proportional increase in the ripeness index was observed in SO4 rootstock. This increase was determined as 109% in the first year and 145% in the second year according to approximately 11-12 days before harvest. During this period, TSS % content increased and acidity % content decreased. Miele and Rizzon (2019) also reported that there was an inverse relationship between these two characteristics during

http://www.aloki.hu ● ISSN 1589 1623 (Print) ● ISSN1785 0037 (Online)
DOI: http://dx.doi.org/10.15666/aeer/2005_43634376

the ripening of grapes. Muñoz-Robredo et al. (2011) determined that Red Globe variety showed a continuous rise in TSS throughout the sampling period, a decrease in titratable acidity during berry development, and an increase in TSS/acidity quotient toward harvest. Segade et al. (2013) reported that similar results were obtained in the same variety at different stages of ripeness.

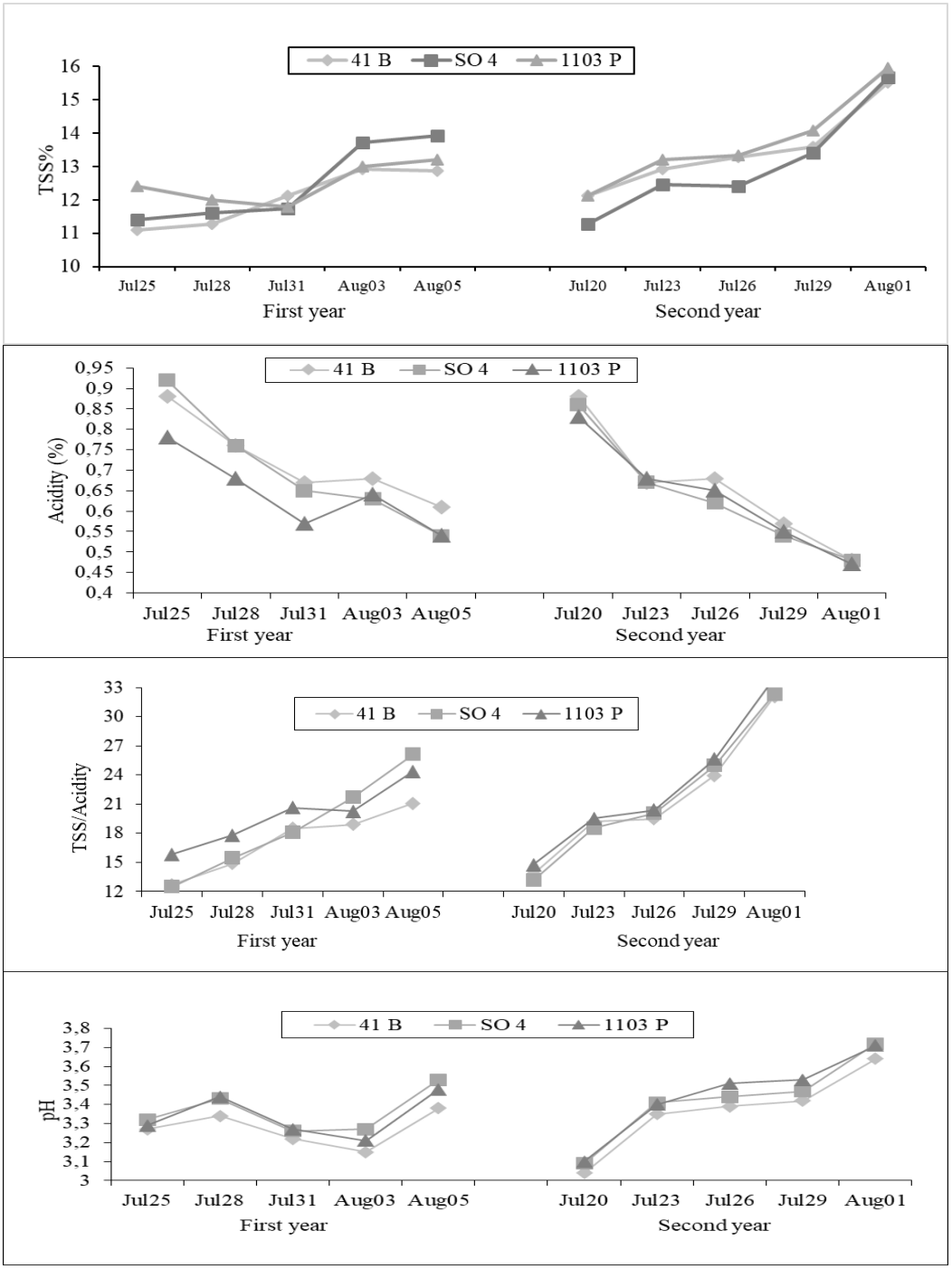

Figure 3. *TSS, acidity, TSS/acidity and pH changes by years in the ripeness progress of Red Globe variety*

http://www.aloki.hu ● ISSN 1589 1623 (Print) ● ISSN1785 0037 (Online)
DOI: http://dx.doi.org/10.15666/aeer/2005_43634376

Table 4 indicates the effect of rootstocks on juice quality of Red Globe variety at the time of harvest. In terms of the first year, the second year, and the average for both years, the effect of rootstocks on TSS content was not found to be significant. While the effect of rootstocks on pH, acidity, TSS/acidity content was found to be significant in the first year, it was not significant in the second year. In terms of the average for both years SO4 rootstock, which gave the highest statistical value in pH and TSS/acid content, was followed by 1103 P rootstock (*Table 4*). Rizk-Alla et al. (2011) found the performance of Red Globe variety on its own root and 5 rootstocks to be significant in terms of TSS, acidity and TSS/acid ratio. In certain other studies, it was reported by Sivilotti et al. (2007) and Cus (2004) that no significant difference was found in terms of these characteristics between, respectively, 7 rootstocks (SO4, 420A, 3309C, 161-49C, Fercal, 1103P, 5BB) and 3 rootstocks (SO4, 1103P and 420A). Furthermore, vegetation period can also affect the differences between rootstocks in term of quality (Sivilotti et al., 2007).

Table 4. *The effects of some rootstocks on juice composition of 'Red Globe' table grapes in the East Mediterranean region*

Rootstock	TSS (%)			pH			Acidity (%)			TSS/acidity		
	1st year	2nd year	Mean	1st year	2nd year	Mean	1st year	2nd year	Mean	1st year	2nd year	Mean
41 B	12.87	15.53	14.20	3.38 b*	3.64	3.51 b	0.61 a	0.48	0.55	21.07 b	32.09	26.58 b
SO4	13.93	15.67	14.80	3.53 a	3.72	3.63 a	0.54 b	0.48	0.51	26.11 a	32.33	29.22 a
1103P	13.20	15.97	14.58	3.48 a	3.71	3.59 ab	0.54 b	0.47	0.51	24.37 ab	33.98	29.17 ab
LSD(*P*=0.05)	ns	ns	ns	**	ns	**	**	ns	ns	**	ns	**

*:Values not associated with the same letter(s) are significantly different; **: Significant at 0.05 level; ns: Not significant

Rootstocks affected some cluster properties and berry properties (Kaplan et al., 2018). Cluster weight differed significantly among the rootstocks. The greatest cluster weight was given by SO4 rootstock, while the smallest cluster weight was recorded on 41B and 1103P rootstocks (*Table 5*). Vines grafted on 41B rootstock yielded a cluster width value lower than SO4 and 1103P rootstocks. The effects of rootstocks on average cluster length (26.17-27.44 cm) are similar in the study. However, it may be suggested to shorten the cluster length for satisfying packaging and marketing needs. This operation called berry thinning is removed with one-third of the bottom part of the cluster. Berry thinning is performed when berries are at pea-size, in order to give more uniform clusters in terms of weight and shape (Zabadal, 2002; Di Lorenzo et al., 2011).

The berry weight is an important aspect in quality grape production which was significantly influenced by the use of different rootstocks (Ghule et al., 2021). In the study, the effects of rootstocks on berry weight and berry width were found to be significant in the first year, while their effects on berry length were found to be significant in both years. According to the values for the average of both years, SO4 and 1103 P rootstocks yielded higher values than 41 B rootstock (*Table 6*).

Rizk-Alla et al. (2011) determined that rootstocks significantly affected berry physical components in Red Globe variety cultivated on its own root and Dogridge, Salt Creek, Freedom, Harmony, 1103P. In another study, where the same variety was cultivated on its own root and Freedom, Salt Creek, 110R, rootstocks also had a significant effect on berry weight and size (Hifny et al., 2016). Also in another study, it

http://www.aloki.hu ● ISSN 1589 1623 (Print) ● ISSN1785 0037 (Online)
DOI: http://dx.doi.org/10.15666/aeer/2005_43634376

was reported that berry weight and berry diameter of Red Globe cultivar were significantly affected by the use of different rootstocks (Ghule et al., 2021).

Table 5. *The effects of some rootstocks on cluster properties of 'Red Globe' table grapes in the East Mediterranean region*

Rootstock	Cluster weight (g)			Cluster width (cm)			Cluster length (cm)		
	1st year	2nd year	Mean	1st year	2nd year	Mean	1st year	2nd year	Mean
41 B	915.19 c*	826.86 b	871.02 b	15.10 b	13.55 b	14.33 b	27.66	24.68	26.17
SO4	1105.75 a	927.84 a	1016.80a	16.38 a	14.60 a	15.49 a	28.77	26.10	27.44
1103P	1012.90 b	913.32 ab	963.11 b	15.79 ab	14.48 a	15.13 a	29.04	25.45	27.25
LSD(*P*=0.05)	**	**	**	**	**	**	ns	ns	ns

*:Values not associated with the same letter(s) are significantly different; **: Significant at 0.05 level; ns: Not significant

Table 6. *The effects of some rootstocks on berry properties of 'Red Globe' table grapes in the East Mediterranean region*

Rootstock	Berry weight (g)			Berry width (mm)			Berry length (mm)			Berry removal force (N)		
	1st year	2nd year	Mean	1st year	2nd year	Mean	1st year	2nd year	Mean	1st year	2nd year	Mean
41B	10.37 b*	9.54	9.96 b	23.93 b	24.26	24.10 b	26.87 b	25.52 b	26.20 b	9.18	6.28	7.73
SO4	11.80 a	10.25	11.02 a	25.12 a	24.68	24.90 a	28.01 a	26.32 a	27.17 a	8.59	6.48	7.54
1103P	11.29 a	9.95	10.62 a	24.31 b	24.53	24.42 ab	28.09 a	26.31 a	27.20 a	8.92	6.16	7.54
LSD(*P*=0.05)	**	ns	**	**	ns	**	**	**	**	ns	ns	ns

*:Values not associated with the same letter(s) are significantly different; **: Significant at 0.05 level; ns: Not significant

In terms of berry physical components, berry removal force was found to be between 7.54-7.74 N in rootstocks according to the average values for both years. Kamiloglu and Demirkeser (2019) determined that berry removal force was 7.30 N in Red Globe variety grafted on 1103 P; while Segade et al. (2013) determined that berry removal force of the same variety grafted on 140 Ru rootstock varied between 4.90 and 7.66 N according to ripeness periods.

In the study, the effects of rootstocks on leaf chlorophyll (chlorophyll a, chlorophyll b, total chlorophyll, and SPAD) contents of Red Globe grape were found to be similar (*Table 7*). Kuljančić et al. (2012) determined the photosynthesis ratio as 6.9 µmol $m^{-2}s^{-1}$, and transpiration ratio as 2.4 mmol $m^{-2}s^{-1}$ in leaves on the main shoot in Sila grape cultivar. These results were found within the range of values obtained in our study. However, there was no statistical difference between rootstocks in terms of these physiological characteristics (photosynthesis ratio and transpiration ratio) (*Table 8*). Although Bica et al. (2000) suggested that rootstocks could have a significant effect on photosynthetic parameters, their study that photosynthesis ratio was similar in Pinot Noir plants grafted on SO4 and 1103P rootstocks. Somkuwar et al. (2015), associating high photosynthesis ratio with leaf area and shoot length, reported that 110 R, which had the highest photosynthesis ratio in their study, could have gained maximum benefit from sunlight due to the increase in leaf area.

http://www.aloki.hu ● ISSN 1589 1623 (Print) ● ISSN1785 0037 (Online)
DOI: http://dx.doi.org/10.15666/aeer/2005_43634376

Table 7. *The effects of rootstocks on chlorophyll content and leaf area for Red Globe grapes grown in the East Mediterranean region*

Rootstock	Chlorophyll 'a' (mg g $^{-1}$ FW)			Chlorophyll 'b' (mg g $^{-1}$ FW)			Total Chlorophyll (mg g $^{-1}$ FW)			SPAD			Leaf area (cm^2)		
	1styear	2ndyear	Mean	1styear	2ndyear	Mean	1styear	2ndyear	Mean	1styear	2ndyear	Mean	1styear	2ndyear	Mean
41 B	0.71	0.90	0.80	0.30	0.41	0.35	1.15	1.52	1.33	29.59	30.40	30.00	177.33	204.13	190.73
SO4	0.72	0.92	0.82	0.29	0.38	0.34	1.16	1.52	1.34	30.11	31.68	30.90	170.54	200.38	185.46
1103P	0.84	0.91	0.87	0.29	0.37	0.33	1.31	1.51	1.41	29.35	31.18	30.26	162.96	199.67	181.31
LSD(*P*=0.05)	ns	ns	ns	ns	ns	ns	ns	ns	ns	ns	ns	ns	ns	ns	ns

FW: Fresh weight, ns: Not significant

Table 8. *The effects of rootstocks on photosynthetic rate, transpiration rate for Red Globe grapes grown in the East Mediterranean region*

Rootstock	Photosynthetic rate (µmol m^{-2} s^{-1})			Transpiration rate (mmol m^{-2} s^{-1})		
	1styear	2ndyear	Mean	1styear	2ndyear	Mean
41 B	6.13	5.16	5.65	2.12	2.69	2.40
SO4	7.40	5.43	6.42	2.10	2.90	2.50
1103P	6.51	4.91	5.71	1.94	2.61	2.28
LSD(*P*=0.05)	ns	ns	ns	ns	ns	ns

ns: Not significant

http://www.aloki.hu ● ISSN 1589 1623 (Print) ● ISSN1785 0037 (Online)
DOI: http://dx.doi.org/10.15666/aeer/2005_43634376

The use of rootstocks can have an important effect on the mineral nutrition of the grafted variety. Little is known about the specific mechanisms used by grape rootstocks to absorb nutrients (Ibacache and Sierra, 2009). Many reports dealt with mineral uptake and distribution of minerals in grapevine; it was noticed that the differences in nutrient uptake and distribution could be attributed to the genotype of rootstock which gives a different absorption capability or tendency for some specific minerals (Rizk Alla et al., 2011). The effects of rootstocks on macro nutrient uptake in Red Globe grape variety were given in *Table 9*. No significant differences were observed in leaf N content among the rootstocks. Similar effects were observed by Dalbo et al. (2011) and Vijaya and Srinivas Rao (2015) when using different rootstocks. However, the effects of rootstocks on P, K, Ca and Mg absorption were statistically significant. It was determined that the effect of 1103 P on the uptake of these elements was higher than other rootstocks. As a matter of fact, Jogaiah et al. (2013) reported that rootstocks with a *Berlandieri x Rupestris* genetic background generally have a good ability for nutrient uptake. Ibacache and Sierra (2009) reported that the effects of Red Globe grape variety, grafted on 10 different American vine stocks, on N (0.86-1.29%), P (0.21-0.42%), K (1.47-3.37%) uptake in leaf petioles were significant; while the effect of Salt Creek rootstock on P uptake and the effect of Harmony rootstock on K uptake were higher than the others. Risk-Alla et al. (2011) found in their study, where they analyzed the leaf mineral content of the same variety on 5 different rootstocks, that the most effective rootstocks were, respectively, Dogridge and Salt Creek on N (0.63-0.72% and P (0.32-0.37%) uptake, and Freedom on K (0.40-0.44%) uptake. In our study, the N content in Red Globe leaves was found between 2.67-2.86% in the first year and 2.52-2.78% in the second year. it was seen that these values were close to the limit values (2.30-2.80%) reported by Bergman (1992). While P content was within the range of limit value (0.25-0.45%) in 1103P and SO4 rootstocks, it was partially low in 41 B rootstock. Weaver (1976) categorized K content values between 0.8% and 1.5% as close to normal level, and above 1.5% as adequate. In our study, rootstocks did not adequately affect K uptake. The lowest K content was determined in 41 B rootstock. At the same time, Ca content was found to be below the limit value (1.5-2.5%) in this rootstock.

Table 9. *The effects of rootstocks some macro element concentrations for Red Globe grapes grown in the East Mediterranean region*

Rootstock	N (%)			P (%)			K (%)			Ca (%)			Mg (%)		
	1st year	2nd year	Mean	1st year	2nd year	Mean	1st year	2nd year	Mean	1st year	2nd year	Mean	1st year	2nd year	Mean
41B	2.86	2.52	2.69	0.23b*	0.23 c	0.23 c	0.82	0.76 b	0.79b	1.18	1.48 b	1.33b	0.24	0.30 ab	0.27b
SO4	2.67	2.78	2.72	0.26 b	0.30 b	0.28b	0.79	0.87a	0.83ab	1.34	1.82 a	1.58ab	0.23	0.29 b	0.26b
1103P	2.72	2.56	2.64	0.38 a	0.35 a	0.37 a	0.91	0.84 a	0.87 a	1.50	1.78 ab	1.64 a	0.27	0.35 a	0.31 a
LSD (*P*=0.05)	ns	ns	ns	**	**	**	ns	**	**	ns	**	**	ns	**	**

*:Values not associated with the same letter(s) are significantly different; **: Significant at 0.05 level; ns: Not significant

Differences between rooting models of different rootstocks may affect water and nutrient uptake (Somkuwar et al., 2008). There are very few studies on the effect of

http://www.aloki.hu ● ISSN 1589 1623 (Print) ● ISSN1785 0037 (Online)
DOI: http://dx.doi.org/10.15666/aeer/2005_43634376

rootstocks on microelement uptake (Vijaya and Srinivas Rao, 2015). In this study, micronutrient element contents in Red Globe leaves were given in *Table 10*.

Table 10. *The effects of rootstocks some micro element concentrations for Red Globe grapes grown in the East Mediterranean region*

Rootstock	Mn (ppm)			Fe (ppm)		
	1st year	2nd year	Mean	1st year	2nd year	Mean
41 B	21.54	31.17	26.36	80.68	124.39 ab	102.53
SO4	21.16	38.68	29.92	74.65	135.96 a	105.30
1103P	22.02	29.48	25.75	80.65	112.40 b	96.52
LSD(*P*=0.05)	ns	ns	ns	ns	**	ns
Rootstock	**Cu (ppm)**			**Zn (ppm)**		
	1st year	2nd year	Mean	1st year	2nd year	Mean
41 B	24.54	8.18	16.36	41.66	16.64	29.15
SO4	19.98	11.11	15.54	41.19	15.06	28.13
1103P	19.66	7.64	13.65	37.88	18.00	27.94
LSD(*P*=0.05)	ns	ns	ns	ns	ns	ns

**: Significant at 0.05 level; ns: Not significant

The effects of rootstocks on Mn, Fe (except for 2nd year), Cu, Zn uptake were not found to be statistically significant. Dalbo et al. (2011) reported in their study that micronutrient accumulation in petioles was not affected by rootstock. According to Gärtel (1993), Mn and Fe contents in Red Globe leaves displayed slight deficiency in the 1st year and they were at an optimal level in the 2nd year of the study, while Cu was at an optimal level in both years. Zn content was found to be higher and at an optimal level in the 1st year (in comparison with the 2nd year).

Conclusion

In modern viticulture, grafting commercial grapevine varieties on interspecific rootstocks is a common practice required for conferring resistance to many biotic and abiotic stresses. Nevertheless, the use of rootstocks is also known to impact grape berry development and quality (Corso et al., 2016).

In the study, no difference was observed in terms of the effects of rootstocks on phenological periods in Red Globe variety. It ripened during the first week of August in Mediterranean ecological conditions, and EHS of bud burst-ripeness period was found to be 1600-1700 dd. The highest value in terms of cluster and berry weights and ripeness index were yielded by SO4 rootstock, which was followed by 1103 P rootstock. According to the averages for two years, it was determined that rootstocks did not have any effect on accumulation of micronutrient elements, while 1103 P yielded higher values than other two rootstocks in terms of macronutrient elements (P, K, Ca, Mg). The effects of rootstocks on chlorophyll a, chlorophyll b and total chlorophyll contents were found to be similar. No significant difference was observed between rootstocks in physiological measurements such as photosynthesis and transpiration ratio.

http://www.aloki.hu ● ISSN 1589 1623 (Print) ● ISSN1785 0037 (Online)
DOI: http://dx.doi.org/10.15666/aeer/2005_43634376

Acknowledgements. The author wishes to thank the coordination unit of scientific research projects, Mustafa Kemal University for financial support.

REFERENCES

[1] Ağaoğlu, Y. S. (2002): Bilimsel ve Uygulamalı Bağcılık. – Cilt II, Asma Fizyolojisi-I. Kavaklıdere Eğitim Yayınları No: 5, 444 s. (in Turkish).
[2] Aktürk, B., Uzun, H. İ. (2019): Bazı sofralık üzüm çeşitlerinin Antalya'daki değişik yörelere uygunlukları ve etkili sıcaklık toplamı istekleri. – Mediterranean Agricultural Sciences 32(3): 267-273. (in Turkish).
[3] Anonymous (2022): Meteorological data. – Available at: https://www.mgm.gov.tr/veridegerlendirme/il-ve-ilceler-istatistik.aspx?k=A&m=HATAY Access date: 22.06.2022.
[4] Arnon, D. L. (1949): Copper enzymes in isolated chloroplast polyphenoloxidase in *Beta vulgaris*. – Plant Physiology 21: 1-5.
[5] Bergman, W. (1992): Nutritional Disorders of Plants. Development, Visual and Analytical Diagnosis. – Gustav Fisher Verlag Jena, Stutgart, New York.
[6] Bica, D., Gay, G., Morando, A., Soave, E. (2000): Effects of rootstocks and *Vitis vinifera* genotype on photosynthetic parameters. – Acta horticulturae 526: 373-379.
[7] Cangi, R., Altun, M. A. (2015): Bazı önemli sofralık üzüm çeşitlerinin Sakarya/Taraklı ekolojisine adaptasyonu. – Tarım Bilimleri Araştırma Dergisi 8(2): 35-39. (in Turkish).
[8] Chanana, Y. R., Gill, M. I. S. (2008): High quality grapes can be produced in Punjab. Proceedings of the international symposium on grape production and processing. – Acta Horticulturae 785: 85-95.
[9] Corso, M., Vannozzi, A., Ziliotto, F., Zouine, M., Maza, E., Nicolato, T., Müller, M. (2016): Grapevine rootstocks differentially affect the rate of ripening and modulate auxin-related genes in Cabernet Sauvignon berries. – Frontiers in Plant Science 7: 69.
[10] Cousins, P. (2005): Evolution, genetics, and breeding: Viticultural applications of the origins of our rootstocks. Grapevine Rootstocks; Current Use, Research and Application. – Proceedings of the 2005 Rootstock Symposium. Pub by MVEC. Pp. 1-7.
[11] Cox, C. M., Favero, A. C., Dry, P. R., McCarthy, M. G., Collins, C. (2012): Rootstock effects on primary bud necrosis, bud fertility, and carbohydrate storage in Shiraz. – Am. J. Enol. Vitic. 63: 277-283.
[12] Cus, F. (2004): The effect of different scion/rootstock combinations on yield properties of cv. 'Cabernet Sauvignon'. – Acta Agriculturae 83: 63-71.
[13] Dalbo, M. A., Schuck, E., Basso, C. (2011): Influence of rootstock on nutrient content in grape petioles. – Rev. Bras. Frutic., Jaboticabal 33(3): 941-947.
[14] Di Lorenzo, R., Gambino, C., Scafidi, P. (2011): Summer pruning in table grape. – Advances in Horticultural Science 25(3): 143.
[15] Gärtel, W. (1993): Grapes. – In: Bennett, W. F. (ed.) Nutrient deficiencies and toxicities in crop plants. – APS Press, St. Paul, MN. pp. 177-183.
[16] Gautier, A., Cookson, S. J., Lagalle, L., Ollat, N., Marguerit, E. (2020): Influence of the three main genetic backgrounds of grapevine rootstocks on petiolar nutrient concentrations of the scion, with a focus on phosphorus. – Oeno One 54(1): 1-13.
[17] Ghule, V. S., Ranpise, S. A., Somkuwar, R. G., Nimbalkar, R. W. C. (2021): Influence of cane biochemical content on yield and quality of Red Globe grapevines grafted on different rootstocks. – The Pharma Innovation Journal 10(6): 1154-1158.
[18] Gu, S. (2003): Effect of rootstocks on grapevines. – Rootstock review.
[19] Hifny, H. A., Baghdady, G. A., Abdrabboh, G. A., Sultan, M. Z., Shahda, M. A. (2016): Effect of rootstocks on growth, yield and fruit quality of Red Globe grape. – Annals of Agric. Sci. 54(2): 339-344.

http://www.aloki.hu ● ISSN 1589 1623 (Print) ● ISSN1785 0037 (Online)
DOI: http://dx.doi.org/10.15666/aeer/2005_43634376

[20] Ibacache, A. G., Sierra, C. B. (2009): Influence of rootstocks on nitrogen, phosphorus and potassium content in petioles of four table grape varieties. – Chilean Journal of Agricultural Research 69(4): 503-508.
[21] Ibacache, A., Albornoz, F., Zurita-Silva, A. (2016): Yield responses in Flame seedless, Thompson Seedless and Red Globe table grape cultivars are differentially modified by rootstocks under semi-arid conditions. – Scientia Horticulturae 204: 25-32.
[22] Ibacache, A., Verdugo-Vásquez, N., Zurita-Silva, A. (2020): Rootstock: Scion combinations and nutrient uptake in grapevines. – Fruit crops, Chapter 21, pp. 297-316.
[23] Jogaiah, S., Oulkar, D. P., Banerjee, K., Sharma, J., Patil, A. G., Maske, S. R., Somkuwar, R. G. (2013): Biochemically induced variations during some phenological stages in Thompson Seedless grapevines grafted on different rootstocks. – S. Afr. J. Enol. Vitic. 34(1): 36-45.
[24] Kacar, B., İnal, A. (2008): Bitki Analizleri. – Nobel Yayınları, Yayın No: 1241, 892 s. Ankara. (in Turkish).
[25] Kamiloğlu, Ö., Demirkeser, Ö. (2019): Phenological and Pomological features of some table grape cultivars in the east mediterranean (Hatay/Turkey) conditions. – II. International Agriculture and Forest Congress, Ege University/İzmir/Turkey. 8-9 November, Proceeding Book, pp. 99-114.
[26] Kapłan, M., Klimek, K., Borowy, A., Najda, A. (2018): Effect of rootstock on yield quantity and quality of grapevine 'Regent'in South-Eastern Poland. – Acta Scientiarum Polonorum-Hortorum Cultus 17(4): 117-127.
[27] Klimek, K., Kapłan, M., Najda, A. (2022): Influence of Rootstock on Yield Quantity and Quality, Contents of Biologically Active Compounds and Antioxidant Activity in Regent Grapevine Fruit. – Molecules 27(7): 1-15.
[28] Koblet, W., Candolfi-Vasconcelos, M. C., Keller, M. (1995): Effects of training system, canopy management practices, crop load and rootstock on grapevine photosynthesis. – Acta Horticulturae 427: 133-140.
[29] Kuljančić, I. D., Paprić, D., Korać, N., Božović, P., Boriscaron, M., Medić, M., Ivaniscaron, D. (2012): Photosynthetic activity in leaves on laterals and top leaves on main shoots of Sila cultivar before grape harvest. – African Journal of Agricultural Research 7(13): 2072-2074.
[30] Li, M., Guo, Z., Jia, N., Yuan, J., Han, B., Yin, Y., Sun, Y., Liu, C., Zhao, S. (2019): Evaluation of eight rootstocks on the growth and berry quality of 'Marselan' grapevines. – Scientia Horticulturae 248: 58-61.
[31] Miele, A., Rizzon, L. A. (2019): Rootstock-scion interaction: 5. Effect on the evolution of Cabernet Sauvignon grape ripening. – Revista Brasileira de Fruticultura 41(3): 1-9.
[32] Muñoz-Robredo, P., Robledo, P., Manríquez, D., Molina, R., Defilippi, B. G. (2011): Characterization of sugars and organic acids in commercial varieties of table grapes. – Chilean journal of agricultural research 71(3): 452.
[33] OIV (2009): Descriptor list for grape varieties and vitis species. – 2nd edition, 178p.
[34] OIV (2017): Distribution of the world's grapevine varieties. – 53p. http://www.oiv.int/public/medias/5888/en-distribution-of-the-worlds-grapevine-varieties.pdf.
[35] OIV (2019): Statistical report on world vitiviniculture. – 22p.
[36] Rizk-Alla, M. S., Sabry, G. H., Abd El-Wahab, M. A. (2011): Influence of some rootstocks on the performance of Red Globe grape cultivar. – Journal of American Science 7(4): 71-81.
[37] Santibáñez, F., Sierra, H., Santibanez, P. (2014): Degree day model of table grape (*Vitis vinifera* L.) phenology in Mediterranean temperate climates. – International Journal of Science, Environment and Technology 3(1): 10-22.
[38] Satisha, J., Somkuwar, R. G., Sharma, J., Upadhyay, A. K., Adsule, P. G. (2010): Influence of rootstocks on growth yield and fruit composition of Thompson Seedless grapes grown in the Pune Region of India. – S. Afr. J. Enol. Vitic. 31(1): 1-8.

http://www.aloki.hu ● ISSN 1589 1623 (Print) ● ISSN1785 0037 (Online)
DOI: http://dx.doi.org/10.15666/aeer/2005_43634376

[39] Seccia, A., Santeramo, F. G., Nardone, G. (2015): Trade competitiveness in table grapes: A global view. – Outlook on Agriculture 44(2): 127-134.
[40] Segade, S. R., Giacosa, S., Torchio, F., de Palma, L., Novello, V., Gerbi, V., Rolle, L. (2013): Impact of different advanced ripening stages on berry texture properties of 'Red Globe'and 'Crimson Seedless' table grape cultivars (*Vitis vinifera* L.). – Scientia Horticulturae 160: 313-319.
[41] Sivilotti, P., Zulini, L., Peterlunger, E., Petrussi, C. (2007): Sensory properties of 'Cabernet Sauvignon' wines as affected by rootstock and season. – Acta Horticulturae 754: 443-448.
[42] Skinkis, P., Walton, V. M., Kaiser, C. (2009): Grape phylloxera biology and management in the Pacific Northwest.Oregon State University. – 25p.
[43] Somkuwar, R. G., Satisha, J., Sharma, J., Ramteke, S. D. (2008): Partitioning of dry matter and nutrient uptake in Thompson Seedless grafted on different rootstocks. – Acta Horticulturae 785: 117-120.
[44] Somkuwar, R. G., Taware, P. B., Bhange, M. A., Sharma, J., Khan, I. (2015): Influence of different rootstocks on growth, photosynthesis, biochemical composition, and nutrient contents in 'Fantasy Seedless' grapes. – International Journal of Fruit Science 15(3): 251-266.
[45] Steel, C. C., Greer, D. H. (2008): Effect of climate on vine and bunch characteristics: Bunch rot disease susceptibility. Proceedings of the international symposium on grape production and processing. – Acta Horticulturae 785: 253-262.
[46] Stell, P., Zulini, L., Peterlunger, E., Petrussi, C. (2007): Sensory properties of 'Cabernet Sauvignon' wines as affected by rootstock and season. – Acta Horticulturae 754: 443-448.
[47] TUIK (2019): Türkiye istatistik kurumu. – http://www.tuik.gov.tr/ bitkiselapp/ bitkisel.zul. (in Turkish).
[48] Valenzuela-Ruiz, M. J., Robles-Contreras, F., Grijalva-Contreras, R. L., Macias-Duarte, R. (2005): Effect of Harmony and Freedom rootstocks on yield and quality of 'Red Globe' table grapes. – Hort. Science 40(4): 1069.
[49] Verma, S. K., Singh, S. K., Krishna, H. (2010): The effect of certain rootstocks on the grape cultivar 'Pusa Urvashi' (*Vitis vinifera* L.). – International Journal of Fruit Science 10(1): 16-28.
[50] Vijaya, D., Srinivas Rao, B. (2015): Effect of rootstocks on petiole mineral nutrient composition of grapes (*Vitis vinifera* L. cv. Thompson Seedless). – Current Biotica 8(4): 367-374.
[51] Weaver, R. J. (1976): Grape Growing. – New York, John Wiley, 371p.
[52] Winkler, A. J., Cook, J. A., Kliewer, W. M., Lider, L. A. (1974): General Viticulture. – Second Revised Edition, University of California Press, Berkeley, California, 710p.
[53] Wooldridge, J., Louw, P. J. E., Conradie, W. J. (2010): Effects of rootstock on grapevine performance, petiole and must composition, and overall wine score of *Vitis vinifera* cv. Chardonnay and Pinot noir. – S. Afr. J. Enol. Vitic. 31(1): 45-48.
[54] Zabadal, T. J. (2002): Growing table grapes in a temperate climate. – Michigan State University Extension, 44p.

http://www.aloki.hu ● ISSN 1589 1623 (Print) ● ISSN1785 0037 (Online)
DOI: http://dx.doi.org/10.15666/aeer/2005_43634376

SOIL PHYSICAL AND CHEMICAL PROPERTIES EFFECT THE SOIL MICROBIAL CARBON, NITROGEN, AND PHOSPHORUS STOICHIOMETRY IN A MANGROVE FOREST, SOUTH CHINA

HU, C.[1†] – HU, G.[1†] – XU, C. H.[1] – LI, F.[2,3] – ZHANG, Z. H.[1*]

[1]*School of Environment and Life Science, Nanning Normal University, Nanning, Guangxi 530001, China*

[2]*Key Laboratory of Agro-ecological Processes in Subtropical Region, Institute of Subtropical Agriculture, Chinese Academy of Sciences, Changsha 410125, China*

[3]*Dongting Lake Station for Wetland Ecosystem Research, Institute of Subtropical Agriculture, Chinese Academy of Sciences, Changsha 410125, China*

[†]*These authors have contributed equally to this work*

[*]*Corresponding author*
e-mail: gxtczzh@126.com; ORCID: 0000-0003-2094-698X

(Received 21st Apr 2022; accepted 26th Jul 2022)

Abstract. Mangrove wetland ecosystem is a coastal ecological key area that combines ecological characteristics of land and marine environments. This study examined soil carbon (C), nitrogen (N), and phosphorus (P) and their stoichiometry in three dominant mangrove species (*Aegiceras corniculatum*, *Kandelia obovata*, and *Avicennia marina*) distributed in the Guangxi Beilun Estuary Nature Reserve, China. Results showed that soil organic carbon (SOC) was highest in *K. obovata*, whereas soil total nitrogen (TN) and phosphorus (TP) were highest in *A. corniculatum*. The C:N, C:P, and N:P ratios in *K. obovata* were greater than those in the others. The microbial biomass C (MBC), N (MBN), and P (MBP) concentrations varied in ranges of 33.45–249.44 mg kg^{-1}, 5.17–9.17 mg kg^{-1}, and 0.17–0.43 mg kg^{-1}, respectively. Similar to soil C, N, and P stoichiometry, *K. obovata* had the highest MBC, MBC:MBN, and MBC:MBP values, whereas the highest MBN and MBN:MBP were found in *A. marina*, and the highest MBP was found in mudflats. Overall, this study demonstrated that the soil stoichiometry and soil microbial biomass responded differently to different plant communities and these differences might be accounted for by variations in the environmental conditions of the three communities.
Keywords: *soil nutrients, ecological stoichiometry, microbial biomass, mangrove forest, estuarine wetland*

Introduction

Mangrove ecosystems are an essential ecotone between terrestrial and marine environments in tropical and subtropical coastlines (Pires et al., 2012). These intertidal forests contribute to coastline protection, reducing the effect of waves and tsunamis, producing detritus to sustain an extensive food web, and acting as nutrient filters between terrestrial and marine ecosystems (Luo et al., 2018). The stability of mangrove ecosystems is influenced by salinity; soil physical and chemical properties, such as nutrient content dynamics; and physiological tolerance (Tripathi et al., 2016).

Ecological stoichiometry focuses on the balance in multiple chemical substances (particularly carbon, C; nitrogen, N; phosphorus, P) in ecological interactions and processes of ecosystems (Elser et al., 2000; Meng et al., 2021). Soil C, N, and P stoichiometry in mangrove ecosystems is not only determined by primary production of the ecosystem and sedimentation processes but is also affected by environmental factors,

http://www.aloki.hu ● ISSN 1589 1623 (Print) ● ISSN1785 0037 (Online)
DOI: http://dx.doi.org/10.15666/aeer/2005_43774389

such as species composition, soil properties, the tidal gradient, and water salinity (Liu et al., 2019; Meng et al., 2021). For example, the absorption of P by sediment particles in coastal waters results in low N:P ratios of mangrove soils under temperate inorganic sediment-rich coastal landforms (Harrison et al., 2005). In addition, C:N:P stoichiometric interactions can enhance or weaken the carbon-climate feedback, and reconciling site-specific mechanisms that regulate C:N:P stoichiometry in mangrove ecosystems is beneficial to improve capacity and predict carbon stocks in coastal wetlands (Rovai et al., 2018). Thus, exploring soil C, N, and P stoichiometry can help to improve our understanding of the potential impacts of nutrients on ecosystem processes under environmental change in mangrove forests.

In addition to the effect of soil C, N, and P stoichiometry, soil microbes also determine the changes associated with the ecological process and function (Bai et al., 2021). Since soil microbial biomass has been proven to be highly correlated with environmental factors, such as soil pH (Rousk et al., 2009), moisture (Fierer et al., 2003), soil organic C (Xu et al., 2014), and biological properties (He et al., 2020), these soil microorganisms affect the changes in ecological processes, such as organic matter decomposition, nutrient cycling, and mineralization (Yang et al., 2010; Rawat et al., 2021). In addition, the variation in soil microbial biomass can indicate the soil fertility and stability (Angst et al., 2018). For example, soil microbial biomass carbon (MBC) is used to predict alterations in soil carbon stocks (Luo et al., 2020; Srivastava et al., 2020). Meanwhile, soil microbial biomass serves as a crucial buffer for soil nitrogen and nitrogen immobilization in fall seasons when nitrogen availability is higher, while releasing nitrogen in early spring when the nitrogen availability is low (Zak et al., 2003). Though extensive research has been carried out on the ecology, structure, and function of the mangrove ecosystem, very limited research is available concerning an array of soil microbial biomass that is a sensitive indicator of environmental change. Therefore, the primary objectives of this study were as follows: to (a) analyze soil and microbial stoichiometry with different mangrove species; (b) explore which environmental variables are most strongly correlated with soil and microbial stoichiometry. This study will provide a basis for the differential restoration of coastal ecosystems in the future.

Materials and Methods

Study area

The Beilun Estuary, Fangchenggang City, Guangxi Zhuang Autonomous Region, P.R. China is located at 21°31′00″–21°37′30″N and 108°00′30″–108°16′30″E with a 150 km coastline, including a land area of 53 km^2 and mangrove forest area of 12.74 km^2 (*Figure 1*). It is dominated by a subtropical climate, and the mean annual temperature, mean annual precipitation, and evaporation are 22.3 °C, 2220.5 mm, and 1400 mm, respectively (Zhou et al., 2020). The rainy season is mainly from June to August. This ecosystem consists of two typical ecological niches (i.e., mudflat and mangrove forest). *Aegiceras corniculatum*, *Kandelia obovata*, and *Avicennia marina* are the three dominant mangrove species in the Beilun estuarine wetland (Zhou et al., 2020).

Sampling

In this study, we chose four sites, each of which was from mudflat to mangrove forests, to collect surface (0–20 cm) soils in May of 2020 (*Table 1*). For each sample, three

http://www.aloki.hu ● ISSN 1589 1623 (Print) ● ISSN1785 0037 (Online)
DOI: http://dx.doi.org/10.15666/aeer/2005_43774389

subsamples were mixed to compose one sample. The soil samples were homogenized and sieved through a mesh size of 2 mm to remove plant debris and roots and then transported to the lab immediately for further analyses. Soil samples were stored at 4 °C to determine the physicochemical characteristics.

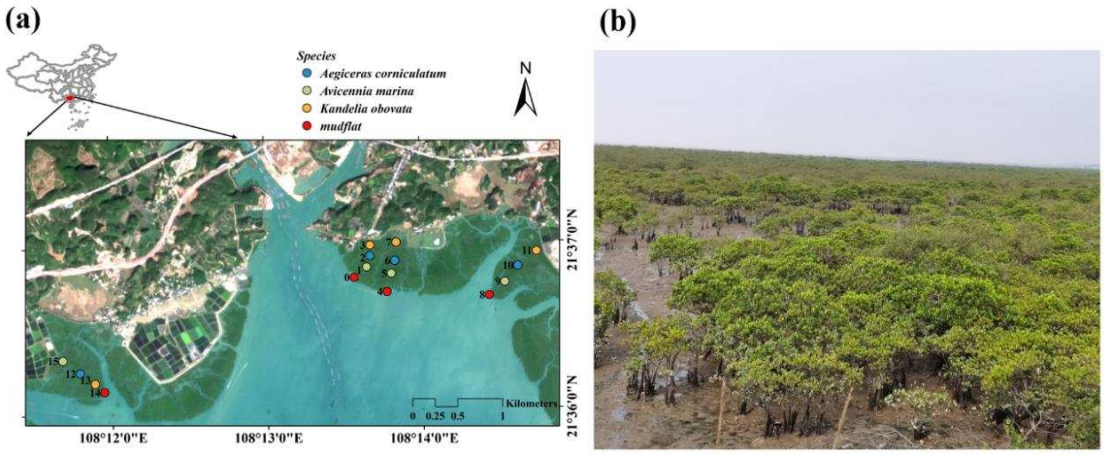

Figure 1. *(a) Map of soil samples collecting locations in mangrove forest ecosystems; (b) sampling environment in the study*

Table 1. *Coordinates and dominant species of sampling sites*

Sampling site	Longitude	Latitude	Dominant species
0	108.226044	21.613317	Mudflat
1	108.2274	21.614351	*A. marina*
2	108.227793	21.615475	*A. corniculatum*
3	108.227816	21.61652	Mudflat
4	108.229551	21.611845	Mudflat
5	108.230035	21.613669	*A. marina*
6	108.230447	21.61495	*A. corniculatum*
7	108.23061	21.616781	*K. obovata*
8	108.240517	21.61133	*K. obovata*
9	108.242201	21.612635	*A. marina*
10	108.243625	21.614211	*A. corniculatum*
11	108.24566	21.615661	*K. obovata*
12	108.19651	21.60421	*A. corniculatum*
13	108.198069	21.60313	*K. obovata*
14	108.199072	21.602287	Mudflat

Soil physical and chemical properties

For the determination of the soil moisture content, soil samples were oven dried at 105 °C for 24 h. The pH was determined in a 1:2.5 (soil:water) slurry using a Delta 320 pH meter (Model Delta 320, Mettler Toledo, Switzerland). The salinity of soil was quantified using the dregs-drying math method. Soil organic carbon (SOC) concentrations were measured by the $K_2Cr_2O_7$–H_2SO_4 oxidation method (Zhang et al., 2009). TN concentrations were measured using a Carlo Erba CNS Analyzer (Carlo Erba, Milan, Italy) (Gallaher et al., 1976). TP concentrations were measured via perchloric-acid

http://www.aloki.hu ● ISSN 1589 1623 (Print) ● ISSN1785 0037 (Online)
DOI: http://dx.doi.org/10.15666/aeer/2005_43774389

digestion followed by ammonium-molybdate colorimetry (Wang et al., 2006). The units (g kg^{-1}) of SOC, TN, and TP concentrations were transformed to mol kg^{-1} to calculate the C:N, C:P, N:P ratios of each soil sample as the molar ratios (atomic ratio).

Soil microbial biomass C, N, and P

Soil MBC, MBN, and MBP concentrations were analyzed by the chloroform fumigation-extraction method after 65 h of incubation (Brookes et al., 1982; Wu et al., 1990). The soil was split into two parts, and one half was placed in a desiccator with chloroform. The desiccator was evacuated until the $CHCl_3$ had boiled for 2 min, and samples were fumigated for 24 h at room temperature. For MBC and MBN analysis (multi N/C 2100, Analytik Jena), the samples were extracted with 0.5 M K_2SO_4 with a soil:solution ratio of 1:5. For MBP analysis (FIALAB, MLE Dresden), a Bray-1 solution (0.03 M NH_4Fe, 0.025 M HCl) with a soil:solution ratio of 1:10 was used. MBC:MBN:MBP ratios were calculated from molar MBC, MBN, and MBP concentrations.

Statistical analysis

One-way analysis of variance and pair-wise comparison tests (Tukey's HSD) were used to compare the concentrations of essential elements in the different mangrove species. Relationships between nutritional elements and microbial biomass were determined by correlation analysis. Multiple comparisons of the means were performed using Tukey's test at the 0.05 significance level. All statistical analyses were performed with SPSS 20.0 (SPSS Inc., Chicago, IL, USA).

The variable importance in the projection (VIP) with the PLSR model was conducted to reflect the importance of soil physical and chemical properties (soil moisture, salinity, pH; soil C, N, and P concentrations; and C:N, C:P, and N:P) for the soil microbial biomass C, N, and P concentrations and stoichiometry. Larger VIP values (≥ 1) represent the most relevant parameter for explaining the dependent variable (Zhou et al., 2017). The VIP values of these properties were calculated with SIMCA-P+13.0 (Umetrics AB, Sweden).

Results

Soil physical properties

Results showed a significant difference in soil properties, such as soil moisture, pH, and salinity, between mudflats and the three mangrove species (*Figure 2*). The average soil moisture contents of mudflats (23.64%) and *A. marina* (23.52%) were significantly lower than those in *A. corniculatum* (29.08%) and *K. obovata* (30.76%). The highest pH (4.97) and lowest salinity (0.99%) were in mudflats, whereas there was no significant difference among the three mangrove species in pH and salinity.

Soil C, N, and P concentrations and stoichiometry

The C, N, and P concentrations and stoichiometry of soil exhibited marked difference, as in *Figure 3*. The concentrations of SOC ranged from 5.05 to 12.63 g kg^{-1}, with an average of 9.95 g kg^{-1}. The TN and TP concentrations varied from 0.38 to 0.60 g kg^{-1} and 0.08 to 0.18 g kg^{-1}, with mean values of 0.49 and 0.14 g kg^{-1}, respectively. The SOC concentration was higher in the *K. obovata* plant community than in the other plant communities, whereas the N and P concentrations in *A. corniculatum* plant communities

http://www.aloki.hu ● ISSN 1589 1623 (Print) ● ISSN1785 0037 (Online)
DOI: http://dx.doi.org/10.15666/aeer/2005_43774389

were both higher than those in the other plant communities. The C:N, C:P, and N:P ratios exhibited the ranges of 21.63 to 26.31, 138.82 to 258.72, and 6.21 to 9.66, respectively. The C:N, C:P, and N:P ratios in *K. obovata* plant communities were greater than those in the other plant communities.

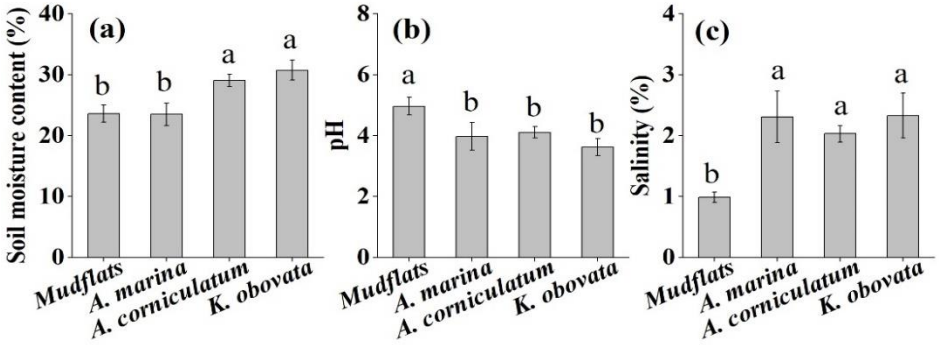

Figure 2. *Characteristics of soil moisture content (a), pH (b), and salinity (c) content for four zones. Values are means ± SE. Different letters indicate significant difference among treatments at 0.05 significance level*

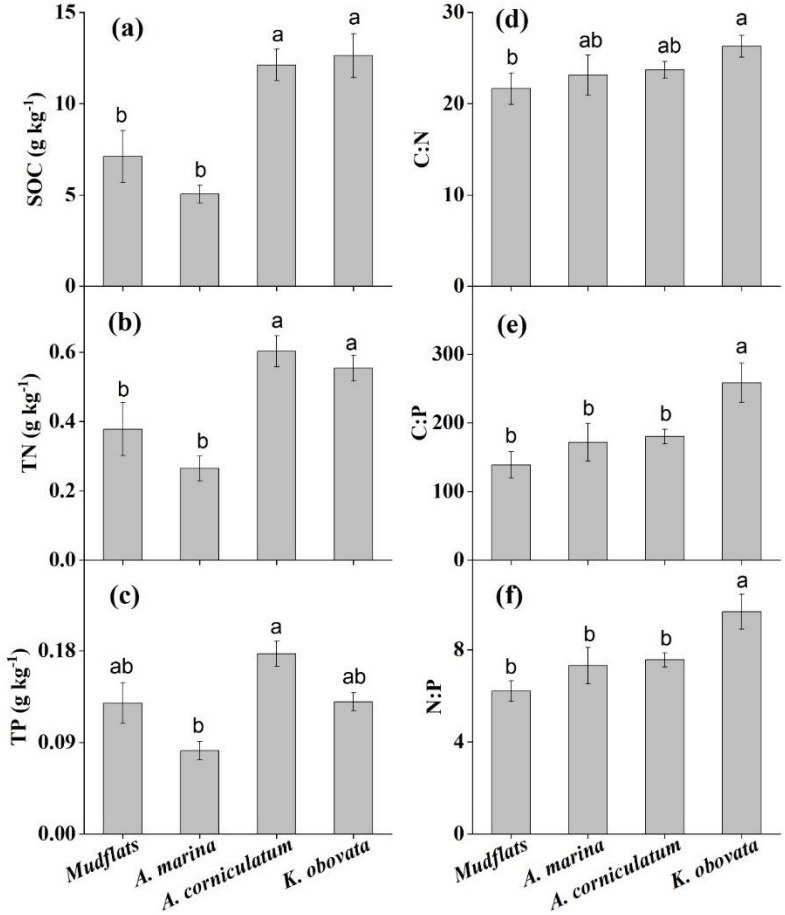

Figure 3. *Concentrations of SOC (a), TN (b) and TP (c), ratios of C:N (d), C:P (e) and N:P (f) for four zones. Values are means ± SE. Different letters indicate significant difference among treatments at 0.05 significance level*

http://www.aloki.hu ● ISSN 1589 1623 (Print) ● ISSN1785 0037 (Online)
DOI: http://dx.doi.org/10.15666/aeer/2005_43774389

Microbial biomass C, N, and P stoichiometry

The microbial biomass concentration (MBC, MBN, MBP) and their stoichiometry (MBC:MBN, MBC:MBP, MBN:NBP ratios) in the studied soil samples are illustrated in *Figure 4*. The MBC, MBN, and MBP varied from 33.45 to 249.44 mg kg^{-1}, 5.17 to 9.17 mg kg^{-1}, and 0.17 to 0.43 mg kg^{-1}, with averages of 150.33 mg kg^{-1}, 6.35 mg kg^{-1}, and 0.26 mg kg^{-1}, respectively. The highest MBC, at a significance level, was observed in *K. obovata* plant communities, followed by that in *A. corniculatum*, mudflats, and *A. marina*. In contrast to that for MBC, significantly higher MBN was shown in *A. marina* than in the other soils. The highest MBP was observed in mudflats. Similar to that with MBC:MBN, a markedly higher MBC:MBP ratio was found in *K. obovata*, whereas a higher MBN:MBP ratio was shown in *A. marina*.

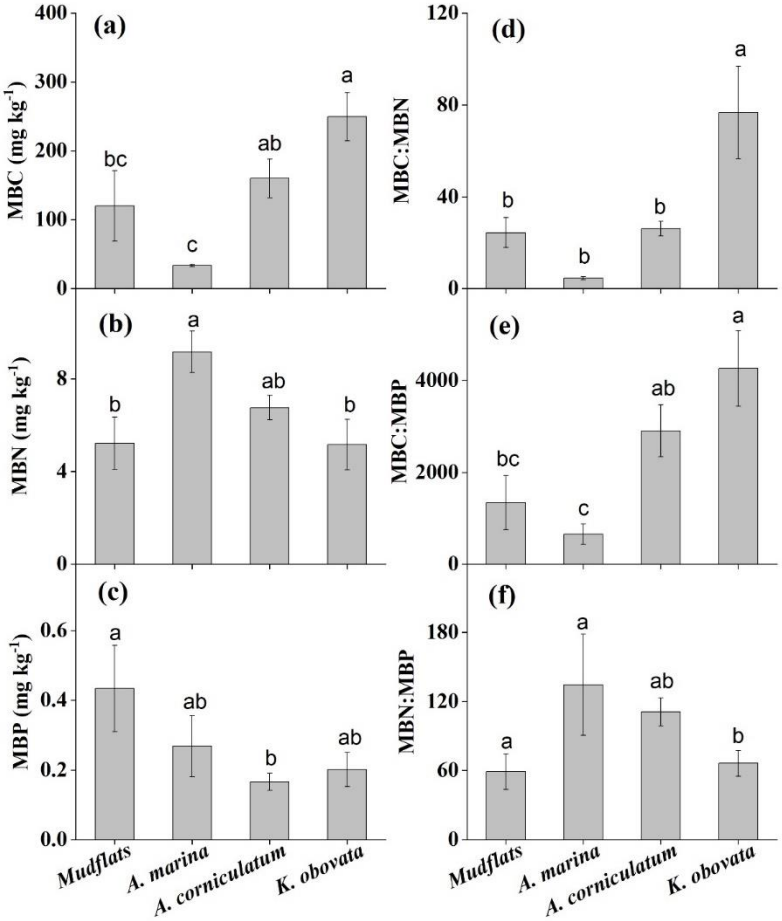

Figure 4. *Characteristics of soil microbial biomass (a-c) and ratios (d-f) for four zones. Values are means ± SE. Different letters indicate significant difference among treatments at 0.05 significance level. MBC, microbial biomass C. MBN, microbial biomass N. MBP, microbial biomass P*

Correlations among soil and microbial biomass stoichiometry, and environment

Soil moisture was significantly positively associated with salinity, concentrations of SOC, TN, MBC, MBN, and ratios of C:N, C:P, N:P, and MBC:MBP, but was negatively associated with MBP concentrations. Soil pH was negatively associated with SOC and

http://www.aloki.hu ● ISSN 1589 1623 (Print) ● ISSN1785 0037 (Online)
DOI: http://dx.doi.org/10.15666/aeer/2005_43774389

ratios of C:N, C:P, N:P, and MBC:MBN but was positively associated with MBP. Soil salinity was positively related to ratios of N:P and MBN:MBP and negatively related to MBP (*Figure 5*).

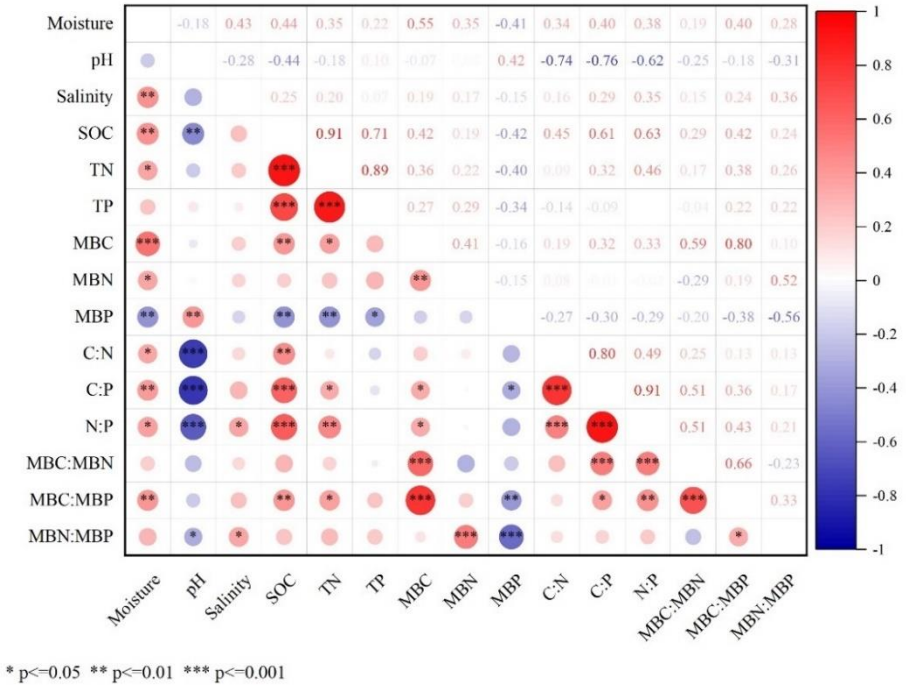

Figure 5. *Pearson's correlations between soil physical, chemical, and biological properties. The color of circle corresponds to the direction of correlations. Positive correlations are shown in blue, while negative correlations in red. '*' indicates significant correlation at P< 0.05; **P< 0.01; ***P< 0.001. MBC, microbial biomass C; MBN, microbial biomass N; MBP, microbial biomass P*

Overall, there were significant correlations among SOC, TN, TP concentrations. Additionally, soil properties were significant correlate with microbial properties. SOC and TN were positively associated with MBC and MBC:MBP but were negatively associated with MBP. TP was negatively associated with MBP. MBC was positively associated with MBP and ratios of C:P, N:P. MBP was negatively associated with ratios of C:P (*Figure 5*).

The weight plots indicated the variables with the highest weights in the optimal model (*Figure 6a*). In the soil and microbial biomass stoichiometry model, the first component was dominated by the soil moisture, with positive PLSR weights. The second component was dominated by pH, with negative PLSR weights (*Figure 6a*). A more convenient expression of the relative importance of the soil physical chemistry factors could be obtained from their VIP values and regression coefficients (*Figure 6b*). For microbial biomass models, the soil moisture was the key variable. All considered variables were related to soil microbial biomass, but those with a VIP < 1 were considered of minor importance for prediction purposes. Therefore, the discussion is limited to variables with a VIP > 1.

http://www.aloki.hu ● ISSN 1589 1623 (Print) ● ISSN1785 0037 (Online)
DOI: http://dx.doi.org/10.15666/aeer/2005_43774389

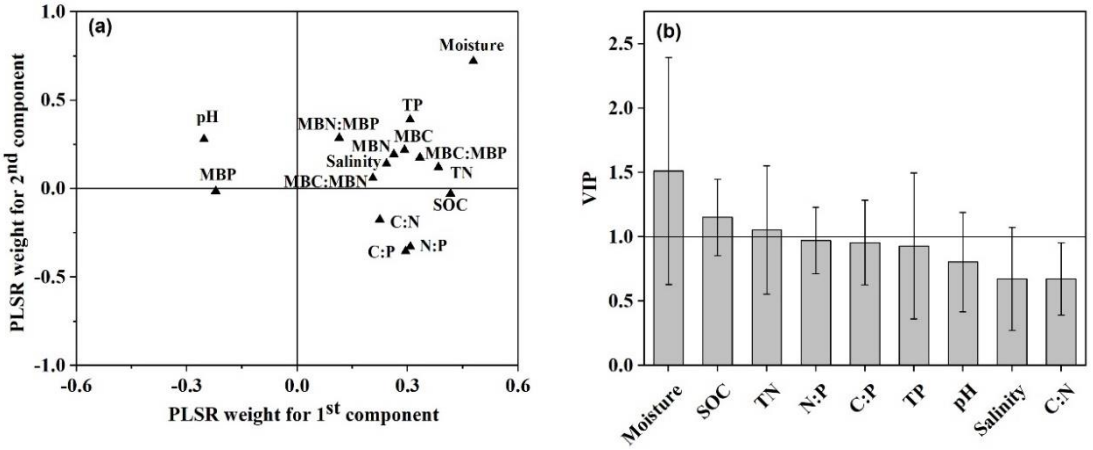

Figure 6. *(a) Weight plots of the first and second PLS components for soil microbial biomass and stoichiometry; (b) Variable importance for the projection (bars) and regression coefficients (lines) of each predictor of soil microbial biomass. The straight solid line indicates a threshold above which predictors are considered to be important for interpretation*

Discussion

All of soil SOC (9.23 g kg^{-1}), TN (0.45 g kg^{-1}), and TP (0.13 g kg^{-1}) in this study area were lower than the mean values reported previously for China (19.33 g kg^{-1}, 1.04 g kg^{-1}, and 0.75 g kg^{-1}, respectively) (Tian et al., 2010), Chongming island (15.94 g kg^{-1}, 0.74 g kg^{-1}, and 0.74 g kg^{-1}, respectively) (Yun et al., 2009), and Minjiang estuary wetland (17.02 g kg^{-1}, 1.02 g kg^{-1}, and 0.24 g kg^{-1}, respectively) (Wang et al., 2012). The difference might be related to various comprehensive factors, such as the source of elements, decomposition process of organic matter, root exudates, and tidal and human disturbances. The N:P ratio (7.69) was approximately equal to that reported in China (Zhou et al., 2020), whereas the ratios of C:N (23.7) and C:P (187.35) were approximately two times higher than those in China (13 and 105, respectively). This could be caused by the activity of soil microorganisms and the oxidation of organic carbon being restrained, as well as the accumulation of SOC in wetlands (Yang et al., 2013; Wang et al., 2014). In addition, mangrove forests are the most important ecosystems for organic carbon sequestration and storage, largely owing to the high SOC levels produced by burial rates, which are higher on average than those in other terrestrial ecosystems (McLeod et al., 2011; Breithaupt et al., 2019).

Soil microbial biomass serves as a pool of nutrients in the soils, which plays an important role in ecosystem sustainability and is a sensitive indicator under the changing environmental conditions. In the present study, the mean concentrations of MBC (33.45-249.44 mg kg^{-1}), MBN (5.17–9.17 mg kg^{-1}), and MBP (0.17–0.43 mg kg^{-1}) in the three mangrove species were lower than those on South Andaman Islands, India (141-489 mg kg^{-1}, 14–38 mg kg^{-1}, and 3.3–15.4 mg kg^{-1}, respectively) (Dinesh and Chaudhuri, 2013). The reason for this might be that land-use changes in mangrove forests in India have altered the soil microbial biomass and microbial community over the long-term. In addition, plants provide the energy to the soil system in the form of litter and root exudates, which eventually are turned into soil microbial biomass (Ohtonen et al., 1999). Several studies suggested that the shifts in stoichiometry of microbial biomass C:N, C:P, and N:P are predictable across a range of biological scales (Sistla et al., 2015; Yao et al.,

http://www.aloki.hu ● ISSN 1589 1623 (Print) ● ISSN1785 0037 (Online)
DOI: http://dx.doi.org/10.15666/aeer/2005_43774389

2019). Globally, the average soil microbial biomass C:N ratio is 7.6, estimated by Xu et al. (2013), and 8.6, estimated by Cleveland and Daniel (2007). This study suggested that the microbial biomass C:N is consistently higher (except for *A. marina*, with a microbial biomass C:N of 4.57) than these global average values. This is probably due to the presence of more organic matter and the low N availability to soil microbes (Rawat et al., 2021). Compared to the results of a study by Dinesh and Chaudhuri (2013), the soil microbial C:P was higher in this study. This could be due to poor soil P availability in the soil (Rawat et al., 2021). Meanwhile, Xu et al. (2013) reported that the soil microbial biomass N:P ratio was more constrained than soil N:P ratios. Cleveland and Daniel (2007) suggested that the soil microbial biomass N:P ratio (6.9) could be an indicator of ecosystem nutrient limitations, and a relatively higher microbial biomass N:P ratio indicates P limitation. Higher biomass N:P ratios were found in the present study, indicating that the mangrove forest might be more likely to be P-limited.

Furthermore, MBC and MBN concentrations were significantly positively correlated with SOC and TN concentrations ($p < 0.01$). The reasons for this might be that soil C and N could promote soil microbial activity, and their availability to the soil microorganisms is possibly increased through root exudates. Soil C availability is one of the vital ecological driving factors for microbial community dynamics and has a crucial effect on the microbial community structure under nutrient-limited conditions. For example, de Vries et al. (2012) indicated that the SOC can provide more readily available C and energy for soil microbial communities. Soil N can also affect the soil microbial composition and MBN by directly supplying N for soil microbial metabolism (Huang et al., 2014). Results in this study are consistent with previous results, suggesting that MBC and MBN concentrations are closely related to changes in the soil microorganism concentrations (Huang et al., 2015). In addition, the positive relationship between soil moisture and microbial biomass C confirms the findings of Curtin et al. (2012) and Rawat et al. (2021). SOC decomposition could be associated with physical protection, thee inhibited diffusion of catabolites, and interactivity with the surface of soil organic matter (Zhao et al., 2020).

In wetlands, larger numbers of microorganisms might require more oxygen to decompose SOC, and when soil moisture exceeds the optimal level, increased water availability can suppress microbial activity. Water-logged soil with limited oxygen availability has been shown to reduce the SOC decomposition rate (Qu et al., 2021). However, the negative relationship between soil moisture and microbial biomass P in our study is not in accordance with the results of the study by Rawat et al. (2021). A possible reason for this might be that frequent drying and rewetting increases the volatility of microbial biomass P (Bagheri et al., 2020). Soil pH is the one of the factors affecting nutrient cycling in soil and microbial biomass in the present study. Low pH might also lead to the higher SOC concentration owing to slow decomposition processes under low pH conditions, and this result agrees with the finding of Liu et al. (2018). Salinity was positively and strongly correlated with N:P and MBN:MBP, which might be due to a shift in the microbial community composition leading to variance in soil nutrients and altering the stoichiometry of microbial biomass, as reported by Hu et al. (2019). However, this finding was contrary to that of Hartzell and Jordan (2012), who proposed that spatiotemporal changes in the dynamics of N and P could shift nutrient availability in the estuaries owing to the mixing of freshwater and seawater.

http://www.aloki.hu ● ISSN 1589 1623 (Print) ● ISSN1785 0037 (Online)
DOI: http://dx.doi.org/10.15666/aeer/2005_43774389

Conclusions

Our results confirmed that the soil and microbial biomass stoichiometry is influenced by plant communities and soil properties in the mangrove forest. However, these results are based on a preliminary field investigation, and further controlled incubation experiments are needed to confirm the mechanisms by which plant communities and soil properties influence soil stoichiometry characteristics.

Acknowledgements. This work was supported by the National Natural Science Foundation of China [31560136]; The Guangxi Science and technology project [2020AC19235]; The Open Fund of Key Laboratory of Agro-ecological Processes in Subtropical Region, Chinese Academy of Sciences [ISA2021104]; The project of improving the basic scientific research ability of young and middle-aged teachers in Guangxi universities [2020KY09026]. We would like to thank Yuanhui Zhou, Kuaikuai Huang, and Qinling Pang who helped with this project. We also thank the anonymous reviewers for their valuable comments and suggestions regarding our article.

Conflict of Interests. The authors declare that they have no competing interests.

REFERENCES

[1] Angst, S., Baldrian, P., Harantova, L., Cajthaml, T., Frouz, J. (2018): Different twig litter (Salix caprea) diameter does affect microbial community activity and composition but not decay rate. – Fems Microbiology Ecology 94(9): fiy126.
[2] Bagheri, S., Mirseyed, H., Etesami, H., Razavipour, T., Astatkie, T. (2020): Short term soil drying-rewetting effects on respiration rate and microbial biomass carbon and phosphorus in a 60-year paddy soil. – 3Biotech 10(11): 492.
[3] Bai, X., Dippold, M. A., An, S., Wang, B., Zhang, H., Loeppmann, S. (2021): Extracellular enzyme activity and stoichiometry: The effect of soil microbial element limitation during leaf litter decomposition. – Ecological Indicators 121: 107200.
[4] Breithaupt, J. L., Smoak, J. M., Sanders, C. J., Troxler, T. G. (2019): Spatial Variability of Organic Carbon, $CaCO_3$ and Nutrient Burial Rates Spanning a Mangrove Productivity Gradient in the Coastal Everglades. – Ecosystems 22: 844-858.
[5] Brookes, P. C., Powlson, D. S., Jenkinson, D. S. (1982): Measurement of microbial biomass phosphorus in soil. – Soil Biology & Biochemistry 14: 319-329.
[6] Cleveland, C. C., Daniel, L. (2007): C:N:P stoichiometry in soil: is there a "Redfield ratio" for the microbial biomass? – Biogeochemistry 85: 235-252.
[7] Curtin, D., Beare, M. H., Hernandez-Ramirez, G. (2012): Temperature and Moisture Effects on Microbial Biomass and Soil Organic Matter Mineralization. – Soil Science Society of America Journal 76(6): 2055-2067.
[8] De Vries, F. T., Manning, P., Tallowin, J. R. B., Mortimer, S. R., Pilgrim, E. S., Harrison, K. A., Hobbs, P. J., Quirk, H., Shipley, B., Cornelissen, J. H. C., Kattge, J., Bardgett, R. D. (2012): Abiotic drivers and plant traits explain landscape-scale patterns in soil microbial communities. – Ecology Letters 15: 1230-1239.
[9] Dinesh, R., Chaudhuri, S. G. (2013): Soil biochemical/microbial indices as ecological indicators of land use change in mangrove forests. – Ecological Indicators 32: 253-258.
[10] Elser, J. J., Sterner, R. W., Gorokhova, E., Fagan, W. F., Markow, T. A., Cotner, J. B., Harrison, J. F., Hobbie, S. E., Odell, G. M., Weider, L. J. (2000): Biological stoichiometry from genes to ecosystems. – Ecology Letters 3: 540-550.
[11] Fierer, N., Schimel, J. P., Holden, P. A. (2003): Variations in microbial community composition through two soil depth profiles. – Soil Biology & Biochemistry 35: 167-176.

http://www.aloki.hu ● ISSN 1589 1623 (Print) ● ISSN1785 0037 (Online)
DOI: http://dx.doi.org/10.15666/aeer/2005_43774389

[12] Gallaher, R. N., Weldon, C. O., Boswell, F. C. (1976): A semi-automated procedure for total nitrogen in plant and soil samples. – Soil Science Society of America Journal 40: 887-889.
[13] Harrison, J. A., Seitzinger, S. P., Bouwman, A. F., Caraco, N. F., Beusen, A. H. W., Vorosmarty, C. J. (2005): Dissolved inorganic phosphorus export to the coastal zone: Results from a spatially explicit, global model. – Global Biogeochemical Cycles 19(4).
[14] Hartzell, J. L., Jordan, T. E. (2012): Shifts in the relative availability of phosphorus and nitrogen along estuarine salinity gradients. – Biogeochemistry 107: 489-500.
[15] He, L., Rodrigues, J. L. M., Soudzilovskaia, N. A., Barcelo, M., Olsson, P. A., Song, C., Tedersoo, L., Yuan, F., Yuan, F., Lipson, D. A., Xu, X. (2020): Global biogeography of fungal and bacterial biomass carbon in topsoil. – Soil Biology & Biochemistry 151: 108024.
[16] Hu, M., Peñuelas, J., Sardans, J., Yang, X., Tong, C., Zou, S., Cao, W. (2019): Shifts in Microbial Biomass C/N/P Stoichiometry and Bacterial Community Composition in Subtropical Estuarine Tidal Marshes Along a Gradient of Freshwater–Oligohaline Water. – Ecosystems 23: 1265-1280.
[17] Huang, X., Liu, S., Wang, H., Hu, Z., Li, Z., You, Y. (2014): Changes of soil microbial biomass carbon and community composition through mixing nitrogen-fixing species with Eucalyptus urophylla in subtropical China. – Soil Biology & Biochemistry 73: 42-48.
[18] Huang, Y. M., Liu, D., An, S. S. (2015): Effects of slope aspect on soil nitrogen and microbial properties in the Chinese Loess region. – Catena 125: 135-145.
[19] Liu, X., Rashti, M. R., Dougall, A., Esfandbod, M., Van Zwieten, L., Chen, C. (2018): Subsoil application of compost improved sugarcane yield through enhanced supply and cycling of soil labile organic carbon and nitrogen in an acidic soil at tropical Australia. – Soil & Tillage Research 180: 73-81.
[20] Liu, S., Xie, Z., Zeng, Y., Liu, B., Li, R., Wang, Y., Wang, L., Qin, P., Jia, B., Xie, J. (2019): Effects of anthropogenic nitrogen discharge on dissolved inorganic nitrogen transport in global rivers. – Global change biology 25: 1493-1513.
[21] Luo, L., Wu, R., Gu, J. D., Zhang, J., Deng, S., Zhang, Y., Wang, L., He, Y. (2018): Influence of mangrove roots on microbial abundance and ecoenzyme activity in sediments of a subtropical coastal mangrove ecosystem. – International Biodeterioration & Biodegradation 132: 10-17.
[22] Luo, R., Luo, J., Fan, J., Liu, D., He, J.S., Perveen, N., Ding, W. (2020): Responses of soil microbial communities and functions associated with organic carbon mineralization to nitrogen addition in a Tibetan grassland. – Pedosphere 30: 214-225.
[23] McLeod, E., Chmura, G. L., Bouillon, S., Salm, R., Bjork, M., Duarte, C. M., Lovelock, C. E., Schlesinger, W. H., Silliman, B. R. (2011): A blueprint for blue carbon: toward an improved understanding of the role of vegetated coastal habitats in sequestering CO_2. – Frontiers in Ecology and the Environment 9: 552-560.
[24] Meng, L., Qu, F., Bi, X., Xia, J., Li, Y., Wang, X., Yu, J. (2021): Elemental stoichiometry (C, N, P) of soil in the Yellow River Delta nature reserve: Understanding N and P status of soil in the coastal estuary. – Science of The Total Environment 751: 141737.
[25] Ohtonen, R., Fritze, H., Pennanen, T., Jumpponen, A., Trappe, J. (1999): Ecosystem properties and microbial community changes in primary succession on a glacier forefront. – Oecologia 119: 239-246.
[26] Pires, A. C. C., Cleary, D. F. R., Almeida, A., Cunha, A., Dealtry, S., Mendonca-Hagler, L. C. S., Smalla, K., Gomes, N. C. M. (2012): Denaturing Gradient Gel Electrophoresis and Barcoded Pyrosequencing Reveal Unprecedented Archaeal Diversity in Mangrove Sediment and Rhizosphere Samples. – Applied and Environmental Microbiology 78: 5520-5528.
[27] Qu, W., Han, G., Wang, J., Li, J., Zhao, M., He, W., Li, X., Wei, S. (2021): Short-term effects of soil moisture on soil organic carbon decomposition in a coastal wetland of the Yellow River Delta. – Hydrobiologia 848: 3259-3271.

http://www.aloki.hu ● ISSN 1589 1623 (Print) ● ISSN1785 0037 (Online)
DOI: http://dx.doi.org/10.15666/aeer/2005_43774389

[28] Rawat, M., Arunachalam, K., Arunachalam, A. (2021): Seasonal dynamics in soil microbial biomass C, N and P in a temperate forest ecosystem of Uttarakhand, India. – Tropical Ecology 62: 377-385.
[29] Rousk, J., Brookes, P. C., Baath, E. (2009): Contrasting Soil pH Effects on Fungal and Bacterial Growth Suggest Functional Redundancy in Carbon Mineralization. – Applied and Environmental Microbiology 75: 1589-1596.
[30] Rovai, A. S., Twilley, R. R., Castaneda-Moya, E., Riul, P., Cifuentes-Jara, M., Manrow-Villalobos, M., Horta, P. A., Simonassi, J. C., Fonseca, A. L., Pagliosa, P. R. (2018): Global controls on carbon storage in mangrove soils. – Nature Climate Change 8: 534.
[31] Sardans, J., Penuelas, J. (2012): The role of plants in the effects of global change on nutrient availability and stoichiometry in the plant-soil system. – Plant Physiol 160: 1741-1761.
[32] Sistla, S. A., Appling, A. P., Lewandowska, A. M., Taylor, B. N., Wolf, A. A. (2015): Stoichiometric flexibility in response to fertilization along gradients of environmental and organismal nutrient richness. – Oikos 124: 949-959.
[33] Srivastava, P., Singh, R., Bhadouria, R., Tripathi, S., Raghubanshi, A. S. (2020): Temporal change in soil physicochemical, microbial, aggregate and available C characteristic in dry tropical ecosystem. – Catena 190: 104553.
[34] Tian, H. Q., Chen, G. S., Zhang, C., Melillo, J. M., Hall, C. A. S. (2010): Pattern and variation of C:N:P ratios in China's soils: a synthesis of observational data. – Biogeochemistry 98: 139-151.
[35] Tripathi, R., Shukla, A. K., Shahid, M., Nayak, D., Puree, C., Mohanty, S., Raja, R., Lal, B., Gautam, P., Bhattacharyya, P., Panda, B. B., Kumar, A., Jambhulkar, N. N., Nayak, A. K. (2016): Soil quality in mangrove ecosystem deteriorates due to rice cultivation. – Ecological Engineering 90: 163-169.
[36] Wang, G. P., Liu, J. S., Wang, J. D., Yu, J. B. (2006): Soil phosphorus forms and their variations in depressional and riparian freshwater wetlands (Sanjiang Plain, Northeast China). – Geoderma 132: 59-74.
[37] Wang, L., Wang, Y. P., Xu, C. X., An, Z. Y. (2012): Pollution Characteristics and Ecological Risk Assessment of Heavy Metals in the Surface Sediments of the Yangtze River. – Huanjing Kexue 33: 2599-2606.
[38] Wang, X. G., Lü, X. T., Han, X. G. (2014): Responses of nutrient concentrations and stoichiometry of senesced leaves in dominant plants to nitrogen addition and prescribed burning in a temperate steppe. – Ecological Engineering 70: 154-161.
[39] Wu, J., Joergensen, R. G., Pommerening, B., Chaussod, R., Brookes, P. C. (1990): Measurement of soil microbial biomass C by fumigation-extraction-an automated procedure. – Soil Biology & Biochemistry 22: 1167-1169.
[40] Xu, X., Thornton, P. E., Post, W. M. (2013): A global analysis of soil microbial biomass carbon, nitrogen and phosphorus in terrestrial ecosystems. – Global Ecology and Biogeography 22: 737-749.
[41] Xu, X., Schimel, J. P., Thornton, P. E., Song, X., Yuan, F., Goswami, S. (2014): Substrate and environmental controls on microbial assimilation of soil organic carbon: a framework for Earth system models. – Ecology Letters 17: 547-555.
[42] Yang, K., Zhu, J., Zhang, M., Yan, Q., Sun, O. J. (2010): Soil microbial biomass carbon and nitrogen in forest ecosystems of Northeast China: a comparison between natural secondary forest and larch plantation. – Journal of Plant Ecology 3: 175-182.
[43] Yang, W., Hao, F., Cheng, H., Lin, C., Ouyang, W. (2013): Phosphorus Fractions and Availability in an Albic Bleached Meadow Soil. – Agronomy Journal 105: 1451.
[44] Yao, L., Rashti, M. R., Brough, D. M., Burford, M. A., Liu, W., Liu, G., Chen, C. (2019): Stoichiometric control on riparian wetland carbon and nutrient dynamics under different land uses. – Science of the Total Environment 697: 134127.
[45] Yun, S., Li, D. Z., Li, H., Zou, Y., Ke, S. Z., Wang, C. Y., Sun, Y. B., Li, L. K., L. I., Zhao, L. Q. (2009): Characteristics of spatial distribution of soil organic matter and total nitrogen

http://www.aloki.hu ● ISSN 1589 1623 (Print) ● ISSN1785 0037 (Online)
DOI: http://dx.doi.org/10.15666/aeer/2005_43774389

as well as the influencing factors in three islands in Chongming. – Journal of Henan Agricultural University 43: 204-209.

[46] Zak, D. R., Holmes, W. E., White, D. C., Peacock, A. D., Tilman, D. (2003): Plant diversity, soil microbial communities, and ecosystem function: are there any links? – Ecology 84: 2042-2050.

[47] Zhang, T. J., Wang, Y. W., Wang, X. G., Wang, Q. Z., Han, J. G. (2009): Organic carbon and nitrogen stocks in reed meadow soils converted to alfalfa fields. – Soil & Tillage Research 105: 143-148.

[48] Zhao, M., Han, G., Li, J., Song, W., Qu, W., Eller, F., Wang, J., Jiang, C. (2020): Responses of soil CO_2 and CH_4 emissions to changing water table level in a coastal wetland. – Journal of Cleaner Production 269: 122316.

[49] Zhou, Y., Xu, J. F., Yin, W., Ai, L., Fang, N. F., Tan, W. F., Yan, F. L., Shi, Z. H. (2017): Hydrological and environmental controls of the stream nitrate concentration and flux in a small agricultural watershed. – Journal of Hydrology 545: 355-366.

[50] Zhou, Y., Zhang, Z., Li, J., Liu, X., Hu, G. (2020): Ecological Stoichiometry of Carbon, Nitrogen and Phosphorus in Plant Leaves and Soils of Mangrove Forests in the Beilun Estuary, Guangxi, China. – Earth and Environment 48: 58-65.

http://www.aloki.hu ● ISSN 1589 1623 (Print) ● ISSN1785 0037 (Online)
DOI: http://dx.doi.org/10.15666/aeer/2005_43774389

ESTIMATING THE PLANT NITROGEN CONTENT OF FOXTAIL MILLET (*SETARIA ITALICA* L.) BASED ON CONTINUOUS WAVELET ANALYSIS

XIA, F.[1,2] – FENG, M. C.[1,2*] – ZHU, S. A.[1,2] – WANG, C.[1,2] – MU, T. T.[1,2] – XIAO, L. J.[1] – YANG, W. D.[1,2] – ZHANG, M. J.[1] – SONG, X. Y.[1,2] – YANG, H.[3] – QIN, M. X.[4]

[1]*Agronomy College, Shanxi Agricultural University, Taigu 030800, Shanxi, China*

[2]*State Key Laboratory of Sustainable Dryland Agriculture (in preparation), Shanxi Agricultural University, Taiyuan 030000, Shanxi, China*

[3]*College of Information Science and Engineering, Shanxi Agricultural University, Taigu 030800, Shanxi, China*

[4]*College of Resource and Environment, Shanxi Agricultural University, Taigu 030800, Shanxi, China*

**Corresponding author*
e-mail: fmc101@163.com; phone: +86-138-3483-8834

(Received 21st Apr 2022; accepted 22nd Jul 2022)

Abstract. The variation in the plant nitrogen content (PNC) directly characterizes the growth of foxtail millet, and estimation of the PNC using hyperspectral techniques is important for effective evaluating the growth of this species. Effective statistical modeling methods can improve the accuracy and reliability of PNC estimates. In this study, field experiments were conducted under different gradients of organic fertilizer to develop an estimation model for determining the PNC in foxtail millet. The continuous wavelet transform (CWT) was used to process the collected reflection spectra and construct partial least square regression (PLSR), random forest (RF) and support vector machine (SVM) estimation models. Among the common wavelet families, Daubechies (db5), Coiflets (coif3), Biorthogonal (bior1.5), Symlets (sym8), haar and rbio3.1 were selected to analyze the correlation with the PNC, and all the wavelet functions had a good correlation with the PNC. The correlation coefficients were 0.834, -0.835, -0.973, -0.784, -0.789 and -0.770, respectively. The CWT technique can significantly improve the prediction accuracy of the PNC. The best PNC estimate was obtained using db5 (R^2_{cal} = 0.859, $RMSE_{cal}$ = 3.415), and the best decomposition scale was 2^4. In addition, the validation data indicate that db5-RF can be used to estimate the PNC (R^2_{val} = 0.935, $RMSE_{val}$ = 1.311, RPD_{val} = 3.32). This study provides a reference for the practical application of PNC analysis in foxtail millet.
Keywords: *hyperspectral data analysis, wavelet transform, partial least square regression, support vector machine, random forest*

Abbreviations: R^2_{cal}, coefficient of determination of the calibration set; $RMSE_{cal}$, root mean square error of the calibration set; R^2_{val}, coefficient of determination of the validation set; $RMSE_{val}$, root mean square error of the validation set; RPD_{val}: residual prediction deviation of the validation set

Introduction

Foxtail millet (*Setaria italica* L.) is a healthy staple food originating in China and is listed as the most common small grain among Chinese crops (Lu et al., 2009). Foxtail millet has a short planting cycle, a high drought tolerance, and a strong ability to adapt to adverse climate conditions; it is widely cultivated in arid and semiarid regions of the world, especially in China and India (Mahajan et al., 2021; Jia et al., 2013). Nitrogen, an essential nutrient for crops, has an important influence on crop photosynthesis and

http://www.aloki.hu ● ISSN 1589 1623 (Print) ● ISSN 1785 0037 (Online)
DOI: http://dx.doi.org/10.15666/aeer/2005_43914407

quality. Therefore, real-time adjustment of the nitrogen supply is an important task to ensure that cereal crops grow well and produce high quality and stable yields, while an effective, non-destructive, and low-cost method or tool for measuring the nitrogen content in the field is also a key step in accurate fertilization (Bechlin et al., 2014; Eitel et al., 2014; Mao et al., 2015).

In recent years, many methods have been used to determine the crop nitrogen status. The traditional method of determining the nitrogen status involves collecting samples from the field and analyzing them based on chemical methods. However, this method is characterized by hysteresis, destructiveness, and high costs (Dong et al., 2010; Tian et al., 2014). Compared with traditional sampling methods, remote sensing methods provide fast, non-destructive, and dynamic monitoring approaches for estimating the physiological parameters and nutrient levels of crops; these methods have attracted a substantial amount of attention in crop nitrogen monitoring (He et al., 2016; Clevers et al., 2017; Hong et al., 2018; Li et al., 2016).

A vegetation index has been used to successfully monitor the nitrogen content of winter wheat leaves (Feng et al., 2016). Tarpley et al. (2000) reported that the red edge position and the near-infrared band can be combined to accurately estimate the nitrogen content in cotton leaves. Ranjan et al. (2012) used hyperspectral remote sensing to build an estimation model of the nitrogen content of wheat leaves and aboveground nitrogen accumulation. The results showed that the estimation accuracy of the vegetation index for the leaf nitrogen content was better than that for aboveground nitrogen accumulation. Li et al. (2018c) analyzed the nutritional status of the leaf nitrogen content and plant nitrogen accumulation in winter wheat in different years and growth stages based on the N-PROSAIL model, and the results showed that this method can effectively estimate the nitrogen status of winter wheat. Stroppiana et al. (2009) estimated the nitrogen content of rice based on hyperspectral data and found that nitrogen regression constructed by using spectral reflectance information from the blue and green light bands can accurately reflect the nitrogen nutritional status of rice. However, the influence of the nitrogen content on crop spectra is hidden in the spectral signal, and the use of band screening or spectral indices (Datt, 1999) in spectral analysis methods leads to the loss of some hidden information in the hyperspectral data, resulting in a relatively low estimation accuracy.

The continuous wavelet transform (CWT) is an effective signal processing method (Blackburn et al., 2008); it uses a wavelet function to decompose spectral reflectance at different scales into a series of wavelet energy coefficients, and correlation analysis is then conducted with the physiological and biochemical parameters of crops (Tao et al., 2012). The wavelet coefficients obtained from spectral data and processing are not sensitive to background interference and the external environment and are highly correlated with physiological parameters. At the same time, the regression model between wavelet coefficients and physiological parameters can be established to improve the precision of the inversion model (Rivard et al., 2008). Ampe et al. (2013) established an estimation model of the chlorophyll content in inland water bodies based on continuous wavelet analysis, and the prediction accuracy of the model exceeded that of the traditional blue–green band ratio method. Wang et al. (2016) reported that SPAD can be estimated using the CWT method with a high coefficient of determination (coefficient of determination (R^2) = 0.7444, root mean square error (RMSE) = 7.359). Cheng et al. (2010) used the CWT to analyze a dataset of 47 plant species and compared it with the vegetation index analysis method. The estimation accuracy of the wavelet

http://www.aloki.hu ● ISSN 1589 1623 (Print) ● ISSN 1785 0037 (Online)
DOI: http://dx.doi.org/10.15666/aeer/2005_43914407

transform approach was much higher than that of the vegetation index-based method. Zhang et al. (2014) used the traditional wheat spectrum and the continuous wavelet characteristic spectrum to determine the physiological condition of wheat. The results showed that the physiological response of the wavelet characteristic spectrum to wheat was stronger than that of the original spectrum, and the proposed approach performed well in estimating the physiological potential. Continuous wavelet analysis adds a new dimension to the establishment of plant physiological parameter estimation models using spectral data (Cheng et al., 2014).

Hyperspectral remote sensing systems with different spectral, spatial, and temporal characteristics provide a large amount of hyperspectral data for the monitoring of nitrogen in cereal crops. However, hyperspectral data usually contain highly correlated bands, and cereal crop nitrogen monitoring models fitted directly with such data are prone to overfitting, which limits the accuracy of such models (Rivera-Caicedo et al., 2017; Thorp et al., 2017). In recent years, machine learning algorithms with higher accuracies have been used to solve the variable covariance problem to a large extent and deal with high-dimensional data (Marang et al., 2021). The effectiveness of machine learning algorithms has been proven in the field of hyperspectral research, and the advantages of theses algorithms, which include the support vector machine (SVM) (Chen et al., 2022) and random forest (RF) (Chen et al., 2020) algorithms, over multiple linear regression in describing the complex relationship between the crop nitrogen status and hyperspectral data are becoming increasingly clear (Tan et al., 2017; Zhou et al., 2018). Thus, this study aimed to clarify and create a monitoring method to estimate the plant nitrogen content PNC of foxtail millet on the basis of the CWT and the partial least square regression (PLSR), SVM and RF algorithms during the growth stages. An appropriate wavelet function was chosen to perform scale 2^1-2^{10} decomposition of the spectral reflectance to obtain the wavelet coefficients and perform correlation analysis. The PLSR, RF and SVM estimation models were constructed based on the optimal decomposition scales obtained from the CWT and the correlation analysis. The accuracy of the four models under different wavelet functions was explored, and the best wavelet function and model were determined to provide a foundation for the practical application of nitrogen content analysis in foxtail millet.

Materials and methods

Experimental design

The experiment was conducted in Shanyin County, Shuozhou city, Shanxi Province (39°11'-39°47' N, 112°25'-113°04' E) from May to October 2019. The local climate in this area is a temperate continental monsoon climate with an average annual temperature of approximately 7 °C and an average annual rainfall of 410 mm. The experiment adopted a split zone design, with the main zone including Jingu21 and Jingu28. The subsidiary zone was treated with sheep dung as an organic fertilizer (the recommended amount was 7881.8 kg·hm^{-2}, organic matter $\geq$ 50% and nitrogen, phosphorus and potassium $\geq$ 5%). The organic fertilizer applications were set as follows: T0: compound fertilizer control treatment (the recommended amount was 750 kg·hm^{-2}; the ratio of nitrogen to phosphorus to potassium was 24:10:6), T1: 5763.6 kg·hm^{-2}, T2: 7881.8 kg·hm^{-2}, T3: 10000 kg·hm^{-2} and T4: 0 kg·hm^{-2}. Each treatment was repeated three times.

http://www.aloki.hu ● ISSN 1589 1623 (Print) ● ISSN 1785 0037 (Online)
DOI: http://dx.doi.org/10.15666/aeer/2005_43914407

Foxtail millet canopy spectrum

The canopy spectra of foxtail millet at the four growth stages BBCH 32, 47, 55, and 70 (Bleiholder et al., 2001) were recorded. BBCH stands for Biologische Bundesanstalt, Bundessortenamt and Chemical industry. The BBCH-scale is based on the well-known cereal code developed by Zadoks et al. (1974). The canopy spectra of plants were determined using a portable FieldSpec Pro hyperspectral radiometer (FR2500, American Analytical Spectral Device, ASD). An ASD non-imaging spectrometer with a band range of 350-2500 nm and a field of view of 25° was used. The sampling interval from 350-1000 nm was 1.4 nm, and the spectral resolution was 3 nm. The sampling interval of the 1000-2500 nm spectrum was 2 nm, and the spectral resolution was 10 nm. To eliminate the influence of environmental conditions spectra were collected in clear and windless weather between 10:00 and 14:00 local time. The instrument was adjusted by white standard calibration each quarter, and the probe was oriented vertically downward at a vertical height of approximately 1 m from the canopy. Three representative sampling points were selected within the plot, ten readings were obtained for each point (n = 30), and the average value was used as the final spectrum of each plot.

PNC determination

The PNC was measured simultaneously with spectral measurements based on canopy spectroscopy. A total of 120 plant samples were used for PNC determination. The selected plants were desiccated at 105 °C for 30 min and then dried at 80 °C to constant weight. The sample was crushed and sieved, 0.5 g of powder was weighed, 5 mL of concentrated H_2SO_4 was added, and the resulting mixture was placed in a digestion oven at 370 °C. Hydrogen peroxide was used as a catalyst. The nitrogen concentration was measured with a Smart-chem 200 automatic chemical analyzer produced by Alliance in France.

CWT

Wavelet analysis can be used to decompose complex spectral signals into wavelet signals of different scales (frequencies). This method can be used to perform multiscale decomposition and mainly involves the extraction of information as a function of time and space frequencies. Wavelet transform types can be divided into the CWT and the discrete wavelet transform (DWT). When the DWT is used to analyze hyperspectral data, determining the output parameters is difficult. Therefore, this study used the CWT to transform the foxtail millet spectrum curves. The wavelet function scales and shifts can be obtained from the following equation (Lin et al., 2021):

$$\Psi_{a,b}(t) = \frac{1}{\sqrt{a}} \Psi\left(\frac{t-b}{a}\right) \quad \text{(Eq.1)}$$

where $\Psi_{a,b}(t)$ is the wavelet function; a is a scale factor; and b is a translation factor. The output of the CWT is given by the following:

$$Wf(a,b) \leq f; \Psi_{a,b} \geq \int_{-\infty}^{+\infty} f(t)\, \Psi_{a,b}(t) dt \quad \text{(Eq.2)}$$

http://www.aloki.hu ● ISSN 1589 1623 (Print) ● ISSN 1785 0037 (Online)
DOI: http://dx.doi.org/10.15666/aeer/2005_43914407

where $Wf(a_i, b_j)$ are the CWT coefficients of a two-dimensional wavelet power scalogram (j = 1, 2, …, n) that is composed of a noe-dimensional scale (i = 1, 2, …, m). *f(t)* is the hyperspectral reflectance data; and t is the spectral band. The wavelet function of the wavelet transform is not unique, the results of different wavelet functions are not the same, and the wavelet function is selected based on the support length, symmetry, vanishing moment, regularity and similarity. In this study, six common wavelet families (Daubechies (db5), Coiflets (coif3), Biorthogonal (bior1.5), Symlet (sym8), haar and rbio3.1) were selected to process the hyperspectral data (Virmani et al., 2013). The original reflectance spectrum data from the samples were decomposed with a 10-layer wavelet in MATLAB, and the decomposition scale of the CWT was set to 2^1, 2^2, 2^3..., and 2^{10}.

Model construction and verification

To evaluate the estimation accuracy and stability of the model, the R^2, RMSE, residual prediction deviation (RPD) and 1:1 line were used (Viscarra et al., 2007). The R^2 and RPD evaluation criteria are shown in *Table 1*. A 1:1 scatter plot was created to visually demonstrate the reliability of the PNC model. The formulas for R^2, RMSE and RPD are as follows (Wang et al., 2020a):

$$R^2 = 1 - \frac{\sum_{i=1}^{n}(y_i - x_i)^2}{\sum_{i=1}^{n}(y_i - \bar{y})^2} \quad \text{(Eq.3)}$$

$$RMSE = \sqrt{\frac{\sum_{i=1}^{n}(x_i - y_i)^2}{n}} \quad \text{(Eq.4)}$$

$$RPD = \frac{SD}{RMSE} \quad \text{(Eq.5)}$$

where n is the number of samples, x_i and y_i are the predicted value and the measured value respectively, $\bar{y}$ is the average of the measured value, and SD is the standard deviation.

Table 1. *Classification of the accuracy of the model based on the R^2 and RPD values*

Parameters	Model accuracy		
	Unacceptable	Acceptable	Excellent
R^2	＜0.50	0.50-0.75	＞0.75
RPD	＜1.40	1.40-2.00	＞2.00

Results

The PNC of foxtail millet

To visually present the characteristics of the PNC data for foxtail millet under the experimental conditions, descriptive statistical analysis was conducted (*Table 2*). For the 120 samples obtained, they were randomly divided into calibration set (n = 90) and validation set (n = 30) in a 3:1 ratio. The maximum values for the PNC correction set and the validation set are 34.042 and 34.052, and the minimum values are 7.134 and 8.006, respectively. The overall distance is large, so there are significant differences in

http://www.aloki.hu ● ISSN 1589 1623 (Print) ● ISSN 1785 0037 (Online)
DOI: http://dx.doi.org/10.15666/aeer/2005_43914407

the data. The skewness is 0.485 and 0.457, respectively. The lower kurtosis and skewness also indicate that the dataset as a whole has an approximately normal distribution and can be further used for modeling and data analysis.

Table 2. *Descriptive statistical analysis for the PNC of foxtail millet*

Data type	Number	Min	Max	Mean	SD	Skewness	Kurtosis
Calibration set	90	7.134	34.042	19.059	8.730	0.485	-0.243
Validation set	30	8.006	34.052	19.488	8.701	0.457	-0.306

Analysis of changes in foxtail millet spectral reflectance

Due to interference from other external factors, the spectral data from 1350-1400 nm, 1800-1950 nm, and 2450-2500 nm were eliminated and not used. *Figure 1* reveals the spectral changes in the canopy of Jingu21 and Jingu28 at different growth stages and fertilization rates. With the T4 treatment as an example, the canopy spectra of the two cultivars were different in different growth stages, but the change trend was similar. Additionally, the spectral reflectance in the near-infrared region in the booting stage and the heading stage was higher than that in the other two growth stages. The change in the canopy structure led to a decrease in the spectral reflectance. In the filling stage, the spectral reflectance of the canopy was lower than that in the other three growth periods (*Fig. 1A, B*).

Figure 1C, D shows the raw spectrum changes of two foxtail millet cultivars at the heading stage under different fertilization rates. The reflectivity decreases in the visible region and increases in the near-infrared region. In the near-infrared region, the reflectivity is as high as 37%-62%, which is mainly due to the multiple reflection scattering of the inner structure of the leaf. With the increase in the nutrient level of the organic fertilizer, the nitrogen content, leaf area index and biomass of the plants increased, and the material accumulation and cell tissue contents increased correspondingly. In addition, the vegetation coverage, palisade tissue thickness, spongy tissue thickness and leaf thickness increased, resulting in an increase in the near-infrared reflectance. The figure also shows that the spectral reflectance of different organic fertilizer nutrient levels has a small difference in the visible range, while the difference gradually becomes larger in the near infrared band. In the near-infrared region, the spectral reflectance of the Jingu21 canopy showed a trend of first increasing and then decreasing. The spectral reflectance of the Jingu28 was T0 > T3 > T2 > T1 > T4.

Based on the spectral data of 120 samples, the spectral reflectance of the canopy spectral of Jingu21 and Jingu28 under different treatments was analyzed for variance. The results are shown in *Figure 2*, in the near-infrared region, Jingu21 and Jingu28 had some difference in spectral reflectance under 5 treatments. At 710-139 nm, 1532-1799 nm, and 1951-2431 nm, the spectral reflectance of Jingu21 differed by up to 5% between different treatments. At 545-1322 nm and 1439-1514 nm, the spectral reflectance of Jingu28 differed significantly between different treatments. It can be seen that there were spectral characteristic differences between foxtail millet under different treatments, and they can be distinguished.

Correlation analysis between the raw spectrum and the PNC

The correlation between the PNC and the spectral reflectance was analyzed and is shown in *Figure 3*. The visible light region (440-716 nm) was positively correlated with

http://www.aloki.hu ● ISSN 1589 1623 (Print) ● ISSN 1785 0037 (Online)
DOI: http://dx.doi.org/10.15666/aeer/2005_43914407

the PNC. The minimum absolute value of the correlation coefficient (R) was 0.249 near 539 nm, and the maximum absolute R value was 0.762 in the 670 nm band. The correlation between the PNC and the raw spectrum reflectance was negative at 717-1349 nm. The maximum absolute R value was 0.592 when the band was 933 nm, and the R value varied widely in the near-infrared region (1350-2158 nm).

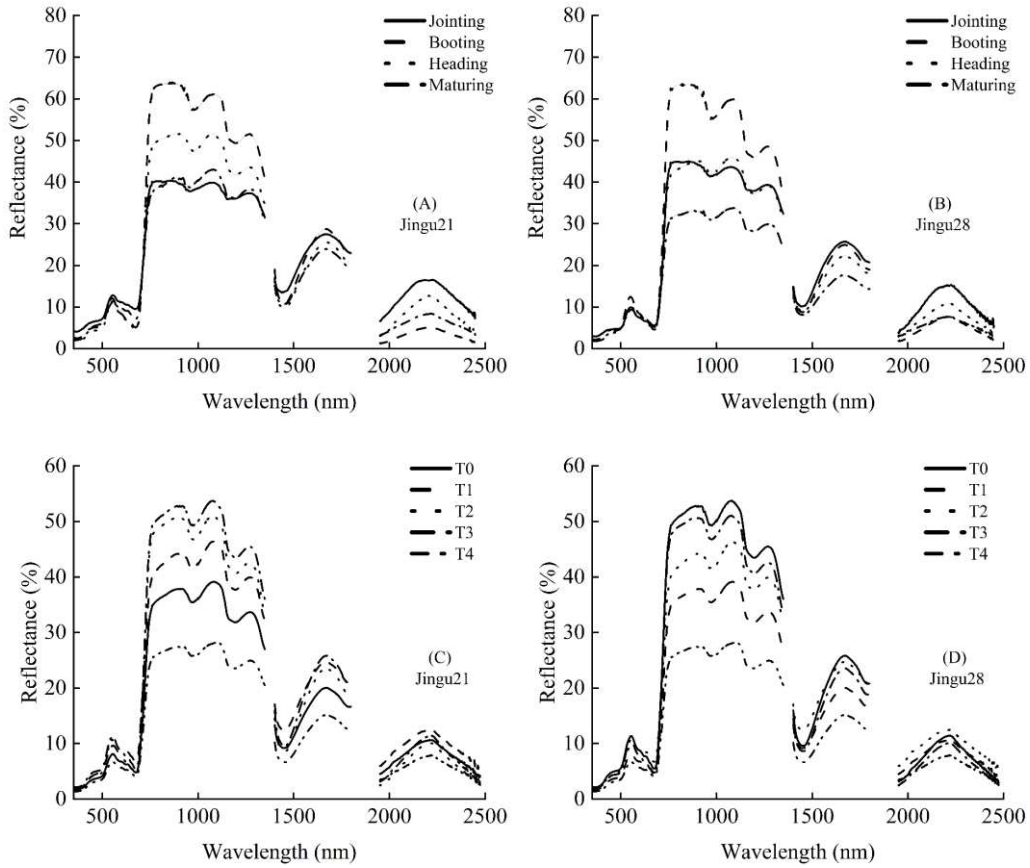

Figure 1. *Spectral curve changes of the two foxtail millet cultivars (Jingu21 and Jingu28). (A) and (B) represent the spectral curve changes at different growth and development stages. (C) and (D) represent the spectral curve changes of different organic fertilizer treatments*

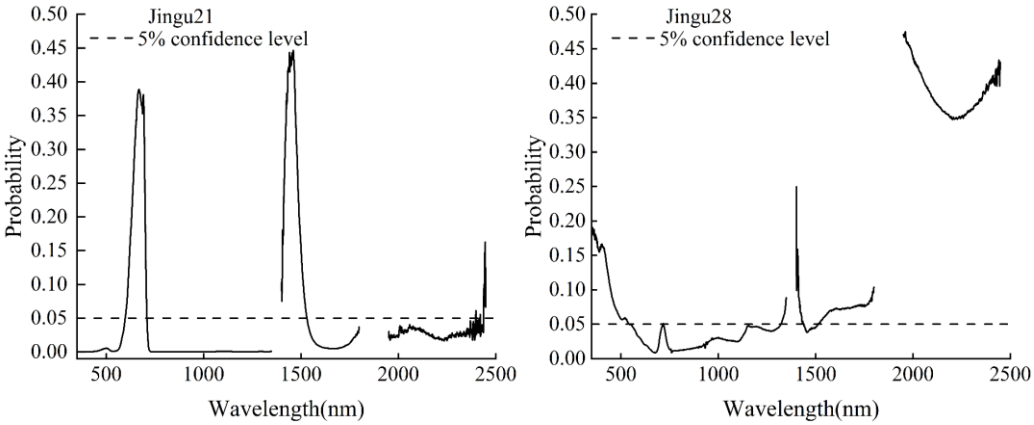

Figure 2. *Results of one-way ANOVA of foxtail millet canopy reflectance among the five treatments at different wavelength*

http://www.aloki.hu ● ISSN 1589 1623 (Print) ● ISSN 1785 0037 (Online)
DOI: http://dx.doi.org/10.15666/aeer/2005_43914407

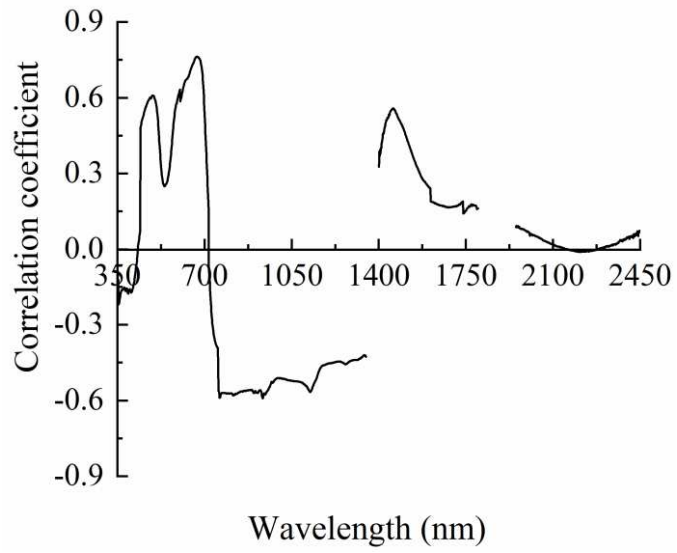

Figure 3. *Coefficient between the raw spectra and the PNC*

Correlation analysis of the wavelet coefficient and the PNC

The correlation between the wavelet coefficients obtained by db5, coif3, bior1.5, sym8, rbio3.1 and haar on the 2^1-2^{10} scale and the PNC was analyzed. The R value is expressed by the color depth in *Figure 4*. The correlation between the PNC and the wavelet coefficients is obviously positive and negative, and the difference in the R values among the different decomposition scales is obvious. Through the CWT, the detailed characteristic information related to the nitrogen content of foxtail millet was released layer by layer, and the wavelet coefficient information of each layer was different.

The maximum R value between the wavelet function and the PNC at different decomposition scales is shown in *Table 3*. bior1.5 showed the best correlation with the PNC, with an absolute value of 0.973 and a corresponding decomposition scale of 1. For coif3, db5, rbio3.1, sym8 and haar, the maximum absolute R values were 0.835, 0.834, 0.789, 0.784 and 0.770, respectively. The corresponding decomposition scales were 4, 4, 1, 4 and 2, respectively.

Table 3. *Comparison of the maximum R values between the wavelet coefficients and the PNC at different scales*

Decomposition scale	Maximum R					
	db5	**coif3**	**bior1.5**	**sym8**	**rbio3.1**	**haar**
2^1	-0.712	0.713	-0.973	-0.516	-0.789	-0.753
2^2	0.777	0.759	-0.809	0.628	-0.731	-0.77
2^3	0.793	0.804	-0.725	-0.721	-0.749	-0.729
2^4	0.834	-0.835	-0.737	-0.784	-0.724	-0.753
2^5	-0.827	0.805	-0.723	-0.722	-0.699	-0.717
2^6	0.698	0.709	-0.704	0.627	-0.655	-0.693
2^7	0.769	-0.626	-0.665	0.561	-0.538	-0.651
2^8	0.449	0.644	-0.505	-0.583	-0.432	-0.518
2^9	0.414	0.375	-0.431	0.353	-0.351	-0.425
2^{10}	-0.294	-0.293	-0.314	0.326	-0.191	-0.314

http://www.aloki.hu ● ISSN 1589 1623 (Print) ● ISSN 1785 0037 (Online)
DOI: http://dx.doi.org/10.15666/aeer/2005_43914407

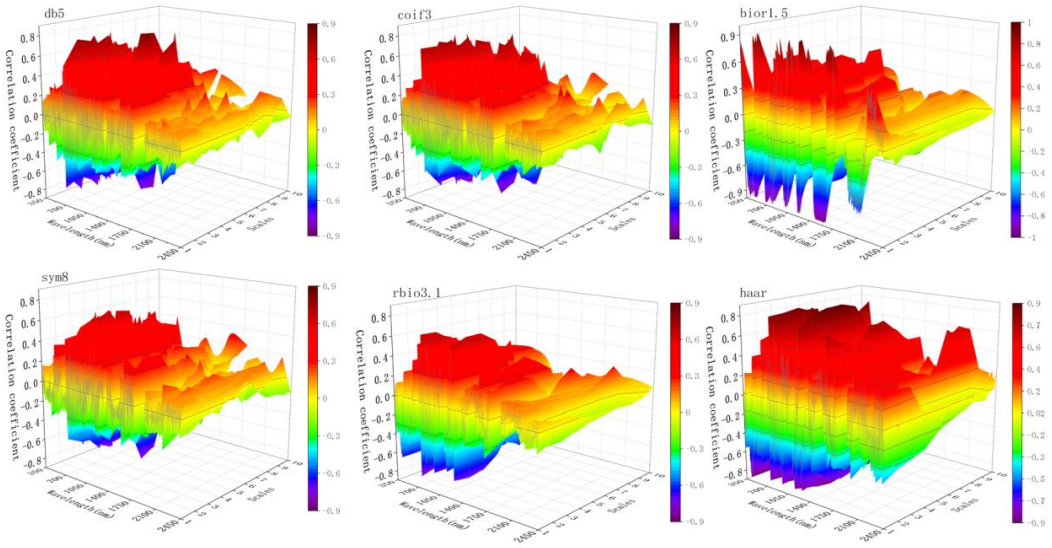

Figure 4. *Correlation analysis between the wavelet coefficients and the PNC based on six kinds of wavelet decomposition (n = 120)*

Establishment and verification of the PNC estimation model

The raw spectrum and CWT spectra were used as independent variables, and the PNC was used as a dependent variable; the PLSR, SVM and RF algorithms were used to characterize the relationship between the PNC and the spectral data. The results of the PNC model are shown in *Figure 5*. The results show that the predictive performances of the CWT spectra for the PNC compared to the raw spectrum and R^2, RMSE and RPD values were all significantly improved. However, significant differences were observed in the prediction accuracy of the different wavelet functions combined with the different machine learning algorithms. db5-RF, coif3-SVM, bior1.5-RF, sym8-RF, rbio3.1-SVM and haar-SVM had the best prediction performance. For the calibration dataset, the RPD values (RPD_{cal}) of the db5-RF, coif3-SVM, bior1.5-RF, sym8-RF, rbio3.1-SVM and haar-SVM models were 2.63, 2.34, 2.76, 2.14, 2.12 and 1.91, respectively, and these values were 168.36%, 60.27%, 181.63%, 118.37%, 45.21% and 30.82% higher than the corresponding values of the raw-spectrum model, respectively. For the validation dataset, the R^2 values (R^2_{val}) of the db5-RF, coif3-SVM, bior1.5-RF, sym8-RF, rbio3.1-SVM and haar-SVM models were 0.935, 0.890, 0.909, 0.874, 0.864 and 0.840, respectively, indicating that the estimation models have high degrees of fit and accuracy. Meanwhile, the RPD values of db5-RF, coif3-SVM, bior1.5-RF, sym8-RF, rbio3.1-SVM and haar-SVM were much greater than 2.0, indicating that these models have ideal predictive robustness and accuracy. Among them, the db5-RF model had the best prediction performance, with an RPD value of 3.32.

The measured and predicted values of the validated model were analyzed by the 1:1 line. As seen from the *Figure 6*, the sample points of both the measured and predicted values are basically distributed around the 1:1 line, and the model accuracy is high, indicating that these models can be used to estimate the PNC. The db5-RF model had the best prediction performance with an RPD value (RPD_{val}) of 3.32, indicating its ability to accurately estimate the PNC of foxtail millet. In summary, the SVM model with a 2^4-scale wavelet coefficient was obtained after db5 decomposition, and was the best model for establishing the canopy spectrum and nitrogen nutrition of foxtail millet.

http://www.aloki.hu ● ISSN 1589 1623 (Print) ● ISSN 1785 0037 (Online)
DOI: http://dx.doi.org/10.15666/aeer/2005_43914407

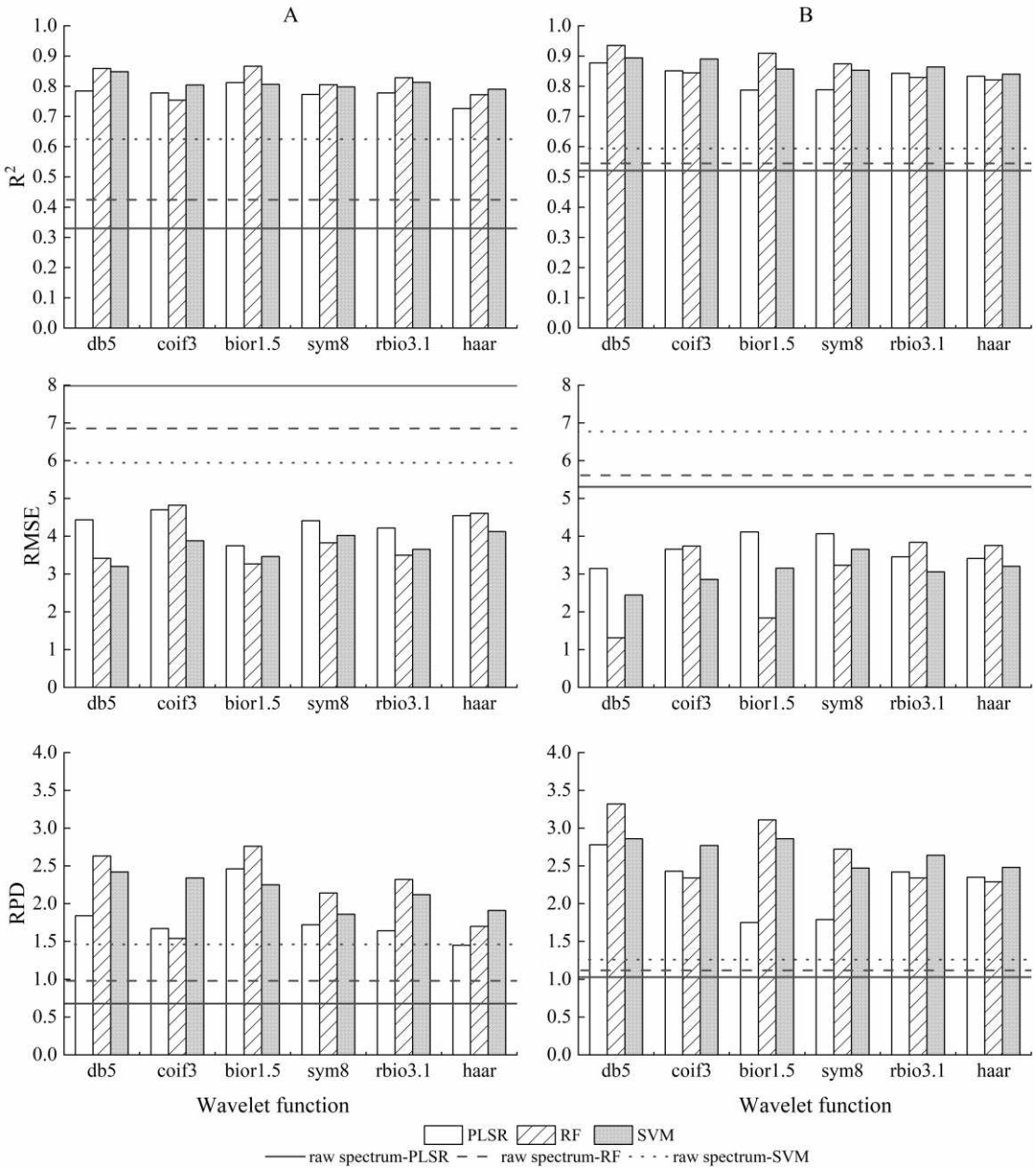

Figure 5. *The PNC model for foxtail millet (n = 120). A represents the calibration set, and B represents the validation set*

Discussion

Remote sensing-based crop phenotypic development provides a new way to monitor crop production and management, and the PNC can be remotely monitored to directly and quickly predict the photosynthetic performance and growth status of a plant using hyperspectral data (Jin et al., 2021; Weiss et al., 2020). In this study, the spectral reflectance of the foxtail millet canopy decreased gradually in the visible region and had a steep reflectance in the near-infrared region under different fertilization rates due to the application of the organic fertilizers, which affected the cellular structure of the vegetation leaves, removing the absorbing and scattering parts, and resulting in higher reflectivity values (Pinty et al., 2009). In the range of 740 to 1250 nm, the spectral

http://www.aloki.hu ● ISSN 1589 1623 (Print) ● ISSN 1785 0037 (Online)
DOI: http://dx.doi.org/10.15666/aeer/2005_43914407

reflectance of Jingu21 and Jingu28 performed differently under different treatments. The reason why the spectral reflectance of Jingu21 increased first and then decreased may be that with the increase of fertilizer, the phloem part of the leaves of foxtail millet decreased, and the utilization rate of photosynthetic products decreased (Cui et al., 2017). At the same time, the main stem of Jingu21 is 20-30 cm higher than that of Jingu28, and the fertilizer is too high, causing the foxtail millet to fall easily; Jingu28 has stronger tillering ability and need more nutrients, and its spectral reflectance increased with the increase of fertilizer amount. The stages of growth of a plant are associated with changes in cell structure, water content, biomass and function, which lead to changes in spectral reflectance during plant development (Bartlett et al., 2011; Li et al., 2014; Yu et al., 2014). Taking the T4 treatment as an example, the spectral reflectance first increased and then decreased with the progression of the growth stage and reached the maximum value at the booting stage. At this stage, the growth and development of foxtail millet are vigorous, photosynthesis is strengthened, and the ability of the plant to absorb nitrogen is enhanced, which affects the absorption and reflection of its canopy spectrum, thus leading to the strong absorption of visible light in this region. In addition, the reflectivity of the near-infrared region increases. In the near-infrared band, the water content of the plant increases its absorption and decreases its reflectivity (Im et al., 2008). This study showed that the spectral reflectance difference of foxtail millet under different treatments reached a significant level of 5%, which was consistent with Zhao et al. (2004). This may be due to the great influence of fertilization on various physiological and biochemical indices of foxtail millet, resulting in significant differences in the reflectance of the canopy spectral curve under different treatments (Serrano et al., 2000).

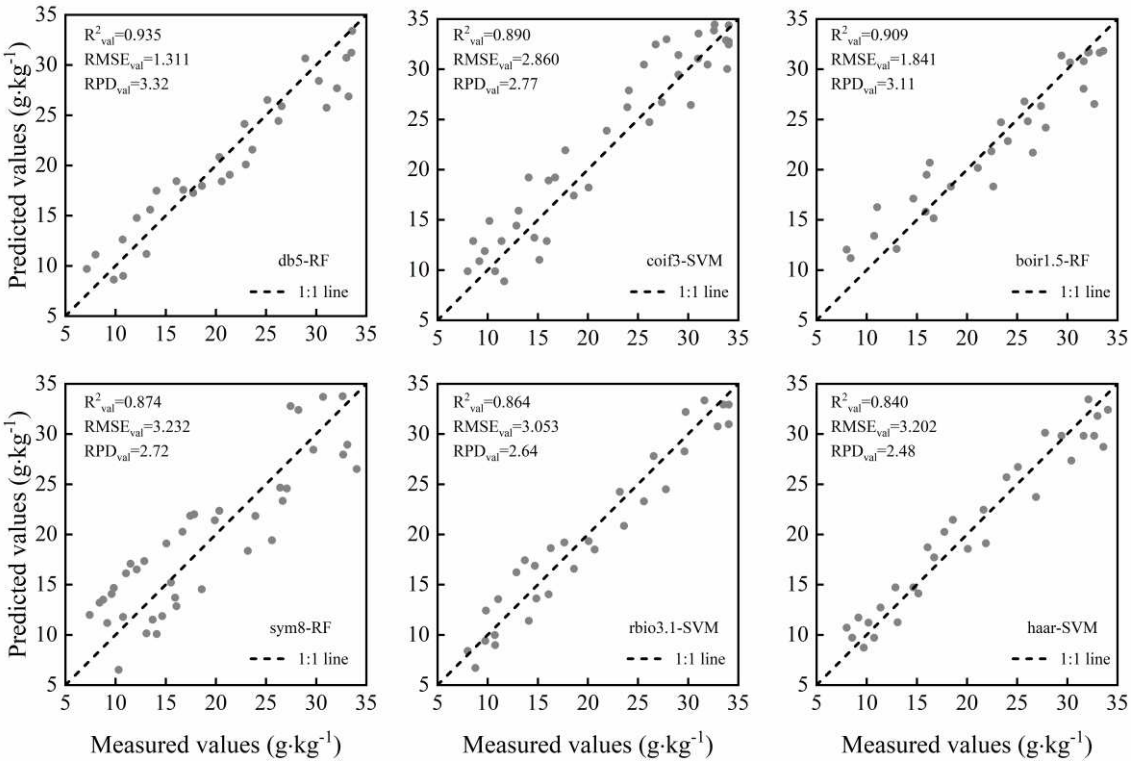

Figure 6. *Scatter plots of the measured and estimated PNCs of the validation set based on six kinds of wavelet functions (n = 30)*

http://www.aloki.hu ● ISSN 1589 1623 (Print) ● ISSN 1785 0037 (Online)
DOI: http://dx.doi.org/10.15666/aeer/2005_43914407

Many studies have shown that the PNC and the spectral reflectance have a good correlation (Guo et al., 2017; Boegh et al., 2021). In this study, we analyzed the correlation between the canopy spectra and the PNC and found that in the visible region, the nitrogen nutrition of foxtail millet was positively correlated with the spectral reflectance. However, in the near-infrared band region, the spectral reflectance was negatively correlated with nitrogen nutrition, which is consistent with the results of Alchanatis et al. (2005). The R value of the visible band was higher than that of the near-infrared band, which is mainly influenced by the canopy and the plant structure and does not reflect sensitivity to the PNC, while the visible band is sensitive to the PNC (Feng et al., 2008).

The wavelet coefficients obtained after the CWT decomposition showed a high correlation with the PNC because wavelet analysis can decompose hyperspectral data in space and frequency (Pinto et al., 2011; Zhang et al., 2020), and the physiological and biochemical composition of vegetation can be predicted by searching for optimal signals at different scales (He et al., 2018). Therefore, the CWT method can change the correlation of the PNC by decomposing the spectral data. The corresponding decomposition scales were found to appear before 2^8 when the R value between the six wavelet functions and the PNC was large. The results suggest that the CWT decomposition scale should be controlled at 2^8 in actual crop nitrogen monitoring. For each wavelet function, the maximum R value corresponds to a different decomposition scale.

The raw spectrum contains a large amount of information related to vegetation, but this information contains some redundancy (Fang et al., 2012), which makes the accuracy of the constructed models less than ideal. However, the CWT method can be used to further decompose the spectral data continuously, and the decomposed wavelet coefficients correspond to the raw spectrum. Thus, the fine signals in the spectral data can be extracted more effectively and the accuracy of the spectral monitoring model can be improved (Wang et al., 2020b). CWT spectral data can achieve a high accuracy in estimating chlorophyll, nitrogen, water, and photosynthetic rate data in vegetation, and such data are superior to the results of traditional methods (Liu et al., 2011; Koger et al., 2003; Yao et al., 2018). In this study, the CWT method was able to extract the weak spectral signal of foxtail millet well and achieve accurate estimation. These results are consistent with the results of previous studies (Li et al., 2018a, b). The different modeling results under different wavelet functions are shown in *Figure 5*, which is related to the nature of the wavelet functions. The performance of Daubechies (db5) in estimating the PNC of foxtail millet was the best. Therefore, the Daubechies family is recommended when estimating the PNC (Fu et al., 2020). However, this study was conducted under experimental conditions. Studies of each agronomic parameter and the different wavelet functions of foxtail millet for different regions, years, cultivars, and fertilization treatments are still needed to provide a theoretical basis to accurately estimate the growth of foxtail millet.

The SVM and RF algorithms, which have been successfully applied to estimate crop nitrogen levels can reveal the complicated nonlinear relationship between spectral characteristics and the crop nitrogen status (Marang et al., 2021). In this study, the SVM and RF models outperformed the PLSR model due to the presence of collinearity among the variables in the spectral data, which led to overfitting. Some overlapping spectral variables may contain invalid information for calibrating the model, such as noise and background, which can lead to inaccurate results. Therefore, a single approach for

http://www.aloki.hu ● ISSN 1589 1623 (Print) ● ISSN 1785 0037 (Online)
DOI: http://dx.doi.org/10.15666/aeer/2005_43914407

modeling the spectral data of vegetation is unfavorable, and optimized machine learning algorithms are increasingly used (Elsherbiny et al., 2021; Lu et al., 2020). However, spectral data contain many useless variables which can lead to complications in the models, and a relationship between the modeling approach and the data attributes may exist (Mehmood et al., 2012). The relationship between the variables and the modeling methods will be discussed in the future.

Conclusion

This study evaluated the performance of the PLSR, RF and SVM models of db5, coif3, bior1.5, sym8, rbio3.1 and haar in estimating PNC. Taking Jingu21 and Jingu28 as examples, the CWT method was performed on the raw spectrum at different decomposition scales to construct the PNC model. The results show that the model constructed by the CWT method is more accurate and reliable than the raw spectrum model. With the validation data, the R^2_{val} values of the db5-RF, coif3-SVM, bior1.5-RF, sym8-RF, rbio3.1-SVM and haar-SVM models were 0.935, 0.890, 0.909, 0.874, 0.864 and 0.840, respectively. The db5-RF model was found to perform the best (R^2_{val} = 0.935, $RMSE_{val}$ = 1.311, RPD_{val} = 3.32). The proposed method provides an intuitive way to monitor the nitrogen nutrient status of foxtail millet and thereby scientifically improve its quality and production.

Acknowledgements. This work was supported by the Research Program Sponsored by the State Key Laboratory of Sustainable Dryland Agriculture (in preparation), Shanxi Agricultural University (No. 202003-6), and the Key Research and Development Program of Shanxi Province, China (201903D211002-01, 201703D211001).

REFERENCES

[1] Alchanatis, V., Schmilovitch, Z., Meron, M. (2005): In-field assessment of single leaf nitrogen status by spectral reflectance measurements. – Precision Agriculture 6(1): 25-39.
[2] Ampe, E. M., Hestir, E. L., Bresciani, M., Salvadore, E. (2013): A wavelet approach for estimating chlorophyll a form inland waters with reflectance spectroscopy. – IEEE Geoscience and Remote Sensing Letters 11(1): 89-33.
[3] Bartlett, M. K., Ollinger, S. V., Hollinger, D. Y., Wicklein, H. F., Richardson, A. D. (2011): Canopy-scale relationships between foliar nitrogen and albedo are not observed in leaf reflectance and transmittance within temperate deciduous tree species. – Botany 89: 491-497.
[4] Bechlin, M. A., Fortunato, F. M., Silva, R. M. D., Ferreira, E. C., Neto, J. A. G. (2014): A simple and fast method for assessment of the nitrogen–phosphorus–potassium rating of fertilizers using high-resolution continuum source atomic and molecular absorption spectrometry. – Spectrochimica Acta Part B: Atomic Spectroscopy 101: 240-244.
[5] Blackburn, G., Ferwerda, J. (2008): Retrieval of chlorophyll concentration from leaf reflectance spectra using wavelet analysis. – Remote Sensing of Environment 112(4): 1614-1632.
[6] Bleiholder, H., Buhr, L., Eicke, H., Feller, C., Hack, H., Hess, M., Klose, R., Lancashire, P. D., MEIER, U., Stauss, R., Weber, E., von den Boom, T. (2001): Growth stages of mono- and dicotyledonous plants. – BBCH Monograph 158.
[7] Boegh, E., Soegaard, H., Broge, N., Hasager, C. B., Jensen, N. O., Schelde, K., Thomsen, A. (2021): Airborne multi-spectral data for quantifying leaf area index, nitrogen con-

http://www.aloki.hu ● ISSN 1589 1623 (Print) ● ISSN 1785 0037 (Online)
DOI: http://dx.doi.org/10.15666/aeer/2005_43914407

centration, and photosynthetic efficiency in agriculture. – Remote Sensing of Environment 81(2-3): 179-193.

[8] Chen, S., Hu, T., Luo, L., He, Q., Li, H. (2020): Rapid estimation of leaf nitrogen content in apple-trees based on canopy hyperspectral reflectance using multivariate methods. – Infrared Physics and Technology 111: 103542.

[9] Chen, D. S., Zhang, F., Tan, M. L., Chan, N. W., Shi, J. C., Liu, C. J., Wang, W. W. (2022): Improved Na^+ estimation from hyperspectral data of saline vegetation by machine learning. – Computers and Electronics in Agriculture 196: 106862.

[10] Cheng, T., Rivard, B., Sánchez-Azofeifa, G. A., Feng, J., Calvo-Polanco, M. (2010): Continuous wavelet analysis for the detection of green attack damage due to mountain pine beetle infestation. – Remote Sensing of Environment 114(4): 899-910.

[11] Cheng, T., RiañO, D., Ustin, S. L. (2014): Detecting diurnal and seasonal variation in canopy water content of nut tree orchards from airborne imaging spectroscopy data using continuous wavelet analysis. – Remote Sensing of Environment 143: 39-53.

[12] Clevers, J. G., Kooistra, L., Marnix, V. D. B. (2017): Using Sentinel-2 data for retrieving LAI and leaf and canopy chlorophyll content of a potato crop. – Remote Sensing 9(5): 405.

[13] Cui, J. H., Zhao, J., Meng, J., Liu, M., Zhao, Y., Song, S. J., Xia, X. Y., Li, S. G. (2017): Effect of ammonium nitrogen and nitrate nitrogen on the morphology and biomass of foxtail millet (*Setaria italic* L.). – Journal of Agricultural Science and Technology 19(10): 66-72.

[14] Datt, B. (1999): Visible/near infrared reflectance and chlorophyll content in Eucalyptus leaves. – International Journal of Remote Sensing 20(14): 2741-2759.

[15] Dong, S. K., Gong, Z. P., Wei, Z. U. (2010): Effects of nitrogen nutrition levels on N-accumulation and yields of soybean. – Plant Nutrition and Fertilizer Science 16: 65-70.

[16] Eitel, J. U. H., Magney, T. S., Vierling, L. A., Brown, T. T., Huggins, D. R. (2014): LiDAR based biomass and crop nitrogen estimates for rapid, non-destructive assessment of wheat nitrogen status. – Field Crops Research 159: 21-32.

[17] Elsherbiny, O., Fan, Y., Zhou, L., Qiu, Z. (2021): Fusion of feature selection methods and regression algorithms for predicting the canopy water content of rice based on hyperspectral data. – Agriculture 11(1): 51.

[18] Fang, Q., Tian, H. (2012): A review of hyperspectral remote sensing in vegetation monitoring. – Remote Sensing Technology and Application 13(1): 62-69.

[19] Feng, W., Yao, X., Zhu, Y., Tian, Y. C., Cao, W. X. (2008): Monitoring leaf nitrogen status with hyperspectral reflectance in wheat. – European Journal of Agronomy 28(3): 394-404.

[20] Feng, W., Zhang, H. Y., Zhang, Y. S., Qi, S. L., Guo, T. C. (2016): Remote detection of canopy leaf nitrogen concentration in winter wheat by using water resistance vegetation indices from in-situ hyperspectral data. – Field Crops Research 198: 238-246.

[21] Fu, Y., Yang, G., Li, Z., Li, H., Li, Z., Xu, X., Chen, L. (2020): Progress of hyperspectral data processing and modelling for cereal crop nitrogen monitoring. – Computers and Electronics in Agriculture 172: 105321.

[22] Guo, B. B., Qi, S. L., Heng, Y. R., Duan, J. Z., Zhang, H. Y., Wu, Y. P., Zhu, Y. J. (2017): Remotely assessing leaf N uptake in winter wheat based on canopy hyperspectral red-edge absorption. – European Journal of Agronomy 82: 113-124.

[23] He, L., Song, X., Feng, W., Guo, B. B., Zhang, Y. S., Wang, Y. H., Wang, C. Y., Guo, T. C. (2016): Improved remote sensing of leaf nitrogen concentration in winter wheat using multi-angular hyperspectral data. – Remote Sensing of Environment 174: 122-133.

[24] He, R. Y., Li, H., Qiao, X. J., Jing, J. B. (2018): Using wavelet analysis of hyperspectral remote-sensing data to estimate canopy chlorophyll content of winter wheat under stripe rust stress. – International Journal of Remote Sensing 39: 4059-4076.

http://www.aloki.hu ● ISSN 1589 1623 (Print) ● ISSN 1785 0037 (Online)
DOI: http://dx.doi.org/10.15666/aeer/2005_43914407

[25] Hong, S., Liu, N., Li, W., Chen, L., Yang, L., Li, M., Zhang, Q. (2018): Water content detection of potato leaves based on hyperspectral image. – IFAC-PapersOnLine 51(17): 443-448.
[26] Im, J., Jensen, J. R. (2008): Hyperspectral remote sensing of vegetation. – Geography Compass 2(6): 1943-1961.
[27] Jia, G. Q., Huang, X. H., Zhi, H., Zhao, Y., Zhao, Q., Li, W. J., Chai, Y., Yang, L. F., Liu, K. Y., Lu, H. Y., Zhu, C. R., Lu, Y. Q., Zhou, C. C., Fan, D. L., Weng, Q. J., Guo, Y. L., Huang, T., Zhang, L., Lu, T. T., Feng, Q., Hao, H. F., Liu, H. K., Li, P., Zhang, N., Li, Y. H., Guo, E. H., Wang, S. J., Wang, S. Y., Liu, J. R., Zhang, W. F., Chen, G. Q., Zhang, B. J., Li, W., Wang, Y. F., Li, H. Q., Zhao, B. H., Li, J. Y., Diao, X. M., Han, B. (2013): A haplotype map of genomic variations and genome-wide association studies of agronomic traits in foxtail millet (*Setaria italica*). – Nature Genetics 45: 957-961.
[28] Jin, X., Zarco-Tejada, P. J., Schmidhalter, U., Reynolds, M. P., Hawkesford, M. J., Varshney, R. K., Yang, T., Nie, C., Li, Z., Ming, B. O., Xiao, Y., Xie, Y., Li, S. (2021): High-throughput estimation of crop traits: A review of ground and aerial phenotyping platforms. – IEEE Geoscience and Remote Sensing Magazine 9(1): 200-231.
[29] Koger, C. H., Bruce, L. M., Shaw, D. R., Reddy, K. N. (2003): Wavelet analysis of hyperspectral reflectance data for detecting pitted morning glory (Ipomoea lacunose) in soybean (Glycine max). – Remote Sensing of Environment 86: 108-119.
[30] Li, F., Mistele, B., Hu, Y., Chen, X., Schmidhalter, U. (2014): Optimising three-band spectral indices to assess aerial N concentration, N uptake and aboveground biomass of winter wheat remotely in China and Germany. – ISPRS Journal of Photogrammetry and Remote Sensing 92: 112-123.
[31] Li, D., Wang, C., Liu, W., Peng, Z., Huang, S., Huang, J., Chen, S. (2016): Estimation of litchi (*Litchi chinensis* Sonn) leaf nitrogen content at different growth stages using canopy reflectance spectra. – European Journal of Agronomy 80: 182-194.
[32] Li, D., Wang, X., Zheng, H., Zhou, K., Yao, X., Tian, Y., Cheng, T. (2018b): Estimation of area and mass based leaf nitrogen contents of wheat and rice crops from water-removed spectra using continuous wavelet analysis. – Plant Methods 14(1): 1-20.
[33] Li, D., Cheng, T., Jia, M., Zhou, K., Lu, N., Yao, X., Cao, W. (2018a): PROCWT: Coupling PROSPECT with continuous wavelet transform to improve the retrieval of foliar chemistry from leaf bidirectional reflectance spectra. – Remote Sensing of Environment 206: 1-14.
[34] Li, Z., Jin, X., Yang, G., Drummond, J., Yang, H., Clark, B., Zhao, C. (2018c): Remote sensing of leaf and canopy nitrogen status in winter wheat (*Triticum aestivum* L.) based on N-PROSAIL model. – Remote Sensing 10(9): 1-18.
[35] Lin, D., Li, G., Zhu, Y., Liu, H., Jiao, Q. (2021): Predicting copper content in chicory leaves using hyperspectral data with continuous wavelet transforms and partial least squares. – Computers and Electronics in Agriculture 187: 106293.
[36] Liu, M., Liu, X., Ding, W., Wu, L. (2011): Monitoring stress levels on rice with heavy metal pollution from hyperspectral reflectance data using wavelet-fractal analysis. – International Journal of Applied Earth Observation and Geoinformation 13(2): 246-255.
[37] Lu, H. Y., Zhang, J. P., Liu, K. B., Wu, N. Q., Li, Y. M., Zhou, K. S., Ye, M. L., Zhang, T. Y., Zhang, H. J., Yang, X. Y., Shen, L. C., Xu, D. K., Li, Q. (2009): Earliest domestication of common millet (Panicum miliaceum) in East Asia extended to 10,000 years ago. – Proceedings of the National Academy of Sciences 106(18): 7367-7372.
[38] Lu, X., Zhang, S., Tian, Y., Li, Y., Wen, R., Tsou, J., Zhang, Y. (2020): Monitoring Suaeda salsa spectral response to salt conditions in coastal wetlands: A case study in dafeng elk national nature reserve, China. – Remote Sensing 12(17): 2700.
[39] Mahajan, P., Bera, M. B., Panesar, P. S., Chauhan, A. (2021): Millet starch: a review. – International Journal of Biological Macromolecules 180(3): 61-79.

http://www.aloki.hu ● ISSN 1589 1623 (Print) ● ISSN 1785 0037 (Online)
DOI: http://dx.doi.org/10.15666/aeer/2005_43914407

[40] Mao, H., Gao, H., Zhang, X., Kumi, F. (2015): Nondestructive measurement of total nitrogen in lettuce by integrating spectroscopy and computer vision. – Scientia Horticulturae 184: 1-7.
[41] Marang, I. J., Filippi, P., Weaver, T. B., Evans, B. J., Whelan, B. M., Bishop, T. F., Roth, G. (2021): Machine learning optimised hyperspectral remote sensing retrieves cotton nitrogen status. – Remote Sensing 13(8): 1428.
[42] Mehmood, T., Liland, K. H., Snipen, L., Sæbø, S. (2012): A review of variable selection methods in partial least squares regression. – Chemometrics and Intelligent Laboratory Systems 118: 62-69.
[43] Pinto, L. A., Galv˜ao, R. K. H., Araújo, M. C. U. (2011): Influence of wavelet transform settings on NIR and MIR spectrometric analyses of diesel, gasoline, corn and wheat. – Journal of the Brazilian Chemical Society 22(1): 179-186.
[44] Pinty, B., Lavergne, T., Widlowski, J. L., Gobron, N., Verstraete, M. (2009): On the need to observe vegetation canopies in the near-infrared to estimate visible light absorption. – Remote Sensing of Environment 113(1): 10-23.
[45] Ranjan, R., Chopra, U. K., Sahoo, R. N., Singh, A. K., Pradhan, S. (2012): Assessment of plant nitrogen stress in wheat (*Triticum aestivum* L.) through hyperspectral indices. – International Journal of Remote Sensing 33(20): 6342-6360.
[46] Rivard, B., Feng, J., Gallie, A., Sanchez-Azofeifa, A. (2008): Continuous wavelets for the improved use of spectral libraries and hyperspectral data. – Remote Sensing of Environment 112(6): 2850-2862.
[47] Rivera-Caicedo, J. P., Verrelst, J., Muñoz-Marí, J., Camps-Valls, G., Moreno, J. (2017): Hyperspectral dimensionality reduction for biophysical variable statistical retrieval. – ISPRS Journal of Photogrammetry and Remote Sensing 132: 88-101.
[48] Serrano, L., Filella, L., Penuelas, J. (2000): Remote sensing of biomass and yield of winter wheat under different nitrogen supplies. – Crop Science 40: 723 − 731.
[49] Stroppiana, D., Boschetti, M., Brivio, P. A., Bocchi, S. (2009): Plant nitrogen concentration in paddy rice from field canopy hyperspectral radiometry. – Field Crop Research 111(1-2): 119-129.
[50] Tan, K., Wang, S., Song, Y., Liu, Y., Gong, Z. (2017): Estimating nitrogen status of rice canopy using hyperspectral reflectance combined with BPSO-SVR in cold region. – Chemometrics and Intelligent Laboratory Systems 172: 68-79.
[51] Tao, C., Rivard, B., Sánchez-Azofeifa, A. G., Féret, J. B., Jacquemoud, S., Ustin, S. L. (2012): Predicting leaf gravimetric water content from foliar reflectance across a range of plant species using continuous wavelet analysis. – Journal of Plant Physiology 169(12): 1134-1142.
[52] Tarpley, L., Reddy, K. R., Sassenrath-Cole, G. F. (2000): Reflectance indices with precision and accuracy in predicting cotton leaf nitrogen concentration. – Crop Science 40(6): 1814-1819.
[53] Thorp, K. R., Wang, G., Bronson, K. F., Badaruddin, M., Mon, J. (2017): Hyperspectral data mining to identify relevant canopy spectral features for estimating durum wheat growth, nitrogen status, and grain yield. – Computers and Electronics in Agriculture 136: 1-12.
[54] Tian, Y. C., Gu, K. J., Chu, X., Yao, X., Cao, W. X., Zhu, Y. (2014): Comparison of different hyperspectral vegetation indices for canopy leaf nitrogen concentration estimation in rice. – Plant and Soil 376(1-2): 193-209.
[55] Virmani, J., Kumar, V., Kalra, N., Khandelwal, N. (2013): SVM-based characterization of liver ultrasound images using wavelet packet texture descriptors. – Journal of Digital Imaging 26(3): 530-543.
[56] Viscarra, R. A., Mcglynn, R. N., Mcbratney, A. B. (2007): Determining the composition of mineral-organic mixes using UV-VIS-NIR diffuse reflectance spectroscopy. – Geoderma 137(1/2): 70-82.

http://www.aloki.hu ● ISSN 1589 1623 (Print) ● ISSN 1785 0037 (Online)
DOI: http://dx.doi.org/10.15666/aeer/2005_43914407

[57] Wang, H. F., Huo, Z. G., Zhou, G. S., Liao, Q. H., Feng, H. K., Wu, L. (2016): Estimating leaf SPAD values of freeze-damaged winter wheat using continuous wavelet analysis. – Plant Physiology and Biochemistry Ppb 98: 39-45.
[58] Wang, G. D., Wang, Q. X., Su, Z. L., Zhang, J. H. (2020a): Predicting copper contamination in wheat canopy during the full growth period using hyperspectral data. – Environmental Science and Pollution Research 27(31): 39029-39040.
[59] Wang, Z., Chen, J., Fan, Y., Cheng, Y., Wu, X., Zhang, J., Yang, F. (2020b): Evaluating photosynthetic pigment contents of maize using UVE-PLS based on continuous wavelet transform. – Computers and Electronics in Agriculture 169: 105160.
[60] Weiss, M., Jacob, F., Duveiller, G. (2020): Remote sensing for agricultural applications: A meta-review. –Remote Sensing of Environment 236: 111402.
[61] Yao, X., Si, H. Y., Cheng, T., Jia, M., Chen, Q., Tian, Y. C., Zhu, Y., Cao, W. X., Chen, C. Y., Cai, J. Y., Gao, R. R. (2018): Hyperspectral estimation of canopy leaf biomass phenotype per ground area using a continuous wavelet analysis in wheat. – Frontiers in Plant Science 9: 1360.
[62] Yu, K., Lenz-Wiedemann, V., Chen, X., Bareth, G. (2014): Estimating leaf chlorophyll of barley at different growth stages using spectral indices to reduce soil background and canopy structure effects. – ISPRS Journal of Photogrammetry and Remote Sensing 97: 58-77.
[63] Zadoks, J. C., Chang, T. T., Konzak, C. F. (1974): A decimal code for the growth stages of cereals. – Weed Research 14(6): 415-421.
[64] Zhang, J., Yuan, L., Pu, R., Loraamm, R. W., Yang, G., Wang, J. (2014): Comparison between wavelet spectral features and conventional spectral features in detecting yellow rust for winter wheat. – Computers and Electronics in Agriculture 100: 79-87.
[65] Zhang, J. Y., Sun, H., Gao, D. H., Qiao, L., Liu, N., Li, M. Z., Zhang, Y. (2020): Detection of canopy chlorophyll content of corn based on continuous wavelet transform analysis. – Remote Sensing 12(17): 2741.
[66] Zhao, D. H., Li, J. L., Song, Z. J., Qi, J. G. (2004): Difference of canopy spectral reflectance to nitrogen nutrient in cotton with different nitrogen applications. – Acta Agronomica Sinica 30(11): 1169-1172.
[67] Zhou, K., Cheng, T., Zhu, Y., Cao, W., Ustin, S. L., Zheng, H., Tian, Y. (2018): Assessing the impact of spatial resolution on the estimation of leaf nitrogen concentration over the full season of paddy rice using near-surface imaging spectroscopy data. – Frontiers in Plant Science 9: 964.

http://www.aloki.hu ● ISSN 1589 1623 (Print) ● ISSN 1785 0037 (Online)
DOI: http://dx.doi.org/10.15666/aeer/2005_43914407

SEASONAL DEVELOPMENT OF TREE SPECIES IN URBAN AND PERI-URBAN FORESTS IN DROUGHT

FEDOROV, N. I.[1,2] – ZHIGUNOVA, S. N.[1,2*] – MARTYNENKO, V. B.[1] – MIKHAYLENKO, O. I.[2]

[1]*Ufa Institute of biology - Subdivision of the Ufa Federal Research Centre of the Russian Academy of Sciences, Prospect Oktyabrya, 69, Ufa 450054, Russia*
(phone: +7-347-235-62-47; fax: +7-347-235-62-47)

[2]*Ufa State Petroleum Technological University, Kosmonavtov St., building 1, 1, Ufa 450062, Russia*
(phone: +7-347-242-03-70; fax: +7-347-243-14-19)

[*]*Corresponding author*
e-mail: Zigusvet@yandex.ru; phone: 8-965-923-04-92

(Received 29th Apr 2022; accepted 22nd Jul 2022)

Abstract. Our study aimed to analyze the impact of extreme drought on the phenological development of *Pinus sylvestris* L. and *Quercus robur* L. forests in Ufa city (Bashkortostan Republic, Russia) and outside it. The study area is located in the northern part of the forest-steppe subzone of the temperate climate zone. The vegetation indices NDVI, GNDVI, and CVI were calculated from cloudless Landsat images for the growing season in the dry year of 2010 and time series of 2008-2017, and they were used to analyze the phenological development of forest vegetation. To plot phenology, we used the Bayesian LSP script which uses Landsat time series data and a Bayesian hierarchical model. Higher temperatures in the city led to the higher pace at the beginning of seasonal development of pine and oak forests. The tendency for the seasonal development of forests outside the city to delay continued in the dry year. At the same time, in the dry year in pine forests both in the city and outside the city the delay of phenological development began earlier than in oak forests. Pine forests respond to a long period of water scarcity more noticeably than oak forests, which is substantially due to the features of root systems of *Quercus robur* that allow them to use deeper moisture reserves.
Keywords: *Pinus sylvestris, Quercus robur, temporal dynamics of vegetation indices, NDVI, GNDVI, CVI, Landsat TM, ETM+, OLI/TIRS*

Introduction

Currently, humanity observes significant climatic changes, which are indicated not only in changes in the temperature regime and redistribution of the summer and winter precipitation, but also in an increase in the frequency of extreme weather events (Karl et al., 1995; Beniston, 2004; Walsh et al., 2020; Cheng et al., 2021; Matkala et al., 2021). Forest communities strongly respond to climate variability (Barber et al., 2000; Lloyd and Fastie, 2002; Hirota et al., 2011), including such extreme weather events as droughts (Martínez-Vilalta and Piñol, 2002; Bigler et al., 2006; Pasho et al., 2011). Droughts can cause deterioration of trees, outbreaks of insect pests and infectious diseases of forest trees, increase in the frequency of forest fires, and other types of stress (Singatullin, 2017; Gulácsi and Kovács, 2018; Hais et al., 2019; Vanhellemont et al., 2019; Avetisyan et al., 2021; Moreno-Fernández et al., 2021; Rohner et al., 2021). Many studies show various cases of forest stand death due to severe drought stress (Pedersen, 1998; Allen et al., 2010; Williams et al., 2010, 2013; Liu et al., 2013; Moreno-Fernández et al., 2021). The vegetation seasonality reflects the reaction of species to inter-annual climate variability, including air temperature variability, daylight hours, and the soil moisture content

http://www.aloki.hu ● ISSN 1589 1623 (Print) ● ISSN 1785 0037 (Online)
DOI: http://dx.doi.org/10.15666/aeer/2005_44094427

(Kramer et al., 2000; Zhang et al., 2005). The influence of drought is primarily manifested in the change in the rhythm of the seasonal development of plants and in the decrease in their productivity (Ahl et al., 2006; Gaertner et al., 2019). Therefore, vegetation phenology is an effective bioindicator of the extreme weather events and a key parameter for understanding and modeling vegetation-climate interactions (Menzel, 2002; Crucifix et al., 2005). Few studies have addressed the relationship between forest dieback and phenological indicators derived from satellite imagery, despite phenology being the main indicator of the interactions between climate and vegetation. A good tool for studying the influence of stress factors on vegetation phenology is the use of various vegetation indices (NDVI, GNDVI, EVI, CVI, PRI, etc.) calculated from the spectral channels of satellite images (Soudani et al., 2008; Fedorov et al., 2019a,b). For example, vegetation indices were used to study the response of trees to drought in temperate deciduous forests (Hwang et al., 2017), to detect forest stress from outbreaks of European spruce bark beetle (Huo et al., 2021), to study inter-annual changes in the productivity of Mediterranean forests in Italy depending on the start of the dry season (Maselli et al., 2014), to assess the drought impact on the productivity of Mediterranean forests in central Chile (Miranda et al., 2020), to study drought resilience of rangelands in southern Cyprus (von Keyserlingk et al., 2021), etc. Most studies used medium- and high-resolution satellite images (MODIS, Landsat, Sentinel).

Urban environment is a specific type of vegetation habitat, and its influence on the temperature regime (the urban heat island) has been well studied (Xian and Crane, 2006; Imhoff et al., 2010; Li et al., 2011; Weng, 2012). This effect is caused by the high proportion of impervious surfaces in cities (asphalt and concrete pavements, building roofs), the low ventilation capacity of urban canyons formed by high-rise buildings, and the heat generated by urban transport (Akbari et al., 2016). The difference in temperature between the city and the suburban areas averages 1-3 °C, however sometimes it can reach 7-15 °C (Tzavali et al., 2015; Aleksashina and Le, 2018). The urban heat island effect decreases with an increase of green areas in the cities (Yuan and Bauer, 2007; Hu and Brunsell, 2013; Anniballe et al., 2014; Zhang et al., 2020). Higher air and ground temperatures in the city affect the rhythm of seasonal vegetation development (Li et al., 2017; Zhigunova et al., 2018). For different tree species the influence of the urban heat island effect on the seasonal development can appear in varying degrees and it depends, among other things, on climate variability. This issue is poorly covered in the literature because of the complexity of the selection sites. They have to include urban and peri-urban forests with tree stands similar in composition and age which would be of sufficient size to study using medium and high resolution satellite images. Otherwise, the pixel size of the satellite raster tile is larger than the studied vegetation sites (Weng et al., 2014). A good option would be to use ultra-high resolution satellite images. However, their use is limited by the low availability in the necessary quantities for the studies of phenological development of the vegetation (Yuan and Bauer, 2007; Zhan et al., 2013; Weng et al., 2014).

Extreme droughts occur in the Southern Urals periodically, and the last one happened in 2010 (Kucherov et al., 2016; Singatullin, 2017). Our previous research has shown that the seasonal development of oak and pine forests in the city and outside it differs significantly (Zhigunova et al., 2018). However, it was not clear how urban heat island-influenced forest ecosystems in the city and forest ecosystems outside the city would respond to extreme drought. The aim of our study was to analyze the impact of the extreme drought of 2010 on the features of the phenological development of pine and oak

http://www.aloki.hu ● ISSN 1589 1623 (Print) ● ISSN 1785 0037 (Online)
DOI: http://dx.doi.org/10.15666/aeer/2005_44094427

forests in the city and outside it, based on the analysis of vegetation indices calculated from the Landsat TM, ETM +, OLI/TIRS.

Materials and Methods

Study area

The Ufa city (Bashkortostan Republic, Russia) is located in the northern part of the forest-steppe subzone of the temperate zone. The climate is moderately continental, relatively humid. The average temperature in January is -12.3 °C and in July is 19.7 °C. The average annual air temperature is 3.8 °C. The average annual precipitation is 589 mm (www.pogodaiklimat.ru). The climate contributed to the spread of oak-linden forests (*Quercus robur* L. and *Tilia cordata* Mill.) which were the main vegetation type in the interfluve of Ufa and Belaya rivers, currently occupied by the Ufa city. The remains of these forests have been preserved in the park areas of the city. *Pinus sylvestris* L. is often used for landscaping in the city, and is also used for reforestation outside it. In this regard, we selected for our study the forest sites in the city and in the peri-urban area that are homogeneous in composition and age with the dominance of *Q. robur* and *P. sylvestris* (*Fig. 1*). The average age of *Q. robur* in different sites in 2010 ranged from 80 to 85 years. The age of *P. sylvestris* in 2010 was 65 and 70 years. No silvicultural activities have been carried out in the sites in the period between the years under consideration. The main factor of the pollution in the area of sites is urban transportation. However, the sites in the urban area were located within the forests at a distance of more than 100 meters from the forest border.

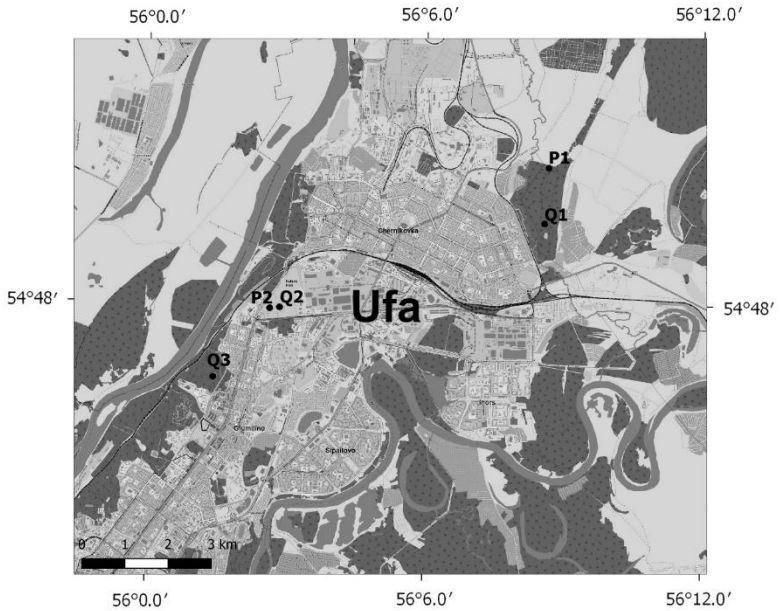

Figure 1. *Location of sites dominated by Quercus robur L. (Q1, Q2, Q3) and Pinus sylvestris L. (P1, P2) in the Ufa city and outside it*

Three oak forest sites and two pine forest sites were selected:

Q1 – an oak forest site with an area of 2.45 hectares outside the city. The coordinates of the center of the site are: 54 ° 49'0 "N, 56 ° 8'34" E. The exposure of the site is South-

http://www.aloki.hu ● ISSN 1589 1623 (Print) ● ISSN 1785 0037 (Online)
DOI: http://dx.doi.org/10.15666/aeer/2005_44094427

Southwest with a 3 ° slope. The forest stand is dominated by *Quercus robur*. The tree layer consists of *Q. robur* (80%), *Acer platanoides* L. (10%), and *Ulmus glabra* Huds. (10%). Tree ground cover is 35%, undergrowth ground cover is 60%. The undergrowth mainly consists of *Acer platanoides*, *Quercus robur*, *Ulmus glabra*, *Padus avium* Mill., *Sorbus aucuparia* L.

Q2 – an oak forest site with an area of 0.73 hectares in the city park. The coordinates of the center of the site are: 54°47'56" N, 56°2'52" E. The exposure is South-Southwest with a 2 ° slope. The tree layer consists of *Quercus robur* (80%) and *Tilia cordata* (20%). Tree ground cover is 45%, undergrowth ground cover is 40%. The undergrowth mainly consists of *Ulmus glabra*, *Acer platanoides*, *Sorbus aucuparia*, and *Corylus avellana* L.

Q3 – an oak forest site with an area of 0.68 hectares in the city park. The coordinates of the center of the site are: 54°47'8" N, 56°1'19" E. The exposure is South with a 26 ° slope. The tree layer consists of *Quercus robur* (80%) and *Acer platanoides* (20%). Tree ground cover is 40%, undergrowth ground cover is 60%. The undergrowth mainly consists of *A. platanoides*, *Euonymus verrucosa* Scop.

P1 – a pine forest site with an area of 1.23 hectares outside the city. The coordinates of the center of the site are: 54°49'44" N, 56°8'39" E. The exposure of the site is West-Northwest with a 3 ° slope. The tree layer consists of *Pinus sylvestris* with the addition of *Tilia cordata*. Tree ground cover is 50%, undergrowth ground cover is 25%. The undergrowth mainly consists of *Sorbus aucuparia*, *Acer platanoides*, *Tilia cordata*, *Padus avium*, *Euonymus verrucosa*, and *Corylus avellana*.

P2 – a pine forest site with an area of 0.70 hectares in the city park. The coordinates of the center of the site are: 54°47'55" N, 56°2'39" E. The exposure of the site is Southeast with a 1 ° slope. The tree layer consists of *Pinus sylvestris*. Tree ground cover is 50%, undergrowth ground cover is 50%. The undergrowth mainly consists of *Acer platanoides*, *Sorbus aucuparia*, *Ulmus glabra*, *Acer negundo* L., *Corylus avellana*, *Euonymus verrucosa*.

The analysis of the seasonal development of tree species

To analyze the seasonal development of oak and pine forests, we selected vegetation indices which, according to literature data, are often used to analyze inter-annual differences in the phenology of tree species. Five vegetation indices are often used in these studies (NDVI, GNDVI, EVI, CVI, PRI) and they are calculated from high and medium resolution satellite images (Li et al., 2019; Ochtyra et al., 2020; Dixon et al., 2021). Thus, in the study of the forests in central Indiana, USA, the vegetation indices NDVI and EVI were used to identify the trees with isohydric and anisohydric behavior in response to drought (Hwang et al., 2017). The authors calculated vegetation indices based on MODIS satellite images, which had sufficient quantity due to the high frequency of the passages of this satellite. We used Landsat satellite images of different generations (TM, ETM+, OLI/TIRS) due to the small size of the sites. These satellites have a temporal resolution of 16 days and some of the images were discarded due to the presence of clouds. Between Landsat satellites of different generations, there are between-sensor differences in the reflectance of individual channels used to calculate vegetation indices (Chen et al., 2021). The studies by Chen et al. show, that the between-sensor differences are more significant when calculating EVI than when calculating NDVI. Therefore, the direct application of the EVI is questionable when analyzing time series based on Landsat data of different generations (Chen et al., 2021). We could not calculate the PRI, which captures the response of woody species to drought well (Hwang et al., 2017; Wong et al.,

http://www.aloki.hu ● ISSN 1589 1623 (Print) ● ISSN 1785 0037 (Online)
DOI: http://dx.doi.org/10.15666/aeer/2005_44094427

2019), since the spectral ranges used in PRI calculation (0.53 and 0.57 mkm) are within the same spectral channel in the Landsat imagery. Therefore, in this study we used three vegetation indices: NDVI, GNDVI, and CVI.

NDVI (Normalized Difference Vegetation Index) is most often used to study the phenology of forest and herbaceous vegetation (Berra et al., 2019; Fedorov et al., 2019a,b; Dixon et al., 2021). The index is based on the ability of vegetation to absorb electromagnetic waves in the visible red light (RED) and reflect them in the near-infrared light (NIR). It is calculated using the formula:

$$NDVI = \frac{NIR - RED}{NIR + RED} \quad \text{(Eq.1)}$$

Chlorophyll strongly absorbs visible red light while the cell structure of the leaves strongly reflects near-infrared light. NDVI can become oversaturated in dense vegetation conditions when the leaf area index (LAI) becomes high.

GNDVI (Green Normalized Difference Vegetation Index) is widely used to study the phenology of vegetation and its response to various stress factors (Gitelson and Merzlyak, 1998; Ahamed et al., 2011; Liu and Treitz, 2016; Zarei et al., 2020). It is an indicator of the photosynthetic activity of the vegetation cover used in assessing the moisture content and nitrogen concentration in plant leaves. GNDVI is similar to NDVI except that green light (GREEN) is used instead of red light. Compared to the NDVI, GNDVI is more sensitive to chlorophyll concentration (Ochtyra et al., 2020). GNDVI is recommended to identify plants under stress and at the stage of seasonal wilting (Ahamed et al., 2011):

$$GNDVI = \frac{NIR - GREEN}{NIR + GREEN} \quad \text{(Eq.2)}$$

CVI (Chlorophyll Vegetation Index) has an increased sensitivity to the chlorophyll content of the foliage. The index was developed to assess the chlorophyll content of crops (Datt et al., 2003; Vincini et al., 2008), but it had also been used for studying tree species (Li et al., 2019):

$$CVI = \frac{NIR}{GREEN} * \frac{RED}{GREEN} \quad \text{(Eq.3)}$$

Vegetation indices were calculated from cloudless images of Landsat TM, ETM +, and OLI / TIRS for the period from 2008 to 2017 with preliminary radiometric and atmospheric correction (Neteler and Mitasova, 2008). We did not use the images from 2018-2020 because of the appearance of the insect pest *Acrocercops brongniardella* (Fabricius, 1798) (Lepidoptera, Gracillariidae) in the peri-urban *Quercus robur* sites.

All calculations were carried out in SAGA GIS v. 7.7.0 and QGIS 3.18.1 with GRASS 7.8.5 support. The average values of the indices for each site were calculated using the Zonal Statistics plugin.

The mean plot of the temporal dynamics of vegetation indices was calculated using a double-logistic function with a “greendown” parameter (Elmore et al., 2012; Melaas et al., 2013; Gao et al., 2021; Zhang et al., 2021). This function combines the spring and autumn seasons into a single equation and allows the gradual reduction of the vegetation

http://www.aloki.hu ● ISSN 1589 1623 (Print) ● ISSN 1785 0037 (Online)
DOI: http://dx.doi.org/10.15666/aeer/2005_44094427

indices values in the middle of summer which is usually observed during the remote sensing of forest canopy greenness. We used a Bayesian method that uses Landsat time series data, and a Bayesian hierarchical model to plot phenology. This method is implemented in the Bayesian_LSP script, developed in the R programming language (Gao et al., 2021). One of the advantages of Bayesian methods is the ability to quantify uncertainty for the estimated parameter by the posterior distribution (Babcock et al., 2021; Gao et al., 2021). This is done by using Markov Chain Monte Carlo (MCMC) sampling (Geyer, 1992). The uncertainties of the estimated parameters are summarized by calculating the 95% credible interval of the estimated posterior distribution. The 95% credible interval of the posterior distribution can be interpreted as a range of values with a 95% probability that contains the true mean of the parameter (Gao et al., 2021).

We analyzed the seasonal dynamics of forests using the temporal dynamics of vegetation indices for the following parameters:

- the SOS and EOS parameters defined as the inflection points on the phenology plot which are used to represent the start of season (SOS) and the end of season (EOS);
- the growing season defined as the time between SOS and EOS (in the plots of NDVI temporal dynamics) which were calculated for each year separately, as well as for the generalized mean phenology plot based on Landsat time series data for 2008-2017;
- the mean value of the vegetation index during the growing season;
- the maximum value of the vegetation index during the growing season;
- the difference between the average value of the vegetation index for the whole growing season of 2010 and the mean value of the vegetation index of the growing season for 10 years (as a percentage);
- the maximum difference between the value of vegetation index in 2010 and the mean value of the vegetation index for 10 years on exact dates (as a percentage).

To characterize the weather conditions in 2008-2017 (mean daily air temperature, precipitation, snow depth), we used the data from meteorological station № 28722 of the Ufa city (aisori-m.meteo.ru).

Results

Features of weather conditions in dry 2010

In the South Ural region, the year 2010 was anomalous in terms of the precipitation and also had a higher temperature during the growing season (*Fig. 2*). The precipitation during the growing season (April-September) in 2010 was only 155.3 mm, which is almost two times lower than the mean values for the last 70 years (311.0 mm). In 2010, in addition to the summer-spring precipitation deficit, there was also less precipitation during the winter which resulted in a significantly lower snow depth. The mean monthly temperatures during the growing season in 2010 exceeded the monthly average from 2 to 5 ° C.

The analysis of the seasonal development of tree species

Abnormal weather conditions in 2010 led to the change in the phenological development of tree species (*Table 1*). The temporal dynamics of vegetation indices (NDVI, GNDVI and CVI) of oak and pine forests in 2010 and the mean temporal dynamics of the vegetation indices of 2008-2017 are shown in *Figures 3-8*.

http://www.aloki.hu ● ISSN 1589 1623 (Print) ● ISSN 1785 0037 (Online)
DOI: http://dx.doi.org/10.15666/aeer/2005_44094427

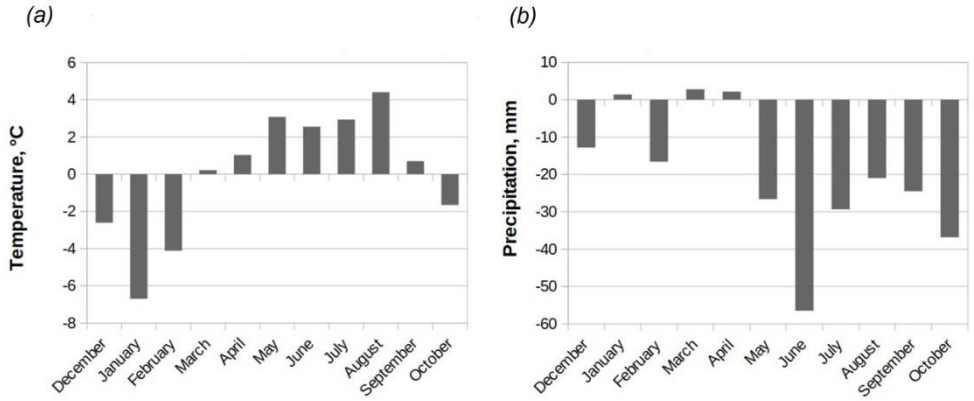

Figure 2. *Deviation from the average values: a) monthly average temperature (from December of the previous year to October of the year under review) in the dry year 2010 from the average values for the last 70 years (1950-2019); b) average monthly precipitation (from December of the previous year to October of the year under review) in the dry year 2010 from the average values for the last 70 years (1950-2019)*

Table 1. *Dates of the start of the growing season (SOS) (the inflection points on the temporal dynamics plots of NDVI) on the sites dominated by Quercus robur L. and Pinus sylvestris L. in the Ufa city and outside it*

Years	Sites[1]				
	Q1	**Q2**	**Q3**	**P1**	**P2**
2010	May 8	May 5	April 30	April 30	April 25
mean	May 10	May 4	May 2	April 30	April 24

[1]Sites dominated by *Quercus robur* L.: **Q1** – outside the city, **Q2** – in the city on a flat area, **Q3** – in the city on a steep southern slope; sites dominated by *Pinus sylvestris* L.: **P1** – outside the city, **P2** – in the city on a flat area

As seen in *Table 1*, the dates of the start of the growing season (SOS) in 2010 in the oak forest sites in the city (Q2 and Q3) and outside the city (Q1) differed slightly from the 10-years average. At the same time, in the oak forests outside the city (Q1), the pace of the NDVI increase during the crown formation (from the early April to the first ten days of May) in 2010 was higher than the average, and in the city the values did not differ (*Fig. 3, Table 1*). The average NDVI values of the whole growing season in 2010 in the oak forests in the city and outside the city in a dry year in all cases were lower than the 10-years average values (*Table 2*). In the second half of July of the dry year there was a sharp NDVI decrease in all sites followed by recovery caused by the rains by the end of summer. Moreover, after the recovery the NDVI values exceeded the average for 10 years.

The analysis of the NDVI temporal dynamics in the pine forests showed that in the city (P2) and outside the city (P1) the dates of the start of the growing season (SOS) in the dry year almost did not differ from the average of 10 years (*Table 1*).

However, the NDVI values during the period from the moment of snow melt to the first ten days of May in the dry year were lower than the average values for 2008-2017. In the pine forests outside the city (P1) at the beginning of June (during the completion of the formation of new needles) the NDVI values were slightly higher than average, and they almost did not differ in the city (*Fig. 4*). The mean NDVI values for the whole

http://www.aloki.hu ● ISSN 1589 1623 (Print) ● ISSN 1785 0037 (Online)
DOI: http://dx.doi.org/10.15666/aeer/2005_44094427

growing season in 2010 in pine forests both in the city and outside it in a dry year were lower than the mean values for 2008-2017 (*Table 2*). In the second half of July of the dry year, in both pine forest sites, as well as in oak forests, there was a sharp decrease in NDVI, followed by their recovery after rains by the end of summer, exceeding the 10-year average.

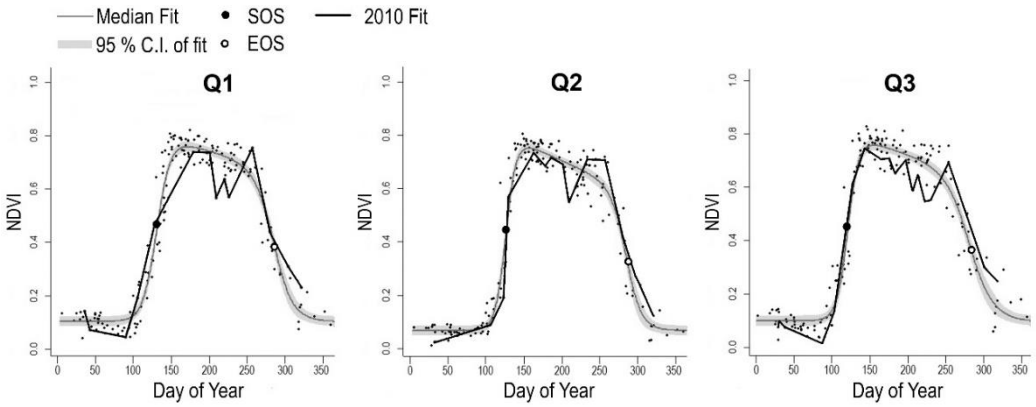

Figure 3. *The temporal dynamics of NDVI on the sites dominated by Quercus robur L. in the Ufa city and outside it.* ***Q1*** *– outside the city,* ***Q2*** *– in the city on a flat area,* ***Q3*** *– in the city on a steep southern slope;* ***Median Fit*** *– average plot of 2008-2017;* ***95% C.I. of fit*** *– 95% credible interval of median fit;* ***SOS*** *– start of season;* ***EOS*** *– end of season;* ***2010 Fit*** *– plot of 2010*

Table 2. *Average (maximum) values of NDVI, GNDVI and CVI during the vegetation period of full crown development on the sites dominated by Quercus robur L. and Pinus sylvestris L. in the Ufa city and outside it*

Sites	2010	Mean $^{2008-2017}$	$\Delta^{2010-mean}$, %	Max $\Delta^{2010-mean}$, %	Date of max $\Delta^{2010-mean}$
NDVI					
Q1	0.6 (0.75)	0.68 (0.82)	12	22.3	2010-07-29
Q2	0.64 (0.73)	0.66 (0.8)	3.5	20.4	2010-07-29
Q3	0.65 (0.74)	0.68 (0.83)	4.7	20.6	2010-08-14
P1	0.48 (0.63)	0.56 (0.71)	15.8	42.3	2010-08-14
P2	0.53 (0.62)	0.59 (0.71)	9	27.3	2010-07-29
GNDVI					
Q1	0.49 (0.64)	0.56 (0.7)	13.7	31.1	2010-08-14
Q2	0.54 (0.64)	0.55 (0.68)	2.5	18.4	2010-07-29
Q3	0.56 (0.63)	0.57 (0.7)	1.9	18.3	2010-08-14
P1	0.37 (0.5)	0.44 (0.58)	16.6	42	2010-08-05
P2	0.42 (0.51)	0.46 (0.58)	8.9	27.5	2010-07-29
CVI					
Q1	2.3 (3.11)	2.52 (3.16)	8.7	32.5	2010-08-14
Q2	2.57 (3.2)	2.45 (3.34)	-4.8	18.4	2010-07-29
Q3	2.53 (3.14)	2.6 (3.21)	2.7	20.8	2010-07-29
P1	1.68 (2.21)	1.86 (2.42)	9.7	28.3	2010-07-29
P2	1.88 (2.24)	1.92 (2.37)	2.4	17.6	2010-08-06

[1] Sites dominated by *Quercus robur* L.: **Q1** – outside the city, **Q2** – in the city on a flat area, **Q3** – in the city on a steep southern slope; sites dominated by *Pinus sylvestris* L.: **P1** – outside the city, **P2** – in the city on a flat area; **Δ 2010-mean** – the difference between the average value of the vegetation indices during the growing season of 2010 and the average value of the vegetation indices during the growing season for 10 years; **Max Δ 2010-mean** – the maximum difference of vegetation indices from the average value of vegetation indices for this date for 10 years

http://www.aloki.hu ● ISSN 1589 1623 (Print) ● ISSN 1785 0037 (Online)
DOI: http://dx.doi.org/10.15666/aeer/2005_44094427

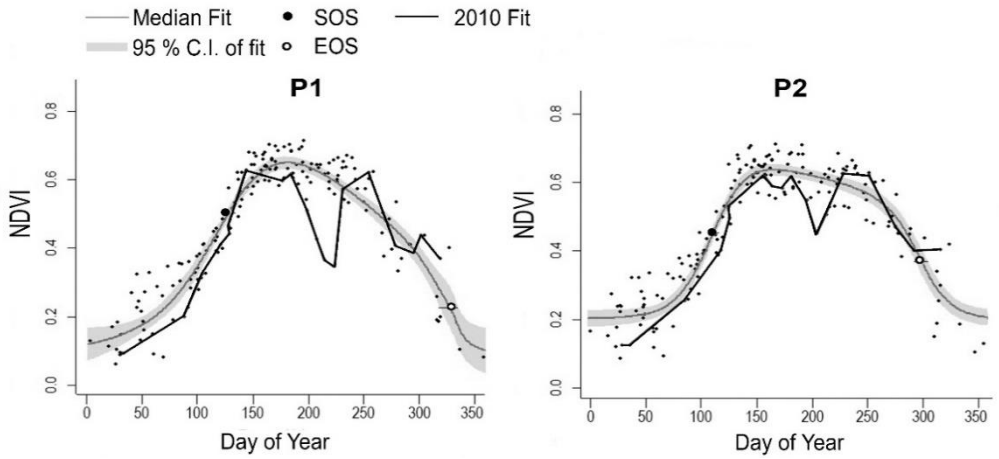

Figure 4. *The temporal dynamics of NDVI on the sites dominated by Pinus sylvestris L. in the Ufa city and outside it.* ***P1*** *– outside the city,* ***P2*** *– in the city;* ***Median Fit*** *– average plot of 2008-2017;* ***95% C.I. of fit*** *– 95% credible interval of median fit;* ***SOS*** *– start of season;* ***EOS*** *– end of season;* ***2010 Fit*** *– plot of 2010*

The analysis of the GNDVI temporal dynamics showed the similar patterns to the NDVI temporal dynamics during the growing season of both studied tree species (*Fig. 5, 6*). However, in the second half of July of the dry year (during the maximum drought), the oak forests outside the city (Q1) showed a stronger decline in the GNDVI values compared to NDVI. The average GNDVI values for the whole growing season in the oak forests outside the city (Q1) in a dry year were significantly lower than the 10-year average. In the oak forests in the city (Q2 and Q3), the average values of GNDVI in 2010 almost coincided with the 10-years average (*Table 2*). By the end of August, the GNDVI values in all oak forest sites exceeded the 10-years average values.

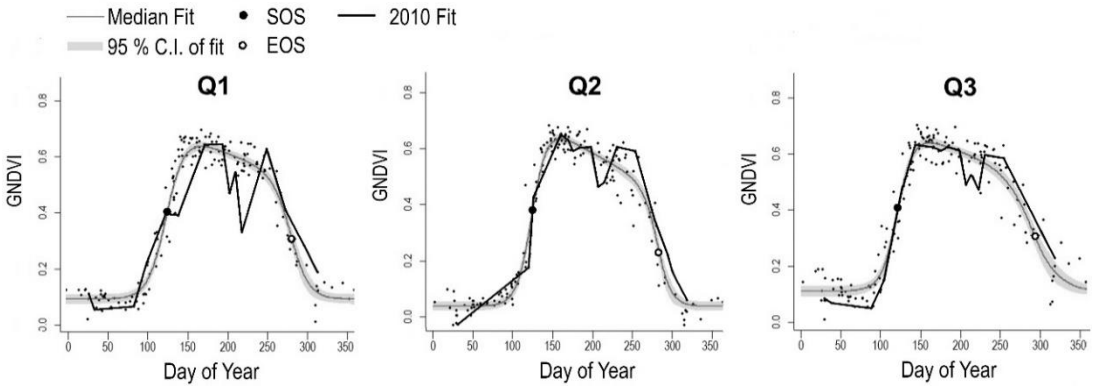

Figure 5. *The temporal dynamics of GNDVI on the sites dominated by Quercus robur L. in the Ufa city and outside it.* ***Q1*** *– outside the city,* ***Q2*** *– in the city on a flat area,* ***Q3*** *– in the city on a steep southern slope;* ***Median Fit*** *– average plot of 2008-2017;* ***95% C.I. of fit*** *– 95% credible interval of median fit;* ***SOS*** *– start of season;* ***EOS*** *– end of season;* ***2010 Fit*** *– plot of 2010*

The GNDVI temporal dynamics in the pine forests both in the city and outside it also had a similar character to the NDVI temporal dynamics (*Fig. 6*). The GNDVI values during the period from the moment of snow melt to the first ten days of May in the dry

http://www.aloki.hu ● ISSN 1589 1623 (Print) ● ISSN 1785 0037 (Online)
DOI: http://dx.doi.org/10.15666/aeer/2005_44094427

year were below the 10-year average. The average GNDVI values for the whole growing season in the dry year were significantly lower than the average for 10 years (*Table 2*). In late summer, after the onset of regular rains, the GNDVI values exceeded the 10-year average.

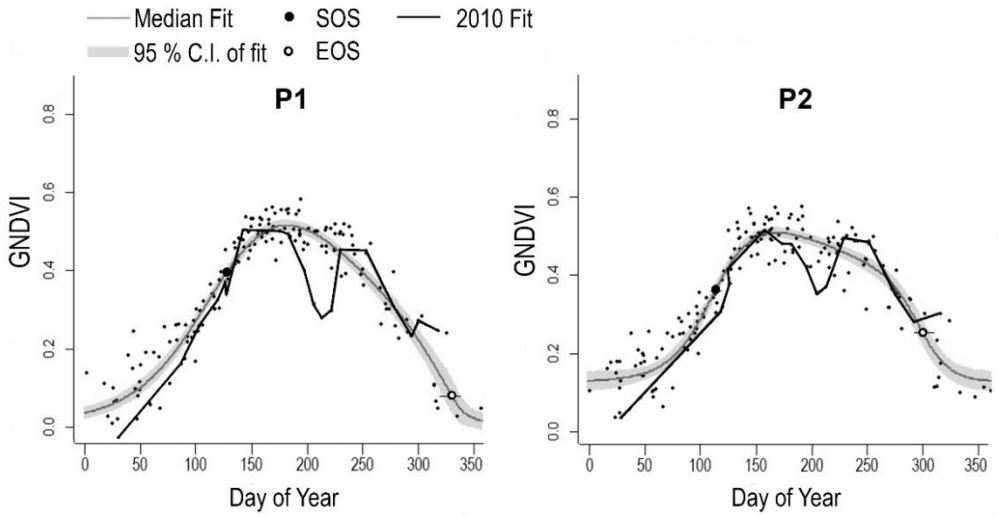

Figure 6. *The temporal dynamics of GNDVI on the sites dominated by Pinus sylvestris L. in the Ufa city and outside it.* ***P1*** *– outside the city,* ***P2*** *– in the city.* ***Median Fit*** *– average plot of 2008-2017;* ***95% C.I. of fit*** *– 95% credible interval of median fit;* ***SOS*** *– start of season;* ***EOS*** *– end of season;* ***2010 Fit*** *– plot of 2010*

The CVI temporal dynamics of oak and pine forests differ significantly from the temporal dynamics of GNDVI and NDVI. *Figures 7* and *8* show that CVI was higher than the average in the first half of summer at the beginning of the drought in 2010 in all studied sites, and during the period of severe drought the CVI dropped. After the rains in the second half of August, the CVI values increased up to the average or higher.

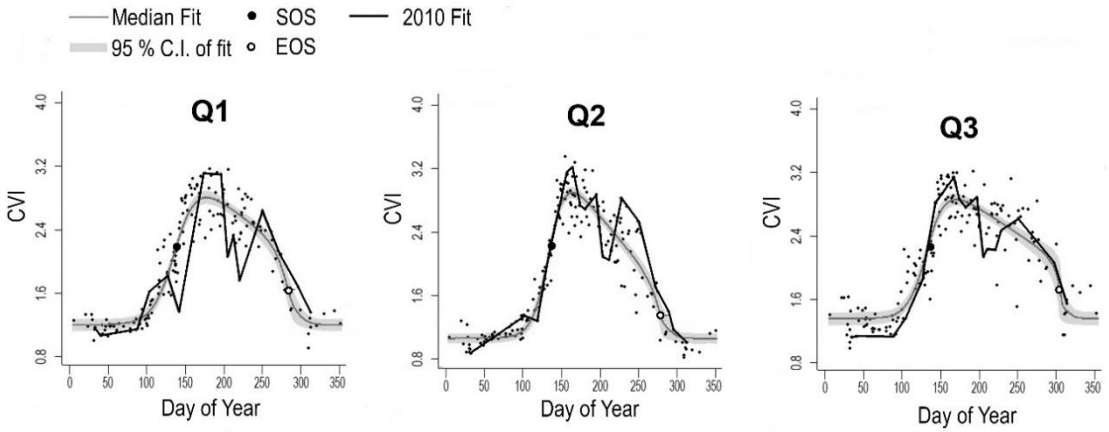

Figure 7. *The temporal dynamics of CVI (**c**) on the sites dominated by Quercus robur L. in the Ufa city and outside it.* ***Q1*** *– outside the city,* ***Q2*** *– in the city on a flat area,* ***Q3*** *– in the city on a steep southern slope;* ***Median Fit*** *– average plot of 2008-2017;* ***95% C.I. of fit*** *– 95% credible interval of median fit;* ***SOS*** *– start of season;* ***EOS*** *– end of season;* ***2010 Fit*** *– plot of 2010*

http://www.aloki.hu ● ISSN 1589 1623 (Print) ● ISSN 1785 0037 (Online)
DOI: http://dx.doi.org/10.15666/aeer/2005_44094427

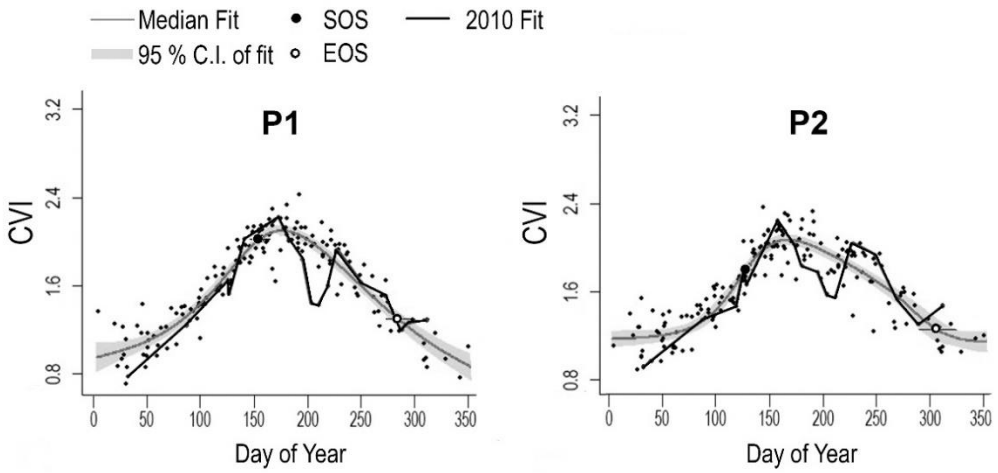

Figure 8. *The temporal dynamics of CVI on the sites dominated by Pinus sylvestris L. in the Ufa city and outside it.* ***P1*** *– outside the city,* ***P2*** *– in the city;* ***Median Fit*** *– average plot of 2008-2017;* ***95% C.I. of fit*** *– 95% credible interval of median fit;* ***SOS*** *– start of season;* ***EOS*** *– end of season;* ***2010 Fit*** *– plot of 2010*

Discussion

The basic strategy of plant adaptation to drought is aimed at maintaining water balance through more efficient water use using morphological and physiological mechanisms (Querejeta et al., 2007; McDowell et al., 2008; Hwang et al., 2017; Rohner et al., 2021). There are changes in transpiration level and a decrease in photosynthesis at the initial drought stages. Further, chlorophyll content in leaves and the total surface area evaporating moisture decrease due to inhibition of the young shoots growth and even partial shedding of the leaves (Kozina et al., 2011; Vanhellemont et al., 2019). Due to this, the vegetation indices also change (Joiner et al., 2018; Miranda et al., 2020; Yang et al., 2020; Avetisyan et al., 2021).

The average annual temperature excess was observed as soon as the second half of April of 2010 (*Fig. 2*), which led to an earlier snow melt-off. This also facilitated the lower amount of winter precipitation (from December to March), which was 19% less than the average precipitation according to the long-term observations. Earlier snow melt-off and higher temperatures during the beginning of crown formation (April-mid-May) led to the acceleration of the phenological development of the oak forests outside the city compared to the 10-year average. At the same time, during this period in the urban oak forests (Q2, Q3) there was no increase in the phenological development pace which was apparently due to the lower moisture supply caused by the earlier convergence of the snow cover in comparison with the peri-urban forest (*Fig. 3*). However, by mid-May, a significant decline in soil moisture began to occur and the phenological development of the oak forests both in the city and outside it slows down.

In general, the development of oak forests in the city and outside the city happened differently. Urban heat island effect lead to an earlier start of the growing season and to the higher pace of the crown development at the beginning of seasonal development (Zhigunova et al., 2018). According to the average data for 2008-2017, there was a lag in phenological development of oak forests outside the city (Q1) from early spring until the complete formation of the crowns (*Fig. 9*). The date of the start of the growing season (SOS) in the oak forest outside the city (Q1) comes on average 6 days later than in the

http://www.aloki.hu ● ISSN 1589 1623 (Print) ● ISSN 1785 0037 (Online)
DOI: http://dx.doi.org/10.15666/aeer/2005_44094427

oak forests in the city park (Q2) and 8 days later than in the oak forests on the southern slope (Q3) (*Table 1, Fig. 9*). The tendency for the development of the peri-urban oak forests to lag behind the development of the urban oak forests continued in the dry year. At the same time, due to drought in 2010 in the peri-urban oak forests the lag in phenological development began during the leaf unfolding. At the same time, the crown development was already underway in the city and the average size of leaves on the flat area of oak forests (Q2) did not yet reach 50%, and on the southern slope (Q3), it was more than 50% of the size of fully developed leaves.

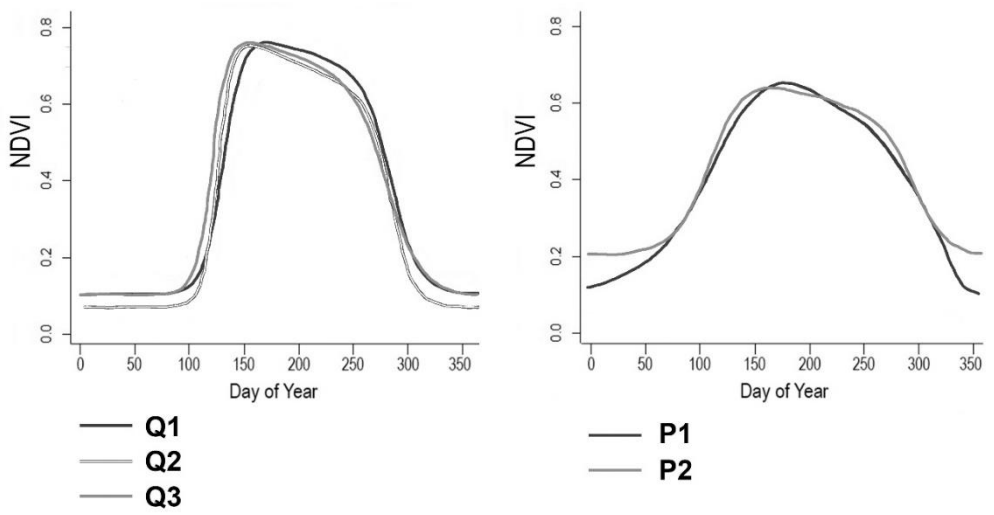

Figure 9. *The averages temporal dynamics of NDVI (average plot of 2008-2017) on the sites dominated by Quercus robur L. and Pinus sylvestris L. in the Ufa city and outside it.* ***Q1, P1*** *– outside the city,* ***Q2, Q3, P2*** *– in the city*

The average NDVI values for the whole growing season in 2010 in the oak forests both outside the city (Q1) and in the city (Q2 and Q3) were lower than the average values for 2008-2017. Lower NDVI values indicate a pronounced suppression of the tree layer with a photosynthetic activity decrease and a slowdown of the new leafy shoots formation (Joiner et al., 2018; Miranda et al., 2020; Avetisyan et al., 2021).

Small intermittent rains in July led to local increases in NDVI, however up to mid-August a downward trend in the NDVI was observed. The maximum decline in NDVI in the oak forests compared to the 10-year average was 20.4% to 22.3% (*Table 2*). In mid-August, regular light rains led to a gradual increase in NDVI and lowering the differences between the values of the dry year and the average values of 2008-2017.

The plots of the NDVI temporal dynamics in the pine forests show that the lag in the phenological development of the urban (P2) and peri-urban (P1) pine forests in contrast to the oak forests in the dry year began from the snow melt-off (*Fig. 4*). This happened because the seasonal development of pine is more dependent on the spring precipitation (Elmore et al., 2012; Kucherov et al., 2016). The suppression of the pine forest in the city from the seasonal development beginning was observed and NDVI did not reach the values of 2017, before regular precipitation at the end of August 2010, which is explained by the intensification of drought in the urban environment (Zhigunova et al., 2018).

Comparison of the prolonged drought response in oak and pine forests is of considerable interest. Comparing the temporal dynamics of the NDVI of the oak and pine

http://www.aloki.hu ● ISSN 1589 1623 (Print) ● ISSN 1785 0037 (Online)
DOI: http://dx.doi.org/10.15666/aeer/2005_44094427

forests in 2010 (*Figs. 3, 4, Table 2*) showed that the pine forests react more strongly to a long period of water deficit in the middle of summer. The maximum decrease in NDVI compared to the 10-years average in the pine forests is 1.5-2 times greater than in the oak forests (*Table 2*). Different responses to prolonged drought can be explained by the difference in the root systems structure of these species. The drought tolerance of plants as a function of root length has been well studied in crops, but this is also true for tree species (Lynch, 2013). Under relatively favorable edaphic conditions, such as study area, *Q. robur* forms a deeper root system. Oak taproots are two to three times longer than the pine roots (Praciak et al., 2013; Prutskoy, 2017). After the prolonged drought in the study area, the groundwater level has changed by 0.84-3.27 m (Abdrakhmanov et al., 2018). The deeper root system allows *Q. robur* to use deeper moisture reserves. Besides, broad-leaved trees can use the water stored in the heartwood during prolonged dry periods while conifers keep their water reserves mainly by real-time absorption (Querejeta et al., 2007; Goldsmith, 2013). The results are also confirmed by the fact that oak is more resistant to summer drought conditions than pine (Merlin et al., 2015; Toïgo et al., 2015; Vanhellemont et al., 2019; Steckel et al., 2020).

Changes of GNDVI and NDVI were similar in both oak and pine forests during the growing season. However, in the absence of precipitation during the period of the most severe drought from the second half of July to mid-August, in oak forests outside the city (Q1) the GNDVI decrease was much more significant than NDVI decrease (*Table 2*). The maximum decline in GNDVI in oak forests compared to the 10-year average is ranged from 18.3% to 31.1% (*Table 2*). At the same time, in the oak forests outside the city a stronger decrease in GNDVI was observed. Perhaps this was due to the fact that the lag in phenology outside the city began at an earlier stage of crown development than in the city. Thus, when assessing the stress caused by drought the informative value of GNDVI in some cases may be higher than NDVI. Literature data confirm that GNDVI has a higher sensitivity to moisture and chlorophyll content in plant leaves as well as to a greater extent reflects the level of plant stress (Ahamed et al., 2011).

The temporal dynamic of CVI (*Figs. 4, 5*) is significantly different from the temporal dynamics of NDVI and GNDVI. In a year with the average precipitation, the plots of temporal dynamics of the CVI in the pine and oak forests show fluctuations in values which are not explained by objective reasons. The CVI values in oak and pine forests in the early summer of 2010 were significantly higher than the average for 2008-2017. The highest CVI values were recorded in the second half of June when the NDVI reached a plateau or had already begun to decline. Thus, no positive correlation was observed between the CVI values and the chlorophyll concentration reflected by the NDVI and GNDVI. This result does not contradict the literature data. Initially, Vincini et al. (2008) found a positive correlation between CVI and chlorophyll content in leaves of crops; however, Ortiz et al. (2011) found a negative correlation of CVI with chlorophyll content of crops and control plots of crops showed lower CVI values than the plots with inhibited herbicide treatment. Also, a negative correlation between CVI and chlorophyll content was shown using the example of mangrove forest (Heenkenda et al., 2015). However, with the prolonged drought in the second half of the summer the CVI values decrease, similarly to NDVI and GNDVI. Thus, NDVI and GNDVI seem to be more informative when analyzing the impact of drought on the phenology of forest vegetation.

http://www.aloki.hu ● ISSN 1589 1623 (Print) ● ISSN 1785 0037 (Online)
DOI: http://dx.doi.org/10.15666/aeer/2005_44094427

Conclusions

Abnormal weather events, the frequency of which increases with the climate change, have a significant impact on the phenological development and condition of urban forests. We have shown that NDVI and GNDVI were most informative and CVI was uninformative when using high-resolution satellite images to study the impact of drought on forest vegetation. Higher temperatures in the city lead to the earlier start of the growing season and to the higher pace at the beginning of seasonal development of pine and oak forests. This tendency for the seasonal development of the peri-urban forests to delay continued in the dry year. Thus, at the beginning of the growing season, the effect of the location on the development of plants were much more intense than the impact of the weather conditions. At the same time, in both urban and peri-urban pine forests in the dry year the delay of the phenological development began earlier than in the oak forests. Pine forests respond to the long period of water scarcity to a greater extent than the oak forests. This is largely explained by the features of *Q. robur* root systems which allow the plants to use deeper moisture reserves.

After the rains at the end of summer, there was an increase in the NDVI and GNDVI values in the urban and peri-urban forests to a level exceeding the 10-year average values. This happened due to the combination of sufficient precipitation and higher air temperature which led to the increase in photosynthetic activity.

Q. robur along with *P. sylvestris* should be used more widely when landscaping the cities located in the forest-steppe subzone of the temperate zone. We especially recommend using oak in places where it has become extinct as a result of the abnormally low winter temperatures of the 20th century, since the oak forests have not been observed in the study area for more than 40 years due to the climate change.

Funding. This research was funded by State Assignment no. 075-00326-19-00 of the Ministry of Education and Science of Russia (topic no. AAAA-A18-118022190060-6) and grant of the Ministry of Education and Science of the Republic of Bashkortostan REC-RMG-2022 "Creating the methodological foundations for evaluating the greenhouse gas balance and determining the carbon sequestration potential in different ecosystems".

Conflicts of Interests. The authors declare no conflict of interests.

REFERENCES

[1] Abdrakhmanov, R., Komissarov, A., Durnaeva, V., Poleva, A. (2018): Monitoring of groundwater in the basin of the middle course of the river Belaya used for local water supply. – Prirodoobustroystvo 5: 7-13.

[2] Ahamed, T., Tian, L., Zhang, Y., Ting, K. C. (2011): A review of remote sensing methods for biomass feedstock production. – Biomass and Bioenergy 35(7): 2455-2469.

[3] Ahl, D. E., Gower, S. T., Burrows, S. N., Shabanov, N. V., Myneni, R. B., Knyazikhin, Y. (2006): Monitoring spring canopy phenology of a deciduous broadleaf forest using MODIS. – Remote Sensing of Environment 104(1): 88-95.

[4] Akbari, H., Cartalis, C., Kolokotsa, D., Muscio, A., Pisello, A. L., Rossi, F., Santamouris, M., Synnefa, A., Wong, N. H., Zinzi, M. (2016): Local climate change and urban heat island mitigation techniques - The state of the art. – Journal of Civil Engineering and Management 22(1): 1-16.

[5] Aleksashina, V. V., Le, M. T. (2018): Influence of the urban heat island effects on the ecology of the megacity. – Problemy Regionalnoy Ekologii 5: 36-40.

http://www.aloki.hu ● ISSN 1589 1623 (Print) ● ISSN 1785 0037 (Online)
DOI: http://dx.doi.org/10.15666/aeer/2005_44094427

[6] Allen, C. D., Macalady, A. K., Chenchouni, H., Bachelet, D., McDowell, N., Vennetier, M., Kitzberger, T., Rigling, A., Breshears, D. D., Hogg, E. H., Gonzalez, P., Fensham, R., Zhang, Z., Castro, J., Demidova, N., Lim, J. H., Allard, G., Running, S. W., Semerci, A., Cobb, N. (2010): A global overview of drought and heat-induced tree mortality reveals emerging climate change risks for forests. – Forest Ecology and Management 259(4): 660-684.

[7] Anniballe, R., Bonafoni, S., Pichierri, M. (2014): Spatial and temporal trends of the surface and air heat island over Milan using MODIS data. – Remote Sensing of Environment 150: 163-171.

[8] Avetisyan, D., Borisova, D., Velizarova, E. (2021): Integrated evaluation of vegetation drought stress through satellite remote sensing. – Forests 12(8): 1-32.

[9] Babcock, C., Finley, A. O., Looker, N. (2021): A Bayesian model to estimate land surface phenology parameters with harmonized Landsat 8 and Sentinel-2 images. – Remote Sensing of Environment 261: 112471.

[10] Barber, V. A., Juday, G. P., Finney, B. P. (2000): Reduced growth of Alaskan white spruce in the twentieth century from temperature-induced drought stress. – Nature 405: 668-673.

[11] Beniston, M. (2004): The 2003 heat wave in Europe: A shape of things to come? An analysis based on Swiss climatological data and model simulations. – Geophysical Research Letters 31(2).

[12] Berra, E. F., Gaulton, R., Barr, S. (2019): Assessing spring phenology of a temperate woodland: A multiscale comparison of ground, unmanned aerial vehicle and Landsat satellite observations. – Remote Sensing of Environment 223: 229-242.

[13] Bigler, C., Bräker, O. U., Bugmann, H., Dobbertin, M., Rigling, A. (2006): Drought as an inciting mortality factor in scots pine stands of the Valais, Switzerland. – Ecosystems 9(3): 330-343.

[14] Chen, F., Wang, C., Zhang, Y., Yi, Z., Fan, Q., Liu, L., Song, Y. (2021): Inconsistency among landsat sensors in land surface mapping: A comprehensive investigation based on simulation. – Remote Sensing 13(7): 1-25.

[15] Cheng, Q., Zhong, F., Wang, P. (2021): Potential linkages of extreme climate events with vegetation and large-scale circulation indices in an endorheic river basin in northwest China. – Atmospheric Research 247: 105256.

[16] Crucifix, M., Betts, R. A., Cox, P. M. (2005): Vegetation and climate variability: A GCM modelling study. – Climate Dynamics 24(5): 457-467.

[17] Datt, B., McVicar, T. R., Van Niel, T. G., Jupp, D. L. B., Pearlman, J. S. (2003): Preprocessing EO-1 Hyperion hyperpsectral data to support the application of agricultural indexes. – IEEE Trans. Geosci. Remote Sens. 41: 1246-1259.

[18] Dixon, D. J., Callow, J. N., Duncan, J. M. A., Setterfield, S. A., Pauli, N. (2021): Satellite prediction of forest flowering phenology. – Remote Sensing of Environment 255: 112197.

[19] Elmore, A. J., Guinn, S. M., Minsley, B. J., Richardson, A. D. (2012): Landscape controls on the timing of spring, autumn, and growing season length in mid-Atlantic forests. – Global Change Biology 18(2): 656-674.

[20] Fedorov, N. I., Zharkikh, T. L., Mikhailenko, O. I., Bakirova, R. T. (2019a): Forecast changes in the productivity of plant communities in the pre-urals steppe site of Orenburg state nature reserve (Russia) in extreme drought conditions using NDVI. – Nature Conservation Research 4: 104-110.

[21] Fedorov, N. I., Zharkikh, T. L., Mikhailenko, O. I., Bakirova, R. T., Martynenko, V. B. (2019b): The use of NDVI for the analysis of the effect of drought on vegetation productivity in the Pre-urals steppe area where a population of the Przewalski horse equus ferus Przewalskii Polj., 1881 had been established. – In: Information Technologies in the Research of Biodiversity. Proceedings of the International Conference. 'Springer Proceedings in Earth and Environmental Sciences', pp. 1-7.

http://www.aloki.hu ● ISSN 1589 1623 (Print) ● ISSN 1785 0037 (Online)
DOI: http://dx.doi.org/10.15666/aeer/2005_44094427

[22] Gaertner, B. A., Zegre, N., Warner, T., Fernandez, R., He, Y., Merriam, E. R. (2019): Climate, forest growing season, and evapotranspiration changes in the central Appalachian Mountains, USA. – Science of the Total Environment 650: 1371-1381.
[23] Gao, X., Gray, J. M., Reich, B. J. (2021): Long-term, medium spatial resolution annual land surface phenology with a Bayesian hierarchical model. – Remote Sensing of Environment 261: 112484.
[24] Geyer, C. J. (1992): Practical Markov Chain Monte Carlo. – Statistical Science 7(4): 473-511.
[25] Gitelson, A. A., Merzlyak, M. N. (1998): Remote sensing of chlorophyll concentration in higher plant leaves. – Advances in Space Research 22(5): 689-692.
[26] Goldsmith, G. R. (2013): Changing directions: the atmosphere-plant-soil continuum. – New Phytologist 199: 4-6.
[27] Gulácsi, A., Kovács, F. (2018): Drought monitoring of forest vegetation using MODIS-based normalized difference drought index in Hungary. – Hungarian Geographical Bulletin 67(1): 29-42.
[28] Hais, M., Hellebrandová, K. N., Šrámek, V. (2019): Potential of Landsat spectral indices in regard to the detection of forest health changes due to drought effects. – Journal of Forest Science 65(2): 70-78.
[29] Heenkenda, M. K., Joyce, K. E., Maier, S. W., de Bruin, S. (2015): Quantifying mangrove chlorophyll from high spatial resolution imagery. – ISPRS Journal of Photogrammetry and Remote Sensing 108: 234-244.
[30] Hirota, M., Holmgren, M., Van Nes, E. H., Scheffer, M. (2011): Global Resilience of Tropical Forest and Savanna to critical transitions. – Science 334: 232-235.
[31] Hu, L., Brunsell, N. A. (2013): The impact of temporal aggregation of land surface temperature data for surface urban heat island (SUHI) monitoring. – Remote Sensing of Environment 134: 162-174.
[32] Huo, L., Persson, H. J., Lindberg, E. (2021): Early detection of forest stress from European spruce bark beetle attack, and a new vegetation index: Normalized distance red & SWIR (NDRS). – Remote Sensing of Environment 255: 112240.
[33] Hwang, T., Gholizadeh, H., Sims, D. A., Novick, K. A., Brzostek, E. R., Phillips, R. P., Roman, D. T., Robeson, S. M., Rahman, A. F. (2017): Capturing species-level drought responses in a temperate deciduous forest using ratios of photochemical reflectance indices between sunlit and shaded canopies. – Remote Sensing of Environment 199: 350-359.
[34] Imhoff, M. L., Zhang, P., Wolfe, R. E., Bounoua, L. (2010): Remote sensing of the urban heat island effect across biomes in the continental USA. – Remote Sensing of Environment 114(3): 504-513.
[35] Joiner, J., Yoshida, Y., Anderson, M., Holmes, T., Hain, C., Reichle, R., Koster, R., Middleton, E., Zeng, F. W. (2018): Global relationships among traditional reflectance vegetation indices (NDVI and NDII), evapotranspiration (ET), and soil moisture variability on weekly timescales. – Remote Sensing of Environment 219: 339-352.
[36] Karl, T. R., Knight, R. W., Plummer, N. (1995): Trends in high-frequency climate variability in the twentieth century. – Nature 377: 217-220.
[37] von Keyserlingk, J., de Hoop, M., Mayor, A. G., Dekker, S. C., Rietkerk, M., Foerster, S. (2021): Resilience of vegetation to drought: Studying the effect of grazing in a Mediterranean rangeland using satellite time series. – Remote Sensing of Environment 255: 112270.
[38] Kozina, L. V., Titova, M. S., Ivaschenko, E. A., Rezinkina, G. A. (2011): Stress factor effect on conifer seedling growth and productivity. – Vestnik KrasGAU 53(2): 96-100.
[39] Kramer, K., Leinonen, I., Loustau, D. (2000): The importance of phenology for the evaluation of impact of climate change on growth of boreal, temperate and Mediterranean forests ecosystems: An overview. – International Journal of Biometeorology 44(2): 67-75.

http://www.aloki.hu ● ISSN 1589 1623 (Print) ● ISSN 1785 0037 (Online)
DOI: http://dx.doi.org/10.15666/aeer/2005_44094427

[40] Kucherov, S. E., Vasilev, D. Y., Muldashev, A. A. (2016): Reconstruction of May–June precipitation in the territory of Bashkiria based on Scots pine tree-ring data from the Bugulma–Belebey Upland. – Russian Journal of Ecology 47(2): 115-124.
[41] Li, J., Song, C., Cao, L., Zhu, F., Meng, X., Wu, J. (2011): Impacts of landscape structure on surface urban heat islands: A case study of Shanghai, China. – Remote Sensing of Environment 115(12): 3249-3263.
[42] Li, F., Song, G., Liujun, Z., Yanan, Z., Di, L. (2017): Urban vegetation phenology analysis using high spatio-temporal NDVI time series. – Urban Forestry and Urban Greening 25: 43-57.
[43] Li, W., El-Askary, H., Qurban, M. A., Li, J., ManiKandan, K. P., Piechota, T. (2019): Using multi-indices approach to quantify mangrove changes over the Western Arabian Gulf along Saudi Arabia coast. – Ecological Indicators 102: 734-745.
[44] Liu, H., Park Williams, A., Allen, C. D., Guo, D., Wu, X., Anenkhonov, O. A., Liang, E., Sandanov, D. V., Yin, Y., Qi, Z., Badmaeva, N. K. (2013): Rapid warming accelerates tree growth decline in semi-arid forests of Inner Asia. – Global Change Biology 19(8): 2500-2510.
[45] Liu, N., Treitz, P. (2016): Modelling high arctic percent vegetation cover using field digital images and high resolution satellite data. – International Journal of Applied Earth Observation and Geoinformation 52: 445-456.
[46] Lloyd, A. H., Fastie, C. L. (2002): Spatial and temporal variability in the growth and climate response of treeline trees in Alaska. – Climatic Change 52(4): 481-509.
[47] Lynch, J. P. (2013): Steep, cheap and deep: An ideotype to optimize water and N acquisition by maize root systems. – Annals of Botany 112(2): 347-357.
[48] Martínez-Vilalta, J., Piñol, J. (2002): Drought-induced mortality and hydraulic architecture in pine populations of the NE Iberian Peninsula. – Forest Ecology and Management 161(1-3): 247-256.
[49] Maselli, F., Cherubini, P., Chiesi, M., Gilabert, M. A., Lombardi, F., Moreno, A., Teobaldelli, M., Tognetti, R. (2014): Start of the dry season as a main determinant of inter-annual Mediterranean forest production variations. – Agricultural and Forest Meteorology 194: 197-206.
[50] Matkala, L., Kulmala, L., Kolari, P., Aurela, M., Bäck, J. (2021): Resilience of subarctic Scots pine and Norway spruce forests to extreme weather events. – Agricultural and Forest Meteorology 296: 108239.
[51] McDowell, N., Pockman, W. T., Allen, C. D., Breshears, D. D., Cobb, N., Kolb, T., Plaut, J., Sperry, J., West, A., Williams, D. G., Yepez, E. A. (2008): Mechanisms of plant survival and mortality during drought: Why do some plants survive while others succumb to drought? – New Phytologist 178(4): 719-739.
[52] Melaas, E. K., Friedl, M. A., Zhu, Z. (2013): Detecting interannual variation in deciduous broadleaf forest phenology using Landsat TM/ETM+ data. – Remote Sensing of Environment 132: 176-185.
[53] Menzel, A. (2002): Phenology: Its importance to the global change community: An editorial comment. – Climatic Change 54(4): 379-385.
[54] Merlin, M., Perot, T., Perret, S., Korboulewsky, N., Vallet, P. (2015): Effects of stand composition and tree size on resistance and resilience to drought in sessile oak and Scots pine. – Forest Ecology and Management 339: 22-33.
[55] Miranda, A., Lara, A., Altamirano, A., Di Bella, C., González, M. E., Julio Camarero, J. (2020): Forest browning trends in response to drought in a highly threatened Mediterranean landscape of South America. – Ecological Indicators 115: 106401.
[56] Moreno-Fernández, D., Viana-Soto, A., Camarero, J. J., Zavala, M. A., Tijerín, J., García, M. (2021): Using spectral indices as early warning signals of forest dieback: The case of drought-prone Pinus pinaster forests. – Science of The Total Environment 793: 148578.
[57] Neteler, M., Mitasova, H. (2008): Open Source GIS: A GRASS GIS Approach. – Third edition, NewYork: Springer.

http://www.aloki.hu ● ISSN 1589 1623 (Print) ● ISSN 1785 0037 (Online)
DOI: http://dx.doi.org/10.15666/aeer/2005_44094427

[58] Ochtyra, A., Marcinkowska-Ochtyra, A., Raczko, E. (2020): Threshold- and trend-based vegetation change monitoring algorithm based on the inter-annual multi-temporal normalized difference moisture index series: A case study of the Tatra Mountains. – Remote Sensing of Environment 249: 112026.
[59] Ortiz, B. V., Thomson, S. J., Huang, Y., Reddy, K. N., Ding, W. (2011): Determination of differences in crop injury from aerial application of glyphosate using vegetation indices. – Computers and Electronics in Agriculture 77(2): 204-213.
[60] Pasho, E., Camarero, J. J., de Luis, M., Vicente-Serrano, S. M. (2011): Impacts of drought at different time scales on forest growth across a wide climatic gradient in north-eastern Spain. – Agricultural and Forest Meteorology 151(12): 1800-1811.
[61] Pedersen, B. S. (1998): The Role of Stress in the Mortality of Midwestern Oaks As Indicated By Growth Prior To Death. – Ecology 79(1): 79-93.
[62] Praciak, A., Pasiecznik, N., Sheil, D., van Heist, M., Sassen, M., Correia, C. S., Dixon, C., Fyson, G., Rushford, K., Teeling, C. (2013): The CABI encyclopedia of forest trees. – Oxfordshire: CABI.
[63] Prutskoy, A. V. (2017): Structural peculiarities of the root systems of pine and of oak in conifer-broadleaf plantings on sandy loam podzolic soil. – Uspekhi sovremennogo yestestvoznaniya 7: 47-53.
[64] Querejeta, J. I., Estrada-Medina, H., Allen, M. F., Jiménez-Osornio, J. J. (2007): Water source partitioning among trees growing on shallow karst soils in a seasonally dry tropical climate. – Oecologia 152(1): 26-36.
[65] Rohner, B., Kumar, S., Liechti, K., Gessler, A., Ferretti, M. (2021): Tree vitality indicators revealed a rapid response of beech forests to the 2018 drought. – Ecological Indicators 120: 106903.
[66] Singatullin, I. K. (2017): Condition of pine forests of the Republic of Tatarstan after the drought of 2010. – Vestnik Omskogo GAU 27(3): 95-101.
[67] Soudani, K., Le Maire, G., Dufrêne, E., François, C., Delpierre, N., Ulrich, E., Cecchini, S. (2008): Evaluation of the onset of green-up in temperate deciduous broadleaf forests derived from Moderate Resolution Imaging Spectroradiometer (MODIS) data. – Remote Sensing of Environment 112(5): 2643-2655.
[68] Steckel, M., del Río, M., Heym, M., Aldea, J., Bielak, K., Brazaitis, G., Černý, J., Coll, L., Collet, C., Ehbrecht, M., Jansons, A., Nothdurft, A., Pach, M., Pardos, M., Ponette, Q., Reventlow, D. O. J., Sitko, R., Svoboda, M., Vallet, P., Wolff, B., Pretzsch, H. (2020): Species mixing reduces drought susceptibility of Scots pine (*Pinus sylvestris* L.) and oak (*Quercus robur* L., Quercus petraea (Matt.) Liebl.) - Site water supply and fertility modify the mixing effect. – Forest Ecology and Management 461: 117908.
[69] Toïgo, M., Vallet, P., Tuilleras, V., Lebourgeois, F., Rozenberg, P., Perret, S., Courbaud, B., Perot, T. (2015): Species mixture increases the effect of drought on tree ring density, but not on ring width, in *Quercus petraea-Pinus sylvestris* stands. – Forest Ecology and Management 345: 73-82.
[70] Tzavali, A., Paravantis, J. P., Mihalakakou, G., Fotiadi, A., Stigka, E. (2015): Urban heat island intensity: A literature review. – Fresenius Environmental Bulletin 24(12B): 4537-4554.
[71] Vanhellemont, M., Sousa-Silva, R., Maes, S. L., Van den Bulcke, J., Hertzog, L., De Groote, S. R. E., Van Acker, J., Bonte, D., Martel, A., Lens, L., Verheyen, K. (2019): Distinct growth responses to drought for oak and beech in temperate mixed forests. – Science of the Total Environment 650: 3017-3026.
[72] Vincini, M., Frazzi, E., D'Alessio, P. (2008): A broad-band leaf chlorophyll vegetation index at the canopy scale. – Precision Agriculture 9(5): 303-319.
[73] Walsh, J. E., Ballinger, T. J., Euskirchen, E. S., Hanna, E., Mård, J., Overland, J. E., Tangen, H., Vihma, T. (2020): Extreme weather and climate events in northern areas: A review. – Earth-Science Reviews 209: 103324.

http://www.aloki.hu ● ISSN 1589 1623 (Print) ● ISSN 1785 0037 (Online)
DOI: http://dx.doi.org/10.15666/aeer/2005_44094427

[74] Weng, Q. (2012): Remote sensing of impervious surfaces in the urban areas: Requirements, methods, and trends. – Remote Sensing of Environment 117: 34-49.
[75] Weng, Q., Fu, P., Gao, F. (2014): Generating daily land surface temperature at Landsat resolution by fusing Landsat and MODIS data. – Remote Sensing of Environment 145: 55-67.
[76] Williams, A. P., Allen, C. D., Millar, C. I., Swetnam, T. W., Michaelsen, J., Still, C. J., Leavitt, S. W. (2010): Forest responses to increasing aridity and warmth in the southwestern United States. – Proceedings of the National Academy of Sciences of the United States of America 107(50): 21289-21294.
[77] Williams, A. P., Allen, C. D., Macalady, A. K., Griffin, D., Woodhouse, C. A., Meko, D. M., Swetnam, T. W., Rauscher, S. A., Seager, R., Grissino-Mayer, H. D., Dean, J. S., Cook, E. R., Gangodagamage, C., Cai, M., Mcdowell, N. G. (2013): Temperature as a potent driver of regional forest drought stress and tree mortality. – Nature Climate Change 3(3): 292-297.
[78] Wong, C. Y. S., D'Odorico, P., Bhathena, Y., Arain, M. A., Ensminger, I. (2019): Carotenoid based vegetation indices for accurate monitoring of the phenology of photosynthesis at the leaf-scale in deciduous and evergreen trees. – Remote Sensing of Environment 233: 111407.
[79] Xian, G., Crane, M. (2006): An analysis of urban thermal characteristics and associated land cover in Tampa Bay and Las Vegas using Landsat satellite data. – Remote Sensing of Environment 104(2): 147-156.
[80] Yang, Y., Anderson, M., Gao, F., Hain, C., Noormets, A., Sun, G., Wynne, R., Thomas, V., Sun, L. (2020): Investigating impacts of drought and disturbance on evapotranspiration over a forested landscape in North Carolina, USA using high spatiotemporal resolution remotely sensed data. – Remote Sensing of Environment 238: 111018.
[81] Yuan, F., Bauer, M. E. (2007): Comparison of impervious surface area and normalized difference vegetation index as indicators of surface urban heat island effects in Landsat imagery. – Remote Sensing of Environment 106(3): 375-386.
[82] Zarei, A., Asadi, E., Ebrahimi, A., Jafari, M., Malekian, A., Mohammadi Nasrabadi, H., Chemura, A., Maskell, G. (2020): Prediction of future grassland vegetation cover fluctuation under climate change scenarios. – Ecological Indicators 119: 106858.
[83] Zhan, W., Chen, Y., Zhou, J., Wang, J., Liu, W., Voogt, J., Zhu, X., Quan, J., Li, J. (2013): Disaggregation of remotely sensed land surface temperature: Literature survey, taxonomy, issues, and caveats. – Remote Sensing of Environment 131(19): 119-139.
[84] Zhang, X., Friedl, M. A., Schaaf, C. B., Strahler, A. H., Liu, Z. (2005): Monitoring the response of vegetation phenology to precipitation in Africa by coupling MODIS and TRMM instruments. – Journal of Geophysical Research D: Atmospheres 110(12): 1-14.
[85] Zhang, J., Gou, Z., Zhang, F., Shutter, L. (2020): A study of tree crown characteristics and their cooling effects in a subtropical city of Australia. – Ecological Engineering 158: 106027.
[86] Zhang, L., Han, W., Niu, Y., Chávez, J. L., Shao, G., Zhang, H. (2021): Evaluating the sensitivity of water stressed maize chlorophyll and structure based on UAV derived vegetation indices. – Computers and Electronics in Agriculture 185: 106174.
[87] Zhigunova, S. N., Mikhaylenko, O. I., Fedorov, N. I. (2018): The Use of Remotely Sensed Data for Analysis of the Influence of the Urban Environment on the Seasonal Growth of Arboreal Vegetation. – Fourth International Scientific Conference Ecology and Geography of Plants and Plant Communities, pp. 254-260.

http://www.aloki.hu ● ISSN 1589 1623 (Print) ● ISSN 1785 0037 (Online)
DOI: http://dx.doi.org/10.15666/aeer/2005_44094427

PLANT DIVERSITY IN KING SALMAN PARK IN RIYADH, SAUDI ARABIA

ALFAGHAM, A.* – BAHAMMAM, N. – ALSAHLI, W. – ALZAHEM, S.

Botany and Microbiology Department, College of Science, King Saud University, 11451 Riyadh, Saudi Arabia
(e-mails: Njood.nb@gmail.com – N. Bahammam; Shaden4004@gmail.com – W. Alsahli; w.h.al_sa1419@hotmail.com – S. Alzahem)

**Corresponding author*
e-mail: aalfaghom@ksu.edu.sa

(Received 29th Apr 2022; accepted 26th Jul 2022)

Abstract. King Salman National Park is located about 22 km north of Riyadh city (Saudi Arabia) and has an area of 340000 m^2. The park is one of the important parks in Riyadh and the Kingdom of Saudi Arabia. This study aims to determine the floristic structure and plant diversity, informing policymakers and conservationists about this protected area. Fifteen sites of the national park, cultivated and non-cultivated, were selected. Density, frequency and diversity indices were evaluated. Twenty species were recorded in the park, including eight species of phanerophyte (40%), followed by seven species of chamaephytes (35%), three species of therophyte (15%) and two species of hemicryptophytes (10%). Rhamnaceae were dominated in the national park with one species (*Ziziphus spina-cristi*) which had the greatest ecological importance in all areas under study (44.77%). Small sandy hills have the highest diversity among all studied sites. Decreasing the effect of visitors and climate change by creating protected areas in the park could increase plant diversity in the park under study.
Keywords: *King Salman National Park, biodiversity, species richness, vegetation*

Introduction

Saudi Arabia covers a huge area of the Arabian Peninsula, it is located in the Middle East in South Asia at 25 degrees north latitude and 45 degrees east longitude. It covers an area of 2.25 million km^2. Saudi Arabia is characterised by a semi-arid to arid climate with hot days, cold nights, and extremely low annual rainfall. Drought-resistant plant species are widely spread in Saudi Arabia, distinguished from plants in non-dry conditions at the morphological, anatomical, and physiological levels. Promoting the conservation of these species could maintain water agriculture used in the world. Plant diversity is essential to human survival, economic well-being, ecosystem function and stability (Singh et al., 2019). Local plant species are more vulnerable to human activity pressures and natural changes, posing a greater danger of extinction. To promote the conservation of these species, in situ conservation measures must be implemented, and the establishment of National parks is the most efficient and cost-effective technique. (Coelho et al., 2020; Abeli et al., 2020). The United Nations Environment Program (2001) reported that habitat destruction, overexploitation, pollution, and species introduction are the main causes of biodiversity loss. These disturbances have been considered an important factor in structuring societies and determining plant dynamics diversity at the local and regional levels (Wilcove et al., 1998; Suratman, 2012; Kehoe et al., 2021). The climate zones favourable for plants will alter, and species diversity will be significantly threatened as a result of climate change. Climate change's impact on species has become a hot topic in studying global species spatial patterns (Tian and

http://www.aloki.hu ● ISSN 1589 1623 (Print) ● ISSN 1785 0037 (Online)
DOI: http://dx.doi.org/10.15666/aeer/2005_44294439

Jiang, 2015). Therefore, regular plant diversity monitoring and high maintenance requirements of national parks are crucial. Plants are keys to life on earth and main components of all ecosystems. Despite their importance, plant diversity is threatened not only by climate change but also by human activities (FAO, 2019).

In vegetation cover management operations, the information from the quantitative inventory will provide a valuable reference for assessing desert ecosystems and improving our knowledge in identifying ecologically beneficial species of particular interest, thus defining conservation efforts to sustain plant biodiversity. For example, the all-taxa biodiversity inventory (ATBI) can help to determine the nature and distribution of biodiversity in the area being managed, in addition to the quantitative analysis studies that could give resources for a wide range of species (Cannon et al., 1998). A study made by El-Sheikh et al., 2013, showed the progressive succession varying among the different habitat types in Thumamah Nature Park, which was an attempt to explain the vegetation dynamics after 30 years of conservation. The escarpment and the rocky upland habitats reflect the relationship between altitude, edaphic factors, and the type of vegetation units in each habitat type after excluding the human impact. A different study talked about regeneration, density, and diversity of woody vegetation in awash national park in Ethiopia. They found that only Acacia senegal, the park's major tree species, exhibited a higher capability for regeneration (Mekonnen, 2009). As a result, if the park's surviving vegetation is to be protected, appropriate management interventions, such as avoiding human intrusion, are required for Awash National Park. The quantitative analysis study of Khadimnagar National Park of Bangladesh described the diversity of plant species (trees, shrubs and herbs) and the structure and composition of the national park, which give them the ability to assess the plant diversity and provide sustainable management strategies to the protected area (Sobuj and Rahman, 2011).

Several new wildlife-protected areas have been established in Saudi Arabia over the last three decades (SA). The number of national parks, newly constituted nature reserves, wildlife sanctuaries, protected landscapes and biosphere reserves have expanded. Saudi Arabia now includes 16 protected areas and 12 national parks (Abuzinada, 2003). King Salman national Park is in Banban, north of Riyadh. It is one of the most important parks in Riyadh.

Moreover, it was opened in March of 2016 and is intended for visitors from inside and outside the country. This study aims to determine this national park's floristic structure and plant diversity, informing policymakers and conservationists about this protected area. As a result, appropriate steps would be taken to preserve and enhance its diversity.

Materials and methods

The study area

The King Salman Wilderness Park is located in Banban, 22 km from the city of Riyadh, on a land area of more than 3.400.000 m^2 in the northwest corner of King Khalid International Airport. Numerous valleys separated by ridges dissect the small hills. The soil ranges from clay loams to sandy on the hills. The desert climate prevails in Riyadh, where the national park is located. Climate is hot and dry. June and July are the hottest, and December and January are the coolest. During the year, there is virtually no rainfall, the average annual temperature is 26.2 °C and the precipitation is about 5 mm per year (*Fig. 1*). The study was carried out through a total of 15 sample plots in all three areas, each area had five plots, 10 m × 10 m sample plots were nested within

http://www.aloki.hu ● ISSN 1589 1623 (Print) ● ISSN 1785 0037 (Online)
DOI: http://dx.doi.org/10.15666/aeer/2005_44294439

each plot. Overall, the first five sites have represented the slope of the valley habitat. The middle five sites represented the depressions habitat. And the last five sites represented the small sandy hill habitat (*Fig. 2*).

Plants identification

Samples were taken from King Salman Wilderness Park, in which this study was carried out in the fall-spring season of 2022 (April/2022). In this field study, some tools were used to obtain these samples. These materials used in field work include plastic bags, scissors, pen, label tapes and a notebook to record the number of species in the study areas. Species were identified in the study site, King Salman Park and confirmed in the herbarium of the plant and microbiology department at King Saud University. The numbers of these species in each site were counted. The analytical characteristics such as abundance, density, relative density, frequency, relative frequency, abundance, relative dominance and Importance Value Index (IVI) were calculated through (Shukla and Chandel, 2000) and (Zhigila et al., 2015). Shannon- Wiener diversity index for trees and herbs species and Simpson's index for all species were also calculated (Michael, 1990).

Data analyses

The data acquired were analyzed quantitatively. The analytical characters used were density, relative density, frequency, relative frequency, abundance, relative abundance cover, importance value, Simpson's index, and Shannon wiener index.

$$\textbf{Density} = \frac{\textbf{Total number r of individuals of a species in all quadrats}}{\textbf{Total number of quadrats studied X Quadrats area}} \quad \text{(Eq.1)}$$

$$\textbf{Relative Density} = \frac{\textbf{Number of individuals of one species}}{\textbf{Total number of all individuals counted}} \times \mathbf{100} \quad \text{(Eq.2)}$$

$$\textbf{Frequency} = \frac{\textbf{Number of quadrats in which the species occurs}}{\textbf{Total number of quadrats sampled}} \quad \text{(Eq.3)}$$

$$\textbf{Relative Frequency} = \frac{\textbf{Frequency of one species}}{\textbf{Total frequency of all species}} \times \mathbf{100} \quad \text{(Eq.4)}$$

$$\textbf{Abundance} = \frac{\textbf{Total number of individuals of a species in all quadrats}}{\textbf{Total number of quadrats in which the species occurred}} \quad \text{(Eq.5)}$$

$$\textbf{Relative Abundance} = \frac{\textbf{The abundance of one species}}{\textbf{Total of all species counted}} \times \mathbf{100} \quad \text{(Eq.6)}$$

$$\textbf{Importance value index = Relative Frequency + Relative Density + Relative Abundance} \quad \text{(Eq.7)}$$

$$\textbf{Simpson diversity index } (C) = \sum_{i=1}^{s} pi^2 \quad \text{(Eq.8)}$$

The value of C ranges between 0 and 1. With this index, 0 represents infinite diversity and 1 no diversity.

$$\textbf{Shannon-Wiener index (H) = -} \sum_{i=1}^{s} \textbf{pi Log pi} \quad \text{(Eq.9)}$$

where $Pi = \frac{Number\ of\ individuals\ of\ one\ species}{Total\ number\ of\ individuals\ in\ the\ samples} \times 100$ or relative sp. abundance.

http://www.aloki.hu ● ISSN 1589 1623 (Print) ● ISSN 1785 0037 (Online)
DOI: http://dx.doi.org/10.15666/aeer/2005_44294439

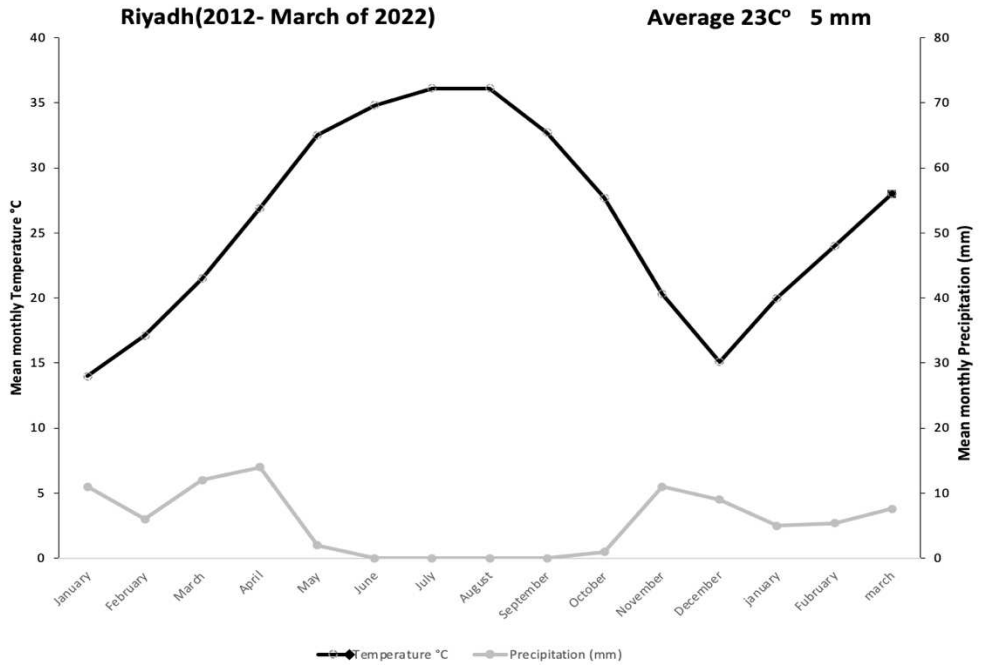

Figure 1. *Average of 2012- March of 22. Mean monthly temperature (°C) and mean monthly precipitation (mm) in King Salman Wilderness Park, Riyadh according to King Khalid international airport station*

Figure 2. *Study area map showing the whole map of Saudi Arabia with focus on the study area. And showing the distribution of the studied Sites in the study area. Sites 1, 2, 3, 4, 5 show Slope of valley habitat. Sites 6, 7, 8, 9, 10 show Depressions habitat. Sites 11, 12, 13, 14, 15 show Small sandy hill habitat*

http://www.aloki.hu ● ISSN 1589 1623 (Print) ● ISSN 1785 0037 (Online)
DOI: http://dx.doi.org/10.15666/aeer/2005_44294439

Results and discussion

Trees and herbs were mainly accrued in King Salman National Park. A species' high important value index (IVI) indicates its dominance and ecological success, as well as its good regeneration power and bigger ecological amplitude, as well as those plants that require monitoring management. In contrast, species classed as low require substantial conservation efforts.

Floristic diversity and composition of plants species

Floral diversity refers to the variety of plants that exist at a given time. In the present study, the cultivated and non-cultivated plants were recorded in March-April at 2022. Twenty taxa, including eight species of phanerophyte (40%), followed by seven species of chamaephytes (35%), three species of therophyte (15%) and two species of hemicryptophytes (10%) were recorded (*Fig. 3*). Phanerophyte is the most represented life form in the national park. The majority of conifer and dicot tree species, as well as numerous palm and cycad species, and tree ferns, come under phanerophyte (Niklas, 2008).

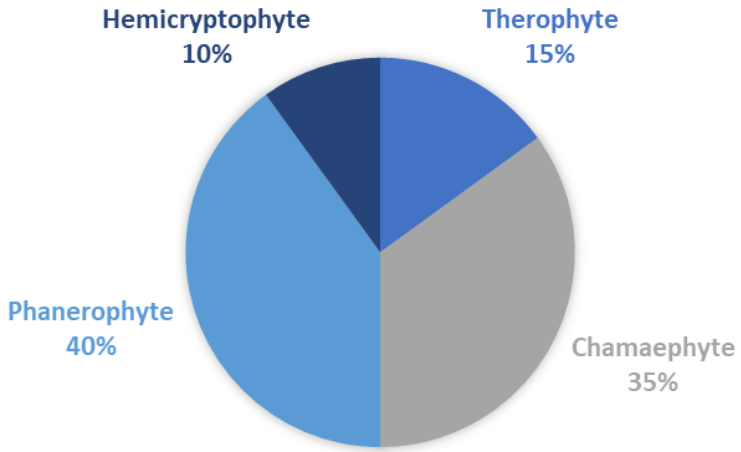

Figure 3. *Life-form spectrum of the recorded species in the study area*

In more detail, eight species of trees under five families were identified. Mimosaceae containing three species followed by Caesalpiniaceae (two species), Fabaceae, Tamaricaceae, Rhamnaceae had the same number of species (one species each) (*Table A1* in the *Appendix*). Moreover, 11 species of shrubs and sub-shrubs under eight families were identified. The family Poaceae, Asteraceae, and Brassicaceae containing two species each, followed by Resedaceae, Polygonaceae, Chenopodiaceae, Boraginaceae, and Malvaceae (one species each). These plant families are widely distributed in Saudi Arabia, especially in the middle region at late winter and the beginning of spring (Migahid, 1996; Chaudhary, 1999). And known to be resistant to drought climate in the desert ecosystem (Maraghni et al., 2019; Akande et al., 2019; Ricks, 1992). They are able to colonize wide spaces and create microsites for the germination and establishment of numerous other species beneath their canopies because of their high germinability, accelerated growth rates during the early stages, and tolerance to high radiation levels (Bedair et al., 2020). However, due to the high impact of the pressure of human trampling on the land which is the major issue of plant diversity declined (Pescott and Stewart, 2014). Rhamnaceae were dominated in the

http://www.aloki.hu ● ISSN 1589 1623 (Print) ● ISSN 1785 0037 (Online)
DOI: http://dx.doi.org/10.15666/aeer/2005_44294439

national park with one spices (*Ziziphus spina-cristi*) which had the most ecological importance in all studied areas (44.77%). The ecological and economic importance of *Ziziphus spina-cristi* is considerable (Zhao et al., 2021). With their thick root structure that stabilizes the soil and protects it from erosion, *Ziziphus spina-cristi* plays a vital role in soil conservation. The firm wood is useful for turning and manufacturing agricultural implements, firewood, and high-quality charcoal, while the leaves provide fodder for cattle. Based on the importance of the *Ziziphus spina-cristi*, King Salman national park emphasises sowing this tree in all park areas. The second dominant family was Caesalpiniaceae represented by *Parkinsonia aculeata* which is one of the aline plant species and widely disturbed trees or shrubs in hot climates which would affect negatively in native plant diversity (Calvo-Alvarado et al., 2022). Due to its thorns it develops dense, impenetrable woods that ruin meadows, clog rivers, and prevent livestock drinking (van Klinken et al., 2009). It was frequently marketed as a forage, hedge, or decorative tree with the ability to endure the driest, saltiest, and most waterlogged environments.

Sorghum halepense and *Pulicaria crispa* (3.11%) had less ecological importance. *Sorghum halepense* L. is a common and noxious herb that is spreading around the world. It showed less abundance in the park, but it spreads quickly and will compete with native species diversity (Travlos et al., 2019). Therefore, the national park maintenance should increase the species spread control (*Fig. 4*).

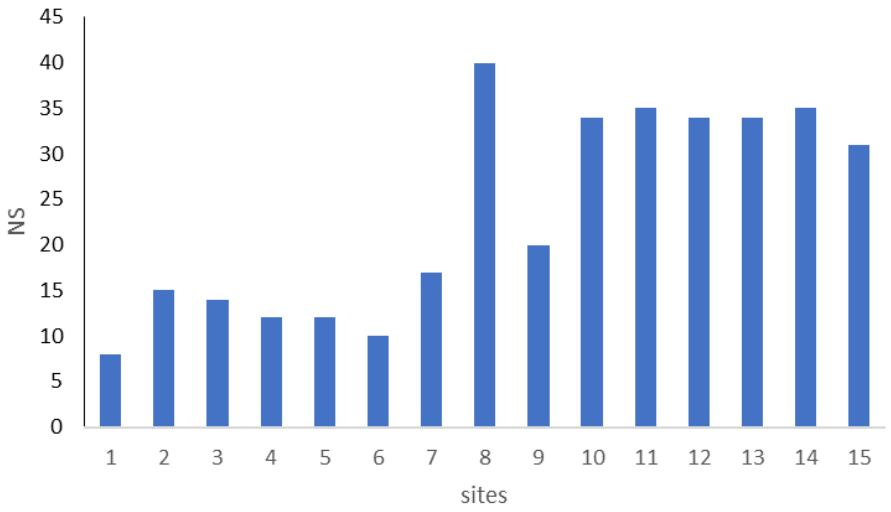

Figure 4. *Number of all organisms of given species (NS) at each site under study*

Habitat diversity

The habitat types in King Salman National Park were divided into three types, the slope of the valley (1, 2, 3, 4 and 5 site), depressions (6, 7, 8, 9 and 10 site) and small sandy hill (11, 12, 13, 14 and 15 site) (*Fig. 2*). The slope of the valley habitat indicates the species' lowest degree of relative evenness, which is confirmed by the high Simson index, illustrating that 4-5 species were dominated in this site (*Table A3*). In the second habitat of the study (depressions), the degree of relative evenness of the species was high only in the ninth site compared with other sites in the same habitat. However, the small sandy hill habitat showed the highest diversity and regular distribution at all sites (11, 12, 13, 14 and 15) (*Table A3*), far from visitors and the nature of rocky soil. This

http://www.aloki.hu ● ISSN 1589 1623 (Print) ● ISSN 1785 0037 (Online)
DOI: http://dx.doi.org/10.15666/aeer/2005_44294439

confirms that repeated use of the same sites by the visitors trampled the vegetation and soil (Bar, 2017), eventually resulting in harm that could cause plant diversity loss (Pescott and Stewart, 2014). Encouraging visitors to use the places designated for picnics and walking paths could help to increase or protect plant diversity and improve ecosystem stability in the national park.

Also, the climate change has tangible impact on the vegetation of National Parks (Scherrer and Pickering, 2001; Jahani and Saffariha, 2021). Due to the drought seasons during last ten years (*Fig. 1*), some important species such as *Acacia spp.* had low relative abundance (*Fig. 5*).

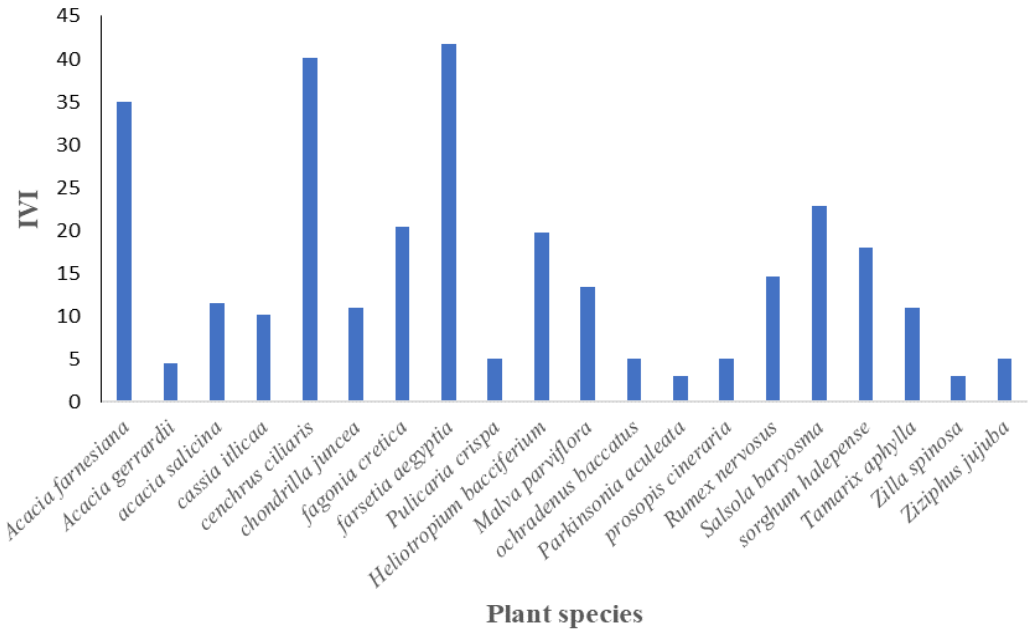

Figure 5. *Importance value index (IVI) of plant species at the 15 sites in King Salman National Park*

Conclusion

- *Ziziphus spina-cristi* dominate the King Salman National Park plants community. Increasing species diversity in the current park could elevate the ecosystem stability in each site.
- The small plant diversity species in the study area could be related to two main factors, the pressure of national park visitors and climate change. Therefore, this study would like to draw attention to the importance of increasing plant diversity in the parks and decreasing the effect of visitors by creating some protected areas in the park.

REFERENCES

[1] Abeli, T., Dalrymple, S., Godefroid, S., Mondoni, A., Müller, J. V., Rossi, G., Orsenigo, S. (2020): Ex situ collections and their potential for the restoration of extinct plants. – Conservation Biology 34: 303-313.

http://www.aloki.hu ● ISSN 1589 1623 (Print) ● ISSN 1785 0037 (Online)
DOI: http://dx.doi.org/10.15666/aeer/2005_44294439

[2] Abuzinada, A. H. (2003): The role of protected areas in conserving biological diversity in the kingdom of Saudi Arabia. – Journal of Arid Environments 54: 39-45.
[3] Akande, O., Ahmad, Y., Shuaib, A., Jeje, C. (2019): Distribution and relative density of trees species in Kainji Lake National Park, Nigeria. – World News of Natural Sciences 22.
[4] Bar, P. (2017): Visitor trampling impacts on soil and vegetation: the case study of Ramat Hanadiv Park, Israel. – Israel Journal of Plant Sciences 64: 145-161.
[5] Bedair, H., Shaltout, K., Ahmed, D., Sharaf El-Din, A., El-Fahhar, R. (2020): Characterization of the wild trees and shrubs in the Egyptian Flora. – Egyptian Journal of Botany 60: 147-168.
[6] Calvo-Alvarado, J. C., Jiménez-Rodríguez, C. D., Solano, J. C., Arias-Rodríguez, O. (2022): Interception and Redistribution of Precipitation by Parkinsonia aculeata L.: Implications for Palo Verde National Park Wetlands, Costa Rica. – Water 14: 311.
[7] Chaudhary, S. A. (1999): Flora of Kingdom Saudi Arabia, Riyadh, Saudi Arabia. – Ministry of Agriculture and Water, Saudi Arabia.
[8] Coelho, N., Gonçalves, S., Romano, A. (2020): Endemic plant species conservation: biotechnological approaches. – Plants 9: 345.
[9] EL-Sheikh, M. A., Thomas, J., Alatar, A. A., Hegazy, A. K., Abbady, G. A., Alfarhan, A. H., Okla, M. I. (2013): Vegetation of Thumamah Nature Park: a managed arid land site in Saudi Arabia. – Rendiconti Lincei 24: 349-367.
[10] FAO (2019): The State of the World's Biodiversity for Food and Agriculture. – In: Bélanger, J., Pilling, D. (eds.) FAO Commission on Genetic Resources for Food and Agriculture Assessments. FAO, Rom.
[11] Jahani, A., Saffariha, M. (2021): Human activities impact prediction in vegetation diversity of Lar National Park in Iran using artificial neural network model. – Integrated Environmental Assessment and Management 17: 42-52.
[12] Kehoe, R., Frago, E., Sanders, D. (2021): Cascading extinctions as a hidden driver of insect decline. – Ecological Entomology 46: 743-756.
[13] Maraghni, M., Gorai, M., Steppe, K., Neffati, M., VAN Labeke, M.-C. (2019): Coordinated changes in photosynthetic machinery performance and water relations of the xerophytic shrub Ziziphus lotus (L.) Lam. (Rhamnaceae) following soil drying. – Photosynthetica 57: 113-120.
[14] Mekonnen, M., Gebrehiwot, K., Birhane, E., Tewoldeberhan, S. (2009): Regeneration, density and diversity of woody vegetation in Awash National Park, Ethiopia. – Journal of the Drylands 2: 101-109.
[15] Michael, P. (1990): Ecological Methods for Field and Laboratory Investigation. – Tata McGrew Hill Publishing Co. Ltd., New Delhi.
[16] Migahid, M. A. (1996): Flora of Saudi Arabia. –King Saudi University, Saudi Arabia.
[17] Niklas, K. J. (2008): Life Forms, Plants. – In: Jorgensen, S. E., Faith, B. (eds.) Encyclopedia of Ecology. Academic Press, Cambridge, MA.
[18] Pescott, O. L., Stewart, G. B. (2014): Assessing the impact of human trampling on vegetation: a systematic review and meta-analysis of experimental evidence. – PeerJ 2: e360.
[19] Ricks, G. (1992): Native & Introduced Species for Naturalistic Landscape in Saudi Arabia. – Engineering Sciences 4.
[20] Scherrer, P., Pickering, C. M. (2001): Effects of grazing, tourism and climate change on the alpine vegetation of Kosciuszko National Park. – Victorian Naturalist 118: 93-93.
[21] Shukla, R., Chandel, P. (2000): Plant Ecology and Soil Science. 9th Ed. – S. Chand & Company Limited, Ramnagor, New Delhi.
[22] Singh, H., Kaur, K., Singh, S., Kaur, P., Singh, P. (2019): Genome-wide analysis of cyclophilin gene family in wheat and identification of heat stress responsive members. – Plant Gene 19: 100197.
[23] Sobuj, N., Rahman, M. (2011): Assessment of plant diversity in Khadimnagar National Park of Bangladesh. – International Journal of Environmental Sciences 2: 79.

http://www.aloki.hu ● ISSN 1589 1623 (Print) ● ISSN 1785 0037 (Online)
DOI: http://dx.doi.org/10.15666/aeer/2005_44294439

[24] Suratman, M. N. (2012): Tree species diversity and forest stand structure of Pahang National Park, Malaysia. – Biodiversity enrichment in a diverse world 19: 45-56.
[25] Tian, Z., Jiang, D. (2015): Mid-Holocene and last glacial maximum changes in monsoon area and precipitation over China. – Chinese Science Bulletin 60: 400-410.
[26] Travlos, I. S., Montull, J. M., Kukorelli, G., Malidza, G., Dogan, M. N., Cheimona, N., Antonopoulos, N., Kanatas, P. J., Zannopoulos, S., Peteinatos, G. (2019): Key aspects on the biology, ecology and impacts of Johnsongrass [Sorghum halepense (L.) Pers] and the role of glyphosate and non-chemical alternative practices for the management of this weed in Europe. – Agronomy 9: 717.
[27] Van Klinken, R. D., Campbell, S. D., Heard, T. A., Mckenzie, J., March, N. (2009): The biology of Australian weeds: 54. 'Parkinsonia aculeata' L. – Plant Protection Quarterly 24: 100-117.
[28] Wilcove, D. S., Rothstein, D., Dubow, J., Phillips, A., Losos, E. (1998): Quantifying threats to imperiled species in the United States. – BioScience 48: 607-615.
[29] Zhao, G., Cui, X., Sun, J., Li, T., Wang, Q., Ye, X., Fan, B. (2021): Analysis of the distribution pattern of Chinese Ziziphus jujuba under climate change based on optimized biomod2 and MaxEnt models. – Ecological Indicators 132: 108256.
[30] Zhigila, D. A., Sawa, F. B., Abdul, S. D., Abba, H. M., Tela, M. (2015): Diversity and Phytogeographic Investigation into the Woody Plants of West Tangaza Forest Reserve, Sokoto State, Nigeria. – International Journal of Plants Research 5: 73-79.

APPENDIX

Table A1. *Nomenclature and life form of plant species at the 15 sites in King Salman National Park*

Family	Scientific name	Common name	Life form
Mimosaceae	*Acacia farnesiana*		Ph
Mimosaceae	*Acacia gerrardii*	AlGhaf	Ph
Mimosaceae	*Acacia salicina*		Ph
Caesalpiniaceae	*Senna italica*	AlAshrik	Ch
Caesalpiniaceae	*Parkinsonia aculeata*		Ph
Fabaceae	*Prosopis cineraria*		Ph
Tamaricaceae	*Tamarix aphylla*	AlAthel	Ph
Rhamnaceae	*Ziziphus spina-cristi*	AlSeder	Ph
Poaceae	*Cenchrus ciliaris*		Ch
Poaceae	*Sorghum halepense*		He
Asteraceae	*Pulicaria crispa*	AlJuthjath	Ch
Asteraceae	*Chondrilla juncea*		He
Brassicaceae	*Zilla spinosa*	AlZilla	Th
Brassicaceae	*Farsetia aegyptia*	AlJurba	Ch
Resedaceae	*Ochradenus baccatus*	AlKurda	Ph
Polygonaceae	*Rumex vesicarius*	AlHumeedh	Th
Chenopodiaceae	*Salsola baryosma*	Salsola	Ch
Boraginaceae	*Heliotropium crispum*	AlRumram	Ch
Malvaceae	*Malva parviflora*	AlKhobeeza	Th
Zygophyllaceae	*Fagonia cretica*		Ch

The life forms are: Th therophyte, Ch chamaephyte, Ph phanerophyte, He hemicryptophyte

http://www.aloki.hu ● ISSN 1589 1623 (Print) ● ISSN 1785 0037 (Online)
DOI: http://dx.doi.org/10.15666/aeer/2005_44294439

Table A2. *The occurrence and importance value index (IVI) of plant species at the 15 sites in King Salman National Park*

Scientific name	1	2	3	4	5	6	7	8	9	10	11	12	13	14	15	T	M	RD	RF	RA	IVI
Acacia farnesiana	3	0	1	4	4	0	0	0	0	0	12	9	6	10	4	53	3.53	1.86	10.00	9.82	21.68
Acacia gerrardii	0	1	0	1	0	0	0	0	0	0	0	0	0	0	0	2	0.13	0.66	2.22	1.67	4.55
Acacia salicina	2	5	1	0	2	0	0	0	0	0	0	0	0	0	0	10	0.67	3.31	4.44	4.17	11.92
Cassia itlicaa	1	2	1	1	1	0	1	0	0	0	0	0	0	0	0	7	0.47	1.74	6.67	1.94	10.35
Cenchrus ciliaris	0	0	0	0	0	0	0	0	0	2	0	0	0	0	0	2	0.13	0.66	1.11	3.33	5.11
Chondrilla juncea	0	0	0	0	0	0	0	0	0	0	6	4	3	7	3	23	1.53	7.62	5.56	7.67	20.84
Fagonia cretica	0	0	0	0	0	0	0	1	0	0	2	4	2	1	2	12	0.80	3.98	6.67	3.33	13.98
Farsetia aegyptia	0	0	0	0	0	0	0	2	0	0	0	0	0	0	0	2	0.13	0.66	1.11	3.33	5.11
Pulicaria crispa	0	0	0	0	0	0	0	1	0	0	0	0	0	0	0	1	0.07	0.33	1.11	1.67	3.11
Heliotropium bacciferium	0	0	0	0	0	0	0	2	0	0	0	0	0	0	0	2	0.13	0.66	1.11	3.33	5.11
Malva parviflora	0	0	0	0	0	0	0	1	0	1	2	0	1	6	3	14	0.93	4.64	6.67	3.89	15.19
Ochradenus baccatus	0	0	0	0	0	0	0	0	0	0	2	6	9	8	3	28	1.87	9.28	5.56	9.33	24.17
Parkinsonia aculeata	1	7	9	2	2	3	5	7	12	16	0	0	0	0	0	64	4.27	21.20	11.11	10.67	42.98
Prosopis cineraria	0	0	0	0	0	0	0	0	0	0	4	3	2	0	0	9	0.60	2.98	3.33	5.00	11.32
Rumex nervosus	·	·	0	0	0	0	0	0	0	0	3	4	6	2	5	20	1.33	6.63	5.56	6.67	18.85
Salsola baryosma	0	0	0	0	0	0	0	0	0	0	0	0	3	1	5	9	0.60	2.98	3.33	5.00	11.32
Sorghum halepense	0	0	0	0	0	1	0	0	0	0	0	0	0	0	0	1	0.07	0.33	1.11	1.67	3.11
Tamarix aphylla	0	0	0	0	0	2	5	12	0	1	2	0	1	0	1	24	1.60	7.95	7.78	5.71	21.44
Zilla spinosa	0	0	0	0	0	0	0	2	0	0	0	0	0	0	0	2	0.13	0.66	1.11	3.33	5.11
Ziziphus spina-cristi	1	0	2	4	3	4	6	12	8	14	2	4	1	0	5	66	4.40	21.86	14.44	8.46	44.77
Total	8	15	14	12	12	10	17	40	20	34	35	34	34	35	31	-	-	100	100	100	300
Mean	0.4	0.8	0.7	0.6	0.6	0.5	0.9	2	1	1.7	1.8	1.7	1.7	1.8	1.6						

T: total, M: mean, RD: relative density, RF: relative frequency. RA: relative abundance. IVI: important value index

http://www.aloki.hu ● ISSN 1589 1623 (Print) ● ISSN 1785 0037 (Online)
DOI: http://dx.doi.org/10.15666/aeer/2005_44294439

Table A3. *Plant diversity measurement in the study area*

Sites	S	N	d	J'	H'(log10)	Lambda'	Habitat
1	5	8	1.924	0.928	0.6489	0.1429	
2	4	15	1.108	0.8447	0.5086	0.3048	
3	5	14	1.516	0.7006	0.4897	0.4066	Slope of valley
4	5	12	1.61	0.8979	0.6276	0.197	
5	5	12	1.61	0.9426	0.6589	0.1667	
6	4	10	1.303	0.9232	0.5558	0.2222	
7	4	17	1.059	0.9046	0.5446	0.2574	
8	9	40	2.169	0.798	0.7615	0.2	Depressions
9	2	20	0.3338	0.971	0.2923	0.4947	
10	5	34	1.134	0.6798	0.4752	0.3779	
11	9	35	2.25	0.8855	0.845	0.1597	
12	7	34	1.701	0.9657	0.8161	0.139	
13	10	34	2.552	0.8846	0.8846	0.1319	Small sandy hill
14	7	35	1.688	0.8665	0.7323	0.1849	
15	9	31	2.33	0.9615	0.9175	9.892E-2	
F	7.448**			0.575	10.322**	3.746*	
P value	0.008			0.578	0.002	0.054	

S = species number. N = individual numbers of species. J = species richness $\hat{H}$ = Shannon Wiener index. Lambda' = Simpson dominance. GPS = Global Positioning System position of the sampling sites. F and P value calculated according to ANOVA one-way. * = ≤ 0.05, ** = ≤ 0.001, *** = ≤ 0.001

Table A4. *The habitats of study samples and their locations*

Sites	GPS	Habitat
1	25.011818, 46.595993	
2	25.012051, 46.597034	
3	25.011298, 46.595172	Slope of valley
4	25.011851, 46.596629	
5	25.010914, 46.596563	
6	25.003241, 46.598145	
7	25.001173, 46.595776	
8	25.001242, 46.595896	Depressions
9	25.000570, 46.597005	
10	25.001262, 46.599238	
11	25.001252, 46.601240	
12	25.002657, 46.603266	
13	25.002099, 46.605138	Small sandy hill
14	25.000526, 46.604654	
15	24.999432, 46.603563	

http://www.aloki.hu ● ISSN 1589 1623 (Print) ● ISSN 1785 0037 (Online)
DOI: http://dx.doi.org/10.15666/aeer/2005_44294439

SPATIAL AND TEMPORAL DISTRIBUTION CHARACTERISTICS OF $PM_{2.5}$ AND VARIATION FACTORS OF THE AQI IN THE BEIJING-TIANJIN-HEBEI REGION FROM 2015 TO 2018

CHENG, M. Y.[1,2] – ZHANG, H.[1] – WAN, L. H.[1,2*]

[1]*College of Geographical Sciences, Harbin Normal University, Harbin 150025, Heilongjiang, China*

[2]*Heilongjiang Provincial Key Laboratory of Geographic Environment Monitoring and Spatial Information Service in Cold Regions, Harbin Normal University, Harbin 150025, Heilongjiang, China*

[*]*Corresponding author*
e-mail: wanluhe@hrbnu.edu.cn; phone: +86-1321-4618-158

(Received 6th May 2022; accepted 23rd Aug 2022)

Abstract. The current air pollution situation in northern China, especially in the Beijing-Tianjin-Hebei region, is particularly critical. How to prevent and control air quality in the Beijing-Tianjin-Hebei region has become the focus of China's environmental protection departments. Based on the hourly monitoring data from available monitoring stations in the Beijing-Tianjin-Hebei region from 2015 to 2018, The annual pollution frequency of the city was calculated, and the temporal and spatial distribution characteristics of the $PM_{2.5}$ concentration are analyzed in the study area from 2015 to 2018 by using the spatial interpolation method. The impact of various air pollutants and ground meteorological factors on air quality are studied using the Pearson correlation analysis method. The results are as follows: (1) With the increase of time, the pollution situation of $PM_{2.5}$ in the Beijing-Tianjin-Hebei region has steadily improved. (2) $PM_{2.5}$ and PM_{10} were the decisive pollutants that had the greatest impact on the AQI. (3) The influence of ground pressure and temperature on the $PM_{2.5}$ concentration and the AQI were more closely related than other meteorological factors. These research results help to deepen the understanding and prediction of air quality changes in the Beijing-Tianjin-Hebei region and provide theoretical support for policy-makers to improve air quality in the region.
Keywords: *variation trend, multiple factors, spatial interpolation, correlation analysis*

Introduction

With increasing awareness of environmental protection, people are paying more attention to air pollution because these problems will not only have an adverse impact on the environment but also damage human health (Kuo et al., 2021). The concentration of fine particles has always been a key indicator of China's environmental quality and a core factor that restricts sustainable development (Qian et al., 2021). Therefore, particulate matter ($PM_{2.5}$) pollution has become a major and urgent challenge facing China and the focus of the central government (Liu et al., 2021). $PM_{2.5}$ pollution in the environment has been associated with a variety of adverse health effects (Ru et al., 2021). Many studies have reported that long term exposure to fine particulate matter ($PM_{2.5}$) will increase the risk of chronic obstructive pulmonary disease (COPD) (Bo et al., 2021). Globally, the number of COPD deaths and the daily deaths caused by environmental $PM_{2.5}$ increased by more than 90% from 1990 to 2019 (Xiaorong et al., 2021). Exposure to long term air pollution, especially fine particulate matter, is a contributor to incidence rate and mortality worldwide and is also known as risk factor for coronary heart disease (CAD) and myocardial infarction (MI) (Slawsky et al., 2021).

http://www.aloki.hu ● ISSN 1589 1623 (Print) ● ISSN 1785 0037 (Online)
DOI: http://dx.doi.org/10.15666/aeer/2005_44414458

Moreover, long term $PM_{2.5}$ exposure is closely related to incidence rate and mortality rate of cancer (Pei et al., 2021). Therefore, understanding and analyzing the temporal and spatial distribution characteristics of $PM_{2.5}$ and the relevant influencing factors of the $PM_{2.5}$ concentration will help to deepen people's understanding of $PM_{2.5}$ and provide a reference for formulating air pollution control policies based on health effects. This is of great significance for controlling air pollution and protecting people's health (Yu et al., 2019).

The air quality index (AQI) can undoubtedly reflect the air quality of a region more directly, and its level directly affects the survival of human beings in a region, although the definition and scope of the AQI vary from country to country (Meng et al., 2021). Scholars all over the world have never stopped studying the regional trend changes and influencing factors of the AQI and its pollutants. Dutta et al. (2021) analyzed the air pollution trends and patterns of the three major cities in India under a temporal and spatial framework and pointed out that the seasonal distribution of the AQI showed that the pollution concentration was high in winter. Bhutiani et al. (2021), based on the temporal and spatial changes of air quality in integrated industrial estate, Haridwar, and its surrounding areas, demonstrated the important role of highway transportation in environmental air quality. Farhadi et al. (2018) analyzed the sensitivity of meteorological parameters and the instability index to the carbon monoxide concentration, particulate matter, and the AQI and discovered that particulate matter was the most important influence on the AQI. Mangayarkarasi et al. (2021) utilized $PM_{2.5}$ as the core factor, then, using the seasonal autoregressive comprehensive moving average and Facebook's Prophet database, proposed an AQI prediction model that provides strong support for the AQI prediction. In particular, during the worldwide novel coronavirus pandemic, regulators need to consider $PM_{2.5}$ and PM_{10} in monitoring ambient air quality so as to prevent potential hazards associated with human exposure (Richard et al., 2021). As the economic and political center of China, the Beijing-Tianjin-Hebei region has a large population density. An analysis of the change trend factors of the AQI in the Beijing-Tianjin-Hebei region not only is conducive for the formulation of environmental protection policies but also plays a reference role in the prevention and control of COVID-19 in the region.

This study set out to: (1) determine the decisive pollutants that affect the AQI and analyze the internal correlations of air pollutants; (2) analyze the temporal and spatial variation law of $PM_{2.5}$ in the Beijing-Tianjin-Hebei region from 2015 to 2018; and (3) explore the important influencing factors of meteorological factors on the AQI and $PM_{2.5}$ concentration changes.

Data and Methods

Study area

The Beijing-Tianjin-Hebei region is located in the north of the North China Plain at a west longitude of 113°7′ 20″–119°50′47″ and a north latitude of 36°3′–42°36′58″ (*Fig. 1*). It is adjacent to the Yanshan Mountains in the north, the North China Plain in the south, the Taihang Mountains in the west, and Bohai Bay in the east. The terrain in the northwest and north is high, and the terrain in the south and east is relatively flat. The area includes a variety of geomorphic features, but it is still dominated by a plain landform with an altitude of -52 to 2836 m (Nuan et al., 2021). The Beijing-Tianjin-Hebei region is one of the four major industrial zones in China that includes two

http://www.aloki.hu ● ISSN 1589 1623 (Print) ● ISSN 1785 0037 (Online)
DOI: http://dx.doi.org/10.15666/aeer/2005_44414458

municipalities directly under the central government (Beijing and Tianjin) and 13 cities in Hebei Province such as Zhangjiakou, Chengde, Qinhuangdao, Tangshan, Langfang, Baoding, Cangzhou, Shijiazhuang, Hengshui, Xingtai, and Handan. It has an extremely important economic and political status (Meng et al., 2021).

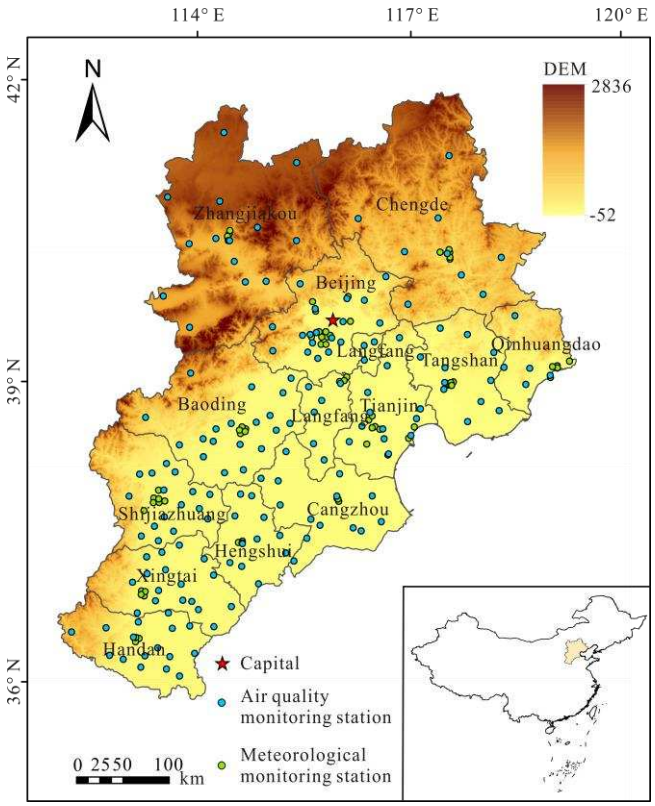

Figure 1. *Study area and monitoring station locations*

Data sources

The hourly air quality data of the Beijing-Tianjin-Hebei region from 2015 to 2018 included the AQI, $PM_{2.5}$, O_3, PM_{10}, NO_2, SO_2, and CO. There exist 72 available air quality monitoring points in the study area (*Fig. 1*), and they publish their data on the national urban air quality real-time release platform of the China Environmental Monitoring Station (http://www.cnemc.cn). The pollutant concentration data used in the calculation in this paper is the hourly data. The IAQI of single category pollutants is calculated by using the concentration limit of single category pollutants and the concentration of pollutants respectively, and the maximum value in the calculation result is the air quality index of this hour or that day.

The hourly meteorological data observed in the Beijing-Tianjin-Hebei region from 2015 to 2018 included the temperature, ground pressure, relative humidity, two-minute average wind speed, two-minute average wind direction, precipitation, and other parameters. There are 171 meteorological monitoring stations in the study area (*Fig. 1*). The China Meteorological Data Network (http://data.cma.cn) Release contains data that are quality controlled. Therefore, actual rate of each data parameter exceeds 99.9%, and the accuracy of the data is near 100%.

http://www.aloki.hu ● ISSN 1589 1623 (Print) ● ISSN 1785 0037 (Online)
DOI: http://dx.doi.org/10.15666/aeer/2005_44414458

Study methods

Correlation analysis

A Pearson correlation analysis is suitable for measuring the degree of correlation between two variables, and this is defined as the quotient of the covariance and standard deviation between two variables. The correlation coefficient is between -1 and 1. When the absolute value is closer to 0, the correlation is weaker. When the absolute value is closer to 1, the correlation is stronger (Yao, 2021). The correlation grades are shown in *Table 1*.

Table 1. *Correlation strength comparison*

Correlation coefficient (r)	Degree of correlation between variables
1.0≧|r|≧0.8	Extremely strong correlation
0.8>|r|≧0.6	Strong correlation
0.6>|r|≧0.4	Moderate correlation
0.4>|r|≧0.2	Weak correlation
0.2>|r|	Weak correlation, Basically irrelevant

Spatial interpolation method

The spatial interpolation algorithm is based on the data of known sample points and is used to deduce unknown data in the same area. An inverse distance weighted interpolation (IDW) combines the advantages of the multiple regression gradient method and the natural proximity method. It is a global interpolation method. Experiments have demonstrated that the predicted sample values on a continuous surface generated by the inverse distance weighted interpolation method are completely equal to the actual measured sample values. Hence, the IDW is an accurate interpolation method (Rahman and Lateh, 2016).

Results

Subsection

The correlations between the concentrations of various kinds of atmospheric pollutants and air quality are shown in *Figure 2*.

The AQI had a very significant and very strong positive correlation with $PM_{2.5}$ and PM_{10}, with correlation coefficients of 0.877 and 0.947, respectively. Among the six types of pollutants, $PM_{2.5}$ and PM_{10} had the greatest impact on the AQI and were determined to be decisive pollutants. With increases in the $PM_{2.5}$ and PM_{10} concentrations, the air quality became significantly worse.

The correlation coefficient of $PM_{2.5}$ with PM_{10} with CO passed the significance level test of $P < 0.05$. $PM_{2.5}$ showed a strong positive correlation with PM_{10} and the CO and NO_2 concentrations, and the correlation coefficients were 0.775, 0.814, and 0.642, respectively.

There was a significant and strong positive correlation between the SO_2 concentration and the NO_2 concentration, and the correlation coefficient was 0.743. There was a significant and strong negative correlation with the O_3 concentration, and the correlation coefficient was -0.777.

http://www.aloki.hu ● ISSN 1589 1623 (Print) ● ISSN 1785 0037 (Online)
DOI: http://dx.doi.org/10.15666/aeer/2005_44414458

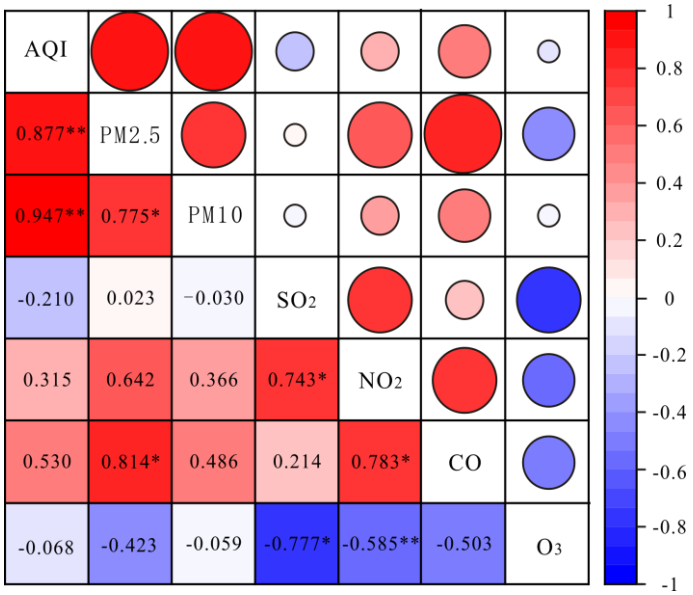

Figure 2. *Correlations between the atmospheric pollutant concentration and the AQI*

There was a significant and strong positive correlation between the NO_2 concentration and the CO concentration, with a correlation coefficient of 0.783, and a very significant and moderate negative correlation with the O_3 concentration, with a correlation coefficient of -0.585. The concentrations of CO and O_3 showed insignificant and moderate negative correlations, respectively. The concentration of O_3 was negatively correlated with the concentration of the other five pollutants, among which the correlation coefficient was the strongest with the concentration of SO_2 and the smallest with the concentration of PM_{10}. The correlation degree between SO_2 and PM_{10} was the weakest.

The annual temporal and spatial distribution characteristics of $PM_{2.5}$

The inverse distance weighted spatial interpolation method was used to interpolate the annual average concentration of $PM_{2.5}$ of 72 air quality monitoring stations in the Beijing-Tianjin-Hebei region from 2015 to 2018, and the continuous surface generated by interpolation is shown in *Figure 3*. From 2015 to 2018, the annual average concentration range of $PM_{2.5}$ in Beijing Tianjin Hebei region was 28–114 ug/m³ (2015, *Fig. 3a*), 26–101 ug/m³ (2166, *Fig. 3b*), 25–90 ug/m³ (2017, *Fig. 3c*), 7–75 ug/m³ (2018, *Fig. 3d*).

From 2015 to 2018, the southern regions of the Beijing-Tianjin-Hebei region, primarily Baoding, Xingtai, Shijiazhuang, Hengshui, and Handan, had the highest annual average concentration of $PM_{2.5}$ compared with other regions that were seriously affected by fine particles. The central region primarily includes Cangzhou, Tianjin, Langfang, Tangshan, and Beijing. The annual average concentration of $PM_{2.5}$ was low and was less affected by fine particles. Zhangjiakou, Chengde, and Qinhuangdao in the northern region had the lowest annual average concentrations of $PM_{2.5}$ and were less affected by fine particles (*Fig. 3*).

Generally speaking, the distribution of $PM_{2.5}$ high concentration areas in the Beijing-Tianjin-Hebei region from 2015 to 2018 was basically unchanged, but the highest value of $PM_{2.5}$ concentration showed a decreasing trend with time. In terms of the spatial

http://www.aloki.hu ● ISSN 1589 1623 (Print) ● ISSN 1785 0037 (Online)
DOI: http://dx.doi.org/10.15666/aeer/2005_44414458

distribution, the annual average concentration of $PM_{2.5}$ from high to low showed distribution characteristics of the highest in the south, the second in the middle, and the lowest in the north.

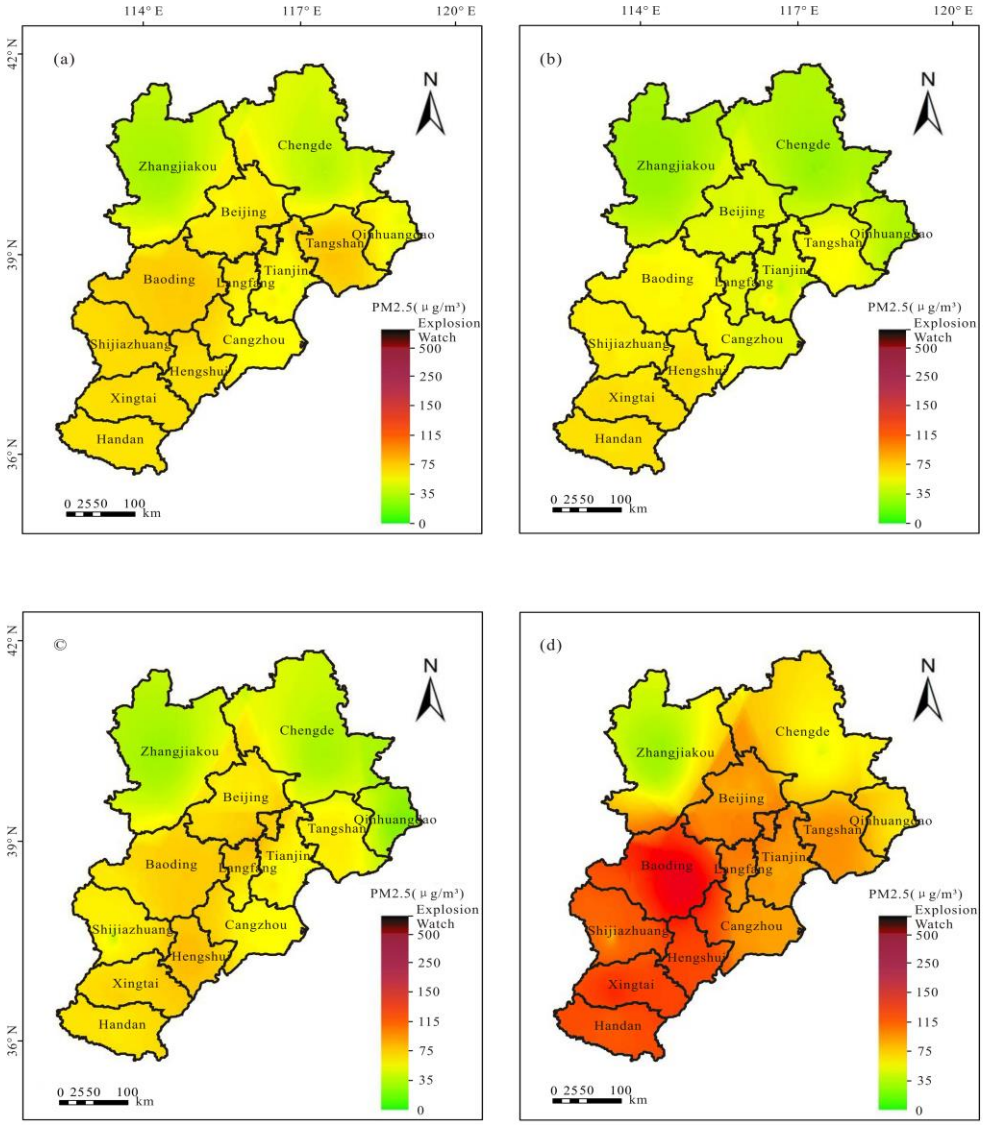

Figure 3. *The annual average concentration distribution of $PM_{2.5}$ from 2015 to 2018*

Seasonal temporal and spatial distribution characteristics of $PM_{2.5}$

According to the climate status of the Beijing-Tianjin-Hebei region in China, the $PM_{2.5}$ concentration data of all the air quality monitoring stations in the Beijing-Tianjin-Hebei region from 2015 to 2018 were divided into four seasons according to the time attribute as shown in *Table 2*.

Table 2. *Season determination*

Seasons	Spring	Summer	Autumn	Winter
Month	3, 4, 5	6, 7, 8	9, 10, 11	12, 1, 2

http://www.aloki.hu ● ISSN 1589 1623 (Print) ● ISSN 1785 0037 (Online)
DOI: http://dx.doi.org/10.15666/aeer/2005_44414458

The seasonal spatial and temporal distribution of the $PM_{2.5}$ concentration in the Beijing-Tianjin-Hebei region during 2015–2018 is shown in *Figure 4*.

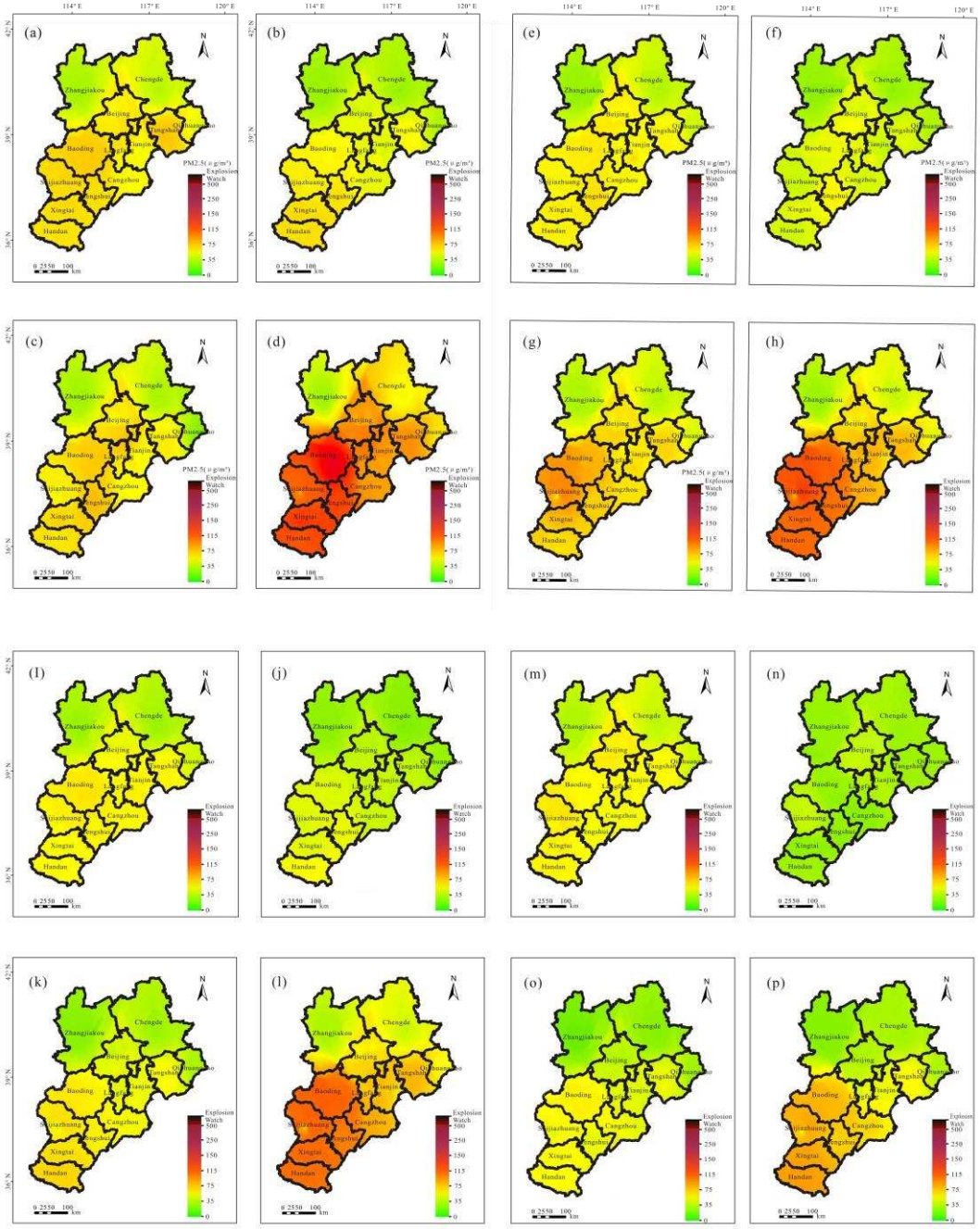

Figure 4. *Seasonal spatial distribution of the $PM_{2.5}$ average concentration from 2015 to 2018*

In the spring of 2015, the minimum concentration of $PM_{2.5}$ in the Beijing-Tianjin-Hebei region was 28 ug/m³, and the maximum value was 97 ug/m³. The average concentration of $PM_{2.5}$ was the highest in the south, followed by the middle, and the lowest in the north (*Fig. 4a*). The minimum average concentration of $PM_{2.5}$ in the Beijing-Tianjin-Hebei region in summer was 24 ug/m³, and the maximum value was 91 ug/m³. The atmospheric environment in the southern part of the Beijing-Tianjin-

http://www.aloki.hu ● ISSN 1589 1623 (Print) ● ISSN 1785 0037 (Online)
DOI: http://dx.doi.org/10.15666/aeer/2005_44414458

Hebei region was most seriously affected by the concentration of $PM_{2.5}$, and the atmospheric environment in the northern portion was least affected by the concentration of $PM_{2.5}$. The concentration of $PM_{2.5}$ was low in most areas, and the overall air quality of the region was the best (*Fig. 4b*). The minimum average concentration of $PM_{2.5}$ in autumn was 23 ug/m³, and the maximum value was 102 ug/m³. The maximum average concentration of $PM_{2.5}$ had an obvious upward trend compared with summer. The high value area of the $PM_{2.5}$ concentration was primarily distributed in the south, and the $PM_{2.5}$ concentration in the north was the lowest (*Fig. 4c*). In winter, the minimum average concentration of $PM_{2.5}$ in the Beijing-Tianjin-Hebei region was 27 ug/m³, and the maximum value was 211 ug/m³. The highest $PM_{2.5}$ concentration was primarily distributed in the south, the lowest $PM_{2.5}$ concentration in the north, and the Beijing-Tianjin-Hebei region has the worst air quality in winter (*Fig. 4d*).

In the spring of 2016, the minimum average concentration of $PM_{2.5}$ in the Beijing-Tianjin-Hebei region was 25 ug/m³, and the maximum value was 80 ug/m³. The atmospheric environment in the south was most affected by the concentration of $PM_{2.5}$, and the concentration of $PM_{2.5}$ in the north was the lowest (*Fig. 4e*). In summer, the minimum average concentration of $PM_{2.5}$ in the Beijing-Tianjin-Hebei region was 22 ug/m³, and the maximum value was 70 ug/m³. The high value areas were primarily distributed in Hengshui and Beijing, and the concentrations of $PM_{2.5}$ in the other areas were low (*Fig. 4f*). The minimum average concentration of $PM_{2.5}$ in autumn was 30 ug/m³, and the maximum value was 126 ug/m³. Compared with summer, the maximum value increased by 56 ug/m³, and the minimum value increased by 8 ug/m³. The high P value area was primarily distributed in the south, and the $PM_{2.5}$ concentrations in other areas were low (*Fig. 4g*). The average concentration in winter was 27 ug/m³, and the maximum value was 170 ug/m³. In addition, the highest concentration displayed a rapid upward trend. The high value area was primarily distributed in the south of the Beijing-Tianjin-Hebei region, followed by the central region (*Fig. 4h*).

In the spring of 2017, the minimum concentration of $PM_{2.5}$ in the Beijing-Tianjin-Hebei region was 27 ug/m³, and the maximum value was 77 ug/m³. The high value area was primarily distributed in Baoding, and the concentrations of $PM_{2.5}$ in Zhangjiakou and Chengde in the north were the lowest (*Fig. 4i*). In summer, the minimum average concentration of $PM_{2.5}$ in the Beijing-Tianjin-Hebei region was 19 ug/m³, and the maximum value was 73 ug/m³. The high value areas were primarily concentrated in the south, of which the atmospheric environmental pollution in Handan was most seriously affected by the concentration of $PM_{2.5}$, and the concentration of $PM_{2.5}$ in the north was low (*Fig. 4j*). The minimum average concentration of $PM_{2.5}$ in autumn was 12 ug/m³, and the maximum value was 85 ug/m³. The high value areas were primarily distributed in Handan and Xingtai in the south. The impact of the $PM_{2.5}$ concentration on the atmospheric environment during autumn was significantly more serious than during spring and summer (*Fig. 4k*). In winter, the minimum average concentration of $PM_{2.5}$ in the Beijing-Tianjin-Hebei region was 25 ug/m³, and the maximum value was 157 ug/m³. Compared with other seasons, the average concentration of $PM_{2.5}$ was the largest in winter, and the pollution degree of the atmospheric environment was also the most seriously affected by the $PM_{2.5}$ concentration. The high value area was primarily distributed in the south, and the $PM_{2.5}$ concentrations in Zhangjiakou and Chengde in the north were the lowest (*Fig. 4l*).

http://www.aloki.hu ● ISSN 1589 1623 (Print) ● ISSN 1785 0037 (Online)
DOI: http://dx.doi.org/10.15666/aeer/2005_44414458

In the spring of 2018, the minimum average concentration range of $PM_{2.5}$ in the Beijing-Tianjin-Hebei region was 9 ug/m³, and the maximum value was 79 ug/m³. The high value areas were primarily distributed in Baoding. The atmospheric environment of Zhangjiakou and Chengde in the north was the least affected by the $PM_{2.5}$ concentration, and the $PM_{2.5}$ concentration was the lowest (*Fig. 4m*). In summer, the minimum average concentration of $PM_{2.5}$ in the Beijing-Tianjin-Hebei region was 17 ug/m³, and the maximum value was 50 ug/m³. In summer, the concentration of $PM_{2.5}$ in the study area was low, and the maximum value pm significantly (*Fig. 4n*). The minimum average concentration of $PM_{2.5}$ in autumn was 19 ug/m³, and the maximum value was 73 ug/m³. The high value areas were primarily distributed in Handan, Baoding, and Shijiazhuang in the south, and the atmospheric environment in the north was least affected by the $PM_{2.5}$ concentration (*Fig. 4o*). In winter, the minimum average concentration of $PM_{2.5}$ in the Beijing-Tianjin-Hebei region was 26 ug/m³, and the maximum value was 113 ug/m³. In winter, the concentration of $PM_{2.5}$ reached the maximum value in a year, and the high value areas were primarily distributed in the south. Zhangjiakou and Chengde in the north were the least affected by the concentration of $PM_{2.5}$, and the concentration of $PM_{2.5}$ was the lowest (*Fig. 4p*).

Overall, from 2015 to 2018, the regional distribution of high $PM_{2.5}$ concentrations in each corresponding season in the Beijing-Tianjin-Hebei region was roughly the same, with high concentrations in the south, followed by the middle and low concentrations in the north. With increased time, the pollution during the four seasons eased from 2015 to 2018, and the overall $PM_{2.5}$ concentration decreased. According to the chronological order of different years, the $PM_{2.5}$ concentration was the highest in winter, with the widest impact on the distribution range, and the pollution was the most serious. The concentration of $PM_{2.5}$ was the lowest in summer. The ranking of the $PM_{2.5}$ concentration from low to high was the following: summer < spring < autumn < winter.

The frequency of exceedance of PM2.5 concentration in cities

The 24-hour mean value data of $PM_{2.5}$ in each city in the study area from 2015 to 2018 are statistically analyzed and compared with the air quality standard of $PM_{2.5}$ (0-35 μg/m^3 is good, 35-75 μg/m^3 is moderate, and more than 75 μg/m^3 is polluted) specified in 《Ambient Air Quality Standard》(GB 3095—1996). *Figure 5a,b* is obtained.

Taking Beijing as an example, from 2015 to 2018, the annual frequency of air quality ($PM_{2.5}$) above moderate level has increased year by year. The annual frequency of good level increases year by year, from 29.32% in 2015 to 34.43% in 2018.The frequency of pollution level days decreases year by year, from 39.18% in 2015 to 20.60% in 2018, with a decrease of 18.58%. The air quality is significantly improved (*Fig. 5*).

Among the cities in Beijing Tianjin Hebei region, the air quality of $PM_{2.5}$ in Hengshui City improved most significantly. The frequency of polluted level days in the whole year decreased by 35.24% from 55.77% in 2015 to 19.76% in 2018, and the good level frequency also increased from 36.26% to 55.35%, an increase of 19.09%. Zhangjiakou is relatively unique, from 2015 to 2018, although the air quality has improved slightly, the change range is the smallest. In 2016, the polluted level frequency even increased in Zhangjiakou, but in 2015, most of the pollution frequencies of other cities in Beijing Tianjin Hebei region were more than 30%. The polluted frequency of Zhangjiakou was 4.93%, and the frequency of good air quality was as high

http://www.aloki.hu ● ISSN 1589 1623 (Print) ● ISSN 1785 0037 (Online)
DOI: http://dx.doi.org/10.15666/aeer/2005_44414458

as 63.84% (*Fig. 5*). The high quality of air quality and the stability of change, it may benefit from the excellent geographical location of Zhangjiakou in Shankou.

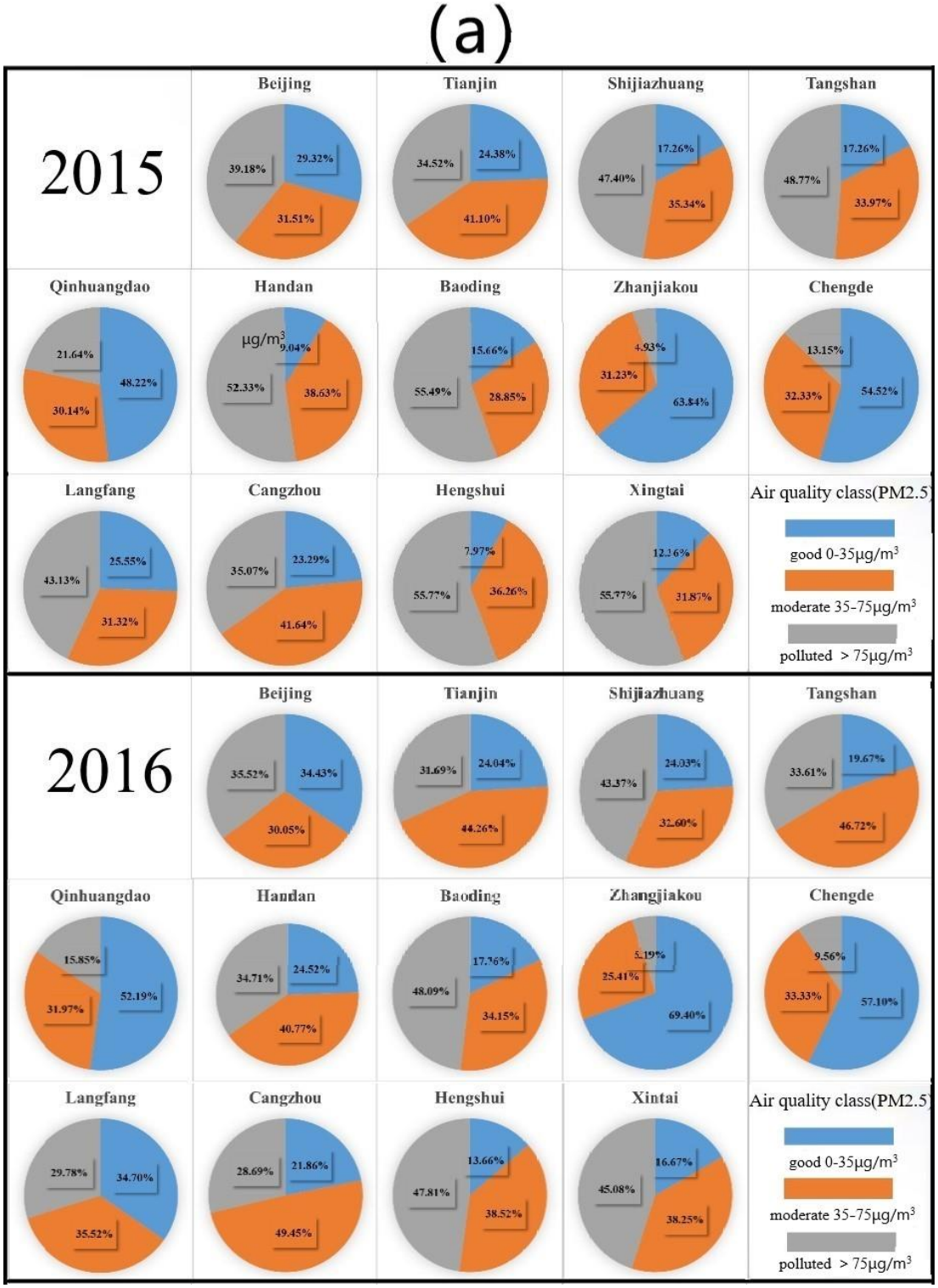

Figure 5(a). *Annual frequency of air quality($PM_{2.5}$) from 2015 to 2016*

http://www.aloki.hu ● ISSN 1589 1623 (Print) ● ISSN 1785 0037 (Online)
DOI: http://dx.doi.org/10.15666/aeer/2005_44414458

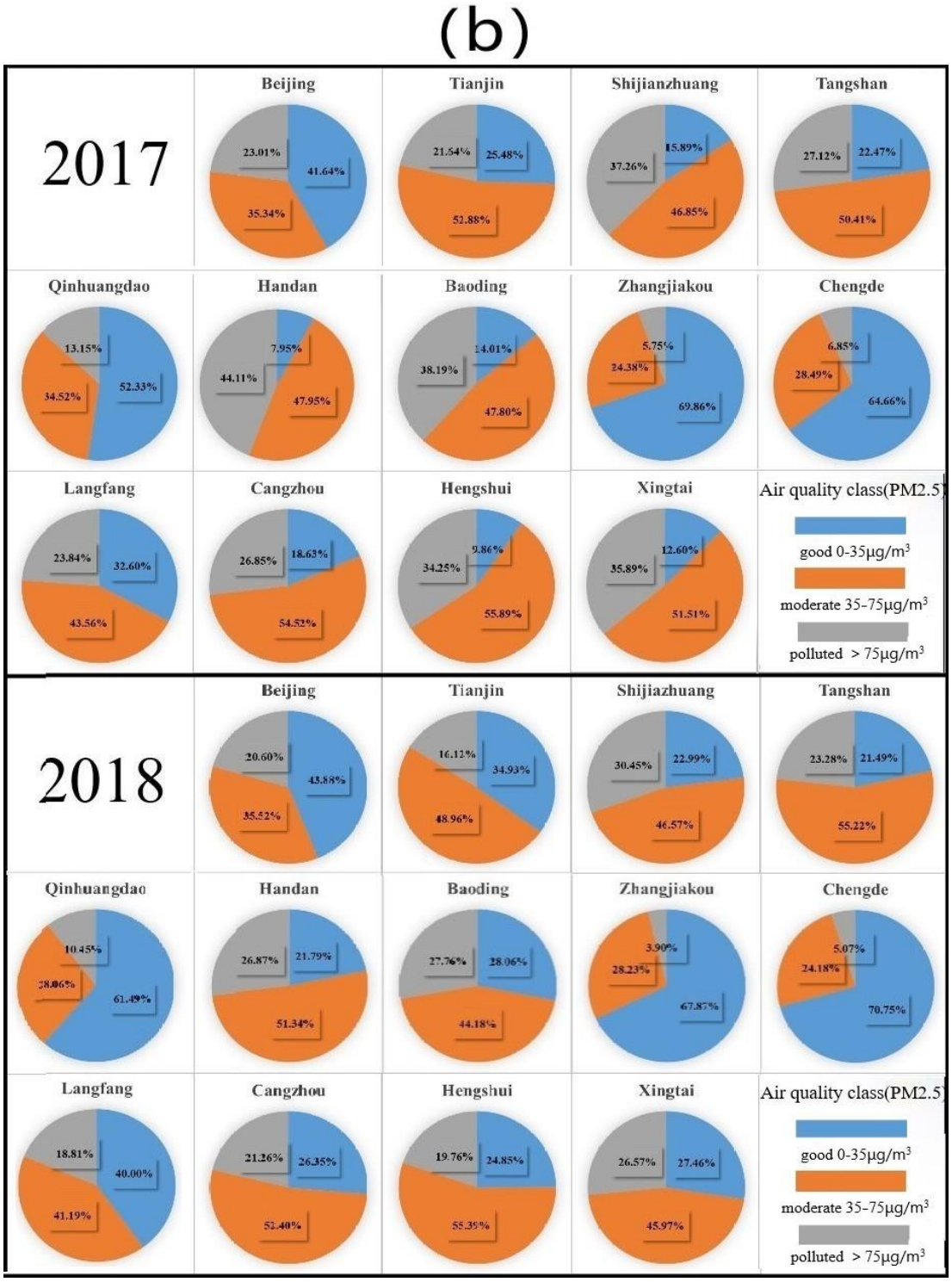

Figure 5(b). *Annual frequency of air quality($PM_{2.5}$) from 2017 to 2018*

Influence of meteorological factors on air quality

A correlation analysis between the meteorological factors, air quality, and air pollutants was conducted, and the results are shown in *Figure 6*.

http://www.aloki.hu ● ISSN 1589 1623 (Print) ● ISSN 1785 0037 (Online)
DOI: http://dx.doi.org/10.15666/aeer/2005_44414458

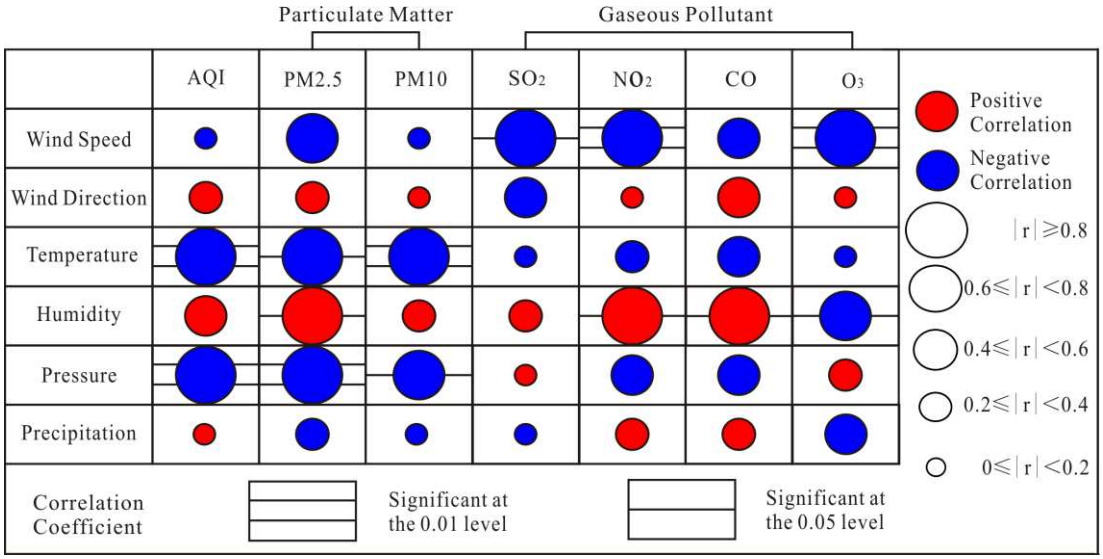

Figure 6. *Correlation of the meteorological factors with the AQI and air pollutants*

Wind speed had a very significant and very strong negative correlation with SO_2 and NO_2, with correlation coefficients of -0.815 and -0.859, respectively. Wind speed had a significant and strong negative correlation with O_3, with correlation coefficient of -0.918, and had no significant negative correlation with the AQI and other pollutants (*Fig. 6*). On the whole, the average wind speed in the study area had a negative correlation with the AQI and the concentrations of six pollutants. This means that when the average wind speed was greater, the smaller the concentration of various pollutants, and the better the air quality.

Wind direction had no significant correlation with the AQI and the six types of pollutants. Wind direction had a medium positive correlation with CO, a medium negative correlation with SO_2, and a weak positive correlation with the AQI and other pollutants (*Fig. 6*). On the whole, the wind direction value is negatively correlated with SO_2 and positively correlated with other air pollutants. The smaller the wind direction (the larger the value means that the wind direction was more east and south) value, the greater the SO_2 content, the smaller the content of other air pollutants, and the smaller the AQI, and the better the air quality. Compared with other pollutant concentrations, the influence of wind direction on SO_2 and CO was more significant.

Temperature had a very significant and very strong negative correlation with the AQI and PM_{10}, and the correlation coefficients were -0.929 and -0.924, respectively. Temperature had a significant and very strong negative correlation with $PM_{2.5}$, and the correlation coefficient was -0.806, but it had no significant negative correlation with other pollutants (*Fig. 6*). The research demonstrated that temperature had a negative correlation with the AQI and the concentration of six pollutants. When the temperature increased, this was conducive to the diffusion of pollutants. In addition, the concentrations of various pollutants were reduced, improving air quality.

Humidity had a significant and very strong positive correlation with $PM_{2.5}$, NO_2, and CO, and the correlation coefficients were 0.812, 0.823, and 0.833, respectively. Humidity had a significant and strong negative correlation with O_3, and the correlation coefficient was -0.790. Humidity had insignificant and medium positive correlations with the AQI, which was related to PM_{10} (*Fig. 6*). The results showed that the relative

http://www.aloki.hu ● ISSN 1589 1623 (Print) ● ISSN 1785 0037 (Online)
DOI: http://dx.doi.org/10.15666/aeer/2005_44414458

humidity was positively correlated with the AQI and the concentrations of five pollutants except O_3. This means that the greater the relative humidity, the smaller the O_3 concentration, but the concentration of other pollutants increased, especially the concentrations of $PM_{2.5}$, NO_2, and CO, which accelerate the accumulation of pollutants and easily cause heavy pollution.

There was a very significant and very strong negative correlation between pressure and the AQI and $PM_{2.5}$, and the correlation coefficients were -0.894 and -0.868, respectively. There was a significant and strong negative correlation between pressure and PM_{10}, and the correlation coefficient was -0.790. The pressure had a moderate positive correlation with NO_2 and CO, a weak positive correlation with O_3, and a very weak positive correlation with SO_2 (*Fig. 6*). The results showed that the greater the near surface pressure, the more favorable the diffusion of the pollutant concentration, the lower the concentrations of various pollutants, and the better the air quality.

Precipitation had a very weak positive correlation with the AQI, a weak positive correlation with NO_2 and CO, a moderate negative correlation with O_3, a weak negative correlation with $PM_{2.5}$, and a very weak negative correlation with PM_{10} and SO_2. The correlations between precipitation and the AQI and the six types of pollutants were not significant (*Fig. 6*). The research showed that when the precipitation increased, the increasing and decreasing trends of various pollutants were different. However, generally speaking, the air quality was developing a favorable trend. In general, changes in temperature, humidity, and pressure had the greatest impact on the changes in the $PM_{2.5}$ concentration in the study area, and temperature and air pressure had the greatest contributions to changes in air quality in the study area.

Discussion

Currently, with the rapid industrial development in the world, the concentration of particulate matter and various air pollutants in the air continues to increase. The impact of various pollutants on air quality has always been a focus of world atmospheric environmental researchers. Mavrakis et al. (2021) studied the effects of early heat wave events on human thermal discomfort and urban air quality in an industrialized plain in the Mediterranean region, and they determined that particulate matter (diameter < 10 μm) had a significant impact on poor air quality. Vehicle emissions, dust events, and the combustion of fossil fuels and other organic compounds can increase the urban PM concentration (He et al., 2021; Grmasha et al., 2021). However, there have been different conclusions regarding the types of primary pollutants in the ambient air due to different regions and seasons. In the autumn of 2014–2018, the ozone concentration in the Pearl River Delta increased sharply and became the primary pollutant in the ambient air (Huang et al., 2021). Liu et al. (2020) determined that in Nanchong City, the $PM_{2.5}$ value showed a downward trend with each year, and $PM_{2.5}$ was the primary atmospheric pollutant. Bogomolova et al. (2021) concluded that $PM_{2.5}$ has the potential to predict novel corona pneumonia. From 2015 to 2018, the impact of PM_{10} and $PM_{2.5}$ on the AQI in the Beijing-Tianjin-Hebei region was far greater than that of other air pollutants (*Fig. 2*). Because $PM_{2.5}$ causes more direct harm to the human body, the primary pollutant affecting air quality in the Beijing-Tianjin-Hebei region was identified as $PM_{2.5}$, which is understandable because the Beijing-Tianjin-Hebei region is one of China's four major industrial zones.

http://www.aloki.hu ● ISSN 1589 1623 (Print) ● ISSN 1785 0037 (Online)
DOI: http://dx.doi.org/10.15666/aeer/2005_44414458

The large-scale temporal and spatial distribution characteristics of $PM_{2.5}$ not only represent the temporal and spatial distribution characteristics of the AQI to a certain extent but also more intuitively reflect the harm caused by regional atmospheric environmental changes to the human body. Wang et al. (2019) and others used the $PM_{2.5}$ data of 338 cities in China from 2014 to 2017 for real-time monitoring, and they found that the annual average value of the $PM_{2.5}$ concentration decreased annually. However, more than two thirds of cities still exceeded the standard value specified by the Chinese government (35 μg/m3). The high concentration of $PM_{2.5}$ was primarily distributed in the Henan Province in the middle of east China (including Shandong, Jiangsu, Anhui, and other provinces) and the Beijing-Tianjin-Hebei region (Li et al., 2019; Zhao et al., 2021). The concentrations of $PM_{2.5}$ in northern and eastern China were higher than that in southern and western China (Zhou et al., 2019), and the primary air pollutant in northern China was also $PM_{2.5}$ (Huimin et al., 2021). There were obvious regional differences in the urban air quality. The average annual concentration of the AQI and $PM_{2.5}$ showed a ranking of the following: northern cities > southern cities, inland cities > coastal cities (Jia and Ye, 2019). The primary reason for the formation of haze is that the concentration of $PM_{2.5}$ is too high. Determining the spatial heterogeneity of the $PM_{2.5}$ concentration and its influencing factors is of great significance for regional air quality control and management. Zhou et al. (2019) showed that the decreasing trend of the $PM_{2.5}$ concentration in the Beijing-Tianjin-Hebei region from 2015 to 2018 agreed with the change trend of China's air quality this year that showed the distribution characteristics of the highest in the south, the second in the middle, and the lowest in the north (*Fig. 3*). This was also caused by the industrial distribution in the Beijing-Tianjin-Hebei region and the decrease in altitude when the terrain in the region decreased from the north to the south (*Fig. 1*). From 2015 to 2018, most cities in Beijing Tianjin Hebei region showed that the frequency of annual pollution days decreased year by year, and the frequency of annual excellent air quality days increased year by year. The frequency of $PM_{2.5}$ in the whole region was roughly the same. The emission of $PM_{2.5}$ was significantly controlled and improved year by year, and the air quality was getting better and better (*Fig. 5*). Different from other cities, Zhangjiakou has a unique and stable change law, which also confirms that the change trend of $PM_{2.5}$ concentration has spatial differences and regional characteristics. Seasonal variation was very evident in the temporal and spatial variation of the $PM_{2.5}$ concentration. Zhang et al. (2019) showed that the air quality in summer and autumn was better than that in spring and winter by using data from national monitoring stations in 2015. In Tibet, the pollutant concentration in winter was even 38% higher than that in summer (Deqing et al., 2021). There were obvious seasonal differences in the air quality and pollutant concentrations in the Beijing-Tianjin-Hebei region (Cheng et al., 2019). The variation in the $PM_{2.5}$ concentration in Shijiazhuang City in the Beijing Tianjin Hebei region was ranked as the following: winter > autumn > spring > summer (Yue et al., 2021). From 2015 to 2018, the spatial distribution of high $PM_{2.5}$ concentration areas in each season in the Beijing-Tianjin-Hebei region was basically the same. The seasonal change was basically consistent with the national $PM_{2.5}$ change trend and was ranked as the following: winter > autumn > spring > summer (*Fig. 4*).

A study that examines the driving factors of air quality change and $PM_{2.5}$ concentration change is conducive for formulating targeted environmental improvement policies. Secondary aerosols contribute greatly to the $PM_{2.5}$ concentration. Low temperature, low wind speed, and high relative humidity will aggravate the

http://www.aloki.hu ● ISSN 1589 1623 (Print) ● ISSN 1785 0037 (Online)
DOI: http://dx.doi.org/10.15666/aeer/2005_44414458

accumulation of regional pollutants in winter (He et al., 2021). In Chengdu, the air quality had a significant positive correlation with the air temperature, air pressure, visibility, and sunshine hours (Cheng et al., 2018). Sindosi et al. (2021) used the city of Ivanina in northern Greece as an example, and they showed that, in addition to meteorological factors, socioeconomic factors also determined the level of atmospheric particulate matter. Bowen et al. (2021) confirmed that changes in the $PM_{2.5}$ concentration were affected by many factors by using the daily air pollutant concentration and meteorological element data of Lanzhou from 2013 to 2020. By utilizing the air pollution index and surface meteorological elements of the Beijing-Tianjin-Hebei region from 2001 to 2010, Shi et al. (2018) confirmed that meteorological factors had an important impact on air pollution. The novel coronavirus pneumonia outbreak occurred at the end of 2019, and the air quality and $PM_{2.5}$ concentration have been shown to be significantly associated with the spread of novel coronavirus pneumonia. Changes in human activity have had a significant impact on air quality during the novel coronavirus pneumonia period (Bogomolova et al., 2021; Gao et al., 2021). The AQI of most cities decreased significantly in NO_2, SO_2, Co, $PM_{2.5}$, and PM_{10}, but the change in O_3 was not significant (Fu et al., 2020). The mortality of the novel coronavirus pneumonia was found to be positively correlated with the mean temperature and the AQI. However, mortality was found to be independent of wind speed, relative humidity, and precipitation (Huang et al., 2020). This suggests that the novel coronavirus pneumonia case fatality rate (CFR) may be predicted by $PM_{2.5}$ and other air pollutants (Hou et al., 2020). The increases in temperature and air pressure in the Beijing-Tianjin-Hebei region from 2015 to 2018 led to a significant decrease in the air quality index in the study area. Wind speed, wind direction, humidity, and precipitation had no significant impact on the air quality index in the study area. The change in the $PM_{2.5}$ concentration in the study area had strong correlations with the temperature, humidity, and air pressure (*Fig. 6*), and the variation in the regional temperature and atmospheric pressure played an important role in the regional air quality trend.

Conclusions

(1) $PM_{2.5}$ and PM_{10} had the greatest impact on the air quality index and were decisive pollutants. PM_{10} and CO had the greatest impact on $PM_{2.5}$, and CO had the greatest impact on PM_{10}.

(2) From 2015 to 2018, the overall air quality of the Beijing-Tianjin-Hebei region obviously recovered and developed in a good direction. From the perspective of the spatial distribution, the $PM_{2.5}$ high value area was primarily concentrated in the south, and the areas least affected were primarily concentrated in Chengde and Zhangjiakou. Overall, the annual average concentrations of $PM_{2.5}$ areas from low to high in the study area were ranked in the following order: north < central < south.

(3) From 2015 to 2018, the concentration of $PM_{2.5}$ decreased during each season, but the spatial distribution of the high value area of the $PM_{2.5}$ concentration during each season remained basically the same. The pollution degree and pollution range were similar in different seasons, ranking as the following: winter > autumn > spring > summer. There was no significant difference in the regional distribution characteristics of the high $PM_{2.5}$ value during the same season.

http://www.aloki.hu ● ISSN 1589 1623 (Print) ● ISSN 1785 0037 (Online)
DOI: http://dx.doi.org/10.15666/aeer/2005_44414458

(4) From 2015 to 2018, the $PM_{2.5}$ air quality of cities in Beijing Tianjin Hebei region improved year by year, the frequency of annual pollution days decreased year by year, and the frequency of annual high-quality air quality days increased year by year.

(5) An increase in temperature and air pressure significantly reduced the air quality index in the study area, and the air quality improved. The influences of wind speed, wind direction, humidity, and precipitation on the air quality index in the study area were not significant. However, a change in the $PM_{2.5}$ concentration in the study area had a strong correlation with temperature, humidity, and air pressure. An increase in temperature and air pressure and a decrease in humidity led to a significant decrease in the air quality index in the study area, and the air quality developed a good trend. Changes in wind speed, wind direction, and precipitation had no significant correlations with changes in the $PM_{2.5}$ concentration in the study area.

REFERENCES

[1] Bhutiani, R., Kulkarni, D. B., Khanna, D. R., Tyagi, V., Ahamad, F. (2021): Spatial and seasonal variations in particulate matter and gaseous pollutants around integrated industrial estate (IIE), SIDCUL, Haridwar: a case study. – Environment, Development and Sustainability 23: 15619-15638.

[2] Bo, Y., Chang, L-Y., Guo, C., Lin, C., Lau, A. K. H., Tam, T., Lao, X. Q. (2021): Reduced ambient PM2.5, better lung function, and decreased risk of chronic obstructive pulmonary disease. – Environment International 156: 10676.

[3] Bogomolova, A., Balk, I., Polkovnikova, N., Ivaschenko, N. (2020): The impact of the COVID-19 related lockdowns on air quality. – International Conference on Sustainability and Climate Change 534: 012010.

[4] Bowen, C., Yuxia, M., Fengliu, F., Yifan, Z., Jiahui, S., Hang, W., Yongtao, G., Yifan, C. (2021): Influence of weather and air pollu-tion on concentration change of PM2.5 using a generalized additive model and gradient boosting machine. – Atmospheric Environment 255: 118437.

[5] Cheng, Y., Zhang, D., Yang, R., Ni, C., Sun, L. (2018): A Study on the Relationship between Meteorological Condition and Air Qual-ity of Chengdu. – Open Journal of Nature Science 6(01): 53-62.

[6] Cheng, Y., Liu, T., Zhao, Y., Wang, Y. (2019): Spatiotemporal Evolution and Socioeconomic Driving Mechanism of Air Quality in Beijing-Tianjin-Hebei and Surrounding Areas ("2+26" Cities). – Economic Geography 39(10): 183-192.

[7] Deqing, Z., Tang, S., Ren, C., Da, Q. (2021): Analysis of the Air Pollution Index and Meteorological Factors and Risk Assessment for Tibet. – Journal of Physics: Conference Series 1838(1): 012047.

[8] Dutta, S., Ghosh, S., Dinda, S. (2021): Urban Air-Quality Assessment and Inferring the Association Between Different Factors: A Comparative Study Among Delhi, Kolkata and Chennai Megacity of India. – Aerosol Science and Engineering 5(1): 93-111.

[9] Farhadi, R., Hadavifar, M., Moeinaddini, M., Amintoosi, M. (2018): Sensitivity Analysis of Meteorological Parameters and Instability Indices on Concentration of Carbon Monoxide, Particulate Matter, and Air Quality Index in Tehran. – ECOPERSIA 6(2): 91-100.

[10] Fu, F., Purvisroberts, K. L., Williams, B. (2020): Impact of the COVID-19 Pandemic Lockdown on Air Pollution in 20 Major Cities around the World. – Atmosphere 11(11): 1189.

[11] Gao, C., Li, S., Liu, M., Zhang, F., Cai, C. (2021): Impact of the COVID-19 Pandemic on Air Pollution in Chinese Megacities from the Perspective of Traffic Volume and Meteorological Factors. – Science of The Total Environment 773(1-4): 145545.

http://www.aloki.hu ● ISSN 1589 1623 (Print) ● ISSN 1785 0037 (Online)
DOI: http://dx.doi.org/10.15666/aeer/2005_44414458

[12] Grmasha, R. A., Al-Azzawi, S., Al-Sareji, O. J., Alardhi, T., Alkhayyat, A. (2021): Engineering, Analysis of Air Quality Index Distribution of PM 10 and PM 2.5 Concentrations in Ambient Air of Al-Hillah City, Iraq. – IOP Conference Series Materials Science and Engineering 1058(1): 012014.
[13] He, C., Hong, S., Mu, H., Tu, P., Huang, J. (2021): Characteristics and Meteorological Factors of Severe Haze Pollution in China. – Advances in Meteorology 2021: 1-15.
[14] Hou, C. K., Qin, Y. F., Liu, Q. L., Yang, X. Y., Wang, H. (2020): Impact of Long-Term Air Pollution on the Case Fatality Rate of COVID-19. – Research Square.
[15] Huang, H., Liang, X., Huang, J., Yuan, Z., Ouyang, H., Wei, Y., Bai, X. (2020): Correlations between Meteorological Indicators, Air Quality and the COVID-19 Pandemic in 12 Cities across China. – Journal of Environmental Health Science and Engineering 18(2): 1491-98.
[16] Huang, C., Liao, Q., Lu, J. (2021): Analysis of Temporal and Spatial Variation Characteristics of Air Quality in the Pearl River Delta during 2015-2019. – IOP Conference Series Earth and Environmental Science 687(1): 012026.
[17] Huimin, Z., Rende, W., Xiaomiao, F., Cheney, A., Jinping, Q. (2021): Spatial characteristics of the PM2.5/PM10 ratio and its indicative significance regarding air pollution in Hebei Province, China. – Environmental Monitoring and Assessment 193: 486.
[18] Jia, Q., Ye, C. (2019): Canonical Correlation Analysis of Composition of Urban Development Land and Air Quality in 35 Large and Medium-sized Cities in China. – Chinese Agricultural Science Bulletin 35(25): 84-93.
[19] Kuo, C. H., Hsiu, L. Y., Yen, L. C. (2021): Convex nonparametric least squares and stochastic semi-nonparametric frontier to estimate the shadow prices of PM2.5 and NO; for Taiwan's transportation modes. – Ecological Indicators 15(9): 659-677.
[20] Li, D., Zhao, Y., Wu, R., Dong, J. (2019): Spatiotemporal Features and Socioeconomic Drivers of PM2.5 Concentrations in China. – Sustainability 11(4): 1201.
[21] Liu, C. L., Guo, C. H., Jiang, Z. B., Chen, L. Y. (2020): Characteristics and Time Series Analysis of Primary Air Pollutants in Nanchong City from 2014 to 2018. – Sichuan Environment 39(02): 42-48.
[22] Liu, G., Dong, X., Kong, Z., Dong, K. (2021): Does national air quality monitoring reduce local air pollution? The case of PM2.5 for China. – Journal of Environmental Management 296(4): 113232.
[23] Mangayarkarasi, R., Vanmathi, C., Khan, M. Z., Noorwali, A., Agarwal, P. (2021): COVID19: Forecasting Air Quality Index and Par-ticulate Matter (PM2.5). – Computers, Materials and Continua 67(3): 3363-3380.
[24] Mavrakis, A., Kapsali, A., Tsiros, I. X., Pantavou, K. (2021): Air quality and meteorological patterns of an early spring heatwave event in an industrialized area of Attica, Greece. – Euro-Mediterranean Journal for Environmental Integration 6: 25.
[25] Meng, J., Wang, M., Xuekelaiti, X. (2021): Characteristics of air pollution and environmental economic efficiency in Beijing-Tianjin-Hebei and surrounding areas. – Arabian Journal of Geosciences 14(12)
[26] Nuan, W., Jie, Y., Lin, Z., Yanbing, W., Zhengyang, H. (2021): Spatial Downscaling of Remote Sensing Precipitation Data in the Beijing-Tianjin-Hebei Region. – Journal of Computer and Communications 09(06): 191-202.
[27] Pei, Y., Xu, R., Coelho, M. S. Z. S., Saldiva, P. H. N., Li, S., Zhao, Q., Mahal, A., Sim, M., Abramson, M. J., Guo, Y. (2021): The impacts of long-term exposure to PM2.5 on cancer hospitalizations in Brazil. – Environment International 154: 106671.
[28] Qian, L., Zheyu, Z., Chaofeng, S., Run, Z., Yang, G., Chen, C. (2021): Spatio-temporal variation and driving factors analysis of PM2.5 health risks in Chinese cities. – Ecological Indicators 129: 107937.

http://www.aloki.hu ● ISSN 1589 1623 (Print) ● ISSN 1785 0037 (Online)
DOI: http://dx.doi.org/10.15666/aeer/2005_44414458

[29] Rahman, M. R., Lateh, H. (2016): Meteorological drought in Bangladesh: assessing, analysing and hazard mapping using SPI, GIS and monthly rainfall data. – Environmental Earth Sciences 75: 1026.
[30] Richard, G., Sawyer, W. E., Izah, S. (2021): Health Implications of Air Quality Index of Fine and Coarse Particulates During Outdoor Combustion of Biomass in the Niger Delta, Nigeria. – International Journal of World Policy and Development Studies 72: 21-26.
[31] Ru, M., Brauer, M., Lamarque, J.-F., Shindell, D. (2021): Exploration of the Global Burden of Dementia Attributable to PM2.5: What Do We Know Based on Current Evidence? – GeoHealth 5(5): e220GH000356.
[32] Shi, H., Critto, A., Torresan, S., Gao, Q. (2018): The Temporal and Spatial Distribution Characteristics of Air Pollution Index and Meteorological Elements in Beijing, Tianjin, and Shijiazhuang, China. – Integrated Environmental Assessment and Management 14(5): 710-721.
[33] Sindosi, O. A., Hatzianastassiou, N., Markozannes, G., Rizos, E. C., Ntzani, E., Bartzokas, A. (2021): PM_{10} Concentrations in a Provincial City of Inland Greece in the Times of Austerity and Their Relationship with Meteorological and Socioeconomic Conditions. – Water Air and Soil Pollution 232: 77.
[34] Slawsky, E., Ward-Caviness, C. K., Neas, L., Devlin, R. B., Cascio, W. E., Russell, A. G., Huang, R., Kraus, W. E., Hauser, E., Diaz-Sanchez, D., Weaver, A. M. (2021): Evaluation of $PM_{2.5}$ air pollution sources and cardiovascular health. – Environmental Epidemiology 5(3): e157.
[35] Wang, Y., Duan, X., Wang, L. (2019): Spatial-Temporal Evolution of $PM_{2.5}$ Concentration and its Socioeconomic Influence Factors in Chinese Cities in 2014–2017. – International Journal of Environmental Research and Public Health 16(6): 985.
[36] Xiaorong, Y., Tongchao, Z., Yuan, Z., Hao, C., Shaowei, S. (2021): Global burden of COPD attributable to ambient PM2.5 in 204 countries and territories, 1990 to 2019: A systematic analysis for the Global Burden of Disease Study 2019. – Science of the Total Environment 796: 148819.
[37] Yao, W., Gui, K., Wang, Y., Che, H., Zhang, X. (2021): Identifying the dominant local factors of 2000-2019 changes in dust loading over East Asia. – Science of The Total Environment 777(D23): 146064.
[38] Yu, G., Wang, F., Hu, J., Liao, Y., Liu, X. (2019): Value Assessment of Health Losses Caused by $PM_{2.5}$ in Changsha City, China. – International Journal of Environmental Research and Public Health 16(11): 2063.
[39] Yue, T., Qiu, J., Wang, J., Fang, C. (2021): Analysis of Spatio-Temporal Variation Characteristics of Main Air Pollutants in Shijiazhuang City. – Sustainability 13(2): 941.
[40] Zhang, Z., Chen, L., Zhang, H., Liu, P. (2019): The Analysis of Spatial-Temporal Distribution Characteristics and Correlation on Air Quality in Beijing-Tianjin-Hebei Region. – Geomatics World 26(03): 31-35.
[41] Zhao, C., Sun, Y., Zhong, Y., Xu, S., Liang, Y., Liu, S., He, X., Zhu, J., Shibamoto, T., He, M. (2021): Health, Spatio-temporal analysis of urban air pollutants throughout China during 2014–2019. – Air Quality Atmosphere & Health 14(10): 1619-1632.
[42] Zhou, L., Zhou, C., Yang, F., Che, L., Wang, B. (2019): Spatio-temporal evolution and the influencing factors of PM2.5 in China between 2000 and 2015. – Journal of Geographical Sciences 29(2): 253-270.

http://www.aloki.hu ● ISSN 1589 1623 (Print) ● ISSN 1785 0037 (Online)
DOI: http://dx.doi.org/10.15666/aeer/2005_44414458

IMPACT OF WETLAND CONVERSION INTO FORESTS AND ARABLE LAND ON SOIL MICROBIAL COMMUNITY STRUCTURE AND DIVERSITY IN THE SANJIANG PLAIN, NORTHEASTERN CHINA

WANG, X.[1,2#] – LI, S. J.[1,2#] – WENG, X. H.[1,2] – SUI, X.[1,2*] – LI, M. S.[3*]

[1]*Engineering Research Center of Agricultural Microbiology Technology, Ministry of Education, Heilongjiang University, Harbin 150500, China*

[2]*Heilongjiang Provincial Key Laboratory of Ecological Restoration and Resource Utilization for Cold Region, School of Life Sciences, Heilongjiang University, Harbin 150080, China*

[3]*Institute of Nature and Ecology, Heilongjiang Academy of Sciences, Harbin, 150040, China*

[#]*Wang Xin and Li Shaojie contributed equally to this work*

**Corresponding authors*
e-mail: xinsui_cool@126.com (X. Sui); lms19861004@163.com (M. S. Li)

(Received 8th May 2022; accepted 26th Jul 2022)

Abstract. Changes in land use patterns lead to changes in soil ecosystem functions, and soil microorganisms can sensitively reflect the evolution of soil quality and different ecosystem functions. Here, three typical land use patterns (wetland, arable land, and forest) in the Sanjiang Plain of northeastern China were selected to study the effect of land use changes on the microbial community structure of wetlands. High-throughput sequencing technology based on bacterial 16S rRNA genes was used to study the community structure of soil bacteria in three land use patterns and to explore the relationship between soil bacterial community and environmental factors. Our findings indicated that the dominant bacterial phyla in soils of different land use patterns were Proteobacteria, Acidobacteria, and Actinobacteria. However, the land use patterns significantly changed the composition and abundance of soil bacterial genera. Combined with the soil bacterial alpha diversity index, the soil bacterial α diversity in wetlands was higher than that in forests and farmlands. Soil bacterial beta diversity varied significantly among land use patterns. The redundancy analysis results showed that soil moisture content was the main factor affecting the bacterial community structure of wetland soils, whereas pH, soil organic carbon, and total nitrogen were the main factors affecting the soil bacterial community structure in forests, and total phosphorus and available phosphorus were the main factors affecting the soil bacterial community structure in arable land.
Keywords: *alpine wetlands, reclamation, high-throughput sequencing, bacterial communities, soil physicochemistry*

Introduction

Soil microbial communities are a central component of the soil biogeochemical cycle, and are involved in regulating ecosystem processes at all scales (Huang et al., 2019). These communities are the driving force for the transformation and cycling of soil organic matter and crucial nutrients such as C and N (Zhang et al., 2022), and are therefore important biological indicators of soil health (Sui et al., 2022). Soil microbial community diversity is influenced by several factors such as soil organic carbon, soil pH, C/N ratio, and nutrient bioavailability (Deng et al., 2020), all of which are regulated by land use patterns (Sui et al., 2019). Different land use patterns have been associated with unique vegetation types and species structure (Li et al., 2013), soil structure (Acín-Carrera et al., 2013), soil water characteristics (Zucco et al., 2014), soil respiration (Sheng et al., 2010),

http://www.aloki.hu ● ISSN 1589 1623 (Print) ● ISSN 1785 0037 (Online)
DOI: http://dx.doi.org/10.15666/aeer/2005_44594475

soil nutrient fertility characteristics (Liu et al., 2010), soil enzyme activity (Tischer et al., 2015), soil microbial biomass, and soil microbial community (Van Leeuwen et al., 2017). Land use not only affects nutrient levels in soil but also nutrient cycling by affecting water, heat, and other environmental conditions, thus affecting the transformation and flow of soil nutrients. In turn, this can directly or indirectly affect the number, composition, and activity of soil microorganisms, resulting in changes in the structure and function of soil microbial communities. Moreover, the diversity of soil microbial communities can also reflect changes in vegetation. The rational use of land plays an important role in improving soil structure and promoting regional ecological restoration. In addition, land use change is an important factor affecting soil properties (Birkhofer et al., 2012). Previous studies have demonstrated that different vegetation (Sui et al., 2021) and management measures (Sánchez-Moreno et al., 2006) can significantly modify soil properties among different land use modes. For example, in the process of land use change, soil aggregates with larger particle sizes are more likely to be lost (Li et al., 2014). Other studies have reported that anthropogenic disturbances such as tillage and fertilizer application led to soil compaction and slabbing, and relatively high powder and clay particle contents resulted in the continuous refinement of large soil particles (Ren et al., 2014). Lv et al. (2011) reported that incorporating more plants into a landscape (i.e., by planting) results in higher levels of litter, which promoted the formation of the root system aggregates and enhanced soil erosion resistance. At the same time, the species diversity increased, the soil physical properties improved, the soil layer thickened, and the bulk density decreased. With the accumulation of a large amount of litter on the surface, soil organic matter accumulated, total nitrogen, available nitrogen, and available potassium increased, and soil fertility exhibited an obvious upward trend (Liu et al., 2005). Tillage and harvesting and utilization of surface vegetation not only accelerates the decomposition and loss of soil organic matter, but also intensifies soil disturbances, soil and water loss, and the loss of other nutrients in the soil, particularly the bioavailable fraction of these nutrients (Zhao et al., 2012). Zhao et al. (2011) found that different land use modes have a significant impact on the contents of soil organic matter, total nitrogen, available phosphorus, and available potassium. Among various land use modes, the average contents of total nitrogen and organic matter in cultivated soil are generally considered low or very low. Most previous studies have focused on the impact of land use changes on soil properties in the study area, whereas the impact of land use-driven soil property changes on microbial community structure and function remains unclear.

The Sanjiang Plain wetland is among the most important freshwater wetland distribution areas in Northeast China, and is also the primary terrestrial environment dominated by black soil (Sui et al., 2021). Due to the particular climatic conditions and geographical location of the study area, its soil is characterized by high humus content and low abundance and diversity of microorganisms (Weng et al., 2022). Therefore, this ecosystem is extremely fragile despite being uniquely suitable for agricultural development. Many studies have characterized the effects of land use changes on community structure and soil physicochemical properties in the wetlands of the Sanjiang Plain (Wu et al., 2010; Xu et al., 2017; Sui et al., 2019). However, the effects of these parameters on the soil microbial community structure have remained largely unexplored. Therefore, our study characterized the effect of land use on soil physicochemical properties and soil microbial functional diversity in typical swampy meadow wetlands, artificial larch forests, and cornfields in the Sanjiang Plain. Moreover, we analyzed the mechanisms of different land use practices on soil microbial

http://www.aloki.hu ● ISSN 1589 1623 (Print) ● ISSN 1785 0037 (Online)
DOI: http://dx.doi.org/10.15666/aeer/2005_44594475

community structural characteristics in the Sanjiang Plain, and clarified the main environmental factors affecting soil microbial community differentiation. Collectively, our findings provide a scientific basis for the preservation and enhancement of soil fertility and the conservation of soil microbial diversity, as well as for the ecological reconstruction and rational use of land resources in the study region.

Materials and methods

Overview of the study sample site

The study area belongs to the ecological transition zone between the Xiaoxinganling Mountains and the Sanjiang Plain, and is located in the Sanhuanpao and Naolihe Nature Reserve of Heilongjiang Province, downstream of the Songhua River in northeastern of China (46° 57’ 55″~47° 14’ 7″N, 130° 24’ 51″~130° 57’ 38″E) (*Fig. 1*). The region exhibits a temperate continental monsoon climate, with an altitude of 65–81 m, an average annual rainfall of 548 mm, an average annual evaporation of 1,155 mm, and an average annual frost-free period of approximately 130 d. The average temperature for five months of the year is below 0 °C, with the average annual temperature being 2.1 °C. The highest temperature occurs in July, with an average temperature of 21.2 °C, and the lowest temperature occurs in January, with an average temperature of -19.4 °C. The freezing and thawing period is from mid-October to mid-May of the following year, with a freezing period of 150 d and a wetland freeze depth of 80 to 125 mm. The vegetation in the reserve is dominated by wet herbaceous and shrub vegetation, with intermittent planted forests. The main vegetation includes *Salix siuzevii*, *Salix sungkianica*, *Salix viminalis*, *Carex lehmanii*, *Acorus calamus* and *Deyeuxia angustifolia*, among others. The characteristics of three land use types were shown in *Table 1*.

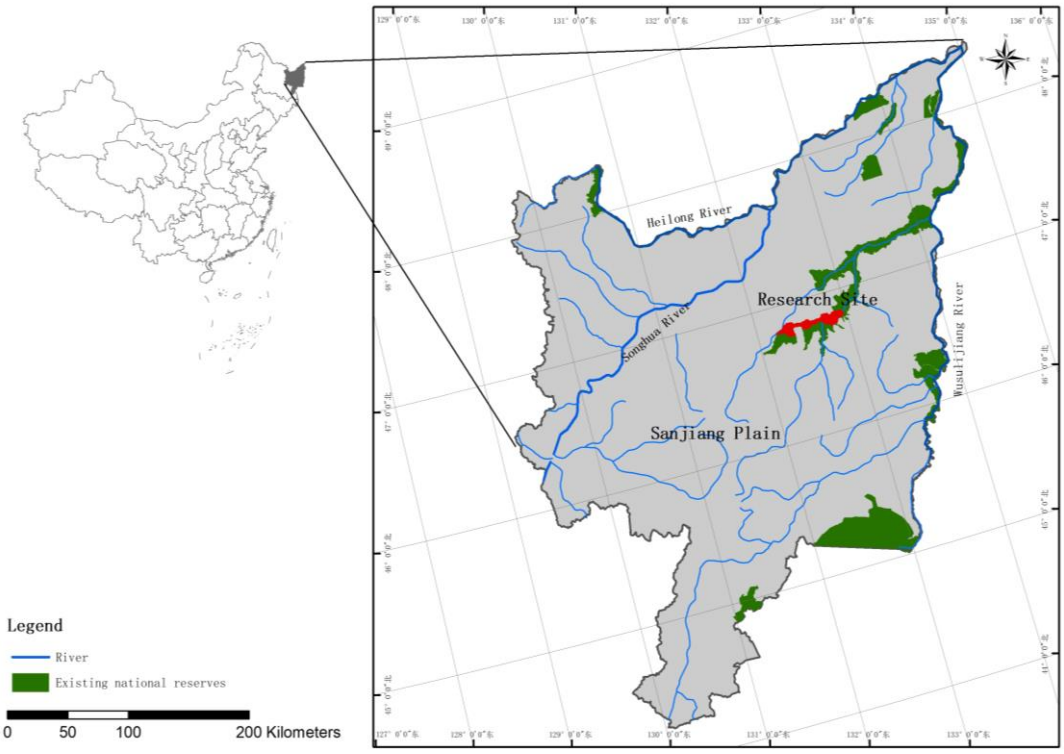

Figure 1. *The location of this research site*

http://www.aloki.hu ● ISSN 1589 1623 (Print) ● ISSN 1785 0037 (Online)
DOI: http://dx.doi.org/10.15666/aeer/2005_44594475

Table 1. *Characteristics of the three land use types in the Sanjiang plain*

Land use type	Primary vegetation species	Position
Wetland	*Deyeuxia angustifolia*, *Stellaria radians*, *Anemone dichotoma*, *Lathyrus quinquenervius*, *Carex appendiculata*	132°21′11″E, 46°51′4″N
Forest	*Pure Populus simonii*, planted in 2010, the average height was about 12 m, the diameter at breast height was about 15 cm, and the average density was 1600 stems ha^{-1}	132°19′15″E, 46°45′7″N
Arable land	The maize plantation was fertilized with 370 kg ha^{-1} y^{-1} of fertilizer (N:P:K) each year in the end of May	132°32′91″E, 46°83′91″N

Sample collection

In June 2019, three standard 50 m × 50 m plots were selected from three different land use sample plots, including a pristine wetland, agricultural land, and forest land (*Fig. 2*), respectively, and soil samples were taken from a 0 to 20 cm depth using a five-point mixed sampling method. After each layer of soil samples were thoroughly mixed, the debris and rhizomes were removed from the samples and passed through a 2 mm sieve, after which a portion of the samples was placed in a 15 mL centrifuge tube, stored in liquid nitrogen, transferred to the laboratory, and stored in a refrigerator at −80 °C refrigerator for DNA extraction and for microbiological analysis. The rest of the soil samples were divided into two parts in the laboratory, one was kept in a refrigerator at 4 °C whereas the other was naturally air-dried for the determination of soil physical and chemical properties.

Determination of physical and chemical properties

For the determination of soil moisture content, the retrieved fresh soil sample was immediately placed in an aluminum box and weighed on a scale accurate to 0.01 g. The sample was then baked at constant temperature in a drying oven preheated to 10 °C ± 2 °C for 8 h, after which moisture content was calculated. Soil pH was determined using an acidity meter with a water to soil ratio of 2.5:1. Soil organic carbon content was determined using a Vario TOC meter (Elementar, Germany). For the analysis of total nitrogen, 0.25 g of soil sample was passed through a 0.149 mm sieve, followed by the addition of 2 g of accelerant mixed with zinc sulfate and copper sulfate and 5 mL of concentrated H_2SO_4 for decoction. The sample was then fixed and filtered after decoction, and total nitrogen determination was conducted with a continuous flow analyzer (Auto Analyzer 3-AA3, SEAL Company, Germany). Total phosphorus was determined via sulfuric acid/perchloric acid dissolution molybdenum antimony anti colorimetry. Fast-acting phosphorus was determined using 0.5 $mol \cdot L^{-1}$ sodium bicarbonate leaching - molybdenum antimony anti-colorimetric.

DNA extraction and high-throughput sequencing

Genomic DNA was extracted from fresh soil samples (n = 18; 0.5 g each) using the power soil DNA extraction kit according to the manufacturer's instructions. PCR was performed on a Geneamp 9700 PCR system (Applied Biosystems, CA, USA). The extracted genomic DNA was detected by 1% agarose gel electrophoresis (CHEF-DR II, Bio-red, Beijing, China). The 338F (5'-ACTCCTACGGGAGGCAGCA-3') and 806R (5'-GGACTACHVGGGTWTCTAAT-3') universal primers were used for bacterial 16S

http://www.aloki.hu ● ISSN 1589 1623 (Print) ● ISSN 1785 0037 (Online)
DOI: http://dx.doi.org/10.15666/aeer/2005_44594475

rRNA gene amplification. The amplified products were detected by 2% agarose gel electrophoresis, recovered from the gel using the AxyPrep DNA gel extraction kit, washed with tris HCl, and verified by 2% agarose gel electrophoresis. The PCR products were quantified using a QuantiFluorTM-ST fluorometer, after which the concentration of the samples was adjusted as needed for sequencing. Sequencing was performed by Beijing Biomaker Technology Co., Ltd. (Beijing, China) using an Illumina HiSeq sequencer.

16S rRNA gene sequence analysis

The original fastq sequence files were quality filtered using Trimmomatic and then spliced by FLASH using the following criteria: (i) sequences less than 50 bp and with an average quality score less than 20 were eliminated; (ii) 2 nucleotide mismatches were allowed and fragments containing ambiguous bases were removed; (iii) sequences with overlapping lengths of more than 10 bp were merged according to their overlapping sequences.

Using UPARSE (version 7.1, http://drive5.com/uparse/), operational taxonomic units (OTUs) were assigned with a 97% similarity threshold and chimeric sequences were identified and removed using UCHIME. All 16S rRNA gene sequences were classified using the RDP classification algorithm (http://rdp.cme.msu.edu/) against the Silva (SSU123) 16S rRNA database.

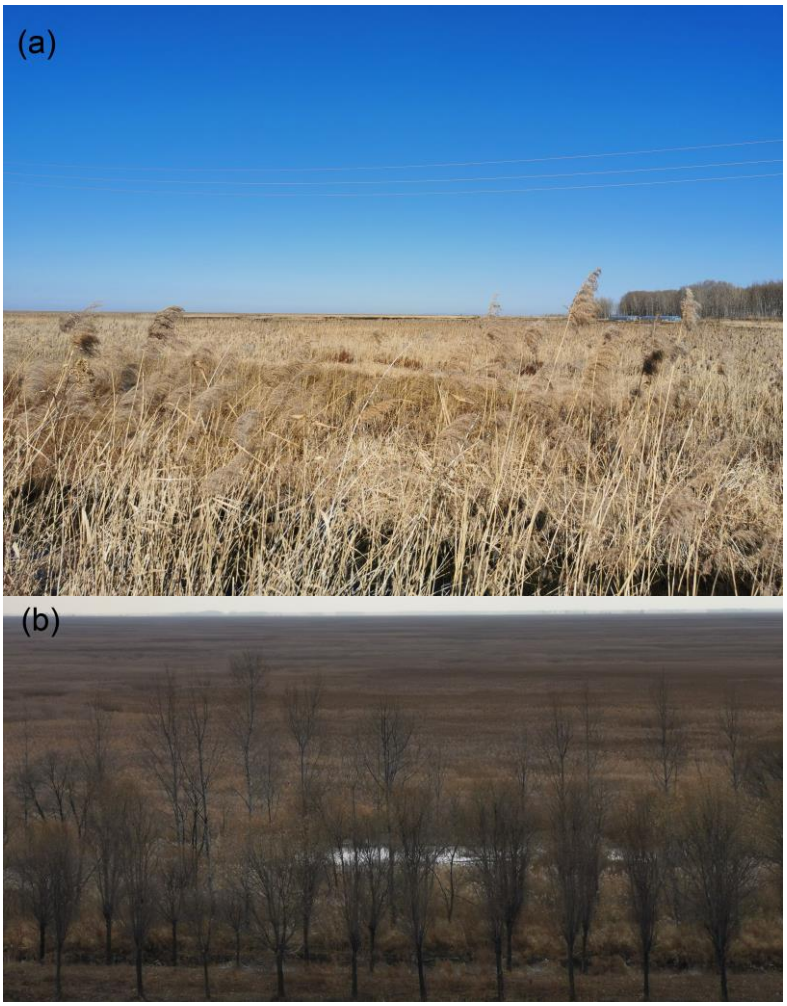

http://www.aloki.hu ● ISSN 1589 1623 (Print) ● ISSN 1785 0037 (Online)
DOI: http://dx.doi.org/10.15666/aeer/2005_44594475

Figure 2. *The habitats of three land use types: (a) wetland; (b) forest; (c) arable land*

Data analysis

For alpha diversity analysis, community richness parameters (Chao1 and ACE indices) and community diversity parameters (Shannon-Wiener indices) were calculated using Mothur version v.1.39.1 (Schloss et al., 2009). Beta diversity was calculated using R v3.3.2 (R Development Core Team, 2017) using "Vegan" package and redundancy analysis (RDA) was conducted based on OTU levels using R v3.3.2 (R Development Core Team, 2017) using "Microeco" package. One-way ANOVA was used to analyze the effects of different site types on soil properties and microbial diversity, and Duncan's test was used to test the significance of the differences between site types for each indicator ($\alpha = 0.05$ and 0.01). The results for all samples were reported as mean ± standard deviation (SD). A P-value < 0.05 was deemed statistically significant.

Results

Effect of different land uses on soil physicochemical properties

Table 2 summarizes the physicochemical properties of the soils of the three land uses. The pH of all three samples was acidic. The arable land exhibited the lowest pH value, followed by the forest soil, with wetland soil exhibiting the highest pH. Compared with arable soil (13.48% soil moisture content) and forest soil (13.19% soil moisture content), the wetland soil (13.66% soil moisture content) had a higher water content ($P < 0.05$). Except the soil available phosphorus ($P > 0.05$), the soil organic matter, total nitrogen and total phosphorus were significantly different between three land use types ($P < 0.05$). Soil organic matter, total nitrogen and total phosphorus in wetland were higher than that in forest and arable land.

OTU of soil bacteria from different land use types

A total of 2049 soil bacterial OTU sequences were identified in the three land use types, of which 1100 soil bacterial OTU sequences were shared among all three land

http://www.aloki.hu ● ISSN 1589 1623 (Print) ● ISSN 1785 0037 (Online)
DOI: http://dx.doi.org/10.15666/aeer/2005_44594475

use types (*Fig. 3*). The highest number of total OTUs was observed in the wetland soil (1856, accounting for 90.58% of the total), followed by forest soil (1837, accounting for 89.65% of the total), and finally arable soil (1292, accounting for 63.06% of the total). Therefore, pristine wetland and forest soils exhibited the highest number of bacterial OTUs, and the number of OTUs specific to wetland soils was the highest (148).

Table 2. *Physicochemical properties of soils with different land use practices*

Land use type	pH	SMC (%)	SOM (g/kg)	TN (g/kg)	TP (g/kg)	AP (mg/kg)
Wetland	5.45 ± 0.16b	73.66 ± 0.27a	52.27 ± 0.51a	4.29 ± 2.77a	6.42 ± 0.89a	28.84 ± 1.74a
Forest	5.85 ± 0.07a	23.19 ± 0.52b	34.01 ± 0.51b	1.13 ± 2.03c	4.23 ± 0.52b	25.45 ± 2.15a
Arable land	4.87 ± 0.11b	15.48 ± 0.82c	23.06 ± 0.08c	3.14 ± 1.11b	3.71 ± 0.14b	23.74 ± 1.23a

SMC, soil moisture content; SOM, soil organic carbon; TN, total nitrogen; TP, total phosphors; AP, available phosphors

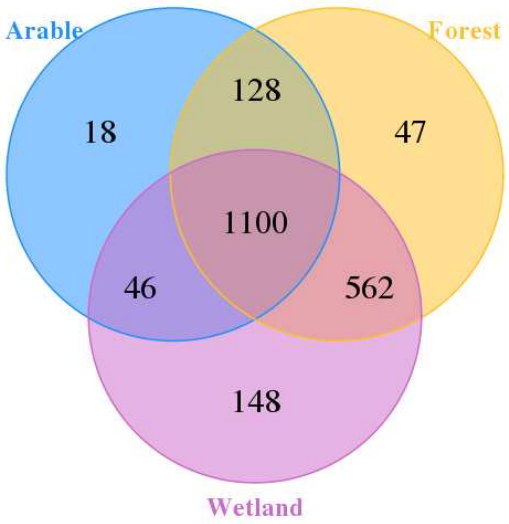

Figure 3. *Venn diagram of bacterial community structure for different land use practices*

For rarefaction curve analysis, a certain number of individuals were randomly selected from the sample, the number of species represented by these individuals was then counted, and the curve was constructed based on the number of individuals and species. As illustrated in *Figure 4,* the rarefaction curves of nine soil samples tended to be flat, indicating that the sequencing data provided an accurate representation of the samples (i.e., more sequencing data would only produce a small amount of new OTUs). Furthermore, the number of soil bacterial OTUs in different land use patterns exhibited the following descending order: wetland > forest > arable land.

Differences in soil microbial alpha and beta diversity under different land use patterns

The α-diversity indices of bacteria in soil samples from three land use types are shown in *Figure 5*. ACE, Chao1, and Shannon indices showed a consistent pattern: wetland > forest > arable land. The differences in soil ACE, Chao1, and Shannon

http://www.aloki.hu ● ISSN 1589 1623 (Print) ● ISSN 1785 0037 (Online)
DOI: http://dx.doi.org/10.15666/aeer/2005_44594475

indices between wetlands and forests were not significant (*Fig. 5,* Duncan test, $P > 0.05$). There were significant differences in the soil ACE, Chao1, and Shannon indices between wetland and arable land (*Fig. 5,* Duncan test, $P < 0.01$). Moreover, there were significant differences in soil ACE, Chao1, and Shannon indices between forest and arable land (*Fig. 5,* Duncan test, $P < 0.05$).

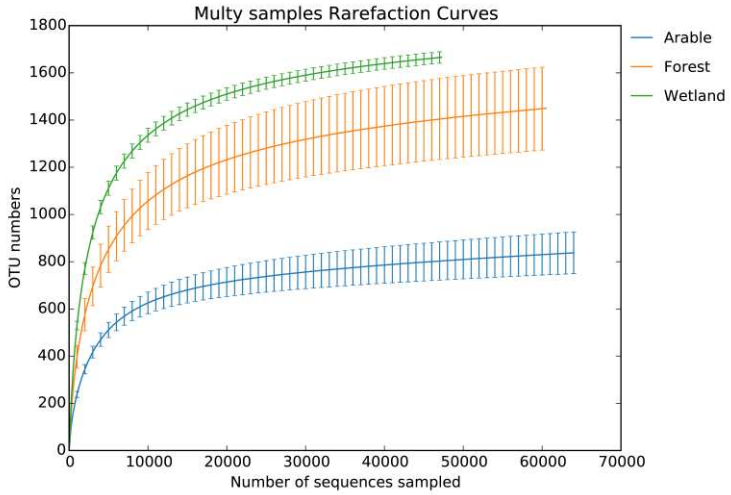

Figure 4. *Bacterial rarefaction curves of different land use modes*

The beta diversity of bacterial communities in different land use modes was measured by PCoA based on the Bray-Curtis distance. As illustrated in *Figure 5,* there were significant differences in bacterial community structure among different land use modes (PERMANOVA: $r = 0.68$, $P < 0.01$). The difference within the samples was not significant, with the main differences occurring only between different samples (*Fig. 6*). These findings indicated that long-term land use change can significantly affect the bacterial community structure of the soil.

Analysis of soil bacterial community structure in different land use modes

From the perspective of the overall bacterial community structure, all OTUs belonged to 33 bacterial phyla. If a given sequence could not be classified as a known phylum, the phyla were uniformly classified as "others." Based on the relative abundance of all phyla levels of the three land types (*Fig. 7a*), the dominant phyla in the sample are Proteobacteria, Acidobacteria, and Actinobacteria. The relative abundances of Proteobacteria, Acidobacteria, and Actinomycetes in wetland soil were 37%, 18%, and 11%, respectively. The relative abundance of the dominant Proteobacteria in forest soil was 39%, Acidobacteria was 17%, and Actinobacteria was 14%. The relative abundance of dominant bacteria in Arable land soil was 67%, Acidobacteria was 5%, and Actinobacteria was 6%.

In terms of relative abundance at the genus level (*Fig. 7b*), the composition of soil bacterial genera was not the same under different land use practices. As seen in *Figure 6b,* the major genera of soil bacteria in arable land were *Cupriavidus*, *Reyranelia*, *Aquabacterium*, and *Azohydromonas*; the major genera of soil bacteria in forest soil were *Bradyrhizobium*, *RB41*, *Rhizobacter*, *Novosphingobium*, and *Sphingomonasc*; the major genera of soil bacteria in wetland were *RB41*,

http://www.aloki.hu ● ISSN 1589 1623 (Print) ● ISSN 1785 0037 (Online)
DOI: http://dx.doi.org/10.15666/aeer/2005_44594475

Flavobacterium, *Bradyrhizobium*, *Massilia,* and *Sphingomonas*. Therefore, we concluded that different land use practices significantly affect the composition of the main genera of soil bacteria.

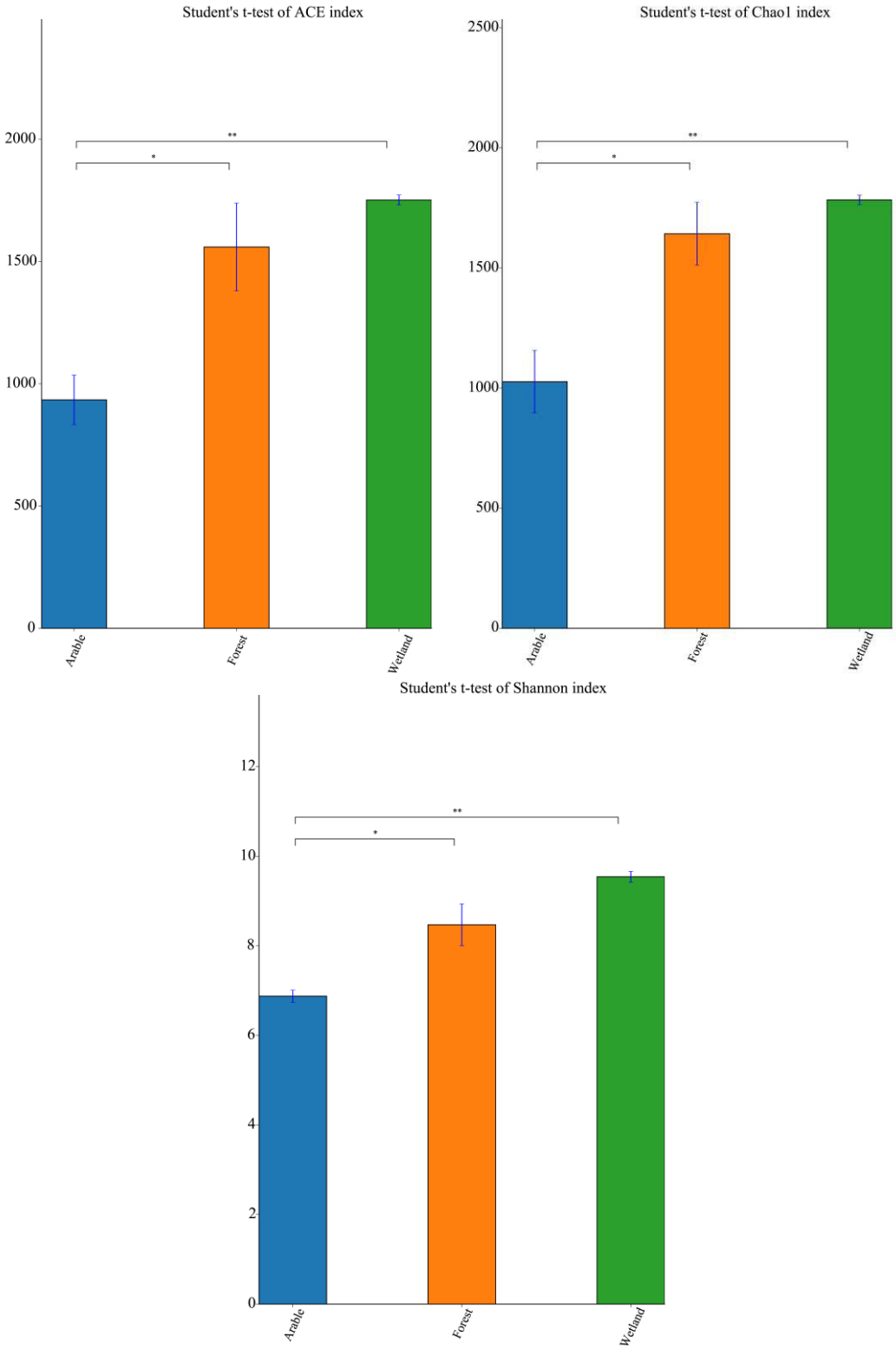

Figure 5. *Alpha diversity of soil bacteria in different land use modes. * and ** indicated the one way-ANOVA, Duncan's test at 0.05 and 0.01 level, respectively*

http://www.aloki.hu ● ISSN 1589 1623 (Print) ● ISSN 1785 0037 (Online)
DOI: http://dx.doi.org/10.15666/aeer/2005_44594475

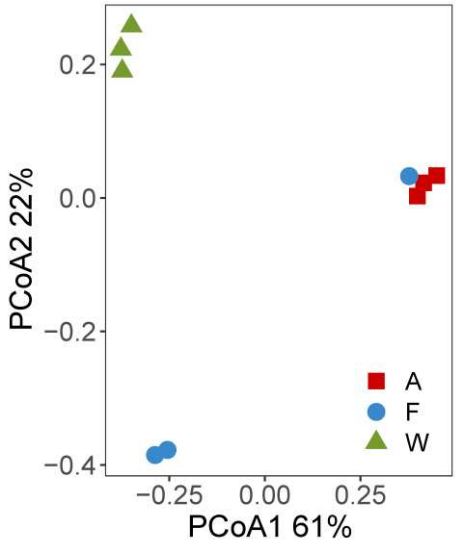

Figure 6. *PCoA diagram of soil bacterial community under different land use modes. A, arable land; F, forest; W, wetland*

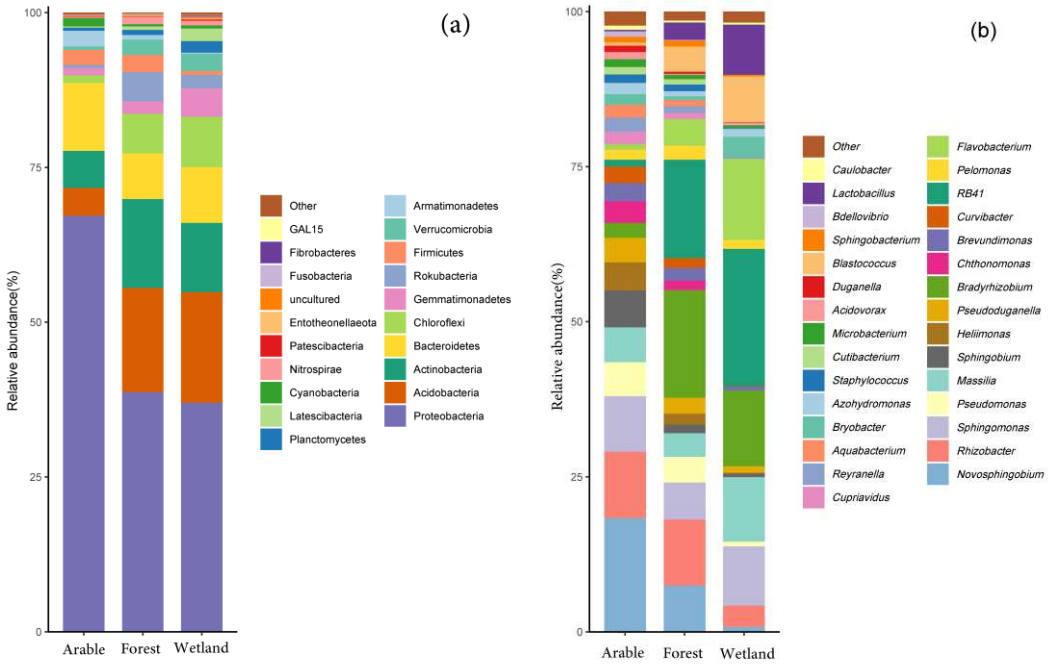

Figure 7. *Structural composition of bacterial communities in different land use practices. Phylum level (a); genus level (b); abundances less than 1% were combined into the category "other"*

Redundancy analysis of soil bacterial communities and physicochemical properties for different land use practices

Figure 8 shows the RDA of the soil physicochemical properties in relation to the community composition of bacteria at the genus level. RDA1 explained 81.31% of all variation, RDA2 explained 7.37% of all information, and the first two axes could

http://www.aloki.hu ● ISSN 1589 1623 (Print) ● ISSN 1785 0037 (Online)
DOI: http://dx.doi.org/10.15666/aeer/2005_44594475

explain 88.68% of the information. Longer rays of pH and TN indicated that they had a greater influence on bacterial community composition, whereas the shorter rays of SOC, AP, and TP values indicated that they had a smaller influence on bacterial community composition.

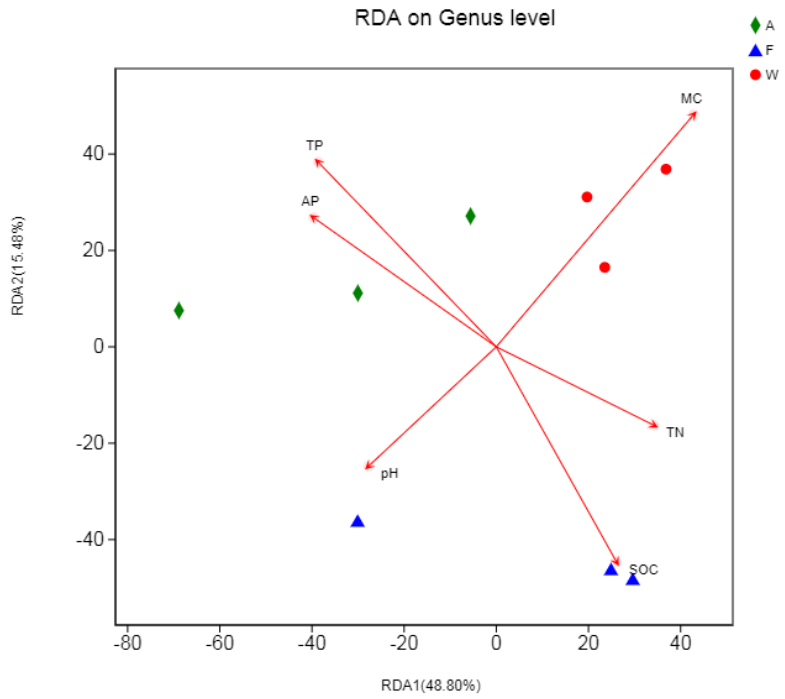

Figure 8. *RDA of soil bacterial community structure and soil physicochemical properties. A: Arable; F: Forest; W: Wetland. MC, soil moisture content; SOM, soil organic carbon; TN, total nitrogen; TP, total phosphors; AP, available phosphors*

Discussion

Changes in the diversity of soil microbial communities can reflect the quality and health of soil ecosystems (Hermans et al., 2020; García-Orenes et al., 2013). The disturbance of natural ecosystems by human activities is the most important direct driver that alters ecosystem service functions. Therefore, studying bacterial community structure and diversity in areas impacted by human activities can provide insights into the structural differences in soil bacterial communities under different land uses (Rampelotto et al., 2013; Cheng et al., 2021). In this study, the soil bacterial ACE, Chao1, and Shannon indices all exhibited the same descending pattern: wetland > forest > arable land. The differences in diversity indices between wetlands and forests were not significant, whereas the differences with farmland soil were significant. This may be due to the high nutrient content of the original wetland soil coupled with the stable ecosystem, which provided a suitable habitat for bacteria. Once reclaimed into agricultural land, the application of chemical fertilizers and tillage resulted in the destruction of the stable soil ecosystem, making it difficult for the original soil bacterial microorganisms to survive, thus reducing microbial diversity. This is consistent with the findings of Zhang et al. (2020), who reported a significant decrease in soil bacterial diversity after the reclamation of wetlands into agricultural

http://www.aloki.hu ● ISSN 1589 1623 (Print) ● ISSN 1785 0037 (Online)
DOI: http://dx.doi.org/10.15666/aeer/2005_44594475

fields. Lynn et al. (2017) also found that the soil bacterial diversity of original wetland was higher than other land use types because the land use disturbed the ecological stability and thus decreased the soil bacteria diversity. Suleiman et al. (2013) also proved that the bacterial diversity in soil decreased from pristine forest and grassland resulted from the deforestation. However, Xu et al. (2016) found that reclamation could significantly increase the soil bacterial diversity index in swampy wetlands, and concluded that reclamation increased the abundance of soil aerobic bacteria as a result of increased aeration of agricultural soils after reclamation. The moderate storm disturbances believed that disturbance had a positive effect on microbial communities by increasing their production and both their community and diversity (Galand et al., 2016). Barba et al. (2019) also proved that disturbance increased the soil microbial diversity. However, we believe that the reason for the inconsistency with the moderate disturbance hypothesis may be that the vegetation diversity on the original wetland was higher (see *Table 1*). After changing to artificial forest and maize, the vegetation on the ground became simple (see *Table 1*), and resulted the composition of litter simple, this directly affected soil microbial nutrient sources, leading to a decrease in soil bacterial diversity. Addition, we also believe that different tillage intensity, tillage treatment, and tillage time will affect soil bacterial diversity. Therefore, additional studies are required to assess the long-term effects of different land use practices on soil bacterial diversity.

Currently, the mechanisms of soil bacterial community generation and maintenance are not fully understood. However, differences in soil bacterial community components can explain the effects of environmental changes on in situ soil bacterial community reconstruction (Xun et al., 2015). The significant differences in soil bacterial β-diversity among different land use practices (*Fig. 5*) indicate that changes in land use practices have modified the structure of soil bacterial communities. This may be because there were significant changes in soil nutrient cycling due to changes in the original aboveground vegetation when the original swampy wetlands were transformed into forests and agricultural lands, as bacteria are closely associated with the diversity of the aboveground vegetation (Sui et al., 2021). Although short-term changes may not be obvious, the input of litter caused by the changes in aboveground vegetation after long-term land change and the long-term changes in plant root exudates and biomass ultimately affect the soil bacterial community structure, which is consistent with the findings of Xu et al. (2021).

We found that the main factors affecting soil bacterial community structure of three land use types were different, among which soil moisture content was the main environmental factor affecting wetland soil bacterial community structure, while available phosphorus and total phosphorus were the main environmental factors affecting farmland soil bacterial community structure, and soil pH, soil organic carbon and total nitrogen were the main environmental factors affecting forest soil bacteria. This may be because the wetland environment was mainly dominated environmental factor (e.g. high water level), especially the original wetland soil has high water content, which may be the main factor affecting the soil bacterial structure. However, due to the application of phosphorus fertilizer, the phosphorus content of the farmland changed, which may be the main reason affecting the farmland soil bacterial community. The above-ground vegetation in forest was mainly affected litter input and the litter contained a large amount of organic carbon and total nitrogen. Many studies showed that wetland soil microbiome were affected by soil water content (Clairmont et al., 2019; Choi et al., 2022), which was consistent with the results of this study. However,

http://www.aloki.hu ● ISSN 1589 1623 (Print) ● ISSN 1785 0037 (Online)
DOI: http://dx.doi.org/10.15666/aeer/2005_44594475

Clairmont et al. (2019) also found that soil microbial community structure was not only affected by soil water content, but also the composition of aboveground vegetation also played an important role. However, since this study did not study the root soil microbial structure, hence, it is necessary to carry out research on the changes of root microorganisms and their driving factors in the future. Soil phosphorus was the main nutrient factor affecting soil microbial structure (Turley et al., 2020). When the phosphorus element in the soil increases, the microbial groups related to the phosphorus element content in the soil microorganisms would change, which lead to the change of the soil microbial community structure. pH, organic carbon and total nitrogen were the main physicochemical factors affecting soil microorganisms (Plassart et al., 2019). Studies have shown that soil pH, organic carbon and nitrogen significantly affected the structure of soil bacterial community in soil forests (Praeg et al., 2020). This is consistent with these results, but the factors affecting soil bacterial structure are complex, and different aboveground vegetation compositions and disturbance intensity will affect soil bacterial community structure, so further research is still needed.

Changes in land use mode did not affect the main phyla of the soil bacterial communities (*Fig. 7a*). The dominant phyla in the three land soils were Proteobacteria, Acidobacteria, and Actinobacteria. According to Wang et al. (2019), different land use modes have an important impact on the bacterial community structure of wetland soil, with Proteobacteria, Acidobacteria, and Actinobacteria being the dominant bacteria in the wetland soil environment. Ogola et al. (2021) also found that Proteobacteria, Acidobacteria, and Actinobacteria play an important role in different soil bacterial communities. Therefore, changes in land use mode will not affect the main dominant flora of soil bacteria, but may still have a significant impact at the genus level. In other words, although the main components of the community did not change at the phylum level, significant effects were observed at the genus level because different land use modes are affected by different soil physical and chemical factors. In this study, the major genera of soil bacteria in arable land were *Cupriavidus*, *Reyranelia*, *Aquabacterium*, and *Azohydromonas*; the major genera of soil bacteria in forest soil were *Bradyrhizobium*, *RB41*, *Rhizobacter*, *Novosphingobium*, and *Sphingomonasc*; the major genera of soil bacteria in wetland were *RB41*, *Flavobacterium*, *Bradyrhizobium*, *Massilia,* and *Sphingomonas*. Specifically, our findings indicated that wetland soil bacteria are mainly affected by soil water content, whereas forest soil bacteria are affected by soil organic carbon and total nitrogen, and arable land soil bacteria is most significantly affected by soil total phosphorus and available phosphorus (*Fig. 8*). This suggested that different bacterial species respond differently to habitat changes. This is consistent with other research findings (Ormeño-Orrillo et al., 2012; De Meyer et al. 2018) indicating that when the habitat changes, the microbial niche will be differentiated, which will lead to the change of species composition (Hartmann et al., 2017). This would explain why different dominant genera of soil bacteria were observed under different land use modes, which is consistent with the findings of Xu et al. (2016) and Sui et al. (2019).

Conclusion

Changing the land use patterns of primitive swamp wetlands in Sanjiang Plain has led to significant changes in soil physical and chemical properties, in addition to causing significant differences in soil bacterial community diversity among different land use types. Different land use habitats have their own distinct dominant flora. The

http://www.aloki.hu ● ISSN 1589 1623 (Print) ● ISSN 1785 0037 (Online)
DOI: http://dx.doi.org/10.15666/aeer/2005_44594475

variations in wetland soil bacterial communities are mainly caused by soil water content. Pristine marsh wetland habitats are a key factor in maintaining high levels of bacterial alpha diversity. The dominant phylum of soil bacteria in each land use type habitat remained stable. However, the bacterial community structure at the genus level was significantly influenced by the physicochemical properties of the soil in each land use type. Collectively, our findings demonstrate that long-term land use changes can significantly change the bacterial community composition and diversity of soil.

Acknowledgements. The work was funded by the Natural Sciences Foundation of Heilongjiang Province (LH2020C088); Heilongjiang Province Postdoctoral Research Start-up Fund Project (LBH-Q21167); the Outstanding Youth Foundation of Heilongjiang University (JCL202006); and the China Scholarship Council Visiting Scholar Program (201908230401). We thank Sci Paper Edit Corporation for language editing. We thank Dr Luo Chunyu for the map editing. We also thank Liyu, who is working the Sanhuanpao National Nature Reserve and Cui Xingbo, who is working in Naolihe Nature Reserve of Heilongjiang Province, for the help of taking samples.

REFERENCES

[1] Acín-Carrera, M., José Marques, M., Carral, P., Álvarez, A. M., López, C., Martín-López, B., González, J. A. (2013): Impacts of land-use intensity on soil organic carbon content, soil structure and water-holding capacity. – Soil Use Manage 29(4): 547-556.

[2] Barba, C., Folch, A., Gaju, N., Sanchez-Vila, X., Carrasquilla, M., Grau-Martínez, A., Martínez-Alonso, M. (2019): Microbial community changes induced by Managed Aquifer Recharge activities: linking hydrogeological and biological processes. – Hydrol. Earth Syst Sci 23: 139-154.

[3] Birkhofer, K., Schöning, I., Alt, F., Herold, N., Klarner, B., Maraun, M., Marhan, S., Oelmann, Y., Wubet, T., Yurkov, A., Begerow, D., Berner, D., Buscot, F., Daniel, R., Diekötter, T., Ehnes, R., Erdmann, G., Christiane, F., Bärbel, Janine, F., Jessica, G., Ellen, G., Christa, K., Gertrud, L., Annabel, L., Heiko, M., Astrid, N., Jörg, N., Andrea, O., Melanie M., P., Stefan, P., Michael, S., Ernst-Detlef, S., Schulze, W., Schulze, Weinert, J., Weisser, W., Wolters, V., Schrumpf, M. (2012): General relationships between abiotic soil properties and soil biota across spatial scales and different land-use types. – PloS one 7(8): e43292.

[4] Cheng, X., Yun, Y., Wang, H., Ma, L., Tian, W., Man, B., Liu, C. (2021): Contrasting bacterial communities and their assembly processes in karst soils under different land use. – Sci Total Environ 751: 142263.

[5] Choi, H., Geronimo, F. K., Jeon, M., Kim, L. H. (2022): Evaluation of bacterial community in constructed wetlands treating different sources of wastewater. – Ecol Eng 182: 106703.

[6] Clairmont, L. K., Stevens, K. J., Slawson, R. M. (2019): Site-specific differences in microbial community structure and function within the rhizosphere and rhizoplane of wetland plants is plant species dependent. – Rhizosphere 9: 56-68.

[7] De Meyer, S. E., Ruthrof, K. X., Edwards, T., Hopkins, A. J., Hardy, G., O'Hara, G., Howieson, J. (2018): Diversity of endemic rhizobia on Christmas Island: implications for agriculture following phosphate mining. – Syst Appl Microbiol 41(6): 641-649.

[8] Deng, J. J., Bai, X. J., Zhou, Y., Zhu, W. X., Yin, Y. (2020): Variations of soil microbial communities accompanied by different vegetation restoration in an open-cut iron mining area. – Sci Total Environ 704: 135243.

http://www.aloki.hu ● ISSN 1589 1623 (Print) ● ISSN 1785 0037 (Online)
DOI: http://dx.doi.org/10.15666/aeer/2005_44594475

[9] Galand, P. E., Lucas, S., Fagervold, S. K., Peru, E., Pruski, A. M., Vétion, G., Guizien, K. (2016): Disturbance increases microbial community diversity and production in marine sediments. – Front Microbial 7: 1950.
[10] García-Orenes, F., Morugán-Coronado, A., Zornoza, R., Scow, K. (2013): Changes in soil microbial community structure influenced by agricultural management practices in a Mediterranean agro-ecosystem. – PloS ONE 8(11): e80522.
[11] Hartmann, M., Brunner, I., Hagedorn, F., Bardgett, R. D., Stierli, B., Herzog, C., Frey, B. (2017): A decade of irrigation transforms the soil microbiome of a semi-arid pine forest. – Mol Ecol 26(4): 1190-1206.
[12] Hermans, S. M., Buckley, H. L., Case, B. S., Curran-Cournane, F., Taylor, M., Lear, G. (2020): Using soil bacterial communities to predict physico-chemical variables and soil quality. – Microbiome 8(1): 1-13.
[13] Huang, Q., Wang, J., Wang, C., Wang, Q. (2019): The 19-years inorganic fertilization increased bacterial diversity and altered bacterial community composition and potential functions in a paddy soil. – Appl Soil Ecol 144: 60-67.
[14] Li, Y., Fan, J., Zhang, L., Zhai, J., Liu, G., Li, J. (2013): The impact of different land use and management on community composition, species diversity and productivity in a typical temperate grassland. – Acta Pratacul Sini 22(1): 1-9.
[15] Li, J., Jiang, C., Hao, Q. (2014): Impact of land use type on stability and organic carbon of soil aggregates in Jinyun Mountain. – Environ Sci 35(12): 4695-4704.
[16] Liu, H., Huang, J. (2005): Dynamics of soil properties under secondary succession forest communities in Mt. Jinyun. – ChinJ Appl Ecol 16(11): 37-42.
[17] Liu, X., He, Y., Zhang, H., Schroder, J., Li, C., Jing, Zhou, J., Zhang, Z. (2010): Impact of land use and soil fertility on distributions of soil aggregate fractions and some nutrients. – Pedosphere 20(5): 666-673.
[18] Lv, W., Zhang, H., Chen, J., Li, J., Wang, X., Wu, Y., Wang, R. (2011): Effects on soil physicochemical properties and anti-erosion caused by plant hedgerows in Three Gorges reservoir area. – J Soil Water Conserv 25(4): 69-73.
[19] Lynn, T. M., Liu, Q., Hu, Y., Yuan, H., Wu, X., Khai, A. A., Ge, T. (2017): Influence of land use on bacterial and archaeal diversity and community structures in three natural ecosystems and one agricultural soil. – Arch Microbiol 199(5): 711-721.
[20] Ogola, H. J. O., Selvarajan, R., Tekere, M. (2021): Local geomorphological gradients and land use patterns play key role on the soil bacterial community diversity and dynamics in the highly endemic indigenous afrotemperate coastal scarp forest biome. – Front Microbiol 12: 592725.
[21] Ormeño-Orrillo, E., Rogel-Hernández, M. A., Lloret, L., López-López, A., Martínez, J., Barois, I., Martínez-Romero, E. (2012): Change in land use alters the diversity and composition of Bradyrhizobium communities and led to the introduction of Rhizobium etli into the tropical rain forest of Los Tuxtlas (Mexico). – Microb Ecol 63(4): 822-834.
[22] Plassart, P., Prévost-Bouré, N. C., Uroz, S., Dequiedt, S., Stone, D., Creamer, R., Lemanceau, P. (2019): Soil parameters, land use, and geographical distance drive soil bacterial communities along a European transect. – Sci Rep 9(1): 1-17.
[23] Praeg, N., Seeber, J., Leitinger, G., Tasser, E., Newesely, C., Tappeiner, U., Illmer, P. (2020): The role of land management and elevation in shaping soil microbial communities: insights from the Central European Alps. – Soil Biol Biochem 150: 107951.
[24] Rampelotto, P. H., de Siqueira Ferreira, A., Barboza, A. D. M., Roesch, L. F. W. (2013): Changes in diversity, abundance, and structure of soil bacterial communities in Brazilian Savanna under different land use systems. – Microb Ecol 66(3): 593-607.
[25] Ren, T., Wang, X., Sun, X., Qiu, Y., Li, D. (2014): Characterization of soil physical properties under different land use types. – J Soil Water Conserv 28(2): 123-126.

http://www.aloki.hu ● ISSN 1589 1623 (Print) ● ISSN 1785 0037 (Online)
DOI: http://dx.doi.org/10.15666/aeer/2005_44594475

[26] Sánchez-Moreno, S., Minoshima, H., Ferris, H., Jackson, L. (2006): Linking soil properties and nematode community composition: effects of soil management on soil food webs. – Nematology 8(5): 703-715.
[27] Schloss, P. D., Westcott, S. L., Ryabin, T., Hall, J. R., Hartmann, M., Hollister, E. B., Weber, C. F. (2009): Introducing mothur: open-source, platform-independent, community-supported software for describing and comparing microbial communities. – Appl Environ Microb 75(23): 7537-7541.
[28] Sheng, H. A. O., Yang, Y., Yang, Z., Chen, G., Xie, J., Guo, J., Zou, S. (2010): The dynamic response of soil respiration to land-use changes in subtropical China. – Glob Chang Biol 16(3): 1107-1121.
[29] Sui, X., Zhang, R., Frey, B., Yang, L., Li, M. H., Ni, H. (2019): Land use change effects on diversity of soil bacterial, Acidobacterial and fungal communities in wetlands of the Sanjiang Plain, northeastern China. – Sci Rep 9(1): 1-14.
[30] Sui, X., Zhang, R., Frey, B., Yang, L., Liu, Y., Ni, H., Li, M. (2021): Soil physicochemical properties drive the variation in soil microbial communities along a forest successional series in a degraded wetland in northeastern China. – Ecol Evol 11(5): 2194-2208.
[31] Sui, X., Zeng, X., Li, M., Weng, X., Frey, B., Yang, L., Li, M. (2022): Influence of Different Vegetation Types on Soil Physicochemical Parameters and Fungal Communities. – Microorganisms 10(4): 829.
[32] Suleiman, A. K. A., Manoeli, L., Boldo, J. T., Pereira, M. G., Roesch, L. F. W. (2013): Shifts in soil bacterial community after eight years of land-use change. – Syst Appl Microbiol 36(2): 137-144.
[33] Tischer, A., Blagodatskaya, E., Hamer, U. (2015): Microbial community structure and resource availability drive the catalytic efficiency of soil enzymes under land-use change conditions. – Soil Biol Biochem 89: 226-237.
[34] Turley, N. E., Bell-Dereske, L., Evans, S. E., Brudvig, L. A. (2020): Agricultural land-use history and restoration impact soil microbial biodiversity. – J Appl Ecol 57(5): 852-863.
[35] Van Leeuwen, J., Djukic, I., Bloem, J., Lehtinen, T., Hemerik, L., De Ruiter, P. C., Lair, G. J. (2017): Effects of land use on soil microbial biomass, activity and community structure at different soil depths in the Danube floodplain. – Eur J Soil Biol 79: 14-20.
[36] Wang, N., Gao, J., Wei, J., Liu, Y., Zhuang, X., Zhuang, G. (2019): Effects of wetland reclamation on soil microbial community structure in the Sanjiang Plain. – Environ Sci 40(5): 2375-2381.
[37] Weng, X. H., Sui, X., Liu, Y. N., Yang, L. B., Zhang, R. T. (2022): Effect of nitrogen addition on the carbon metabolism of soil microorganisms in a Calamagrostis angustifolia wetland of the Sanjiang Plain, northeastern China. – Ann Microbiol 72(1): 1-14.
[38] Wu, H. T., Wu, D. H., Lu, X. G., Yin, X. M. (2010): Spatial distribution of ant mounds and effects on soil physical properties in wetlands of the Sanjiang plain, China. – Acta Ecol Sin 30(5): 270-275.
[39] Xu, F., Cai, T., Yang, X., Ju, C., Tang, Q. (2016): Effect of cultivation and natural restoration on soil bacterial community diversity in marshland in the Sanjiang Plain. – Acta Ecol Sin 36(22): 7412-7421.
[40] Xu, S. Q., Zhang, B., Ma, L. N., Hou, A. X., Tian, L., Li, X. J., Tian, C. J. (2017): Effects of marsh cultivation and restoration on soil microbial communities in the Sanjiang Plain, Northeastern China. – Eur J Soil Biol 82: 81-87.
[41] Xu, A., Liu, J., Guo, Z., Wang, C., Pan, K., Zhang, F., Pan, X. (2021): Soil microbial community composition but not diversity is affected by land-use types in the agro-pastoral ecotone undergoing frequent conversions between cropland and grassland. – Geoderma 401: 115165.
[42] Xun, W., Huang, T., Zhao, J., Ran, W., Wang, B., Shen, Q., Zhang, R. (2015): Environmental conditions rather than microbial inoculum composition determine the

http://www.aloki.hu ● ISSN 1589 1623 (Print) ● ISSN 1785 0037 (Online)
DOI: http://dx.doi.org/10.15666/aeer/2005_44594475

bacterial composition, microbial biomass and enzymatic activity of reconstructed soil microbial communities. – Soil Biol Biochem 90: 10-18.

[43] Zhang, T., Xu, F., Huai, B. D., Yang, X., Sui, W. (2020): Effects of land use changes on soil bacterial community diversity in the riparian wetland along the downstream of Songhua River. – Environ Sci 41(9): 4273-4283.

[44] Zhang, R. T., Liu, Y. N., Zhong, H. X., Chen, X. W., Sui, X. (2022): Effects of simulated nitrogen deposition on the soil microbial community diversity of a Deyeuxia angustifolia wetland in the Sanjiang Plain, Northeastern China. – Ann Microbiol 72(1): 1-13.

[45] Zhao, R., Zhang, Y., Zhang, Q., Chen, B., Zhang, J. (2011): Effects of different land use types on soil nutrients conditions in cultivated land—A case study of Taiyuan. – Chin Agricul Sci Bull 27(14): 262-266.

[46] Zhao, J., Zhang, D., Liu, C., Xu, C. (2012): The effect of different land use patterns on soil properties in alpine of eastern Qilian mountains. – Acta Ecol Sin 32(2): 548-556.

[47] Zucco, G., Brocca, L., Moramarco, T., Morbidelli, R. (2014): Influence of land use on soil moisture spatial–temporal variability and monitoring. – J Hydrol 516: 193-199.

http://www.aloki.hu ● ISSN 1589 1623 (Print) ● ISSN 1785 0037 (Online)
DOI: http://dx.doi.org/10.15666/aeer/2005_44594475

LAND USE AND LANDSCAPE PATTERN CHANGES IN NAIMAN BANNER OF HORQIN SANDY LAND, CHINA

YUE, X. Y.[1*] – YUE, W.[2] – CHANG, X. L.[3]

[1]*Shandong Key Laboratory of Eco-Environmental Science for Yellow River Delta, Binzhou University, Binzhou 256603, China*

[2]*School of Geography, Geomatics and Planning, Jiangsu Normal University, Xuzhou 221116, China*

[3]*School of Resources and Environmental Engineering, Ludong University, Yantai 264025, Shandong, China*

**Corresponding author*
e-mail: yuexiyuan393@126.com; phone: +86-183-6380-0513

(Received 9th May 2022; accepted 26th Jul 2022)

Abstract. Quantifying the spatial-temporal dynamics of land use and landscape patterns is important for land management and ecological conservation in an ecologically fragile region. This study focused on Naiman Banner on the southern edge of Horqin sandy land, one of the largest sandy lands in northern China. Based on remote sensing (RS) and geographical information system (GIS), the spatial-temporal changes of land use and landscape pattern were investigated in Naiman Banner from 2002 to 2018. The results showed that the area of cropland and construction land area increased by 586.75 km^2 and 215.05 km^2, respectively. Meanwhile, the area of grassland, forest land, sandy land and water body decreased by 488.55 km^2, 177.44 km^2, 88.88 km^2 and 46.89 km^2, respectively. Forest land and grassland were mainly replaced by cropland, and sandy land was mainly converted into grassland. The area of cropland expanded towards the north of the study area. The largest patch index of cropland and construction land increased, while that of grassland decreased. The landscape change was mainly characterized by the largest patch index increased, which suggested the landscape became more homogeneous. The study is meaningful in the land use management and ecological environment protection in Naiman Banner of Horqin sandy land.
Keywords: *landscape metrics, spatial-temporal change, agricultural expansion, remote sensing, geographical information system*

Introduction

Land use and land cover change (LUCC) reflects the interactions between human and the environment (Bagaria et al., 2021). LUCC is one of the important aspects of studying global and regional environmental changes (Inalpulat and Genc, 2021; Deus and Tenedório, 2021). Monitoring the negative effects of LUCC has become a major priority for many scholars worldwide (Obeidat et al., 2019; Mohamed et al., 2020). Remote sensing (RS) and geographic information system (GIS) are efficient and cost-effective tools to assess LUCC (Mohamed et al., 2020). Based on RS, GIS technologies and statistical analysis methods, the trend and magnitude of land use changes can be well quantified (Minta et al., 2018). Recently, LUCC analysis has contributed to understanding land use changes in some ecologically vulnerable regions, such as wetland (Ansari and Golabi, 2019), oasis (Liu et al., 2021), sandy land (Liang and Yang, 2016) and coastal areas (Daniela and Marco, 2017). In addition, landscape pattern is defined as spatial arrangements of landscape patches (Wang et al., 2020). Quantifying landscape pattern changes is a major part of landscape ecology (Wan et al., 2015; Wu, 2013). Landscape

http://www.aloki.hu ● ISSN 1589 1623 (Print) ● ISSN 1785 0037 (Online)
DOI: http://dx.doi.org/10.15666/aeer/2005_44774488

metrics can be used to promote the quantification of landscape pattern changes at the class and landscape levels, for example, the fragmentation, diversity and heterogeneity of landscape (Deus and Tenedório, 2021; Obeidat et al., 2019).

In arid and semi-arid regions, human activities such as overgrazing, deforestation and land reclamation resulted in desertification (Duan et al., 2014). With the development of social economy and population growth, land degradation is widespread in arid and semi-arid regions (Hirche et al., 2011; Jiang et al., 2013), threatening the survival of local people, and impeding socioeconomic development and ecosystem security in the local areas. With RS and GIS technologies, much attention has been paid to studying the degradation of sand land ecosystem, like the study of desertification dynamics (Dawelbait and Morari, 2012; Guo et al., 2020), land use changes (Ge et al., 2016), and landscape pattern changes at regional scales (Hirche et al., 2011). It is beneficial to understand these changes in achieving the sustainable management of land.

Horqin sandy land, located in agro-pastoral ecotone, is one of the largest sandy lands in northern China (Ge et al., 2016). The eco-environment of Horqin sandy land is vulnerable to global climate change and human activities (Guo et al., 2020). In recent decades, local government and people have taken positive measures such as the grazing ban policy, pasture fences and forestation to restore the degraded sandy land, and the eco-environment of Horqin sandy land has been improved (Zhang et al., 2012). With rapid economic development, population growth, and agricultural reclamation activities, land use changes in Horqin sandy land were affected (Li et al., 2017; Zhou et al., 2017). Many previous studies focused on desertification monitoring (Duan et al., 2019; Wang et al., 2017) and grassland restoration (Yuan et al., 2012; Miao et al., 2015) in Horqin sandy land, little attention has been paid to land use and landscape pattern changes in Horqin sandy land in recent years. Moreover, the trend and magnitude of land use changes in recent years was ignored in the study area. In this study, a representative area was selected in Naiman Banner on the southern edge of Horqin sandy land, northern China. The RS and GIS techniques were applied to characterize its changes in land use and landscape patterns. The objectives of our study were: (1) to investigate the land use changes; (2) to examine the main changes in landscape patterns.

Materials and methods

Study area

Naiman Banner is located in the south of Horqin sandy land (120°19′40″-121°31′44″E, 42°14′10″-43°32′20″N), and it is one of the counties in Inner Mongolia, China (*Fig. 1*). The topography of the study area is low in the north and high in the south, and the elevation ranges from 186 m to 792 m. The climate is characterized by the temperate continental climate, with an average temperature 6.8 °C (Zhou et al., 2014). The long-term mean annual precipitation is 360 mm, 75% of which is from June to September (Zuo et al., 2017). The study region covers an area of about 8100 km^2, with a population of 450,000 in 2018. Naiman Banner is mainly composed of cropland and grassland.

Data sources and processing

Landsat images in 2002, 2008 (Landsat 5 Thematic Mapper) and 2018 (Landsat 8 Operational Land Imager) were acquired from the United States Geological Survey (http://earthexplorer.usgs.gov/). All remote sensing images with a spatial resolution of

http://www.aloki.hu ● ISSN 1589 1623 (Print) ● ISSN 1785 0037 (Online)
DOI: http://dx.doi.org/10.15666/aeer/2005_44774488

30 m were selected in August, and the satellite images were mosaiced and geo-referenced. Land use types were classified by using visual interpretation in ArcGIS software after field surveys. According to the national standard of current land use classification (GB/T21010-2017), the land use was classified into six classes, including cropland, forest land, grassland, water body, construction land, and sandy land (*Fig. 2*). We used the Kappa coefficient to evaluate land use classification accuracy based on the field survey (Lamine et al., 2018), and the Kappa index was greater than 0.85. The field survey was conducted in June to July 2002, 2008 and 2018, and 180 verification points were collected by using geographic positioning system (GPS). The population and number of livestock were obtained from the Inner Mongolia statistical yearbook (2003-2018) and Tongliao statistical yearbook (2019).

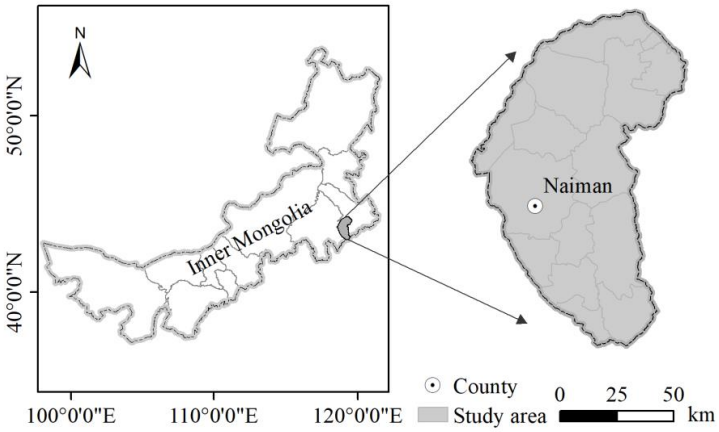

Figure 1. *Location of the study area*

Land use change rate

Land use change rate reflects the changes of different land use types (Alawamy et al., 2020). The formula of annual change rate as follows:

$$V = \frac{(A_j - A_i)}{T} \quad \text{(Eq.1)}$$

where V is the annual change rate (km^2/year). A_i is the area of specific land use type at time i, and A_j is the area of specific land use type at time j. T is time intervals.

Land use transformation

The transition matrix was widely used to detect the conversions among different land use types (Lin et al., 2018; Daniela and Marco, 2017). In our study, the analysis of transition matrix that was obtained by the spatial overlay method in GIS software used to identify the land use transformations.

Landscape pattern analysis

Landscape metrics were used to depict the spatial-temporal characteristics of landscape pattern changes such as landscape fragmentation and heterogeneity (Dadashpoor et al., 2019). We selected widely-adopted landscape metrics that can

http://www.aloki.hu ● ISSN 1589 1623 (Print) ● ISSN 1785 0037 (Online)
DOI: http://dx.doi.org/10.15666/aeer/2005_44774488

reflect the composition and configuration of landscape pattern (Yu and Ng, 2008; Deus and Tenedório, 2021). Landscape metrics selected in the study are as follows: the number of patches (NP), mean patch size (MPS), largest patch index (LPI), interspersion and juxtaposition index (IJI) and Shannon's diversity index (SHDI) (*Table 1*). Landscape metrics were calculated by using FRAGSTATS software.

Table 1. *Landscape metrics used in the study (adopted from Obeidat et al., 2019)*

Metrics	Units	Abbreviation	Description	Justification
Number of patches	None	NP	Total number of patches in the landscape	Fragmentation
Mean patch size	km^2	MPS	The average size of patches	Fragmentation
Largest patch index	%	LPI	The ratio of largest patch area to investigated area	Dominance
Interspersion and juxtaposition index	%	IJI	Degree of interspersion of patch types	Uniformity
Shannon's diversity index	None	SHDI	Proportional abundance of each patch type multiplied by that proportion	Diversity

Results

Land use dynamics

The area of cropland and construction land increased from 3291.85 km^2 and 34.28 km^2 in 2002 to 3878.60 km^2 and 249.33 km^2 in 2018, respectively (*Fig. 2*; *Table 2*). In contrast, the area of grassland, forest land, water body and sandy land decreased by 488.55 km^2, 177.44 km^2, 46.89 km^2 and 88.88 km^2 from 2002 to 2018, respectively. Cropland was the most dominant land use type, and its area proportion shows an increasing trend from 40.64% in 2002 to 47.88% in 2018. Grassland had the largest decrease during the study period, and the proportion of grassland decreased from 40.00% to 33.97%. The construction land area was accounted for 0.42% of the study area in 2002, and rapidly increased to 3.08% in 2018.

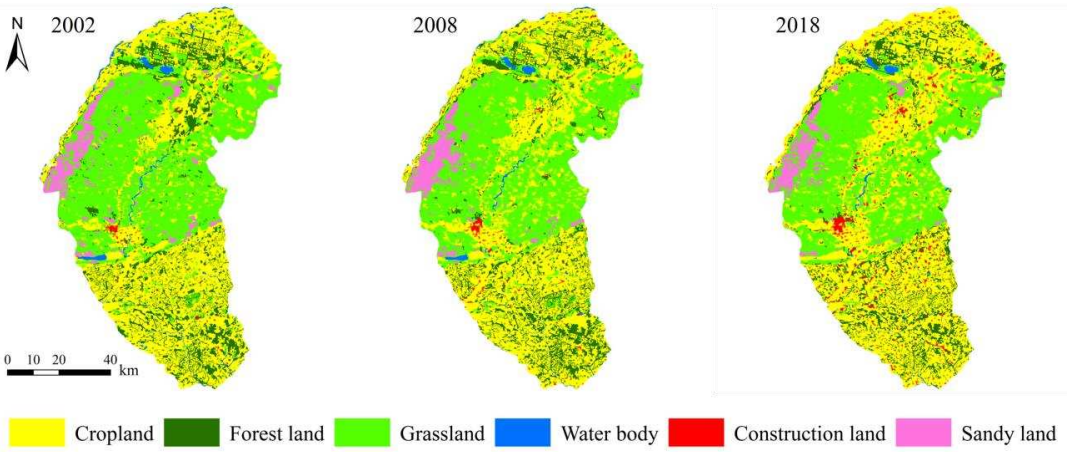

Figure 2. *Land use classification map of the study area in 2002, 2008 and 2018*

During 2002-2008, the annual change rate of cropland and construction land was positive (*Fig. 3*), while that of forest land, grassland, water body and sandy land was negative. The annual change rate of cropland was the highest (44.75 km^2/year), followed by construction land (4.97 km^2/year). The annual change rate of grassland witnessed the biggest reduction (38.51 km^2/year). During 2008-2018, cropland

http://www.aloki.hu ● ISSN 1589 1623 (Print) ● ISSN 1785 0037 (Online)
DOI: http://dx.doi.org/10.15666/aeer/2005_44774488

decreased at the rate of 31.82 km^2/year, while construction land increased at the rate of 18.52 km^2/year. The annual change rate of construction land during 2008-2018 was three times larger than that during 2002-2008.

Table 2. *Changes in area and percentage of land use types*

Land use type	2002		2008		2018	
	Area (km^2)	Percentage (%)	Area (km^2)	Percentage (%)	Area (km^2)	Percentage (%)
Cropland	3291.85	40.64	3560.37	43.95	3878.60	47.88
Forest land	1061.47	13.10	1047.55	12.93	884.03	10.91
Grassland	3240.14	40.00	3009.09	37.15	2751.59	33.97
Water body	108.75	1.34	81.96	1.01	61.86	0.76
Construction land	34.28	0.42	64.12	0.79	249.33	3.08
Sandy land	364.50	4.50	337.84	4.17	275.62	3.40

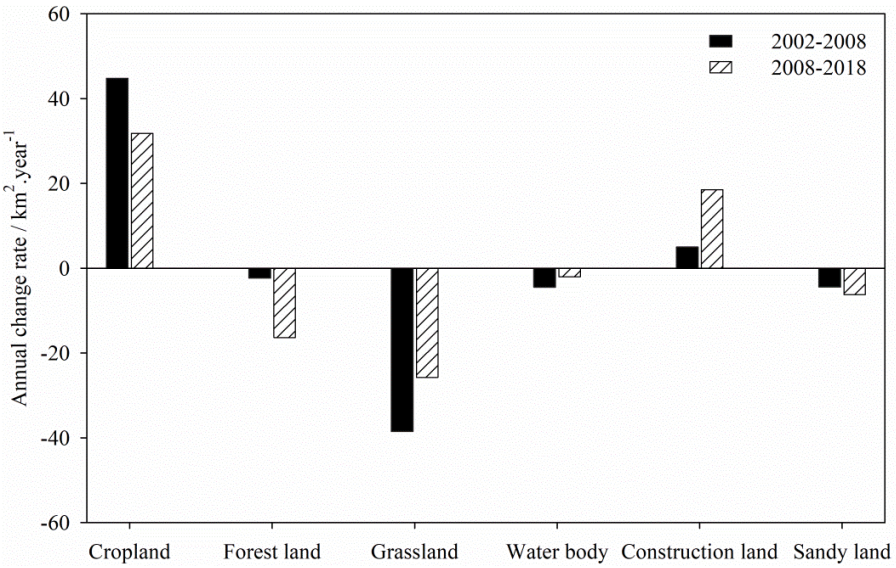

Figure 3. *The annual change rate of each land use types*

Land use conversions

From 2002 to 2008, grassland and forest land were mainly converted to cropland (*Table 3*). About 418.06 km^2 and 386.73 km^2 of grassland and forest land turned into cropland, respectively. The increased area of construction land was related to the transition of cropland and forest land. About 14.83 km^2 and 13.15 km^2 of cropland and forest land were occupied by construction land, respectively. Water body was mainly converted to cropland, and sand land mainly converted to grassland. From 2008 to 2018, 436.49 km^2 and 74.62 km^2 of forestland were converted to cropland and construction land, respectively (*Table 4*). A total of 109.13 km^2 of sandy land was transformed into grassland. Grassland was mainly converted into cropland and forest land, and the large water body area was converted into cropland.

During 2002-2008, the transition to cropland was mainly in the middle and north of Naiman Banner (*Fig. 4*). The transition to grassland occurred in the south and north. Sandy land conversions were primarily distributed in the middle. During 2008-2018, cropland gradually expanded towards the south of Naiman Banner, and grassland

http://www.aloki.hu ● ISSN 1589 1623 (Print) ● ISSN 1785 0037 (Online)
DOI: http://dx.doi.org/10.15666/aeer/2005_44774488

shrunk in the south, middle and north. The transitions to grassland and construction land were mainly concentrated in the south and north. The water body transition occurred in the middle of the study area.

Table 3. *Land use transitions from 2002 to 2008 (km^2)*

2002	2008					
	Cropland	**Forest land**	**Grassland**	**Water body**	**Construction land**	**Sandy land**
Cropland	2717.05	355.84	193.57	10.31	14.83	0.32
Forest land	386.73	583.41	75.22	2.70	13.15	0.19
Grassland	418.06	101.24	2606.47	4.26	9.14	100.93
Water body	32.55	4.38	7.14	64.55	0.04	0.07
Construction land	5.21	1.59	1.45	0.01	26.04	-
Sandy land	0.94	0.76	125.37	0.18	0.95	236.27

Table 4. *Land use transitions from 2008 to 2018 (km^2)*

2008	2018					
	Cropland	**Forest land**	**Grassland**	**Water body**	**Construction land**	**Sandy land**
Cropland	3008.21	329.50	126.85	12.27	83.60	0.15
Forest land	436.49	469.17	64.21	2.46	74.62	0.24
Grassland	389.25	81.03	2447.90	6.99	34.51	49.53
Water body	36.40	2.45	2.80	40.01	0.32	0.04
Construction land	7.54	1.44	0.53	0.15	54.50	-
Sandy land	0.60	0.49	109.13	0.07	1.83	225.67

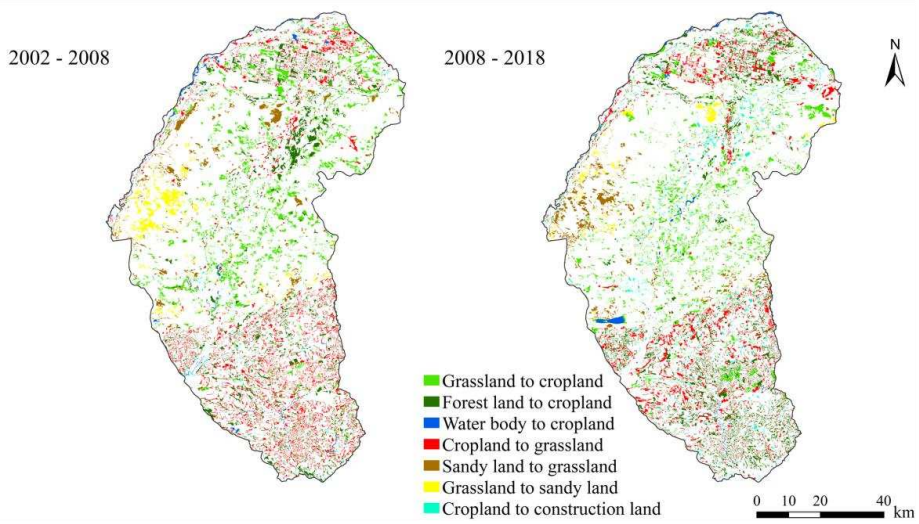

Figure 4. *Spatial change of land use transitions*

Landscape pattern changes

At the class level, the number of patches (NP) of forest land was the highest, and that of the water body was the lowest (*Fig. 5*). The NP of construction land increased, while

http://www.aloki.hu ● ISSN 1589 1623 (Print) ● ISSN 1785 0037 (Online)
DOI: http://dx.doi.org/10.15666/aeer/2005_44774488

that of forest land, grassland and sandy land decreased from 2002 to 2018. The NP of construction land drastically increased from 108 in 2002 to 571 in 2018. The mean patch size (MPS) of grassland was the highest, while that of the construction land was the lowest. Except for forest land and water body, the MPS of cropland, grassland, construction land and sandy land increased from 2002 to 2018. The largest patch index (LPI) of cropland was the largest, and that of water body the lowest. The LPI of cropland increased from 21.87% to 24.64% during 2002-2018, and that of construction land increased from 0.10% to 0.36%. In contrast, the LPI of grassland decreased by 4.95%. Except for the cropland and water body, the interspersion and juxtaposition index (IJI) of forest land, grassland and construction land decreased from 2002 to 2018.

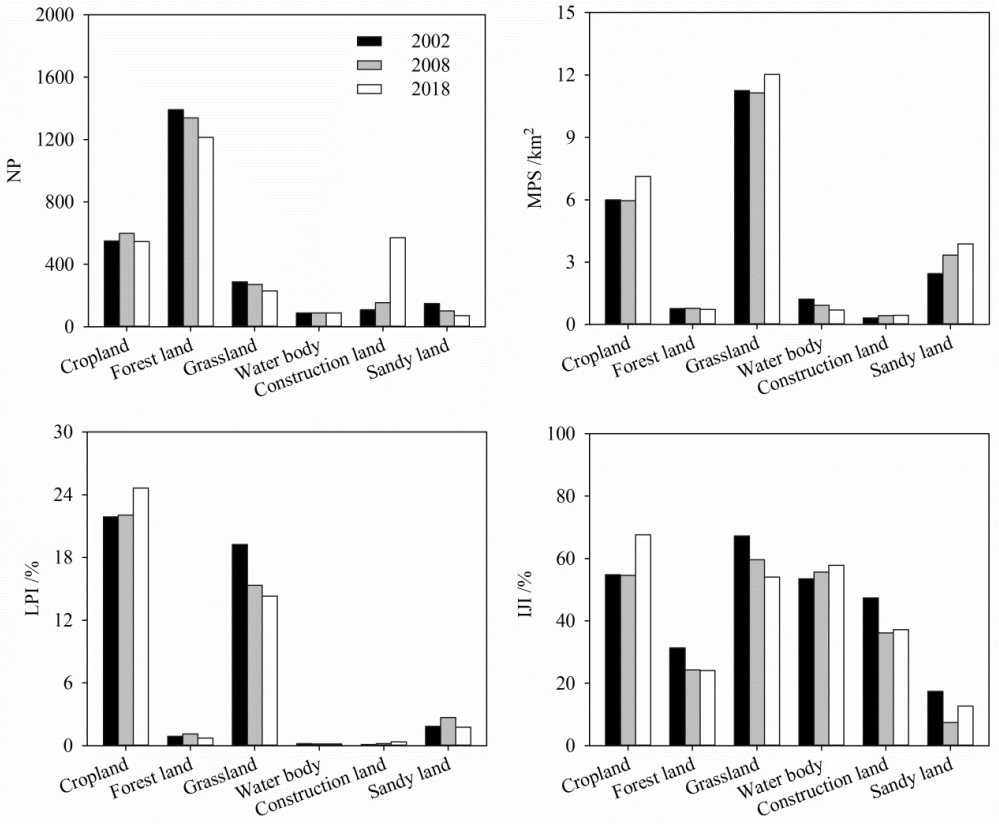

Figure 5. *Landscape pattern metrics of different land use types*

At the landscape level, the NP slightly decreased during 2002-2008 and then increased by 171 during 2008-2018 (*Table 5*). The LPI increased from 21.87% in 2002 to 22.06% in 2008 and to 24.64% in 2018. The IJI decreased from 52.53% in 2002 to 49.08% in 2008 and increased from 49.08% in 2008 to 55.83% in 2018. Shannon's diversity index (SHDI) changed a little during 2002-2018.

Table 5. *Landscape level metrics in Naiman Banner*

Year	NP	LPI	IJI	SHDI
2002	2576	21.87	52.53	1.22
2008	2548	22.06	49.08	1.21
2018	2719	24.64	55.83	1.22

http://www.aloki.hu ● ISSN 1589 1623 (Print) ● ISSN 1785 0037 (Online)
DOI: http://dx.doi.org/10.15666/aeer/2005_44774488

Discussion

The major land use change was characterized by the rapidly expansion of cropland and construction land during 2002-2018. In particular, the area of cropland expanded from the north to south in Naiman Banner of Horqin sandy land. The agricultural expansion was mainly attributed to population growth and farmers pursuing economic interests in Horqin sandy land (Li et al., 2017). This result is in line with the previous study showing that cropland increased from 2074.93 km^2 in 1975 to 3314.42 km^2 in 2005 in Naiman Banner (Zhang et al., 2009). Moreover, the previous study also identified the loss of grassland was mainly the result of cropland expansion during 1975-2005. In contrast, we observed forest land and grassland were mainly occupied by cropland during 2002-2018. These results reflected that the pattern of cropland expansion significantly changed. Forest land and grassland were reclaimed first in the study area because their soil fertility was higher than that of cropland (Liu and Zhao, 2010). In addition, forest land and grassland near cropland were susceptible to agricultural reclamation activities. Therefore, the phenomenon of expanding cropland by grassland and deforestation was observed in Naiman Banner during the study period.

Agricultural land is the major consumer of water resources in Horqin sandy land (Zheng et al., 2012). In our study area, agricultural irrigation largely depends on underground water, and cropland expansion always causes excessive water use (Ainiwaer et al., 2019). The water body is largely converted to cropland in the study area, which further aggravating the water shortage. Additionally, the previous study reported that over-cultivation might cause desertification in the agro-pastoral ecotone (Zhou et al., 2017). Thus, the local government should control land reclamation, protect water resources, and minimize the impact of aimless reclamation on land degradation in this region.

Previous studies showed that build-up areas rapidly expanded in Horqin sandy land (Li et al., 2017; Yue et al., 2017). The increased area and mean patch size of construction land indicated its expansion in our study area. The expansion rate of construction land changed differently during the 2002-2008 and 2008-2018 periods. The area of construction land expanded quickly during 2008-2018, reflecting the periodic characteristics of urban development in the study area. The result was similar to the previous study where the urban development speed in Dalate Banner, Inner Mongolia, differed during two periods (Chang et al., 2007). Population growth associated with socioeconomic development accelerated urban development in Horqin sandy land (Yue et al., 2017), resulting in new construction land.

At the landscape level, we observed a rather fragmented landscape in Naiman Banner. This could be explained by the significant increase in the number of patches of construction land. It reflected that human activities played an important role in influencing landscape fragmentation in the study area, chiming with many previous studies (Fan and Ding, 2016; Hou and Gao, 2020). An increase in the largest patch index at the landscape level was mainly due to the significant expansion of cropland in our study area. It was because the increase of cropland in the largest patch index was the biggest during the study period. The small patches of cropland merged into large patches during agricultural development, decreasing the NP of cropland. A similar landscape pattern was also observed in the agro-pastoral ecotone of northern China (Zhou et al., 2017).

Among socio-economic factors, previous studies have reported that agricultural expansion and residential development were caused by regional population growth

http://www.aloki.hu ● ISSN 1589 1623 (Print) ● ISSN 1785 0037 (Online)
DOI: http://dx.doi.org/10.15666/aeer/2005_44774488

(Japelaghi et al., 2019). In our study, the number of populations significantly increased from 2002 to 2018 (*Fig. 6*), which was one of the most important factors causing the land use changes in Naiman Banner. In particular, more food and dwelling area were needed with the growth of populations (Ge et al., 2016; Japelaghi et al., 2019), which further causing land reclamation in the study area. Although grassland reclamation can bring economic benefit, it also can lead to land degradation due to soil erosion. Except for population growth, land use changes were also attributed to the regional environmental protection policies and ecological restoration projects (Li et al., 2017). The main anti-desertification projects implemented in this area, included the Three-North Shelterbelt Project started in 1978, the Grain for Green Project started in 2002, and the Beijing-Tianjin Sandstorm Source Control Project during 2001-2010 (Duan et al., 2014; Li et al., 2017). In recent years, the local government has been controlling the number of livestock which significantly decreased during 2009-2018 (*Fig. 6*). The grazing exclusion policy was carried out, which further reduced the vegetation destruction in Horqin sandy land (Miao et al., 2015). The straw checkerboard barriers in sandy land lightened soil erosion and promoted the recovery of degraded sandy land in the study area. The area of sandy land in the study area was reduced and mainly transformed into grassland, which is consistent with the results of previous studies (Duan et al., 2014; Wang et al., 2017).

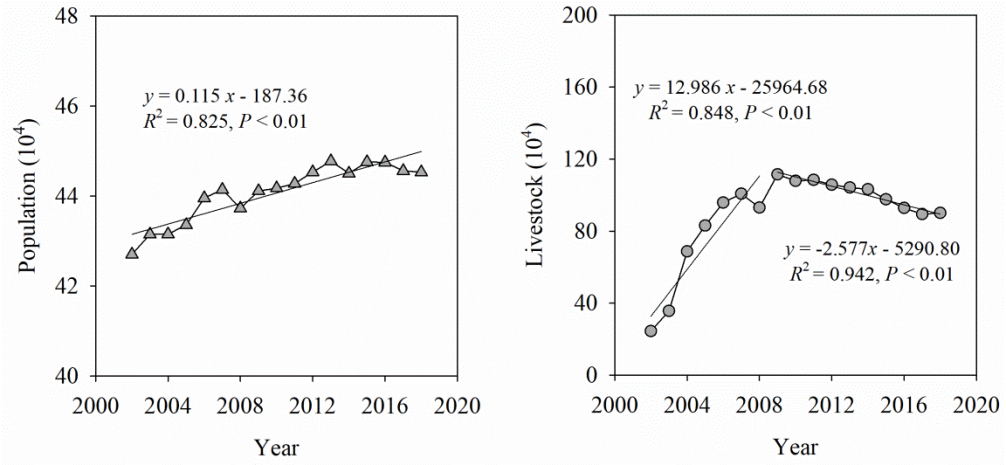

Figure 6. *Changes of population and the number of livestock in Naiman Banner from 2002 to 2018*

Conclusion

The land use changes in Naiman Banner of Horqin sandy land, China, was dramatic from 2002 to 2018. The analysis of LUCC showed that the rapid expansion of cropland was mainly at the expense of grassland and forest land, and the increases in the area of construction land was mainly at the cost of cropland and forest land during the last 16 years. Land use changes affected the composition and configuration of landscape in this study. During the study, the increase in the largest patch index and mean patch size of cropland revealed the overdevelopment of agriculture. Population growth resulted in agricultural reclamation and construction land expansion led to land use conversions, affecting the landscape patterns of Naiman Banner. The decision-makers should protect grassland and forest land and mitigate the negative effects of agricultural reclamation on

http://www.aloki.hu ● ISSN 1589 1623 (Print) ● ISSN 1785 0037 (Online)
DOI: http://dx.doi.org/10.15666/aeer/2005_44774488

the ecological environment in Horqin sandy land. Sustainable land management approaches and conservation policies may contribute to solving regional ecological problems, especially land degradation.

Acknowledgements. This study was supported by the National Natural Science Foundation of China (41271193) and Doctor Program of Binzhou University (2018Y23). The authors thank all the members of Naiman Desertification Research Station, Chinese Academy of Sciences (CAS), for their assistance in the field.

REFERENCES

[1] Ainiwaer, M., Ding, J., Wang, J., Nasierding, N. (2019): Spatiotemporal dynamics of water table depth associated with changing agricultural land use in an arid zone oasis. – Water 11: 673.

[2] Alawamy, J. S., Balasundram, S. K., Hanif, A. H. M., Sung, C. T. B. (2020): Detecting and analyzing land use and land cover changes in the region of Al-Jabal Al-Akhdar, Libya using time-series landsat data from 1985 to 2017. – Sustainability 12: 1-24.

[3] Ansari, A., Golabi, M. H. (2019): Prediction of spatial land use changes based on LCM in a GIS environment for desert wetlands - a case study: Meighan wetland, Iran. – International Soil and Water Conservation Research 7: 64-70.

[4] Bagaria, P., Nandy, S., Mitra, D., Sivakumar, K. (2021): Monitoring and predicting regional land use and land cover changes in an estuarine landscape of India. – Environmental Monitoring and Assessment 193: 124.

[5] Chang, X., Chen, Y., Cui, B. (2007): Urbanization progress influence upon regional desertification process in semi-arid zone. – Arid Land Geography 30: 321-327.

[6] Dadashpoor, H., Azizi, P., Moghadasi, M. (2019): Land use change, urbanization, and change in landscape pattern in a metropolitan area. – Science of The Total Environment 655: 707-719.

[7] Daniela, R., Marco, V. (2017): Land use and landscape pattern changes driven by land reclamation in a coastal area: the case of Volturno delta plain, Campania region, southern Italy. – Environmental Earth Sciences 76: 694.

[8] Dawelbait, M., Morari, F. (2012): Monitoring desertification in a Savannah region in Sudan using landsat images and spectral mixture analysis. – Journal of Arid Environments 80: 45-55.

[9] Deus, R. F., Tenedório, J. A. (2021): Coastal land-use and land-cover change trajectories: are they sustainable? – Sustainability 13: 8840.

[10] Duan, H., Wang, T., Xue, X., Liu, S., Guo, J. (2014): Dynamics of aeolian desertification and its driving forces in the Horqin sandy land, northern China. – Environmental Monitoring and Assessment 186: 6083-6096.

[11] Duan, H., Wang, T., Xue, X., Yan, C. (2019): Dynamic monitoring of aeolian desertification based on multiple indicators in Horqin sandy land, China. – Science of The Total Environment 650: 2374-2388.

[12] Fan, Q., Ding, S. (2016): Landscape pattern changes at a county scale: a case study in Fengqiu, Henan province, China from 1990 to 2013. – Catena 137: 152-160.

[13] Ge, X., Dong, K., Luloff, A. E., Wang, L., Xiao, J. (2016): Impact of land use intensity on sandy desertification: an evidence from Horqin sandy land, China. – Ecological Indicators 61: 346-358.

[14] Guo, B., Zang, W., Han, B., Yang, F., Luo, W., He, T., Fan, Y., Yang, X., Chen, S. (2020): Dynamic monitoring of desertification in Naiman Banner based on feature space models with typical surface parameters derived from landsat images. – Land Degradation & Development 31: 1573-1592.

http://www.aloki.hu ● ISSN 1589 1623 (Print) ● ISSN 1785 0037 (Online)
DOI: http://dx.doi.org/10.15666/aeer/2005_44774488

[15] Hirche, A., Salamani, M., Abdellaoui, A., Benhouhou, S., Valderrama, J. M. (2011): Landscape changes of desertification in arid areas: the case of south-west Algeria. – Environmental Monitoring and Assessment 179: 403-420.
[16] Hou, W., Gao, J. (2020): Spatially variable relationships between karst landscape pattern and vegetation activities. – Remote Sensing 12: 1134.
[17] Inalpulat, M., Genc, L. (2021): Quantification of LULC changes and urbanization effects on agriculture using historical landsat data in North-west Anatolia, Turkey. – Polish Journal of Environmental Studies 30: 3999-4007.
[18] Japelaghi, M., Gholamalifard, M., Shayesteh, K. (2019): Spatio-temporal analysis and prediction of landscape patterns and change processes in the central Zagros region, Iran. – Remote Sensing Applications: Society and Environment 15: 100244.
[19] Jiang, D., Miao, R., Toshio, O., Zhou, Q. (2013): Effects of fence enclosure on vegetation restoration and soil properties in Horqin sandy land. – Ecology and Environmental Sciences 22: 40-46.
[20] Lamine, S., Petropoulos, G. P., Singh, S. K., Szabó, S., Bachari, N. E. I., Srivastava, P. K., Suman, S. (2018): Quantifying land use/land cover spatio-temporal landscape pattern dynamics from hyperion using SVMs classifier and FRAGSTATS®. – Geocarto International 33: 862-878.
[21] Li, J., Xu, B., Yang, X., Qin, Z., Zhao, L., Jin, Y., Zhao, F., Guo, J. (2017): Historical grassland desertification changes in the Horqin sandy land, northern China (1985-2013). – Scientific Reports 7: 3009-3021.
[22] Liang, P., Yang, X. (2016): Landscape spatial patterns in the Maowusu (Mu Us) sandy land, northern China and their impact factors. – Catena 145: 321-333.
[23] Lin, W., Cen, J., Xu, D., Du, S., Gao, J. (2018): Wetland landscape pattern changes over a period of rapid development (1985–2015) in the ZhouShan Islands of Zhejiang province, China. – Estuarine, Coastal and Shelf Science 213: 148-159.
[24] Liu, R., Zhao, H. (2010): Effect of land use changes on soil properties in Horqin sandy land. – Ecology and Environmental Sciences 19: 2079-2084.
[25] Liu, C., Zhang, F., Carl Johnson, V., Duan, P., Kung, H.-T. (2021): Spatio-temporal variation of oasis landscape pattern in arid area: human or natural driving? – Ecological Indicators 125: 107495.
[26] Miao, R., Jiang, D., Musa, A., Zhou, Q., Guo, M., Wang, Y. (2015): Effectiveness of shrub planting and grazing exclusion on degraded sandy grassland restoration in Horqin sandy land in Inner Mongolia. – Ecological Engineering 74: 164-173.
[27] Minta, M., Kibret, K., Thorne, P., Nigussie, T., Nigatu, L. (2018): Land use and land cover dynamics in Dendi-Jeldu hilly-mountainous areas in the central Ethiopian highlands. – Geoderma 314: 27-36.
[28] Mohamed, M., Anders, J., Schneider, C. (2020): Monitoring of land use/land cover in Syria from 2010 to 2018 using multitemporal landsat imagery and GIS. – Land 9: 226.
[29] Obeidat, M., Awawdeh, M., Lababneh, A. (2019): Assessment of land use/land cover change and its environmental impacts using remote sensing and GIS techniques, Yarmouk river basin, north Jordan. – Arabian Journal of Geosciences 12: 685.
[30] Wan, L., Zhang, Y., Zhang, X., Qi, S., Na, X. (2015): Comparison of land use/land cover change and landscape patterns in Honghe national nature reserve and the surrounding Jiansanjiang region, China. – Ecological Indicators 51: 205-214.
[31] Wang, Y., Zhang, J., Tong, S., Guo, E. (2017): Monitoring the trends of aeolian desertified lands based on time-series remote sensing data in the Horqin sandy land, China. – Catena 157: 286-298.
[32] Wang, L. T., Wang, S. X., Zhou, Y., Zhu, J. F., Zhang, J. Z., Hou, Y. F., Liu, W. L. (2020): Landscape pattern variation, protection measures, and land use/land cover changes in drinking water source protection areas: a case study in Danjiangkou reservoir, China. – Global Ecology and Conservation 21: e00827.

http://www.aloki.hu ● ISSN 1589 1623 (Print) ● ISSN 1785 0037 (Online)
DOI: http://dx.doi.org/10.15666/aeer/2005_44774488

[33] Wu, J. (2013): Key concepts and research topics in landscape ecology revisited: 30 years after the Allerton Park workshop. – Landscape Ecology 28: 1-11.
[34] Yu, X., Ng, C. (2008): An integrated evaluation of landscape change using remote sensing and landscape metrics: a case study of Panyu, Guangzhou. – International Journal of Remote Sensing 27: 1075-1092.
[35] Yuan, J., Ouyang, Z., Zheng, H., Xu, W. (2012): Effects of different grassland restoration approaches on soil properties in the southeastern Horqin sandy land, northern China. – Applied Soil Ecology 61: 34-39.
[36] Yue, X., Hou, M., Chang, X., Zuo, X., Liu, L., Lv, D. (2017): Impact of urbanization process on landscapes in the Horqin sandy land. – Arid Zone Research 34: 912-920.
[37] Zhang, J., Chang, X., Cai, M., Li, J. (2009): Effects of land use on desertification in typical regions in the Horqin sandy land. – Arid Zone Research 26: 39-44.
[38] Zhang, G., Dong, J., Xiao, X., Hu, Z., Sheldon, S. (2012): Effectiveness of ecological restoration projects in Horqin sandy land, China based on spot-vgt NDVI data. – Ecological Engineering 38: 20-29.
[39] Zheng, X., Zhu, J. J., Yan, Q. L., Song, L. N. (2012): Effects of land use changes on the groundwater table and the decline of Pinus sylvestris var. Mongolica plantations in southern Horqin sandy land, northeast China. – Agricultural Water Management 109: 94-106.
[40] Zhou, Y., Chang, X., Ye, S., Zheng, Z., Lv, S. (2014): Analysis on regional vegetation changes in dust and sandstorms source area: a case study of Naiman Banner in the Horqin sandy region of northern China. – Environmental Earth Sciences 73: 2013-2025.
[41] Zhou, J., Zhang, F., Xu, Y., Gao, Y., Xie, Z. (2017): Evaluation of land reclamation and implications of ecological restoration for agro-pastoral ecotone: case study of Horqin Left Back Banner in China. – Chinese Geographical Science 27: 772-783.
[42] Zuo, X. A., Yue, X. Y., Lv, P., Yu, Q., Chen, M., Zhang, J., Luo, Y., Wang, S., Zhang, J. (2017): Contrasting effects of plant inter- and intraspecific variation on community trait responses to restoration of a sandy grassland ecosystem. – Ecology and Evolution 7: 1125-1134.

http://www.aloki.hu ● ISSN 1589 1623 (Print) ● ISSN 1785 0037 (Online)
DOI: http://dx.doi.org/10.15666/aeer/2005_44774488

DISTRIBUTION OF CLIMATIC SUITABILITY OF *PELLIONIA SCABRA* BENTH. (*URTICACEAE*) IN CHINA

CHEN, T.[1] – ACMA, F. M.[1] – AMOROSO, V. B.[1] – MEDECILO GUIANG, M. M.[1*] – HUANG, B.[2*]

[1]*Department of Biology, Central Mindanao University, University Town, Musuan 8714, Maramag, Bukidnon, Philippines*

[2]*School of Pharmaceutical Sciences, Hunan University of Medicine, Huaihua, Hunan 418000, China*

**Corresponding authors*
e-mail: f.mariamelanie.guiang@cmu.edu.ph; huangbinsg@163.com

(Received 11th May 2022; accepted 26th Jul 2022)

Abstract. *Pellionia scabra* Benth. (PSB), a traditional Chinese medicinal plant, is widely used as folk treatment for rheumatic diseases. Assessing the impact of climate change on habitat suitability is critical for PSB resource utilization and ecological conservation. In this study, the maximum entropy model (MaxEnt) and the Geographic Information System (ARCGIS) were applied to predict the distribution of PSB, and the contribution of variables was evaluated using Jackknife test. The area under the receiver operating characteristic curve (AUC) of the PSB geographic distribution model reached a very good standard, indicating that the model prediction results can be used in this study. The potential distribution of PSB was mainly in Guangxi, Guangdong, Fujian, Hunan, Jiangxi, Zhejiang, Taiwan, Chongqing, Guizhou, southeast of Sichuan, southwest of Hubei, and south of Anhui (adaptability index > 0.5). The comprehensive analysis of the contribution rate of climatic factors and jackknife experiment showed that the precipitation of driest quarter (35.4%), precipitation of driest month (25.0%), annual precipitation (11.4%), mean diurnal range (7.9%) and precipitation of wettest quarter (3.9%) were the most important factors affecting the potential distribution of PSB.
Keywords: *Maxent, ARCGIS, climate change, geographic information system, traditional Chinese medicine, Jackknife test*

Introduction

Pellionia scabra Benth. (PSB) is plant species under the family Urticaceae. *P. scabra* is also known as alias rock amaranth (Hunan) and *Pellionia scabra* (Taiwan) (Liu, 2001; Yang et al., 1996). It is widely distributed in south China, southwest China, central China, east China, Taiwan China, Vietnam and Japan and is found at 300-1200 m above sea level (Wang et al., 2013). In the Chinese folk, this species is mainly used for the treatment of eye red swelling and pain, toothache, contusion sore furuncle swelling and pain, burns and scald, snake bites, trauma bleeding and other diseases (Wang et al., 2013). In recent years, PSB has been clinically used to treat patients with coronary heart disease and further found to have a good effect on the treatment of patients with hyperlipidemia (Zhu et al., 1994). Due to the important medicinal properties of this species, the wild resources of PSB have been greatly depleted, and the natural habitat of these plants may be gradually reduced due to climate change. Most previous studies have focused on its taxonomy (Lin et al., 2002), while others have focused on its chemical and nutritional composition (Wang et al., 2013; Zhu et al., 1994). However, so far, there has been little ecological research on the conservation and utilization of PSB resources.

In recent years, with the great promotion of ecological restoration, more stakeholders have begun to pay attention to the utilization and planting of species resources.

http://www.aloki.hu ● ISSN 1589 1623 (Print) ● ISSN 1785 0037 (Online)
DOI: http://dx.doi.org/10.15666/aeer/2005_44894498

Therefore, the research on the potential distribution and prediction of species resources has become necessary. The working principle of MaxEnt model is to determine the ecological niche occupied by species based on the known distribution information and ecological environmental factor variables, to predict the potential geographical distribution model of species (Ye et al., 2021; Song et al., 2020; Ji et al., 2021). Compared with Climax, Garp, Bioclim, Domain and other models, MaxEnt is the most widely used software to predict the potential distribution of species. At the same time, combined with the calibration, reclassification, modeling, and display functions of Arcgis, the ecological suitability map of species can make the potential geographical distribution of species more accurate, intuitive and specific (Zhang et al., 2021a; Zhuo et al., 2020; Wang et al., 2019; Li et al., 2022).

This study combines the MaxEnt model and Arcgis software to evaluate the suitable distribution areas of PSB under different climatic conditions. The objectives of the study were to (1) investigate the important climatic factors affecting the distribution of PSB; (2) analyse the data calculated by MaxEnt model in combination with ArcGIS10.5 analysis and mapping functions, and to comprehensively evaluate the suitable distribution areas of PSB in China. The results of the study can provide reference for the exploitation and utilization of PSB as traditional Chinese medicine and environmental resource management.

Materials and methods

Species data source

The distribution information of *P. scabra* was obtained from the Chinese Virtual Herbarium (http://www.cvh.ac.cn), the China National Nature Reserve Specimen Resource Sharing Platform (http://www.papc.cn/), and the field survey (*Fig. 1*), excluding the repeated longitude and latitude coordinates. A total of 67 PSB distribution information were collected, as shown in *Figure 2*. The data is divided into three columns by species name, longitude, and latitude, and stored in ".csv" format.

Climatic factor data

Climatic factors data from Worldclim website (https://www.worldclim.org/data/index.html), which mainly includes BIO1 (Annual Mean Temperature), BIO2 (Mean Diurnal Range), BIO3 (Isothermality), BIO4 (Temperature Seasonality), BIO5 (Max Temperature of Warmest Month), BIO6 (Min Temperature of Coldest Month), BIO7 (Temperature Annual Range), BIO8 (Mean Temperature of Wettest Quarter), BIO9 (Mean Temperature of Driest Quarter), BIO10 (Mean Temperature of Warmest Quarter), BIO11 (Mean Temperature of Coldest Quarter), BIO12 (Annual Precipitation), BIO13 (Precipitation of Wettest Month), BIO14 (Precipitation of Driest Month), BIO15 (Precipitation Seasonality), BIO16 (Precipitation of Wettest Quarter), BIO17 (Precipitation of Driest Quarter), BIO18 (Precipitation of Warmest Quarter), BIO19 (Precipitation of Coldest Quarter) were accessed which has a total of 19 comprehensive climatic factors were included in the study. The above 19 comprehensive climate factor data were imported into ArcMap10.5 and stored in ".asc" format with the Species Distribution Model (SDM) Toolbox. The vector maps of administrative departments and provincial boundaries in China were used for basic map analysis by the National basic geographic information system, and the suitability distribution maps of species were generated by ArcMap10.5.

http://www.aloki.hu ● ISSN 1589 1623 (Print) ● ISSN 1785 0037 (Online)
DOI: http://dx.doi.org/10.15666/aeer/2005_44894498

Figure 1. *Pellionia scabra Benth. collected in the wild*

Figure 2. *Distribution map of Pellionia scabra Benth*

Maximum entropy model

The ".csv" format of PSB distribution and 19 integrated climatic factors data were imported into MaxEnt3.3.3. 25% species distribution points were set as the test date, and the remaining 75% was the training date. The maximum number of iterations was 10^6, and the model operation was repeated 10 times. According to the response curve, receiver-operating characteristic (ROC) and area under the receiver operating characteristic curve (AUC) were used to test the accuracy of MaxEnt model prediction results, jackknife method was used to test the weight, and other parameters were default software values.

http://www.aloki.hu ● ISSN 1589 1623 (Print) ● ISSN 1785 0037 (Online)
DOI: http://dx.doi.org/10.15666/aeer/2005_44894498

Reliability and accuracy analysis

ROC curve is a highly recognized indicator for predicting and evaluating the potential distribution of species. AUC value is the area value under the ROC curve, which is used to evaluate the fitting degree of the model in species distribution prediction. When the AUC value ranges from 0.9 to 1, the model performance was excellent, 0.8–0.9 was very good, 0.7–0.8 was good, 0.6–0.7 was fair and 0.5–0.6 was poor.

Screening of climatic factors

The distribution prediction results of MaxEnt simulation were imported into ArcMap for superposition operation, and the PSB climatic suitability zoning map based on dominant factors was drawn. According to the concept of ecological similarity and the reclassification function of ArcMap, manual classification was carried out, and finally four grade regions were divided, including high suitability area (≥50%), medium suitability area (30%-50%), low suitability area (10%-30%) and non-suitability area (≤10%).

Results

Accuracy evaluation

The prediction accuracy of the model is measured by value of AUC, which ranges from 0 to 1. The value of AUC is proportional to the strength of the model's judgment ability. The average training data of ROC curve of MaxEnt model is 0.976, greater than 0.9, and tends to 1, indicating that the PSB growth environment suitability calculated by MaxEnt model has high accuracy and reliability. As shown in *Figure 3*.

Figure 3. *ROC curve of Maxent model for Pellionia scabra Benth.*

http://www.aloki.hu ● ISSN 1589 1623 (Print) ● ISSN 1785 0037 (Online)
DOI: http://dx.doi.org/10.15666/aeer/2005_44894498

Main climatic factors

Climatic factors are the key to the quality formation of medicinal plants, and their selection will affect the accuracy prediction of the model. A total of 19 climatic factors were established in this model. After 10 calculations of MaxEnt model, there were 16 climatic factors with contribution rate remaining, and 9 climatic factors with contribution rate > 1% were selected for analysis. The total contribution rate of nine climatic factors was 96.7%, including precipitation of driest quarter (bio17), precipitation of driest month (bio14), annual precipitation (bio12), mean diurnal range (bio2), mean temperature (bio10), precipitation of wettest quarter (bio16), mean temperature of wettest quarter (bio8), temperature seasonality (bio4) and isothermality (bio3). The results are shown in *Table 1*. As can be seen from the jackknife analyses (*Fig. 4*), the weight order of each climatic factor on PSB distribution is as follows: precipitation of driest quarter (bio17), precipitation of driest month (bio14), annual precipitation (bio12), precipitation of coldest quarter (bio19), mean diurnal range (bio2), precipitation of wettest quarter (bio16), precipitation of wettest month (bio13), temperature annual range (bio7), precipitation of warmest quarter (bio18), min temperature of coldest month (bio6), mean temperature of driest quarter (bio9), annual mean temperature (bio1), Mean temperature of coldest quarter (bio11). After comprehensive analysis of the contribution rate of climatic factors and the results of jackknife analyses, the intersection part of climatic factors is taken. The influencing factors were precipitation of driest quarter (35.4%), precipitation of driest month (25.0%), annual precipitation (11.4%), mean diurnal range (7.9%) and precipitation of wettest quarter (3.9%). The cumulative contribution rate was 83.6%, and they were the main climatic factors affecting PSB suitability.

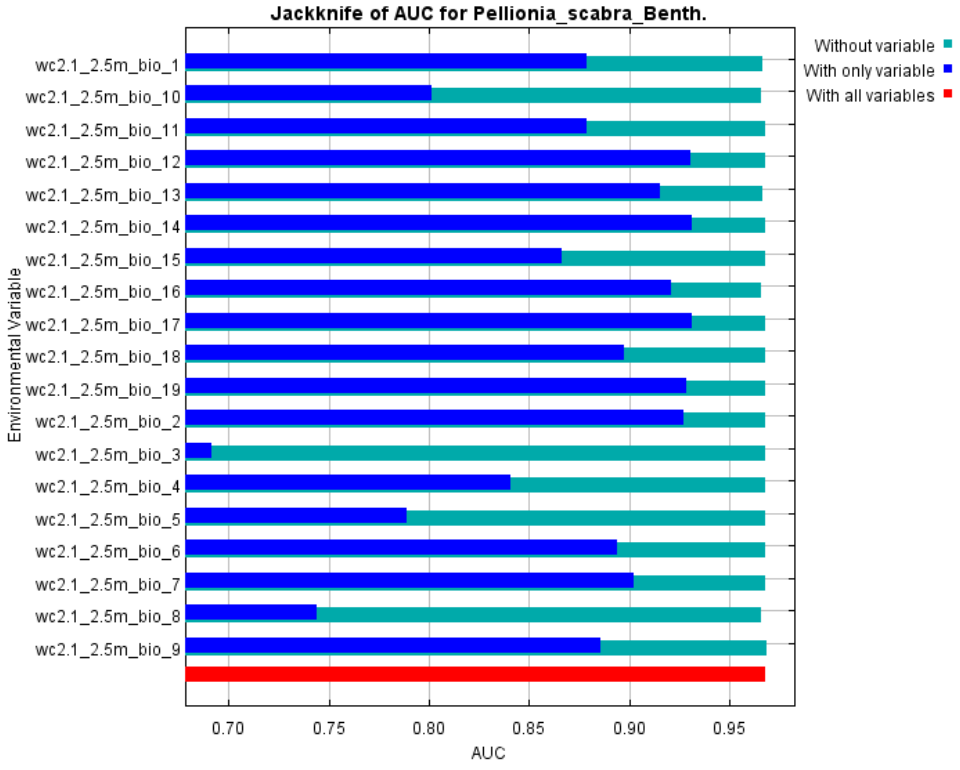

Figure 4. *Results of the jackknife test of variables' contribution in modelling potentive distribution of Pellionia scabra Benth.*

http://www.aloki.hu ● ISSN 1589 1623 (Print) ● ISSN 1785 0037 (Online)
DOI: http://dx.doi.org/10.15666/aeer/2005_44894498

Table 1. *Climatic factors affecting the distribution of Pellionia scabra Benth.*

Factors	Name	Percent contribution (%)
bio17	Precipitation of driest quarter	35.4
bio14	Precipitation of driest month	25.0
bio12	Annual precipitation	11.4
bio2	Mean diurnal range (mean of monthly (max temp - min temp))	7.9
bio10	Mean temperature	7.1
bio16	Precipitation of wettest quarter	3.9
bio8	Mean temperature of wettest quarter	3.6
bio4	Temperature seasonality (standard deviation ×100)	1.6
bio3	Isothermality (bio2/bio7) (×100)	1.1

Climatic suitability zoning

The results of MaxEnt model operation were imported into ArcGIS10.5 software to obtain the climatic suitability of PSB, as shown in *Figure 5*. As can be seen from *Figure 5*, the distribution of PSB is mainly concentrated in the south of the Yangtze River, and the most suitable distribution areas include Guangxi, Guangdong, Fujian, Hunan, Jiangxi, Zhejiang, Taiwan, Chongqing, Guizhou, southeast of Sichuan, southwest of Hubei, and south of Anhui (*Table 2*).

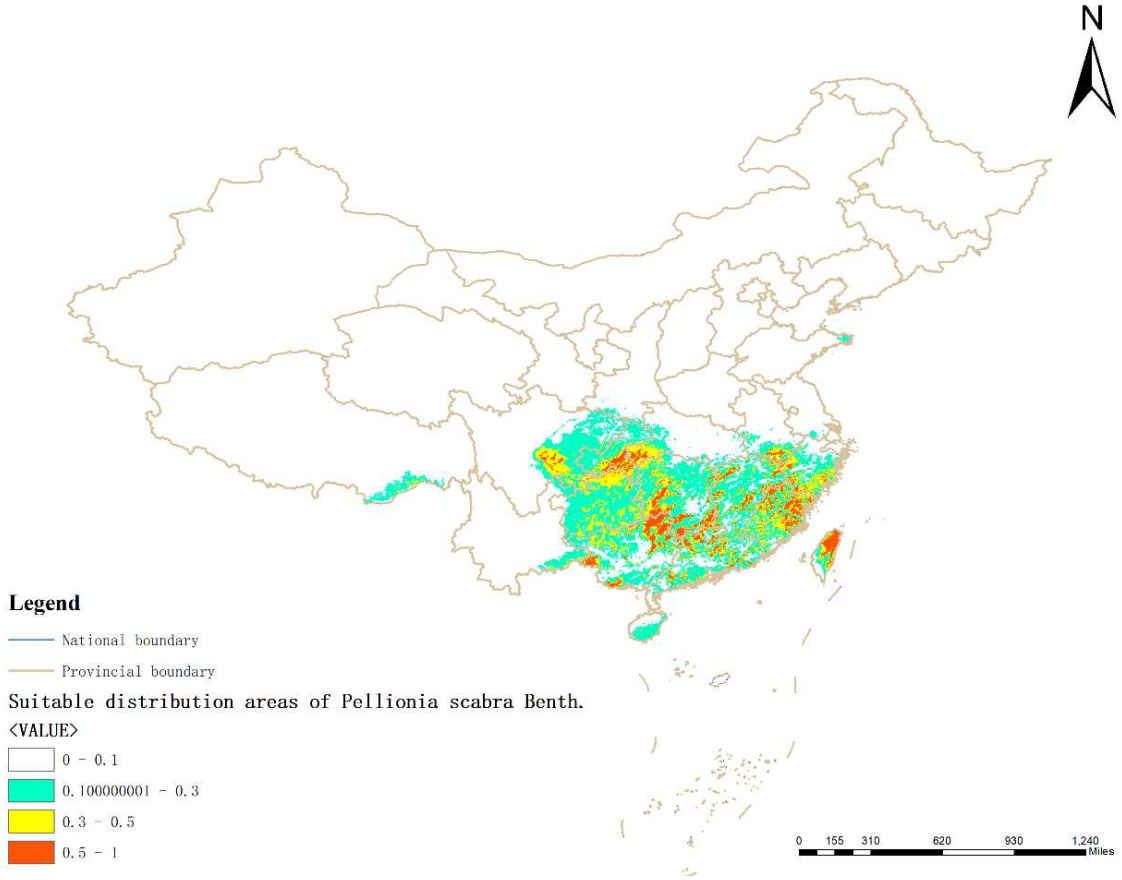

Figure 5. *Pellionia scabra Benth. climatic suitability distribution area*

http://www.aloki.hu ● ISSN 1589 1623 (Print) ● ISSN 1785 0037 (Online)
DOI: http://dx.doi.org/10.15666/aeer/2005_44894498

Table 2. *Climatic suitability distribution area of Pellionia scabra Benth. in China*

Province	Climatic suitability distribution area
Guangxi	Guilin, Liuzhou, Baise, Chongzuo, Fangchenggang, Hezhou, Guigang, Yulin, Laibin, Hechi, Nanning
Guangdong	Shaoguan, Qingyuan, Zhaoqing, Heyuan, Maoming, Yangjiang, Jiangmen, Chaozhou, Shantou, Jieyang, Shanwei, Huizhou, Meizhou, Shenzhen, Dongguan
Fujian	Ningde, Nanping, Fuzhou, Shanming, Putian, Zhangzhou, Longyan, Quanzhou
Hunan	Yueyang, Zhuzhou, Chenzhou, Yongzhou, Hengyang, Huaihua, Jishou, Zhangjiajie, Shaoyang, Changde
Jiangxi	Jiujiang, Shangrao, Jingdezhen, Pingxiang, Yichun, Ganzhou, Fuzhou, Yingtan
Zhejiang	Hangzhou, Quzhou, Lishui, Wenzhou, Taizhou, Ningbo
Taiwan	Keelung, Taipeh, Ilan, Taoyuan, Hsinchu, Miaoli, Taichung, Nantou, Hualien,
Chongqing	Qianjiang, Youyang, Xiushan, Shizhu, Fengdu, Fuling, Nanchuan, Jiangjin, Wansheng, Qijiang, Pengshui, Wulong
Sichuan	Luzhou, Yibin, Neijiang, Leshan, Meishan, Ziyang, Yaan, Chengdu
Hubei	Enshi
Guizhou	Zunyi, Tongren, Qiandongnan
Anhui	Chizhou, Xuancheng, Huangshan

Discussion

MaxEnt model can find the maximum entropy of species distribution rule through incomplete information of species distribution (Phillips et al., 2006; Zhang et al., 2021b; Shogren et al., 2020), so as to predict the existence probability of species and determine the distribution area of species. In general, the sample quantity and sample on the space distribution of the directly related to the accuracy of the model prediction results and reliability (Cao et al., 2021), the more sample size model prediction results more accurate, but studies show MaxEnt model rules of procedure in the small sample size in the process of the simulation can offset excessive fitting trend (Zhao et al., 2018; Xu et al., 2022; Li et al., 2020), showing the predictions of a high quality. In this study, MaxEnt model was used to analyse the 67 distribution points of PSB, 25% of which were the test date and the remaining 75% were the training date. The adoption of the above approach was mainly based on a large number of literature studies (Cao et al., 2021; Xu et al., 2022; Zhan et al., 2022; Shi et al., 2021), which yielded conclusions with a high degree of accuracy and feasibility. Furthermore, the area under the subject operating characteristic (ROC) curve (AUC) provides a further measure of the accuracy of the model predictions. The accuracy test of the ROC curve shows that the AUC value is higher than 0.9, indicating that the model has a good prediction effect on PSB distribution area and has high reliability (Kottas et al., 2014). The jackknife experiment of MaxEnt model and the analysis of the response curve of climatic factors showed that precipitation (precipitation of driest quarter, precipitation of driest month, annual precipitation, Precipitation of Wettest Quarter) and temperature (mean diurnal range) are the main climatic factors affecting the difference of PSB's geographical spatial distribution, which is consistent with PSB preferring to live in shady places and near small streams.

ArcGIS analysis shows that PSB is mainly distributed in the Yangtze River basin and the provinces south of the Yangtze River, including Guangxi, Guangdong, Guizhou,

http://www.aloki.hu ● ISSN 1589 1623 (Print) ● ISSN 1785 0037 (Online)
DOI: http://dx.doi.org/10.15666/aeer/2005_44894498

southeastern Sichuan, Hunan, Jiangxi, southern Anhui, Zhejiang, Fujian, and Taiwan, in agreement with the descriptions in Flora of China. However, there are still some differences between the predicted distribution area and the actual distribution area of PSB. The results show that the low suitability area of PSB is widely distributed, especially in the south and southeast of Tibet, the south and east of Jiangsu, and the east of Shandong, which is larger than the current known distribution area of PSB.

PSB is a kind of common subshrub plant, which mainly grow in the valley stream or forest, and has unique application value in water environment protection and medicine. Based on our findings, this method can be used to predict the potential distribution of other medicinal plants, providing a valuable tool for species conservation and distribution. However, there are still some aspects of this study that need improvement. First, the potential distribution area predicted by the model may overestimate the actual ecological position of the species. This is because the species may not be able to spread to potential areas due to human disturbance, topographic barriers and species competition. Secondly, ecological factors other than those selected in this study may also influence the distribution range of PSB. Finally, a combination of an appropriate increase in sample size and field surveys would make the study of PSB regionalisation more comprehensive and reasonable.

Conclusions

Based on the results and discussions presented above, the conclusions are the following:

(1) MaxEnt and Arcgis were used to model the climatic suitability of PSB, and correlation analysis was conducted on 19 climate factor variables. 5 climatic factors such as precipitation of driest quarter (bio17), precipitation of driest month (bio14), annual precipitation (bio12), mean diurnal range (bio19) and precipitation of wettest quarter (bio2), contributed more to the prediction results of PSB distribution. The cumulative contribution rate was 83.6%, and they were the main climatic factors affecting PSB suitability.

(2) PSB suitable areas in China are mainly distributed in Guangxi, Guangdong, Fujian, Hunan, Jiangxi, Taiwan, Chongqing, Guizhou. Southeast of Sichuan, Southwest of Hubei, and South of Anhui. Low suitability areas are distributed in Hainan, southern Shaanxi, southern and eastern Jiangsu, southeastern Yunnan, northeastern Sichuan, western Hunan, southern and southeastern Xizang, southwestern Anhui, and eastern Shandong.

(3) Of course, in practice, the distribution areas of plants need further field surveys. the prediction accuracy of the MaxEnt model increases with the sample size and eventually stabilises, so to improve the accuracy of the model prediction results, the sample size should be appropriately selected according to the differences of different species, and the sample size and the number of ecological factors should be appropriately increased.

Acknowledgements. This work was financially supported by the Scientific Research Foundation of Hunan Provincial Education Department (20B415), the Reform Project of Hunan Provincial Education Department (HNJG-2020-1218).

http://www.aloki.hu ● ISSN 1589 1623 (Print) ● ISSN 1785 0037 (Online)
DOI: http://dx.doi.org/10.15666/aeer/2005_44894498

REFERENCES

[1] Cao, Z., Zhang, L., Zhang, X., Guo, Z. (2021): Predicting the potential distribution of Hylomecon japonica in China under current and future climate change based on Maxent model. – Sustainability 13(20): 11253.
[2] Ji, W., Gao, G., Wei, J. (2021): Potential global distribution of Daktulosphaira vitifoliae under climate change based on MaxEnt. – Insects 12(4): 347.
[3] Kottas, M., Kuss, O., Zapf, A. (2014): A modified Wald interval for the area under the ROC curve (AUC) in diagnostic case-control studies. – BMC Medical Research Methodology 14: 26.
[4] Li, G., Huang, J., Guo, H., Du, S. (2020): Projecting species loss and turnover under climate change for 111 Chinese tree species. – Forest Ecology and Management 477: 118488.
[5] Li, Y., Shao, W., Jiang, J. (2022): Predicting the potential global distribution of Sapindus mukorossi under climate change based on MaxEnt modelling. – Environmental Science and Pollution Research International 29(15): 21751-21768.
[6] Lin, Q., Duan, L. D., Li, M. H. (2002): A new synonym of Pellionia scabra Benth. – Journal of Systematics and Evolution 40(5): 477-479.
[7] Liu, K. (2001): Flora of Hunan. – HSTP Publishing, Changsha.
[8] Phillips, S. J., Anderson, R. P., Schapire, R. E. (2006): Maximum entropy modeling of species geographic distributions. – Ecological Modelling 190(3-4): 231-259.
[9] Shi, X., Yin, Q., Sang, Z., Zhu, Z., Jia, Z., Ma, L. (2021): Prediction of potentially suitable areas for the introduction of Magnolia wufengensis under climate change. – Ecological Indicators 127: 107762.
[10] Shogren, C., Paine, T. (2020): Predicting the potential invasive range of Klambothrips myopori (Thysanopetra: Phlaeothripidae). – Journal of Economic Entomology 113(3): 1202-1210.
[11] Song, R., Ma, Y., Hu, Z., Li, Y., Li, M., Wu, L., Li, C., Dao, E., Fan, X., Hao, Y., Bayin, C. (2020): MaxEnt modeling of Dermacentor marginatus (Acari: Ixodidae) distribution in Xinjiang, China. – Journal of Medical Entomology 57(5): 1659-1667.
[12] Wang, L., Liao, W. B., Qiu, W. Z. (2013): Study on the nutrient composition of Pellionia scabra. – Acta Scientiarum Naturalium Universitatis Sunyatseni 52(6): 119-123.
[13] Wang, R., Yang, H., Luo, W., Wang, M., Lu, X., Huang, T., Zhao, J., Li, Q. (2019): Predicting the potential distribution of the Asian citrus psyllid, Diaphorina citri (Kuwayama), in China using the MaxEnt model. – PeerJ 7: e7323.
[14] Xu, W., Zhu, S., Yang, T., Cheng, J., Jin, J. (2022): Maximum entropy niche-based modeling for predicting the potential suitable habitats of a traditional medicinal plant (Rheum nanum) in Asia under climate change conditions. – Agriculture 12(5): 610.
[15] Yang, Y. P., Shih, B. L., Liu, H. Y. (1996): Flora of Taiwan. – ECFT Publishing, Taipei.
[16] Ye, P., Zhang, G., Zhao, X., Chen, H., Si, Q., Wu, J. (2021): Potential geographical distribution and environmental explanations of rare and endangered plant species through combined modeling: a case study of Northwest Yunnan, China. – Ecology and Evolution 11(19): 13052-13067.
[17] Zhan, P., Wang, F., Xia, P., Zhao, G., Wei, M., Wei, F., Han, R. (2022): Assessment of suitable cultivation region for Panax notoginseng under different climatic conditions using MaxEnt model and high-performance liquid chromatography in China. – Industrial Crops and Products 176(6): 114416.
[18] Zhang, H., Song, J., Zhao, H., Li, M., Han, W. (2021a): Predicting the distribution of the Invasive Species Leptocybe invasa: combining MaxEnt and Geodetector models. – Insects 12(2): 92.
[19] Zhang, Y., Tang, J., Ren, G., Zhao, K., Wang, X. (2021b): Global potential distribution prediction of Xanthium italicum based on Maxent model. – Scientific Reports 11(1): 16545.

http://www.aloki.hu ● ISSN 1589 1623 (Print) ● ISSN 1785 0037 (Online)
DOI: http://dx.doi.org/10.15666/aeer/2005_44894498

[20] Zhao, X. J., Gong, J. X., Zhao, S. S., Meng, H. X., Yan, B. Q., Qi, X. Y. (2018): Impact of sample size and spatial distribution on species distribution model. – Journal of Lanzhou University (Natural Sciences) 54(2): 208-215.
[21] Zhu, G. D., Qiu, C. B. (1994): Studies on the Chemical Constituents of Pellionia scabra. – Journal of Chinese Medicinal Materials 6: 33-56.
[22] Zhuo, Z., Xu, D., Pu, B., Wang, R., Ye, M. (2020): Predicting distribution of Zanthoxylum bungeanum Maxim. in China. – BMC Ecology 20(1): 46.

http://www.aloki.hu ● ISSN 1589 1623 (Print) ● ISSN 1785 0037 (Online)
DOI: http://dx.doi.org/10.15666/aeer/2005_44894498

CLIMATE CHANGE-INDUCED RANGE SHIFTS IN CHINESE ASH (*FRAXINUS CHINENSIS*) ALONG THREE GEOGRAPHICAL DIMENSIONS IN CHINA AT THE LATE 21ST CENTURY

LI, G. Q.[1*] – AN, K. L.[2] – LI, Y. R.[2]

[1]*State Key Laboratory of Soil Erosion and Dryland Farming on the Loess Plateau, Institute of Soil and Water Conservation, Northwest A&F University, Yangling, Xianyang 712100, China*

[2]*College of Forestry, Northwest A&F University, Yangling, Xianyang 712100, China*

**Corresponding author*
e-mail: liguoqing@nwsuaf.edu.cn; phone: +86-29-8701-2411; fax: +86-29-8701-2210

(Received 12th May 2022; accepted 26th Jul 2022)

Abstract. In the present study, we establish a set of indicator systems to characterize the shifts in total range and core range of Chinese ash (*Fraxinus chinensis*) at three geographical dimensions under climate change scenarios in China by the year of 2070. The results show that current core range and total range areas were 1.3×10^6 km^2 and 3.3×10^6 km^2, accounting for 13.5% and 34.4% of the land area in China. The size of core range and total range areas will increase in varying degrees, depending on the CO2 emission concentration path. The average of future core range and total range areas were 1.95×10^6 km^2 and 3.7×10^6 km^2 across climate change scenarios, accounting for 20.3% and 38.5% of the land area in China. But, there was a difference in the centroid shift velocity and direction between the core and total ranges at the horizontal gradient. The average shift speed of total range is 11.39 km/decade toward northwest and that for core range is 9.32 km/decade toward northeast across climate scenarios. The average shift speed of the core range -9.05 m/decade downward and that for total range is 17.15 m/decade upward across climate change scenarios. This study indicates that the response of total range and core distribution range to climate change is not synchronous. Considering poleward or northward shift will underestimate about 2.2-20.1% for total range and 21.2-56.3% for core range. Thus, the study have important guiding significance for determining the potential shift route and adjust the shift speed for planting the tree species in response to future climate change. The indicator systems used here have a wide range of practicability and can applied to any species, region, or time.
Keywords: *Fraxinus chinensis, shift velocity, bioclimatic envelope model, centroid method, forest management, suitable habitat*

Introduction

Global climate is changing with human interference; temperature and rainfall patterns have changed dramatically, which will inevitably lead to changes in the structure and function of natural ecosystems at different organizational levels (Geest et al., 2018; Zhang et al., 2019). At the species level, the shift in species range, rather than evolution and extinction, are currently considered the most likely strategy for adapting to climate change (Aitken et al., 2008; Kosanic et al., 2019). Many biological taxa have shifted their ranges along latitudinal and altitudinal gradients in the past few decades (Chen et al., 2011) and the direction of shifts in ranges is mainly related to temperature gradient (Lenoir et al., 2008; Lenoir and Svenning, 2015). However, this is currently not fully demonstrated by many studies. Species can shifted and migrated in multiple directions because the limitation of species range is not only temperature, but also other environmental and biological variables (Aitken et al., 2008; Lafleur et al., 2010; Huang et al., 2018). In particular, species that are sensitive to both temperature and precipitation may move in other directions (Li et al., 2021; Harsch and

http://www.aloki.hu ● ISSN 1589 1623 (Print) ● ISSN 1785 0037 (Online)
DOI: http://dx.doi.org/10.15666/aeer/2005_44994513

HilleRisLambers, 2016). Besides, due to the location relationship between land, ocean, mountain and plateau, the distribution patterns of temperature and precipitation gradient will affect the velocity and direction of range shift for particular species (Burrows et al., 2014; Huang et al., 2018).

For the protection, management, and introduction of specific species in the context of climate change, it is necessary to quantitatively characterize the potential distribution range (Li et al., 2020), as well as the likely range shift velocity and direction of the species (Iverson et al., 2008), which are crucial for our understanding of whether the species can keep up with climate change in the natural state, and knowing where there is still afforestation potential and where the species will face threats under future climate change conditions (Booth, 2016). The basic method of characterizing the potential range of species is mainly based on the climate envelope modeling (Booth et al., 2014; Gobeyn et al., 2019). A climate envelope model quantitatively characterizes the realized climatic niche of the species based on the relationship between the species occurrence data and the climate variables, and then applies the realized climatic niche onto current and future scenarios to project the current and future ranges (Peterson et al., 2011).

Characterizing velocity and direction of range shift is usually performed using the centroid method (Huang et al., 2016, 2018), which mainly calculates the latitude, longitude, and altitude centroids of the current and future potential distribution ranges, and estimates the direction and velocity of range shifts through certain calculations. However, a global meta-analysis have shown that few studies used a multidimensional approach focusing on at least two geographical dimensions (e.g. latitude and elevation) simultaneously to assess range shifts at the leading edge, the trailing edge or the optimum position (Lenoir and Svenning, 2015). What is more, previous studies have focused more on the total range and less on the core range of species (Huang et al., 2017, 2018; Robinson et al., 2015). Whether the dynamics of the core range is consistent with that of the total range remains to be studied for many target species, as the dynamics of core range play an important role in the construction of nature reserves or seedling breeding centers for protection and utilization purpose.

Chinese ash (*Fraxinus chinensis*) is a deciduous tree, which has major commercial use for breeding Ericerus pela to produce white wax, as well as used for woody products and traditional Chinese medicine (DFRPSAASE, 1994). Due to its strong sprout capacity and salt and drought tolerance (Ren et al., 2022), the species has a significantly ecological use for mountain soil conservation and urban greening projects (Zhang et al., 2022). With the improvement of urbanization level (Yang and Wang, 2019) and the strengthening of ecological restoration projects in China (Bryan et al., 2018), Chinese ash has been widely introduced to many regions of China. Numbers of breeding bases have also been established across the country. All these facts indicate the natural dispersal is not a limit factor in determining the species distribution. Previous studies investigated the reproductive technology (Xu and Ye, 2014; Zhang et al., 2007), pest control (Diao and Ding, 2004; Ma, 2022), and physiological response (Zhang et al., 2022), which have contributed greatly to the conservation and rational use of Chinese ash. In terms of the response of this species to climate change, Wang et al. (2012) suggested that Chinese ash had a phenological response with an average advance of 1.1 days/decade during 1952 to 2007 in ten years. However, the way in which future climate change is likely to affect the range shifts of this species along three geographical dimensions is still unknown, which is essential for development of climate change adaptation strategies for the species.

http://www.aloki.hu ● ISSN 1589 1623 (Print) ● ISSN 1785 0037 (Online)
DOI: http://dx.doi.org/10.15666/aeer/2005_44994513

Here we established a set of indicator systems to characterize the shifts in total range and core range at three geographical dimensions for Chinese ash (*Fraxinus chinensis*) under future climate change based on the bioclimatic envelope model and centroid method. The aims of this study were to 1) estimated the current and future total and core ranges of Chinese ash in China, 2) characterized the velocity and direction of total and core range shifts under future climate. This study theoretically makes sense for describing the three-dimensional range shift dynamics to elucidate the response of species to climate change. In practice, it is of great significance for the adaptive management of Chinese ash to cope with climate change.

Materials and methods

Species and climate databases

Occurrence data

The specimen data for Chinese ash was obtained from the Chinese Virtual Herbarium (http://www.cvh.ac.cn, 2382 specimens) and Global Biodiversity Information Facility (http://www.gbif.org, 1426 specimens) databases. The duplicate specimens and specimens without locational information or coordinates were removed. Then, the remaining specimens were rasterized onto a raster layer with 10-arcmin resolution. Currently, there is a general assumption that specimen data can represent the climatic requirements of the species in the study of species distribution models (Soberon and Nakamura, 2009; Booth, 2018). Here, a grid cell was considered a suitable habitat when one or more specimens were located in it. However, it is an open question whether a grid cell could be defined as suitable habitat if only one individual lives there. This is beyond the scope of this study. Finally, the binary occurrence map with 10-arcmin resolution was converted into points, and we obtained 293 records with latitudinal and longitudinal values (DOI: 10.6084/m9.figshare.19736284.v1).

Climatic variables

We integrated a set of climatic factors based on BIOCLIM (Hijmans et al., 2005; Booth, 2018), Holdridge life zone model (Holdridge, 1947) and Kira's index system (Kira, 1945). An excess of climatic factors can cause overfitting for simulating process, so we only selected 8 of the 19 BIOCLIM variables based on our previous research. A total of 13 climatic factors were used to define the climatic niches of in China, which were widely used in research on the relationship between species/vegetation and climate, at a regional or global scale (e.g. Li et al., 2018; Huang et al., 2018). The 13 climatic variables are introduced in Table 1.

Current and future climate layers

The basic climatic layers of current and future climate scenarios were obtained from the WorldClim database (http://www.worldclim.org/). In the database, the current climatic layers were generated from thin plate smoothing splines using latitude, longitude, altitude, monthly temperature, and precipitation data from the averages of 51-year (1950–2000) climate station records (Hijmans et al., 2005).

The future climatic layers were generated from many general circulation models (GCMs) with four representative concentration pathways (RCP2.6, RCP4.5, RCP6.0,

http://www.aloki.hu ● ISSN 1589 1623 (Print) ● ISSN 1785 0037 (Online)
DOI: http://dx.doi.org/10.15666/aeer/2005_44994513

and RCP8.5). Here, the climatic layers of future scenarios were averaged by combining seven GCMs to deal with the uncertainty of GCMs under four representative concentration pathways (Huang et al., 2018). The seven GCMs were from seven modeling centers of six countries: BCC-CSM1-1, CCSM4, GISS-E2-R, HadGEM2-AO, IPSL-CM5A-LR, MIROC-ESM-CHEM, and NorESM1-M.

Table 1. *Description of 13 climatic variables*

Nr.	Variable	Abbreviation	Unit
1	Annual mean temperature	AMT	°C
2	Maximum temperature of the warmest month	MTWM	°C
3	Minimum temperature of the coldest month	MTCM	°C
4	Annual range of temperature	ART	°C
5	Annual precipitation	AP	mm
6	Precipitation of the wettest month	PWM	mm
7	Precipitation of the driest month	PDM	mm
8	Precipitation of seasonality	PSD	mm
9	Annual biotemperature	ABT	°C
10	Warmth index	WI	°C
11	Coldness index	CI	°C
12	Potential evapotranspiration rate	PER	/
13	Humidity index	HI	mm/°C

The time-period from 2061 to 2080 was selected as the target future, in which the annual temperature in China will increase from 6.4 °C to 8.2–10.6 °C and the annual precipitation will increase from 576 mm to 603–623 mm based on ensemble average results of the seven GCMs in contrast to that of 1950-2000. All climatic layers used be obtained from DOI: 10.6084/m9.figshare.19736284.v1.

Simulation and range shift calculation processes

Simulation process

We used a Maxent model as a bioclimatic envelope model to simulate the current and future range of Chinese ash under current and future scenarios in China (Phillips et al., 2006; Elith et al., 2010). MaxEnt is a machine learning algorithm written in Java, and it can be used on all modern computing platforms. The software is freely available on the Internet (https://biodiversityinformatics.amnh.org/open_source/maxent/). The Maxent performance was evaluated using 10-fold cross-validation of all records and characterized by the area under the receiver operating characteristic curve (AUC) and predicted accuracy (Fielding and Bell, 1997). A jackknife test (systematically leaving out each variable) and the regularized gain change [log of the number of grid cells minus the log loss (average of the negative log probabilities of the sample locations)] were then used to evaluate which climatic factors were the most important in determining the climatic suitability of the species.

In this study, the Maxent model expresses the climatic suitability of a grid cell as a function of its 13 climatic variables in China together, with 293 sample records where the species was observed, where the climatic suitability takes the form (*Eq. 1*):

http://www.aloki.hu ● ISSN 1589 1623 (Print) ● ISSN 1785 0037 (Online)
DOI: http://dx.doi.org/10.15666/aeer/2005_44994513

$$P(x) = \exp(c_1 \times f_1(x) + c_2 \times f_2(x) + c_3 \times f_3(x) + ...) / Z \quad \text{(Eq.1)}$$

where c_1, c_2, c_3,… are constants; f_1, f_2, f_3,… are the features (or variables), and Z is a scaling constant that ensures that P sums to 1 over all grid cells. Then, the simulated Maxent models were projected on the current and future climate scenarios to obtain five suitability maps for Chinese ash, with one map of the current condition and four maps of future conditions.

We converted the five climatic suitability maps into two types of maps: total range maps and core range maps. The total range maps were converted from these climatic suitability maps with an optimal threshold of maximum sensitivity and specificity [max(tp/(tp + fn) + tn/(tn + fp)), tp is true positive value, fn is false negative value, fp is false positive value and tn is true negative value] (Fielding and Bell, 1997). The core range maps were also generated from climatic suitability maps with two times the optimal threshold. Finally, we obtained 10 range maps with five total range maps and five core range maps, each with one current map and four maps for four RCPs.

Range shift calculation process

The change in size of area under current and future scenarios was characterized by three indices: the expansion area, loss area, and stability area, which were calculated by the sum of the area of each occurring grid cell. The centroids of species range at three geographical dimensions were computed based on the following formulae (*Eqs. 2–4*):

$$Lon_c = \sum_{i=1}^{n} (Lon_i / n) \quad \text{(Eq.2)}$$

$$Lat_c = \sum_{i=1}^{n} (Lat_i / n) \quad \text{(Eq.3)}$$

$$Alt_c = median(Alt_i) \quad \text{(Eq.4)}$$

where Lon_c, Lat_c, and Alt_c represent the longitude, latitude and altitude centroids on the range map (using Geographic Coordinate System: GCS_WGS_1984; Angular Unit: degree), respectively, and n represents the number of occurring grid cells. The reason we used arithmetic means for longitude and latitude, but median for altitude was that occupancy grids value of longitude and latitude generally shows normal distribution pattern, while that of altitude value generally shows skewed distribution pattern.

The shift velocities of range centroids along the longitudinal, latitudinal, and vertical directions were calculated using the following formulae (*Eqs. 5–7*):

$$SV_{lon} = (Lon_f - Lon_c) / n \quad \text{(Eq.5)}$$

$$SV_{lat} = (Lat_f - Lat_c) / n \quad \text{(Eq.6)}$$

$$SV_{alt} = (Alt_f - Alt_c) / n \quad \text{(Eq.7)}$$

where SV_{lon}, SV_{lat}, and SV_{alt}, represent shift velocities of range centroids along the longitudinal, latitudinal, and vertical directions. Lon_f, Lat_f, Lon_c, Lat_c, represent the

http://www.aloki.hu ● ISSN 1589 1623 (Print) ● ISSN 1785 0037 (Online)
DOI: http://dx.doi.org/10.15666/aeer/2005_44994513

longitude and latitude of centroids under future and current climate scenarios (using Projected Coordinate System: Clarke_1866_Albers; Linear Unit: meter), respectively. Alt_f and Alt_c represent the altitudes of centroids under future and current climate scenarios, respectively. The divisor n represent the time period between current and target future scenarios [the median value of 1950-2000 (current period, 1975) and 2060-2080 (future period, 2070) were used to determine n value (9.5 decades) in this study]. The total shift velocities (SV) of ranges on earth surface were calculated using the following formula (*Eq. 8*):

$$SV = \sqrt{SV_{lon}^2 + SV_{lat}^2} \quad \text{(Eq.8)}$$

We also calculated the altitude changes along the longitudinal and latitudinal gradients (the range of the species was divided into bands with one-degree width along the two gradients, and the median value of altitude in each band represented the centroid of that band. All statistical analyses were performed on R software.

Results

Maxent performance and total and core distributions of Chinese ash

The results of the ten cross-validations showed that the Maxent prediction accuracy is high. The test AUC reached 0.83, and the prediction accuracy rate was 71%. We found that MTCM, AP, and CI were the most important climatic factors determining the distribution of Chinese ash. The three factors could explain 84% of the variance, and could be divided into thermal group (MTCM and CI, 59.5%) and humidity group (AP, 24.5%). It appeared that thermal condition was more important than humidity condition in controlling the distribution ranges of the species.

Both climatic suitability map and total range map (optimal threshold is 0.26) are shown in *Fig.1AB*. They show that the total range of Chinese ash spreads throughout almost all provinces in the southeast of China. The total range area can occupy 34.4% (3.3×10^6 km^2) of the land area in China. The core range map is generated from suitability maps with threshold of 0.52 (two times the optimal threshold, *Fig.1C*). It indicates that the core areas (with high suitability) are mainly concentrated in center part of China, occupying 13.5% (1.3×10^6 km^2) of the country's land area. The results of the ten cross-validations showed that the Maxent prediction accuracy is high. The test AUC reached 0.83 (*Fig. 1D*).

Range expansion and loss under future climate change scenarios

The increase or decrease of the future total range area and core range areas show that the overall range of Chinese ash is relatively stable in response to future climate change (*Fig.2*). The results show that the average of future core range and total range areas were 1.95×10^6 km^2 and 3.7×10^6 km^2 across climate change scenarios, accounting for 20.3% and 38.5% of the land area in China. The stable area occupies 3.0–3.2 $\times 10^6$ km^2 for the total range and 1.0–1.1 $\times 10^6$ km^2 for the core range of the species; the loss area occupies 0.1–0.26 $\times 10^6$ km^2 for total range and 0.17–0.21 $\times 10^6$ km^2 for the core range; the expansion area occupies 0.4–0.8 $\times 10^6$ km^2 for the total range and 0.7–1.1 $\times 10^6$ km^2 for the core range. Generally, the dynamics of suitability range were more sensitive at high concentration path (e.g. RCP8.5) than that of low concentrations path (e.g.

http://www.aloki.hu ● ISSN 1589 1623 (Print) ● ISSN 1785 0037 (Online)
DOI: http://dx.doi.org/10.15666/aeer/2005_44994513

RCP2.6). The location of expansion area in the total range was mainly distributed in the northern boundary and that of loss area was mainly distributed in the south boundary. The size of expansion area is larger than that of loss area in both core and total ranges of Chinese ash.

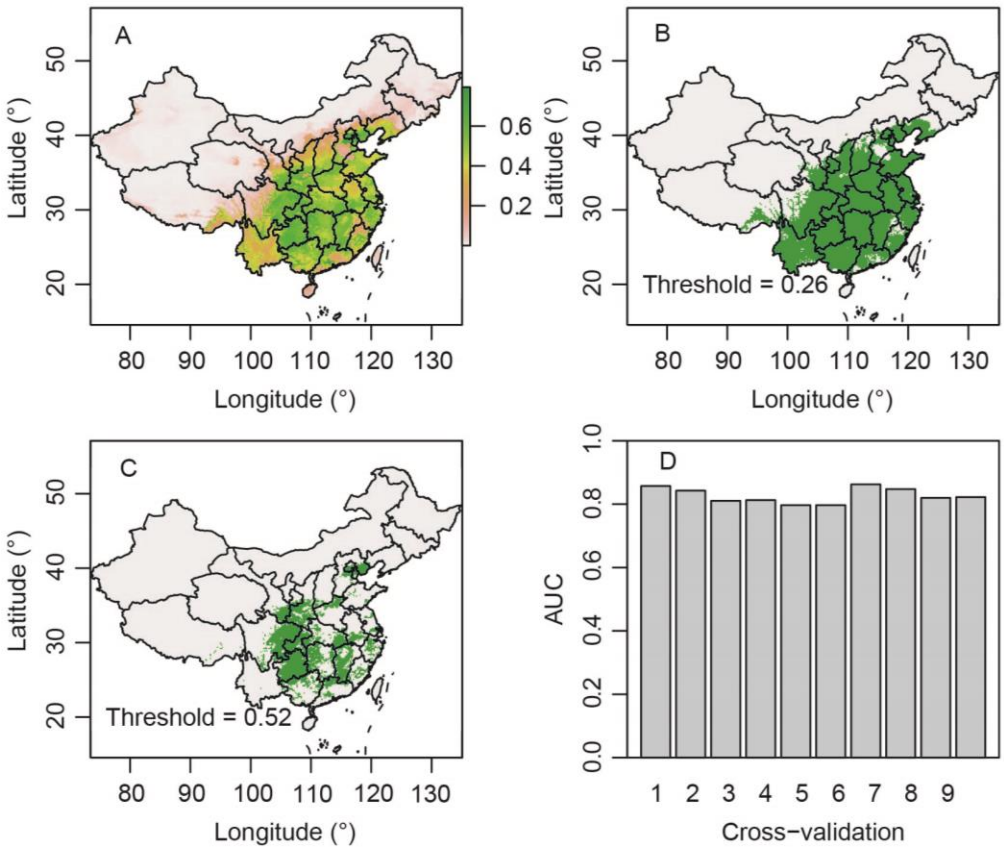

Figure 1. *Current climatic suitability maps based on all occurrence data and Maxent model. (A) Probability map; (B) Total range map (threshold = 0.26). (C) Core range map (threshold = 0.52). (D) Area under the receiver operating characteristic curve (AUC) of 10 cross-validations*

Centroid shifts along three geographical dimensions

The shift pattern of the total range and core range of Chinese ash in horizontal and vertical directions is shown in *Fig.3*. The results show that the centroid of total range is located in Changyang Tujia Autonomous County (*Fig.3A*), the future centroids will shift to the northwest, the shift velocity is 7.86–14.92 km/decade (1.65–8.76 km/decade along the longitudinal gradient; 7.49–12.08 km/decade along the latitudinal gradient); the centroid of the core range is located in Shimen County (*Fig.3C*), the future centroid will shift to the northeast, the velocity is about 6.30–12.33 km/decade (5.36–8.67 km/decade along longitudinal gradient; 3.30–9.72 km/decade along latitudinal gradient). The altitude will shift to a higher altitude in the total range, from 507.5 m in the current climate, to 585–755 m in the future climate (*Fig.3B*), with a centroid shift velocity of 8.2–26.1 m/decade. The altitude will shift to a lower altitude in the core range, from 505 m in current climate to 405–433 m in the future climate (*Fig.3D*), with a centroid shift velocity from -10.5 to -7.6 m/decade.

http://www.aloki.hu ● ISSN 1589 1623 (Print) ● ISSN 1785 0037 (Online)
DOI: http://dx.doi.org/10.15666/aeer/2005_44994513

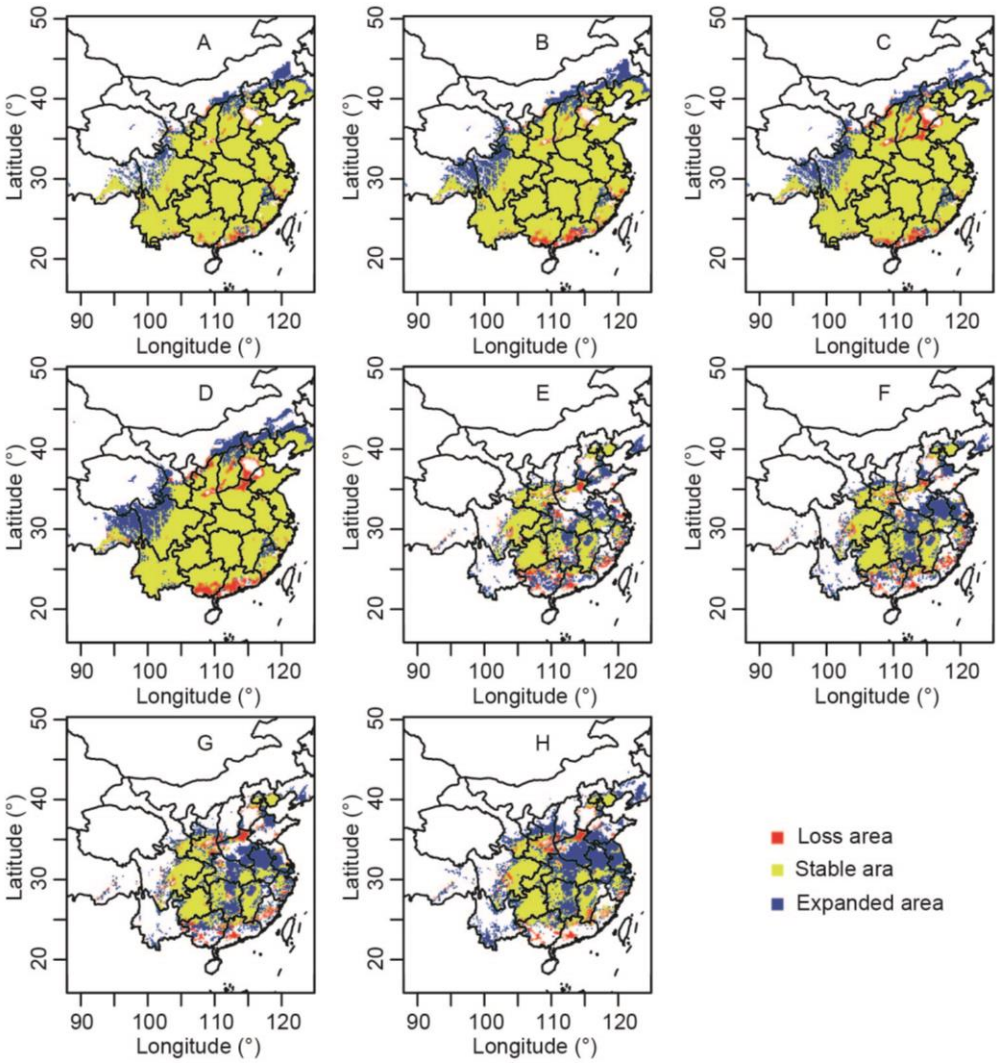

Figure 2. *Expansion of area, loss of area, and stability of area by overlap of current and future total range maps. Total range shift under RCP2.6 (A), RCP4.5(B), RCP6.0 (C) and RCP8.5(D); Core range shift under RCP2.6 (E), RCP4.5(F), RCP6.0 (G) and RCP8.5(H)*

We analyzed the altitude centroids along the longitudinal and latitudinal gradients in the total range and core range maps (*Fig.4*). It shows that there is no obvious rising trend along the longitudinal gradient, regardless of the core range or the total range (*Fig.4A, C*). In the latitudinal gradient, there was a significant trend in raising altitude in the total range maps, especially in the area where the latitude was higher than 30° (*Fig.4B*). In contrast, the shift of altitude in the core range has an upward or downward trend in the latitudinal gradient, but it is less violent than that for the total range (*Fig.4C*). Between 30–35°, there is a phenomenon of altitude decrease in the core range (*Fig.4D*).

Discussion

Climate change induced range shifts in three geographical dimensions

We studied the effects of climate change on the distribution of an afforestation tree species, Chinese ash, and established a procedure that describes the speed and direction

http://www.aloki.hu ● ISSN 1589 1623 (Print) ● ISSN 1785 0037 (Online)
DOI: http://dx.doi.org/10.15666/aeer/2005_44994513

of range shift in both total and core ranges for the target species in three geographical dimensions. Our study found that the size of total range area of Chinese ash will increase, mainly due to the increase of area in the northwest of China; that is, the expansion of the leading edge. This study is consistent with most of the results from similar research, such as on *Hippophae rhamnoides* subsp. *Sinensis* (Huang et al., 2018) and *Pinus tabuliformis* (Li et al., 2016). Besides, future climate change will lead to a loss in area of the southern boundary of Chinese ash; that is, its trailing edge shrinks. However, the shrink area of trailing edge is smaller than the expansion area of leading edge in total range. In total, the overall area of Chinese ash trees is large and will continue to increase in the future, which means that Chinese ash do not face the danger of extinction according to the theory of species–area curves (Thomas et al., 2004). When undertaking the adaptive management of Chinese ash to cope with climate change, the enhancement of dispersal ability of individual tree species, such as building corridors, artificial introductions, etc., should be performed more priority near the leading edge than that of the trailing edge.

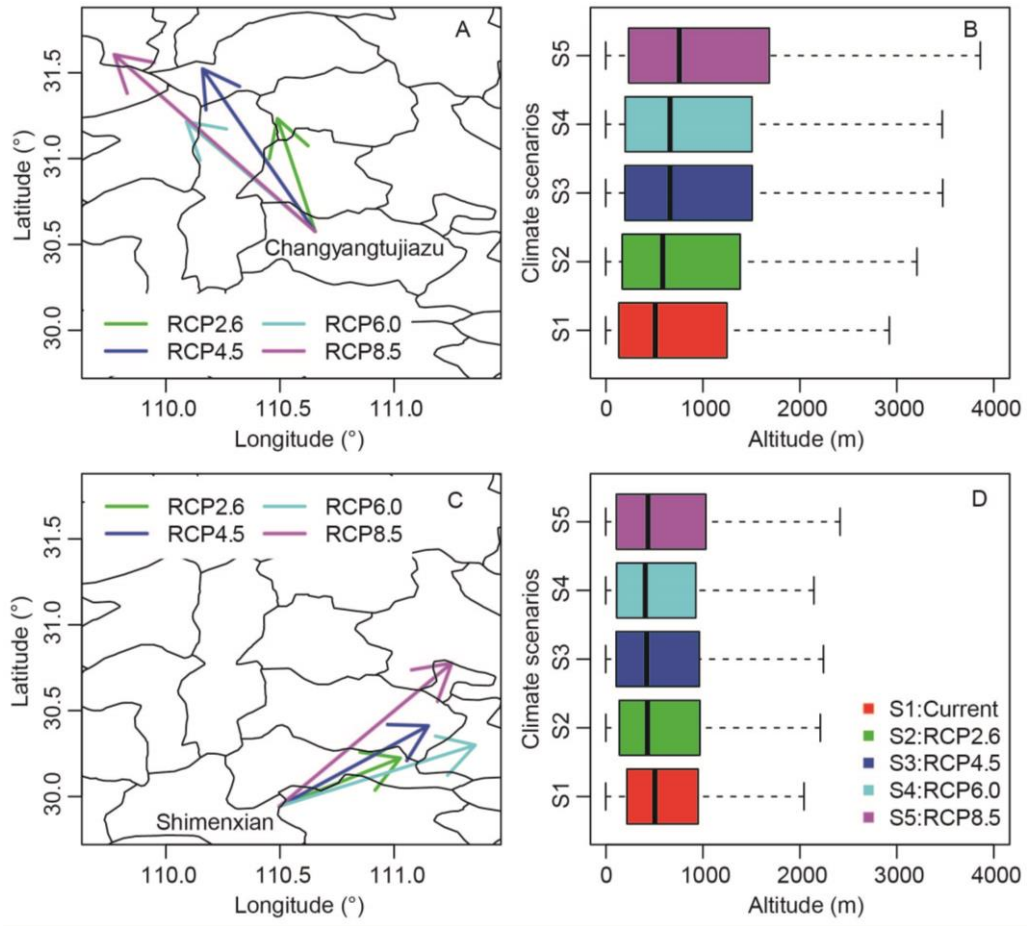

Figure 3. *Total range shift of ash in horizontal (A) and vertical (B) gradients; core range shift of ash in horizontal (C) and vertical (D) gradients*

In contrast to the total range, the range size change of the core range has similar expansion dynamics with it. However, the change in core range is more drastic than total range, especially for the proportion of expansion area. The loss area for the core

http://www.aloki.hu ● ISSN 1589 1623 (Print) ● ISSN 1785 0037 (Online)
DOI: http://dx.doi.org/10.15666/aeer/2005_44994513

range and the total range are small, and the average loss area is about 0.18×10^6 km^2 across climate scenarios. But, the expansion area in the core range is 37.5-75% more than that in total range, and the average expansion area for the core range is 0.9×10^6 km^2 across climate scenarios. It means that the core range is more sensitive to climate change than that for the total range. It also means that future climate change is conducive to the survival of this species from the perspective of climate suitability. The degree of benefits is increasing with the increase of CO2 concentration path. It means that future climate change will bring more opportunities to reforestation in high CO2 concentration path than that in low CO2 concentration path. Species range shift is the better way to adapt to climate change than plasticity and gene mutation (Aitken et al., 2008). But how fast and in which direction should Chinese ash adapts to climate change in three-dimensional geographical space in the late 21st century?

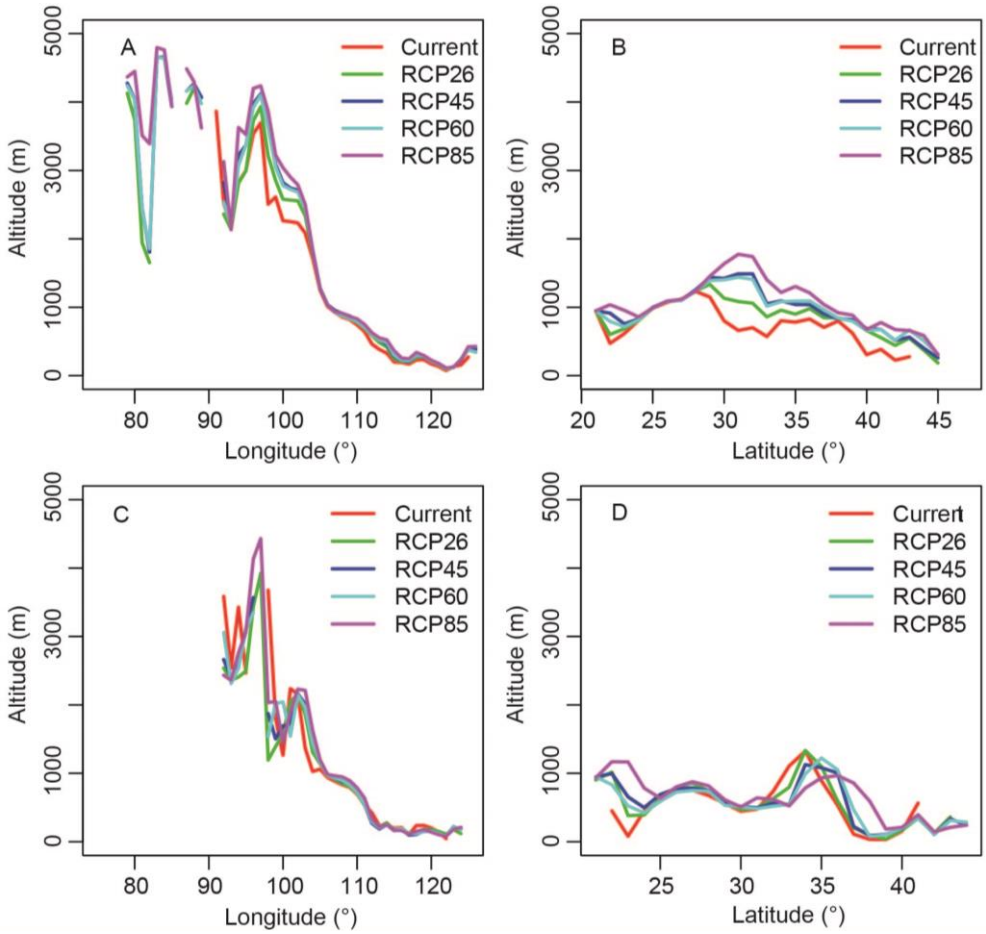

Figure 4. *Altitude centroid shifts in total range along the longitudinal (A) and latitudinal (B) gradients; altitude centroid shifts in core range along the longitudinal (C) and latitudinal (D) gradients*

Our study suggested that the shift velocity of range for Chinese ash is relatively slow at the horizontal gradients, reaching only 6.30–12.33 km/decade to northeast for core range and 7.86–14.92 km/decade to northwest for total range. One reason may be that Chinese ash occupies a wider climate niche and the driving factor of range shift is mainly the expansion of the leading edge rather than the contraction from the trailing edge. At the

http://www.aloki.hu ● ISSN 1589 1623 (Print) ● ISSN 1785 0037 (Online)
DOI: http://dx.doi.org/10.15666/aeer/2005_44994513

same time, we should note that although the shift velocity of the total range is similar to that of the core range, the direction of the range shift is not strictly following the shift to poleward or northward. This is inconsistent with the traditional understanding (Chen et al., 2011; Lenoir and Svenning, 2015). Traditionally, species should shift to the north to track the constancy of temperature (Burrows et al., 2014). This traditional understanding was based on the assumption that temperature is the main limit climatic factor affecting species distribution. However, this study found that annual precipitation is still one of the limiting factors for Chinese ash. Our research did not support this hypothesis, so the shift direction of the core range and the total range is different from the traditional northward viewpoint. It indicated that simply considering poleward or northward shift will underestimate the actual shift velocity of Chinese ash species (underestimating about 2.2-20.1% for total range and 21.2-56.3% for core range).

On the altitude gradient, we found that the altitude centroid of the total range will increase slightly with a velocity of 8.2–26.1 m/decade, but that of the core range will decrease slightly with a velocity of -10.5 – -7.6 m/decade in the future scenarios. This means that the shift direction of the core range and the total range on the vertical gradient is completely opposite. The shift direction of the core range challenges the traditional understanding (upward shift) to a certain extent (Lenoir et al., 2008). The shift direction of core range was simulated to downward, which may be related to the increase in annual precipitation in low-altitude areas along the eastern coast of China, and then the increase in annual precipitation offsets the potential threat of temperature rise to the suitability of Chinese ash (Harsch et al., 2016; Huang et al., 2018). Downward shifts also mean that Chinese ash may face more intense interference from persistent human activities in the future, especially land use change. Therefore, much attention should be focused on both the impact of climate change and land use on suitability of Chinese ash in the future studies.

Uncertainty and future efforts

The modern bioclimatic envelope model began with the development of the BIOCLIM program in 1984 (Booth et al., 2014). The development of improved methods of climatic interpolation as part of the BIOCLIM project has allowed reliable estimates to be made for locations that are some distance from existing meteorological stations across the whole world (Hijmans et al., 2005; Fick and Hijmans, 2017). Important advances are now being made with providing data on soil conditions across the world (Booth, 2018). However, extensive testing will be required before the reliability of these data is determined for China. Besides, soil factors cannot be obtained in the future, which also limits the use of soil factors as prediction variables. Here we have concentrated on determining the climate niche and dimensions of potential ranges for Chinese ash under current and future scenarios. These range maps may be overestimated the range of the species according to Eltonian Noise Hypothesis, which believes that limitation of small-resolution factors (e.g. soil factors) can be papered over on large-resolution (Soberon and Nakamura, 2009). Therefore, the range shift maps should assist managers' plan the rational conservation and use of Chinese ash under changing climates. Currently, a large amount of free land use and disturbance data can be obtained (Chen et al., 2017; Mu et al., 2022). Combined with our predicted range maps and these land use and disturbance data, a further detailed planning can be realized. Thus, it is conducive to climate suitability decision-making.

http://www.aloki.hu ● ISSN 1589 1623 (Print) ● ISSN 1785 0037 (Online)
DOI: http://dx.doi.org/10.15666/aeer/2005_44994513

Species velocity based on projections of changes in climatic niche alone (as is the case here) does not inform about species' dispersal ability. Aubin et al. (2016) defined tree dispersal ability as seed dispersal distance, dispersal vector and seed mass. Instead, species velocity as defined here was a way of quantifying species exposure to climate change (Glick et al., 2011). The inherent assumption of this research was that species has infinite dispersal capacity. However, in reality, it is difficult for species to achieve such a situation under natural conditions and further research is needed on whether the species can keep up with the pace of climate change. Interestingly, human assistant migration, such as afforestation and planting trees, could enhance the dispersal ability of species and this can break through the limit of tree migration. Numerous afforestation and greening projects have been carried out in China (Bran et al., 2018) and the species can play an important role in vegetation greening and construction. Our study provides significance guiding for the specific shift direction of planting tree species in response to future climate change, thus determining the potential shift route and adjust the shift speed.

Conclusion

We developed an indicator system to characterize the range shift of the total and core ranges of *Fraxinus chinensis* at three geographical dimensions under future climate change using the bioclimatic model and centroid methods. We found that the current core range and total range areas were 1.3×10^6 km^2 and 3.3×10^6 km^2, accounting for 13.5% and 34.4% of the country's land area. The core range and total range areas will increase under future climate change scenarios. The centroid shift velocity and direction of the core and the total ranges are 6.30–12.33 km/decade to northeast and 7.86–14.92 km/decade to northwest at the horizontal gradient. The driving force of range shift of the core and total ranges mainly comes from the expansion of the leading edge rather than the retreat of the trailing edge. At the vertical gradient, the shift direction of altitude in the total range is upward (8.2–26.1 m/decade), while the shift direction of altitude in the core range is downward (-10.5 – -7.6 m/decade). This study indicates that the response of total range and core distribution range to climate change is not synchronous. Simply considering poleward or northward shift will underestimate about 2.2–20.1% for total range and 21.2–56.3% for core range. Thus, the study has important guiding significance for determining the potential shift route and adjust the shift speed for planting the tree species in response to future climate change. The indicator system used has a wide range of practicability and can be applied to any species, region, or time.

Acknowledgements. The project was supported financially by National Natural Science Foundation of China (31971488).

REFERENCES

[1] Aitken, S. N., Yeaman, S., Holliday, J. A., Wang, T., Curtis-McLane, S. (2008): Adaptation, migration or extirpation: climate change outcomes for tree populations. – Evolutionary Applications 1: 95-111.

[2] Aubin, I., Munson, A. D., Cardou, F., Burton, P. J., Isabel, N., Pedlar, J. H., Paquette, A., Taylor, A. R., Delagrange, S., Kebli, H., Messier, C., Shipley, B., Valladares, F., Kattge, J., Boisvert-Marsh, L., McKenney, D. (2016): Traits to stay, traits to move: a review of

http://www.aloki.hu ● ISSN 1589 1623 (Print) ● ISSN 1785 0037 (Online)
DOI: http://dx.doi.org/10.15666/aeer/2005_44994513

functional traits to access sensitivity and adaptive capacity of temperate and boreal trees to climate change. – Environmental Reviews 24: 164-186.

[3] Booth, T. H. (2016): Estimating potential range and hence climatic adaptability in selected tree species. – Forest Ecology Management 366: 175-183.

[4] Booth, T. H. (2018): Why understanding the pioneering and continuing contributions of BIOCLIM to species distribution modelling is important. – Austral Ecology 43: 852-860.

[5] Booth, T. H., Nix, H. A., Busby, J. R., Hutchinson, M. F. (2014): BIOCLIM: the first species distribution modelling package, its early applications and relevance to most current MAXENT studies. – Diversity and Distribution 20: 1-9.

[6] Bryan, B. A., Gao, L., Ye, Y. Q., Sun, X. F., Connor, J. D., Crossman, N. D., Stafford-smith, M., Wu, J., He, C., Yu, D., Liu, Z., Li, A., Huang, Q., Ren, H., Deng, X., Zheng, H., Niu, J., Han, G., Hou, X. (2018): China's response to a national land-system sustainability emergency. – Nature 559: 193-204.

[7] Burrows, M. T., Schoeman, D. S., Richardson, A. J., Molinos, J. G., Hoffmann, A., Buckley, L. B., Moore, P. J., Brown, C. J., Bruno, J. F., Duarte, C. M., Halpern, B. S., Hoegh-Guldberg, O., Kappel, C. V., Kiessling, W., O'Connor, M. I., Pandolfi, J. M., Parmesan, C., Sydeman, W., Ferrier, S., Williams, K. J., Poloczanska, E. S. (2014): Geographical limits to species-range shifts are suggested by climate velocity. – Nature 507: 492-495.

[8] Chen, I. C., Hill, J. K., Ohlemuller, R., Roy, D. B., Thomas, C. D. (2011): Rapid range shifts of species associated with high levels of climate warming. – Science 333: 1024-1026.

[9] Chen, B.; Xu, B.; Zhu, Z.; Yuan, C.; Suen, H. P.; Guo, J.; Xu, N.; Li, W.; Zhao, Y.; Yang, J. (2019): Stable classification with limited sample: transferring a 30-m resolution sample set collected in 2015 to mapping 10-m resolution global land cover in 2017. – Science Bulletin 64: 370-373.

[10] DFRPSAASE (1994): Delectis Florae Reipublicae Popularis Sinicae Agendae Academiae Sinicae Edita. – In: Flora Reipublicae Popularis Sinicae. Science Press, Beijing.

[11] Diao, Z. E., Ding, F. B. (2004): Occurrence and control of white-stiped longhorn, *Batocera horsfildi* (Hope) (Coleoptera: Cerambycidae) on Chinese ash, *Fraxinus chinese* Roxb. – Entomological Journal of East China 13: 49-52.

[12] Elith, J., Phillips, S. J., Hastie, T., Dudik, M., Chee, Y. E., Yates, C. (2010): A statistical explanation of MaxEnt for ecologists. – Diversity and Distribution 17: 43-57.

[13] Fick, S. E., Hijmans, R. J. (2017): WorldClim 2: new 1 km spatial resolution climate surfaces for global land areas. – International Journal of Climatology 37: 4302-4315.

[14] Fielding, A. H., Bell, J. F. (1997): A review of methods for the assessment of prediction errors in conservation presence/absence models. – Environmental Conservation 24: 38-49.

[15] Geest, K., Sherbinin, A., Kienberger, S., Zommers, Z., Sitati, A., Roberts, E., James, R. (2019): The Impacts of Climate Change on Ecosystem Services and Resulting Losses and Damages to People and Society. In: Mechler, R., Bouwer, L., Schinko, T., Surminski, S., Linnerooth-Bayer, J. (eds.) Loss and Damage from Climate Change. Climate Risk Management, Policy and Governance. – Springer, Cham.

[16] Glick, P., Stein, B. A., Edelson, N. A. (2011): Scanning the Conservation Horizon: A Guide to Climate Change Vulnerability Assessment. – National Wildlife Federation, Washington, DC.

[17] Gobeyn, S., Mouton, A. M., Cord, A. F., Kaim, A., Volk, M., Goethals, P. (2019): Evolutionary algorithms for species distribution modelling: a review in the context of machine learning. – Ecological Modelling 392: 179-195.

[18] Harsch, M. A., HilleRisLambers, J. (2016): Climate warming and seasonal precipitation change interact to limit species distribution shifts across western North America. – PLoS ONE 11: e0159184.

http://www.aloki.hu ● ISSN 1589 1623 (Print) ● ISSN 1785 0037 (Online)
DOI: http://dx.doi.org/10.15666/aeer/2005_44994513

[19] Hijmans, R. J., Cameron, S. E., Parra, J. L., Jones, P. G., Jarvis, A. (2005): Very high resolution interpolated climate surfaces for global land areas. – International Journal of Climatology 25: 1965-1978.
[20] Holdridge, L. R. (1947): Determination of world plant formations from simple climatic data. – Science 105: 367-368.
[21] Huang, Q. Y., Sauer, J. R., Dubayah, R. O. (2017): Multidirectional abundance shifts among North American birds and the relative influence of multifaceted climate factors. – Global Change Biology 23: 3610-3622.
[22] Huang, J. H., Li, G. Q., Li, J., Zhang, X. Q., Yan, M. J., Du, S. (2018): Projecting the range shifts in climatically suitable habitat for Chinese sea buckthorn under climate change scenarios. – Forests 9: 9.
[23] Iverson, L. R., Prasad, A. M., Matthews, S. N., Peters, M. (2008): Estimating potential habitat for 134 eastern US tree species under six climate scenarios. – Forest Ecology and Management 254: 390-406.
[24] Kira, T. (1945): A New Classification of Climate in Eastern Asia as the Basis for Agricultural Geography. – Horticultural Institute, Kyoto University, Japan.
[25] Kosanic, A., Kavcic, I., vanKleunen, M., Harrison, S. (2019): Climate change and climate change velocity analysis across Germany. – Scientific Reports 9: 2196.
[26] Lafleur, B., Pare, D., Munson, A. D., Bergeron, Y. (2010): Response of northeastern North American forests to climate change: will soil conditions constrain tree species migration. – Environmental Reviews 18: 279-289.
[27] Lenoir, J., Gegout, J. C., Marquet, P. A., de Ruffray, P., Brisse, H. (2008): A significant upward shift in plant species optimum elevation during the 20th century. – Science 320: 1768-1771.
[28] Lenoir, J., Svenning, J. C. (2015): Climate-related range shifts - a global multidimensional synthesis and new research directions. – Ecography 38: 15-28.
[29] Li, G. Q., Xu, G. H., Guo, K., Du, S. (2016): Geographical boundary and climatic analysis of *Pinus tabulaeformis* in China: insights on its afforestation. – Ecological Engineering 86: 75-84.
[30] Li, G. Q., Zhang, X. Q., Huang, J. H., Wen, Z. M., Du, S. (2018): Afforestation and climatic niche dynamics of black locust (*Robinia pseudoacacia*). – Forest Ecology Management 407: 184-190.
[31] Li, G., Huang, J., Guo, K., Du, S. (2020): Projecting species loss and turnover under climate change for 111 Chinese tree species. – Forest Ecology and Management 477: 118488.
[32] Li, G., Paul, C. R., Huang, J. (2021): Black locust (*Robinia pseudoacacia* L.) range shifts in China: application of a global model in climate change futures. – Climate Change Ecology 2: 100036.
[33] Ma, J. (2022): Occurrence and control measures of diseases and pests for *Fraxinus chinensis*. – Seed Science and Technology 8: 82-84.
[34] Mu, H., Li, X., Wen, Y., Huang, J., Du, P., Su, W., Miao, S., Geng, M. (2018): A global record of annual terrestrial Human Footprint dataset from 2000 to 2018. – Scientific Data 9: 176.
[35] Peterson, A. T., Soberon, J., Pearson, R. G., Andersen, R. P., Martinez-Meyer, E., Nakamura, M., Araujo, M. B. (2011): Ecological Niches and Geographic Distributions; Monographs in Population Biology. No. 49. – Princeton University Press, Princeton, NJ.
[36] Phillips, S. J., Anderson, R. P., Schapire, R. E. (2006): Maximum entropy modeling of species geographic distributions. – Ecology Modelling 190: 231-259.
[37] Ren, H. (2022): Key points of *Fraxinus chinensis* afforestation technology. – World Tropical Agricultural Information 4: 41-42.
[38] Robinson, L. M., Hobday, A. J., Possingham, H. P., Richardson, A. J. (2015): Trailing edges projected to move faster than leading edges for large pelagic fish habitats under climate change. – Deep-Sea Res Pt Ii 113: 225-234.

http://www.aloki.hu ● ISSN 1589 1623 (Print) ● ISSN 1785 0037 (Online)
DOI: http://dx.doi.org/10.15666/aeer/2005_44994513

[39] Soberon, J., Nakamura, M. (2009): Niches and distributional area: concepts, methods, and assumptions. – Proceedings of the National Academy of Sciences of the United States of America 106: 19644-19650.
[40] Thomas, C. D., Cameron, A., Green, R. E., Bakkenes, M., Beaumont, L. J., Collingham, Y. C., Erasmus, B. F. N., de Siqueira, M. F., Grainger, A., Hannah, L., Hughes, L., Huntley, B., van Jaarsveld, A. S., Midgley, G. F., Miles, L., Ortega-Huerta, M. A., Peterson, A. T., Phillips, O. L., Williams, S. E. (2004): Extinction risk from climate change. – Nature 427: 145-148.
[41] Wang, H. J., Dai, J. H., Ge, Q. S. (2012): The spatiotemporal characteristics of spring phenophase changes of *Fraxinus chinensis* in China from 1952-2007. – Science China Earth Science 55: 991-1000.
[42] Xu, S. Y., Ye, J. F. (2014): Advances in research on tree reproduction of Chinese ash (*Fraxinus chinensis*). – Protection Forest Science and Technology 2: 44-45.
[43] Yang, X. J., Wang, X. K. (2019): Regional difference of urbanization speed in China and its main influencing factors. – Ecological Science 38: 36-44.
[44] Zhang, L. J., Shen, H. L., Cui, J. G., Zhou, Q. (2007): Advances in somatic embryogenesis of *Fraxinus* species. – Biotechnology Bulletin 3: 31-34.
[45] Zhang, W., Brandt, M., Penuelas, J., Guichard, F., Tong, X., Tian, F., Fensholt, R. (2019): Ecosystem structural changes controlled by altered rainfall climatology in tropical savannas. – Nature Communications 10: 671.
[46] Zhang, Z. G., Li, B., Shi, K. Q., Yang, J. J., Wang, H. P., Li, H., Shi, H. Y. (2022): Response of five introduced *Fraxinus chinensis* species to drought stress in Yili area. – Agricultural Research in the Arid Areas 2: 9-16.

http://www.aloki.hu ● ISSN 1589 1623 (Print) ● ISSN 1785 0037 (Online)
DOI: http://dx.doi.org/10.15666/aeer/2005_44994513

EFFECTS OF EXOGENOUS ABSCISIC ACID ON SALT TOLERANCE OF WATERMELON SEEDLINGS UNDER NaCl STRESS

FENG, X. Y. – CHEN, S. Y. – YANG, S. M. – AN, X. Q. – LIU, Y. Y. – LU, H. L. – YANG, C. Q. – QIN, Y. G.*

College of Horticulture, Sichuan Agricultural University, Chengdu 611130, China

**Corresponding author*
e-mail: qinyaoguo@sina.com

(Received 15th May 2022; accepted 26th Jul 2022)

Abstract. Effects of exogenous abscisic acid (ABA) treatment on growth, chlorophyll fluorescence parameters, and antioxidant enzyme activities of watermelon seedlings under NaCl stress were investigated in this study to explore physiological mechanism of ABA-induced salt tolerance response of watermelon. Results showed that NaCl stress significantly reduced the growth and photosynthetic efficiency of watermelon seedlings and affected activities of antioxidant enzymes. ABA treatment at a certain concentration significantly reduced salt injury index and increased fresh and dry weights of watermelon seedlings under NaCl stress. The maximum photosynthetic efficiency, actual photosynthetic efficiency, relative electron transport rate, and photochemical quenching of photosystem II of watermelon seedlings under NaCl stress increased first and then decreased with the increase of ABA concentration, while non-photochemical quenching, quantum yield of regulated energy dissipation, and quantum yield of non-regulated energy dissipation showed the opposite trend. ABA treatment increased activities of superoxide dismutase, catalase, and peroxidase in plants and reduced the content of malondialdehyde. Treatment with ABA concentrations of 1 and 5 $mg \cdot L^{-1}$ demonstrated an enhanced effect that can improve salt tolerance and effectively alleviate injury of watermelon seedlings under NaCl stress.
Keywords: *ABA, salt stress, salt tolerance, salt injury, photosynthesis*

Introduction

Soil salinization is a global problem that affects 20% of arable land and 33% of irrigated agricultural land worldwide and severely reduces crop yields (Wu et al., 2021). Watermelon (*Citrullus lanatus* (Thunb.) Matsum. et Nakai), a widely cultivated annual trailing herb from the gourd family, is used as a fruit for consumption and demonstrates high edibility and medicinal value. Secondary salinization of soil in facilities has occurred in recent years due to irrigation methods, fertilization, soil texture, groundwater level, and other factors (Huan et al., 2007). The secondary salinization of soil has seriously affected the yield and quality of watermelon and hindered the sustainable development of watermelon facility cultivation. Therefore, investigating physiological and biochemical changes of watermelon under salt stress as well as methods for improving the salt tolerance of plants is urgently necessary.

Abscisic acid (ABA) is a key plant hormone produced in response to abiotic stress conditions and an activator and regulator of abiotic stress resistance mechanism in plants (Hauser et al., 2017). Accumulation of ABA increases significantly under drought, cold, and salt stress (Jiang and Zhang, 2004). Drought resistance mechanism of *Camellia oleifera* was controlled by maintaining the growth of root system to obtain the required water, increasing contents of osmotic substances in leaves to maintain water holding capacity, and reducing water transpiration by increasing ABA and other hormone contents in leaves (He et al., 2020). Spraying ABA regulated the osmotic

http://www.aloki.hu ● ISSN 1589 1623 (Print) ● ISSN 1785 0037 (Online)
DOI: http://dx.doi.org/10.15666/aeer/2005_45154524

protection and antioxidant mechanisms of grape leaves and promoted metabolic response under water stress (Pontin et al., 2021). Exogenous ABA improved cold tolerance of wheat, and the ultrastructure of chloroplasts also changed evidently to maintain the photosynthetic activity (Venzhik et al., 2016). Alfalfa seedlings were stressed with alkaline solution after pretreatment with ABA. Compared with the control, ABA pretreatment significantly reduced leaf injury and increased fresh weight, water content, and survival rate of alfalfa seedlings under alkaline condition (Wei et al., 2021). A long-term study on salt tolerance induced by ABA revealed the mechanism of ABA regulation at the molecular level and demonstrated that salt stress symptoms of *Vicia faba* could be alleviated by continuously changing transcription pattern of key genes and improving photosynthesis (Sagervanshi et al., 2021). A study on the effect of ABA on *Toona sinensis* seedlings under salt stress showed that ABA participated in signal transduction under NaCl stress, promoted synthesis of related proteins, maintained integrity of cell membrane structure, alleviated osmotic and ion stresses caused by excessive salt in plants, and maintained water balance of plants (Yao et al., 2020). However, effects of ABA treatment on photosynthetic parameters and antioxidant enzyme activities of watermelon seedlings remain to be elucidated.

Watermelon was used as the research material in this work to explore effects of different concentrations of exogenous ABA treatment on the growth and physiological indicators of watermelon seedlings under NaCl stress and obtain the appropriate ABA concentration. This study aims to provide a theoretical basis for reasonably solving the problem of salt injury in watermelon production.

Materials and Methods

Test materials

Seeds of watermelon cultivar ‘Zaojia’ were provided by New Century Agricultural High-technology Development Center of Changji, Xinjiang, China. ABA was purchased from Beijing Solarbio Science & Technology Co., Ltd., China.

Sowing

Seeds were first disinfected with 1% methanal solution for 30 min and then rinsed several times with sterile distilled water. Seeds were then incubated at 30℃ for germination after soaking for 6 h. Peat, vermiculite, and perlite were mixed at a volume ratio of 2:1:1 and then placed into plastic pots (10 cm×10 cm). Seeds were germinated and then sown into a substrate. The plastic pots were placed in a controlled growth chamber under conditions of 28℃/22℃ (day/night), relative humidity of 75% ± 5%, and photoperiods of 12 h (PAR 200 $\mu mol \cdot m^{-2} \cdot s^{-1}$) after sowing.

Experimental treatments

Watermelon seedlings with emergence of two true leaves were sprayed with different concentrations of exogenous ABA. Seedlings were irrigated with 1/2 strength Hoagland’s nutrient solution containing 180 mM of NaCl (50 mL per plant) after 1 day and then every day onward. The optimal concentration of NaCl stress was determined to be 180 mM from a pre-experiment. Another treatment without NaCl stress and ABA spraying was set as the control. Thirty plants were used for each treatment. The six treatments are listed below.

http://www.aloki.hu ● ISSN 1589 1623 (Print) ● ISSN 1785 0037 (Online)
DOI: http://dx.doi.org/10.15666/aeer/2005_45154524

Control: 0 mg·L^{-1} ABA + 0 mM NaCl
ABA0: 0 mg·L^{-1} ABA + 180 mM NaCl
ABA1: 1 mg·L^{-1} ABA + 180 mM NaCl
ABA5: 5 mg·L^{-1} ABA + 180 mM NaCl
ABA25: 25 mg·L^{-1} ABA + 180 mM NaCl
ABA50: 50 mg·L^{-1} ABA + 180 mM NaCl

Determination of indicators

Second leaves from the bottom of four randomly selected seedlings in each treatment were used for measurement after 6 days of NaCl stress. Chlorophyll fluorescence parameters, including maximum photosynthetic efficiency (*F*v/*F*m), actual photosynthetic efficiency (Y(II)), relative electron transport rate (rETR), photochemical quenching (qL), non-photochemical quenching (NPQ), quantum yield of regulated energy dissipation (Y(NPQ)), and quantum yield of non-regulated energy dissipation (Y(NO)) of photosystem II (PSII), were measured using a portable modulated chlorophyll fluorimeter (PAM-2500, Walz, Germany) after 30 min of dark adaptation.

Second leaves of randomly selected seedlings were harvested from each treatment after 6 days of NaCl stress. Superoxide dismutase (SOD) activity was measured by the method of Giannapoliti and Ries (1977); catalase (CAT) activity was determined according to Aebi's assay (1984); peroxidase (POD) activity was measured using a procedure described by Li and Yi (2012); the content of malondialdehyde (MDA) was assayed as described by Hodges et al. (1999). Measurement of these indicators was performed in three biological replicates using two plants per replicate.

Symptoms of leaf injury in each treatment were investigated and recorded and the salt injury index was calculated according to Zhen et al. (2010) after 10 days of NaCl stress. Meanwhile, 10 plants were randomly selected from each treatment for fresh and dry weight measurements.

Statistical analysis

The experimental data were statistically analyzed using two-way ANOVA through the SPSS software, version 27 (IBM SPSS, Chicago, USA). Duncan multiple range test was used to compare differences among different treatments.

Results

Effects of exogenous ABA on salt injury index and fresh and dry weights of watermelon seedlings under NaCl stress

The investigation and comparison of the salt injury index of watermelon seedlings pretreated with exogenous ABA under NaCl stress (*Figure 1*) revealed that the certain concentrations (1 and 5 mg·L^{-1}) of ABA treatment alleviated symptoms of salt injury and significantly reduced the salt injury index, which decreased by 26.8% and 19.6% compared with that at a concentration of 0 mg·L^{-1}, whereas an excessive concentration led to the aggravation of the degree of injury (*Figure 2A*). Data in *Figure 2B* showed a significant decrease in fresh and dry weights of watermelon seedlings under NaCl stress compared with the control, indicating that seedling growth was evidently inhibited. However, the inhibition effect was alleviated with a certain concentration of ABA. The fresh weight of seedlings treated with 1 mg·L^{-1} of ABA was significantly higher than

http://www.aloki.hu ● ISSN 1589 1623 (Print) ● ISSN 1785 0037 (Online)
DOI: http://dx.doi.org/10.15666/aeer/2005_45154524

that of seedlings treated with 0, 25, and 50 mg·L^{-1} of ABA but showed no significant differences compared with that of seedlings treated with 5 mg·L^{-1} of ABA. ABA treatment at a concentration of 1 mg·L^{-1} was significantly higher than that of 0 and 50 mg·L^{-1} while no significant differences were observed between the treatment of 1, 5, and 25 mg·L^{-1} for the dry weight of seedlings under NaCl stress. Overall, fresh and dry weights of watermelon seedlings under NaCl stress increased first and then decreased with increasing ABA treatment concentration.

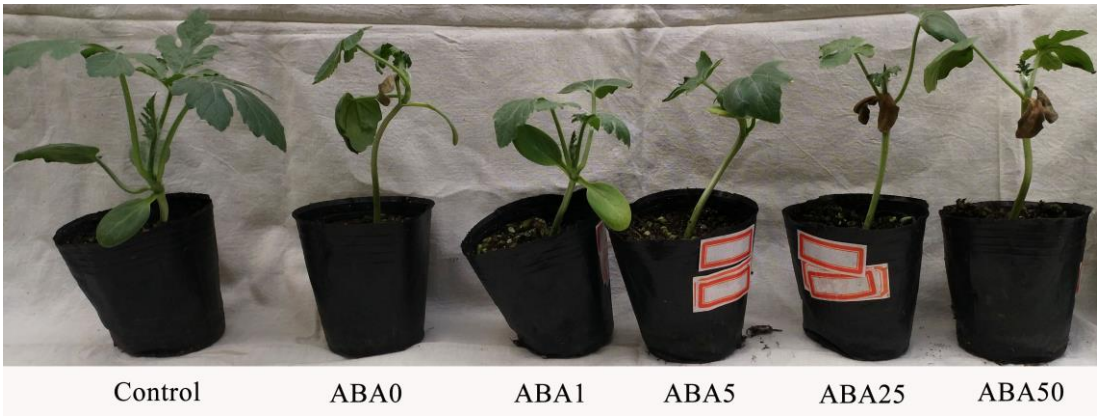

Figure 1. *Effect of ABA on watermelon seedling growth under NaCl stress. Control: seedlings grown in substrate under normal conditions; ABA0: seedlings grown in substrate with 180 mM NaCl; ABA1: seedlings pretreated with 1 mg·L^{-1} ABA, grown in substrate with 180 mM NaCl; ABA5: seedlings pretreated with 5 mg·L^{-1} ABA, grown in substrate with 180 mM NaCl; ABA25: seedlings pretreated with 25 mg·L^{-1} ABA, grown in substrate with 180 mM NaCl; ABA50: seedlings pretreated with 50 mg·L^{-1} ABA, grown in substrate with 180 mM NaCl. The photograph was taken after 10 days of NaCl stress*

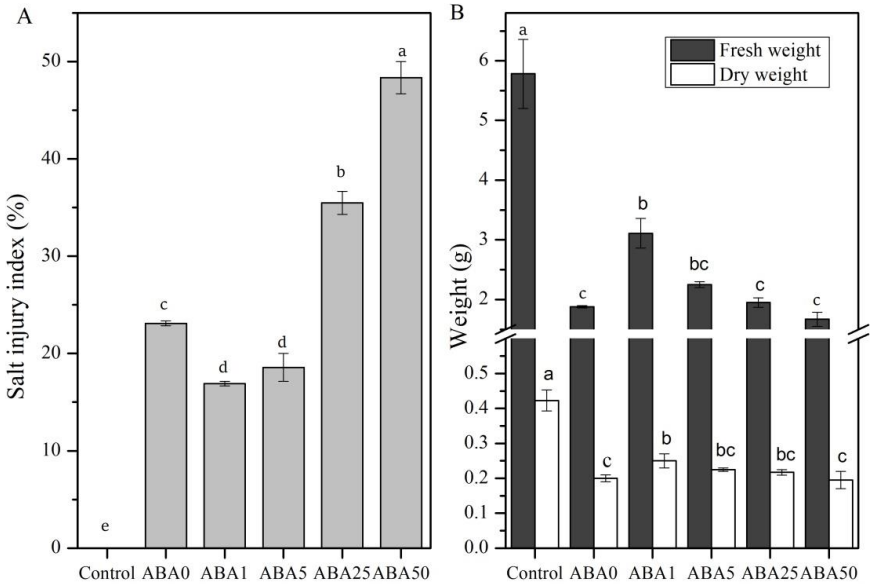

Figure 2. *Effects of exogenous ABA on salt injury index and fresh and dry weights of watermelon seedlings under NaCl stress. (A) Salt injury index; (B) Fresh weight and dry weight. Bars represent mean ± standard error of mean and those labeled with different lowercase letters are significantly different ($p < 0.05$)*

http://www.aloki.hu ● ISSN 1589 1623 (Print) ● ISSN 1785 0037 (Online)
DOI: http://dx.doi.org/10.15666/aeer/2005_45154524

Effects of exogenous ABA on chlorophyll fluorescence parameters of watermelon seedlings under NaCl stress

As shown in *Figure 3*, significant differences existed in chlorophyll fluorescence parameters of watermelon seedlings due to NaCl stress and exogenous ABA treatments. *Fv*/*Fm*, Y(II), rETR, and qL of watermelon seedlings were significantly lower than those of the control while NPQ, Y(NPQ), and Y(NO) were significantly higher than those of the control under NaCl stress alone. *Fv*/*Fm*, Y(II), rETR, and qL values increased initially and then decreased with the increase of ABA concentration. *Fv*/*Fm* was higher when the exogenous ABA concentration was 1 $mg \cdot L^{-1}$, while Y(II), rETR, and qL were higher when the exogenous ABA concentration was 25 $mg \cdot L^{-1}$. NPQ, Y(NPQ), and Y(NO) first decreased and then increased with the increase of exogenous ABA concentration. Y(NO) of ABA treatments at low and medium concentrations was significantly lower than that of the non-ABA treatment.

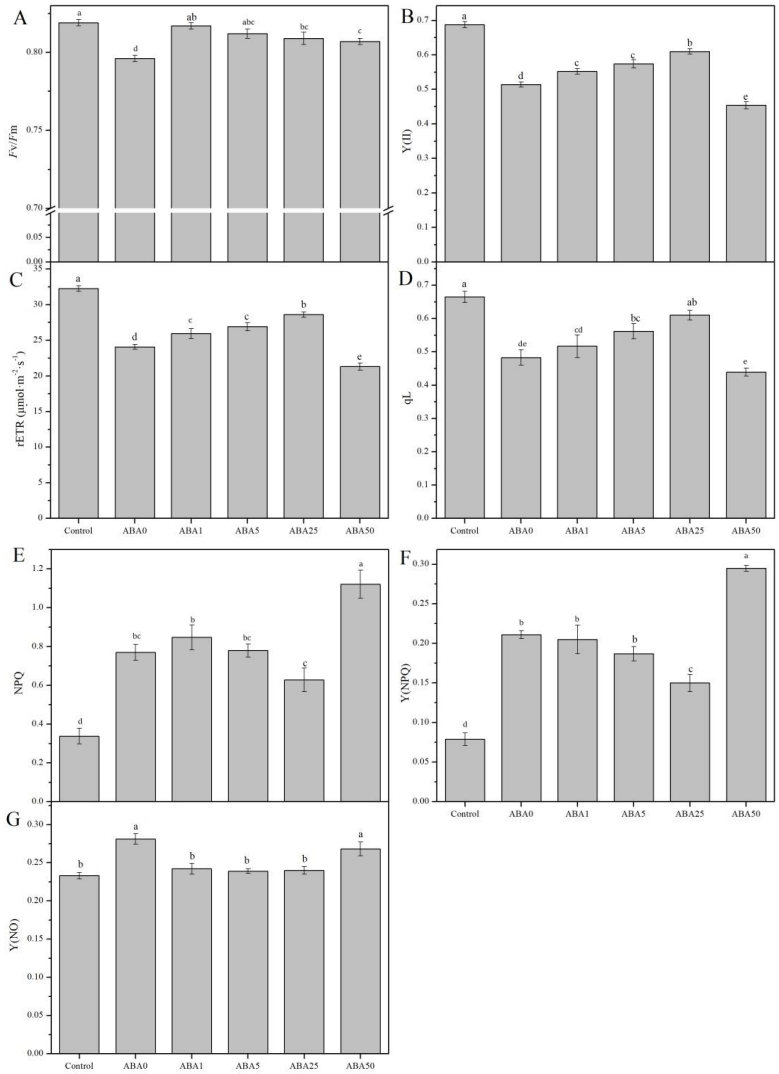

Figure 3. *Effect of exogenous ABA on chlorophyll fluorescence parameters of watermelon seedlings under NaCl stress. (A) Fv/Fm; (B) Y(II); (C) rETR; (D) qL; (E) NPQ; (F) Y(NPQ); (G) Y(NO). Bars represent mean ± standard error of mean and those labeled with different lowercase letters are significantly different ($p < 0.05$)*

http://www.aloki.hu ● ISSN 1589 1623 (Print) ● ISSN 1785 0037 (Online)
DOI: http://dx.doi.org/10.15666/aeer/2005_45154524

Effects of exogenous ABA on antioxidant enzyme activities and MDA content of watermelon seedlings under NaCl stress

Figure 4 shows that NaCl stress and exogenous ABA treatment exerted significant effects on antioxidant enzyme activities and MDA content of watermelon seedlings. SOD activity, POD activity, and MDA content of watermelon seedlings were significantly higher than those of the control under NaCl stress. SOD, CAT, and POD activities first increased and then decreased with the increase of ABA treatment concentration. SOD and CAT activities when seedlings were treated with 5 $mg \cdot L^{-1}$ of ABA were significantly higher than those of seedlings treated with 0 $mg \cdot L^{-1}$ of ABA. POD activity was higher in 25 $mg \cdot L^{-1}$ of ABA treatment than that in 0 $mg \cdot L^{-1}$ of ABA treatment. The results showed that activities of antioxidant enzymes can improve via exogenous ABA. By contrast, the content of MDA decreased first and then increased with the increase of ABA treatment concentration and reached a low value when the ABA treatment concentration was 1 $mg \cdot L^{-1}$, which indicated that a certain concentration of ABA treatment can reduce the MDA content.

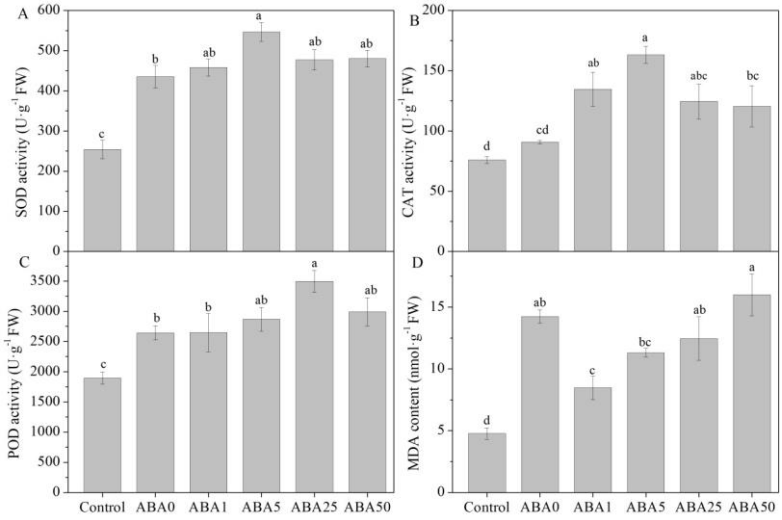

Figure 4. *Effects of exogenous ABA on antioxidant enzyme activities and MDA content of watermelon seedlings under NaCl stress. (A) SOD activity; (B) CAT activity; (C) POD activity; (D) MDA content. Bars represent mean ± standard error of mean and those labeled with different lowercase letters are significantly different ($p < 0.05$)*

Discussion

Salt stress is considered an obstruction of nonhalophytic plants that results in physiological drought of plants, reduces enzyme activity, changes membrane permeability, and affects the normal growth of plants (Hu et al., 2018). For example, germination of cottonseed was inhibited (Chen et al., 2021) and dry weight of tomato seedlings was significantly reduced under NaCl stress (Hu et al., 2021). Salt stress leads to the inhibition of absorption and transport of plant nutrients and results in the imbalance of mineral nutrients (Farissi et al., 2014). The low water potential in soil due to salt stress reduces not only the water potential (Flowers and Colmer, 2010) and stomatal conductance of leaves (Rahnama et al., 2010) but also the content of CO_2 entering stomata while inhibiting photosynthesis, thereby reducing carbon fixation and

http://www.aloki.hu ● ISSN 1589 1623 (Print) ● ISSN 1785 0037 (Online)
DOI: http://dx.doi.org/10.15666/aeer/2005_45154524

biomass accumulation (Munns, 2010; Setia et al., 2013). Watermelon seedlings in this experiment showed evident symptoms of salt injury and fresh and dry weights significantly reduced under NaCl stress. Low concentrations of ABA treatments reduced the salt injury index and increased fresh and dry weights of seedlings, thereby indicating enhanced growth compared with those under NaCl stress alone, which demonstrated that a certain concentration of ABA treatment can improve salt tolerance and alleviate the inhibition of salt stress on the growth of watermelon seedlings. However, an excessively high concentration of ABA exerted a negative effect on plant growth. This finding is similar to the results obtained in the experiment where ABA was applied to alleviate the toxicity of NaCl to grape plants. The weight, leaf number, leaf area, and bud dry weight of grape plants under NaCl stress were lower than those without NaCl stress. However, these indicators increased with an ABA treatment of 100 μM (Karimi et al., 2021). The study of physiological characteristics of Tartary buckwheat under salt stress demonstrated that applying an appropriate amount of ABA can improve seedling fresh weight and root activity (Lu et al., 2021). Similar results were also obtained for tomato (Martínez-Andújar et al., 2021; Xue et al., 2021).

Chlorophyll fluorescence kinetics is a fast, sensitive, and non-invasive approach often used to explore and evaluate the effect of environmental stress on the photosynthetic performance of plants (Krause and Weis, 1984; Baker, 2008). Each chlorophyll fluorescence parameter demonstrates a certain biological meaning. *F*v/*F*m and Y(II) represent the maximum and actual photosynthetic quantum yield of PSII, respectively; qL represents the proportion of light energy absorbed by PSII for photochemistry; rETR represents the relative electron transport rate; NPQ reflects the proportion of dissipation of excess light energy by heat emission; and Y(NPQ) and Y(NO) reflect the part of energy that is dissipated in the form of heat via the regulated mechanism and passively dissipated in the form of heat and fluorescence, respectively (Maxwell and Johnson, 2000; Klughammer and Schreiber, 2008; Kalaji et al., 2014). Values of *F*v/*F*m, Y(II), qL, and rETR of watermelon seedlings under NaCl stress were significantly lower than those of the control in this experiment. This finding suggested that PSII of leaves was damaged to a certain extent. However, the significant increase of chlorophyll fluorescence parameters after ABA treatment compared with those without ABA treatment suggested that a suitable concentration of ABA can enhance the photochemical efficiency of leaves. Small values of NPQ, Y(NPQ), and Y(NO) under a certain concentration of ABA treatment suggested low heat dissipation and high light energy conversion efficiency. These results indicated that ABA treatment can improve the photosynthetic efficiency to a certain extent and protect the photosynthesis of leaves, thereby alleviating the injury caused by excess light energy to photosynthetic apparatus of watermelon seedlings under NaCl stress.

SOD, CAT, and POD are key enzymes in the antioxidant defense system of scavenging reactive oxygen species in plants. The increase of activities of these enzymes indicates that the ability of scavenging reactive oxygen enhances and the membrane lipid peroxidation reduces to maintain the normal metabolism of cells (Moradi and Ismail, 2007). Activities of SOD, CAT, and POD of watermelon seedlings under NaCl stress increased and reflected the stress response of plants themselves in this study. The ABA treatment significantly increased the activities of SOD, CAT, and POD in watermelon seedlings under NaCl stress and effects increased first and then decreased with the increase of ABA concentration. MDA is the end product of membrane lipid peroxidation and its content is an important indicator of the degree of

http://www.aloki.hu ● ISSN 1589 1623 (Print) ● ISSN 1785 0037 (Online)
DOI: http://dx.doi.org/10.15666/aeer/2005_45154524

membrane lipid peroxidation directly related to the injury degree of cell membranes (Yang et al., 2012). In this experiment, MDA content in the leaves of watermelon seedlings was significantly elevated by NaCl stress compared with the control. This result suggested that NaCl stress caused injury to the cell membrane system. However, ABA protected the integrity of cell membranes to some extent by reducing membrane lipid peroxidation, inhibiting the accumulation of MDA, and thus effectively alleviating the injury of NaCl stress on watermelon seedlings.

Conclusions

ABA treatment within a certain concentration range can improve the salt tolerance in watermelon seedlings by increasing biomass of plants, exerting a beneficial effect on photosynthetic efficiency of leaves to a certain extent, enhancing activities of SOD, CAT, and POD, and reducing the content of MDA in plants, and thus effectively alleviate the injury of NaCl stress on watermelon seedlings. ABA treatment of 1 and 5 $mg \cdot L^{-1}$ exerted acceptable effects on alleviating the injury caused by NaCl stress; however, effects were very poor when the ABA concentration was increased to 50 $mg \cdot L^{-1}$. This finding indicated that low ABA concentrations exert alleviating effects whereas high ABA concentrations exert negative effects. ABA has protective effect on plants depending on the treatment concentration.

Acknowledgements. This work was supported by the Science and Technology Plan Project of Sichuan (grant number 2015NZ0039).

REFERENCES

[1] Aebi, H. (1984): Catalase in vitro. – Methods in enzymology 105: 121-126.
[2] Baker, N. R. (2008): Chlorophyll fluorescence: a probe of photosynthesis in vivo. – Annual Review of Plant Biology 59: 89-113.
[3] Chen, L., Lu, B., Liu, L. T., Duan, W. J., Jiang, D., Li, J., Zhang, K., Sun, H. C., Zhang, Y. J., Li, C. D., Bai, Z. Y. (2021): Melatonin promotes seed germination under salt stress by regulating ABA and GA3 in cotton (*Gossypium hirsutum* L.). – Plant Physiology and Biochemistry 162: 506-516.
[4] Farissi, M., Faghire, M., Bargaz, A., Bouizgaren, A., Makoudi, B., Sentenac, H., Ghoulam, C. (2014): Growth, nutrients concentrations, active enzymes involved in plant nutrition of alfalfa populations under saline conditions. – Journal of Agricultural Science & Technology 16: 301-314.
[5] Flowers, J., Colmer, D. (2010): Salinity tolerance in halophytes. – New Phytologist 179(4): 945-963.
[6] Giannapoliti, C. N., Ries, S. K. (1977): Superoxide dismutase: I. occurrence of higher plants. – Plant Physiology 59: 309-314.
[7] Hauser, F., Li, Z., Waadt, R., Schroeder, J. I. (2017): SnapShot: abscisic acid signaling. – Cell 171: 1708-1708.
[8] He, X. S., Xu, L. C., Pan, C., Gong, C., Wang, Y. J., Liu, X. L., Yu, Y. C. (2020): Drought resistance of *Camellia oleifera* under drought stress: changes in physiology and growth characteristics. – PloS one 15: e0235795.
[9] Hodges, D. M., De Long, J. M., Forney, C. F., Prange, R. K. (1999): Improving the thiobarbituric acid-reactive substances assay for estimating lipid peroxidation in plant tissues containing anthocyanin and other creaming compounds. – Planta 207: 604-611.

http://www.aloki.hu ● ISSN 1589 1623 (Print) ● ISSN 1785 0037 (Online)
DOI: http://dx.doi.org/10.15666/aeer/2005_45154524

[10] Hu, T., Zhang, G. X., Zheng, F. C., Cao, Y. (2018): Research progress of plant salt stress response. – Molecular Plant Breeding 16: 3006-3015.
[11] Hu, E. M., Liu, M., Zhou, R., Jiang, F. L., Sun, M. T., Wen, J. Q., Zhu, Z. H., Wu, Z. (2021): Relationship between melatonin and abscisic acid in response to salt stress of tomato. – Scientia Horticultura 285: 110176.
[12] Huan, H. F., Zhou, J. M., Duan, Z. Q., Wang, H. Y., Gao, Y. F. (2007): Contributions of greenhouse soil nutrients accumulation to the formation of the secondary salinization: a case study of Yixing City, China. – Agrochimica 51: 207-221.
[13] Jiang, M. Y., Zhang, J. H. (2004): Abscisic acid and antioxidant defense in plant cells. – Acta Botanica Sinica 46: 1-9.
[14] Kalaji, H. M., Schansker, G., Ladle, R. J., Goltsev, V., Bosa, K., Allakhverdiev, S. I., Zivcak, M. (2014): Frequently asked questions about in vivo chlorophyll fluorescence: practical issues. – Photosynthesis research 122: 121-158.
[15] Karimi, R., Ebrahimi, M., Amerian, M. (2021): Abscisic acid mitigates NaCl toxicity in grapevine by influencing phytochemical compounds and mineral nutrients in leaves. – Scientia Horticulturae 288: 110336.
[16] Klughammer, C., Schreiber, U. (2008): Complementary PS II quantum yields calculated from simple fluorescence parameters measured by PAM fluorometry and the saturation pulse method. – PAM application notes 1: 201-247.
[17] Krause, G. H., Weis, E. (1984): Chlorophyll fluorescence as a tool in plant physiology. – Photosynthesis research 5: 139-157.
[18] Li, L. H., Yi, H. L. (2012): Effect of sulfur dioxide on ROS production, gene expression and antioxidant enzyme activity of Arabidopsis plants. – Plant Physiology and Biochemistry 58: 46-53.
[19] Lu, Q. H., Wang, Y. Q., Xu, J. P., Cai, X. Y., Yang, H. B. (2021): Effect of ABA on physiological characteristics and expression of salt tolerance-related genes in Tartary buckwheat. – Acta Physiologiae Plantarum 43: 73.
[20] Martínez-Andújar, C., Martínez-Pérez, A., Albacete, A., Martínez-Melgarejo, P. A., Dodd, I. C., Thompson, A. J., Pérez-Alfocea, F. (2021): Overproduction of ABA in rootstocks alleviates salinity stress in tomato plants. – Plant, Cell & Environment 44: 2966-2986.
[21] Maxwell, K., Johnson, G. N. (2000): Chlorophyll fluorescence-a practical guide. – Journal of experimental botany 51: 659-668.
[22] Moradi, F., Ismail, A. M. (2007): Responses of photosynthesis, chlorophyll fluorescence and ROS-scavenging systems to salt stress during seedling and reproductive stages in rice. – Annals of botany 99: 1161-1173.
[23] Munns, R. (2010): Physiological processes limiting plant growth in saline soils: some dogmas and hypotheses. – Plant Cell & Environment 16: 15-24.
[24] Pontin, M., Murcia, G., Bottini, R., Fontana, A., Bolcato, L., Piccoli, P. (2021): Nitric oxide and abscisic acid regulate osmoprotective and antioxidative mechanisms related to water stress tolerance of grapevines. – Australian Journal of Grape and Wine Research 27: 392-405.
[25] Rahnama, A., James, A., Poustini, K., Munns, R. (2010): Stomatal conductance as a screen for osmotic stress tolerance in durum wheat growing in saline soil. – Functional Plant Biology 37: 255-263.
[26] Sagervanshi, A., Naeem, A., Geilfus, C., Kaiser, H., Muhling, K. H. (2021): One-time abscisic acid priming induces long-term salinity resistance in *Vicia faba*: Changes in key transcripts, metabolites, and ionic relations. – Physiologia Plantarum 172: 146-161.
[27] Setia, R., Gottschalk, P., Smith, P., Marschner, P., Baldock, J., Setia, D., Smith, J. (2013): Soil salinity decreases global soil organic carbon stocks. – Science of the Total Environment 465: 267-272.

http://www.aloki.hu ● ISSN 1589 1623 (Print) ● ISSN 1785 0037 (Online)
DOI: http://dx.doi.org/10.15666/aeer/2005_45154524

[28] Venzhik, Y., Talanova, V., Titov, A. (2016): The effect of abscisic acid on cold tolerance and chloroplasts ultrastructure in wheat under optimal and cold stress conditions. – Acta Physiologiae Plantarum 38: 63.
[29] Wei, T. J., Wang, M. M., Jin, Y. Y., Zhang, G. H., Liu, M., Yang, H. Y., Jiang, C. J., Liang, Z. W. (2021): Abscisic acid priming creates alkaline tolerance in Alfalfa seedlings (*Medicago sativa* L.). – Agriculture 11: 608.
[30] Wu, H., Li, H., Zhang, W., Tang, H., Yang, L. (2021): Transcriptional regulation and functional analysis of *Nicotiana tabacum* under salt and ABA stress. – Biochemical and Biophysical Research Communications 570: 110-116.
[31] Xue, F. L., Liu, W. L., Cao, H. L., Song, L. J., Ji, S. S., Tong, L. (2021): Stomatal conductance of tomato leaves is regulated by both abscisic acid and leaf water potential under combined water stress. – Physiologia Plantarum 172: 2070-2078.
[32] Yang, Z., Yu, J., Merewitz, E., Huang, B. (2012): Differential effects of abscisic acid and glycine betaine on physiological responses to drought and salinity stress for two perennial grass species. – Journal of the American Society for Horticultural Science 137: 96-106.
[33] Yao, X. M., Ou, C., Zhang, Y. L., Yang, L. M., Xu, M., Wang, Q. Q., Qu, C. Q. (2020): Effects of abscisic acid on ion absorption and photosynthesis of *Toona sinensis* seedlings under salt stress. – Journal of Northeast Forestry University 48: 27-32.
[34] Zhen, A., Bie, Z. L., Huang, Y., Liu, Z. X., Li, Q. (2010): Effects of scion and rootstock genotypes on the anti-oxidant defense systems of grafted cucumber seedlings under NaCl stress. – Soil Science and Plant Nutrition 56: 263-271.

APPENDIX

Two-way ANOVA (related to Figure 2)

Factors	P value (salt injury index)	P value (Fresh weight)	P value (dry weight)
NaCl	0.000	0.000	0.000
ABA	0.000	0.077	0.556

Two-way ANOVA (related to Figure 3)

Factors	P value (*Fv*/*Fm*)	P value (Y(II))	P value (rETR)	P value (qL)	P value (NPQ)	P value (Y(NPQ))	P value (Y(NO))
NaCl	0.000	0.000	0.000	0.000	0.000	0.000	0.000
ABA	0.002	0.000	0.000	0.001	0.000	0.000	0.001

Two-way ANOVA (related to Figure 4)

Factors	P value (SOD)	P value (CAT)	P value (POD)	P value (MDA)
NaCl	0.002	0.388	0.042	0.000
ABA	0.114	0.036	0.117	0.012

http://www.aloki.hu ● ISSN 1589 1623 (Print) ● ISSN 1785 0037 (Online)
DOI: http://dx.doi.org/10.15666/aeer/2005_45154524

RESEARCH ON WATER MOVEMENT PARAMETERS OF INFERIOR SOIL OF DIFFERENT SITE TYPES IN MINING AREAS

CHEN, G.[1] – LIU, H.[2*] – WEI, Z. M.[1]

[1]*Water Conservancy and Civil Engineering College of Inner Mongolia Agricultural University, Hohhot, China*

[2]*Institute of Water Resources for Pastoral Area Ministry of Water Resources, Hohhot, China*

**Corresponding author*
e-mail: liuhuycy@163.com; phone/fax: +86-471-459-0554

(Received 16th May 2022; accepted 26th Jul 2022)

Abstract. The present research aims to explore the difference in water movement parameters of inferior soils in different site types; the undisturbed soil, mine-accumulated soil and ecologically modified soil in Wujiata Mining Area, Yiqi, Erdos City, Inner Mongolia, were taken as the research objects. The soil texture, soil diffusivity and water characteristic curve were measured through laboratory tests, and the soil water characteristic curve model suitable for inferior soils in mining areas was selected, and the variation laws of soil hydrodynamic characteristics such as water retention characteristics, effective water content and water conductivity characteristics of inferior soils in different site types were discussed. The Van Genuchten (VG) model shows the best fitting effect on the soil water characteristic curve model of inferior soils of different site types in mining areas. Under the same pressure head, the water characteristic curves of different horizons of soil are quite different; under the condition of 0-7000 cm pressure head, the water-holding capacity of undisturbed soil, mine-accumulated soil and ecologically modified soil decreases with the increase of depth. The soil water characteristic curve changes greatly in the low-pressure head section (<1000 cm) and relatively gently in the middle and high-pressure head section (>1000 cm). The water-holding capacity of ecologically modified soil is obviously enhanced. Ecological restoration can improve the poor soil structure in the research area, optimize the soil structure, and control the soil erosion obviously.
Keywords: *inferior soil, soil water, water characteristic curve, unsaturated hydraulic conductivity*

Introduction

Soil water is an important part of water balance and water cycle, and the research on soil water movement and its law has always been highly attended in soil water research (Sun et al., 2021; Li and Song, 2020; Zhang and Wang, 2003). With the continuous integration and development of computer science and "3S" and other fields, the research direction of soil water has been further expanded. The traditional soil water research based on single-point infiltration process and indoor simulation has gradually changed into the improvement and coupling of soil water movement model. On the other hand, some scholars began to focus on numerical simulation at the scale of "watershed" and studied soil water movement by combining with "3S" technology (Li et al., 2015; Wei et al., 2015; Zhang and Wang, 2007). The hydrus-1d model and the RETC software are often used to determine the unsaturated water movement parameters of the soil (Ma et al., 2017) by means of capacitance and water content (Wang et al., 2021), to obtain the infiltration characteristics of the soil and to analyze the differences (Zhao et al., 2022; Dong et al., 2017) in the hydraulic characteristics of different soil layers (Hu et al., 2017; Gu et al., 2021). hydrus-1d models are often used to study the infiltration patterns of soil water (Pan et al., 2021) and to investigate the influence of soil hydraulic parameters on the long-range correlation of soil water under different climatic conditions (Li et al., 2022).

http://www.aloki.hu ● ISSN 1589 1623 (Print) ● ISSN 1785 0037 (Online)
DOI: http://dx.doi.org/10.15666/aeer/2005_45254537

The results show that soil structure and soil texture have an obvious influence on soil water movement. Excellent soil texture and soil structure are capable obviously promoting soil water movement, so many researchers have made researches on the topic, but the research on poor soil is rare. Soil in mining areas can be regarded as a typical representative of poor-quality soil because of the damage of soil structure during excavation. Research on the water movement and its law of inferior soil plays an important role in researching the ecological restoration of mining areas, and has a great influence on maintaining the structural and functional stability of ecosystems (Yadav and Kumar, 2017; Lehmann et al., 2018; Dong et al., 2018).

Aiming at the soil environmental problems caused by open-pit mining in Western Inner Mongolia, the present research plans to take undisturbed soil, mine-accumulated soil and ecologically modified soil in Wujiata mining area of Yiqi, Erdos City as the research objects, set up sample plots in soil areas with different site types, and take stratified sampling. By measuring the soil texture, soil diffusivity and water characteristic curve of inferior soil in different site types in the mining area, the change laws of soil hydrodynamic characteristics, such as water holding or retention characteristics, effective water content and hydraulic conductivity characteristics of inferior soils in different site types can be analyzed. Then, the physical and chemical properties of different soils and their correlation can be further studied, thereby finally concluding the change laws and response mechanisms of soil physical and chemical properties, which served as theoretical support and scientific basis for ecosystem restoration in mining areas.

Research methods and data sources

Overview of the research area

The research area is located in Wujiata Mining Area (39 15’ 16 “N, 110 05’ 56” E), Yiqi, Erdos City, Inner Mongolia. The research area is located in Mu Us Sandland, with fragile ecology, low annual average temperature of only 7.3 ℃, as well as low annual precipitation, ranging from 325 mm to 460 mm all the year round, as a semi-arid continental monsoon climate. It is located in the sandy land and has a long sunshine exposure time, with its high annual evaporation ranging from 2297.4 mm to 2838.7 mm, its annual average wind speed of 3.6 $m \cdot s^{-1}$. The terrain in the research area is complex, mainly hills and valleys. Due to the influence of geographical distribution, geomorphology and hydrogeological conditions, zonal soil and hidden soil are distributed in the research area, and aeolian sand accounts for about 70% of the research area, which is the main soil type.

Research methods

In this research, samples were collected and tested from three different site types: undisturbed soil, mine-accumulated soil and ecologically modified soil. The sampling period is 2018. The sampling point map is shown in *Figure 1*. The vegetation in the undisturbed soil sample plot is a mixed structure of natural grassland and artificial shrubs, and the artificial shrubs are distributed in intermittent strips, mainly *Salix psammophila* and *Caragana korshinskii*. After two years of natural recovery, the soil sample plot is covered with short-lived plants such as *Sarcophora*, associated *Corispermum declinatum*, etc. The vegetation coverage is less than 15%, the height is below 20 cm, and it is

http://www.aloki.hu ● ISSN 1589 1623 (Print) ● ISSN 1785 0037 (Online)
DOI: http://dx.doi.org/10.15666/aeer/2005_45254537

distributed in patches, and there is almost no vegetation in some sections. The soil is bare and wind erosion is extremely serious. Since 2011, the ecological soil sample plot has been transformed by adopting the biological control measures, which combine arbor, shrub and grass. Arbors and *Salix psammophila* grids have been planted on the slope of the dump to prevent wind and sand. Grass seeds, *Caragana korshinskii* and sea buckthorn (*Hippophae rhamnoides* L.) have been planted in the grids, and pine trees have been planted on both sides of the road to form a green area where twisted strips, sea buckthorn (*Hippophae rhamnoides* L.) and grasses are planted.

Figure 1. *The sampling point map*

The undisturbed soil sampling point is numbered as 1#, the mine-accumulated soil sampling point is numbered as 2#, and the ecologically modified soil sampling point is numbered as 3#. Each sampling point takes 30 cm as a horizon of soil, with 3 horizons in total. Three bags of samples are randomly collected from each soil horizon in each sampling point. During sampling, the ring knife method is applied to measure the dry bulk density of undisturbed soil, mine-accumulated soil and ecologically modified soil. The mechanical composition of soil is measured and analyzed by laser particle size analyzer, the soil water diffusivity is measured by horizontal soil column method, the semi-infinite horizontal soil column imbibition experiment, and the soil pressure head and water content are measured by pressure film method. In RETC software, Van Genuchten (VG) and Brooks & Corey (BC) models are used to fit the soil water characteristic curve. The expression formula of VG and BC models are:

(1) Van Genuchten (VG) model:

$$\theta(h) = \theta_{res} + \frac{\theta_{sat} - \theta_{res}}{\left(1 + \left|\alpha h\right|^{n}\right)^{\frac{n-1}{n}}} \quad \text{(Eq.1)}$$

where θ represents the water content, $cm^3 \cdot cm^{-3}$; θ_{res} represents the residual water content, $cm^3 \cdot cm^{-3}$; θ_{sat} represents saturated water content, $cm^3 \cdot cm^{-3}$; h represents the pressure head, cm; and α and n are empirical fitting parameters.

http://www.aloki.hu ● ISSN 1589 1623 (Print) ● ISSN 1785 0037 (Online)
DOI: http://dx.doi.org/10.15666/aeer/2005_45254537

(2) Brooks & Corey (BC) model:

$$\theta = \begin{cases} \theta_r + (\theta_s - \theta_r)(\alpha h)^{-m} & (\alpha h > 1) \\ \theta_s & (\alpha h \le 1) \end{cases} \quad \text{(Eq.2)}$$

where θ represents the water content, $cm^3 \cdot cm^{-3}$; θ_r represents the residual water content, $cm^3 \cdot cm^{-3}$; θ_s represents saturated water content, $cm^3 \cdot cm^{-3}$; h represents the pressure head, cm; and α and n are empirical fitting parameters.

Results and analysis

Soil texture

Because of the different site types of inferior soil, the bulk density of soil shows obvious differences in different soil horizons; but the bulk density of the same soil has little difference in different soil horizons. The dry bulk density of different horizons of undisturbed soil is as follows: 1.778 $g \cdot cm^{-3}$, 1.751 $g \cdot cm^{-3}$, 1.499 $g \cdot cm^{-3}$; the dry bulk density of different soil horizons of mine-accumulated soil is as follows: 1.747 $g \cdot cm^{-3}$, 1.563 $g \cdot cm^{-3}$, 1.468 $g \cdot cm^{-3}$; the dry bulk density of different soil horizons of ecologically modified soil is as follows: 1.602 $g \cdot cm^{-3}$, 1.665 $g \cdot cm^{-3}$, 1.578 $g \cdot cm^{-3}$; the average dry bulk density of each soil sample is as follows: 1.676 g/cm^{-3}, 1.593 g/cm^{-3} and 1.615 $g \cdot cm^{-3}$. It can be seen that the average bulk density of undisturbed soil in the mining area is higher than that of ecologically improved soil and mine-accumulated soil. Three kinds of dry bulk density all change with the change of soil horizon, and the general change laws of dry bulk density of each soil sample according to the depth of soil horizon are detailed as follows: 0 ~ 30 cm > 30 ~ 60 cm > 60 ~ 90 cm.

The content of soil particle size components measured by soil particle size experiment is shown in *Table 1,* and the soil texture is analyzed in combination with the classification map of American soil texture. It is obvious from *Table 1* that the three kinds of soil samples belong to sandy soil, and in terms of the content, grit > powder > cosmid.

Table 1. *Composition of soil particles*

Soil sample	Soil horizon (cm)	Grit (%)	Powder particle (%)	Cosmid (%)
1#	0 ~ 30	95.73	3.97	0.30
	30 ~ 60	94.48	5.28	0.24
	60 ~ 90	95.62	4.17	0.21
2#	0 ~ 30	87.47	11.89	0.64
	30 ~ 60	86.33	13.07	0.60
	60 ~ 90	88.54	10.95	0.51
3#	0 ~ 30	95.72	4.11	0.17
	30 ~ 60	96.98	2.92	0.10
	60 ~ 90	98.29	1.61	0.10

The average particle composition of undisturbed soil is 95.28% grit, 4.47% powder and 0.25% cosmid; the average particle composition of mine-accumulated soil is 87.45%

http://www.aloki.hu ● ISSN 1589 1623 (Print) ● ISSN 1785 0037 (Online)
DOI: http://dx.doi.org/10.15666/aeer/2005_45254537

grit, 11.97% powder and 0.58% cosmid; the average particle composition of ecologically improved soil is 97.00% grit, 2.88% powder and 0.12% cosmid. Ecologically modified soil has the highest content of grit, followed by undisturbed soil, and finally mine-accumulated soil. With the increase of the depth, in ecological modified soil the particle composition of grit gradually increases, and the particle composition of powder and cosmid gradually decreases; in undisturbed soil and mine-mine-accumulated soil, the particle composition of grit decreases at first and then increases, while that of powder increases at first and then decreases, while that of cosmid decreases, like that of ecological modified soil, but when the particle composition of cosmid in ecological modified soil decreases to a certain value, it tends to become stable. Ecological restoration has improved the soil particle size and pore structure in the mining area, and the soil structure has undergone favorable changes, which have been significantly improved (Song et al., 2022).

Model fitting of soil moisture characteristic curve

The pressure film instrument method is used to measure the soil pressure head and water content in the mining area. Taking the water content θ as the ordinate and the pressure head h as the abscissa, the soil water characteristic curves of three soils at different depths of 0 ~ 30 cm, 30 ~ 60 cm and 60 ~ 90 cm are shown in *Figures 2*, *3* and *4*.

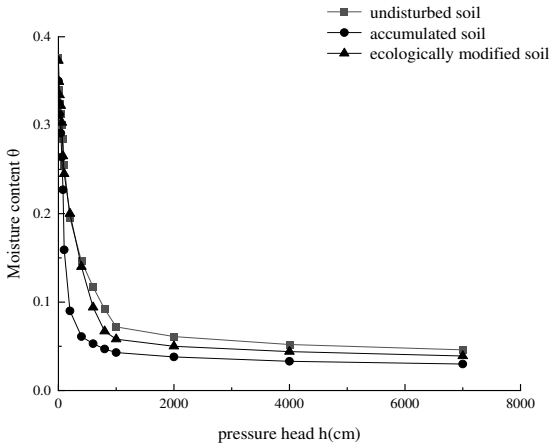

Figure 2. *0 ~ 30 cm soil moisture characteristic curve*

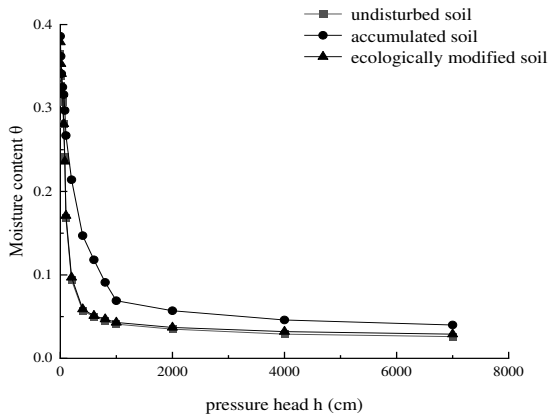

Figure 3. *30 ~ 60 cm soil moisture characteristic curve*

http://www.aloki.hu ● ISSN 1589 1623 (Print) ● ISSN 1785 0037 (Online)
DOI: http://dx.doi.org/10.15666/aeer/2005_45254537

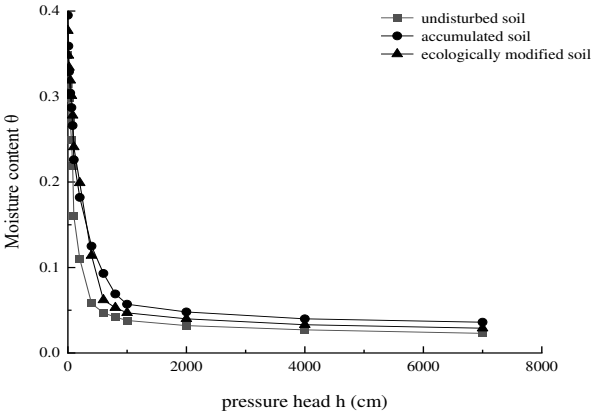

Figure 4. *60 ~ 90 cm soil moisture characteristic curve*

It is shown from *Figures 2-4*: with the increase of pressure head, the wet weight of soil gradually decreases, and the soil moisture content gradually decreases. The soil moisture content at the buried depth of 0 ~ 30 cm is higher than 30 ~ 60 cm and 60 ~ 90 cm. The minimum pressure head is 0 cm and the maximum pressure head is 7000 cm. Under different soil depths, the change of soil water content of undisturbed soil, mine-accumulated soil and ecological modified soil is the most obvious at the pressure head of 100 cm.

The overall change trend of soil water characteristic curve is basically the same, and three different types of inferior soils are all in "L" shape at the same depth. The water content θ decreases with the increase of the pressure head. 1000 cm pressure head is an obvious milestone. Before the pressure head reaches this milestone, the water content θ decreases obviously, and the curve shows a rapid downward trend. After that, the change is relatively gentle, and the curve begins to show a horizontal trend. Separately, in the same depth soil horizon, obvious differences can be observed in the water characteristic curves of different kinds of site soils. When the pressure head is the same (for example, 2000 cm at the depth of 0 ~ 30 cm), the water content of undisturbed soil, mine-accumulated soil and ecologically modified soil are 0.038, 0.061 and 0.05 respectively. The soil water characteristic curve changes greatly in the low-pressure head section (<1000 cm) and relatively gently in the middle and high-pressure head section (>1000 cm).

It can be clearly seen from the figure that the ecological restoration has an impact on the soil water characteristic curve, and it moves up as a whole compared with the soil water characteristic curve of mine-accumulated soil. In another word, under the same soil water suction, the soil moisture content of ecologically modified soil is larger than that of mine-accumulated soil and less than that of undisturbed soil. The main reason is that, after ecological restoration, the soil pore structure is improved, the soil porosity is reduced, and the water retention is enhanced. Compared with the original soil, there is still a gap, but the overall improvement has been obvious.

Soil water characteristic curve reflects the relationship between soil water and potential energy, and fully shows the dynamic characteristics of soil water, so it can be called an important basis for researching and analyzing soil water (Su et al., 2018; Fredlund, 2019; Lu et al., 2014). Soil structure, texture and other factors have great influence on soil water, so it is often necessary to combine these factors when analyzing

http://www.aloki.hu ● ISSN 1589 1623 (Print) ● ISSN 1785 0037 (Online)
DOI: http://dx.doi.org/10.15666/aeer/2005_45254537

soil water characteristic curve (Lu and Likos, 2006). Under the same pressure head, the water content of mine-accumulated soil decreases rapidly. Combined with the soil texture, it can be clearly shown that the mine-accumulated soil has a high content of powder particles. In this case, compared with the other two kinds of soils, there are more macropores in the overall structure, which leads to this situation. In the low-pressure head section (<1000 cm), the part of the curve shows a steep and straight trend. With the increase of pressure head, the curve trend changes gently, and the overall change trend is obvious.

In RETC software, Van Genuchten (VG) model and Brooks & Corey (BC) model are used to fit the soil water characteristic curves for three site types.

It is shown from *Table 2* that the R^2 of each soil sample at different soil depths is larger, reaching above 0.99, with a high degree of fitting. It shows that Van Genuchten (VG) model can simulate the soil water characteristic curves of three site types. The residual water content θ_{sat} of all soil samples decreases with the depth, except for the depth of 30 ~ 60 cm in ecologically modified soil, with the most drastic decrease from the depth of 30 ~ 60 cm to the depth of 60 ~ 90 cm, and the minimum residual water content θ_{sat} of mine-accumulated soil at the depth of 60 ~ 90 cm is only 0.0001. Compared with the undisturbed soil, the saturated water content (θ_{sat}) of the mine-accumulated soil and the ecologically modified soil shows a rising trend, and the residual water content θ_{sat} of the mine-accumulated soil at the depth of 60 ~ 90 cm is the largest, 0.36702.

Table 2. *Fitting parameters of Van Genuchten (VG) model*

Soil sample	Soil horizon (cm)	θ_{res}	θ_{sat}	α	n	R^2
1#	0 ~ 30	0.03645	0.33211	0.01402	2.56173	0.99384
	30 ~ 60	0.03334	0.34623	0.01337	2.61185	0.99394
	60 ~ 90	0.02089	0.32776	0.01647	2.03820	0.99267
2#	0 ~ 30	0.02060	0.35582	0.01351	1.53046	0.99284
	30 ~ 60	0.01168	0.36702	0.01118	1.64694	0.99448
	60 ~ 90	0.00001	0.37531	0.01954	1.55163	0.99192
3#	0 ~ 30	0.01533	0.35756	0.01235	1.70200	0.99225
	30 ~ 60	0.03478	0.36187	0..01448	2.51940	0.99596
	60 ~ 90	0.01285	0.35464	0.01069	1.86914	0.99092

It can be shown from *Table 3* that R^2 of fitting parameters of Brooks & Corey (BC) model is all up to 0.97, which is less than Van Genuchten (VG) model, but it can also simulate soil moisture characteristic curve well. The residual water content (θres) is obviously different from Van Genuchten (VG) model, and it is 0.00001 for multi-horizon soil. There is little difference in saturated water content. Compared with undisturbed soil, the saturated water content (θsat) of mine-accumulated soil and ecologically modified soil shows a rising trend. The value α is the reciprocal of soil water suction value at the inflection point when the water characteristic curve is close to saturation. The larger the value α is, the worse the soil water holding capacity is. It is shown from the parameters fitted by the two models, α of the ecologically modified soil at the depth of 0 ~ 30 cm and 60 ~ 90 cm is less than that of the mine-accumulated soil, and the water holding capacity is better, but the depth of 30 ~ 60 cm is the opposite. m and n are shape coefficients, reflecting the bending degree of the fitted curve. Compared

http://www.aloki.hu ● ISSN 1589 1623 (Print) ● ISSN 1785 0037 (Online)
DOI: http://dx.doi.org/10.15666/aeer/2005_45254537

with the undisturbed soil, the other two soils show a downward trend, and the mine-accumulated soil is less than the other two soils at different depths. On the whole, the Van Genuchten (VG) model shows a better fitting effect on soil water characteristic curves of three site types in mining areas.

Table 3. *Fitting parameters of the Brooks & Corey (BC) model*

Soil sample	Soil horizon (cm)	θ_{res}	θ_{sat}	α	m	R^2
1#	0 ~ 30	0.03076	0.31950	0.01972	1.08333	0.98884
	30 ~ 60	0.00884	0.34333	0.02613	0.70469	0.98261
	60 ~ 90	0.00001	0.32033	0.02921	0.59970	0.98261
2#	0 ~ 30	0.00001	0.34667	0.02538	0.39795	0.97830
	30 ~ 60	0.00001	0.35350	0.01901	0.46268	0.98403
	60 ~ 90	0.00001	0.36100	0.03006	0.44907	0.97842
3#	0 ~ 30	0.00001	0.35200	0.02450	0.44706	0.98019
	30 ~ 60	0.01372	0.35767	0.02692	0.73615	0.98718
	60 ~ 90	0.00001	0.34450	0.01906	0.57468	0.98008

Soil diffusivity

It is shown from the measured data that the soil water diffusivity decreases with the decrease of water content. Further comparative analysis of soil samples concludes the relationship between soil diffusivity $D(\theta)$ and water content θ in three different sites, as shown in *Figures 5*, *6* and *7*.

It can be clearly shown from the figure that the soil curves of each site type have a good exponential relationship. Obviously, the diffusivity is proportional to the water content θ, but when it reaches a critical value at a certain point, the critical values of different soil types at different depths are different. When it exceeds this critical value, the diffusivity begins to show a downward trend. The soil diffusivity $D(\theta)$ and water content of the same site type are significantly different at different depths ($p < 0.05$). The difference between curves of different site soils at the same depth is also very obvious.

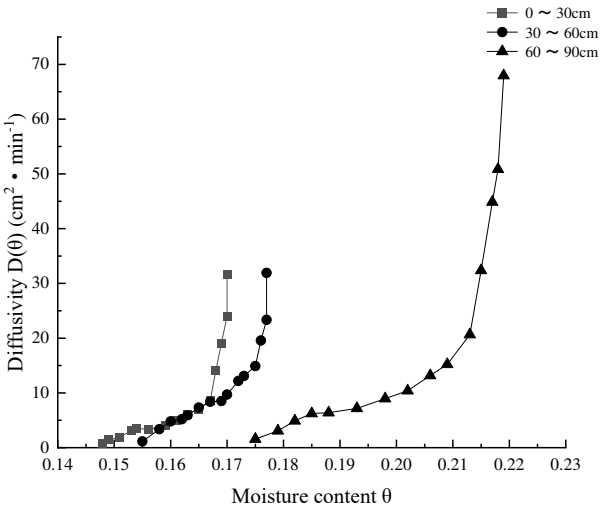

Figure 5. *The relationship between soil water diffusion rate D (θ) and θ at different depths of undisturbed soil*

http://www.aloki.hu ● ISSN 1589 1623 (Print) ● ISSN 1785 0037 (Online)
DOI: http://dx.doi.org/10.15666/aeer/2005_45254537

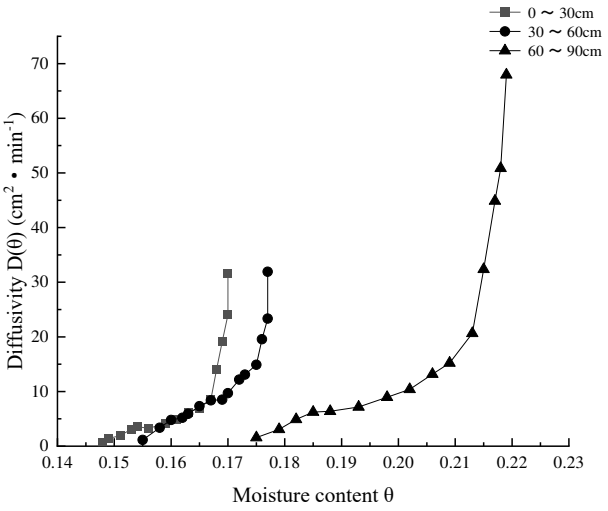

Figure 6. *The relationship between soil water diffusion rate D (θ) and θ at different depths of mine-accumulated soil*

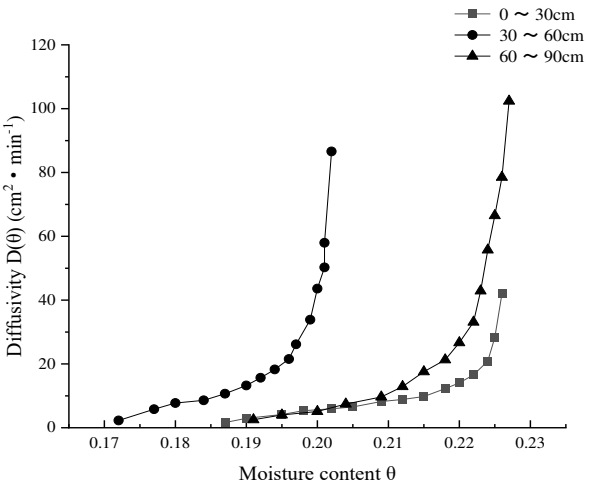

Figure 7. *The relationship between water diffusion rate D (θ) and θ in different depths of ecologically modified soil*

Comparing the soils of three site types, it is obvious that: The maximum diffusivity of the deposited soil is 268.957 $cm^2 \cdot min^{-1}$ at the depth of 30 ~ 60 cm. Among the three soils, the undisturbed soil has the smallest diffusivity, and the diffusivity of each horizon of soil is less than 70 $cm^2 \cdot min^{-1}$, and that at the depth of 0 ~ 60 cm is less than 32 $cm^2 \cdot min^{-1}$. Compared with the mine-accumulated soil, the diffusion rate of the ecologically improved soil at the depth of 30 ~ 60 cm decreased to 86.579 $cm^2 \cdot min^{-1}$, with a decrease rate of 67%, after ecological restoration measures combining arbor, shrub and grass are taken.

Firstly, it is analyzed from the perspective of soil physical properties. Soil can affect the diffusivity through its surface soil solid particles and capillary pores, and different soil texture will have different effects on diffusivity (He and Wang, 2019; Carrick et al., 2011; Laio et al., 2009; Laio, 2006; Kawamoto et al., 2006). The adsorption of soil is directly proportional to its surface area. When the θ increment is the same, the water in

http://www.aloki.hu ● ISSN 1589 1623 (Print) ● ISSN 1785 0037 (Online)
DOI: http://dx.doi.org/10.15666/aeer/2005_45254537

sandy soil spreads faster because of matrix suction, while cohesive soil does the opposite. Secondly, the more and larger the pores in the soil, the more obvious the effect of promoting the diffusion of water is. When θ decreases, the force applied changes from capillary force to adsorption force, and the water in the soil also changes from capillary water to bound water. At the same time, the binding force on the surface of soil particles increases, which is unfavorable to the diffusion of water. On the contrary, when θ increases, the number of water-filled capillaries in soil increases, and the pores become larger, which further promotes the diffusion of water.

The relationship between diffusivity $D(\theta)$ and water content θ in each soil horizon is established by using exponential equation and measured data, and the curve fitting is performed according to the data of diffusivity $D(\theta)$ and water content θ. The fitting results are shown in *Table 4*.

Table 4. *Diffusion rate fitting results*

Soil sample	Soil horizon (cm)	Fitting formula	R^2
1#	0 ~ 30	$D(\theta) = 1E-08e^{70.282\theta}$	0.9266
	30 ~ 60	$D(\theta) = 1E-07e^{62.127\theta}$	0.9185
	60 ~ 90	$D(\theta) = 2E-05e^{44.876\theta}$	0.9319
2#	0 ~ 30	$D(\theta) = 1E-04e^{39.748\theta}$	0.9275
	30 ~ 60	$D(\theta) = 4E-05e^{43.234\theta}$	0.9272
	60 ~ 90	$D(\theta) = 3E-06e^{45.719\theta}$	0.9613
3#	0 ~ 30	$D(\theta) = 1E-05e^{39.729\theta}$	0.9451
	30 ~ 60	$D(\theta) = 1E-07e^{59.589\theta}$	0.9479
	60 ~ 90	$D(\theta) = 3E-08e^{59.583\theta}$	0.9627

Generally, the diffusivity is affected by soil water content, bulk density, particle composition, porosity and other factors. Under a certain dry bulk density, the more cosmid content, the greater capillary porosity, the faster diffusion rate and the less water content. Similarly, under a certain cosmid content, the larger the dry bulk density, the larger the capillary porosity, the faster the diffusion rate and the less the water content.

Discussion

In arid and semi-arid areas, soil water is often the most important limiting factor that can affect ecology. The structural and functional stability of the ecosystem is closely related to it. Mining in the mining area will cause the destruction of soil structure, and change in the soil structure, porosity and moisture content. With the changes of these factors, the water movement will also change, thereby causing serious damage to surface water and underground water system. The research results of Lv Jingjie et al. show that the soil moisture content in the mine-accumulated soil area decreases. Compared with the other two site types, the drastic spatial variation worsens the living environment of the surface vegetation and seriously damages the surface landscape (Ma et al., 2013; Zhang et al., 2009; Lv et al., 2005).

As an index of basic physical properties of soil, soil bulk density can significantly affect soil water permeability, air permeability, water holding capacity and solute transport. The soil bulk density of different soil horizons of mine-accumulated soil is

http://www.aloki.hu ● ISSN 1589 1623 (Print) ● ISSN 1785 0037 (Online)
DOI: http://dx.doi.org/10.15666/aeer/2005_45254537

less than that of undisturbed soil and ecologically modified soil. With the stability of soil subsidence, the soil bulk density difference with other two site types tends to decrease. Mining subsidence in mining area significantly affects the physical characteristics of surface soil. It is considered that subsidence causes the migration of fine-grained materials on soil slopes, resulting in sandy phenomenon, among which soil water content is the most affected factor. Relevant research shows that many factors affect the characteristic curve of soil water, among which porosity, bulk density, texture and human activities are regarded as the major affecting factors. There is a good positive correlation between unsaturated soil diffusivity and water content θ, and the former can increase with the increase of θ. The water content θ is greatly influenced by soil texture, bulk density and other factors, and then has different effects on diffusivity.

After two years' natural recovery, the mine-accumulated soil in Wujiata mining area has been covered by short-lived plants such as *Chenopodium album*, *Chenopodium glabra*, *Salsola salsa*, and *Salsola collina*. The vegetation coverage is less than 15%, and the height is below 20 cm. the plants are distributed in patches, and there is almost no vegetation in some sections. At present, it is still in the quicksand vegetation structure dominated by pioneer plants. After seven years of ecological restoration, the vegetation structure of the modified soil sample plot is close to the original soil, and the soil erosion is basically controlled. However, it has not reached the level of undisturbed soil landform vegetation, it still needs longer time to recover.

Conclusions

In this paper, the undisturbed soil, mine-accumulated soil and ecologically modified soil in Wujiata mining area, Yiqi, Erdos City, Inner Mongolia are selected as three inferior soils with different site types. All three soils are sandy.

With the increase of the depth of the three inferior soils, the relative content of cosmid in the soil structure decreases, and the bulk density also decreases. Van Genuchten (VG) model shows the best effect on simulating the water characteristic curve of inferior soil in different site types in the mining area. The soil moisture characteristic curves of three different soils in different depth horizons show the same trend as a whole, and all of them show a good "L" shape. When the inferior soil is pressurized, the water content is inversely proportional to it, and then decreases. Under the condition of 0-7000 cm pressure head, the water content θ of undisturbed soil, mine-mine-accumulated soil and ecologically modified soil decreases with the increase of depth, or the water holding capacity is inversely related to the depth. The soil water characteristic curve changes greatly in the low-pressure head section (<1000 cm) and relatively gently in the middle and high-pressure head section (>1000 cm). The water-holding capacity of the ecologically modified soil is enhanced. Ecological restoration is capable of improving the inferior soil structure in the research area, and optimizing the overall structure obviously; making the vegetation structure close to the original soil vegetation, enhancing the ability to regulate water, and controlling the soil erosion basically.

REFERENCES

[1] Carrick, S., Buchan, G., Almond, P., Smith, N. (2011): Atypical early-time infiltration into a structured soil near field capacity: The dynamic interplay between sorptivity, hydrophobicity, and air encapsulation. – Geoderma 160(3-4): 579-89.

http://www.aloki.hu ● ISSN 1589 1623 (Print) ● ISSN 1785 0037 (Online)
DOI: http://dx.doi.org/10.15666/aeer/2005_45254537

[2] Dong, Y. Y., Hu, S. J., Zhao, C. Y., Zhu, H., Wang, D. D., Ding, Z. Y. (2017): One-dimensional horizontal infiltration test for determining permeability coefficient of aeolian sandy soil in interdune at the southern edge of Gurbantünggüt Desert. – Arid Land Ceography 40(04): 729-736.
[3] Dong, S. Y., Guo, Y., Yu, X. (2018): Method for quick prediction of hydraulic conductivity and soil-water retention of unsaturated soils. – Transportation Research Record 2672(52): 108-17.
[4] Fredlund, D. G. (2019): State of practice for use of the soil-water characteristic curve (SWCC) in geotechnical engineering. – Canadian Geotechnical Journal 56(8): 1059-69.
[5] Gu, J. Y., Yang, B. G., Wei, Y. J., Cai, C. F. (2021): Analysis on the difference of soil hydraulic properties in different soil layers of Benggang. – Journal of Soil and Water Conservation 35(2): 61-67.
[6] He, D., Wang, E. L. (2019): On the relation between soil water holding capacity and dryland crop productivity. – Geoderma 353(11-24).
[7] Hu, C. W., Wang, H., Liu, C., Yuan, H., Li, Y. Y. (2017): Difference analysis of hydraulic characteristics of typical soils in South China. – Journal of Soil and Water Conservation 31(2): 97-102.
[8] Kawamoto, K., Moldrup, P., Ferre, T. P. A., Tuller, M., Jacobsen, O. H., Komatsu, T. (2006): Linking the Gardner and Campbell models for water retention and hydraulic conductivity in near-saturated soil. – Soil Science 171(8): 573-84.
[9] Laio, F. (2006): A vertically extended stochastic model of soil moisture in the root zone. – Water Resources Research 420(2): 10.
[10] Laio, F., Tamea, S., Ridolfi, L., D'Odorico, P., Rodriguez-Iturbe, I. (2009): Ecohydrology of groundwater-dependent ecosystems: 1. Stochastic water table dynamics. – Water Resources Research 45(5): 207.
[11] Lehmann, P., Merlin, O., Gentine, P., Or, D. (2018): Soil texture effects on surface resistance to bare-soil evaporation. – Geophysical Research Letters 45(19): 10398-405.
[12] Li, Y., Song, W. F. (2020): Advances in numerical simulation of soil moisture movement. – Subtropical Soil and Water Conservation 32(2): 26-31.
[13] Li, C. M., Yang, Y. G., Qin, Z. D., Zou, S. B., Li, J. C. (2015): Simulation and prediction on variations of groundwater in mining area based on FEFLOW and GIS. – Arid Land Geography 38(2): 359-367.
[14] Li, L., Wu, D. D., Wang, T. J., Di, C. L. (2022): Effects of soil hydraulic parameters on long-range correlation of soil moisture based on numerical simulation. – Journal of Soil and Water Conservation 36(1): 80-85 + 94.
[15] Lu, N., Likos, W. J. (2006): Suction stress characteristic curve for unsaturated soil. – Journal of Geotechnical and Geoenvironmental Engineering 132(2): 131-42.
[16] Lu, N., Kaya, M., Godt, J. W. (2014): Interrelations among the soil-water retention, hydraulic conductivity, and suction-stress characteristic curves. – Journal of Geotechnical and Geoenvironmental Engineering 140(5): 10.
[17] Lv, J. J., Hu, C. Y., He, X. (2005): Studied on the influences of coal mining collapse on the soil water dynamics of fixed dune. – Journal of Arid Land Resources and Environment S1: 152-156.
[18] Ma, Y. B., Gao, Y., Zhang, Y., Zhang, L. W., Huang, Y. R. (2013): Infuence of collapse and cracks of rolling loess area because of coal mining to the soil moisture of slope surface. – Soil and Water Conservation in China (11): 54-57 + 79.
[19] Ma, M. H., Zhang, S. H., Wang, H. X., Yang, H. C., Li, Q. (2017): Parameters of unsaturated soil moisture movement: a case study of red soil in Kunming. – Journal of Beijing Normal University (Natural Science) 53(1): 38-42.
[20] Pan, Z. H., Li, P., Xiao, T. (2021): The law of water infiltration in loess based on numerical simulation. – Journal of Northwest University (Natural Science Edition) 51(3): 470-484.

http://www.aloki.hu ● ISSN 1589 1623 (Print) ● ISSN 1785 0037 (Online)
DOI: http://dx.doi.org/10.15666/aeer/2005_45254537

[21] Song, L., Li, J. H., Zhou, T., Fredlund, D. G. (2017): Experimental study on unsaturated hydraulic properties of vegetated soil. – Ecological Engineering 103(207-16）.

[22] Su, S., Yang, Y. G., Huang, L. (2018): Dynamic characteristics of soil water in different sites during ecological restoration in mining area. – Bulletin of Soil and Water Conservation 38(01): 18-23.

[23] Sun, F. H., Xiao, B., Li, S. L., Wang, F. F. (2021): Effects of moss-dominated biocrusts on surface soil-water movement parameters in the Chinese Loess Plateau. – Transactions of the Chinese Society of Agricultural Engineering 37(14): 79-88.

[24] Wang, J. K., Guo, Y. F., Qi, W., Yao, Y. F., Wang, H. (2021): Horizontal infiltration characteristics and applicable models of Pisha sandstone soil in Inner Mongolia. – Journal of Inner Mongolia Agricultural University (Natural Science Edition) 42(5): 46-52.

[25] Wei, G. X., Wang. D. J., Wang. G., Li. C. B., Zhu, F., Xu, T. (2007): Application of GIS technique and FEFLOW to numerical simulation of groundwater system in Jiuquan East Basin. – Journal of Lanzhou University (Natural Sciences) 6: 1-6.

[26] Yadav, R. R., Kumar, L. K. (2017): One-dimensional spatially dependent solute transport in semi-infinite porous media: an analytical solution. – International Journal of Engineering, Science and Technology 9(4): 20-27.

[27] Zhang, C., Wang, H. X. (2003): A brief review of advances in soil water research. – Agricultural Research in the Arid Areas 4: 117-120 + 125.

[28] Zhang, X., Wang, J., Liu, C. Y. (2009): Influences of coal mining subsidence on soil water loss and its mechanisms. – Journal of Anhui Agricultural Sciences 37(11): 5058-5062.

[29] Zhao, W., Zhao, J., Wei, Z. M., Yin, C. Y., Liu, H., Zhu, B. (2022): Effect of aeolian sandy soil improved by gasification slag on soil water physical properties. – Research of Soil and Water Conservation 29(02): 64-69.

http://www.aloki.hu ● ISSN 1589 1623 (Print) ● ISSN 1785 0037 (Online)
DOI: http://dx.doi.org/10.15666/aeer/2005_45254537

CROSS SEASONAL INHERITANCE AND IMPACT OF AMBIENT WATER MICROBIOTA ON THE GUT MICROBIOTA OF *RHINOGOBIO CYLINDRICUS* GÜNTHER

CHEN, X. J.[1*] – ZHU, Q. G.[1] – YANG, Z.[1] – ZHAO, N.[1] – NI, J. J.[2,3]

[1]*Key Laboratory of Ministry of Water Resources for Ecological Impacts of Hydraulic-Projects and Restoration of Aquatic Ecosystem, Institute of Hydroecology, Ministry of Water Resources and Chinese Academy of Sciences, Wuhan, China*

[2]*Research and Development Center, Guangdong Meilikang Bio-Science Ltd., Dongguan, China*

[3]*Dongguan Key Laboratory of Medical Bioactive Molecular Developmental and Translational Research, Guangdong Medical University, Dongguan, China*

[*]*Corresponding author*
e-mail: chenxiaojuan@mail.ihe.ac.cn

(Received 17th May 2022; accepted 22nd Jul 2022)

Abstract. The gut microbiota (GM) participates in various physiological processes in fish. Although there are many host- and environment-related factors affecting the composition of fish GM, there are relatively few reports on the inheritance of fish GM across seasons and the impact of environmental water microbiota (WM) on fish GM. Here, we aimed to identify the differences in the composition of *Rhinogobio cylindricus* GM (RGM) in autumn and summer, and to determine how the summer RGM affected the autumn RGM. Samples of R. cylindricus were collected in summer and autumn and the composition of GM was analyzed through high-throughput sequencing of 16S rDNA. Our results showed that the alpha diversity indices of RGM in autumn were significantly higher than those in summer. The RGM collected in summer and autumn showed significant differences. The relative abundances of the most dominant operational taxonomic units (OTUs) were significantly different between the summer and autumn RGM samples. The proportions of OTUs in autumn RGM from summer RGM were significantly lower than those in WM. Moreover, there was no sampling site difference in the proportion of RGM compared with that of WM. Our results provide important insight into understanding the maintenance mechanisms of RGM.
Keywords: *composition, dispersal limitation, habitat, inheritance, operational taxonomic unit, maintenance mechanism*

Introduction

The gut microbiota (GM) participates in various physiological processes, such as digestion (Ghanbari et al., 2015; Liu et al., 2016), growth (Li et al., 2019), metabolism (Butt and Volkoff, 2019), and immune response in fish (Galindo-Villegas et al., 2012; Stagaman et al., 2017). Although studies have established that the composition of GM is affected by many factors, such as habitat (Ni et al., 2012, 2014), feeding habits (Li et al., 2014), development (Li et al., 2017; Yukgehnaish et al., 2020), and host genetic variation (Li et al., 2014; Smith et al., 2015; Yukgehnaish et al., 2020), the underlying mechanisms are still unclear.

Rhinogobio cylindricus Günther is an endemic fish species in upper Yangtze River, widely distributed in the mainstream of the Yangtze River and its tributaries (Liu et al., 2012, 2019). *R. cylindricus* captured monthly from Yibin to Wanzhou river section of the upper Yangtze River from July 2010 to July 2012 showed that their main foods were algae, molluscs, and aquatic insects. In terms of quantity percentage, algae and molluscs

http://www.aloki.hu ● ISSN 1589 1623 (Print) ● ISSN 1785 0037 (Online)
DOI: http://dx.doi.org/10.15666/aeer/2005_45394551

are the majority (93.12%), whereas in terms of weight percentage, algae, molluscs, and aquatic insects account for the majority (78.38%) (Xiong et al., 2015). Historically, *R. cylindricus* is one of the most popular species in the Yangtze River region, and wild resources have decreased owing to overfishing, construction of hydraulic projects, and other anthropogenic influences (Liu et al., 2012). To protect wild *R. cylindricus*, its basic biology (Xiong, 2013), feeding habits (Xiong et al., 2013), population genetic diversity (Liu et al., 2012; Shao et al., 2013), population parameters and resources (Xiong et al., 2015), and morphological characteristics (Wang et al., 2012) have been studied. We analyzed the composition of *R. cylindricus* GM (RGM) collected from four different sampling sites in the upper Yangtze River and found that there were no significant differences in RGM among different sampling sites, although significant differences were noted in their habitat water microbiota (WM) (Chen et al., 2021).

Considering the important roles of GM in various fish physiological processes, maintaining the stability of the GM composition and clarifying the factors affecting its composition are of great significance for protecting wild *R. cylindricus*. Since there are seasonal differences in the food composition of *R. cylindricus* (Xiong et al., 2013), which are important factors affecting fish GM (Ni et al., 2014; Wang et al., 2018; Li et al., 2019), we speculated that there were significant differences in the composition of GM between autumn and summer. However, the extent to which the autumn RGM was inherited from the summer GM remains unclear. To identify any difference in the composition of RGM in autumn and summer, and to determine how the summer RGM affected the autumn RGM, we collected samples of *R. cylindricus* in summer and autumn and analyzed the composition of GM through high-throughput sequencing of 16S rDNA. Our results provide an important insight into the maintenance mechanisms of a wide range of RGM.

Materials and Methods

Sampling area and sample collection

R. cylindricus samples were collected from Mudong (29.577 °N, 106.843 °E), Jiangjin (29.348 °N, 106.429 °E), and Heijiang (28.805 °N, 105.843 °N) in June and July (summer) of 2019 and October and November (autumn) of 2020 (*Fig. 1*), as previously described (Chen et al., 2021). The total length and body length of each sample were measured using a vernier caliper, and the body weight was weighed using an electronic balance.

DNA extraction and high-throughput sequencing

Gut microbial DNA was extracted using a PowerSoil DNA extraction kit (QIAGEN, Hilden, Germany). The V4-V5 hypervariable region of the prokaryotic 16S rDNA was amplified using primers 515F and 909R, as previously described (Xiang et al., 2018). Polymerase chain reaction (PCR) was performed and the amplicons were sequenced using a HiSeq system (Illumina, USA) at Guangdong Meilikang Bio-Science, Ltd. (Dongguan, China), as previously described (Ni et al., 2019; Chen et al., 2020).

http://www.aloki.hu ● ISSN 1589 1623 (Print) ● ISSN 1785 0037 (Online)
DOI: http://dx.doi.org/10.15666/aeer/2005_45394551

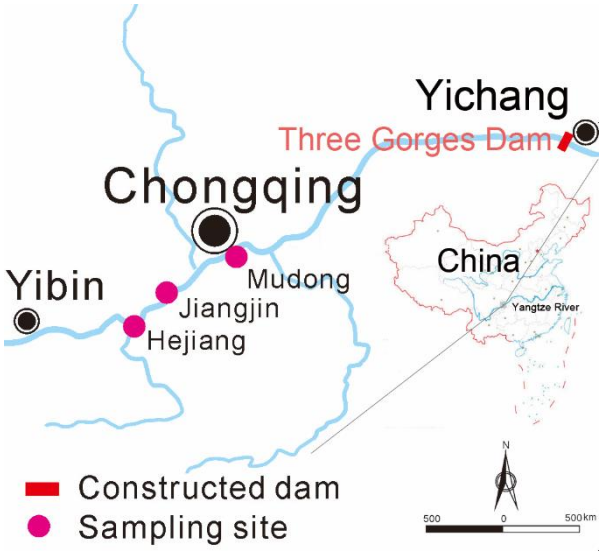

Figure 1. *Distribution of sampling sites*

The raw sequences were merged and quality-controlled and chimeric sequences were removed as previously described using FLASH version 1.2.8 (Magoč and Salzberg, 2011), QIIME 1.9.0 (Caporaso et al., 2010), and UCHIME 4.2.40 (Edgar et al., 2011), respectively. The remaining sequences were clustered into operational taxonomic units (OTUs) at 97% identity using UPARSE version 7.0.1090 (Edgar, 2013). Taxonomic assignment of each OTU was conducted using RDP classifier 2.2 (Wang et al., 2007) with the Greengene gg_13_8_otus dataset.

Merged sequences were deposited in the NCBI Sequence Read Archive database with accession number PRJNA824943.

Data analysis

Data are presented as the mean ± standard error for each group. The Wilcoxon rank-sum and Kruskal-Wallis tests were conducted using R version 4.0.3 (R Core Team, 2020). Permutational multivariate analysis of variance (PERMANOVA) (Anderson, 2001) was used to test the significance of the differences between groups using the R vegan package (Dixon, 2003). Principal co-ordinates analysis (PCoA) based on weighted Unifrac distance was conducted using QIIME 1.9.0. Boxplots were constructed using the ggpubr R package (https://www.rdocumentation.org/packages/ggpubr/versions/0.4.0). Microbial source tracking analysis was conducted using SourceTracker (Knights et al., 2011). Statistical significance was set at $p < 0.05$.

Results

A total of 77 summer samples and 34 autumn samples were collected and measured total length, body length, and body weight. The total length (Wilcoxon test, $\chi 2 = 13.755$, $p < 0.001$; *Fig. 2A*), body length (Wilcoxon test, $\chi 2 = 14.784$, $p < 0.001$; *Fig. 2B*), and body weight (Wilcoxon test, $\chi 2 = 7.353$, $p = 0.007$; *Fig. 2C*) of autumn *R. cylindricus* samples were significantly larger than those of summer samples.

http://www.aloki.hu ● ISSN 1589 1623 (Print) ● ISSN 1785 0037 (Online)
DOI: http://dx.doi.org/10.15666/aeer/2005_45394551

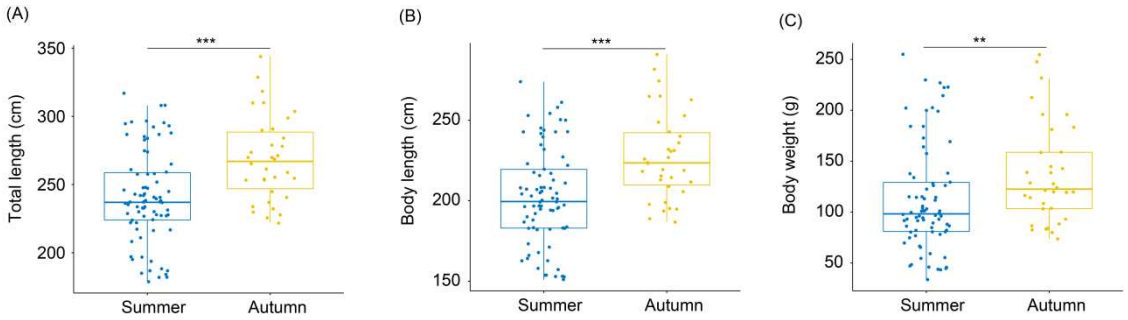

Figure 2. *Wilcoxon tests of total length (A), body length (B), and body weight (C) of R. cylindricus samples collected in summer and autumn. **, $p < 0.01$; ***, $p < 0.001$*

A total of 112 samples (33, 23, and 22 samples collected from Hejiang, Jiangjin, and Mudong in summer, and 6, 13, and 15 samples collected from Hejiang, Jiangjin, and Mudong in autumn, respectively) were anlyzed their GM composition. After sequence quality control and chimera removal, 21,236 sequences were randomly re-sampled from each sample for subsequent analyses. A total of 34,949 OTUs were detected in the samples. The alpha-diversity indices of RGM in autumn were significantly higher than those in summer (Wilcoxon rank sum test, $p < 0.001$ for OTU number, Shannon, Simpson, and Chao1 indices; *Fig. 3A-3D*). Therefore, the coverage of sequencing of RGM in autumn was significantly lower than that in summer (Wilcoxon rank-sum test, $p < 0.001$; *Fig. 3E*). In summer, the OTU number and Chao1 index of RGM collected from Hejiang were significantly higher than those at other sampling sites (Kruskal-Wallis rank sum test, $p < 0.001$; *Fig. 3A and 3D*), whereas the OTU number and Chao1 index of RGM collected from Hejiang were significantly lower than those collected from Jiangjin and Mudong (Kruskal-Wallis rank sum test, $p < 0.05$; *Fig. 3A and 3D*). The alpha-diversity indices of autumn WM were between those of the RGM collected in summer and autumn (*Fig. 3A-3D*).

PCoA results based on weighted UniFrac distances also showed significant differences in RGM collected in summer and autumn (PERMANOVA, $F = 64.265$, $p = 0.005$; *Fig. 3F*), and they were significantly different from the WM composition (PERMANOVA, $F = 80.392$, $p = 0.005$; *Fig. 3F*). However, the composition of the RGM collected at different sampling sites was not significantly different in autumn (PERMANOVA, $F = 1.372$, $p = 0.090$), although the autumn WM composition among sampling sites was significantly different (PERMANOVA, $F = 2.214$, $p = 0.005$).

Except for a few OTUs whose phylum could not be determined, the other OTUs were divided into 78 prokaryotic phyla, among which AC1, Acidobacteria, Actinobacteria, Bacteroidetes, Chlorobi, Chloroflexi, Cyanobacteria, Elusimicrobia, Firmicutes, Fusobacteria, Gemmatimonadetes, KSB3, Nitrospirae, OP3, OP8, Planctomycetes, Proteobacteria, Spirochaetes, Tenericutes, WS3, and Thermi dominated the microbiota (*Fig. 3G*). The relative abundances of the dominant phyla in RGM were significantly different between the summer and autumn samples. The relative abundances of Firmicutes, Fusobacteria, Proteobacteria, and Tenericutes in the summer samples were significantly higher than those in the autumn samples, whereas those of AC1, Acidobacteria, Bacteroidetes, Chlorobi, Chloroflexi, Cyanobacteria, Elusimicrobia, Gemmatimonadetes, KSB3, Nitrospirae, OP3, OP8, Planctomycetes, Spirochaetes, and WS3 in the autumn samples were significantly higher than those in the summer samples

http://www.aloki.hu ● ISSN 1589 1623 (Print) ● ISSN 1785 0037 (Online)
DOI: http://dx.doi.org/10.15666/aeer/2005_45394551

(*Appendix1*). The relative abundances of the dominant phyla in the autumn WM were also significantly different from those in the autumn RGM (*Appendix 1*).

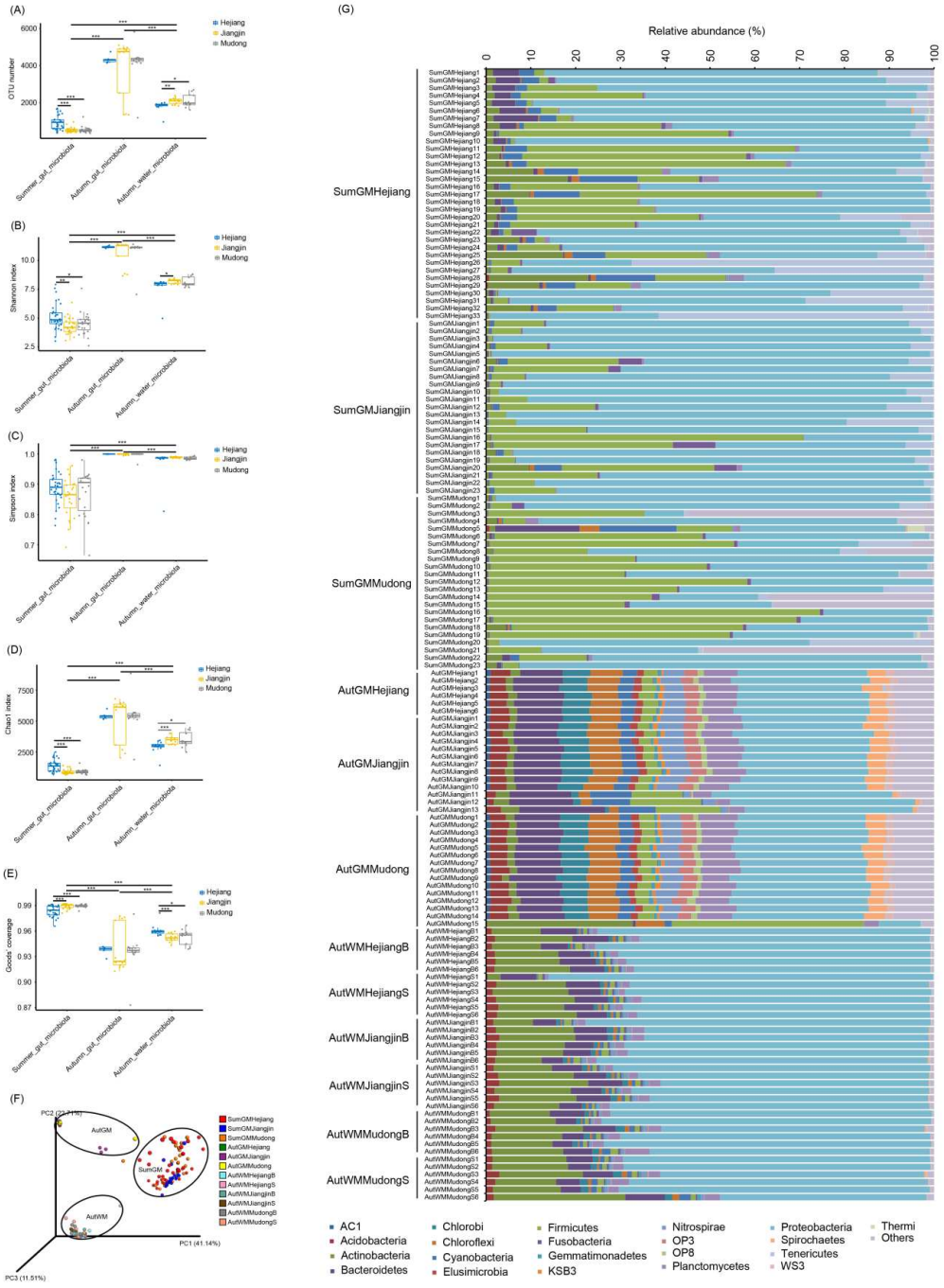

Figure 3. *Alpha-diversity indices and composition of Rhinogobio cylindricus gut microbiota and ambient water microbiota. (A), OTU number; (B), Shannon index; (C), Simpson index; (D), Chao1 index; (E), Good's coverage; (F), PCoA profile showed composition changes of R. cylindricus gut microbiota and ambient water microbiota; (G), dominant phylum composition of R. cylindricus gut microbiota and ambient water microbiota. SumGM, gut microbiota of Rhinogobio cylindricus collected in summer; WinGM, gut microbiota of Rhinogobio cylindricus collected in autumn; and WinWM, ambient water microbiota collected in autumn. *, $p < 0.05$; **, $p < 0.01$; ***, $p < 0.001$*

http://www.aloki.hu ● ISSN 1589 1623 (Print) ● ISSN 1785 0037 (Online)
DOI: http://dx.doi.org/10.15666/aeer/2005_45394551

LEfSe results showed that the relative abundances of the most dominant OTUs were significantly different between the summer and autumn *R. cylindricus* samples (*Fig. 4A*), whereas at the sampling time, the relative abundance of only a few dominant genera exhibited significant differences among sampling sites (*Fig. 4B*). Among the dominant genera that could be identified to the genus level, *Phormidium*, *Enterococcus*, *Lactococcus*, *Epulopiscium*, *Clostridium*, *Ochrobactrum*, *Sphingomonas*, *Ralstonia*, *Aeromonas*, *Escherichia*, *Plesiomonas*, *Vibrio*, *Stenotrophomonas*, *Mycoplasma*, *Deinococcus*, and *Mycobacterium* significantly enriched in the summer RGM; *Synechococcus*, *Ruminococcus*, *Oscillospira*, *Nitrospira*, *GOUTA19*, *LCP_6*, *Crenothrix*, *Halomonas*, *Treponema*, and *Bacteroides* significantly enriched in autumn RGM; whereas *Planctomyces*, *Rhodobacter*, *Aquabactenum*, *Comamonas*, *Hydrogenophaga*, *Limnohabitans*, *Rhodoferax*, *Polynucleobacter*, *Methylotenera*, *Acinetobacter*, *Perlucidibaca*, *Pseudoalteromonas*, and *Flavobacterium* significantly enriched in autumn WM (*Fig. 4A*). For autumn *R. cylindricus* GM, only LCP_6 and *Ralstonia* significantly enriched in Jiangjin, whereas *Bacillus* and *Hyphomicrobium* significantly enriched in Mudong (*Fig. 4B*).

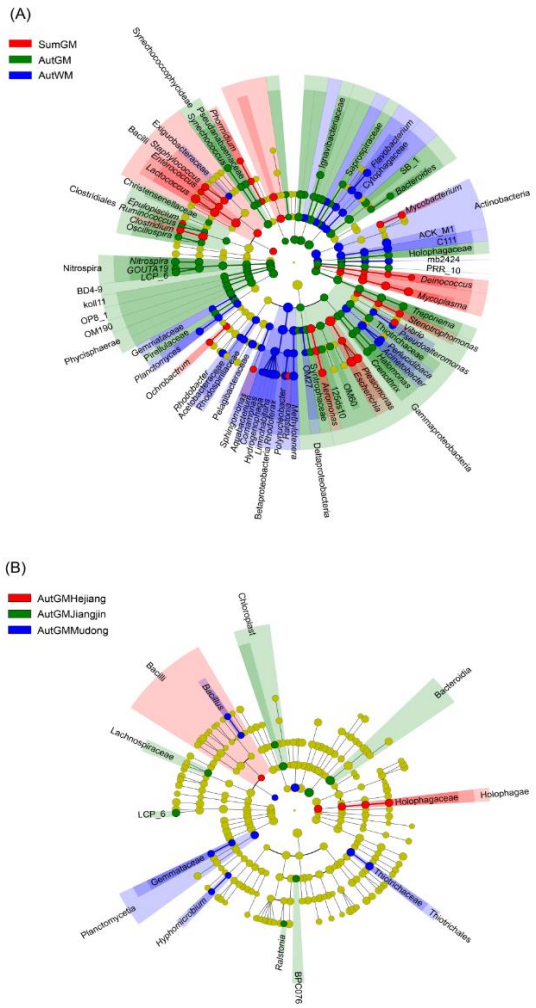

Figure 4. *Cladogram plots emerged LEfSe results. (A) different genera among SumGM, AutGM, and AutWM; (B) different genera of R. cylindricus gut microbiota at different sampling sites*

http://www.aloki.hu ● ISSN 1589 1623 (Print) ● ISSN 1785 0037 (Online)
DOI: http://dx.doi.org/10.15666/aeer/2005_45394551

Source tracking results showed that only a small number of OTUs in autumn RGM were from summer RGM and were significantly fewer than those from autumn WM (Wilcoxon test, $p < 0.001$; *Fig. 5* and *Appendix 2*). Only 0.45 ± 0.10%, 0.53 ± 0.06%, and 0.79 ± 0.06% OTUs in autumn RGM collected from Hejiang were from summer RGM collected from Hejiang, Jiangjin, and Mudong, respectively (*Fig. 5*). Only 4.71 ± 2.28%, 3.42 ± 1.66%, and 4.32 ± 2.02% OTUs in autumn RGM collected from Jiangjin were from summer RGM collected from Hejiang, Jiangjin, and Mudong, respectively (*Fig. 5*). Only 1.93 ± 1.22%, 1.27 ± 0.90%, and 0.96 ± 0.25% OTUs in autumn RGM collected from Mudong were from summer RGM collected from Hejiang, Jiangjin, and Mudong, respectively (*Fig. 5*). There were no significant differences in the proportions of OTUs from different sampling sites in the autumn RGM (Wilcoxon test, $p > 0.05$). The OTU proportion of RGM in the autumn from summer RGM collected from Jiangjin was significantly higher than that in the *R. cylindricus* samples collected from the other two sampling sites (Kruskal-Wallis test, $\chi 2 = 13.473$, $p = 0.001$; *Fig. 5* and *Appendix 2*). The OTU proportions of autumn RGM collected from Hejiang were 6.08 ± 0.33% and 5.65 ± 0.37% from surface and bottom WM, respectively (*Fig. 5*). The OTU proportions of autumn RGM collected from Jiangjin were 5.88 ± 0.58% and 6.36 ± 0.57% from surface and bottom WM, respectively (*Fig. 5*). The OTU proportions of autumn RGM collected from Mudong were 5.41 ± 0.39% and 5.66 ± 0.36% from surface and bottom WM, respectively (*Fig. 5*). The OTU proportions of autumn RGM from the surface and bottom WM were not significantly different (Wilcoxon test, $p > 0.05$; *Fig. 5* and *Appendix 2*). These results indicate that the proportions of OTUs in autumn RGM from summer RGM were significantly lower than those from habitat WM. Moreover, there was no sampling site difference in the proportion of RGM from WM.

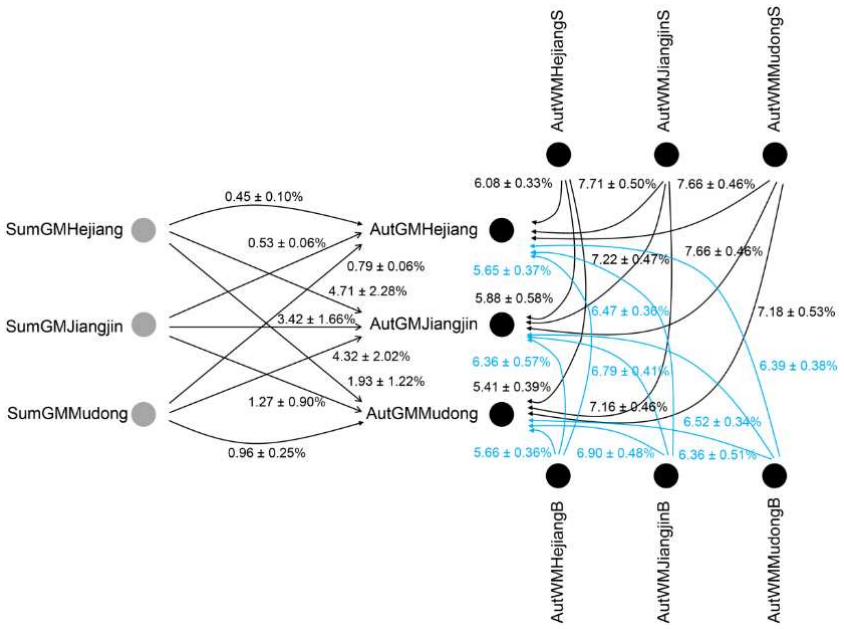

Figure 5. *Proportions of autumn R. cylindricus gut microbiota from summer R. cylindricus gut and autumn water microbiota. The proportions were calculated using SourceTracker script. Light blue indicates the proportions of autumn R. cylindricus gut microbiota from bottom water microbiota*

http://www.aloki.hu ● ISSN 1589 1623 (Print) ● ISSN 1785 0037 (Online)
DOI: http://dx.doi.org/10.15666/aeer/2005_45394551

Discussion

GM plays important roles in fish growth, development, immunity, and health (Pérez et al., 2010; Galindo-Villegas et al., 2012; Stagaman et al., 2017; Xiong et al., 2019). Dysbiosis of the GM often leads to diseases in fish (Nie et al., 2017; He et al., 2017). Therefore, understanding the maintenance mechanism and influencing factors of fish GM not only has important ecological and theoretical value but is also significant for its production (Liu et al., 2021). At present, it has been confirmed that habitat (Ni et al., 2012, 2014; Kuang et al., 2020; Kim et al., 2021), feeding habit (Li et al., 2014), development (Yan et al., 2016; Li et al., 2017), season (Tarnecki et al., 2017; Egerton et al., 2018), and species (Li et al., 2014; Huang et al., 2020) affect the composition of fish GM. Our results showed that RGM composition collected in summer and autumn exhibited significant differences, indicating that there were significant seasonal differences in the composition of RGM (*Fig. 3F*). This may be due to differences in the dietary niche breadth and consumed detritus of R. cylindricus between summer and autumn (Liu et al., 2019).

Although there are many host- and environment-related factors affecting the composition of fish GM, there are relatively few reports on the its inheritance across seasons, and the impact of environmental WM on fish GM. Liu et al. (2021) reported that 12.69 ± 3.63% OTUs of largemouth bass (*Micropterus salmoides*) GM came from ambient WM in ponds, and the proportion increased with an increase in culture time. They also found that the proportion of ambient sediment microbiota was 7.03 ± 3.47%. Our results showed that 5.41% to 7.71% of the OTUs of autumn RGM came from ambient WM, and less than 5% of the OTUs of autumn RGM came from summer RGM (*Fig. 5*). These results showed that RGM underwent reconstruction greatly from summer to autumn, which might be caused by the significant decrease in water temperature upstream of the Yangtze River and changes in the food composition of *R. cylindricus* after autumn.

Fish GM contains a variety of opportunistic pathogens such as *Aeromonas*, *Flavobacterium*, and *Vibrio* (Ni et al., 2012; Derome et al., 2016; Xiong et al., 2019; Emam et al., 2019); these pathogens were the dominant genera identified in this study. Moreover, *Aeromonas* and *Vibrio* were significantly enriched in summer RGM, whereas *Flavobacterium* was significantly enriched in autumn WM. *Clostridium* species have been reported to attenuate inflammation and allergic diseases effectively owing to their distinctive biological activities (Guo et al., 2020), and *Clostridium* was significantly enriched in summer RGM. These results imply that *R. cylindricus* has a higher risk of bacterial diseases caused by opportunistic pathogens from GM in summer than in autumn, which is consistent with the fact that fish are more prone to bacterial diseases in summer (Toranzo et al., 2005; Gauger et al., 2006; Marcos-López et al., 2010; Loch and Faisal, 2015).

Although we found that RGM was significantly different in summer and autumn, and the proportion of bacteria in autumn RGM from autumn WM was significantly higher than that from summer RGM in this study. We did not clarify the entire changing process of RGM from summer to autumn because of the large sampling time interval. Additionally, owing to the limitations tied to sampling, we did not study the annual change pattern of the RGM. These issues require further investigation.

http://www.aloki.hu ● ISSN 1589 1623 (Print) ● ISSN 1785 0037 (Online)
DOI: http://dx.doi.org/10.15666/aeer/2005_45394551

Conclusions

The alpha-diversity indices of the RGM in autumn were significantly higher than those in summer. The RGM collected in summer and autumn showed significant differences. The relative abundances of the most dominant OTUs were significantly different between summer and autumn RGM. The proportions of OTUs in autumn RGM from summer RGM were significantly lower than those in habitat WM. Moreover, there was no sampling site difference in the proportion of RGM compared with that of WM. These results implied that RGM had weak cross seasonal inheritance, and was more affected by ambient water microbiota than cross seasonal inheritance.

Ethical approval. All experimental protocols were approved by the Ethics Committee of the Institute of Hydroecology, Ministry of Water Resources, and the Chinese Academy of Sciences (approval number IHE[2019]030001). Fishing for studies was approved by the local fishery administrations of the Department of Agriculture Affairs of Sichuan province and Chongqing city.

Acknowledgements. This research was funded by the National Natural Science Foundation of China, grant number 51879171.

REFERENCES

[1] Anderson, M. J. (2001): A new method for non-parametric multivariate analysis of variance. – Austral Ecology 26(1): 32-46.
[2] Butt, R. L., Volkoff, H. (2019): Gut microbiota and energy homeostasis in fish. – Frontiers in Endocrinology 10: 9.
[3] Caporaso, J. G., Kuczynski, J., Stombaugh, J., Bittinger, K., Bushman, F. D., Costello, E. K., Fierer, N., Peña, A. G., Goodrich, J. K., Gordon, J. I. (2010): QIIME allows analysis of high-throughput community sequencing data. – Nature Methods 7: 335-336.
[4] Chen, X., He, D., Zhou, L., Cao, Y., Li, Z. (2020): Influence of hydropower stations on the water microbiota in the downstream of Jinsha River, China. – PeerJ 8: e9500.
[5] Chen, X., Zhu, Q., Yang, Z., Sun, H., Zhao, N., Ni, J. (2021): Filtering effect of *Rhinogobio cylindricus* gut microbiota relieved influence of the Three Gorges Dam on the gut microbiota composition. – Water 13: 2697.
[6] Derome, N., Gauthier, J., Boutin, S., Llewellyn, M. (2016): Bacterial opportunistic pathogens of fish. – In: Hurst, C. J. (ed.) The Rasputin Effect: When Commensals and Symbionts Become Parastitic. Advances in Environmental Microbiology 3: 81-108.
[7] Dixon, P. (2003): VEGAN, a package of R functions for community ecology. – Journal of Vegetation Science 14(6): 927-930.
[8] Edgar, R. C. (2013): UPARSE: Highly accurate OTU sequences from microbial amplicon reads. – Nature Methods 10: 996-998.
[9] Edgar, R. C., Haas, B. J., Clemente, J. C., Quince, C., Knight, R. (2011): UCHIME improves sensitivity and speed of chimera detection. – Bioinformatics 27(16): 2194-2200.
[10] Egerton, S., Culloty, S., Whooley, J., Stanton, C., Ross, R. P. (2018): The gut microbiota of marine fish. – Frontiers in Microbiology 9: 873.
[11] Emam, A. M., Hashem, M., Gadallah, A. O., Haridy, M. (2019): An outbreak of Vibrio alginolyticus infection in aquarium-maintained dark-spotted (*Himantura uarnak*) and Tahitian (*H. fai*) stingrays. – The Egyptian Journal of Aquatic Research 45(2): 153-158.
[12] Galindo-Villegas, J., García-Moreno, D., de Oliveira, S., Meseguer, J., Mulero, V. (2012): Regulation of immunity and disease resistance by commensal microbes and chromatin modifications during zebrafish development. – Proceedings of the National Academy of Sciences of United States of American 109(39): E2605-E2614.

http://www.aloki.hu ● ISSN 1589 1623 (Print) ● ISSN 1785 0037 (Online)
DOI: http://dx.doi.org/10.15666/aeer/2005_45394551

[13] Gauger, E., Smolowitz, R., Uhlinger, K., Casey, J., Gómez-Chiarri, M. (2006): *Vibrio harveyi* and other bacterial pathogens in cultured summer flounder, *Paralichthys dentatus*. – Aquaculture 260: 10-20.
[14] Ghanbari, M., Kneifel, W., Dornig, K. J. (2015): A new view of the fish gut microbiome: advances from next-generation sequencing. – Aquaculture 448: 464-475.
[15] Guo, P., Zhang, K., Ma, X., He, P. (2020): Clostridium species as probiotics: potentials and challenges. – Journal of Animal Science and Biotechnology 11: 24.
[16] He, S. X., Wang, Q. M., Li, S. N., Ran, C., Guo, X. Z., Zhang, Z., Zhou, Z. G. (2017): Antibiotic growth promoter olaquindox increases pathogen susceptibility in fish by inducing gut microbiota dysbiosis. – Science China Life Sciences 60: 1260-1270.
[17] Huang, Q., Sham, R. C., Deng, Y., Mao, Y., Wang, C., Zhang, T., Leung, K. M. Y. (2020): Diversity of gut microbiomes in marine fishes is shaped by host-related factors. – Molecular Ecology 29(24): 5019-5034.
[18] Kim, P. S., Shin, N.-R., Lee, J.-B., Kim, M.-S., Whon, T. W., Hyun, D.-W., Yun, J.-H., Jung, M.-J., Kim, J. Y., Bae, J.-W. (2021): Host habitat is the major determinant of the gut microbiome of fish. – Microbiome 9: 166.
[19] Knights, D., Kuczynski, J., Charlson, E. S., Zaneveld, J., Mozer, M. C., Collman, R. G., Bushman, F. D., Knight, R., Kelley, S. T. (2011): Bayesian community-wide culture-independent microbial source tracking. – Nature Methods 8: 761-763.
[20] Kuang, T., He, A., Lin, Y., Huang, X., Liu, L., Zhou, L. (2020): Comparative analysis of microbial communities associated with the gill, gut, and habitat of two filter-feeding fish. – Aquaculture Reports 18: 100501.
[21] Li, J., Ni, J., Li, J., Wang, C., Li, X., Wu, S., Zhang, T., Yu, Y., Yan, Q. (2014): Comparative study on gastrointestinal microbiota of eight fish species with different feeding habits. – Journal of Applied Microbiology 117(6): 1750-1760.
[22] Li, X., Zhou, L., Yu, Y., Ni, J., Xu, W., Yan, Q. (2017): Composition of gut microbiota in the gibel carp (*Carassius auratus gibelio*) varies with host development. – Microbial Ecology 74: 239-249.
[23] Li, X., Ringø, E., Hoseinifar, S. H., Lauzon, H. L., Birkbeck, H., Yang, D. (2019): The adherence and colonization of microorganisms in fish gastrointestinal tract. – Reviews in Aquaculture 11(3): 603-618.
[24] Liu, H. Y., Xiong, F., Duan, X. B., Chen, D. Q., Liu, S. P., Zhang, F. R., Yang, D., Yu, L. N. (2012): A first set of polymorphic microsatellite loci isolated from *Rhinogobio cylindricus*. – Conservation Genetetics Resources 4: 307-310.
[25] Liu, H., Guo, X., Gooneratne, R., Lai, R., Zeng, C., Zhan, F., Wang, W. (2016): The gut microbiome and degradation enzyme activity of wild freshwater fishes influenced by their trophic levels. – Scientific Reports 6: 24340.
[26] Liu, F., Wang, J., Liu, H. (2019): Seasonal variations in food resource partitioning among four sympatric gudgeon species in the upper Yangtze River. – Ecology and Evolution 9(12): 7227-7236.
[27] Liu, Q., Lai, Z., Gao, Y., Wang, C., Zeng, Y., Liu, E., Mai, Y., Yang, W., Li, H. (2021): Connection between the gut microbiota of largemouth bass (*Micropterus salmoides*) and microbiota of the pond culture environment. – Microorganisms 9: 1770.
[28] Loch, T. P., Faisal, M. (2015): Emerging flavobacterial infections in fish: A review. – Journal of Advanced Research 6(3): 283-300.
[29] Magoč, T., Salzberg, S. (2011): FLASH: Fast length adjustment of short reads to improve genome assemblies. – Bioinformatics 27: 2957-2963.
[30] Marcos-López, M., Gale, P., Oidtmann, B. C., Peeler, E. J. (2010): Assessing the impact of climate change on disease emergence in freshwater fish in the United Kingdom. – Transboundary and Emerging Diseases 57(5): 293-304.
[31] Ni, J., Yu, Y., Zhang, T., Gao, L. (2012): Comparison of intestinal bacterial communities in grass carp, *Ctenopharyngodon idellus*, from two different habitats. – Chinese Journal of Oceanology and Limnology 30: 757-765.

http://www.aloki.hu ● ISSN 1589 1623 (Print) ● ISSN 1785 0037 (Online)
DOI: http://dx.doi.org/10.15666/aeer/2005_45394551

[32] Ni, J., Yan, Q., Yu, Y., Zhang, T. (2014): Factors influencing the grass carp gut microbiome and its effect on metabolism. – FEMS Microbiology Ecology 87(3): 704-714.
[33] Ni, J., Huang, R., Zhou, H., Xu, X., Li, Y., Gao, P., Zhong, K., Ge, M., Chen, X., Hou, B., Yu, M., Peng, B., Li, Q., Zhang, P., Gao, Y. (2019): Analysis of the relationship between the degree of dysbiosis in gut microbiota and prognosis at different stages of primary hepatocellular carcinoma. – Frontiers in Microbiology 10: 1458.
[34] Nie, L., Zhou, Q. J., Qiao, Y., Chen, J. (2017): Interplay between the gut microbiota and immune responses of ayu (*Plecoglossus altivelis*) during *Vibrio anguillarum* infection. – Fish & Shellfish Immunology 68: 479-487.
[35] Pérez, T., Balcázar, J. L., Ruiz-Zarzuela, I., Halaihel, N., Vendrell, D., de Blas, I., Múzquiz, J. L. (2010): Host-microbiota interactions within the fish intestinal ecosystem. – Mucosal Immunology 3: 355-360.
[36] R Core Team. (2020): R: A language and environment for statistical computing. – R Foundation for Statistical Computing. R Core Term, Vienna. URL https://www.R-project.org/.
[37] Shao, K., Yan, S., Zhao, Y., Xiong, M., Xu, N. (2013): Seventeen microsatellite loci isolated from *Rhinogobio cylindricus* (Gunther), and their cross-amplification in six Gobioninae species. – Conservation Genetics Resources 5: 339-342.
[38] Smith, C. C. R., Snowberg, L. K., Caporaso, J. G., Knight, R., Bolnick, D. I. (2015): Dietary input of microbes and host genetic variation shape among-population differences in stickleback gut microbiota. – THE ISME Journal 9: 2515-2526.
[39] Stagaman, K., Burns, A. R., Guillemin, K., Bohannan, B. J. M. (2017): The role of adaptive immunity as an ecological filter on the gut microbiota in zebrafish. – The ISME Journal 11: 1630-1639.
[40] Tarnecki, A. M., Burgos, F. A., Ray, C. L., Arias, C. R. (2017): Fish intestinal microbiome: diversity and symbiosis unravelled by metagenomics. – Journal of Applied Microbiology 123(1): 2-17.
[41] Toranzo, A. E., Magariños, B., Romalde, J. L. (2005): A review of the main bacterial fish diseases in marinculture systems. – Aquaculture 246(1-4): 37-61.
[42] Wang, Q., Garrity, G. M., Tiedje, J. M., Cole, J. R. (2007): Naïve Bayesian classifier for rapid assignment of rRNA sequences into the new bacterial taxonomy. – Applied and Environmental Microbiology 73(16): 5261-5267.
[43] Wang, M. R., Yang, S. R., Liu, F., Li, M. Z., Dan, S. G., Liu, H. Z. (2012): Age and growth of *Rhinogobio cylindricus* Günther in the upper reaches of the Yangtze River. – Acta Hydrobiologica Sinica 36: 262-269.
[44] Wang, A. R., Ran, C., Ringø, E., Zhou, Z. G. (2018): Progress in fish gastrointestinal microbiota research. – Reviews in Aquaculture 10(3): 626-640.
[45] Xiang, J., He, T., Wang, P., Xie, M., Xiang, J., Ni, J. (2018): Opportunistic pathogens are abundant in the gut of cultured giant spiny frog (*Paa spinosa*). – Aquaculture Research 49(5): 2033-2041.
[46] Xiong, X. (2013): Study on basic biology and resource of *Rhinogobio cylindricus* Günther. – Chongqing Normal University, Chongqing. Master's thesis.
[47] Xiong, X., Li, Y., Tian, H., Jia, X., Duan, X., Liu, S., Chen, D. (2013): Growth and feeding habits of *Rhinogobio cylindricus* Günther in the upper reaches of Yangtze River. – Chinese Journal of Ecology 32(4): 905-911.
[48] Xiong, F., Liu, H. Y., Duan, X. B., Liu, S. P., Chen, D. Q. (2015): Population parameters and population abundance of Rhinogobio cylindricus in Zhuyangxi section of the upper Yangtze River. – Acta Ecologica Sinica 35(22): 7320-7327.
[49] Xiong, J., Nie, L., Chen, J. (2019): Current understanding on the roles of gut microbiota in fish disease and immunity. – Zooligical Research 40(2): 70-76.
[50] Yan, Q., Li, J., Yu, Y., Wang, J., He, Z., Van Nostrand, J. D., Kempher, M. L., Wu, L., Wang, Y., Liao, L., Li, X., Wu, S., Ni, J., Wang, C., Zhou, J. (2016): Environmental

http://www.aloki.hu ● ISSN 1589 1623 (Print) ● ISSN 1785 0037 (Online)
DOI: http://dx.doi.org/10.15666/aeer/2005_45394551

filtering decreases with fish development for the assembly of gut microbiota. – Environmental Microbiology 18(12): 4739-4754.

[51] Yukgehnaish, K., Kumar, P., Sivachandran, P., Marimuthu, K., Arshad, A., Paray, B. A., Arockiaraj, J. (2020): Gut microbiota metagenomics in aquaculture: factors influencing gut microbiome and its physiological role in fish. – Review in Aquaculture 12(3): 1903-1927.

APPENDIX

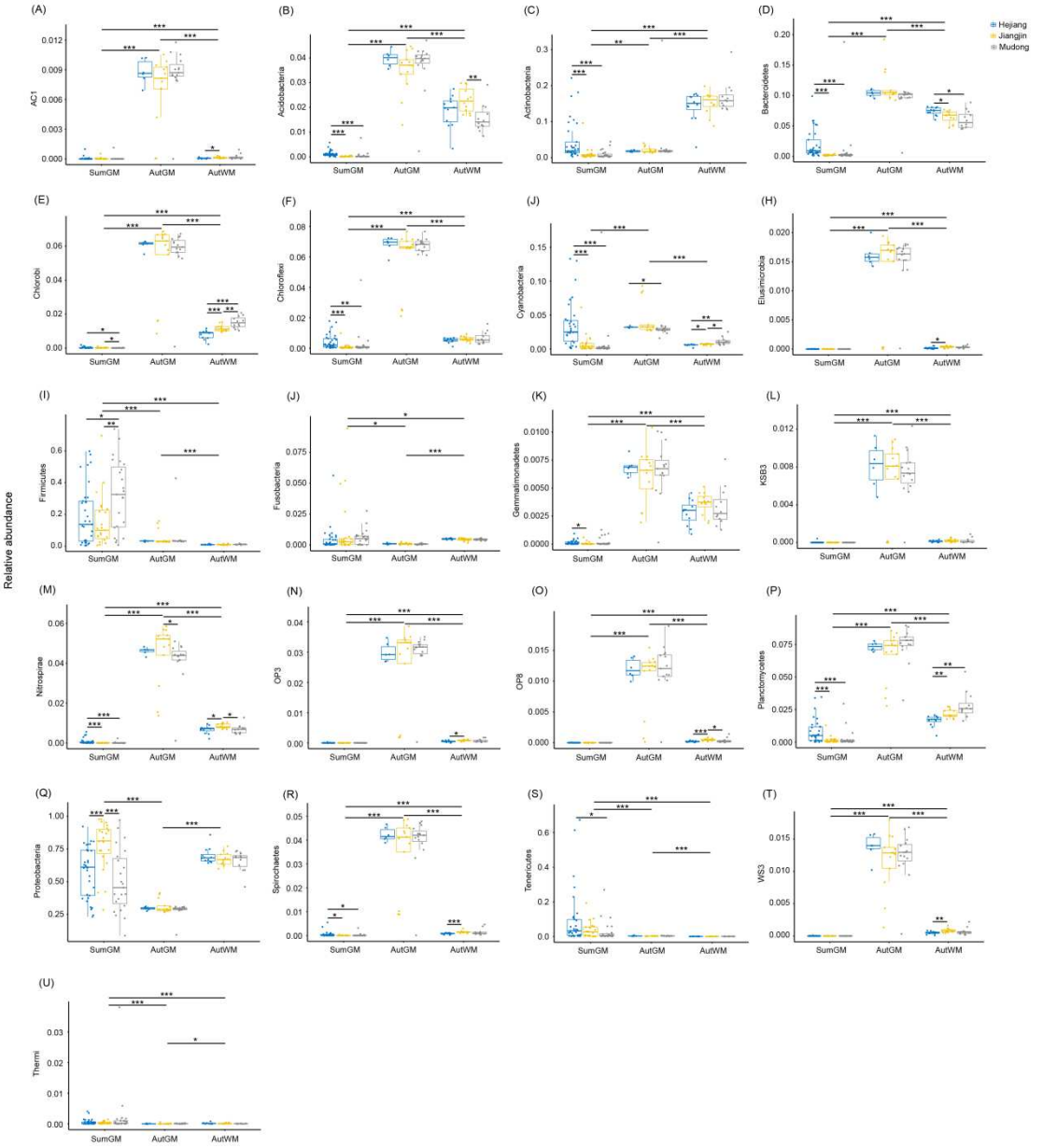

Appendix 1. *Changes of dominant phyla of Rhinogobio cylindricus gut microbiota and ambient water microbiota. SumGM, gut microbiota of R. cylindricus collected in summer; WinGM, gut microbiota of R. cylindricus collected in autumn; and WinWM, ambient water microbiota collected in autumn. *, $p < 0.05$; **, $p < 0.01$; ***, $p < 0.001$*

http://www.aloki.hu ● ISSN 1589 1623 (Print) ● ISSN 1785 0037 (Online)
DOI: http://dx.doi.org/10.15666/aeer/2005_45394551

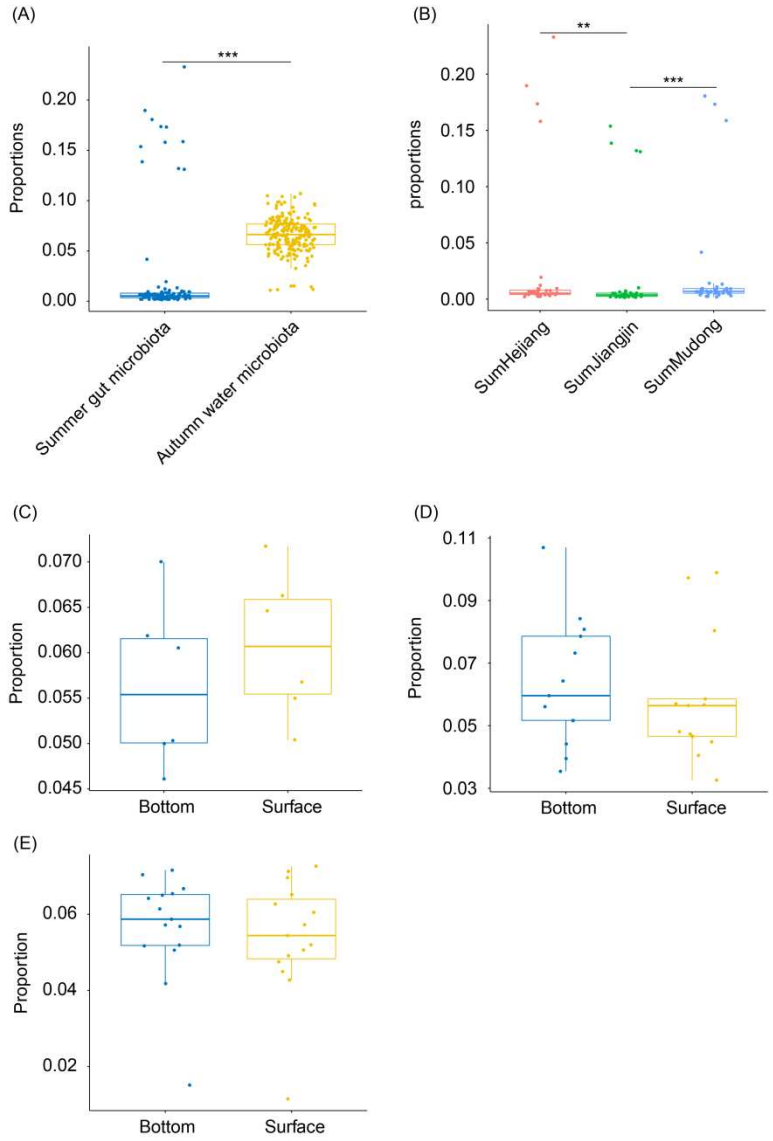

Appendix 2. *Proportion of autumn R. cylindricus gut microbiota (RGM) from summer RGM and autumn water microbiota. (A) Proportion of autumn RGM from summer RGM and autumn water microbiota, (B) Proportion of autumn RGM from summer RGM collected from different sampling sites, (C) Proportion of autumn RGM from autumn water microbiota collected from Hejiang, (D) Proportion of autumn RGM from autumn water microbiota collected from Jiangjin, and (E) Proportion of autumn RGM from autumn water microbiota collected from Mudong. **, $p < 0.01$; ***, $p < 0.001$*

http://www.aloki.hu ● ISSN 1589 1623 (Print) ● ISSN 1785 0037 (Online)
DOI: http://dx.doi.org/10.15666/aeer/2005_45394551

CONVERSION OF WETLANDS TO FARMLAND AND FORESTS REDUCES SOIL MICROBIAL FUNCTIONAL DIVERSITY AND CARBON USE INTENSITY

WANG, Q. B.[1,2] – WANG, Z. Y.[2] – WU, L. H.[2] – YANG, D. Q.[2] – DING, C. H.[2] – WANG, M.[2] – WANG, R.[2] – FU, X.[2] – WANG, Z. B.[2*]

[1]*Pharmaceutical Department of the First Affiliated Hospital of Guangdong Pharmaceutical University, Clinical Pharmacy Department of Guangdong Pharmaceutical University, Guangzhou 510080, China*

[2]*Key Laboratory of Basic and Application Research of Beiyao (Ministry of Education), Heilongjiang University of Chinese Medicine, Harbin 150040, China*

**Corresponding author*
e-mail: wzbmailbox@126.com

(Received 2nd Jun 2022; accepted 2nd Sep 2022)

Abstract. Changes in land use types typically lead to changes in soil ecosystem functions, and soil microorganisms can sensitively reflect soil quality and the evolution of different ecosystem functions. To characterize the impact of land use changes on the microbial function of wetlands, our study assessed three typical land use types (wetland, farmland, and forest land) in the Sanjiang Plain, and Biolog microplate technology was used to study the changes in the use intensity and functional diversity of different soil microbial carbon sources, as well as their relationship with soil physicochemical properties. Our findings indicated that the physical and chemical properties of soil changed significantly in different land use types ($P < 0.05$). The functional diversity and carbon source metabolism of wetland soil were significantly higher than those of farmland and forest. Furthermore, the utilization intensity of compound carbon sources was significantly higher than that of forests and farmland, whereas amino acids, esters, alcohols, amines, and acid carbon sources did not change significantly. Soil water content, total phosphorus, organic carbon, available phosphorus, and other physical and chemical factors affected soil microbial function in different land use types. This study provides key insights into the mechanisms through which land use changes affect soil microbial functions in the Sanjiang Plain, and it also serves as a theoretical basis for the protection and sustainable utilization of wetlands in the future.
Keywords: *Sanjiang Plain, reclamation, functional diversity, soil physicochemical, carbon source utilization efficiency*

Introduction

Soil microorganisms are an important part of soil ecosystems and have important roles in organic matter decomposition, nutrient cycling, promotion or inhibition of plant growth, and various soil physical processes (Sui et al., 2022). Studies have shown that several microbial activity indicators such as soil microbial biomass, respiration intensity, and changes in microbial community structure and functional diversity can sensitively reflect soil quality and health status. Therefore, these biological indicators are indispensable for soil environmental quality evaluation (Weng et al., 2022).

Changes in land use patterns affect the cycle and supply of soil nutrients, directly causing changes in soil texture and subsurface microbial community structure (Sui et al., 2019; Turley et al., 2020), which in turn leads to changes in soil microbial diversity. In recent years, Biolog Eco microplates have been used to study microbial diversity in a variety of media including sediments (Lopes et al., 2016) and activated sludge (Paixão

http://www.aloki.hu ● ISSN 1589 1623 (Print) ● ISSN 1785 0037 (Online)
DOI: http://dx.doi.org/10.15666/aeer/2005_45534564

et al., 2007). This method can be used to quickly characterize environmental samples and has therefore been applied in many fields. Deng et al. (2018) employed this technology to study the impact of different land use patterns on the diversity of soil microbial communities in the mountainous areas of Liaodong. Zhu et al. (2018) also found that cultivated land exhibited the lowest soil microbial metabolic activity among different land uses, whereas grasslands exhibited the strongest soil microbial metabolic activity and therefore, the highest microbial biomass carbon, followed by forest lands. Moreover, among six types of carbon sources, carbohydrates, amino acids, and carboxylic acids exhibited the highest relative utilization rates. Qin et al. (2017) reported that forest land can retain more soil nutrients, in addition to possessing higher bacterial and fungal diversity. Current research on soil microbial diversity has largely focused on natural soils such as forest land and grassland, and changes in land use patterns are known to significantly affect soil microbial activity and functional groups. However, very few studies have assessed the functional diversity of wetland soils, especially under different land use patterns.

The Sanjiang Plain Wetland is the largest concentration of freshwater wetlands in China and this ecosystem is highly biodiverse. The wetland ecosystem in the Sanjiang Plain is essential for the process of protecting regional biological resource diversity and maintaining the integrity of ecosystem functions (Sui et al., 2021). Therefore, this study employed Biolog microplate technology to study the changes in soil microbial functional diversity and carbon source utilization capacity under different land use patterns in the Sanjiang Plain. Moreover, the correlation between the soil carbon source metabolic diversity of microorganisms and environmental factors was also discussed. Understanding the functions of wetland ecosystems in the Sanjiang Plain provides a theoretical basis for the protection and sustainable utilization of wetland ecosystems in the future.

Materials and methods

Research area

The study site is located in the Sanjiang Plain in Heilongjiang Province (133°37′–133°45′E, 47°43′–47°52′N) and has an average elevation of 5.14–51.5 m. The site belongs to the mid-temperate continental monsoon climate zone and is mostly dry in spring. The region is windy, hot, and rainy in summer and cold with moderate snowing in winter, with an average annual temperature of 2.3 °C. The average precipitation is 454 mm. The freezing period begins in early November and the thawing period is in early May. The three land use methods selected in this area were the following: (1) Pristine wetlands, with an area of approximately 500 hm², the vegetation is mainly composed of *Deyeuxia angustifolia*, *Stellaria radians*, *Anemone dichotoma* and *Thalictrum simplex*. (2) Farmlands, which were transformed via swamp wetland reclamation 10 years ago, with an area of approximately 500 hm²; corn is the main crop in this area. (3) Forest, with an area of approximately 500 hm². This large artificial pure forest was planted in wetland soil 20 years ago.

Sample collection

In October 2021, three standard 10 m × 10 m plots were selected from the original wetland, farmland, and forest sample plots. Within each sampling plot, Fifteen to 20 soil

http://www.aloki.hu ● ISSN 1589 1623 (Print) ● ISSN 1785 0037 (Online)
DOI: http://dx.doi.org/10.15666/aeer/2005_45534564

samples (0–20 cm) were obtained. After the top layer (0–20 cm) of soil samples was evenly mixed, the gravel and rhizomes in the samples were removed and then sieved through a 2 mm sieve. A portion of the sample was placed in a 15 mL centrifuge tube, stored in liquid nitrogen, transferred to the laboratory and stored at -80 °C for DNA extraction and microbiological analysis. The rest of the soil samples were divided into two parts in the laboratory, one was kept at 4 °C, and the other was air-dried for the determination of soil physicochemical properties.

Determination of physical and chemical properties of soil samples

Determination of soil moisture content: 0.01 g of fresh soil samples were accurately weighed and placed in an aluminum dish, after which they were maintained at 10 ± 2 °C. The samples were then dried in a constant temperature drying chamber for 8 h, then weighed again to determine the moisture content. pH: soil pH was measured with a pH meter at a water-soil ratio of 2.5:1. Soil organic matter: soil organic carbon content was measured with a Vario TOC instrument produced by Elementar, Germany. Total nitrogen: 0.25 g of soil sample was accurately weighed and passed through a 0.149 mm sieve. Next, 2 g of accelerator mixed with zinc sulfate and copper sulfate and 5 mL of concentrated H_2SO_4 were added for digestion.

Biolog-Eco microplate test

The Biolog-Eco microplate culture method was used to detect the carbon metabolism capacity of the wetland soil microbial community. A portion of the soil sample was activated at 25 °C for 1 d, after which 10 g of the activated fresh soil was placed in a 200 mL conical flask. Next, 90 mL of 0.85% sterile NaCl solution was added to the flask, after which the flask was mixed and sealed. Afterward, the samples were placed in a shaker for 0.5 h at 200 r•min^{-1}. Then, the soil suspension diluted to 10^{-3} was inoculated into the microplate with a pipette. Each experiment was repeated three times, and the microplate was continuously cultured at 25 °C for 168 h. During the culture, the absorbance value at a wavelength of 590 nm was recorded every 24 h.

Data analysis

Average well color development (AWCD) was calculated as follows:

$$\text{AWCD} = \sum(C_i - R)/31 \quad \text{(Eq.1)}$$

In the formula, C_i is the absorbance value of the carbon sources at 590 nm; R is the absorbance value of the control well; the carbon source well with C_i-R < 0 is denoted as 0 in the calculation.

Soil microbial diversity index calculation:

$$\text{Shannon index: H} = P_i \ln P_i \quad \text{(Eq.2)}$$

$$\text{Simpson index: D} = 1 - (\sum P_i)^2 \quad \text{(Eq.3)}$$

$$\text{Margalef index: D} = (P_i\text{-}1)/\ln P_i \quad \text{(Eq.4)}$$

http://www.aloki.hu ● ISSN 1589 1623 (Print) ● ISSN 1785 0037 (Online)
DOI: http://dx.doi.org/10.15666/aeer/2005_45534564

In the formula, P_i is the ratio of the difference between the absorbance values of the i-*th* carbon source well and the control well (n_i) to the sum of the relative absorbance values of all wells.

Data analysis was performed using Excel 2010. The SPSS 25.0 software was used for one-way analysis of variance (ANOVA) and Duncan tests at a 0.05 significance level. One-way ANOVA was conducted to identify variations in soil physicochemical parameters, soil microbial α-diversity, and the microbial utilization of different carbon sources in different land use types, after which Duncan tests were conducted. Scatter plots with trend lines were generated in Excel 2010 and SigmaPlot 10.0 was used to draw histograms. Analysis of soil microbial alpha diversity, redundancy analysis (RDA), and principal coordinates analysis (PCoA) were conducted in R (version 3.3.2) using the 'vegan' package (R Core Team, 2022). Permutational multivariate analysis of variance (PERMANOVA) between all habitats and each land use type were performed in R software (version 3.3.2) using the "vegan" package (R Core Team, 2022).

Results

Changes in soil physical and chemical properties under different land use patterns

Table A1 (see *Appendix*) summarizes the physical and chemical properties of the soil in the three land use modes. There were significant differences in soil pH, moisture content (MC), soil organic carbon (SOC), total nitrogen (TN), total phosphor (TP), available phosphor (AP), and available nitrogen (AN) among different land use types ($P < 0.05$). Overall, the soil SOC, TN, TP, AP, MC and AN of the original wetland were the highest. The pH values of the different soil types exhibited the following descending order: forest > farmland > wetland. MC exhibited the following order: wetland > forest > farmland.

Soil microbial alpha diversity of the wetland in Sanjiang Plain

To further determine the effect of different land uses on soil microbial functional diversity, the AWCD value at 168 h of cultivation was selected for α diversity analysis. As indicated in *Table 1,* all indices except for the Margalef richness index showed significant differences. Particularly, the Shannon, Simpson, and AWCD indices were the highest in the original wetlands and the lowest in the farmland. This indicated that the functional diversity of soil microorganisms decreased significantly after the wetlands were converted into farmland.

Table 1. *α-Diversity of soils with different land use types*

Land use type	Shannon	Simpson	Margalef	AWCD
Wetland	3.4 ± 0.03a	0.96 ± 0.00a	9.8 ± 0.46a	1.14 ± 0.08a
Farmland	3.3 ± 0.03b	0.96 ± 0.00b	12.0 ± 1.76a	0.88 ± 0.02b
Forest	3.3 ± 0.03a	0.96 ± 0.00ab	12.0 ± 0.83a	0.89 ± 0.06b

The values represent the mean ± standard deviation (n = 3); different lowercase letters indicate significant differences among different treatments based on Duncan tests ($P < 0.05$)

The relationship between soil microbial functional diversity indices and soil physicochemical properties in Sanjiang Plain is shown in *Table 2*. Except for MC and

http://www.aloki.hu ● ISSN 1589 1623 (Print) ● ISSN 1785 0037 (Online)
DOI: http://dx.doi.org/10.15666/aeer/2005_45534564

TN, the environmental factors pH, AN, AP, TP, and SOC were all correlated with AWCD, the Shannon index, the Simpson index, and the Margalef index. AWCD was positively correlated with AN and TP but negatively correlated with pH. The Margalef index was correlated with AN and negatively correlated with TP. The Shannon index was positively correlated with AP and SOC. The Simpson index was positively correlated with AN, AP, and SOC.

Table 2. *Correlation between soil environmental factors and soil microbial functional diversity in different land use types*

	pH	AN	AP	TP	TN	SOC	MC
Simpson	-0.54	0.67*	0.81**	0.45	0.32	0.89**	0.41
Shannon	-0.41	0.54	0.78*	0.32	0.14	0.87**	0.52
Margalef	0.59	-0.72*	-0.62	-0.77*	-0.55	-0.58	-0.08
AWCD	-0.69*	0.82**	0.64	0.81**	0.62	0.64	0.04

*$P < 0.05$; **$P < 0.01$

Carbon source metabolic activity of soil microorganisms in different land use types

The AWCD reflects the overall ability of the microbial community to utilize a single carbon source in the Biolog-ECO plate and is an important indicator of the functional diversity of the microbial community (Song et al., 2019). As shown in *Figure 1,* the soil microbial community AWCD increased with cultivation time in all of the examined land use types. The AWCD values of the soils of all plots remained low from 0 to 48 h. After 48 h, the AWCD values of the original wetland soil microorganisms increased rapidly, but the increase rate of the forest and farmland soils was slow. This indicated that the utilization of carbon sources by soil microbes began after 48 h. In general, the AWCD values of 31 carbon sources under different land use patterns exhibited the following trend: wetland > forest > farmland. It is also worth noting that there was no significant difference in AWCD values between forest and farmland ($P > 0.05$). However, both of them were significantly different from the original wetland ($P < 0.05$).

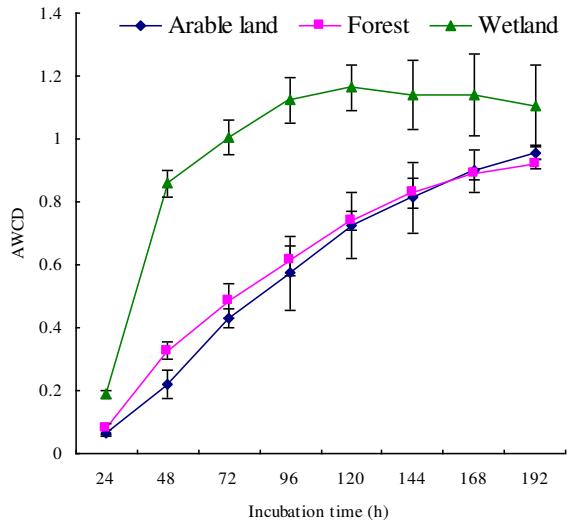

Figure 1. *AWCD of the soil microbial community in different land use types of the Sanjiang plain. The data and error bar were expressed as the mean ± standard deviation*

http://www.aloki.hu ● ISSN 1589 1623 (Print) ● ISSN 1785 0037 (Online)
DOI: http://dx.doi.org/10.15666/aeer/2005_45534564

There are 31 carbon sources in the Biolog-ECO board, which can be divided into six categories, namely 7 carbohydrates, 6 amino acids, 4 esters, 3 alcohols, 3 amines, and 8 organic acids. *Figure 2* illustrates the utilization of different carbon sources by soil microorganisms under different land use patterns in the Sanjiang Plain. Overall, only the carbohydrate carbon sources showed significant differences ($P < 0.05$) under different land use patterns, whereas the other five types of carbon sources did not show significant differences. However, the utilization intensity of all 6 types of carbon sources reached a maximum in wetland soil. This indicated that the wetland soil microorganisms had the highest utilization activity of the six types of carbon sources.

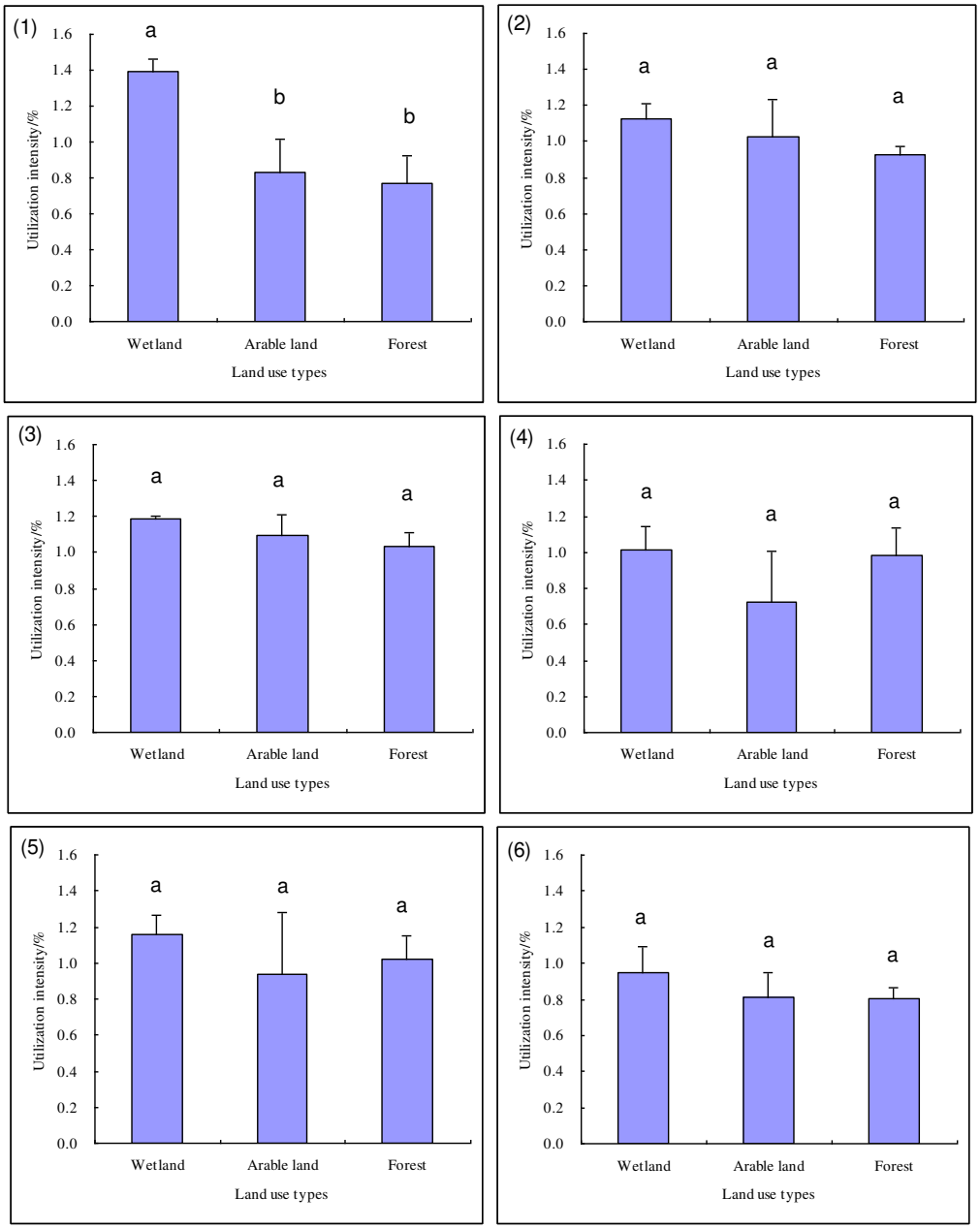

Figure 2. *Changes in the microbial utilization of different carbon sources in different land use types. Different lowercase letters indicate significant differences among different nitrogen treatments based on Duncan tests ($P < 0.05$). (1): carbohydrates; (2): amino acids; (3): alcohols; (4): esters, (5): amines; (6): organic acids*

http://www.aloki.hu ● ISSN 1589 1623 (Print) ● ISSN 1785 0037 (Online)
DOI: http://dx.doi.org/10.15666/aeer/2005_45534564

As illustrated in *Figure 3,* there were significant differences in the metabolic activities of 31 carbon sources in soil microbial communities under three different land use methods. Wetland soil microorganisms mainly used α-cyclodextrin, α-D-lactose, glycogen, 4-hydroxy benzoic acid, and D-xylose. Farmland soil microorganisms mainly used L-asparagine, D-galactonic acid-γ-lactone, γ-hydroxybutyric acid, D-cellobiose, and L-serine. Forest soil microorganisms mainly used L-asparagine, D-mannitol, phenylethyl-amine, D-galacturonic acid, and L-serine. The PCoA results showed that the variance contribution rates of Pco1 and Pco2 were 45% and 17%, respectively (see *Fig. 4*). Overall, there were significant differences in the soil microbial community functions between wetlands, farmland, and forests (*Figure 4; Table A2*).

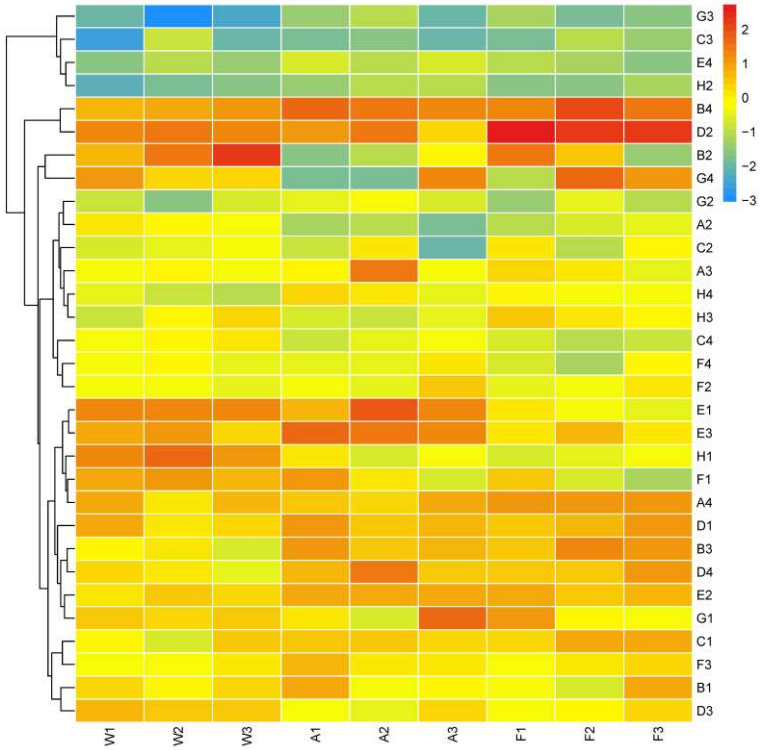

Figure 3. *Metabolic activity heat map of soil microbial community in different land use types in the Sanjiang Plain. W(1-3): wetland, A(1-3): farmland, F(1-3): forest. G3–α-ketobutyric acid; C3–2-hydroxy benzoic acid; E4–L-threonine; H2–D, L-α-glycerol phosphate; B4–L-asparagine; D2–D-mannitol; B2–D-xylose; G4–phenylethyl-amine; G2–α-D-glucose-1-phosphate; A2–β-methyl-D-glucoside; C2–i-erythritol; A3–D-galactonic acid-γ-lactone; H4–putrescine; H3–D-malic acid; C4–L-phenylalanine; F4–glycyl-L-glutamic acid; F2–D-glucosaminic acid; E1–α-cyclodextrin; E3–γ-hydroxybutyric acid; H1–α-D-lactose; F1–Glycogen; A4–L-arginine; D1–tween 80; B3–D-galacturonic acid; D4–L-serine; E2–N-acetyl-d-glucosamine; G1–D-cellobiose; C1–tween 40; F3–itaconic acid; B1–pyruvic acid methyl ester; D3–4-hydroxy benzoic acid*

Relationship between soil microbial carbon utilization activity and soil physicochemical properties

Redundancy analysis (RDA) was performed on the AWCD values of soil microbial communities in the Sanjiang Plain wetland cultivated for 168 h under different land use patterns (*Figure 5*). The first two RDA axes explained 48.29% and 17.98% of the

http://www.aloki.hu ● ISSN 1589 1623 (Print) ● ISSN 1785 0037 (Online)
DOI: http://dx.doi.org/10.15666/aeer/2005_45534564

variance, respectively. The soil microbial community exhibited obvious spatial differences in carbon source utilization under different land use patterns. Particularly, changes in land utilization patterns had an impact on the ability of wetland soil microbes to utilize different carbon sources. Additionally, the RDA results demonstrated that MC, TP, SOC, and AP were among the soil environmental factors that had the greatest impact on soil microbial function. Among them, forests were significantly positively correlated with MC, pH, SOC, and AP, whereas wetlands were positively correlated with TN, TP, AN, AP, and SOC, and farmland was positively correlated with pH, TN, AN, and TP.

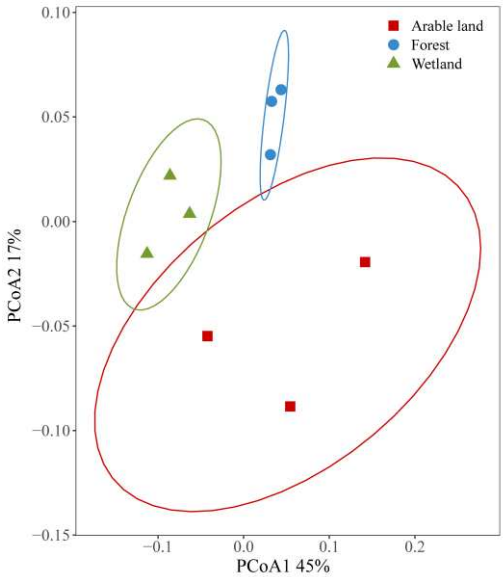

Figure 4. *PCoA of soil carbon source metabolism of the different land use types*

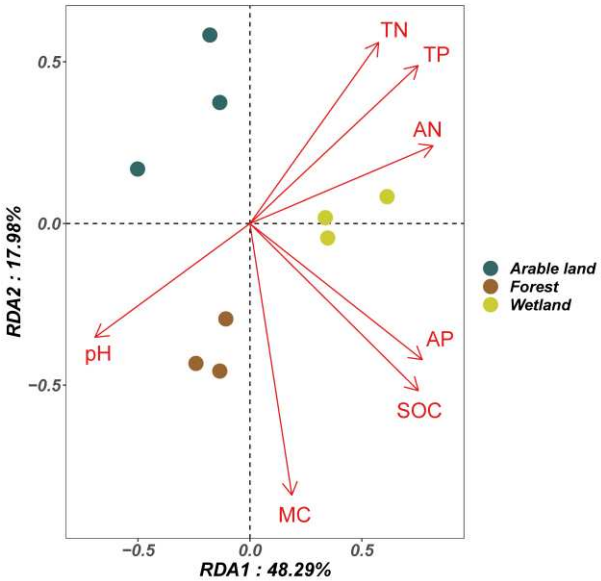

Figure 5. *Redundancy analysis of soil carbon sources and soil physicochemical properties of the different land use types*

APPLIED ECOLOGY AND ENVIRONMENTAL RESEARCH 20(5):4553-4564.
http://www.aloki.hu ● ISSN 1589 1623 (Print) ● ISSN 1785 0037 (Online)
DOI: http://dx.doi.org/10.15666/aeer/2005_45534564

Discussion

Effects of land use patterns on soil microbial functional diversity

Different land use patterns significantly affected the functional diversity of soil microbial communities. The AWCD of the original wetland was significantly higher than that of the farmland and forest (*Table 1*). This indicated that the soil microbial carbon source utilization ability decreased after the transformation of the original wetland. Moreover, the results of the Shannon index study also showed that the soil microbial functional diversity of the original wetland was significantly higher than that of the forests and farmland. In other words, the diversity and ability of soil microbes to utilize carbon sources decreased once the wetlands were converted into forests and farmlands. This may be due to the stability of the original wetland soil ecosystem. When wetlands are converted into farmlands and forests, the soil microbial structure changes due to the disturbance of aboveground vegetation and human activities (Sui et al., 2019; Guo et al., 2021). Jia et al. (2020) also found that after the original wasteland was converted into cultivated land, the microbial carbon source utilization rate decreased.

Land use can directly change the physicochemical properties and structure of soil, thereby affecting the soil microbial community and playing an important role in shaping its diversity (Burton et al., 2010). In a previous study that assessed the functional diversity of soil microorganisms in different land use types in the Sanjiang Plain, the authors found that there were significant differences in the soil microbial alpha functional diversity in the different land types, and the diversities of the original wetland and forest were significantly higher than those of farmlands. In primitive wetlands and forest ecosystems, the soil environment is conducive to the reproduction and growth of microorganisms due to the high diversity of aboveground vegetation, which results in high functional diversity. Therefore, the diversity of soil microbial species decreases and harmful microorganisms increase in farmland ecosystems, and the functional diversity of farmland soil microorganisms will be significantly lower than that in wetlands and forests. Zhang et al. (2015) compared the soil microbial functional diversity of primitive wetlands and paddy fields, and the results were consistent with this study, suggesting that microbial metabolic diversity is related to carbon input. Moreover, this study also found that soil microbial Shannon diversity was positively correlated with organic carbon utilization. Therefore, the soil microbial Shannon diversity of farmland soil was lower due to low carbon input and agricultural disturbances.

Effects of land use patterns on soil microbial carbon source metabolism

This study found that there were significant differences in soil carbohydrate carbon sources when the original wetland was converted into forest and farmland, and the utilization intensity of carbohydrate carbon sources in wetland soil microorganisms was significantly higher than that in forest and farmland soils. However, no significant differences were observed in the utilization of amino acids, esters, alcohols, amines, and organic acids. There is currently no consensus regarding the utilization patterns of different types of carbon sources by soil microorganisms. This may be because microbial communities are highly sensitive to soil environmental changes and stresses, resulting in changes in microbial carbon utilization patterns related to changes in environmental parameters (Kumar et al., 2017). Moreover, different carbon source types

http://www.aloki.hu ● ISSN 1589 1623 (Print) ● ISSN 1785 0037 (Online)
DOI: http://dx.doi.org/10.15666/aeer/2005_45534564

have different functional groups (e.g., carbohydrates: R-C = O; amino acids: -NH2 and -COOH; carboxylic acids: -COOH; phenolic compounds: -OH; amines: -NH2; polymers: monomers). Carbohydrate carbon sources are the most widely used carbon sources by soil microorganisms, and decreases in carbohydrate utilization may be related to a decrease in the overall diversity of soil microorganisms. Sui et al. (2019) studied soil microbial diversity in different succession stages in the Sanjiang Plain and found that wetland soil microbial diversity was significantly higher than that of forests. Therefore, this may explain why carbohydrate utilization in wetland soil was higher than that in forest and farmland. However, our findings indicated that although the differences in the utilization of amino acids, esters, alcohols, amines, and organic acids were not significant, the utilization intensity of these carbon sources by wetland soil microorganisms was still higher than in forests and farmlands. This may be because the forest and farmland in this study had not been transformed from wetlands for a long time, and the original microbial composition in the soil may not have changed significantly. Therefore, the utilization of other carbon source types by soil microorganisms has not changed significantly. However, Wang et al. (2017) studied the metabolic intensity of soil microbial carbon sources in the Xiaoyezhang wetlands, larch plantations, and soybean fields in the Sanjiang Plain, and found that the utilization of all types of carbon sources were significantly different.

Currently, there are many methodological difficulties and obstacles in the determination of soil microbial functional diversity. On the one hand, the Biolog analysis method can only reflect the functional diversity of microorganisms from the perspective of metabolic characteristics, but cannot reflect the diversity of specific species. Only the culturable microorganisms that can utilize the carbon source on the plate can be reflected. Furthermore, after the mixed culture is added into the wells of the Biolog microplate, synergistic effects or countermeasure effects will cause the final color in the microplate to not necessarily represent the simple sum of the colors produced by various microorganisms alone. Therefore, a combination of techniques is needed to comprehensively characterize changes in soil microbial function. High-throughput sequencing technology has proven to be a very powerful tool in microbial ecology research. Therefore, this technology must also be implemented in ecology studies to fully and accurately reflect the functional diversity of soil microorganisms. This approach would provide important insights into the factors that shape the structure of microbial communities and the response of microorganisms to environmental changes. In turn, this would improve our understanding of the dynamics of natural or managed ecosystems.

Conclusion

Our findings demonstrated that changes in the land use types in the Sanjiang Plain resulted in significant variations in soil microbial functional diversity and carbohydrate utilization. The α-diversity of wetland soil microorganisms was significantly higher than that of forest and farmland soils. Moreover, the utilization of different carbon sources by wetland soil microorganisms was also higher than that of forest and farmland microbes. The differences in soil microbial functional diversity, carbon source utilization capacity, and microbial functional diversity of carbon source utilization under different land use patterns were related to soil physicochemical factors. Soil MC, TP, SOC, and AP are the most important environmental factors affecting soil microbial

http://www.aloki.hu ● ISSN 1589 1623 (Print) ● ISSN 1785 0037 (Online)
DOI: http://dx.doi.org/10.15666/aeer/2005_45534564

function. Collectively, our findings revealed the impact of soil microbial functions on wetland ecosystems and provide a theoretical basis for the future management and sustainable utilization of wetland ecosystems.

Acknowledgements. This study was supported by the "Touyan" Innovation Team Program of Heilongjiang Province, China (Grant Number: [2019] No. 5).

REFERENCES

[1] Burton, J., Chen, C., Xu, Z., Ghadiri, H. (2010): Soil microbial biomass, activity and community composition in adjacent native and plantation forests of subtropical Australia. – J Soil Sediment 10(7): 1267-1277.

[2] Deng, J. J., Zhu, W. X., Zhou, Y. B., Yin, Y., Bai, X. J., Zhang, H. Z., Zhang, Y. M., Qin, S. J. (2018): Effects of different land use patterns on the soil microbial community diversity in montane region of eastern Liaoning Province, China. – Chin J Appl Ecol 29(7): 2269-2276.

[3] Guo, X., Zhou, Y. (2021): Effects of land use patterns on the bacterial community structure and diversity of wetland soils in the Sanjiang Plain. – J Soil Sci Plant Nut 21(1): 1-12.

[4] Jia, P. L., Li, M., Feng, H. Y. 2020: Soil microbial diversity of black soil under different land use patterns in northeast China. – Transactions of the Chinese Society of Agricultural Engineering (Transactions of the CSAE) 36(20): 171-178.

[5] Kumar, U., Shahid, M., Tripathi, R., Mohanty, S., Kumar, A., Bhattacharyya, P., Nayak, A. K. (2017): Variation of functional diversity of soil microbial community in sub-humid tropical rice-rice cropping system under long-term organic and inorganic fertilization. – Ecol Indic 73: 536-543.

[6] Lopes, J. C., Peixoto, V., Coutinho, A., Mota, C., Fernandes, S. (2016): Determination of the community-level physiological profiles (CLPP) using BiologTM ECO-plates in the river Minho estuary sediments (Northern Portugal). – In: Front Mar Sci Conference Abstract: IMMR| International Meeting on Marine Research.

[7] Paixão, S. M., Sàágua, M. C., Tenreiro, R., Anselmo, A. M. (2007): Assessing microbial communities for a metabolic profile similar to activated sludge. – Water Environ Res 79: 536-546.

[8] Qin, H., Li, C. X., Ren, Q. S. (2017): Effects of different land use patterns on soil bacterial and fungal biodiversity in the hydro-fluctuation zone of the Three Gorges Reservoir region. – Acta Ecol Sini 37(10): 3494-3504.

[9] R Core Team (2022): R: A language and environment for statistical computing. – R Foundation for Statistical Computing, Vienna, Austria. URL https://www.R-project.org/.

[10] Song, X. C., Wang, H. L., Qin, W. D., Deng, X. J., Tian, H. D., Tan, Y. B., Cao, J. Z. (2019): Effects of stand type of artificial forests on soil microbial functional diversity. – J Appl Ecol 30(3): 841-848.

[11] Sui, X., Zhang, R. T., Frey, B., Yang, L. B., Li, M. H., Ni, H. W. (2019): Land use change effects on diversity of soil bacterial, acidobacterial and fungal communities in wetlands of the Sanjiang Plain, northeastern China. – Sci Rep 9(1): 1-14.

[12] Sui, X., Zhang, R. T., Frey, B., Yang, L. B., Liu, Y. N., Ni, H. W., Li, M. H. (2021): Soil physicochemical properties drive the variation in soil microbial communities along a forest successional series in a degraded wetland in northeastern China. – Ecol Evol 11(5): 2194-2208.

[13] Sui, X., Zeng, X. N., Li, M. S., Weng, X. H., Frey, B., Yang, L. B., Li, M. H. (2022): Influence of different vegetation types on soil physicochemical parameters and fungal communities. – Microorganisms 10(4): 829.

http://www.aloki.hu ● ISSN 1589 1623 (Print) ● ISSN 1785 0037 (Online)
DOI: http://dx.doi.org/10.15666/aeer/2005_45534564

[14] Turley, N. E., Bell-Dereske, L., Evans, S. E., Brudvig, L. A. (2020): Agricultural land-use history and restoration impact soil microbial biodiversity. – J Appl Ecol 57(5): 852-863.
[15] Wang, J. F., Sui, X., Zhang, R. T., Xu, N., Yang, L. B., Liu, Y. N., Fu, X. L., Chai, C. R., Xu, M. Y., Xing, J. H., Zhong, H. X., Ni, H. W., Li, M. H. (2017): Effects of different land use on soil bacterial functional diversity in Sanjiang Plain, Northeast China. – J Residuals Sci Tech 14(1): 91-98.
[16] Weng, X. H., Sui, X., Liu, Y. N., Yang, L. B., Zhang, R. T. (2022): Effect of nitrogen addition on the carbon metabolism of soil microorganisms in a Calamagrostis angustifolia wetland of the Sanjiang Plain, northeastern China. – Ann Microbiol 72(1): 1-14.
[17] Zhang, J., Hu, W., Liu, Y. Z., Ge, G., Wu, L. (2015): Response of soil microbial functional diversity to different land-use types in wetland of Poyang Lake, China. – Acta Ecol Sini 35(4): 965-971.
[18] Zhu, K., Wang, R., Li, G. (2018): The response of microbial biomass carbon and metabolic characteristics of albic soil to land use change. – J Agro-Environ Sci 37(10): 2194-2201.

APPENDIX

Table A1. *Physicochemical properties of soils with different land use practices*

Land use types	pH	MC (%)	SOC (g/kg)	TN (g/kg)	TP (g/kg)	AP (mg/kg)	AN (mg/kg)
Wetland	4.5 ± 0.13c	43.5 ± 2.79a	55.4 ± 0.97a	4.2 ± 0.22a	7.0 ± 0.55a	47.5 ± 1.70a	365.9 ± 19.11a
Farmland	5.5 ± 0.13b	18.2 ± 0.70c	27.3 ± 2.15c	3.3 ± 0.09b	5.1 ± 0.40b	28.7 ± 0.63c	194.6 ± 5.52b
Forest	6.1 ± 0.21a	28.5 ± 4.76c	45.1 ± 1.52b	1.8 ± 0.21c	3.5 ± 0.51c	38.7 ± 1.39b	141.0 ± 11.13c

MC, soil moisture content; SOM, soil organic carbon; TN, total nitrogen; TP, total phosphorus; AP, available phosphors; AN, available nitrogen. The values represent the mean ± standard deviation (n = 3), different lowercase letters indicate significant differences among different treatments ($P < 0.05$)

Table A2. *Permanova analysis of soil microbial community functions comparing two types along different land use types in Sanjiang Plain, northeastern China*

Land use types	R^2	*P*
Habitat	0.48	< 0.05
Wetland versus farmland	0.45	< 0.05
Farmland versus forest	0.65	< 0.05
Forest versus wetland	0.58	< 0.05

http://www.aloki.hu ● ISSN 1589 1623 (Print) ● ISSN 1785 0037 (Online)
DOI: http://dx.doi.org/10.15666/aeer/2005_45534564

STRUCTURE, VARIATION, AND CO-OCCURRENCE OF ARCHAEAL COMMUNITIES ASSOCIATED WITH POLYMER- AND ASP-FLOODED PETROLEUM RESERVOIR BLOCKS

WANG, J. L.[1] – WANG, C. J.[1] – BIAN, L. H.[2] – HU, M.[2] – QU, L.[2] – REN, G. L.[2*]

[1]*College of Science, Traditional Chinese Medicine Biotechnology Innovation Center in Jilin Province, Beihua University, Jilin 132013, China*

[2]*College of Bioengineering, Daqing Normal University, Heilongjiang Provincial Key Laboratory of Oilfield Applied Chemistry and Technology, Daqing 163712, China*

**Corresponding author*
e-mail: Rengl2020@163.com

(Received 9th Jul 2022; accepted 2nd Sep 2022)

Abstract. The response of archaeal communities to the enhancement of the oil recovery process in the extreme environments of oil reservoirs has rarely been investigated. In this study, archaeal communities in polymer- and alkaline-surfactant-polymer (ASP)-flooded production wells were evaluated via Illumina high-throughput sequencing targeting 16S rRNA genes. The composition of the archaeal community differed significantly among enhanced oil recovery production wells. *Methanothermobacter* was dominant in the polymer- and ASP-flooded production blocks. *Methanoculleus* accounted for numerous archaeal communities inhabiting the polymer-flooded blocks but were hardly detected in the ASP-flooded blocks; the trends for *Methanolinea* were the opposite. Redundancy analysis indicated that the archaeal communities in polymer- and ASP-flooded production blocks were closely related to physical and chemical factors, such as strong alkalinity and high salinity, which together accounted for 75.03% of the total variance. We applied network analysis to the co-occurrence pattern of archaeal communities in oil reservoirs. The archaeal communities in oil reservoirs were non-random, and that the community structure was more stable in the polymer- than in the ASP-flooded production wells. The polymer flooding process led to a more complex archaeal network than that of ASP flooding. Our results indicated that enhanced oil recovery mediates the coexistence of archaeal species in deep oil reservoirs. This study contributes to our understanding of the contemporary coexistence theory in microbial ecosystems in extreme environments. Revealing the influence of polymer flooding and ASP flooding on community composition and co-occurrence patterns of archaea could facilitate the implementation of MEOR technology in the future.

Keywords: *archaeal community, network analysis, polymer flooding, ASP flooding, enhanced oil recovery, deep subsurface environments*

Introduction

Subsurface petroleum reservoir ecosystems represent a deep subsurface environment with high salinity and pressure, low water activity, and high hydrophobicity, which is extreme for microbial life (Cai et al., 2015; Pannekens et al., 2019). Nevertheless, oil reservoirs consist of multiphase media (including water, organic materials, and crude oil), which allow microorganisms to thrive (Kobayashi et al., 2012; Abilio et al., 2021) and harbor a wide distribution of anaerobic microorganisms, including most hydrocarbon-oxidizing, sulfur-oxidizing, sulfate-reducing, fermentative, and methanogenic bacteria (Chia, 2014; Singh and Choudhary, 2021). In recent years, the microbial communities associated with deep oil reservoirs have received increasing attention from researchers (l'Haridon et al., 1995; Ollivier et al., 1997; Grabowski et al., 2005; Li et al., 2007; Zhao et al., 2021; Yun et al., 2022). Numerous anaerobic microorganisms, such as sulfidogens

http://www.aloki.hu ● ISSN 1589 1623 (Print) ● ISSN 1785 0037 (Online)
DOI: http://dx.doi.org/10.15666/aeer/2005_45654578

(Lenchi et al., 2021), sulfate reducers (Rajbongshi and Gogoi, 2021), methanogens (Nilsen and Torsvik, 1996; Dengler et al., 2022), and iron and manganese reducers (Dong et al., 2022) have been isolated and recognized from different oil reservoirs. Methanogenic archaea are very common in subsurface petroleum reservoir ecosystems, in which liquid petroleum hydrocarbons are the primary organic matter (Magot et al., 2000). In these oil reservoirs, hydrocarbons are degraded by various bacteria into methanogenic substrates, such as CO_2, acetate, and H_2. Methanogenesis is the last degradation procedure of organic matter by methanogenic archaea in the subsurface petroleum reservoir and, therefore, of great significance for understanding the ecological pattern of oil reservoir archaea from the perspective of scientific significance and industrial applications, such as microbial enhanced oil recovery (MEOR) (Aitken et al., 2004; Rathi et al., 2018; Tyne et al., 2021; Du et al., 2022).

Many large oil fields worldwide, including the DaQing, have recently entered the late stage of high water cut production. Oil recovery in such reservoirs faces differing degrees of annual decline. However, the consumption and demand for oil are growing, and oil will continue to be a major contributor to the world economy in the coming decades (Al Adasani and Bai, 2011; Chen et al., 2019; Baumeister et al., 2022). Approximately 70% of the total crude oil in a reservoir remains after the use of only conventional oil recovery methods (Yang et al., 2004; Kang et al., 2011). In recent years, chemical flooding has become a very important tertiary oil recovery technology. Chemical EOR flooding technologies, such as alkaline, surfactant, polymer, alkaline surfactant, alkaline polymer (AP), and alkaline-surfactant-polymer (ASP) flooding, are increasingly used in oil fields (Shutang and Qiang, 2010; Firozjaii and Saghafi, 2020). Polymer and ASP flooding technologies have been applied in oil reservoirs globally for 30 years (Chang et al., 2006). However, the diversity and composition of the archaea community in polymer- and ASP-flooded reservoirs have rarely been reported.

Due to the natural advantages of indigenous microbial communities, such as archaea in the process of microbial oil flooding, revealing the community composition and co-occurrence pattern of archaea in polymer flooding and ASP flooding reservoirs could facilitate the implementation of future oil recovery technologies. In this study, a 16S rRNA gene library was analyzed to study the archaeal community structure in different EOR processes at the DaQing Oilfield located in Heilongjiang province, China. We aimed to reveal additional archaeal diversity, which will increase our understanding of the complex community that inhabits the subterranean petroleum-rich system. The composition of archaeal communities present in two EOR production blocks (polymer- and ASP-flooded) was investigated to determine the archaeal co-occurrence pattern response to EOR treatment. Considering the contrasting processes and mechanisms of polymer and ASP flooding, we hypothesized that (I) the community composition of archaea was significantly different in polymer- and ASP-flooded production blocks, and (II) the community co-occurrence networks from these sample sets were non-random. EOR methods mediated the organization and complexity of co-occurrence networks and stability.

Materials and methods

Sample collection and total DNA extraction

The research was conducted in the DaQing Oilfield in Northeast China. The temperature of the oil-bearing layer of the reservoir was approximately 45 °C. Polymer and ASP flooding technologies were applied in 1995 and 2014 in the Daqing Oil Field,

http://www.aloki.hu ● ISSN 1589 1623 (Print) ● ISSN 1785 0037 (Online)
DOI: http://dx.doi.org/10.15666/aeer/2005_45654578

respectively. The pH of the production water samples obtained from polymer- and ASP-flooded blocks were 11.18 and 8.22, respectively (INESA Instrument, Shanghai, China). In August 2019, A total of 66 oil-water samples were collected from polymer-flooded (29 wells) and ASP-flooded (37 wells) production wells and were immediately stored in 10 L plastic containers. To avoid oxygen intrusion, the containers were filled to maintain anaerobic conditions. We transported the containers in a cooler filled with ice blocks within 48 h to the lab for DNA extraction. Before collecting the samples, we autoclaved all the containers and rinsed them with water samples for collection. The water samples (2 L) were centrifuged repeatedly at 12,000 g at 4 °C for 30 min to precipitate microbial cells (Beckman, United States). The filters were used for genomic extraction, placed in a buffer, and immediately frozen in a freezer at −80 °C until the DNA was isolated (Pham et al., 2009; Tully et al., 2012). The Axygene bacterial genomic DNA extraction kit (Takara) was used to extract genomic DNA from the precipitate. The quality of DNA was checked on an agarose gel and either used in the analysis described below or stored at −20 °C.

Amplification and analysis of 16S rRNA genes

Total genomic DNA was extracted from the production water and used to construct the archaeal library. Archaeal 16S rRNA sequences were amplified using archaea-specific primer set Arch524f (5'-TGYCAGCCGCCGCGGTAA-3') and Arch958r (5'-YCC GGC GTT GAM TCC AAT T-3') (DeLong, 1992). The polymerase chain reaction (PCR) mixture contained 2 μL of dNTP (2.5 mM), 0.2 μL of Ex Taq (5 U/μL), 2.5 μL of 10 × PCR buffer, primers 27f/1492r (20 μM) at 0.4 μl, 4 μL of template DNA (100 ng), and 15.5 μl of sterile water. The genomic DNA from the water sample was used as the template for amplification with final reaction concentrations of 1.5–3 ng/μL. The PCR amplification program contained a 5-min initial denaturation at 95 °C, followed by 5 cycles at 94 °C for 30 s, 55 °C for 30 s, and 72 °C for 1 min, 30 cycles at 92 °C for 30 s, 55 °C for 30 s, and 72 °C for 1 min, and a final extension at 72 °C for 10 min. The 16S rRNA PCR clones were used to construct a library that was sequenced.

Illumina MiSeq sequencing

Purified amplicons were pooled in equimolar ratios and paired-end sequenced (2 × 250) on an Illumina MiSeq platform (Illumina, SanDiego, USA) according to the standard protocols by Majorbio Bio-Pharm Technology Co. Ltd. (Shanghai, China).

Statistical analysis

The variation in the composition of the archaeal community inhabiting the ASP- and polymer-flooded production blocks was visualized using nonmetric multidimensional scaling (NMDS) with 1000 iterations, using the function metaMDS () of the VEGAN package in R (Van Geel et al., 2018). To explicitly test whether archaeal communities differed among different EOR application oil reservoirs, we used PerMANOVA (1000 permutations), applying the Adonis () function of VEGAN package in R on the archaeal OTU data matrix (Oksanen et al., 2017). The Wilcoxon rank-sum test was performed to determine the microbial populations with statistical differences. The relationships between environmental factors and archaeal communities were assessed via redundancy analysis (RDA), using the rda () function of the VEGAN package in R. The co-occurrence of operational taxonomic units

http://www.aloki.hu ● ISSN 1589 1623 (Print) ● ISSN 1785 0037 (Online)
DOI: http://dx.doi.org/10.15666/aeer/2005_45654578

(OTUs) in archaeal communities across the two EOR production blocks was analyzed. To reduce the network complexity and facilitate the identification of the core soil community, we selected OTUs with more than 20 sequences for further analysis. The correlation between two OTUs was considered statistically robust if the Spearman correlation coefficient (ρ) was > 0.6 and the Benjamini Hochberg adjusted p-value was < 0.01 (Barberán et al., 2012). The visualization of the co-occurrence network was conducted using the Fruchtermann–Feingold layout of the interactive platform Gephi version 0.9.2. The within-module connectivity (Zi) and among-module connectivity (Pi) were used to divide the network nodes into four sub-categories: (1) nodes with Zi > 2.5 and Pi > 0.62 were defined as network hubs; (2) nodes with Zi < 2.5 and Pi < 0.62 were defined as peripherals; (3) nodes with Zi < 2.5 and Pi > 0.62 were defined as connectors; and (4) nodes with Zi > 2.5 and Pi < 0.62 were defined as module hubs (Olesen et al., 2007).

Results

Overall pyrosequencing information

After quality control, 1,936,270 sequences ranging from 202–549 bp (the length of most sequences was 445 bp) were obtained from Illumina MiSeq sequencing from 37 ASP-flooded production well samples, whereas 1,435,920 sequences ranging from 190–549 bp (the length of most sequences was 448 bp) were obtained from 29 polymer-flooded samples. Based on 97% similarity, 914 OTUs were detected (*Table A1*) that belonged to 8 phyla, 17 classes, 27 orders, 39 families, 57 genera, and 112 species. The species accumulation curves (*Fig. A1*) tended to reach saturation plateaus as the sample number increased, indicating that the number of archaeal sequences obtained represented the archaeal communities well.

Archaeal community composition in polymer-flooded and alkaline-surfactant-polymer (ASP)-flooded production wells

Six genera, including *Methanothermobacter* (18.11%), *Methanoculleus* (15.22%), *Methanolinea* (16.74%), *Methanofollis* (10.59%), *Methanobacterium* (8.50%), and *Candidatus Methanomethylicus* (5.60%) were predominant (relative abundance > 5%) in the polymer-flooded wells and accounted for 74.74% of the total sequences. Five genera, including *Methanothermobacter* (33.69%), *Methanosaeta* (16.70%), *Methanolinea* (13.14%), *Methanobacterium* (9.27%), and *Methanolobus* (7.58%) were predominant (relative abundance > 5%) in the ASP-flooded wells and accounted for 80.39% of the total sequences (*Fig. 1*).

The relative abundance of each archaeal taxonomic group varied between the two EOR technologies (*Fig. 2*). Remarkably, the relative abundance of archaeal genera associated with the polymer-flooded blocks differed significantly from that of the ASP-flooded production wells. Based on the Wilcoxon rank-sum test, the Methanosaeta phylotypes were less abundant in the polymer-flooded blocks than in the ASP production wells. Methanoculleus and Methanofollis were significantly higher in polymer- than in the ASP-flooded wells. The relative abundance of *Candidatus Methanomethylicus* and *Methanolinea*–the dominant archaeal populations in the water-flooded wells–decreased in the ASP-and polymer-flooded wells, whereas *Methanosaeta* became the dominant archaeal population in the ASP-flooded wells.

http://www.aloki.hu ● ISSN 1589 1623 (Print) ● ISSN 1785 0037 (Online)
DOI: http://dx.doi.org/10.15666/aeer/2005_45654578

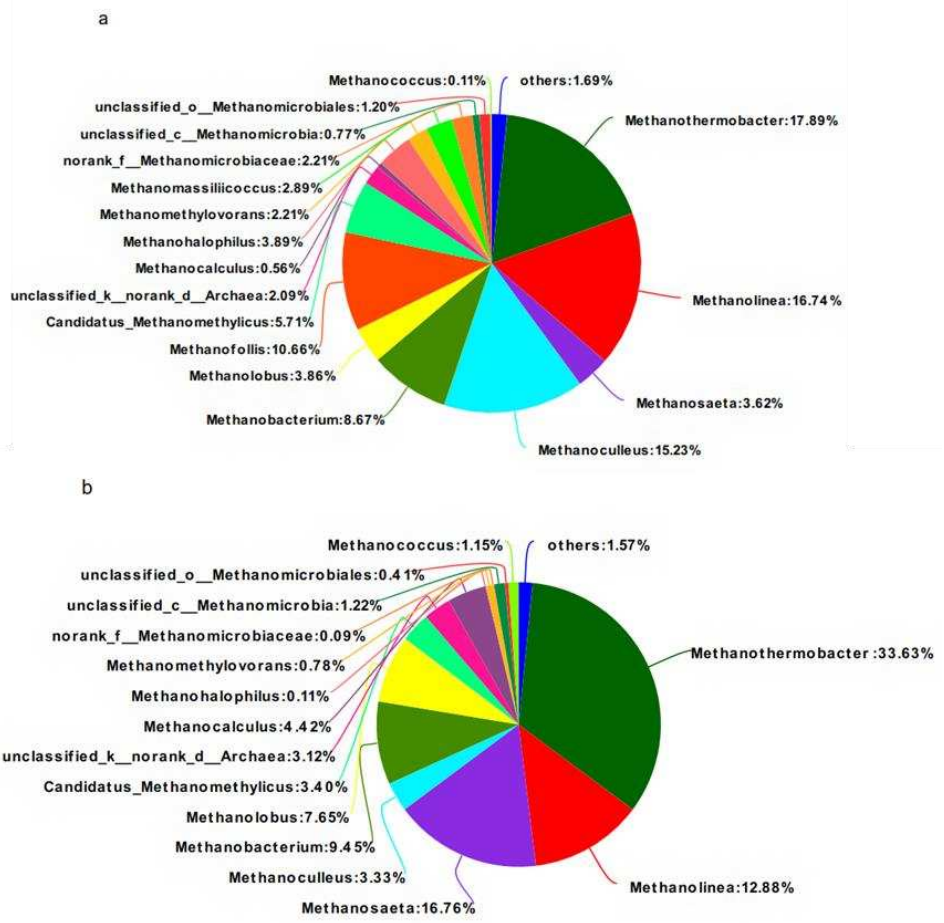

Figure 1. *Archaeal community compositions at the genus level in polymer flooded (a) and ASP flooded (b) production wells*

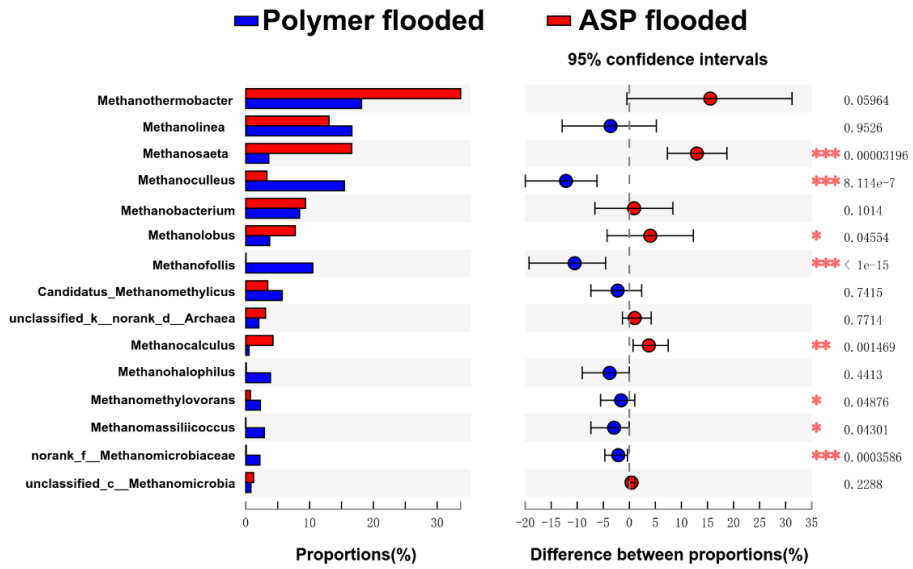

Figure 2. *Wilcoxon rank-sum test revealed the archaeal populations with significant differences in the relative abundance between water flooded, polymer flooded and ASP flooded production wells. *P < 0.05, **P < 0.01, ***P < 0.001*

http://www.aloki.hu ● ISSN 1589 1623 (Print) ● ISSN 1785 0037 (Online)
DOI: http://dx.doi.org/10.15666/aeer/2005_45654578

NMDS ordination (*Fig. 3*) and PerMANOVA revealed a significant effect of EOR flooding technology on the taxonomic composition of archaeal communities ($R^2 = 0.0755$, $P = 0.001$). There was a clear separation between the archaeal communities in the polymer- and ASP-flooded wells from oil recovery.

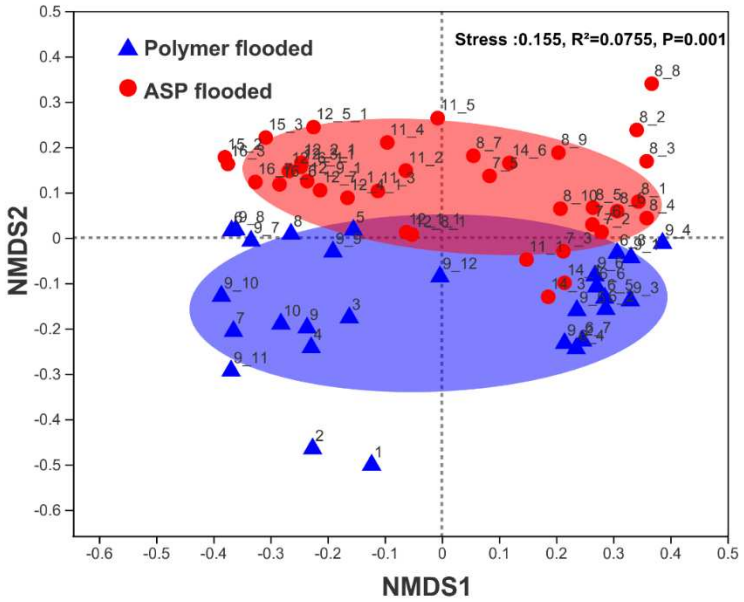

Figure 3. *Nonmetric multidimensional scaling (NMDS) ordination plot of archaeal communities from ASP flooded wells and polymer flooded wells. PERMANOVA analysis showed significant differences in archaeal communities between polymer flooded and ASP flooded production wells*

Archaeal co-occurrence network analysis

We applied correlation-based network analysis to explore the co-occurrence patterns of archaeal communities across two EOR practices by combining all archaea originating from each EOR technology production well (*Fig. 4*). The modularity indexes were 0.745 and 0.739 in the polymer- and ASP-flooded blocks, respectively (*Table A2*), revealing that the networks had a modular structure. The polymer-flooded network consisted of 539 nodes linked by 4665 edges. In contrast, the ASP-flooded network consisted of 689 nodes with 5031 edges. The genera in the network were primarily distributed into eight major genera, of which the most abundant were Methanosaeta (16.67%), Methanothermobacter (14.44%), Methanoculleus (14.25%), and Candidatus Methanomethylicus (8.21%). In the ASP network, Methanosaeta (19.71%), Methanothermobacter (17.10%), Candidatus Methanomethylicus (7.68%), and unclassified Archaea (11.15%) appeared most frequently, indicating environmental adaptation. Compared to that in the polymer-flooded network, the clustering coefficient of the ASP network decreased by 0.019, the network density of the polymer-flooded network increased by 0.011, and the average degree of the polymer-flooded network was higher than that of the ASP-flooded network (*Table A2*), indicating that the archaeal community structure was more complex in polymer-flooded than in ASP-flooded networks and that the application of ASP technology reduced the interspecific relationship of the archaeal community.

http://www.aloki.hu ● ISSN 1589 1623 (Print) ● ISSN 1785 0037 (Online)
DOI: http://dx.doi.org/10.15666/aeer/2005_45654578

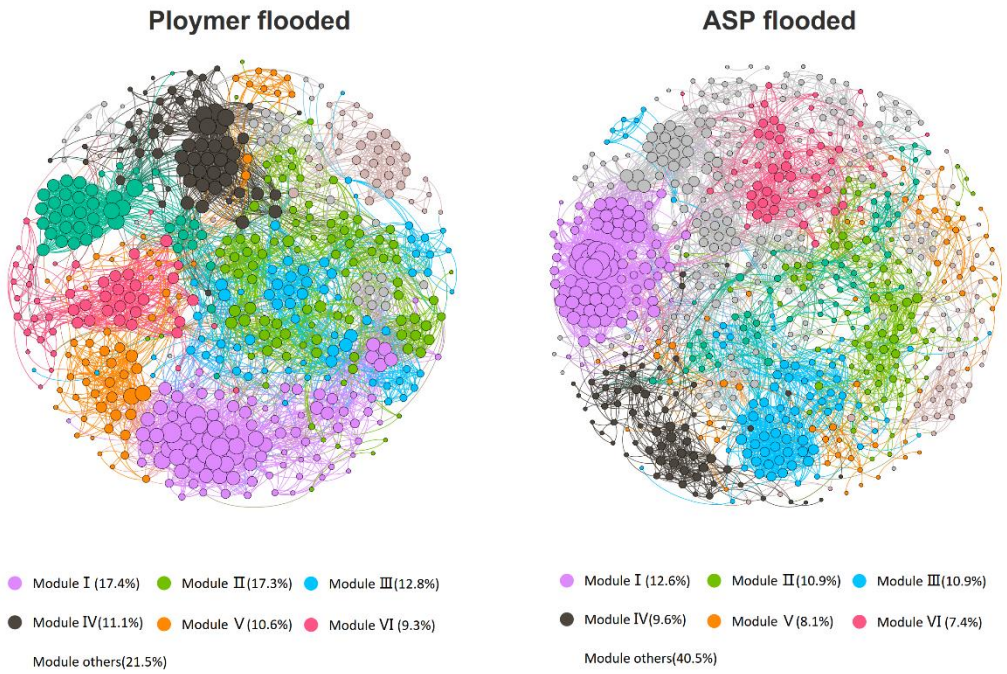

Figure 4. *The co-occurrence patterns among OTUs revealed by network analysis. The nodes were colored according to different types of modularity classes, respectively. A connection stands for a strong (Spearman's $r > 0.6$ or $r < -0.6$) and significant (P-value < 0.01) correlation. The size of each node is proportional to the number of connections (i.e., degree)*

To evaluate the possible topological roles of taxa in the networks based on the within-module connectivity (Zi) and the among-module connectivity (Pi) values, we classified the network nodes into four categories: network hubs, module hubs, connectors, and peripherals (*Fig. A2*). Peripherals were the most abundant nodes in each network with most links inside their modules (*Fig. 4*). No network hubs or module hubs were identified in any of the two networks (*Fig. A2*). In contrast, multiple nodes were classified as connectors in polymer-flooded and ASP networks (*Table A3*). Seventy-five nodes, i.e., Methanosaeta (21 OTUs), Methanoculleus (14 OTUs), Candidatus Methanomethylicus (7 OTUs), Methanolinea (7 OTUs), Methanobacterium (5 OTUs), Methanothermobacter (3 OTUs), and others (18 OTUs), were defined as connectors in the polymer-flooded network. In contrast, the ASP network contained 66 connector nodes, primarily Methanosaeta (16 OTUs), Methanoculleus (7 OTUs), Candidatus Methanomethylicus (10 OTUs), Methanolinea (7 OTUs), Methanobacterium (5 OTUs), Methanothermobacter (3 OTUs), and others (18 OTUs).

Relationship between AMF and soil factors

The different EOR technologies had distinct effects on oil reservoir characteristics (*Table 1*). CO_3^{2-}, Na^+, and pH were significantly higher in ASP-flooded production wells than in polymer-flooded production wells ($p < 0.05$), whereas Ca^{2+} was significantly lower in polymer-flooded production wells. Cl^-, SO_4^{2-}, HCO_3^-, and Mg^{2+} between the polymer- and ASP-flooded processes were not significantly different. To further determine the environmental variables associated with changes in the archaeal community structure, RDA was applied to the contextual parameters in *Table A4,*

http://www.aloki.hu ● ISSN 1589 1623 (Print) ● ISSN 1785 0037 (Online)
DOI: http://dx.doi.org/10.15666/aeer/2005_45654578

revealing that the archaeal community structure was formed by primary environmental characteristics. The first two RDA axes explained 75.03% of the variance in the composition of archaeal communities among different EOR processes (*Fig. 5*). Forward selection in RDA revealed that pH ($P = 0.011$) was the strongest driver of archaeal community assembly in the oil reservoir.

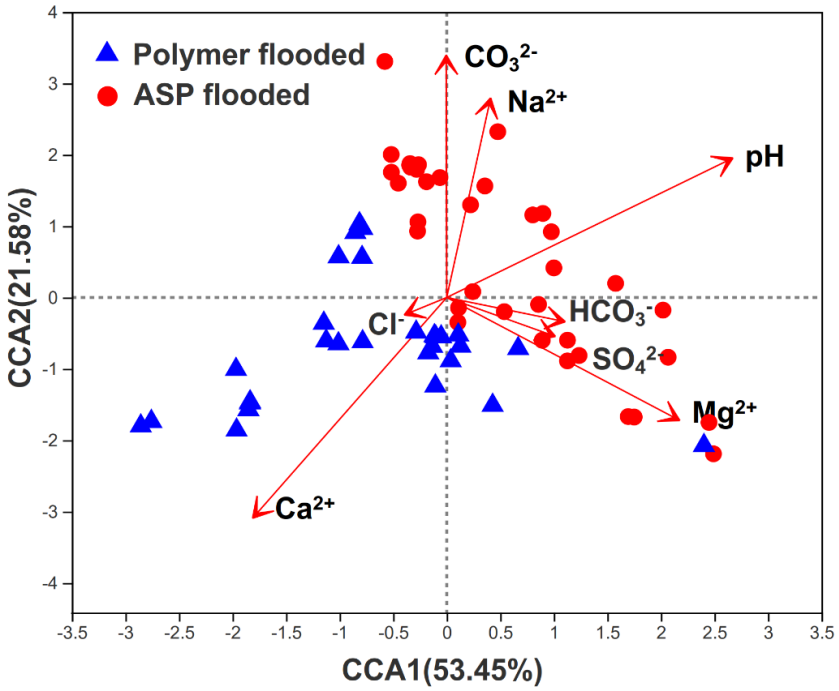

Figure 5. *Redundancy analysis (RDA) of the AMF community based on the OTU matrix from different treatments as affected by different EOR process. Different color points represent different treatments: Polymer flooded (blue) and ASP flooded (red). Arrows represent environmental factors*

Table 1. *Physical and chemical characteristics of samples collected from different EOR treatment*

	pH	CO_3^{2-} (g/L)	HCO_3^- (g/L)	Cl^- (g/L)	SO_4^{2-} (g/L)	Mg^{2+} (mg/L)	Na^+ (g/L)	DOM (g/L)	Ca^{2+} (mg/L)
Polymer	8.22 ± 0.46b	0.40 ± 0.06b	3.52 ± 0.43a	1.22 ± 0.35a	0.12 ± 0.08a	10.52 ± 1.12b	1.94 ± 0.20b	6.64 ± 0.56a	30.20 ± 2.54b
ASP	11.18 ± 1.09a	3.93 ± 1.4a	3.35 ± 0.19a	0.99 ± 0.24a	0.10 ± 0.01a	13.44 ± 0.96a	3.62 ± 0.21a	7.99 ± 1.12a	52.36 ± 1.37a

Data with different lowercase letters indicate significant levels at $P < 0.05$

Discussion

Archaeal communities in oil reservoirs have been investigated for many years (Zhao et al., 2012). This study investigated the influence of polymer and ASP flooding processes on the composition of archaeal communities inhabiting an oil reservoir exploited by decades of water flooding. The archaeal communities in the two EOR flooded oil reservoirs were dominated by *Methanothermobacteraceae* and *Methanosaetaceae*, in which *Methanothermobacter* and *Methanosaeta* were the principal groups (*Fig. 1*). Our results agreed with those of a previous investigation on

http://www.aloki.hu ● ISSN 1589 1623 (Print) ● ISSN 1785 0037 (Online)
DOI: http://dx.doi.org/10.15666/aeer/2005_45654578

archaeal communities in aqueous and oil phases from four production wells from the Chengdong petroleum reservoir in the Shengli Oilfield (Liang et al., 2018) and showed that *Methanothermobacter* was the most common archaea. In the polymer- and ASP-flooded production blocks, *Methanothermobacter*–a common type of *methanogen* in many high-temperature oil reservoirs–was the major division (Wang et al., 2012). *Methanothermobacter* is a type of hydrogenotrophic methanogen that produces methane from CO_2 (Wasserfallen et al., 2000). Some isolates use formate as an electron donor and sulfate as an electron acceptor (Wasserfallen et al., 2000). *Methanosaeta* and *Methanosarcina* are acetoclastic methanogens; *Methanosarcina* utilizes CO_2 and hydrogen to produce methane (Oren, 2014). The NMDS results suggested that the archaeal community structure was significantly different between polymer- and ASP-flooded production wells (*Fig. 3*) and corroborated previous investigations on microbial communities in diverse oil reservoirs, which showed that the microbial community was significantly influenced by reservoir environments. The bacterial and archaeal communities were remarkably affected by extreme reservoir environments, such as high temperature, steam soaking, high pressure, and hypersalinity (Gao et al., 2016, 2019). Crucially, the injection of alkali could result in an extremely alkaline environment in ASP-flooded oil reservoirs, with a pH of up to 11.18, which is much higher than the pH 8.22 of most polymers-flooded environments and exceeds the survival limits of most microbial populations. In the present study, archaeal communities were primarily affected by pH (*Fig. 5*). The strong correlation between pH and archaea distribution could be explained by the relatively narrow growth tolerance exhibited by most archaeal taxa. Indeed, each type of microorganism has an optimal pH value, and a slight change in pH might favor distinct archaeal taxa (Xue et al., 2017). The aforementioned factors made the environmental significance different in the polymer- and ASP-flooded production wells and affected the composition of the archaeal community.

The results of the co-occurring network analysis (*Fig. 4*) suggested the existence of non-random assembly patterns in archaeal communities in polymer- and ASP-flooded networks, as shown by the high modularity index of the network (*Fig. 4*). The non-random assembly pattern of the microbiota may be dominated by deterministic factors, such as nutritional and competitive interactions and niche differentiation (Barberán et al., 2012; Ju et al., 2014).

Compared to the ASP-flooded network, the clustering coefficient of the polymer-flooded network increased by 0.019 (*Table A3*). The average degree of polymer flooding increased by 2.71 compared to the ASP network (*Table A3*), indicating that archaeal associations were tighter in polymer-flooded than ASP-flooded production wells. This agrees with the results of our previous investigation on bacterial communities in diverse oil reservoirs: the bacterial community network was more complex in polymer-flooded than in ASP-flooded production wells (Ren G, 2020). The difference may be explained by changes in taxa that are sensitive to alkali, surfactants, or hydrolyzed polyacrylamide. In particular, the increase in the pH of formation water reduced the connections of the archaeal community in the network of the ASP-flooded blocks and may indicate that the pH of the formation water served as a major selective force in the EOR production blocks.

Multiple nodes were classified as connectors in the polymer- and ASP-flooded networks (*Table A4*). The significance of a taxon in a microbial network may be less influenced by its abundance and instead, depend on its connectivity (Peura et al., 2015). Euryarchaeota (70 OTUs nodes) and Nanoarchaeaeota (2 OTUs) were defined as

http://www.aloki.hu ● ISSN 1589 1623 (Print) ● ISSN 1785 0037 (Online)
DOI: http://dx.doi.org/10.15666/aeer/2005_45654578

connectors in the polymer-flooded network, whereas Euryarchaeota (58 OTUs) and Thaumarchaeota (2 OTUs) were defined in the ASP network. These "key" OTUs identified as hubs are rich OTUs, some of which are rare and may be important participants in ecosystem functions (Comte et al., 2016). In accordance with a previous study (2015), Keystone taxa, such as connectors, are defined by interaction with multiple members and are deemed to play important roles in the overall community (Berry and Widder, 2014).

Conclusions

This study revealed the characteristics of archaeal communities in polymer- and ASP-flooded production wells. Our results indicated that EOR technologies significantly altered the composition of the archaeal community and that different EOR methods significantly influenced the distribution of archaeal communities. Furthermore, the polymer flooding process could make the network of archaea communities more complex and tight than ASP flooding. Considering the critical roles of indigenous microbial communities, such as archaea, in microbial enhanced oil recovery (MEOR) process, revealing the influence of polymer flooding and ASP flooding on community composition and co-occurrence patterns of archaea could facilitate the implementation of MEOR technology in the future. Future work is needed to investigate how to use an upgraded method to stimulate the indigenous archaea, and increase the stability of archaeal co-occurrence patterns to enhance oil recovery.

Acknowledgements. This work was supported by the Heilongjiang Natural Science Foundation Joint Guiding Project (LH2020C069).

Conflict of interests. The authors declare that the research was conducted in the absence of any commercial or financial relationships that could be construed as potential conflict of interests.

Author contributions. WJL, QLN and RGL proposed and organized the overall project. WCJ, HM, BLH and QLN performed the majority of the experiments. WJL and RGL gave assistance in lab work and laboratory analyses. WJL and BLH wrote the main manuscript text. HM, WCJ and QLN contributed insightful discussions. All authors reviewed the manuscript.

REFERENCES

[1] Abilio, A., Wolodko, J., Eckert, R. B., Skovhus, T. L. (2021): Review and Gap Analysis. – Eckert, R. B., Skovhus, T. L. (eds.) Failure Analysis of Microbiologically Influenced Corrosion. CRC, Boca Raton, FL.
[2] Aitken, C. M., Jones, D. M., Larter, S. (2004): Anaerobic hydrocarbon biodegradation in deep subsurface oil reservoirs. – Nature 431: 291-294.
[3] Al Adasani, A., Bai, B. (2011): Analysis of EOR projects and updated screening criteria. – Journal of Petroleum Science and Engineering 79: 10-24.
[4] Barberán, A., Bates, S. T., Casamayor, E. O., Fierer, N. (2012): Using network analysis to explore co-occurrence patterns in soil microbial communities. – The ISME Journal 6: 343-351.
[5] Baumeister, C., Korobilis, D., Lee, T. K. (2022): Energy markets and global economic conditions. – Review of Economics and Statistics 104: 828-844.
[6] Berry, D., Widder, S. (2014): Deciphering microbial interactions and detecting keystone species with co-occurrence networks. – Frontiers in Microbiology 5: 219-219.

http://www.aloki.hu ● ISSN 1589 1623 (Print) ● ISSN 1785 0037 (Online)
DOI: http://dx.doi.org/10.15666/aeer/2005_45654578

[7] Cai, M., Nie, Y., Chi, C.-Q., Tang, Y.-Q., Li, Y., Wang, X.-B., Liu, Z.-S., Yang, Y., Zhou, J., Wu, X.-L. (2015): Crude oil as a microbial seed bank with unexpected functional potentials. – Scientific Reports 5: 1-12.
[8] Chang, H., Zhang, Z., Wang, Q., Xu, Z., Guo, Z., Sun, H., Cao, X., Qiao, Q. (2006): Advances in polymer flooding and alkaline/surfactant/polymer processes as developed and applied in the People's Republic of China. – Journal of Petroleum Technology 58: 84-89.
[9] Chen, J., Zhang, W., Wan, Z., Li, S., Huang, T., Fei, Y. (2019): Oil spills from global tankers: status review and future governance. – Journal of Cleaner Production 227: 20-32.
[10] Chia, N. (2014): Halomonas sulfidaeris-dominated microbial community inhabits a 1.8 km-deep subsurface Cambrian Sandstone reservoir. – Environmental Microbiology 16: 1695.
[11] Comte, J., Lovejoy, C., Crevecoeur, S., Vincent, W. (2016): Co-occurrence patterns in aquatic bacterial communities across changing permafrost landscapes. – Biogeosciences 13: 175-190.
[12] DeLong, E. F. (1992): Archaea in coastal marine environments. – Proceedings of the National Academy of Sciences 89: 5685-5689.
[13] Dengler, L., Meier, J., Grünberger, F., Bellack, A., Rachel, R., Grohmann, D., Huber, H. (2022): Methanofollis propanolicus sp. nov., a novel archaeal isolate from a Costa Rican oil well that uses propanol for methane production. – Archives of Microbiology 204: 1-6.
[14] Dong, H., Zhang, F., Xu, T., Liu, Y., Du, Y., Wang, C., Liu, T., Gao, J., He, Y., Wang, X. (2022): Culture-dependent and culture-independent methods reveal microbe-clay mineral interactions by dissimilatory iron-reducing bacteria in an integral oilfield. – Science of the Total Environment 156577.
[15] Du, C. A., Song, Y., Yao, Z., Su, W., Zhang, G., Wu, X. (2022): Developments in in-situ microbial enhanced oil recovery in Shengli oilfield. – Energy Sources, Part A: Recovery, Utilization, and Environmental Effects 44: 1977-1987.
[16] Firozjaii, A. M., Saghafi, H. R. (2020): Review on chemical enhanced oil recovery using polymer flooding: fundamentals, experimental and numerical simulation. – Petroleum 6: 115-122.
[17] Gao, P., Tian, H., Wang, Y., Li, Y., Li, Y., Xie, J., Zeng, B., Zhou, J., Li, G., Ma, T. (2016): Spatial isolation and environmental factors drive distinct bacterial and archaeal communities in different types of petroleum reservoirs in China. – Scientific Reports 6: 20174.
[18] Gao, P., Tan, L., Li, Y., Guo, F., Ma, T. (2019): Composition of bacterial and archaeal communities in an alkali-surfactant-polyacrylamide-flooded oil reservoir and the responses of microcosms to nutrients. – Frontiers in Microbiology 10: 2197.
[19] Grabowski, A., Nercessian, O., Fayolle, F., Blanchet, D., Jeanthon, C. (2005): Microbial diversity in production waters of a low-temperature biodegraded oil reservoir. – FEMS Microbiology Ecology 54: 427-443.
[20] Ju, F., Xia, Y., Guo, F., Wang, Z., Zhang, T. (2014): Taxonomic relatedness shapes bacterial assembly in activated sludge of globally distributed wastewater treatment plants. – Environmental Microbiology 16: 2421-2432.
[21] Kang, X., Zhang, J., Sun, F., Zhang, F., Feng, G., Yang, J., Zhang, X., Xiang, W. (2011): A review of polymer EOR on offshore heavy oil field in Bohai Bay, China. – In: SPE Enhanced Oil Recovery Conference, Society of Petroleum Engineers.
[22] Kobayashi, H., Endo, K., Sakata, S., Mayumi, D., Kawaguchi, H., Ikarashi, M., Miyagawa, Y., Maeda, H., Sato, K. (2012): Phylogenetic diversity of microbial communities associated with the crude-oil, large-insoluble-particle and formation-water components of the reservoir fluid from a non-flooded high-temperature petroleum reservoir. – Journal of Bioscience and Bioengineering 113: 204-210.
[23] L'Haridon, S., Reysenbacht, A.-L., Glenat, P., Prieur, D., Jeanthon, C. (1995): Hot subterranean biosphere in a continental oil reservoir. – Nature 377: 223-224.

http://www.aloki.hu ● ISSN 1589 1623 (Print) ● ISSN 1785 0037 (Online)
DOI: http://dx.doi.org/10.15666/aeer/2005_45654578

[24] Lenchi, N., Kebbouche- S., Gana,, Servais, P., Gana, M. L., Llirós, M. (2021): Identification and phylogenetic analyses of anaerobic sulfidogenic bacteria in two algerian oilfield water injection samples. – Geomicrobiology Journal 38: 732-740.
[25] Li, H., Yang, S.-Z., Mu, B.-Z. (2007): Phylogenetic diversity of the archaeal community in a continental high-temperature, water-flooded petroleum reservoir. – Current Microbiology 55: 382-388.
[26] Liang, B., Zhang, K., Wang, L.-Y., Liu, J.-F., Yang, S.-Z., Gu, J.-D., Mu, B.-Z. (2018): Different diversity and distribution of archaeal community in the aqueous and oil phases of production fluid from high-temperature petroleum reservoirs. – Frontiers in Microbiology 9: 841.
[27] Magot, M., Ollivier, B., Patel, B. K. (2000): Microbiology of petroleum reservoirs. – Antonie van Leeuwenhoek 77: 103-116.
[28] Nilsen, R. K., Torsvik, T. (1996): Methanococcus thermolithotrophicus isolated from North Sea oil field reservoir water. – Applied and Environmental Microbiology 62: 728-731.
[29] Oksanen, F. J., Blanchet, F. G., Friendly, M., Kindt, R., Legendre, P., McGlinn, D., Minchin, P., O'Hara, R. B., Simpson, G., Solymos, P., et al. (2017): vegan: Community Ecology Package. – R package version 2.4-4. https://CRAN. R-project.org/package=vegan.
[30] Olesen, J. M., Bascompte, J., Dupont, Y. L., Jordano, P. (2007): The modularity of pollination networks. – Proceedings of the National Academy of Sciences of the United States of America 104: 19891-19896.
[31] Ollivier, B., Cayol, J.-L., Patel, B., Magot, M., Fardeau, M.-L., Garcia, J.-L. (1997): Methanoplanus petrolearius sp. nov., a novel methanogenic bacterium from an oil-producing well. – FEMS Microbiology Letters 147: 51-56.
[32] Oren, A. (2014): The Family Methanosarcinaceae. – Rosenberg, E. et al. (eds.) The Prokaryotes: Other Major Lineages of Bacteria and the Archaea. Springer, Berlin, pp. 259-281.
[33] Pannekens, M., Kroll, L., Müller, H., Mbow, F. T., Meckenstock, R. U. (2019): Oil reservoirs, an exceptional habitat for microorganisms. – New Biotechnology 49: 1-9.
[34] Peura, S., Bertilsson, S., Jones, R. I., Eiler, A. (2015): Resistant microbial cooccurrence patterns inferred by network topology. – Applied and Environmental Microbiology 81: 2090.
[35] Pham, V. D., Hnatow, L. L., Zhang, S., Fallon, R. D., Jackson, S. C., Tomb, J. F., DeLong, E. F., Keeler, S. J. (2009): Characterizing microbial diversity in production water from an Alaskan mesothermic petroleum reservoir with two independent molecular methods. – Environmental Microbiology 11: 176-187.
[36] Rajbongshi, A., Gogoi, S. B. (2021): A review on anaerobic microorganisms isolated from oil reservoirs. – World Journal of Microbiology and Biotechnology 37: 1-19.
[37] Rathi, R., Lavania, M., Kukreti, V., Lal, B. (2018): Evaluating the potential of indigenous methanogenic consortium for enhanced oil and gas recovery from high temperature depleted oil reservoir. – Journal of Biotechnology 283: 43-50.
[38] Ren, G., W. J., Qu, L., Li, W., Hu, M., Bian, L., Zhang, Y., Le, J., Dou, X., Chen, X., Bai, L., Li, Y. (2020): Compositions and co-occurrence patterns of bacterial communities associated with polymer- and ASP-flooded petroleum reservoir blocks. – Front. Microbiol 11: 580363.
[39] Shutang, G., Qiang, G. (2010): Recent progress and evaluation of ASP flooding for EOR in Daqing oil field. – In: SPE EOR Conference at Oil & Gas West Asia. Society of Petroleum Engineers.
[40] Singh, N. K., Choudhary, S. (2021): Bacterial and archaeal diversity in oil fields and reservoirs and their potential role in hydrocarbon recovery and bioprospecting. – Environmental Science and Pollution Research 28: 58819-58836.

http://www.aloki.hu ● ISSN 1589 1623 (Print) ● ISSN 1785 0037 (Online)
DOI: http://dx.doi.org/10.15666/aeer/2005_45654578

[41] Tully, B. J., Nelson, W. C., Heidelberg, J. F. (2012): Metagenomic analysis of a complex marine planktonic thaumarchaeal community from the Gulf of Maine. – Environmental Microbiology 14: 254-267.
[42] Tyne, R., Barry, P., Lawson, M., Byrne, D., Warr, O., Xie, H., Hillegonds, D., Formolo, M., Summers, Z., Skinner, B. (2021): Rapid microbial methanogenesis during CO2 storage in hydrocarbon reservoirs. – Nature 600: 670-674.
[43] Van Geel, M., Jacquemyn, H., Plue, J., Saar, L., Kasari, L., Peeters, G., van Acker, K., Honnay, O. … Ceulemans, T. (2018): Abiotic rather than biotic filtering shapes the arbuscular mycorrhizal fungal communities of European seminatural grasslands. – The New phytologist 220: 1262-1272.
[44] Wang, L.-Y., Duan, R.-Y., Liu, J.-F., Yang, S.-Z., Gu, J.-D., Mu, B.-Z. (2012): Molecular analysis of the microbial community structures in water-flooding petroleum reservoirs with different temperatures. – Biogeosciences 9: 4645-4659.
[45] Wasserfallen, A., Nölling, J., Pfister, P., Reeve, J., De Macario, E. C. (2000): Phylogenetic analysis of 18 thermophilic Methanobacterium isolates supports the proposals to create a new genus, Methanothermobacter gen. nov., and to reclassify several isolates in three species, Methanothermobacter thermautotrophicus comb. nov., Methanothermobacter wolfeii comb. nov., and Methanothermobacter marburgensis sp. nov. – International Journal of Systematic and Evolutionary Microbiology 50: 43-53.
[46] Xue, Ren, Leng, H. D., Yao, X. H. (2017): Soil bacterial community structure and co-occurrence pattern during vegetation restoration in karst rocky desertification area. – Front Microbiol. https://doi.org/10.3389/fmicb.2017.02377.
[47] Yang, F., Wang, D., Yang, X., Sui, X., Chen, Q., Zhang, L. (2004): High concentration polymer flooding is successful. – In: SPE Asia Pacific Oil and Gas Conference and Exhibition. Society of Petroleum Engineers.
[48] Yun, Y., Gui, Z., Su, T., Tian, X., Wang, S., Chen, Y., Su, Z., Fan, H., Xie, J., Li, G. (2022): Deep mining decreases the microbial taxonomic and functional diversity of subsurface oil reservoirs. – Science of the Total Environment 821: 153564.
[49] Zhao, L., Ma, T., Gao, M., Gao, P., Cao, M., Zhu, X., Li, G. (2012): Characterization of microbial diversity and community in water flooding oil reservoirs in China. – World Journal of Microbiology and Biotechnology 28: 3039-3052.
[50] Zhao, J.-Y., Hu, B., Dolfing, J., Li, Y., Tang, Y.-Q., Jiang, Y., Chi, C.-Q., Xing, J., Nie, Y., Wu, X.-L. (2021): Thermodynamically favorable reactions shape the archaeal community affecting bacterial community assembly in oil reservoirs. – Science of the Total Environment 781: 146506.

APPENDIX

Table A1. *The rarefied sample OTU matrix data. See electronic appendix*

Table A2. *Topological indices of each network in root AMF of the three grasslands*

	Polymer flooded	**ASP flooded**
Clustering coefficient	0.584	0.563
Modularity	0.745	0.739
Network density	0.032	0.021
Number of nodes	539	689
Number of edges	4665	5031
Average degree	17.31	14.60

http://www.aloki.hu ● ISSN 1589 1623 (Print) ● ISSN 1785 0037 (Online)
DOI: http://dx.doi.org/10.15666/aeer/2005_45654578

Table A3. *Network nodes in polymer and ASP flooded production wells. See electronic appendix*

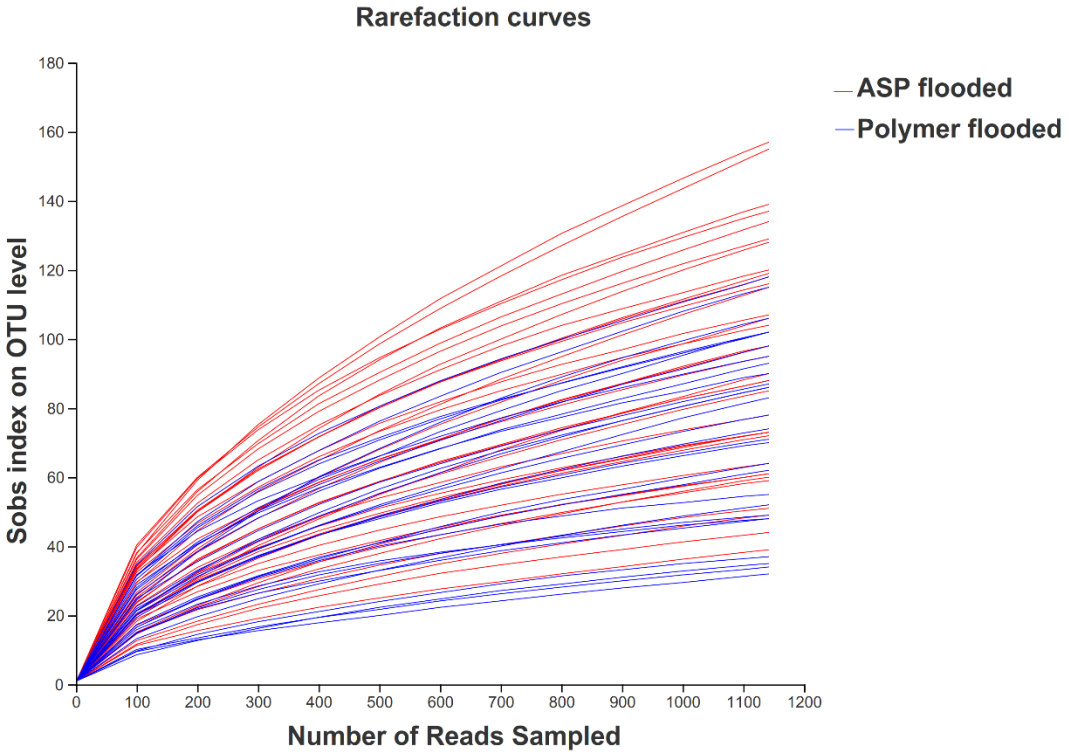

Figure A1. *Taxa accumulation curves of AMF in all samples*

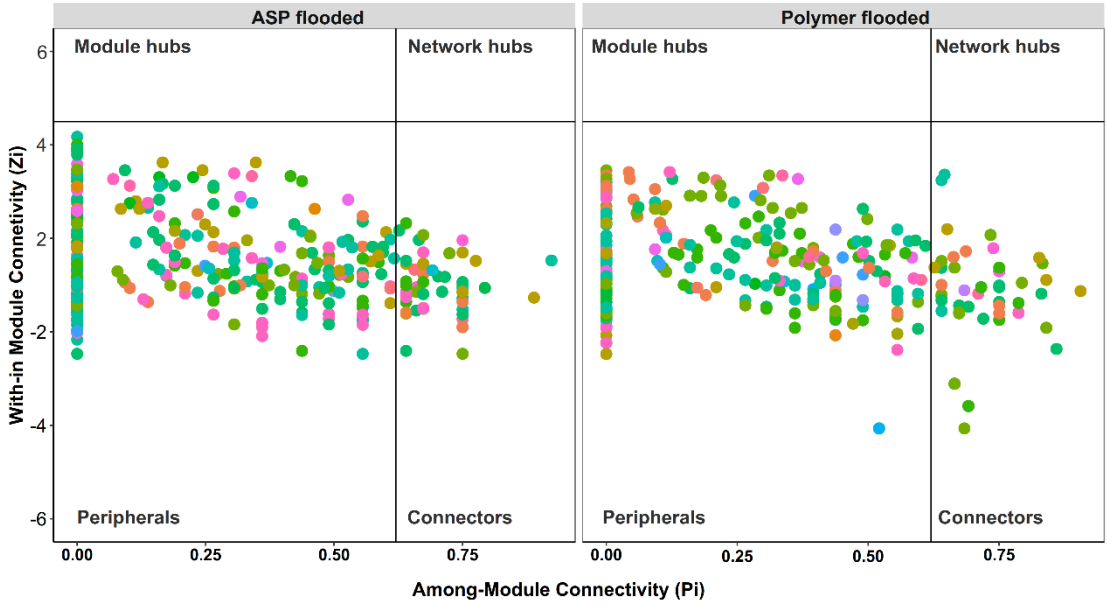

Figure A2. *Zi-Pi plot showing the distribution of OTUs based on their topological roles. Each symbol represents an OTU. The topological role of each OTU was determined according to the scatter plot of within-module connectivity (Zi) and among-module connectivity (Pi)*

http://www.aloki.hu ● ISSN 1589 1623 (Print) ● ISSN 1785 0037 (Online)
DOI: http://dx.doi.org/10.15666/aeer/2005_45654578

Applied Ecology and Environmental Research

International Scientific Journal

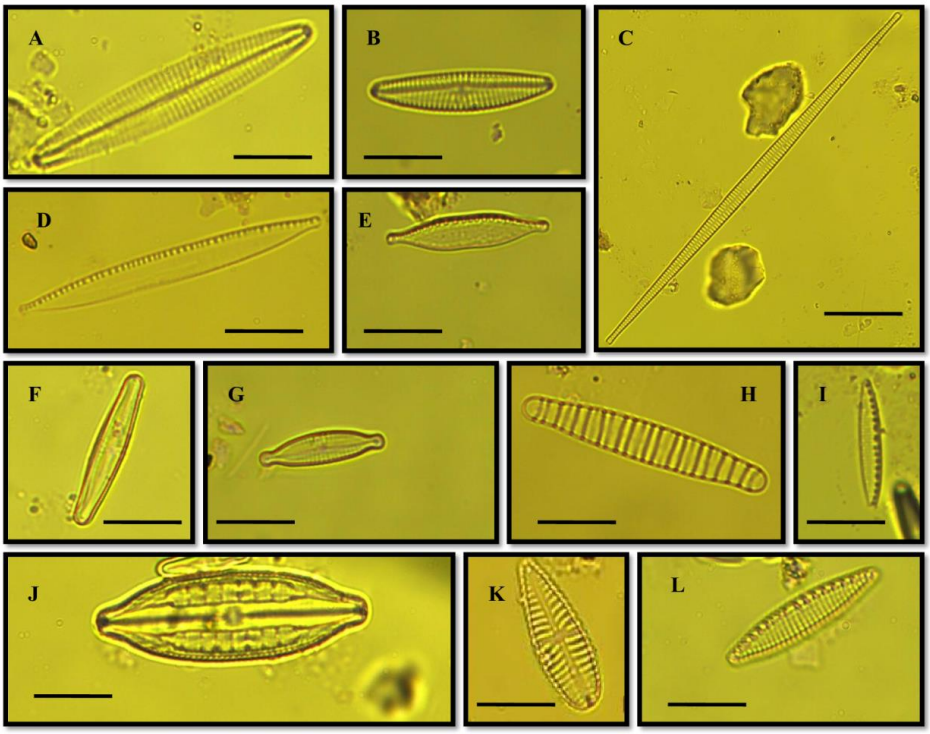

VOLUME 20 * NUMBER 5 * 2022

Published: September 30, 2022
http://www.aloki.hu
ISSN 1589 1623 / ISSN 1785 0037
DOI: http://dx.doi.org/10.15666/aeer